Volume 175 Number 1

THE BIOLOGICAL BULLETIN

AUGUST, 1988

Published by the Marine Biological Laboratory

THE
BIOLOGICAL BULLETIN

PUBLISHED BY
THE MARINE BIOLOGICAL LABORATORY

AUGUST, 1988

Printed and Issued by
LANCASTER PRESS, Inc.
PRINCE & LEMON STS.
LANCASTER, PA

THE BIOLOGICAL BULLETIN

THE BIOLOGICAL BULLETIN is published six times a year by the Marine Biological Laboratory, MBL Street, Woods Hole, Massachusetts 02543.

Subscriptions and similar matter should be addressed to THE BIOLOGICAL BULLETIN, Marine Biological Laboratory, Woods Hole, Massachusetts. Single numbers, $20.00. Subscription per volume (three issues), $55.00 ($110.00 per year for six issues).

Communications relative to manuscripts should be sent to Dr. Charles B. Metz, Editor, or Pamela Clapp, Associate Editor, at the Marine Biological Laboratory, Woods Hole, Massachusetts 02543.

POSTMASTER: Send address changes to THE BIOLOGICAL BULLETIN, Marine Biological Laboratory, Woods Hole, MA 02543.

Second-class postage paid at Woods Hole, MA, and additional mailing offices.
ISSN 0006-3185

INSTRUCTIONS TO AUTHORS

The Biological Bulletin accepts outstanding original research reports of general interest to biologists throughout the world. Papers are usually of intermediate length (10–40 manuscript pages). Very short papers (less than 10 manuscript pages including tables, figures, and bibliography) will be published in a separate section entitled "Short Reports." A limited number of solicited review papers may be accepted after formal review. A paper will usually appear within four months after its acceptance.

The Editorial Board requests that manuscripts conform to the requirements set below; those manuscripts which do not conform will be returned to authors for correction before review.

1. ***Manuscripts.*** Manuscripts, including figures, should be submitted in triplicate. (Xerox copies of photographs are not acceptable for review purposes.) The original manuscript must be typed in double spacing (*including* figure legends, footnotes, bibliography, etc.) on one side of 16- or 20-lb. bond paper, 8½ by 11 inches. Manuscripts should be proofread carefully and errors corrected legibly in black ink. Pages should be numbered consecutively. Margins on all sides should be at least 1 inch (2.5 cm). Manuscripts should conform to the *Council of Biology Editors Style Manual*, 4th Edition (Council of Biology Editors, 1978) and to American spelling. Unusual abbreviations should be kept to a minimum and should be spelled out on first reference as well as defined in a footnote on the title page. Manuscripts should be divided into the following components: Title page, Abstract (of no more than 200 words), Introduction, Materials and Methods, Results, Discussion, Acknowledgments, Literature Cited, Tables, and Figure Legends. In addition, authors should supply a list of words and phrases under which the article should be indexed.

2. ***Figures.*** The dimensions of the printed page, 7 by 9 inches, should be kept in mind in preparing figures for publication. We recommend that figures be about 1½ times the linear dimensions of the final printing desired, and that the ratio of the largest to the smallest letter or number and of the thickest to the thinnest line not exceed 1:1.5. Explanatory matter generally should be included in legends, although axes should always be identified on the illustration itself. Figures should be prepared for reproduction as either line cuts or halftones. Figures to be reproduced as line cuts should be unmounted glossy photographic reproductions or drawn in black ink on white paper, good-quality tracing cloth or plastic, or blue-lined coordinate paper. Those to be reproduced as halftones should be mounted on board, with both designating numbers or letters and scale bars affixed directly to the figures. All figures should be numbered in consecutive order, with no distinction between text and plate figures. The author's name and an arrow indicating orientation should appear on the reverse side of all figures.

3. ***Tables, footnotes, figure legends, etc.*** Authors should follow the style in a recent issue of *The Biological Bulletin* in preparing table headings, figure legends, and the like. Because of the high cost of setting tabular material in type, authors are asked to limit such material as much as possible. Tables, with their headings and footnotes, should be typed on separate sheets, numbered with consecutive Roman numerals, and placed after the Literature Cited. Figure legends should contain enough information to make the figure intelligible separate from the text. Legends should be typed double spaced, with consecutive Arabic numbers, on a separate sheet at the end of the paper. Footnotes should be limited to authors' current addresses, acknowledgments or contribution numbers, and explanation of unusual abbreviations. All such footnotes should appear on the title page. Footnotes are not normally permitted in the body of the text.

4. ***A condensed title*** or running head of no more than 35 letters and spaces should appear at the top of the title page.

5. ***Literature cited.*** In the text, literature should be cited by the Harvard system, with papers by more than two authors cited as Jones *et al.*, 1980. Personal communications and material in preparation or in press should be cited in the text only, with author's initials and institutions, unless the material has been formally accepted and a volume number can be supplied. The list of references following the text should be headed LITERATURE CITED, and must be typed double spaced on separate pages, conforming in punctuation and arrangement to the style of recent issues of *The Biological Bulletin*. Citations should include complete titles and inclusive pagination. Journal abbreviations should normally follow those of the U. S. A.

Standards Institute (USASI), as adopted by BIOLOGICAL ABSTRACTS and CHEMICAL ABSTRACTS, with the minor differences set out below. The most generally useful list of biological journal titles is that published each year by BIOLOGICAL ABSTRACTS (BIOSIS List of Serials; the most recent issue). Foreign authors, and others who are accustomed to using THE WORLD LIST OF SCIENTIFIC PERIODICALS, may find a booklet published by the Biological Council of the U.K. (obtainable from the Institute of Biology, 41 Queen's Gate, London, S.W.7, England, U.K.) useful, since it sets out the WORLD LIST abbreviations for most biological journals with notes of the USASI abbreviations where these differ. CHEMICAL ABSTRACTS publishes quarterly supplements of additional abbreviations. The following points of reference style for THE BIOLOGICAL BULLETIN differ from USASI (or modified WORLD LIST) usage:

A. Journal abbreviations, and book titles, all underlined (for *italics*)

B. All components of abbreviations with initial capitals (not as European usage in WORLD LIST *e.g. J. Cell. Comp. Physiol.* NOT *J. cell. comp. Physiol.*)

C. *All* abbreviated components must be followed by a period, whole word components *must not* (*i.e. J. Cancer Res.*)

D. Space between all components (*e.g. J. Cell. Comp. Physiol.*, not *J.Cell.Comp.Physiol.*)

E. Unusual words in journal titles should be spelled out in full, rather than employing new abbreviations invented by the author. For example, use *Rit Vísindafjélags Islendinga* without abbreviation.

F. All single word journal titles in full (*e.g. Veliger, Ecology, Brain*).

G. The order of abbreviated components should be the same as the word order of the complete title (*i.e. Proc.* and *Trans.* placed where they appear, not transposed as in some BIOLOGICAL ABSTRACTS listings).

H. A few well-known international journals in their preferred forms rather than WORLD LIST or USASI usage (*e.g. Nature, Science, Evolution* NOT *Nature, Lond., Science, N.Y.; Evolution, Lancaster, Pa.*)

6. ***Reprints, charges.*** Authors will be charged the excess over $100 of the total of (a) $30 for each printed page beyond 15, (b) $30 for each table, (c) $15 for each formula more complex than a single line with simple subscripts or superscripts, and (d) $15 for each figure, with figures on a single plate all considered one figure and parts of a single figure on separate sheets considered separate figures. Reprints may be ordered at time of publication and normally will be delivered about two to three months after the issue date. Authors (or delegates for foreign authors) will receive page proofs of articles shortly before publication. They will be charged the current cost of printers' time for corrections to these (other than corrections of printers' or editors' errors).

Reference: *Bio Bull.* 175: 1–64. (August, 1988)

THE MARINE BIOLOGICAL LABORATORY

NINETIETH REPORT, FOR THE YEAR 1987—ONE-HUNDREDTH YEAR

I. Trustees

Including Action of the 1987 Annual Meeting

Officers

Prosser Gifford, *Chairman of the Board of Trustees,* Woodrow Wilson International Center for Scholars, Smithsonian Building, Washington, DC 20560

Denis M. Robinson, *Honorary Chairman of the Board of Trustees,* 200 Ocean Lane, Key Biscayne, FL 33149

Robert Manz, *Treasurer,* Helmer and Associates, Weston, MA 02193

Harlyn O. Halvorson, *President of the Corporation and Director,* Marine Biological Laboratory, Woods Hole, MA 02543

David D. Potter, *Clerk,* Harvard Medical School, Cambridge, MA 02138

Emeriti

John B. Buck, National Institutes of Health
Aurin Chase, Princeton University
George H. A. Clowes Jr., The Cancer Research Institute
Seymour S. Cohen, Woods Hole, MA
Arthur L. Colwin, Key Biscayne, FL
Laura Hunter Colwin, Key Biscayne, FL
D. Eugene Copeland, Marine Biological Laboratory
Sears Crowell, Indiana University
Alexander T. Daignault, Boston, MA
Teru Hayashi, Miami, FL
Hope Hibbard, Oberlin College (deceased 5/11/88)
Lewis Kleinholz, Reed College
Maurice Krahl, Tucson, AZ
Charles B. Metz, University of Miami
Keith Porter, University of Maryland
C. Ladd Prosser, University of Illinois
John S. Rankin, Ashford, CT (deceased 12/12/87)
S. Meryl Rose, Waquoit, MA
John Saunders Jr., Waquoit, MA
George T. Scott, Woods Hole, MA (deceased 9/18/87)
Mary Sears, Woods Hole, MA
Homer P. Smith, Woods Hole, MA
Carl C. Speidel, University of Virginia (deceased 1982)
W. Randolph Taylor, University of Michigan
George Wald, Woods Hole, MA

Class of 1991

Robert B. Barlow Jr., Syracuse University
James M. Clark, Edna McConnell Clark Foundation
Laszlo Lorand, Northwestern University
Lionel I. Rebhun, University of Virginia
Carol L. Reinisch, Tufts University School of Veterinary Medicine
Brian M. Salzberg, University of Pennsylvania
Howard A. Schneiderman, Monsanto Company
Sheldon J. Segal, The Rockefeller Foundation

Class of 1990

John E. Dowling, Harvard University
Gerald D. Fischbach, Washington University School of Medicine
Robert D. Goldman, Northwestern University
John E. Hobbie, Marine Biological Laboratory
Richard E. Kendall, Massachusetts Governor's Office
Irving W. Rabb, Boston, Massachusetts

Joan V. Ruderman, Duke University
Ann E. Stuart, University of North Carolina
D. Thomas Trigg, Wellesley, MA

Class of 1989

Garland E. Allen, Washington University
Peter B. Armstrong, University of California, Davis
Robert W. Ashton, Gaston Snow Beekman and Bogue
Jelle Atema, Marine Biological Laboratory
John G. Hildebrand, University of Arizona
Thomas J. Hynes Jr., Meredith and Grew, Inc.
Robert Mainer, The Boston Company
Birgit Rose, University of Miami
Gerald Weissmann, New York University

Class of 1988

Clay M. Armstrong, University of Pennsylvania
Joel P. Davis, Seapuit, Inc.
Ellen R. Grass, The Grass Foundation
Judith P. Grassle, Marine Biological Laboratory
Holger W. Jannasch, Woods Hole Oceanographic Institution
George M. Langford, University of North Carolina
Andrew Szent-Györgyi, Brandeis University
Kensal E. Van Holde, Oregon State University
Stanley W. Watson, Woods Hole Oceanographic Institution

Standing Committees

Executive Committee of the Board of Trustees

Prosser Gifford*
Harlyn O. Halvorson*
Ray L. Epstein*
Robert Manz*
John E. Dowling, 1990
Gerald D. Fischbach, 1989
John G. Hildebrand, 1988
Sheldon J. Segal, 1989
Andrew Szent-Györgyi, 1988
D. Thomas Trigg, 1990

Animal Care Commitee

Carol L. Reinisch, Chairman
Ray L. Epstein*
Linda Huffer*
Edward Jaskin
Andrew H. Mattox*
Roxanna Smolowitz
Felix Strumwasser
J. Richard Whittaker

Buildings and Grounds Committee

Kenyon S. Tweedell, Chairman
Lawrence B. Cohen
Richard D. Cutler*
Alan Fein
Daniel L. Gilbert
Clifford V. Harding Jr.
Ferenc I. Harosi
Donald B. Lehy*
Thomas H. Meedel
Philip Person
Lionel I. Rebhun
Thomas S. Reese
Evelyn Spiegel

Employee Relations Committee

John V. K. Helfrich, Chairman
Judith Ashmore
Florence Dwane
Edward Enos
William A. Evans
John B. MacLeod

Fellowships Committee

Thoru Pederson, Chairman
Judith P. Grassle
John G. Hildebrand
George M. Langford
Eduardo Macagno
Carol L. Reinisch

Housing, Food Service and Day Care Committee

Jelle Atema, Chairman
Robert B. Barlow Jr.
Gail D. Burd
LouAnn King*
Thomas S. Reese
Joan V. Ruderman
Ann E. Stuart

Institutional Biosafety

Raymond E. Stephens, Chairman
Paul J. DeWeer
Paul T. Englund
Harlyn O. Halvorson*
Paul Lee
Donald B. Lehy*
Joseph Martyna
Andrew H. Mattox*
Al Senft

Instruction Committee

Judith P. Grassle, Chairman
Ray L. Epstein*
Brian Fry
John G. Hildebrand
Hans Laufer
Joan V. Ruderman
Brian M. Salzberg
Roger D. Sloboda
Andrew Szent-Györgyi

Investment Committee

D. Thomas Trigg, Chairman
Prosser Gifford*
William T. Golden
Mauriee Lazarus
Robert Manz*
John W. Speer*
W. Nicholas Thorndike

Library Joint Management Committee

Harlyn O. Halvorson, Chairman*
Garland E. Allen
George D. Griee
John W. Speer*
John H. Steele

Library Joint Users Committee

Garland E. Allen, Chairman
Wilfred B. Bryan
A. Farmanfarmaian

* *ex-officio*

Jane Fessenden*
Lionel F. Jaffe
Laurence P. Madin
John Schlee
Frederic Serchuk
Oliver C. Zafiriou

Marine Resources Committee

Robert D. Goldman, Chairman
William D. Cohen
Richard D. Cutler*
Louis Leibovitz
Toshio Narahashi
George D. Pappas
Rober D. Sloboda
Melvin Spiegel
Antoinette Steinacher
John Valois*

Radiation Safety Committee

Paul J. DeWeer, Chairman
Richard L. Chappell
Sherwin J. Cooperstein
Daniel S. Grosch
Louis M. Kerr*
Andrew H. Mattox*
Harris Ripps
Walter S. Vincent

Research Services Committee

Birgit Rose, Chairman
Peter B. Armstrong
Robert B. Barlow Jr.
Richard D. Cutler*
Ray L. Epstein*
Barbara Ehrlich
John G. Hildebrand
Laurinda Jaffe
Samuel S. Koide
Andrew H. Mattox*
Bryan Noe
Joel Rosenbaum
Rudi Strickler

Research Space Committee

Joseph Sanger, Chairman
Clay M. Armstrong
David Landowne
Hans Laufer
Laszlo Lorand
Eduardo Macagno
Jerry Melillo
Roger D. Sloboda
Evelyn Spiegel
Steven Treistman
Ivan Valiela

Safety Committee

John E. Hobbie, Chairman
Daniel L. Alkon
D. Eugene Copeland
Richard D. Cutler*
Edward Enos*
Alan Fein
Louis M. Kerr*
Alan M. Kuzirian
Donald B. Lehy*
Andrew H. Mattox*
Edward A. Sadowski*
Paul A. Steudler

Trustees' Committees

Audit Committee

Robert Mainer, Chairman
Robert Manz*
Sheldon J. Segal
D. Thomas Trigg
Kensal E. Van Holde

* *ex-officio*

Investment Committee

D. Thomas Trigg, Chairman
William T. Golden
Maurice Lazarus
Robert Manz*
W. Nicholas Thorndike

Compensation Committee

Thomas J. Hynes Jr., Chairman
James M. Clark
John E. Dowling
Irving W. Rabb

Committee on Laboratory Goals

Gerald D. Fischbach, Chairman
Michael V. L. Bennett
Harlyn O. Halvorson
John G. Hildebrand
John E. Hobbie
David D. Potter
Joan V. Ruderman
J. Richard Whittaker

Centennial Committee

James D. Ebert, Chairman
Pamela Clapp, Coordinator*
Garland E. Allen
Robert B. Barlow, Jr.
Paul R. Gross
Harlyn O. Halvorson*
Olivann Hobbie
Richard E. Kendall
John Pfeiffer
Keith Porter
Frank Press
C. Ladd Prosser
John S. Reed
D. Thomas Trigg
John Valois

II. Members of the Corporation

Including Action of the 1987 Annual Meeting

Life Members

Abbott, Marie, c/o Vaughn Abbott, Flyer Rd., East Hartland, CT 06027

Adolph, Edward F., University of Rochester, School of Medicine and Dentistry, Rochester, NY 14642

Beams, Harold W., Department of Biology, University of Iowa, Iowa City, IA 53342

Behre, Ellinor, Black Mountain, NC 28711

Bernheimer, Alan W., Department of Microbiology, New York University Medical Center, 550 First Ave., New York, NY 10016

Bertholf, Lloyd M., Westminster Village #2114, 2025 E. Lincoln St., Bloomington, IL 61701

Bishop, David W., Department of Physiology, Medical College of Ohio, C. S. 10008, Toledo, OH 43699

Bold, Harold C., Department of Botany, University of Texas, Austin, TX 78712

Bridgman, A. Josephine, 715 Kirk Rd., Decatur, GA 30030

Buck, John B., NIH, Laboratory of Physical Biology, Room 112, Building 6 Bethesda, MD 20892

Burbanck, Madeline P., Box 15134, Atlanta, GA 30333

Burbanck, William D., Box 15134, Atlanta, GA 30333

Carpenter, Russell, L., 60-H Lake St., Winchester, MA 01890

Chase, Aurin, Professor of Biology Emeritus, Princeton University, Princeton, NJ 08544

Clark, Arnold M., 48 Wilson Rd., Woods Hole, MA 02543

Clarke, George L., Address unknown (deceased 8/23/87)

Cohen, Seymour S., 10 Carrot Hill Rd., Woods Hole, MA 02543

Colwin, Arthur, 320 Woodcrest Rd., Key Biscayne, FL 33149

Colwin, Laura Hunter, 320 Woodcrest, Key Biscayne, FL 33149

Copeland, D. E., 41 Fern Lane, Woods Hole, MA 02543

Costello, Helen M., Carolina Meadows, Villa 137, Chapel Hill, NC 27514

Crouse, Helen, Institute of Molecular Biophysics, Florida State University, Tallahassee, FL 32306

Diller, Irene C., Rydal Park, Apartment 660, Rydal, PA 19046 (deceased 2/88)

Elliott, Alfred M., 428 Lely Palm Ext., Naples, FL 33962-8903 (deceased 1/20/88)

Failla, Patricia M., 2149 Loblolly Lane, Johns Island, SC 29455

Ferguson, Frederick P., National Institute of General Medical Science, NIH, Bethesda, MD 20892

Ferguson, James K. W., 56 Clarkehaven St., Thornhill, Ontario L4J 2B4 CANADA

Fries, Erik F. B., 41 High Street, Woods Hole, Ma 02543

Gilman, Lauren C., Department of Biology, University of Miami, PO Box 24918, Coral Gables, FL 33124 (deceased 12/87)

Graham, Herbert, 36 Wilson Rd., Woods Hole, MA 02543

Green, James W., 409 Grand Ave., Highland Park, NJ 08904

Grosch, Daniel S., Department of Genetics, Gardner Hall, North Carolina State University, Raleigh, NC 27607

Hamburger, Viktor, Professor Emeritus, Washington University, St. Louis, MO 63130

Hamilton, Howard L., Department of Biology, University of Virginia, Charlottesville, VA 22901

Hibbard, Hope, c/o Jeanne Stephens, 374 Morgan St., Oberlin, OH 44074 (deceased 5/11/88)

Hisaw, F. L., 5925 SW Plymouth Drive, Corvallis, OR 97330

Hollaender, Alexander, Council for Research Planning, 1717 Massachusetts Ave. NW, Washington, DC 20036

Humes, Arthur, Marine Biological Laboratory, Woods Hole, MA 02543

Johnson, Frank H., Department of Biology, Princeton University, Princeton, NJ 08540

Kaan, Helen W., Royal Megansett Nursing Home, Room 205, P. O. Box 408, N. Falmouth, MA 02556

Karush, Fred, Department of Microbiology, University of Pennsylvania School of Medicine, Philadelphia, PA 19104

Kille, Frank R., 1111 S. Lakemont Ave. #444, Winter Park, FL 32792

Kingsbury, John M., Department of Botany, Cornell University, Ithaca, NY 14853

Kleinholz, Lewis, Department of Biology, Reed College, Portland, OR 97202

Lauffer, Max A., Department of Biophysics, University of Pittsburgh, Pittsburgh, PA 15260

LeFevre, Paul G., 15 Agassiz Road, Woods Hole, MA 02543

Levine, Rachmiel, 2024 Canyon Rd., Arcadia, CA 91006

Lochhead, John H., 49 Woodlawn Rd., London SW6 6PS, England, U. K.

Lynn, W. Gardner, Department of Biology, Catholic University of America, Washington, DC 20017

Magruder, Samuel R., 270 Cedar Lane, Paducah, KY 42001

Manwell, Reginald, D., Syracuse University, Lyman Hall, Syracuse, NY 13210

Miller, James A., 307 Shorewood Drive, E. Falmouth, MA 02536

Milne, Lorus J., Department of Zoology, University of New Hampshire, Durham, NH 03824

Moore, John A., Department of Biology, University of California, Riverside, CA 92521

Moul, E. T., 43 F. R. Lillie Rd., Woods Hole, MA 02543

Nace, Paul F., 5 Bowditch Road, Woods Hole, MA 02543

Page, Irving H., Box 516, Hyannisport, MA 02647

Pollister, A. W., 313 Broad Street, Harleysville, PA 19438

Prosser, C. Ladd, Department of Physiology and Biophysics, Burrill Hall 524, University of Illinois, Urbana, IL 61801

Provasoli, Luigi, Haskins Laboratories, 165 Prospect Street, New Haven, CT 06510

Prytz, Margaret McDonald, 21 McCouns Lane, Oyster Bay, NY 11771

Rankin, John S., Jr., Box 97, Ashford, CT 06278 (deceased 12/12/87)
Renn, Charles E., Route 2, Hempstead, MD 21074
Richards, A. Glenn, 942 Cromwell Ave., St. Paul, MN 55114
Richards, Oscar W., Pacific University, Forest Grove, OR 97462
Rockstein, Morris, 8045 SW 107 Ave., #201, Miami, FL 33173
Ronkin, Raphael R., 3212 McKinley St., NW, Washington, DC 20015
Sanders, Howard, Woods Hole Oceanographic Institution, Woods Hole, MA 02543
Scharrer, Berta, Department of Anatomy, Albert Einstein College of Medicine, 1300 Morris Park Avenue, Bronx, NY 10461
Schlesinger, R. Walter, University of Medicine and Dentistry of New Jersey, Department of Microbiology, Rutgers Medical School, P. O. Box 101, Piscataway, NJ 08854
Schmitt, F. O., Room 16-512, Massachusetts Institute of Technology, Cambridge, MA 02139
Scott, Allan C., 1 Nudd St., Waterville, ME 04901
Scott, George T., 10 Orchard St., Woods Hole, MA 02543 (deceased 9/17/87)
Shemin, David, 33 Lawrence Farm Rd., Woods Hole, MA 02543
Smith, Homer P., 8 Quissett Ave., Woods Hole, MA 02543
Smith, Paul F., P. O. Box 264, Woods Hole, MA 02543
Sonnenblick, B. P., 91 Chestnut St., Millburn, NJ 07041
Speidel, Carl C., 1873 Field Rd., Charlottesville, VA 22903 (deceased 1982)
Steinhardt, Jacinto, 1508 Spruce St., Berkeley, CA 94709
Stunkard, Horace W., American Museum of Natural History, Central Park West at 79th St., New York, NY 10024
Taylor, Robert E., 20 Harbor Hill Rd., Woods Hole, MA 02543
Taylor, W. Randolph, Department of Biology, University of Michigan, Ann Arbor, MI 48109
Taylor, W. Rowland, 152 Cedar Park Road, Annapolis, MD 21401
TeWinkel, Lois E., 4 Sanderson Ave., Northampton, MA 01060
Trager, William, The Rockefeller University, 1230 York Ave., New York, NY 10021
Wainio, Walter W., 331 State Rd., Princeton, NJ 08540 (deceased 12/87)
Wald, George, 21 Lakeview Ave., Cambridge, MA 02138
Waterman, T. H., Yale University, Biology Department, Box 6666, 610 Kline Biology Tower, New Haven, CT 06510
Weiss, Paul A., Address unknown
Wichterman, Ralph, 31 Buzzards Bay Ave., Woods Hole, MA 02543
Wiercinski, Floyd J., Department of Biology, Northwestern Illinois University, Chicago, IL 60625
Wilber, Charles G., Department of Zoology, Colorado State University, Fort Collins, CO 80523
Young, D. B., 1137 Main St., N. Hanover, MA 02339
Zinn, Donald J., P. O. Box 589, Falmouth, MA 02541
Zorzoli, Anita, 18 Wilbur Blvd., Poughkeepsie, NY 12603
Zweifach, Benjamin W., c/o Ames, University of California, La Jolla, CA 92037

Regular Members

Ache, Barry W., Whitney Marine Laboratory, University of Florida, Rt. 1 Box 121, St. Augustine, FL 32086
Acheson, George H., 25 Quissett Ave., Woods Hole, MA 02543
Adams, James A., Department of Biological Sciences, Tennessee State University, 3500 John Merritt Blvd., Nashville, TN 37203
Adelberg, Edward A., Department of Human Genetics, Yale University Medical School, P. O. Box 3333, New Haven, CT 06510
Adelman, William J., Jr., NIH, Bldg. 9, Rm. 1E-127, Bethesda, MD 20892
Afzelius, Bjorn, Wenner-Gren Institute, University of Stockholm, Stockholm, Sweden
Alberte, Randall S., Oceanic Biology Program, Code 1122B, Office of Naval Research, 800 North Quincy St., Arlington, VA 22217-5000
Alkon, Daniel, Laboratory of Cellular and Molecular Neurobiology, NINDDS/NIH, Bldg. 5, Rm. 435, Bethesda, MD 20892
Allen, Garland E., Department of Biology, Washington University, St. Louis, MO 63130
Allen, Nina S., Department of Biology, Wake Forest University, Box 7325, Reynolds Station, Winston-Salem, NC 27109
Allen, Suzanne T., Department of Medicine, Worcester Memorial Hospital 119 Belmont St., Worcester, MA 01605
Amatniek, Ernest, 4797 Boston Post Rd., Pelham Manor, NY 10803
Anderson, Everett, Department of Anatomy, LHRBB, Harvard Medical School, 45 Shattuck St., Boston, MA 02115
Anderson, J. M., 110 Roat St., Ithaca, NY 14850
Armet-Kibel, Christine, Biology Department, University of Massachusetts-Boston, Boston, MA 02125

Armstrong, Clay M., Department of Physiology, Medical School, University of Pennsylvania, Philadelphia, PA 19174

Armstrong, Peter B., Department of Zoology, University of California, Davis, CA 95616

Arnold, John M., Pacific Biomedical Research Center, 209 Snyder Hall, 2538 The Mall, Honolulu, HI 96822

Arnold, William A., 102 Balsam Rd., Oak Ridge, TN 37830

Ashton, Robert W., Gaston Snow Beekman and Bogue, 14 Wall St., Suite 1600 New York, NY 10005

Atema, Jelle, Marine Biological Laboratory, Woods Hole, MA 02543

Atwood, Kimball C., P. O. Box 673, Woods Hole, MA 02543

Augustine, George J., Section of Neurobiology, Department of Biological Sciences, University of Southern California, Los Angeles, CA 90089-0371

Austin, Mary L., 506 1/2 N. Indiana Ave., Bloomington, IN 47401

Ayers, Donald E., Marine Biological Laboratory, Woods Hole, MA 02543

Bacon, Robert, P. O. Box 723, Woods Hole, MA 02543

Baker, Robert G., New York University Medical Center, 550 First Ave., New York, NY 10016

Baldwin, Thomas O., Department of Biochemistry and Biophysics, Texas A&M University, College Station, TX 77843

Bang, Betsy, 76 F. R. Lillie Rd., Woods Hole, MA 02543

Barlow, Robert B., Jr., Institute for Sensory Research, Syracuse University, Merrill Lane, Syracuse, NY 13210

Barry, Daniel T., Department of Physical Medicine and Rehabilitation, ID204, University of Michigan Hospital, Ann Arbor, MI 48109-0042

Barry, Susan R., Department of Physical Medicine and Rehabilitation, ID204, University of Michigan Hospital, Ann Arbor, MI 48109-0042

Bartell, Clelmer K., 2000 Lake Shore Drive, New Orleans, LA 70122

Bartlett, James H., Department of Physics, Box 1921, University of Alabama, Tuscaloosa, AL 35489

Bass, Andrew H., Seely Mudd Hall, Department of Neurobiology and Behavior, Cornell University, Ithaca, NY 14853

Battelle, Barbara-Anne, Whitney Laboratory, Rt. 1, Box 121, St. Augustine, FL 32086

Bauer, G. Eric, Department of Anatomy, University of Minnesota, Minneapolis, MN 55455

Beauge, Luis Alberto, Instituto de Investigacion Medica, Casilla de Correo 389, 5000 Cordoba, Argentina

Beck, L. V., School of Experimental Medicine, Department of Pharmacology, Indiana University, Bloomington, IN 47401

Begenisich, Ted, Department of Physiology, University of Rochester, Rochester, NY 14642

Begg, David A., LHRRB, Harvard Medical School, 45 Shattuck St., Boston, MA 02115

Bell, Eugene, Organogenesis, Inc., 83 Rogers St., Cambridge, MA 02142

Benjamin, Thomas L., Department of Pathology, Harvard Medical School, 25 Shattuck St., Boston, MA 02115

Bennett, M. V. L., Albert Einstein College of Medicine, Department of Neuroscience, 1300 Morris Park Ave., Bronx, NY 10461

Bennett, Miriam F., Department of Biology, Colby College, Waterville, ME 04901

Berg, Carl J., Jr., Bureau of Marine Research, 13365 Overseas Highway, Marathon, FL 33050

Berne, Robert M., University of Virginia, School of Medicine, Charlottesville, VA 22908

Bezanilla, Francisco, Department of Physiology, University of California, Los Angeles, CA 90052

Biggers, John D., Department of Physiology, Harvard Medical School, Boston, MA 02115

Bishop, Stephen H., Department of Zoology, Iowa State University, Ames, IA 50010

Blaustein, Mordecai P., Department of Physiology, School of Medicine, University of Maryland, 655 W. Baltimore Street, Baltimore, MD 21201

Bloom, Kerry S., Department of Biology, University of North Carolina, Chapel Hill, NC 27514

Bodian, David, Address unknown

Bodznick, David A., Department of Biology, Wesleyan University, Middletown, CT 06457

Boettiger, Edward G., 29 Juniper Point, Woods Hole, MA 02543

Boolootian, Richard A., Science Software Systems, Inc., 3576 Woodcliff Rd., Sherman Oaks, CA 91403

Borei, Hans G., Long Cove, Stanley Point Road, Minturn, ME 04659

Borgese, Thomas A., Department of Biology, Lehman College, CUNY, Bronx, NY 10468

Borisy, Gary G., Laboratory of Molecular Biology, University of Wisconsin, Madison, WI 53706

Borst, David W., Jr., Department of Biological Sciences, Illinois State University, Normal, IL 61761

Bosch, Herman F., 17 Damon Drive, Falmouth, MA 02540

Bowles, Francis P., P. O. Box 674, Woods Hole, MA 02543

Boyer, Barbara C., Department of Biology, Union College, Schenectady, NY 12308

Brandhorst, Bruce P., Biology Department, McGill University, 1205 Avenue Dr. Penfield, Montreal, P. Q., CANADA H3A 1B1

Brehm, Paul, Department of Physiology, Tufts Medical School, Boston, MA 02111

Brinley, F. J., Neurological Disorders Program, NINCDS, 812 Federal Building, Bethesda, MD 20892

Brown, Joel E., Department of Ophthalmology, Box 8096 Sciences Center, Washington University, 660 S. Euclid Ave., St. Louis, MO 63110

Brown, Stephen C., Department of Biological Sciences, SUNY, Albany, NY 12222

Burd, Gail Deerin, Department of Molecular and Cellular Biology, Biosciences West, Room 305, University of Arizona, Tucson, AZ 85721

Burdick, Carolyn J., Department of Biology, Brooklyn College, Brooklyn, NY 11210

Burger, Max, Department of Biochemistry, Biocenter, Klingelbergstrasse 70, CH-4056 Basel, Switzerland

Burky, Albert, Department of Biology, University of Dayton, Dayton, OH 45469

Burstyn, Harold Lewis, 216 Bradford Parkway, Syracuse, NY 13224

Bursztajn, Sherry, Neurology Department—Program in Neuroscience, Baylor College of Medicine, Houston, TX 77030

Bush, Louise, 7 Snapper Lane, Falmouth, MA 02540

Calabrese, Ronald L., Department of Biology, Emory University, 1555 Pierce Drive, Atlanta, GA 30322

Candelas, Graciela C., Department of Biology, University of Puerto Rico, Rio Piedras, PR 00931

Carew, Thomas J., Department of Psychology, Yale University, P. O. Box 11A, Yale Station, New Haven, CT 06520

Cariello, Lucio, Stazione Zoologica, Villa Comunale, Naples, ITALY

Carlson, Francis D., Department of Biophysics, Johns Hopkins University, Baltimore, MD 21218

Carriere, Rita M., Department of Anatomy, Box 5, SUNY, Brooklyn, 450 Clarkson Ave., Brooklyn, NY 11203

Case, James, Department of Biological Sciences, University of California, Santa Barbara, CA 93106

Cassidy, Rev. J. D., St. Rose Priory, Springfield, KY 40069

Cebra, John J., Department of Biology, Leidy Labs, G-6, University of Pennsylvania, Philadelphia, Pa 19174

Chaet, Alfred B., University of West Florida, Pensacola, FL 32504

Chambers, Edward L., Department of Physiology and Biophysics, University of Miami, School of Medicine, P. O. Box 016430, Miami, FL 33101

Chang, Donald C., Department of Physiology and Molecular Biophysics, Baylor College of Medicine, One Baylor Plaza, Houston, TX 77030

Chappell, Richard L., Department of Biological Sciences, Hunter College, Box 67, 695 Park Ave., New York, NY 10021

Chauncey, Howard H., 30 Falmouth St., Wellesley Hills, MA 02181

Charlton, Milton P., Physiology Department MSB, University of Toronto, Toronto, Ontario, Canada M5S 1A8

Child, Frank M., Department of Biology, Trinity College, Hartford, CT 06106

Chisholm, Rex L., Department of Cell Biology and Anatomy, Northwestern University Medical School, 303 E. Chicago Avenue, Chicago, IL 60611

Citkowitz, Elena, 410 Livingston St., New Haven, CT 06511

Clark, Eloise E., Vice President for Academic Affairs, Bowling Green State University, Bowling Green, OH 43403

Clark, Hays, Property Management Ltd., 125 Mason St., Greenwich, CT 06830

Clark, James M., Shearson Lehman Brothers Inc., 14 Wall St., 9th Floor, New York, NY 10005

Clark, Wallis H., Jr., Bodega Marine Lab, P. O. Box 247, Bodega Bay, CA 94923

Claude, Philippa, Primate Center, Capitol Court, Madison, WI 53706

Clay, John R., Laboratory of Biophysics, NIH, Building 9, room 1E-127, Bethesda, MD 20892

Clowes, George H. A., Jr., The Cancer Research Institute, 194 Pilgrim Rd., Boston, MA 02215

Clutter, Mary, Office of the Director, Room 518, National Science Foundation, Washington, DC 20550

Cobb, Jewel Plummer, California State University, Fullerton, CA 92634

Cohen, Adolph I., Department of Ophthalmology, School of Medicine, Washington University, 660 S. Euclid Ave., St. Louis, MO 63110

Cohen, Carolyn, Roisenstiel Basic Medical Sciences Research Center, Brandeis University, Waltham, MA 02254

Cohen, Lawrence B., Department of Physiology, Yale University School of Medicine, B-106 SHM, P. O. Box 3333, New Haven, CT 06510-8026

Cohen, Maynard, Department of Neurological Sciences, Rush Medical College, 600 South Paulina, Chicago, IL 60612

Cohen, Rochelle S., Department of Anatomy, University of Illinois at Chicago, 808 S. Wood Street, Chicago, IL 60612

Cohen, William D., Department of Biological Sciences, Hunter College, 695 Park Ave., New York, NY 10021

Cole, Jonathan J., Institute for Ecosystems Studies, Cary Arboretum, Millbrook, NY 12545 (resigned 3/7/88)

Coleman, Annette W., Division of Biology and Medicine, Brown University, Providence, RI 02912

Collier, Jack R., Department of Biology, Brooklyn College, Brooklyn, NY 11210

Collier, Marjorie McCann, Biology Department, Saint Peter's College, Kennedy Boulevard, Jersey City, NJ 07306

Cook, Joseph A., The Edna McConnell Clark Foundation, 250 Park Ave., New York, NY 10017

Cooperstein, S. J., University of Connecticut, School of Medicine, Farmington Ave., Farmington, CT 06032

Corliss, John O., Department of Zoology, University of Maryland, College Park, MD 20742

Cornell, Neal W., 6428 Bannockburn Drive, Bethesda, MD 20817

Cornwall, Melvin C., Jr., Department of Physiology L714, Boston University School of Medicine, 80 E. Concord St., Boston, MA 02118

Corson, David Wesley, Jr., 1034 Plantation Lane, Mt. Pleasant, SC 29464

Corwin, Jeffrey T., Bekesy Lab of Neurobiology, 1993 East-West Road, University of Hawaii, Honolulu, HI 96822

Costello, Walter J., College of Medicine, Ohio University, Athens, OH 45701

Couch, Ernest F., Department of Biology, Texas Christian University, Fort Worth, TX 76129

Cremer-Bartels, Gertrud, Universitats Augenklinik, 44 Munster, West Germany

Crow, Terry J., Department of Physiology, University of Pittsburgh, School of Medicine, Pittsburgh, PA 15261

Crowell, Sears, Department of Biology, Indiana University, Bloomington, IN 47405

Crowther, Robert, Marine Biological Laboratory, Woods Hole, MA 02543

Currier, David L., P. O. Box 2476, Vineyard Haven, MA 02568

Daignault, Alexander T., 280 Beacon St., Boston, MA 02116

Dan, Katsuma, Tokyo Metropolitan University, Meguro-ku, Tokyo, Japan

D'Avanzo, Charlene, School of Natural Science, Hampshire College, Amherst, MA 01002

David, John R., Seeley G. Mudd Building, Room 504, Harvard Medical School, 250 Longwood Ave., Boston, MA 02115

Davidson, Eric H., Division of Biology, California Institute of Technology Pasadena, CA 91125

Davis, Bernard D., 23 Clairemont Road, Belmont, MA 02178

Davis, Joel P., Seapuit, Inc., P. O. Box G, Osterville, MA 02655

Daw, Nigel W., 78 Aberdeen Place, Clayton, MO 63105

DeGroof, Robert C., Squibb Mark, 105 Carnegie Center, Princeton, NJ 08543

DeHaan, Robert L., Department of Anatomy, Emory University, Atlanta, GA 30322

DeLanney, Louis E., Institute for Medical Research, 2260 Clove Drive, San Jose, CA 95128

DePhillips, Henry A., Jr., Department of Chemistry, Trinity College, Hartford, CT 06106

DeTerra, Noel, 215 East 15th St., New York, NY 10003

Dettbarn, Wolf-Dietrich, Department of Pharmacology, School of Medicine, Vanderbilt University, Nashville, TN 37127

DeWeer, Paul J., Department of Physiology, School of Medicine, Washington University, St. Louis, MO 63110

Dixon, Keith E., School of Biological Sciences, Flinders University, Bedford Park, South Australia

Donelson, John E., Department of Biochemistry, University of Iowa, Iowa City IA 52242

Dowdall, Michael J., Department of Zoology, School of Biological Sciences, University of Nottingham, University Park, Nottingham N672 UH, England, UK

Dowling, John E., The Biological Laboratories, Harvard University, 16 Divinity St., Cambridge, MA 02138

DuBois, Arthur Brooks, John B. Pierce Foundation Laboratory, 290 Congress Ave., New Haven, CT 06519

Dudley, Patricia L., Department of Biological Sciences, Barnard College, Columbia University, New York, NY 10027

Duncan, Thomas K., P. O. Box 662, Woods Hole, MA 02543

Dunham, Philip B., Department of Biology, Syracuse University, Syracuse, NY 13244

Dunlap, Kathleen, Department of Psychology, Tufts Medical School, Boston, MA 02111

Ebert, James D., Office of the Director, Chesapeake Bay Institute, The Johns Hopkins University, Suite 340, The Rotunda, 771 West 40th St., Baltimore, MD 21211

Eckberg, William R., Department of Zoology, Howard University, Washington, DC 20059

Edds, Kenneth T., Department of Anatomical Sciences, SUNY, Buffalo, NY 14214

Eder, Howard A., Albert Einstein College of Medicine, 1300 Morris Park Ave., Bronx, NY 10461

Edstrom, Joan E., 2515 Milton Hills Drive, Charlottesville, VA 22901

Edwards, Charles, Rm. 403, Bldg. 10, NIADDK/NIH, Bethesda, MD 20892

Egyud, Laszlo G., 18 Skyview, Newton, MA 02150

Ehrenstein, Gerald, NIH, Bethesda, MD 20892

Ehrlich, Barbara E., Division of Cardiology, University of Connecticut Health Center, Farmington, CT 06032

Eisen, Arthur Z., Division of Dermatology, Washington University, St. Louis, MO 63110

Eisenman, George, Department of Physiology, University of California Medical School, Los Angeles, CA 90024

Elder, Hugh Young, Institute of Physiology, University of Glasgow, Glasgow, Scotland, U. K.

Elliott, Gerald F., The Open University Research Unit, Foxcombe Hall, Berkeley Rd., Boars Hill, Oxford, England, UK

Englund, Paul T., Department of Biological Chemistry, Johns Hopkins School of Medicine, Baltimore, MD 21205

Epel, David, Hopkins Marine Station, Pacific Grove, CA 93950

Epstein, Herman T., Department of Biology, Brandeis University, Waltham, MA 02254

Epstein, Ray L., Marine Biological Laboratory, Woods Hole, MA 02543

Erulkar, Solomon D., 318 Kent Rd., Bala Cynwyd, PA 19004

Essner, Edward S., Kresge Eye Institute, Wayne State University, 540 E. Canfield Ave., Detroit, MI 48201

Farb, David H., SUNY Health Science Center, Brooklyn, NY 11203

Farmanfarmaian, A., Department of Biological Sciences, Nelson Biological Laboratory, Rutgers University, P. O. Box 1059, Piscataway, NJ 08854

Fein, Alan, Physiology Department, University of Connecticut Health Center, Farmington, CT 06032

Feinman, Richard D., Box 8, Department of Biochemistry, SUNY Health Science Center, Brooklyn, NY 11203

Feldman, Susan C., Department of Anatomy, University of Medicine and Dentistry of New Jersey, New Jersey Medical School, 100 Bergen St., Newark, NJ 07103

Fessenden, Jane, Marine Biological Laboratory, Woods Hole, MA 02543

Festoff, Barry W., Neurology Service (127), Veterans Administration Medical Center, 4801 Linwood Blvd., Kansas City, MO 64128

Fink, Rachel D., Clapp Biology Laboratory, Mount Holyoke College, South Hadley, MA 01075

Finkelstein, Alan, Albert Einstein College of Medicine, 1300 Morris Park Ave., Bronx, NY 10461

Fischbach, Gerald, Department of Anatomy and Neurobiology, Washington University School of Medicine, St. Louis, MO 63110

Fischman, Donald A., Department of Cell Biology and Anatomy, Cornell University Medical College, 1300 York Ave., New York, NY 10021

Fishman, Harvey M., Department of Physiology, University of Texas Medical Branch, Galveston, TX 77550

Flanagan, Dennis, 12 Gay St., New York, NY 10014

Fox, Maurice S., Department of Biology, Massachusetts Institute of Technology, Cambridge, MA 02138

Frank, Peter W., Department of Biology, University of Oregon, Eugene, OR 97403

Franzini, Clara, Department of Biology G-5, School of Medicine, University of Pennsylvania, Philadelphia, PA 19174

Frazier, Donald T., Department of Physiology and Biophysics, University of Kentucky Medical Center, Lexington, KY 40536

Freeman, Gary L., Department of Zoology, University of Texas, Austin, TX 78172 (resigned 3/31/88)

Freinkel, Norbert, Center for Endocrinology, Metabolism & Nutrition, Northwestern University Medical School, 303 E. Chicago Avenue, Chicago, IL 60611

French, Robert J., Department of Medical Physiology, University of Calgary, 3330 Hospital Dr., NW, Calgary, Alberta, T2N 4N1 Canada

Freygang, Walter J., Jr., 6247 29th St., NW, Washington, DC 20015

Fry, Brian, Marine Biological Laboratory, Woods Hole, MA 02543

Fukui, Yoshio, Department of Cell Biology and Anatomy, Northwestern University Medical School, Chicago, IL 60201

Fulton, Chandler M., Department of Biology, Brandeis University, Waltham, MA 02154

Furshpan, Edwin J., Department of Neurophysiology, Harvard Medical School, Boston, MA 02115

Fuseler, John W., Department of Biology, University of Southwestern Louisiana, Lafayette, LA 70504

Futrelle, Robert P., College of Computer Science, Northeastern University, 360 Huntington Avenue, Boston, MA 02115

Fye, Paul, P. O. Box 309, Woods Hole, MA 02543 (deceased 3/11/88)

Gabriel, Mordecai, Department of Biology, Brooklyn College, Brooklyn, NY 11210

Gadsby, David C., Laboratory of Cardiac Physiology, The Rockefeller University, 1230 York Avenue, New York, NY 10021

Gainer, Harold, Section of Functional Neurochemistry, NIH, Bldg. 36 Room 4D-20, Bethesda, MD 20892

Galatzer-Levy, Robert M., 180 N. Michigan Avenue, Chicago, IL 60601

Gall, Joseph G., Carnegie Institution, 115 West University Parkway, Baltimore, MD 21210

Gallant, Paul E., Laboratory of Preclinical Studies, Bldg. 36, NIAAA/NIH, 1250 Washington Ave., Rockville, MD 20892

Gascoyne, Peter, Department of Experimental Pathology, Box 85E, University of Texas System Cancer Center, M. D. Anderson Hospital and Tumor Insti-

tute, Texas Medical Center, 6723 Bertner Avenue, Houston, TX 77030

Gelfant, Seymour, Department of Dermatology, Medical College of Georgia, Augusta, GA 30904

Gelperin, Alan, Department of Biology, Princeton University, Princeton, NJ 08540

German, James L., III, The New York Blood Center, 310 East 67th St., New York, NY 10021

Gibbs, Martin, Institute for Photobiology of Cells and Organelles, Brandeis University, Waltham, MA 02254

Giblin, Anne E., Ecosystems Center, Marine Biological Laboratory, Woods Hole, MA 02543

Gibson, A. Jane, Wing Hall, Cornell University, Ithaca, NY 14850

Gifford, Prosser, The Wilson Center, Smithsonian Building, 1000 Jefferson Drive, SW, Washington, DC 20590

Gilbert, Daniel L., NIH, Bldg. 9, Room IE-124, Bethesda, MD 20892

Giudice, Giovanni, Via Archirafi 22, Palermo, Italy

Glusman, Murray, Department of Psychiatry, Columbia University, 722 W. 168th St., New York, NY 10032

Golden, William T., 40 Wall St., Room 4201, New York, NY 10005

Goldman, David E., 63 Loop Rd., Falmouth, MA 02540

Goldman, Robert D., Department of Cell Biology and Anatomy, Northwestern University, 303 E. Chicago Ave., Chicago, IL 60611

Goldsmith, Paul K., NIH, Bldg. 10, Room 9C-101, Bethesda, MD 20892

Goldsmith, Timothy H., Department of Biology, Yale University, New Haven, CT 06510

Goldstein, Moise H., Jr., ECE Department, Borten Hall, Johns Hopkins University, Baltimore, MD 21218

Goodman, Lesley Jean, Department of Biological Sciences, Queen Mary College, Mile End Road, London, E1 4NS, England, U. K.

Goudsmit, Esther, M., Department of Biology, Oakland University, Rochester, MI 48063

Gould, Robert Michael, Institute for Basic Research in Developmental Disabilities, 1050 Forest Hill Rd., Staten Island, NY 10314

Gould, Stephen J., Museum of Comparative Zoology, Harvard University, Cambridge, MA 02138

Govind, C. K., Zoology Department—Scarborough, University of Toronto, 1265 Military Trail, West Hill, Ontario, Canada, M1C 1A4

Graf, Werner, Rockefeller University, New York, NY 10021

Grant, Philip, Department of Biology, University of Oregon, Eugene, OR 97403

Grass, Albert, The Grass Foundation, 77 Reservoir Rd., Quincy, MA 02170

Grass, Ellen R., The Grass Foundation, 77 Reservoir Rd., Quincy, MA 02170

Grassle, Judith, Marine Biological Laboratory, Woods Hole, MA 02543

Green, Jonathan P., Department of Biology, Roosevelt University, 430 S. Michigan Avenue, Chicago, IL 60605 (resigned 2/5/88)

Greenberg, Everett Peter, Department of Microbiology, Stocking Hall, Cornell University, Ithaca, NY 14853

Greenberg, Michael J., C. V. Whitney Lab, Rt. 1, Box 121, St. Augustine, FL 32086

Greif, Roger L., Department of Physiology, Cornell University, Medical College, New York, NY 10021 (resigned 10/87)

Griffin, Donald R., The Rockefeller University, 1230 York Ave., New York, NY 10021

Gross, Paul R., Office of the Vice President and Provost, University of Virginia, Charlottesville, VA 22906-9014

Grossman, Albert, New York University, Medical School, New York, NY 10016

Gruner, John, Department of Neurosurgery, New York University Medical Center, 550 First Ave., New York, NY 10016

Gunning, A. Robert, P. O. Box 165, Falmouth, MA 02541

Gwilliam, G. P., Department of Biology, Reed College, Portland, OR 97202

Hall, Linda M., Department of Genetics, Albert Einstein College of Medicine 1300 Morris Park Ave., Bronx, NY 10461

Hall, Zack W., Department of Physiology, University of California, San Francisco, CA 94143

Halvorson, Harlyn O., Marine Biological Laboratory, Woods Hole, MA 02543

Hamlett, Nancy Virginia, Department of Biology, Swarthmore College, Swarthmore, PA 19081

Hanna, Robert B., College of Environmental Science and Forestry, SUNY, Syracuse, NY 13210

Harding, Clifford V., Jr., P. O. Box 452, Woods Hole, MA 02543

Harosi, Ferenc I., Laboratory of Sensory Physiology, Marine Biological Laboratory, Woods Hole, MA 02543

Harrigan, June F., 7415 Makaa Place, Honolulu, HI 96825

Harrington, Glenn W., Department of Microbiology, School of Dentistry, University of Missouri, 650 E. 25th St., Kansas City, MO 64108

Harris, Andrew L., Department of Biophysics, Johns Hopkins University, 34th & Charles Sts., Baltimore, MD 21218

Haschemeyer, Audrey E. V., Department of Biological

Sciences, Hunter College, 695 Park Ave., New York, NY 10021

Hastings, J. W., Harvard University, 16 Divinity Street, Cambridge, MA 02138

Hauschka, Theodore S., RD1, Box 781, Damariscotta, ME 04543

Hayashi, Teru, 7105 SW 112 Place, Miami, FL 33173

Hayes, Raymond L., Jr., Department of Anatomy, Howard University, College of Medicine, 520 W St., NW, Washington, DC 20059

Henley, Catherine, 5225 Pooks Hill Rd., #1127 North, Bethesda, MD 20034

Hepler, Peter K., Department of Botany, University of Massachusetts, Amherst, MA 01003

Herndon, Walter R., University of Tennessee, Department of Botany, Knoxville, TN 37996-1100

Hessler, Anita Y., 5795 Waverly Ave., La Jolla, CA 92037

Heuser, John, Department of Biophysics, Washington University, School of Medicine, St. Louis, MO 63110

Hiatt, Howard H., Brigham and Women's Hospital, 75 Francis Street, Boston, MA 02115

Highstein, Stephen M., Department of Otolaryngology, Washington University, St. Louis, MO 63110

Hildebrand, John G., Arizona Research Laboratories, Division of Neurobiology, 603 Gould-Simpson Science Building, University of Arizona, Tucson, AZ 85721

Hill, Susan D., Department of Zoology, Michigan State University, E. Lansing, MI 48824

Hillis-Colinvaux, Llewellya, Department of Zoology, The Ohio State University, 484 W. 12th Ave., Columbus, OH 43210

Hillman, Peter, Department of Biology, Hebrew University, Jerusalem, ISRAEL

Hinegardner, Ralph T., Division of Natural Sciences, University of California, Santa Cruz, CA 95064

Hinsch, Gertrude, W., Department of Biology, University of South Florida, Tampa, FL 33620

Hobbie, John E., Ecosystems Center, Marine Biological Laboratory, Woods Hole, MA 02543

Hodge, Alan J., Marine Biological Laboratory, Woods Hole, MA 02543

Hoffman, Joseph, Department of Physiology, School of Medicine, Yale University, New Haven, CT 06510

Hollyfield, Joe G., Baylor School of Medicine, Texas Medical Center, Houston, TX 77030

Holtzman, Eric, Department of Biological Sciences, Columbia University, New York, NY 10017

Holz, George G., Jr., Department of Microbiology, SUNY, Syracuse, NY 13210

Hoskin, Francis C. G., Department of Biology, Illinois Institute of Technology, Chicago, IL 60616

Houghton, Richard A., III, Woods Hole Research Center, P. O. Box 296, Woods Hole, MA 02543

Houston, Howard E., 2500 Virginia Ave., NW, Washington, DC 20037

Howarth, Robert, Section of Ecology & Systematics, Corson Hall, Cornell University, Ithaca, NY 14853

Hoy, Ronald R., Section of Neurobiology and Behavior, Cornell University, Ithaca, NY 14850

Hubbard, Ruth, 67 Gardner Road, Woods Hole, MA 02543

Hufnagel, Linda A., Department of Microbiology, University of Rhode Island, Kingston, RI 02881

Hummon, William D., Department of Zoology, Ohio University, Athens, OH 45701

Humphreys, Susie H., 710 Waukegan Rd., Glenview, IL 60025

Humphreys, Tom D., University of Hawaii, PBRC, 41 Ahui St., Honolulu, HI 96813

Hunter, Robert D., Department of Biological Sciences, Oakland University, Rochester, NY 48063

Hunter, W. Bruce, Box 321, Lincoln Center, MA 01773

Hunziker, Herbert E., Esq., P. O. Box 547, Falmouth, MA 02541

Hurwitz, Charles, Basic Science Research Lab, Veterans Administration Hospital, Albany, NY 12208

Hurwitz, Jerard, Memorial Sloan Kettering Institute, 1275 York Avenue, New York, NY 11021

Huxley, Hugh E., Department of Biology, Rosenstiel Basic Medical Sciences Research Center, Brandeis University, Waltham, MA 02254

Hynes, Thomas J., Jr., Meredith and Grew, Inc., 160 Federal Street, Boston, MA 02110

Ilan, Joseph, Department of Anatomy, Case Western Reserve University, Cleveland, OH 44106

Ingoglia, Nicholas, Department of Physiology, New Jersey Medical School, 100 Bergen St., Newark, NJ 07103

Inoué, Saduyki, McGill University Cancer Centre, Department of Anatomy, 3640 University St., Montreal, PQ, Canada, H3A 2B2

Inoué, Shinya, Marine Biological Laboratory, Woods Hole, MA 02543

Issadorides, Marietta, R., Department of Psychiatry, University of Athens, Monis Petraki 8, Athens, 140 Greece

Isselbacher, Kurt J., Massachusetts General Hospital, 32 Fruit Street, Boston, MA 02114

Izzard, Colin S., Department of Biological Sciences, SUNY, Albany, Albany, NY 12222

Jacobson, Antone G., Department of Zoology, University of Texas, Austin, TX 78712

Jaffe, Lionel, Marine Biological Laboratory, Woods Hole, MA 02543

Jahan-Parwar, Behrus, Center for Laboratories & Research, New York State Department of Health, Empire State Plaza, Albany, NY 12201

Jannasch, Holger W., Department of Biology, Woods Hole Oceanographic Institution, Woods Hole, MA 02543

Jeffery, William R., Department of Zoology, University of Texas, Austin, TX 78712

Jenner, Charles E., Department of Zoology, University of North Carolina, Chapel Hill, NC 27514 (resigned 8/87)

Jones, Meredith L., Division of Worms, Museum of Natural History, Smithsonian Institution, Washington, DC 20560

Josephson, Robert K., School of Biological Sciences, University of California, Irvine, CA 92664

Kabat, E. A., Department of Microbiology, College of Physicians and Surgeons Columbia University, 630 West 168th St., New York, NY 10032

Kaley, Gabor, Department of Physiology, Basic Sciences Building, New York Medical College, Valhalla, NY 10595

Kaltenbach, Jane, Department of Biological Sciences, Mount Holyoke College, South Hadley, MA 01075

Kaminer, Benjamin, Department of Physiology, School of Medicine, Boston University, 80 East Concord St., Boston, MA 02118

Kammer, Ann E., Department of Zoology, Arizona State University, Tempe, AZ 85281

Kane, Robert E., University of Hawaii, PBRC, 41 Ahui St., Honolulu, HI 96813

Kaneshiro, Edna S., Department of Biological Sciences, University of Cincinnati, Cincinnati, OH 45221

Kao, Chien-yuan, Department of Pharmacology (Box 29), State University of New York, Downstate Medical Center, 450 Clarkson Avenue, Brooklyn, NY 11203

Kaplan, Ehud, The Rockefeller University, 1230 York Ave., New York, NY 10021

Karakashian, Stephen J., Apt. 16-F, 165 West 91st St., New York, NY 10024

Karlin, Arthur, Department of Biochemistry and Neurology, Columbia University, 630 West 168th St., New York, NY 10032

Katz, George M., Fundamental and Experimental Research, Merck Sharpe and Dohme, Rahway, NJ 07065

Kean, Edward L., Department of Ophthalmology and Biochemistry, Case Western Reserve University, Cleveland, OH 44101

Kelley, Darcy Brisbane, Department of Biological Sciences, 1018 Fairchild, Columbia University, New York, NY 10032

Kelly, Robert E., Department of Anatomy, College of Medicine, University of Illinois, P. O. Box 6998, Chicago, IL 60680

Kemp, Norman E., Department of Biology, University of Michigan, Ann Arbor, MI 48104

Kendall, John P., Faneuil Hall Associated, One Boston Place, Boston, MA 02108

Kendall, Richard E., 26 Green Harbor Rd., East Falmouth, MA 02536

Keynan, Alexander, Hebrew University, Jerusalem, ISRAEL

Kiehart, Daniel P., Department of Cellular and Developmental Biology, Harvard University, 16 Divinity Avenue, Cambridge, MA 02138

Klein, Morton, Department of Microbiology, Temple University, Philadelphia, PA 19103

Klotz, I. M., Department of Chemistry, Northwestern University, Evanston, IL 60201

Koide, Samuel S., Population Council, The Rockefeller University, 66th St. and York Ave., New York, NY 10021

Konigsberg, Irwin R., Department of Biology, Gilmer Hall, University of Virginia, Charlottesville, VA 22903

Kornberg, Sir Hans, The Master's Lodge, Christ's College, Cambridge CB2 3BU England, UK

Kosower, Edward M., Ramat-Aviv, Tel Aviv, 69978 ISRAEL

Krahl, M. E., 2783 W. Casas Circle, Tucson, AZ 85741

Krane, Stephen M., Massachusetts General Hospital, Boston, MA 02114

Krassner, Stuart M., Department of Developmental and Cell Biology, University of California, Irvine, CA 92717

Krauss, Robert, FASEB, 9650 Rockville Pike, Bethesda, MD 20814

Kravitz, Edward A., Department of Neurobiology, Harvard Medical School, 25 Shattuck St., Boston, MA 02115

Kriebel, Mahlon E., Department of Physiology, B.S.B., Upstate Medical Center, 766 Irving Ave., Syracuse, NY 13210

Kristan, William B., Jr., Department of Biology B-022, University of California San Diego, San Diego, CA 92093

Kuhns, William J., University of North Carolina, 512 Faculty Lab Office, Bldg. 231-H, Chapel Hill, NC 27514

Kusano, Kiyoshi, Illinois Institute of Technology, Department of Biology, 3300 South Federal St., Chicago, IL 60616

Kuzirian, Alan M., Marine Biological Laboratory, Woods Hole, MA 02543

Laderman, Aimlee, P. O. Box 689, Woods Hole, MA 02543

LaMarche, Paul H., Eastern Maine Medical Center, 489 State St., Bangor, ME 04401

Landis, Dennis M. D., Department of Developmental Genetics and Anatomy, Case Western Reserve Medical School, 2119 Abington Road, Cleveland, OH 44106

Landis, Story C., Department of Pharmacology, Case Western Reserve University Medical School, 2119 Abington Road, Cleveland, OH 44106

Landowne, David, Department of Physiology, Yale University School of Medicine, 333 Cedar St., New Haven, CT 06510

Langford, George M., Department of Physiology, Medical Sciences Research Wing 206H, University of North Carolina, Chapel Hill, NC 27514

Lasek, Raymond J., Case Western Reserve University, Department of Anatomy, Cleveland, OH 44106

Laster, Leonard, University of Oregon, Health Sciences Center, Portland, OR 97201

Laufer, Hans, Biological Science, Molecular and Cell Biology, Group U-125, University of Connecticut, Storrs, CT 06268

Lazarow, Paul B., The Rockefeller University, 1230 York Avenue, New York, NY 10021

Lazarus, Maurice, Federated Department Stores, Inc., 50 Cornhill, Boston, MA 02108

Leadbetter, Edward R., Department of Molecular and Cell Biology, U-131, University of Connecticut, Storrs, CT 06268

Lederberg, Joshua, President, The Rockefeller University, 1230 York Ave., New York, NY 10021

Lederhendler, Izja I., Laboratory of Cellular and Molecular Neurobiology, NINCDS/NIH, Park 5 Building, Room 435, Bethesda, MD 20892

Lee, John J., Department of Biology, City College of CUNY, Convent Ave. and 138th St., New York, NY 10031

Lehy, Donald B., Marine Biological Laboratory, Woods Hole, MA 02543

Leibovitz, Louis, Laboratory for Marine Animal Health, Marine Biological Laboratory, Woods Hole, MA 02543

Leighton, Joseph, 1201 Waverly Rd., Gladwyne, PA 19035

Leighton, Stephen, NIH, Bldg. 13 3W13, Bethesda, MD 20892

Leinwand, Leslie Ann, Department of Microbiology and Immunology, Albert Einstein College of Medicine, 1300 Morris Park Ave., Bronx, NY 10461

Lerman, Sidney, Laboratory for Ophthalmic Research, Emory University, Atlanta, GA 30322

Lerner, Aaron B., Yale University, School of Medicine, New Haven, CT 06510

Lester, Henry A., 156-29 California Institute of Technology, Pasadena, CA 91125

Levin, Jack, Clinical Pathology Service, VA Hospital—113A, 4150 Clement St., San Francisco, CA 94121

Levinthal, Cyrus, Department of Biological Sciences, Columbia University, 435 Riverside Drive, New York, NY 10025

Levitan, Herbert, Department of Zoology, University of Maryland, College Park, MD 20742

Linck, Richard W., Department of Anatomy, Jackson Hall, University of Minnesota, 321 Church Street, S. E., Minneapolis, MN 55455

Lipicky, Raymond J., Department of Cardio-Renal/HFD 110, FDA Bureau of Drugs, Rm. 16B-45, 5600 Fishers Lane, Rockville, MD 20857

Lisman, John E., Department of Biology, Brandeis University, Waltham, MA 02254

Liuzzi, Anthony, 320 Beacon St., Boston, MA 02116

Llinas, Rodolfo R., Department of Physiology and Biophysics, New York University Medical Center, 550 First Ave., New York, NY 10016

Loewenstein, Werner R., Department of Physiology and Biophysics, University of Miami, P. O. Box 016430, Miami, FL 33101

Loewus, Frank A., Institute of Biological Chemistry, Washington State University, Pullman, WA 99164

Loftfield, Robert B., Department of Biochemistry, School of Medicine, University of New Mexico, 900 Stanford, NE, Albuquerque, NM 87131

London, Irving M., Massachusetts Institute of Technology, Cambridge, MA 02139

Longo, Frank J., Department of Anatomy, University of Iowa, Iowa City, IA 52442

Lorand, Laszlo, Department of Biochemistry and Molecular Biology, Northwestern University, Evanston, IL 60208

Luckenbill-Edds, Louise, 155 Columbia Ave., Athens, OH 45701

Luria, Salvador E., 48 Peacock Farm Rd., Lexington, MA 02173

Macagno, Eduardo R., 1003B Fairchild, Columbia University, New York, NY 10022

MacNichol, E. F., Jr., 45 Brewster Street, Cambridge, MA 02138

Maglott-Duffield, Donna R. S., 1014 Baltimore Road, Rockville, MD 20851

Maienschein, Jane Ann, Department of Philosophy, Arizona State University, Tempe, AZ 85281

Mainer, Robert, The Boston Company, One Boston Place, MA 02108

Malbon, Craig Curtis, Department of Pharmacological Sciences, Health Sciences Center, SUNY, Stony Brook, Stony Brook, NY 11794-8651

Malkiel, Saul, Allergic Diseases, Inc., 130 Lincoln St., Worcester, MA 01605

Manalis, Richard S., Department of Biological Sciences, Indiana University—Purdue University at Fort Wayne, Fort Wayne, IN 46805

Mangum, Charlotte P., Department of Biology, College of William and Mary, Williamsburg, VA 23185

Margulis, Lynn, Department of Biology, Boston University, 2 Cummington St., Boston, MA 02215

Marinucci, Andrew C., 102 Nancy Drive, Mercerville, NJ 08619

Marsh, Julian B., Department of Biochemistry and Physiology, Medical College of Pennsylvania, 3300 Henry Ave., Philadelphia, PA 19129

Martin, Lowell V., Marine Biological Laboratory, Woods Hole, MA 02543

Martinez-Palomo, Adolfo, Seccion de Patologia Experimental, Cinvesav-ipn, 17000 Mexico, D.F. A.P., 14-740, Mexico

Maser, Morton, P. O. Box EM, Woods Hole, MA 02543

Mastroianni, Luigi, Jr., Department of Obstetrics and Gynecology, University of Pennsylvania, Philadelphia, PA 19174

Mathews, Rita W., Department of Medicine, New York University Medical Center, 550 First Ave., New York, NY 10016

Matteson, Donald R., Department of Physiology, G4, School of Medicine, University of Pennsylvania, Philadelphia, PA 19104

Mautner, Henry G., Department of Biochemistry, Tufts University, 136 Harrison Ave., Boston, MA 02111

Mauzerall, David, The Rockefeller University, 1230 York Ave., New York, NY 10021

Mazia, Daniel, Hopkins Marine Station, Pacific Grove, CA 93950

Mazzella, Lucia, Laboratorio di Ecologia del Benthos, Stazione Zoologica di Napoli, P.ta S. Pietro 80077, Ischia Porto (NA), Italy

McCann, Frances, Department of Physiology, Dartmouth Medical School, Hanover, NH 03755

McCloskey, Lawrence R., Department of Biology, Walla Walla College, College Place, WA 99324 (resigned 10/87)

McLaughlin, Jane A., P. O. Box 187, Woods Hole, MA 02543

McMahon, Robert F., Department of Biology, Box 19498, University of Texas, Arlington, TX 76019

Meedel, Thomas, Marine Biological Laboratory, Woods Hole, MA 02543

Meinertzhagen, Ian A., Department of Psychology, Life Sciences Center, Dalhousie University, Halifax, Nova Scotia, Canada B3H 451

Meinkoth, Norman A., 431W Woodland Avenue, Springfield, PA 19064 (deceased 4/87)

Meiss, Dennis E., 462 Solano Avenue, Hayward, CA 94541

Melillo, Jerry A., Ecosystems Center, Marine Biological Laboratory, Woods Hole, MA 02543

Mellon, Richard P., P. O. Box 187, Laughlintown, PA 15655

Mellon, DeForest, Jr., Department of Biology, University of Virginia, Charlottesville, VA 22903

Menzel, Randolf, Institut fir Tierphysiologie, Free Universitat of Berlin, 1000 Berlin 41, FEDERAL REPUBLIC OF GERMANY (resigned 10/87)

Metuzals, Janis, Department of Anatomy, Faculty of Medicine, University of Ottawa, Ottawa, Ontario, CANADA K1N 9A9

Metz, Charles B., 7220 Southwest 124th St., Miami, FL 33156

Milkman, Roger, Department of Zoology, University of Iowa, Iowa City, IA 52242

Mills, Eric L., Oceanography Dept., Dalhousie University, Halifax, Nova Scotia B3H 4J1, Canada

Mills, Robert, 10315 44th Avenue, W' 12 H Street, Bradenton, FL 33507-1535

Mitchell, Ralph, Pierce Hall, Harvard University, Cambridge, MA 02138

Miyamoto, David M., Department of Biology, Drew University, Madison, NJ 07940

Mizell, Merle, Department of Biology, Tulane University, New Orleans, LA 70118

Moore, John W., Department of Physiology, Duke University Medical Center, Durham, NC 27710

Moore, Lee E., Department of Physiology and Biophysics, University of Texas, Medical Branch, Galveston, TX 77550

Morin, James G., Department of Biology, University of California, Los Angeles, CA 90024

Morrell, Frank, Department of Neurological Sciences, Rush Medical Center, 1753 W. Congress Parkway, Chicago, IL 60612

Morrill, John B., Jr., Division of National Sciences, New College, Sarasota, FL 33580 (resigned 12/87)

Morse, M. Patricia, Marine Science Center, Northeastern University, Nahant MA 01908

Morse, Richard S., 193 Winding River Rd., Wellesley, MA 02181

Morse, Robert W., Box 574, N. Falmouth, MA 02556

Morse, Stephen Scott, The Rockefeller University, 1230 York Ave., Box 2, New York, NY 10021-6399

Moscona, A. A., Department of Molecular Genetics and Cell Biology, University of Chicago, 920 East 58th St., Chicago, IL 60637

Mote, Michael I., Department of Biology, Temple University, Philadelphia, PA 19122

Mountain, Isabel, Vinson Hall #112, 6251 Old Dominion Drive, McLean, VA 22101

Mullins, Lorin J., University of Maryland, School of Medicine, Baltimore MD 21201

Musacchia, Xavier J., Graduate School, University of Louisville, Louisville, KY 40292

Nabrit, S. M., 686 Beckwith St., SW, Atlanta, GA 30314

Nadelhoffer, Knute, Marine Biological Laboratory, Woods Hole, MA 02543

Naka, Ken-ichi, National Institute for Basic Biolgy, Okazaki, Japan 444

Nakajima, Shigehiro, Department of Biological Sciences, Purdue University, West Lafayette, IN 47907

Nakajima, Yasuko, Department of Biological Sciences, Purdue University, West Lafayette, IN 47907

Narahashi, Toshio, Department of Pharmacology, Medical Center, Northwestern University, 303 East Chicago Ave., Chicago, IL 60611

Nasatir, Maimon, Department of Biology, University of Toledo, Toledo, OH 43606

Nelson, Leonard, Department of Physiology, Medical College of Ohio, Toledo, OH 43699

Nelson, Margaret C., 119 Forest Home Drive, Ithaca, NY 14850

Nicholls, John G., Biocenter, Klingelbergstr 70, Basel 4056, Switzerland

Nicosia, Santo V., Department of Pathology, University of South Florida, College of Medicine, Box 11, 12901 North 30th St., Tampa, FL 33612

Nielsen, Jennifer B. K., Merck Sharp & Dohme Laboratories, Bldg. 50-G, Room 226, Rahway, NJ 07065

Noe, Bryan D., Department of Anatomy, Emory University, Atlanta, GA 30345

Obaid, Ana Lia, Department of Physiology and Pharmacy, University of Pennsylvania, 4001 Spruce St., Philadelphia, PA 19104

Ochoa, Severo, 530 East 72nd St., New York, NY 10021 (resigned 3/87)

Odum, Eugene, Department of Zoology, University of Georgia, Athens, GA 30701 (resigned 1/87)

Oertel, Donata, Department of Neurophysiology, University of Wisconsin, 283 Medical Science Bldg., Madison, WI 53706

O'Herron, Jonathan, Lazard Freres and Company, 1 Rockefeller Plaza, New York, NY 10020

Olins, Ada L., University of Tennessee-Oak Ridge, Graduate School of Biomedical Sciences, Biology Division ORNL, P. O. Box Y, Oak Ridge, TN 37830

Olins, Donald E., University of Tennessee-Oak Ridge, Graduate School of Biomedical Sciences, Biology Division ORNL, P. O. Box Y, Oak Ridge, TN 37830

O'Melia, Anne F., 16 Evergreen Lane, Chappaqua, New York 10514

Oschman, James L., 9 George Street, Woods Hole 02543

Palmer, John D., Department of Zoology, University of Massachusetts, Amherst, MA 01002

Palti, Yoram, Department of Physiology and Biophysics, Israel Institute of Technology, 12 Haaliya St., Bat-Galim, POB 9649, Haifa, Israel

Pant, Harish C., NINCDS/NIH, Bldg. 36, Room 4D-20, Bethesda, MD 20892

Pappas, George D., Department of Anatomy, College of Medicine, University of Illinois, 808 South Wood St., Chicago, IL 60612

Pardee, Arthur B., Department of Pharmacology, Harvard Medical School, Boston, MA 02115

Pardy, Rosevelt L., School of Life Sciences, University of Nebraska, Lincoln, NE 68588

Parmentier, James L., Becton Dickinson, P. O. Box 12016, Research Triangle Park, NC 27709

Passano, Leonard M., Department of Zoology, Birge Hall, University of Wisconsin, Madison, WI 53706

Pearlman, Alan L., Department of Physiology, School of Medicine, Washington University, St. Louis, MO 63110

Pederson, Thoru, Worcester Foundation for Experimental Biology, Shrewsbury, MA 01545

Perkins, C. D., 400 Hilltop Terrace, Alexandria, VA 22301

Person, Philip, Oral Health Director, Research Testing Labs, Inc., 167 E. 2nd St., Huntington Station, NY 11746

Peterson, Bruce J., 82 Hillcrest Dr., Falmouth, MA 02540

Pethig, Ronald, School of Electronic Engineering Science, University College of N. Wales, Dean St., Bangor, Gwynedd, LL57 IUT, UK

Pettibone, Marian H., Division of Worms, W-213, Smithsonian Institution, Washington, DC 20560 (resigned 11/87)

Pfohl, Ronald J., Department of Zoology, Miami University, Oxford, OH 45056

Pierce, Sidney K., Jr., Department of Zoology, University of Maryland, College Park, MD 20740

Poindexter, Jeanne S., Science Division, Long Island University, Brooklyn Campus, Brooklyn, NY 11201

Pollard, Harvey B., NIH, F Building 10, Room 10B17, Bethesda, MD 20892

Pollard, Thomas D., Department of Cell Biology and Anatomy, Johns Hopkins University, 725 North Wolfe St., Baltimore, MD 21205

Pollock, Leland W., Department of Zoology, Drew University, Madison, NJ 07940

Poole, Alan F., 114 Metoxit Road, Waquoit, MA 02536

Porter, Beverly H., 13617 Glenoble Drive, Rockville, MD 20853

Porter, Keith R., Department of Biology, University of Maryland, Catonsville, MD 21228

Porter, Mary E., Department MCD Biology, Campus Box 347, University of Colorado, Boulder, CO 80309

Potter, David, Department of Neurobiology, Harvard Medical School, Boston, MA 02115

Potts, William T., Department of Biology, University of Lancaster, Lancaster, England, UK

Poussart, Denis, Department of Electrical Engineering, Universite Laval, Quebec, Canada

Pratt, Melanie M., Department of Anatomy and Cell Biology, University of Miami School of Medicine (R124), P. O. Box 016960, Miami, FL 33101

Prendergast, Robert A., Department of Pathology and Ophthalmology, Johns Hopkins University, Baltimore, MD 21205

Presley, Phillip H., Carl Zeiss, Inc., 1 Zeiss Drive, Thornwood, NY 10594

Price, Carl A., Waksman Institute of Microbiology, Rutgers University, P. O. Box 759, Piscataway, NJ 08854

Price, Christopher H., Biological Science Center, Boston University, 2 Cummington St., Boston, MA 02215 (resigned 11/87)

Prior, David J., Department of Biological Sciences, University of Kentucky, Lexington, KY 40506

Prusch, Robert D., Department of Life Sciences, Gonzaga University, Spokane, WA 99258

Przybylski, Ronald J., Case Western Reserve University, Department of Anatomy, Cleveland, OH 44104

Purves, Dale, Department of Anatomy, Washington University School of Medicine, 660 S. Euclid Ave., St. Louis, MO 63110

Quigley, James, Department of Microbiology and Immunology Box 44, SUNY Downstate Medical Center, 450 Clarkson Ave., Brooklyn, NY 11203

Rabin, Harvey, DuPont Biomed. Prod.-BRL-2, 331 Treble Cove Road, No. Billerica, MA 01862

Raff, Rudolf A., Department of Biology, Indiana University, Bloomington, IN 47405

Rakowski, Robert F., Department of Physiology and Biophysics, UHS/The Chicago Medical School, 3333 Greenbay Rd., N. Chicago, IL 60064

Ramon, Fidel, Dept. de Fisiologia y Biofisca, Centrol de Investigacion y de, Estudius Avanzados del Ipn, Apurtado Postal 14-740, Mexico, D.F. 07000

Ranzi, Silvio, Sez Zoologia Sc Nat, Via Coloria 26, I20133, Milano, Italy

Rastetter, Edward B., Ecosystems Center, Marine Biological Laboratory, Woods Hole, MA 02543

Ratner, Sara, Department of Biochemistry, Public Health Research Institute, 455 First Ave., New York, NY 10016

Rebhun, Lionel I., Department of Biology, Gilmer Hall, University of Virginia, Charlottesville, VA 22901

Reddan, John R., Department of Biological Sciences, Oakland University, Rochester, MI 48063

Reese, Barbara F., Marine Biological Laboratory, Woods Hole, MA 02543

Reese, Thomas S., Marine Biological Laboratory, Woods Hole, MA 02543

Reiner, John M., 2150 Grand Boulevard, Schenectady, NY 12309

Reinisch, Carol L., Tufts University School of Veterinary Medicine, 203 Harrison Avenue, Boston, MA 02115

Reuben, John P., Department of Biochemistry, Merck Sharp and Dohme, P. O. Box 2000, Rahway, NJ 07065

Reynolds, George T., Department of Physics, Jadwin Hall, Princeton University, Princeton, NJ 08540

Rice, Robert V., 30 Burnham Dr., Falmouth, MA 02540

Rich, Alexander, Department of Biology, Massachusetts Institute of Technology, Cambridge, MA 02139

Rickles, Frederick R., University of Connecticut, School of Medicine, VA Hospital, Newington, CT 06111

Ripps, Harris, Department of Ophthalmology, University of Illinois College of Medicine, 1855 W. Taylor Street, Chicago, IL 60611

Roberts, John L., Department of Zoology, University of Massachusetts, Amherst, MA 01002 (resigned 10/87)

Robinson, Denis M., 200 Ocean Lane Drive, Key Biscayne, FL 33149

Rose, Birgit, Department of Physiology R-430, University of Miami School of Medicine, P. O. Box 016430, Miami, FL 33149

Rose, S. Meryl, Box 309W, Waquoit, MA 02536

Rosenbaum, Joel L., Department of Biology, Kline Biology Tower, Yale University, New Haven, CT 06520

Rosenberg, Philip, School of Pharmacy, Division of Pharmacology, University of Connecticut, Storrs, CT 06268

Rosenbluth, Jack, Department of Physiology, New York University School of Medicine, 550 First Ave., New York, NY 10016

Rosenbluth, Raja, 3380 West 5th Ave., Vancouver 8, BC, Canada V6R 1R7

Roslansky, John, Box 208, Woods Hole, MA 02543

Roslansky, Priscilla F., Box 208, Woods Hole, MA 02543

Ross, William N., Department of Physiology, New York Medical College, Valhalla, NY 10595

Roth, Jay S., 18 Millfield Street, Woods Hole, MA 02543

Rowland, Lewis P., Neurological Institute, 710 West 168th St., New York, NY 10032

Ruderman, Joan V., Department of Zoology, Duke University, Durham, NC 27706

Rushforth, Norman B., Case Western Reserve University, Department of Biology, Cleveland, OH 44106

Russell-Hunter, W. D., Department of Biology, Lyman Hall 029, Syracuse University, Syracuse, NY 13210

Saffo, Mary Beth, Institute of Marine Sciences, 272 Applied Sciences, University of California, Santa Cruz, CA 95064

Sager, Ruth, Dana Farber Cancer Institute, 44 Binney St., Boston, MA 02115

Salama, Guy, Department of Physiology, University of Pittsburgh, Pittsburth, PA 15261

Salmon, Edward D., Department of Zoology, University of North Carolina, Chapel Hill, NC 27514

Salzberg, Brian M., Department of Physiology, University of Pennsylvania, 4010 Locust St., Philadelphia, PA 19174

Sanborn, Richard C., 5862 North Olney St., Indianapolis, IN 46220

Sanger, Jean M., Department of Anatomy, School of Medicine, University of Pennsylvania, 36th and Hamilton Walk, Philadelphia, PA 19174

Sanger, Joseph, Department of Anatomy, School of Medicine, University of Pennsylvania, 36th and Hamilton Walk, Philadelphia, PA 19174

Sato, Eimei, Department of Animal Science, Faculty of Agriculture, Kyoto University, Kyoto 606, Japan

Sato, Hidemi, Sugashima Marine Biological Laboratory, Nagoya University, Sugashima-cho, Toba-chi, Mie-Ken 517, Japan

Sattelle, David B., AFRC Unit-Department of Zoology, University of Cambridge, Downing St., Cambridge CB2 3EJ, England, UK

Saunders, John W., Jr., P. O. Box 381W, Waquoit, MA 02536

Saz, Arthur K., Medical and Dental Schools, Georgetown University, 3900 Reservoir Rd., NW, Washington, DC 20051

Schachman, Howard K., Department of Molecular Biology, University of California, Berkeley, CA 94720

Schatten, Gerald P., Integrated Microscopy Facility for Biomedical Research, University of Wisconsin, 1117 W. Johnson St., Madison, WI 53706

Schatten, Heide, Department of Zoology, University of Wisconsin, Madison, WI 53706

Schiff, Jerome A., Institute for Photobiology of Cells and Organelles, Brandeis University, Waltham, MA 02154

Schmeer, Arline C., Mercenene Cancer Research Institute, Hospital of Saint Raphael, New Haven, CT 06511

Schnapp, Bruce J., Marine Biological Laboratory, Woods Hole, MA 02543

Schneider, E. Gayle, Department of Obstetrics and Gynecology, Yale University School of Medicine, 333 Cedar St., New Haven, CT 06510

Schneiderman, Howard A., Monsanto Company, 800 North Lindberg Blvd., D1W, St. Louis, MO 63166

Schotte, Oscar E., Department of Biology, Amherst College, Amherst, MA 01002 (deceased 4/12/88)

Schuel, Herbert, Department of Anatomical Sciences, SUNY, Buffalo, Buffalo, NY 14214

Schuetz, Allen W., School of Hygiene and Public Health, Johns Hopkins University, Baltimore, MD 21205

Schwartz, James H., Center for Neurobiology and Behavior, New York State Psychiatric Institute—Research Annex, 722 W. 168th St., 7th Floor, New York, NY 10032

Scofield, Virginia Lee, Department of Microbiology and Immunology, UCLA School of Medicine, Los Angeles, CA 90024

Sears, Mary, P. O. Box 152, Woods Hole, MA 02543

Segal, Sheldon J., Population Division, The Rockefeller Foundation, 1133 Avenue of the Americas, New York, NY 10036

Seliger, Howard H., Johns Hopkins University, McCollum-Pratt Institute, Baltimore, MD 21218 (resigned 1/31/88)

Selman, Kelly, Department of Anatomy, College of Medicine, University of Florida, Gainesville, FL 32601

Senft, Joseph, English Village Apartments, Bldg. 24, C-1, Lower State Rd., North Wales, PA 19454

Shanklin, Douglas R., 134 Grove Park Circle, Memphis, TN 38117

Shapiro, Herbert, 6025 North 13th St., Philadelphia, PA 19141

Shaver, Gaius R., Ecosystems Center, Marine Biological Laboratory, Woods Hole, MA 02543

Shaver, John R., 615 Jones St., Lansing, MI 48912-1718

Sheetz, Michael P., Department of Cell Biology and Physiology, Washington University Medical School, 606 S. Euclid Ave., St. Louis, MO 63110

Shepard, David C., P. O. Box 44, Woods Hole, MA 02543

Shepro, David, Department of Biology, Boston University, 2 Cummington St., Boston, MA 02215

Sher, F. Alan, Immunology and Cell Biology Section, Laboratory of Parasitic Disease, NIAID, Building 5, Room 114, NIH, Bethesda, MD 20892

Sheridan, William F., Biology Department, University of North Dakota, Grand Forks, ND 58202

Sherman, I. W., Division of Life Sciences, University of California, Riverside, CA 92502

Shilo, Moshe, Department of Microbiological Chemistry, Hebrew University, Jerusalem, ISRAEL

Shoukimas, Jonathan J., 45 Dillingham Avenue, Falmouth, MA 02540

Siegel, Irwin M., Department of Ophthalmology, New

York University Medical Center, 550 First Avenue, New York, NY 10016

Siegelman, Harold W., Department of Biology, Brookhaven National Laboratory, Upton, NY 11973

Silver, Robert B., Laboratory of Molecular Biology, University of Wisconsin, 1525 Linden Drive, Madison, WI 53706

Sjodin, Raymond A., Department of Biophysics, University of Maryland, Baltimore, MD 21201

Skinner, Dorothy M., Oak Ridge National Laboratory, Biology Division, Oak Ridge, TN 37830

Sloboda, Roger D., Department of Biological Sciences, Dartmouth College, Hanover, NH 03755

Sluder, Greenfield, Cell Biology Group, Worcester Foundation for Experimental Biology, 22 Maple Ave., Shrewsbury, MA 01545

Smith, Michael A., Jl Sinabung, Buntu #7, Semarang, Java, Indonesia

Smith, Ralph I., Department of Zoology, University of California, Berkeley, CA 94720

Sorenson, Martha M., Depto de Bioquimica-RFRJ, Centro de Ciencias da Saude-I. C. B., Cidade Universitaria-Fundad, Rio de Janeiro, Brasil 21.910

Speck, William T., Case Western Reserve University, Department of Pediatrics, Cleveland, OH 44106

Spector, A., College of Physicians and Surgeons, Columbia University, Black Bldg., Room 1516, New York, NY 10032

Speer, John W., Marine Biological Laboratory, Woods Hole, MA 02543

Spiegel, Evelyn, Department of Biological Sciences, Dartmouth College, Hanover, NH 03755

Spiegel, Melvin, Department of Biological Sciences, Dartmouth College, Hanover, NH 03755

Spray, David C., Albert Einstein College of Medicine, Department of Neurosciences, 1300 Morris Park Avenue, Bronx, NY 10461

Steele, John Hyslop, Woods Hole Oceanographic Institution, Woods Hole, MA 02543

Steinacher, Antoinette, Dept. of Otolaryngology, Washington University, School of Medicine, 4911 Barnes Hospital, St. Louis, MO 63110

Steinberg, Malcolm, Department of Biology, Princeton University, Princeton, NJ 08540

Stephens, Grove, Department of Developmental and Cell Biology, University of California, Irvine, CA 92717

Stephens, Raymond E., Marine Biological Laboratory, Woods Hole, MA 02543

Stetten, DeWitt, Jr., Senior Scientific Advisor, NIH, Bldg. 16, Room 118, Bethesda, MD 20892

Stetten, Jane Lazarow, 2 W Drive, Bethesda, MD 20814

Steudler, Paul A., Ecosystems Center, Marine Biological Laboratory, Woods Hole, MA 02543

Stokes, Darrell R., Department of Biology, Emory University, Atlanta, GA 30322

Stommel, Elijah W., 766 Palmer Avenue, Falmouth, MA 02540

Stracher, Alfred, Downstate Medical Center, SUNY, 450 Clarkson Ave., Brooklyn, NY 11203

Strehler, Bernard L., 2235 25th St., #217, San Pedro, CA 90732

Strumwasser, Felix, Marine Biological Laboratory, Woods Hole, MA 02543

Stuart, Ann E., Department of Physiology, Medical Sciences Research Wing 206H, University of North Carolina, Chapel Hill, NC 27514

Sugimori, Mutsuyuki, Department of Physiology and Biophysics, New York University Medical Center, 550 First Avenue, New York, NY 10016

Summers, William C., Huxley College, Western Washington University, Bellingham, WA 98225

Sussman, Maurice, 72 Carey Lane, Falmouth, MA 02540

Szabo, George, Harvard School of Dental Medicine, 188 Longwood Avenue, Boston, MA 02115

Szent-Gyorgyi, Andrew, Department of Biology, Brandeis University, Waltham, MA 02254

Szent-Gyorgyi, Eva Szentkiraly, Department of Biology, Brandeis University, Waltham, MA 02254

Szuts, Ete Z., Laboratory of Sensory Physiology, Marine Biological Laboratory, Woods Hole, MA 02543

Tamm, Sidney L., Boston University Marine Program, Marine Biological Laboratory, Woods Hole, MA 02543

Tanzer, Marvin L., Department of Oral Biology, Medical School, University of Connecticut, Farmington, CT 06032

Tasaki, Ichiji, Laboratory of Neurobiology, Bldg. 36, Rm. 2B-16, NIMH/NIH, Bethesda, MD 20892

Taylor, Douglass L., Biological Sciences, Mellon Institute, 440 Fifth Avenue, Pittsburgh, PA 15213

Teal, John M., Department of Biology, Woods Hole Oceanographic Institution, Woods Hole, MA 02543

Telfer, William H., Department of Biology, University of Pennsylvania, Philadelphia, PA 19174

Thorndike, W. Nicholas, Wellington Management Company, 28 State St., Boston, MA 02109

Trager, William, Rockefeller University, 1230 York Ave., New York, NY 10021

Travis, D. M., Veterans Administration Medical Center, Fargo, ND 58102

Treistman, Steven N., Worcester Foundation for Experimental Biology, Shrewsbury, MA 01545

Trigg, D. Thomas, 125 Grove St., Wellesley, MA 02181

Trinkaus, J. Philip, Department of Biology, Box 6666, Yale University, New Haven, CT 06510

Troll, Walter, Department of Environmental Medicine,

College of Medicine, New York University, New York, NY 10016

Troxler, Robert F., Department of Biochemistry, School of Medicine, Boston University, 80 East Concord St., Boston, MA 02118

Tucker, Edward B., The City University of New York, Baruch College, Box 502, 17 Lexington Ave., New York, NY 10010

Turner, Ruth D., Mollusk Department, Museum of Comparative Zoology, Harvard University, Cambridge, MA 02138

Tweedell, Kenyon S., Department of Biology, University of Notre Dame, Notre Dame, IN 46656

Tytell, Michael, Department of Anatomy, Bowman Gray School of Medicine, Winston-Salem, NC 27103

Ueno, Hiroshi, Laboratory of Biochemistry, The Rockefeller University, 1230 York Ave., New York, NY 10021

Uretz, Robert B., Division of Biological Sciences, University of Chicago, 950 East 59th St., Chicago, IL 60637

Valiela, Ivan, Boston University Marine Program, Marine Biological Laboratory, Woods Hole, MA 02543

Vallee, Richard, Cell Biology Group, Worcester Foundation for Experimental Biology, Shrewsbury, MA 01545

Valois, John, Marine Biological Laboratory, Woods Hole, MA 02543

Van Holde, Kensal, Department of Biochemistry and Biophysics, Oregon State University, Corvallis, OR 97331

Villee, Claude A., Parcel B, Room 122, Harvard Medical School, 25 Shattuck St., Boston, MA 02115

Vincent, Walter S., School of Life and Health Sciences, University of Delaware, Newark, DE 19711

Waksman, Byron, National Multiple Sclerosis Society, 205 East 42nd St., New York, NY 10017

Wall, Betty, 9 George St., Woods Hole, MA 02543

Wallace, Robin A., Whitney Marine Lab, 9505 A1A South, St. Augustine, FL 32086

Wang, An, Wang Laboratories, Inc., One Industrial Ave., Lowell, MA 01851

Wang, Ching Chung, Department of Pharmaceutical Chemistry, University of California, San Francisco, CA 94143

Warner, Robert C., Department of Molecular Biology and Biochemistry, University of California, Irvine, CA 92717

Warren, Kenneth S., The Rockefeller Foundation, 1133 Avenue of the Americas, New York, NY 10036

Warren, Leonard, Department of Therapeutic Research, School of Medicine, Anatomy-Chemistry Building, University of Pennsylvania, Philadelphia, PA 19174

Watson, Stanley, Department of Biology, Woods Hole Oceanographic Institution, Woods Hole, MA 02543

Webb, H. Marguerite, Marine Biological Laboratory, Woods Hole, MA 02543

Weber, Annemarie, Department of Biochemistry and Biophysics, School of Medicine, University of Pennsylvania, Philadelphia, PA 19104

Webster, Ferris, Box 765, Lewes, DE 19958

Weidner, Earl, Department of Zoology and Physiology, Louisiana State University, Baton Rouge, LA 70803

Weiss, Dieter, G., Institut fur Zoologie, Technische Universitat Munchen, 8046 Garching, Federal Republic of Germany

Weiss, Leon P., Department of Animal Biology, School of Veterinary Medicine, University of Pennsylvania, Philadelphia, PA 19104

Weissmann, Gerald, New York University, 550 First Avenue, New York, NY 10016

Werman, Robert, Neurobiology Unit, The Hebrew University, Jerusalem, ISRAEL

Westerfield, R. Monte, The Institute of Neuroscience, University of Oregon, Eugene, OR 37403

Wexler, Nancy Sabin, 15 Claremont Avenue, Apt. 92, New York, NY 10027

White, Roy L., Department of Neuroscience, Albert Einstein College, 1300 Morris Park Avenue, Bronx, NY 10461

Whittaker, J. Richard, Marine Biological Laboratory, Woods Hole, MA 02543

Wigley, Roland L., 35 Wilson Road, Woods Hole, MA 02543

Wilson, Darcy B., Medical Biology Institute, 11077 North Torrey Pines Road, La Jolla, CA 92037

Wilson, Edward, O., Museum, Comparative Zoology, Harvard University, Cambridge, MA 02138 (resigned 10/87)

Wilson, T. Hastings, Department of Physiology, Harvard Medical School, Boston, MA 02115

Wilson, Walter L., 743 Cambridge Drive, Rochester Hills, MI 48063

Witkovsky, Paul, Department of Ophthalmology, New York University Medical Center, 550 First Ave., New York, NY 10016

Wittenberg, Jonathan B., Department of Physiology and Biochemistry, Albert Einstein College, 1300 Morris Park Ave., New York, NY 10016

Wolfe, Ralph, Department of Microbiology, 131 Burrill Hall, University of Illinois, Urbana, IL 61801

Wolken, Jerome J., Department of Biological Sciences, Carnegie Mellon University, 440 Fifth Ave., Pittsburgh, PA 15213

Worgul, Basil V., Department of Ophthalmology, Columbia University, 630 West 168th St., New York, NY 10032

Wu, Chau Hsiung, Department of Pharmacology, Northwestern University Medical School, 203 E. Chicago Ave., Chicago, IL 60611

Wyttenbach, Charles R., Department of Physiology and Cell Biology, University of Kansas, Lawrence, KS 66045

Yeh, Jay Z., Department of Pharmacology, Northwestern University Medical School, 303 E. Chicago Ave., Chicago, IL 60611

Young, Richard W., Mentor O & O, Inc., 3000 Longwater Dr., Norwell, MA 02061-1610

Zackroff, Robert, 66 White Horn Drive, Kingston, RI 02881

Zigman, Seymour, School of Medicine and Dentistry, University of Rochester, 260 Crittenden Blvd., Rochester, NY 14620

Zigmond, Richard E., Department of Pharmacology, Harvard Medical School, 250 Longwood Ave., Boston, MA 02115

Zimmerberg, Joshua J., Bldg. 12A, Room 2007, NIH, Bethesda, MD 20892

Zottoli, Steven J., Department of Biology, Williams College, Williamstown, MA 01267

Zucker, Robert S., Department of Physiology, University of California, Berkeley, CA 94720

Associate Members

Ackroyd, Dr. Frederick W.
Adams, Dr. Paul
Adelberg, Dr. and Mrs. Edward A.
Ahearn, Mr. and Mrs. David
Alden, Mr. John M.
Allen, Miss Camilla K.
Allen, Dr. Nina S.
Amon, Mr. Carl H. Jr
Anderson, Mr. J. Gregory
Anderson, Drs. James L. and Helene M.
Armstrong, Dr. and Mrs. Samuel C.
Arnold, Mrs. Lois
Atwood, Dr. and Mrs. Kimball C., III
Ayers, Mr. and Mrs. Donald
Baker, Mrs. C. L.
Ball, Mrs. Eric G.
Ballantine, Dr. and Mrs. H. T., Jr.
Bang, Mrs. Frederik B.
Bang, Miss Molly
Banks, Mr. and Mrs. William L.
Barkin, Mr. and Mrs. Mel A.
Barrows, Mrs. Albert W.
Baum, Mr. Richard T.
Baylor, Drs. Edward and Martha
Beers, Dr. and Mrs. Yardley
Belcsir, Mr. Tasos
Bennett, Dr. and Mrs. Michael V. L.
Berg, Mr. and Mrs. C. John
Bernheimer, Dr. Alan W.
Bernstein, Mr. and Mrs. Norman
Berwind, Mr. David McM.
Bicker, Mr. Alvin
Bigelow, Mrs. Robert O.
Bird, Mr. William R.
Bleck, Dr. Thomas B.
Boche, Mr. David
Bodeen, Mr. and Mrs. George H.
Boettiger, Dr. and Mrs. Edward G.
Boettiger, Mrs. Julie
Bolton, Mr. and Mrs. Thomas C.
Bonn, Mr. and Mrs. Theodore H.
Borgese, Dr. and Mrs. Thomas
Bowles, Dr. and Mrs. Francis P.
Bradley, Dr. and Mrs. Charles C.
Bradley, Mr. Richard
Brown, Mrs. Frank A., Jr.
Brown, Mr. and Mrs. Henry
Brown, Mr. and Mrs. James
Brown, Mrs. Neil
Brown, Dr. and Mrs. Thornton
Broyles, Dr. Robert H.
Buck, Dr. and Mrs. John B.
Buckley, Mr. George D.
Bunts, Mr. and Mrs. Frank E.
Burt, Mrs. Charles E.
Bush, Dr. Louise
Buxton, Mr. and Mrs. Bruce E.
Buxton, Mr. E. Brewster
Calkins, Mr. and Mrs. G. N., Jr.
Campbell, Dr. and Mrs. David G.
Carlson, Dr. and Mrs. Francis
Carlton, Mr. and Mrs. Winslow G.
Case, Dr. and Mrs. James
Chandler, Mr. Robert
Chase, Mr. Tom H.
Child, Dr. and Mrs. Frank M.
Church, Dr. Wesley
Claff, Mr. and Mrs. Mark
Clark, Dr. and Mrs. Arnold
Clark, Mr. and Mrs. Hays
Clark, Mr. and Mrs. James McC.
Clark, Mrs. Leonard B.
Clark, Mr. and Mrs. Leroy, Jr.
Clarke, Dr. Barbara J.
Clement, Mrs. Anthony
Clowes Fund, Inc.
Clowes, Dr. and Mrs. Alexander W.
Clowes, Mr. Allen W.
Clowes, Dr. and Mrs. G. H. A., Jr.
Coburn, Mr. and Mrs. Lawrence
Cohen, Mrs. Seymour S.
Coleman, Dr. and Mrs. John
Connell, Mr. and Mrs. W. J.
Cook, Dr. and Mrs. Paul W., Jr.
Copeland, Dr. and Mrs. D. Eugene
Copeland, Mr. Frederick C.
Copeland, Mr. and Mrs. Preston S.
Costello, Mrs. Donald P.
Crabb, Mr. and Mrs. David L.
Crain, Mr. and Mrs. Melvin C.
Cramer, Mr. and Mrs. Ian D. W.
Crane, Mrs. John O.
Crane, Josephine B., Foundation
Crane, Mr. Thomas S.
Cross, Mr. and Mrs. Norman C.
Crossley, Miss Dorothy
Crossley, Miss Helen
Crowell, Dr. and Mrs. Sears
Currier, Mr. and Mrs. David L.

Daignault, Mr. and Mrs. Alexander T.
Daniels, Mr. and Mrs. Bruce G.
Davidson, Dr. Morton
Davis, Mr. and Mrs. Joel P.
Day, Mr. and Mrs. Pomeroy
Decker, Dr. Raymond F.
DeMello, Mr. John
DiBerardino, Dr. Marie A.
Dickson, Dr. Willim A.
Dierolf, Dr. Shirley H.
Drummey, Mr. and Mrs. Charles E.
Drummey, Mr. Todd A.
DuBois, Dr. and Mrs. Arthur B.
Dudley, Dr. Patricia
DuPont, Mr. A. Felix, Jr.
Dutton, Mr. and Mrs. Roderick L.
Ebert, Dr. and Mrs. James D.
Egloff, Dr. and Mrs. F. R. L.
Elliott, Mrs. Alfred M.
Enos, Mr. Edward, Jr.
Eppel, Mr. and Mrs. Dudley
Estabrook, Mr. Gordon C.
Evans, Mr. and Mrs. Dudley
Farley, Miss Joan
Farmer, Miss Mary
Faull, Mr. J. Horace, Jr.
Ferguson, Dr. and Mrs. James J., Jr.
Fisher, Mrs. B. C.
Fisher, Mr. Frederick S., III
Fisher, Dr. and Mrs. Saul H.
Folino, Mr. John W., Jr.
Forbes, Mr. John M.
Ford, Mr. John H.
Fowlkes, Mr. Aaron
Francis, Mr. and Mrs. Lewis W., Jr.
Frenkel, Dr. Krystina
Fribourgh, Dr. James H.
Friendship Fund
Fries, Dr. and Mrs. E. F. B.
Frosch, Dr. and Mrs. Robert A.
Fye, Mrs. Paul M.
Gabriel, Dr. and Mrs. Mordecai L.
Gagnon, Mr. Michael
Gaiser, Mrs. David W.
Gallagher, Mr. Robert O.
Garfield, Miss Eleanor
Garrey, Dr. Walter E.
Gellis, Dr. and Mrs. Sydney
Gephard, Mr. Stephen
German, Dr. and Mrs. James L., III
Gewecke, Mr. and Mrs. Thomas H.
Gifford Mr. and Mrs. Cameron
Gifford, Mr. John A.
Gifford, Dr. and Mrs. Prosser
Gilbert, Drs. Daniel L. and Claire
Gilbert, Mrs. Carl J.
Gildea, Dr. Margaret C. L.
Gillette, Mr. and Mrs. Robert S.
Glad, Mr. Robert
Glass, Dr. and Mrs. H. Bentley
Glazebrook, Mr. James
Glazebrook, Mrs. James R.
Goldman, Mrs. Mary
Goldring, Mr. Michael
Goldstein, Dr. and Mrs. Moise H., Jr.
Goodwin, Mr. and Mrs. Charles
Gould, Miss Edith
Grace, Miss Priscilla B.
Grant, Dr. and Mrs. Philip
Grassle, Mrs. J. F.
Green, Mrs. Davis Crane
Greer, Mr. and Mrs. W. H., Jr.
Griffin, Mrs. Robert W.
Griffith, Dr. and Mrs. B. Herold
Grosch, Dr. and Mrs. Daniel S.
Gross, Mrs. Mona
Gunning, Mr. and Mrs. Robert
Haakonsen, Dr. Harry O.
Haigh, Mr. and Mrs. Richard H.
Hall, Mr. and Mrs. Peter A.
Hall, Mr. Warren C.
Halvorson, Dr. and Mrs. Harlyn O.
Hamstrom, Miss Mary Elizabeth
Harrington, Mr. Robert D., Jr.
Harvey, Dr. and Mrs. Richard B.
Hassett, Mr. and Mrs. Charles
Hastings, Dr. and Mrs. J. Woodland
Haubrich, Mr. Robert R.
Hay, Mr. John
Hays, Dr. David S.
Hedberg, Mrs. Frances
Hedberg, Dr. Mary
Hersey, Mrs. George L.
Hiatt, Dr. and Mrs. Howard
Hichar, Mrs. Barbara
Hill, Mrs. Samuel E.
Hirschfeld, Mrs. Nathan B.
Hobbie, Dr. and Mrs. John
Hocker, Mr. and Mrs. Lon
Hodge, Mrs. Stuart
Hokin, Mr. Richard
Hornor, Mr. Townsend
Horwitz, Dr. and Mrs. Norman H.
Hoskin, Dr. and Mrs. Francis C. G.
Houston, Mr. and Mrs. Howard E.
Howard, Mr. and Mrs. L. L.
Hoyle, Dr. Merrill C.
Huettner, Dr. and Mrs. Robert J.
Hutchison, Mr. Alan D.
Hynes, Mr. and Mrs. Thomas J., Jr.
Inouë, Dr. and Mrs. Shinya
Issokson, Mr. and Mrs. Israel
Jackson, Miss Elizabeth B.
Jaffe, Dr. and Mrs. Ernst R.
Janney, Mrs. F. Wistar
Jewett, G. F., Foundation
Jewett, Mr. and Mrs. G. F., Jr.
Jones, Mr. and Mrs. DeWitt C., III
Jones Mr. and Mrs. Frederick, II
Jones, Mr. Frederick S., III
Jordan, Dr. and Mrs. Edwin P.
Kaan, Dr. Helen W.
Kahler, Mrs. Robert W.
Kaminer, Dr. and Mrs. Benjamin
Karplus, Mrs. Alan K.
Karush, Dr. and Mrs. Fred
Kelleher, Mr. and Mrs. Paul R.
Kendall, Mr. and Mrs. Richard E.
Keosian, Mrs. Jessie
Keoughan, Miss Patricia
Ketchum, Mrs. Paul
Kien, Mr. and Mrs. Pieter
Kinnard, Mrs. L. Richard
Kirschenbaum, Mrs. Donald
Kissam, Mr. and Mrs. William M.

Kivy, Dr. and Mrs. Peter
Koller, Dr. Lewis R.
Korgen, Dr. Ben J.
Kuffler, Mrs. Stephen W.
Laderman, Mr. and Mrs. Ezra
Lafferty, Miss Nancy
Larmon, Mr. Jay
Laster, Dr. and Mrs. Leonard
Laufer, Dr. and Mrs. Hans
Laufer, Jessica, and Weiss, Malcolm
LaVigne, Mrs. Richard J.
Lawrence, Mr. Frederick V.
Lawrence, Mr. and Mrs. William
Leatherbee, Mrs. John H.
LeBlond, Mr. and Mrs. Arthur
Leeson, Mr. and Mrs. A. Dix
LeFevre, Dr. Marian E.
Lehman, Miss Robin
Lemann, Mrs. Lucy B.
Lenher, Dr. and Mrs. Samuel
Leprohon, Mr. Joseph
Levine, Mr. Joseph
Levine, Dr. and Mrs. Rachmiel
Levitz, Dr. Mortimer
Levy, Mr. Stephen R.
Lindner, Mr. Timothy P.
Little, Mrs. Elbert
Livingstone, Mr. and Mrs. Robert
Loeb, Mrs. Robert F.
Lovell, Mr. and Mrs. Hollis R.
Lovering, Mr. Richard C.
Low, Miss Doris
Lowe, Dr. and Mrs. Charles V.
Lowengard, Mrs. Joseph
Mackey, Mr. and Mrs. William K.
MacLeish, Mrs. Margaret
MacNary, Mr. and Mrs. B. Glenn
MacNichol, Dr. and Mrs. Edward F., Jr.
Maher, Miss Anne Camille
Mahler, Mrs. Henry
Mahler, Mrs. Suzanne
Mansworth, Miss Marie
Marsh, Dr. and Mrs. Julian
Martyna, Mr. and Mrs. Joseph C.
Mason, Mr. Appleton
Mastroianni, Dr. and Mrs. Luigi, Jr.
Mather, Mr. and Mrs. Frank J., III
Matherly, Mr. and Mrs. Walter
Matthiessen, Dr. and Mrs. G. C.
McCusker, Mr. and Mrs. Paul T.
McElroy, Mrs. Nella W.
McIlwain, Dr. Susan G.
Meigs, Mr. and Mrs. Arthur
Meigs, Dr. and Mrs. J. Wister
Melillo, Dr. and Mrs. Jerry M.
Mellon, Richard King, Trust
Mellon, Mr. and Mrs. Richard P.
Mendelson, Dr. Martin
Metz, Dr. and Mrs. Charles B.
Meyers, Mr. and Mrs. Richard
Millbury, Mr. Edward Van R.
Miller, Dr. Daniel A.
Miller, Mr. and Mrs. Paul
Mixter, Mr. and Mrs. William J., Jr.
Mizell, Dr. and Mrs. Merle
Monroy, Mrs. Alberto
Montgomery, Dr. and Mrs. Charles H.
Montgomery, Dr. and Mrs. Raymond B.
Moore, Drs. John and Betty
Morgan, Miss Amy
Morse, Mrs. Charles L., Jr.
Morse, Dr. M. Patricia
Moul, Dr. and Mrs. Edwin T.
Mountain, Dr. Isabel M.
Murray, Dr. David M.
Myles-Tochko, Dr. Christina J.
Nace, Dr. and Mrs. Paul
Nace, Mr. Paul F., Jr.
Neall, Mr. William G.
Nelson, Dr. and Mrs. Leonard
Nelson, Dr. Pamela
Newton, Mr. William F.
Nickerson, Mr. and Mrs. Frank L.
Norman, Mr. and Mrs. Andrew E.
Norman Foundation
Norris, Mr. and Mrs. Barry
Norris, Mr. and Mrs. John A.
Norris, Mr. William
O'Herron, Mr. and Mrs. Jonathan
Olszowka, Miss Janice S.
O'Neil, Mr. and Mrs. Barry T.
O'Rand, Mr. and Mrs. Michael
Ortins, Mr. and Mrs. Armand
O'Sullivan, Dr. Renee Bennett
Pappas, Dr. and Mrs. George D.
Park, Mrs. Franklin A.
Park, Mr. and Mrs. Malcolm S.
Parmenter, Dr. Charles
Parmenter, Miss Carolyn L.
Peltz, Mr. and Mrs. William L.
Pendergast, Mrs. Claudia
Pendleton, Dr. and Mrs. Murray E.
Perkins, Mr. and Mrs. Courtland D.
Person, Dr. and Mrs. Philip
Peterson, Mr. and Mrs. E. Gunnar
Peterson, Mr. and Mrs. E. Joel
Peterson, Mr. Raymond W.
Petty, Mr. Richard F.
Petty, Mr. William
Pfeiffer, Mr. and Mrs. John
Plough, Mr. and Mrs. George H.
Plough, Mrs. Harold H.
Pointe, Mr. Albert
Pointe, Mr. Charles
Porter, Dr. and Mrs. Keith R.
Pothier, Dr. and Mrs. Aubrey
Press, Drs. Frank and Billie
Proskauer, Mr. Joseph H.
Proskauer, Mr. Richard
Prosser, Dr. and Mrs. C. Ladd
Psaledakis, Mr. Nicholas
Psychoyos, Dr. Alexandre
Putnam, Mr. Allan Ray
Putnam, Mr. and Mrs. William A., III
Raymond, Dr. and Mrs. Samuel
Reese, Miss Bonnie
Reingold, Mr. Stephen C.
Reynolds, Dr. and Mrs. George
Reynolds, Mr. Robert M.
Reznikoff, Mrs. Paul
Ricca, Dr. and Mrs. Renato A.
Righter, Mr. Harold
Riina, Mr. and Mrs. John R.
Robb, Mrs. Alison A.

Roberts, Miss Jean
Roberts, Mrs. Mervin F.
Robertson, Mrs. C. W.
Robinson, Dr. Denis M.
Root, Mrs. Walter S.
Rosenthal, Miss Hilde
Roslansky, Drs. John and Priscilla
Ross, Dr. and Mrs. Donald
Ross, Dr. Robert
Ross, Dr. Virginia
Roth, Dr. and Mrs. Stephen
Rowe, Mr. Don
Rowe, Mr. and Mrs. William S.
Rubin, Dr. Joseph
Rugh, Mrs. Roberts
Ryder, Mr. and Mrs. Francis C.
Sager, Dr. Ruth
Sardinha, Mr. George H.
Saunders, Dr. and Mrs. John W.
Saunders, Mrs. Lawrence
Saunders, Lawrence, Fund
Sawyer, Mr. and Mrs. John E.
Saz, Mrs. Ruth L.
Schlesinger, Dr. and Mrs. R. Walter
Scott, Mrs. George T.
Scott, Mr. and Mrs. Norman E.
Sears, Mr. Clayton C.
Sears, Mr. and Mrs. Harold B.
Sears, Mr. Harold H.
Seaver, Mr. George
Segal, Dr. and Mrs. Sheldon J.
Senft, Dr. and Mrs. Alfred
Shapiro, Mr. and Mrs. Howard
Shapley, Dr. Robert
Shemin, Dr. and Mrs. David
Shepro, Dr. and Mrs. David
Siegel, Mr. and Mrs. Alvin
Simmons, Mr. Tim
Singer, Mr. and Mrs. Daniel M.
Smith, Drs. Frederick E. and Marguerite A.
Smith, Mrs. Homer P.
Smith, Mr. Van Dorn C.
Snyder, Mr. Robert M.
Solomon, Dr. and Mrs. A. K.
Speck, Dr. William T.
Specht, Mr. and Mrs. Heinz
Spiegel, Dr. and Mrs. Melvin
Spotte, Mr. Stephen
Steele, Mrs. John H.
Stein, Mr. Ronald
Steinbach, Mrs. H. Burr
Stetson, Mrs. Thomas J.
Stetten, Dr. Gail
Stetten, Dr. and Mrs. H. DeWitt, Jr.
Stewart, Mr. and Mrs. Peter
Strehler, Dr. and Mrs. Bernard
Stunkard, Dr. Horace
Sudduth, Dr. William
Swanson, Dr. and Mrs. Carl P.
Swope, Mrs. Gerard, Jr.
Swope, Mr. and Mrs. Gerard L.
Szent-Györgyi, Dr. Andrew
Tabor, Mr. George H.
Taylor, Mr. James K.
Taylor, Dr. and Mrs. W. Randolph
Tietje, Mr. and Mrs. Emil D., Jr.
Timmins, Mrs. William
Todd, Mr. and Mrs. Gordon F.
Tolkan, Mr. and Mrs. Norman N.
Trager, Mrs. William
Trigg, Mr. and Mrs. D. Thomas
Troll, Dr. and Mrs. Walter
Tucker, Miss Ruth
Tully, Mr. and Mrs. Gordon F.
Ulbrich, Mr. and Mrs. Volker
Valois, Mr. and Mrs. John
Van Buren, Mrs. Harold
Van Holde, Mrs. Kensal E.
Veeder, Mrs. Ronald A.
Vincent, Mr. and Mrs. Samuel W.
Vincent, Dr. Walter S.
Wagner, Mr. Mark
Waksman, Dr. and Mrs. Byron H.
Ward, Dr. Robert T.
Ware, Mr. and Mrs. J. Lindsay
Warren, Dr. Henry B.
Warren, Dr. and Mrs. Leonard
Watt, Mr. and Mrs. John B.
Weeks, Mr. and Mrs. John T.
Weinstein, Miss Nancy B.
Weisberg, Mr. and Mrs. Alfred M.
Wheeler, Dr. and Mrs. Paul S.
Whitehead, Mr. and Mrs. Fred
Whitney, Mr. and Mrs. Geoffrey G., Jr.
Wichterman, Dr. and Mrs. Ralph
Wickersham, Mr. and Mrs. A. A. Tilney
Wiese, Dr. Konrad
Wilhelm, Dr. Hazel S.
Wilson, Mr. and Mrs. T. Hastings
Winn, Dr. William M.
Winsten, Dr. Jay A.
Witting, Miss Joyce
Wofinsohn, Mrs. Wolfe
Woodwell, Dr. and Mrs. George M.
Yntema, Mrs. Chester L.
Young-Wallace, Miss Nina L.
Zinn, Dr. and Mrs. Donald J.
Zipf, Dr. Elizabeth

III. Certificate of Organization

(On File in the Office of the Secretary of the Commonwealth)

No. 3170

We, Alpheus Hyatt, President, William Stanford Stevens, Treasurer, and William T. Sedgwick, Edward G. Gardiner, Susan Mims and Charles Sedgwick Minot being a majority of the Trustees of the Marine Biological Laboratory in compliance with the requirements of the fourth section of chapter one hundred and fifteen of the Public Statutes do hereby certify that the following is a true copy of the agreement of association to constitute said Corporation, with the names of the subscribers thereto:

We, whose names are hereto subscribed, do, by this agreement, associate ourselves with the intention to constitute a Corporation according to the provisions of the one hundred and fifteenth chapter of the Public Statutes of the Commonwealth of Massachusetts, and the Acts in amendment thereof and in addition thereto.

The name by which the Corporation shall be known is THE MARINE BIOLOGICAL LABORATORY.

The purpose for which the Corporation is constituted is to establish and maintain a laboratory or station for scientific study and investigations, and a school for instruction in biology and natural history.

The place within which the Corporation is established or located is the city of Boston within said Commonwealth.

The amount of its capital stock is none.

In Witness Whereof, we have hereunto set our hands, this twenty seventh day of February in the year eighteen hundred and eighty-eight, Alpheus Hyatt, Samuel Mills, William T. Sedgwick, Edward G. Gardiner, Charles Sedgwick Minot, William G. Farlow, William Stanford Stevens, Anna D. Phillips, Susan Mims, B. H. Van Vleck.

That the first meeting of the subscribers to said agreement was held on the thirteenth day of March in the year eighteen hundred and eighty-eight.

In Witness Whereof, we have hereunto signed our names, this thirteenth day of March in the year eighteen hundred and eighty-eight, Alpheus Hyatt, President, William Stanford Stevens, Treasurer, Edward G. Gardiner, William T. Sedgwick, Susan Mims, Charles Sedgwick Minot.

(Approved on March 20, 1988 as follows:

I hereby certify that it appears upon an examination of the within written certificate and the records of the corporation duly submitted to my inspection, that the requirements of sections one, two and three of chapter one hundred and fifteen, and sections eighteen, twenty and twenty-one of chapter one hundred and six, of the Public Statutes, have been complied with and I hereby approve said certificate this twentieth day of March A.D. eighteen hundred and eighty-eight.

Charles Endicott
Commissioner of Corporations)

IV. Articles of Amendment

(On File in the Office of the Secretary of the Commonwealth)

We, James D. Ebert, President, and David Shepro, Clerk of the Marine Biological Laboratory, located at Woods Hole, Massachusetts 02543, do hereby certify that the following amendment to the Articles of Organization of the Corporation was duly adopted at a meeting held on August 15, 1975, as adjourned to August 29, 1975, by vote of 444 members, being at least two-thirds of its members legally qualified to vote in the meeting of the corporation:

Voted: That the Certificate of Organization of this corporation be and it hereby is amended by the addition of the following provisions:

"No Officer, Trustee or Corporate Member of the corporation shall be personally liable for the payment or satisfaction of any obligation or liabilities incurred as a result of, or otherwise in connection with, any commitments, agreements, activities or affairs of the corporation.

"Except as otherwise specifically provided by the Bylaws of the corporation, meetings of the Corporate Members of the corporation may be held anywhere in the United States.

"The Trustees of the corporation may make, amend or repeal the Bylaws of the corporation in whole or in part, except with respect to any provisions thereof which shall by law, this Certificate or the bylaws of the corporation, require action by the Corporate Members."

The foregoing amendment will become effective when these articles of amendment are filed in accordance with Chapter 180, Section 7 of the General Laws unless these articles specify, in accordance with the vote adopting the amendment, a later effective date not more than thirty days after such filing, in which event the amendment will become effective on such later date.

In Witness whereof and Under the Penalties of Perjury, we have hereto signed our names this 2nd day of September, in the year 1975, James D. Ebert, President; David Shepro, Clerk.

(Approved on October 24, 1975, as follows:

I hereby approve the within articles of amendment and, the filing fee in the amount of $10 having been paid, said articles are deemed to have been filed with me this 24th day of October, 1975.

Paul Guzzi
Secretary of the Commonwealth)

V. Bylaws of the Corporation of the Marine Biological Laboratory

(Revised August 16, 1985)

I. (A) The name of the Corporation shall be The Marine Biological Laboratory. The Corporation's purpose shall be to establish and maintain a laboratory or station for scientific study and investigation, and a school for instruction in biology and natural history.

(B) Marine Biological Laboratory admits students without regard to race, color, sex, national and ethnic origin to all the rights, privileges, programs and activities generally accorded or made available to students in its courses. It does not discriminate on the basis of race, color, sex, national and ethnic origin in employment, administration or its educational policies, admissions policies, scholarship and other programs.

II. (A) The members of the Corporation ("Members") shall consist of persons elected by the Board of Trustees, upon such terms and conditions and in accordance with such procedures, not inconsistent with law or these Bylaws, as may be determined by said Board of Trustees. Except as provided below, any Member may vote at any meeting either in person or by proxy executed no more than six months prior to the date of such meeting. Members shall serve until their death or resignation unless earlier removed with or without cause by the affirmative vote of two-thirds of the Trustees then in office. Any member who has attained the age of seventy years or has retired from his home institution shall automatically be designated a Life Member provided he signifies his wish to retain his membership. Life Members shall not have the right to vote and shall not be assessed for dues.

(B) The Associates of the Marine Biological Laboratory shall be an unincorporated group of persons (including associations and corporations) interested in the Laboratory and shall be organized and operated under the general supervision and authority of the Trustees.

III. The officers of the Corporation shall consist of a Chairman of the Board of Trustees, President, Director, Treasurer and Clerk, elected or appointed by the Trustees as set forth in Article IX.

IV. The Annual Meeting of the Members shall be held on the Friday following the Second Tuesday in August in each year at the Laboratory in Woods Hole, Massachusetts, at 9:30 a.m. Subject to the provisions of Article VIII(2), at such meeting the Members shall choose by ballot six Trustees to serve four years, and shall transact such other business as may properly come before the meeting. Special meetings of the Members may be called by the Chairman or Trustees to be held at such time and place as may be designated.

V. Twenty five Members shall constitute a quorum at any meeting. Except as otherwise required by law or these Bylaws, the affirmative vote of a majority of the Members voting in person or by proxy at a meeting attended by a quorum (present in person or by proxy) shall constitute action on behalf of the Members.

VI. (A) Inasmuch as the time and place of the Annual Meeting of Members are fixed by these Bylaws, no notice of the Annual Meeting need be given. Notice of any special meeting of Members, however, shall be given by the Clerk by mailing notice of the time and place and purpose of such meeting, at least 15 days before such meeting, to each Member at his or her address as shown on the records of the Corporation.

(B) Any meeting of the Members may be adjourned to any other time and place by the vote of a majority of those Members present or represented at the meeting, whether or not such Members constitute a quorum. It shall not be necessary to notify any Members of any adjournment.

VII. The Annual Meeting of the Trustees shall be held promptly after the Annual Meeting of the Corporation at the Laboratory in Woods Hole, Massachusetts. Special meetings of the Trustees shall be called by the Chairman, the President, or by any seven Trustees, to be held at such time and place as may be designated. Notice of Trustees' meetings may be given orally, by telephone, telegraph or in writing; and notice given in time to enable the Trustees to attend, or in any case notice sent by mail or telegraph to a Trustee's usual or last known place of residence, at least one week before the meeting shall be sufficient. Notice of a meeting need not be given to any Trustee if a written waiver of notice, executed by him before or after the meeting is filed with the records of the meeting, or if he shall attend the meeting without protesting prior thereto or at its commencement the lack of notice to him.

VIII. (A) There shall be four groups of Trustees:

(1) Trustees (the "Corporate Trustees") elected by the Members according to such procedures, not inconsistent with these Bylaws, as the Trustees shall have determined. Except as provided below, such Trustees shall be divided into four classes of six, one class to be elected each year to serve for a term of four years. Such classes shall be designated by the year of expiration of their respective terms.

(2) Trustees ("Trustees-at-large") approved by members according to such procedures, not inconsistent with these Bylaws, as the Trustees shall have determined. Except as provided below, such Trustees-at-large shall be divided into four classes of *four,* one class to be elected each year to serve for a term of four years. Such classes shall be designated by the year of expiration of their respective terms. It is contemplated that, unless otherwise determined by the Trustees for good reason, Trustees-at-large, shall be individuals who have not been considered for election as Corporate Trustees.

(3) Trustees ex officio, who shall be the Chairman, the President, the Director, the Treasurer, and the Clerk.

(4) Trustees emeriti, who shall include any Member who has attained the age of seventy years (or the age of sixty-five and has retired from his home institution) and who has served a full elected term as a regular Trustee, provided he signifies his wish to serve the Laboratory in that capacity. Any Trustee who qualifies for emeritus status shall continue to serve as a regular Trustee until the next Annual Meeting whereupon his office as regular Trustee shall become vacant and be filled by election by the Members or by the Board, as the case may be. The Trustees ex officio and emeriti shall have all the rights of the Trustees, except that Trustees emeriti shall not have the right to vote.

(B) The aggregate number of Corporate Trustees and Trustees-at-large elected in any year (excluding Trustees elected to fill vacancies which do not result from expiration of a term) shall not exceed ten. The number of Trustees-at-large so elected shall not exceed four and unless otherwise determined by vote of the Trustees, the number of Corporate Trustees so elected shall not exceed six. Corporate Trustees shall always constitute a majority on the Board of those elected or approved by the Corporation.

(C) The Trustees and Officers shall hold their respective offices until their successors are chosen in their stead.

(D) Any Trustee may be removed from office at any time with or without cause, by vote of a majority of the Members

entitled to vote in the election of Trustees; or for cause, by vote of two-thirds of the Trustees then in office. A Trustee may be removed for cause only if notice of such action shall have been given to all of the Trustees or Members entitled to vote, as the case may be, prior to the meeting at which such action is to be taken and if the Trustee so to be removed shall have been given reasonable notice and opportunity to be heard before the body proposing to remove him.

(E) Any vacancy in the number of Trustees, however arising, may be filled by the Trustees then in office unless and until filled by the Members at the next Annual Meeting.

(F) A Corporate Trustee or a Trustee-at-large who has served an initial term of at least two years duration shall be eligible for re-election to a second term, but shall be ineligible for re-election to any subsequent term until two years have elapsed after he last served as Trustee.

IX. (A) The Trustees shall have the control and management of the affairs of the Corporation. They shall elect a Chairman of the Board of Trustees who shall be elected annually and shall serve until his successor is selected and qualified and who shall also preside at meetings of the Corporation. They shall elect a President of the Corporation who shall also be the Vice Chairman of the Board of Trustees and Vice Chairman of meetings of the Corporation, and who shall be elected annually and shall serve until his successor is selected and qualified. They shall annually elect a Treasurer who shall serve until his successor is selected and qualified. They shall elect a Clerk (a resident of Massachusetts) who shall serve for a term of four years. Eligibility for re-election shall be in accordance with the content of Article VIII(F) as applied to corporate or Board Trustees. They shall elect Board Trustees as described in Article VIII(B). They shall appoint a Director of the Laboratory for a term not to exceed five years, provided the term shall not exceed one year if the candidate has attained the age of 65 years prior to the date of the appointment. They may choose such other officers and agents as they may think best. They may fix the compensation and define the duties of all the officers and agents of the Corporation and may remove them at any time. They may fill vacancies occurring in any of the offices. The Board of Trustees shall have the power to choose an Executive Committee from their own number as provided in Article X, and to delegate to such Committee such of their own number as provided in Article X, and to delegate to such Committee such of their own powers as they may deem expedient in addition to those powers conferred by Article X. They shall from time to time elect Members to the Corporation upon such terms and conditions as they shall have determined, not inconsistent with law or these Bylaws.

(B) The Board of Trustees shall also have the power, by vote of a majority of the Trustees then in Office, to elect an Investment Committee and any other committee and, by like vote, to delegate thereto some or all of their powers except those which by law, the Articles of Organization or these Bylaws they are prohibited from delegating. The members of any such committee shall have tenure and duties as the Trustees shall determine; provided that the Investment Committee, which shall oversee the management of the Corporation's endowment funds and marketable securities, shall include the Chairman of the Board of Trustees, the Treasurer of the Corporation, and the Chairman of the Corporation's Budget Committee, as ex officio members, together with such Trustees as may be required for not less than two-thirds of the Investment Committee to consist of Trustees. Except as otherwise provided by these Bylaws or determined by the Trustees, any such committee may make rules for the conduct of its business; but, unless otherwise provided by the Trustees or in such rules, its business shall be conducted as nearly as possible in the same manner as is provided by these Bylaws for the Trustees.

X. (A) The Executive Committee is hereby designated to consist of not more than ten members, including the ex officio Members (Chairman of the Board of Trustees, President, Director and Treasurer); and six additional Trustees, two of whom shall be elected by the Board of Trustees each year, to serve for a three-year term. Beginning with the members elected for terms ending in 1990, one of the Trustees elected to serve on the Executive Committee should be a Trustee-at-large. This procedure will be repeated in the class of 1991, and henceforth the Trustees will elect to the Executive Committee Trustees to ensure that the composition of the Committee is four Corporate Trustees and two Trustees-at-large.

(B) The Chairman of the Board of Trustees shall act as Chairman of the Executive Committee, and the President as Vice Chairman. A majority of the members of the Executive Committee shall constitute a quorum and the affirmative vote of a majority of those voting at any meeting at which a quorum is present shall constitute action on behalf of the Executive Committee. The Executive Committee shall meet at such times and places and upon such notice and appoint such subcommittees as the Committee shall determine.

(C) The Executive Committee shall have and may exercise all the powers of the Board during the intervals between meetings of the Board of Trustees except those powers specifically withheld from time to time by vote of the Board or by law. The Executive Committee may also appoint such committees, including persons who are not Trustees, as it may from time to time approve to make recommendations with respect to matters to be acted upon by the Executive Committee or the Board of Trustees.

(D) The Executive Committee shall keep appropriate minutes of its meetings and its action shall be reported to the Board of Trustees.

(E) The elected Members of the Executive Committee shall constitute a standing "Committee for the Nomination of Officers," responsible for making nominations, at each Annual Meeting of the Corporation, and of the Board of Trustees, for candidates to fill each office as the respective terms of office expire (Chairman of the Board, President, Director, Treasurer, and Clerk).

XI. A majority of the Trustees, the Executive Committee, or any other committee elected by the Trustees shall constitute a quorum; and a lesser number than a quorum may adjourn any meeting from time to time without further notice. At any meeting of the Trustees, the Executive Committee, or any other

committee elected by the Trustees, the vote of a majority of those present, or such different vote as may be specified by law, the Articles of Organization or these Bylaws, shall be sufficient to take any action.

XII. Any action required or permitted to be taken at any meeting of the Trustees, the Executive Committee or any other committee elected by the Trustees as referred to under Article IX may be taken without a meeting if all of the Trustees or members of such committee, as the case may be, consent to the action in writing and such written consents are filed with the records of meetings. The Trustees or members of the Executive Committee or any other committee appointed by the Trustees may also participate in meeting by means of conference telephone, or otherwise take action in such a manner as may from time to time be permitted by law.

XIII. The consent of every Trustee shall be necessary to dissolution of the Marine Biological Laboratory. In case of dissolution, the property shall be disposed of in such a manner and upon such terms as shall be determined by the affirmative vote of two-thirds of the Board of Trustees then in office.

XIV. These Bylaws may be amended by the affirmative vote of the Members at any meeting, provided that notice of the substance of the proposed amendment is stated in the notice of such meeting. As authorized by the Articles of Organization, the Trustees, by a majority of their number then in office, may also make, amend, or repeal these Bylaws, in whole or in part, except with respect to (a) the provisions of these Bylaws governing (i) the removal of Trustees and (ii) the amendment of these Bylaws and (b) any provisions of these Bylaws which by law, the Articles of Organization or these Bylaws, requires action by the Members.

No later than the time of giving notice of the meeting of Members next following the making, amending or repealing by the Trustees of any Bylaw, notice thereof stating the substance of such change shall be given to all Corporation Members entitled to vote on amending the Bylaws.

Any Bylaw adopted by the Trustees may be amended or repealed by the Members entitled to vote on amending the Bylaws.

XV. The account of the Treasurer shall be audited annually by a certified public accountant.

XVI. Except as otherwise provided below, the Corporation shall, to the extent legally permissible, indemnify each person who is, or shall have been, a Trustee, director or officer of the Corporation or who is serving, or shall have served, at the request of the Corporation as a Trustee, director or officer of another organization in which the Corporation directly or indirectly has any interest, as a shareholder, creditor or otherwise, against all liabilities and expenses (including judgments, fines, penalties and reasonable attorneys' fees and all amounts paid, other than to the Corporation or such other organization, in compromise or settlement) imposed upon or incurred by any such person in connection with, or arising out of, the defense or disposition of any action, suit or other proceeding, whether civil or criminal, in which he or she may be a defendant or with which he or she may be threatened or otherwise involved, directly or indirectly, by reason of his or her being or having been such a Trustee, director or officer.

The Corporation shall provide no indemnification with respect to any matter as to which any such Trustee, director or officer shall be finally adjudicated in such action, suit or proceeding not to have acted in good faith in the reasonable belief that his or her action was in the best interests of the Corporation. The Corporation shall provide no indemnification with respect to any matter settled or compromised, pursuant to a consent decree or otherwise, unless such settlement or compromise shall have been approved as in the best interests of the Corporation, after notice that indemnification is involved, by (i) a disinterested majority of the Board of Trustees or of the Executive Committee or, (ii) a majority of the Corporation's Members.

Indemnification may include payment by the Corporation of expenses in defending a civil or criminal action or proceeding in advance of the final disposition of such action or proceeding upon receipt of an undertaking by the person indemnified to repay such payment if it is ultimately determined that such person is not entitled to indemnification under the provisions of this Article XVI, or under any applicable law.

As used in this Article, the terms "Trustee," "director" and "officer" include their respective heirs, executors, administrators and legal representatives, and an "interested" Trustee, director or officer is one against whom in such capacity the proceeding in question or another proceeding on the same or similar grounds is then pending.

To assure indemnification under this Article of all persons who are determined by the Corporation or otherwise to be or to have been "fiduciaries" of any employee benefit plan of the Corporation which may exist from time to time, this Article shall be interpreted as follows: (i) "another organization" shall be deemed to include such an employee benefit plan, including without limitation, any plan of the Corporation which is governed by the Act of Congress entitled "Employee Retirement Income Security Act of 1974," as amended from time to time ("ERISA"); (ii) "Trustee" shall be deemed to include any person requested by the Corporation to serve as such for an employee benefit plan where the performance by such person of his or her duties to the Corporation also imposes duties on, or otherwise involves services by, such person to the plan or participants or beneficiaries of the plan; (iii) "fines" shall be deemed to include any excise taxes assessed on a person with respect to an employee benefit plan pursuant to ERISA; and (iv) actions taken or omitted by a person with respect to an employee benefit plan in the performance of such person's duties for a purpose reasonably believed by such person to be in the interest of the participants and beneficiaries of the plan shall be deemed to be for a purpose which is in the best interests of the Corporation.

The right of indemnification provided in this Article shall not be exclusive of or affect any other rights to which any Trustee, director or officer may be entitled under any agreement, statute, vote of members or otherwise. The Corpora-

tion's obligation to provide indemnification under this Article shall be offset to the extent of any other source of indemnification or any otherwise applicable insurance coverage under a policy maintained by the Corporation or any other person. Nothing contained in this Article shall affect any rights to which employees and corporate personnel other than Trustees, directors or officers may be entitled by contract, by vote of the Board of Trustees or of the Executive Committee or otherwise.

VI. Report of the Director

Standing the Test of Experience

As the development of an organism can only be understood from the standpoint of genetic continuity, . . . *so the development of the Laboratory, if it is to be fairly understood, must be examined, not in the light of what may transpire in a week or even a whole session, but in the light of its continuous history. Each session may be regarded as a developmental phase, as the promise of the germinal inception unfolded to the extent determined by all the cooperating factors. But each phase or stage is the fulfilment of all that have gone before and the prophecy of all that are to follow.*

In order to know whether we have fulfilled well or ill, we must go back to the germ in its first stage, and see what promise it contained and what general policy and means were proposed for the fulfilment. If we have pursued one purpose and one method from the beginning, we ought now to be in a position to see whether theory has stood the test of experience.

—C. O. Whitman, Eighth Annual Report, 1895, p. 18

The centennial anniversary of an institution is an appropriate occasion for looking back—and an equally appropriate occasion for looking around and looking forward.

In the years leading up to the Marine Biological Laboratory's centennial, historians have examined this embryonic organism—its origins and its early developmental phases. Historians and philosophers, within the corporation and without, have asked what has happened at the MBL, and what role the laboratory has played in spurring the remarkable growth of American biology. (Some of the best of those studies are available in a special issue of *The Biological Bulletin*, vol 168, no 3.)

While the historians have been looking back, other members of the MBL community have been taking a careful look around, asking what the laboratory is today, and forward, asking what role it will play in the next decades of American biology—and enterprise several orders of magnitude larger and vastly more complex than it was in C. O. Whitman's time. An *ad hoc* Committee on Long Range Goals spent two years taking a hard look forward, and submitted its report on the laboratory's future to the corporation in June of 1987.

In the second half of the laboratory's one-hundredth year, we have been working to draw together into one workable plan all the ideas inspired by the approach of the centennial year. Well-acquainted now with the laboratory's illustrious and unusual history, we are confident that the experiences of the past 100 years show us the way forward. Thus, although the centennial celebration has just begun, the centennial self-examination has already shown us where the laboratory must go in the next decade—if it is to continue to make important contributions to the national biological research effort.

Clearly, the MBL's unparalleled summer programs of teaching and research must remain the laboratory's *raison d'être*. Just as clearly, we must redouble our efforts to apply the most modern biological approaches in our summer courses and in our research programs.

We must continue to provide tutorial laboratory courses at the cutting edge of science. For nearly a century now, MBL summer courses have attracted faculty and students from the best institutions in the world. Taken together, the MBL summer courses represent a collection of scientific talent that cannot be duplicated at any one university. To ensure the continued health of these one-of-a-kind courses, we must seek over the next decade an educational endowment fund that will cover course expenses not covered by tuition or grants.

To sustain and improve our present research technologies and to provide a stable base for summer programs, we will have to encourage new year-round research programs in areas of traditional MBL strength. The new programs will supplement the important existing programs and create a critical mass of year-round investigators in neurobiology, cell biology, and developmental biology. We should build strong year-round programs in microbiology and in molecular genetics, molecular evolution, and other areas of research that employ the tools and techniques of modern molecular biology. And of course we must maintain the strong and still-expanding year-round Ecosystems Center.

We must continue to capitalize on marine organisms as models for the study of human diseases. As we've known for some time now, we will have to develop new facilities and expertise for cultivating, rearing, and studying the many marine animals that are so critical to biomedical research. And to complement modern molecular approaches, we will need an updated and modernized facility for warm-blooded animals.

While we look to expand our year-round programs and modernize our research facilities, we must continue to nourish our traditional programs and resources. We will maintain our relationship with the Boston University Marine Program, an association that supports traditional areas of MBL research, provides us with another window on environmental science, and ensures a continuous tie to academia. And having completed a $2.5 mil-

lion library endowment campaign in 1987, we've already begun to look for ways to modernize and strengthen this renowned biological science resource.

The demands of modern biological research and teaching are great—and accelerating. To meet those demands, to take the laboratory where it must go in the exciting decade of biology that lies immediately ahead, we have accelerated greatly our development efforts in 1987. We have asked those who have supported us in the past to maintain their support and to increase it where possible, and we have worked very hard to identify sources of support beyond the core of foundations and friends who have historically been so generous and loyal to the MBL.

To support the new development efforts, we have made an effort to improve communications—with the trustees who run the laboratory, with the individuals and foundations who support the laboratory, and with the many individuals and institutions who are potential supporters. The emphasis on communications has inspired two new publications: a monthly newsletter (*MBL Update*) from the director to the trustees and an annual development report (this year titled *MBL 87*) to acknowledge and thank everyone who has supported the laboratory in the past year.

While we have tried to improve communications with our far-flung network of friends, we have tried simultaneously to improve routine communications within the laboratory. Associate Director Ray Epstein has instituted weekly meetings of the top management staff and monthly meetings of other staff members. The year-round scientists have begun meeting monthly to identify common problems and to search for solutions; those meetings, now formalized as the Forum for Year-Round Scientists, provide a way for the scientific staff to bring their concerns directly to the administrative staff who are responsible for the area of operation that needs attention. Also within the laboratory, the Employee Relations Committee has begun to publish a staff newsletter (*ERC News*).

If the years leading up to the Centennial have been a valuable period of self-examination for the MBL community, the centennial year of 1988 brings the opportunity to share our history and our aspirations with the world at large. Mindful of the many ways the centennial can contribute to the health of the laboratory, we have tried to shape a centennial that will be both celebratory and useful. We have encouraged activities that contribute to one or more of our centennial goals: to search our past for guidance about our future; to bring the story of our past and of our future before a new audience; to give our neighbors, on the Cape and across the country, a glimpse into a modern research laboratory; to raise public understanding of science by fostering sophisticated yet accessible discussions of science, science education, science communication, and science and public policy; and to mount scientific symposia and other scientific events that make an immediate contribution to the central activities of the laboratory—teaching and research in basic biology.

Having noted some of the directions the laboratory must move in the near future, I'd like to close this 100th director's report with an observation about continuity.

We know the MBL as the summer home of neurobiology, embryology, and cell biology; as the place where ideas are brought together, fertilized, and allowed to develop (with occasional interesting mutations); as an institution where whole areas of inquiry can take root quickly; as the training ground of the next generation of American biologists; and as the only major biological institution that recreates itself each year. These fond visions of the laboratory are reconfirmed every year by the scientists, students, scholars, writers, and others who come to the laboratory for the first time. But until you look closely at the historical record, (until you've viewed the laboratory in light of its continuous history, as Whitman suggested it must be viewed) you're apt to miss one of the outstanding features of this institution: throughout its one hundred seasons, through twelve directorships and many more institutional changes, the MBL has remained true to the course set by its original director, Charles Otis Whitman.

In the First Annual Report of 1888, Whitman outlined the essential design of the MBL in a few brief paragraphs:

> *The new Laboratory at Wood's Holl is nothing more, and, I trust, nothing less, than a first step towards the establishment of an ideal biological station, organized on a basis broad enough to represent all important features of the several types of laboratories hitherto known in Europe and America . . .*
>
> *The research department should furnish just the elements required for the organization of a thoroughly efficient department of instruction. Other things being equal, the investigator is always the best instructor. The highest grade of instruction in any science can only be furnished by one who is thoroughly imbued with the scientific spirit, and who is actually engaged in original work. Hence the propriety—and, I may say, the necessity—of linking the function of instruction with that of investigation . . . To limit the work of the Laboratory to teaching would be a most serious mistake; and to exclude teaching would shut out the possibilities of the highest development. The combination of the two functions in mutually stimulating relations is a feature of the Laboratory to be strongly commended.*
>
> —C. O. Whitman, First Annual Report, 1888, pp. 16–17

Reflecting on this statement seven years later, Whitman wrote, "Here [in the 1888 Report] we see sketched

the elemental basis of our germ-organization . . . The *aim* was a permanent biological station; the *function* was to be instruction and investigation; the *formative principle* relied upon was co-operation." (Eighth Annual Report, 1895, p. 19)

Taken together, these two passages provide a nearly complete index of features and functions (in the double sense of rules and roles) that shaped the early development of the laboratory, still guide its growth today, and will continue to do so into the future.

The essential principles of the laboratory are:

1. The MBL is equally devoted to investigation and instruction; and these are interdependent functions of the institution.
2. The MBL is independent, democratic, and national in character.
3. The MBL is cooperative in spirit and design.
4. The MBL is an institution for teaching and research in basic biology.
5. The MBL is unrestricted in biological scope.
6. The MBL fosters collaboration, interaction, and the exchange of ideas.
7. The MBL is equally dedicated to attracting top-flight investigators and training young scientists.
8. The organization and administration of the MBL is flexible and responsive to the need for change.

Throughout its first century, the laboratory has managed—sometimes against great odds—to remain true to this ambitious set of principles.

Our plans for the first decade of the laboratory's second century grow out of the recommendations of the forward-looking Committee on Long Range Goals. At the same time, our plans are perfectly in keeping with the principles that have served the MBL—and American biology—so well for 100 years.

The close of our first century finds us in a fortunate position. We have a proud and successful history. We have a good base on which to build. And we can look forward with a vision that was elucidated clearly in the laboratory's first decade and adhered to steadfastly ever after. I'm confident that over the next few years that vision will guide us into a future that is relentlessly bright.

VII. Report of the Treasurer

I want first to call your attention to the strength of the Laboratory's balance sheet at the end of 1987. Current assets exceeded current liabilities by almost $2,000,000 compared to about $760,000 at the end of 1986. This increase is due mainly to the generous five-year grant of $750,000 by the MacArthur Foundation in support of the Parasitology course, and a multi-year grant by the Mellon Foundation to the Ecosystems Center. Such long-term funding considerably improves the financial stability of the MBL and allows the Director to plan and optimize the scientific program of the Laboratory.

Another factor contributing to the increase in net current assets is the net growth of the repairs and replacement reserve by $61,401, even after acquisition of fixed assets and repayment of debt principal of $173,572. We are continuing to make progress towards our goal of funding depreciation expense from current operations. The need for such reserves is real, and it is underscored by the fact that in 1988 we have expended the balance available for housing repairs and replacements on renovations.

Endowed fund balances increased by approximately $475,000 in 1987 while quasi-endowment balances were down slightly. The former is due principally to the generous support of the library endowment by the Bay Foundation, which enabled us to meet the challenge of the Mellon Match Grant. In this roller-coaster year in the financial markets we have reason to be satisfied with our portfolio management. Net realized and unrealized losses amounted to approximately $60,000 on portfolios in excess of $10,000,000. We had lightened up on equities in advance of the crash, but I will admit to some concern about such a market decline in the year following my recommendation that we show investments at market value on the balance sheet. I hope you will agree that it is better to see clearly on the balance sheet "how we did" than having to dive into the footnotes to find out.

The statement of Support, Revenue, Expenses and Changes in Fund Balances shows how the Laboratory's operations fared this year. The Total Current Unrestricted Funds (Housing Enterprises) has an excess of revenue over expenses of $290,894, which is gratifying. I reiterate my statement of last year that this cannot be considered a "surplus" because it is before taking account of depreciation expenses. We were only able to contribute $32,274 to Repairs and Replacements from the Housing Enterprise Fund, which is of concern to the Executive Committee. A program is in place to restore the Housing budget to more robust financial health. We were able to set aside $145,701 for the Repairs and Replacement Reserve this year out of the current unrestricted fund, a great improvement over 1986.

The overall operating results of the Laboratory in 1987 were quite good, but there are some trends that merit attention and concern. For the third straight year total expenditures on research declined—from $4,048,000 in 1985 to $3,864,000 in 1987. That actually understates the amount by which year-round research at the Laboratory has decreased since a significant portion of the expenses of the departing NINCDS program have not been administered by the Laboratory and are therefore not in our accounts. The major financial effect of this shrinking

of the research base is to cause an increase in our overhead rates. While our proposed rate for 1988 is not high in comparison to other research institutions, the size of the increase in one year has placed a potential burden on our year-round scientists.

Recovery of indirect costs for the summer program declined slightly, from $525,000 in 1986 to $521,000 in 1987. While this is not a major amount, and is still significantly above 1985's total of $468,000, any decrease in revenues from the core of the Laboratory's program should alert us for causes and to look carefully at future prospects.

Operating expenses of support activities were relatively stable in 1987, but this stability masks the fact that during the transition between full-time directors some positions were not staffed, and under the new administration, some necessary positions have been added.

In 1988 we expect expenses to rise more rapidly than revenues, and your Executive Committee has approved a budget for 1988 with a deficit of revenues to expenses of $88,000. This budget received the most careful review by the Executive Committee—a substantial portion of its meetings from September through January were devoted to it. The decision to incur a deficit was based on the following factors: the need to maintain excellent support of science at the MBL, the soundness of the Laboratory's financial condition, and reasonable prospects of improved grant funding in the near term. We also felt that the longer term financial prospects of the Laboratory were bright and that any major retrenchment of expenditures might balance the budget in the short term but jeapordize the resources on which future growth depends.

The Executive Committee's deliberations on the budget were an exemplary exercise in financial review. Out of them came a commitment to continued funding of excellence in science and a renewed awareness that that is a difficult challenge. All of us enter this Second Century dedicated to the greatness of the Laboratory and committed to the effort of sustaining that distinction.

Coopers
&Lybrand

certified public accountants

To the Trustees of
Marine Biological Laboratory
Woods Hole, Massachusetts

We have examined the balance sheet of Marine Biological Laboratory as of December 31, 1987 and the related statement of support, revenues, expenses and changes in fund balances for the year then ended. Our examination was made in accordance with generally accepted auditing standards and, accordingly, included such tests of the accounting records and such other auditing procedures as we considered necessary in the circumstances. We previously examined and reported upon the financial statements of the Laboratory for the year ended December 31, 1986, which condensed statements are presented for comparative purposes only.

In our opinion, the financial statements referred to above present fairly the financial position of Marine Biological Laboratory at December 31, 1987 and its support, revenues, expenses and changes in fund balances for the year then ended, in conformity with generally accepted accounting principles applied on a basis consistent with that of the preceding year.

Coopers & Lybrand

Boston, Massachusetts
April 15, 1988

MARINE BIOLOGICAL LABORATORY

BALANCE SHEETS

December 31, 1987 and 1986

Assets	*1987*	*1986*
Cash and savings deposits	$ 531,705	$ 238,120
Money market securities (Notes B and H)	850,000	50,000
Accounts receivable, net of allowance for uncollectible accounts	586,776	425,840
Receivables due for costs incurred on grants and contracts	595,925	562,375
Other assets	19,199	8,663
Total current assets	2,583,605	1,284,998
Investments, at market (Notes B and H)	10,268,985	10,093,443
Land, buildings and equipment (Notes B and C)	19,304,410	19,193,896
Less accumulated depreciation	(7,707,689)	(7,143,565)
	11,596,721	12,050,331
Total assets	$24,449,311	$23,428,772

Liabilities and fund balances	*1987*	*1986*
Accounts payable and accrued expenses	$ 449,140	$ 333,859
Deferred income	92,800	117,282
Current portion of long-term debt	78,654	73,001
Total current liabilities	620,594	524,142
Mortgage and note payable (Note G)	1,185,315	1,249,182
Current unrestricted fund balances:		
Current unrestricted funds	84,572	55,890
Housing enterprise funds	—	—
	84,572	55,890
Current restricted fund balances:		
Unexpended grants	459,179	201,556
Unexpended gifts	1,113,768	457,699
Unexpended income of endowment funds	80,387	86,137
	1,653,334	745,392
Endowment fund balances:		
Income for unrestricted purposes	2,671,519	2,658,967
Income for restricted purposes	3,053,692	2,592,671
	5,725,211	5,251,638
Quasi-endowment fund balances:		
Unrestricted	792,538	826,455
Restricted	3,766,195	3,835,526
	4,558,733	4,661,981
Plant fund balances:		
Unrestricted	10,375,536	10,770,932
Repairs and replacement reserve	231,016	169,615
Restricted	15,000	—
	10,621,552	10,940,547
Total liabilities and fund balances	$24,449,311	$23,428,772

The accompanying notes are an integral part of the financial statements.

MARINE BIOLOGICAL LABORATORY

STATEMENT OF SUPPORT, REVENUES, EXPENSES AND CHANGES IN FUND BALANCES

for the year ended December 31, 1987
(with comparative totals for 1986)

	Current Funds								*Plant Funds*				
	Current Unrestricted Fund	*Housing Enterprises Fund*	*Total Current Unrestricted Fund*	*Current Restricted Fund*	*Endowment Funds*		*Quasi-endowment Funds*		*Unrestricted*	*Restricted*	*Repairs and Replacement Reserve*	*1987 Total All Funds*	*1986 Total All Funds*
					Unrestricted	*Restricted*	*Unrestricted*	*Restricted*					
Support and Revenues													
Grant reimbursement of direct costs:													
Instruction				$ 359,811								$ 359,811	$ 333,191
Research				3,653,808								3,653,808	3,327,603
Recovery of indirect costs related to research and instruction:													
Summer program	$ 521,338		$ 521,338									521,338	525,924
Year-round program	1,773,586		1,773,586									1,773,586	1,699,208
Other	23,769		23,769									23,769	32,107
Instruction	10,827		10,827									10,827	63,536
Tuition				320,495								320,495	287,415
Support activities													
Dormitory		$ 765,895	765,895									765,895	679,378
Dining hall	721,841		721,841									721,841	441,564
Library	207,857		207,857									207,857	240,315
Biological Bulletin	171,457		171,457									171,457	172,676
Research services	453,422		453,422									453,422	351,251
Marine resources	163,708		163,708									163,708	158,539
Other				95,684								95,684	500
Investment income	348,900		348,900	209,378								558,278	521,823
Gifts (Note I)	560,344		560,344	1,734,298		$ 446,032		$ 3,000		$15,000		2,758,674	1,899,099
Miscellaneous revenue	101,243		101,243									101,243	153,729
Total support and revenues	5,058,292	765,895	5,824,187	6,373,474		446,032		3,000		15,000		12,661,693	10,887,858

Expenses:													
Instruction				1,263,867								1,263,867	960,727
Research	43,426		43,426	3,821,113								3,864,539	3,960,219
Scholarships and stipends				200,067								200,067	194,397
Support activities:													
Dormitory		587,432	587,432									587,432	491,551
Dining hall	654,722		654,722									654,722	439,994
Library	509,577		509,577									509,577	528,103
Biological Bulletin	139,795		139,795									139,795	150,551
Research services	632,882		632,882									632,882	565,513
Marine resources	365,900		365,900									365,900	363,496
Administration	1,112,519	79,275	1,191,794									1,191,794	1,111,623
Sponsored projects administration	333,630		333,630									333,630	291,624
Plant operations	1,074,135		1,074,135								11,616	1,085,751	1,116,940
Depreciation									$ 564,124			564,124	563,911
Disposal									4,844			4,844	63,519
Other				215,994				3,926				219,920	180,765
Total expenses	4,866,586	666,707	5,533,293	5,501,041				3,926	568,968		11,616	11,618,844	10,982,933
Excess (deficit) of support and revenues over expenses	191,706	99,188	290,894	872,433		446,032		(926)	(568,968)	15,000	(11,616)	1,042,849	(95,075)
Transfers among funds:													
Acquisition of fixed assets									104,958		(104,958)	—	—
Repayment of debt		(68,614)	(68,614)						68,614			—	—
Mellon match transfer				(10,000)		10,000						—	—
Repairs and replacement	(145,701)	(32,274)	(177,975)								177,975	—	—
To support ecosystems operations				29,886				(29,886)				—	—
Other transfers	(17,323)	1,700	(15,623)	15,623								—	—
Total transfers among funds	(163,024)	(99,188)	(262,212)	35,509		10,000		(29,886)	173,572		73,017	—	—
Realized gains on investments					$ 187,328	108,668	$ 30,536	324,255				650,787	527,606
Unrealized gains (loss) on investment					(174,776)	(103,679)	(64,453)	(362,774)				(705,682)	335,815
Total gain (loss) on investments					12,552	4,989	(33,917)	(38,519)				(54,895)	863,421
Net change in fund balances	28,682		28,682	907,942	12,552	461,021	(33,917)	(69,331)	(395,396)	15,000	61,401	987,954	768,346
Fund balances, beginning of year	55,890		55,890	745,392	2,658,967	2,592,671	826,455	3,835,526	10,770,932		169,615	21,655,448	20,887,102
Fund balances, end of year	$ 84,572		$ 84,572	$1,653,334	$2,671,519	$3,053,692	$792,538	$3,766,195	$10,375,536	$15,000	$231,016	$22,643,402	$21,655,448

The accompanying notes are an integral part of the financial statements.

Notes to Financial Statements

A. *Purpose of the Laboratory*

The purpose of Marine Biological Laboratory (the "Laboratory") is to establish and maintain a laboratory or station for scientific study and investigations, and a school for instruction in biology and nature history.

B. *Significant Accounting Policies*

Basis of Presentation—Fund Accounting

In order to ensure observance of limitations and restrictions placed on the use of resources available to the Laboratory, the accounts of the Laboratory are maintained in accordance with the principles of "fund accounting." This is the procedure by which resources are classified into separate funds in accordance with specified activities or objectives.

Externally restricted funds may only be utilized in accordance with the purposes established by the donor or grantor of such funds. However, the Laboratory retains full control over the utilization of unrestricted funds. Restricted gifts, grants, and other restricted resources are accounted for in the appropriate restricted funds. Restricted current funds are reported as revenue when received and as related costs are incurred.

Endowment funds are subject to restrictions requiring that the principal be invested with income available for use for restricted or unrestricted purposes by the Laboratory. Quasi-endowment funds have been established by the Laboratory for the same purposes as endowment funds; however, the principal of these funds may be expended for various restricted and unrestricted purposes.

Fixed Assets

Fixed assets are recorded at cost. Depreciation is computed using the straight-line method over estimated useful lives of fixed assets.

Reclassifications

The financial statements for 1987 reflect certain changes in classification of revenue and expenses. Similar reclassifications have been made to amounts previously reported in order to provide consistency of the financial statements.

Contracts and Grants

Revenues associated with contracts and grants are recognized in the statement of support, revenues, expenses and changes in fund balances when received and as related costs are incurred. The Laboratory reimbursement of indirect costs relating to government contracts and grants is based on negotiated indirect cost rates with adjustments for actual indirect costs in future years. Any over or underrecovery of indirect costs is recognized through future adjustments of indirect cost rates.

Investments

Investments purchased by the Laboratory are carried at market value. Money market securities are carried at cost which approximates market value. Investments donated to the Laboratory are carried at fair market value at the date of the gift. For determination of gain or loss upon disposal of investments, cost is determined based on the average cost method

The Laboratory is the beneficiary of certain endowment investments which are held in trust by others. These investments are reflected in the financial statements. Every ten years the Laboratory's status as beneficiary is reviewed to determine that the Laboratory's use of these funds is in accordance with the intent of the funds. The market value of these investments are $3,334,500 and $3,333,054 at December 31, 1987 and 1986.

Investment Income and Distribution

The Laboratory follows the accrual basis of accounting except that investment income is recorded on a cash basis. The difference between such basis and the accrual basis does not have a material effect on the determination of investment income earned on a year-to-year basis. Investment income includes income from the investments of specific funds and from the pooled investment account. Income from the pooled investment account is distributed to the participating funds on the basis of their proportionate share at market value adjusted for any addition or disposals to pooled funds.

C. *Land, Buildings, and Equipment*

The following is a summary of the unrestricted plant fund assets:

	1987	*1986*
Land	$ 689,660	$ 689,660
Buildings	16,385,099	16,333,358
Equipment	2,229,651	2,170,878
	19,304,410	19,193,896
Less accumulated depreciation	(7,707,689)	(7,143,565)
	$11,596,721	$12,050,331

D. *Retirement Fund*

The Laboratory has a noncontributory defined benefit pension plan for substantially all employees. Contributions are intended to provide for benefits attributed to the service date, but also those expected to be earned in the future.

Actuarial present value of accumulated benefit obligation including vested benefits of $1,514,493 as of January 1, 1987	$1,566,992
Projected benefit obligation	2,328,190
Plan assets at fair value	2,371,245
Projected benefit obligation less than plan assets	43,055
Unrecognized net (gain) or loss	68,948
Prior service cost not yet recognized in net periodic pension cost	—
Unrecognized net obligation at December 31, 1987	(293,525)
Prepaid pension cost (pension liability) recognized in the statement of financial position	$ (181,522)
Net pension cost for fiscal year ending December 31, 1987:	
Service cost—benefits earned during the period	172,293
Interest cost on projected benefit obligation	157,845
Actual return on plan assets	600
Net amortization and deferral	(231,898)
Net periodic pension cost	$ 98,840

The actuarial present value of the projected benefit obligation was determined using a discount rate of 6.5% and rates of increase in compensation levels of 6%. The expected long-term rate of return on assets was 8%.

In addition, the Laboratory participates in the defined contribution pension program of the Teachers Insurance and Annuity Association. Expenses amounted to $103,386 in 1987 and $106,535 in 1986.

E. *Pledges and Grants:*

As of December 31, 1987 and 1986, the following amounts remain to be received on gifts and grants for specific research and instruction programs, and are expected to be received as follows:

	December 31, 1987		*December 31, 1986*	
	Unrestricted	*Restricted*	*Unrestricted*	*Restricted*
1988	$10,000	$ 951,400	$10,000	$40,764
1989	—	596,000	—	5,764
1990	—	250,000	—	—
	$10,000	$1,797,400	$10,000	$46,528

F. *Interfund Borrowings:*

Interfund balances at December 31 are as follows:

Current Funds	*1987*	*1986*
Due from plant funds	$ 3,240	$ 76,275
Due to restricted endowment fund	(120,875)	(115,909)
Due to restricted quasi-endowment funds	(3,000)	(200,750)
Due from current restricted fund	64,318	64,318
	$ (56,317)	$(176,066)

G. *Mortgages and Notes Payable.*

The mortgage note payable with a term of 26 years is in the amount of $1.3 million bearing interest based on the bank's prime rate plus three quarters percent (.75%) on a floating basis for the initial five year period with a floor of 7.50% and a ceiling of 13.00%. The interest rate at December 31, 1987 was 9.75%. The mortgage loan is collateralized by a first mortgage on the land and properties known as Memorial Circle, with recourse in the event of default limited to this land and property and the related revenue. Monthly principal and interest payments of $15,000 commenced January 19, 1987.

Other notes payable consist of the following:

Unsecured note with interest at 7.90% with monthly principal and interest payments of $221.20	$ 7,048
Unsecured note with interest at 6.90% with monthly principal and interest payments of $394.71	8,901
	$15,949

At December 31, 1987, these mortgages and notes payable had aggregate future annual principal payments as follows:

	Amount
1988	$ 78,654
1989	83,899
1990	86,492
1991	94,127
1992	102,957
Thereafter	817,840
	1,263,969
Less current portion	78,654
	$1,185,315

H. *Investments*

The following is a summary of the cost and market value of investments at December 31, 1987 and 1986 and the related investment and distribution of investment income for the years ended December 31, 1987 and 1986.

	Cost		*Market*		*Investment Income*	
	1987	*1986*	*1987*	*1986*	*1987*	*1986*
Endowment and Quasi-endowment						
U.S. Government securities	$1,299,763	$2,278,843	$1,270,857	$ 2,384,842	$218,919	$240,056
Corporate fixed income	2,136,500	947,287	2,134,363	933,749	104,583	85,871
Common stocks	4,088,042	4,069,893	5,545,523	6,101,973	204,776	178,837
Preferred stock	9,611	9,611	14,973	17,975	1,019	3,214
Money market securities	1,292,097	639,155	1,287,520	639,155	42,911	29,667
Real estate	15,749	15,749	15,749	15,749	—	—
Total	8,841,762	7,960,538	10,268,985	10,093,443	572,208	537,645
Less custodian fees					(54,290)	(51,646)
					517,918	485,999
Unrestricted Current Fund						
Money market securities	850,000	50,000	850,000	50,000	40,360	35,824
Total investments	$9,691,762	$8,010,538	$11,118,985	$10,143,443	$558,278	$521,823

I. *Gift Support for Instructions.*

Unrestricted Gifts includes $314,309 of gifts for the support of the Laboratory's instruction program available for indirect costs attributable to the instruction program.

VIII. Report of the Librarian

"A man will turn over half a library to write one book"—if so, scientists throughout the world, including 34 Nobel Prize winners, have "turned over" the MBL Library an amazing number of times in the past 100 years. When established in 1888, Dr. Whitman, the laboratory's first Director, stated in his first report:

> *A library is a necessity in such a laboratory. Boston libraries are near enough to be of great service, but we cannot depend on them alone. In addition to textbooks and standard works, we MUST have, at a minimum to begin with, all the important journals now printed in the four principal languages. It is most earnestly to be hoped that adequate means may be found to meet this all-important requisite.*

Today, one hundred years later, the library has 5000 separate titles of scientific journals, printed in 30 languages, bound in 165,000 volumes. Somehow, over the years "adequate means" have been found to expand the collection to its present size and to keep it available to the scientific community on a 24-hour basis. In 1888 an "invaluable addition" of a $1,000 gift gave the journal collection its beginning ("owing to Mrs. Glendower Evans liberality"); in 1988 the completion of an endowment gift of $2.5 million ensures its future.

Until 1902 the library depended entirely on donations for books and subscription costs. The 1902 treasurer's report lists the first library expense—$9.29. The Laboratory did not commit real funds until 1905 when Cornelia Clapp served as librarian during the summer months. In 1913 it was recommended that a trained assistant be hired to carry on throughout the year "a systematic campaign to develop the library since the peculiarly free methods used in this library with free access to the shelves demand constant study to take account of losses, repairs and disarrangements."

In 1919 Priscilla B. Montgomery was hired as a year-round Assistant Librarian. The following year the Dewey Decimal Classification system was introduced "after careful consideration of the various schemes in general use—it seems to be the one most familiar to biologists."

The main part of the Lillie building was completed in 1924, and a major portion of it was devoted to the Library, which consisted of five floors of stacks and a large reading room with serial racks along the walls. Three hundred and seventy-eight titles were received at the time. Deborah Lawrence was hired as secretary, and the three staff salaries totaled $5,650 for the year.

In 1929 The General Education Fund gave $50,000 for the purchase of back sets, serials, and books, and the following year the Director of the newly founded Woods Hole Oceanographic Institution donated $5,000 for the purchase of oceanographic books and journals. Ten years later a gift from the Rockefeller Foundation of $110,000 made the addition of the library wing possible. MBL was asked to raise from other sources an additional $25,000 to fill gaps in the journal collection (back sets). The addition cost less than planned, and the extra money was spent "to rebuild the Eel Pond wall, install a book-lift in the stacks, pave the parking lot, and re-grade the lawn around Lillie." The basement floor of the new library wing would house "temporarily, apparatus for sterilizing glassware and distilling water."

A $25,000 gift was received in 1941 from Carnegie for purchase of foreign journals whenever the market opened again in Europe. Library purchases were limited to the United States and England throughout the war years, although subscriptions were continued for German, French, and Russian publications. They were stored in a Scandinavian country, and by 1947 most had been received by the MBL Library.

Mrs. Montgomery retired in 1947, and Deborah Lawrence was named Librarian. In 1952 WHOI contributed $1,200 annually for their books and journals. In 1956 the reprint collection passed the 200,000 mark, and the first Xerox machine appeared in 1963. The first major physical changes since 1940 were made in 1964, the year Jane Fessenden was named librarian. Tile flooring was placed on all five stacks, and fluorescent lighting was added in the stacks, reading rooms, and offices. Reserve desks received locked cabinets and new lights, and four labs were renovated into library offices. A xerox room and a Rare Book Room were also added to the office area. In 1966 the book collection was recataloged from the Dewey system to Library of Congress. Fifteen thousand books changed numbers and positions on the shelves, confusing most of the users. Twelve private carrels were added on the third floor.

By 1970, WHOI was contributing $15,000 annually and in 1971 the reprints were moved to the basement stack and further collection of reprints ended. The collection numbered 250,000 when moved. At the same time, the entire journal collection was moved to cover four stacks instead of three and, we changed the arrangement of titles by dropping the articles "the, les, des," etc.

The book collection expanded in 1971 when the MBL Associates gave their annual gift to the Library—$10,500. The following year they donated another $6,000 which was also added to the growth of the book collection. At the same time WHOI added $25,000 specifically for books. Space was not available in the existing book section, therefore Room 306 on the third floor (the equivalent of three laboratories) was renovated for library stacks. Books on ocean engineering, physics, mathematics, and marine policy were shelved there.

In 1975 the first annual meeting of the East Coast Marine Science Librarians was held in Woods Hole; 49 librarians representing 25 institutions met to discuss areas of mutual cooperation. Today membership numbers 140, representing 120 institutions. That same year H. M.

Hirohito, Emperor of Japan, came to Woods Hole and spent an hour in the library catalog room. All offices, reading rooms, and hallways were painted for the occasion.

The library budget was increasing rapidly, and a number of proposals were made to further involve the Woods Hole Oceanographic. One proposal, submitted to the members of the Corporation in 1976, recommended the creation of a separate corporation for the library, supported by both MBL and WHOI and governed by a separate Board of Trustees. This met with such opposition from the members that the annual meeting was re-convened three times before final adjournment. Not until 1979 was an agreement finally reached. It was a cost sharing plan in which both institutions share certain activities of the library on a 50–50 basis. That agreement is still in effect today. That same year the R. K. Mellon Foundation gave $450,000 for the renovation of the Lillie building. The library was included in that renovation. Demolition and construction began by 1982. The library now covers about one-half of the Lillie building; eleven laboratories were torn down and an area of the third floor, over the present library space, was converted to stack space for the entire book collection. All five floors of existing stacks now house the journal collection, and the Rare Books and Archives occupy three rooms on the first floor.

In 1983 we initiated a User Survey. This involved recording the use of every journal for a nine month period. We found, in brief, that 53% of the 4765 titles were used during this period and 76% involved the years 1980–1983. In 1985, after years of discussions, the National Marine Fisheries Service in Woods Hole placed their library collection in the MBL Library, thus making the MBL Library the main library for all four institutions in Woods Hole. The scientists at the Fisheries have been using the library since the founding of the laboratory. The minutes of 1889 record that the Fisheries contributed both books and pamphlets to the original collection compiled that first summer of 1888.

The uniqueness of this library lies in the fact that for 100 years scientists—members of the MBL Corporation— have owned it. It has always been run by, and for, the scientists. Hopefully, it always will be. Stephen Jay Gould, in the preface of his book, "Ontogeny and Phylogeny" referred to the library as:

> *". . . an institution that has its own humanity and seems to me more an organism than a place—the Library of the Marine Biological Laboratory at Woods Hole. Where else would an idiosyncratic worker like me find a library open all the time, free from the rules and bureaucracy that stifle scholarship and 'protect' books only by guarding them from use. It is an anomaly in a suspicious and anonymous age. May it survive as it is, despite all the improbabilities."*

IX. Educational Programs

Summer

BIOLOGY OF PARASITISM

Course directors

Englund, Paul T., Johns Hopkins University School of Medicine
Sher, Alan, NIAID/NIH

Other faculty, staff, and lecturers

Beverley, Stephen, Harvard University School of Medicine
Bloom, Barry, Albert Einstein College of Medicine of Yashiva University
Boothroyd, John, Stanford University Medical School
Burakoff, Steven J., Harvard University School of Medicine
Burns, James M., Jr., Hahnemann Medical College & Hospital
Butterworth, Anthony, University of Cambridge, UK
Cerami, Anthony, Rockefeller University
Coffman, Robert, DNAX, Research Institute of Molecular & Cellular Biology
Doering, Tamara L., Johns Hopkins University School of Medicine
Donelson, John, University of Iowa
Dvorak, James, NIAID/NIH
Dwyer, Dennis, NIAID/NIH
Farley, Patrick J., Hamilton College
Germain, Ronald, NIAID/NIH
Glaven, Judy, George Washington University
Hart, Gerald W., Johns Hopkins University School of Medicine
Henkle, Kim, University of Iowa
Hereld, Dale, Johns Hopkins University School of Medicine
Joiner, Keith, NIAID/NIH
Kumar, Nirbhay, Johns Hopkins University School of Hygiene & Public Health
Long, Carole A., Hahnemann Medical College & Hospital
Maizels, Richard, Imperial College of Science and Technology, London, UK
Martinez-Palomo, Adolfo, National Polytechnical Institute, Mexico
Miller, Louis, NIAID/NIH
Modi, Govind, Yale University School of Public Health
Nelson, George, Liverpool School of Tropical Medicine, UK
Nussenzweig, Victor, New York University Medical Center
Nutman, Thomas, NIAID/NIH
Pearce, Edward J., NIAID/NIH
Pedersen, Peter, Johns Hopkins University School of Medicine

Pereira, Miercio, Tufts University School of Medicine
Pfefferkorn, Elmer, Dartmouth College Medical School
Quinn, Thomas, NIH/Johns Hopkins University
Sacks, David, NIAID/NIH
Scott, Phillip, NIAID/NIH
Shapiro, Terry, Johns Hopkins University School of Medicine
Shevach, Ethan, NIAID/NIH
Smith, Cassandra, Columbia University
Sollner-Webb, Barbara, Johns Hopkins University School of Medicine
Spielman, Andrew, Harvard School of Public Health
Turner, Mervyn J., Merck, Sharp & Dohme Research Laboratory
Walters, Laurel, Yale University School of Public Health
Wang, Ching C., University of California, School of Pharmacy, San Francisco
Wang, Charlotte, University of California, Berkeley
Ward, Samuel, Carnegie Institution of Washington
Warren, Kenneth S., The Rockefeller Foundation
Wassom, Donald L., University of Wisconsin School of Veterinary Medicine
Wellems, Thomas E., NIAID/NIH
Young, Richard, Massachusetts Institute of Technology

Students

Acosta-Gio, Enrique A., National University of Mexico, Mexico
Alvarez, Raquel M., Jewish Hospital of St. Louis
Aslund, Lena A., Uppsala University, Sweden
Barry, Wendy C., International Lab. for Research on Animal Diseases, Kenya
Cerami, Carla J., Columbia University
Gordon, Dalia L., University of Washington
Herwaldt, Barbara L., Washington University School of Medicine
Karam, Marc V., Onchocerciasis Control Programme in W. Africa, W. Africa
Klinkert, Mo Q., University of Heidelberg, FRG
Mani, Sridhar, City College, CUNY
Prioli, Reginaldo P., Tufts University School of Medicine
Rossi, Cesare, California Institute of Technology
Sherman, David R., Vanderbilt University
Sjolander, Anders J., University of Stockholm, Sweden
Slatter, Andrew F. G., Oxford University, UK
Tendler, Miriam, Oswaldo Cruz Institute, Brazil

EMBRYOLOGY: A COURSE IN MODERN DEVELOPMENTAL BIOLOGY

Course directors

Brandhorst, Bruce, McGill University, Canada
Jeffery, William, University of Texas, Austin

Other faculty, staff, and lecturers

Assman, Sally, University of Connecticut
Bates, William R., Kyoto University, Japan
Beach, Rebecca, University of Texas, Austin
Bloom, Theodora, Cambridge University, UK
Burdsal, Carol, Duke University
Chambers, Edward L., University of Miami
Cheng, Andrew, NIAID/NIH
Colman, Alan, University of Warwick, UK
Crowther, Robert, Marine Biological Laboratory
Elinson, Richard, University of Toronto, Canada
Etkin, Larry, M. D. Anderson Hospital and Tumor Institute
Ford, Christopher, Sussex University, UK
Gimlich, Robert, M. D. Anderson Hospital and Tumor Institute
Grainger, Robert, University of Virginia
Gurdon, John, Cambridge University, UK
Humphreys, Tom, University of Hawaii
Hunt, Tim, Cambridge University, UK
Iwao, Yasuhiro, Yamaguchi University, Japan
Jaffe, Laurinda, University of Connecticut Health Center
Jaffe, Lionel, Marine Biological Laboratory
Kado, Raymond T., C. N. R. S., France
Kitajima, Takashi, University of California, Berkeley
Kline, Douglas, University of Connecticut Health Center
Koenig, Gerd, Max Planck Institute, FRG
Krieg, Paul, University of Adelaide, Australia
Longo, Frank, University of Iowa
Lorraine, Anne, University of Texas, Austin
Maller, James, University of Colorado
Masui, Yoshio, University of Toronto, Canada
Maxson, Robert E., University of Southern California School of Medicine
Melton, Douglas, Harvard University
Olins, Joshua, Earlham College
Ouellette, Francis, McGill University, Canada
Perreault, Sally, EPA, Division of Developmental Biology
Poccia, Dominic, Amherst College
Raff, Rudolf A., Indiana University
Ruderman, Joan, Duke University
Saavedra, Carol, McGill University, Canada
Sargent, Thomas, NIH
Satoh, Noriyuki, Kyoto University, Japan
Shibuya, Ellen, University of Toronto, Canada
Sluder, Greenfield, Worcester Foundation for Experimental Biology
Solursh, Michael, University of Iowa
Specksnyder, Johanna, University of Utrecht, Netherlands
Stephens, Laurie, University of California, Berkeley

Swalla, Billie J., University of Texas, Austin
Trinkaus, John Philip, Yale University
Turner, Paul, University of California, Berkeley
Vacquier, Victor, University of California, San Diego
Velleca, Mark A., Washington University School of Medicine
Venuti, Judy, University of Texas, Austin
Waugh, Larry, Brandeis University
White, Mary E., University of Texas, Austin
Whittaker, J. Richard, Marine Biological Laboratory
Wilt, Fred H, University of California, Berkeley
Winkler, Matthew M., University of Texas, Austin
Zucker, Robert S., University of California, Berkeley

Students

Beanan, Maureen J., Indiana University
Beer, Donna M., University of Massachusetts, Amherst
Bloom, Theodora L.**, University of Cambridge, UK
Coffin, J. Douglas, SUNY Health Science Center at Syracuse
Cox, Cheryl A., Indiana University
Drysdale, Thomas A., University of Toronto, Canada
Foster, Barbara A., University of California, San Francisco
Gewalt, Sally L., University of North Carolina
Govind, Shubha, Princeton University
Han, Jin K., University of California, Davis
Jongejan-Zivkovic, Danica D., University of Utrecht, Netherlands
Kelly, Gregory M., University of Manitoba, Canada
Koenig, Gerd**, Max-Planck-Institut, FRG
Mandley, Elizabeth N., University of California, Riverside
Miranda, Louis M., University of Texas Health Science Center, Dallas
Monpetit, Isabelle, McGill University, Canada
Motta, Chiara Maria, University of Naples, Italy
Niemeyer, Christina C., Baylor College of Medicine
Nuelle, Jon R., University of Texas, Austin
Satterwhite, Lisa L., Johns Hopkins University
Shilling, Fraser M., University of Southern California
Simoncini, Luciana, University of Washington
Sturm, Karin S., Linus Pauling Institute of Science & Medicine
Vogel, Bruce E., Rutgers University
Vogel, Jacalyn, Illinois State University
Zhang, Wei WZ, University of Texas Health Science Center, Houston

MARINE ECOLOGY

Course director

Frank, Peter W., University of Oregon

Other faculty, staff, and lecturers

Aller, Robert, SUNY, Stony Brook
Buss, Leo W., Yale University
Caraco, Nina, Institute of Ecosystem Studies, Cary Arboretum
Carlton, James, Williams College
Caron, David A., Woods Hole Oceanographic Institution
Caswell, Hal, Woods Hole Oceanographic Institution
Cavanaugh, Colleen, Harvard College
Cole, Jonathan J., Institute of Ecosystem Studies, Cary Arboretum
Davis, Cabell S., Woods Hole Oceanographic Institution
Farrington, John W., Woods Hole Oceanographic Institution
Foreman, Kenneth, BUMP/Marine Biological Laboratory
Freadman, Marvin, BUMP/Marine Biological Laboratory
Fry, Brian, Marine Biological Laboratory
Gallagher, Eugene P., University of Massachusetts, Boston
Giblin, Anne, Marine Biological Laboratory
Hartman, Jean Marie, Harvard University
Jenkins, William J., Woods Hole Oceanographic Institution
Mann, Kenneth, Bedford Institute of Oceanography, Canada
Marcy, Maribel, Vassar College
Myers, Phillip E., University of South Carolina
Nixon, Scott, University of Rhode Island
Osman, Richard W., Philadelphia Academy of Natural Sciences
Peterson, Bruce J., Marine Biological Laboratory
Petraitis, Peter S., University of Pennsylvania
Platt, Trevor, Bedford Institute of Oceanography, Canada
Porter, James, University of Georgia
Porter Karen, University of Georgia
Pregnall, Marshall A., Vassar College
Reinisch, Carol L., Tufts University School of Veterinary Medicine
Rhoads, Donald C., Science Applications International Corp.
Rice, Donald, Chesapeake Biological Laboratory, Universityof Maryland
Roth, Nina, Vassar College
Sarda, Raphael, BUMP/Marine Biological Laboratory
Strickler, Rudi, BUMP/Marine Biological Laboratory
Valiela, I., BUMP/Marine Biological Laboratory

Students

Bisbal, Gustavo A., Instituto Nacional de Investigacion y Desarrollo, Argentina

** Advanced Research Training Program Participants

Birne, Patricia P. B., University College, Ireland
Charrier Melillan, Maria Elena, Universidad Nacional de Mar del Plata, Argentina
Dell'Arciprete, Olga Patricia, Instituto Nacional de Investigacion y Desarrollo, Argentina
Fernandez, Miriam E., Instituto de Biologica Marina y Pesquera "A. Storni," Argentina
Krishnan, Thankavel, Annamalai University, India
Roberts, Michael S., Wesleyan University
Sadovsky, Sebastian, Universidade Federal do Espirito, Brazil
Shierwater, Bernd, Braunschweig University, FRG
Varela, Diana E., Centro Nacional Patagonico, Argentina

MICROBIOLOGY: MOLECULAR ASPECTS OF CELLULAR DIVERSITY

Course directors

Wolfe, Ralph, University of Illinois
Greenberg, Peter, Cornell University

Other faculty, staff, and lecturers

Berg, Howard C., Harvard University
Blakemore, Richard, University of New Hampshire
Cordts, Marcia L., Cornell University
Dimarco, Anthony A., University of Illinois
Dore, Joel, University of Illinois
Dworkin, Martin, University of Minnesota
Frankel, Richard, Massachusetts Institute of Technology
Gertman, Eva, Queen's University, Canada
Gest, Howard, Indiana University
Gibson, Jane, Cornell University
Kashket, Eva, Boston University School of Medicine
Konisky, Jordan, University of Illinois
Kropinski, Andrew M., Queen's University, Canada
Krulwich, Terry, Mt. Sinai School of Medicine
Marrs, Barry, E. I. DuPont De Nemours & Co.
Michel, Tomas A., University of California, Davis
Mulligan, Martin E., University of Chicago
Olson, Karl, University of Illinois
Saulnier, Michelle, Queen's University, Canada
Scolnick, Pablo, E. I. DuPont De Nemours & Co.
Shapiro, Lucy, Columbia University
Spormann, Alfred M., Philipps Universitat, FRG
Stetter, Karl, University of Regensberg, FRG
Thayer, Rudolf, Phillips Universitat, FRG
Widdel, Friedrich W., University of Illinois

Students

Albertson, Nan H., University of Goteborg, Sweden
Arnold, Robert G., University of Arizona
Boehme, Susan E., North Carolina State University
Conway, Noellette M., Woods Hole Oceanographic Institution
Garcia-Pichel, Ferran, University of Oregon
Henry, Elizabeth A., Harvard University
Holden, Eric G., University of Massachusetts, Amherst
Hughes, Robert E., Yale University
Kolibachuk, Dana, Cornell University
Leisinger, Thomas, Mikrobiologisches Institut, Switzerland
Mack, E. Erin, University of Puget Sound
Moran, Mary Ann, University of Georgia
Parales Rebecca E., Cornell University
Roberts, A. Lynn, Massachusetts Institute of Technology
Robins, Jeff P., University of Massachusetts
Rood, Brian E., University of Florida
Schauder, Rolf, University of Ulm, FRG
Seeler, Jacob S., Boston University
Sment, Karen A., University of Illinois
Teiser, Markolf L. O., University of Oregon

NEURAL SYSTEMS AND BEHAVIOR

Course directors

Carew, Tom, Yale University
Kelley, Darcy, Columbia University

Other faculty, staff, and lecturers

Bate, Michael, University of Cambridge, UK
Borst, Axel, Max-Planck Institute, FRG
Bottjer, Sarah, University of Southern California, Los Angeles
Byrne, John H., University of Texas Medical School
Calabrese, Ronald, Emory University
Cleary, Leonard, University of Texas Medical School
Constantine-Paton, M., Yale University
Dodd, Frank, Cornell University
Eisner, Thomas, Cornell University
Fernald, Russell D., University of Oregon
Gorlick, Dennis L., Columbia University
Hoskins, Sally, Columbia University
Jacobs, Gwen, University of California, Berkeley
Kent, Karla, University of Arizona
Lasansky, Richard, Hebron Academy
Levine, Richard B., University of Arizona
Macagno, Eduardo, Columbia University
Marcus, Emilie, Yale University
Menzel, Randolf, University of Berlin, FRG
Nusbaum, Michael, Brandeis University
Smith, Brian H., University of California, Berkeley
Stevens, Charles F., Yale University School of Medicine
Streichert, Laura, University of California, Riverside
Tompkins, Laurie, Temple University
Van Essen, David C., California Institute of Technology
Walsh, John P., University of California, Los Angeles
Weeks, Janis C., University of California, Berkeley

Wenning-Erxleben, Angela, University of Konstanz, FRG
Williams, Heather, Rockefeller University
Wyman, Robert J., Yale University

Students

Born, Richard T., Harvard Medical School
Brainard, Michael S., Stanford University
Braun, Gotz, Institut fur Tierphysiologie, FRG
Casagrand, Janet L., Case Western Reserve University
Comfort, Nathaniel, Cornell University
Corfas, Gabriel, Weizmann Institute of Science, Israel
Evans, Bruce D., Emory University
Gallman, Eve A., University of North Carolina
Gilbert, Cole, Indiana University
Gruner, Wendy, SUNY, Stony Brook
Harty, T. Patrick, University of Pittsburgh
Ito, Minami, Osaka University, Japan
Liberstat, Frederic, The Hebrew University of Jerusalem, Israel
Lubischer, Jane L., University of California, Los Angeles
Matsumoto, Rae R., Brown University
Mendonca, Mary T., University of Texas, Austin
Orchinik, Miles, Oregon State University
Rinaman, Linda M., University of Pennsylvania
Wright, William G., Yale University
Wyttenbach, Robert Alan, Cornell University.

NEUROBIOLOGY

Course director

Karlin, Arthur, Columbia University

Other faculty, staff, and lecturers

Andrews, S. B., NINCDS, NIH
Armstrong, Katie, Rice University
Catterall, William, University of Washington School of Medicine
Cepko, Connie, Harvard University
Chark, Amitabh, Columbia University
Cheng, Toni, NINCDS/NIH
Clapham, David, Brigham and Women's Hospital
Claudio, Toni, Yale University
Correira, Frederick F., Albert Einstein College of Medicine of Yeshiva University
Czajkowski, Cynthia, Columbia University
Dale, Nicholas, Columbia University
Ehrlich, Barbara, University of Connecticut
Fischbach, Gerald D., Washington University School of Medicine
Frank, Eric, University of Pittsburgh
Gadsby, David C., Rockefeller University
Hall, Linda M., Albert Einstein College of Medicine of Yeshiva University
Hess, Peter, Harvard University
Inoue, Tomo, McGill University, Canada
Jessell, Thomas, Columbia University
Jones, Stephen W., Case Western Reserve University
Kaesmarek, L., Yale University
Kao, Peter, Columbia University
Landis, Dennis, Case Western Reserve University
Landis, Story, Case Western Reserve University
Llinas, Rudolfo, New York University Medical Center
Mac Kinnon, Roderick, Brandeis University
Majerus, Phil, Washington University School of Medicine
Mandel, Gail, Tufts University School of Medicine
Marder, Eve, Brandeis University
Matsumoto, Steven, Harvard University
Maue, Robert Alan, Tufts University School of Medicine
Mc Nab, Robert M., Yale University
Miller, Christopher, Brandeis University
Moosekar, Mark S., Yale University
Raviola, Elio, Harvard University
Reese, Thomas S., NINCDS/NIH, MBL
Rosen, Ora, Memorial Sloan Kettering Cancer Center
Schnapp, Bruce, NINCDS/NIH, MBL
Schuetze, Stephen M., Columbia University
Sheetz, Michael, Washington University
Siegel, Ruth E., Case Western Reserve University
Siegelbaum, Steven A., Columbia University
Silman, Israel, Weizmann Institute of Science, Israel
Smith, Carolyn, University of Pittsburgh
Smith, Steve, Yale University
Spudich, John, Albert Einstein College of Medicine of Yashiva University
Sternweis, Paul C., University of Texas Health Science Center
Teyler, T., Northeastern Ohio University
Vallee, Richard, Worcester Foundation for Experimental Biology
Van Wagoner, David R., Case Western Reserve University
Vicini, Stefano, Georgetown University

Students

Aoki, Chiye, Cornell University Medical College
Banin, Eyal, Hebrew University of Jerusalem, Israel
Freed, Michael, NINCDS/NIH
Gilford, Andrew N., St. Andrews University, Scotland
Hsu, Hsiao-Lan, Johns Hopkins University
Kernan, Maurice J., University of Wisconsin
Larmet, Yves, Centre National de la Recherche Scientifique, France
Merzdorf, Christa S., Harvard University
Muly III, Emil C., Duke University Medical Center
Sands, Steven B., University of California, Irvine
Van Vactor, David L., Jr., University of California, Los Angeles
Vogel, Steven S., Columbia University

PHYSIOLOGY: CELL AND MOLECULAR BIOLOGY

Course director

Goldman, Robert, Northwestern University Medical School

Other faculty, staff, and lecturers

Albrecht-Buehler, Guenter, Northwestern University Medical School
Asai, David J., Purdue University
Bartles, James, Northwestern University Medical School
Bloom, Kerry, University of North Carolina
Broschat, Kay O., University of Miami School of Medicine
Burgess, David, University of Miami School of Medicine
Chisholm, Rex L., Northwestern University Medical School
Chou, Ying-Hao, Northwestern University Medical School
Collins, Christine, Worcester Foundation for Experimental Biology
Dahl, Stephen, Wesleyan University
Desrosier, David, Brandeis University
Dessev, George N., Northwestern University Medical School
Earnshaw, William, Johns Hopkins University
Foltz, Kathy, Purdue University
Fuchs, Elaine, University of Chicago
Fukui, Yoshio, Northwestern University Medical School
Giroux, Craig, NIEMS
Goldman, Anne, Northwestern University Medical School
Hammarback, James, Worcester Foundation for Experimental Biology
Han, Peter S., Earlham College
Helfman, David, Cold Spring Harbor Laboratories
Hinds, Kristin, Showa University Research Institute
Hinds, Lael, Colorado College
Hughes-Fulford, Millie, NASA, University of California Medical Center, S. F.
Jamieson, James, Yale University
Kenna, Margaret, University of North Carolina
Lindberg, Uno, University of Stockholm, Sweden
Litman, Gary W., Showa University Research Institute
Mayrand, Sandra, Worcester Foundation for Experimental Biology
Mc Knight, Steven, Carnegie Institution of Washington
Morris, N. Ronald, Rutgers University
Obar, Robert, Worcester Foundation for Experimental Biology
Pederson, Thoru, Worcester Foundation for Experimental Biology
Penman, Sheldon, Massachusetts Institute of Technology
Petes, Tom, University of Chicago
Pollard, Thomas, Johns Hopkins University Medical School
Reinisch, Carol, Tufts University School of Veterinary Medicine
Rich, Alexander, Massachusetts Institute of Technology
Ruderman, Joan, Duke University
Shamblott, Mike J., Showa University Research Institute
Sloboda, Roger D., Dartmouth College
Sluder, Greenfield, Worcester Foundation for Experimental Biology
Smith, Allison M., University of Strathclyde, Scotland
Spudich, James, Stanford University
Steinert, Peter, National Cancer Institute
Steinhardt, Richard, University of California, Berkeley
Tisty, Thea, University of North Carolina
Vallee, Richard, Worcester Foundation for Experimental Biology
Vikstrom, Karen L., Northwestern University
Wieben, Eric D., Mayo Clinic, Rochester, Minnesota
Wilson, Darcy B., Medical Biological Institute
Yeh, Elaine, University of North Carolina
Yin, Helen, Harvard Medical School
Zeev, Avri Ben, Weizmann Institute of Science, Israel

Students

Barton, Nelson, R., University of Miami School of Medicine
Berryman, Mark A., University of Virginia
Carlos, Ruben, University of Hawaii
Cowles, Elizabeth A., Michigan State University
Curry, Alice M., Yale University
Cyr, Janet L., University of Texas Health Science Center, Dallas
Dohrmann, Cord E., Duke University
Dolan, Liam, University of Pennsylvania
Dong, Feng, Oregon State University
Feng, Sunlian, Wesleyan University
Ferber, Daniel M., Johns Hopkins University
Hagstrom, James E., Mayo Graduate School of Medicine
Harding, Fiona, University of Rochester
Harding, Susan M., University of Alabama
Healy, Aileen M., Tufts University
Hughes-Fulford, Millie, NASA/University of California Medical Center
Kronidou, Nafsika, Dartmouth College
Kuppe, Andreas, University of Oregon
Lee, Youngsook, University of Connecticut
Liang, Bruce T., Harvard Medical School
Mackey, Harris M., Columbia Medical School
Miller, Rita K., Northwestern University

Plopper, George E., Harvard University
Racoosin, Esther L., Harvard Graduate School of Arts and Sciences
Roberts, Denise M., University of Virginia
Roy, Linda M., Medical University of South Carolina
Ryan, Maureen C., Rush University
Sandor, Laurie Wright, Oklahoma University
Saunders, Kim B., Harvard Medical School
Sawin, Kenneth Eric, Stanford University
Strong, Theresa V., University of Alabama
Sympson, Carolyn J., University of Louisville School of Medicine
Thomas, Linda A., University of California, San Francisco
Turner, Christopher E., University of North Carolina
Walker, Richard A., University of North Carolina
Yutzey, Katherine E., Purdue University

Spring

ANALYTICAL AND QUANTITATIVE LIGHT MICROSCOPY IN BIOLOGY, MEDICINE AND MATERIALS SCIENCE

May 14–20, 1987

Course director

Inoué, Shinya, Marine Biological Laboratory

Other faculty, staff, lecturers

Ellis, Gordon W., University of Pennsylvania
Lanni, Frederick, Carnegie-Mellon University
Luby-Phelps, Katherine, Carnegie-Mellon University
Lutz, Douglas A., Harvard University
Salmon, Edward D., University of North Carolina
Taylor, D. Lansing, Carnegie-Mellon University

Commercial faculty

Aikens, Richard, Photometrics, Ltd.
Brenner, Mel, Nikon, Inc.
Chaisson, Richard, Olympus Corporation of America
Claypool, David J., Atlantex & Zieler Instrument Corp.
Cohen, David, Universal Imaging Corporation
Esser, Hermann J., Optical Elements Corp.
Goldberg, Michael, Research Imaging Systems, Inc.
Hannaway, Wyndham, G. W. Hannaway Associates
Hinsch, Jan, E. Leitz, Inc.
Howard, Michael, Quanta Systems, Inc.
Keller, Ernst, Carl Zeiss, Inc.
Klotsche, Richard, COHU, Inc.
Korkidis, Katherine, Spex Industries, Inc.
Mengers, Paul, Quantex Corporation
Olwell, Patricia, E. Leitz, Inc.
Ota, Bob, Trident Electronics
Presley, Phillip H., Carl Zeiss, Inc.
Taylor, Richard, Colorado Video
Thomas, Paul, DAGE-MTI
Wick, Robert, Photonic Microscopy, Inc.

Students

Blumenfeld, Hal, Howard Hughes Medical Institute
Chen, Nong-Ruay, Cornell University
Cheng, Toni, Marine Biological Laboratory/NIH
Collin, Carlos E., NINCDS/NIH, Marine Biological Laboratory
Dissing, Steen, University of Copenhagen, Denmark
Faltermeier, Bernd, Carl Zeiss, Inc.
Fink, Rachel D., Mount Holyoke College
Frostig, Ron D., Rockefeller University
Gibson, Sarah Frisken, Carnegie-Mellon University
Holmes, Tim, University of Missouri
Hutchison, Nancy J., Fred Hutchinson Cancer Research Center
Jamieson, James D., Yale University School of Medicine
Lechleiter, James D., Tufts University School of Medicine
Lowy, Robert Joel, National Institutes of Health
Martin, James C., University of Alabama
Pratt, Melanie, M., University of Miami School of Medicine
Salzman, Gary C., Los Alamos National Laboratory
Sardet, Christian, Station Zoologique, France
Stump, Robert F., University of New Mexico School of Medicine
Telzer, Bruce R., Pomona College
Teragawa, Carolyn K., University of California, Irvine
Weiss, Dieter G., Technische Universitat Munchen, FRG

Short Courses

CELL AND MOLECULAR BIOLOGY OF PLANTS

August 3–15, 1987

Directors

Dure, Leon S., University of Georgia
Key, Joe L., University of Georgia

Lecturers

Binns, Andrew, University of Pennsylvania
Chua, Nam-Hai, Rockefeller University
Crouch, Martha, Indiana University
Darvill, Alan, University of Georgia
Fraley, Rob, Monsanto Company
Guilfoyle, Tom, University of Missouri
Hallick, Richard, University of Arizona
Haselkorn, Robert, University of Chicago
Levings III, C. S., North Carolina State University
Long, Sharon, Stanford University
Meagher, Richard, University of Georgia
Meyerowitz, Elliott, California Institute of Technology
Quail, Peter, University of Wisconsin
Ryan, Clarence A., Washington State University
Silflow, Carolyn, University of Minnesota
Timberlake, William, University of Georgia

Verma, Desh Pal S., McGill University
Wessler, Susan, University of Georgia
Yoder, Olin, Cornell University

Students

App, Alva, A., Rockefeller Foundation
Armbrust, Ginger, WHOI/MIT
Basson, Bruce R., University of North Carolina
Baumgarten, Miriam, Columbia University
Becker, David W., Pomona College
Brady, Kevin P., Indiana University
Bruemmer, Joseph H., USDA
Couch, Jennifer, Pennsylvania State University
Diebold, Ronald, Marquette University
Heeyong, Tai, Pennsylvania State University
Jayne, Susan M., Ciba-Geigy Corp.
Lahners, Kristine, Ciba-Geigy Corp.
Palenik, Brian, WHOI/MIT
Robertson, Borre, University of Tromso, Norway
Rusnak, Suzanne, Parma City School, OH
Sasavage, Nancy, Bethesda Research Laboratories
Toenniessen, Gary H., Rockefeller Foundation
Waddle, James A., University of California
Ward, Michael R., University of California

MOLECULAR AND CELLULAR IMMUNOLOGY

August 3–15, 1987

Course directors

Reinisch, Carol, Tufts University School of Veterinary Medicine
Wilson, Darcy, Medical Biological Institute

Other faculty, staff and lecturers

Bevan, Michael J., Scripps Clinic and Research Foundation
Broedeur, Peter, Tufts University
Hogg, Nancy, Imperial Cancer Research Fund, England
Janeway, Charles A., Jr., Yale University School of Medicine
Kabat, Elvin A., Columbia University
Leskowitz, Sidney, Tufts University School of Medicine
Morse, Herbert C., III, NIH
Mosier, Donald E., Medical Biological Institute
Prendergast, Robert A., Johns Hopkins Hospital
Rosenwasser, Larry J., Tufts New England Medical Center
Springer, Timothy, Dana-Farber Cancer Institute
Strominger, J., Harvard University
Sunshine, Geoffrey, Tufts University School of Veterinary Medicine
Valentine, Fred T., New York University Medical Center
Weissmann, Gerald, New York University Medical Center
Winchester, Robert, New York, NY
Wortis, Henry H., Tufts University School of Medicine

Students

Allen, Suzanne T., Worcester Memorial Hospital
Carlson, David L., University of California, Davis
Chang, Yueh-jong, Indiana State University
Fitzgerald, Kathleen A., Bristol-Myers
Harshan, K. V., All India Institute of Medical Sciences, India
Hayflick, Joel S., Oregon Health Sciences University
Marx, James J., Jr., Marshfield Medical Research Foundation
Miller, Lynn, Hampshire College
Pender, Daniel J., Columbia University
Petty, Richard F., Brick Township School, Brielle, NJ
Read, Dorothy L., Southeastern Massachusetts University
Saugstad, Julie A., University of Oklahoma
Tomlinson, Gail E., Children's Hospital National Medical Center
Zaroogian, Gerald E., United States Environmental Protection Agency

CELLULAR NEUROBIOLOGY IN THE LEECH

August 5–25, 1987

Course director

Nicholls, John G., University of Basel, Switzerland

Other faculty, staff, and lecturers

Blackshaw, Susanna, University of Glasgow, Scotland
Calabrese, Ronald, Harvard University
Cohen, Lawrence G., Yale University School of Medicine
Friesen, W. Otto, University of Virginia
Kristan, William B., Jr., University of California, San Diego
Macagno, Eduardo, Columbia University
Muller, Kenneth J., University of Miami School of Medicine
Payton, Brian W., Memorial University of Newfoundland, Canada
Ross, William, New York Medical College
Salzberg, Brian M., University of Pennsylvania
Stent, Gunther S., University of California, Berkeley
Weisblat, David, University of California, Berkeley
Zipser, Birgit, Michigan State University

Students

Clarke, William P., Mount Sinai School of Medicine
Gleizer, Lidia, University of California, Berkeley
Gu, Xiao-nan, University of Miami School of Medicine
Karrer, Tracy A., Yale University
Nakagawa, Liria, University of Basel, Switzerland
Passani, M. Beatrice, Columbia University
Szczupak de Rodgers, Instituto Nacional de Investigacion, Argentina
Venable, Nancy L., University of Basel, Switzerland

Wallace, Mark T., Temple University
Wedeen, Cathy J., University of California, Berkeley
Wittenberg, George F., University of California, San Diego
Xiao, Chun, Yale University School of Medicine

HISTORY OF BIOLOGY: HEREDITY AND DEVELOPMENT

August 2–15, 1987

Course directors

Garland, Allen E., Washington University
Fantini, Bernardino, University of Rome, Italy
Maienschein, Jane, Arizona State University

Other faculty, staff, and lecturers

Churchill, Frederick, Indiana University
Gilbert, Scott, Swarthmore College
Groeben, Christiane, Naples Zoological Station, Italy
Grmek, Mirko, L'Ecole des Hautes Etudes, Le Sorbonne, France
Olby, Robert, University of Leeds, UK
Roe, Shirley A., Harvard University

Students

Ascuitto, James, Mahwah High School, NJ
Bogin, Mary, Cornell University
Burian, Richard M., Virginia Polytechnic Institute and State University
Cadwallader, Joyce V., Saint Mary-of-the-Woods College
Cronin, Eunice A., Belmont Abbey College
De Jonghe-Murphy, Viviane, Stamford, CT
Doering, Grant R., College of the Academy of the New Church
Fausto-Sterling, Anne, Brown University
Gariepy, Thomas P., Stonehill College
Hammonds, Evelynn M., Harvard University
Howard, Heidi, Harvard University
Jungek, John R., Beloit College
Karustis, Marlene, Mt. St. Mary's Academy
Leach, Berton J., Rockville, MD
Lewin, Susan O., Shodair Children's Hospital
Lyons, Sherrie L., University of Chicago
Miles, Sara Joan, Wheaton College
Mylott, Anne, Indiana University
Opitz, John M., Montana State University
Paracer, Surindar, Worcester State College
Richardson, Robert C., University of Cincinnati
Sawin, Clark T., Tufts University
Shaver, John R., University of Puerto Rico
Sloan, Jan Butin, Kansas City Art Institute
Swetlitz, Marc, University of Chicago
Walley, Willis Wayne, Delta State University
Weidman, Nadine M., Bryn Mawr College
Wimsatt, William, University of Chicago

X. Research and Training Programs

Summer

Principal Investigators

Alford, Simon, St. Georges Hospital Medical School, U. K.
Anderson, Winston A., Howard University
Angstadt, James D., Emory University
Armstrong, Clay M., University of Pennsylvania
Armstrong, Peter B., University of California, Davis
Arnold, John, University of Hawaii
Atwood, Kimball, Woods Hole, MA
Augustine, George, University of Southern California
Barlow, Robert B., Jr., Syracuse University
Barry, Daniel, University of Michigan
Barry, Michael A., Albert Einstein College of Medicine of Yeshiva University
Barry, Susan R., University of Michigan
Bass, Andrew, Cornell University
Beauge, Luis A., Instituto de Investigacion Medica, Argentina
Begenisich, Ted, University of Rochester
Bennett, Michael V. L., Albert Einstein College of Medicine of Yeshiva University
Bezanilla, Francisco, University of California, Los Angeles
Bloom, George S., University of Texas Health Science Center, Dallas
Bodznick, David, Wesleyan University
Borgese, Thomas A., Lehman College
Boron, Walter F., Yale University School of Medicine
Borst, David W., Illinois State University
Brady, Scott T., University of Texas Health Science Center, Dallas
Brehm, Paul, Tufts University School of Medicine
Brezina, Vladimir, University of California, Los Angeles
Brown, Joel E., Washington University School of Medicine
Burdick, Carolyn J., Brooklyn College
Burger, Max M., University of Basel, Switzerland
Burgos, Mario, University of Cuyo, Mendoza, Argentina
Butt, Arthur M., East Carolina University School of Medicine
Chang, Donald C., Baylor College of Medicine
Chappell, Richard L., Hunter College
Charlton, Milton P., University of Toronto, Canada
Cinelli, Angel R., University of Pennsylvania School of Dental Medicine
Clark, John M., University of Massachusetts, Amherst
Cohen, Avis H., Cornell University
Cohen, Lawrence B., Yale University School of Medicine
Cohen, William D., Hunter College
Cooperstein, Sherwin J., University of Connecticut Health Center

De Weer, Paul, Washington University School of Medicine
Delaney, Kerry, Princeton University
Dunlap, Kathleen, Tufts University School of Medicine
Eckberg, William E., Howard University
Ehrlich, Barbara E., University of Connecticut Health Center
Feinman, Richard D., SUNY Health Science Center, Brooklyn
Fishman, Harvey M., University of Texas Medical Branch
Gadsby, David C., Rockefeller University
Gainer, Harold, NINCDS/NIH
Gilbert, Daniel L., NINCDS/NIH
Gilbert, Susan P., Pennsylvania State University
Giuditta, Antonio, University of Naples, Italy
Gonzalez-Serratos, Hugo, University of Maryland School of Medicine
Gould, Robert M., New York State Institute for Basic Research
Govind, C. K., University of Toronto, Canada
Graf, Werner, Rockefeller University
Greengard, Paul, Rockefeller University
Haimo, Leah, University of California, Riverside
Halvorson, Harlyn O., Brandeis University
Hess, Stephen D., University of Southern California, Los Angeles
Highstein, Stephen M., Washington University School of Medicine
Hill, Susan D., Michigan State University
Hoskin, Francis C. G., Illinois Institute of Technology
Humphreys, Tom, University of Hawaii
Ingoglia, Nicholas, New Jersey Medical School
Josephson, Robert K., University of California, Irvine
Kaminer, Benjamin, Boston University School of Medicine
Keynan, Alexander, Hebrew University of Jerusalem, Israel
Kornberg, Hans, University of Cambridge, UK
Kriebel, Mahlon E., SUNY Health Science Center, Syracuse
Landowne, David, University of Miami School of Medicine
Langford, George M., University of North Carolina School of Medicine
Lasek, Raymond J., Case Western Reserve University
Laufer, Hans, University of Connecticut
Lechleiter, James D., Tufts University School of Medicine
Levin, Jack, University of California School of Medicine
Levis, Richard A., Rush Medical Center
Lewbart, Gregory A., University of Pennsylvania Veterinary School
Lichtman, Jeff W., Washington University School of Medicine
Lipicky, Raymond J., Food and Drug Administration
Lisman, John, Brandeis University
Llinas, Rudolfo, New York University Medical Center
Loewenstein, Werner R., University of Miami School of Medicine
Lorand, Laszlo, Northwestern University
Malbon, Craig C., SUNY, Stony Brook
Marcum, James, Harvard Medical School
Matsumura, Fumio, Michigan State University
Matteson, Donald R., University of Maryland School of Medicine
McMahon, Douglas G., Harvard University
Mendelson, Bruce, University of Pittsburgh School of Medicine
Metuzals, J., University of Ottawa, Canada
Moore, John W., Duke University Medical Center
Mullins, Lorin J., University of Maryland School of Medicine
Narahashi Toshio, Northwestern University Medical School
Nelson, Leonard, Medical College of Ohio
Noe, Bryan D., Emory University School of Medicine
Pappas, George D., University of Illinois College of Medicine
Pierson, Beverly K., University of Puget Sound
Pumplin, David W., University of Maryland School of Medicine
Purves, Dale, Washington University School of Medicine
Quigley, James P., SUNY Health Science Center, Brooklyn
Rakowski, Robert F., University of Health Sciences/ The Chicago Medical School
Rebhun, Lionel I., University of Virginia
Rickles, Frederick R., University of Connecticut Health Center
Ripps, Harris, University of Illinois College of Medicine
Rose, Birgit, University of Miami School of Medicine
Ruderman, Joan, Duke University
Russell, John M., University of Texas Medical Branch, Galveston
Saez, Juan C., Albert Einstein College of Medicine of Yeshiva University
Salzberg, Brian M., University of Pennsylvania
Sanger, Jean M., University of Pennsylvania School of Medicine
Sanger, Joseph W., University of Pennsylvania School of Medicine
Segal, Sheldon J., Rockefeller Foundation
Silver, Robert B., University of Wisconsin
Sloboda, Roger D., Dartmouth College
Smith, Stephen J., Yale University School of Medicine
Speck, William T., Case Western Reserve University/ University Hospitals of Cleveland
Steinacker, Antoinette, Washington University Medical School

Stuart, Ann E., University of North Carolina
Suprenant, Kathy A., University of Kansas
Tablin, Fern, University of California, Davis
Telzer, Bruce R., Pomona College
Tilney, Lewis G., University of Pennsylvania
Treistman, Steven N., Worcester Foundation for Experimental Biology
Trinkaus, John Philip, Yale University
Troll, Walter, New York University Medical Center
Tucker, Edward B., Baruch College
Tytell, Michael, Wake Forest University, Bowman Gray School of Medicine
Vincent, Walter, University of Delaware
Weiss, Dieter G., Technical University of Munich at Garching, FRG
Weissmann, Gerald, New York University Medical Center
Wiens, T. J., University of Manitoba, Canada
Wu, Jian-young, Yale University School of Medicine
Yeh, Jay Z., Northwestern University
Zigman, Seymour, University of Rochester Medical Center
Zukin, R. Suzanne, Albert Einstein College of Medicine of Yeshiva University

Other Research Personnel

Abramson, Charles, Downstate Medical Center
Adler, Elizabeth, University of Toronto, Canada
Adra, Chaker N., University of Ottawa, Canada
Alberghina, Mario, University of Catania, Italy
Albrecht, Kenneth, University of Connecticut
Altamirano, Anibal, University of Texas Medical Branch, Galveston
Armstrong, Margaret, University of California, Davis
Baccetti, Baccio, Howard University
Baker, Margaret, Cornell University
Baker, Robert G., New York University Medical Center
Bamrungphol, Wattana, University of Pennsylvania
Berry, Dwight, Howard University
Blumer, Jeffrey L., Case Western Reserve University
Breitwieser, Gerdna E., University of Texas Medical Branch, Galveston
Brewton, Kevin, Howard University
Brosius, Denton, Albert Einstein College of Medicine of Yeshiva University
Brown, Anthony, Case Western Reserve University
Browne, Carol, Wake Forest University
Brozen, Reed, Yale University
Buchanan, JoAnn, Yale University School of Medicine
Callaway, Joseph Charles, University of Washington
Caputo, Carlo, Instituto Venezolanode Investigaciones Cientifican, Venezuela
Cariello, Lucio, Zoological Station, Italy
Chen, Eric, Northwestern University Medical School
Chow, Robert H., University of Pennsylvania
Cohen, Avrum, University of Chicago
Cohen, Sarah R., Yale University
Cole, Neil M., University of Michigan
Contanche, Douglas A., Medical University of South Carolina
Cota-Penuelas, Gabriel, University of Pennsylvania
Couch, Ernest F., Texas Christian University
Cruise, Enid, Howard University
Dailey, Jessica, Northwestern University
Davidson, Sarah, New York University Medical Center
Deak, Peter, University of Connecticut
DiFranco, Marino, Central University of Venezuela
Di Polo, Reinaldo, Instituto Venezolanode Investigaciones Cientifican, Venezuela
Dome, Jeffrey S., University of Pennsylvania School of Medicine
Dowling, John E., Harvard University
Duffy, Steven, University of Toronto, Canada
Duran, Carlos L., Lehman College
Eatock, Ruth Anne, University of Rochester
Ferkowie, Michael, Michigan State University
Fink, Rachel D., Mount Holyoke College
Flacker, Jonathan, University of Chicago School of Medicine
Flores, Roberto, University of Pennsylvania School of Dental Medicine
Forman, Robin, Medical College of Virginia
Fox, Geoffrey Q., Max Planck Institut fur Biophysikalische Chemie, FRG
Frank, Dorothy M., Case Western Reserve University School of Medicine
Frederick, Judith L., University of Puget Sound
Freepong-Buodo, Anthony, Howard University
Gao, Pei-qing, Baylor College of Medicine
Garcia, Richard, Baruch College
George, Edwin B., Case Western Reserve University
Gershfeld, Norman, NIAMS/NIH
Gill-Kumar, Pritam, Food and Drug Administration
Grassi, Daniel, Ft. Lauderdale
Graubard, Catherine, Albert Einstein College of Medicine of Yeshiva University
Greif, Peter C., Food and Drug Administration
Greiner, Francine, Emory University School of Medicine
Grob, Marianne, Friedrich Miescher-Institut, Switzerland
Gruner, John A., New York University Medical Center
Hamosh, Leora Y., University of Michigan
Haneji, Tatsuji, Population Council, Rockefeller University
Hernandez, Michael R., University of Texas Medical Branch, Galveston
Herring, Alex McNeely, University of North Carolina
Hill, Christine, Mount Holyoke College
Hines, Michael, Duke University Medical Center

Hogan, Emilia, Yale University School of Medicine
Holmstrom, Diane, University of Puget Sound
Homola, Ellen, University of Connecticut
Hopp, Hans, Yale University School of Medicine
Hollis, Vincent W., Jr., Howard University
Hunt, John R., Baylor College of Medicine
Jumblatt, James, Tufts University
Kadam, Arjun L., Population Council, Rockefeller University
Kaplan, Ehud, Rockefeller University
Keller, Franz, Technical University of Munich at Garching, FRG
Kissee, Linda, Illinois State University
Khier, J., Albert Einstein College of Medicine of Yeshiva University
Knudsen, Knud, Food and Drug Administration
Koide, Samuel S., Population Council, Rockefeller University
Kosik, Kenneth S., Brigham & Women's Hospital
Landau, Matthew, University of Connecticut
Lehman, Herman K., Syracuse University
Leidigh, Christopher, Brown University
Leopold, Philip L., University of Texas Health Science Center, Dallas
Leuchtag, H. Richard, Texas Southern University
Levitan, Herbert, W/L. Cohen
Li, Hui, Illinois State University
Lindgren, Clark A., Duke University Medical Center
Llinas, Rafael, Washington University School of Medicine
Lowe, Kris, New College of University of South Florida
Luca, Frank, Duke University
Luthi, Theres, University of Basel, Switzerland
Maldonado, Pedro E., University of Miami School of Medicine
Matsumura, Fumihiko, Michigan State University
Mauney, Donald, University of North Carolina School of Medicine
McGuinness, Teresa, Rockefeller University
McIlveen, Anita, University of Connecticut
McKee, Juliet M., University of Kansas
Menichini, Enrico, Instituto di Biologia Cellulare, Italy
Meyer, Monica A., Thomas Jefferson University
Milgram, Sharon L., Emory University School of Medicine
Misevic, Gradimir, Friedrich Miescher-Institut, Switzerland
Murray, Sandra, University of Pittsburgh
Mushynski, Walter E., McGill University, Canada
Nealey, Tara A., University of Rochester
Nicholas, Craig J., Syracuse University
Nishio, Matomo, Northwestern University Medical School
Obaid, Ana Lia, University of Pennsylvania School of Dental Medicine
Oberhauser, Andres, University of Pennsylvania
Osses, Luis R., University of Southern California, Los Angeles
Palazzo, Robert E., University of Virginia
Pant, Harish, NINDCDS/NIH
Parsons, Thomas D., University of Pennsylvania
Pearce, Joanne, University of Toronto, Canada
Perozo, Eduardo, University of California, Los Angeles
Porter, Charles W., Rockefeller University
Powers, Maureen K., Vanderbilt University
Rasgado-Flores, Hector, University of Maryland School of Medicine
Repucci, Anthony, Case Western Reserve University
Requena, J., Instituto Internacional de Estudios Avanzados, Venezuela
Riesen, William, Yale University
Robinson, Phyllis R., Brandeis University
Robitaille, Yves, Montreal Neurological Institute, Canada
Rodriguez, Richard, Baruch College
Rooks, Arthur, University of North Carolina School of Medicine
Rudolph, Rebecca E., University of Puget Sound
Salvati, Serafina, N. Y. S. U. for Basic Research in Developmental Disabilities
Sanchez, Ivelisse, Hunter College
Sands, Peter J., New York University Medical Center
Sanger, Jean M., University of Pennsylvania School of Medicine
Schiminovich, David, Yale University
Schneider, Eric J., Wesleyan University
Schneider, Melissa R., Hamilton College
Seitz-Tutter, Dieter, Technical University of Munich at Garching, FRG
Shockley, Ronald, University of California, Irvine
Spires, Sherrill, University of Rochester
Spray, David C., Albert Einstein College of Medicine of Yeshiva University
Stadler, Herbert, Max Planck Institut fur Biophysikalische Chemie, FRG
Stokes, Darrell R., Emory University
Sugimori, Mutsuyuki, New York University Medical Center
Swandulla, Dieter, University of Pennsylvania
Swenson, Katherine, Harvard Medical School
Sydlik, Mary Anne, Syracuse University
Tanguy, Joelle, Ecole Normale Superieure, France
Tricas, Timothy C., Washington University School of Medicine
Ueno, Hiroshi, Rockefeller University
Vandenberg, Carol A., University of California, Los Angeles
Vaysse, Pierre, Albert Einstein College of Medicine of Yeshiva University

Verselis, Vytautas, Albert Einstein College of Medicine of Yeshiva University
Vilijn, Marie-Helene, Albert Einstein College of Medicine of Yeshiva University
Vogel, Jacalyn M., Eastern Illinois University
Waxman, Stephen G., Yale University School of Medicine
Webb, Christina Kae, University of California, Los Angeles
Weiss, Jerry S., Northwestern University Medical School
Weiss, Leo, Venice, CA
Westendorf, Joanne M., Duke University
White, Roy L., Albert Einstein College of Medicine of Yeshiva University
Whittembury, Jose, Case Western Reserve University
Xiao, Chun, Yale University School of Medicine
Zakevicius, Jane M., University of Illinois College of Medicine
Zavilowitz, Joseph, Albert Einstein College of Medicine of Yeshiva University
Zecevic, Dejan, Institute of Biological Research, Yugoslavia
Zhang, Lan, Syracuse University

Library Readers

Adelberg, Edward A., Yale Medical School
Alkon, Dan, NIH
Allen, Garland, Washington University
Anderson, Everett, Harvard Medical School
Apter, Nathaniel S., Nova University
Bang, Betsy, MBL
Bauer, G. Eric, University of Minnesota Medical School
Boettiger, Julie, Temple University
Buck, John, NIH
Cape Cod Planning & Economic Development
Candelas, Graciela, University of Puerto Rico
Carriere, Rita, Downstate Medical Center, SUNY
Cathcart, Tom, Mississippi State University
Child, Frank, Trinity College
Chambers, Edward L., University of Miami
Chinard, Francis P., New Jersey Medical School
Churchill, Fred, History of Biology Course
Clark, Arnold, MBL
Cobb, Jewel Plummer, California State University
Cohen, Leonard A., American Health Foundation
Cohen, Seymour S., MBL
Corliss, Bruce H., Duke University
Dancis, Joseph, New York School of Medicine
DeToledo-Morrell, Leyla, Rush Presbyterian St. Lukes Medical Center
Dodge, Frederick A., IBM Research
Duncan, Thomas, Nichols College
Ebert, James, Carnegie Institute of Washington
Eder, Howard A., Albert Einstein College of Medicine
Farb, David, SUNY
Farmanfarmaian, A., Rutgers University
Feingold, David S., New England Medical Center
Fisher, Saul H., NYU Medical Center
Frenkel, Krystyna, New York University Medical Center
Friedler, Gladys, Boston University School of Medicine
Fussell, Catharine P., The Pennsylvania State University
Galatzer-Levy, Robert, University of Chicago
German, James L., The New York Blood Center
Gibbs, Terrell T., SUNY Health Science Center at Stony Brook
Goldstein, Moise H., Jr., Johns Hopkins University, EECS Department
Goodgal, Sol H., Pennsylvania School of Medicine
Grant, Philip, University of Oregon
Greelish, Stephen J., Liberty Mutual Research Center
Grossman, Albert, NYU
Guttenplan, Joseph B., New York University Dental Center
Harding, Clifford V., Kresge Eye Institute, Wayne State University
Haubrich, Robert, Denison University
Herskovitz, Theodore T., Fordham University
Hildebrand, John G., University of Arizona
Hill, Richard W., Michigan State University
Hoffman, Peter R.
Hostetler, Karl Y., University of California
Hughes-Fulford, Millie, Johnson Space Center
Ilan, Joseph, Case Western Reserve University
Ilan, Judith, Case Western Reserve University
Inoue, Sadayuki, McGill University
Jarvik, Murry E., U.C.L.A.
Kaltenbach, Jane C., Mount Holyoke College
Kaplan, Ilene M., Union College
Karush, Fred, University of Pennsylvania
Kelly, Robert, University of Illinois, College of Medicine
Kemlow, Kenneth M., Wilkes College
King, Kenneth, Jr., Children's Hospital
Kisten & Babitsky, Private Lawyers
Klein, David L., University of California San Francisco
Koulish, Sasha, College Staten Island, CUNY
Krane, Stephen M., Massachusetts General Hospital
Kravitz, Edward A., Harvard Medical School
Laderman, Aimlee, MBL
Lazarow, Normand H., Mayo Clinic
Leach, Berton J.
Lee, John J., City College NY
Leighton, Joseph, Medical College of Pennsylvania
Levine, Rachmiel, City of Hope Medical Center
Levitz, Mortimer, New York University Medical Center
Lewis, Larry, Millersville University

Luckenbill-Edds, Louise, Ohio University
Maienschein, Jane, Arizona State University
Marine Research Inc., Marine Research Inc.
Mautner, Henry G., Tufts University School of Medicine
McCann-Collier, Marjorie, Saint Peter's College
McNabb, F. M. Anne, Virginia Polytechnic Institute & State University
Mecurio, Arthur M., Harvard Medical School
Mecurio, Kimberly, MBL
Meinertzhagen, I. A., Dalhousie University
Mitchell, Ralph, Harvard University
Mizell, Merle, Tulane University
Morrell, Frank, Rush Presbyterian St. Lukes Medical Center
Moyer, Carolyn F., E. G. & G. Mason Research Institute
Musacchia, X. J., University of Louisville
Nagel, Ronald L., Albert Einstein College of Medicine
Nickerson, Peter A., SUNY at Buffalo
Nowotny, Alois H., University of Pennsylvania
Olby, Robert, History of Biology Course
Oschmann, James, MBL
Ott, Karen J., University of Evansville
Paton, David
Person, Philip, VA Medical Center, Brooklyn, NY
Pierce, Sidney K., University of Maryland
Pollen, Don, University of Massachusetts Medical Center
Prusch, Robert D., Gonzaga University
Reiner, John M., Albany Medical College
Reynolds, George T., Princeton University
Ringer, Steven, Childrens Hospital
Rosenkranz, Herbert S., Case Western Reserve University
Roth, Jay S., University of Connecticut
Rowland, Lewis P., Neurological Institute
Rudmann, Daniel G., Kenyon College
Russell-Hunter, W. D., Syracuse University
SMU Library, Southeastern Massachusetts University
Schippers, Jay, WAFRA Advisory
Seaver, George, Seaver Engineering
Shapley, Robert, Rockefeller University
Shemin, David, Northwestern University School of Medicine
Shepard, Frank, Woods Hole Data Base
Shepro, David, Boston University
Shriftman, Mollie Starr, North Nassau Mental Health Center
Sluder, Greenfield, Worcester Foundation for Experimental Biology
Spector, Abraham, Columbia University
Spiegel, Evelyn, Dartmouth College
Spiegel, Melvin, Dartmouth College
Stephens, Philip J., Villanova University
Stephenson, William K., Earlham College
Stracher, Alfred, State University of New York
Szent-Gyorgyi, Andrew G., Brandeis University
Szentkiralyi, Eva M., Brandeis University
Tashiro, Jay Shiro, Kenyon College
Tellez, Alexander, Harvard University
Tessie, Richard, University of Montreal
Tilney, Lewis, University of Pennsylvania
Trager, William, The Rockefeller University
True, Merrill, MBL
Tweedell, Kenyon S., University of Notre Dame
Vaida, Akhil B., Hahneman University
Van Holde, Kensal E., Oregon State University
Wagenbach, Gary, Carleton College
Wainio, Walter, Rutgers University
Warren, Leonard, Wistar Institute
Webb, H. Marguerite, MBL
Weidner, Earl H., Louisiana State University
Wheeler, George, Brooklyn College
Whittaker, J. Richard, MBL
Wichterman, Ralph, MBL
Wilber, Charles G., Colorado State University
Williams, Wendy, Cape Cod Times
Wirth, Dyann, HSPH/TPH
Wittenberg, Jonathan, Albert Einstein College of Medicine
Wittenberg, Beatrice, Albert Einstein College of Medicine
Wolken, Jerome J., Carnegie Mellon University
Yow, F. W., Kenyon College
Zacks, Sumner I., The Miriam Hospital/Brown University
Zigmond, Richard E., Harvard Medical School
Zottoli, Steven J., Williams College

Year-Round Programs

Adelman, William J., Jr., Director, and Chief, Section on Neural Membranes, Laboratory of Biophysics, Marine Biological Laboratory, NINCDS/NIH

The Section on Neural Membranes concentrates on the biophysical mechanisms underlying the conduction of the nerve impulse, synaptic transmission, and muscular transmission. The primary research animal is the Woods Hole squid, *Loligo pealei.*

Staff

Clay, John
Fohlmeister, Jorgen
Goldman, David
Hodge, Alan
Muller, Ruthanne
Rice, Robert
Ross, Darci
Vick, Sherry

Alkon, Daniel L., Chief, Section on Neural Systems, Laboratory of Biophysics, Marine Biological Laboratory, NINCDS/NIH

The Section on Neural Systems studies the cellular basis of learning and memory. Investigators relate changes in behavior caused by associative learning to biochemical and biophysical transformation of specific nerve cells using a California nudibranch, *Hermissenda crassicornis*.

Staff

Bank, Barry
Chen, Chong
Collin, Carlos
Garner, Lisa
Hopp, Hans
Ikeno, Hide
Kuzirian, Alan
Lederhendler, Izja
Loturco, Joe
Nelson, Tom
Tyndal, Clyde

Boston University Marine Program

Staff[1]

Hahn, Dorothy, Administrative Secretary
Sunley, Madeline, Administrative Consultant

Graduate students

Alber, Merryl
Banta, Gary
Barshaw, Diana
Borroni, Paola
Brooks, Cydney
Bryden, Cindy
Chen, Chong
Corroto, Frank
Costa, Joseph
Coughlin, David
Cowan, Diane
Ellis, Sarah
Elskus, Adria
Foreman, Kenneth
Gallager, Scott
Glick, Stephen
Hahn, Jill
Hersh, Douglas
Krieger, Yutta
Lavalli, Kari
Mercurio, Kim
Merrill, Carl
Moore, Paul
Mulsow, Sandor
Scott, Marsha
Tamse, Armando
Trager, Geoffrey
Trott, Thomas
Webb, Jacqueline
White, David
Wood, Susan

Undergraduates

Bower, Patricia
Carlon, David
Coburn, Cara
Corker, Amy
Cromarty, Stuart
Dawson, Steffany
Dolan, Paula
Gaspar, Kathy
Hill, Christine
Howard, Katherine
Hoffman, Jennifer
Kaska, David
Kelly, Jennifer
Marsich, Victor
Mc Watters, Brian
Sammon, Leslie
Santa Ana, Jeff
Schad, Andrea
Souders, Donna
Taft, Natalie
Weisman, Kitty
Zeller, Robert

Visiting investigators

D'Avanso, Charlene, Hampshire College
Poole, Alan, Boston University
Rietsma, Carol, SUNY, New Paltz

[1] Note: All staff of Boston University unless otherwise indicated.

Atema, Jelle, Professor of Biology, Boston University

Organisms use chemical signals as their main channel of information about the environment. These signals are transported in the marine environment by turbulent currents, viscous flow, and molecular diffusion. Receptor cells extract signals through various filtering processes. Currently, the lobster with its exquisite sense of taste and smell is our major model to study the signal filtering capabilities of the whole animals and its narrowly tuned receptor cells. Research focuses on amino acids (food signals) and pheromones (courtship), neurophysiology of receptor cells, and computer modeling of odor plumes.

Staff

Voigt, Rainer, Research Associate

Freadman, Marvin, Visiting Assistant Professor of Biology, Boston University

Principal research interests: comparative animal physiology, respiratory and circulatory physiology, physiology and hydromechanics of animal locomotion. Current research: (1) mechanisms of thrust production in marine fishes, drag relations in swimming fishes; (2) influence of hydrodynamic phenomena on circulatory and respiratory function in fishes; (3) determinants of circulatory system function in horseshoe crab, *Limulus polyphemus;* (4) locomotor muscle function at varying temperatures and levels of performance.

Humes, Arthur G., Professor of Biology Emeritus, Boston University

Research interests include systematics, development, host specificity, and geographical distribution of copepods associated with marine invertebrates. Current research is on taxonomic studies of copepods from invertebrates in the tropical Indo-Pacific area, and poecilostomatoid and siphonostomatoid copepods from deep-sea hydrothermal vents and cold seeps.

Strickler, Rudi J., Professor of Biology, Boston University

Use high-speed cinematography and special laser light optical systems with target tracking devices to observe zooplankton-algae, carnivorous-herbivorous zooplankton, and fish-zooplankton interactions. Lab and field results show the degree to which abiotic forces influence the evolution of species, feeding guilds, and predator-prey interactions. Additional topics in the feeding ecology of crinoids, bryozoans and other suspension feeding invertebrates enhance perception of the first consumer level in the aquatic food chain.

Staff

Costello, John, Research Associate

Tamm, Sidney L., Associate Professor of Biology, Boston University

We investigate the mechanism and control of diverse types of motility and behavior on the organismal, cellular, and subcellular levels. Techniques include electrophysiology, microinjection, laser microsurgery, cytochemistry and histochemistry, video-enhanced phase contrast and interference contrast mi-

croscopy, biochemistry, transmission and scanning EM, and freezer-etch EM. Other studies include the role of massive actin filament bundles, biology of prokaryotic-eukaryotic cell associations, fluid dynamics and biomechanical coordination of cilia, and predator-prey interactions of herbivorous-carnivorous macroplankton.

Staff

Tamm, Signhild, Research Associate

Valiela, Ivan, Professor of Biology, Boston University

Research emphasis is on structure and function of salt marsh ecosystems and coastal embayments, including the processes of predation, herbivory, decomposition, and nutrient cycles. A parallel line of work, with more applied aspects, is eutrophication in coastal marine communities and interactions between watersheds and coastal waters.

Staff

Dzierzewsky, Michelle, Research Assistant
Lohmann, Denah, Research Assistant
Sarda, Rafael, Research Associate
Taylor, Margery, Research Assistant

Visiting Investigators

Woodward, Helen, Undergraduate Researcher

Copeland, D. Eugene, Investigator, Marine Biological Laboratory

Electron microscopy of luminescent organs (photophores) in deep sea fish; gas secretion in swimbladders of deep sea fish; and osmoregulatory tissue in *Limulus*.

The Ecosystems Center

The Center was established in 1975 to promote research and education in ecosystems ecology. Nine scientists study the terrestrial and aquatic ecology of a wide variety of ecosystems ranging from northern Europe (trace gas emission from acid-rain affected forests) to the Alaskan Arctic (long-term studies of the control tundra, lake, and stream biota) to Buzzards Bay (controls of anaerobic decomposition). Many projects, such as those dealing with sulfur transformations in lakes and nitrogen cycling in the forest floor, investigate the movements of nutrients and make use of the Center's mass spectrometry laboratory (directed by Brian Fry) to measure the stable isotopes of carbon, nitrogen, and sulfur. The research results are applied wherever possible to questions of the successful management of the natural resources of the earth. In addition, the ecological expertise of the staff is made available to public affairs groups and government agencies who deal with such problems as acid rain, ground water contamination, and possible carbon dioxide-caused climate change. There are opportunities for postdoctoral fellows.

Administrative staff

Hobbie, John E., Director
Helfrich, John V. K.
Semino, Suzanne
Griffin, Elisabeth A.

Scientific staff

Hobbie, John E., Senior Scientist
Melillo, Jerry M., Associate Scientist
Peterson, Bruce J., Associate Scientist
Shaver, Gaius R., Associate Scientist
Fry, Brian D., Assistant Scientist
Giblin, Anne E., Assistant Scientist
Nadelhoffer, Knute J., Assistant Scientist
Rastetter, Edward B., Assistant Scientist
Steudler, Paul A., Research Specialist

Consultants

Bowles, Francis P.
Jordan, Marilyn J.

Education staff appointments

Bowden, Richard D., Postdoctoral Fellow
Kling, George W., Postdoctoral Fellow
Mc Ivor, Carole, Postdoctoral Fellow
Raich, James, Postdoctoral Fellow

Technical staff

Banta, Gary, Research Assistant
Dornblaser, Mark, Research Assistant
Downs, Margaret, Research Assistant
Hooper, David, Research Assistant
Kicklighter, David, Research Assistant
Laundre, Jim, Research Assistant
Mc Kerrow, Alexa, Research Assistant
Michener, Bob, Research Assistant
O'Brien, Margaret, Research Assistant
Regan, Kathleen, Research Assistant
Tucker, Jane, Research Assistant
Turner, Andrea R., Research Assistant
White, David, Research Assistant

Fein, Alan, Investigator, Laboratory of Sensory Physiology, Marine Biological Laboratory, and Department of Physiology, Boston University School of Medicine

Physiology and biochemistry of invertebrate photoreceptors. Research into the inositol polyphosphate pathway in transduction in *Limulus* ventral photoreceptors in response to light and squid photoreceptors. Recent work: studying oxygen consumption in *Limulus* ventral photoreceptors in response to light.

Staff

Payne, Richard, Assistant Scientist
McBride, Jim, Technician
Wood, Susan, Boston University Marine Program Graduate Student

Grassle, Judith P., Senior Scientist, Marine Biological Laboratory

Studies on the population genetics and ecology of marine invertebrates living in disturbed environments, especially of sibling species in the genus *Capitalla* (Polychaeta).

Staff

Mills, Susan W., Research Assistant

Halvorson, Harlyn O., President and Director, Marine Biological Laboratory

Research focuses on the regulation of phosphate metabolism in *Acinetobacter lwoffi* in particular, synthesis and utilization of polymerized inorganic phosphate (polyphosphate), and the process of spore germination in *Bacillus subtilis*.

Staff

Chikarmane, Hemant, Research Associate
Pratt, Sara, Research Assistant

Visiting investigators

Atwood, Kim, Columbia University
Kornberg, Hans, University of Cambridge
Keynan, Alex, Memorial Sloan Kettering Cancer Center
Vincent, Walter, University of Delaware
Doig, Stephen, Science Writing Fellow, *The Miami Herald*

Harosi, Ferenc I., Investigator, Associate Scientist, Marine Biological Laboratory, Boston University School of Medicine

Native and analogue visual pigment studies in situ. The major technique is microspectrophotometry. Retinal photoreceptors are obtained from amphibian, lizard, fish and primate eyes.

Staff

Zahajszky, Tibor, Research Associate

Visiting investigators

Cornwall, Carter, Boston University School of Medicine
Hawryshyn, Craig W., McMaster University, Hamilton, Ontario, Canada
Petry, Heywood M., SUNY, Stony Brook

Inoué, Shinya, Distinguished Scientist, Marine Biological Laboratory, and the University of Pennsylvania

Mechanism of mitosis and related motility. Development of high resolution 3-D video microscope systems.

Staff

Anniballi, Dyon, Programming Engineer, Cornell University College of Engineering
Boyd, Steven, Programming Engineer, Cornell University College of Engineering
Green, Daniel, Programming Engineer, University of Illinois, School of Engineering
Inoue, Theodore, Programming Engineer, Cornell University College of Engineering
Rubinow, Jerry, Programming Engineer, Cornell University College of Engineering
Shimomura, Sachi, Research Assistant, Stanford University
Taracka, Robert, Research Assistant
Woodward, Bertha M., Laboratory Manager

Visiting investigators

Bajer, Andrew S., University of Oregon
Burgos, Mario H., University of Cuyo, Mendoza, Argentina
Fukui, Yoshio, Northwestern University Medical School
Kiehart, Daniel P., Harvard University
Salmon, Edward D., University of North Carolina
Sardet, Christian, Biol. Cell. Marine, Ville France-Sur-Mer
Silver, Robert B., University of Wisconsin

Jaffe, Lionel, Senior Scientist, Marine Biological Laboratory, and Director, National Vibrating Probe Facility

We are exploring the roles of ionic currents, gradients, and waves in controlling development. We focus on controls *of* pattern and *by* calcium ions.

Staff

Kuhtreiber, Wiel, Physiologist
Shipley, Alan, Technician
Williams, Phillip C., Engineer
Speksnijder, Annelies, Postdoctoral Fellow, Royal Veterinary University, Denmark

Visiting investigators

Asman, Sally, Harvard University
Baumann, Steve, EPA, Research Triangle Park, NC
Biggers, John, Harvard Medical School
Bowdan, Elizabeth, University of Massachusetts
Chen, Tsung-Hsien, Academia Sinica, Taiwan
Crawford, Karen, Swarthmore College
Cullander, Chris, University of California, S. F.
Devlin, Leah, University of Rhode Island
Dickey, Joe, Clemson College
Diehl-Jones, W. L., University of Manitoba, Canada
Fink, Rachael, Mount Holyoke College
Holtug, Klars, Royal Veterinary University, Denmark
Kunkel, Joseph, University of Massachusetts
Mladenov, Phillip, Mount Allison University, New Brunswick, Canada
Payne, Richard, University of Maryland
Pethig, Ron, University College of North Wales, U. K.
Sardet, Christian, Station Marine Villelfranche sur mer, France
Trinkaus, John, Yale University
Troxell, Cindy, University of Colorado
Ver Achtert, Barend, University of Leuven, Belgium
Wyman, Robert, Yale University

Leibovitz, Louis, Director, Laboratory for Marine Animal Health, Marine Biological Laboratory, and Professor, Department of Avian & Aquatic Animal Medicine, New York State College of Veterinary Medicine

The laboratory provides diagnostic, consultative, research and educational services to the institutions and scientists of the Woods Hole community concerned with marine animal health. Diseases of wild, captive, and cultured animals are investigated.

Staff

Abt, Donald A., Co-Investigator, University of Pennsylvania
Bullis, Robert A., Senior Research Associate, Cornell University
Hansen, Sandra B., Secretary, Cornell University
McCafferty, Michelle, Histological Technician, Cornell University
Moniz, Priscilla C., Administrative Secretary
Wadman, Elizabeth A., Microbiological Technician, Cornell University

Visiting investigators

Koulish, Sasha, College of Staten Island, CUNY
Lewbart, Gregory, University of Pennsylvania

Rabinowitz, Michael, Investigator, Marine Biological Laboratory, and Instructor in Neurology, Harvard Medical School

Measurement of lead in baby teeth to see if lead exposure at different ages, recorded at different sites within teeth, are related to child development.

Staff

Lewandowski, Ann, Research Assistant, Harvard Medical School

Reese, Thomas S., Chief, Laboratory of Neurobiology, Marine Biological Laboratory, NINCDS/NIH

The Laboratory of Neurobiology is concerned with the secretory mechanism underlying synaptic transmission, the mechanism of organelle movement underlying axoplasmic transport, and the organization of neural cytoplasm.

Staff

Andrews, S. Brian, Research Associate
Bechtold-Imhof, Ruth, Research Assistant
Cheng, Toni, Research Associate
Chludzinski, John, Research Technician
Coyle, Jo-Anne, Secretary
Gallant, Paul, Research Associate
Garbus-Gooch, Cynthia, Research Assistant
Hammar, Katherine, Research Assistant
Khan, Shahid, Visiting Research Associate
Reese, Barbara F., Research Technician
Sheetz, Michael P., Visiting Research Associate
Schnapp, Bruce J., Research Associate
Tatsuoka, Hozumi, Research Associate
Terasaki, Mark, Research Associate

Reinisch, Carol L., Investigator, Marine Biological Laboratory, and Chairperson, Department of Comparative Medicine, Tufts University School of Medicine

Our laboratory is studying hematopoietic neoplasia, a leukemia-like disease of soft shell clams. Monoclonal antibodies developed by this laboratory and techniques in molecular biology are used to investigate the differences between normal and leukemic cells and their ontogeny.

Staff

Miosky, Donna, Laboratory Technician
Smolowitz, Roxanna, Postdoctoral Fellow

Shimomura, Osamu, Senior Scientist, Marine Biological Laboratory, and Boston University School of Medicine

Biochemical studies of the various types of bioluminescent systems. Preparation of the improved forms of aequorin for measuring intracellular free calcium

Staff

Shimomura, Akemi, Research Assistant

Visiting investigators

Musicki, Branislav, Harvard University
Nakamura, Hideshi, Harvard University

Stephens, Raymond E., Investigator, Marine Biological Laboratory, and Boston University School of Medicine

Biochemistry of microtubules in cilia, flagella, and the cytoplasm; mechanosensitivity and the control of ciliary movement.

Staff

Good, Michael J., Research Assistant
Oleszko-Szuts, Susan, Research Associate
Stommel, Elijah W., Research Associate, St. Elizabeth's Hospital

Visiting investigator

Holz, George G., Tufts University School of Medicine

Strumwasser, Felix, Director, Laboratory of Neuroendocrinology, Boston University School of Medicine, and Marine Biological Laboratory

This laboratory studies the molecular and cellular bases of two neural programs that regulate different important behaviors in the model mollusc *Aplysia*. Research is conducted on the mechanisms of the neuronal circadian oscillators located in the eyes. These circadian oscillators drive the circadian activity rhythm of the animal, which is concerned with the daily timing of food gathering and of prolonged rest. Additional research is conducted on a group of neuroendocrine cells that produce a peptide, "egg-laying hormone," that initiates egg laying and associated behaviors. The laboratory is interested in how the three-dimensional shape of this peptide hormone allows a highly specific interaction with its receptor and the intracellular processes that are triggered by it.

Staff

Eason, Barbara, Laboratory Assistant
Glick, David, Senior Postdoctoral Fellow
Hellmich, Mark, Graduate Student
Viele, Daniel P., Senior Research Assistant

Sussman, Raquel, Associate Scientist, Marine Biological Laboratory

Investigation of the molecular mechanism of DNA damage-inducible functions. Present studies deal with the structure-function relationships of λ repressor analyzed by immunological techniques.

Staff

McLaughlin, Jane, Research Assistant
Cornuel, Catherine, Research Assistant

Szuts, Ete Z., Investigator/Assistant Scientist, Marine Biological Laboratory, Laboratory of Sensory Physiology, and Department of Physiology, Boston University School of Medicine

Biochemical reactions (phosphorylation, inositide metabolism) that mediate the light-induced response of retinal photo-

receptors in both vertebrates (frog and cattle) and invertebrates (squid and *Limulus*).

Staff

Trapp, Susan C., Research Assistant

Visiting investigators

Clay, John R., Laboratory of Biophysics, NINCDS/NIH
Eckberg, William R., Howard University
Wood, Susan F., Boston University Marine Program

Whittaker, J. Richard, Senior Scientist, Marine Biological Laboratory

This research group studies the early gene control of cellular differentiation pathways (cell lineage determination) in embryos of tunicates and other marine invertebrate species.

Staff

Crowther, Robert, Research Assistant
Loescher, Jane L., Research Assistant
Meedel, Thomas H., Assistant Scientist

Visiting investigators

Arnold, John M., University of Hawaii
Collier, J. R., Brooklyn College
Heady, Judith E., University of Michigan-Dearborn (Sabbatical year, 1987–88)
Johnson, Carl D., Cambridge NeuroScience Research

Intern (Undergraduate)

Zeller, Robert, Boston University

XI. Honors

Friday Evening Lectures

Pickett-Heaps, Jeremy, University of Colorado at Boulder, 26 June, "*Mitosis—Some Novel Prospects Concerning an Old Enigma*"

Dowling, John, Harvard University, 3 July, Lang Lecture, "*Neuromodulation: The Eyes Have It*"

Tilney, Lewis, University of Pennsylvania, 10 July, "*What Actin Tells Us If We Listen*"

Greengard, Paul, The Rockefeller University, 16, 17 July, Forbes Lectures, "*Neuronal Phosphoproteins as Mediators of Signal Transduction: Presynaptic Effects; Neuronal Phosphoproteins as Mediators of Signal Transduction: Postsynaptic Effects*"

Alkon, Daniel, NINCDS, NIH, and Marine Biological Laboratory, 24 July, NIH Centennial Lecture, "*Cellular Substrates of Associative Memory: What the Snail's Eye Tells the Rabbit's Brain*"

Davidson, Eric H., California Institute of Technology, 31 July, "*Spatial Patterns of Differential Gene Expression in the Early Sea Urchin Embryo*"

Swazey, Judith P., The Acadia Institute, 6 August, Hiroshima Day Lecture, "*But I Have Promises to Keep: Reflections on the Moral Life of Science*"

Raven, Peter, Missouri Botanical Garden, 7 August, Monsanto Biotechnology Lecture, "Population, Poverty and Politics in the Tropics"

Randi, James, Conjurer, Lecturer and MacArthur Fellow, 14 August, "*Search for the Chimera*"

Capuzzo, Judith McDowell, Woods Hole Oceanographic Institution, 21 August, "*Cross Ecosystem Comparison of Waste Disposal Impacts: The Scientific Basis for Decision Making of Environmental Issues*"

Gerbi, Susan, Brown University, 28 August, "*Evolution of a Molecular Machine: The Ribosome*"

Frank A. Brown, Jr. Memorial Readership

Hill, Richard W., Michigan State University

Robert Day Allen Fellowship

Suprenant, Kathy A., University of Kansas

Frederik B. Bang Fellowship Fund

Lewbart, Gregory A., University of Pennsylvania Veterinary School
Tablin, Fern, University of California School of Veterinary Medicine

Stephen W. Kuffler Fellowships

Barry, Susan R., University of Michigan
Ehrlich, Barbara E., University of Connecticut Health Center

H. B. Steinbach Fellowships

Bass, Andrew H., Cornell University
Gilbert, Susan P., Pennsylvania State University

MBL Summer Fellowships

Barry, Michael A., Albert Einstein College of Medicine
Borst, David W., Illinois State University
Marcum, James A., Harvard Medical School
Pierson, Beverly K., University of Puget Sound

Biology Club of New York

Roberts, Michael W., Wesleyan University

Father Arsenius Boyer Scholarship Fund

Dell'Arciprete, Olga Patricia, Instituto National de Investigacion, Argentina

Gary N. Calkins Memorial Scholarship

Dell'Arciprete, Olga Patricia, Instituto National de Investigacion, Argentina

Frances S. Claff Memorial Scholarship

Roberts, Michael S., Wesleyan University

Edwin Grant Conklin Memorial Scholarship

Bisbal, Gustavo A., Instituto National de Investigacion, Argentina

Lucretia Crocker Endowment Fund

Dell'Arciprete, Olga Patricia, Instituto National de Investigacion, Argentina
Krishnan, Thankavel, Annamalai University, India

Aline D. Gross Scholarship

Bloom, Theodora L., University of Cambridge, U. K.
Simoncini, Luciana, University of Southern California

Caswell Grave Scholarship

Fernandez, Miriam E., Instituto de Biologia Marina y Pesquera, Argentina
Krishnan, Thankavel, Annamalai University, India

Merkel H. Jacobs Scholarship

Sadovsky, Sebastian, Universidade Federal do Espirito, Brazil

Arthur Klorfein Fund Scholarship

Govind, Shubha, Princeton University
Koenig, Gerd, Max Planck Institut fur Entwicklungsbiologie, FRG
Monpetit, Isabelle, McGill University, Canada
Sturm, Karin S., Linus Pauling Institute of Science & Medicine
Zhang, Wei WZ, University of Texas Health Science Center

Jacques Loeb Fellowship

Sadovsky, Sebastian, Universidade Federal do Espirito, Brazil

Lucille P. Markey Charitable Trust Scholarship

Banin, Eyal, Hebrew University, Hadassah Medical School, Israel
Barton, Nelson R., University of Miami Medical School
Bisbal, Gustavo A., Instituto Nacional de Investigacion, Argentina
Byrne, Patricia P. B., University College, Ireland
Charrier Melillan, Maria Elena, Universidad Nacional, Argentina
Cyr, Janet L., University of Texas Health Science Center
Dong, Feng, Oregon State University
Drysdale, Thomas A., University of Toronto, Canada
Ferber, Daniel M., The Johns Hopkins University
Gifford, Andrew N., St. Andrews University, Scotland
Ito, Minami, Osaka University, Japan
Jongejan-Zivkovic, Danica D., University of Utrecht, The Netherlands
Kelly, Gregory M., University of Manitoba, Canada
Kernan, Maurice J., University of Wisconsin
Kronidou, Nafsika, Dartmouth College
Kuppe, Andreas, University of Oregon
Larmet, Yves, Centre National de la Recherche Scientifique, France
Libersat, Frederic, The Hebrew University of Jerusalem, Israel
Mackey, Harris M., Columbia Medical School
Miller, Rita K., Northwestern University
Plopper, George E., Harvard University
Racoosin, Esther L., Harvard Graduate School of Arts and Sciences
Saunders, Kim B., Harvard Medical School
Sawin, Kenneth Eric, Stanford University
Sjolander, Anders J., University of Sweden, Stockholm
Slatter, Andrew F. G., Oxford University, UK
Tendler, Miriam, Oswaldo Cruz Institute, Brazil
Turner, Christopher, E., University of North Carolina
Walker, Richard A., University of North Carolina
Yutzey, Katherine E., Purdue University

S. O. Mast Founders Scholarship

Sadovsky, Sebastian, Universidade Federal do Espirito, Brazil

Allen R. Memhard Scholarship

Sadovsky, Sebastian, Universidade Federal do Espirito, Brazil
Roberts, Michael S., Wesleyan University

Faith Miller Endowment

Byrne, Patricia P. B., University College, Ireland

James S. Mountain Memorial Fund Scholarship

Ferber, Daniel M., The Johns Hopkins University
Miller, Rita K., Northwestern University
Plopper, George E., Harvard University
Racoosin, Esther L., Harvard Graduate School of Arts and Sciences
Saunders, Kim B., Harvard Medical School

Planetary Biology Internship

Sment, Karen A., University of Illinois

Society of General Physiologists

Gruner, Wendy, SUNY, Stony Brook
Satterwhite, Lisa L., Johns Hopkins University
Saunders, Kim B., Harvard Medical School
Van Vactor, David L., Jr., University of California, Los Angeles

Marjorie W. Stetten Scholarship Fund

Montpetit, Isabelle, McGill University, Canada

Surdna Foundation Scholarship

Braun, Gotz, Institut fur Tierphysiologie, FRG
Corfas, Gabriel, Weizmann Institute of Science, Israel
Govind, Shubha, Princeton University

Han, Jin K., University of California, Davis
Sadovsky, Sebastian, Universidade Federal do Espirito, Brazil

William Morton Wheeler Family Founders' Scholarship

Roberts, Michael S., Wesleyan University

XII. Institutions Represented

U. S. A.

Academy of Natural Sciences of Philadelphia
Alabama, University of
Albert Einstein College of Medicine of Yeshiva University
American Bionetics, Inc.
Ames Division, Miles Laboratories
Amherst College
Arizona State University
Arizona, University of
Atlantex & Zeiler Instrument Corp.
Axon Instruments, Inc.
Baylor College of Medicine
Beckman Instruments, Inc.
Bellco Glass, Inc.
Belmont Abbey College
Beloit College
Bethesda Research Laboratories
Bio-Rad
Bioanalytical Systems, Inc.
Biodyne Electronics
Boston University
Boston University School of Medicine
Brandeis University
Brick Township School, Brielle, N. J.
Brigham & Women's Hospital
Brinkman Instruments, Inc.
Brown University
Bryn Mawr College
California Institute of Technology
California, University of, School of Medicine, San Francisco
California, University of, School of Pharmacy, San Francisco
California, University of, School of Veterinary Medicine
California, University of, Berkeley
California, University of, Davis
California, University of, Irvine
California, University of, Los Angeles
California, University of, Riverside
California, University of, San Diego
California, University of, San Francisco
Cambridge Instruments, Inc. (Reichert-Jung)
Cambridge Neuroscience Research
Cambridge Technology
Carnegie Institution of Washington
Carnegie-Melon University
Case Western Reserve University
Case Western Reserve University School of Medicine
Chicago, University of
Chicago, University of, School of Medicine
Children's Hospital National Medical Center
Ciba Corning Diagnostics Corporation
Ciba-Geigy Corp.
Cincinnati, University of
Cincinnati, University of, School of Medicine
Clemson College
COHU, Inc.
Cold Spring Harbor Laboratories
College of the Academy of the New Church
Colorado College
Colorado, University of
Colorado Video
Columbia University
Connecticut, University of
Connecticut, University of, Health Center
Cornell University
Cornell University Medical College
Cornell University College of Engineering
Crimson Camera
Dagan Corporation
Dage-MTI, Inc.
Dartmouth College
Dartmouth College Medical School
David Kopf Instruments
Delaware, University of
Delta State University
Donsanto Corporation
DuPont Company (Sorvall)
DuPont, E. I. DeNemours & Co.
Duke University
Duke University Medical Center
E-C Apparatus Corporation
E.G.&G.
Earlham College
East Carolina University School of Medicine
Eastern Airlines, Inc.
Eastern Illinois University
Emory University
Emory University School of Medicine
Florida, University of
Flow Laboratories, Inc.
Food and Drug Administration
Fred Hutchinson Cancer Research Center
G. W. Hannaway Associates
General Scanning
George Washington University
Georgetown University
Georgia, University of
Gilson Medical Electronics, Inc.
Grass Instrument Company

Hacker Instruments, Inc.
Hahnemann Medical College & Hospital
Hamilton College
Hampshire College
Harvard Graduate School of Arts and Sciences
Harvard Medical School
Harvard School of Public Health
Harvard University
Harvard University School of Medicine
Hawaii, University of
Hebron Academy
Hoefer Scientific Instruments
Houston Instruments
Howard Hughes Medical Institute
Howard University
ICN Biomedicals, Inc.
Illinois Institute of Technology
Illinois State University
Illinois, University of
Illinois, University of, College of Medicine
Indec Systems, Inc.
Indiana University
Institute For Basic Research in Developmental Disabilities
International Biotechnologies, Inc.
Iowa, University of
Isco, Inc.
JEOL
Jewish Hospital of St. Louis
Johns Hopkins University
Johns Hopkins University School of Medicine
Johns Hopkins University School of Hygiene & Public Health
Kansas City Art Institute
Kansas, University of
Kip & Zonan
LKB Instruments, Inc.
Lab-Line Instruments
Leitz, E., Inc.
Linus Pauling Institute of Science & Medicine
Los Alamos National Laboratory
Louisville University of, School of Medicine
Ludlum Measurements, Inc.
M. D. Anderson Hospital
Mahwah High School, N. J.
Marquette University
Mary Flagler Cary Arboretum, Institute of Ecosystem Studies
Maryland, University of
Maryland, University of, School of Medicine
Maryland, University of, Chesapeake Biological Laboratory
Massachusetts Institute of Technology
Massachusetts, University of, Amherst
Massachusetts, University of, Boston
Mayo Clinic, Rochester, MN
Mayo Graduate School of Medicine
Medical Biological Institute
Medical College of Ohio
Medical College of Virginia
Medical Systems Corporation
Medical University of South Carolina
Memorial Sloan Kettering Cancer Center
Merck, Sharp & Dohme Research Laboratory
Miami, University of
Miami, University of, School of Medicine
Michigan State University
Michigan, University of
Millipore Corporation
Minnesota, University of
Missouri, University of
Monsanto Company
Montana State University
Mount Holyoke College
Mountfield Corporation
Mt. St. Mary's Academy
National Aeronautical & Space Administration
National Cancer Institute
National Institute on Alcohol Abuse and Alcoholism/NIH
National Institute of Allergy and Infectious Diseases/NIH
National Institute of Environmental Health Sciences/NIH
National Institutes of Mental Health/NIH
National Institute of Neurological and Communicative Disorders and Strokes/NIH
New Brunswick Scientific Co., Inc.
New College of University of South Florida
New Hampshire, University of
New Jersey Medical School
New Mexico, University of, School of Medicine
New York State Institute for Basic Research
New York State Institute for Basic Research in Developmental Disabilities
New York University Medical Center
New York, City University of, Bernard M. Baruch College
New York, City University of, Brooklyn College
New York, City University of, City College
New York, City University of, Hunter College
New York, City University of, Lehman College
New York, City University of, Mt. Sinai School of Medicine
New York, State University of, Downstate Medical Center
New York, State University, Health Science Center at Stony Brook
New York, State University, Upstate Medical Center
New York, State University at Stony Brook

NIEMS
Nikon, Inc.
North Carolina State University
North Carolina, University of
North Carolina University of, School of Medicine
Northeastern University
Northwestern University Medical School
Northwestern University
Oklahoma, University of
Olympus Corporation of America
Optical Elements Corp.
Oregon State University
Oregon, University of
Parma City School, OH
Pennsylvania State University
Pennsylvania, University of
Pennsylvania, University of, School of Dental Medicine
Pennsylvania, University of, School of Medicine
Pennsylvania, University of, Veterinary School
Pharmacia, Inc.
Photometrics, Ltd.
Photonic Microscopy, Inc.
Pittsburgh, University of, School of Medicine
Pomona College
Princeton University
Puerto Rico, University of
Puget Sound, University of
Purdue University
Quanta Systems, Inc.
Quantex Corporation
R & M Biometrics Corporation
R/C Electronics
RadioAnalytic, Inc.
Research Imaging Systems, Inc.
Research Institute of Molecular & Cellular Biology
Rhode Island, University of
Rice University
Rochester, University of
Rochester, University of, Medical Center
Rockefeller Foundation
Rockefeller University
Rush Medical Center
Rush University
Rutgers University
Saint Mary-of-the-Woods College
Saint Elizabeth's Hospital, MA
Savant Instruments, Inc.
Schleicher & Schuell, Inc.
Science Applications International Corp.
Shodair Children's Hospital
Showa University Research Institute
South Carolina, University of
South Florida, University of
Southern California, University of
Southern California, University of, Los Angeles
Southern California, University of, School of Medicine
Southern Louisiana State University
Spex Industries, Inc.
Stanford University
Stanford University Medical School
Stonehill College
Sutter Instrument Company
Swarthmore College
Syracuse University
Technical Products International, Inc.
Temple University
Texas Christian University
Texas Southern University
Texas, University of, Austin
Texas, University of, Health Science Center, Dallas
Texas, University of, Health Science Center, Houston
Texas, University of, Medical Branch, Galveston
Texas, University of, Medical School
Thomas Jefferson University
Trident Electronics
Tufts New England Medical Center
Tufts University
Tufts University School of Medicine
Tufts University School of Veterinary Medicine
United States Environmental Protection Agency
United States Food and Drug Administration
Universal Imaging Corp.
University Hospitals of Cleveland
Vanderbilt University
Vassar College
Virginia Polytechnic Institute and State University
Virginia, University of
Wake Forest University, Bowman Gray School of Medicine
Washington State University
Washington University
Washington University School of Medicine
Washington, University of
Washington, University of, School of Medicine
Waters Associates
Wesleyan University
Wheaton College
Williams College
Wisconsin, University of
Wisconsin, University of, School of Veterinary Medicine
Woods Hole Oceanographic Institution
Worcester Foundation for Experimental Biology
Worcester Memorial Hospital
Worcester State College
World Precision Instruments
Yale University
Yale University School of Medicine
Yale University School of Public Health
Zeiss, Carl, Inc.

Foreign Institutions

Academia Sinica, Taiwan
Adelaide, University of, Australia
Aerolineas Argentinas
All India Institute of Medical Sciences, India
Annamalai University, India
Basel, University of, Switzerland
Bedford Institute of Oceanography, Canada
Berlin, University of, FRG
Biol. Cell. Marine, Ville France-Sur-Mer, France
Braunschweig University, FRG
Cambridge University, UK
Cambridge, University of, UK
Catania, University of, Italy
Central University of Venezuela
Centre National de la Recherche Scientifique, France
Centro National Patagonico, Argentina
Cuyo, University of, Mendoza, Argentina
Copenhagen, University of, Denmark
Ecole Normale Superieure, France
Friedrich Miescher-Institut, Switzerland
Glasgow, University of, Scotland
Goteborg, University of, Sweden
Hadassah Medical School, Israel
Hebrew University of Jerusalem, Israel
Heidelberg, University of, FRG
Imperial College of Science and Technology, UK
Institut fur Tierphysiologie, FRG
Institute of Biological Research, Yugoslavia
Instituto de Biologia, Argentina
Instituto de Histologia y Embriologia, Argentina
Instituto de Investigacion Medica, Argentina
Instituto di Biologia Cellulare, Italy
Instituto Internacional de Estudios Avanzados, Venezuela
Instituto Nacional de Investigacion, Argentina
Instituto Venezolanode Investigaciones Cientifican, Venezuela
International Lab. for Research on Animal Diseases, Kenya
Japan, University of, Japan
Konstanz, University of, FRG
Kyoto University, Japan
L'Ecole des Hautes Etudes, Le Sorbonne, France
Leeds, University of, UK
Leuven, University of, Belgium
Liverpool School of Tropical Medicine, UK
Manitoba, University of, Canada
Max-Planck Institute, FRG
McGill University, Quebec, Canada
Memorial University of Newfoundland, Canada
Mikrobiologisches Institut, Switzerland
Montreal Neurological Institute, Canada
Mount Allison University, New Brunswick, Canada
Naples Zoological Station, Italy
Naples, University of, Italy
National Polytechnical Institute, Mexico
National University of Mexico, Mexico
Onchocerciasis Control Programme in W. Africa, W. Africa
Osaka University, Japan
Oswaldo Cruz Institute, Brazil
Ottawa, University of, Canada
Oxford University, UK
Philipps Universitat, FRG
Queen's University, Canada
Regensberg, University of, FRG
Rome, University of, Italy
Royal Veterinary University, Denmark
St. Andrews University, Scotland
St. Georges Hospital Medical School, UK
Station Zoologique, France
Stockholm, University of, Sweden
Strathclyde, University of, Scotland
Sussex University, UK
Sweden, University of, Stockholm
Technical University of Munich at Garching, FRG
Toronto, University of, Canada
Toyohashi University of Technology, Japan
Tromso, University of, Norway
Ulm, University of, FRG
Universidad Nacional de Mar del Plata, Argentina
Universidade Federal do Espirito, Brazil
Universita Degli Studi Di Napoli, Italy
University College, Ireland
University College of North Wales, UK
Uppsala University, Sweden
Utrecht, University of, Netherlands
Warwick, University of, UK
Weizmann Institute of Science, Israel
Yamaguchi University, Japan
Zoological Station, Italy
Zoologisches Institut der Universitat, Heidelberg, FRG

XIII. Laboratory Support Staff

Including Persons Who Joined or Left the Staff During 1987

Biological Bulletin

Metz, Charles, B., Editor
Bauer, Diane
Clapp, Pamela L.
Mountford, Rebecca J.

Buildings and Grounds

Cutler, Richard D., Services, Projects, and Facilities Manager
Lehy, Donald B., Superintendent

Anderson, Lewis B.
Baldic, David P.
Blunt, Hugh F.
Bourgoin, Lee E.
Brunette, Clifford J.
Carini, Robert J.
Collins, Paul J.
Conlin, Henry P.
Finegan, Timothy B.
Fuglister, Charles K.
Gibbons, Roberto G.

Gonsalves, Walter W., Jr.
Illgen, Robert F.
Jennings, David A.
Lewis, Ralph H.
Lochhead, William M.
Lunn, Alan G.
MacLeod, John B.
McAdams, Herbert, III
Mills, Stephen A.
Rattacasa, Frank
Rossetti, Michael
Schoepf, Claude
Schwamb, Peter J.
Varao, John
deVeer, Robert L.
Ward, Frederick
Weeks, Gordon W.
Whittaker, William
Windle, Irvin

Controller's Office

Speer, John W., Controller
Binda, Ellen F.
Campbell, Ruth B.
Davis, Doris C.
Gilmore, Mary F.
Godin, Frances T.
Hobbs, Roger W., Jr.
Hough, Rose A.
Mahan, Joan M.
O'Brien-Sibson, Patricia J.
Oliver, Elizabeth
Tollios, Constantine

Copy Service Center

Gibson, Caroline F.
Jackson, Jacquelyn F.
Mountford, Rebecca J.

Development Office

Ayers, Donald E., Director
Lyons, Elaine D.
Thimas, Lisa T.

Director's Office

Halvorson, Harlyn O., President/Director
Whittaker, J. Richard, Acting Director
Berthel, Dorothy
Clark, Catharine T.
Epstein, Ray L.
Kinneally, Kathleen R.

Gray Museum

Armstrong, Ellen P.
Montiero, Eva

Housing

King, LouAnn D., Conference Center and Housing Manager
Adolf, Bozena
Andrews, Loretta
Baptiste, Winnie
Chamberlain, Bonny
Eddy, Kristine A.
Ellsworth, Lynne M.
Hamilton, Heather A.
Heins, Christine
Johnson, Frances N.
Kuil, Elisabeth
Leach, Adele
Lewis, Sheryl H.
Lewis, Shirley A.
McNamara, Noreen
Palmer, Doreen P.
Price, Dale L.
Ruff, Corinne M.

Library

Fessenden, Jane, Librarian
Ashmore, Judith A.
Corbett, Marguerite
Mirra, Anthony J.
Mountford, Rebecca J.
Munson, Robin
Nelson, Heidi
Norton, Catherine N.
Pratson, Patricia G.
deVeer, Joseph M.

Marine Resources

Valois, John J., Manager
DeGiorgis, Joseph
Enos, Edward G., Jr.
Enos, Joyce B.
Fahle, Scott
Fisher, Harry T., Jr.
Frank, Donald S.
Hanley, Janice S.
Moniz, Priscilla
Tassinari, Eugene

Animal Care

Povio, Sandra
Tripp, Gretchen

MBL Associates Liaison

Scanlon, Deborah

Public Information Office

Liles, George W., Jr., Director
Anderson, Judith L.
Crosby, Carol
Dzierzeski, Michelle J.
Hoff, Linde R.
Pauk, Christine

Research Services

Mattox, Andrew H., Safety Officer
Barnes, Franklin D.
Evans, William A.
Geggatt, Richard E.
Golder, Linda M.
Golder, Robert J.
Hall, Lionel G., Jr.
Hodge, Alan J.
Kerr, Louis M.
Martin, Lowell V.
Mercurio, Kimberley
Monteiro, Dana
Myette, Vincent J.
Nichols, Francis H., Jr.
Ross, Darcy
Sadowski, Edward A.
Sanger, Richard H., Jr.
Sylvia, Frank E.

Sponsored Programs

Howard, Joan E., Coordinator
Roth, Joyce J., Assistant Administrator
Casiles, Phyllis B.
Dwane, Florence
Ferzoco, Susan J.
Huffer, Linda
O'Brien-Sibson, Patricia J.

Telephone Office

Baker, Ida M.
Geggatt, Agnes L.
Grace, Patricia A.

1987 Summer Support Staff

Allen, Tania L.
Armstrong, Nicholas B.
Armstrong, Timothy C.
Ashmore, Lynne E.
Becker, Sharron A.
Beetlestone, Linda
Beliveau, Christine A.
Burdick, Jonathan R.
Burr, Michelle
Burr, Suzanne
Butler, Kelly A.
Cadwalader, George, Jr.
Callagy, Kristen
Campbell, Andrew
Carrier, Michelle A.
Child, Malcolm S.
Collins, Jessica J.
Dickman, Michael C.
Dino, Victor H.
Donovan, Christine B.
Donovan, Jason P.
Felcyn, George D.
Hahn, Heidi
Hines, Kristen
Hodapp, John M.
Illingworth, Dawn
Ingersoll, David
Ireland, Lisa
Mackey, William T.
Magennis, Colleen A.
Magennis, Maureen P.
Manheim, Francesca
Marini, Michael F.
Martyna, Jonathan W.
McMenamin-Balano, Jonathan
Montroll, Charles
Nelson, Christen L.
Pachter, Jane E.
Parsons, Marc L.
Peal, Richard W.
Philbin, Linda M.
Remsen, Andrew W.
Richardson, Keith W.
Rickles, Andrew H.
Rose, Christine M.
Sadovsky, Sebastian
Shaw, Trevor P.
Shay, Pamela L.
Sheetz, Jonathan P.
Shipley, Michael
Sirrico, Jennifer M.
Sohn, Marcus
Stevens, Lisa D.
Sun, Ya-ping
Sylvia, James A.
Valois, Francis X.
Wetzel, Ernest D.
Woodward, Helen

Reference: *Biol. Bull.* **175**: 65–78. (August, 1988)

Development of Nerve Cells in Hydrozoan Planulae: II. Examination of Sensory Cell Differentiation Using Electron Microscopy and Immunocytochemistry

VICKI J. MARTIN

Department of Biological Sciences, University of Notre Dame, Notre Dame, Indiana 46556

Abstract. The development of sensory cells in hydrozoan planulae of *Halocordyle disticha* was examined using transmission electron microscopy and light immunocytochemistry. Sensory cells arise in the anterior end of the planula in the ectoderm at 24 hours postfertilization. These cells extend from the free surface of the planula to a ganglionic plexus located just above the mesoglea. The cytomorphosis of sensory cells is characterized by the appearance of a single apical cilium, microtubules, mitochondria, one to several Golgi complexes, electron-dense droplets, dense-cored vesicles, and neurites. The basal end of the sensory cell forms one to several processes (neurites) which contribute to the ganglionic plexus. Apical specialization of the sensory cell precedes basal differentiation. Sensory cells increase in number as planulae develop and many become organized into clusters of 3–6 cells distributed along the entire length of the planula. Within some of these clusters, two morphological types of sensory cells are discernible: light sensory cells and dark sensory cells. Light sensory cells outnumber the dark sensory cells and are the first sensory cells to appear at 24 hours postfertilization. Use of immunocytochemical techniques on wholemounts and paraffin-embedded sections of planulae demonstrates the presence of FMRFamide-like immunoactivity associated with some of the sensory cells. Such FMRFamide-like expression is first detected at 24 hours postfertilization in the anterior ectoderm of the planula. By 96 hours postfertilization, the spatial distribution of FMRFamide-like positive sensory cells is such that many are found in clusters along the entire anterior-posterior axis of the planula. There is, however, an abundance of FMRFamide-like positive cells in the anterior region of the planula just prior to metamorphosis. The apices and cell bodies of the sensory cells exhibit intense immunostaining, whereas the basal processes stain faintly. This study identifies neuropeptide-like substances in nerve cells of cnidarian larvae and demonstrates a developmental correlation between the time of appearance of the synthetic machinery of sensory cells with the pattern of expression of the FMRFamide-like peptide.

Received 26 October 1987; accepted 31 May 1988.

Introduction

Early light microscopists defined two types of nerve cells in cnidarians: sensory cells and ganglionic cells (Burnett and Diehl, 1964). Sensory cells are oriented perpendicular to the mesoglea with their apical ends contacting the outer free surface of the animal and their basal ends drawn out into processes. Ganglionic cells exhibit round perikarya and lie in the basal part of the ectoderm with their axes oriented parallel to the mesoglea. Furthermore, Westfall and associates have demonstrated that, in hydra, many types of sensory cells and ganglionic cells exist which can be classified as unipolar, bipolar, or multipolar depending on the number of processes extending from the perikaryon (Yu *et al.*, 1985).

Chemical synapses with electron-dense and dense-cored vesicles have been observed in the nervous systems of adult hydrozoans, scyphozoans, and anthozoans (Horridge and Mackay, 1962; Lentz and Barrnett, 1965; Jha and Mackie, 1967; Davis *et al.*, 1968; Westfall, 1970, 1973; Westfall *et al.*, 1971; Stokes, 1974; Peteya, 1975; Yamasu and Yoshida, 1976; Singla, 1978; Spencer, 1979). However, only recently has a specific peptide been identified in adult cnidarians that might be acting as a neurotransmitter (Grimmelikhuijzen and Graff, 1986; Grimmelikhuijzen and Groeger, 1987). Electron-dense droplets and dense-cored vesicles also have been identified in planular nervous systems (Martin, 1988), and

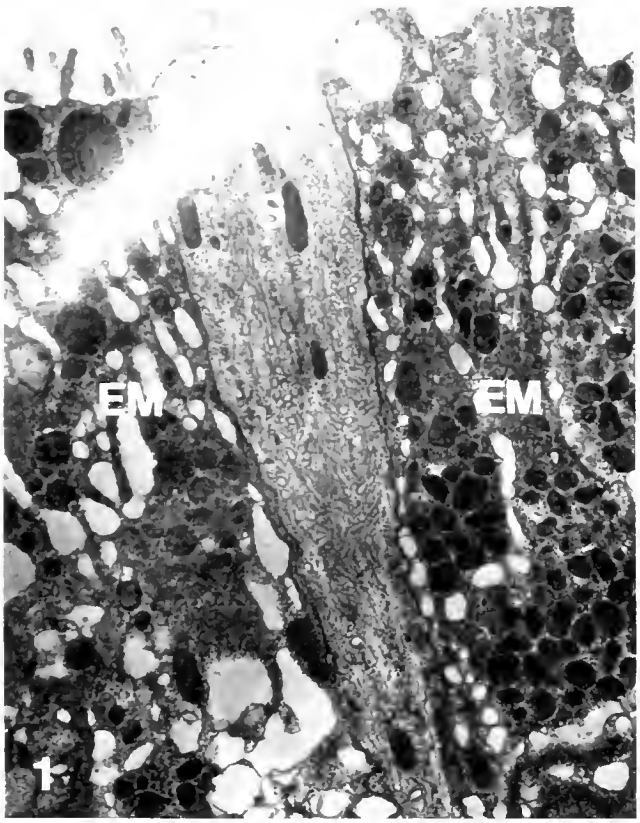
EM
EM
1

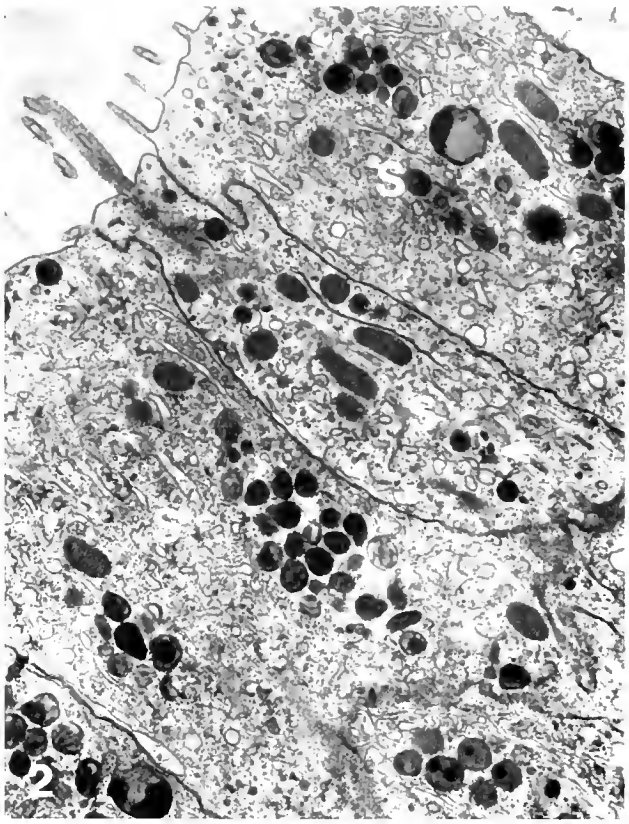
S
2


P
P
G
GP
B
M


D
D

Kolberg and Martin (1988) have demonstrated catecholamines in association with planular nerves. Furthermore, they provide evidence that such catecholamines may be functioning as neurotransmitters, neurohormones, or neuromodulators during embryogenesis (Kolberg and Martin, 1988).

A reagent (anti-FMRFamide) is available which will stain cells containing peptides ending in -Arg-Phe-NH_2. The work of Grimmelikhuijzen and associates suggests that, when this antiserum is applied to cnidarians, the peptides bound to it are likely to be related to pGlu-Gly-Arg-Phe-amide (PQGRFa) which is present in large amounts in nervous systems of adult anthozoans and probably also in scyphozoans and hydrozoans (Grimmelikhuijzen and Graff, 1986; Grimmelikhuijzen and Groeger, 1987). The question is: how early in development, and in what cells, is the gene for this peptide (or peptide family) expressed? The planula larva is a good system in which to examine this problem because the number of cell types in the larva is small, their arrangement is simple, and neither the variety nor the arrangement are very far from those of the adult (Martin and Thomas, 1980; Martin *et al.*, 1983; Thomas *et al.*, 1987; Martin, 1988).

In this study, the development of the planula of the marine hydrozoan *Halocordyle disticha* was followed with transmission electron microscopy to determine when sensory nerve cells appeared and when the synthetic machinery of these cells appeared. Different aged planulae were exposed to FMRFamide antiserum, and the pattern of expression of the FMRFamide-like peptide was correlated with the electron microscopic findings.

Materials and Methods

Mature colonies of *Halocordyle disticha* were collected from wharf pilings in Morehead City, North Carolina. Fronds from male and female colonies were placed together in large finger bowls of filtered seawater. The bowls were placed in the dark at 6:00 pm, and at 9:00 pm, early cleavage embryos were collected, placed in small finger bowls of seawater, and reared at 23°C.

Eight-hour embryos, as well as 10-, 16-, 24-, 48-, 72-, 96-, and 120-hour planulae, were prepared for transmission electron microscopy. The animals were fixed for 1 hour in 2.5% glutaraldehyde, pH 7.4, in 0.2 *M* phosphate buffer. They were postfixed for 1 hour in 2% osmium tetroxide, pH 7.2, in 1.25% sodium bicarbonate. The specimens were dehydrated in an ethanol series, infiltrated, and embedded in Spurr's embedding medium. Serial thin-sections were cut with a Porter-Blum MT-2B ultramicrotome, placed on 150-mesh copper grids, and stained with 3.5% uranyl acetate in ethanol followed by lead hydroxide. The grids were examined and photographed with a Hitachi H-600 transmission electron microscope. Thick plastic sections were also cut, placed on subbed glass slides, and stained with methylene blue-azure II.

To better visualize the basal processes of sensory cells, early cleavage embryos were cultured in seawater containing 0.01 *M* hydroxyurea until they reached the mature planula stage (Martin, 1985, 1986). These treated larvae were then prepared for transmission electron microscopy. Embryos reared continuously in hydroxyurea contain reduced numbers of ganglionic cells and slightly fewer ganglionic neurites, yet possess the same number of sensory cells as do comparable controls (Martin, 1985, 1986, pers. obs.). The sensory cells of hydroxyurea-grown planulae are morphologically identical to those of comparable controls, and their basal processes are more easily traceable due to the reduced size of the ganglionic plexus (Martin, 1985, 1986, pers. obs.).

Planulae of eight different ages, wholemounts and paraffin sections, were tested for their ability to bind a rabbit antiserum raised to FMRFamide (Immuno Nuclear Corporation). The planular ages included 10-, 16-, 24-, 36-, 48-, 72-, 96-, and 120-hour planulae. To visualize

Figure 1. Single light sensory cell (S) in the anterior ectodermal region of a 24 hour planula. The cytoplasm is filled with microtubules, Golgi cisternae, some rough endoplasmic reticulum, and a few mitochondria. EM, epitheliomuscle cell. ×8400.

Figure 2. Cluster of three light sensory cells (S) in the mid ectodermal region of a 72 hour planula. Each cell possesses an apical cilium and a cytoplasm rich in microtubules, Golgi cisternae, electron-dense droplets (arrow), and dense cored vesicles. ×11,200.

Figure 3. Ganglionic nerve cell (G) and ganglionic plexus (GP) at the base of the ectoderm in a 72 hour planula. Basal neurite extensions (P) of light sensory cells (arrow) and dark sensory cells (not visible here) project into and help constitute the ganglionic plexus. Neurites of the plexus contain microtubules, mitochondria, electron-dense droplets, and dense-cored vesicles. M, mesoglea. ×10,000.

Figure 4. Cluster of light (S) and dark (D) sensory cells in the ectoderm of a mature hydroxyurea-grown planula. From the early cleavage stage, animals were continuously cultured in 0.01 *M* hydroxyurea in seawater. All cells in treated planulae are morphologically identical to those in control planulae. Photographs of treated embryos (Figs. 4, 6, 9) were included because excellent planes of section illustrating clustering of sensory cells and sensory cell processes were obtained from these embryos. ×7000.

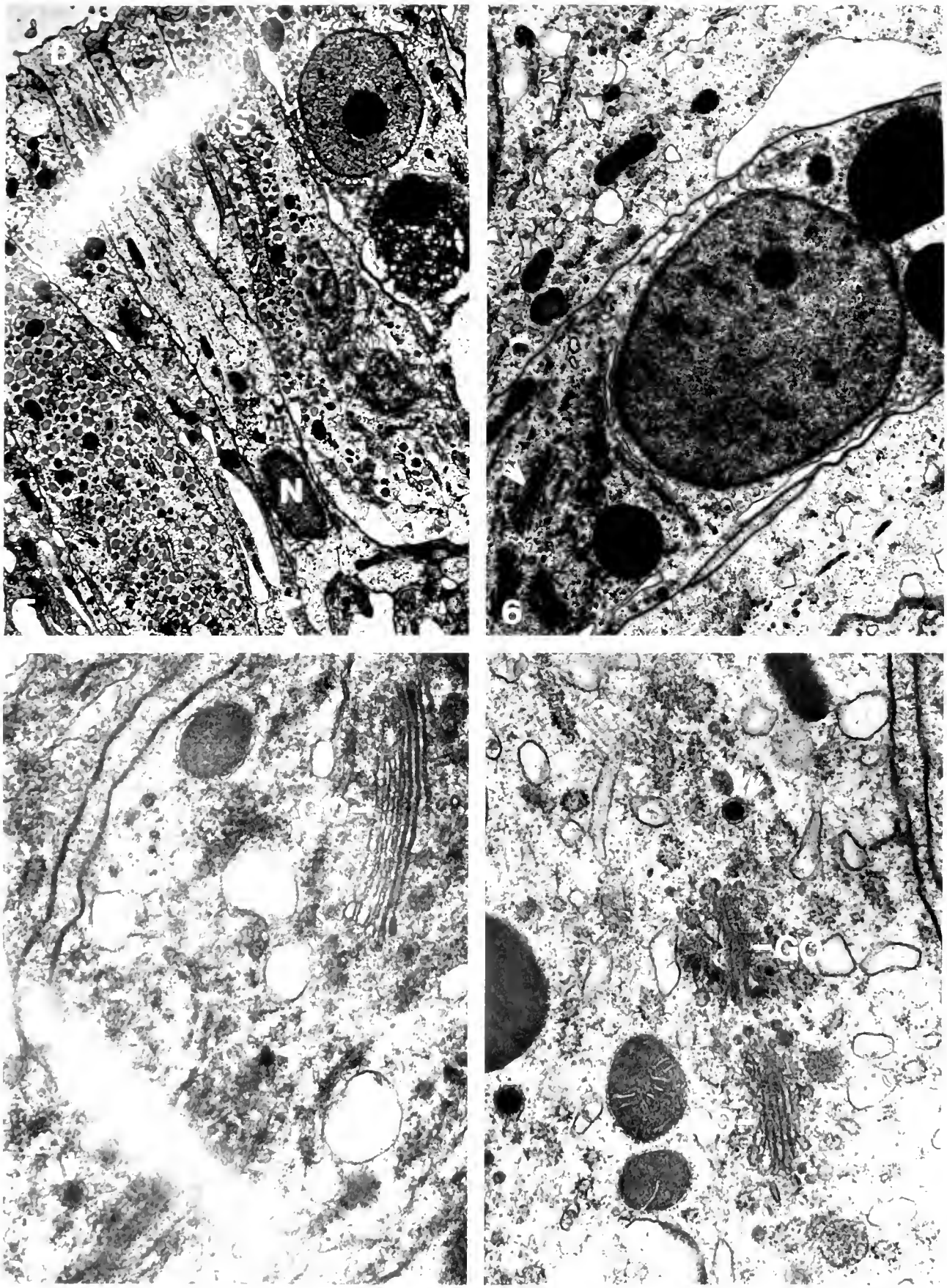
N
6

the binding of FMRFamide antiserum on wholemounts of planulae, the procedure presented by Koizumi and Bode (1986) was followed with some modifications. Planulae were fixed for 1 hour in 10% formalin in seawater. After fixation, the animals were washed 3 times, for 15 minutes each, in 10 m*M* phosphate-buffered saline (PBS, pH 7.2). Incubation with the FMRFamide antiserum was for 18 hours, with the primary antibody diluted 1:200 with 10 m*M* PBS, pH 7.2, containing 2% neonatal calf serum (Irvine Scientific), 0.3% Triton X-100, and 0.1% sodium azide. The incubation was carried out with the planulae in lid-covered 96 well tissue culture plates that were resting on a rotating shaker platform set at 60 rpm. After the first incubation period, the primary antibody was pulled off with a pipette, and the animals were washed for three 15-minute changes in 10 m*M* PBS, pH 7.2. Incubation with the second antibody was for 1 hour in fluorescein isothiocyanate (FITC)-conjugated goat anti-rabbit immunoglobins (U. S. Biochemical Corporation) diluted 1:120 in 10 m*M* PBS, pH 7.2, containing 10% fetal calf serum, 0.3% Triton X-100, and 0.1% sodium azide. The second incubation was also in 96 well plates rotated at 60 rpm. After the second incubation, the animals were washed 3 times, for 15 minutes each, in fresh 10 m*M* PBS, pH 7.2. Wholemount preparations were examined for fluorescently labelled cells with a Zeiss microscope equipped with epifluorescence.

To visualize binding of FMRFamide antiserum to paraffin sections of planulae, the following procedure was followed. Samples fixed in formalin were dehydrated through an alcohol series, infiltrated and embedded in paraffin, and serially sectioned at 8 μm. Approximately nine sections were mounted in the center of a single glass slide, three rows one above the other, and each row containing three sections. The slides were rehydrated to distilled water, and the sections were surrounded by an outer ring of vacuum grease (the grease ring was just to the outside of the sections). The grease was applied in a moist chamber to prevent the sections from drying.

The protocol for indirect immunofluorescence for paraffin sections was identical to that described for wholemounts. The FMRFamide antiserum was placed in the grease-created well thus immersing the sections. Such slides were placed in a lid-covered moist chamber and rotated at 40–60 rpm for 18 hours. PBS rinses and incubation in the second antibody were also carried out in the moist chamber. After incubation, the grease was carefully removed from the slides, and the sections were covered with mineral oil and examined for fluorescently labeled cells. Some of the paraffin sections were subsequently stained with azure B after their initial examination for immunofluorescence.

For wholemounts and paraffin sections, the binding specificity of the FMRFamide antiserum was determined by preincubating a 1:200 dilution of the antiserum with either 1 or 10 μg/ml synthetic FMRFamide (Peninsula Lab) for 24 hours at 4°C before using it to stain the samples.

Results

Sensory cells begin to arise in the ectoderm of the planula at 24 hours postfertilization (Fig. 1). They first appear as single cells scattered in the anterior region of the planula. As development progresses, these cells increase in number and become distributed along the entire length of the planula, many arranged in clusters of 3–6 cells (Fig. 2). Sensory cells are columnar and extend from the free surface of the planula to a ganglionic plexus located just above the mesoglea (Fig. 3). Sensory cells are characterized by an apical cilium, a medially to basally located nucleus, and small basal neurite extensions which project into and help constitute the ganglionic plexus.

Two morphological types of sensory cells are identifiable at the fine-structural level: a light sensory cell and a dark sensory cell (Fig. 4); the light sensory cell has a more electron-lucent cytoplasm than does the dark sensory cell. The light and dark sensory cells can be distinguished on the basis of their distribution and time of appearance, their cytology, and their neurite processes.

First, the light cells are in the vast majority, and they appear first in planulae that are only 24 hours old (Fig. 1). I have, as yet, only seen dark sensory cells in the most

Figure 5. A cluster of sensory cells containing one dark sensory cell (D) and several light sensory cells (S) in the anterior ectoderm of a 72 hour planula. The dark sensory cell has a cytoplasm rich in microtubules, mitochondria aligned in rows between the microtubules, electron-dense droplets, and dense-cored vesicles. The nucleus (N) of the dark sensory cell is mid to basally located, and the basal extension is bipolar (arrows). ×5000.

Figure 6. Medially located nucleus of a dark sensory cell. A single Golgi complex (arrow) is found in close association with the nucleus, as are numerous granules and vesicles. ×11,900.

Figure 7. Cytoplasm of a dark sensory cell in a maturing planula. Electron-dense droplets (single arrow) and dense-cored vesicles (double arrows) are abundant in the Golgi region (GO) of the cell. ×41,000.

Figure 8. Cytoplasm of a light sensory cell in a mature planula. Multiple Golgi complexes (GO) appear throughout the apical cytoplasm, as do electron-dense droplets (arrow) and dense-cored vesicles (double arrows). ×41,000.

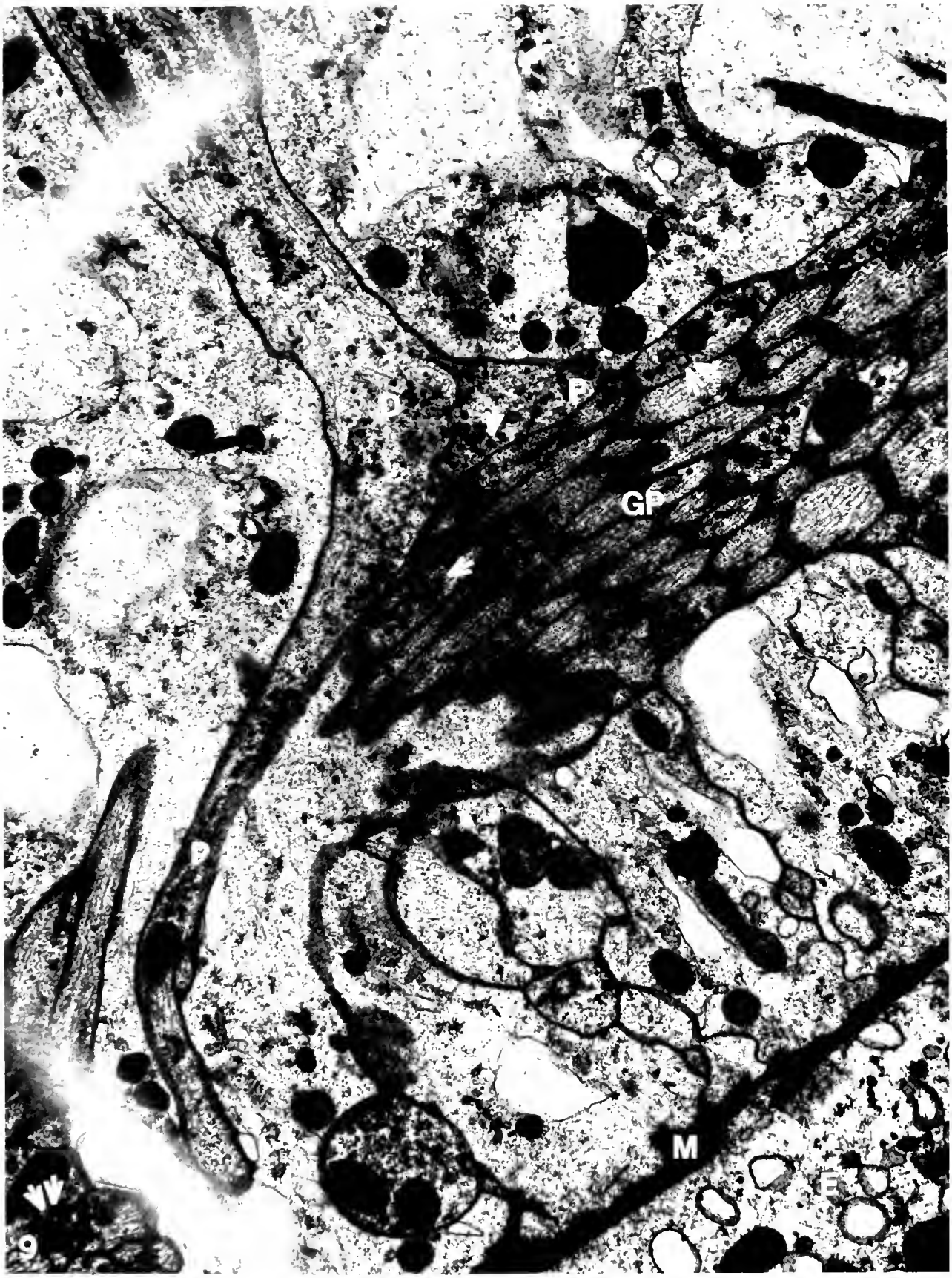

Figure 9 Basal portion of a presumed sensory cell (D) in a mature hydroxyurea-grown planula. The base of the cell forms two processes (P) that contribute to the ganglionic plexus (GP). Mitochondria, microtubules, electron-dense droplets, multivesicular bodies, and dense-cored vesicles (double arrows) fill the sensory neurites and are abundant in the other neurites of the ganglionic plexus. E, endoderm; M, mesoglea. × 49,200

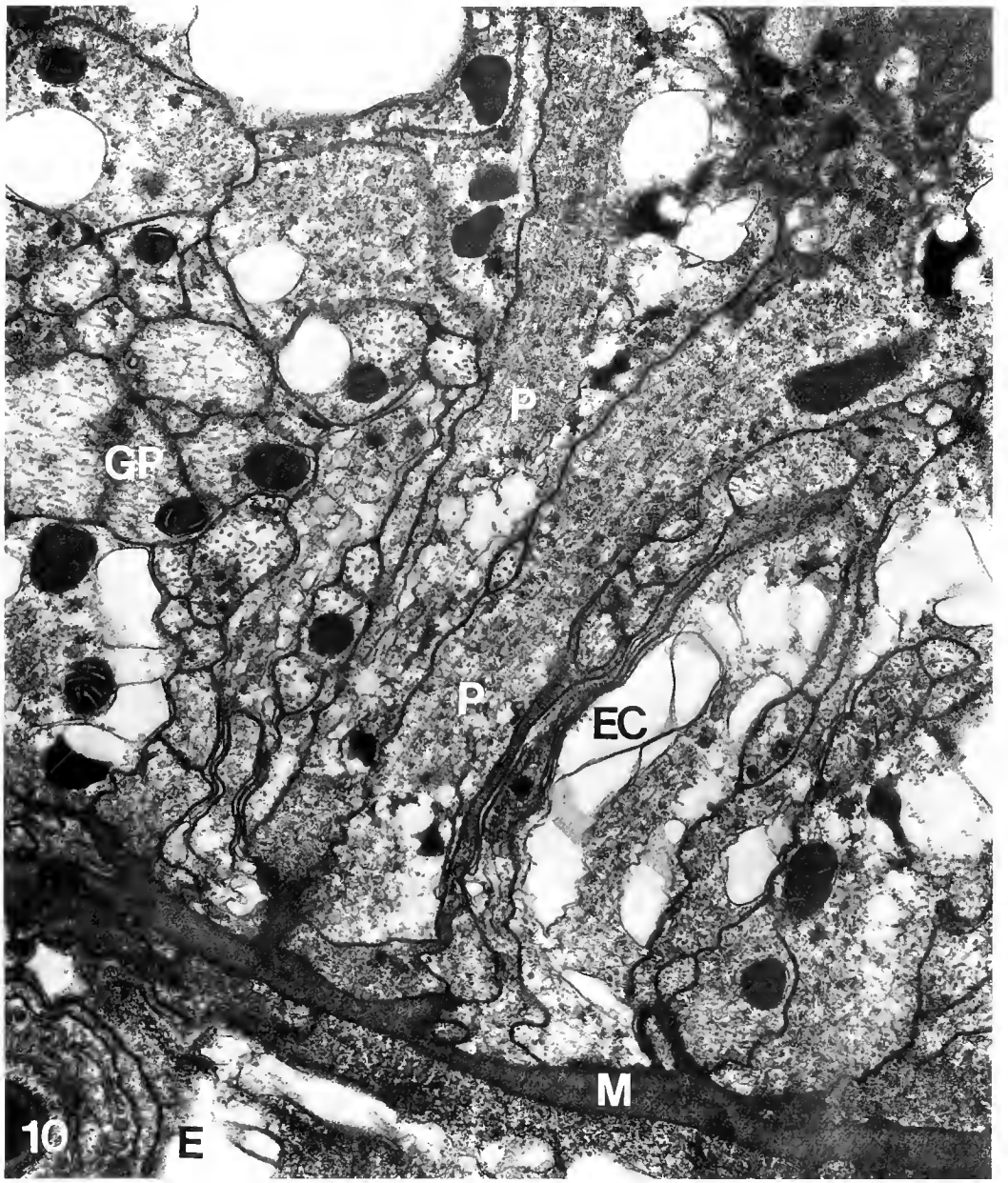

Figure 10. Basal regions of light sensory cells in a maturing planula. Basal processes (P) from two light sensory cells extend into the ganglionic plexus (GP). Numerous microtubules occupy the cytoplasm of these processes, however, electron-dense droplets and dense-cored vesicles have not yet appeared. The appearance of these droplets and vesicles in the basal extensions constitutes the last phase of sensory cell differentiation. E, endoderm; EC, ectoderm; M, mesoglea. ×19,000.

mature planulae (36–96 hours postfertilization depending on temperature: just prior to attachment). Furthermore, the dark sensory cells do not appear in all sensory cell clusters (Fig. 2), and when they are present, they generally occur singly or in pairs (Fig. 5). Light sensory cells may occur singly along the length of the mature planula, but dark sensory cells have only been seen among the clusters.

The cytoplasm of the dark sensory cells contains numerous bundles of microtubules, rows of mitochondria dispersed in between the microtubule bundles, generally a single Golgi complex in close proximity to the nucleus, and electron-dense, non-membrane bound droplets and dense-cored, membrane-bound vesicles (Figs. 4–7). The cytoplasm of light sensory cells also contains numerous bundles of microtubules, many Golgi complexes in the

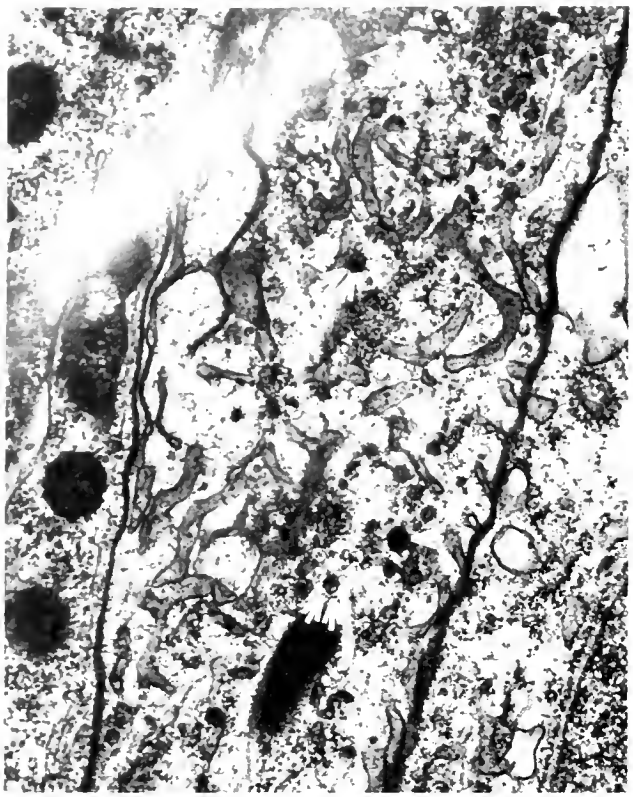

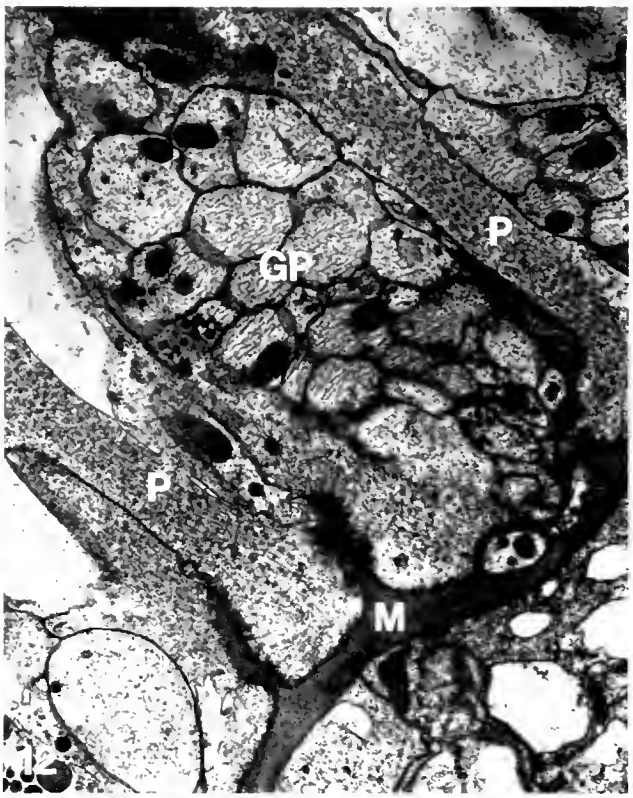
P
GP
P
M

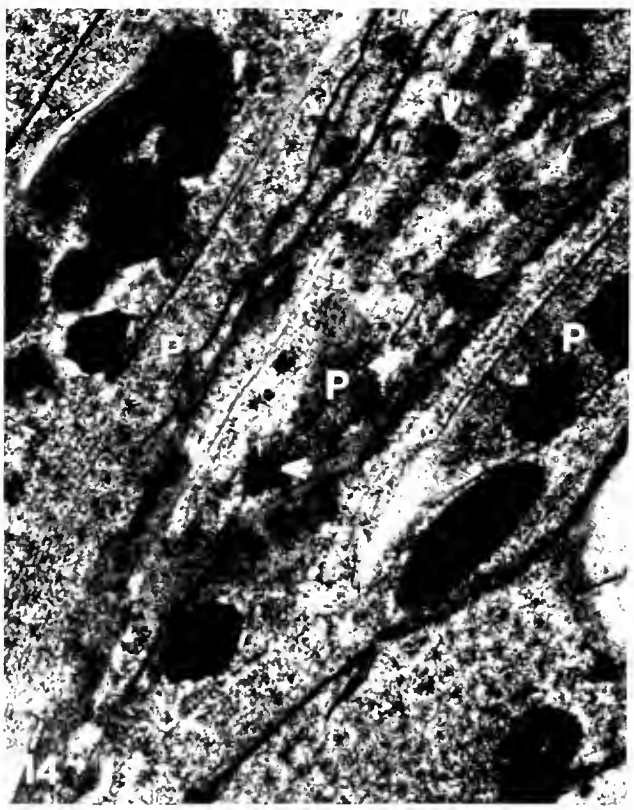
P
P
P

upper apical regions, and electron-dense, non-membrane bound droplets and dense-cored, membrane-bound vesicles (Figs. 1, 2, 4, and 8). However, there are fewer mitochondria than in dark sensory cells, and the mitochondria are not arranged in the distinct rows that characterize the dark cells (Fig. 4).

The basal extensions of dark sensory cells contain numerous mitochondria, microtubules, electron-dense droplets and dense-cored vesicles and often bifurcate to form two neurites that project into the ganglionic plexus (Fig. 9). In contrast, the basal processes of light sensory cells have not been seen to bifurcate, and they appear to contain fewer droplets and vesicles than do the processes of dark sensory cells (Fig. 10). Thus, the dark sensory cells appear to be bipolar, whereas the light cells may be considered as unipolar.

During the development of both types of sensory cells, the apical region of each cell becomes specialized before the basal region (Figs. 7, 8, 11–13). One or several Golgi complexes, depending on the type of sensory cell, form early in close association with the nucleus. Droplets and vesicles soon appear within the region of the Golgi (Figs. 7, 8, 13). Concurrent with the appearance of the Golgi, mitochondria and microtubules fill the apical cytoplasm. Next, the basal regions of the cells become specialized to form neurites. Mitochondria, microtubules, droplets, and vesicles appear within the forming basal neurites (Figs. 9, 14).

FMRFamide-like immunoactivity is observed in paraffin sections and wholemounts of planulae of *Halocordyle disticha* (Figs. 15, 17–26). Such immunoactivity is first detected in single cells in the ectoderm at 24 hours postfertilization in the anterior region of the planula (Fig. 15). Before 24 hours animals lack immunostaining (Fig. 16). As the planulae mature, the immunostaining increases and appears scattered along the planular anterior-posterior axis (Figs. 17–22). The appearance and distribution of the FMRFamide-like positive cells corresponds to the appearance and distribution of some of the sensory cells as viewed by transmission electron microscopy. As planulae age, some of the positively staining cells appear in clusters (Figs. 18–22) and display the characteristic morphology of sensory cells: columnar cells in the ectoderm with tiny tortuous processes that project toward the mesoglea. An examination of the FMRF-amide-like positive cells in paraffin sections confirms that they are sensory cells (Fig. 28). When such sections are subsequently stained with azure B, the immunopositive cells stain faintly as they lack apical granules. The only other columnar cells in the ectoderm, glandular and epitheliomuscle cells, possess numerous large apical granules; such granules stain darkly. Thus, epitheliomuscle cells and glandular cells stain darker with azure B than do the sensory cells. Furthermore, light azure B-staining sensory cells are first detected at 24 hours postfertilization, whereas dark azure B-staining cells are visible shortly after gastrulation (10–12 hours postfertilization). No distinction between dark and light sensory cells, as seen via transmission electron microscopy, is possible at the light microscopic level.

Examination of paraffin sections from different aged planulae and from different axial regions of the planula illustrates the abundance and distribution of immunopositive cells with respect to axial location and developmental time. All FMRFamide-like expression, with the exception of a few scattered fluorescent dots in the endoderm, is confined to the planular ectoderm (Figs. 15, 17–23). Developmental expression of the FMRFamide-like peptide by sensory cells is such that it is first detected in the upper apical two-thirds of the cell and last, if at all, in the basal region (Figs. 15, 17–22). The upper portion of the cell exhibits brilliant immunostaining while the basal processes stain weakly. Hence, the first immunopositive cells to appear at 24 hours exhibit intense fluorescence in their apical regions and little or no staining in their basal ends (Fig. 15). Examination of different axial regions of mature planulae indicates that FMRFamide-like immunopositive cells are found along the entire planular axis by 48–72 hours postfertilization (Figs. 18–22). However, there does appear to be more immunopositive cells at the anterior end of the planula than at the posterior end (Figs. 20–22). Just prior to metamor-

Figure 11. Apical region of a differentiating light sensory cell in a 72 hour planula. Apical differentiation of sensory cells precedes basal differentiation as Golgi complexes, microtubules, electron-dense droplets (single arrow), and dense-cored vesicles (double arrows) fill the apical cytoplasm. Electron-dense droplets, dense-cored vesicles, microtubules, and mitochondria form later in the basal processes. ×32,000.

Figure 12. Immature basal extensions of light sensory cells. The processes (P) are not yet filled with electron-dense droplets, dense-cored vesicles, or mitochondria. These neurites extend into a well-formed ganglionic plexus (GP). M, mesoglea. ×15,000.

Figure 13. Golgi region in the apex of a light sensory cell. Electron-dense droplets and dense-cored vesicles (arrows) are found in the area of the Golgi. ×63,000.

Figure 14. Differentiating basal processes (P) of light sensory cells. These processes become filled with mitochondria, electron-dense droplets (arrows), and dense-cored vesicles (not visible). Compare this micrograph with Figure 12 illustrating immature basal processes of light sensory cells. ×31,000.


E
15


E
16


A
E
17 P


E
18


E
19


A
E
20 P

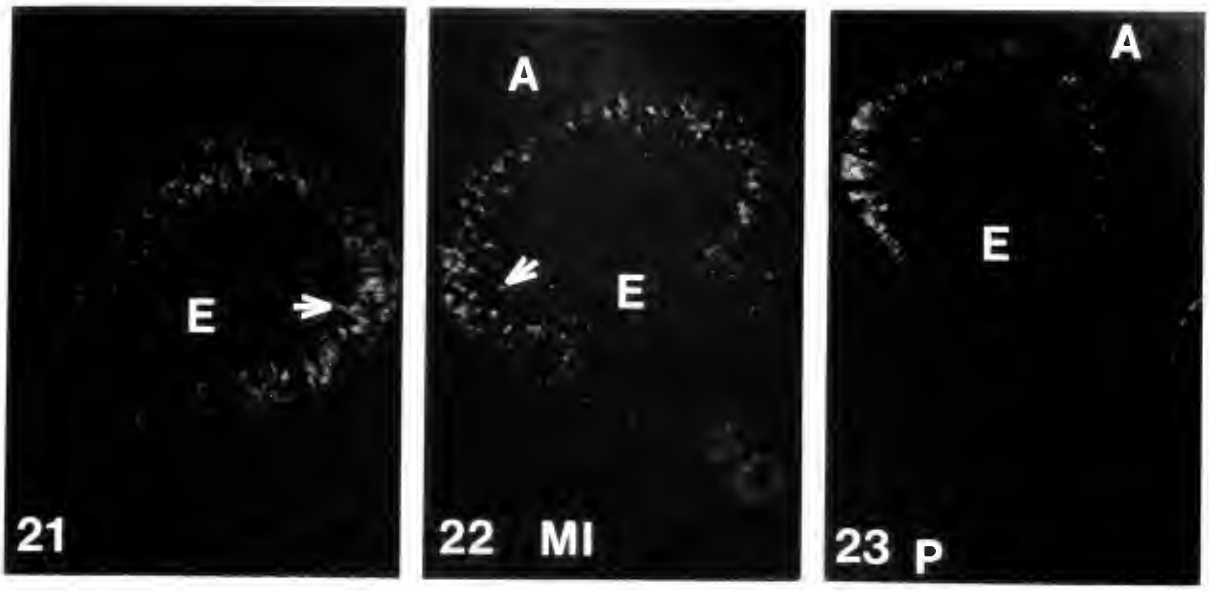

Figure 21. Slightly oblique paraffin section through the anterior region of a young 96 hour planula. Basal processes (arrow) of some sensory cells exhibit weak FMRFamide-like activity. E, endoderm. ×150.

Figure 22. Longitudinal paraffin section of a young 96 hour planula. Immunopositive cells are abundant in the anterior region (A) and a few are visible along the mid-sides (MI) of the animal. The arrow denotes the location of the mesoglea. E, endoderm. ×220.

Figure 23. Longitudinal paraffin section of a mature 120 hour planula just prior to metamorphosis. Immunopositive cells are present in the anterior (A) region of the planula, however, they are absent from the more posterior (P) regions of the animal. E, endoderm. ×100.

Figure 15. Paraffin section through the anterior region of a 24 hour planula. A few FMRFamide-positive cells first appear in the anterior region of the planula at this stage of development. These cells probably correspond to some of the first sensory cells seen via transmission electron microscopy. The FMRFamide-like peptide is first expressed in the apices of these cells (as indicated here) and only later in the mid to basal regions of the cells. Expression of the peptide-like material at this time is confined to a few ectodermal cells, as the endoderm (E) lacks immunostaining. The single arrow denotes the outer edge of the ectoderm, whereas the double arrows indicate the mesoglea. ×230.

Figure 16. Paraffin section through the anterior region of a 16 hour planula. These embryos do not express the FMRFamide-like peptide, as indicated by their lack of immunostaining. The arrow indicates the outer margin of the ectoderm. E, endoderm. ×250.

Figure 17. Longitudinal paraffin section of a 36 hour planula. As development proceeds, the number of cells expressing the FMRFamide-like peptide increases, as demonstrated by the larger number of positive-staining cells at 36 hours compared to 24 hours (Fig. 15). By 36 hours, immunopositive cells are visible in the anterior region (A) of the planula and also along the sides of the planula. For the most part, the immunostaining at this stage is strongest in the apical regions of cells. The arrow indicates the location of the mesoglea. E, endoderm; P, posterior. ×150.

Figure 18. Paraffin cross section through the mid region of a 72 hour planula. The number of immunopositive cells has increased by 72 hours, and many of these cells associate to form intense immunopositive clusters (arrows) along the length of the planula. E, endoderm. ×200.

Figure 19. Oblique paraffin section of a 72 hour planula. Single immunopositive cells and clusters of immunopositive cells are visible in the planular ectoderm. By 72 hours, in those cells that express the FMRFamide-like peptide, the immunostaining is not confined solely to the apices of the cells but has extended to include the mid regions of the cells, and in some cases the basal regions of the cells (arrow). Faint staining of basal processes is seen in the anterior region of the planula and decreases towards the posterior end of the planula. E, endoderm. ×220.

Figure 20. Oblique paraffin section of a 72 hour planula. Immunopositive sensory cells are found in the ectoderm along the entire anterior-posterior axis of the planula. There appears to be more immunopositive cells in the anterior region (A) of the planula than in the more posterior regions (P). A few immunopositive small cells are visible in the anterior endoderm (E) at this stage, and these cells represent a subpopulation of interstitial cells differentiating along the ganglionic cell line. ×200.

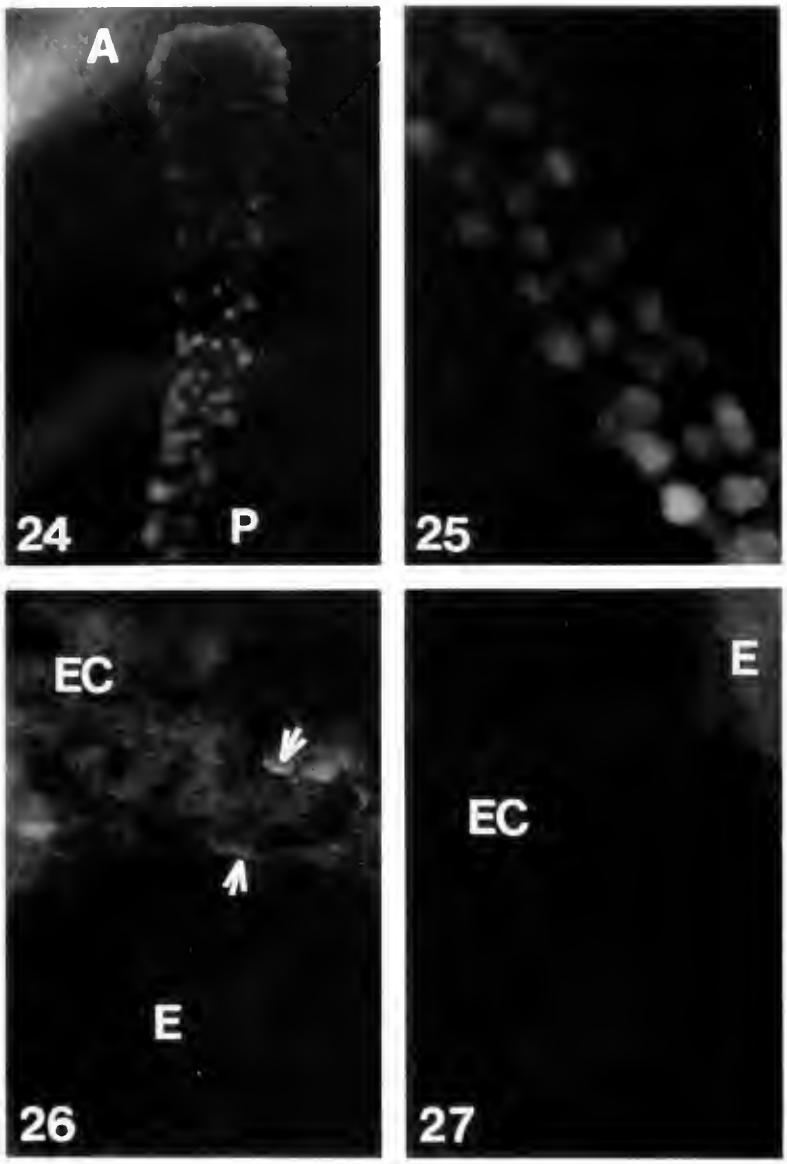

Figure 24. Distribution of clusters of immunopositive cells in a wholemount of a 96 hour planula. These cells are found in the anterior (A), middle, and posterior (P) regions of the planula. ×80.

Figure 25. Wholemount of the mid to posterior region of a 96 hour planula showing the distribution of FMRFamide-like positive clusters of cells. ×90.

Figure 26. Wholemount of a mature planula showing the anterior region. Processes (arrows) stain faintly and are located in the ectodermal region of the ganglionic plexus and also just above the plexus. E, endoderm; EC, ectoderm. ×250.

Figure 27. Wholemount of a mature planula showing the posterior region. There are no positive staining processes detected in this area. E, endoderm; EC, ectoderm. ×250.

phosis, a large number of immunopositive cells are detected in the extreme anterior region of the planula (Fig. 23). Basal processes of sensory cells located in the anterior region of the planula stain more intensely than do those of sensory cells distributed in the mid to posterior region of the animal (Figs. 21–23).

The spatial distribution of cells expressing the FMRFamide-like peptide is easily visualized using wholemounts of planulae (Figs. 24–27). In mature planulae (96 h) clusters of immunopositive cells are visible as large dots scattered along the length of the animal. A few of these FMRFamide-like positive clusters first appear in the anterior region of the late 24 hour planula and later in the mid to posterior regions of the mature planula. In wholemounts, the basal processes of the sensory cells are very difficult to visualize as they are tiny and stain only

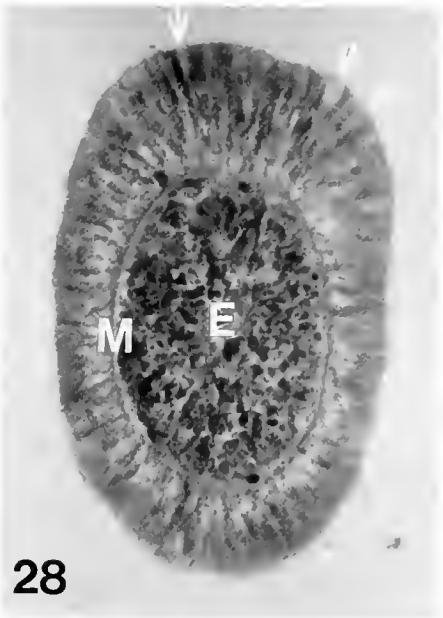

Figure 28. Paraffin section through the anterior region of a maturing planula stained with azure B. Light staining sensory cells (arrows) are found among darker staining epitheliomuscle cells and glandular cells. Dark staining cells outnumber the light staining cells. When processed for immunocytochemistry the light cells exhibit a positive response for FMRFamide-like activity. E, endoderm; M, mesoglea. ×250.

faintly (Fig. 26). Visualization of weak immunopositive basal processes is more obvious in paraffin sections (Fig. 21).

Wholemounts and paraffin sections of planulae stained with FMRFamide antiserum preabsorbed with 10 μg/ml synthetic FMRFamide do not exhibit any immunopositive staining. Furthermore, treatment of samples with antiserum preabsorbed with 1 μg/ml FMRFamide results in very dim staining of cells.

Discussion

Using immunocytochemistry and radioimmunoassays, Grimmelikhuijzen and associates identified substances resembling vertebrate or invertebrate neuropeptides in the nervous systems of adult cnidarians (Grimmelikhuijzen and Graff, 1985, 1986; Grimmelikhuijzen and Groeger, 1987). The most common neuropeptides seen were those related to the molluscan neuropeptide Phe-Met-Arg-Phe-amide (FMRFamide). When anti-FMRFamide was applied to adult cnidarians, cells containing peptides ending in -Arg-Phe-NH_2 bound the antiserum. Recently, Grimmelikhuijzen and co-workers isolated and sequenced a specific neuropeptide, pGlu-Gly-Arg-Phe-amide (antho-RFamide), from sea anemones and pennatulids (Grimmelikhuijzen and Graff, 1985, 1986; Grimmelikhuijzen and Groeger, 1987).

In this study hydrozoan planulae of different developmental ages were tested for their ability to bind a rabbit antiserum raised to FMRFamide to determine if peptides ending in -Arg-Phe-NH_2 were present in larval cnidarians and, if so, to determine when in development the gene for such a peptide (or peptide family) was expressed. Planulae of *Halocordyle disticha* exhibited a positive staining response when exposed to anti-FMRFamide, indicating that peptides ending in -Arg-Phe-NH_2 are present in cnidarian larvae. The expression of the FMRFamide-like peptide was first observed at 24 hours postfertilization in the ectoderm in association with some of the sensory cells. As planulae matured, the number of immunopositive sensory cells increased, and such cells were seen along the entire length of the planula. Just prior to metamorphosis a large number of FMRFamide-positive cells appeared in the anterior ectoderm (attachment end), suggesting the involvement of the FMRFamide-like peptide in planular attachment or metamorphosis.

The time of appearance of the synthetic machinery of planular sensory cells, and the pattern of appearance of FMRFamide-like immunofluorescence, appear to be correlated. Ultrastructural examination of planulae reveals that the planular nervous system begins to form in the ectoderm at 24 hours in development. A few sensory cells are found in the anterior end of the planula at this time, and as planulae age, the number of sensory cells increase. Furthermore, as sensory cells differentiate, their apical regions become specialized before their basal regions. One of the first differentiative events detected in the sensory cell is the formation of one to several Golgi complexes in close association with the nucleus. Shortly after the formation of the Golgi complexes, electron-dense droplets and dense-cored vesicles appear in the apical cytoplasm, and only later in the forming basal neurites. Individual immunopositive cells first appear at 24 hours in the anterior ectoderm of the planula and, most probably, correspond to the first sensory cells seen via transmission electron microscopy. As development progresses, many of these immunopositive cells become organized into clusters along the length of the planula. Furthermore, such immunopositive cells exhibit brilliant immunofluorescence first in their apical regions, and only later do they show a dim staining in their basal regions. Such a spatial and temporal staining response in the immunopositive cells is expected in view of the ultrastructural findings concerning time of appearance and location of the Golgi complexes, droplets, and vesicles.

The presence of peptides in the nervous systems of planulae suggest that: (1) peptides may play crucial roles in the development of these larvae; and (2) peptides may be important for metamorphosis. In either case, the sim-

ple nervous system of the planula provides an excellent system with which to analyze neuropeptide action on developmental processes. Also, because the planula can be easily visualized, maintained, and acquired throughout the entire metamorphic process, it offers a unique developmental model for examining the temporal appearance of new neuropeptides and for analyzing possible switches that may occur in neuropeptide phenotype (*i.e.*, plasticity of neuropeptide expression) as an animal passes from the embryonic condition to the adult state.

Acknowledgments

This research was supported by National Science Foundation Grants DCB-8702212 and DCB-8711245.

Literature Cited

Burnett, A., and N. Diehl. 1964. The nervous system of *Hydra* I. Types, distribution and origin of nerve elements. *J Exp. Zool* **157:** 217–226.

Davis, L., A. Burnett, and J. Haynes. 1968. Histological and ultrastructural study of the muscular and nervous systems in hydra. *J Exp. Zool.* **167:** 295–332.

Grimmelikhuijzen, C., and D. Graff. 1985. Arg-Phe-amide-like peptides in the primitive nervous systems of coelenterates. *Peptides* **6:** 477–483.

Grimmelikhuijzen, C., and D. Graff. 1986. Isolation of pGlu-Gly-Arg-Phe-NH_2 (Antho-RFamide), a neuropeptide from sea anemones. *Proc. Natl Acad. Sci. USA* **83:** 9817–9821.

Grimmelikhuijzen, C., and A. Groeger. 1987. Isolation of the neuropeptide pGlu-Gly-Arg-Phe-amide from the pennatulid *Renilla kollikeri. FEBS Lett* **211:** 105–108.

Horridge, G., and B. Mackay. 1962. Naked axons and symmetrical synapses in coelenterates. *Q J Microsc. Sci.* **103:** 531–541.

Jha, R., and G. Mackie. 1967. The recognition, distribution and ultrastructure of hydrozoan nerve elements. *J Morphol.* **123:** 43–62.

Koizumi, O., and H. Bode. 1986. Plasticity in the nervous system of adult *Hydra* I. The position-dependent expression of FMRFamide-like immunoreactivity. *Dev. Biol.* **116:** 407–421.

Kolberg, K., and V. Martin. 1988. Morphological, cytochemical and neuropharmacological evidence for the presence of catecholamines in hydrozoan planulae. *Development* **103:** 1–10.

Lentz, T., and R. Barrnett. 1965. Fine structure of the nervous system of hydra. *Am. Zool.* **5:** 341–356.

Martin, V. 1985. Interstitial cells are required for polyp morphogenesis during metamorphosis of planulae. *Am. Zool.* **25:** 61A.

Martin, V. 1986. Development of nerve cells in hydrozoan planulae of *Pennaria tiarella. Am. Zool* **26:** 53.

Martin, V. 1988. Development of nerve cells in hydrozoan planulae: I. Differentiation of ganglionic cells. *Biol. Bull* **174:** 319–329.

Martin, V., and M. Thomas. 1980. Nerve elements in the planula of the hydrozoan *Pennaria tiarella. J Morphol.* **166:** 27–36.

Martin, V., F. Chia, and R. Koss. 1983. A fine structural study of metamorphosis of the hydrozoan *Mitrocomella polydiademata. J Morphol* **176:** 261–287.

Peteya, D. 1975. The ciliary-cone sensory cell of anemones and cerianthids. *Tissue Cell* **7:** 243–252.

Singla, C. 1978. Fine structure of the neuromuscular system of *Polyorchis penicillatus* (Hydromedusae, Cnidaria). *Cell Tissue Res.* **193:** 163–174.

Spencer, A. 1979. Neurobiology of *Polyorchis* II. Structure of effector systems. *J Neurobiol.* **10:** 95–117.

Stokes, D. 1974. Morphological substrates of conduction in the colonial hydroid *Hydractinia echinata* I. An ectodermal nerve net. *J Exp. Zool* **190:** 19–46.

Thomas, M., G. Freeman, and V. Martin. 1987. The embryonic origin of neurosensory cells and the role of nerve cells in metamorphosis in *Phialidium gregarium* (Cnidaria, Hydrozoa). *Int J Invertebr. Reprod Dev* **11:** 265–287.

Westfall, J. 1970. Ultrastructure of synapses in a primitive coelenterate. *J Ultrastruct Res.* **32:** 237–246.

Westfall, J. 1973. Ultrastructural evidence for neuromuscular systems in coelenterates. *Am. Zool.* **13:** 237–246.

Westfall, J., S. Yamataka, and P. Enos. 1971. Ultrastructural evidence of polarized synapses in the nerve net of hydra. *J Cell Biol.* **51:** 318–323.

Yamasu, T., and M. Yoshida. 1976. Fine structure of complex ocelli of a cubomedusan *Tamoya bursaria. Cell Tissue Res.* **170:** 325–339.

Yu, S., J. Westfall, and J. Dunne. 1985. Light and electron microscopic localization of a monoclonal antibody in neurons *in situ* in the head region of *Hydra. J Morphol.* **184:** 183–193.

Reference: *Biol. Bull.* **175:** 79–93. (August, 1988)

The Dynamics of Oogenesis and the Annual Ovarian Cycle of *Stichopus californicus* (Echinodermata: Holothuroidea)

SCOTT SMILEY

Friday Harbor Laboratories and Department of Zoology, University of Washington, Seattle, Washington 98195

Abstract. The major cytological stages of oogenesis in the holothurian *Stichopus californicus* are morphologically separated in distinct classes of tubules, the discrete anatomical units comprising the ovary. Primordial germ cells are in the connective tissue compartment of the gonad basis. Mitotic oogonia are in the smallest and most anterior set of primary ovarian tubules. Oocytes in the early prophase stages of meiosis I are in secondary tubules located more posteriorly. Diplotene oocytes occur in larger, more posterior secondary tubules. The most advanced oocytes are in the most posterior fecund tubules. *S. californicus* oocytes bear nuage, a subcellular marker common to many germ line cells. The striking axial polarization of these oocytes, evident as the egg axis, is indistinguishable from the apical basal axial polarization in epithelial germ line cells. These axes are congruent throughout the developmental history of the oocyte. I present a model for the annual cycle of the *S. californicus* ovary and assess its application to other holothurians. I infer function from the structure of oogenesis presented here; and contrast this information with what is known about oogenesis in the other echinoderm classes.

Introduction

The only detailed histological investigation of holothurian oogenesis is that of Théel (1901) who reported annual cycling of the gonadal tubules in the synallactid aspidochirote *Mesothuria intestinalis*. Because *M. intestinalis* is hermaphroditic, a fine structural study of oogenesis in a gonochoric holothurian will be useful. It would also be of interest because many comparative anatomists consider holothurian gonads primitive (Hyman, 1955; Smiley, 1988b). The simplicity of the holothurian ovary makes it a promising model for all echinoderm gonads. Such a study will also shed light on the development of polarization within the holothurian oocyte. These oocytes bear an apical protuberance, making them among the most visibly polarized in the animal kingdom (Smiley and Cloney, 1985). The protuberance is the site of polar body formation during meiosis, and marks the animal pole of the egg axis (Smiley and Cloney, 1985). Analysis of the development of epithelial cellular polarization in the early germ line cells is also of interest because of its likely importance in the development of embryonic pattern.

In this paper, I present a detailed fine structural analysis of oogenesis in the aspidochirote holothurian *Stichopus californicus*. I also report on an analysis of the annual cycle of this ovary, from resorption of the spent fecund tubules, through oogenesis, culminating in the inception of vitellogenesis in oocytes that will be spawned in the next reproductive season.

Materials and Methods

Stichopus californicus adults, collected by dredging or diving in nearby waters, were maintained in running seawater aquaria at the Friday Harbor Laboratories, University of Washington, from 1980 through 1985. Ovaries from more than 150 individual *S. californicus* were fixed in all months of the year except December. Dissection was done rapidly and all stages of fixation were done on ice using described methods (Smiley and Cloney, 1985).

Received 8 December 1987; accepted 15 April 1988.

Present address: Department of Biochemistry and Biophysics, University of California, San Francisco, San Francisco, California 94143.

Tissues were dehydrated in acetone and embedded in epon. Semithin (1 μm) sections were examined from each of several blocks made from each ovary fixed. Thin sections from more than 25 individuals were examined in a Philips 301 electron microscope.

S. californicus juveniles were raised from eggs fertilized *in vitro*, as described previously (Smiley, 1986, 1988a). After settlement, fingerbowls containing juveniles were barely submerged in aquaria. This allowed suspended food to flow into the bowls, which were cleaned weekly by rinsing. Maintained in this manner, juvenile *S. californicus* grow well their first fall and winter. Juveniles were fixed in January and February following fertilizations in May, June, and July. *Stichopus californicus*, Clark's (1901) generic redesignation of *Holothuria californica* Stimpson (1857) is also referred to as *Parastichopus californicus* Deichmann (1937).

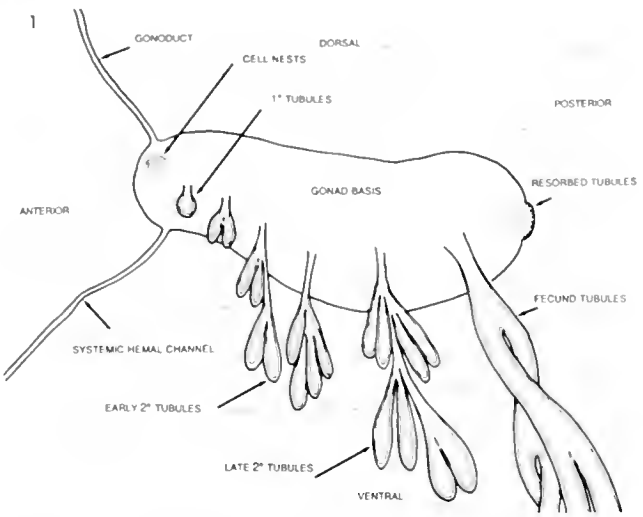

Figure 1. Diagrammatic depiction of a left lateral view of the *Stichopus californicus* ovary. This ovary is bilaterally symmetric about the dorsal mesentery.

Results

The results are organized into two parts. The first is a description of the anatomy and histology of the ovary, including the fecund tubules before and after spawning, and progressing anteriorly. This section gives the light microscopical level distinctions between classes of tubules. The second part covers the fine structural changes in the ovarian inner epithelium. This includes a detailed analysis of the dynamics of the somatic and germ line cells beginning with the cell nests of the gonad basis and culminating in vitellogenesis in the most posterior tubules.

Anatomy and histology of the ovary

Fecund tubules. The ovary of *Stichopus californicus* consists of three classes of tubules attached to a central *gonad basis* (Fig. 1): fecund, secondary, and primary tubules. While the three size classes are distinguished by a number of criteria, they represent stages in a continuum, in which the fecund tubules are the most posterior and the largest. These attach to the most posterior regions of the basis and bifurcate many times along their length. They contain vitellogenic oocytes in the months prior to spawning, and post vitellogenic oocytes in the weeks immediately before.

The fine structural organization of fecund ovarian tubules in *S. californicus* was recently reported (Smiley and Cloney, 1985). Tubules are the structural unit in holothurian gonads, and each consists of three tissues. Outermost is a *complex peritoneum* composed of peritoneal epithelial cells, nerves, and muscle cells. Innermost is the *inner epithelium* composed of oocytes and somatic inner epithelial cells of two types. Lying between the basal laminae of the peritoneum and the inner epithelium is the *connective tissue compartment* composed of fibers, the mesenchymal cells, and the genital hemal sinus. The genital hemal sinus is not lined by cells but is a lacuna within the connective tissue compartment. The oocyte basal lamina (oolamina) limits direct connection of the oocyte and the jelly space with the fluid in the genital hemal sinus. No outer sac of tissues surrounds holothurian gonads.

Spent tubules. Spawning evacuates post-vitellogenic oocytes from the fecund tubules (Smiley and Cloney, 1985). Just after spawning, spent tubules are a maximum of 4 cm long, and their pigmentation has decreased markedly. A week later, they have shrunken and become a rust color owing to phagocytosis (Fig. 9). This phagocytic action reduces the ovarian inner epithelium to few identifiable structures; the most obvious are the oocyte oolaminae (Fig. 9). The densely staining material in peritoneal cells and coelomocytes are birefringent residual bodies, products of phagocytic activity. A month after spawning, only pigmented plaques on the posterior of the gonad basis remain, testifying to the former presence of spent fecund tubules (Fig. 1). Since these tubules are lost, subsequent generations of oocytes must be recruited from other ovarian tubules.

Secondary tubules. The secondary tubules are just anterior to fecund tubules on the gonad basis (Fig. 1). They average 2.5 cm in length and 0.35 mm in diameter. They branch once or twice along their length, and each branched portion is slightly elongate. Their histology is similar to the fecund tubules, but the peritoneal epithelial cells are more columnar in secondary tubules (Fig. 2), and the genital hemal sinus is less extensive, giving the connective tissue compartment a more fibrous appearance. Fibroblasts, morula cells, and especially petal-

oid amoebocytes are more common in the connective tissue compartment of secondary tubules. Secondary tubules can be divided into two categories. Late secondary tubules are more posterior on the basis; early ones are more anterior.

In late secondary tubules, coincident with the onset of vitellogenesis in the fall, somatic inner epithelial cells form the inner wall of the ovary, and surround the oocytes (Fig. 10). Together, the inner epithelium and connective tissue compartment of these tubules form stubby longitudinal folds (Fig. 2) that run short distances along the length of the tubule. These develop into the long deep longitudinal folds in fecund tubules (Smiley and Cloney, 1985). Some inner epithelial cells form a follicle around the oocytes; these adhere to the oocyte surface, and a jelly space is not present. The lumen of late secondary tubules is much less occluded by oocytes than that of fecund tubules. Sexes can be reliably identified from late secondary tubules, after oocytes have formed germinal vesicles.

The peritoneum of early secondary tubules is thinner than in late secondary tubules, but is otherwise similar. The inner epithelium in early secondary tubules is simple in spite of its stratified appearance (Fig. 3). Here, longitudinal folds are reduced in size compared to late secondary tubules. The monociliated somatic cells are smaller than oocytes and have nuclei with denser peripheral heterochromatin. Even by electron microscopy, it is not possible to distinguish between oocytes and spermatocytes in early secondary tubules, or between oogonia and spermatogonia in primary tubules. The ovarian lumen of early secondary tubules is not seriously occluded by oocytes or longitudinal folds (Fig. 2) and is more expansive than in late secondary tubules. Within it is weakly staining hemal fluid containing morula cells and petaloid amoebocytes.

Primary tubules. The primary tubules, the smallest and most anterior on the gonad basis, are often difficult to discern even with magnification (Fig. 1). The most anterior are less than 2 mm in length, 0.25 mm in diameter, and do not bifurcate along their length. Those primary tubules closest to secondary tubules are slightly larger than those more anterior, and they may branch, but the tips of their branches are globose rather than elongate. The distinction between primary and secondary tubules is made on size, position, and cytology. There are no longitudinal folds of the inner epithelium and the connective tissue compartment in primary tubules (Fig. 4).

The histological organization of primary tubules is similar to the other tubules (Smiley and Cloney, 1985), but the connective tissue compartment is substantially smaller, particularly the genital hemal sinus. The lumen of primary tubules also contains hemal fluid which appears to be identical with that found in the genital hemal sinus of late secondary and fecund tubules. In spite of the adhering junctions between cells of the inner epithelium, fluids and mesenchymal cells within the lumen appear to mix freely with those in the genital hemal sinus. I conclude that the lumen of primary and early secondary tubules is in direct connection with, if not a part of, the ovarian connective tissue compartment.

Gonad basis. The gonad basis in *S. californicus* is a 5 to 7 mm long saddle-shaped thickening (Fig. 1) of the dorsal mesenteric connective tissue compartment (Smiley and Cloney, 1985; Cameron and Fankboner, 1986). It is totally enclosed by the dorsal mesenteric perivisceral peritonea (Fig. 6), which are structurally identical to, and continuous with, the investing peritonea of the ovarian tubules (Smiley and Cloney, 1985). The dorsal mesentery results from the lateral fusion of the left and right somatocoels during metamorphosis (Smiley, 1986), and the peritonea of the gonad basis and tubules have the same ontogeny.

The gonoduct inserts into the dorsal anterior aspect of the gonad basis and ascends within the connective tissue compartment of the dorsal mesentery to the gonopore located anteriorly in interambulacrum *CD* (Hyman, 1955). In all specimens sectioned (Fig. 8), the thinner wall of the gonoduct faces one side of the dorsal mesentery, and the long axis of its elliptical lumen is parallel with it. The duct is lined with a simple epithelium composed of columnar and exaggeratedly columnar monociliated cells. No *genital cord* (Théel, 1901; Haanen, 1914) is present adjacent to the gonoduct in *Stichopus californicus,* nor is there any genital rachis (Smiley, 1988b). Entering the basis at a ventral anterior aspect is a channel connecting the genital hemal sinus of the gonad with the dorsal hemal structures of the gut (Fig. 1).

The composition and structure of the connective tissue compartment in the gonad basis is complex (Figs. 6, 7). Within it, muscle cells run between the fibers of the connective tissue matrix. Lacunae are found in the connective tissue of the gonad basis, but based on evidence from serial semithin sections, neither the genital hemal sinus of late secondary and fecund tubules, nor the central lumina of primary and early secondary tubules are in direct connection with these lacunae. The gonad basis contains a reduced central lumen continuous with lumina from more advanced tubules (Fig. 6). Columnar somatic inner epithelial cells of the less advanced tubules partially occlude the opening near the point of their insertion onto the gonad basis. At the most anterior lateral aspect of the gonad basis, the connective tissue compartment contains small cell nests, about 50 μm in diameter (Fig. 7), similar to those described for *Holothuria parvula* (Kille, 1942). In *S. californicus,* each cell nest has a reduced central lumen isolated from the lumen of the gonad basis. The nests are separated from the connective tissue compartment by a basal lamina (Fig. 13).

Cytology of the inner epithelial cells

Primordial germ cells in the gonad basis. The cells comprising the cell nests are easily differentiated into two

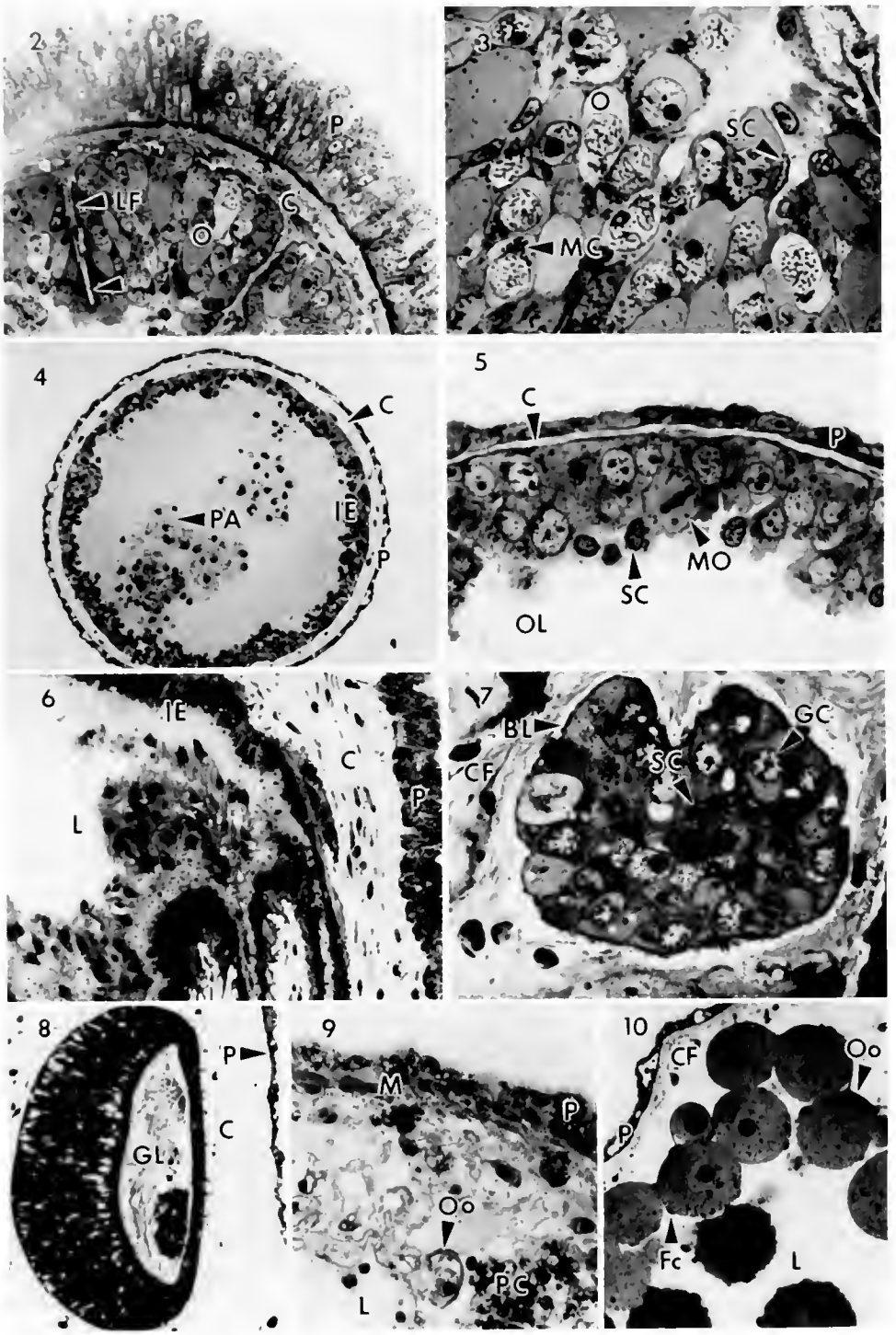

Figure 2. Light micrograph of a cross section of an early secondary tubule. C, connective tissue compartment, LF, incipient longitudinal folds, O, oocyte, P, peritoneum. The arrows demark a longitudinal fold. 480×.

Figure 3. Light micrograph of the inner epithelium in an early secondary tubule. MC, mitochondrial cloud in a spireme stage oocyte, O, oocyte, SC, inner epithelial somatic cell. 910×.

Figure 4. Light micrograph of a cross section of a primary tubule. C, connective tissue compartment, IE, inner epithelium, P, peritoneum, PA, petaloid amoebocytes within the lumen. 175×.

Figure 5. Light micrograph of details on the inner epithelium of a primary tubule. C, connective tissue compartment, MO, mitotic oogonium, OL, ovarian lumen, P, peritoneum, SC, somatic cell of the inner epithelium. 1050×.

types found in approximately equal abundance (Fig. 13). The smaller type, averaging about 6 μm in diameter, have more electron-dense cytoplasm, nuclei with distinct peripheral heterochromatin, prominent centrioles and a cilium; these are interpreted as somatic cells. The larger cells (Fig. 13), averaging about 10 μm in diameter, have more electron-lucent cytoplasm, nuclei with reduced peripheral heterochromatin, prominent centrioles (Fig. 18), and appear to bear a cilium. The cytoplasm in the larger cells (Fig. 13) contains aggregations of mitochondria and associated electron-dense bodies (Fig. 19), here called *type I nuage*. Nuage is germ line specific electron-dense granules, unbound by membranes, and has been described for germ line cells from other species (Eddy, 1975; Kessel, 1983). These criteria indicate that the larger cells (Figs. 7, 13) are *primordial germ cells* (*PGCs*), the progenitors of the mitotic gonial cells, themselves precursors of spermatocytes or oocytes. PGCs lack yolk, are bound to neighboring cells with adhering junctions (Fig. 19), and appear attached to the thickened basal lamina (Fig. 13).

Oogonial mitoses in primary tubules. The inner epithelium of primary tubules contains two distinct cell types, somatic cells and oogonia (Fig. 5). The smaller cells, with more basophilic cytoplasm and nuclei with more distinct peripheral heterochromatin are somatic cells, homologous with the smaller cells in cell nests within the gonad basis. These monociliated cells are not organized into a simple epithelium typical of late secondary and fecund tubules. Their jumbled arrangement makes the organization difficult to classify (Fig. 5). TEM reveals that all cells have adhering junctions attaching them to their neighbors, and the basal most cells rest on a basal lamina, therefore the inner cells of primary tubules form a true epithelium.

Within primary tubules, germ line cells of the inner epithelium are less electron dense, and their nuclei show substantially less peripheral heterochromatin than somatic cells. They average about 10 μm in diameter, lack yolk, and contain type I nuage. Like the somatic cells, these are bound to neighbors by adhering junctions, and appear attached to the thickened basal lamina. Germ line mitoses are frequently encountered, and are restricted to the primary tubules (Fig. 5) in *S. californicus*. Mitoses indicate that these germ line cells are oogonia, which correspond to PGCs in cell nests. The criteria supporting this conclusion include: (1) they are part of the inner epithelium of the tubules, (2) they are larger and are morphologically similar to other germ line cells, (3) their staining pattern is more like germ cells than somatic cells, and (4) because TEM reveals that they contain type I nuage.

The frequency of mitotic figures among the oogonia of primary tubules is higher than that found in any other ovarian tissues of *S. californicus*. The plane of the division spindles in oogonia is parallel to the inner epithelium, preventing daughter cells from being pushed into the tubule lumen at mitosis. Oogonia occur throughout the length of the primary tubule; indicating there is no discrete zone of mitotic proliferation in this tissue. Peritoneal epithelial cells in primary tubules also divide, although not as frequently as oogonia.

Prophase of meiosis I in early secondary tubules. In the inner epithelium of secondary tubules, the somatic cells cannot be distinguished as parietal or follicular. These cells are bound to other inner epithelial cells, somatic and germ line, by adhering junctions; or they may be closely applied to the surface of adjacent cells but showing no junctions. The somatic cells are smaller than germ line cells and have nuclei with peripheral heterochromatin.

The germ line cells here are quite small relative to those in late secondary tubules, and their chromosomes are in configurations characteristic of early prophase stages of meiosis (compare Fig. 21). These cells average about 15 μm in diameter, lack yolk, have adhering junctions with adjacent cells, contain nuage, and appear to be associated with a special basal lamina, the oolamina. Because of the small oocyte size, oolaminae in early secondary tubules extend over a greater area at the basal surface of the oocyte than in the fecund tubules (Smiley and Cloney, 1985), but it has the same staining properties and fine structure. The differences in relative size of the oolamina in secondary and fecund tubules are probably a result of oocyte growth.

An aggregation of densely staining particles lies adja-

Figure 6. Light micrograph of the gonad basis. C. connective tissue compartment, IE. inner epithelium, L. lumen, P. peritoneum. 375×.

Figure 7. Light micrograph of a cell nest within the connective tissue compartment of the gonad basis. BL. basal lamina limiting the nest, CF. connective tissue fibers, GC. germ line cell, SC. somatic cell. 1025×.

Figure 8. Light micrograph of the gonoduct. C. connective tissue compartment of the dorsal mesentery, GL. gonoduct lumen, P. peritoneum. Note the absence of a genital cord. 255×.

Figure 9. Light micrograph of a cross section of a resorbing spent tubule. M. muscle cells of the complex peritoneum, L. ovarian lumen, Oo. oolamina, P. peritoneum, PC. petaloid amoebocytes containing lipofuscin granules. 525×.

Figure 10. Light micrograph of a cross section of a late secondary tubule. CF. connective tissue fibers, Fc. follicular inner epithelial cells, L. ovarian lumen, Oo. oolamina, P. peritoneum. 250×.

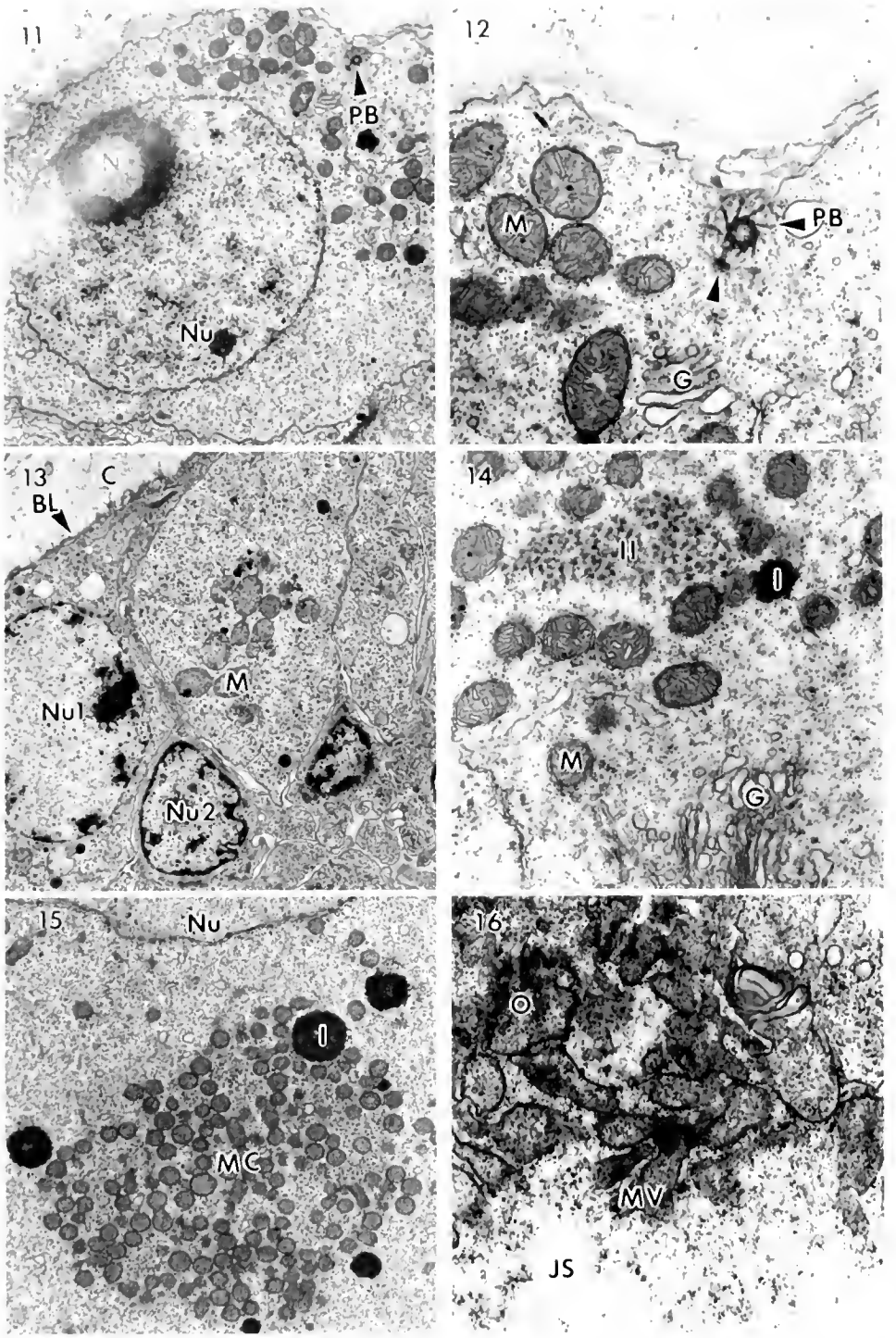

Figure 11. TEM of a germ line cell from a late primary tubule. N, nucleolus, Nu, nucleus, PB, pericentriolar body (satellite structures). 6980×.

Figure 12. TEM at higher magnification of the centriolar satellite structure in Figure 11. G, Golgi body, M, mitochondrion, PB, pericentriolar body (satellite structures). Arrowhead points to microtubules radiating from the centriole. 21,700×.

Figure 13. TEM of cell nest within the gonad basis. BL, basal lamina separating cell nest from, C, connective tissue compartment, M, mitochondria, Nu1, nucleus of a germ line cell, Nu2, nucleus of a somatic cell. 5770×.

Figure 14. TEM showing nuage in a spireme stage oocyte from an early secondary tubule. G, Golgi body, M, mitochondrion, I, type I nuage, II, type II nuage. 13,330×.

Figure 15. TEM showing mitochondrial cloud from a previtellogenic oocyte in a secondary tubule. MC, mitochondrial cloud, Nu, nucleus of oocyte, I, type I nuage. Type II nuage is located between the mitochondria of the cloud. 8200×.

Figure 16. TEM vegetal microvilli in an oocyte from a late secondary tubule just beginning vitellogenesis. Many of the particulate densities are precipitated lead stain, an artifact. JS, jelly space, MV, microvilli, O, oocyte. 20,000×.

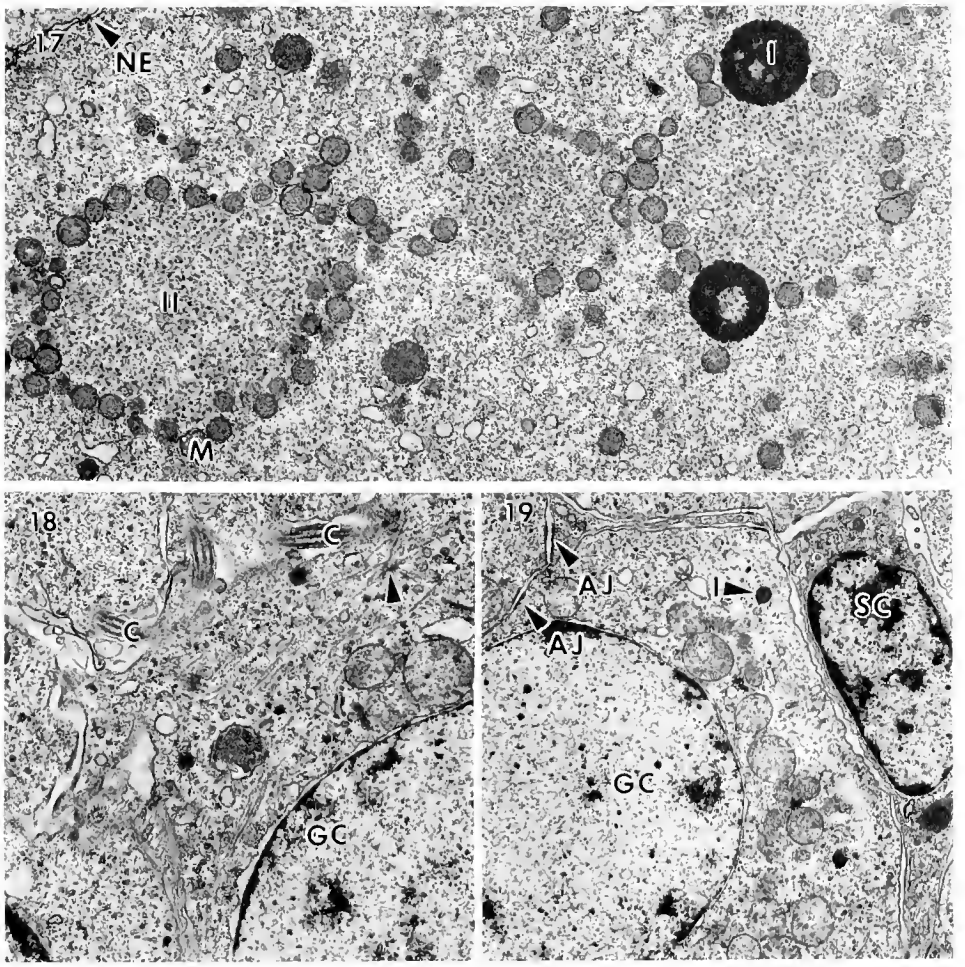

Figure 17. TEM showing unusual spherical aggregations of mitochondria. M. spherical aggregations of mitochondria, NE. nuclear envelope, I. type I nuage, II. type II nuage. 13,060×.

Figure 18. TEM of cilia found on somatic and germ line cells within the cell nests. C. cilium, GC. germ line cell nucleus. Arrowhead marks an apical centriole in this germ line cell. 11,150×.

Figure 19. TEM showing intercellular junctions between adjacent inner epithelial cells in the cell nests. AJ. adhering junctions, GC. germ line cell, SC. somatic cell, I. type I nuage. 8360×.

cent to the nucleus, in the vegetal region of prediplotene oocytes of the secondary tubules (Fig. 3). These are not yolk, but a cloud of mitochondria (Fig. 15). As oogenesis progresses these mitochondria become arranged in striking spherical aggregations which enclose granular electron-dense material (Figs. 14, 17), here called *type II nuage*, which is ultrastructurally indistinguishable from similar nuage found in other echinoderm oocytes (Millonig *et al.*, 1968; Eddy, 1975). Type I nuage (Fig. 14) is also present in these oocytes. Oocytes of secondary tubules have a centriole located in the peripheral cytoplasm (Figs. 11, 12). The centriole has a full compliment of satellite structures (Fig. 12) as would be expected in a cilium producing centriole, yet holothurian oocytes are not known to bear a cilium and none were found in these sections. The centriole and the mitochondrial cloud define the future egg axis, judged by their relationship to the oolamina. It is possible that the centriole acts to fashion the oocyte protuberance, which contains dense arrays of microtubules (Smiley and Cloney, 1985).

Diplotene oocytes in late secondary tubules. The term previtellogensis is used here to include all phases of oocyte development beginning with the production of oocytes in the mitotic proliferation of oogonia, and extending to the inception of active vitellogenesis. Cytologically, the earlier portions of oocyte previtellogenesis can be referred to as spireme stages (Wilson, 1925), describing the characteristic chromosome morphologies. The spireme stages of leptotene, pachytene, and zygotene are evidently accomplished rapidly in *S. californicus* since they are only rarely encountered in sections. The chromosomes decondense at diplotene; the nucleus enlarges and assumes an expanded germinal vesicle configuration, giving the oocyte its most recognizable morphol-

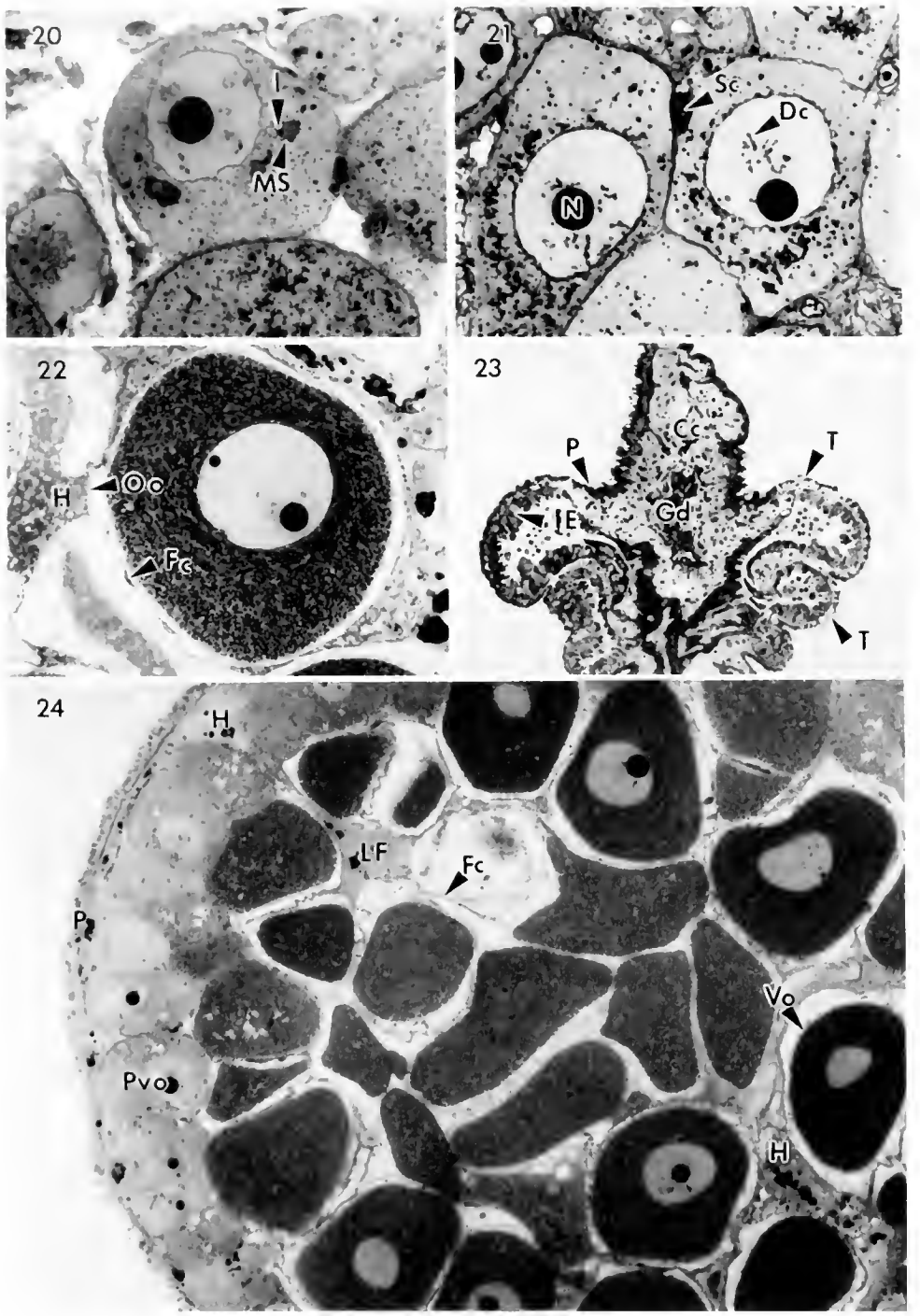

Figure 20. Light micrograph of previtellogenic oocytes in a late secondary tubule. MS, spherical aggregations of mitochondria (see Fig. 17). I, type I nuage. 1130×.

Figure 21. Light micrograph of diplotene configuration to chromosomes of secondary tubule oocytes. D, diplotene chromosomes, N, nucleolus, Sc, somatic cells. 940×.

Figure 22. Light micrograph of early vitellogenic oocyte in the late secondary or early fecund tubule. Fc, follicle cells, H, genital hemal sinus of the connective tissue compartment, Oo, oolamina. 375×.

Figure 23. Light micrograph of frontal section through the developing gonad of a juvenile *S. californicus*. CC, connective tissue compartment, Gd, gonoduct, IE, inner epithelium, P, peritoneum, T, tubules. 75×.

Figure 24. Light micrograph of a cross section of a vitellogenic tubule. Fc, follicle, H, genital hemal sinus, LF, longitudinal fold, P, peritoneum, Pvo, previtellogenic oocytes, Vo, vitellogenic oocytes. 180×.

ogy. The diplotene stage extends into the vitellogenic period, and is terminated when the chromosomes enter diakinesis. Diplotene has the longest duration of any of these stages in *S. californicus* (Fig. 20) and most oocytes in late secondary tubules have their chromosomes in this configuration.

The morphology of oocytes and somatic cells in secondary tubules changes greatly during early oocyte growth and differentiation. When tubules have advanced to where their oocytes are in the diplotene stage, somatic inner epithelial cells adhere to the surface of the oocyte (Fig. 10). During the transition from early to late secondary tubules, these somatic cells form junctional complexes between themselves, creating a true follicle around the oocyte, but it is only in late secondary tubules that the parietal inner epithelium is clearly identifiable (Fig. 24). When a follicle is present around secondary tubule oocytes, the jelly space is absent. Oocytes adhere to the connective tissue layer of the ovary (Fig. 10) by their oolamina in all but the most advanced secondary tubules (Smiley and Cloney, 1985), and attempts to manually dislodge oocytes with fine needles were unsuccessful. Oocytes here average about 40 μm in diameter, contain type I and II nuage, and for the most part lack yolk. The large diplotene germinal vesicle nucleus is probably active in synthesizing messages required for further development, but no specific information on this point is available.

Vitellogenesis in smaller fecund tubules. Stichopus californicus oocytes start to accumulate yolk late in the fall, beginning at about the end of October in the San Juan Archipelago population. The onset of vitellogenesis occurs only in late secondary tubules, and is heralded by a substantial increase in cellular debris found in the genital hemal sinus of these tubules (Fig. 22), during the resorptive period and torpor that follows spawning (Fankboner and Cameron, 1985; Cameron and Fankboner, 1986). Vitellogenesis initially proceeds at a leisurely pace, determined by the slow increase in dense basophilic granules in oocytes of animals fixed during November. By late November, there is a marked increase in the number of granules per oocyte section, indicating that the pace of vitellogenesis has increased. The pace continues to increase until mid January when it appears to level off. The accumulation of cellular debris within the genital hemal sinus is paralleled by elaboration of microvilli at the vegetal pole of the oocyte adjacent to the oolamina (Fig. 16).

TEM reveals that the majority of these granules are yolk platelets (Smiley and Cloney, 1985; Fig. 23), but some are mitochondria, and others type I nuage. During vitellogenesis the spherical aggregations of mitochondria that surrounded nuage in early secondary tubules break up. The mitochondria and nuage disperse within the ooplasm and are not localized to the perinuclear vegetal region. Vitellogenesis is detectable earlier in more centrally located oocytes (Fig. 24). Oocytes near the periphery of tubules are the last to show an increase in size and in accumulation of the dense basophilic yolk granules diagnostic of vitellogenesis. The average diameter of oocytes increases during the late fall and through winter and early spring in *S. californicus*.

The juvenile gonad. In juvenile *Stichopus californicus*, the gonad has started to develop by three to four months after metamorphosis (Fig. 23). The initial structures to form include an expanded central connective tissue component of the gonad basis, a developing gonoduct, and two to four pairs of tubules, similar to the conditions reported for *Holothuria parvula* (Kille, 1942). The tubules are small and unbranched. The most posterior tubules are slightly larger than those more anterior, but the germ line cells within their inner epithelia are all in the proliferative oogonial stage, as determined by the presence of mitotic figures in serially sectioned gonads. Juveniles are difficult to raise, and consequently are rare. I took serial 1 μm sections of the gonads from the four specimens I raised, and found no genital rachis (Hyman, 1955; Smiley, 1988b) present in any of these specimens.

Discussion

Structural aspects of oogenesis in Stichopus californicus

This data shows that the gametogenic holothurian ovary consists of three classes of ovarian tubules, which can be defined by their size, their location along the gonad basis, and the cytological stage of the germ line cells within them. These results are harmonious with and expand upon those of Théel (1901), Mitsukuri (1903), and Kille (1942) concerning the function of the smaller ovarian tubules anterior on the basis in other holothurians. However, my results are in conflict with the arguments of Delage and Hérouard (1903) who suggested that the function of the smaller tubules was to provide a fluid that augmented the spawn. The tubules represent a continuum between the smallest most anterior primary tubules, and the largest most posterior fecund tubules. This continuum is broken by the annual episodic cytological changes in the development of the oocytes. All primary tubules, whether larger or smaller, contain only oogonia. All secondary tubules, whether early or late, contain previtellogenic oocytes. The onset of vitellogenesis in secondary tubules during the fall is a convenient marker for determining the initial stage of the fecund tubules.

This description of the resorption of spent tubules, the progressive increase in size of the secondary tubules during autumn, and the localization of separate functions to particular classes of tubules supports the hypothesis that tubules are progressively recruited to a more posterior position along the flanks of the gonad basis as they develop. Direct testing of this hypothesis is not easy. Vital

dye markers disappear long before a year has passed, *S. californicus* eviscerates when tagged, and animals kept in aquaria for more than a few months shrink in size, and fail to develop oocytes properly (Smiley, pers. obs.). In the field, individuals range freely and readily change depth (Courtney, 1927). The most direct test of this hypothesis would be to mark mitotic oogonial cells with radioactive thymidine. A sizable number of animals would have to be tagged to insure significant recovery, and doses of the marker would have to be initially high to be detected reliably. Because the morphological evidence is so compelling, use of this much radioisotope is probably not warranted.

Oocyte polarity and attachment

Holothurian oocytes are among the most visibly polarized in the animal kingdom (Smiley and Cloney, 1985). In fully formed oocytes, this polarization is referred to as the egg axis, which passes from the oocyte protuberance at the animal pole, through the eccentric germinal vesicle, to the oolamina at the vegetal pole. This axial polarization develops gradually as oocytes increase in size and is continuously congruent with an epithelial cell polarization of the germ line cells that is evident from the time they are first identifiable in the cell nests. This epithelial character of the polarization is defined by the presence of a luminal apical surface, the apical centriole, junctional complexes with adjacent cells, and a basal lamina.

The centriole of *S. californicus* oocytes is apical (animal quadrant), and similar in position to those in oocytes of the asteroid *Pisaster ochraceus* (Schroeder and Otto, 1984; Schroeder, 1985). This is in contrast to reports in *Xenopus* oocytes of a basal centriole (in the vegetal quadrant) which is associated with the mitochondrial cloud (Al-Mukhtar and Webb, 1971; Coggins, 1973), a position not homologous to that in any other epithelial cell. I contend that these workers have mistakenly assigned a basal position to this centriole because they assumed a vegetal location for the aggregated mitochondria of the Balbiani body. But, the terms 'Balbiani body' and 'yolk nucleus' actually mean any basophilic zone near the germinal vesicle (Nørrevang, 1968), and neither aggregated mitochondria nor Golgi bodies are restricted to the vegetal quadrant or to the mitochondrial cloud according to other investigators (Heasman *et al.*, 1984; Wylie *et al.*, 1985).

Wilson (1925) suggested promorphological homology for the vegetal location of the oocyte centrioles through his comparison of oocytes with spermatozoa which have a centriole basal to the nucleus. However, his depiction of spermatozoa is inverted compared to their true promorphological architecture. The trailing flagellum is actually an apical cilium; and the centrioles of spermatozoa are apical to the nucleus. In other words, sperm swim backwards. Consequently, if the centriole is indeed vegetal in *Xenopus* oocytes, one would expect to identify centrioles in two different axial positions in premetamorphic tadpole gonocytes. Al-Mukhtar and Webb did not report this observation. Recent analyses using immunocytochemical methods did not identify a vegetally located centriole in *Xenopus* (Palacek *et al.*, 1985; Dent and Klymkowsky, 1988). Given these arguments, it seems prudent to reinvestigate the axial pattern in *Xenopus* prediplotene oocytes using these techniques.

In some previous descriptions of other holothurians (Inaba, 1930) and other echinoderms (Boveri, 1901), oocytes were often thought to be attached to the somatic ovary by their vegetal surfaces. Other investigators hold that oocytes are attached by the animal surface (Lindahl, 1932; Monné, 1946, Holland *et al.*, 1975). In *Stichopus californicus*, both views are correct depending on the stage of oogenesis. In early stages, oocytes are connected to the somatic ovary by the oolamina at their vegetal pole. In more advanced stages, the protuberance, an animal pole elaboration, connects oocytes to the cells of the somatic ovary. Sections through less fully developed ovaries might lead one to erroneously conclude that holothurian oocytes are always attached by their oolaminae. Information derived from thicker sections of poorly fixed and paraffin embedded specimens might also lead to erroneous conclusions.

Origin of the germ cells

If we accept type I nuage as a more critical marker of germ line cells than either alkaline phosphatase or dense RNA accumulation (Eddy, 1975), then PGCs can be reliably identified only with TEM or immunocytochemistry (Strome and Wood, 1982, 1983). Between the somatocoels in newly metamorphosed *S. californicus* there is set of mesenchymal cells which contain dense RNA accumulations characteristic of germ line cells, but these do not have unambiguous type I nuage as determined by TEM (Smiley, 1986). In the present study, I show that when *Stichopus californicus* is six months old, gonadogenesis has begun, and unambiguous PGCs are located in the connective tissue compartment of the dorsal mesentery. The location and timing of the appearance of these germ line cells is consistent with previous reports of the onset of holothurian gonadogenesis (Cuénot, 1948; Wootton, 1949). These results support the views of Nieuwkoop and Sutasurya (1981) who concluded that echinoderm germ cells first become visible some months after settlement. However, primordial germ cells have been described in newly metamorphosed echinoids (Houk and Hinegardner, 1980).

These arguments should not be interpreted to mean either that germ line cells of holothurians or other echinoderms show an irrevokable lineage restriction, or that

there is an inviolable restriction barring other cell types from becoming germ line cells. The results of Kille (1942), on posterior half regenerates of *Holothuria parvula* following binary fission, suggest that at least peritoneal epithelial cells can transform into germ line cells under some conditions. Théel (1901) described cell aggregations lying against the ascending gonoduct in the dorsal mesentery of adult *Mesothuria intestinalis*, as a genital cord, which contained cells that he interpreted to be PGCs. The histological description of the genital cord in *M. intestinalis* does not match that of the cell nests in the gonad basis of *S. californicus*, but the location and description of *M. intestinalis* PGCs themselves are quite similar to those of *S. californicus* reported here. Presumptive PGCs occur in cell nests lodged within the dorsal mesentery of the aspidochirote *Holothuria parvula* (Kille, 1942). Until PGCs have been described in holothurians from different taxa, we must assume that the differences in location and structure of the germ line bearing tissues reflect intraordinal variations.

Cytological aspects of oogenesis

Nuage. This is the first specific identification of nuage in a holothurian oocyte. Nuage is electron-dense material, lacking a unit membrane, which is found in the cytoplasm of germ line cells where it commonly occurs in two forms (Eddy, 1975, Kessel, 1983). Type I nuage is about 1 μm in diameter and is a granular electron-dense material (Fig. 17) forming rough spheres. Type II nuage consists of minute particulate electron-dense granules surrounded by a homogeneous matrix which is slightly more electron dense than ordinary cytoplasm and which excludes ribosomes (Figs. 14, 17). Both types of nuage are often associated with mitochondria, especially in female germ line cells (Fig. 17; and Millonig *et al.*, 1968). The relationship between nuage and the mitochondrial yolk cloud is likely to be a fundamental one judging from the association between these elements in the oocytes of species from numerous phyla (Eddy, 1975). To date there is no detailed explanation for this association.

In echinoderms, a number of different names have been applied to nuage including 'dense lumps' in oocytes of the crinoid *Nemaster rubignosa* (Holland, 1971) and probably the extruded nucleoli in oocytes of the holothurian *Thyone briareus* (Kessel, 1966). Type I and type II nuage have been reported in oocytes of adult echinoids (Millonig *et al.*, 1968). Houk and Hinegardner (1980) found structures similar to type I nuage, which they called goniosomes, in cells presumed to be PGCs in newly metamorphosed *Lytechinus pictus*, and types I and II nuage were found in oocytes of *Xenopus laevis* (Al-Mukhtar and Webb, 1971; Coggins, 1973). Available reports suggest that all animals probably have some form of germ line specific granule, whether it be called nuage (Eddy, 1975), polar granules as in *Drosophila melanogaster*, or P granules as in *Caenorhabditis elegans* (Wolf *et al.*, 1983). Nuage appears to be germ line specific, because somatic cells have not been shown to contain it (Eddy, 1975). Determination of the origin of germ line cells in other echinoderms may be facilitated by using nuage as a marker. Nuage is distinct from the *heavy* (dense) *bodies*, large granular inclusions surrounded by annulate lamellae often encountered in a variety of echinoderm oocytes (Afzelius, 1957; Eddy, 1975; Kessel, 1966; see Smiley and Cloney, 1985, Fig. 22).

Nuage is no longer aggregated in *S. californicus* oocytes after the onset of vitellogenesis. The spherical aggregations of mitochondria which surround type II nuage disperse, presumably carrying nuage along with them. A similar dispersal was noted in echinoids (Millonig *et al.*, 1968). If nuage is a germ line determinant, then its dispersal may be expected in those animals, such as echinoderms, where regulative development is the rule. If the nuage were not to disperse it would be absent from isolated blastomeres which then would lack the germ line determinant, a condition incompatible with numerous surgical studies on echinoderm embryos (Hörstadius, 1973). In support of this assessment is a recent report by Wylie *et al.* (1985), which suggests that the mitochondrial cloud of *Xenopus laevis* disperses throughout the vegetal ooplasm when the oocyte becomes fully formed. In this case mitochondria and nuage remain somewhat localized to the vegetal quadrant.

Mitochondrial cloud. This structure (Fig. 15) has been referred to as the yolk nucleus, the Balbiani body, and the Balbiani vitelline body in other oocytes (Nørrevang, 1968; Guraya, 1979), as well as the mitochondrial cloud (Heasman *et al.*, 1984; Wylie *et al.*, 1985). The definitions for these terms appear to be capricious; they refer to a number of structures having only a juxtanuclear position and basophilic staining characteristics in common (Nørrevang, 1968; Guraya, 1979). The term 'mitochondrial cloud' is at least accurately descriptive and is used here.

In *S. californicus*, the mitochondrial cloud is always found in the vegetal hemisphere of developing oocytes, close to the nuclear envelope. In sections through secondary tubules (Figs. 2, 3), adjacent oocytes appear to have their mitochondrial clouds in opposing orientation. But the complex topology of the inner epithelium shows that this is not the case (Smiley and Cloney, 1985). In these oocytes, as well as in those of *Xenopus laevis*, the vegetal mitochondrial cloud appears to be the site for mitochondrial proliferation (Heasman *et al.*, 1984), judging by the frequency with which dumbell-shaped mitochondria are encountered. However, the identity of the bio-

chemical pathways controlling this proliferation are not known. Among other echinoderms, a mitochondrial cloud is found in crinoid oocytes (Holland, 1976). The report that echinoid oocytes contain yolk nuclei (Verhey and Moyer, 1967) must be reinterpreted, because the micrographs these investigators present as documentation of their claim show only annulate lamellae (their Fig. 20).

Vitellogenesis. Intense vitellogenesis begins in the late secondary tubules after the autumnal resorption of the viscera in *Stichopus californicus*. At this time, the genital hemal sinus contains cellular debris and unidentifiable particulate matter, and the number of yolk granules in oocytes increases. Vitellogenesis begins in oocytes at the center of the *S. californicus* ovary, but an explanation for this is not readily apparent. It appears likely that oocyte growth constricts passage of hemal fluid through the genital hemal sinus toward the interior of the tubule (Smiley and Cloney, 1985). But rapid growth of central oocytes, occluding only the most central parts of the ovary, would still allow the peripheral oocytes access to an unrestricted hemal sinus.

Yolk proteins appear to be preferentially taken up at the vegetal pole of the *S. californicus* oocyte, based on fine structural information alone. Elongate microvilli are found at the vegetal surface of *S. californicus* oocytes during the post resorptive period of vitellogenesis (Fig. 16). Similar structures have been described at the presumptive vegetal pole of an asteroid oocyte (Beijnink *et al.*, 1984). Some elasipod holothurians have very large eggs, and uptake occurs over the entire egg surface (Eckelbarger, pers. comm.).

Recent studies of echinoid vitellogenesis indicate that cells within the echinoid ovary, either accessory cells or oocytes or both, may synthesize some of the yolk glycoproteins (Ozaki *et al.*, 1986; Shyu *et al.*, 1986). Cells explicitly homologous to the accessory cells do not occur either in any holothurian yet described (Smiley and Cloney, 1985) or in crinoids (Holland *et al.*, 1975). Consequently, these classes require a different mode of nutrient replenishment, which may be provided by the coelomocytes of the perivisceral coelomic fluid. The most abundant protein found in echinoid coelomic fluid shows immunocytochemical cross reactivity with the egg 23S yolk glycoprotein (Giga and Ikai, 1985a, b). Coelomocytes in the coelomic fluid may be the largest single source for all yolk glycoproteins, at least in *Dendraster excentricus* (Harrington and Ozaki, 1986), but ovary (Ozaki *et al.*, 1986) and gut (Shyu *et al.*, 1986) also produce yolk precursor proteins. Results from the experiments of Shyu *et al.* (1986), while documenting that the coelomic fluid contains large amounts of the yolk precursor proteins in *Strongylocentrotus purpuratus*, appear to contradict the conclusion that coelomocytes are a major source. Shyu *et al.* (1986) did not include a divalent cation chelator in their coelomocyte culture medium, and they only labeled for about one quarter the time that Harrington and Ozaki did. In the absence of 10–50 m*M* EDTA, echinoid petaloid amoebocytes undergo an irreversible clotting reaction (Otto *et al.*, 1979; Edds, 1980). This suggests that the failure of Shyu *et al.* to record radiolabeled amino acid incorporation into vitellogenin in the coelomocytes might be due to differences in the duration of labeling or to the clotting response. Future research into holothurian vitellogenesis should include an examination of coelomocytes to see if they are a rich source of vitellogenins. If they prove to be, then the absence of a discrete nutrient storage organ in this class might be explained, and the pathway of nutrient replenishment proposed by Smiley and Cloney (1985) supported.

The annual cycle of the S. californicus *ovary*

The results of this study demonstrate that holothurian oogenesis follows the same cytological course that has been described for a number of other animals in different phyla (Wilson, 1925). In all non parthenogenetic animals, the PGCs, proliferating oogonia, spireme stages of meiosis I prophase, diplotene, and diakinesis sequence is followed in exact order. Repetition of this order, coupled with the localization of these clearly interpretable cytological stages into discrete and linearly ordered structures within the *S. californicus* ovary, offers a simple explanation of the annual ovarian cycle in holothurians.

The cytology of the germ line cells of cell nests, primary and secondary tubules, and the complete resorption of spent fecund tubules support the idea that more anterior tubules are progressively recruited to a more posterior position on the gonad basis with the same timing as that shown by changes in the cytological stages in the oocyte nuclei. This suggestion was also made in other aspidochirotes by Mitsukuri (1903) for *Stichopus japonicus*, Kille (1942) for *Holothuria parvula*, and Deichmann (1948) for *Neostichopus grammatus*, and for the dendrochirote *Thyone briareus* by Kille (1939). This notion of progressive recruitment is attractive in *S. californicus* because it is a large animal that doubtless lives for many more than six years, and probably spawns in all but the first three (Fankboner and Cameron, 1985; Cameron and Fankboner, 1986). If progressive recruitment of new tubules did not occur in *S. californicus*, then after its sixth year the animal would be without spawn.

The Model

My results provide the information necessary to propose a model of how the annual cycle of the *S. californicus* ovary progresses. The annual cycle begins with the resorption of spent tubules in year **N**, and can be summarized as follows. Some of the nutrients derived from

phagocytosis of the spent tubules are taken up into the genital hemal sinus of the secondary tubules, as indicated in Figure 22. Concurrent with the increase of material in the genital hemal sinus, vitellogenesis begins in these oocytes. Therefore, from late fall to early spring, secondary tubules become the fecund tubules of year **N + 1** and are located at the posterior of the gonad basis. Immediately after resorption of the spent tubules, the genital hemal sinus and lumina of primary tubules and hemal lacunae in the connective tissue compartment also become occluded with debris and nutrients. The primary tubules, having completed the oogonial proliferative divisions, become the secondary tubules of year **N + 1** and are now located further back on the basis. During the fall, winter, and early spring, oocytes in these new secondary tubules (year **N + 1**) undergo the early prophase stages of meiosis I, culminating in diplotene. Nests of cells within the gonad basis emerge from the connective tissue compartment during the early fall. Surrounded by the perivisceral peritoneum, they become the primary tubules of year **N + 1** and are found in the anterior location characteristic of primary tubules.

General applicability of the model

Hyman (1955) suggested that resorption of spawned tubules would prove to be the rule among holothurians. If spent tubules are resorbed after spawning, it is likely that progressive recruitment of tubules also occurs, with anterior less advanced tubules moving to a more posterior location concomitant with advancement in the cytological development of the germ line cells. Progressive recruitment of ovarian tubules has been strongly suggested in several aspidochirotes; *Stichopus californicus* (this study), *Mesothuria intestinalis* (Théel, 1901), as well as in the dendrochirote *Thyone briareus* (Kille, 1939). However, there is too little comparative information on oogenesis in apodan, molpadian, dactylochirote, and elasipod holothurians to assess the applicability of this model to them. The best information supporting this model are the surgical experiments of Kille (1939) with the dendrochirote *Thyone briareus*. These showed that of all the ovarian tissues, the gonad basis alone can regenerate oocytes. When only fecund tubules were ablated, new oocyte-bearing tubules regenerated from the basis. When the entire gonad including the basis was removed, regeneration failed. Kille's (1942) study of the gonad in *Holothuria parvula*, an animal which also reproduces asexually through binary fission, provides additional support for this model.

The data and analysis presented in this paper, while considerably more precise in determining cell and tissue level changes, is limited by this precision, and cannot supplant population level surveys. Information derived by the gonad index method may be applicable in assessing this model's generality. From the data presented here, it is clear that these gonad index studies measure vitellogenesis and not the process of oogenesis. A number of species have been investigated in this way, including *Stichopus californicus* (Cameron and Fankboner, 1986), *Stichopus japonicus* (Tanaka, 1958), *Thelenota ananas* and *Microthele nobilis* (Conand, 1983), and the data they present are entirely consistent with the pattern described here (see Smiley *et al.*, for a more complete review). Consistency, not confirmation or refutation, is all that can be expected from such studies, because gonad index assessments only measure average changes in populations. Analysis of reproductive cycle data derived from gonad indices of populations of many different holothurians shows that most species have the general features predicted by this model. This includes marked diminishment in gonad index after spawning, the subsequent further reduction in index corresponding to phagocytosis of spent tubules, the measurable lowest size corresponding to the basis and more anterior tubules, and the gradual build up in index as vitellogenesis for the next season commences (Smiley *et al.*, 1988).

This model may not account for the gonad index data of male holothurians of any order, nor of small and hermaphroditic holothurians, such as *Cucumaria curata* (Rutherford, 1973), or *Rhabdomolgus ruber* (Menker, 1970). Because many Arctic, Antarctic, and deep sea species are thought to produce eggs continuously (Feral and Magniez, 1985; Tyler *et al.*, 1985) they may also pose problems for this model.

Comparisons with other echinoderm classes

The anatomical and histological simplicity of this holothurian ovary offers unique information that is applicable to understanding the dynamics of oogenesis in other echinoderm ovaries (Smiley, 1984, 1986, 1988b; Smiley and Cloney, 1985; Smiley *et al.*, 1988). It is difficult to study microscopic morphological changes among a synchronously developing population of oocytes in other echinoderms. Primordial germ cells, mitotic oogonia, and early meiotic prophase staged oocytes are considerably smaller than previtellogenic or vitellogenic oocytes; they can be quite difficult to locate within the inner epithelium. This difficulty is reflected in the limited reports on the earliest stages of oogenesis in other echinoderms (Holland *et al.*, 1975; Walker, 1982). These same structural problems have prevented biochemical analysis of oogenesis in any echinoderm. Given the identifiable and discrete localization of the major cytological stages in oogenesis in the holothurian ovary, such biochemical analyses may now be possible.

Unanswered questions

This study offers a number of important observations and analyses which require more detailed investigation. Among these are the possible signalling role of the resorptive phase and the onset of torpor in driving subsequent oogenesis. There is no clear description of the earliest stages of development in the PGCs of any holothurian, nor of their ultimate source. If cells other than those containing nuage are capable of transforming into PGCs (Kille, 1942), then the conditions under which this transformation can occur are important to know. This knowledge would allow a more detailed analysis of the mechanisms of coordinated control over the regulatory pathways for differentiation in an echinoderm, an elusive problem made more difficult by the extreme regulative development of these animals. The mechanisms of control over the proliferative divisions of the mitotic oogonia are not known, nor is the control of entry into the prophase stages of meiosis I or the biochemical details of these changes. Even if the onset of vitellogenesis is controlled by resorption of the viscera, a mechanism that could explain how the interior oocytes of late secondary tubules are directed to begin vitellogenesis prior to the peripheral oocytes is elusive. We have very little information on the relative contribution of the oocyte itself on yolk formation in any holothurian species. Finally, the reasons for the general resorption of the viscera of this holothurian each fall, even in those individuals that have not yet reached sexual maturity (Fankboner and Cameron, 1985), remain a mystery.

Acknowledgments

Much of this work was done at the Friday Harbor Laboratories. I thank the administration, faculty, staff, visiting scientists, and graduate students for helping me in all phases of this work. I especially thank K. P. Irons for her substantial efforts that improved this paper. C. Chaffee, R. Cloney, K. Eckelbarger, R. Emlet, M. Hille, R. Langelan, J. Otto, J. Pearse, T. Pennington, T. Schroeder, R. Strathmann, C. Walker, and an anonomous reviewer all offered good suggestions and helpful criticisms. I gratefully acknowledge support from an NIH Developmental Biology Training Grant (HD-00266) and a Damon Runyon-Walter Winchell Cancer Fund Postdoctoral Fellowship (DRG-895) during the tenure of this

Literature Cited

Afzelius, B. A. 1957. Electron microscopy on the basophilic structures of the sea urchin egg. *Z. Zellforsch. Mikrosk. Anat. Abt. Histochem.* **45:** 660–675.

Al-Mukhtar, K. A. K., and A. C. Webb. 1971. An ultrastructural study of primordial germ cells, oogonia and early oocytes in *Xenopus laevis*. *J. Embryol. Exp. Morphol.* **26:** 195–217.

Beijnink, F. B., C. W. Walker, and P. A. Voogt. 1984. An ultrastructural study of relationships between the ovarian haemal system, follicle cells, and primary oocytes in the sea star *Asterias rubens*. *Cell Tiss. Res.* **238:** 339–347.

Boveri, T. 1901. Die polaritat von Ovocyte, Ei, und Larve des *Strongylocentrotus lividus*. *Zool. Jahrb. Anat.* **14:** 630–653.

Cameron, J. L., and P. V. Fankboner. 1986. Reproductive biology of the commercial sea cucumber *Parastichopus californicus*. I. Reproductive periodicity and spawning behavior. *Can. J. Zool.* **64:** 168–175.

Clark, H. L. 1901. The holothurians of the Pacific coast of North America. *Zool. Anz.* **24:** 162–171.

Coggins, L. W. 1973. An ultrastructural and radioautographic study of early oogenesis in the toad *Xenopus laevis*. *J. Cell. Sci.* **12:** 71–93.

Conand, C. 1983. Sexual cycle of three commercially important holothurian species from the lagoon of New Caledonia. *Bull. Mar. Sci.* **31:** 523–543.

Courtney, W. D. 1927. Fertilization in *Stichopus californicus*. *Publ. Puget Sound Biol. Stn.* **5:** 257–260.

Cuénot, L. 1948. Anatomie, éthologie, et systématique des échinodermes. In *Traité de Zoologie*. **11:** 3–275. (P. P. Grassé), ed. Masson & Cie, Paris. 1077 pp.

Deichmann, E. 1937. The Templeton Crocker Expedition LX. Holothurians from the Gulf of California, the west coast of Lower California and Clarion Island. *Zoologica* **22:** 161–176.

Deichmann, E. 1948. The holothurian fauna of South Africa. *Ann. Nat. Mus.* **11:** 325–376.

Delage, Y., and E. Hérouard. 1903. *Traité de Zoologie Concrète*. Tome III. *Les Échinodermes*. Schleicher Freres, Paris. 495 pp.

Dent, J. A., and M. W. Klymkowsky. 1988. Wholemount analysis of cytoskeletal reorganization and function during oogenesis and early embryogenesis in *Xenopus*. In *The Cell Biology of Fertilization*. H. Schatten, and G. Schatten, eds. Academic Press, New York. (in press).

Edds, K. T. 1980. The formation and elongation of filopodia during transformation of sea urchin coelomocytes. *Cell Motility* **1:** 131–140.

Eddy, E. M. 1975. Germ plasm and the differentiation of the germ cell line. *Int. Rev. Cytol.* **43:** 229–280.

Fankboner, P. V., and J. L. Cameron. 1985. Seasonal atrophy of the visceral organs in a sea cucumber. *Can. J. Zool.* **63:** 2888–2892.

Feral, J. P., and P. Magniez. 1985. Level, content and energetic equivalent of the main biochemical constituents of the subantarctic molpadid holothurian *Eumolpadia violacea* at two seasons of the year. *Comp. Biochem. Physiol.* **81A:** 415–422.

Giga, Y., and A. Ikai. 1985a. Purification of the most abundant protein in the coelomic fluid of a sea urchin which immunocytochemically cross reacts with 23S glycoprotein in the sea urchin egg. *J. Biochem.* **98:** 19–26.

Giga, Y., and A. Ikai. 1985b. Purification and physical characterization of 23S glycoprotein from sea urchin (*Anthocidaris crassispina*) eggs. *J. Biochem.* **98:** 237–243.

Guraya, S. S. 1979. Recent advances in the morphology, cytochemistry, and function of Balbiani's vitelline body in animal oocytes. *Int. Rev. Cytol.* **59:** 249–321.

Haanen, W. 1914. Anatomische und histologische studien an *Mesothuria intestinalis*. *Zeit. Wiss. Zool.* **109:** 185–255.

Harrington, F. E., and H. Ozaki. 1986. The major yolk glycoprotein precursor in echinoids is secreted by coelomocytes into the coelomic plasma. *Cell Differ.* **19:** 51–57.

Heasman, J., J. Quarmby, and C. C. Wylie. 1984. The mitochondrial cloud of *Xenopus* oocytes: the source of germinal granule material. *Dev. Biol.* **105:** 458–469.

Holland, N. D. 1971. The fine structure of the ovary of the feather star *Nemaster rubiginosa. Tissue Cell.* **3:** 163–177.

Holland, N. D. 1976. The fine structure of the yolk nucleus in oocytes of *Antedon bifida. J. Mar. Biol. Assoc. U. K.* **56:** 59–63.

Holland, N. D., J. G. Grimmer, and H. Kubota. 1975. Gonadal development during the annual reproductive cycle of *Comanthus japonica. Biol. Bull.* **148:** 219–242.

Hörstadius, S. 1973. *Experimental Embryology of Echinoderms.* Clarendon Press, Oxford. 192 pp.

Houk, M. S., and R. T. Hinegardner. 1980. The formation and early differentiation of sea urchin gonads. *Biol. Bull.* **159:** 280–294.

Hyman, L. H. 1955. *The Echinoderms. The Invertebrates Vol. IV.* McGraw-Hill, New York. 763 pp.

Inaba, D. 1930. Notes on the development of a holothurian *Caudina chilensis. Sci. Rept. Tohôku Imp. Univ. Ser.* **4, 5:** 215–248.

Kessel, R. G. 1966. Some observations on the oocyte of *Thyone briarcus* with special reference to the relationship of the Golgi complex and endoplasmic reticulum in the formation of yolk. *J. Ultrastruct. Res.* **16:** 305–319.

Kessel, R. G. 1983. Urochordata-Ascidiacea. Pp. 655–734 in *Reproductive Biology of Invertebrates. Vol. 1. Oogenesis, Oviposition, and Oosorption.* K. G. Adiyodi, and R. G. Adiyodi, eds. John Wiley & Sons.

Kille, F. R. 1939. Regeneration of gonad tubules following extripation in the sea cucumber *Thyone briareus. Biol. Bull.* **76:** 70–79.

Kille, F. R. 1942. Regeneration of the reproductive system following binary fission in the sea cucumber *Holothuria parvula. Biol. Bull.* **83:** 55–66.

Lindahl, P. E. 1932. Zur Kenntnis des Ovarialeies bei dem Seeigel. *Roux's Arch.* **126:** 373–390.

Menker, D. 1970. Lebenzyklus, Jungendentwicklung und Geschlechtorgane von *Rhabdomolgus ruber. Mar. Biol.* **6:** 167–186.

Millonig, G., M. Bosco, and L. Giambertone. 1968. Fine structural analysis of oogenesis in sea urchins. *J. Exp. Zool.* **169:** 293–314.

Mitsukuri, K. 1903. Notes on the habits and life history of *Stichopus japonicus. Annot. Zool. Japn* **5:** 1–21.

Monné, L. 1946. Some observations on the polar and dorsoventral organization of the sea urchin egg. *Ark. Zool.* **38A** (No. 15): 1–13.

Nieuwkoop, P. A., and L. A. Sutasurya. 1981. *Primordial Germ Cells of the Invertebrates.* Cambridge Univ. Press. New York. 258 pp.

Nörrevang, A. 1968. Electron microscopic morphology of oogenesis. *Int. Rev. Cytol.* **23:** 113–186.

Otto, J., R. Kane, and J. Bryan. 1979. Formation of filopodia in coelomocytes: localization of fascin, a 58 kilodalton actin cross linking protein. *Cell* **17:** 285–293.

Ozaki, H., O. Moriya, and F. E. Harrington. 1986. A glycoprotein in the accessory cells of the echinoid ovary and its role in vitellogenesis. *Roux's Arch. Dev. Biol.* **195:** 74–79.

Palacek, J., V. Habrova, J. Nedvidek, and A. Romanovsky. 1985. Dynamics of tubulin structures in *Xenopus laevis. J. Embryol. Exp. Morphol.* **87:** 75–86.

Rutherford, J. C. 1973. Reproduction, growth, and mortality of the holothurian *Cucumaria pseudocurata. Mar. Biol.* **22:** 167–176.

Schroeder, T. E. 1985. Physical interactions between asters and the cortex in echinoderm eggs. In *The Cellular and Molecular Biology of Invertebrate Development.* R. H. Sawyer and R. M. Showman, eds. *Belle W. Baruch Library in Marine Science.* **15:** 69–89.

Schroeder, T. E. 1985. Physical interactions between asters and the cortex in echinoderm eggs. In *The Cellular and Molecular Biology of Invertebrate Development.* R. H. Sawyer and R. M. Showman, eds. *Belle W. Baruch Library in Marine Science.* **15:** 69–89.

Schroeder, T. E., and J. J. Otto. 1984. Cyclic assembly-disassembly of cortical microtubules during maturation and early development of starfish oocytes. *Dev. Biol.* **103:** 493–503.

Shyu, A-B., R. A. Raff, and T. Blumenthal. 1986. Expression of the vitellogenin gene in female and male sea urchin. *Proc. Natl. Acad Sci U.S.A* **83:** 3865–3869.

Smiley, S. 1984. A description and analysis of the structure and dynamics of the ovary, of ovulation, and of oocyte maturation in the holothurian *Stichopus californicus.* M.Sc. Thesis, Univ. Washington, Seattle. 119 pp.

Smiley, S. 1986. Metamorphosis of *Stichopus californicus:* and its phylogenetic implications. *Biol. Bull.* **171:** 611–631.

Smiley, S. 1988a. Investigations into the purification and identification of the oocyte maturation hormone of *Stichopus californicus.* In *Echinoderm Biology: Proceedings of the 6th International Echinoderm Conference.* R. D. Burke, P. V. Mladenov, P. Lambert, and R. L. Parsley, eds. Balkema Press, Rotterdam. (in press).

Smiley, S. 1988b. The phylogenetic relationships of holothurians: a cladistic analysis of the extant echinoderm classes. Ch. 6 in *Echinoderm Phylogeny and Evolutionary Biology.* C. R. C. Paul, and A. B. Smith, eds. Symposium British Museum (Natural History). Oxford Univ. Press. (in press).

Smiley, S., and R. A. Cloney. 1985. Ovulation and the fine structure of the *Stichopus californicus* fecund ovarian tubules. *Biol. Bull.* **169:** 342–363.

Smiley, S., F. S. McEuen, and C. Chaffee. 1988. Holothurian reproductive biology. Ch. 8 in *A Treatise of Invertebrate Reproduction. Vol. 6.* A. C. Geise, and J. S. Pearse, eds. Blackwell Scientific Publishers (in press).

Strome, S., and W. B. Wood. 1982. Immunofluorescence visualization of germ line specific cytoplasmic granules in embryos, larvae, and adults of *Caenorhabditis elegans. Proc. Natl. Acad. Sci. U.S.A.* **79:** 1558–1563.

Strome, S., and W. B. Wood. 1983. Generation of assymetry and segregation of germline granules in early *C. elegans* embryos. *Cell* **35:** 15–25.

Tanaka, Y. 1958. Seasonal changes occurring in the gonad of *Stichopus japonicus. Bull. Fac. Fish Hokkaido Univ.* **9:** 29–36.

Théel, H. 1901. A singular case of hermaphroditism in holothuroids. *Bihang till Kungl. Svenska Vetensk. Acad. Handl.* **27:** Afd. 4., No. 6.

Tyler, P. A., A. Muirhead, D. S. M. Billett, and J. D. Gage. 1985. Reproductive biology of the deep sea holothurians *Laetmogone violacea* and *Benthogone rosacea* (Elasipoda: Holothurioidea). *Mar. Ecol. Prog. Ser.* **23:** 269–277.

Verhey, C. A., and F. H. Moyer. 1967. Fine structural changes during sea urchin oogenesis. *J. Exp. Zool.* **164:** 195–207.

Walker, C. W. 1982. Nutrition of gametes. Pp. 449–468 in *Echinoderm Nutrition.* M. Jangoux, and J. M. Lawrence, eds. Balkema, Rotterdam.

Wilson, E. B. 1925. *The Cell in Development and Heredity. 3rd* ed. MacMillan Pubs., New York. 1296 pp.

Wolf, N., J. Priess, and D. Hirsh. 1983. Segregation of germline granules in early embryos of *Caenorhabditis elegans:* an electron microscopic analysis. *J. Embryol. Exp. Morphol.* **73:** 297–306.

Wootton, D. M. 1949. The development of *Thyonepsolus nutriens.* Ph.D. Dissertation, Stanford Univ. 90 pp.

Wylie, C. C., S. Holwill, M. O'Driscoll, A. Snape, and J. Heasman. 1985. Germ plasm and germ cell determination in *Xenopus laevis* as studied by cell transplantation analysis. *Cold Spring Harb. Symp. Quant. Biol.* **50:** 37–44.

Reference: *Biol Bull* 175: 94–101. (August, 1988)

Assessment of Ciguatera Dinoflagellate Populations: Sample Variability and Algal Substrate Selection

PHILLIP S. LOBEL[1], DONALD M. ANDERSON[1], AND MONIQUE DURAND-CLEMENT[2]

[1]*Woods Hole Oceanographic Institution, Woods Hole, Massachusetts 02543, and*
[2]*Unite INSERM 303, Marine Station, 06250 Villefranche Sur Mer, France*

Abstract. Preliminary assessment is made of two key components in ciguatera ecology. First, we examined the numerical variability of *Gambierdiscus toxicus* as an epiphyte on the macroalgae, *Dictyota* and *Galaxaura*. Variability was examined by a statistical bootstrap technique to determine the minimum number of samples required to adequately estimate the abundance of *G. toxicus* at one station and to test for statistically significant differences between two stations. A minimum of 10 replicates were needed at the relatively low *G. toxicus* abundance found at our study site. Second, we demonstrated the feasibility of conducting controlled laboratory experiments to assess the short-term colonization behavior of *G. toxicus* on selected macroalgae offered in varying mass and surface area ratios. To assess *G. toxicus* abundance and distribution, the number of cells per unit of host alga must be standardized. We show that contradictory conclusions can be reached depending on whether the number of dinoflagellate cells is normalized to algal biomass or surface area.

Introduction

The continuing enigma of ciguatera, namely the stochastic variability of fish toxicity in time and space, must have its basis in the ecology and population dynamics of the benthic dinoflagellates that produce ciguatoxin and maitotoxin. Several dinoflagellate species have been implicated as producing chemical compounds that likely result in fish toxicity (Yasumoto *et al.*, 1987). One of these *Gambierdiscus toxicus*, appears to be most significant in ciguatera ecology. Despite the identification over a decade ago of the most likely progenitors of the toxins and numerous field and laboratory studies throughout the tropics (reviewed in Withers, 1982; Ragelis, 1984; Salvat, 1985; Anderson *et al.*, 1985; Anderson and Lobel, 1987), the state of knowledge about ciguatera and *G. toxicus* physiology and ecology remains "very primitive indeed" (Scheuer and Bagnis, 1985).

Clearly, one reason for this situation is the complex and gradual manner in which small quantities of the highly potent ciguatoxin and related toxins move through the food chain to the higher predators. We believe that a contributing factor has been the lack of a standardized, statistically rigorous methodology for examining the distribution and abundance of the ciguatera dinoflagellates in time and space. In this preliminary study, we addressed the question: "How many samples of a macroalgal species must be collected at one time and at one site and depth to adequately quantify the abundance of *G. toxicus*?" Strictly speaking, the results of our data analysis are valid only for one study site at one point in time and for the two macroalgal hosts we examined, but these data and methodologies document the large errors associated with inadequate sample size and provide a means to determine the minimum number of samples needed to test for statistically significant differences between stations. In addition, we tested the feasibility of conducting laboratory studies of the preference of *G. toxicus* for a particular macroalgal host. Analysis of these data demonstrate the misleading nature of dinoflagellate abundance expressed per gram of host alga and provide a good argument for yet another change to common enumeration methodologies—namely the normalization of dinoflagellate abundance to host surface area rather than biomass (Bomber *et al.*, 1985). Ciguatera is a complex ecological phenomenon that is poorly understood. It seems appropriate to re-evaluate commonly accepted

Received 19 October 1987; accepted 31 May 1988.

methodologies and assumptions and to test the feasibility of addressing certain fundamentally important behavioral and physiological issues in the laboratory.

Materials and Methods

Study site

This field study was conducted at St. Barthelemy (17°54'N, 62°50'W) in the Caribbean (French West Indies) from 8 to 20 August 1986. Extensive collections were made at the "Pointe de Negre" site located on the south side of the island, about 3 km from the port of Gustavia. Laboratory facilities and logistics on the island were provided by the New England Biolabs Foundation.

Macroalgal collection and dinoflagellate enumeration

Two macroalgal species were selected for intensive study, *Dictyota* sp. (probably *D. bartayresii* and maybe mixed with *D. dichotoma* and *D. divaricata*) and *Galaxaura* sp. (probably *G. corneum*). Both species were epiphytized by *G. toxicus*. *Dictyota* is a brown alga and *Galaxaura* is a red articulated coralline alga. The growth form of each is a complex 3-D structure of branches. Both algae were growing abundantly in close proximity.

All specimens were collected between 5–6.5 m depth at the Pointe de Negre study site on 17 and 19 August 1986. Specimens were picked, placed in individual plastic bags that were sealed underwater, and transported to the laboratory in the dark at ambient water temperature. The bags were then vigorously shaken and kneaded to dislodge *G. toxicus*. The 20–250 μm size fraction was collected by pouring the contents through Nitex sieves. The adequacy of this method was confirmed by successive shaking and washing, which produced few additional dinoflagellates.

The collected material was backwashed into a vial with approximately 10 ml of filtered seawater. *G. toxicus* individuals were enumerated with a compound microscope at 100× total magnification. A minimum of one ml of the concentrated suspension was scanned for each sample. Macroalgae were blot-dried and weighed. Masses ranged between 1 and 20 grams. Dinoflagellate abundance was initially expressed as cells per gram blot dry weight of host algae. Subsequent measurements of algal surface area per gram blot dry weight allow the data to be normalized to surface area as well.

Preference studies

Two laboratory experiments were conducted. One used equal biomass amounts of macroalgae and the other combined two algae in different proportions. In all treatments, algae were rinsed several times to remove most epiphytes (determined by visual inspection of algae under a dissecting microscope) and placed in pairs in 125-ml beakers with filtered seawater. A known number of *G. toxicus* cells were then added (final concentration approximately 80 ml^{-1}). The samples were maintained for 24 hours in an incubator at 26°C on a 12:12 L:D cycle at approximately 50 μEinst m^{-2} s^{-1}. Beakers were mildly swirled every 4 h (except overnight) to evenly distribute those dinoflagellates which had not yet settled. When the experiments were terminated, the number of *G. toxicus* cells on each alga and those remaining unattached in the beaker were counted separately. Because of the differences in algal morphology, the results are expressed as the percentage of all *G. toxicus* attached to the algae, as cells per unit mass and as cells per surface area. Two *G. toxicus* isolates were used–strain T3 isolated from Gambier Islands by R. Bagnis and strain SB01 isolated from Lorient, St. Barthelemy, by M. Durand-Clement in July 1986. They were grown in modified ES medium (Durand, 1984).

Macroalgae measurements

Surface area, wet weight, and displacement volume were assessed for the macroalgae *Galaxaura* and *Dictyota*. Surface area is the most difficult measurement to obtain accurately. We used three methods for surface area calculations. One technique consisted of dipping a dried macroalgal sample in a detergent solution that is supposed to adhere to the algal surface in a layer of consistent thickness (Harrod and Hall, 1962). By knowing the weight of solution that coats a standard area of plastic sheeting, the surface area of an alga can be calculated. We encountered numerous problems with this method and did not obtain consistent or reliable data. Clearly, this concept has potential, and modifications made by Bomber (1985, pers. comm.) using wet specimens and full strength detergent might be necessary, but problems exist with how the solution coats and is adsorbed by different algae. Other techniques involved morphological measurements of surface area. Enlarged silhouettes of *Dictyota* were analyzed using a computer and a digitizer graphics unit since that species' shape is essentially two-dimensional. *Galaxaura* was measured in pieces under a microscope with a micrometer. *Galaxaura's* shape is tubular, and painstaking measurements were made of all individual pieces in a sample. Surface area by these latter two methods provided consistant data.

Results

Algal mass measurement

The primary problem we encountered was the measurement of algal characteristics for valid interspecific comparison of host-alga selection by *G. toxicus*. The

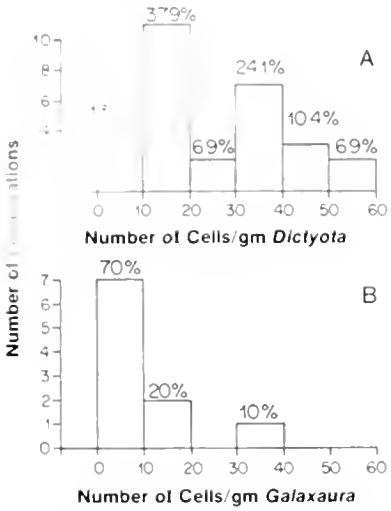

Figure 1. Frequency distribution of the number of *Gambierdiscus toxicus* cells on (A) *Dictyota* and (B) *Galaxaura*. Percentage relative frequency is specified above each column.

common measure of 'cells per gram blot-dry weight' is suitable for *intra*specific comparison of *G. toxicus* on a host alga. This measurement had the advantage of being easy and rapid in the field. However, the best measurement for *inter*specific host algal comparisons is 'cells per surface area.'

The surface area of *Dictyota* was 105 ± 31 (range 67–151) cm^2 gm^{-1} (n = 13). The surface area of *Galaxaura* was 31 ± 8 (range 25–42) cm^2 gm^{-1} (n = 4). Conversion of the number of *G. toxicus* cells per gm alga to cells per cm^2 was obtained by dividing by 105 for *Dictyota* and 31 for *Galaxaura*. The variance in surface areas is probably due in large part to measurement error, but the possibility of allometric variation in these algae also needs to be examined.

Field abundance

Gambierdiscus toxicus was present at the study site, but in relatively low abundance. Every *Dictyota* sample (n = 29) hosted at least 5 cells g^{-1} blot-dry weight. Eighty-six percent of the collection had greater than 10 cells g^{-1} (Fig. 1A). The mean (±S.D.) number of *G. toxicus* on *Dictyota* was 24 ± 14 (range 5–56) cells g^{-1} or 23 cells per 100 cm^2. Only half of the *Galaxaura* samples (n = 10) were epiphytized by *G. toxicus* and another 20% had fewer than 10 cells g^{-1} (Fig. 1B). The mean (±S.D.) abundance of *G. toxicus* on *Galaxaura* was 6 ± 10 (range 0–30) cells g^{-1} or 19 cells per 100 cm^2. The number of *G. toxicus* per gram of host alga was not a function of the size of individual *Dictyota* (Fig. 2) or *Galaxaura* samples, based on linear, exponential, log, or power function regression tests.

Sampling statistics

We collected many (n = 29) specimens of *Dictyota* to evaluate the sample size necessary for statistical analysis of the distribution and abundance of *G. toxicus*. We also examined this for *Galaxaura* but with, as it turned out, too few samples.

The analysis used was a statistical "bootstrapping" routine (Diaconis and Efron, 1983). The graphs (Figs. 3, 4) show 25 random combinations (with replacement) from the sample set for each sample size. The sample size range for *Dictyota* was 2 to 29 and for *Galaxaura* was 2 to 10. Thus, for each incremental sample size to n = 25, calculations were made based on the total sample pool.

The analysis is presented in three plots each for *Dictyota* (Fig. 3) and *Galaxaura* (Fig. 4): (A) the mean number of *G. toxicus* cells per gram of alga, (B) standard error of these means, and (C) the percentage change in the standard error as sample size increases. The first plot shows the spread in possible averages among 25 sample sets for a given sample size. It illustrates the wide variability obtainable at small sample sizes, especially n < 10 drawn from the same sample pool. The second plot quantifies this variability as the standard error of the means. It decreases substantially with increasing sample size. The third plot defines the degree to which results fluctuate as the percentage change in the standard error with the incremental addition of samples.

At small sample sizes the variability in the means is due more to random sample selection than actual differences in the density of *G. toxicus* at a site. This variability is greater for *Galaxaura*, since 50% of the samples lacked *G. toxicus* cells. Thus, fewer samples of *Dictyota* than *Galaxaura* would more accurately assess *G. toxicus* abundance. A sample size of n = 10 to 15 *Dictyota* sam-

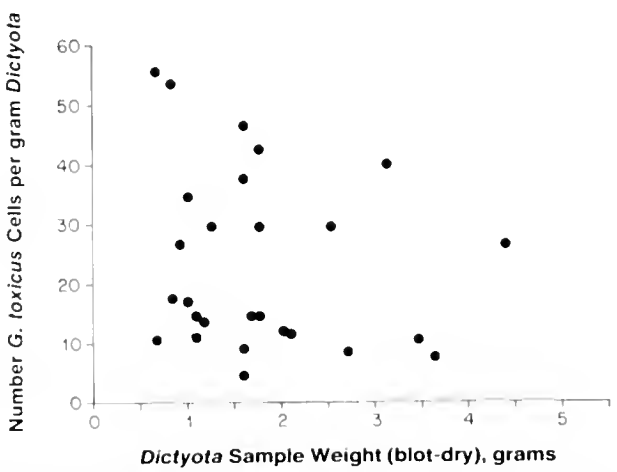

Figure 2. Relationship between the number of *Gambierdiscus toxicus* cells per gm of *Dictyota* as a function of the sample weight of individual *Dictyota* masses (n = 29). No statistical correlation was found.

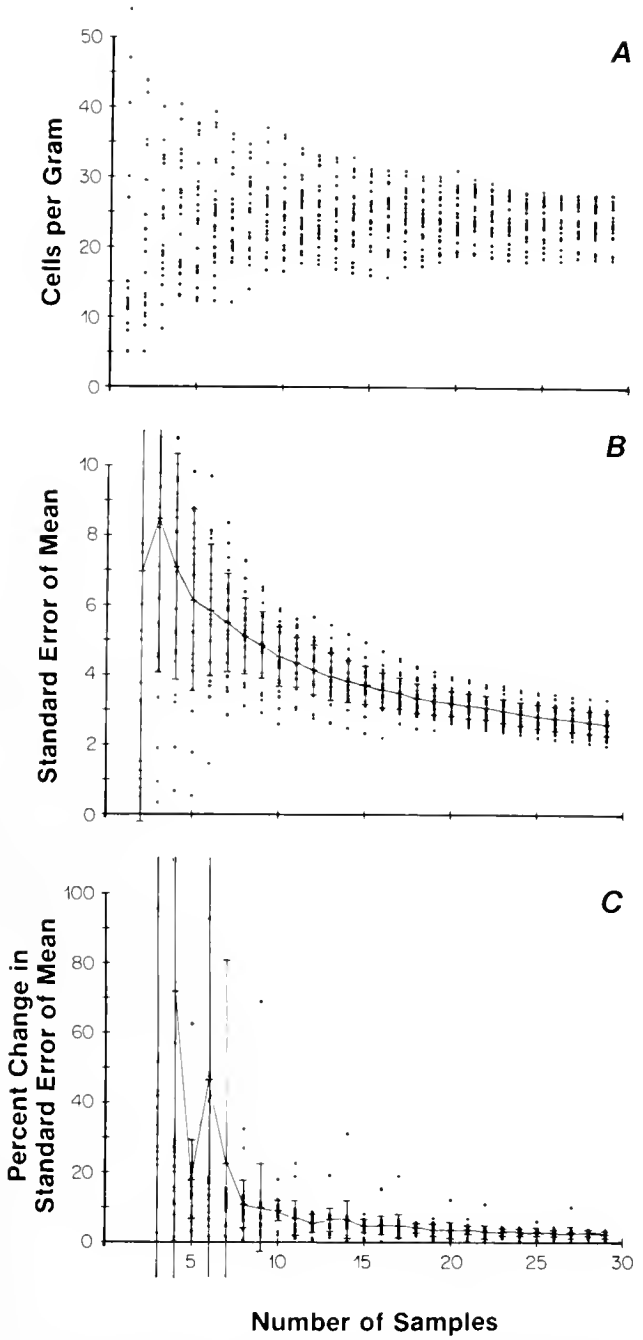

Figure 3. *Dictyota.* (A) Variations in means for given sample sizes drawn from the total pool of 29 samples calculated by the "bootstrap" method. The mean was calculated 25 times for each sample size. At sample sizes less than n = 5, some points exceed the limit of the ordinate. (B) Standard error of the means in Figure 5 calculated 25 times with the overall average connected by a solid line across all sample sizes. This indicates the variance associated with a mean calculated for a given sample size. As sample size increases, this variance decreases. (C) Percent change in the standard error of the means from n to n + 1 calculated 25 times for each n. The overall average is connected by a solid line across all n's. In this case, as sample size increased, the percentage change in possible means decreased substantially up to about n = 15 after which additional samples did not significantly affect the mean.

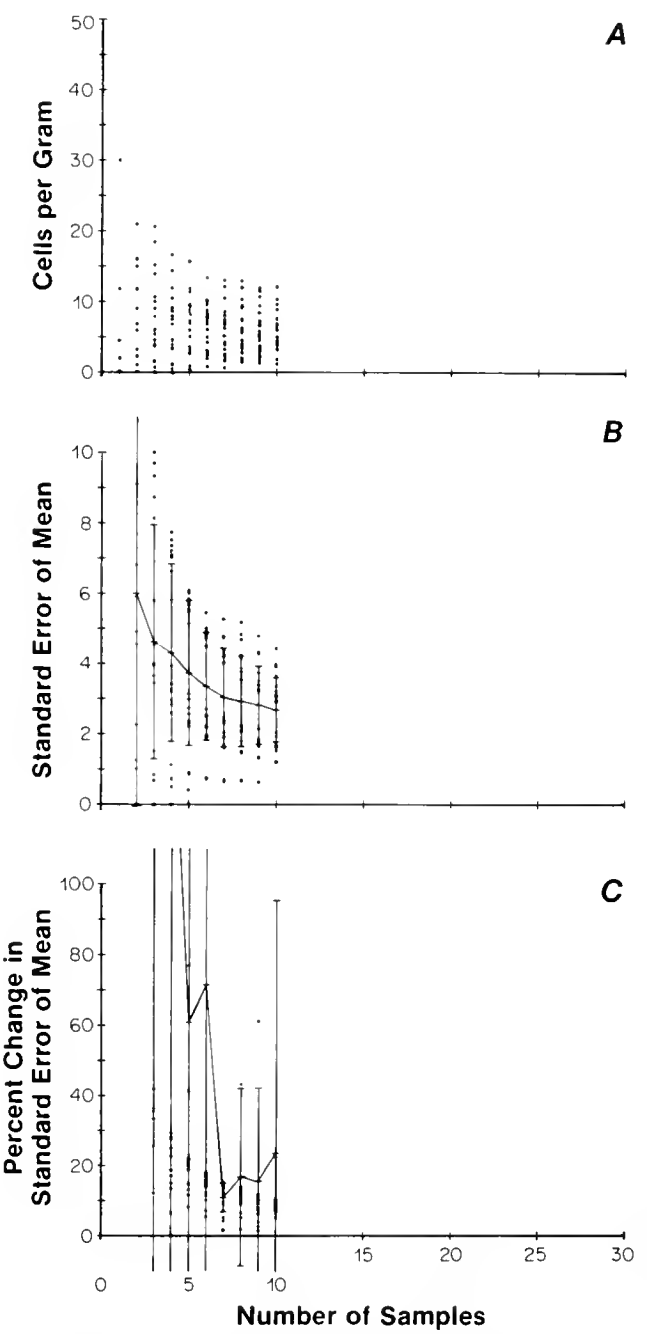

Figure 4. *Galaxaura.* (A) Variations in means. (B) Standard error of the means calculated in A. (C) Percent change in the standard error of the means. In this case, n = 10 was insufficient to determine the point at which additional samples would not significantly affect the results. See Figure 3 for details.

ples would be statistically adequate using parametric analyses to estimate the abundance of *G. toxicus* (Fig. 3). For comparison to other collections, these analyses can be used to determine the variance values that would be significantly different for specified sample sizes. Given the means and standard errors calculated above, the val-

ues of sample means, which would be significantly different at $P < .05$ and $P < .01$ assuming the same degree of standard error, can be simply specified by a *t*-test. It would be necessary to generate a new set of plots in other studies with different *G. toxicus* abundance and distribution.

Substrate selection

Several experiments were designed to evaluate the feasibility of determining if the *G. toxicus* abundance on different macroalgae is the result of stochastic processes or a demonstration of active substrate preference and selection. Preference was evaluated by counting the number of dinoflagellate cells on each of the macroalgal choices (which were offered alone or in pairs in several different mass ratios) after 24 hours. Although in some cases the mass of the algal choices were the same, comparisons are complicated by the different morphologies. For example, *Dictyota* is flat and *Galaxaura* is round, but both have equivalent mass to volume ratios (*i.e.*, 1.05 and 0.96, respectively), although *Dictyota* has more than triple the surface area compared to the same mass of *Galaxaura*. In control trials where only one macroalga was available, approximately the same fraction of the introduced *G. toxicus* population chose to settle on *Dictyota* and *Galaxaura* (55 and 51%, respectively) after 24 h.

A detailed breakdown of the *Dictyota:Galaxaura* selectivity is given in Table I, which shows the effects of differential availability of the competing host algae. The data are expressed in three ways. When the number of attached cells on each host species was expressed as a percentage of the total attached cells, the *Dictyota* portion varied systematically between 24 and 74% as the *Dictyota:Galaxaura* mass ratio changed from 0.25 to 2.0 between treatments. Stated differently, when *Dictyota* only represented 20% of the macroalgal biomass, 24% of the cells selected it as a host. At the other extreme, when *Dictyota* represented 67% of the biomass, 74% of the cells selected it. Alternatively, if the *G. toxicus* abundance was normalized to the mass of the host species, the number on *Dictyota* was between 1.3 and 2.0 times greater than that on *Galaxaura* for the four treatments.

Comparative analysis of the number of *G. toxicus* cells per unit surface area on different algae suggests a different picture. *Dictyota* has approximately three-times greater surface area per gram wet weight than does *Galaxaura* (ratio D. : G. cm^2/gm is 3.4). On a per unit surface area basis, the number of cells on *Dictyota* was between 1.7 and 2.7 times less than on *Galaxaura*. The number of *G. toxicus* per gram and per cm^2 of *Dictyota* or *Galaxaura* remained remarkably consistent even when the ratio of the macroalgal masses varied eight-fold.

At Pointe de Negre, the number of *G. toxicus* cells per gram of *Dictyota* was significantly greater (a ratio of 4:1) than on *Galaxaura* (*t*-test, $t = 3.6449$, DF = 37, $P < 0.01$). The two macroalgal species were common and present in approximately equal abundance at the study site.

Discussion

Numerous investigators world-wide have conducted field surveys to elucidate the *in situ* population biology of *G. toxicus* and the other ciguatera dinoflagellates. To date, reports on the distribution and abundance of these dinoflagellates have been uniformly based on small sample sizes ($n < 10$), with the dinoflagellate numbers being variously described in terms of: (A) the maximum number of cells per gram of host algae (genera or species not always specified; Carlson *et al.*, 1984; Ballantine *et al.*, 1985; Carlson and Tindall, 1985; Taylor, 1985; Taylor and Gustavson, 1983); (B) cells per gram of a specified alga (Shimizu *et al.*, 1982; Bagnis *et al.*, 1985a; Ballantine *et al.*, 1985; Taylor, 1985); (C) cells per gram of multiple unspecified algae (Bagnis *et al.*, 1985b; Caire *et al.*, 1985; Gillespie *et al.*, 1985a, b; Taylor and Gustavson, 1983); and (D) cell counts per algal surface area (Bomber *et al.*, 1985). The purposes of these surveys varied, as did the macroalgal species distributions, but the lack of a coherent picture of *G. toxicus* ecology (Scheuer and Bagnis, 1985; Anderson and Lobel, 1987) nevertheless argues that a re-examination of commonly used methodologies and assumptions is warranted. A desirable initial goal should be the standardization of sampling and enumeration procedures.

One of the first questions facing any field survey is the number of macroalgal species to sample and the number of replicates of each species to include. The major logistical constraints of time, money, and distance to cover often have led researchers to sample multiple species of macroalgae, each collected with few if any replicates at a given site. The statistical analysis of our Pointe de Negre data makes it clear that small sample sizes are inherently misleading, and that only when the *Dictyota* sample size exceeded $n = 10$ did the variance reach acceptable levels. Of course, a sample size of 10 is minimal for any parametric statistical test. Given the high variance that we observed for small sample sizes, non-parametric tests would have been of dubious merit. The issue of sample variance is further complicated by the level of absolute numerical abundance of cells per sample. Phytoplankton ecologists recognized early that the accuracy of a count varies as a function of the square root of the number counted (Lund *et al.*, 1958). To obtain twice the accuracy, four times the number of organisms must be counted. Consequently, there is a critical population level below which field survey data will not resolve substrate preference or biogeography with certainty.

Table I

Gambierdiscus toxicus *substrate preference with differing amounts of macroalgal hosts*

	Dictyota (=*D*)	*Galaxaura* (=*G*)	Ratio *D*:*G* # cells g^{-1}	Ratio *D*:*G* # cells/cm^2	Ratio *G*:*D* # cells/cm^2
Treatment 1: Mass ratio 0.25 *D*:*G*					
blot weight, g	0.2	0.8			
% of total macroalgal biomass	20%	80%			
% of total macroalgal surface area	46%	54%			
% attached cells*	24%	76%			
# cells per g	2750	2167	1.3		
# cells per cm^2	26	69		0.25	2.7
Treatment 2: Mass ratio 0.5 *D*:*G*					
blot weight, g	0.4	0.8			
% total macroalgal biomass	33%	67%			
% of total macroalgal surface area	63%	37%			
% attached cells*	49%	51%			
# cells per gram	3168	1625	2.0		
# cells per cm^2	30	52		0.58	1.7
Treatment 3: Mass ratio 1.0 *D*:*G*					
blot weight, g	0.4	0.4			
% of total macroalgal biomass	50%	50%			
% of total macroalgal surface area	75%	25%			
% attached cells*	60%	40%			
# cells per gram	3250	2168	1.5		
# cells per cm^2	31	70		0.44	2.3
Treatment 4: Mass ratio 2.0 *D*:*G*					
blot weight, g	0.8	0.4			
% of total macroalgal biomass	67%	33%			
% of total macroalgal surface area	87%	13%			
% attached cells*	74%	26%			
# cells per g	2188	1500	1.5		
# cells per cm^2	21	48		0.44	2.3

* Attached cells on each species as a percent of the total cells attached to macroalgae.

Another problem encountered in attempts to compare field distributional data for *G. toxicus* is that the species of host macroalgae collected for the various surveys differ so dramatically. This is not only a reflection of the difficulty in finding one or two macroalgal species distributed throughout all coastal marine habitats, but it also indicates that little is known about the differential abundance of *G. toxicus* and other benthic dinoflagellates on particular macroalgal species. If researchers could go to a site and know that they could obtain meaningful data on *G. toxicus* abundance by sampling only one or two algal species, sampling statistics could be improved and ecological issues more easily resolved. Given that it seems desirable to designate key macroalgae that are significantly associated with ciguatera dinoflagellates, we argue that an experimentally derived hierarchy of host species is needed. A laboratory procedure to determine this hierarchy is described here. Algae to be examined in the laboratory should include representatives of the flora found in each of the coastal marine habitats (e.g., tidepool, forereef, backreef, lagoon, etc.).

Adhering to our belief that more can be learned from a statistically relevant number of replicates of one or two key host species rather than an equal number of samples split between the various macroalgae present in a study area, we focused our attention on *Dictyota* and *Galaxaura* during our field study. We chose these species because of their circumtropical distribution, because they are abundant at most shallow and deep reef environments, and because they have been cited as supporting high *G. toxicus* populations (especially *Dictyota;* Carlson, 1984; Carlson *et al.,* 1984; Ballantine *et al.,* 1985; Carlson and Tindall, 1985; Gillespie *et al.,* 1985a; Taylor, 1985; Taylor and Gustavson, 1983). Ballantine *et al.* (1985) studied the seasonal abundance of *G. toxicus* on *Dictyota* at Puerto Rico and found typical densities ranging between 100–300 cells g^{-1} with a maximum of 8000. They recognized the huge variability in cell counts among samples collected close to one another, and noted that *Dictyota* appeared to be preferred as a substrate over the seagrass *Thalassia testudinum.* Elsewhere in the Caribbean, *G. toxicus* was also found to be significantly more abundant in association with *Dictyota* spp. than sympatric *Spyridea filamentosa* and *Cladophora hetero-*

nema (Carlson, 1984; Carlson and Tindall, 1985). *Spyridea* in turn was considered a preferred host for *G. toxicus* based on field distributions in Hawaii (Shimizu *et al.*, 1982).

These data are discussed here because they emphasize the value in establishing comparable macroalgal species (or an established hierarchy of species) as substrates to be collected in field surveys, but they are also examples of how preference has been inferred without suitable background information. The relatively obvious source of error that, with one exception (Bomber *et al.*, 1985), has largely been ignored in field studies to date is that cell counts normalized to mass are only comparable between macroalgal hosts if these hosts have the same surface area per unit mass. The value of this concept was first recognized by Bomber *et al.* (1985) who saw no correlation between the field abundance of another epiphytic dinoflagellate, *Prorocentrum lima,* and the mass of macroalgal species. The dinoflagellate distribution was best explained on the basis of available surface area. On first inspection, our laboratory data might be seen as evidence for active preference of *G. toxicus* for *Dictyota,* since the dinoflagellate abundance per gram of host alga was always higher on *Dictyota* than on *Galaxaura.* In fact, when the dinoflagellate abundance is normalized to host surface area, the opposite conclusion is reached—namely that the preference is for *Galaxaura.* As seen in Table I, the percentage of all attached cells that selected *Galaxaura* was always higher than the percentage of available macroalgal surface area represented by *Galaxaura,* typically 1.5–2 times higher. If attachment were simply surface area dependent, a 1:1 correspondence would be expected. This apparent preference is also seen in the ratio of cells cm^{-2} on *Galaxaura versus Dictyota,* which varies between 1.7 and 2.7. A simple surface area dependence with no preference would again be evidenced by values closer to 1.0.

In this context, it is noteworthy that we typically saw four times as many *G. toxicus* cells (per gram) on *Dictyota* than on *Galaxaura* at Pointe de Negre (Figs. 3A, 4A). This corresponds to a nearly equal dinoflagellate abundance per cm^2 (*i.e.,* a ratio near 1.0 as discussed above), so active preference seems unlikely. However, these data might be the end result of an initial colonization based on preference, as seen in our short-term laboratory experiments, followed by differential growth or mortality of the dinoflagellate on each macroalga. The separation and quantification of these two processes clearly requires further study that is beyond the scope of this paper. Our intent is to emphasize the difficulties associated with comparisons between different macroalgal hosts and the ease with which incorrect interpretations can be made if data are expressed in commonly accepted units of cells g^{-1} of host algae. Bomber (1985) reports that macroalgal species can be divided into three general groups on the basis of surface area g^{-1}, with differences spanning a factor of four between species. Until surface area mass^{-1} relationships are determined for other important macroalgae, we argue that *G. toxicus* abundance data cannot be interpreted either in terms of substrate preference or geographic distribution patterns. Only data for the same host species would be comparable, and then only if the number of replicate samples is sufficient.

Another fascinating and unexpected result from the preference experiments is that a relatively constant number of *G. toxicus* cells attached to each gram or cm^2 of our host algae, even when each host species' fractional biomass varied eight-fold. One possible interpretation is that there is a "carrying capacity" for each species. Given reports of much higher numbers of *G. toxicus* per gram of *Dictyota* by Ballantine *et al.* (1985), it seems more likely that we are seeing colonization that was still in progress when the experiment was terminated after 24 h. This consistency is reassuring and argues that the studies of the dynamics of *G. toxicus* substrate attachment and preference are feasible in the laboratory. We have shown that valuable information can be obtained by comparing the short-term colonization behavior of *G. toxicus* when offered different macroalgal hosts. These results suggest that there is preference expressed in the early stages of colonization. Our next step is to extend these experiments in time so as to evaluate other factors that will affect the final abundance of dinoflagellates, namely host chemistry, dinoflagellate growth, water turbulence effects, light effects, and so forth.

In summary, we have initiated a ciguatera research program that we hope will generate field data that are not only statistically sound but that also will allow comparisons to be drawn with results from other researchers throughout the world. Central to this approach is a focus on one or two key macroalgal host species, as well as the collection of sufficient replicates for our abundance estimates to be a valid representation of the real *G. toxicus* distribution. Normalization of these data to host surface area would be more informative and less subject to misinterpretation than the more common units of cells g^{-1}. Finally, we have demonstrated the ease with which substrate preference studies can be conducted in the laboratory. We recognize that the natural abundance and distribution of *G. toxicus* in the field is a reflection of both substrate attachment and the resulting growth and mortality of the established dinoflagellate population. This complex phenomenon must first be separated into discrete components, however, each to be studied in isolation if we are ever to fully comprehend the spatial and temporal dynamics of ciguatera.

Acknowledgments

We gratefully acknowledge the assistance of J. Aubin, B. Keafer, D. Kulis, and the support of D. Combs and

M. Kellett. We thank D. Smith for the computer programming and J. Weinberg for discussion about statistical bootstrap methods. This research was supported in part by the New England Biolabs Foundation, by the Office of Sea Grant in the National Oceanic and Atmospheric Administration through grants NA84AA-D-00033 (R/B 56 and R/B 86 and NA86AA-D-SG090 (R-V76), and by the National Science Foundation (OCE-8614210). Contribution No. 6614 from Woods Hole Oceanographic Institution.

Literature Cited

Anderson, D. M., and P. S. Lobel. 1987. The continuing enigma of ciguatera. *Bio. Bull.* **172:** 89–107.

Anderson, D. M., A. W. White, and D. G. Baden, eds. 1985. *Toxic Dinoflagellates.* Elsevier, New York. 561 pp.

Bagnis, R., J. Bennett, C. Prieur, and A. M. Legrand. 1985a. The dynamics of three benthic dinoflagellates and the toxicity of ciguateric surgeonfish in French Polynesia. Pp. 177–182 in *Toxic Dinoflagellates.* D. M. Anderson, A. W. White, and D. G. Baden, eds. Elsevier, New York.

Bagnis, R., J. Bennett, M. Barsinas, M. Chebret, G. Jacquet, I. Lechat, Y. Mitermite, Ph. Perolat, and S. Rongeras. 1985b. Epidemiology of ciguatera in French Polynesia from 1960 to 1984. Pp. 475–482 in *Proceedings of the 5th International Coral Reef Congress,* B. Salvat, ed. Antenne Museum-EPHE. Vol. **4.**

Ballantine, D. L., A. T. Bardales, T. R. Tosteson, and H. Dupont-Durst. 1985. Seasonal abundance of *Gambierdiscus toxicus* and *Ostreopsis* sp. in coastal waters of southwest Puerto Rico. Pp. 417–422 in *Proceedings of the 5th International Coral Reef Congress,* B. Salvat, ed. Antenne Museum—EPHE. Vol. **4.**

Bomber, J. W. 1985. Ecological studies of benthic dinoflagellates associated with ciguatera from the Florida Keys. M. S. Thesis, Florida Inst. Tech. 104 pp.

Bomber, J. W., D. R. Norris, and L. E. Mitchell. 1985. Benthic dinoflagellates associated with ciguatera from the Floriday Keys. II. Temporal, spatial and substrate heterogeneity of *Prorocentrum lima.* D. M. Anderson, *et al.,* eds. In *Toxic Dinoflagellates.* Elsevier, New York. 561 pp.

Caire, J. F., A. Raymond, and R. Bagnis. 1985. Ciguatera: study of the setting up and the evolution of *Gambierdiscus toxicus* population on an artificial substrate introduced in an atoll lagoon with follow-up of associated environmental factors. Pp. 429–435 in *Proceedings of the 5th International Coral Reef Congress,* B. Salvat, ed. Antenne Museum—EPHE. Vol. **4.**

Carlson, R. D. 1984. Distribution, periodicity and culture of benthic/epiphytic dinoflagellates in a ciguatera endemic region of the Caribbean. Ph.D. Thesis, Southern Illinois Univ. 308 pp.

Carlson, R. D., G. Morey-Gaines, D. R. Tindall, and R. W. Dickey. 1984. Ecology of toxic dinoflagellates from the Caribbean Sea: effects of macroalgal extracts on growth in culture. Pp. 271–287 in *Seafood Toxins,* E. P. Ragelis, ed. Am. Chem. Soc. Symp. Ser. No. 262, Washington, DC.

Carlson, R. D., and D. R. Tindall. 1985. Distribution and periodicity of toxic dinoflagellates in the Virgin Islands. Pp. 171–176 in *Toxic Dinoflagellates,* D. M. Anderson *et al.,* eds. Elsevier, New York.

Diaconis, P., and B. Efron. 1983. Computer-intensive methods in statistics. *Sci. Am.* **248:** 116–130.

Durand, M. 1984. Etude biologique, cytologique et toxicologique de *Gambierdiscus toxicus* en culture, dinoflagelle responsable de la ciguatera. *These de 3eme Cycle.* Université Paris VII, France.

Gillespie, N. C., M. J. Holmes, J. B. Burke, and J. Doley. 1985a. Distribution and periodicity of *Gambierdiscus toxicus* in Queensland, Australia. Pp. 183–188 in *Toxic Dinoflagellates,* D. M. Anderson *et al.,* eds. Elsevier, New York.

Gillespie, N. C., R. Lewis, J. Burke, and M. Holmes. 1985b. The significance of the absence of ciguatoxin in a wild population of *Gambierdiscus toxicus.* Pp. 437–442 in *Proceedings of the 5th International Coral Reef Congress.* B. Salvat, ed. Antenne Museum—EPHE. Vol. **4.**

Harrod, J. J., and R. E. Hall. 1962. A method for determining the surface areas of various aquatic plants. *Hydrobiolica* **20:** 173–178.

Lund, J. W. G., C. Kipling, and E. D. LeCren. 1958. The inverted microscope method for estimating algal numbers and the statistical bias of estimates by counting. *Hydrobiolica* **11:** 143–170.

Ragelis, E. P., ed. 1984. *Seafood Toxins.* Am. Chem. Soc. Symp. Ser. No. 262, Washington, DC. 460 pp.

Salvat, B., ed. 1985. *Proceedings of the 5th International Coral Reef Congress.* Antenne Museum—EPHE. Vol. **4.** 598 pp.

Scheuer, P. J., and R. Bagnis. 1985. Ciguatera and other reef seafood poisoning, introduction. Pp. 401–402 in *Proceedings of the 5th International Coral Reef Congress,* B. Salvat, ed. Antenne Museum—EPHE. Vol. **4.**

Shimizu, Y. H., Shimizu, P. J. Scheuer, Y. Hokama, M. Oyama, and J. T. Miyahara. 1982. *Gambierdiscus toxicus,* a ciguatera-causing dinoflagellate from Hawaii. *Bull. Jpn. Soc. Sci. Fish.* **48:** 811–813.

Taylor, F. J. R. 1985. The distribution of the dinoflagellate *Gambierdiscus toxicus* in the eastern Caribbean. Pp. 423–428 in *Proceedings of the Fifth International Coral Reef Congress,* B. Salvat, ed. Antenne Museum—EPHE. Vol. **4.**

Taylor, F. J. R., and M. S. Gustavson. 1983. An underwater survey of the organism chiefly responsible for "ciguatera" fish poisoning in the eastern Caribbean region: the benthic dinoflagellate *Gambierdiscus toxicus.* In *Proceedings of the Seventh International Diving Science Symposium,* A. Stefanon and N. J. Flemming, eds.

Withers, N. W. 1982. Ciguatera fish poisoning. *Annu. Rev. Med.* **33:** 97–111.

Yasumoto, T., N. Seino, Y. Murakami, and M. Murata. 1987. Toxins produced by benthic dinoflagellates. *Biol. Bull.* **172:** 128–131.

Reference: *Biol. Bull.* 175: 102–110. (August, 1988)

Ontogeny of Osmoregulation and Salinity Tolerance in Two Decapod Crustaceans: *Homarus americanus* and *Penaeus japonicus*

G. CHARMANTIER[1], M. CHARMANTIER-DAURES[1], N. BOUARICHA[1], P. THUET[1], D. E. AIKEN[2], AND J.-P. TRILLES[1]

[1]*Laboratoire de Physiologie des Invertébrés, Université des Sciences et Techniques du Languedoc, Pl. E. Bataillon, 34060 Montpellier Cédex, France, and* [2]*Department of Fisheries and Oceans, Invertebrate Biology and Aquaculture, Biological Station, St. Andrews, New Brunswick E0G 2X0, Canada*

Abstract. Osmoregulation and salinity tolerance were studied in larvae and post-larvae of two species of crustaceans, *Homarus americanus* and *Penaeus japonicus*, that have different types of embryonic development.

In both species, salinity tolerance decreased through the larval stages, was at a minimum at metamorphosis, and increased in post-larval stages. In *H. americanus*, the lethal salinity for 50% of the animals (24 h LS50) at 20°C was about 17‰ at metamorphosis, and about 10.5–12‰ in stages IV and V. In *P. japonicus*, the 24 h LS50 at 25°C was about 25‰ at metamorphosis, and about 7–10‰ from the sixth post-larval stage onwards.

In both species, larvae were hyper-osmoconformers and the osmoregulatory pattern changed after metamorphosis to the juvenile/adult type. In *H. americanus*, stages IV and V slightly hyper-osmoregulated in low salinities. In *P. japonicus*, post-larvae hyper-hypo-regulated, and their regulatory capacity increased up to the fifth post-larval stage.

In young stages of *H. americanus* and *P. japonicus*, osmoregulation and salinity tolerance appear correlated, and are modified at metamorphosis. These results are discussed with regard to their ecological and physiological implications and to previous studies on other species.

Introduction

Most studies on crustacean osmoregulation deal with adult forms (review in Mantel and Farmer, 1983), and only a few data are available on larval and post-larval osmoregulation. These are summarized in Table I. Depending on species, the osmoregulatory abilities can vary among the successive larval stages or remain unchanged. The adult type of regulation is also established at variable stages in different species. Numerous studies have been concerned with larval and post-larval salinity tolerance, but few have attempted to correlate the salinity tolerance of different developmental stages with their corresponding osmoregulatory capabilities in a given species.

The objective of this study conducted with the American lobster *Homarus americanus* H. Milne Edwards, 1837, and the shrimp *Penaeus japonicus* Bate, 1888, was to determine the salinity tolerance of larval and post-larval stages of these species, to define the ontogeny of their osmoregulation, and to attempt to correlate osmoregulatory abilities and salinity tolerance. *H. americanus* and *P. japonicus* are both economically important, and any knowledge of their larval and post-larval environmental tolerance and physiology can be valuable for their management and potential culture. Moreover, their patterns of post-embryonic development are different, offering the opportunity for comparisons of larval physiology.

In the genus *Homarus*, larval development comprises one prelarva and three zoea or mysis larvae—stages I to III—before a metamorphosis leading to post-larvae—stage IV or megalopa—and then to juvenile stages. In *H. americanus*, osmoregulation has been studied in adults (Dall, 1970) and juveniles (Charmantier *et al.*, 1981, 1984a); information on ionic regulation (Charmantier *et al.*, 1984b) and preliminary data on osmoregulation (Charmantier *et al.*, 1984c) are also available for the early post-embryonic stages of this species. Osmotic and ionic

Received 8 February 1988; accepted 29 April 1988.

Table I

Summary of studies on larval/post-larval crustacean osmoregulation

Species	Larval/ post-larval development	Type(s) of osmoregulation during post-embryonic development	Type of osmoregulation in adults
Rhithropanopeus harrisii (1)	4 zoeae	Hyper-osmoconform from 10 to 40 ‰ Slight hyper-regulation in lowest salinities. Except osmoconform in diecdysial stage V	Hyper-hypo-regulation (2)
Cardisoma guanhumi (3)	5 zoeae	Hyper-osmoconform <20 ‰ Tendency to hyper-regulate in 30–40 ‰ in 3rd, 4th, 5th zoeae	Hyper-hypo-regulation (4) (5)
Callinectes sapidus (6)	7 zoeae several megalopae	Hyper-isoregulation in 1st, 2nd zoeae and late megalopa. Osmoconform in 7th zoea. Hyper-osmoconform in other stages	Hyper-hypo-regulation (7)
Hepatus epheliticus (6)	3 zoeae	Hyper-isoregulation in 1st zoea. Slightly hypo-regulate in 40 ‰ in following stages. Larvae approaching megalopa and settling crab stages gradually osmoconform	Supposedly osmoconform (6)
Libinia emarginata (6)	2 zoeae 1 megalopa	1st zoea and late megaloga osmoconform. Slight hypo-regulation in 40 ‰ in 2nd zoea and early megalopa	Osmoconform (6) (8)
Sesarma retieulatum (9)	3 zoeae 1 megalopa	Hyper-regulate from 10–35 ‰. Slight hyper-regulation in 40 ‰	Hyper-hypo-regulation (9)
Clibanarius vittatus (10)	5 zoeae 1 megalopa	Hyper-osmoconform from 200 to 1200 mosm · kg^{-1}	Hyper-regulation Isosmotic regulation (11)
Macrobrachium petersi (12)	9 larval stages	Hyper-hypo-regulation Stronger ability in 1st stage and in post-larvae	Hyper-hypo-regulation (12)
Uca subcylindrica (13)	2 zoeae 1 megalopa	Slight hyper-regulation in zoeae I–II Slight hyper-hypo-regulation in megalopa	Hyper-hypo-regulation (13)
Callianassa jamaica louisianensis (14)	2 zoeae	Slight hyper-regulation in media <800–900 mosm · kg^{-1}	Hyper-hypo-regulation (15)

(1) Kalber and Costlow (1966)
(2) Smith (1967)
(3) Kalber and Costlow (1968)
(4) Pearse (1932)
(5) Quinn and Lane (1966)
(6) Kalber (1970)
(7) Ballard and Abbott (1969)
(8) Gilles (1970)
(9) Foskett (1977)
(10) Young (1979a)
(11) Young (1979b)
(12) Read (1984)
(13) Rabalais and Cameron (1985)
(14) Felder *et al.* (1986)
(15) Felder (1978)

regulation of *H. gammarus* has been studied in juveniles (Charmantier *et al.*, 1984d).

In contrast to the simple post-embryonic development of homarid lobsters, the penaeid shrimps have numerous larval instars beginning with nauplii stages, which is an exception among decapod crustaceans. The post-embryonic development of *Penaeus japonicus* goes through six nauplius stages, three zoeae, and three mysis. The third mysis stage ends with a metamorphosis: the succeeding post-larval stages can be named either by their stage (*e.g.*, PL5, fifth post-larva) or by the time elapsed since metamorphosis (*e.g.*, P5, 5 days after metamorphosis). Although osmoregulation has been studied extensively in penaeid shrimps (review in Charmantier, 1987b), only ionic regulation is known in *P. japonicus* (Exbrayat and Bourguet, 1982). Preliminary data have also been gathered on osmoregulation of their larvae (Charmantier, 1986).

Materials and Methods

This study was conducted at two different locations: St. Andrews (New Brunswick, Canada) for *Homarus americanus* and Montpellier (Hérault, France) for *Penaeus japonicus*. Standardized methods were used for both species and two of us were members of both the

Canadian and French groups who performed the experiments.

Animals

Homarus americanus larvae were obtained during the summer from lobsters captured in Passamaquoddy Bay and held at the lobster culture facility at the Biological Station at St. Andrews. After hatching, larvae were transferred to 40-l planktonkreisels (Hughes *et al.*, 1974) supplied with flow-through seawater at a salinity of 30–31‰, a temperature of 20°C under natural photoperiod. Larvae were fed three times a day with frozen adult *Artemia*. As each larval stage lasts several days, molting stages were obtained according to the time elapsed from the preceeding molt, and three groups of animals, postmolt stage A, stage C and premolt stage D, were selected.

Larvae of *P. japonicus* were obtained in early spring from the Ifremer Station (Deva-Sud) at Palavas (Hérault). They were reared in semi-recirculated systems using a clear water technique at a salinity of 35–36‰, a temperature of 25–27°C and under an artificial photoperiod (12L/12D) (Aquacop, 1983; Laubier, 1986). Larvae were fed with algae or *Artemia* nauplii according to their stage. Each larval stage lasted 24 h or less, so it was not possible to select animals according to molting stages.

Preparation of media

Dilute media were prepared by addition of tap water to seawater and high salinity media were prepared by adding "Instant Ocean Synthetic Sea Salts" (Aquarium Systems, Inc.) to seawater. All experiments were conducted at 20°C (*Homarus*) or 25°C (*Penaeus*). Salinities were expressed according to the osmotic pressure in mosm·kg^{-1} and to the salt content of the medium in ‰. Osmotic pressure was measured on an Advanced Instruments 31 LA or Roebling osmometer, and salinity on a YSI 33 salinometer. A value of 3.4 ‰ is equivalent to 100 mosm·kg^{-1}.

Survival bioassays

To determine salinity tolerance, acute static bioassays were conducted with animals held in test media ranging from fresh water (~10 mosm·kg^{-1}) to seawater (~900–1100 mosm·kg^{-1}) and differing by increments of 100 mosm·kg^{-1} (3.4‰). Penaeid shrimp larvae were held communally in plastic containers holding 0.5 l of medium; due to agonistic behavior, lobster larvae were held in individual compartments partly immersed in 3.5-l containers. All media were aerated. Animals were not fed during the bioassays. The duration of lobster experiments was 48–96 h. The shrimp experiments lasted 24–96 h due to the shorter duration of the stages.

Each bioassay was run on a group of 10 animals and replicated. Animals were counted and dead animals removed at 0.5, 1, 2, 3, 6, 12, 24, and 48 or 96 h according to the prescriptions of Sprague (1969) in toxicity studies. The criteria for death were total lack of movement, immobility of the scaphognathite (lobster) and of the heart (both species), and lack of response after repeated touches with a probe. Median times to 50% mortality (LT50) and their 95% confidence limits were determined from a computer program (Lieberman, 1983) based on the probit technique of Lichtfield and Wilcoxon (1949) and Finney (1962). Median lethal salinities (LS50) and 95% confidence intervals were calculated by standard techniques of probit analysis (Finney, 1962; Davies, 1971) computerized on the Letcur program (Zitko, 1982). LS50 were calculated at 24 and 48 h, and at 96 h in some longer lasting post-larval stages.

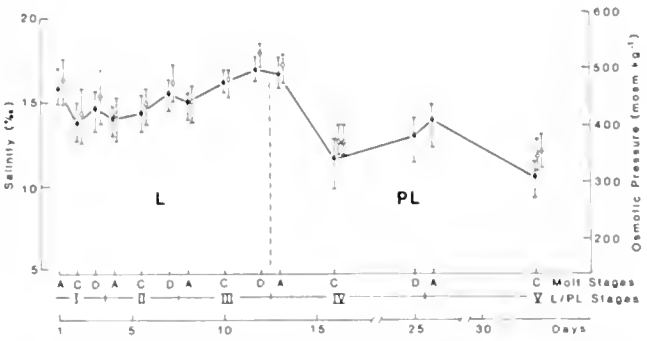

Figure 1. Salinity tolerance in larval (I, II, III) and post-larval (IV, V) *Homarus americanus* at 20°C. Variations in LS50 in ‰ and mosm·kg^{-1} according to larval (L)/post-larval (PL) and molt stages and to days of development. Each point represents the mean value of at least two determinations from 10 animals, with 95% confidence interval. Closed circles: 24 h LS50; open circles: 48 h LS50; open triangles: 96 h LS50.

Osmoregulation

Animals were reared at different selected salinities in recirculated planktonkreisels (lobster) or 0.5-l plastic containers (shrimp). Individuals were dried on filter paper and hemolymph was sampled by inserting a micropipette into the heart. This operation was conducted under mineral oil in the smallest stages in order to avoid rapid evaporation and desiccation. In shrimp, reproducible data were obtained only from stage zoea 2, *i.e.*, more than 1.3 mm long. Osmotic pressure of hemolymph was measured on a Kalber-Clifton micro-osmometer requiring 30-50 nl, with reference to the osmotic pressure of the medium.

Results

Homarus americanus: *salinity tolerance*

The ability of *H. americanus* to tolerate low salinities varied with post-embryonic development (Fig. 1). After

a slight decrease early in stage I, the 24 h LS50 increased through stages I, II, and III from about 410 mosm·kg^{-1} (14‰) to a maximum (corresponding to a minimum tolerance) of 500 mosm·kg^{-1} (17‰) in stages III D and IV A–B preceding and following metamorphosis. In post-larval stages IV and V (in molting stage C), salinity tolerance reached its maximum, with 24 h LS50 values down to 340 mosm·kg^{-1} (11.6‰) and 310 mosm·kg^{-1} (10.5‰); however, LS50 increased during the molt from stage IV to stage V. The 48-h LS50, although higher by 10–40 mosm·kg^{-1} (0.3–1.4‰), followed the same pattern of variation. Molting between larval stages was possible in respectively 0%, about 50%, and more than 80% of the larvae in media of ≤400, 500–600 and ≥700 mosm·kg^{-1} (13.6, 17–20.4, 23.8‰).

H. americanus: *osmoregulatory ability*

Adaptation time. After a rapid transfer from seawater at 850 mosm·kg^{-1} (29‰) to a dilute medium of 500 mosm·kg^{-1} (17‰), the hemolymph osmotic pressure stabilized within 1 h in stages I and II, 2 h in stage III and 3–6 h in stage IV (Fig. 2). Osmotic adaptation to concentrated media of 1100 and 1300 mosm·kg^{-1} (37 and 44‰) was completed in 1–3 h. In all subsequent experiments we kept the animals 6–24 h in each medium before sampling.

Osmoregulation. The types of osmoregulation were

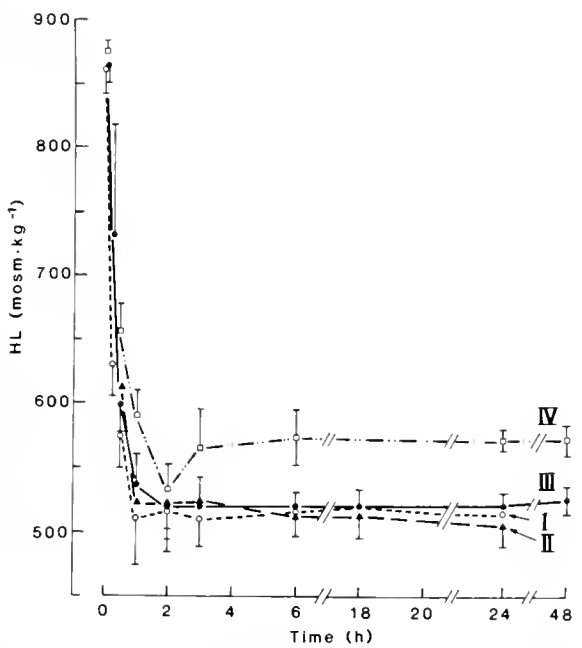

Figure 2. Change in hemolymph osmotic pressure (HL) in stages I–IV of *Homarus americanus* after rapid transfer from seawater (850 mosm·kg^{-1}, 29‰) to a dilute medium (500 mosm·kg^{-1}, 17‰) at 20°C. Each point represents the mean value of determinations from 12–15 animals, with 95% confidence interval.

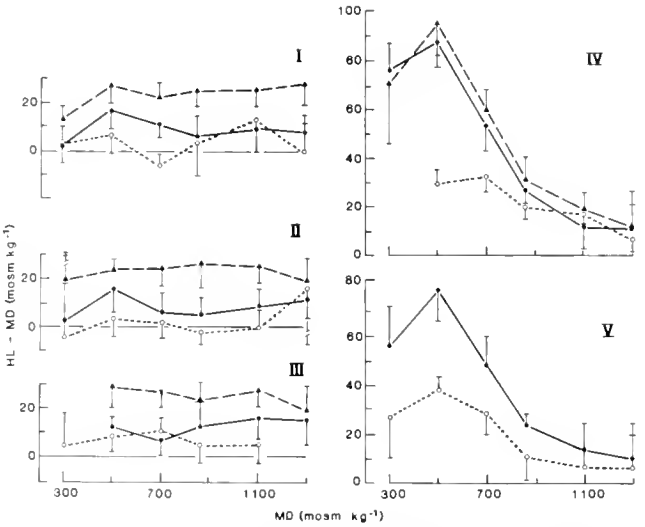

Figure 3. Variations in the difference between the osmotic pressures of hemolymph and medium (HL-MD) according to the osmotic pressure of the medium (MD) in stages I–V of *Homarus americanus* at 20°C. Each point represents the mean value of determinations from 12–20 animals (except in extreme salinities: 5–16 animals) with 95% confidence interval. ○ ---- ○: post-molt; ●——●: stage C; ▲ - - - ▲: premolt.

similar in larval stages I, II, and III. In molting stage C, these larvae hyper-osmoconformed over the whole range of salinity, the osmotic pressures of hemolymph and medium differing by about 10–20 mosm·kg^{-1}. Their regulation was slightly more hyper-osmotic in premolt and nearly isosmotic in post-molt (Fig. 3).

The pattern of osmoregulation changed after metamorphosis. Stage IV and V post-larvae in molting stage C hyper-osmoconformed in high salinities and seawater and their regulation was slightly hyper-osmotic in dilute media (hemolymph-medium difference of about 80 mosm·kg^{-1} in a 500 mosm·kg^{-1} or 17‰ medium). No significant difference was found in the regulation of premolt post-larvae, but the ability to hyper-regulate in dilute media significantly decreased in post-molt stages IV and V (hemolymph-medium difference of about 30–35 mosm·kg^{-1} in a 500 mosm·kg^{-1} or 17‰ medium) (Fig. 3).

Penaeus japonicus: *salinity tolerance*

Tolerance of low salinities varied with the developmental stages of *P. japonicus* (Fig. 4). The 24 h LS50 increased during larval development from about 460–600 mosm·kg^{-1} (16–20‰) in nauplii and zoeae 1 up to 730 mosm·kg^{-1} (25‰) just prior to and after metamorphosis in mysis 3 and first post-larval stages (PL1). Salinity tolerance increased progressively thereafter up to stage PL6, P12, *i.e.*, 12 days after metamorphosis (24 h LS50 about 300 mosm·kg^{-1} or 10‰) and more slowly up to stage

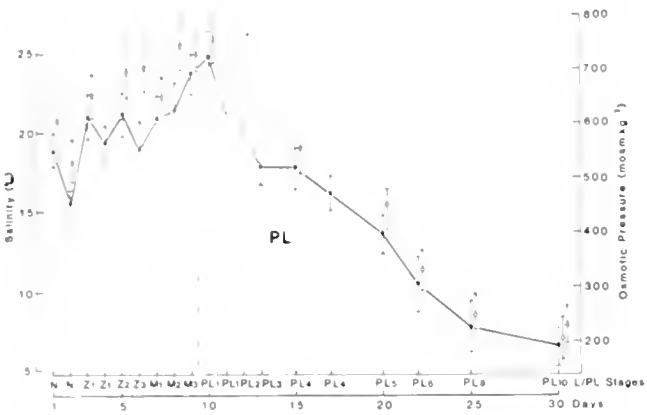

Figure 4. Salinity tolerance in larval (L) and post-larval (PL) *Penaeus japonicus* at 25°C. Variations in LS50 in ‰ and mosm·kg^{-1} according to larval/post-larval stages and days of development. Each point represents the mean value of at least two determinations from 10 animals, with 95% confidence interval. N, nauplius; Z, zoea; M, mysis; Pl, post-larval stage. Closed circles: 24 h LS50; open circles: 48 h LS50; open triangles: 96 h LS50.

PL10, P20 (24 h LS50 about 200 mosm·kg^{-1} or 7‰). The 48 h LS50, higher than the 24 h LS50 by 20–150 mosm·kg^{-1} (0.7–5.1‰), followed the same pattern of variation. Molting between larval stages was possible in 0%, about 50%, and 60–100% of the larvae in media of ≤400, 600–700, and ≥800 mosm·kg^{-1} (13.6, 20.4–23.8, 27.2‰), respectively.

P. japonicus: *osmoregulatory ability*

Adaptation time. After a rapid transfer from seawater (1050 mosm·kg^{-1} or 35.5‰) to a dilute medium (500 mosm·kg^{-1} or 17‰), the hemolymph osmotic pressure stabilized in 1 h in stage zoea 3, 3 h in fourth post-larval stage (PL4), and 6 h in stage PL10 (Fig. 5). In all subsequent experiments, we kept the animals 6–24 h in each medium before sampling.

Osmoregulation. Larval stages (zoea 2 and 3, mysis 1–3) hyper-osmoconformed over the whole range of tested salinities: the osmotic pressures of hemolymph and medium differed by about 10–40 mosm·kg^{-1}. In stage mysis 3, which lasted 2 days, regulation was slightly more hyper-osmotic towards the end of the stage, *i.e.*, in premolt animals (Fig. 6). At the end of the larval period, most of the animals died in the dilute media and the few survivors tended to osmoconform.

The pattern of osmoregulation changed after metamorphosis. Starting from the end of first post-larval stage (PL1) which lasted 2 days, the regulation shifted to slightly hyper-osmotic in dilute media and hypo-osmotic in seawater. Hyper- and hypo-osmoticity increased progressively thereafter up to PL5–PL6, P10–P12. From these stages onwards, the difference between the osmotic pressures of hemolymph and media reached about 300, 200, and −150 mosm·kg^{-1} in 300, 500, and 1000 mosm·kg^{-1} media (corresponding salinities: 10, 17, 34‰), respectively. The isosmoticity medium changed progressively from 900 mosm·kg^{-1} (30.5‰) in PL1 to 800 mosm·kg^{-1} (27‰) in PL5–PL6 (Fig. 6).

Discussion

Salinity tolerance

In *Homarus americanus*, salinity tolerance at 20°C expressed by the 24 h LS50 varies from 14–17‰ in larvae down to 10.5–12‰ in post-larvae and is minimum at metamorphosis—about 17‰. These results are in agreement with previous data: in *H. gammarus* and *H. americanus*, respectively, Gompel and Legendre (1927) and Templeman (1936) found that the larval period could progress to metamorphosis and stage IV only at 15–17.5°C in salinities above 17‰. Sastry and Vargo (1977) observed that larvae developed to stage V in salinities above 20‰ at 15°C and 15‰ at 20°C. Thus, from these studies, the minimum salinity compatible with larval development and metamorphosis can be estimated to be

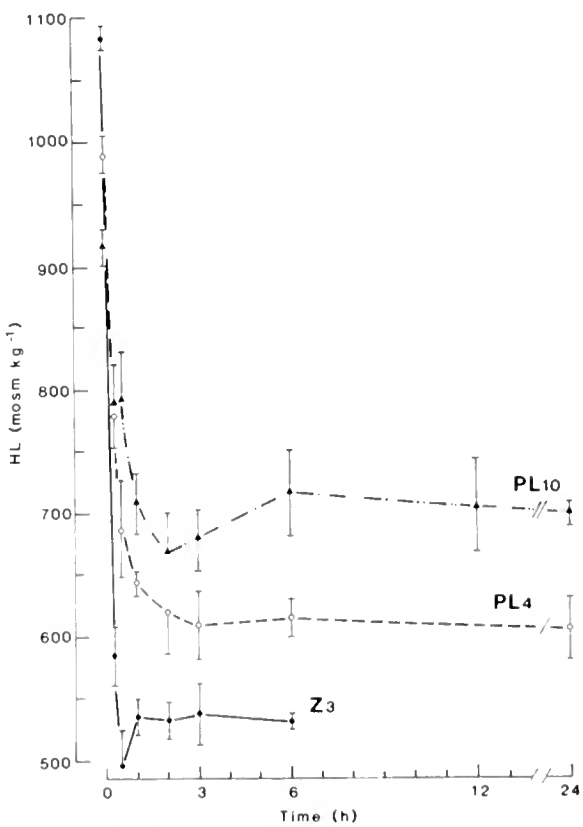

Figure 5. Change in hemolymph osmotic pressure (HL) in stages zoea 3 and post-larvae 4 and 10 of *Penaeus japonicus* after rapid transfer from seawater (1050 mosm·kg^{-1}, 35.5‰) to a dilute medium (500 mosm·kg^{-1}, 17‰) at 25°C. Each point represents the mean value of determinations from 10–15 animals, with 95% confidence interval.

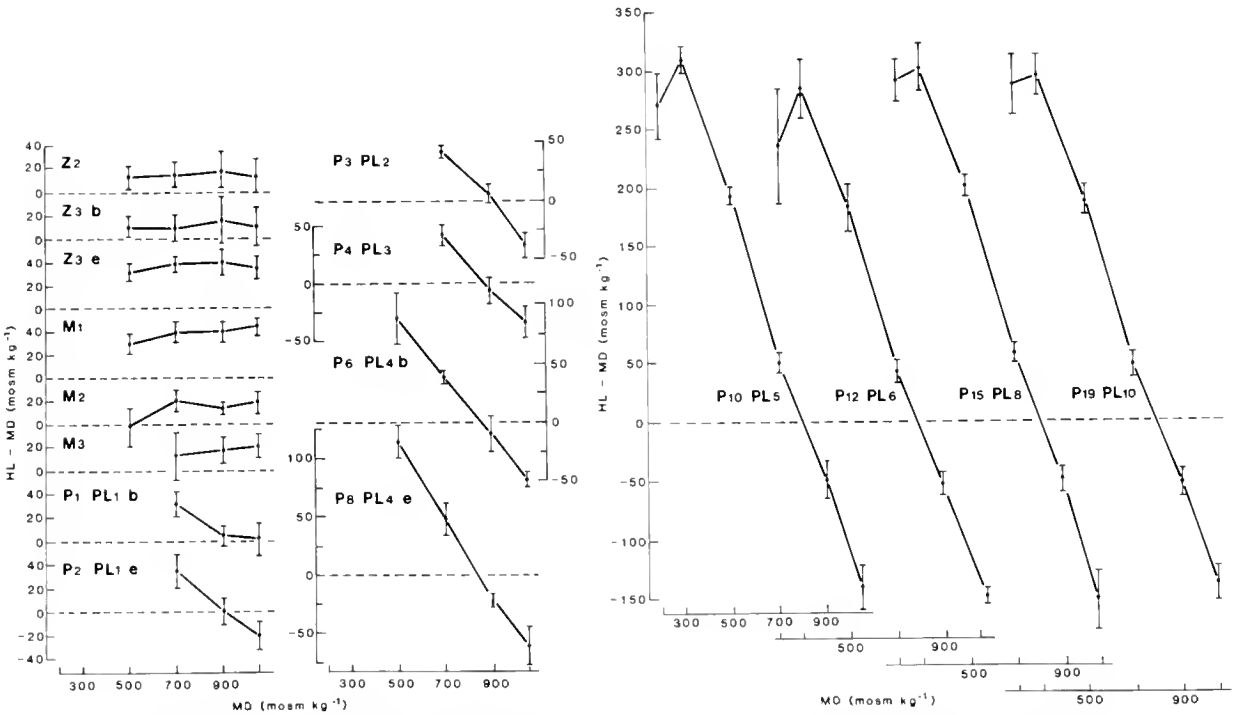

Figure 6. Variations in the difference between the osmotic pressures of hemolymph and medium (HL-MD) according to the osmotic pressure of the medium (MD) in larval and post-larval stages of *Penaeus japonicus* at 25°C. Each point represents the mean value of determinations from 10–15 animals (except in some low salinities, 5), with 95% confidence interval. Z, zoea; M, mysis; P, number of days after metamorphosis; PL, post-larval stage; b, beginning; e, end.

about 17‰ at 20°C. After metamorphosis, the values of LS50 found in post-larvae are similar to those observed in one-year-old juveniles (10‰: Charmantier, unpub. data) and compatible with the lethal limits known in adults (8‰: McLeese, 1956). The salinity tolerance of post-larvae decreases at the time of molt, which is a frequent observation among crustaceans.

In *P. japonicus,* the 24-h LS50 at 25°C varies from 16–20‰ to 25‰ in larval stages with a maximum value at metamorphosis. It decreases progressively to 10‰ from post-larval stage PL1 to PL6, and to 7‰ in stage PL10. In *P. japonicus* (Hudinaga, 1942), *P. duorarum* (Ewald, 1965), *P. marginatus* (Gopalakrishnan, 1976), and *Metapenaeus bennettae* (Preston, 1985), zoea larvae are less resistant to low salinity than mysis, which is not the case in our study. There are two possible explanations of this. The different feeding conditions could interfere with the effect of salinity. Preston (1985) observed that "starvation was a more potent factor than the effects of temperature and salinity in determining survival through the protozoeal larval stages." On the other hand, most of these studies were conducted for long periods to complete the larval development, which is not the case in our stage-by-stage study. After metamorphosis, the values of LS50 from PL6-PL8 were similar to those found in juveniles of the same species (8‰: Dalla Via, 1986; 6‰: Thuet *et al.,* unpub. data).

In *H. americanus* and *P. japonicus,* the 48 or 96 h values of LS50 are higher than those at 24 h. The difference is highest in the stages that last less than 48 h (*Penaeus* larval stages, young *Homarus* in molting stage D). High mortality occurs in the lowest salinities when these animals attempt to molt.

Adaptation time

In *H. americanus* and *P. japonicus* the time required for osmotic equilibration to a dilute medium is about 1–2 h in larvae, and 3–6 h in early post-larvae. It is between 12 and 24 h in juvenile lobster (Charmantier *et al.,* 1984a) and adult shrimp (Charmantier, unpub. data), and about 75 h in adult lobster (Dall, 1970). Therefore, adaptation time is size dependent. In larvae of other species, adaptation time is similar to that of young stages of *Homarus* and *Penaeus* (Kalber and Costlow, 1966, 1968; Kalber, 1970; Foskett, 1977; Felder *et al.,* 1986). Foskett (1977) stressed the physiological and ecological importance of rapid adaptation of hemolymph osmotic pressure to changes in the salinity of the medium. This may be particularly true in the case of larval *Homarus* and *Penaeus* which are planktonic and thus exposed to sud-

den changes in salinity following heavy rainfall. These rapid changes also require the existence of intracellular osmotic adaptation, especially in the hyper-osmoconforming larval stages of the two species.

Osmoregulation

In *H. americanus*, larval stages I–III hyper-osmoconform and post-larval stages IV and V slightly hyper-regulate in dilute media. The adult type of osmoregulation (Dall, 1970), which is identical to juvenile regulation (Charmantier *et al.*, 1981, 1984a), is acquired at stage IV, following metamorphosis. We found the same pattern of changes in the osmotic regulation of larvae and post-larvae of *H. gammarus* (Thuet *et al.*, 1988), confirming the physiological likeness of the two species.

The molt cycle affects osmotic regulation in *H. americanus* in two ways. In premolt larvae in stages I–III, the osmotic pressure of the hemolymph increases in all media. Similar variations have been shown in the larvae of *Rhithropanopeus harrisii* (Kalber and Costlow, 1966) and *Cardisoma guanhumi* (Kalber and Costlow, 1968). These authors suggested that a hyperosmotic internal medium would favor uptake of water at molt. In *H. americanus*, the tendency toward increased hyper-regulation before ecdysis is lost after metamorphosis, but postmolt post-larvae demonstrate a lower ability to hyper-regulate than do stage C animals. The decrease in hemolymph osmotic pressure or ion concentration is well known in postmolt adult crustaceans, where it is related to the water intake at molt, as exemplified by different lobsters (Travis, 1955; Glynn, 1968). Thus the effect of molting on osmotic regulation is different before and after metamorphosis. This could be related to variations in the permeability of the cuticle in larvae and post-larvae and to changes in the mechanisms involved, as discussed later.

In *P. japonicus*, zoeal and mysis larval stages hyper-osmoconform and the type of osmoregulation changes to hyper-hypo-regulation after metamorphosis. In post-larvae, the ability to regulate increases progressively up to stages PL5-PL6. In *P. japonicus*, the adult type of regulation is hyper-hypo-osmotic as in most species of penaeid shrimps (see review in Charmantier, 1987b); thus this type of regulation appears soon after metamorphosis but its efficiency is only gradually established over 10–12 days at 25°C.

A few studies have addressed the evolution of osmoregulatory abilities during the post-embryonic development of decapod crustaceans (Table I). In several species larvae are hyper-osmoconformers, for example *Rhithropanopeus harrisii* (Kalber and Costlow, 1966), *Callinectes sapidus* (Kalber, 1970), *Sesarma reticulatum* (Foskett, 1977), *Clibanarius vittatus* (Young, 1979a). *H. americanus* and *P. japonicus* larvae exhibit a similar type of osmoregulation. In other species such as *Cardisoma guanhumi* (Kalber and Costlow, 1968), *Hepatus epheliticus*, *Libinia emarginata* (Kalber, 1970), *Uca subcylindrica* (Rabalais and Cameron, 1985), *Callianassa jamaicense louisianensis* (Felder *et al.*, 1986), *Macrobrachium petersi* (Read, 1984), some capability for hypo- or hyper-regulation exists in certain larval stages. Thus, most decapod larvae that have been studied are osmoconformers or weak regulators. However, in species confronted with very low salinities in their natural environment, like *M. petersi*, larvae can efficiently regulate the osmotic concentration of their hemolymph.

In several of these species, the osmotic response varies little throughout the larval and post-larval development. Thus Foskett (1977) noted "no clear trend toward development of adult osmoregulatory patterns toward the end of larval life." However, recent findings and our own results contradict this generalization. Larvae of *M. petersi*, except in stage I, are incapable of osmoregulating in fresh water. This capacity re-appears in post-larvae, whose regulation is similar to that of juveniles and adults (Read, 1984). In *U. subcylindrica*, the hyper-hypo-regulation pattern of adults appears in megalopae and in the crab I stage (Rabalais and Cameron, 1985). The adult type of regulation is also present from post-larvae onwards in *H. americanus* and *P. japonicus*. Thus it can be stated that metamorphosis marks a profound change in the osmoregulatory abilities of these species. More generally, metamorphosis can be considered a combination of morphological, ecological, behavioral, and physiological changes (Charmantier *et al.*, 1984b; Charmantier, 1987a). In *P. japonicus*, the morphological metamorphosis is spread over several post-larval stages, which could be related to the progressive increase in osmoregulatory ability from PL1 to PL5. In *H. americanus*, on the contrary, both osmoregulatory and morphological changes are rapidly established in stage IV.

Na^+-K^+ ATPase is known to be implicated in ion transport. In *H. gammarus* the activation of this enzyme in dilute media is significantly higher in stage IV than in the preceding larval stages (Thuet *et al.*, 1988) which seems directly related to the hyper-regulation appearing from this stage onwards.

Evidence for neuroendocrine control of larval osmoregulation was first given by Kalber and Costlow (1966) in zoeae of *R. harrisii*. By eyestalk ablation and implantation the existence of neuroendocrine control of sodium regulation in *H. americanus* (Charmantier *et al.*, 1984b) and of osmoregulation in *H. americanus* and *H. gammarus* (Charmantier, unpub. data) has also been demonstrated. In *Homarus*, developed and functional effector organs such as gills coexist from stage IV with the neuroendocrine control of hydromineral metabolism. This could explain the establishment of the adult type of osmoregulation after metamorphosis. Different studies are underway to examine these hypotheses.

Relation between osmoregulation and salinity tolerance

Larvae of *H. americanus* and *P. japonicus* are weak regulators and their salinity tolerance is comparatively moderate or low. At metamorphosis, salinity tolerance is minimum while the pattern of osmoregulation changes. In post-larvae, the ability to osmoregulate increases either quickly (*Homarus*) or progressively (*Penaeus*) and so do their respective salinity tolerances. Thus, in both species, there is a strong correlation between increased ability to osmoregulate, in particular to hyper-regulate in low salinities, and improved salinity tolerance.

This implies a relationship between salinity-tolerant hyper-regulating stages on one hand and the probability that they will encounter low-salinity media on the other. This relation is not obvious in the case of *Homarus,* the different stages of which live in coastal waters where the salinity may fluctuate. Hyper-osmoconforming larvae could then rely on isosmotic intracellular regulation as they remain at the surface as planktonic stages, while, according to an hypothesis of Foskett (1977), the higher-density hyper-osmotic post-larval stages would be adapted to seek and settle on the bottom. The above mentioned relation is more evident in *P. japonicus,* in which sea-dwelling larvae hyper-osmoconform while, after their coast-bound migration, post-larvae living in coastal or estuarine environments and thus submitted to salinity fluctuations, strongly hyper-hypo-regulate and are widely tolerant of low salinities. As in the lobster, the stages during which hyper-regulation becomes fully established, *i.e.,* PL5/PL6, are also the stages of bottom settlement (Hudinaga, 1942), which enhances Foskett's hypothesis. Dall (1981) and Castille and Lawrence (1981) found in different species of penaeid shrimp that, compared to sea-living adults, coastal and estuarine juveniles displayed stronger hyper-regulation and better tolerance of low salinity. Such is also the case in *P. japonicus* (Charmantier *et al.,* unpub. data). Thus, throughout the development of some species of penaeid shrimp, osmoregulation and ecology are closely linked, although other factors such as bottom selection, food availability, and presence of predators may interfere with the choice of the biotope (Dall, 1981). In two other species in which the young stages encounter salinity extremes in their environment, *Macrobrachium petersi* (Read, 1984) and *Uca subcylindrica* (Rabalais and Cameron, 1985), a clear correlation has also been demonstrated between osmoregulatory ability and salinity tolerance.

In conclusion, the various studies conducted on young crustaceans reveal different patterns of ontogeny of osmoregulation. In one group of brachyuran species mentioned by Foskett (1977), osmoregulation varies little with developmental stage and no general trend can be found. In *M. petersi* (Read, 1984), which migrate between fresh and saline water for reproduction, the adult type of regulation is established as early as the first larval stage. In a third group of species, like *U. subcylindrica* (Rabalais and Cameron, 1985), *H. americanus,* and *P. japonicus* (this study), metamorphosis marks the appearance of the adult type of regulation. Further studies on other species should complement these ontogenetical groups. Since survival in low salinities appears correlated with the ability of *H. americanus* and *P. japonicus* to hyper-regulate in young stages, additional evidence of a relationship between the osmoregulatory ability, salinity tolerance and ecology of young stages of crustaceans should come from future studies.

Acknowledgments

A portion of this work was supported by the Ministère Français des Relations Extérieures and the National Research Council of Canada. The balance was supported by the Ifrémer (Institut Français de Recherches sur la Mer).

We thank Susan Waddy, Wilfred Young-Lai, and Dr. Zitko of St. Andrews, Raymond Mounet-Guillaume of Montpellier, and Jean-Marie Ricard, Gilles Le Moullac, Olivier Avalle, and Lucien Mazara at the Deva-Sud, Ifrémer Station in Palavas for their assistance.

Literature Cited

Aquacop. 1983. Penaeid larval rearing in the Centre Océnographique du Pacifique. In *Handbook of Mariculture,* J. P. Mc'Vey, ed., 1, Crustacean Aquaculture. CRC Press. 123 pp.

Ballard, B. S., and W. Abbott. 1969. Osmotic accommodation in *Callinectes sapidus* Rathbun. *Comp. Biochem. Physiol.* **29:** 671–687.

Castille, F. L., Jr., and A. L. Lawrence. 1981. A comparison of the capabilities of juvenile and adult *Penaeus setiferus* and *Penaeus stylirostris* to regulate the osmotic, sodium and chloride concentrations in the hemolymph. *Comp. Biochem. Physiol.* **68A:** 677–680.

Charmantier, G. 1986. Variation des capacités osmorégulatrices au cours du développement post-embryonnaire de *Penaeus japonicus* Bate, 1888 (Crustacea, Decapoda). *C. R. Hebd. Séanc. Acad. Sci. Paris* **303:** 217–222.

Charmantier, G. 1987a. Le développement larvaire et la métamorphose chez les Homards (Crustacea, Decapoda). *Océanis* **13:** 137–165.

Charmantier, G. 1987b. L'osmorégulation chez les crevettes Penaeidae (Crustacea, Decapoda). *Océanis* **13:** 179–196.

Charmantier, G., M. Charmantier-Daures, and D. E. Aiken. 1981. Contrôle neuroendocrine de la régulation osmotique et ionique chez les juvéniles et les larves de *Homarus americanus* H. Milne Edwards, 1837. *C. R. Hebd. Séanc. Acad. Sci. Paris* **293:** 831–834.

Charmantier, G., M. Charmantier-Daures, and D. E. Aiken. 1984a. Neuroendocrine control of hydromineral regulation in the American lobster *Homarus americanus* H. Milne-Edwards, 1837 (Crustacea, Decapoda). 1. Juveniles. *Gen. Comp. Endocrinol.* **54:** 8–19.

Charmantier, G., M. Charmantier-Daures, and D. E. Aiken. 1984b. Neuroendocrine control of hydromineral regulation in the American lobster *Homarus americanus* H. Milne-Edwards, 1837 (Crustacea, Decapoda). 2. Larval and post-larval stages. *Gen. Comp. Endocrinol.* **54:** 20–34.

Charmantier, G., M. Charmantier-Daures, and D. E. Aiken. 1984c. Variation des capacités osmorégulatrices des larves et post-larves de

Homarus americanus H. Milne-Edwards, 1837 (Crustacea, Decapoda). *C. R. Hebd. Séanc. Acad. Sci. Paris* **299:** 863–866.

Charmantier, G., P. Thuet, and M. Charmantier-Daures. 1984d. La régulation osmotique et ionique chez *Homarus gammarus* (L.) (Crustacea, Decapoda). *J. Exp. Mar. Biol. Ecol.* **76:** 191–199.

Dall, W. 1970. Osmoregulation in the lobster *Homarus americanus*. *J. Fish. Res. Board Can.* **27:** 1123–1130.

Dall, W. 1981. Comparative regulatory ability and juvenile habitat preference in some penaeid prawns. *J. Exp. Mar. Biol. Ecol.* **55:** 219–232.

Dalla Via, G. J. 1986. Salinity responses of the juvenile penacid shrimp *Penaeus japonicus* I. Oxygen consumption and estimations of productivity. *Aquaculture* **55:** 297–306.

Davies, R. G. 1971. *Computer Programming in Quantitative Biology*. Academic Press, London.

Ewald, J. J. 1965. The laboratory rearing of the pink shrimp, *Penaeus duorarum* (Burkenroad). *Bull. Mar. Sci.* **15:** 436–449.

Exbrayat, J.-M., and J.-P. Bourguet. 1982. Variations du milieu intérieur de *Penaeus japonicus* en fonction de certaines conditions naturelles (cycle de mue et âge) et de certaines conditions expérimentales (épédonculation et ablation des organes Y). *Bull. Soc. Zool. Fr.* **107:** 33–51.

Felder, D. L. 1978. Osmotic and ionic regulation in several western Atlantic Callianassidae (Crustacea, Decapoda, Thalassinidea). *Biol. Bull.* **54:** 409–429.

Felder, J. M., D. L. Felder, and S. C. Hand. 1986. Ontogeny of osmoregulation in the estuarine ghost shrimp *Callianassa jamaicense louisianensis* Schmitt (Decapoda, Thalassinidea). *J. Exp. Mar. Biol. Ecol.* **99:** 91–105.

Finney, D. J. 1962. *Probit Analysis: a Statistical Treatment of the Sigmoid Response Curve*. Second Edition, Cambridge Univ. Press, London.

Foskett, J. K. 1977. Osmoregulation in the larvae and adults of the grapsid crab *Sesarma reticulatum* Say. *Biol. Bull.* **153:** 505–526.

Gilles, R. 1970. Osmoregulation in the stenohaline crab *Libinia emarginata* Leach. *Arch. Int. Physiol. Biochim.* **78:** 91–99.

Glynn, J. P. 1968. Studies on the ionic, protein and phosphate changes associated with the moult cycle of *Homarus vulgaris*. *Comp. Biochem. Physiol.* **26:** 937–946.

Gompel, M., and R. Legendre. 1927. Effets de la température, de la salure et du pH sur les larves des Homards. *C. R. Séanc. Soc. Biol.* **97:** 1058–1060.

Gopalakrishnan, K. 1976. Larval rearing of red shrimp *Penaeus marginatus*. *Aquaculture* **9:** 145–154.

Hudinaga, M. 1942. Reproduction, development and rearing of *Penaeus japonicus* Bate. *Japn. J. Zool.* **10:** 305–393, Pl. 16–46.

Hughes, J. T., R. A. Shleser, and G. Tchobanoglous. 1974. A rearing tank for lobster larvae and other aquatic species. *Prog. Fish Cult.* **36:** 129–132.

Kalber, F. A. 1970. Osmoregulation in decapod larvae as a consideration in culture techniques. *Helgol. Wiss. Meeresunters.* **20:** 697–706.

Kalber, F. A., and J. D. Costlow, Jr. 1966. The ontogeny of osmoregulation and neurosecretory control in the decapod crustacean *Rhithropanopeus harrisii*. *Am. Zool.* **6:** 221–229.

Kalber, F. A., and J. D. Costlow, Jr. 1968. Osmoregulation in larvae of the land crab *Cardisoma guanhumi* Latreille. *Am. Zool.* **8:** 411–416.

Laubier, A. 1986. Les crevettes penaeides. Pp. 459–491 in *L'Aquaculture*, G. Barnabé, coordin. 1, Part 3. Technique et Documentation, Lavoisier.

Lieberman, H. R. 1983. Estimating LD50 using the probit technique: a basic computer program. *Drug Chem. Toxicol.* **6:** 111–116.

Litchfield, J. T., and F. Wilcoxon. 1949. The reliability of graphic estimates of relative potency from dose-percent effect curves. *J. Pharmacol. Exp. Ther.* **108:** 18–25.

Mantel, L. H., and L. L. Farmer. 1983. Osmotic and ionic regulation. Pp. 53–161 in *The Biology of Crustacea, Vol. 5*. Internal Anatomy and Physiological Regulation, L. H. Mantel, ed. Academic Press, NY.

McLeese, D. W. 1956. Effects of temperature, salinity and oxygen on the survival of the American lobster. *J. Fish. Res. Board Can.* **13:** 247–272.

Pearse, A. S. 1932. Freezing-points of blood of certain littoral and estuarine animals. *Carnegie Inst. Wash. Publ. n° 435* **28:** 93–102.

Preston, N. 1985. The combined effect of temperature and salinity on hatching success and the survival, growth, and development of the larval stages of *Metapenaeus bennettae* (Racek and Dall). *J. Exp. Mar. Biol. Ecol.* **85:** 57–74.

Quinn, D. J., and C. E. Lane. 1966. Ionic regulation and Na-K stimulated ATPase activity in the land crab, *Cardisoma guanhumi*. *Comp. Biochem. Physiol.* **19:** 533–543.

Rabalais, N. N., and J. N. Cameron. 1985. The effects of factors important in semi-arid environments on the early development of *Uca subcylindrica*. *Biol. Bull.* **168:** 147–160.

Read, G. H. L. 1984. Intraspecific variation in the osmoregulatory capacity of larval, post-larval, juvenile and adult *Macrobrachium petersi* (Hilgendorf). *Comp. Biochem. Physiol.* **78A:** 501–506.

Sastry, A. N., and S. L. Vargo. 1977. Variation in the physiological responses of crustacean larvae to temperature. Pp. 401–423 in *Physiological responses of marine biota to pollutants*, F. J. Vernberg, A. Calabrese, F. P. Thorberg, and W. G. Vernberg, eds. Academic Press, NY.

Smith, R. I. 1967. Osmotic regulation and adaptive reduction of water-permeability in a brackish-water crab, *Rhithropanopeus harrisii* (Brachyura, Xanthidae). *Biol. Bull.* **133:** 643–658.

Sprague, J. B. 1969. Measurement of pollutant toxicity to fish. I. Bioassay methods for acute toxicity. *Water Res.* **3:** 793–821.

Templeman, W. 1936. The influence of temperature, salinity, light and food conditions on the survival and growth of the larvae of the lobster (*Homarus americanus*). *J. Biol. Board Can.* **2:** 485–497.

Thuet, P., M. Charmantier-Daures, and G. Charmantier. 1988. Relation entre osmorégulation et activités d'ATPase Na^+-K^+ et d'anhydrase carbonique chez Parves et postlarves de *Homarus gammarus* (L.) (Crustacea: Decapoda). *J. Exp. Mar. Biol. Ecol.* **115:** 249–261.

Travis, D. F. 1955. The molting cycle of the spiny lobster *Panulirus argus* (Latreille). III. Physiological changes which occur in the blood and urine during the normal molting cycle. *Biol. Bull.* **109:** 484–503.

Young, A. M. 1979a. Osmoregulation in larvae of the striped hermit crab *Clibanarius vittatus* (Bosc). (Decapoda:Anomura:Diogenidae). *Est. Coast. Mar. Sci.* **9:** 595–601.

Young, A. M. 1979b. Osmoregulation in three hermit crab species, *Clibanarius vittatus* (Bosc), *Pagurus longicarpus* Say and *P. pollicaris* Say (Crustacea:Decapoda:Anomura). *Comp. Biochem. Physiol.* **63A:** 377–382.

Zitko, V. 1982. Letcur, the lethality curve program. *Can. Tech. Rep. Fish. Aquat. Sci.* **1134:** 10 pp.

Reference: *Biol. Bull.* **175**: 111–121. (August, 1988)

Swimming Speed and Oxygen Consumption in the Bathypelagic Mysid *Gnathophausia ingens*

DAVID L. COWLES[1] AND JAMES J. CHILDRESS[2]

[1]*Department of Biology, Loma Linda University, Riverside, California 92515-8247 and*
[2]*Marine Science Institute, University of California, Santa Barbara, California 93106*

Abstract. The energetic costs of swimming were determined for the bathypelagic mysid *Gnathophausia ingens*. Individuals over a large size range spontaneously swam at speeds from 5 to 6.5 cm/s. To maintain this speed, smaller animals swam at much higher relative swimming speeds than did larger animals. Routine rates of oxygen consumption were thus considerably higher in the smaller instars. The relationship between standard rates of oxygen consumption and animal size was slightly less than the standard log-log allometric slope of 0.75. Within the speed range of 0–8 cm/s, oxygen consumption appeared to increase as a linear function of speed. Cost of transport was very high at low speeds. At 5.5 cm/s, cost of transport was lower than that measured for other crustaceans, but higher than that of fish. Swimming efficiency increased with speed. While the lower cost of transport and higher swimming efficiency may contribute to *G. ingens'* reduced rates of oxygen consumption as compared to those of shallower-living crustaceans, the major factor appears to be *G. ingens'* lower level of swimming activity.

Introduction

It is well known that deep-living pelagic fish and crustaceans have metabolic rates considerably lower than those of shallower-living pelagic species (Childress, 1969, 1971b, 1975, 1977; Smith and Hessler, 1974; Torres *et al.*, 1979; Smith, 1978; Smith and Laver, 1981; Cowles, 1987). This reduction is of an order of magnitude or more, and can be only partially accounted for by changes in temperature, pressure, and animal protein content with depth (Childress, 1975; Mickel and Childress, 1982). Lower metabolic rates at depth have generally been attributed to selection for energy conservation due to food limitation at depth (Childress and Nygaard, 1973, 1974; Bailey and Robison, 1986). A more recent hypothesis contends that, for deeper-living animals such as fish and crustaceans which rely on vision for detection of predators or prey, the reduction in metabolic rate is related to a decrease in activity and the capacity for activity, which is allowed by the shorter reactive distances at depth and consequent relaxation of selection for capacities for rapid swimming (Childress *et al.*, 1980; Childress and Mickel, 1985).

For any active pelagic species, locomotory activity may be expected to play a prominent role in determining the overall metabolic rate. Activity may be critical for feeding, escape from predation, vertical migrations, finding a mate, and maintaining station in the water column. However, little is known of the normal activity levels of deep-living pelagic crustaceans nor of the amount of metabolic energy such activity requires. A few studies have been made on swimming speeds and rates of aerobic metabolism of shallow-living pelagic crustaceans. Torres *et al.* (1982) and Torres and Childress (1983) used an annular chamber to measure swimming activity and rate of oxygen consumption in the shallow-living *Euphausia pacifica*. Kils (1979a, b) measured mean rates of oxygen consumption and recorded average swimming speeds for the Antarctic krill, *Euphausia superba*. No comparable data, however, are available for deep-living crustaceans. Mickel and Childress (1978, 1982) and Quetin and Childress (1980) measured pleopod beat rates and oxygen consumption in the mysid *Gnathophausia ingens* strapped to a fixed underwater frame. It is not clear, however, what correlation exists between pleopod beat rates and swimming speeds in swimming crustaceans.

Gnathophausia ingens Dohrn (1870) is a large cosmopolitan bathypelagic mysid from the family Lophogastri-

Received 30 October 1987; accepted 31 May 1988.

dae. The species is negatively buoyant in seawater and appears to be an active swimmer. Most of the population of this species off California live at depths of 400 to 900 meters (Childress, 1975). Since the species can be maintained in the laboratory for long periods of time, more has been learned about its physiology than that of nearly any other large pelagic crustacean (Childress, 1968, 1969, 1971b; Fuzessery and Childress, 1975; Belman and Childress, 1976; Childress and Price, 1978, 1983; Mickel and Childress, 1978, 1982; Quetin and Childress, 1980; Hiller-Adams and Childress, 1983a, b, c; Cowles, 1987). Like many deep-sea animals, its rate of aerobic metabolism is significantly lower than that of comparable epipelagic animals.

In this study we measured the relationship between routine swimming speeds and rates of oxygen consumption in *G. ingens*. These data were used to characterize energetic costs of swimming for this species. Swimming energetics of *G. ingens* were then compared to those of shallower-living crustaceans and of fish to evaluate *G. ingens'* relative swimming abilities and costs in comparison to those of other active pelagic swimmers.

Materials and Methods

Seventy-two *Gnathophausia ingens* of instars 5–11 (Childress and Price, 1978, 1983) were obtained from depths of 450–750 meters from San Clemente, Catalina, and Santa Cruz basins off Southern California, using a 10-foot square Tucker Trawl fitted with a thermally insulated cod end (Childress *et al.*, 1978). The mysids were maintained in the laboratory in 5.5°C seawater in 1-liter plastic containers and were fed once a week to satiation with an alternating diet of salmon and shrimp. Individuals kept in the laboratory were starved at least twenty-four hours before being used for an experiment. Length of stay in the laboratory before use in an experiment ranged from one hour to six months, with the majority being used within twenty days.

Swimming speed and rate of oxygen consumption were measured in a recirculating swim tunnel similar to that described by Cowles *et al.* (1986). Modifications included an increase in diameter to 10.16 cm, the total enclosure of the tunnel for respiration measurements, and the connection of the tunnel to a computer-based data acquisition and control system for continuous data logging. Ultraviolet sterilized, 0.2 μm filtered seawater containing 25 mg/l each of streptomycin and penicillin was used during oxygen consumption experiments to minimize background microbial respiration. A dark cover was placed over the chamber to minimize disturbance to the animal during the experiment.

Experimental animals were sealed individually in the swim tunnel and allowed to swim at spontaneous speeds while speed and oxygen consumption were measured continuously. Individual experiments varied in length from four to thirty hours. An experiment was terminated when it had proceeded long enough so that at least several hours of steady oxygen consumption data had been obtained, preferably at a range of speeds. The animal was then removed, weighed wet, and returned to a holding tank of chilled seawater. Later the live, anesthetized animal's underwater weight was determined in 5.5°C seawater, and the animal was dried to determine dry mass.

Data obtained from the swim tunnel were used to calculate rate of oxygen consumption [MO_2, micromoles O_2/ (mg wet wt × h)] as a function of absolute (S_a, cm/s) and relative (S_r, lengths/s) for each mysid. The mean absolute (S_{mar}) and relative (S_{mrr}) swimming speeds and rate of oxygen consumption (MO_{2mr}) for the entire session in the swim tunnel were calculated for each mysid, with the assumption that these speeds, swum spontaneously by the mysid, represent routine swimming speeds. In addition, the maximum swimming speed maintained for at least one minute, identified as the maximum short-term swimming speed, was noted for each individual.

Data for all animals from each instar were grouped together, and the mean S_{mar}, S_{mrr}, MO_{2mr}, and wet, dry, and underwater weights were calculated for each instar. Best fit mean-square linear and power regressions for the relationship between S_{mar}, S_{mrr} and MO_{2mr} were calculated for each instar and for all the instars combined. Swimming speeds and rates of oxygen consumption for each instar were compared by analysis of variance and by a regression of these variables against carapace length. The best-fit equation relating rate of oxygen consumption (MO_2) to swimming speed (S_a) and body mass (grams wet weight) was determined by least squares multiple regression. All references to statistical significance in these experiments were based on the 95% confidence level. References to rates of oxygen consumption conform to the terminology conventions of Piiper *et al.* (1971).

Results

Swimming speeds and rates of oxygen consumption

Upon first being placed in the swim tunnel, many of the animals swam rapidly and erratically for some time. Maximum short-term speeds were usually recorded during this early period (Table 1). Maximum short-term speeds varied from 10.3 to 18.2 centimeters per second (1 length per second for the larger instars, 2 lengths per second for the smaller).

After this initial acclimation period of one to three hours, most individuals swam at a characteristic speed that varied little throughout the rest of the experiment.

Table I

Swimming speeds and rates of oxygen consumption of Gnathophausia ingens *maintained in the laboratory for less than 30 days, by instar*

		Mean weight (g)			Mean length		Swimming speed* Mean				Maximum cm/s		Rate of oxygen consumption	
Instar	n	Wet	Dry	Under water	Carapace mm	Total cm	S_{mar} cm/s	s.d.	S_{mrr} length/s	s.d.	Short	Sustained	MO_{2mrr}#	s.d.
5	7	0.718	0.114	0.015	15.9	5.2	3.5	2.6	0.67	0.49	10.3	7.5	0.0125	0.00943
6	13	1.27	0.260	0.021	20.2	6.2	5.8	1.7	0.93	0.27	12.8	8.6	0.0116	0.00811
7	14	2.22	0.382	0.030	24.3	7.2	6.2	2.3	0.86	0.32	15.4	10.3	0.00575	0.00307
8	13	4.07	0.772	0.047	30.0	8.5	6.3	2.2	0.74	0.26	18.2	11.6	0.00453	0.00229
9	10	7.12	1.321	0.086	35.9	9.9	5.1	1.1	0.51	0.10	18.2	12.2	0.00271	0.00172
5–9	72	3.10	0.472	0.040	25.6	7.5	5.6	2.1	0.76	0.32	18.2	12.2	0.00725	0.00641

* Mean speeds are the average swimming speeds of all individuals of the instar combined. Maximum "short" speeds are the highest speeds maintained by any individual of the instar for 1 minute; maximum sustained speeds are the highest speeds sustained by any individual in the instar for at least 20 minutes.

MO_2 units = micromoles O_2/(mg wet wt × h).

No significant differences in swimming speed between day and night were observed. Swimming speed and the accompanying rates of oxygen consumption were significantly lower for animals that had been maintained in the laboratory for thirty days or longer ($P < .005$ and .0002, respectively). Mean routine swimming speeds (S_{mar}, cm/s) and rates of oxygen consumption [MO_{2mr}, micromoles O_2/ (mg wet wt × h)] for each instar are summarized in Table I. This table contains data for only those animals that had been in the laboratory for less than thirty days. Except for the smallest individuals (instar 5), routine absolute swimming speed averaged around 5 to 6.5 cm/s for all animals, regardless of instar. Instar 5 animals swam significantly more slowly than the other instars ($P < .05$), but there was no significant difference in absolute swimming speeds among instars 6 through 9 (Fig. 1A). The slope of a regression of S_{mar} *versus* animal length for instars 6 through 9 was not significantly different from zero ($P = .52$).

Significant trends in mean relative routine swimming speeds (S_{mrr}) were found among the instars. The relative routine swimming speeds of each of the instars 6 through 8 were significantly higher than those of all larger instars. A regression of S_{mrr} *versus* animal length for instars 6 through 9 had a highly significant downward trend ($P < .001$), indicating the slower relative swimming speeds of the larger instars. Most instar 5 animals swam at a slower relative speed than predicted by this regression, but faster than the largest instars (Fig. 1B).

The body angle of the swimming mysids changed with swimming speed. At low speeds the body angled upward anteriorly, becoming more horizontal as speed increased. For any given absolute swimming speed, body angle was greater for the smaller instars. By 8 cm/s the body was essentially horizontal. This trend is similar to that reported by Kils (1979b) for swimming *Euphausia superba*, and that reported by Cowles *et al.* (1986) for passive body movements of dead *G. ingens*.

In the animals for which pleopod beat rate was recorded, no significant relationship was found between pleopod beat rate and swimming speed within the narrow range of swimming speeds observed. The pleopods beat at around 150–230 strokes per minute, regardless of swimming speed. The relationship between pleopod beat rate, swimming speed, and body angle for one individual is shown in Figure 2.

Significant differences in rates of oxygen consumption were measured between instars. With the exception of instar 5, routine mass-specific metabolic rates (MO_{2mr}) were significantly higher for the smaller instars than for larger ones (Fig. 1C).

Most individual animals swam at a typical speed for that individual, with little deviation throughout the experiment. The maximum sustained speed, defined as the highest swimming speed maintained for at least 20 minutes, recorded for any animal of a particular instar was typically less than twice the average swimming speed of individuals from that instar. Few animals swam at a large enough range of speeds to determine the relationship between swimming speed and rate of oxygen consumption. In those that did, the relationship was approximately linear (Fig. 3).

The best-fit equation relating rate of oxygen consumption (MO_2) to swimming speed (S_a) and body mass (g wet wt) was:

$$MO_2 = 0.00289 - 0.00216 \log_{10} g + 0.00156 S_a - 0.00167 (\log_{10} g) \times S_a \quad (1)$$

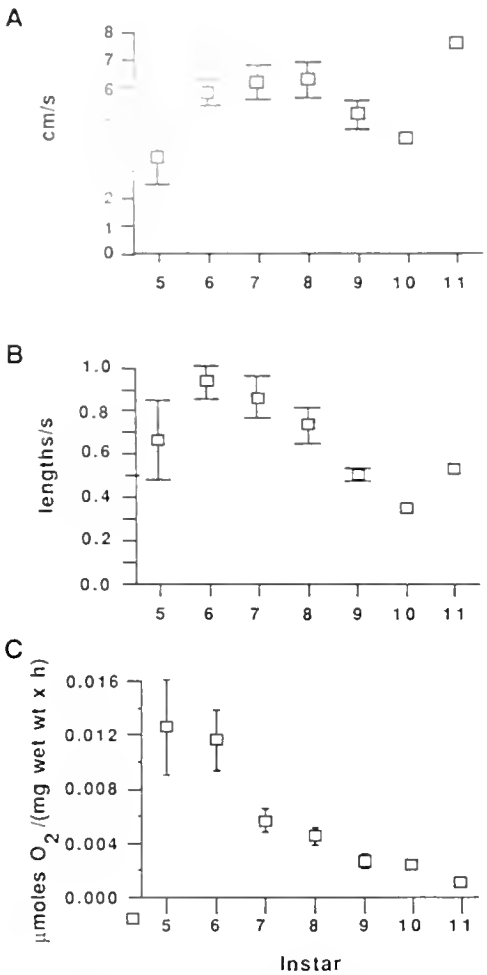

Figure 1. A. Mean swimming speeds, in centimeters per second, for each instar. B. Mean swimming speeds, in lengths per second, for each instar. C. Mass-specific routine oxygen consumption rates, in micromoles of oxygen per milligram wet mass per hour, for each instar in swim tunnel. Error bars are standard error.

(R^2 = 0.45, Standard error of estimate 0.00456, P slope = 0 ≪ .001)

The increase in MO_2 with increase in relative swimming speed (S_r) was approximately the same for each instar, increasing by an amount equal to the standard rate of aerobic metabolism for each 0.1 to 0.25 length per second increase in speed.

Animal size and rates of oxygen consumption

For any given absolute swimming speed, MO_{2mr} of the smaller instars was higher than that of the larger instars (Fig. 4). This effect was reduced but not eliminated by converting swimming speeds to lengths per second for each instar. The smaller animals thus had higher rates of oxygen consumption than did the larger animals at any given swimming speed.

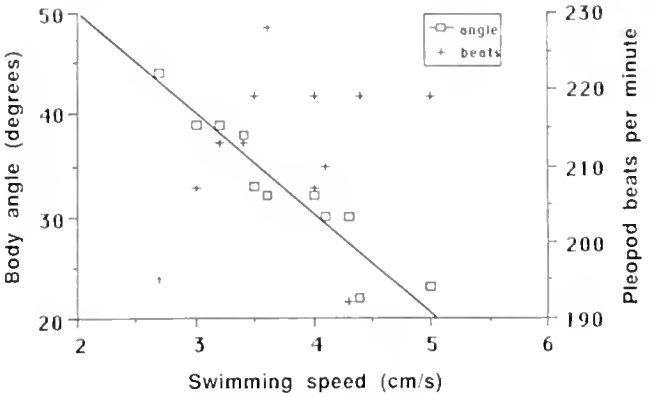

Figure 2. The relationship between swimming speed, body angle, and pleopod beat rate for one instar 6 *Gnathophausia ingens*. Body angle from horizontal (squares) decreases significantly with swimming speed ($P < .001$). There is no significant correlation between pleopod beat rate (crosses) and swimming speed.

The best-fit allometric equation relating mean standard total rate of oxygen consumption (MO_{2tms}, micromoles O_2/h), as calculated using equation 1, to animal wet mass (WWT, grams) was:

$$MO_{2tms} = 2.76\ WWT^{0.547\pm0.179} \quad (2)$$

The fact that the smaller instars spontaneously swam at higher relative speeds than did the larger instars led to an allometric relationship between wet mass and mean routine total rate of oxygen consumption (MO_{2tmr}) which was significantly different from the relationship between wet mass and standard oxygen consumption. The best-fit equation for routine rates of oxygen consumption was:

$$MO_{2tmr} = 8.28\ WWT^{0.307\pm.238} \quad (3)$$

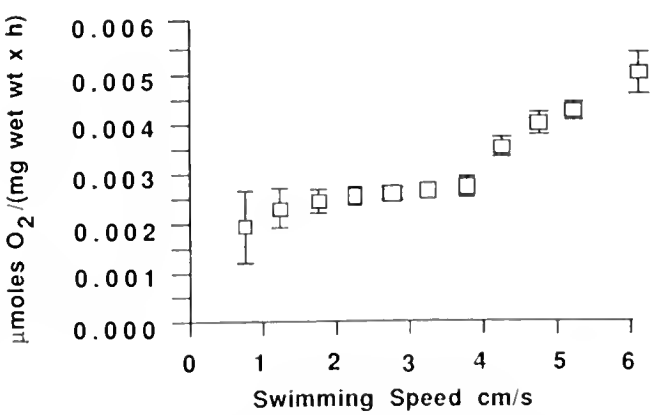

Figure 3. Relationship of swimming speed (X, cm/s) to rate of oxygen consumption (Y, micromoles O_2/ (mg wet wt × h) for one *Gnathophausia ingens*. Error bars are standard deviation.

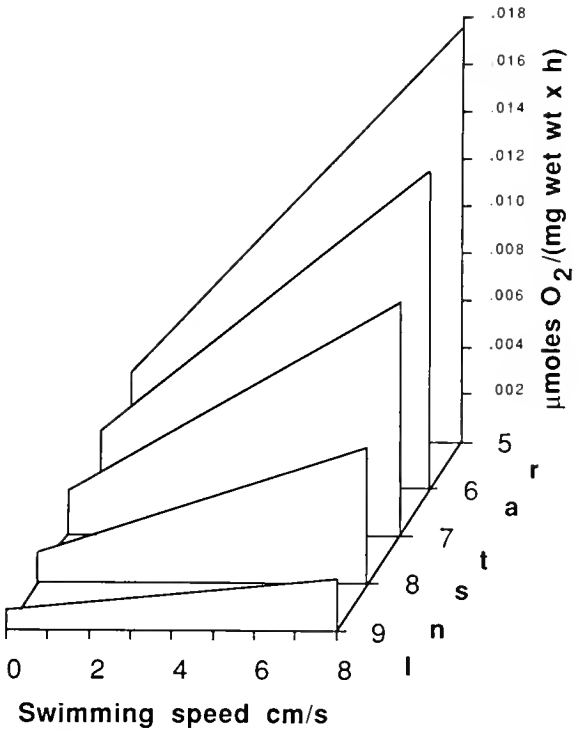

Figure 4. A comparison of the best-fit linear regressions of mass-specific rate of oxygen consumption [micromoles O_2/ (mg wet wt × h)] as a function of absolute swimming speed (cm/s) for *Gnathophausia ingens* instars 5–9, based on equation 1.

Discussion

Swimming speeds

Comparison of *G. ingens'* routine swimming speed of 5 to 6.5 centimeters per second (0.5 to 1 body length per second) to that of other, shallower-living pelagic crustaceans is difficult, since few comparable measurements have been reported (Table II). All shallow-living species cited are smaller than the deep-living *G. ingens* but swim at faster relative speeds. *G. ingens* is also capable of swimming much faster than its routine speeds, as demonstrated by several animals that swam at over 18 cm/s (over 2 lengths/s) for several minutes when first introduced to the swim chamber, and by the maximum sustained speeds of 7.5–12.2 centimeters per second (1–1.5 lengths/s) (Table I). However, these relative speeds for *G. ingens* are as little as one tenth that of the shallower-living species when the difference in body length is taken into account. If the highest speeds cited above for each species are taken as an estimate of the animals' burst speeds, *G. ingens'* burst speeds are also markedly lower than those of shallower-living pelagic crustaceans.

To attain the routine swimming speeds of 5 to 6.5 cm/s, the swimming speed of most *G. ingens* instars, the smaller instars had to swim at relative speeds of nearly twice as many body lengths per second as compared to the larger instars. The routine swimming speeds of the smaller instars thus approached more closely to their maximum sustained speeds (Table I). This may be why the absolute swimming speeds of instar 5 animals were somewhat lower than those of most of the larger instars. If instar 5 animals were to swim at 5 to 6.5 centimeters per second, as the larger instars did, they would be swimming at 1 to 1.25 lengths/s, or nearly the maximum sustained relative speed (1.4 lengths/s) attained by any instar.

Swimming speeds and rates of aerobic metabolism

Due to the relatively restricted range of routine swimming speeds selected by *G. ingens* in this experiment, it was not possible to determine conclusively the shape of the relationship between swimming velocity and rate of oxygen consumption. However, several lines of evidence indicate that the relationship is linear over the limited range of speeds studied. In the few animals that swam at a wide range of speeds, the relationship between velocity and rate of oxygen consumption appeared to be approximately linear, as shown in Figure 3. When data from all individuals of a given instar were pooled, the best-fit relationship in each instar measured was linear over the range of speeds tested. Stepwise linear regression indicated that rate of oxygen consumption was related directly to swimming speed, and not to the logarithm nor

Table II

Comparison of crustacean swimming speeds reported in the literature

Species	Length (cm)	cm/s	Lengths/s	Reference
Gnathophausia ingens	5.2–9.9	5.0–6.5	0.5–1	This paper
Euphausia superba	4–5	5.6	1.25	Kils (1979a)
Mysis relicta	3	5–10	2–3	Robertson *et al.* (1968)
Neomysis americana	11.4	6–8	5–7	Hargreaves (1981)
	0.6–1.7	3–10	5–6	Hargreaves (1981)
Acanthomysis sp.	0.7	9–10	10–14	Allen (1978)
Mysidium columbiae			20	Steven (1961)

to the square of speed. In addition, Cowles *et al.* (1986) showed that drag on a dead mysid's body increases linearly with velocity over the speed range at which these animals were swimming. Since thrust in a steadily swimming animal is equal to drag (Wu, 1977), thrust and metabolic energy consumption would also increase linearly with swimming speed in these animals if drag on a dead mysid is representative of drag on a live, swimming mysid.

A linear relationship between swimming velocity and rate of oxygen consumption has also been reported for several other crustacean species. Halcrow and Boyd, (1967) found a linear relationship for the amphipod *Gammarus oceanicus,* as did Torres and Childress, (1983) for *Euphausia pacifica.* A number of other crustaceans, however, have been found to have nonlinear relationships between swimming velocity and rate of oxygen consumption. The basis for these differences is not clear. However, it appears likely that at higher speeds the relationship between velocity and oxygen consumption in *G. ingens* would begin to conform more closely to an exponential relationship (Hargreaves, 1981; Webb, 1975a; Cowles *et al.,* 1986).

Size dependency of oxygen consumption

It has been shown for numerous organisms that the slope of the allometric equation of the logarithm of total oxygen consumed (Y) *versus* the logarithm of the animal's mass (X) generally falls in the range of 0.67 to 1, usually being about 0.75 (Kleiber, 1947; Wolvekamp and Waterman, 1960; Wu, 1977; Schmidt-Nielsen, 1979). This relationship holds for standard or basal metabolism (Winberg, 1956, 1961; Hemmingsen, 1960; Brett, 1965; Brett and Glass, 1973; Wilkie, 1977; Peters, 1983), for routine metabolism (Job, 1957), and for active metabolism (Brett, 1965, Brett and Glass, 1973; Taylor *et al.,* 1981; Prothero, 1979). Childress (1971a) and Hiller-Adams and Childress (1983c) found a similar relationship between animal size and routine oxygen consumption in *G. ingens.* The standard rates of aerobic metabolism determined in this study were generally lower than these rates (Fig. 5). The routine rates of oxygen consumption reported by Childress (1971a) and Hiller-Adams and Childress (1983c) were similar to rates associated with swimming speeds of 0.25 lengths/s in this study.

Though the slope of the allometric relationship between size and standard metabolic rate (equation 2) was lower than the 0.75 generally found for such relationships, the difference was barely significant. On the other hand, the slope of the allometric regression of the animals' routine metabolic rates *versus* wet mass was highly significantly less than 0.75 (equation 3), and for the

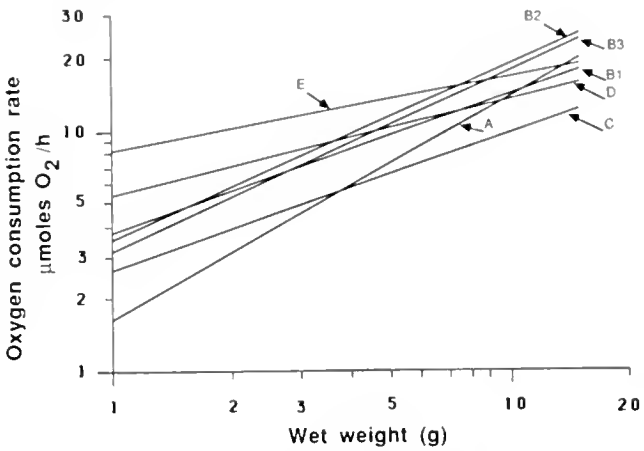

Figure 5. A comparison of the best-fit least-squares linear regressions of the allometric relationship between total rate of oxygen consumption (Y, micromoles O_2/h) *versus* wet mass (X, grams), from several studies of *Gnathophausia ingens'* oxygen consumption rate. Lines: A: from Childress (1971). B1–B3: from Hiller-Adams and Childress (1983c). C to E: rates of oxygen consumption as measured in this study. C: standard rate (0 cm/s). D: oxygen consumption rate at 0.25 lengths per second swimming speed. E: routine oxygen consumption rates.

smaller instars the rates of oxygen consumption were significantly higher than those previously reported for *G. ingens* (Fig. 5). This trend reflects the higher relative swimming speeds and rates of oxygen consumption of the smaller instars under the conditions of the swim tunnel. In this experiment, the animals swam freely in the tunnel at a speed they set themselves, restrained only by connection to a movable force transducer. In previous reports (Childress, 1971a; Hiller-Adams and Childress, 1983c), oxygen consumption was measured within a small enclosed respiration chamber in which the animals lay, beating their pleopods. Since these animals were free to set their own pleopod beat rates within the confines of the chamber, it may be assumed that the rates of oxygen consumption measured under these conditions were routine rates. The fact that the slopes of the allometric relationships obtained under these conditions were similar to the expected slopes of 0.75 supports this assumption. However, in light of the data obtained in the present study, it appears that the definition of routine activity as applied to active, negatively buoyant crustaceans such as *G. ingens* needs to be refined. It appears that the animals in the enclosed chambers, which were not free to swim about, assumed a uniform level of activity that was similar in all instars and equivalent to a swimming speed of approximately 0.25 lengths per second. The present experiment shows that when free to swim through the water, however, the smaller instars assume a much higher level of spontaneous activity than the larger instars do. "Routine" activity levels are markedly different for the different instars if the animal is in a free-swim-

ming state, as in this experiment, but not if the animal is not free to swim about, as in the Childress (1971a) and Hiller-Adams and Childress (1983c) experiments. If one is interested in comparing rates of oxygen consumption at some standard level of activity, then the rates measured by Childress (1971a) and Hiller-Adams and Childress (1983c) will do. However, this study shows that if one is estimating actual energy expenditures as may occur under routine conditions in the field, one must account for the different levels of routine activity the different instars assume when left to swim freely.

Cost of transport

The energy expenditure of an actively moving animal can be described in terms of cost of transport, or the amount of energy required to move a given distance through the medium. Cost of transport is influenced by a number of variables including speed, mode of transport, animal size and shape, and medium. For calculating cost of transport, the linear relationship between swimming speed and rate of oxygen consumption was recalculated in terms of energy expended per unit distance [calories/(g × km)]. A respiratory quotient (RQ) of 0.79 was used, reflecting metabolism of a mixture of carbohydrate, protein, and fat (Bartholomew, 1977). When this RQ is used, 1 micromole of oxygen is equivalent to 0.1075 calories. Instar 8 was selected as an average animal for cost of transport estimation. Instar 8 animals weighed an average of 4.07 grams, and the relationship between speed and rate of oxygen consumption is given in equation 1. Using these data, this animal's energy expenditure per unit distance (CT, calories per gram-kilometer) [cal/(g × km)] while swimming is:

$$CT = 1.63\left(\frac{3.87}{S_a} + 1\right) \quad (4)$$

This relationship is shown graphically in Figure 6. As can be seen, the energy required per unit distance is very high for low swimming speeds, dropping rapidly with increasing speed at low speeds and then much more gradually at speeds above 3 cm/s. This relationship makes it clear that, for *G. ingens*, lowest costs of transport per unit distance are incurred at speeds above 3 cm/s. This fits well with the empirical observation that these mysids swim at a characteristic speed of 5 to 6.5 cm/s. Slower swimming speeds would be energetically expensive, entailing a high cost per unit distance. On the other hand, equation 4 predicts that swimming faster than 5 or 6 cm/s would at best result in only minimal reduction in cost of transport. In reality, higher swimming speeds are likely to result in even higher costs than predicted, due to increasing turbulence and to the exponential increase in drag with speed predicted by hydrodynamic equations

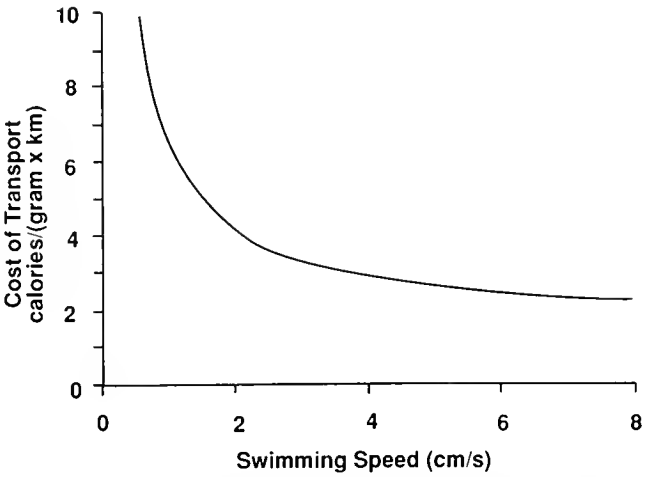

Figure 6. Cost of transport (CT, calories per gram-kilometer) as a function of swimming speed (S_a, cm/s) for *Gnathophausia ingens* of instar 8. Equation: $CT = 1.63\,[(3.87/S_a) + 1]$

(Webb, 1975a). Over the 0 to 8 cm/s range of swimming speeds measured in this experiment, change in body angle with speed appears to mask these effects, but at higher speeds they can be expected to become more prominent, resulting in an increase in cost of transport at higher speeds.

In terms of energy expenditure per unit time, higher swimming speeds also have higher costs due to the increase in metabolic rate with speed. *G. ingens'* routine swimming speeds thus appear to be intermediate between the very low speeds, with their high costs of transport per unit distance, and very high speeds, with their high metabolic costs per unit time and distance.

At a speed of 5.5 cm/s, a 4.07 gram *G. ingens* would have a cost of transport of 2.78 cal/(g × km), or 11.3 cal/km. This value is slightly higher than values estimated from the regression lines shown in Schmidt-Nielsen, (1972) Tucker, (1975), Beamish, (1978), and Hargreaves, (1981), all of which are for swimming fish. None of these authors state the equation for their regression lines; however, Schmidt-Nielsen's data are calculated from data given by Brett (1965) for swimming sockeye salmon of 3.38 to 1432 grams. A regression of Brett's data (for salmon in 15°C water), converted to the units of equation 4, is:

$$CT = 2.05\ WWT^{-0.254\pm0.054} \quad (5)$$

A 4.07 gram *G. ingens* swimming at 5.5 cm/s would have a cost of transport of 2.78 cal/(g × km), while the above equation predicts that cost of transport for a fish of the same size would be 1.43 cal/(g × km).

Torres (1984), using data from Brett and Glass (1973) for a size range of sockeye salmon, calculated net cost of transport for swimming fish. Torres' equation is:

$$CT_n = 1.416\ WWT^{-0.25} \quad (6)$$

(CT_n in this equation is net cost of transport [cal/(g × km)], therefore standard metabolic rate must be subtracted from the active metabolic rate before using this equation.) While this equation is based on salmon data, Torres has shown that the cost of transport of a number of other fish species falls near this line as well. For an instar 8 *G. ingens* swimming at 5.5 cm/s, the net cost of transport would be 1.82 cal/(g × km), while the value Torres' equation predicts for a fish of similar size is 0.997. *G. ingens'* cost of transport thus appears to be twice as high as that of fish of similar size. This trend has been noted for other crustaceans as well. Torres (1984) compiled net cost of transport data for a number of crustacean species and calculated an equation for crustacean net cost of transport analogous to equation 6. For crustaceans Torres' best-fit regression is:

$$CT_n = 6.26\ WWT^{-0.28} \quad (7)$$

This equation predicts a net cost of transport for a 4.07 gram crustacean swimming at 5.5 cm/s of 4.23 cal/(g × km), twice as high as the 1.82 calculated for *G. ingens*. Thus, *Gnathophausia ingens'* net cost of transport appears to be relatively low for crustaceans, which use paddle propulsion, but is higher than that for fish, which use an undulatory propulsion mode.

Swimming efficiency

Swimming efficiency, the ratio of the mechanical power required to overcome the drag an animal experiences while swimming to the metabolic power the animal uses for swimming, is a useful way to compare the efficiency of different propulsive mechanisms. Swimming efficiency has been determined for a number of fish, including salmon (Osborne, 1961; Webb, 1973, 1975a) and trout (Webb, 1971a, b), which swim in the subcarangiform mode, and *Cymatogaster aggregata* (Webb, 1975b) and goldfish (Smit, 1965, Smit *et al.*, 1971), which use pectoral fin propulsion. Calculated swimming efficiencies for the subcarangiform swimmers were low at low speeds, increasing to 15.8% at critical swimming speeds for trout and to 26% for salmon. Efficiency for *Cymatogaster aggregata* at critical swimming speed was 9.2 to 14%. Efficiency tends to increase with fish size and swimming speed (Webb, 1975a), and appears to be higher for the subcarangiform mode than for pectoral fin propulsion.

Previous studies of swimming efficiency in hard-bodied organisms such as crustaceans have mainly been estimates based on what is known about muscle efficiency and efficiency in fish. Klyashtorin and Yarzhombek (1973) used various efficiencies cited in the literature for ATP conversion, muscle efficiency, and paddle propulsion efficiency to arrive at an estimate of 5% for crustacean swimming efficiency. Hargreaves (1981) used similar calculations, along with the fish swimming efficiencies cited above, to estimate crustacean swimming efficiency at 10%. Nachtigall (1977) used a swimming efficiency of 10% for swimming water beetles, based in part on a calculation of 30% efficiency for the rowing apparatus.

Torres (1984) made a more direct calculation of swimming efficiency in the euphausiid *E. pacifica* by measuring rate of oxygen consumption at various swimming speeds and comparing these values to estimated drag based on hydrodynamic formulas. On the basis of this partly empirical data, he calculated swimming efficiency to vary from 0.014% at 1 cm/s to 2.85% at 20 cm/s. If the animal's drag were higher than his estimates based on hydrodynamic formulas, then the animal's swimming efficiency would be correspondingly higher.

Swimming efficiency in *G. ingens* may be calculated based on oxygen consumption data from this experiment (equation 1) and on drag data from Cowles *et al.* (1986). For an instar 8 individual (carapace length 3.0 cm), swimming efficiency E_s is described by the equation:

$$E_s = 2.96 \times 10^{-3} (S_a) \quad (8)$$

At a swimming speed of 5.5 cm/s, swimming efficiency would be 1.6 percent. This efficiency is higher than the 0.097 to 0.133% reported by Torres (1984) for *E. pacifica* swimming at this speed, but is below that reported for fish.

Equation 8 indicates that *G. ingens'* swimming efficiency increases linearly with speed. At 8 cm/s, efficiency for an instar 8 animal would be 2.4%. Swimming efficiency also increases with speed for fish (Webb, 1975a), and for *E. pacifica* (Torres, 1984), though not linearly. In fish, the increase in efficiency with speed is thought to be linked to changes in propeller and muscle efficiency. It is not known whether this is also true for *G. ingens*. Efficiency and the changes in efficiency with speed of the multiple-paddle mode of propulsion used by *G. ingens* and many other pelagic crustaceans have not been adequately studied. Kils (1979b) found that *Euphausia superba* changes many aspects of the pleopod stroke with increases in speed over the range of 0–15 cm/s, including increasing abduction of the protopodites, increasing degree of spreading of propulsive setae, holding pleopods closer to the body on the return stroke, directing the propulsive stroke more directly to the posterior, and bringing the whole body into a more nearly horizontal orientation. These adjustments result in changes in the flow direction and size of the wake and in increased swimming velocity. Change in pleopod beat rate is small over this entire range of speeds, increasing from 150 to 180 beats per minute. Increase in swimming speed is accom-

plished by a linear increase in the transport distance per beat rather than an increase in pleopod beat rate. *E. superba* thus appears to control swimming speed by modifying stroke efficiency at speeds up to 15 cm/s. At this speed maximum stroke efficiency appears to have been reached, and further increases in speed are brought about by changes in stroke rate. Mickel and Childress (1978) and Quetin and Childress (1980) observed that the pleopod beat rate of *G. ingens* strapped to a frame is remarkably constant, remaining at an average of between 140 and 210 beats per minute or stopping completely. *G. ingens* in the swim tunnel also maintained a similarly high, stable rate of pleopod beats, even with changes of swimming speed of at least a factor of two. It thus appears likely that *G. ingens* also adjusts swimming speed largely by changes in stroke characteristics, as does *E. superba*. Which parameters of the stroke are varied and how these changes contribute to stroke efficiency remain to be determined.

One likely factor influencing the increase in swimming efficiency in *G. ingens* with increasing speed is the change in body attitude (Fig. 2). At low speeds the animal swims with its body angled upward, directing a larger proportion of its thrust downward and thereby increasing lift. As speed increases, the body assumes a more horizontal orientation, so that a larger vector percentage of thrust is directed directly backward. This trend is likely to result in increasing efficiency in the generation of forward thrust with increasing speed, as observed. Eventually, however, the animal reaches a speed at which it assumes a nearly horizontal orientation in the water. The speed varies between instars, but by 8 cm/s most animals are nearly horizontal. This speed, at which increases in efficiency due to changes in body angle would be maximized, would correspond to an efficiency of 1.8% for *G. ingens* of instar 8.

Calculations for other instars, such as those carried out above for instar 8, indicate that swimming efficiency also increases with size in *G. ingens*. At 5.5 cm/s, efficiency for an instar 5 individual would be 0.8%, while that of an instar 9 individual would be 5.36%. Such a trend has also been noted for fish (Webb, 1975a).

Gnathophausia ingens *as a bathypelagic crustacean*

As an active pelagic crustacean, *G. ingens* appears to be more efficient and has lower costs of transport than shallower species, such as *E. pacifica*. However, the order of magnitude reduction in rate of oxygen consumption of the bathypelagic *G. ingens* can only be partially accounted for by these relatively small increases in swimming efficiency or reductions in cost of transport. The most obvious factor contributing to *G. ingens'* low rate of oxygen consumption is its reduced swimming speed relative to surface-living crustaceans. *G. ingens'* routine relative swimming speeds are as low as one tenth those measured for shallower-living crustaceans, and its maximum speeds appear to be lower by the same factor. On the other hand, *G. ingens* is not inactive. The mysid swims constantly and shows no tendency for hanging motionless in the water. These observations are consistent with present hypotheses regarding the selective factors responsible for the low metabolic rates of deep-living pelagic species, and provide experimental evidence of reduced activity levels in deep-living animals.

Acknowledgments

We thank the crews of the research vessels *New Horizon* and *Velero* for their help in gathering *G. ingens* for this research, and George Hilton for his help in statistical analysis. Our thanks also to A. Alldredge, A. Ebeling, M. S. Gordon, and the other reviewers for their helpful comments on the manuscript. This research was supported in part by NSF grants OCE78-08933, OCE81-10154, and OCE85-00237 to J. J. Childress.

Literature Cited

Allen, D. M. 1978. Population dynamics, spatial and temporal distributions of mysid crustaceans in a temperate marsh estuary. Ph. D. dissertation, Lehigh University.

Bailey, T. G., and B. H. Robison. 1986. Food availability as a selective factor on the chemical compositions of midwater fishes in the eastern North Pacific. *Mar. Biol.* **91:** 131–141.

Bartholomew, George A. 1977. Energy metabolism. Pp. 57–110 in *Animal Physiology: Principles and Adaptations,* 3rd edition, M. S. Gordon, ed. MacMillan, New York.

Beamish, F. W. H. 1978. Swimming capacity. Pp. 101–188 in *Fish Physiology,* Vol VII: *Locomotion,* W. S. Hoar and D. J. Randall, eds. Academic Press, New York.

Belman, B. W., and J. J. Childress. 1976. Circulatory adaptations to the oxygen minimum layer in the bathypelagic mysid *Gnathophausia ingens. Biol. Bull.* **150:** 15–37.

Brett, J. R. 1965. The relation of size to rate of oxygen consumption and sustained swimming speed of sockeye salmon (*Oncorhynchus nerka*) *J. Fish Res. Board Can.* **22:** 1491–1501.

Brett, J. R., and N. R. Glass. 1973. Metabolic rates and critical swimming speeds of sockeye salmon (*Oncorhynchus nerka*) in relation to size and temperature. *J. Fish. Res. Board Can.* **30:** 379–387.

Childress, J. J. 1968. Oxygen minimum layer: vertical distribution and respiration of the mysid *Gnathophausia ingens. Science* **160:** 1242–1243.

Childress, J. J. 1969. The respiratory physiology of the oxygen minimum layer mysid *Gnathophausia ingens.* Ph. D. dissertation, Stanford University, California. 142 pp.

Childress, J. J. 1971a. Respiratory adaptations to the oxygen minimum layer in the bathypelagic mysid *Gnathophausia ingens. Biol. Bull.* **141:** 109–121.

Childress, J. J. 1971b. Respiratory rate and depth of occurrence of midwater animals. *Limnol. Oceanogr.* **16:** 104–106.

Childress, J. J. 1975. The respiratory rates of midwater crustaceans as a function of depth of occurrence and relation to the oxygen minimum layer off southern California. *Comp. Biochem. Physiol.* **50A:** 787–799.

Childress, J. J. 1977. Physiological approaches to the biology of midwater organisms. Pp. 301–324 in *Oceanic Sound Scattering Prediction*, N. R. Andersen and B. J. Zahuranec, ed. Plenum Press, New York.

Childress, J. J., A. L. Barnes, L. B. Quetin, and B. H. Robison. 1978. Thermally protecting cod ends for the recovery of living deep-sea animals. *Deep-Sea Res.* **25:** 419–422.

Childress, J. J. and T. J. Mickel. 1985. Metabolic rates of animals from the hydrothermal vents and other deep-sea habitats. *Biol. Soc. Wash. Bull.* **6:** 249–260.

Childress, J. J., and M. H. Nygaard. 1973. The chemical composition of midwater fishes as a function of depth of occurrence off southern California. *Deep-Sea Res.* **20:** 1093–1109.

Childress, J. J., and M. H. Nygaard. 1974. The chemical composition and buoyancy of midwater crustaceans as a function of depth of occurrence off Southern California. *Mar. Biol.* **27:** 225–238.

Childress, J. J., and M. H. Price. 1978. Growth rate of the bathypelagic crustacean *Gnathophausia ingens* (Mysidacea: Lophogastridae). I. Dimensional growth and population structure. *Mar. Biol.* **50:** 47–62.

Childress, J. J., and M. H. Price. 1983. Growth rate of the bathypelagic crustacean *Gnathophausia ingens* (Mysidacea: Lophogastridae): II. Accumulation of material and energy. *Mar. Biol.* **76:** 165–177.

Childress, J. J., S. M. Taylor, G. M. Cailliet, and M. H. Price. 1980. Patterns of growth, energy utilization and reproduction in some meso- and bathypelagic fishes off southern California. *Mar. Biol.* **61:** 27–40.

Clutter, R. I. 1969. The microdistribution and social behavior of some pelagic mysid shrimps. *J. Exp. Mar. Biol. Ecol.* **3:** 125–155.

Cowles, D. L. 1987. Factors affecting the aerobic metabolism of midwater crustaceans. Ph. D. dissertation, University of California, Santa Barbara.

Cowles, D. L., J. J. Childress, and D. L. Gluck. 1986. New method reveals unexpected relationship between velocity and drag in the bathypelagic mysid *Gnathophausia ingens*. *Deep-Sea Res.* **33:** 865–880.

Dohrn, A. 1870. Untersuchungen uber Bau und Entwicklung der Arthropoden. 10. Beitragen zur Kenntnis der Malacostraken und ihrer Larven. *Z. Wiss. Zool.* **20:** 607–625.

Fuzessery, Z., and J. J. Childress. 1975. Comparative chemosensitivity to the oxygen minimum layer in the bathypelagic mysid *Gnathophausia ingens*. *Biol. Bull.* **149:** 522–538.

Halcrow, K., and C. M. Boyd. 1967. The oxygen consumption and swimming activity of the amphipod *Gammarus oceanicus* at different temperatures. *Comp. Biochem. Physiol.* **23:** 233–242.

Hargreaves, B. R. 1981. Energetics of crustacean swimming. Pp. 453–490 in *Locomotion and Exercise of Arthropods*, C. F. Herreid and C. R. Fourtner, eds. Plenum Press, New York.

Hemmingsen, A. M. 1960. Energy metabolism as related to body size and respiratory surfaces, and its evolution. *Rep. Steno Mem. Hosp. Nordisk Insulinlaboratorium* **9:** 21–110.

Hiller-Adams, P., and J. J. Childress. 1983a. Effects of feeding, feeding history, and food deprivation on respiration and excretion rates of the bathypelagic mysid *Gnathophausia ingens*. *Biol. Bull.* **165:** 182–196.

Hiller-Adams, P., and J. J. Childress. 1983b. Effects of prolonged starvation on O_2 consumption, NH_4^+ excretion, and chemical composition of the bathypelagic mysid *Gnathophausia ingens*. *Mar. Biol.* **77:** 119–127.

Hiller-Adams, P., and J. J. Childress. 1983c. Effects of season on the bathypelagic mysid *Gnathophausia ingens*: water content, respiration, and excretion. *Deep-Sea Res.* **30:** 629–638.

Job, S. V. 1957. The routine-active oxygen consumption of the milk fish. *Proc. Indian Acad. Sci.* **45:** 302–313.

Kils, U. 1979a. Performance of antarctic krill *Euphausia superba*, at different levels of oxygen saturation. *Meeresforschung* **27:** 35–48.

Kils, U. 1979b. The swimming behavior, swimming performance and energy balance of antarctic krill, *Euphausia superba*. German Ph. D. dissertation, Kiel University, 1979. English translation is *BIOMASS Scientific Series* **3.** 121 pp.

Kleiber, M. 1947. Body size and metabolic rate. *Physiol. Rev.* **27:** 511–541.

Klyashtorin, L. B., and A. A. Yarzhombek. 1973. Energy consumption in active movements of planktonic organisms. *Oceanology* **13:** 575–580.

Mickel, T. J., and J. J. Childress. 1978. The effect of pH on oxygen consumption and activity in the bathypelagic mysid *Gnathophausia ingens*. *Biol. Bull.* **154:** 138–147.

Mickel, T. J., and J. J. Childress. 1982. Effects of pressure and pressure acclimation on activity and oxygen consumption in the bathypelagic mysid *Gnathophausia ingens*. *Deep-Sea Res.* **29:** 1293–1301.

Nachtigall, W. 1977. Swimming mechanics and energetics of locomotion of variously sized water beetles—dytiscidae, body length 2 to 35 mm. Pp 269–283 in *Scale Effects in Animal Locomotion*, T. J. Pedley, ed. Academic Press, London.

Osborne, M. F. M. 1961. Hydrodynamic performance of migratory salmon. *J. Exp. Biol.* **38:** 365–390.

Peters, R. H. 1983. *The Ecological Implications of Body Size*. Cambridge Univ. Press, New York. 329 pp.

Piiper, J., P. Dejours, P. Haab, and H. Rahn. 1971. Concepts and basic quantities in gas exchange physiology. *Respir. Physiol.* **13:** 292–304.

Prothero, J. W. 1979. Maximal oxygen consumption in various animals and plants. *Comp. Biochem. Physiol.* **64A:** 463–466.

Quetin, L. B., and J. J. Childress. 1980. Observations on the swimming activity of two bathypelagic mysid species maintained at high hydrostatic pressures. *Deep-Sea Res.* **27A:** 383–391.

Robertson, A., C. F. Powers, and R. F. Anderson. 1968. Direct observations on *Mysis relicta* from a submarine. *Limnol. Oceanogr.* **13:** 700–702.

Schmidt-Nielsen, K. 1972. Locomotion: Energy cost of swimming, flying, and running. *Science* **177:** 222–228.

Schmidt-Nielsen, K. 1979. *Animal Physiology*, second edition. Cambridge University Press, Cambridge, UK. 560 pp.

Smit, H. 1965. Some experiments on the oxygen consumption of goldfish (*Carassius auratus* L) in relation to swimming speed. *Can. J. Zool.* **43:** 623–633.

Smit, H., J. M. Amelink-Koutsaal, J. Vijverberg, and J. C. Von Vaupel-Klein. 1971. Oxygen consumption and efficiency of swimming goldfish. *Comp. Biochem. Physiol.* **39A:** 1–28.

Smith, K. L., Jr. 1978. Metabolism of the abyssopelagic rattail *Coryphaenoides armatus* measured *in situ*. *Nature* **274:** 362–364.

Smith, K. L., Jr., and R. R. Hessler. 1974. Respiration of benthopelagic fishes: *in situ* measurements at 1230 meters. *Science* **184:** 72–73.

Smith, K. L., Jr., and M. B. Laver. 1981. Respiration of the bathypelagic fish *Cyclothone acclinidens*. *Mar. Biol.* **61:** 261–266.

Steven, D. M. 1961. Shoaling behavior in a mysid. *Nature* **192:** 280–281.

Taylor, C. R., G. M. O. Maloiy, E. R. Weibel, V. A. Langman, J. M. Z. Kamau, H. J. Seeherman, and N. C. Heglund. 1981. Design of the mammalian respiratory system: Scaling maximum aerobic capacity to body mass—wild and domestic animals. *J. Exp. Biol.* **86:** 9–18.

Torres, J. J. 1984. Relationship of oxygen consumption of swim-

ming speed in *Euphausia pacifica*. II. Drag, efficiency and a comparison with other swimming organisms. *Mar. Biol.* **78:** 231–237.

Torres, J. J., B. W. Belman, and J. J. Childress. 1979. Oxygen consumption rates of midwater fishes as a function of depth of occurrence. *Deep-Sea Res.* **26A:** 185–197.

Torres, J. J., and J. J. Childress. 1983. Relationship of oxygen consumption to swimming speed in *Euphausia pacifica*. I. Effects of temperature and pressure. *Mar. Biol.* **74:** 79–86.

Torres, J. J., J. J. Childress, and L. B. Quetin. 1982. A pressure vessel for the simultaneous determination of oxygen consumption and swimming speed in zooplankton. *Deep-Sea Res.* **29:** 631–639.

Tucker, V. A. 1975. The energetic cost of moving about. *Am. Sci.* **63:** 413–419.

Webb, P. W. 1971a. The swimming energetics of trout. I. Thrust and power output at cruising speeds. *J. Exp. Biol.* **55:** 489–520.

Webb, P. W. 1971b. The swimming energetics of trout. II. Oxygen consumption and swimming efficiency. *J. Exp. Biol.* **55:** 521–540.

Webb, P. W. 1973. Effects of partial caudal-fin amputation on the kinematics and metabolic rate of underyearling sockeye salmon (*Oncorhynchus nerka*) at steady swimming speeds. *J. Exp. Biol.* **59:** 565–581.

Webb, P. W. 1975a. Hydrodynamics and energetics of fish propulsion. *Bull. Fish. Res. Board Can.* **190:** 1–159.

Webb, P. W. 1975b. Efficiency of pectoral-fin propulsion of *Cymatogaster aggregata*. Pp. 573–584 in *Swimming and Flying in Nature*, T. Y. T. Wu, C. J. Brokaw, and C. Brennan, eds. Plenum Press, New York.

Wilkie, D. R. 1977. Metabolism and Body size. Pp. 23–36 in *Scale Effects in Animal Locomotion*, T. J. Pedley, ed. Academic Press, New York.

Winberg, G. G. 1956. Rate of metabolism and food requirements of fishes. (In Russian). Translated in *Fish. Res. Board Can. Trans. Ser.* **194.** 239 pp.

Winberg, G. G. 1961. *New information on metabolic rate in fishes.* (In Russian). Translated in *Fish. Res. Board Can. Trans. Ser.* **362.** 11 pp.

Wolvekamp, H. P., and T. H. Waterman. 1960. Respiration. Pp. 35–100. *The physiology of Crustacea*, Vol I, T. H. Waterman, ed. Academic Press, New York.

Wu, T. Y. 1977. Introduction to the scaling of aquatic animal locomotion. Pp. 203–232 in *Scale Effects in Animal Locomotion*, T. J. Pedley, ed. Academic Press, New York.

Reference: *Biol Bull* **175**: 122–131. (August, 1988)

Energy Metabolism During Anoxia and Recovery in Shell Adductor and Foot Muscle of the Gastropod Mollusc *Haliotis lamellosa:* Formation of the Novel Anaerobic End Product Tauropine

GERD GÄDE

Institut für Zoologie IV, Universität Düsseldorf, Universitätsstr. 1, D-4000 Düsseldorf 1, Federal Republic of Germany

Abstract. Metabolic responses to experimental anoxia and subsequent recovery, and to exercise were investigated in two different muscular tissues of the ormer, *Haliotis lamellosa*. The tissues are employed for different tasks by the animal. The foot is mainly responsible for slow gliding movements. The shell adductor muscle pulls down the shell for protection and in righting an animal which has been dislodged from the rocks. Tissue-specific differences in anaerobic energy metabolism occur. During 6 h of experimental anoxia, energy for both muscles was provided by arginine phosphate and co-fermentation of glycogen and aspartate. Glycolysis in the shell adductor muscle led mainly to the formation of the novel end product tauropine; D-lactate production predominated in the foot. This pattern is consistent with observed enzymatic profiles in the two muscles and with the equilibrium constants of the respective enzymes, tauropine and D-lactate dehydrogenase. Recovery from anaerobiosis was characterized by a rapid return of the phosphagen pool and the energy charge to the aerobic state. A protracted time-course was observed for the clearance of glycolytic end products.

Exercise, primarily powered by the shell adductor muscle, was mainly fueled by glycolysis resulting mostly in the accumulation of tauropine.

Introduction

In recent years different enzymes that terminate anaerobic glycolysis, so-called opine dehydrogenases, have been identified in the tissues of many marine invertebrates (for a review, see Gäde and Grieshaber, 1986). The products formed (octopine, strombine, or alanopine) via the reductive condensation of pyruvate with the respective amino acid (arginine, glycine or alanine) are collectively known as opines:

$$\text{pyruvate} + \begin{matrix}\text{arginine}\\ \text{glycine}\\ \text{alanine}\end{matrix} + \text{NADH} + \text{H}^+ \underset{\text{alanopine dehydrogenase}}{\overset{\text{octopine dehydrogenase}\atop\text{strombine dehydrogenase}}{\rightleftharpoons}} \begin{matrix}\text{octopine}\\ \text{strombine}\\ \text{alanopine}\end{matrix} + \text{NAD}^+ + \text{H}_2\text{O}.$$

Recently, a unique compound was detected in muscle extracts of the prosobranch gastropod, the abalone *Haliotis discus hannai* (Sato *et al.*, 1985). It was identified as D-rhodoic acid (now termed tauropine), previously isolated from some red algae (Kuriyama, 1961). The responsible enzyme, rhodoic acid dehydrogenase or tauropine dehydrogenase, catalyzing the reaction: pyruvate + taurine + NADH + $H^+ \rightleftharpoons$ tauropine + NAD^+ + H_2O, has been found in muscle tissue of the Japanese abalone as well as in the European ormer, *Haliotis lamellosa* (Sato and Gäde, 1986), and subsequently purified and characterized in detail in the latter species (Gäde, 1986). Certain features of this enzyme suggest a role in maintaining cytoplasmic redox balance during hypoxic conditions in the ormer (Gäde, 1986).

Various invertebrates can withstand hypoxic conditions in their habitats. Their metabolism during such a period of environmental anoxia is characterized by co-fermentation of aspartate and glycogen leading to the ac-

Received 15 March 1988; accepted 31 May 1988.

cumulation of the end products succinate, alanine and (in some cases) propionate and acetate. The rate of energy production is low, but the yield of ATP increased (reviewed by de Zwaan, 1977; Schöttler, 1980; Livingstone, 1982; Gäde, 1983a; Storey, 1985). During excessive locomotory activity, the capacities of muscle tissue to synthesize ATP rapidly by aerobic means are limited and energy provisions are met during functional anoxia via anaerobic glycolysis resulting in the accumulation of lactate or the opines. The rate of energy production is high, but the efficiency is low (references as above and Gäde, 1980; de Zwaan and van den Thillart, 1985; Gäde and Meinardus, 1986; Gäde and Grieshaber, 1986; Gäde, 1987a).

The present study concerns the anaerobic energy metabolism of muscle tissue in the ormer *Haliotis lamellosa*. The strategies used to provide energy during environmental and functional anoxia are of paramount importance for the survival of this species. The ormer is epifaunal in the littoral zone, attached by its foot to wave-swept rocks. The broad shell acts as a protective shield. It is pulled down tightly by the large shell adductor muscle (the right retractor or columella muscle) during low tide or vigorous wave action. When dislodged, ormers are extremely vulnerable to predators, especially since they often lie upside down. Therefore, these gastropods typically right themselves as fast as possible. This, again, is achieved mainly by relatively active movements of the large shell adductor muscle and with less input of the foot (unpub. obs.).

Previous studies revealed interesting patterns of dehydrogenase distribution in muscle tissue of the ormer (Gäde, 1986). Most tauropine dehydrogenase activity is found in the shell adductor muscle, which contains only minute levels of D-lactate dehydrogenase activity. In the foot muscle D-lactate dehydrogenase displays the highest activity. This almost mutually exclusive distribution of the dehydrogenases, combined with the different involvement of the muscle tissues during environmental (both tissues) and functional (mainly shell adductor) anoxia, led us to compare the energetics of the two muscle tissues. Furthermore, we investigated the metabolic events during recovery in well-aerated seawater, immediately following experimental anoxia, since data on the fate of the accumulated end products and re-charging of the depleted high energy phosphates are rather scarce (see review by Ellington, 1983).

This paper shows unequivocally that the fermentation of glycogen to the novel end product tauropine maintains cytoplasmic redox balance during experimental as well as functional anoxia in the shell adductor muscle. D-lactate is the main fermentation product in the foot during 6 h of anoxia. Both glycolytic end products are apparently oxidized very slowly *in situ*. Comparison of the glycolytic rates during experimental and functional anoxia reveals a 10-fold increase in the shell adductor, but only an enhancement by a factor of 2 in the foot muscle.

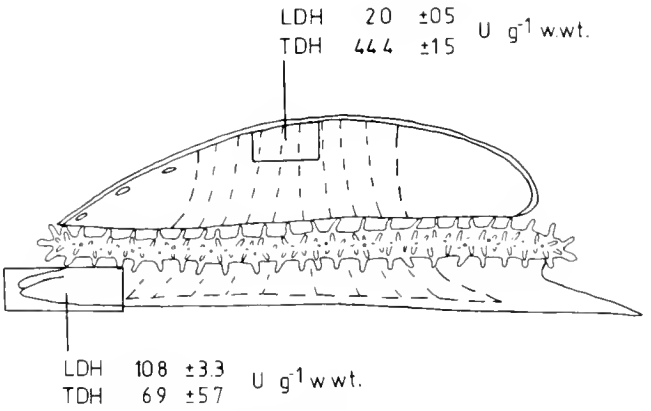

Figure 1. The sites of tissue-sampling (shell adductor muscle and foot) in the ormer, *Haliotis lamellosa*. The boxes identify the sites. Additionally, the enzyme activities for D-lactate dehydrogenase (LDH) and tauropine dehydrogenase (TDH) for each tissue are given as means ± 1 S.D. (n = 4) in units per gram wet weight (U g^{-1} wt wgt).

Materials and Methods

Animals and tissues

Specimens of the ormer *Haliotis lamellosa* (5–7 cm maximal shell length) were collected by local fishermen from the Bay of Naples, Italy, during October 1986. Animals were maintained in flowing seawater (22–24°C) at the Stazione Zoologica. Animals were used in experiments four to six days after collection.

Due to different profiles in the enzyme activities for pyruvate reductases (see Introduction), muscle tissue from two different organs were used in this study (Fig. 1): we compared the metabolic changes occurring in the shell adductor muscle to those in the foot. The dorsal part of the shell adductor (near the attachment of this muscle to the shell), and the anterior edge of the foot just below the head, were always excised for study (Fig. 1).

Biochemicals

Biochemicals were from Sigma Chemical Company (Deisenhofen, FRG) and Boehringer GmbH (Mannheim, FRG). All other chemicals were of reagent grade quality and came from Merck (Darmstadt, FRG). Tauropine dehydrogenase (EC 1.5.1.?), used to determine taurine and tauropine, was purified from the shell adductor muscle of *H. lamellosa* as outlined previously (Gäde, 1987b). D-lactate dehydrogenase (EC 1.1.1.28) and octopine dehydrogenase (EC 1.5.1.11), used to assay for D-lactate, arginine phosphate, and arginine, respectively,

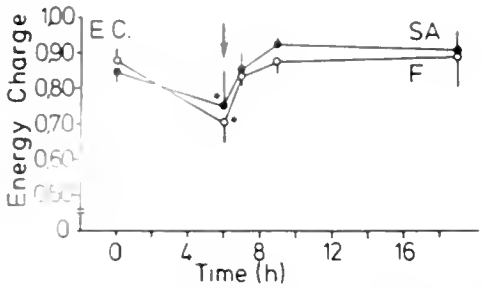

Figure 2. Alterations in the adenylate energy charge (E.C.) in the shell adductor (SA; solid circles) and foot (F; open circles) muscle of *Haliotis lamellosa* during environmental anoxia and recovery (onset marked by arrow). Each value is a mean ± 1 S.D. (for n, see Materials and Methods). The asterisks denotes a significant change compared to controls.

were purified from muscle tissue of the horseshoe crab, *Limulus polyphemus* (Carlsson and Gäde, 1985), and from the adductor muscles of the scallop, *Pecten jacobaeus* (Gäde and Carlsson, 1984), respectively.

Experimental procedure

Metabolic responses to environmental hypoxia and recovery. Twenty specimens of *H. lamellosa* were incubated in wash bottles (10 animals each) filled with about 2 l of seawater (22–24°C) that had been gassed with pure nitrogen until P_{O_2} (monitored with an oxygen electrode) reached almost zero mm Hg. After the animals were inserted, the wash bottles were flushed with a constant, slow stream of nitrogen gas. After 6 h of anoxic incubation, seven animals were removed, and their shell adductor and foot muscles excised, blotted, and frozen in liquid nitrogen. The remaining ormers were returned to well-aerated seawater, and subsets of four animals were removed at various intervals (1, 3, and 13 h) and treated as above. Furthermore, a zero time group of seven gastropods were chosen for the controls. The frozen tissues were subsequently transported from Naples to Düsseldorf on dry ice and stored at −35°C.

Metabolic responses to functional hypoxia. Four animals were exercised for 12 to 15 min in a large aquarium with flowing-seawater system. To induce exercise, the animals were placed upside-down on their shells; their righting movements involved, primarily, relatively vigorous contractions of the shell adductor muscle. When the animals had regained their normal posture, they were immediately inverted again. This work was continued for up to 15 min, when movements became much slower and the animals appeared to be exhausted. Shell adductor and foot muscles were then removed and treated as above.

Metabolite assays

Neutralized perchloric acid extracts were prepared from the frozen tissues of *H. lamellosa* according to previously published methods (Gäde *et al.*, 1978; Carlsson and Gäde, 1986). The levels of ATP, ADP, AMP, arginine, and arginine phosphate were determined spectrophotometrically by the methods of Lamprecht and Trautschold (1974), Jaworeck *et al.* (1974), and Gäde (1985a); the determinations were made immediately after neutralization of the extracts to eliminate sample losses.

Other metabolites were quantitated spectrophotometrically after storage of the extracts at −25°C. The methods used were those of Gawehn and Bergmeyer (1974) for D-lactate, Graβl (1974a, b) for L- and D-alanine, Bergmeyer *et al.* (1974) for aspartate, Williamson (1974) for succinate, and Gäde (1987b) for taurine. Tauropine was determined enzymatically using tauropine dehydrogenase in an assay system almost identical to that used for octopine quantification (Gäde, 1985b).

All metabolite data were analysed for significant

Table I

Alterations in the levels of adenylates (μmoles g^{-1} wt·wgt) in shell adductor and foot muscle of Haliotis lamellosa *during experimental anoxia and subsequent recovery*

Time (h) of anoxia or recovery	(n)	Shell adductor muscle				Foot muscle			
		ATP	ADP	AMP	Sum	ATP	ADP	AMP	Sum
Anoxia:									
0	7	3.25 ± 0.99*	0.96 ± 0.20	0.23 ± 0.16	4.44 ± 1.23	0.73 ± 0.31	0.14 ± 0.06	0.03 ± 0.01	0.90 ± 0.32
6	7	3.00 ± 0.68	1.43 ± 0.49	0.54 ± 0.36	4.97 ± 0.34	0.62 ± 0.32	0.51 ± 0.13	0.10 ± 0.04	1.23 ± 0.45
Recovery:									
1	4	3.04 ± 0.54	0.85 ± 0.17	0.19 ± 0.15	4.08 ± 0.64	0.41 ± 0.20	0.13 ± 0.08	0.02 ± 0.01	0.56 ± 0.28
3	4	3.81 ± 0.35	0.64 ± 0.08	0.05 ± 0.03	4.50 ± 0.36	0.70 ± 0.19	0.19 ± 0.08	0.03 ± 0.01	0.42 ± 0.25
13	4	3.09 ± 0.66	0.58 ± 0.21	0.09 ± 0.06	3.76 ± 0.50	0.91 ± 0.25	0.19 ± 0.11	0.04 ± 0.01	1.14 ± 0.38

* All values are given as mean ± SD.

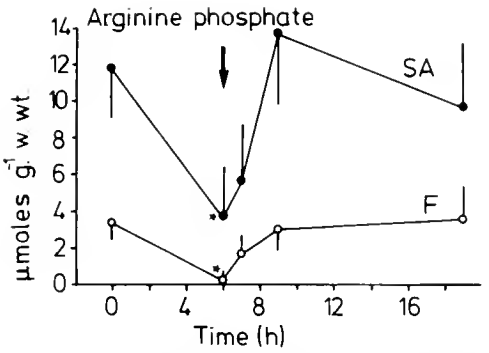

Figure 3. Time-course of the levels of arginine phosphate in the shell adductor (SA; solid circles) and foot (F; open circles) muscle of *Haliotis lamellosa* during experimental anoxia and recovery. For further details, see Figure 2.

changes (anaerobic *versus* controls) by analysis of variance (ANOVAR) using confidence limits of $P \leqq 0.05$.

Results

Metabolic responses to environmental hypoxia and recovery

The levels of the adenylates in the shell adductor muscle and foot during 6 h anoxia and recovery are listed in Table I. The calculated adenylate energy charge (E.C. = ATP + ½ ADP ÷ ATP + ADP + AMP) is depicted in Figure 2. In control animals the adenylate content of the shell adductor muscle was more than 4-fold compared with the foot muscle. This was also true for the individual adenylates ATP, ADP, and AMP. The concentrations of ADP and AMP increased during anoxia, but, due to high variations, these changes were not statistically significant in either tissue, whereas the value of the energy charge declined significantly in both tissues. Upon recovery, ADP and AMP levels as well as the energy charge returned to near the control state after one h. For both tissues, 13 h of recovery after anoxia led to marginally higher values of the energy charge as estimated for control animals.

The sum of the arginine containing compounds (arginine and arginine phosphate) in control animals was about 4-fold higher in the shell adductor muscle (31 µmoles/g w. wt.) than in the foot muscle (7 µmoles/g w. wt.), and it stayed virtually constant throughout the experiment (results not shown). Arginine phosphate levels fell drastically in the shell adductor during anoxia. A significant drop was also seen in the foot (Fig. 3). Concomitantly, the arginine levels rose as a mirror image (results not shown). During recovery, arginine phosphate levels rose more slowly than the energy charge value in both tissues and reached initial levels after 3 h.

The aspartate levels in both tissues were the same in control ormers and there was a significant decline in both tissues upon anoxic incubation (Fig. 4). Whereas aspartate levels were not restored in the shell adductor during recovery, the levels increased slowly, but steadily, in the foot muscle. However, after 13 h of recovery, aspartate levels still differed from pre-anoxic exposure levels.

Levels of D- and L-alanine in control animals were 3- to 4-fold higher in the shell adductor than in the foot (Fig. 5). During anoxia, both stereoisomers accumulated significantly in the foot muscle; L-alanine accumulated in the shell adductor muscle. Alanine levels in the foot muscle returned to control levels during recovery (Fig. 5), but recovery was not evident in the shell adductor muscle.

Initial succinate levels in control animals were slightly higher in the shell adductor compared to the foot (Fig.

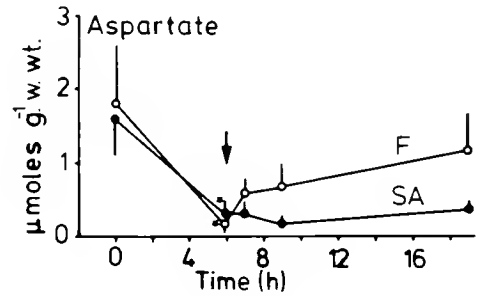

Figure 4. Time-course of the levels of aspartate in the shell adductor (SA; solid circles) and foot (F; open circles) muscle of *Haliotis lamellosa* during experimental anoxia and recovery. For further details, see Figure 2.

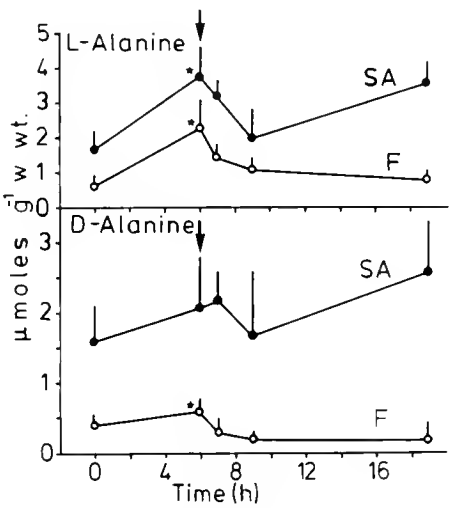

Figure 5. Time-course of the levels of L-alanine (upper panel) and D-alanine (lower panel) in the shell adductor (SA; solid circles) and foot (F; open circles) muscle of *Haliotis lamellosa* during experimental anoxia and recovery. For further details, see Figure 2.

6). Anoxic incubation resulted in a significant increase in both tissues. In the foot muscle, initial values were rapidly achieved after 1 h of recovery. In contrast, succinate levels in the shell adductor declined more slowly, and took 3 h to reach pre-anoxic levels.

Taurine levels were about twice as high in the shell adductor as in the foot of control abalones. No significant changes occurred in the foot. There was a significant decline in the shell adductor muscle during anoxia without any restoration in the recovery period (Figs. 7, 8). Substantial accumulations of tauropine were evident in the shell adductor muscle during anoxia, while a small, but significant, formation occurred in the foot muscle. In the latter tissue, the main anaerobic end product was D-lactate, which also accumulated in the adductor, but to a much lesser extent (50%) than tauropine (Figs. 7, 8). D-lactate levels were rapidly cleared to 50% of the anoxic level during the first hour of recovery in the foot. Both tauropine and D-lactate levels remained high in the shell adductor after 3 h of recovery. Even after 13 h of recovery these levels were still higher than the initial concentrations before anoxia.

No significant changes in the levels of glucose-6-phosphate (0.50 and 0.15 μmoles/g w. wt. in shell adductor and foot muscle, respectively) were observed during anoxic incubation and recovery (results not shown).

Metabolic responses to functional hypoxia

The levels of the adenylates, arginine-containing compounds, and various other metabolites in the shell adductor muscle and the foot during exercise are listed in Table II. There was no significant change in the energy charge or in the levels of arginine phosphate in either tissue. Aspartate levels were marginally, but significantly, diminished in the shell adductor, whereas a small, but significant rise in the levels of L-alanine was observed in the foot. As main glycolytic end products, levels of D-lactate (marginally) and tauropine (primarily) were elevated significantly in the shell adductor muscle, whereas the D-lactate levels were doubled in the foot without any significant rise in the tauropine levels.

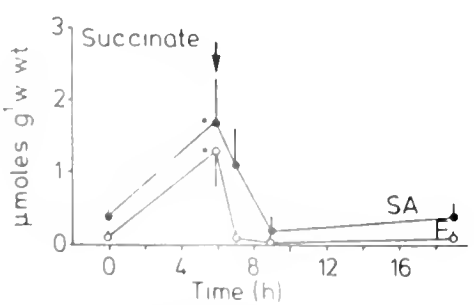

Figure 6. Time-course of the levels of succinate in the shell adductor (SA, solid circles) and foot (F; open circles) muscle of *Haliotis lamellosa* during experimental anoxia and recovery. For further details, see Figure 2.

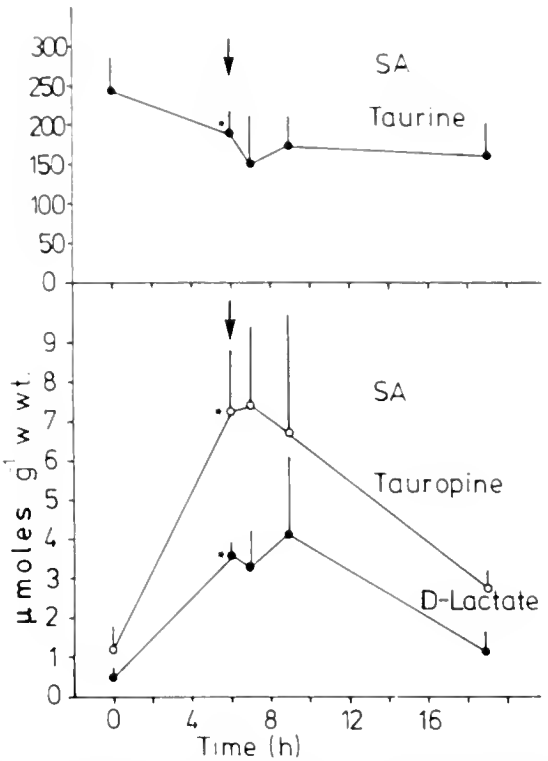

Figure 7. Time-course of the levels of taurine (upper panel) and (lower panel) D-lactate (solid circles) and tauropine (open circles) in the shell adductor muscle (SA) of *Haliotis lamellosa* during experimental anoxia and recovery. For further details, see Figure 2.

Discussion

This study in the ormer is a good example of the principle that anaerobic energy metabolism in a muscle is specifically matched to the function of the muscle. It reflects adaptation to specific metabolic need of the tissue. The two investigated tissues, the foot and the shell adductor muscle, are employed by the animal for different tasks. The foot is mainly responsible for slow gliding movements that very likely are supported by aerobic metabolism. In contrast, the shell adductor muscle pulls the ormer's shield-like shell tightly to the substratum to preclude dessication during low tide and to prevent dislodging by wave action. The shell adductor also rights an animal that has been detached from the rocks. Thus, the shell adductor muscle is metabolically more active than the foot and performs burst contractions which, in general, rely on anaerobic metabolism. However, when the whole animal has to cope with hypoxic or even anoxic conditions, both tissues need to have the capacity for maintaining metabolism anaerobically.

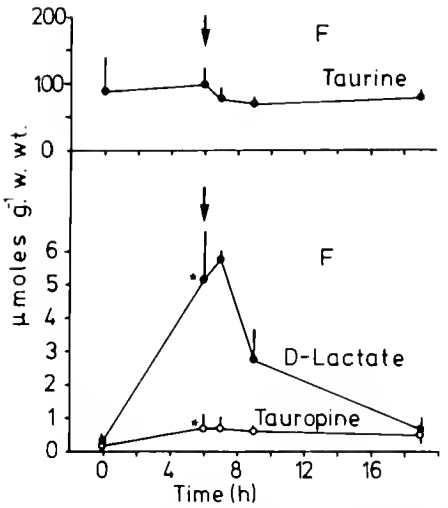

Figure 8. Time-course of the levels of taurine (upper panel) and (lower panel) D-lactate (solid circles) and tauropine (open circles) in the foot (F) of *Haliotis lamellosa* during experimental anoxia and recovery. For further details, see Figure 2.

This partitioning in function is also reflected in the metabolism of the two tissues. Compared to foot muscle, the shell adductor contains 4-fold higher levels of high-energy phosphates, ATP (and, in fact, the total adenylate pool), and arginine phosphate, suggesting a higher metabolic rate. This is confirmed when the energy demand for both tissues is calculated from the decreased levels of the phosphagens and the increased levels of glycolytic products occurring during experimental anoxia (Table III): the ATP production rate (μmoles g^{-1} wt wgt min^{-1}) for the shell adductor muscle is about twice as high as for the foot. In both tissues the bulk of the energy is provided by anaerobic glycolysis (between 70 and 80%), the remainder by the phosphagen (Table III). Again, the glycolytic flux (calculated in nmoles glycosyl units g^{-1} wt wgt min^{-1}; Table III) is also 1.5-fold higher in the shell adductor.

The main qualitative difference between the two tissues is the involvement of two different glycolytic end products in anaerobic metabolism. Whereas glycogen breakdown in foot results in the production of D-lactate, glycolysis in the shell adductor is terminated with the formation of the novel end product tauropine. Thus, the tauropine/tauropine dehydrogenase system—functionally analogous to the lactate/lactate dehydrogenase system—is active in the shell adductor muscle to maintain cytoplasmic redox balance. This pattern of end product formation in the different tissues is in agreement with the enzymatic complement of the respective tissue: lactate dehydrogenase is the predominant pyruvate reductase present in the foot; tauropine dehydrogenase is almost exclusively present in the shell adductor (Gäde, 1986).

We now ask why tauropine dehydrogenase turns up in this mollusc, and why taurine is used as a substrate for a dehydrogenase. Opine dehydrogenases which use the amino acids L-arginine, glycine, and L-alanine for the condensation reaction with pyruvate are already known (see review by Gäde and Grieshaber, 1986). Obviously, the opine dehydrogenases that have evolved are those that would make use of the most abundant amino acids in the species. The same is true for the amino acid taurine. From the amino acids used for opine production (arginine, glycine, alanine, taurine) it is the one with the highest concentration in the shell adductor muscle of the ormer (Gäde, 1986 and this study for arginine). There seems a sort of "co-evolution" of the most abundant amino acid and the corresponding opine dehydrogenase; thus, the specificity of the enzyme for the amino acid may be evolutionarily altered as a consequence of the "makeup" of the pool of amino acids in the different tissues. The mechanism of this is not understood yet, however another example is in the literature. In the polychaete worm *Aphrodite aculeata*, strombine dehydrogenase was found in pharynx muscle containing extremely high levels of glycine, whereas alanopine dehydrogenase was present in body wall musculature (Storey, 1983). Siegmund (1986; also cited in Grieshaber and Kreutzer, 1986) compared the concentrations of those amino acids involved in the action of octopin-, strombine-, and alanopine dehydrogenase from various marine invertebrates (coelenterates, molluscs, and annelids) to the amounts of octopine, strombine, and alanopine actually formed during environmental anoxia. He showed that in the species investigated the most abundant of these amino acids was used as a substrate for opine formation. This was the case for alanine/alanopine in *Littorina littoralis, L. littorea, Nucella lapillus,* and *Glycera convoluta,* and for glycine/strombine in *Halichondra panicea, Mytilus edulis, Crassostrea angulata, Pharus legumen, Solen marginatus, Ensis siligua, Lutraria lutraria, Arenicola marina, Nephtys hombergi, Pherusa plumosa,* and *Pectinaria koreni.* However, tauropine production was not analyzed, but in many of the species taurine concentrations are higher than those of the other amino acids determined. Thus, with the present small data base available—tauropine dehydrogenase has additionally only reported from muscle tissue of the brachiopod *Glottidea pyramidata* (Doumen and Ellington, 1987)—it is not possible to conclude from a high taurine concentration to the presence of tauropine dehydrogenase and/or production of tauropine.

Another question concerning *H. lamellosa* is: what is the significance of tissue-specific differences in pyruvate metabolism? We speculate that the driving force that led to the appearance of tauropine dehydrogenase in the shell adductor muscle is the requirement for burst activ-

Table II

Levels of adenylates, various [illegible] (μmoles g⁻¹ wt·wgt) and adenylate energy charge in shell adductor and foot muscle of Ha[illegible] *during exercise (15 min)*

Meta[illegible]	Shell adductor muscle		Foot muscle	
	Control (n = 7)	Exercise (n = 4)	Control (n = 7)	Exercise (n = 4)
ATP	3.25 ± 0.99*	2.65 ± 0.11	0.73 ± 0.31	1.00 ± 0.59
ADP	0.96 ± 0.20	1.02 ± 0.18	0.14 ± 0.06	0.20 ± 0.07
AMP	0.23 ± 0.16	0.14 ± 0.07	0.03 ± 0.01	0.05 ± 0.02
Sum	4.44 ± 1.23	3.81 ± 0.28	0.90 ± 0.32	1.25 ± 0.64
Energy charge	0.85 ± 0.04	0.83 ± 0.03	0.88 ± 0.03	0.86 ± 0.06
Arginine	19.63 ± 4.38	21.25 ± 4.00	3.56 ± 1.23	5.54 ± 2.46
Arginine phosphate	11.77 ± 2.92	9.88 ± 3.37	3.42 ± 1.18	4.41 ± 3.91
Sum	31.40 ± 2.31	31.13 ± 4.65	6.98 ± 2.27	9.95 ± 6.17
D-lactate	0.50 ± 0.10	0.86 ± 0.16**	0.33 ± 0.19	0.77 ± 0.15**
Tauropine	1.22 ± 0.57	5.83 ± 2.09**	0.23 ± 0.10	0.40 ± 0.26
Taurine	243.2 ± 39.50	168.90 ± 22.0**	91.6 ± 50.5	84.0 ± 23.9
L-alanine	1.72 ± 0.46	2.83 ± 1.48	0.56 ± 0.28	1.26 ± 0.57**
D-alanine	1.60 ± 0.45	1.09 ± 0.74	0.37 ± 0.18	0.18 ± 0.15
Aspartate	1.61 ± 0.47	0.60 ± 0.48**	1.77 ± 0.80	1.05 ± 0.66
Succinate	0.36 ± 0.14	0.40 ± 0.25	0.11 ± 0.03	0.10 ± 0.09

* All values given as mean ± SD.
** Significant to control.

ity creating functional anoxia during the righting movements. Such active muscle work needs a rapid activation of glycolytic energy production, which eventually leads to an increased redox status (NADH/NAD^+ ratio). Based on theoretical considerations of thermodynamic properties of opine and lactate dehydrogenases, it was proposed that the large amino acid pool used for opine production is decisive for maintaining the NADH/NAD^+ ratio lower than using the lactate pathway (see review by Fields, 1983). Most other arguments for the possible advantages of opine synthesis *versus* lactate formation (*e.g.*, lack of disturbance of internal osmolarity and less acidification) have been dismissed, as discussed recently by Grieshaber and Kreutzer (1986).

Besides glycogen and arginine phosphate breakdown, the amino acid aspartate provides energy during anoxia. The simultaneous depletion of aspartate and accumulation of succinate and alanine in both tissues indicates cofermentation of glycogen and aspartate as known to occur in other invertebrates during lack of oxygen (see, for example, Gäde, 1983a, 1987a; Kreutzer *et al.*, 1985). The observation of only very small amounts of succinate

Table III

Comparison of energy yield (μmoles ATP g⁻¹ wt·wgt), rate of energy consumption (μmoles ATP g⁻¹ wt·wgt min⁻¹), and glycolytic flux (nmoles glycosyl units g⁻¹ wt·wgt min⁻¹) in shell adductor and foot muscle of Haliotis lamellosa *during experimental anoxia and exercise**

	ATP equivalents (μmoles g⁻¹ wt wgt) from		Rate of consumption of ATP (μmoles g⁻¹ wt·wgt min⁻¹)	Glycolytic flux (nmoles glycosyl unit g⁻¹ wt·wgt min⁻¹)
	Glycolysis**	Phosphagen		
Six-hour experiment				
shell adductor	18.9 (70%)***	8.2	0.08	16.3
foot	12.2 (79%)	3.2	0.04	10.2
Exercise				
shell adductor	[illegible] (81%)	2.2	0.77	206
foot	[illegible] (100%)	—	0.10	22.7

* For calculations see Meinardus-Hager and Gäde, 1987.
** The small increase of succinate was assumed to derive by aspartate breakdown and is included in this calculation.
*** Contribution of glycolysis as percentage of total equivalents of ATP is given in brackets.

formed in both tissues of the ormer during anoxia and no production of propionate makes it highly unlikely that succinate is derived from glycogen by the so-called phosphoenolpyruvate carboxykinase route. This pathway is apparently only operative in "good anaerobes" tolerating prolonged hours of anoxia (see Introduction). The lack of propionate (and acetate) formation in the ormer is then indicative that this species can tolerate anoxic conditions for only a fraction of the time compared to species such as certain blue mussels, oysters, and many annelids. Indeed, preliminary experiments with specimens of *H. lamellosa* showed that these animals were unable to survive experimental anoxia longer than eight hours.

Recovery in both muscles of *H. lamellosa* was quite similar. Levels of the high-energy phosphates and succinate were rapidly restored, but asparate levels increased slowly (and only) in the foot. Similar changes have been reported during recovery in the foot of the cockles, *Cardium edule* (Gäde and Meinardus, 1981) and *C. tuberculatum* (Meinardus-Hager and Gäde, 1987), and the adductor muscle of the file shell, *Lima hians* (Gäde, 1983b).

Levels of the respective glycolytic end products in the tissues of the ormer, D-lactate and tauropine, were not cleared during the first h (foot) or 3 h (shell adductor) of recovery, but also did not significantly increase during this time period. Thus, it is highly unlikely that an anaerobic initial phase of recovery occurs as observed in tissues of the bivalves *Mytilus edulis* (de Zwaan *et al.*, 1983), *M. squamosus* (Nicchitta and Ellington, 1983), and *Crassostrea gigas* (Eberlee *et al.*, 1983).

The power output during exercise in the ormer is low relative to the jet propulsion of cephalopods and scallops or the jumps of the cockle, *C. tuberculatum*. The present study shows that energy demand increases for both muscles in comparison to experimental anoxia: about 10-fold for the shell adductor and about 2-fold in the foot (Table III). Since the energy is mainly or exclusively (foot) derived from glycolysis, the same increases are calculated for the glycolytic fluxes (Table III). These increases are small when compared to *C. tuberculatum*, where during jumping the glycolytic rate is enhanced 100-fold above the resting rate (Gäde and Meinardus-Hager, 1986). The calculations in Table III also show that the shell adductor muscle is particularly involved in exercise of the ormer; its rate of energy consumption and its glycolytic flux are about 8- to 9-fold higher than those of the foot. The bulk of the energy during exercise came from glycolytic tauropine formation in the shell adductor muscle, although there was also some D-lactate production. Thus, anaerobic breakdown of glycogen to tauropine also supports exercise metabolism, as it did metabolism during experimental anoxia.

The formation, during both experimental and functional anoxia, of both glycolytic end products—tauropine and D-lactate—in the shell adductor muscle may be explained by theoretical considerations of the equilibrium constants of the respective reactions. Since the degree of product formation is determined by the equilibrium constant (K_{eq}) of a reaction, we measured the K_{eq} constants for the reactions catalysed by tauropine (TDH) and D-lactate dehydrogenase (D-LDH). These were $K_{eq}(TDH) = ([pyruvate] \times [taurine] \times [NADH] \times [H^+]) \times ([tauropine] \times [NAD^+])^{-1} = 7.15 \times 10^{-13}$ *M* (Gäde, 1986) and K_{eq}(D-LDH) = $([pyruvate] \times [NADH] \times [H^+]) \times ([D\text{-lactate}] \times [NAD^+])^{-1} = 1.3 \times 10^{-12}$ (Gäde and Meinardus-Hager, 1986).

We can use these values to assess whether this theoretical equilibrium is reached *in vivo* by both enzymes. The actual equilibrium is given by the mass action ratio, *e.g.*, $MAR_{LDH} = ([pyruvate] \times [NADH] \times [H^+]) \times ([D\text{-lactate}] \times [NAD^+])^{-1}$ and $MAR_{TDH} = ([pyruvate] \times [taurine] \times [NADH] \times [H^+]) \times ([tauropine] \times [NAD^+])^{-1}$.

These ratios, however, were not calculated because data for neither the internal proton concentration, nor the $NAD^+/NADH$ ratio, are available for the shell adductor muscle. However, assuming that the reaction catalysed by LDH is at or near equilibrium in most biological systems, we can obtain indirect information on the equilibrium situation of the TDH reaction using the K_{eq} values (see above). The ratio $K_{eq}(TDH)/K_{eq}$(D-LDH) has the value of 0.55 *M* and corresponds to the quotient $([D\text{-lactate}] \times [taurine]) \times ([tauropine])^{-1}$, since TDH and LDH share common substrates such as pyruvate, NADH, H^+, and NAD^+ (see above). Thus, if we use the concentrations of D-lactate, taurine, and tauropine measured in the shell adductor, the calculated ratio should be close to the theoretical value, 550 m*M*, if *both* reactions are near equilibrium (our assumption).

Table IV shows that the reactions are not exactly at the theoretical equilibrium, but the "close equilibrium" of neither reaction changed much during anoxia and subsequent recovery. Thus, the formation of primarily tauropine and a little D-lactate is according to the equilibrium constants of the reactions. In contrast, after exercise the quotient was 10-fold lower than the theoretical value indicating that the reactions of D-LDH and/or TDH are in "disequilibrium." Our data do not indicate which reaction that is, but a recent paper on a similar phenomenon in foot muscle of *C. tuberculatum* argues for a "disequilibrium" of D-LDH because of its low activity and the enhanced production of pyruvate and NADH due to the increased glycolytic flux (see details in Gäde and Meinardus-Hager, 1986; pages 197 and 198). The same arguments can be applied to the ormer during exercise: D-LDH activity in the shell adductor is much lower than TDH activity and glycolytic flux is enhanced.

Table IV

Calculation of the quotient $\frac{[\text{taurine}]}{[\text{alanopine}]}$ *for shell adductor muscle of* Haliotis lamellosa *during experimental anoxia, recovery, and exercise**

	Control	6-h anoxia	1-h recovery	3-h recovery	13-h recovery	Exercise
Quotient (mM	199	190	133	217	133	50

* Tissue concentrations calculated from data presented in Table II and Figures 7 and 8 under the assumption that the water content of the tissues is 50%.

In conclusion, the energy metabolism in both the shell adductor and foot muscle is powered by co-fermentation of glycogen and aspartate and transphosphorylation during experimental anoxia. According to differences in tissue activities, as well as thermodynamic properties of the two pyruvate reductases (TDH, LDH), tauropine is the preferred end product in the shell adductor, while D-lactate accumulation occurs in the foot. Recovery in well-aerated seawater reverses most of the metabolic changes seen during anoxia, but the time courses for high-energy phosphates (fast) and glycolytic end products (slow) are quite different, as in other molluscs. Enhanced glycolysis and maintenance of redox balance by the reaction of tauropine dehydrogenase are the main features of exercise in the shell adductor, and the foot is only minimally involved during this behavior.

Acknowledgments

The author thanks Dr. Georg Meinardus-Hager for help with the experiments, Dr. W. Ross Ellington (The Florida State University, Tallahassee) for commenting on and correcting the manuscript, and the staff of the Stazione Zoologica di Napoli for their hospitality. Financial support was provided in part by grants from the Deutsche Forschungsgemeinschaft (Ga 241/4-3 and Gr 456/12-1) and by a Heisenberg Fellowship awarded from the Deutsche Forschungsgemeinschaft (Ga 241/5-2).

Literature Cited

Bergmeyer, H. U., E. Bernt, H. Möllering, and G. Pfleiderer. 1974. L-Aspartat und L-Asparagin. Pp. 1741–1745 in *Methoden der Enzymatischen Analyse*, Vol. 2, H. U. Bergmeyer, ed. Verlag Chemie, Weinheim.

Carlsson, K.-H., and G. Gade. 1985. Isolation and characterisation of tissue-specific isoenzymes of D-lactate dehydrogenase from muscle and hepatopancreas of *Limulus polyphemus*. *J. Comp. Physiol.* **B155:** 723–731.

Carlsson, K.-H., and G. Gade. 1986. Metabolic adaptation of the horseshoe crab, *Limulus polyphemus*, during exercise and environmental hypoxia and subsequent recovery. *Biol. Bull.* **171:** 217–235.

Doumen, C., and W. R. Ellington. 1987. Isolation and characterization of a taurine-specific opine dehydrogenase from the pedicles of the brachiopod, *Glottidea pyramidata*. *J. Exp. Zool.* **243:** 25–31.

Eberlee, J. C., J. M. Storey, and K. B. Storey. 1983. Anaerobiosis, recovery from anoxia and the role of strombine and alanopine in the oyster, *Crassostrea virginica*. *Can. J. Zool.* **61:** 2682–2689.

Ellington, W. R. 1983. The recovery from anaerobic energy metabolism in invertebrates. *J. Exp. Zool.* **228:** 431–444.

Fields, J. H. A. 1983. Alternatives to lactic acid: possible advantages. *J. Exp. Zool.* **228:** 445–457.

Gäde, G. 1980. Biological role of octopine formation in marine molluscs. *Mar. Biol. Lett.* **1:** 121–135.

Gäde, G. 1983a. Energy metabolism of arthropods and mollusks during environmental and functional anaerobiosis. *J. Exp. Zool.* **228:** 415–429.

Gäde, G. 1983b. Energy production during anoxia and recovery in the adductor muscle of the file shell, *Lima hians*. *Comp. Biochem. Physiol.* **76B:** 73–77.

Gäde, G. 1985a. Arginine and arginine phosphate. Pp. 424–431 in *Methods of Enzymatic Analysis*, Vol. VIII, H. U. Bergmeyer, ed. Verlag Chemie, Weinheim.

Gäde, G. 1985b. Octopine. Pp. 419–423 in *Methods of Enzymatic Analysis*, Vol. VIII, H. U. Bergmeyer, ed. Verlag Chemie, Weinheim.

Gäde, G. 1986. Purification and properties of tauropine dehydrogenase from the shell adductor muscle of the ormer, *Haliotis lamellosa*. *Eur. J. Biochem.* **160:** 311–318.

Gäde, G. 1987a. Leben ohne Sauerstoff: Die Rolle der anaeroben Glykolyse bei aquatischen wirbellosen Tieren. *Verh. Dtsch. Zool. Ges.* **80:** 93–110.

Gäde, G. 1987b. A specific enzymatic method for the determination of taurine. *Biol. Chem. Hoppe-Seyler* **368:** 1519–1523.

Gäde, G., and K.-H., Carlsson. 1984. Purification and characterisation of octopine dehydrogenase from the marine nemertean *Cerebratulus lacteus* (Anopla; Heteronemertea): comparison with scallop octopine dehydrogenase. *Mar. Biol.* **79:** 39–45.

Gäde, G., and M. K. Grieshaber. 1986. Pyruvate reductases catalyze the formation of lactate and opines in anaerobic invertebrates. *Comp. Biochem. Physiol.* **83B:** 255–272.

Gäde, G., and G. Meinardus. 1981. Anaerobic metabolism in the common cockle *Cardium edule*. V. Changes in the levels of metabolites in the foot during aerobic recovery after anoxia. *Mar. Biol.* **65:** 113–116.

Gäde, G., and G. Meinardus-Hager. 1986. Anaerobic energy metabolism in Crustacea, Xiphosura and Mollusca: lactate fermentation versus multiple fermentation products. *Zool. Beitr. N. F.* **30:** 187–203.

Gäde, G., E. Weeda, and P. A. Gabbott. 1978. Changes in the level of octopine during the escape responses of the scallop *Pecten maximus* L. *J. Comp. Physiol.* **124:** 121–127.

Gawehn, K., and H. U. Bergmeyer. 1974. D-Laktat. Pp. 1538–1541 in *Methoden der Enzymatischen Analyse*, Vol. 2, H. U. Bergmeyer, ed. Verlag Chemie, Weinheim.

Graßl, M. 1974a. L-Alanin. Pp. 1727–1730 in *Methoden der Enzy-*

matischen Analyse, Vol. 2, H. U. Bergmeyer, ed. Verlag Chemie, Weinheim.

Graßl, M. 1974b. D-Alanin. Pp. 1731–1734 in *Methoden der Enzymatischen Analyse,* Vol. 2, H. U. Bergmeyer, ed. Verlag Chemie, Weinheim.

Grieshaber, M. K., and U. Kreutzer. 1986. Opine formation in marine invertebrates. *Zool. Beitr. N. F.* **30:** 205–229.

Jaworeck, D., W. Gruber, and H. U. Bergmeyer. 1974. Adenosin-5'-diphosphat und Adenosin-5'-monophosphat. Pp. 2179–2181 in *Methoden der Enzymatischen Analyse,* Vol. 2, H. U. Bergmeyer, ed. Verlag Chemie, Weinheim.

Kreutzer, U., B. Siegmund, and M. K. Grieshaber. 1985. Role of coupled substrates and alternative end products during hypoxia tolerance in marine invertebrates. *Mol. Physiol.* **8:** 371–392.

Kuriyama, M. 1961. Ninhydrin reactive substances in marine algae—III. On the chemical structure of "unknown A" isolated from red algae. *Bull. Jpn. Soc. Sci. Fish.* **27:** 699–702.

Lamprecht, W., and I. Trautschold. 1974. ATP. Bestimmung mit Hexokinase und Glucose-6-phosphat-Dehydrogenase. Pp. 2151–2159 in *Methoden der Enzymatischen Analyse,* Vol. 2, H. U. Bergmeyer, ed. Verlag Chemie, Weinheim.

Livingstone, D. R. 1982. Energy production in the muscle tissue of different kinds of molluscs. Pp. 257–274 in *Exogenous and Endogenous Influences on Metabolic and Neural Control,* Vol. 1, A. D. F. Addink and N. Spronk, eds. Pergamon Press, Oxford.

Meinardus-Hager, G., and G. Gäde. 1987. Recovery from environmental anaerobiosis and muscular work in the cockle, *Cardium tuberculatum:* oxygen debt and metabolic responses. *J Exp. Zool.* **242:** 291–301.

Nicchitta, C. V., and W. R. Ellington. 1983. Energy metabolism during air exposure and recovery in the high intertidal bivalve mollusc *Geukensia demissa granosissima* and the subtidal bivalve molluscs *Modiolus squamosus. Biol. Bull.* **165:** 708–722.

Sato, M., and G. Gäde. 1986. Rhodoic acid dehydrogenase: a novel amino acid-linked dehydrogenase from muscle tissue of *Haliotis* species. *Naturwissenschaften* **73:** 207–209.

Sato, M., N. Kanno, and Y. Sato. 1985. Isolation of D-rhodoic acid from the abalone muscle. *Bull. Jpn. Soc. Sci. Fish.* **51:** 1681–1683.

Schöttler, U. 1980. Der Energiestoffwechsel bei biotopbedingter Anaerobiose: Untersuchungen an Anneliden. *Verh. Dtsch. Zool. Ges.* **73:** 228–240.

Siegmund, B. 1986. Funktionsbedingte und biotopbedingte Hypoxien: Zur Bedeutung der Opine im anaeroben Energiestoffwechsel. Ph. D. Thesis, Universität Düsseldorf.

Storey, K. B. 1983. Tissue-specific alanopine dehydrogenase and strombine dehydrogenase from the sea mouse, *Aphrodite aculeata* (Polychaeta). *J. Exp. Zool.* **225:** 369–378.

Storey, K. B. 1985. A re-evaluation of the Pasteur effect: New mechanisms in anaerobic metabolism. *Mol. Physiol.* **8:** 439–461.

Williamson, J. R. 1974. Succinat. Pp. 1661–1666 in *Methoden der Enzymatischen Analyse,* Vol. 2, H. U. Bergmeyer, ed. Verlag Chemie, Weinheim.

de Zwaan, A. 1977. Anaerobic energy metabolism in bivalve molluscs. *Oceanogr. Mar. Biol.* **15:** 103–187.

de Zwaan, A., and G. van den Thillart. 1985. Low and high power output modes of anaerobic metabolism: Invertebrate and vertebrate strategies. In *Circulation, Respiration, and Metabolism,* R. Gilles, ed. Springer-Verlag, Berlin, Heidelberg.

de Zwaan, A., A. M. T. de Bont, W. Zurburg, B. L. Bayne, and D. R. Livingstone. 1983. On the role of strombine formation in the energy metabolism of adductor muscle of a sessile bivalve. *J. Comp. Physiol.* **149:** 557–563.

Reference: *Biol Bull* 175: 132–136 (August, 1988)

Control of Cnida Discharge: II. Microbasic p-Mastigophore Nematocysts are Regulated by Two Classes of Chemoreceptors

GAIL E. MUIR GIEBEL, GLYNE U. THORINGTON, RENEE Y. LIM, AND DAVID A. HESSINGER[1]

Department of Physiology and Pharmacology, School of Medicine, Loma Linda University, Loma Linda, California 92350

Abstract. Using tentacles of the sea anemone, *Aiptasia pallida,* Thorington and Hessinger (1984, 1988a, b) recently identified two classes of chemoreceptors involved in sensitizing cnidocytes to discharge cnidae in response to mechanical stimuli. Discharge of cnidae was quantified by measuring adhesive force between the tentacles and a test object. This measurement is assumed to reflect the contribution of the three types of cnidae present in the tentacles of *A. pallida:* the adherent spirocysts and two types of penetrant nematocysts, the predominant microbasic p-mastigophores and the basotrichous isorhizas. In the present paper we directly measure the discharge of the microbasic p-mastigophores and show that mastigophore-containing cnidocytes are sensitized by representative agonists for these two classes of chemoreceptors. We also show that under certain conditions the number of discharged microbasic p-mastigophores correlates linearly to a major component of the measured adhesive force. This enables us to calculate the contribution to adhesive force made by individual mastigophores.

Introduction

Nearly one hundred years ago, Nagel (1892) suggested that chemicals derived from prey elicit feeding in cnidarians. Recently, two groups of prey-derived chemicals, including N-acetylated sugars and a variety of amino compounds, were identified as being involved in prey capture. In the tentacles of the sea anemone *Aiptasia pallida,* these chemicals act via at least two classes of chemoreceptors to increase the sensitivity of cnidocytes to mechanical stimuli that trigger the discharge of cnidae (Thorington and Hessinger, 1984, 1988a, b). Using mucin-labelled colloidal gold, the receptors for the N-acetylated sugars have been located on the surface of supporting cells adjacent to cnidocytes in the tentacles of the sea anemone, *Haliplanella luciae* (Watson and Hessinger, 1988a, b). As previously discussed (Thorington and Hessinger, 1988a), our working model of the role of cnidocyte-sensitizing chemoreceptors places the N-acetylated sugars as the initial sensitizers that are detected as macromolecular conjugates on the surfaces of prey as mucins, glycoproteins, and chitin. The amino sensitizers, on the other hand, are secondary sensitizers that leak from prey that have been punctured by penetrant nematocysts responding to the conjugated N-acetylated sugars.

The two classes of cnidocyte-sensitizing chemoreceptors were identified in *A. pallida* by measuring cnida-mediated adhesion of tentacles to test probes following appropriate chemical and mechanical stimulation of cnidocytes (Thorington and Hessinger, 1984, 1988a, b). Since adhesive force represents the force required to separate a tentacle from the test probe (Thorington and Hessinger, 1988a), it is an aggregate measure of contributions from all three types of discharging cnidae present in these tentacles. In this paper we show that the majority of the adhesive force is due to the discharge of the microbasic p-mastigophore nematocysts. The cnidocytes housing these nematocysts are chemosensitized to discharge the nematocysts in a dose-dependent manner by the agonists glycine, which represents the amino sensitizing agents, and N-acetylneuraminic acid (NANA),

Received 16 February 1988; accepted 31 May 1988.

[1] To whom all correspondence should be addressed

which represents N-acetylated sugar agents. These findings validate the underlying assumptions of adhesive force measurements; specifically, that the measured adhesive force is mediated by discharged cnidae, and that the magnitude of adhesive force is proportional to the number of cnidae discharged. From these data we calculate the contribution of individual microbasic p-mastigophores to adhesive force.

Materials and Methods

Maintenance of sea anemones

Sea anemones (*A. pallida,* Miami strain) were cloned in glass trays containing natural seawater and fed daily with *Artemia* nauplii (Hessinger and Hessinger, 1981). Forty animals of similar size were selected and placed in separate finger bowls, which were cleaned daily. These anemones were maintained on a 12/12 h photoperiod using white fluorescent lights at an intensity of 5.5 klux (66 $\mu Es^{-1}\ m^{-2}$) and ambient temperatures of 24 ± 1°C. Animals were starved for 72 h prior to experiments.

Experimental animals and test solutions

Natural seawater was from the Kerckoff Marine Laboratory of Caltech at Corona del Mar, California. Experimental conditions and test solutions were essentially as previously reported (Thorington and Hessinger, 1988a). Glycine and N-acetylneuraminic acid (NANA), each representing the amino and the N-acetylated sugar sensitizers, respectively, were tested at specified concentrations in natural, filtered (Whatman type 1) seawater adjusted to pH 7.65 with 1 *N* HCl or NaOH. The seawater in the finger bowls was replaced with solutions containing specified concentrations of one of these agents. The anemones were allowed to adapt for 10 min before cnidocyte responsiveness was measured.

Assays of cnidocyte responsiveness

Cnidocyte responsiveness to combined chemical and tactile stimulation was determined both by measuring adhesive force and by microscopically counting discharged mastigophores that had adhered to the test probes used to measure adhesive force.

Measurements of adhesive force. Adhesive force was measured using test probes consisting of insect pins with nylon heads (0.8 ± 0.01 mm diameter) (Thorington and Hessinger, 1988a). The pin heads were coated with ~0.06 mm of 30% (w/v) gelatin, stored at 4°C in a humidified container, and used within 24 h. To measure adhesive force, the test probes were attached to a force transducer (Model FT-03, Grass Instruments) and a strip-chart recorder (Thorington and Hessinger, 1988b). The transducer was calibrated with gravitometric weights, and adhesive force measurements were expressed in hybrid units of mg-force (mgf). Each bowl, containing a single sea anemone in the test solution of sensitizer in seawater, was raised by hand until the test probe contacted the tentacle just behind its tip. After contact the bowl was lowered slowly until the tentacle and the coated pinhead separated. The force necessary to separate the probe from the tentacle was recorded.

Counting discharged mastigophores. After probes had been used to measure adhesive force they were processed as follows so that the mastigophores adhering to them could be counted. The gelatin-coated ends of probes were placed in individual microtiter wells (Microtest 11, Falcon Plastics) containing 40 μl of an enzyme and detergent solution (1% Trizyme, Amway Products). The solution was prepared in distilled water, clarified by centrifugation at 2000 × *g* for 30 min, and then frozen in 1.5 ml aliquots until used. Probes were incubated in Trizyme for 4 h at room temperature to hydrolyze the gelatin and to release from the probe the mastigophores and other types of cnida, each of which is protease-resistant (Blanquet and Lenhoff, 1966). Probes were then removed and mastigophores remaining in each well enumerated using an inverted light microscope at 200×.

Collection and analysis of data

Separate animals were tested at each concentration of sensitizer. Five to ten probes (one per tentacle) were used on each animal to determine both adhesive force and the number of discharged mastigophores. Daily experimental means were calculated from these measurements. Replicate experiments for both glycine and NANA were performed on four different days. Each data point expressed in the figures represents the mean of the daily experimental means (n = 4). Range bars indicate the standard error of the mean. Linear regression analysis and determination of maximum response (E_{max}) and of sensitizer concentrations that produce a half-maximum response ($K_{0.5}$) were performed with the aid of a computer-assisted graphics and data-formatting program (Dorgan and Hessinger, 1984).

Results

Glycine as a representative amino sensitizer

The dose-response curves for glycine showing the mean adhesive force (Fig. 1, triangles) and the mean number of discharged mastigophores (Fig. 1, circles) are each biphasic. These dose-response curves coincide somewhat; each has a broad area of sensitization at lower concentrations of glycine, a maximum effect (E_{max}) at about 10^{-6} *M* glycine, and a broad region of apparent desensitization at still higher concentrations. Three

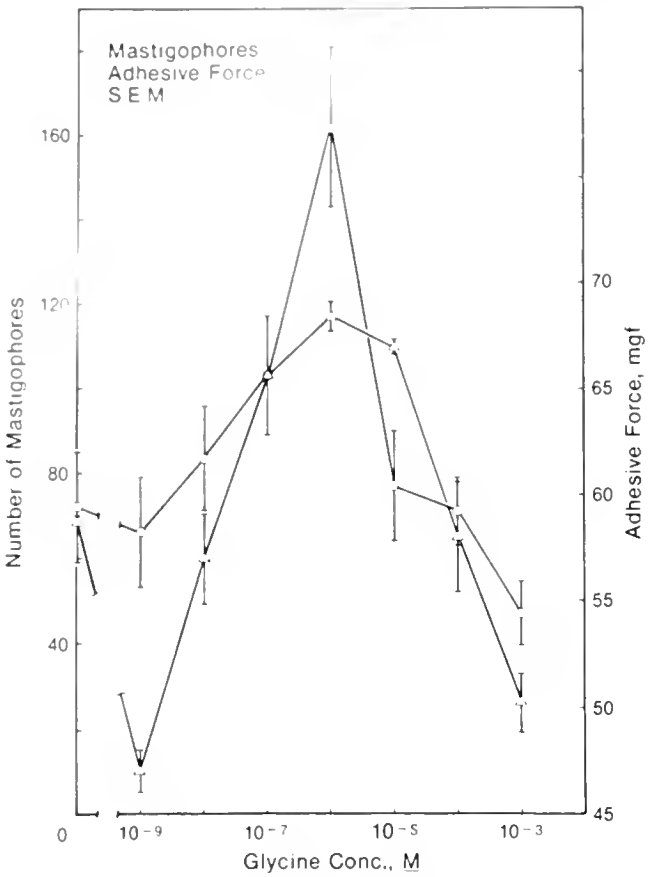

Figure 1. The effects of glycine on adhesive force (mgf) and on the number of discharged mastigophores adhering to test probes. Values for adhesive force (triangles) and for the number of discharged mastigophores (circles) are expressed as means of the daily means of separate measurements with vertical bars representing standard errors.

differences are apparent. First, the measurement of adhesive force initially decreases at 10^{-9} *M* glycine before increasing to the maximum effect, while the number of discharged mastigophores shows no such decrease at 10^{-9} *M*. Second, the magnitude of the maximum increase in adhesive force at E_{max} *versus* naive controls is by 15%, whereas the magnitude of the maximum increase in discharged mastigophores is by more than 100% (Fig. 1). Third, the concentrations of glycine which yield the half-maximum effect (*i.e.*, $K_{0.5}$) are somewhat different for adhesive force measurements at 5.0×10^{-8} *M* than for the number of discharged mastigophores at 1.6×10^{-7} *M*.

NANA as a representative N-acetylated sugar sensitizer

The effects of different concentrations of NANA on mean adhesive force (Fig. 2, triangles) and on the mean number of discharged mastigophores (Fig. 2, circles) are also biphasic and essentially coincidental. Each dose-response curve has regions of sensitization at low concentrations of NANA, E_{max} values occurring at 10^{-5} *M* NANA, and regions of apparent desensitization at still higher concentrations. On the other hand, the magnitude of the increase of adhesive force is by 25%, whereas the magnitude of the increase in the number of discharged mastigophores is by nearly 200%. In addition, the concentration to give the half-E_{max} (*i.e.*, the $K_{0.5}$ value) for adhesive force at 3.2×10^{-7} *M* is about four times as much as that for the discharged mastigophores at 7.8×10^{-8} *M*.

Proportionality of nematocysts discharged to adhesive force

The number of discharged mastigophores is directly proportional to the measured adhesive force for sensitizing doses of agonists up to 10^{-6} *M* glycine and 10^{-5} *M* NANA (Fig. 3). The calculated line for these data, when extrapolated, intercepts the abscissa to the right of the origin. This indicates that the measured adhesive force consists of at least two components, one that is independent of mastigophores and one that is dependent upon mastigophores. Thus, under these experimentally controlled conditions tentacles exhibit an adhesiveness of

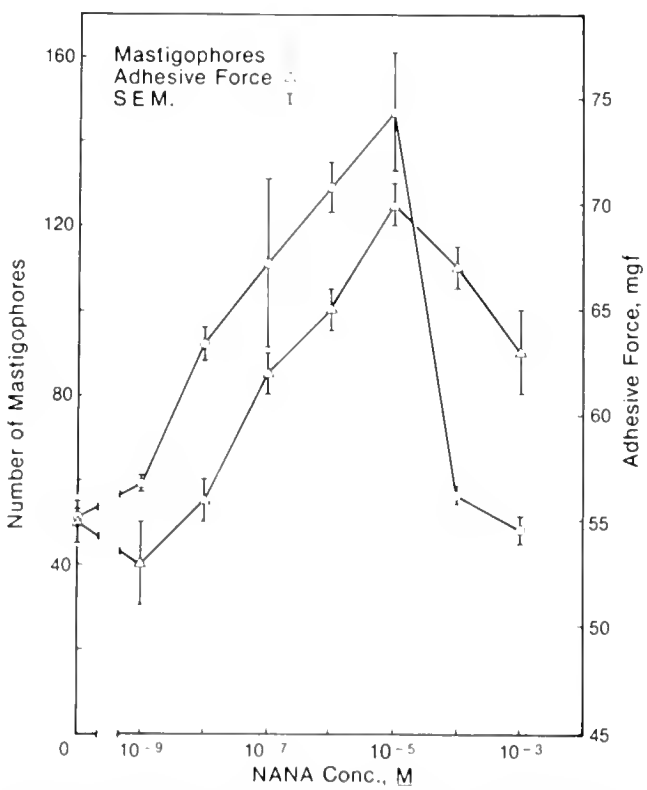

Figure 2. The effects of N-acetylneuraminic acid (NANA) on adhesive force (mgf) and on the number of discharged mastigophores adhering to test probes. Data expressed as in Figure 1.

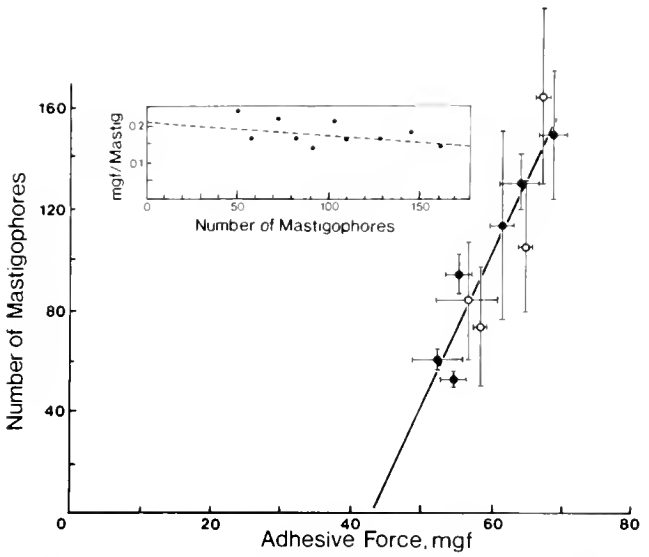

Figure 3. Correlation of discharged mastigophores to measured adhesive force (mgf). Horizontal and vertical bars represent standard errors of the mean (95% confidence limits) for adhesive force and for the number of discharged mastigophores, respectively. Plotted values represent all data measured at sensitizing concentrations of glycine (empty circles) and NANA (filled in circles) from Figures 1 and 2 ($R = 0.92$). Insert: data points obtained by subtracting 43.3 mgf from each mean measurement of adhesive force and dividing by the number of discharged mastigophores and then plotting these values as a function of the number of mastigophores discharged. Ordinate-intercept of calculated line (dashed line) is 0.217 ± 0.028 mgf.

approximately 43.3 mgf that is unrelated to the discharge of mastigophores (Fig. 3). This mastigophore-independent component of adhesiveness can be subtracted from each mean measurement of adhesive force. The resulting value can be expressed as the mean, corrected adhesive force per mastigophore. We find that the contribution of each mastigophore to the adhesive force measurement is slightly dependent on the number of mastigophores discharged (Fig. 3, insert). On the other hand, at desensitizing doses of sensitizers the number of discharged mastigophores does not correlate with measured adhesive force (data not shown).

Discussion

Discharge of mastigophores is influenced by two chemoreceptor classes

The adhesion of tentacles to test objects has been used by researchers to detect *in situ* cnida discharge (Williams, 1968; Lubbock, 1979). More recently, using a novel and sensitive technique to quantify adhesion, Thorington and Hessinger (1984, 1988a, b) identified two classes of chemoreceptors that sensitize cnidocytes to discharge cnidae in response to mechanical stimuli.

There are possible limitations, however, associated with using adhesive force to study responsiveness of cnidocytes. One such possible limitation is that measured adhesive force is an aggregate indicator of the discharge of several types of cnidae and, therefore, cannot distinguish between the different types of responding cnidocytes. In the present paper we have shown that a specific type of cnidocyte—those bearing the predominant nematocyst in the tentacles of *A. pallida,* the microbasic p-mastigophore—respond in a biphasic, dose-dependent manner to the chemosensitizers glycine and NANA (Figs. 1, 2, circles). Similar dose-response curves are obtained by measuring adhesive force under identical conditions (Figs. 1, 2, triangles; Thorington and Hessinger, 1988a). Thus, we conclude that the discharge of mastigophores in this anemone is influenced by the two classes of sensitizing chemoreceptors that detect N-acetylated sugars and a variety of amino compounds, including glycine.

Williams (1968), using the sea anemone *Haliplanella luciae,* concluded that the discharge of spirocysts, an adherent and non-penetrating type of cnida, but not that of mastigophores, was sensitized by food extracts. In contrast, using *A. pallida,* we find that the discharge of mastigophores is sensitized by optimum concentrations of both glycine and NANA (Figs. 1, 2, circles), each likely to be constituents of their natural diet. Similar findings for the effects of NANA on the discharge of mastigophores of *H. luciae* have been found by Watson and Hessinger (in press).

In sea anemones the cnidome of the tentacle consists of the adherent spirocysts and the penetrant nematocysts. In acontiate sea anemones such as *A. pallida* and *H. luciae,* the cnidome of the tentacles is made up of spirocysts, microbasic p-mastigophores, and basitrichous isorhizas (Hand, 1955). Of these three types of cnidae the basitrichous isorhizas comprise a comparatively small portion of the total cnidae in the tentacles of *A. pallida* (Giebel, unpub. obs.) and *H. luciae* (Watson and Mariscal, 1983) and are likely to contribute relatively little to the adhesive force measurements.

Dose responses for nematocyst discharge and adhesive force compared

The major difference between the dose-response curves for adhesive force and for the number of discharged mastigophores (Figs. 1, 2) is a proportionally greater increase in the number of discharged mastigophores at E_{max} values than in adhesive force. For example, the maximum increase in number of discharged mastigophores is 100% and 200% for glycine and NANA, respectively, as compared to only 15% and 25% increases in adhesive force, respectively. These differences in max-

imum effects are not surprising since adhesive force is a composite measure of several contributing factors, including cnida-mediated and non-cnida-mediated (*i.e.*, "stickiness") factors of which the discharged mastigophores is only one.

Contribution of various tentacle factors to adhesive force

The data in this paper show that within the range of sensitizing doses of glycine and NANA, the measurements of adhesive force correlate linearly with the number of discharged mastigophores (Fig. 3). By extrapolating this plot to the abscissa we estimate the adhesive force expected in the absence of discharged mastigophores to be approximately 43 mgf (Fig. 3). Therefore, contributions to adhesive force up to 43 mgf are independent of mastigophores and due to, most probably, a combination of factors, including discharged spirocysts and any inherent "stickiness" of the surface mucus. Recently we obtained measurements for the mucus. The mucus on the tentacle surface contributes approximately 30 mgf to the measure of tentacle adhesive force (Thorington and Hessinger, in prep.) in the absence of cnida discharge.

The difference between 43 mgf (due to surface mucus plus discharged spirocysts) and 30 mgf (due to surface mucus alone) is approximately 13 mgf, possibly accounted for by the sum of all discharged spirocysts. However, this is not to say that the contribution of spirocysts is constant at different concentrations of sensitizer. At sensitizing doses of glycine and NANA, contributory increments in excess of 43 mgf are due to discharged mastigophores. From the slope of the linear correlation between the number of discharged nematocysts and the measured adhesive force we calculate that the contribution of each discharged mastigophore to adhesive force is approximately 0.17 mgf. A comparable value, which is somewhat dependent upon the number of discharged mastigophores, is obtained as the ordinate intercept of a plot when 43 mgf is subtracted from the adhesive force measurements and then plotted as mgf/mastigophore *versus* the number of discharged mastigophores (Fig. 3, insert). The slight dependence of the calculated adhesive force per mastigophore upon the number of discharged mastigophores (Fig. 3, insert) is possibly due to a softening effect of discharged mastigophores on the gelatin coating of the probe.

The correlation between number of discharged mastigophores and adhesive force occurs only at stimulatory doses of the tested sensitizing agents. At higher than optimum doses of sensitizer the measurement of adhesive force does not correlate very well with the number of adhering nematocysts, possibly indicating that dramatic changes in other contributions to adhesive force, such as from discharged spirocysts, may also occur.

Conclusions

In summary, we have shown that the discharge of microbasic p-mastigophore nematocysts is under the controlling influence of at least two classes of chemoreceptor systems, one that is responsive to amino compounds as represented by glycine, and another that is responsive to N-acetylated sugars as represented by NANA. Furthermore, the majority of the increase in adhesive force in response to these chemosensitizers is due to the discharge of the microbasic p-mastigophores. In addition, we have shown that under defined conditions the number of discharged nematocysts is proportional to the measured adhesive force. Thus, measurements of adhesive force can be used to quantify the extent of total cnidae discharged.

Acknowledgments

We thank Drs. G. Watson, P. McMillan, and C. Clausen for their valuable advice in relation to this project. Funded in part by BRSG grant RR 05352-24 and NSF grant DCB-8609859 to D.A.H.

Literature Cited

Blanquet, R., and H. M. Lenhoff. 1966. A disulfide-linked collagenous protein of nematocysts capsules. *Science* **154:** 152–153.

Dorgan, L., and D. A. Hessinger. 1984. GRAFPAC, a graphics and format package for the Apple II and (IIe) computer. Copyright 1984.

Hand, C. 1955. The sea anemones of central California part III. The acontiarian anemones. *Wasmann J. Biol.* **13:** 189–202.

Hessinger, D. A., and J. A. Hessinger. 1981. Methods for rearing sea anemones in the laboratory. Pp. 153–179 in *Marine Invertebrates.* Committee on Marine Invertebrates, National Academy Press, Washington, D. C.

Lubbock, R. 1979. Chemical recognition and nematocyte excitation in a sea anemone. *J. Exp. Biol.* **83:** 283–292.

Nagel, W. 1892. Das geschmacksinn der actinien. *Zool. Anz.* **15:** 334–338.

Thorington, G. U., and D. A. Hessinger. 1984. Identification and partial characterization of cnidocyte chemoreceptors on the sea anemone, *Aiptasia pallida. J. Cell Biol.* **99**(4): 221a.

Thorington, G. U., and D. A. Hessinger. 1988a. Control of cnida discharge: I. Evidence for two classes of chemoreceptor. *Biol. Bull.* **174:** 163–171.

Thorington, G. U., and D. A. Hessinger. 1988b. Chemical control of cnida discharge. In *Biology of Nematocysts,* D. A. Hessinger and H. M. Lenhoff, eds. Academic Press, Orlando. (In press.)

Watson, G. M., and D. A. Hessinger. 1988a. Receptor-mediated endocytosis of a chemoreceptor involved in triggering the discharge of cnidae in a sea anemone tentacle. *Tissue Cell* **19:** 747–755.

Watson, G. M., and D. A. Hessinger. 1988b. Localization of a purported chemoreceptor involved in triggering cnida discharge in sea anemones. In *Biology of Nematocysts,* D. A. Hessinger and H. M. Lenhoff, eds. Academic Press, Orlando. (In press.)

Watson, G. M., and R. N. Mariscal. 1983. Comparative ultrastructure of catch tentacles and feeding tentacles in the sea anemone *Haliplanella. Tissue Cell* **15:** 939–953.

Williams, R. B. 1968. Control of the discharge of cnidae in *Diadumene luciae* (Verrill). *Nature* **219:** 959.

Reference: *Biol. Bull.* **175:** 137–143. (August, 1988)

Aspects of Entrainment of CHH Cell Activity and Hemolymph Glucose Levels in Crayfish*

JANINE L. KALLEN, N. R. RIGIANI, AND H. J. A. J. TROMPENAARS

Zoölogisch Laboratorium, Faculteit der Wiskunde en Natuurwetenschappen, Katholieke Universiteit, Toernooiveld, 6525 ED Nijmegen, The Netherlands

Abstract. We investigated the effects of several experimental conditions, such as constant darkness, light/dark phase-shift, covered eyes, eyestalks and rostral regions, and optic tract sectioning, on the entrainment of daily blood glucose rhythmicity in the crayfish. Hemolymph glucose determination over a 24 h period and a morphometrical study on the secretory activity of the Crustacean Hyperglycemic Hormone (CHH)-producing cells in the eyestalk using immunocytochemistry were carried out. Our results indicate that *Astacus leptodactylus* exhibits an endogenous circadian blood glucose rhythm entrained by the light/dark schedule.

The light stimuli that control the rhythm are not detected by the compound eyes nor by the caudal photoreceptor but most probably by a photoreceptor located elsewhere in the eyestalk. After disruption of the neural connection between the optic lobes and the cerebral ganglion, blood glucose rhythmicity persists, which indicates that the biological clock of the blood glucose rhythm is located within the optic lobes.

Introduction

The Crustacean Hyperglycemic Hormone (CHH)-producing system of the crayfish *Astacus leptodactylus* consists of a number of neurosecretory perikarya located on the rostral latero-ventral side of the medulla terminalis ganglionic X-organ (MTGX). The axons of these cells pass through the medulla terminalis (MT) and terminate in the sinus gland. The location and morphology of this cell system has been described in detail (for *Astacus leptodactylus* see Van Herp and Van Buggenum, 1979; Gorgels-Kallen and Van Herp, 1981; Gorgels-Kallen and Voorter, 1984; for other decapod species see Jaros and Keller, 1979; Gorgels-Kallen *et al.*, 1982; Van Herp *et al.*, 1984).

Under constant light/dark conditions, the CHH cell system of *Astacus leptodactylus* reveals a daily rhythmicity in the synthetic activity of the perikarya, transport of CHH-material to the sinus gland, and release of CHH into the hemolymph which results in a 24 h rhythm of blood glucose level (Gorgels-Kallen and Voorter, 1985). Similar results are described for the prawn *Palaemon serratus* (Van Herp *et al.*, 1984). Diurnal rhythmicity of hemolymph glucose content is also described for the crayfish *Orconectes limosus* (Hamann, 1974) and for the freshwater field crab *Oziotelphusa senex senex* (Reddy *et al.*, 1981). Hamann (1974) examined the day/night rhythmicity of blood glucose content of *Orconectes limosus* under various conditions. His findings signified the importance of light signals as entraining stimuli to maintain blood glucose rhythmicity and indicated the presence of an endogenous pacemaker. Furthermore, we recently described the presence of synaptic input on the ramifications of CHH axons in the MT neuropileum (Gorgels-Kallen, 1985). All the above mentioned findings point to the presence of a system controlling the entrainment of CHH metabolism.

The present work was undertaken in an effort to obtain additional information on the role of the prevailing environmental light/dark conditions in the entrainment of daily rhythmicity of CHH cell activity and, as a consequence, the hemolymph glucose level in *Astacus leptodactylus*. Based on Hamann's (1974) experiments, the daily blood glucose rhythm was examined under various conditions in order to study its exogenous or endogenous character and to learn more about the location of photo-

Received 3 March 1988; accepted 31 May 1988.

* Results were presented at the 'Réunion des Carcinologistes de Langue Française,' Concarneau, France (6–9 June 1987).

receptor(s) and oscillator(s) involved in modulation. Furthermore, since we are immunocytochemically able to determine the secretory activity of individual CHH cells (Gorgels-Kallen and Voorter, 1984, 1985), we investigated the effect of the experimental conditions on the cellular activity of the CHH cell system.

Materials and Methods

Animals and blood sampling

Crayfish of the species *Astacus leptodactylus* (Nordmann), were imported from Turkey via a commercial dealer and kept in the laboratory in running tap water (13–15°C), and fed weekly with pieces of meat or fish. Except when otherwise stated, animals were kept under light/dark conditions (LD 12:12, light on 8.00 am). Experiments were performed with adult female and male crayfish of equal size and in intermolt stage. Blood samples, obtained from 5 to 10 animals per sample time, were collected over a 24 h period at regular intervals. 100 μl of hemolymph was drawn into a calibrated capillary pipet which was inserted between the coxa and the basis of the left cheliped. Samples were taken in duplicate from each animal and frozen immediately. The blood glucose level was determined using the Gluco-Quant Test Combination (Boehringer Mannheim GmbH).

Experimental conditions

Constant darkness. Crayfish were kept in constant darkness (code DD). Blood samples were taken at the start of the experiment and 6, 11, and 35 days after the onset of DD conditions.

Phase-shift. Crayfish kept under normal LD conditions were exposed to a 12 h phase-shift (code PS) accomplished by lengthening the light period with 12 hours at the onset of the experiment. Hemolymph samples were taken at the start of the experiment and 6, 12, and 18 days after introduction of the phase-shift.

Covered retinas and rostral regions. Several experiments were performed covering different regions of the eyestalk and the rostrum. Either both retinas (code RR), both eyestalks (code EE), or the rostral cephalic region including the eyestalks (code CR) were painted using a black textile dye (Silka; Talens, Apeldoorn, The Netherlands) which formed a completely opaque, water-resistant coverage. Before painting blood samples were taken. The experimental conditions were maintained for 35 days, then hemolymph was again sampled.

Optic tract operation. Between the hard exoskeleton of the eyestalk and rostrum there is a softer region enabling articulation of the eyestalk. In order to disrupt the neural connection between the optic ganglia and CHH cell system with the cerebral ganglion, a fine pointed cauterization needle or a microdissection scalpel was pushed through the soft region to section the optic tract locally (code NO). Blood samples were taken before the start of the experiment and 35 days after operation. At the end of the experiment, crayfish were sacrificed and the eyestalks were microscopically examined to check the success of the optic tract section, the condition of the isolated ganglia and the normal course of the blood circulation.

Light microscopy

From animals kept under the above described experimental and control conditions, eyestalks were ablated at 12.00 am and fixed in Bouin Hollande fluid (24 h) containing 10% of a saturated aqueous solution of sublimate. The fixed material was embedded in Paraplast (57°C). The immunocytochemical staining was based on the peroxidase-antiperoxidase (PAP)-method (Sternberger, 1974) and was performed on 7 μm sections with an overnight incubation at 4°C for the anti-CHH. The primary antiserum was raised in rabbits against a purified hyperglycemic fraction derived from eyestalks of *Astacus leptodactylus* (for further details of the purification of the antigen and the production of the antiserum see Gorgels-Kallen and Van Herp, 1981). The procedure of the immunostaining followed Van Herp and Van Buggenum (1979), with the primary antiserum applied in a dilution series. For each experiment the optimal dilution of the primary antiserum proved to be 1/150, which conforms to the optimal dilution used for eyestalks from animals kept under normal LD and laboratory conditions. The specificity of the immunostaining was tested as described previously (Gorgels-Kallen and Van Herp, 1981).

The secretory cell stages of individual CHH cells were determined on the basis of the observed differences in staining intensity which enables the arbitrary division of the immunoreactive cells into three categories: +, ++, and +++, representing the cells with least intense, moderately intense, and most intense immunostaining, respectively. In a previous study, morphometric analyses of the cells at both the light and electron microscopic levels led to the following characterization of the three cell stages: + cells show the weakest immunoreaction which is correlated to the low content of CHH granules in their cytoplasm. The cells possess a large nucleus which points to a high level of mRNA production. ++ Cells show an intermediate immunoreaction. In their cytoplasm the content of granules is increased. These cells possess the largest nuclear and cytoplasmic volumes, which indicate high synthetic activity. +++ Cells show an intense immunoreaction which is correlated with the largest numerical density of CHH granules in their cytoplasm. The synthetic level of these cells is low as documented by

their small cytoplasmic and nuclear volumes. Moreover, the CHH granules show a lower electron density and an increased diameter as compared with those of + and ++ cells. These facts point to the occurrence of a maturation process, indicating that the secretory granules are youngest in the + cells and oldest in the +++ cells, which indicates different degrees of synthetic activity of the three distinguished cell stages. For a detailed description of the morphology and the results of a morphometric study of the CHH cell stages we refer to our previous study (Gorgels-Kallen and Voorter, 1984) and to our study on the secretory dynamics of the CHH cells in the course of the day/night cycle (Gorgels-Kallen and Voorter, 1985). The numbers of +, ++, and +++ cells were counted in the left eyestalks from three specimens per experimental or control condition. In addition, the cytoplasmic and nuclear volumes of five of each of the +, ++, and +++ cells, per eyestalk, were calculated according to Weibel's (1979) method and as described in detail previously (for illustration see Fig. 3; Gorgels-Kallen and Voorter, 1984, 1985).

Results

Hemolymph glucose rhythmicity

Control experiments. Figure 1a represents the results of the glucose determination in the hemolymph for all specimens used in the DD and PS experiment, determined during normal 12 h light and 12 h dark conditions. The blood glucose values show the usual rhythmicity: around 4 hours after the onset of the dark period the glucose level doubles compared to the level found in the daytime.

Constant darkness. Figures 1b–d show the blood glucose levels over a 24 h period, measured after 6 (Fig. 1b), 11 (Fig. 1c), and 35 days (Fig. 1d) under constant darkness conditions. After 6 days absence of the light stimulus, the circadian hemolymph glucose pattern still persists, although the maximum decreases around midnight. After 11 days the normal rhythm is tempered: yet, at midnight an increased variation of the mean glucose level can still be seen. Constant darkness for 35 days results in total absence of any daily rhythm. Furthermore, the data show that removing the periodic changes in light intensity leads to consistently low glucose levels during the whole 24 h period.

Phase-shift. Figures 1e–g show the hemolymph glucose values over a 24 h period measured 6 (Fig. 1e), 12 (Fig. 1f), and 18 days (Fig. 1g) after the introduction of a 12 h shift in the normal LD pattern, by lengthening one light period by 12 hours. Six days after the phase-shift blood glucose rhythmicity is disturbed. The graph shows three zones with an increase followed by a decrease in blood glucose content and increased variation in the

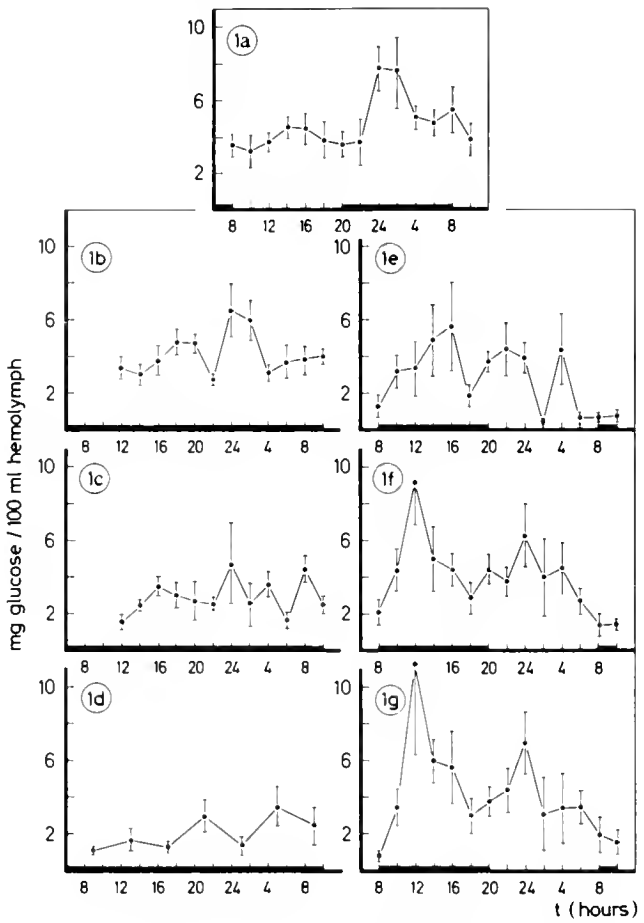

Figure 1. (a–g) Daily hemolymph glucose pattern: (a) under normal light/dark conditions (LD 12:12; n = 10); (b) after 6 days constant darkness (n = 5); (c) after 11 days constant darkness (n = 5); (d) after 35 days constant darkness (n = 5); (e) six days after a 12 h phase shift (n = 5); (f) twelve days after a 12 h phase-shift (n = 5); (g) eighteen days after a 12 h phase-shift (n = 5). Means ± SEM.

mean glucose values for most sample points. After 12 days the normal circadian blood glucose pattern reappears; the maximum in glucose level is found at 12 a.m., 4 hours after the onset of the "new" dark period. However, during the light period at 12 pm a second smaller peak is seen. This glucose pattern persists and even becomes more pronounced 18 days after the start of the experiment. At 12 am, the new midnight, the mean glucose level increases firmly whereas at 12 pm, the former midnight, a second smaller, although distinct rise in blood glucose content is found.

Painted eyestalks and rostral regions. Prevention of light perception via the ommatidia (light percepting units forming the compound eye) does not abolish circadian rhythmicity in the hemolymph glucose content (Fig. 2b). During the dark period the glucose level still doubles. The amplitude and mean glucose levels during the total 24 h period are closely comparable to the con-

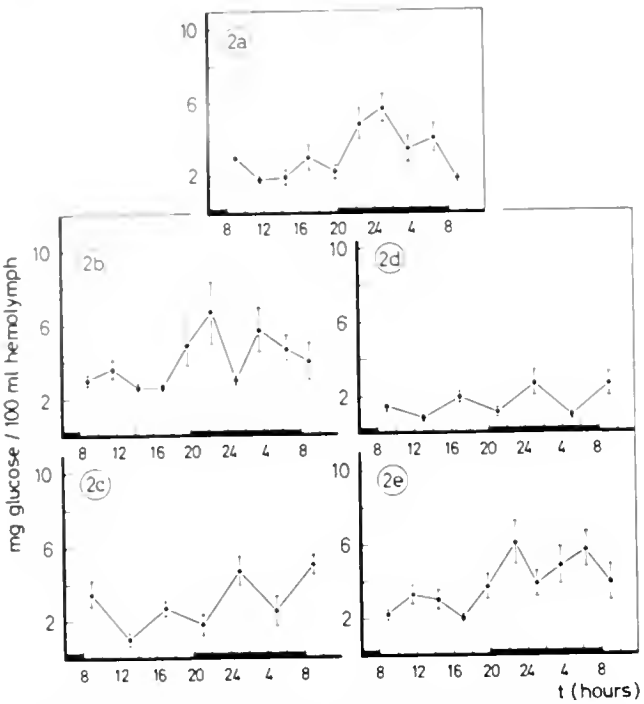

Figure 2. (a–e) Daily hemolymph glucose pattern after several experimental conditions: (a) under normal light/dark conditions before the start of the experiment (LD 12:12; n = 5); (b) thirty-five days after covering of the compound eyes (code RR; n = 5); (c) thirty-five days after covering of the whole eyestalks (code EE; n = 5); (d) thirty-five days after covering of the whole eyestalks and the rostral region of the cephalothorax (code CR; n = 5); (e) thirty-five days after section of the optic tract (code NO; n = 5). Means ± SEM.

trol values obtained from these specimens before starting the experiments (Fig. 2a). Yet, some influence must be noticed. The nocturnal rise in glucose is found immediately at the start of the dark period and the mean values show increased variation. After painting the whole eyestalks, an increased glucose level during the dark period is still seen, although the amplitude is very reduced (Fig. 2c). Covering the whole eyestalks including the rostral part of the cephalothorax leads to a complete absence of circadian blood glucose rhythmicity and during the whole 24 h period the glucose levels consistently stay very low (Fig. 2d).

Optic tract operation. Disruption of the connection between the eyestalk and the cerebral ganglion by sectioning the optic nerve does not interfere with the persistance of a daily rhythmicity in hemolymph glucose content (Fig. 2e).

Secretory activity of the CHH cells

We investigated the effect of a change in environmental conditions on the secretory activity of the CHH cells. Animals that exhibit both a change (DD experiment), and no change (RR experiment) in hemolymph glucose rhythmicity were used. The results of this morphometric investigation are presented in Table I. Animals kept in constant darkness have a ratio between the number of +, ++, and +++ cells which differs from the ratio found for crayfish kept under control conditions. The number of +++ cells increases accompanied by a decrease in the number of ++ cells. The morphometric data reveal an increase in the cellular volume of the +++ cells. Immunocytochemical staining of the eyestalks of the RR animals reveals that both the proportion of +, ++, and +++ cells, and their cellular and nuclear volumes, are similar to those of the control animals. Disruption of the optic nerve produces a ratio of the +, ++, and +++ cells different to the ratio found for control animals. The number of + cells increases firmly, accompanied by a decrease in ++ cells. The morphometric results reveal increased cellular and nuclear volumes of the + cells. Furthermore, the overall conditions of these operated eyestalks were normal: blood circulation was not affected and no signs of degenerating eyestalk tissues were observed, nor regeneration of the sectioned optic nerve.

Discussion

Blood glucose levels found in *Astacus leptodactylus* after exposing the animals to constant dark conditions reveal that the normal 24 h rhythm persists for many cycles. The rise in blood glucose content around midnight remains clearly distinguishable after 6 days of constant darkness; after 11 days the rhythm is tempered, but the high variation in the mean glucose content at 12 pm still indicates a masked presence of the nocturnal peak. Introduction of a 12 h phase-shift results in a very slow adaptation of the 24 h rhythm to the newly imposed light schedule. Six days after the onset of the phase-shift, the normal blood glucose rhythm is still disturbed. This disturbance is expressed as: (a) a high variation in the mean glucose levels of most sample points, and (b) three periods with an increase followed by a decrease. This result corresponds to the description of the so-called transient phase, *i.e.*, a temporary loss of synchrony among the various units involved in a particular circadian rhythm, which results in frequency beats modulating the free-running period (Pavlidis, 1973). Twelve days after introduction of the phase-shift, the normal circadian blood glucose rhythm is restored, adapted to the new light/dark scheme, *i.e.*, around 4 hours after the onset of the dark period a firm blood glucose peak is detected. However, even 18 days after the phase-shift the "old" glucose peak still can be seen.

In his introduction of the symposium "Biological Clocks" (Cold Spring Harbor, 1960) Aschoff underlines the importance of the establishment of the free-running

Table I

Morphometric data on the CHH-producing cells of the crayfish, Astacus leptodactylus, *determined after control and experimental conditions. Mean (±SEM)*

Experimental condition	Cell stage + Number of cells/eyestalk	+ Cellular volume ($\times 10^3\ \mu m^3$)	+ Nuclear volume ($\times 10^3\ \mu m^3$)	++ Number of cells/eyestalk	++ Cellular volume ($\times 10^3\ \mu m^3$)	++ Nuclear volume ($\times 10^3\ \mu m^3$)	+++ Number of cells/eyestalk	+++ Cellular volume ($\times 10^3\ \mu m^3$)	+++ Nuclear volume ($\times 10^3\ \mu m^3$)
Control	9 (±2)	30.7 (±3)	5.2 (±0.4)	19 (±1)	35.3 (±3)	6 (±0.6)	6 (±1)	22.8 (±2)	3.3 (±0.2)
	(n1 = 3)	(n2 = 15)	(n2 = 15)	(n1 = 3)	(n2 = 15)	(n2 = 15)	(n1 = 3)	(n2 = 15)	(n2 = 15)
DD	11 (±2)	34.2 (±3)	4.5 (±0.3)	13 (±1)^s	38.4 (±2)	5.2 (±0.7)	13 (±2)^s	28.3 (±1)^s	4 (±0.2)^s
	(n1 = 5)	(n2 = 25)	(n2 = 25)	(n1 = 5)	(n2 = 25)	(n2 = 25)	(n1 = 5)	(n2 = 25)	(n2 = 25)
RR	10 (±2)	32.3 (±2)	5.6 (±0.5)	19 (±3)	39.2 (±3)	5.7 (±0.4)	8 (±2)	22.4 (±2)	3.4 (±0.3)
	(n1 = 3)	(n2 = 15)	(n2 = 15)	(n1 = 3)	(n2 = 15)	(n2 = 15)	(n1 = 3)	(n2 = 15)	(n2 = 15)
NO	21 (±4)^s	42 (±4)^s	4.2 (±0.4)^s	6 (±2)^s	32.2 (±2)	4 (±0.3)^s	8 (±2)	24.4 (±2)	3.3 (±1)
	(n1 = 5)	(n2 = 25)	(n2 = 25)	(n1 = 5)	(n2 = 25)	(n2 = 25)	(n1 = 5)	(n2 = 25)	(n2 = 25)

Control: Results obtained from eyestalks of crayfish kept under normal light/dark schedule (LD 12:12).
DD: Results obtained from eyestalks of crayfish kept under constant darkness for 35 days.
RR: Results obtained from eyestalks of crayfish kept under normal light/dark schedule, however, with covered compound eyes for 35 days.
NO: Results obtained from eyestalks of crayfish kept under normal light/dark schedule and 35 days after disruption of the connection between the cerebral and optic ganglia.
n1 = number of measured eyestalks from different animals.
n2 = number of cells counted; 5 cells per cell stage per eyestalk.
s = significantly different from control data; Student's *t*-test, $P < 0.05$.

period of individual organisms in order to establish a periodicity as an endogenous one. However, establishment of the free-running period of the blood glucose rhythm in crayfish in this way is not possible, since repeated sampling of hemolymph from the same specimen leads, within several hours, to hyperglycemia caused by stress. Hamann's (1974) method of measuring the circadian hemolymph glucose levels from individual crayfish via an extracorporeal circulatory system only succeeded for a few cycles and cannot be performed with large numbers of animals. As such, blood glucose rhythmicity can only be depicted by sampling different groups of crayfish as described in this paper. However, despite the fact that we were not able to determine one of the major characteristics of circadian rhythm, we believe that the above mentioned results, *i.e.*, (a) the persistance of the rhythm for many cycles without external periodic light stimuli, and (b) the slow adaptation of the rhythm to changed light/dark conditions, allow us to postulate that the daily blood glucose level in *Astacus leptodactylus* is generated within the organism and therefore may be called endogenous or circadian.

Furthermore, since prolonged exposure of the animals to constant darkness eliminates hemolymph glucose rhythmicity and changing the external light stimuli produces entrainment, our data show the final indispensability of the prevailing light/dark cycle as a Zeitgeber in entrainment of the daily blood glucose rhythm. The importance of an external light stimulus can also be seen from the results on the determination of the secretory activity of the CHH cells after 35 days DD conditions: an increased number of enlarged +++ cells and a decreased number of actively producing ++ cells is found. These data point to a reduced production of CHH and increased storage in the perikarya.

Covering both retinas does not abolish reception of a light entraining signal, as blood glucose rhythmicity still persists. This is also supported by the results of the determination of secretory activity of the CHH cells: the resultant data are closely comparable to those of control animals. Painting both eyestalks results in a very faint nocturnal blood glucose increase and covering both eyestalks and the rostral region of the cephalothorax leads to a complete disappearance of rhythmicity and a consistently low glucose level during the whole 24 h period: the resulting hemolymph glucose graph is closely comparable to the graph obtained after constant DD conditions. Comparable experiments with the crayfish *Orconectes limosus,* performed by Hamann (1974), show the same blood glucose patterns. Therefore it appears that the eyestalks (optic lobes) have a dominant role in perception of light, but the presence of an involved photoreceptor in the rostral region of the cephalothorax cannot be excluded. The effect of disruption of the optic tract further

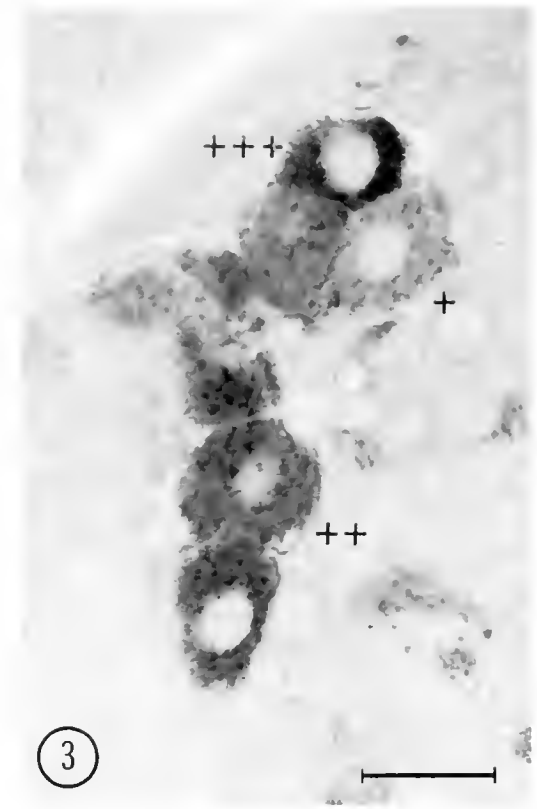

Figure 3. PAP-staining of CHH-producing cells in the MTGX, illustrating +, ++, and +++ cells. Bar represents 50 nm. + cells: mean cell volume $32.5 \times 10^3\ \mu m^3$, mean nuclear volume $5.5 \times 10^3\ \mu m^3$; ++ cells: mean cell volume $38.8 \times 10^3\ \mu m^3$, mean nuclear volume $5.6 \times 10^3\ \mu m^3$; +++ cells: mean cell volume $27.8 \times 10^3\ \mu m^3$, mean nuclear volume $4.1 \times 10^3\ \mu m^3$. (Morphometrical data from Gorgels-Kallen and Voorter, 1984).

supports the importance of the entraining function of the eyestalk: daily rhythmicity of the hemolymph glucose level is not affected after disturbance of the neural connection between the cerebral and optic ganglia. This result points to the presence of a pacemaker or biological clock of the glucose rhythm located in the optic lobes, although hormonal modulation from a pacemaker located elsewhere cannot be ruled out. Indeed, such hormonal influence is not disturbed by the optic tract operation, since microscopic investigation of these eyestalks did not reveal any irregularities concerning blood circulation or the condition of eyestalk structures. However, the secretory activity of the CHH cells of these NO animals does not show the same picture as found in control animals. Yet, as the blood glucose rhythmicity is comparable to control animals, it could be that CHH release is modulated by an oscillator located in the eyestalk. However, that regulation of CHH synthesis is more complex and (also) affected by a pacemaker located elsewhere. Another possibility might be that the CHH cells not only produce a hyperglycemic factor but also other hormonally active substances. Synthesis of hyperglycemic hormone might be affected by optic nerve section, while the synthesis of other hormones might go on undisturbed. Such an effect can be visualized immunocytochemically. Our results exclude any regulatory effect caused by the caudal photoreceptor described for the first time in crayfish by Prosser (1934).

Our data are supported by the work of Page and Larimer (1972), who studied the entrainment of the circadian locomotor activity in the crayfish *Procambarus clarkii*. They found that removal of the caudal photoreceptor, removal of the ommatidia of both eyes, or removal of both the ommatidia and the lamina ganglionaris, did not effect entrainment of rhythmicity in locomotion. Comparable results were also obtained by Pollard and Larimer (1977) regarding circadian rhythmicity of the heart rate in *Procambarus clarkii*. Page and Larimer (1976) demonstrated the existence of a photoreceptor in the brain in the same species. In contrast with these findings are data by Glantz *et al.* (1983), who intracellularly recorded the electrical activity of neurosecretory cells in the eyestalk induced by illumination of retinal fields. Fuentes-Pardo and Inclán-Rubio (1987) recently described the participation of the caudal photoreceptor in synchronizing the circadian locomotor rhythm in *Procambarus bouvieri*. Williams (1985) proposed, after his evaluation of the impact of optic tract section on the locomotor activity of the shore crab *Carcinus maenas*, the presence of a presumptive neural clock in the cerebral ganglion involved in regulation of locomotor rhythm.

In conclusion, we postulate that *Astacus leptodactylus* exhibits an endogenous circadian hemolymph glucose rhythm entrained by the prevailing light/dark schedule. Neither the retinas nor the caudal photoreceptor represent the main modulating receptors for blood glucose level and synthetic activity of the CHH cells. The present results indicate that the eyestalks possess the major receptors for the entraining light stimulus and also contain the oscillatory center for the blood glucose rhythm.

Acknowledgments

The authors are grateful to Prof. Dr. J. M. Denucé and Dr. F. van Herp for discussing the manuscript. We thank the Illustration Services of the Faculty of Sciences for preparing the figures, and Mrs. E. Derksen for typing the manuscript.

Literature Cited

Aschoff, J. 1960. Exogenous and endogenous components in circadian rhythms. In *Biological Clocks. Cold Spring Harb. Symp. Quant. Biol.* **25:** 11–28.

Fuentes-Pardo, B., and I. Inclán-Rubio. 1987. Caudal photoreceptors synchronize the circadian rhythms in crayfish. I. Synchronization of ERG and locomotor circadian rhythm. *Comp. Biochem. Physiol.* **86A:** 523–527.

Glantz, R. M., M. D. Kirk, and H. Aréchiga. 1983. Light input to crustacean neurosecretory cells. *Brain Res.* **265:** 307–311.

Gorgels-Kallen, J. L. 1985. Appearance and innervation of CHH-producing cells in the eyestalk of the crayfish *Astacus leptodactylus* examined after tracing with Lucifer Yellow. *Cell Tissue Res.* **240:** 385–391.

Gorgels-Kallen, J. L., and F. Van Herp. 1981. Localization of crustacean hyperglycemic hormone (CHH) in the X-organ sinus gland complex in the eyestalk of the crayfish *Astacus leptodactylus* (Nordmann, 1842). *J. Morphol.* **170:** 347–355.

Gorgels-Kallen, J. L., and C. E. M. Voorter. 1984. Secretory stages of individual CHH-producing cells in the eyestalk of the crayfish *Astacus leptodactylus* determined by means of immunocytochemistry. *Cell Tissue Res.* **273:** 291–298.

Gorgels-Kallen, J. L., and C. E. M. Voorter. 1985. The secretory dynamics of the CHH-producing cells in the eyestalk of the crayfish *Astacus leptodactylus,* in the course of the day/night cycle. *Cell Tissue Res.* **241:** 361–366.

Gorgels-Kallen, J. L., F. Van Herp, and R. S. E. W. Leuven. 1982. A comparative immunocytochemical investigation of the crustacean hyperglycemic hormone (CHH) in the eyestalks of some decapod crustacea. *J. Morphol.* **174:** 161–168.

Hamann, A. 1974. Die neuroendokrine Steuerung tagesrhythmischer Blutzuckerschwankungen durch die Sinusdrüse beim Flusskrebs. *J. Comp. Physiol.* **89:** 197–214.

Jaros, P. P., and R. Keller. 1979. Immunocytochemical identification of hyperglycemic hormone-producing cells in the eyestalk of *Carcinus maenas. Cell Tissue Res.* **204:** 379–385.

Page, T. L., and J. L. Larimer. 1972. Entrainment of the circadian locomotor activity rhythms in crayfish. *J. Comp. Physiol.* **78:** 107–120.

Page, T. L., and J. L. Larimer. 1976. Extraretinal photoreception in entrainment of crustacean rhythms. *Photochem. Photobiol.* **23:** 245–251.

Pavlidis, T. 1973. Biological phenomena attributable to populations of oscillators. Pp. 159–186 in *Biological Oscillators: Their Mathematical Analysis,* T. Pavlidis, ed. Academic Press, New York.

Pollard, T. G., and J. L. Larimer. 1977. Circadian rhythmicity of heart rate in the crayfish, *Procambarus clarkii. J. Comp. Physiol.* **57:** 221–226.

Prosser, C. L. 1934. Action potential in the nervous system in the crayfish. II. Responses to illumination of the eye and caudal ganglion. *J. Cell. Comp. Physiol.* **4:** 363–377.

Reddy, C. S. D., M. Raghupathi, V. R. Pursushotham, and B. P. Naidu. 1981. Daily rhythms in levels of blood glucose and hepatopancreatic glycogen in the freshwater field crab *Oziotelphusa senex senex* (Fabricius). *Indian J. Exp. Biol.* **19:** 403–404.

Sternberger, L. A. 1974. *Immunocytochemistry.* Prentice Hall, Inc., Englewood Cliffs, New Jersey.

Van Herp, F., and H. J. M. Van Buggenum. 1979. Immunocytochemical localization of hyperglycemic hormone (HGH) in the neurosecretory system in the eyestalk of the crayfish *Astacus leptodactylus. Experientia* **35:** 1527–1528.

Van Herp, F., A. Van Wormhoudt, W. A. J. Van Venrooy, and C. Bellon-Humbert. 1984. Immunocytochemical study of crustacean hyperglycemic hormone (CHH) in the eyestalks of the prawn *Palaemon serratus* (Pennant) and some other Palaemonidae, in relation to variations in the blood glucose level. *J. Morphol.* **182:** 85–94.

Weibel, E. R. 1979. *Stereological Methods. Practical Methods for Biological Morphometry,* Vol. I. Academic Press, London. 415 pp.

Williams, J. A. 1985. Evaluation of optic tract section on the locomotor activity rhythm of the shore crab *Carcinus maenas. Comp. Biochem. Physiol.* **82A:** 447–453.

Reference: *Biol. Bull.* 175: 144–153. (August, 1988)

Electrophysiological and Histological Observations on the Eye of Adult, Female *Diastylis rathkei* (Crustacea, Malacostraca, Cumacea)

V. B. MEYER-ROCHOW AND M. LINDSTRÖM

Department of Biological Sciences, University of Waikato, Hamilton, New Zealand, and Tvärminne Zoological Station, University of Helsinki, SF-10900 Hanko, Finland

Abstract. The approximately 200 μm wide eye of *Diastylis rathkei* consists of two closely apposed eye halves with four lenticular complexes measuring 40 μm in diameter in each. Each lenticular complex consists of a lens rich in 30 nm electron-opaque glycogen-like particles made up of smaller (5–6 nm) subunits, and a rhabdom comprising regularly aligned microvilli. The retinula cell somata, which are in a proximal location, are linked with the distally placed rhabdom via approximately 10 μm thick, cellular strands. The strands are surrounded by cells crowded with reflecting organelles of *ca.* 0.8 μm in diameter.

Dark/light adaptational changes affect the position of uniformly spherical organelles measuring 0.4–0.5 μm in diameter and presumed to contain carotenoids, the overall size of the rhabdom, and the diameter of individual microvilli. The latter measure 75 nm in the light-adapted state and 90–120 nm in the dark-adapted state. There is ultrastructural evidence (swollen and abundant endoplasmic reticulum and widely distributed glycogen-like particles) that, under light-adapted conditions, the retinula cells are in a phase of intense metabolic activity.

A multilamellar structure, similar in appearance to that found in the organ of Bellonci of other crustaceans, but also resembling a trophospongium, was noticed in close proximity to the eye within the optic lobe. Extracellular electrophysiological recordings obtained with NaCl-filled glass electrodes consisted of a cornea-negative potential change and reached a maximum amplitude of nearly 400 μV to 300 ms flashes of white light.

Superimposed spectral response curves from eight different animals, based on a criterion amplitude of 50 μV, were nearly congruent in shape and displayed one single sensitivity peak to light of 512–549 nm in wavelength. Intensity/response curves obtained to light of 472, 549, and 628 nm wavelengths and the single spectral sensitivity peak strongly suggest that only one type of excitatory visual pigment is involved in the visual process of *D. rathkei*.

It is concluded that in spite of its tiny size, the eye of *D. rathkei* could be useful in the coordination of reproduction and synchronization of vertical migrations.

Received 2 February 1988; accepted 31 May 1988.

Introduction

Cumaceans are an order of peracaridan crustaceans traditionally placed near the Isopoda (Siewing, 1956; Fryer, 1967). Certain species of Cumacea, including *Diastylis rathkei*, regularly occur in the plankton, sometimes hundreds of meters above the seabottom (Fricke, 1931; Forsman, 1938). It is thought that the males, which have considerably larger eyes than the females (Zimmer, 1941), seek the latter in the open water at night during the mating season (Forsman, 1938).

At certain times of the year, these small crustaceans can be very abundant (1214/m^2: Kaestner, 1959) and represent an important component of the diet of various species of fishes; yet virtually all we know about the cumacean photoreceptor goes back almost 60 years to a study of *D. rathkei* by Fricke (1931), who asserted that the cumacean eye was a degenerated compound eye. Though in some species of cumaceans, *e.g., Nannastacus euxinicus*, two clearly separated, lateral eyes are present (Bacescu, 1951), this view was challenged by Mayrat (1981), who claimed the cumacean eye was a dorsal ocellus. Arguments for and against either opinion were sum-

marized by Meyer-Rochow (1988) and supplemented with ultrastructural observations on the larval eye of *D. rathkei*. However, a detailed examination of the structure and function of the eyes of the adults is still lacking. Since male and female *D. rathkei* differ in their behavior to a light source (Forsman, 1938; Zimmer, 1941) and the short-lived males are much less common than the females, this paper is concerned with one form only: the female sex.

Materials and Methods

Collection and maintenance of organisms

In early April, live, adult specimens of the cumacean *Diastylis rathkei* were dredged from the sandy bottom of the Baltic Sea southwest off the Danish island of Langeland in approximately 40 m depth. The animals, all females, were taken to the Zoological Institute of the University of Kiel and kept in brackish water aquaria. Within a week, during which time histological preparations of the *D. rathkei* eye were being made, 10 individuals in a 2 liter thermos bottle were taken by one of us (V. B. Meyer-Rochow) to Finland in an airplane and subsequently housed at Tvärminne Zoological Station at 6°C in total darkness. Individuals were picked at random for both anatomical and physiological observations.

Histology

Eyes of daytime specimens as well as night specimens were carefully extirpated under a dissecting microscope at 10:00 h and 24:00 h, respectively. A paraformaldehyde/glutaraldehyde mixture of 7.4 pH, buffered in Millonig's phosphate and adjusted with 3 g d-glucose/100 ml for reasons of osmolarity matching Baltic Sea water, served as the initial fixative, in which the eyes stayed for about 40 h. They were then washed in buffer and post-fixed for 1.5 h in 2% osmiumtetroxide using the same buffer. The specimens were then embedded in Spurr's medium.

One μm sections were stained with toluidine-blue for light microscopy. Gold or silver sections were stained with uranyl acetate and lead citrate for electron microscopy. Four light-adapted and two dark-adapted specimens were examined.

Electrophysiology

Experimental procedures closely followed those reported by Lindström and Meyer-Rochow (1987). During preparation, using infra-red image converters mounted on a Wild-5 stereo-microscope, each animal was illuminated by light that had passed through two Kodak Wratten 87 gelatin filters and a heat filter. These were inserted in the ray path of white light coming from a 15 W microscope lamp. The incident light leaving the 3 mm wide tip of a light guide perpendicular to the eye, was centered around the hole through which the recording electrode was lowered some 40–50 μm into the eye. The light spot made by the stimulating light flash covered the entire eye. The light output had been calculated in absolute units ($qu \cdot cm^{-2} \cdot s^{-1}$) by an Airam UVM-8LX luxmeter calibrated by Airam Laboratories for a wavelength of 564 nm (Donner and Lindström, 1980). Based on these readings, we estimate the quantal amount of the flashes of light on the eye to elicit a response to have been 3.4 $\times 10^{10}$ $qu \cdot cm^{-2} \cdot s^{-1}$. Measurements of light levels in the field at the site of capture are unavailable, but Lindström and Nilsson (1983) mention summer and autumn figures of 10^{12} and 10^{9} $qu \cdot cm^{-2} \cdot s^{-1}$, respectively, for a depth of 100 m at "Norwegian northern latitudes." The stimulus time was usually set at 300 ms.

Tips of glass electrodes drawn with an Ealing microelectrode puller were cut off to an outer diameter of approx. 10 μm. The measuring electrode was filled with a 1 *M* NaCl solution and connected to a Tektronix 5031 dual beam storage oscilloscope. Setting-up procedures averaged no longer than 5–10 minutes. Thereafter the test animals were given 30 minutes of total darkness to recuperate from the operation. In the spectral sensitivity studies a criterion response of 50 uV was employed. All recordings were made in the AC-setting.

Results

Histology

Gross anatomy. The eye consists of two symmetrical eye halves on a common forward-projecting ocellar lobe, separated from each other along the midline by a 1 μm wide gap (Fig. 1). There are four bright red retinal complexes in each eye half, but facets or corneal lenses are not developed. The integument covering the eye is transparent and uniformly 5 μm thick. Distally, each retinal complex possesses a lenticular structure (diameter approx. 40 μm) and is in intimate contact with the microvilli of a rhabdom that is produced by retinula cells. The large nuclei (Fig. 2) of these cells are located some 100–150 μm more proximally near the center of the dome-shaped eye.

Cytoplasmic strands of approx. 10 μm diameter swerve in an arc through a massively developed layer of reflecting material and connect retinula cell bodies and rhabdom (Fig. 1). The rhabdom/lens interface is characterized by unclear cell boundaries that give the impression that the two form a functional unit (Figs. 3, 4). The lens component of each such complex, contrary to Fricke (1931), appears to contain more than one nucleus (Fig. 3). Apart from the large, chromatin-rich nuclei on the proximal or lateral sides of the lens, each lens is made

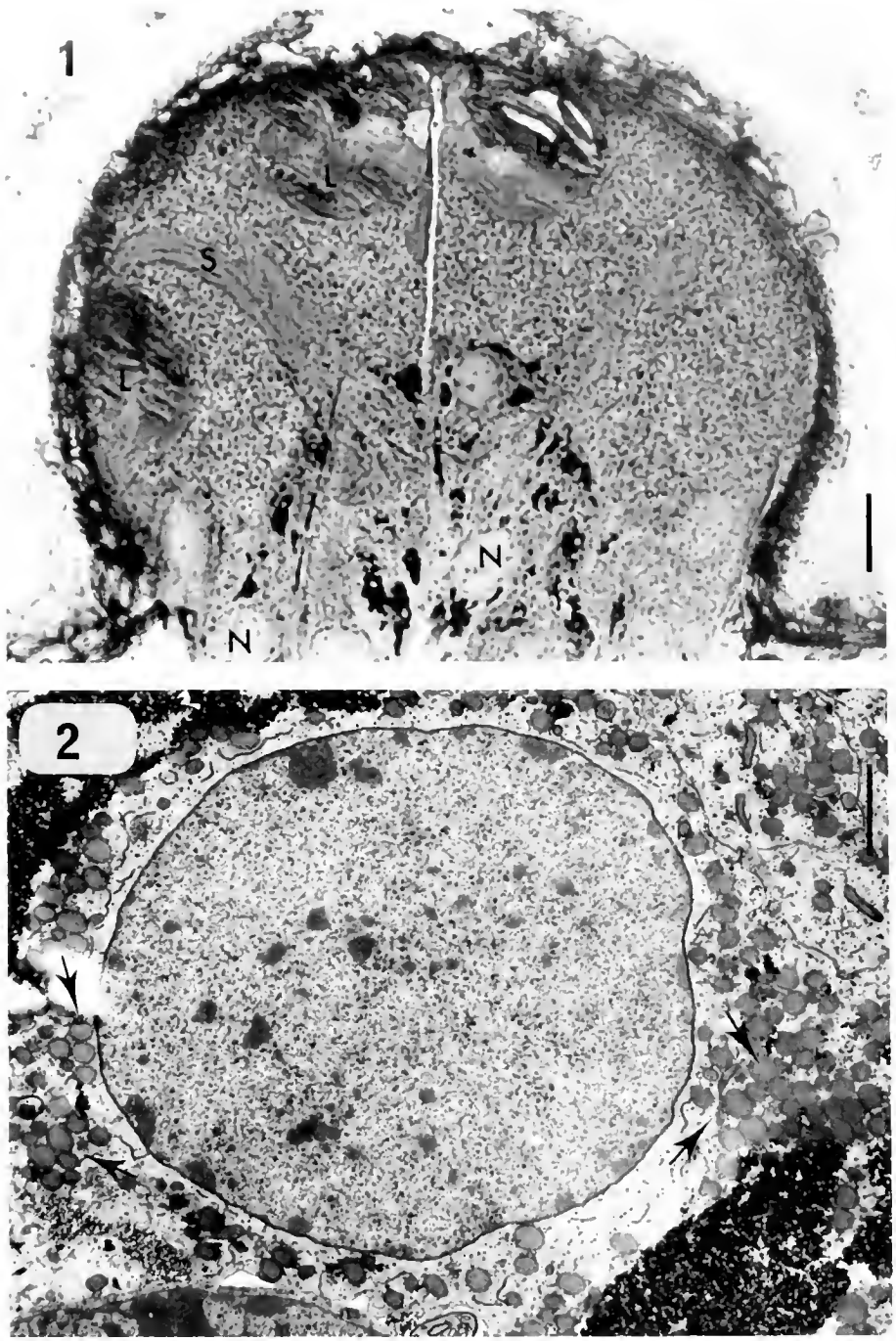

Figure 1. Light micrograph of horizontal section through the eye of an adult female. The symmetrical eye halves joined along the midline are apparent and lenticular complexes (L), retinula cell strands (S), and nuclei (N) are clearly visible. Scale = 20 μm.

Figure 2. Electron micrograph of proximally located retinula cell nucleus with surrounding clusters of electron-opaque glycogen particles and presumed carotinoid bodies (arrows). Scale = 2 μm.

up of a dense aggregation of electron-opaque particles, measuring 30 nm in diameter (Figs. 3, 4). These particles are composed of 40–50 smaller subunits of approx. 6 nm in size (Fig. 5).

Cumacean retinula cells contain uniformly shaped 0.4–0.5 μm large, spherical organelles (Fig. 3). These are identical in appearance and location with bodies identified as carotinoid grains in the crustacean chromatophore (Elofsson and Hallberg, 1973). They are thought to be present in the photoreceptive cells of other peraca-

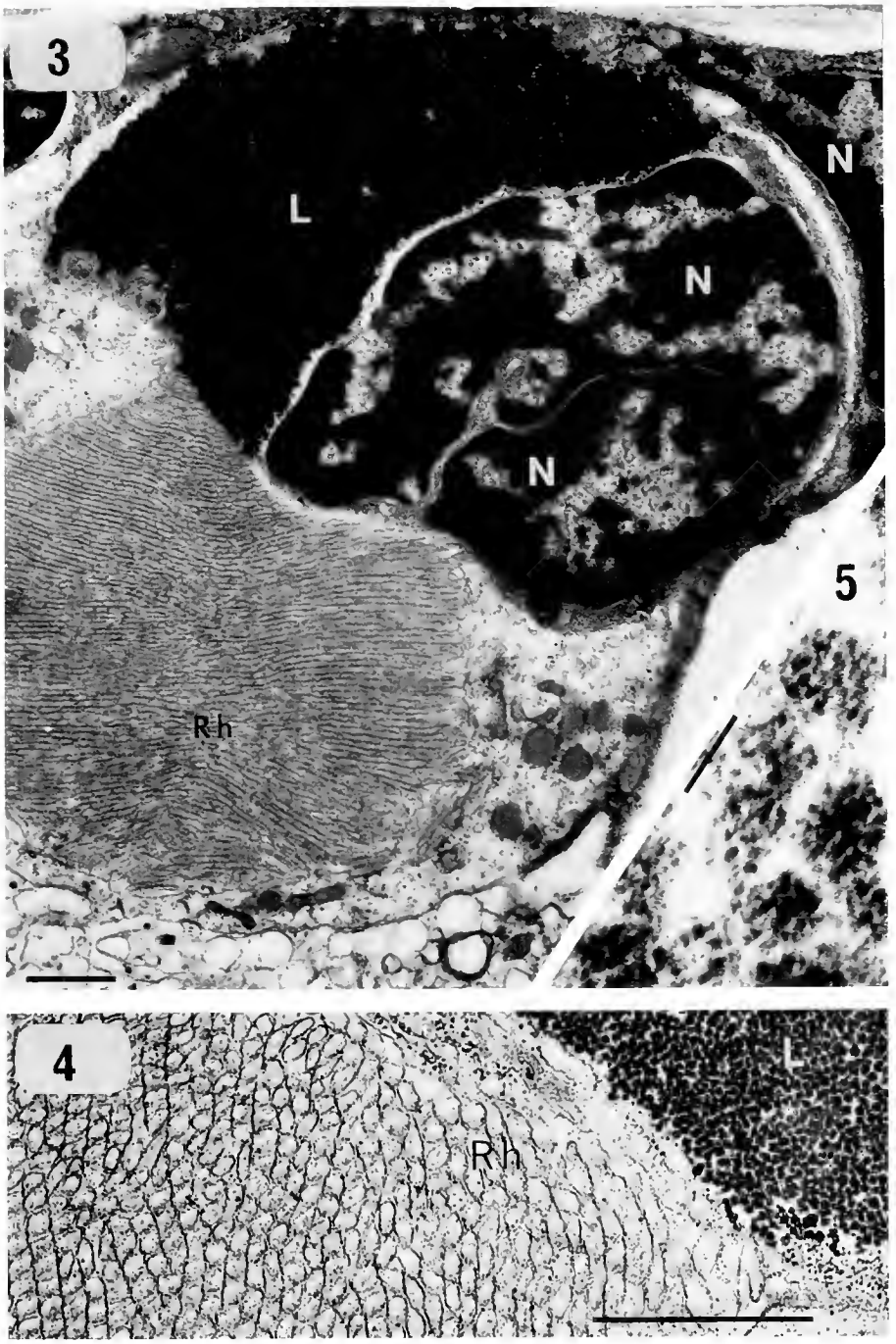

Figure 3. Oblique section through single lenticular complex (L), showing dense aggregations of glycogen-like particles and nuclei (N) as well as the regular alignment of microvilli in the distal portion of the rhabdom (Rh). Scale = 1 μm.

Figure 4. The borderline between lens (L) and rhabdom (Rh) is fuzzy, which should facilitate cell/cell interactions. Scale = 1 μm.

Figure 5. Each glycogen-like granule consists of a variable number of minute (approx. 5–6 nm), spherical subunits. Scale = 30 nm.

rids (*e.g.*, Amphipoda: Michel and Anders, 1954; Hallberg *et al.*, 1980; Meyer-Rochow, 1985; Mysidacea: Hallberg, 1977; Isopoda: Nilsson, 1983). Dark, ommochrome-containing screening pigment granules or melanosomes do not apparently exist in the eye of *D. rathkei,* but reflecting organelles do. The interstitial cells that surround

the retinula cells and isolate individual retinulae (Fig. 6), are crowded with reflecting vesicles of 0.7–0.8 μm in diameter which, on occasions, contained a protein skeleton.

A 14 μm [illegible] multitubular structure was seen in the optic ganglion. This could be mistaken for a rhabdom (Fig. [illegible] part of the organ of Bellonci' (Renaud-Mornant *et al.*, 1977). However, because of its proximity to glial cells, it probably represents a trophospongium (Scharrer, 1964; Eguchi and Meyer-Rochow, 1983). No further observations on it or the higher visual centers were made.

Dark/light adaptational changes. Fricke (1931) observed that the yellow pigment inside the retinula cells of *Cuma rathkei* was not stationary but had the ability to migrate towards or away (= up and down) from the lenticular apparatus. A dark-adapted eye, in which most of the carotenoid pigment is withdrawn and only the whitish reflecting organelles remain, changes within 4 minutes into the light-adapted condition upon exposure to daylight (Fricke, 1931). Ultrastructurally, at night the eye (Fig. 9) had considerably more voluminous rhabdoms than during the day (Fig. 8) and the diameters of the individual microvilli in the "night eye" were significantly enlarged over those of the "day eye" (*i.e.*, 0.09–0.125 μm *versus* 0.075 μm). A centrally placed cytoskeletal rod was also more obvious within the dark-adapted microvilli. An actual change in shape of the microvillar transverse profile upon dark and light adaptation, as claimed by Yoshida and Kaga (1983), was not seen.

The border between rhabdom and cytoplasm in the light adapted eye, however, gave the impression of greater jaggedness in comparison to the dark adapted condition. Also there were consistently more tiny ribosome-like dark particles and Golgi bodies in the cytoplasm of the light adapted eye (Fig. 8), and the endoplasmic reticulum was more obvious and more widely distributed. Longitudinally arranged microtubules, along which glycogen-like particles from storage areas near the proximally located retinula cell nuclei could possibly be transported and carotenoid pigment bodies could slide, were identified in both the dark and light adapted eyes (see discussion on transport mechanisms in the crustacean cell: Frixione *et al.*, 1979; Rao and Fingerman, 1983). However, large, empty cisternae and a lack of multi-vesicular and Golgi bodies were predominantly confined to the dark adapted cells. No obvious difference with regard to rise and abundance of mitochondria between dark and light adapted states was seen, but occasionally tiny vesicles (50 nm diameter) budded off the cristae in light adapted mitochondria.

Electrophysiology

Results were obtained from eight of ten animals tested. Responses were generally small and rarely reached the maximum amplitude of 360 μV, recorded in one animal to the highest available flash of white light. The ERGs were typical cornea-negative responses of the slow type with little or no positive component (Fig. 10) similar to the responses of the isopod *Porcellio loewis* (Benguerrah and Carricaburu, 1976).

The spectral response curves (Fig. 11) had but one smooth sensitivity peak in the vicinity of 512–549 nm. Responses to long ultraviolet radiation were down by one sensitivity log unit from the maximum, whereas to light of wavelengths greater than 600 nm the drop was even steeper. The curves of the 8 successfully tested animals were remarkably congruent and fitted a Dartnell nomogramme of a rhodopsin visual pigment with λ_{max} at 530 nm.

Intensity/response curves to light flashes of 472 nm, 549 nm, and 628 nm were, of course, horizontally shifted and had different maximal amplitudes. They shared more or less the same slope over the linear part of the curve with only the 628 nm curve being slightly less steep (Fig. 12). The fact that there was not even an obvious difference to the V/logI curve obtained by using flashes of white light is interpreted as evidence that there is only a single excitatory visual pigment present in the photoreceptor of *D. rathkei* and that the ERG-recordings correctly reflect the eyes' spectral capacity in the scotopic state.

Discussion

There is nothing about the overall anatomy or ultrastructure of the eye of *D. rathkei* that would preclude it from being functional photoreceptors. Absolute sensitivity is high and spectral sensitivity appears to match the downwelling spectrum of the prevalent light. In fact, the presence of internal lenses of a diameter close to 40 μm and a rhabdom only 20 μm away from the center of the lens would result in an F-number of only 0.5, indicative of considerable light-gathering power in each lenticular complex. We know little about the optical quality or properties of the lens, or whether a radial gradient of refractive index exists as, for example, in the eye of the aquatic beetle *Cybister* (Meyer-Rochow, 1973), that could produce a focus in the distal end of the rhabdom. However, even if the lenticular refractive index only "*liegt etwas uber dem des Seewassers*" (Fricke, 1931), each retinular complex in the eye of *D. rathkei* obtains a further boost in photon-capture from the all-abundant reflecting organelles.

Similarities in lenticular ultrastructure between *D. rathkei* and other arthropods exist. The tiny, compact clusters of electron-opaque particles making up the bulk of the lens or crystalline cones have repeatedly been claimed to represent glycogen material (Perrelet, 1970; Eakin and Kuda, 1971; Elofsson and Odselius, 1975).

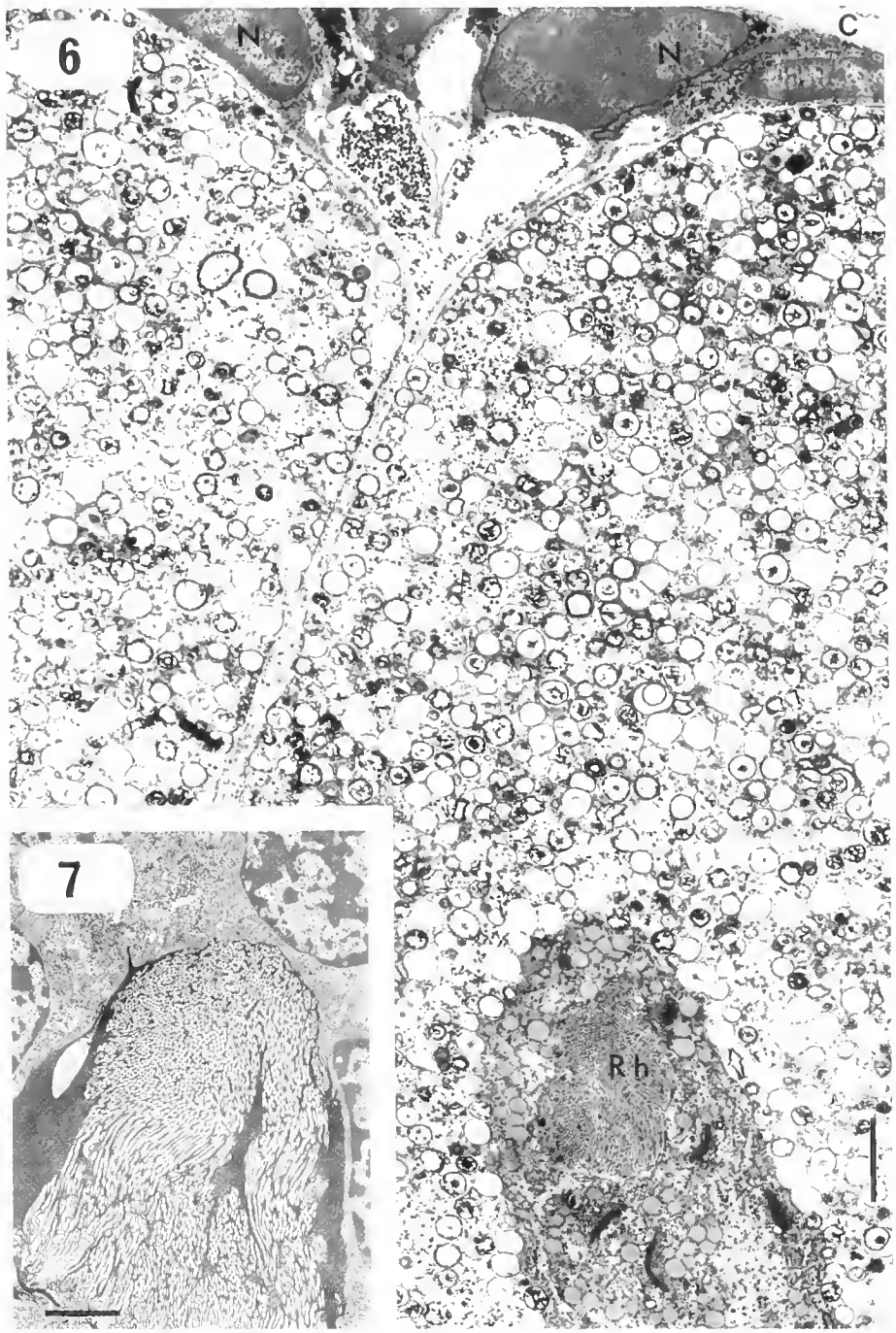

Figure 6. Inward-projecting narrow elongations of hypodermal cells (N), under the cuticle (C), separate the two eye halves, whose major components are cells that are crowded with circular vesicles which are thought to be reflecting in nature, to isolate individual retinular (Rh) complexes, and thus to improve photon capture. Scale = 2 μm.

Figure 7. A short distance behind the eye, this multi-tubular structure, at first glance resembling a rhabdom and probably identical to what Ståhl (1938) interpreted as the "X-organ" in the eye-bladder of *D. rathkei*, was located. Scale = 2 μm.

The granular fine structure in the center of the crystalline cone in the eye of the mantis *Ciulfina* resembles that of the *D. rathkei* lens, but Horridge and Duelli (1979) state that "the crystalline cone in histological and electron microscope sections is obviously made of material that is richer in protein than the surrounding tissue." Be this as it may, there seems little controversy about the chemical nature of the intracellular 'islands' of granular inclusions

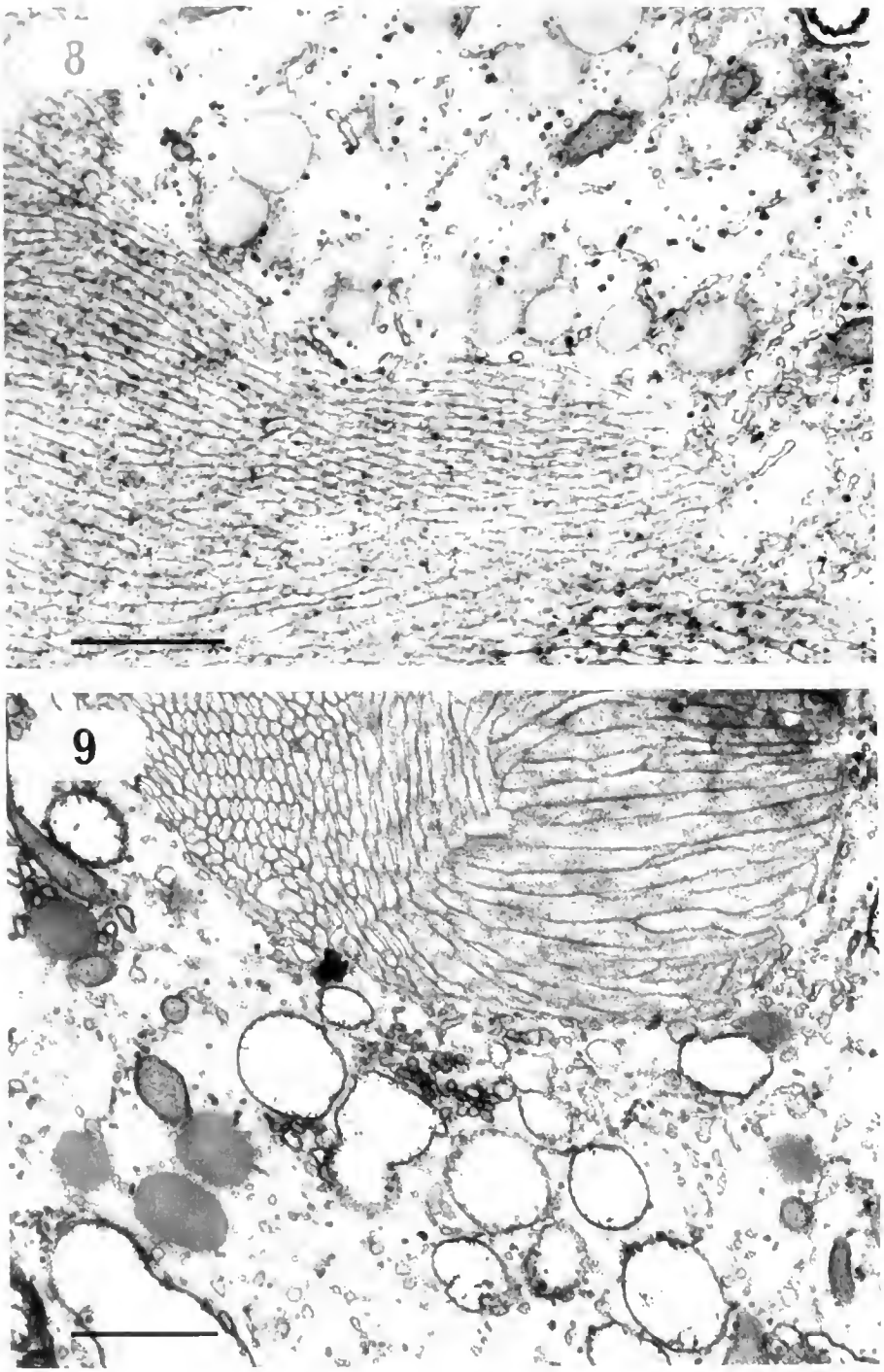

Figure 8. In the light adapted condition the total rhabdom volume is reduced, carotenoid organelles migrate towards the rhabdom edge, and microvilli are 75 nm in diameter. Scale = 1 μm.

Figure 9. In the dark adapted eye the rhabdom volume is enlarged, electron-empty cisternae instead of carotenoid bodies are more numerous around the edge of the rhabdom, and microvillus diameters have become noticeably wider and more variable. Scale = 1 μm.

near the retinula cell nuclei, for they are identical to those reported from the eye of the tick *Amblyomma americanum* (Ill and Cromroy, 1977) and intracerebral ocelli of several species of isopods, in which specific glycogen tests revealed their true character (Martin, 1976). The great abundance of tiny black particles in virtually the

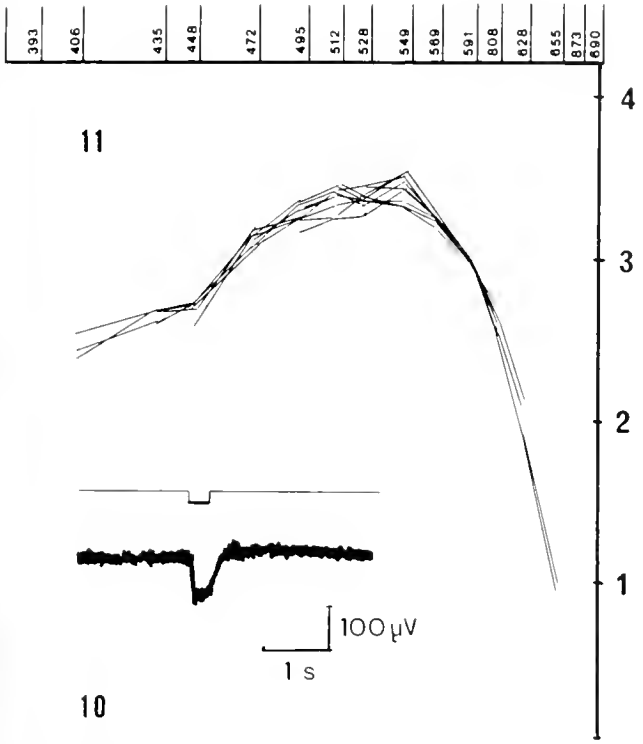

Figure 10. The extracellularly recorded ERG responses are cornea-negative potential changes with little or no positive component.

Figure 11. The superimposed spectral response curves of eight animals based on a criterion response of 50 µV, clearly demonstrate a single sensitivity peak in the range of 512–549 nm wavelengths.

entire retinula cell plasma of the light-adapted eye suggests the involvement of glycogen as an energy source during the energy consuming process of light perception (Hamdorf and Kaschef, 1964; Evequoz *et al.*, 1983). The hypertrophied nature of the endoplasmic reticulum is consistant with, and probably signifies, intense visual pigment synthesis.

The unquestionable increase in microvillus diameter during dark adaptation is somewhat surprising as this would offset the possible gain in sensitivity made by an overall enlargement of rhabdom volume. However, increases in microvillus diameters of a similar magnitude under dark conditions have been reported (Nässel and Waterman, 1979) in the crab *Grapsus grapsus*, in *Gryllus bimaculatus* (Hoff, 1985), and can also be calculated from electron micrographs on the eye of the brine shrimp *Artemia salina* (Hertel, 1980). They are also in agreement with observations by Yoshida and Kaga (1983) if we assume that their "dumbbell-shaped" microvilli in the light-adapted condition actually represented an oblique section through two rows of microvilli. Yoshida and Kaga (1983) state that in the cumacean *Dimorphostylis asiatica* the change from the 30–50 nm wider dark adapted to the narrower light adapted microvillar ultrastructure is completed in 10 minutes at 130 lux illumination, but that it requires 3 times longer in reverse. Although not specifically tested in *D. rathkei*, this time course would agree with pigment granule displacements in arthropods that display such dark/light adaptational changes (Meyer-Rochow and Horridge, 1975; Frixione *et al.*, 1979; Hallberg *et al.*, 1980).

The reasons as well as the trigger for *D. rathkei* to occur more frequently in the plankton at certain times of the year (Valentin, pers. comm.) are not fully understood. However, in agreement with crustacean larvae with adults living lower intertidally (Forward and Cronin, 1979), the spectral response curves in *D. rathkei* lack a strong UV-component and resemble those of the barnacle *Balanus amphitrite* (Stratten and Ogden, 1971). According to Stratten and Ogden (1971) an increase in the slope of the response/intensity function points to increased light adaptation. It also narrows the spectral response curve if only a single photopigment is present. This means then that in addition to the filtering properties of the cuticle and lens, the self-screening of the rhabdom and the transmission characteristics of the screening pigments (see also discussions in Goldsmith, 1978, and Meyer-Rochow and Eguchi, 1984), the changing environmental light intensity, not only between day and night, but also between different seasons, must affect the shape of the spectral response curve. That seasons, time of day, and temperature affect the shape of the spectral response curves in various species of crustaceans, has indeed been shown (Nosaki, 1969; Meyer-Rochow and Eguchi, 1984; Hariyama *et al.*, 1986).

The eye of *D. rathkei*, at least when dark adapted, seems useless as an analyzer of color or as an image-

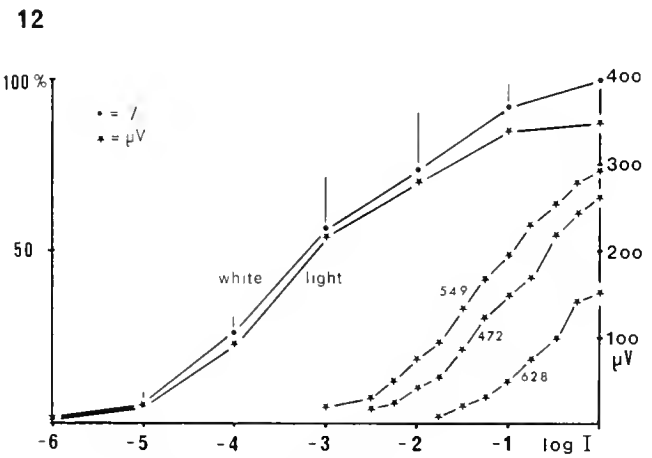

Figure 12. Normalised intensity/response curves (dotted) and responses in µV (ordinate on the right) to flashes of white light and light of 472, 549, and 628 nm wavelength. The slopes of the V/logI functions are identical apart from that of the 628 nm curve which is slightly less steep.

forming photoreceptor. However, it is quite capable of registering small changes in the quantity and quality of environmental light. Thus it must be of some use to the animal, even though the latter spends most of its life buried in the sand (Kaestner, 1959). Segerstråle (1970) invoked photoreception and not the perception of environmental temperature *per se* as the principal agent involved in the coordination of reproduction in the Baltic Sea amphipod *Pontoporeia affinis*. *P. affinis* eyes are also tiny and consist of no more than 30–40 facets (Donner, 1971). Our study of the eye of *D. rathkei* suggests that photoreceptive properties and changes of the latter, perhaps in conjunction with the seasonal fluctuation of consumed carotenoids (Czeczuga, 1980), could be equally important in Cumacea. One could speculate that they are involved in coordinating vertical migrations and synchronising mating activities.

Acknowledgments

The authors thank the Alexander von Humboldt Foundation (Bonn, West Germany) and the Finnish Academy of Sciences for the support rendered towards this project in Germany and Finland, respectively. Further, V. B. Meyer-Rochow acknowledges the help of Dr. Stephan (University of Kiel, W. Germany) and the crew of research cutter "Alkor" in catching the animals, and he is indebted to the Meat Industry Research Institute of New Zealand for making available electron microscope facilities. Finally V. B. Meyer-Rochow expresses his gratitude to Professor Dr. W. Noodt and the staff of the Zoological Museum (University of Kiel) for their fine hospitality.

Literature Cited

Bacescu, M. 1951. *Nannastacus euxinicus* n.sp. Cumaceu nou gasit in apele marii negre. *Communic. Acad. Rep. Pop. Rumania* **1:** 582–592.

Benguerrah, A., and P. Carricaburu. 1976. L'électrorétinogramme chez les crustacés isopodes. *Vision Res.* **16:** 1173–1177.

Czeczuga, B. 1980. Changes occurring during the annual cycle in the carotenoid content of *Gammarus lacustris* G. O. Sars (Crustacea: Amphipoda) specimens from the river Narew. *Comp. Biochem. Physiol.* 66B: 569–572.

Donner, K. O. 1971. On vision in *Pontoporeia affinis* and *P. femorata* (Crustacea, Amphipoda). *Commentat. Biol.* **41:** 1–17.

Donner, K. O., and V. Lindström. 1980. Sensitivity to light and circadian activity in *Pontoporeia affinis* (Crustacea, Amphipoda). *Ann. Zool. Fenn.* **17:** 2[illegible]

Eakin, R. M., and A. Kuda. 1972. Glycogen in lens of tunicate tadpole. *J. Exp. Zool.* **180:** [illegible]70)

Eguchi, E., and V. B. Meyer-Rochow. 1983. Trophospongium-like structures in an insect eye: response of retinula cells of *Papilio xuthus* (Lepidoptera) to irradiation with ultraviolet light. *Cell Tissue Res.* **231:** 519–526.

Elofsson, R., and E. Hallberg. 1973. Correlation of ultrastructure and chemical composition of crustacean chromatophore pigment. *J. Ultrastruc. Res.* **44:** 421–429.

Elofsson, R., and R. Odselius. 1975. The anostracan rhabdom and the basement membrane—an ultrastructural study of the *Artemia* compound eye. *Acta Zool.* **56:** 141–153.

Evequoz, V., A. Stadelmann, and M. Tsacopoulos. 1983. The effect of light on glycogen turnover in the retina of the intact honeybee drone (*Apis mellifera*). *J. Comp. Physiol.* **150:** 69–75.

Forsman, B. 1938. Untersuchungen über die Cumaceeen des Skageraks. *Zool. Bid. Upp.* **18:** 1–162.

Forward, R. B., and T. W. Cronin. 1979. Spectral sensitivity of larvae from intertidal crustaceans. *J. Comp. Physiol.* **133:** 311–315.

Fricke, H. 1931. Die Komplexaugen von *Diastylis rathkei*. *Zool. Jahrb. Abt. Anat. Ontogenie Tiere* **53:** 701–724.

Frixione, E., H. Arechiga, and V. Tsutsumi. 1979. Photomechanical migrations of pigment granules along the retinula cells of the crayfish. *J. Neurobiol.* **10:** 573–590.

Fryer, G. 1967. IV—Studies on the functional morphology and feeding mechanism of *Monodella argentarii* Stella (Crustacea: Thermosbaenaceae). *Trans. R. Soc. Edinb.* **66:** 49–90.

Goldsmith, T. H. 1978. The spectral absorption of crayfish rhabdoms: pigment, photo-product, and pH-sensitivity. *Vision Res.* **18:** 463–473.

Hallberg, E. 1977. The fine structure of the compound eyes of mysids (Crustacea: Mysidacea). *Cell Tissue Res.* **184:** 45–65.

Hallberg, E., M. Andersson, and D.-E. Nilsson. 1980. Responses of the screening pigments in the compound eye of *Neomysis integer* (Crustacea: Mysidacea). *J. Exp. Zool.* **212:** 397–402.

Hallberg, E., H. L. Nilsson, and R. Elofsson. 1980. Classification of amphipod compound eyes—the fine structure of the ommatidial units (Crustacea, Amphipoda). *Zoomorphology* **94:** 279–306.

Hamdorf, K., and A. H. Kaschef. 1964. Der Sauerstoffverbrauch des Facettenauges von *Calliphora erythrocephala* in Abhängigkeit von der Temperatur und dem Ionenmilieu. *Z. V. Physiol.* **48:** 251–265.

Hariyama, T., V. B. Meyer-Rochow, and E. Eguchi. 1986. Diurnal changes in structure and function of the compound eye of *Ligia exotica* (Crustacea; Isopoda). *J. Exp. Biol.* **123:** 1–26.

Hertel, H. 1980. The compound eye of *Artemia salina* (Crustacea). I: Fine structure when light and dark adapted. *Zool. Jahrb. Physiol.* **84:** 1–14.

Hoff, R. 1985. Diurnal ultrastructural changes in the compound eye of *Gryllus bimaculatus* (Orthoptera, Grylloideal) in particular the dorsal rim area. *Zool. Beitr.* **29:** 87–102.

Horridge, G. A., and P. Duelli. 1979. Anatomy of the regional differences in the eye of the mantis *Ciulfina*. *J. Exp. Biol.* **80:** 165–190.

Hu, W. A. P., and H. L. Cromroy. 1977. The microanatomy of the eye of *Amblyomma americanum* (Acari: Ixodidae) and resultant implications of its structure. *J. Med. Entomol.* **13:** 685–698.

Kaestner, A. 1959. *Lehrbuch der Speziellen Zoologie Teil I: Wirbellose.* VEB Gustav Fischer Verlag, Jena.

Lindström, M., and V. B. Meyer-Rochow. 1987. Near infra-red sensitivity of the eye of the crustacean *Mysis relicta*? *Biochem. Biophys. Res. Commun.* **147:** 747–752.

Lindström, M., and H. L. Nilsson. 1983. Spectral and visual sensitivities of *Cirolana borealis* Lilljeborg, a deep-water isopod (Crustacea: Flabellifera). *J. Exp. Mar. Biol. Ecol.* **69:** 243–256.

Martin, G. 1976. Nouvelles donnés ultrastructurales sur les yeux et les ocelles médians de deux d'épicarides (Crustacés isopodes). *Bull. Soc. Zool. Fr.* **101:** 457–464.

Mayrat, A. 1981. Nouvelle définition des yeux simples et composés chez les arthropodes. Le cas des amphipodes et des cumacés. *Arch. Zool. Exp. Gén. Notes Rev.* **12:** 225–236.

Meyer-Rochow, V. B. 1973. The dioptric system of the eye of *Cybister* (Dytiscidae: Coleoptera). *Proc. R. Soc. Lond.* **183B:** 159–178.

Meyer-Rochow, V. B. 1985. A study of unusual intracellular organelles and ultrastructural organisation of the eye of *Gammarus oceanicus* (Segerstråle 1947) fixed in the midnight sun of the Spitsbergen (Svålbard) summer. *Biomed. Res.* **6:** 353–365.

Meyer-Rochow, V. B., and E. Eguchi. 1984. The effects of temperature and light on particles associated with crayfish visual membrane: a freeze-fracture analysis and electrophysiological study. *J Neurocytol.* **13:** 935–959.

Meyer-Rochow, V. B., and G. A. Horridge. 1975. The eye of *Anoplognathus* (Coleoptera, Scarabaeidae). *Proc. R. Soc. Lond.* **188B:** 1–30.

Michel, A., and F. Anders. 1954. Über die Pigmente in Auge von *Gammarus pulex*. *Naturwissenschaften* **41:** 72.

Nässel, D. R., and T. H. Waterman. 1979. Massive diurnally modulated photoreceptor membrane turnover in crab light and dark adaptation. *J. Comp. Physiol.* **131:** 205–216.

Nilsson, D.-E. 1983. Evolutionary links between apposition and super-position optics in crustacean eyes. *Nature* **302:** 818–821.

Nosaki, H. 1969. Electrophysiological study of colour encoding in the compound eye of crayfish. *Procambarus clarkii*. *Z. V. Physiol.* **64:** 318–323.

Perrelet, A. 1970. The fine structure of the retina of the honeybee drone. *Z. Zellforsch.* **108:** 530–562.

Rao, K. R., and M. Fingerman. 1983. Regulation of release and mode of action of crustacean chromatophorotropins. *Am. Zool.* **23:** 517–527.

Renaud-Mornant, J., J. Pochon-Masson, and J. Chaigneau. 1977. Mise en évidence et ultrastructure d'un organe de Bellonci chez un crustacé Mystacocaride. *Ann. Sci. Nat. Zool. Biol. Animale.* 12e series, **19:** 459–478.

Scharrer, E. 1964. A specialized trophospongium in large neurons of *Leptodora* (Crustacea). *Z. Zellforsch.* **61:** 803–812.

Segerstråle, S. G. 1970. Light control of the reproductive cycle of *Pontoporeia affinis* Lindström (Crustacea, Amphipoda). *J. Exp. Mar. Biol. Ecol.* **5:** 272–275.

Siewing, R. 1956. Morphologische Untersuchungen an Cumaceen (*Cumopsis goodsiri* v. Beneden). *Zool. Jahrb. Anat. Ontogenie Tiere* **72:** 522–559.

Ståhl, F. 1938. Preliminary report on the colour changes and the incretory organs in the heads of some crustaceans. *Ark. Zool.* **30B:** 1–3.

Stratten, W. P., and T. E. Ogden. 1971. Spectral sensitivity of the barnacle eye, *Balanus amphitrite*. *J. Gen. Physiol* **57:** 435–447.

Yoshida, M., and K.-I. Kaga. 1983. Photoinduced ultrastructural changes in microvilli of a cumacea *Dimorphostylis asiatica*. *Zool. Mag.* **92:** 529.

Zimmer, C. 1941. Cumacea. Pp. 1–222 in *Bronn's Klassen & Ordnungen des Tierreichs*, Vol. 5(4). Akad. Verlagsges, Leipzig.

Reference: *Biol. Bull.* 175: 154–166. (August, 1988)

Inorganic Aspects of the Blood Chemistry of Ascidians. Ionic Composition, and Ti, V, and Fe in the Blood Plasma of *Pyura chilensis* and *Ascidia dispar*

DOMINGO A. ROMAN, JUSTA MOLINA, AND LIDIA RIVERA

Departamento de Química, Facultad de Ciencias Básicas, Campus Coloso, Universidad de Antofagasta, Casilla 1240 Antofagasta, Chile

Abstract. Iron, titanium, and vanadium analysis were performed on the tunicates *Pyura chilensis* Molina, 1782, and *Ascidia dispar*, and the inorganic chemistry of blood was investigated. The major ionic characterization of the blood plasma and cytosolic solutions were determined. Gel chromatography was used to secure information on the possible existence of metal organic complexes.

Pyura chilensis accumulates Fe and Ti, and *Ascidia dispar* accumulates Fe, Ti, and V in blood cells in this quantitative order. Significant levels of metals are associated with cell residues (membrane cells), although this may be, to some extent, dependent on the cell lysis technique.

The elution behavior of plasma in Sephadex G-75 and LH-20 gels and the respective absorption spectra of the fractions showed evidence of organic metal complexes in the plasma of both tunicate species.

Introduction

For years tunicates have piqued the curiosity of biologists because of their unusual physiological peculiarities and because they may have given rise to the vertebrates (Berril, 1955). Among the physiological peculiarities that distinguish these organisms from others are the following: (i) They need a low tension of oxygen (Goodbody, 1974). To date, no reversible binding of oxygen has been detected nor the unequivocal existence of a proteic O_2 transport compound that transports O_2 through the blood (Macara *et al.*, 1979a; Agudelo *et al.*, 1982). (ii) They are entirely ammonotelic in their protein metabolism, but are uricotelic with respect to nucleic acid metabolism. Therefore, they differ from most invertebrates that are wholly ammonotelic, accumulating uric acid and purines in nephrocyte vacuoles (Goodbody, 1974; Wright, 1981). The functional importance of this storage remains obscure. (iii) They are capable of humoral and cellular immunological responses (Wright, 1981) and are rich in bio-active substances (Roman, 1986). (iv) They accumulate metal ions.

With respect to metal ions, tunicates are known for the uptake of selected metals from seawater and for accumulating them in their blood (Carlisle, 1968; Swinehart *et al.*, 1974; Senozan, 1974; Biggs and Swinehart, 1976). Members of the order Enterogona can accumulate vanadium (Kustin *et al.*, 1975; Kustin and McLeod, 1977; Macara *et al.*, 1979b; Biggs and Swinehart, 1979; Botte *et al.*, 1979; Dingley *et al.*, 1981; Hori and Michibata, 1981; Rowley, 1982; Dingley *et al.*, 1982). However, the type of coordination compound(s) in which the metal is involved in the blood is unknown (Carlson, 1975; Tullius *et al.*, 1980; Dingley *et al.*, 1982; Hawkins *et al.*, 1983a; Bruening *et al.*, 1985; Frank *et al.*, 1986). Members of the order Pleurogona, sub-order Stolidobranchiata, accumulate iron (Endean, 1955a, b, c; Agudelo *et al.*, 1982; Agudelo *et al.*, 1983a, b; Agudelo *et al.*, 1985), but nothing is known about its function in blood cells (Hawkins *et al.*, 1983b). In plasma, iron is associated with transferrin-like metalloproteins (Martin *et al.*, 1984; Finch and Huebers, 1986).

Hawkins *et al.* (1983c) proposed that ascidian taxonomy reflects a separation into vanadium- and iron-containing species. Tunicates accumulate other metals besides vanadium and iron (Monniot, 1978; Macara *et al.*, 1979c; Agudelo *et al.*, 1981; Rowley, 1982), which may

Received 6 July 1987; accepted 20 May 1988.

not be essential elements subjected to selective accumulation mechanisms. Sessile filter feeding animals are very sensitive to their immediate environment, and significant amounts of contaminating metallic elements could be taken up by ascidians (Papadopoulou and Kanias, 1977).

In processes in which metals are accumulated in blood cells, it is logical that metals make a transient or permanent appearance in blood plasma. Once metals gain access to the body interior, they must be appropriately distributed, but because of its hydrolysis property some of these metals cannot be held in solution, in the interior media, without some mechanism to prevent its precipitation.

No metalloproteins such as hemocyanin have been reported in ascidian blood plasma. However, Hawkins *et al.* (1980a) and Webb and Chrystal (1981) studied the metal binding properties—including spectral characterization and metal contents—of some tunicates (Hawkins *et al.*, 1980b). They found preliminary evidence of metal complexing. This was confirmed by Martin *et al.* (1984) in the plasma of *Pyura stolonifera,* by demonstrating an iron-binding protein of about 40,000 daltons molecular weight with one iron-binding site considered as one *Pyura* transferrin (Finch and Huebers, 1986).

In this work, the Ti, V, and Fe contents were determined in several tissues. Also, the major characterization and chromatographic elutive behavior on Sephadex G-75 and LH-20 gels of *Pyura chilensis* Molina, 1782, and *Ascidia dispar* blood plasma were examined. These are two phylogenetically diverse ascidians.

Materials and Methods

Chemicals were from Merck. 3,3'-dimethylnaphthidine was from Eastman organic chemicals and ophenanthroline hydrochloride was from Riedel-De Haen. Sephadex G-75, LH-20 gels and blue dextran 2000 were from Pharmacia Fine Chemicals. Deionized water was prepared from distilled water passed through a disposable demineralizer cartridge (Corning 3508-B).

Specimens of *P. chilensis* and *A. dispar* were collected at Bahía Mejillones del Sur (Antofagasta-Chile) from marine pools, in which they were found as encrusting fouling organisms. *P. chilensis* afixes itself to ropes while *A. dispar* attaches itself to painted floating metallic barrels where they coexist with hydrozoans and bryozoans. Before drawing blood, specimens were maintained for some time in seawater at room temperature, and then were gently squeezed to remove most of the seawater.

Blood samples of both species were obtained by cutting the base of the body. Blood cells were removed from the plasma by centrifuging (2500 rpm; 10 min). Plasma was kept at 4–5°C while carried to the laboratory and was used as soon as possible.

Cellular residues presumably consisted of cell membranes. No distinction was made between cell surface and intracellular membranes. Cell samples were rinsed with seawater and then subjected to two different cell lysis processes. In the first procedure, cells were subjected to three freeze-thaw cycles in deionized water media (1.4 parts of triturated ice + 2 parts of $CaCl_2 \times 6H_2O$ freeze/room temperature), gently squeezed with a cell teflon homogenizer, and then centrifugated at 8000 rpm. In the second procedure cells were subjected twofold to an excess of methanolic solution of 0.75% HCl (Hawkins, pers. comm.) and centrifuged at 8000 rpm. In both cases the cytosolic solution and methanolic extract were made up to the original volume from which the cells were obtained. Whole blood samples of *P. chilensis* were subjected to the first cell lysis procedure, but without deionized water. A Sorvall refrigerated centrifuge was used.

Metal analysis

Prior to the Ti, V, and Fe determinations in specimens and tissues, a qualitative analysis was performed on digested blood cells. Cells rinsed with microfiltered seawater were digested with binary $HNO_3/HClO_4$ acid system (Jones *et al.*, 1982), performing assays for Cu, Mn, Fe, Ni, Co, Ti, V, and Nb (Feigl and Anger, 1972). Mn and Fe were also subjected to semi-quantitative assays with Merkoquant sticks.

Pyura chilensis and *Ascidia dispar* were analyzed individually. Tissues including blood were obtained from 10–20 specimens of *P. chilensis* and 30–50 specimens of *A. dispar.* Bodies were separated from tunics and rinsed with filtered seawater. Tunics were gently scrubbed with a plastic brush to remove dirt and rinsed in a similar manner. Siphons and tunics were cut off with a hard acrylic knife. Specimens and tissues, including some samples of plasma, cells, and cellular residues, were then dried at 110°C to constant weight, digested with a binary acid procedure (Jones *et al.*, 1982), and then treated according to the respective metal analysis.

In tissues, iron was determined with 1,10-phenanthroline (Sandell, 1959; Fries, 1972), and Ti and V were separated (Korkisch, 1969; Fukasawa and Yamane, 1977) prior to their determinations. Titanium was determined according to Qureshi *et al.* (1968), and vanadium using the methods of Bannard and Burton (1968) and Fukasawa and Yamane (1977). In the fractions, iron was determined using 2,4,6-tri-2 pyridyl-1,3,5-triazine (Collins *et al.*, 1959; Box, 1981), and vanadium and titanium as above, without separating them after digestion of the fractions with a binary $HNO_3/HClO_4$ acid system (Jones *et al.*, 1982).

Blank controls were used in every metal analysis, and except in the fractions, all the determinations were performed in triplicate.

Determination of the major ionic composition and relative reduced feature of the fluids

Chlorinity and salinity were determined conductimetrically with respect to standard seawater at 25°C (conductimeter Radiometer CDM 2e, with a standard cell CDC 104). Chloride was determined by Mohr titration and sulphate by direct titration with barium perchlorate using Thorin as indicator. Subsequently, cations were removed by passing the sample through a strong acid cation exchange resin column (Fritz and Yamamura, 1955), except in seawater in which case sulphate was determined gravimetrically as $BaSO_4$. Successive determination of calcium and magnesium were made by potentiometric titration with a calcium ion selective electrode (Roman *et al.*, 1982); Na, K, and Li analysis were performed by flame emission spectrophotometry on a Radiometer FLM-3; pH measurements were made potentiomatrically on a Radiometer pH Meter 26 with glass membrane electrode. All major component determinations were made in triplicate.

The relative reduced feature of the plasma and cytosolic solutions were tested by two redox potentiometric titrations (non-standard biochemical methods). In the first, aliquot samples (10–20 ml) in polypropylene vessel were put into a Radiometer TTA-80 titration assembly, acidified with 0.75% HCl, and then titrated with a standard solution 0.1 *N* $KMnO_4$. In the second, aliquot samples (10–20 ml) were acidified with 2 ml of concentrated $HClO_4$, treated with 5 ml of a standard solution 0.1 *N* $K_2Cr_2O_7$, and then titrated with a standard solution of Fe(II).

Chromatographic fractionation of blood plasma

Fractionations were performed on Sephadex G-75 and LH-20 gels, in thermostated chromatography columns (Pharmacia Fine Chemicals K26/40) loaded with 4 g of Sephadex G-75 and 13 g of Sephadex LH-20, respectively. The column temperature was 20°C, but all samples and eluants were cooled at 4–5°C. Plasma samples were concentrated by freeze-dry (Freezer-dryer-5 Labconco), five-fold for *P. chilensis* and two-fold for *A. dispar* before running the chromatography procedures. The void volume of the column (V_0) was determined using blue dextran-2000, and the bed volume (V_t) was calculated according to the height and diameter of the gel column.

In G-75 chromatography the sample volumes were 6 and 10 ml for *A. dispar* and *P. chilensis;* the eluants were 0.01 *M* NaCl and 0.06 *M* acetic acid, respectively, cooled and deaereated, collecting fractions of 10 ml (plasma of *A. dispar*) and 6 ml (plasma of *P. chilensis*). The absorbance at 278, 288, 310, 375, 454, and 675 nm (plasma of *P. chilensis*), 265 and 322 nm (plasma of *A. dispar*), and the metal analysis in all fractions were monitored with respect to eluant solutions, previously passed through the respective column, as reference or blank, respectively.

In LH-20 chromatography, to minimize inhomogeneities in the column the gel was packed after swelling in deaereated methanol. One bed volume column of each of the following eluants: water, 25, 50 and 75% methanol in water (v/v), were then passed through the column, followed by 99.8% methanol, collecting two 10 ml fractions per eluant for use as reference or blank solutions. The column was then loaded with the sample (10 ml). Chromatography was performed using 1.5 bed volume of each cooled deaereated methanol/water gradient from 0 to 99.8% methanol according to Macara *et al.* (1979b), collecting 6 ml (plasma chromatography of *P. chilensis*) and 10 ml (plasma chromatography of *A. dispar*) fractions. Absorbance at 272, 288, 310, 320, 375, 454, and 675 nm (plasma of *P. chilensis*), 266, 280, 326 and 660 nm (plasma of *A. dispar*), and metal analysis in all fractions were monitored. Ultra-violet and visible spectra were recorded for whole plasma and the peak-fractions from the eluting patterns, employing a Beckman 35 spectrophotometer. All other absorciometric measurements were also made using this instrument.

Results

Metal analysis

Metal concentrations found on specimens and various tissues of tunicates are listed as mg/Kg dry weight (Table I). Concentrations for plasma are given in mg/l. Ni, Co, Mn, and Nb were not detected in blood cells. Higher concentrations of iron and titanium, and iron, titanium, and vanadium were found in *P. chilensis* and *A. dispar* blood cells, respectively. Although V was not detected in *P. chilensis* blood cells and was found in *A. dispar* blood cells, only trace levels of it were found in both blood plasmas. Ti was not detected in *P. chilensis* blood plasma.

Results of the metal analysis in cell lysate (cytosolic solution), calculated by the difference between the metal contents in whole blood cells and in blood cell residues, are tabulated as percentage of metals in Tables IIa, b, c, respectively. Here, the cellular residues were not washed with acid prior to analysis. Aqueous and 0.75% HCl/methanol cell lysis procedures were considered (*P. chilensis*). These results show that iron content in cell residues from aqueous and HCl/methanol cell lysis procedures are low and comparable, but the titanium content, surprisingly, was higher and greater in the cellular residues than in the cytosolic solution for both cell lysis procedures, but higher in cell residues from HCl/methanol lysis method. Therefore, it is possible that metallic precipitation by extensive hydrolysis (Agudelo *et al.*, 1983b,

Table I

Relative distribution of Fe, Ti, and V contents (mg/kg dry) in Pyura chilensis *and* Ascidia dispar

	P. chilensis			*A. dispar*		
	Fe	Ti	V	Fe	Ti	V
Specimen	191.8	n.d.	n.d.	94.1	107.2	25.7
Body (without tunic)	84.3	n.d.	n.d.	717.4	53.1	25.4
Siphons	70.7	n.d.	n.d.	86.4	16.2	34.8
Tunic	243.9	n.d.	1.5	74.3	125.6	0.4
Blood plasma	45.0	n.d.	1.9	93.7	61.4	22.0
	[a](1.5	n.d.	0.06	2.9	2.1	0.8)
Blood cells	1,105.4	277.8	n.d.	2,181.5	1,552.5	692.9
Blood cell residues[b]	7.4	132.8	n.d.	586.4	784.1	163.7
Blood cell residues[c]	17.3	258.9	n.d.	d	d	d

[a] mg/l; [b]from lysed cell preparations produced by subjecting the cell samples to several freeze-thaw cycles in deionized water media and then centrifuging them at 8000 rpm; [c]from lysed cell preparations produced by subjecting the cell samples to treatment with methanolic solution of 0.75% HCl centrifuging them at 8000 rpm; [d]not determined; n.d. = not detected.

1985) may have been minimized during water cell lysis in the conditions of this work. Thus, it appears that more attention should be focused on tunicate blood cell lysis procedures.

Table IIa

Relative iron distribution in blood cells as determined in pooled samples

Species	Cytosolic[d,e] solution	Cell residues
P. chilensis	99.3%	0.7%
P. chilensis	98.4%[f]	1.6%[f]
A. dispar	73.1%	26.9%

Table IIb

Relative titanium distribution in blood cells as determined in pooled samples

P. chilensis	52.2%	47.8%
P. chilensis	6.8%[f]	93.2%[f]
A. dispar	49.5%	50.5%

Table IIc

Relative vanadium distribution in blood cells as determined in pooled samples

A. dispar	76.4%	23.6%

[d] Calculated by difference between contents in whole blood cells and in blood cells residues (Table I); [e]in respect to lysed cells preparations produced by subjecting the cell samples to several freeze-thaw cycles in deionized water media/centrifuging them at 8000 rpm; [f]with respect to lysed cell preparations produced by subjecting the cell samples to treatment with a methanolic solution of 0.75% HCl/centrifuging them at 8000 rpm.

Ion composition and reduced tendency of blood fluids

The pH and ionic composition of plasma, lysed whole blood, and cytosolic solutions, for both species, are shown in Tables III and IV. The sulphate content in *A. dispar* plasma was greater than in *P. chilensis*, but both contents were lower than in seawater. In the cytosolic solutions, *e.g.*, aqueous intracellular media, the concentrations of sulphate were low with respect to the plasma. Calcium and magnesium contents in *P. chilensis* plasma are higher than in *A. dispar*. In *P. chilensis* some enrichment occurred with respect to seawater, which also occurs for sodium and potassium. Calcium, magnesium, sodium, and potassium contents also were lower in whole lysed blood than in plasma (*P. chilensis*). In *P. chilensis* blood cells, the sodium concentration in the cytosolic solution is only 50% of the *A. dispar* cytosolic solution. However, potassium concentration is very low.

The pH of the whole lysed blood (*P. chilensis*) was nearly alkaline, the salinity almost equal to the seawater from which the specimens were obtained. The sulphate concentration was only 62% of its concentration in blood plasma.

Plasmas, 0.75% HCl/methanolic extracts from blood cells, and cytosolic solutions had reducing tendency in both species in respect to dichromate and permanganate, respectively.

Spectral-separative chromatographic behavior of iron, titanium, and vanadium in plasma

P. chilensis plasma is pink-orange and *A. dispar* plasma is greenish-yellow. Figure 1 shows the UV-visible spectra of both species' plasma. The bands 265–290, 300–330, and 675 nm regions were common to both

Table III

Ionic composition of the plasma of Pyura chilensis *and* Ascidia dispar

	Plasma *P. chilensis*	Plasma *A. dispar*	Surface coastal seawater[a]
Chlorinity ‰	19.38	18.64	19.44
Salinity ‰	32.35	33.67	35.13
Cl⁻ (g/l)	19.86	19.05	19.51
SO_4 (g/l)	0.60	0.79	2.60
Ca^{2+} (g/l)	0.51	0.34	0.44
Mg^{2+} (g/l)	1.54	1.14	1.33
Na^+ (g/l)	15.68	9.34	11.16
K^+ (g/l)	0.78	0.42	0.40
Li^+ (mg/l)	0.87	0.84	1.32
pH	6.77	6.48	8.03
Na/K	0.33	0.30	0.23
Ca/Mg	20.10	22.20	27.90

[a] Surface coastal seawater of Bahía Mejillones del Sur.

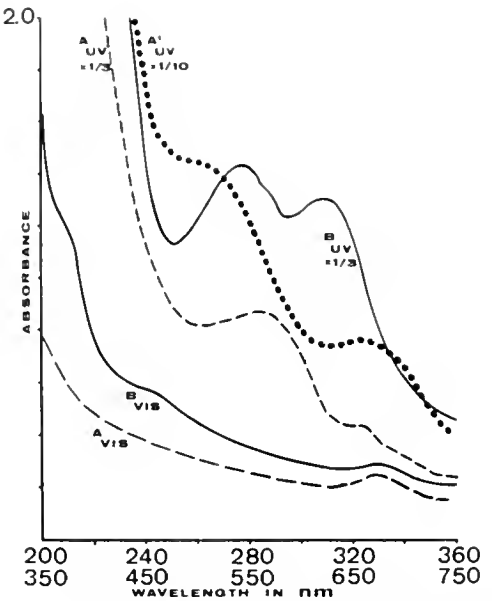

Figure 1. Ultraviolet-visible spectra of blood plasma of *Ascidia dispar* (concentrated twofold by freeze-dry and acidified at pH 3 with acetic acid, that also was the reference solution A_{UV} ···; fresh, water as reference $A_{UV,VIS}$ – – –), and *Pyura chilensis* (fresh, water as reference $B_{UV\,VIS}$ solid line). Cell pathlength 1 cm. Dilution shown were applicable.

spectra, with a light bathochromic effect in the UV bands of *A. dispar* plasma with respect to the *P. chilensis* UV spectrum of plasma, which also shows a shoulder in the 280–290 nm zone.

The elution patterns detected at 265 nm for *A. dispar* and at 310 nm for *P. chilensis* are given in Figure 2a. None of the *P. chilensis* fractions were colored, but fractions 9–11 were yellowish in *A. dispar* plasma chromatography. The elution profiles of iron and vanadium for *P. chilensis*, and iron, titanium, and vanadium for *A. dispar* are also presented in Figure 2b. In both species patterns, two peaks were obtained with respect to absorbance, each one in fractions 3, 4; 6–9 (*A. dispar*), and 5, 6; 10–12 (*P. chilensis*). The first band eluted was in the void volume of the column (V_0 = 30 ml) and should have contained compounds with greater molecular weight or at least comparable to the upper exclusion limit of the G-75 column bed. The second band eluted was at a greater volume than V_t(V_e = 61 and 67 ml for *P. chilensis* and *A. dispar* plasmas, respectively) and should have contained compounds with less molecular weight or comparable to the lowest exclusion limit of the G-75 column bed. This also should be valid for the yellow fractions (9–11) from *A. dispar* plasma chromatography. The absorbance profile at 322 nm showed equal characteristics for *A. dispar*, and the same occurred with the profiles at 278, 288, 375, 454, and 675 nm for *P. chilensis*.

Four peaks were obtained for *P. chilensis* with respect to the iron content in fractions, whose elution volumes (V_e) were 13, 25, 55, and 67 ml. The second peak had the same values of the chromatographic behavior parameter (V_e/V_o, V_e/V_t, K_{av}) of the first band in function of absorbance at 310 nm, and so on. These fractions (5, 6) should have contained iron compounds of high molecular weight, found for the first iron band. The other peaks should correspond to iron compounds of low molecular weight. Vanadium was also eluted after the bed volume.

Table IV

Ionic composition of lysed whole blood and cytosolic solutions of Pyura chilensis *and* Ascidia dispar[a]

	Lysed whole blood of *P. chilensis*[b]	Cytosolic solution of *P. chilensis*[c]	Cytosolic solution of *A. dispar*[c]
Chlorinity ‰	19.74	n.m.	n.m.
Salinity ‰	35.66	n.m.	n.m.
Cl⁻ (g/l)	19.57	n.m.	n.m.
SO_4 (g/l)	0.37	0.070	0.051
Ca^{2+} (g/l)	0.30	n.d.	n.m.
Mg^{2+} (g/l)	1.03	n.d.	n.m.
Na^+ (g/l)	9.59	0.051	0.104
K^+ (mg/l)	484.90	11.20	0.30
Li^+ (mg/l)	0.94	n.d.	0.02
pH	7.82	7.01	7.36
Na/K	0.29	4.6	346.7
Ca/Mg	19.8	—	—

[a] Analysis on lysed whole blood of *A. dispar* were not made due to lack of samples; [b] from subjecting the samples of blood to several freeze-thaw cycles and then centrifuging at 8000 rpm; [c] from subjecting the cell samples to several freeze-thaw cycles with deionized water and then centrifuging them at 8000 rpm; n.m. = not measured; n.d. = not detected.

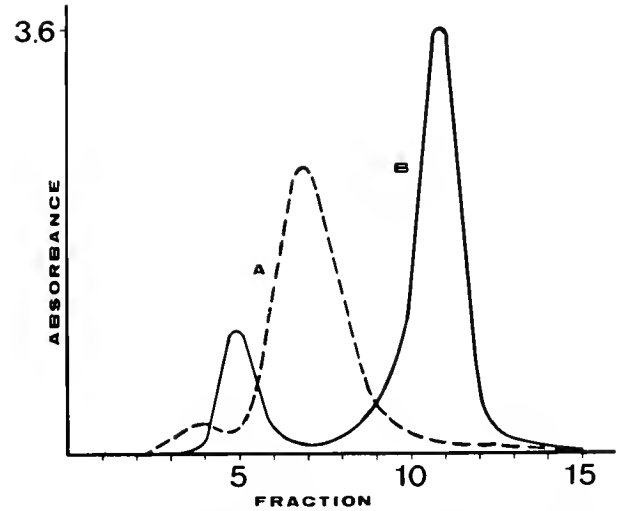

Figure 2a. Elution patterns of blood plasma of *Ascidia dispar* from Sephadex G-75 chromatography at 270 nm (6 ml concentrated twofold by freeze-drying, 6 ml fractions, A dash line), and *Pyura chilensis* at 310 nm (10 ml concentrated fivefold by freeze-drying, 6 ml fractions, B solid line).

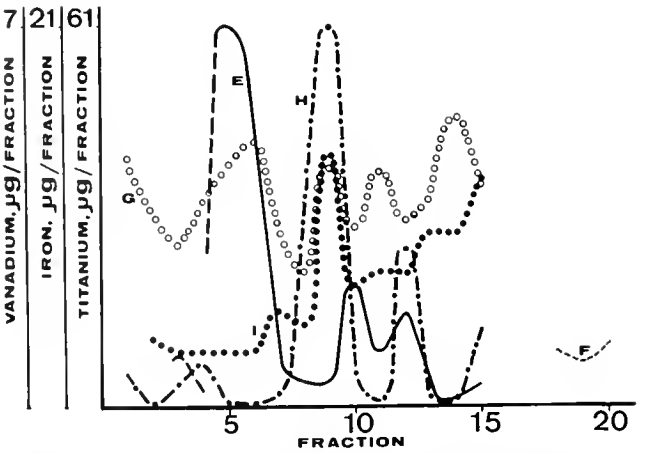

Figure 2b. Elution patterns of metal contents per fraction from Sephadex G-75 chromatography: in plasmas of *Pyura chilensis* (iron E solid line; vanadium F~), and *Ascidia dispar* (iron G open circles; titanium H –·–·–; vanadium I closed circles). Conditions, samples, and fraction volumes are of Figure 2a.

Four bands were also obtained for *A. dispar* with respect to iron content in fractions (V_e = 57, 87, 107, and 137 ml). None had the same values of the chromatographic parameters of the bands in function of absorbance at 265 nm. The four V_e values are greater than the V_t, therefore they should not contain iron compounds of high molecular weight. However, for titanium (three bands, V_e = 37, 87, and 117 ml) the first peak is superposed and similar in the profile at 265 nm, which should mean that it corresponds to titanium compounds with a high molecular weight. The other bands are after the bed volume. The eluted vanadium show increasing contents after fraction 10, for which only two bands were considered (V_e = 67 and 87 ml), both after the bed volume, where the first is superposed with the second peak at 265 nm.

The elution profiles for *P. chilensis* and *A. dispar* blood plasma chromatography on Sephadex LH-20, employing methanol/water gradient as eluants are given in Figures 3 and 4. None of the fractions were colored. At 272 nm, two major bands and one shoulder were obtained for *P. chilensis*, each in fractions 6–9, 11–13, and 14–15. At 310 nm, three bands and two shoulders were obtained, each in fractions 6–9, 11–12, 14–15, and 18–19, respectively. Profiles were also detected at 288 nm (which is superposed with the profile at 272 nm), 320, 375 nm (which were superposed with the profile at 310 nm), and at 454, and 675 nm, which were superposed between them (no bands were obtained in fractions 5–6, 7–8, 10–11, and 15–16).

In *A. dispar*, 6 peaks and 1 shoulder were obtained at 266 nm, each in fractions 4–6, 9, 15–16 (shoulder), 21–22, 25, 29, and 34 (small). At 326 nm one major band was obtained (fractions 3–6), although two small peaks were also observed at fractions 29 and 34, respectively. In addition, patterns were detected at: 288 nm (that was not superposed with the profile at 266 nm, only for the shoulder, fraction 11) and at 660 nm (no bands were obtained in fractions 2–3 and 33–34).

Iron was eluted in all LH-20 chromatography of *P. chilensis* plasma. The V_e of the main bands were at 49, 61, 85, 97, 115, 133, and 235 ml. The first three bands were superposed with the respective eluting peaks at 272 nm, and also with three eluting bands of the profile at 310, and with two peaks of eluting profile at 675 nm. Most of the main iron bands in the profiles were observed at a greater volume than V_t of the bed column, and after fraction number 20, appeared not to have association with the patterns at 272, 288, 310, 375, 454, and 675 nm. Vanadium was not considered in this opportunity.

Iron was also found in all LH-20 chromatography of *A. dispar*, and the V_e of the main peaks were obtained at 35, 55 (shoulder), 115, 145, 165, 195, 215, 265, 295, and 330 ml, in which the chromatographic parameters of any of them correlates with the eluting peaks with respect to absorbance eluting patterns. Titanium was not found in fractions 7–14, and the V_e of the main bands were obtained at 45, 155, 185, 205, 265, and 305 ml. The second titanium eluting band correlates with the respective peaks in the profile at 266 nm, and the fourth is superposed with the patterns at 266 and 280 nm. Vanadium was found in all the chromatography, but most was

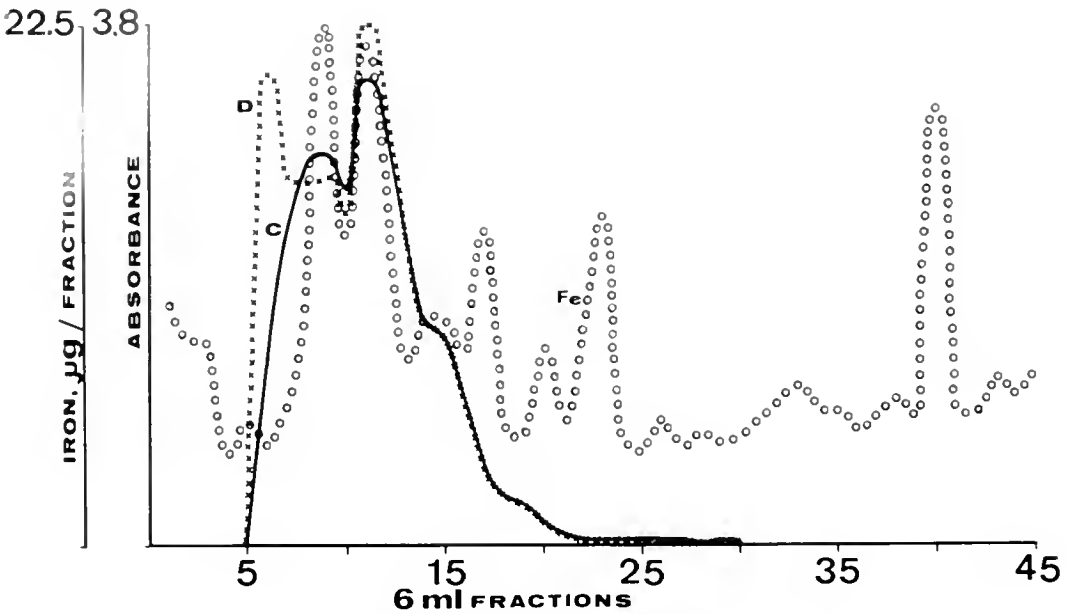

Figure 3. Elution patterns of blood plasma of *Pyura chilensis* from Sephadex LH-20 chromatography at 272 nm (C solid line) and 310 nm (D × × ×), and elution profile of iron (circles). 10 ml concentrated fivefold by freeze-drying, 6 ml fractions.

eluted from fractions 1–17 (V_e = 5, 25, 75, 95, 115, 145, 265, 285, and 335 ml).

Fractions 5 and 11 absorption spectra from Sephadex G-75 chromatography of *P. chilensis* blood plasma are shown in Figure 5a. Fraction 5, that also corresponds to the second iron-band in the respective eluting profile (Fig. 2b), had an absorption band at 276 nm with one shoulder at 400–425 nm. Fraction 11 shows absorption maxima at 270, 310, and 460 nm with a shoulder at 360–375 nm, and is not in the area of an iron-band, although it is between the third and fourth iron-band, in the respective eluting pattern (Fig. 2b).

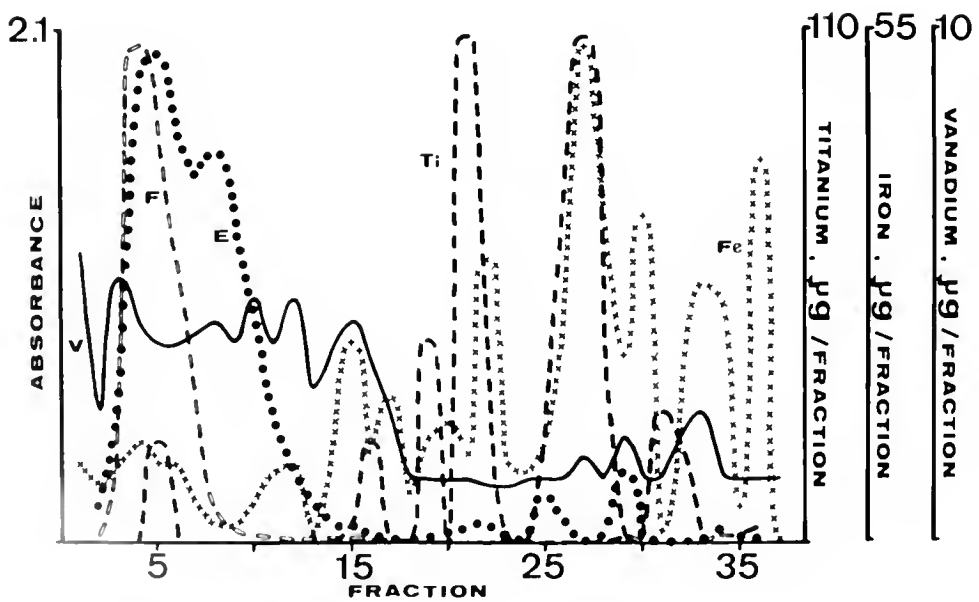

Figure 4. Elution patterns of blood plasma of *Ascidia dispar* from Sephadex LH-20 chromatography at 266 nm (E dots) and 326 nm (F ○ ○ ○), and elution profiles of iron (× × ×), titanium (dash line), and vanadium (solid line). 10 ml concentrated twofold by freeze-drying, 10 ml fractions.

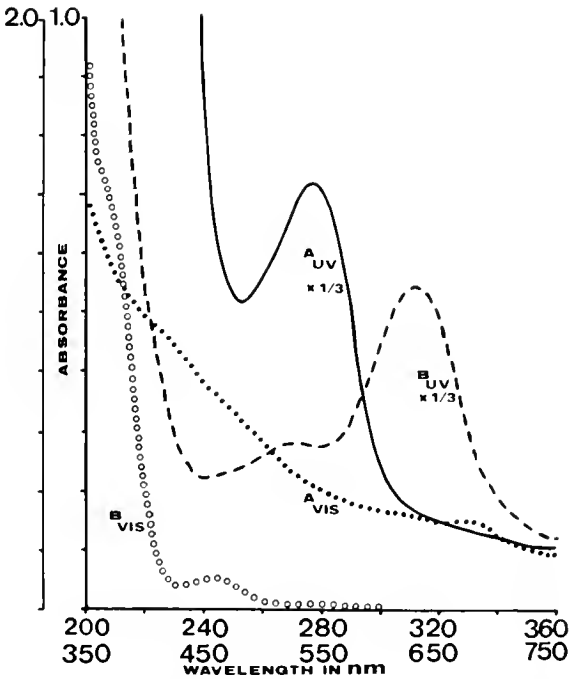

Figure 5a. Absorption spectra of fractions 5 (A_{UV} solid line, A_{VIS} dots) and 11 (B_{UV} dash line, B_{VIS} circles) from Sephadex G-75 chromatography of blood plasma of *Pyura chilensis*.

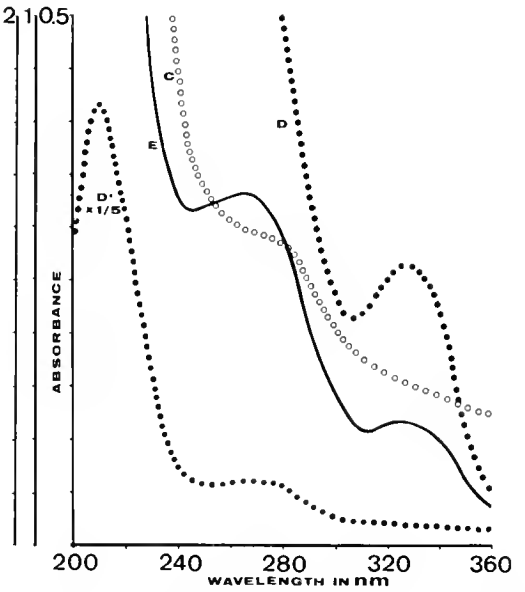

Figure 5b. Ultraviolet spectra of fractions 4 (C circles), 7 (D, D' dots), and 11 (E solid line) from Sephadex G-75 chromatography of blood plasma of *Ascidia dispar*. Dilution shown were applicable.

Ultraviolet spectra of fractions 4, 7 and 11 from Sephadex G-75 chromatography of *A. dispar* blood plasma are shown in Figure 5b. Fraction 4 had an absorption shoulder at 265–285 nm and also corresponds to the first titanium-band in the respective profile (Fig. 2b). Fraction 7 shows absorption bands at 210, 260–280, and 326 nm, and it corresponds to the first vanadium band (Fig. 2b). Fraction 11 (yellowish) had two absorption maxima, at 266 and 326 nm, respectively, and corresponds to the third iron band (Fig. 2b).

Ultraviolet spectra of fractions 5, 8, 17, 21, 25, 29, and 36 from Sephadex LH-20 chromatography of *A. dispar* blood plasma are shown in Figure 6a. Fractions 3–5 had absorption maxima at 266–270 and 322–324 nm, corresponding moreover to the border-line zone between the first iron band and the respective iron shoulder, and to the first titanium band (Fig. 4). Fraction 8 also had two absorption bands, at 262 and 320 nm, which only appear to be associated with the third vanadium peak (Fig. 4). Fraction 17 had ultraviolet bands at 232 nm and in the zone of 280 nm, corresponding to the fourth iron peak in Figure 4. Fraction 21 had one absorption band at 280 nm and two small shoulders at 274–276 nm and 286–288 nm, respectively. This fraction also corresponds to the first titanium band (Fig. 4). Fraction 25 had ultraviolet bands at 230 and 270 nm, and one shoulder at 292–294 nm. This fraction appears not to be associated with any metal. Fraction 29 had the following absorption maxima: at 210, 232 (shoulder), 270, and 292–294 nm (shoulder), and should correspond to the same group of compounds as fraction 25 (have similar UV spectra). Fraction 36 had three ultraviolet maxima, at 218 (not shown), 296, and 328 nm, and it corresponds to the last iron band (Fig. 4). Fraction 34 had a spectrum similar to fraction 36, except for the band at 296 nm, which in fraction 34 appears as a shoulder in the zone of 280 nm. Also, fraction 34 correspond to the penultimate iron peak (Fig. 4). The visible spectra of fractions only showed absorption increasing monotonically with a decreasing wavelength.

Ultraviolet spectra of fractions 6, 8, and 11 from Sephadex LH-20 chromatography of *P. chilensis* blood plasma are shown in Figure 6b. Fraction 6 had absorption maxima at 280 nm and in the 310–320 nm zone. It appeared not to be associated with any principal iron band (Fig. 3) although it is in the borderline of a minor iron peak (fraction 5). Fraction 8–9 also had two ultraviolet bands, at 270 and 302–306 nm, but are in the first principal iron peak zone (Fig. 3). Fraction 11 had an absorption shoulder band at 260–280 nm and another that tends to disappear at 286–288 nm. This fraction is in the second principal iron peak zone (Fig. 3). In the 12–24 fraction range, the absorption spectra showed no bands. From fractions 25 to 29, the ultraviolet spectra only showed one light band at 266 nm. The visible spectra of fractions also consisted in absorptions increasing monotonically with decreasing wavelength.

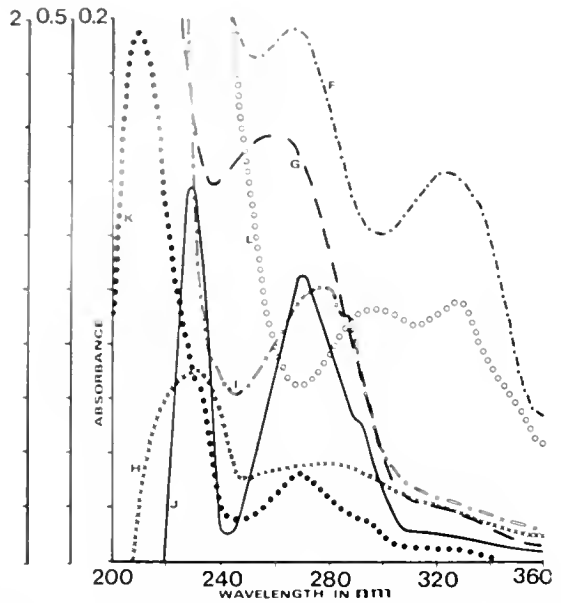

Figure 6a. Ultraviolet spectra of fractions 5 (F – · – · –), 8 (G dash line), 17 (H × × ×), 21 (I ○ □ ○), 25 (J solid line), 29 (K dots), and 36 (L circles) from Sephadex LH-20 chromatography of blood plasma of *Ascidia dispar*.

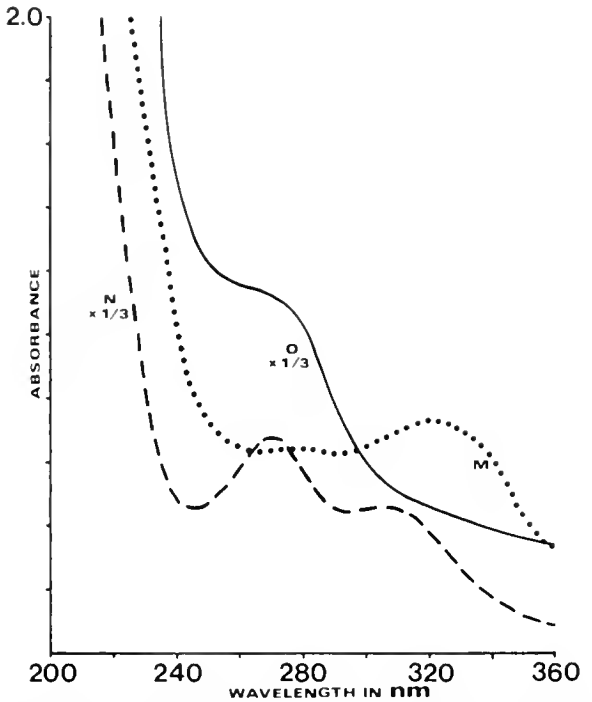

Figure 6b. Ultraviolet spectra of fractions 6 (M dots), 8 (N dash line), and 11 (O solid line) from Sephadex LH-20 chromatography of blood plasma of *Pyura chilensis*

Discussion

The analysis reported here should support the conclusion that *P. chilensis* is an iron and titanium accumulator, and that *A. dispar* is an iron, titanium, and vanadium accumulator. In both species the predominant metal was iron, which in the case of *P. chilensis* is consistent with ascidian phylogeny with respect to vanadium- and iron-containing species (Hawkins *et al.*, 1983c). In the order Pleurogona, all of its family species are iron accumulators (Swinehart *et al.*, 1974; Agudelo *et al.*, 1982). However, *A. dispar* appears to be an iron-predominant species, although, it also accumulates titanium and vanadium at greater levels than considered non-biological (Saxby, 1969; Hawkins *et al.*, 1983c) with respect to metal contents in blood cells. Results from the whole body (specimens) are not reliable because when the animal is removed it immediately begins to lose blood. In the sub-orders Aplousobranchia and Phlebobranchia, the majority contain vanadium in their blood (Hawkins *et al.*, 1983c; Michibata *et al.*, 1986). Titanium has been reported in *Ciona intestinalis* (Noddack and Noddack, 1939) and *Eudistoma ritteri* (Levine, 1961, 1962a,b), but according to Goodbody (1974), there is no concrete evidence that titanium would be concentrated in blood cells. In the present work evidence is presented of this metal in the blood cells of *P. chilensis* and *A. dispar*.

However, some of these results could be only apparent from the biochemical point of view, because they may be influenced by the ascidians immediate environment *e.g.*, the floating metallic barrels of marine pools where fixation occurs. TiO_2 and Fe_2O_3 are frequently used as pigments in many paints (Orna, 1980). Because of their ability to accumulate metallic trace elements from seawater, tunicates also have been suggested to serve as marine pollution indicators (Papadopoulou and Kanias, 1977). Therefore, the Ti in *P. chilensis*, and the higher concentrations of Fe and Ti in *A. dispar*, may also be associated with this aspect, rather than being considered essential elements subjected to selective accumulation mechanisms. The accumulation of uncommon metals by ascidians in significant concentrations is still an open question. For instance, something similar to what happens to Ti, occurs to Nb (Rayner-Canham, 1984).

Iron is the predominant metal in *P. chilensis* cytoplasm, but in *A. dispar* 26.9% could be in cell membranes. Titanium is almost distributed likewise in both species' cytoplasm and cell membranes. Vanadium is predominant in *A. dispar* cytoplasm cells, although 23.6% could be bound to membrane cells. Therefore, variable fraction of metals, which may depend on the species, are associated with blood cell membranes of tunicates.

Blood plasma of both species were nearly neutral, with a lower salinity than the habitat seawater and with low concentrations of sulphate ions. Besides, the Ca/Mg concentration ratios were greater (0.33 for *P. chilensis* and

0.30 for *A. dispar*) compared with the seawater (0.23). The Na/K concentration ratios were lower (20.1 for *P. chilensis* and 22.2 for *A. dispar*) than in seawater (27.9).

Calcium and magnesium were not detected in the cytosolic solutions, and the Na/K concentration ratios were very different (4.6 for *P. chilensis* and 346.7 for *A. dispar*). Nevertheless, both were nearly neutral and their sulphate ion contents were low, reaching 11.7% and 6.5% of their contents in plasmas of *P. chilensis* and *A. dispar*, respectively. This implies that the low concentration of sulphate in plasmas (in respect to the concentration of sulphate in seawater), is not the result of the accumulation into cytoplasmic blood cell solutions. Considerable controversy still exists on the intracellular pH and concentration of sulphate in the intact blood cells of tunicates (Dingley *et al.*, 1982; Hawkins *et al.*, 1983a; Frank *et al.*, 1986).

To obtain more knowledge about the behavior of some major tunicate blood components, plasma-cell interaction was abruptly induced in the blood itself (due to lack of *A. nigra* blood, this experiment was carried out only with *P. chilensis* blood). Blood cells apparently were not lysed under whole blood lysis procedures, according to microscope observations and to differential UV-spectra of plasma, cytosolic solution and lysed whole blood samples. The results (Table IV), are consistent with the fact that the blood cells of *P. chilensis* are not acidic and it seems that interactions could occur between plasma and cellular compounds, that could account for the decrease of sulphate, calcium, magnesium, sodium, and potassium concentrations in whole lysed blood solution, in respect to their concentrations in blood plasma. Part of these components could be taken up by some compound(s) of the cellular membranes. It is also possible that sulphate, calcium, and magnesium in particular, interact with some intracellular compounds, which would mean, for instance, that sulphate is consumed by intracellular compounds of cytosolic solutions. Due to the complexometric titration method by means of which calcium and magnesium were determined (Roman *et al.*, 1982), it is feasible that intracellular strong metal ligands take up part of the calcium and magnesium of the plasma. Therefore, this could be the first evidence of sulphate consumption by blood cell components of tunicates, as hypothesized by Hawkins *et al.* (1983b). It should explain its low concentration in ascidian blood plasma as compared to the blood plasma of other marine animals (Burton, 1973).

Both plasmas and cytosolic solutions were reducing with respect to permanganate and dichromate, respectively. However, deproteinization prior to the titration were not made. However, in the case of the back titration of dicromate method, the sample was acidified with concentrated perchloric acid, a deproteinizant (Carr *et al.*, 1983). In the pioneering studies of Endean (1985a) similar assays were tested, and Muzzarelli (1973) used back titration of dicromate for chitin determination. Hawkins *et al.* (1980a) have detected N-acetylaminosugar compounds in the blood plasma of tunicates. Other reducing components that have been reported in ascidian blood include some reduced form of metals, the tunichrome like compounds and the so called apoferreacids (Macara *et al.*, 1979a, b, c; Agudelo *et al.*, 1982, 1983b, 1985; Hawkins *et al.*, 1983b; Bruening *et al.*, 1985; Frank *et al.*, 1986).

Maintaining iron and vanadium in reduced forms in specialized blood cells, and also in some extension in the plasma in the case of iron (Agudelo *et al.*, 1983b; Roman, unpub. results from *P. praeputialis*), required more investigation in adequately controlled artificial conditions.

The plasma spectra (Fig. 1) are similar for *P. chilensis* and *A. dispar*. The main differences are the presence of a shoulder at 375–385 nm, and the existence of pink-orange compound(s) having an absorption band at 450–475 nm in the plasma spectrum of *P. chilensis*. *P. stolonifera* pink compound(s) had a visible band at 497 nm (Hawkins *et al.*, 1980a). The plasmas UV- spectra of *A. nigra* (Kustin *et al.*, 1976), *A. ceratodes* (Hawkins *et al.*, 1980a), *Podoclavella moluccensis*, *Polycarpa pedunculata* (Hawkins *et al.*, 1980b), and *P. stolonifera* (Hawkins *et al.*, 1980a) also have bands at 260–275 nm and 300–330 nm ranges. A band at 335 nm (Agudelo *et al.*, 1982) was only detected in plasma of *B. ovifera*. The main similarity of the visible spectra of *P. chilensis* and *A. dispar* plasma is the band at the 675 nm zone.

Anion exclusion, cation retardation, and other problems occur in the chromotography of metal-containing substances on Sephadex G and LH types. This is due to the small amounts of donor groups present in the material (Pharmacia Fine Chemicals, 1977; Kura *et al.*, 1977; Johnson and Evans, 1980; Lönnerdall and Hoffman, 1981). To minimize this problem, 0.01 *M* NaCl and 0.06 *M* acetic acid solutions were used as eluents with Sephadex G-75, and methanol/water gradient with Sephadex LH-20 chromatography, respectively. Some level of methanol was always maintained in the separative process and prior to the sample run, the column was conditioned with methanol p.a. As Sephadex LH-20 was used with a mixture of polar solvents, adsorption and partition effects must be considered to play major role in the separation. Gel filtration effects can be disregarded.

The elution behavior of plasmas of *P. chilensis* and *A. dispar* from Sephadex G-75, were similar in respect to absorbance *versus* fraction collected (Fig. 2b), but the patterns for metal contents *versus* fraction collected (Fig. 2b), were not similar in function to the same metal considered. In *P. chilensis* plasma, evidence of iron com-

pounds with a high molecular weight was found (fraction 5–6), in addition to iron bands corresponding to low molecular weight iron compounds. However, these might correspond to iron compounds of high molecular weight that showed greater affinity for the gel phase than for the aqueous phase. In *A. dispar*, no evidence of high molecular weight iron compounds was found. However, these were found in the case of titanium (fraction 4). Low molecular weight compounds of iron and titanium, or metal compounds that showed greater affinity for the stationary phase were also detected. In both plasmas vanadium appears to exist as low molecular weight compounds, unless the high molecular weight compounds were retarded by adsorption phenomena.

The absorption spectra of the fractions associated with high molecular weight iron compounds (Fig. 5a, fraction 5), cannot correspond to an Fe (III) hydrolytic polymer, which only showed a shoulder at 470 nm (Flynn, 1984). The absorption spectrum of fraction 11 (Fig. 5a) appears to correspond to G-75 low molecular weight organic pigment that could be a tunichrome-like compound(s). The absorption spectra of fractions 5 and 11 account for the spectrum plasma of *P. chilensis*, so these results appear not to be "artifacts."

The ultraviolet spectra of the fractions associated with apparently high molecular weight titanium compounds, from *A. dispar* plasma chromatography on Sephadex G-75 (Fig. 5b, fraction 4), only shows a shoulder at 270–286 nm. This absorption zone was also checked for the indication of a high molecular weight iron compound(s), but no visible bands were observed. The ultraviolet spectra of fractions 7 and 11 (Fig. 5b) appeared to correspond to closely related compounds, apparently of low molecular weight, associated with vanadium and iron, respectively. Their UV spectral features suggest that tunichrome-like compounds may also be involved in these fractions (Bruening *et al.*, 1985). In comparison with the absorption spectrum of the whole blood plasma of *A. dispar* (Fig. 1), in the chromatographic fractions, the absorption peak at 675 nm zone was not observed.

The elution behavior of plasma of *P. chilensis* and *A. dispar* on Sephadex LH-20 with methanol/water gradient, showed similar patterns for absorbance, and iron contents *versus* fraction collected (Fig. 3, 4). For *P. chilensis* plasma, chromatographic evidence of iron-compounds were obtained, and the same occurs for iron, titanium, and vanadium compounds in *A. dispar* plasma, respectively, which appear not to be inorganic hydrolytic products of metal ions.

In *A. dispar*, the absorption spectra of fractions 3–5 (Fig. 6a) appear to be associated with iron and titanium-compounds, but according to the spectra of fractions 4, 7, and 11 from Sephadex G-75 (Fig. 5b), the titanium compound(s) should tend to absorb at 260–290 nm zone. Iron, vanadium-compounds and tunichrome like substances also absorb at 320–330 nm. The ultraviolet spectrum of fraction 8 (Fig. 6a), should correspond then to vanadium compound(s). The ultraviolet spectrum of fraction 17 may correspond to iron compounds of proteinaceous nature, due to the band at 280 nm zone, and the same seems to occur in fraction 21 for titanium compound(s). Fractions 25–29 (Fig. 4) were not associated to any metal ions, and by their spectra appear to correspond to closely related compounds. Fractions 34–36 are related to iron, and by their spectral features should correspond to iron compound(s) similar to those obtained from the interaction between iron and fractions 8–13 G-75 chromatography of *A. ceratodes* plasma (Hawkins *et al.*, 1980a). Therefore, compounds of fractions 3–5 should be closely related to iron compound(s) of fractions 34–36.

In *P. chilensis* plasma chromatography on Sephadex LH-20 gel, fraction 6 (Fig. 3) appear not to be associated with iron, and their spectrum (Fig. 6b) could correspond to tunichrome-like substances similar to spectrum of fraction 11 from Sephadex G-75 (Fig. 5a). However, fractions 8, 9 (Fig. 3) are related to a main iron peak, then those should contain iron compound(s), whose absorption peaks show (Fig. 6b) hipsochromic shifts in respect to the spectrum of fraction 6. Hiper- and hipochromic effects in the bands can also be observed. Fraction 11 is in the zone of the second iron peak (Fig. 3), and by their ultraviolet spectra (Fig. 5a), may correspond to iron compound(s) of proteinaceous nature.

It is likely that by dilution the visible absorption maxima were not observed in the spectra of fractions coming from LH-20 chromatography of blood plasmas.

The complicated hydrolytic processes of iron (Flynn, 1984), titanium (Pascal, 1963, Ciavatta *et al.*, 1985) and vanadium (Kustin and Macara, 1982) in a pH media close to neutrality, such as the blood plasma of tunicates, suggests that these elements could be found as coordination compounds with proteic or non proteic organic ligands. The ligands that have been associated with metals, in tunicate plasma, are proteins (Hawkins *et al.*, 1980a; Webb and Chrystal, 1981; Agudelo *et al.*, 1983b) and N-acetylaminosugar compounds (Hawkins *et al.*, 1980a, b). However, Agudelo *et al.* (1983b) considers that these last compounds could correspond to tunichrome-like substances. It also has been suggested that α-hydroxycarboxylic acids residues could be involved in the metal complexation by tunicates (Rayner-Canham, 1984).

The matter of protein metal-binding, and the study of ligating systems for metals in the blood plasma of ascidians *P. chilensis* and *A. dispar* was scarcely treated here. However, information was obtained about the presence of Fe, Ti complexes, and likely vanadium complexes in blood plasma of species under study. Therefore, it is rea-

sonable to suppose that they are involved in the dynamic processes (storage/carrier) of metals in tunicate blood. Accordingly, the high molecular weight metal compound(s) should be "transferrin"-like metalloproteins, which has been recently shown in the blood plasma of *P. stolonifera* (Martin *et al.*, 1984; Finch and Huebers, 1986).

Between pH 2.5–3.5, tunichrome solutions appear green, due to the broad band in the zone near 660 nm (Macara *et al.*, 1979b). We found an absorption peak around 675 nm in both plasmas and in fraction 5 from Sephadex G-75 chromatography of *P. chilensis* plasma. This should arise from iron-compound(s) of high molecular weight with respect to the exclusion limit of the gel. It has recently been suggested that in the d-d transition energy at 660 nm zone, two nitrogen atoms from the coordination by ligands like D-glucosamine (Micera *et al.*, 1985) could be involved. This was not observed when the amino group was protected, as occurs in the case of N-acetyl-D-glucosamine. Therefore, more attention should be focus in the tunicates blood compounds that show absorption bands at 660–675 nm zone, due to their potential association with metal binding.

Literature Cited

Agudelo, M. I., K. Kustin, and E. Robinson. 1981. Blood chemistry of *Boltenia ovifera*. *Comp. Biochem. Physiol.* **72A:** 161–166.

Agudelo, M. I., K. Kustin, and G. C. McLeod. 1983a. The intracellular pH of the blood cells of the tunicate *Boltenia ovifera*. *Comp. Biochem. Physiol.* **75A:** 211–214.

Agudelo, M. I., K. Kustin, G. C. McLeod, W. E. Robinson, and R. T. Wang. 1983b. Iron accumulation in tunicate blood cells. I. Distribution and oxidation state of iron in the blood of *Boltenia ovifera*, *Styela clava*, and *Molgula manhattensis*. *Biol. Bull.* **165:** 100–109.

Agudelo, M. I., K. Kustin, and W. E. Robinson. 1985. Iron accumulation in tunicate blood cells. II. Whole body and blood cell iron uptake by *Styela clava*. *Biol. Bull.* **169:** 152–163.

Bannard, L. G., and J. D. Burton. 1968. The spectrophotometric determination of vanadium(V) with 3,3'-dymethylnaphtidine. *Analyst* **93:** 142–147.

Berril, N. J. 1955. *The Origin of Vertebrates.* Oxford University Press.

Biggs, W. R., and J. H. Swinehart. 1976. *Vanadium in Selected Biological Systems*, Vol. 6, H. Sigel, ed. M. Dekker and Co. Pp. 141–196.

Biggs, W. R., and J. H. Swinehart. 1979. Studies of the blood of *Ascidia ceratodes*. Total blood counts, differential blood cell counts, hematocrit values, seasonal variation, and fluorescent characteristics of blood cells. *Experientia* **35:** 1047–1049.

Botte, L., S. Scippa, and M. De Vicentiis. 1979. Ultrastructural localization of vanadium in the blood cells of Ascidiacea. *Experientia* **35:** 1228–1230.

Box, J. D. 1981. Interference due to crystal formation in the spectrophotometric determination of iron(II) using 2,4,6-tri (2'-pyridyl)-1,3,5-triazine. *Analyst* **106:** 1227–1229.

Bruening, R. C., E. M. Oltz, J. Furukawa, K. Nakanishi, and K. Kustin. 1985. Isolation and structure of tunichrome B-1, a reducing blood pigment from the tunicate *Ascidia dispar* L. *J. Am. Chem Soc.* **107:** 5298–5300.

Burton, R. F. 1973. The significance of ionic concentration in the internal media of animals. *Biol. Rev.* **48:** 195–231.

Carlisle, D. B. 1968. Vanadium and other metals in ascidians. *Proc. R. Soc Biol. Sci.* **171B:** 31–41.

Carlson, R. M. K. 1975. Nuclear magnetic resonance spectrum of living tunicate blood cells and the structure of the native vanadium chromogen. *Proc. Natl Acad. Sci. USA.* **72:** 2217–2221.

Carr, R. S., M. B. Bally, P. Thomas, and J. M. Neff. 1983. Comparison of methods for determination of ascorbic acid in animal tissues. *Anal. Chem.* **55:** 1229–1232.

Ciavatta, L., D. Ferri, and G. Riccio. 1985. On the hydrolysis of the titanium(IV) ion in chloride media. *Polyhedron* **4:** 15–21.

Collins, P. F., D. Harvey, and G. F. Smith. 1959. 2,4,6-tripyridyl-s-triazine a reagent for iron determination of iron in limestone, and refractories. *Anal. Chem.* **31:** 1862–1867.

Dingley, A. L., K. Kustin, I. G. Macara, and G. C. McLeod. 1981. Accumulation of vanadium by tunicate cells occur via a specific anion transport system. *Biochim Biophys. Acta* **649:** 493–502.

Dingley, A. L., K. Kustin, I. G. Macara, G. C. McLeod, and M. F. Roberts. 1982. Vanadium-containing tunicate blood cells are not highly acidic. *Biochim. Biophys. Acta* **720:** 384–389.

Endean, R. 1955a. Studies on the blood and test of some Australian ascidians. I. The blood of *Pyura stolonifera* (Heller). *Aust. J. Mar. Freshw. Res.* **6:** 35–59.

Endean, R. 1955b. Studies on the blood and test of some Australian ascidians. II. The test of *Pyura stolonifera* (Heller). *Aust. J. Mar. Freshw. Res.* **6:** 139–156.

Endean, R. 1955c. Studies on the blood and test of some Australian ascidians. III. The formation of the test of *Pyura stolonifera* (Heller). *Aust. J. Mar. Freshw. Res.* **6:** 157–164.

Feigl, F., and V. Anger. 1972. *Spot Tests in Inorganic Analysis*, 6th ed. Elsevier Publishing Co. Pp. 94–523.

Finch, C. A., and H. A. Huebers. 1986. Iron metabolism. *Clin. Physiol. Biochem.* **4:** 5–10.

Flynn, Ch. M., Jr. 1984. Hydrolysis of inorganic iron(III) salts. *Chem. Rev.* **84:** 31–41.

Frank, P., R. M. K. Carlsnn, and K. O. Hodgson. 1986. Vanadyl ion EPR as a noninvasive probe of pH in intact vanadocytes from *Ascidia ceratodes*. *Inorg. Chem.* **25:** 470–478.

Fries, J. 1972. *Analisis de trazas. Métodos fotométricos comprobados.* Merck. Pp. 102–103.

Fritz, J. S., and S. S. Yamamura. 1955. Rapid microtitration of sulphate. *Anal. Chem.* **27:** 1461–1464.

Fukasawa, T., and T. Yamane. 1977. Determination of trace vanadium in natural waters by a combined ion-exchange-catalytic photometric method. *Anal. Chim. Acta* **88:** 147–153.

Goodbody, I. 1974. The physiology of ascidians. *Adv. Mar. Biol.* **12:** 1–149.

Hawkins, C. J., P. M. Merefield, D. L. Parry, W. R. Biggs, and J. H. Swinehart. 1980a. Comparative study of the blood plasma of the ascidians *Pyura stolonifera* and *Ascidia ceratodes*. *Biol. Bull.* **159:** 656–668.

Hawkins, C. J., D. L. Parry, and C. Pierce. 1980b. Chemistry of the blood of the ascidian *Podoclavella moluccensis*. *Biol. Bull.* **159:** 669–680.

Hawkins, C. J., G. A. J. James, D. L. Parry, J. H. Swinehart, and A. L. Wood. 1983a. Intracellular acidity in the ascidians. *Comp. Biochem. Physiol.* **76B:** 559–565.

Hawkins, C. J., D. L. Parry, B. J. Wood, and P. Clark. 1983b. Formation of an iron-sulphur cluster by the reduction of sulphate with the blood pigment of an ascidian in the presence of iron. *Inorg. Chim. Acta* **78:** L29–L31.

Hawkins, C. J., P. Kott, D. L. Parry, and J. H. Swinehart.

1983c. Vanadium content and oxidation state related to ascidian phylogeny. *Comp. Biochem. Physiol.* **76B:** 555–558.

Hori, R., and H. Mi[illegible]a 1981. Observations on the ultrastructure of the test of C[illegible]*sta*, with special reference to the localization of vanadium [illegible]ron. *Protoplasma* **108:** 9–19.

Johnson, P. [illegible]d G. W. Evans. 1980. Binding of zinc and copper to some [illegible]tration media. *J. Chromatogr.* **188:** 405–407.

Jones, J. [illegible], S. G. Capar, and T. C. O'Haver. 1982. Critical evaluation of multi-element scheme using plasma emission and hydride evolution atomic-absorption spectrometry for the analysis of plant and animal. *Analyst* **107:** 353–377.

Korkisch, J. 1969. *Modern Methods for the Separation of Rarer Metal Ions.* Pergamon Press. Pp. 400–407.

Kura, G., A. Koyama, and T. Tarutani. 1977. Chromatographic study of some inorganic ions on Sephadex gel in thiocyanate media. *J. Chromatogr.* **144:** 245–252.

Kustin, K., K. V. Ladd, and G. C. McLeod. 1975. Site and rate of vanadium assimilation in the tunicate *Ciona intestinalis*. *J. Gen. Physiol.* **65:** 315–328.

Kustin, K., D. S. Levine, G. C. McLeod, and W. A. Curby. 1976. The blood of *Ascidia nigra* blood cell frequency distribution and valence of vanadium in living blood cells. *Biol. Bull.* **150:** 426–441.

Kustin, K., and G. C. McLeod. 1977. *Interactions Between Metal Ions and Living Organisms in Sea Water.* In Topics in current chemistry, Number 69. Inorganic biochemistry II. Springer-Verlag, New York. Pp. 1–36.

Kustin, K., and I. G. Macara. 1982. The new biochemistry of vanadium. *Comments Inorg. Chem.* **2:** 1–22.

Levine, E. P. 1961. Occurrence of titanium, vanadium, chromium and sulphuric acid in the ascidians *Eudistoma ritteri*. *Science* **133:** 1352–1353.

Levine, E. P. 1962a. Studies on the structure, reproduction, development and accumulation of metals in the colonial ascidian *Eudistoma ritteri*. *Science* **133:** 1352–1353.

Levine, E. P. 1962b. Studies on the structure, reproduction, development and accumulation of metals in the colonial ascidian *Eudistoma ritteri* Van Name, 1945. *J. Morphol.* **111:** 105–137.

Lonnerdal, B., and B. Hoffman. 1981. Alkaline reduction of dextran gels and crosslinked agarose to overcome non specific binding of trace elements. *Biol. Trace Element Res.* **3:** 301–307.

Macara, I. G., G. C. McLeod, and K. Kustin. 1979a. Vanadium in tunicates: oxygen-binding studies. *Comp. Biochem. Physiol.* **62A:** 821–826.

Macara, I. G., G. C. McLeod, and K. Kustin. 1979b. Isolation, properties and structural studies on a compound from tunicate blood cells that may be involved in vanadium accumulation. *Biochem. J.* **181:** 457–465.

Macara, I. G., G. C. McLeod, and K. Kustin. 1979c. Tunichromes and metal ion accumulation in tunicate blood cells. *Comp. Biochem. Physiol.* **63B:** 299–302.

Martin, A. W., E. Huebers, H. Huebers, J. Webb, C. A. Finch. 1984. A monosited transferrin from a representative deuterostome. *Blood* **64:** 1047–1052.

Micera, G., S. Deiana, A. Dessi, P. Decock, B. Dubois, and H. Kozlowski. 1985. Copper(II) compexation by D-glucosamine. Spectroscopic and potentiometric studies. *Inorg. Chim. Acta* **107:** 45–48.

Michibata, H., T. Terada, N. Anada, K. Yamakawa, and T. Numakunai. 1986. The accumulation and distribution of vanadium, iron, and manganese in some solitary ascidians. *Biol. Bull.* **171:** 672–681.

Monniot, F. 1978. Connaissances actuelles sur les ions metalliques chez les ascidies. *Actualités de Biochimie Marine.* Colloque GABIN, la Rochelle. Pp. 185–194.

Muzzarelli, R. A. A. 1973. *Natural Chelating Polymer.* International series of monographs in analytical chemistry. Pergamon Press, Hungary. Vol. 55, Pp. 95–96.

Noddak, I., and W. Noddak. 1939. Die häufigkeiten der schwermetalle in meerestieren. *Ark. Zool.* **32:** 1–35.

Orna, M. V. 1980. Chemistry and artist' colors, part I, II, III. *J. Chem. Educ.* **57:** 256–258; 264–267; 267–269.

Papadopoulou, C., and G. D. Kanias. 1977. Tunicate species as marine pollution indicators. *Mar. Pollut. Bull.* **8:** 229–231.

Pascal, P. 1963. *Nouveau Traité de Chemie Minérale.* Masson et Cie. Editeurs. Tome IX.

Qureshi, M., J. P. Rawat, and F. Khan. 1968. A study of interference in the spectrophotometric determination of titanium with sulfosalicylic acid. *Anal. Chim. Acta* **41:** 164–166.

Rayner-Canham, G. W. 1984. Some niobium(V) complexes and their relevance to the uptake of niobium by ascidians. *Polyhedron* **3:** 1029–1031.

Roman, D. A., L. Rivera, C. Espejo, E. I. Brito. 1982. Aplicación del electrodo selectivo de Ca en las determinaciones sucesivas de Ca y Mg en agua de mar, agua intersticial y sangre de tunicados. *Resumenes II Jornadas de Ciencias del Mar,* 21–24 Septiembre 1982. Comité de Ciencias del Mar. Depto. Oceanología, Universidad de Concepción, Pp. 22.

Roman, D. A. 1986. Algunos aspectos de farmacología marina. Tunicados. *Rev. Chil. Educ. Quim.* **11:** 3–12.

Rowley, A. F. 1982. The blood cells of *Ciona intestinalis:* an electron probe X-ray microanalytical study. *J. Mar. Biol. Assoc. U. K.* **62:** 607–620.

Sandell, E. B. 1959. *Colorimetric Determination of Traces of Metals.* Interscience Publishers, Inc., New York, third ed. Pp. 537–542.

Saxby, J. D. 1969. Metal-organic chemistry of the geochemical cycle. *Rev. Pure Appl. Chem.* **19:** 131–150.

Senozan, N. M. 1974. Vanadium in the living world. *J. Chem. Educ.* **51:** 503–505.

Sephadex LH-20. 1977. Technical report. Pharmacia Fine Chemicals. Uppsala, Sweden. Pp. 1–23.

Swinehart, J. H., W. R. Biggs, D. J. Halko, and N. C. Schroeder. 1974. The vanadium and selected metal contents of some ascidians. *Biol. Bull.* **146:** 302–312.

Tullius, T. D., W. O. Gillum, R. M. K. Carlson, and K. O. Hodgson. 1980. Structural study of the vanadium complex in living ascidian blood cells by X-ray absorption spectroscopy. *J. Am. Chem. Soc.* **102:** 5670–5676.

Webb, J., and P. Chrystal. 1981. Protein binding of iron in blood plasma of the ascidian *Hermania momus*. *Mar. Biol.* **63:** 107–112.

Wright, R. K. 1981. *Urochordates.* Pp. 565–626 in *Invertebrate Blood Cells,* N. A. Ratcliffe and A. F. Rowley, eds. Academic Press, London.

Reference: *Biol. Bull.* **175:** 167–174. (August, 1988)

The Behavioral Response of Spiny Lobsters to ATP: Evidence for Mediation by P_2-like Chemosensory Receptors

RICHARD K. ZIMMER-FAUST[1], RICHARD A. GLEESON[2], AND WILLIAM E. S. CARR[2]

[1]*Marine Science Institute, University of California, Santa Barbara, California 93106 and* [2]*The Whitney Marine Laboratory and Department of Zoology, University of Florida, St. Augustine, Florida 32086*

Abstract. The results of both behavioral and electrophysiological studies with the California spiny lobster, *Panulirus interruptus*, support the hypothesis that a locomotory response evoked by ATP in seawater may be mediated by chemoreceptors akin to P_2-type purinoceptors. Behavioral results consistent with this hypothesis are: (1) an activity sequence of ATP > ADP > AMP or adenosine; (2) the behavior is also evoked by ATP analogs with modifications in both the adenine and ribose moieties; and (3) the slowly degradable analogs, β,γ-methylene ATP and β,γ-imido ATP (AMPPNP) are active. Extracellular recordings from single chemosensory cells show that ATP-sensitive cells are present in the antennule of *P. interruptus* and exhibit marked similarities to the P_2-like chemoreceptors identified earlier in *P. argus*. Although the ranked order of behavioral activity to ATP and eight analogs parallels that measured physiologically, important differences include: (1) AMPPNP is relatively more active physiologically; and (2) the behavioral sensitivity to ATP, ADP, and AMP is greater than that measured physiologically. Since degradation of ATP proceeds rapidly in animal flesh and in seawater, it is proposed that ATP may represent a particularly appropriate signal molecule for foraging by the lobster as it is indicative of recently injured or freshly killed organisms.

Introduction

Receptors for purine nucleotides, referred to as purinergic receptors or purinoceptors, occur in various internal tissues of mammals (see Burnstock, 1978). One type of purinergic receptor, the P_2-type, is most sensitive to the nucleotide adenosine triphosphate (ATP) (Burnstock, 1978). Interestingly, chemoreceptors stimulated by ATP, which exhibit properties similar to P_2-type receptors, have been demonstrated electrophysiologically in the olfactory organ of the Florida spiny lobster, *Panulirus argus* (Carr *et al.*, 1986). However, their role in the chemically mediated behavior of *P. argus* has not been explored.

Recently, in the California spiny lobster, *P. interruptus*, ATP was shown to be a potent chemoattractant, evoking a locomotory response associated with the recognition and finding of food (Zimmer-Faust, 1987; Zimmer-Faust and Dyson-Hudson, in prep.). When the effectiveness of adenosine and adenine nucleotides was compared, the potency sequence for the locomotory response was: ATP > ADP > AMP or adenosine. This sequence was identical to that found by Carr *et al.* (1986) in the physiological studies with *P. argus*.

Collectively, the above findings provided the impetus for initiating an integrated behavioral and physiological study to ascertain if the behavioral response of *P. interruptus* to ATP might be mediated by P_2-like chemoreceptors. In this study, we have extended the behavioral data for *P. interruptus* using a series of ATP analogs to permit comparison with the physiological results from *P. argus*. We also demonstrate physiologically that *P. interruptus* has ATP-sensitive chemoreceptors which exhibit major similarities to those characterized in *P. argus*. Together, our findings reveal that *P. interruptus* does have P_2-like chemoreceptors which may mediate its behavioral response to ATP.

Received 29 February 1988; accepted 31 May 1988.

Materials and Methods

Collection and maintenance of animals

Specimens of *P. interruptus* were captured by hand on reefs near Santa Barbara, California. Before use in behavioral studies, lobsters were held for 7 to 14 days in large circular tanks. A continuous flow of seawater maintained the temperature at 15 to 17°C, and a 12:12 D:L cycle was imposed. Only hard-shelled animals (n = 108) of 60 to 72 mm carapace length were used; each was tattoo marked on the ventral sternites for individual recognition (Kuris, 1971). Lobsters were fed live mussels (*Mytilus californianus* and *M. edulis*) and sea urchins (*Strongylocentrotus purpuratus*) *ad libitum;* all food was removed 24 h before tests.

Specimens of *P. interruptus* used for electrophysiological studies were shipped by overnight courier from Santa Barbara to the Whitney Laboratory (St. Augustine, Florida) where they were held together in a tank with a flow-through seawater supply maintained at 14 to 16°C. Specimens of *P. argus* were collected in the Florida Keys and held at ambient seawater temperature in flow-through tanks at the Whitney Laboratory. All animals were fed a diet of fish, squid, and shrimp.

Behavioral assays

Individual lobsters were assayed for locomotory responses to chemical solutions in rectangular aquaria, 30 × 30 × 13 cm, a size shown previously to permit both careful control of stimulus flow and rapid testing, without inhibiting behavior (Zimmer-Faust and Case, 1983). Earlier studies revealed excellent agreement between the locomotory responses evoked by chemostimulants in natural habitats and in the small aquaria used for assays in the current study (*e.g.,* Zimmer-Faust and Case, 1982; Zimmer-Faust *et al.,* 1984). Seawater entered each aquarium at a flow rate of 2 ml/s from a head-tank maintained under constant hydrostatic pressure. A three-way valve was used to introduce a 25-ml volume of each test solution into the seawater flow. Dilution associated with stimulus delivery was determined in 18 trials by introducing a fluorescent dye (sodium fluorescein) and continuously monitoring fluorescence using optical fiber probes attached to the antennules of unrestrained animals (see Zimmer-Faust and Stanfill, 1986; Zimmer-Faust *et al.,* in press). Maximum concentrations contacting the antennules were determined to be 7.57×10^{-3} ($\pm 3.62 \times 10^{-3}$ S.D.) times the injected concentration, with dye peaks attained 29.8 s (±5.8 s S.D.) after initial dye input. Concentrations presented herein are corrected for this dilution.

A locomotory response by *P. interruptus* is defined as forward ambulatory movement to a distance greater than one carapace length. Previously, ATP was found to stimulate other behaviors associated with appetitive feeding (Zimmer-Faust, 1987); however, these other behaviors were more variable than forward ambulatory motion. Individual lobsters were tested only once every 72 to 96 h for a maximum of 5 tests during a 20-day period. Animals were put into experimental aquaria 45 to 60 min prior to testing and usually settled within 30 to 40 min. Observations were initiated 1 min before introduction of a chemical solution and continued for 4 min afterwards; lobsters were tested only if they were inactive during the first minute of observation. Each assay consisted of a randomized presentation of a test or control stimulus with the exception that identical solutions were never repetitively presented to the same animal. All trials were conducted according to a double-blind protocol. At least 20 different lobsters were assayed with each test solution; seawater alone was the control.

Electrophysiological recordings

Extracellular recordings were made from ATP-sensitive sensory cells in the olfactory organ (lateral filament of the antennule) of both *P. interruptus* and *P. argus.* The preparation was similar to that used by Carr *et al.* (1986) and has been described in detail (*e.g.,* Gleeson and Ache, 1985). The essential features of the preparation were as follows. An excised, lateral filament was placed in an olfactometer and maintained via arterial perfusion with *Panulirus* saline. Selected volumes of chemical stimuli were injected into a carrier stream of artificial seawater (ASW) which continuously flowed through the tuft of olfactory sensilla on the filament at a rate of 3 ml/min. Suction electrodes were used to obtain action potential recordings from the axons of individual sensory cells innervating the sensilla. These recordings were made from the antennular nerve which was exposed at the proximal end of the filament and separated into small bundles within a bath of *Panulirus* saline.

ATP-sensitive cells were identified by their initiation of action potentials (impulses) following the introduction of a search stimulus of ATP (10 μM, *ca.* 20 μl) into the carrier flow of ASW; ASW alone was presented in an identical manner as the control. The response of a cell to defined chemicals was determined by injecting a 190 μl volume of each test substance into the carrier flow. Conductivity measurements showed that this volume generated a stimulus profile in the olfactometer that reached the injected concentration within one second and remained constant for approximately two seconds before beginning to wash out. [Note: due to an error in conductivity measurements, the stimulus profile reported previously (Carr *et al.,* 1986) overestimated the time a stimulus remains at the injected concentration.] Intervals of

4 min were maintained between stimulus presentations, during which time ASW continuously flowed over the filament. In each trial, stimuli were presented in a random sequence except in dose-response determinations where an ascending concentration series was used. Single cell responses were recorded using an amplitude/time window discriminator, the output of which was monitored with a microprocessor to measure and store the time intervals between impulses for on-line or subsequent display and analysis of the response. In this report, cell responses are expressed as the total number of evoked impulses.

Relevant physiological results obtained for *P. argus* (Carr *et al.*, 1986) are included in some figures and summarized in the text to facilitate their comparison with the results obtained with *P. interruptus*.

Chemical solutions

All chemicals were from Sigma Chemical Company. Structural formulae of ATP and the analogs included in the study are shown in Figure 1. For behavioral assays, solutions were prepared immediately before tests in membrane-filtered (0.45 μm) seawater and adjusted to pH 7.8. Aliquots were stored on dry ice and warmed to ambient seawater temperature just prior to use. Solutions for physiological studies were prepared as stocks in ASW, adjusted to pH 7.8, stored at −70°C, and aliquots were brought to room temperature just prior to use.

Results

Behavior

Figure 2 shows the results of the behavioral assays comparing the stimulatory activity of ATP and nine structurally related substances. Although ATP was the most stimulatory substance, all of the analogs, except for 8-bromo-ATP and adenosine, were significantly more effective than seawater alone (G-test for Independence with Williams' correction: $G \geq 7.60$, d.f. = 1, $P < 0.01$, all comparisons). We observed no responses to seawater in 66 trials. The rank order of behavioral activity for these analogs parallels that previously measured physiologically in ATP-sensitive cells of *P. argus* (Fig. 2). A Kendall's Tau analysis of these ranks revealed a highly significant association ($\tau = 0.721$, n = 10, $P < 0.008$). The most notable exception to this ranking concerns the stable analog, β,γ-imido ATP (AMPPNP), which in the physiological tests proved to be more stimulatory than ATP itself. Behaviorally, the relative activity of ADP and AMP was greater than that measured physiologically; however, the behavioral activity induced by these analogs was significantly less than that for ATP (G-Test with Williams' correction: $G \geq 4.31$, d.f. = 1, $P < 0.05$, both comparisons).

To characterize the dose-response (D-R) relationships of selected analogs, behavioral assays were conducted over a range of concentrations with ATP and with three analogs having structural modifications in either the nitrogenous base, the ribose, or the triphosphate moiety. The results revealed that the slopes of the D-R curves for ATP and the analogs were not significantly different (Fig. 3). This finding is consistent with the notion that the actions of these substances are mediated by a common population of receptors. The rank order of potencies found in this analysis was ATP > dATP > CTP ≅ AMP-PNP. This ranking confirmed the order of activities observed earlier with the single-dose determinations (see Fig. 2).

Physiology

Physiological studies revealed that *P. interruptus*, like *P. argus*, has a distinct population of olfactory cells that are selectively activated by ATP. In both species, the response of these cells is characterized by a short burst of impulses, the duration of which is generally only a few hundred milliseconds in spite of the fact that the stimulus is present for several seconds (Fig. 4A). A comparison of the D-R relationships for these cells reveals similar sensitivities in the two species. In *P. interruptus*, however, the D-R function exhibits a significantly steeper slope [Test for Parallelism (Tallarida and Murray, 1981): $P < 0.05$], with a response maximum of approximately 17 impulses (Fig. 4B); the cells in *P. argus* show a maximum response of about 11 impulses.

Comparisons of the stimulatory capacities of the adenine nucleotides and adenosine on the ATP-best cells of both species show marked similarities. In both species the activity sequence is ATP ⩾ ADP > AMP and adenosine (Fig. 5A). In both species ADP is a very poor stimulant and, like AMP and adenosine, is virtually inactive. Moreover, the ATP-best cells in both species show greater responses to the slowly degradable analog, AMP-PNP, than to ATP itself (Fig. 5B). A similar specificity for ATP in the cells of both species was also indicated in trials in which 10 μM glutamate, taurine, betaine, and glycine were each individually tested. None of these substances elicited responses from any of the nine cells examined in *P. interruptus*, and only glycine evoked a response (a single impulse) in one of the seven cells tested in *P. argus*.

Discussion

This study shows that the behavioral response to ATP exhibited by the California spiny lobster, *P. interruptus*, may be mediated by chemoreceptors related to the P_2-

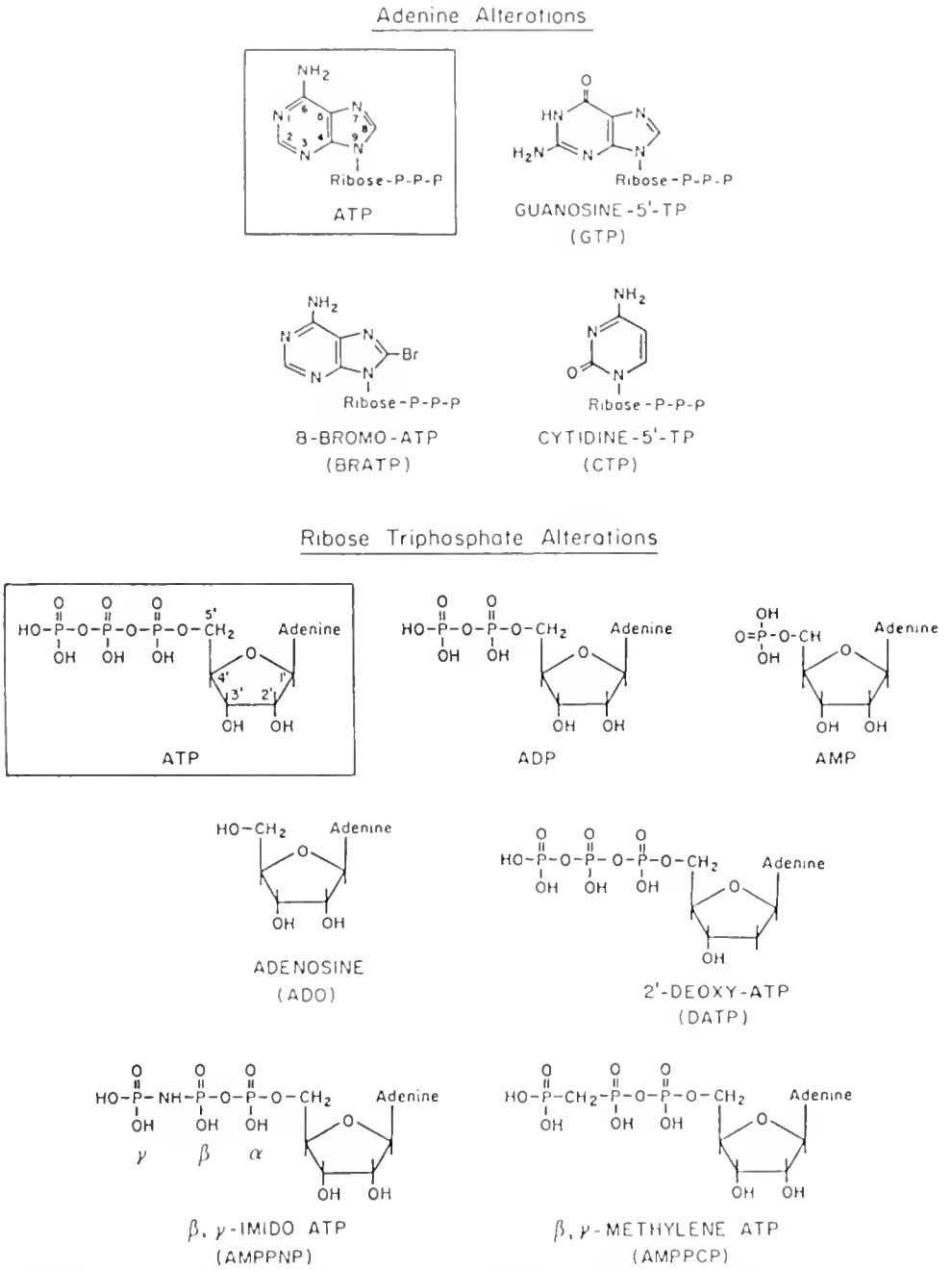

Figure 1. Structural formulae of ATP and analogs tested physiologically and/or behaviorally in *Panulirus interruptus*.

type purinoceptors described by Burnstock (1978). Data supporting this hypothesis include: (1) structure activity relationships (SAR) for the behavior which show congruence with the SAR for P_2-like chemoreceptors previously described in *P. argus* (Carr *et al.*, 1986); and (2) the electrophysiological identification of ATP-sensitive chemoreceptors in *P. interruptus* that are virtually identical in their sensitivity, specificity, and temporal response characteristics to those described in *P. argus*.

The stimulation of the oriented locomotory response in *P. interruptus* by adenine nucleotides and adenosine shows a potency sequence of ATP > ADP > AMP or adenosine. This behavior is also evoked by ATP analogs with modifications in the adenine moiety (*e.g.*, GTP, CTP), the ribose moiety (2'-deoxy ATP), and the triphosphate moiety (AMPPNP, AMPPCP) (see Fig. 2). However the analog 8-Bromo-ATP is only a weak behavioral stimulant. These SAR are consistent with the hypothesis

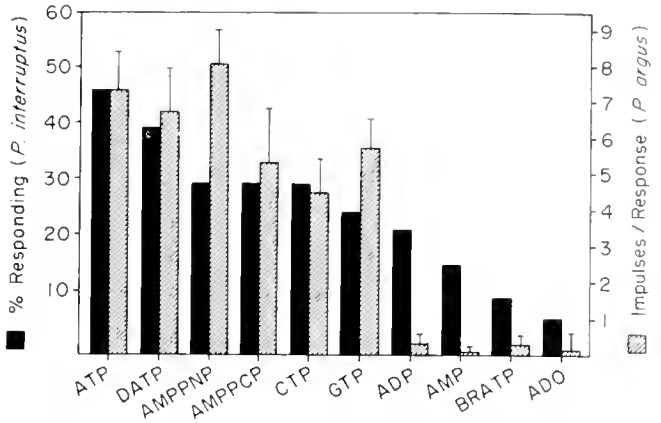

Figure 2. Relative activities of ATP and analogs as determined by behavioral assays in *Panulirus interruptus* (solid bars) and by physiological recordings from ATP-best cells in *P. argus* (hatched bars). In behavioral experiments each compound was tested on at least 20 lobsters at a concentration of 2.3 μM. In physiological studies each compound was tested at 100 μM on at least six cells; bars represent mean responses ± SEM. The physiological data are derived in part from Carr *et al.*, (1986). Abbreviations as in Figure 1.

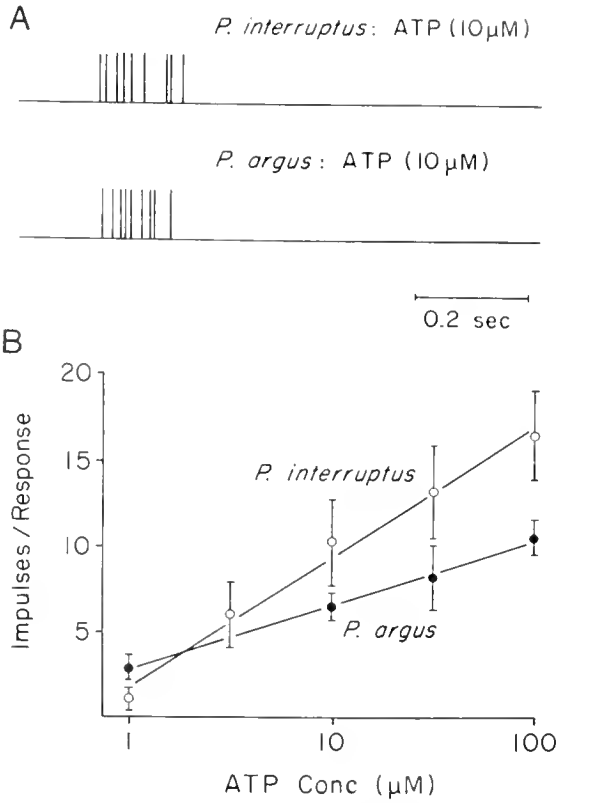

Figure 4. Response properties of ATP-sensitive cells in two lobster species. A. Computer-generated impulse trains depicting typical response profiles following stimulation with ATP. B. Dose-response functions for stimulation with 1 to 100 μM ATP. For each species, the points represent mean values ± SEM for 11 ATP-sensitive cells. Data for *Panulirus argus* are from Carr *et al.* (1986).

that the locomotory behavior is mediated by chemoreceptors akin to the P_2-type purinoceptors that have been found by various workers to exhibit the following SAR: (1) potency sequence of ATP > ADP > AMP or adenosine (Burnstock, 1978); (2) broad sensitivity to nucleotide triphosphates including those with modifications in both the adenine and the ribose moieties (Maguire and Satchell, 1981; Phillis and Wu, 1981; Lukacsko and Krell, 1982); (3) tolerates modifications in the triphosphate moiety such as those represented by the slowly degradable analogs, AMPPNP and AMPPCP (Burnstock and Kennedy, 1985); (4) does not tolerate the deletion of a phosphate group (*e.g.*, as in ADP) (Lukacsko and Krell, 1982); and (5) often not strongly stimulated by the analog, 8-Bromo-ATP (see Maguire and Satchell, 1979).

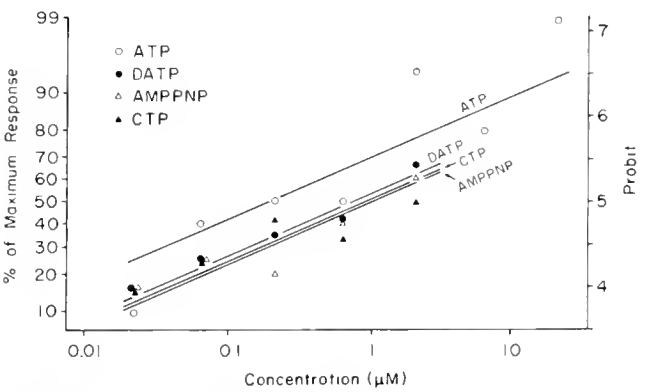

Figure 3. Dose-response relationships for ATP and analogs tested behaviorally in *Panulirus interruptus*. Each point represents data from at least 20 lobsters. The procedure of Potency Probit Analysis (PPA) (Daum and Givens, 1963) showed that the slopes of the individual regression lines are not significantly different, and can be depicted as the parallel lines shown above. Relative potencies obtained by PPA were: ATP = 1.0; 2'deoxyATP (DATP) = 0.257; CTP = 0.188*; β,γ-imidoATP (AMPPNP) = 0.177*. Asterisks indicate potencies significantly less than ATP ($P < 0.05$).

The physiological recordings from the antennules of *P. interruptus* clearly showed that receptor cells selectively sensitive to ATP and related analogs do exist. Furthermore, these cells exhibit marked similarities to the ATP-sensitive cells described earlier in *P. argus* (Carr *et al.*, 1986). A unique property of these cells in both species is that the response is characterized by a brief burst of impulses. Each response terminates abruptly after only a few hundred milliseconds even when the chemical stimulus is continuously introduced over a period of several seconds (see Fig. 4). These "phasic" responses indicate that the cells are rapidly adapted, or desensitized, by stimulatory molecules. This rapid desensitization contrasts markedly with the longer, more "tonic," responses exhibited by other types of antennular chemoreceptor

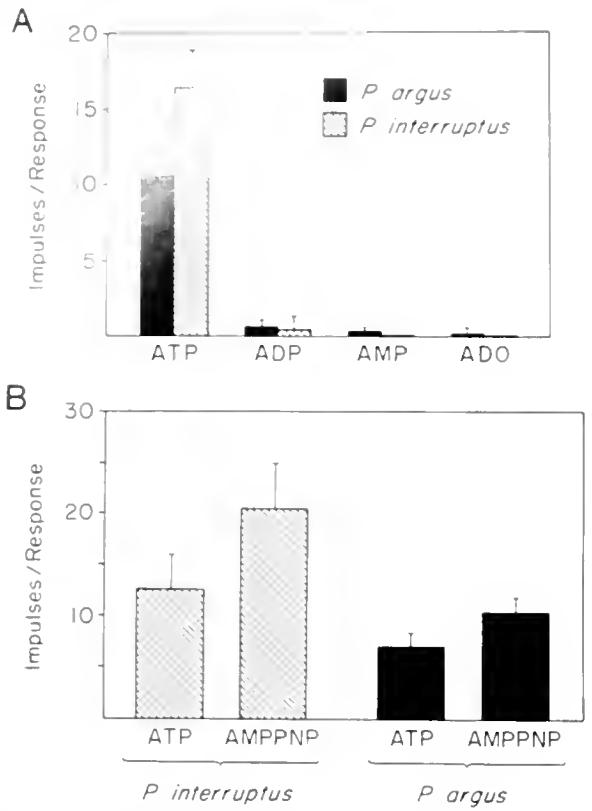

Figure 5. A. Relative activities of adenine nucleotides and adenosine on ATP-sensitive cells of two lobster species. Each compound was presented at a concentration of 100 μM. Bars represent mean responses ± SEM for 11 cells in *Panulirus interruptus* and at least 6 cells in *P. argus*. B. Relative activity of 10 μM ATP and 10 μM β,γ-imidoATP (AMPPNP) on ATP-sensitive cells. Bars are mean values ± SEM for four cells in *P. interruptus* and six cells in *P. argus*. Data for *P. argus* taken from Carr *et al.* (1986).

cells; *e.g.*, see responses of taurine-best cells (Fuzessery *et al.*, 1978) and AMP-best cells (Derby *et al.*, 1984). Since P_2-type purinoceptors are also rapidly desensitized by ATP and related analogs (Burnstock and Kennedy, 1985), it would appear that the ATP-sensitive chemoreceptors exhibit yet another property characteristic of P_2 receptors.

An important discrepancy in the behavioral and physiological data for *P. interruptus* is that the behavioral sensitivity to ATP is approximately 30-fold greater than that determined physiologically for the ATP-sensitive cells (compare D-R curves for ATP in Figs. 3 and 4B). If our physiological and behavioral sensitivity measurements are both accurate, this discrepancy would appear to be inconsistent with the hypothesis that these cells mediate the ATP-stimulated locomotory response; *i.e.*, suggesting that an as yet unidentified population of chemoreceptors with a lower threshold for ATP is responsible for inducing the behavior. However, another possible explanation for the difference could be that convergence of peripheral neurons in the CNS (van Drongelen *et al.*, 1978) plays a role in enhancing the behavioral sensitivity to ATP. Indeed, in several insect species, convergence of many pheromone receptor cells onto fewer neurons in the CNS is believed to give rise to extremely high pheromone sensitivity as measured both behaviorally and in central neurons (Boeckh and Boeckh, 1979; Mankin and Mayer, 1983; Olberg, 1983; Boeckh and Selsam, 1984). For example, in the American cockroach, *Periplaneta americana*, Boeckh and Selsam (1984) demonstrated that deutocerebral neurons exhibit a 100-fold greater sensitivity than the pheromone receptor cell population that projects to them. This was attributed to the fact that the central neurons receive inputs from many peripheral receptor cells and, consequently, can respond to concentrations that activate only a small fraction of the peripheral cells. Hence it is conceivable that a similar amplification occurs in the CNS of the lobster to produce behavioral thresholds for ATP that are lower than predicted from the observed physiological sensitivities of the receptor cells. Finally, because we do not have information on ATP-sensitive chemoreceptors associated with other appendages such as the walking legs (*e.g.*, Derby and Atema, 1982), it is quite possible that inputs from these appendages may contribute importantly to the behavioral response.

Two significant discrepancies are evident when comparisons are made between the behavioral and physiological results obtained with the ATP analogs used in the current study. First, ADP and AMP are better stimulants of the behavioral response in *P. interruptus* than would be predicted from the physiological studies which revealed that both of these nucleotides are virtually nonstimulatory to the ATP-sensitive cells (see Fig. 2). Again, convergence, as discussed above, may result in the behavioral sensitivity to these analogs; also the integration of inputs from other receptor cells is likely since substances presented in the behavioral assays are not restricted to interacting exclusively with the ATP-sensitive cells described herein. Indeed, Spencer (1986) demonstrated strong responses to ADP and AMP in multiunit recordings from antennular chemosensory neurons in *P. interruptus*. Furthermore, sensory cell populations exhibiting selective sensitivity to AMP (Derby *et al.*, 1984) and ADP (Carr *et al.*, in press) have been described in *P. argus*. A second discrepancy between the behavioral and physiological results is that the slowly degradable analog, AMPPNP, is more effective than ATP when tested physiologically (see Fig. 5B), but less effective than ATP when tested behaviorally (see Figs. 2, 3). This suggests that a lobster is capable of discriminating ATP from AMPPNP via some response difference of the ATP-cell population and/or via inputs from other cells which exhibit a differ-

ential sensitivity to these compounds. The mechanisms underlying these intriguing behavioral/physiological differences remain to be determined.

The widespread effects of purine nucleotides, especially ATP, upon visceral muscles of several of the lower vertebrates prompted Burnstock (1975) to propose that ATP may represent one of the most primitive transmitters. If ATP was in fact a primitive transmitter, then receptors for ATP might also occur among many invertebrate organisms as well. Indeed, there is now substantial evidence that receptors activated by ATP or related adenine nucleotides, are frequently represented among the invertebrates (*e.g.*, Mato *et al.*, 1978; Barber *et al.*, 1982; Yatani *et al.*, 1982; Carr and Thompson, 1983; Derby *et al.*, 1984; Chase and Wells, 1986; Derby *et al.*, 1987; Hoyle and Greenberg, 1988). In addition to the P_2-like receptors present on the olfactory organ of the two species of spiny lobsters, ATP-sensitive chemoreceptors are known to occur in several species of insects including the tsetse fly (Mitchell, 1976), the assassin bug (Smith, 1979; Friend and Smith, 1982), the black fly (Sutcliffe and McIver, 1979), the mosquito (Galun *et al.*, 1984, 1985), and others (see review by Friend and Smith, 1977).

The capacity of ATP to serve as a behavioral stimulant of the spiny lobster is probably related to the fact that this nucleotide occurs in high concentrations in fresh tissues of prey organisms such as crustaceans and molluscs (*e.g.*, see Carr and Derby, 1986). Good signal molecules in the sea should be those for which a high "signal to noise" ratio is maintained (*e.g.*, see Fuzessery *et al.*, 1978; Atema, 1985; Carr, 1987). Because processes that maintain very low background concentrations ("noise") of ATP in seawater do exist, this molecule may be a particularly appropriate signal for recognizing recently killed or injured prey organisms. Processes minimizing noise levels of ATP in seawater include nucleotidases in tissues that rapidly dephosphorylate ATP after death (see Zimmer-Faust, 1987), plus dephosphorylating enzymes present on the outer surfaces of many planktonic organisms which quickly degrade nucleotides released into the sea (Ammerman and Azam, 1985). Hence the presence of ATP in seawater could provide a reliable indicator that an injured or freshly killed organism is nearby.

Acknowledgments

This research was supported by NSF Grant BNS-8607513. We thank Mr. Jon LaCommare for assistance with the behavioral assays and Ms. Marsha Lynn Milstead for the illustrations.

Literature Cited

Ammerman, J. W., and F. Azam. 1985. Bacterial 5′-nucleotidase in aquatic ecosystems: a novel mechanism of phosphorus regeneration. *Science* **227:** 1338–1340.

Atema, J. 1985. Chemoreception in the sea: adaptations of chemoreceptors and behavior to aquatic stimulus conditions. *Soc. Exp. Biol. Semin. Ser.* **39:** 387–423.

Barber, J. T., E. G. Ellgaard, and K. Herskowitz. 1982. The attraction of larvae of *Culex pipiens quinquefasciatus* Say to ribonucleic acid and nucleotides. *J. Insect Physiol.* **28:** 585–588.

Boeckh, J., and V. Boeckh. 1979. Threshold and odor specificity of pheromone-sensitive neurons in the deutocerebrum of *Antheraea pernyi* and *A. polyphemus* (Saturnidae). *J. Comp. Physiol. A. Sens. Neural Behav. Physiol* **132:** 235–242.

Boeckh, J., and P. Selsam. 1984. Quantitative investigation of the odour specificity of central olfactory neurones in the American cockroach. *Chem. Senses* **9:** 369–380.

Burnstock, G. 1978. A basis for distinguishing two types of purinergic receptors. Pp. 107–118 in *Cell Membrane Receptors for Drugs and Hormones: A Multidisciplinary Approach*, R. W. Straub and L. Bolis, eds. Raven Press, New York.

Burnstock, G. 1975. Comparative studies of purinergic nerves. *J. Exp. Zool.* **194:** 103–134.

Burnstock, G., and C. Kennedy. 1985. Is there a basis for distinguishing two types of P_2-type purinoceptors? *Br. J. Pharmacol.* **73:** 617–624.

Carr, W. E. S. 1987. The molecular nature of chemical stimuli in the aquatic environment. Pp. 3–27 in *Sensory Biology of Aquatic Animals*, J. Atema, R. R. Fay, A. N. Popper, and W. N. Tavolga, eds. Springer-Verlag, New York.

Carr, W. E. S., and C. D. Derby. 1986. Behavioral chemoattractants for the shrimp, *Palaemonetes pugio*: identification of active components in food extracts and evidence of synergistic mixture interactions. *Chem. Senses* **11:** 49–64.

Carr, W. E. S., and H. W. Thompson. 1983. Adenosine 5′-monophosphate, an internal regulatory agent, is a potent chemoattractant for a marine shrimp. *J. Comp. Physiol. A Sens. Neural Behav. Physiol.* **153:** 47–53.

Carr, W. E. S., H. G. Trapido-Rosenthal, and R. A. Gleeson. In press. Stimulants of feeding behavior in marine organisms: receptor and perireceptor events provide insight into mechanisms of mixture interactions. In *Perception of Complex Tastes and Smells*. D. G. Laing, W. S. Cain, B. W. Ache, and R. L. McBride, eds. Academic Press, Sydney.

Carr, W. E. S., R. A. Gleeson, B. W. Ache, and M. L. Milstead. 1986. Olfactory receptors of the spiny lobster: ATP-sensitive cells with similarities to P_2-type purinoceptors of vertebrates. *J. Comp. Physiol. A. Sens. Neural Behav. Physiol.* **158:** 331–338.

Chase, R., and M. J. Wells. 1986. Chemotactic behaviour in *Octopus*. *J. Comp. Physiol. A Sens. Neural Behav. Physiol.* **158:** 375–381.

Daum, R. J., and C. Givens. 1963. *Potency Probit Analysis*. US Dept. Agriculture, Biometrical Services, Beltsville, MD. 23 pp.

Derby, C. D., B. W. Ache, and W. E. S. Carr. 1987. Purinergic modulation in the brain of the spiny lobster. *Brain Res.* **421:** 57–64.

Derby, C. D., and J. Atema. 1982. Chemosensitivity of walking legs of the lobster *Homarus americanus*: neurophysiological response spectrum and thresholds. *J. Exp. Biol.* **98:** 303–315.

Derby, C. D., W. E. S. Carr, and B. W. Ache. 1984. Purinergic olfactory cells of crustaceans: response characteristics and similarities to internal purinergic cells of vertebrates. *J. Comp. Physiol. A. Sens. Neural Behav. Physiol.* **155:** 341–349.

van Drongelen, W., A. Holley, and K. Døving. 1978. Convergence in the olfactory system: quantitative aspects of odour sensitivity. *J. Theor. Biol.* **71:** 39–48.

Friend, W. G., and J. J. B. Smith. 1977. Factors affecting feeding by bloodsucking insects. *Annu. Rev. Entomol.* **22:** 309–331.

Friend, W. G., and J. J. B. Smith. 1982. ATP analogues and other phosphate compounds as g[illegible]ng stimulants for *Rhodnius prolixus* *J Insect Physiol* 28B [illegible]

Fuzessery, Z. M., W. [illegible], and B. W. Ache. 1978. Antennular chemosensitivity [illegible] spiny lobster, *Panulirus argus*: studies of taurine sensit[illegible]rs. *Biol. Bull* **154:** 226–240.

Galun, R., N. O[illegible]d M. Zecharia. 1984. Effect of plasma components on [illegible]ng response of the mosquito *Aedes aegypti* L. to adenine nu[illegible]tides. *Physiol. Entomol.* **9:** 403–408.

Galun, R., L. C. Koontz, R. W. Gwadz, and J. M. C. Ribeiro. 1985. Effect of ATP analogues on the gorging response of *Aedes aegypti*. *Physiol. Entomol.* **10:** 275–281.

Gleeson, R. A., and B. W. Ache. 1985. Amino acid suppression of taurine-sensitive chemosensory neurons. *Brain Res.* **335:** 99–107.

Hoyle, C. H. V., and M. J. Greenberg. 1988. Actions of adenyl compounds in invertebrates from several phyla: evidence for internal purinoceptors. *Comp. Biochem. Physiol* **90C:** 113–122.

Kuris, A. M. 1971. Population interactions between a shore crab and two symbionts. Ph.D. Dissertation, University of California, Berkeley. 345 pp.

Lukacsko, P., and R. D. Krell. 1982. Responses of the guinea-pig urinary bladder to purine and pyrimidine nucleotides. *Eur J Pharmacol.* **80:** 401–406.

Maguire, M. H., and D. G. Satchell. 1979. Specificity of adenine nucleotide receptor sites: inhibition of the guinea pig taenia coli by adenine nucleotide analogs. Pp. 33–43 in *Physiological and Regulatory Functions of Adenosine and Adenine Nucleotides*, H. P. Baer, and G. I. Drummond, eds. Raven Press, New York.

Maguire, M. H., and D. G. Satchell. 1981. Purinergic receptors in visceral smooth muscle. Pp. 49–92 in *Purinergic Receptors*, G. Burnstock, ed. Chapman and Hall, London.

Mankin, R. W., and M. S. Mayer. 1983. Stimulus-response relationships of insect olfaction: correlations among neurophysiological and behavioral measures of response. *J Theor Biol.* **100:** 613–630.

Mato, J. M., B. Jastorff, M. Morr, and T. M. Konijn. 1978. A model for cyclic AMP-chemoreceptor interaction in *Dictyostelium discoideum*. *Biochem Biophys. Acta* **544:** 309–314.

Mitchell, B. K. 1976. Physiology of an ATP receptor in labellar sensilla of the tsetse fly *Glossina morsitans morsitans* Westw. (Diptera: Glossinidae). *J Exp Biol* **65:** 259–271.

Olberg, R. M. 1983. Interneurons sensitive to female pheromone in the deutocerebrum of the male silkworm moth, *Bombyx mori*. *Physiol Entomol* **8:** 419–428.

Phillis, J. W., and P. H. Wu. 1981. The role of adenosine and its nucleotides in central synaptic transmission. *Prog Neurobiol.* **16:** 187–239.

Smith, J. J. B. 1979. The feeding response of *Rhodnius prolixus* to blood fractions, and the role of ATP. *J. Exp. Biol.* **78:** 225–232.

Spencer, M. 1986. The innervation and chemical sensitivity of single aesthetasc hairs. *J Comp. Physiol. A Sens Neural Behav Physiol.* **158:** 59–68.

Sutcliffe, J. F., and S. B. McIver. 1979. Experiments on biting and gorging behaviour in the black fly, *Simulium venustum*. *Physiol. Entomol* **4:** 393–400.

Tallarida, R. J., and R. B. Murray. 1981. *Manual of Pharmacologic Calculations with Computer Programs* Springer, New York. Pp. 11–12.

Yatani, A., Y. Tsuda, N. Akaike, and A. M. Brown. 1982. Nanomolar concentrations of extracellular ATP activate Ca channels in snail neurones. *Nature* **296:** 169–171.

Zimmer-Faust, R. K. 1987. Crustacean chemical perception: towards a theory on optimal chemoreception. *Biol. Bull.* **172:** 10–29.

Zimmer-Faust, R. K., and J. F. Case. 1982. Odors influencing foraging behavior of the California spiny lobster, *Panulirus interruptus*, and other decapod crustacea. *Mar Behav. Physiol.* **9:** 35–58.

Zimmer-Faust, R. K., and J. F. Case. 1983. A proposed dual role of odor in foraging by the California spiny lobster, *Panulirus interruptus* (Randall). *Biol. Bull.* **164:** 341–353.

Zimmer-Faust, R. K., W. C. Michel, J. E. Tyre, and J. F. Case. 1984. Chemical induction of feeding in California spiny lobster, *Panulirus interruptus* (Randall): responses to molecular weight fractions of abalone. *J. Chem. Ecol.* **10:** 957–971.

Zimmer-Faust, R. K., and M. E. Stanfill. 1986. What do aquatic animals smell? *Am. Zool.* **26:** 9A.

Zimmer-Faust, R. K., J. M. Stanfill, and S. B. Collard III. In press. A fast, multichannel fluorometer for investigating aquatic chemoreception and odor trails. *Limnol. Oceanogr.* **33.**

Reference: *Biol. Bull.* **175:** 175–179. (August, 1988)

Growth Rate of Jamaican Coral Reef Sponges After Hurricane Allen*

CLIVE R. WILKINSON AND ANTHONY C. CHESHIRE

Australian Institute of Marine Science, P.M.B. No. 3, Townsville M.C. 4810, Queensland, Australia

Abstract. Growth rate estimates for five coral reef sponges on the Discovery Bay fore-reef are presented. These were determined from the size of individual sponges growing on the coral rubble that was deposited when Hurricane Allen struck the north coast of Jamaica in August 1980. Sponges collected in February 1986 were weighed and their growth rates determined using the MIX program, originally developed to analyze size-frequency data in fish populations. Sponge doubling times were between 232 and 304 days, with evidence that early exponential growth may be slowing down after four years. The fastest growing sponges were those with small populations of symbiotic cyanobacteria, indicating that there may be a selective advantage for those sponges with photosynthetic symbionts.

Introduction

Hurricane Allen passed within 50 km of the north coast of Jamaica on 6 August 1980. Large seas generated by winds in excess of 250 km per hour caused extensive damage to the coral reefs in the vicinity of the Discovery Bay Marine Laboratory (Woodley, 1980; Woodley *et al.*, 1981). The damage, however, was patchy; it was extensive in some areas and minor in those areas where local topography resulted in the attenuation or deflection of the waves (Woodley *et al.*, 1981). Prior to the hurricane, the fore-reef slope contained extensive, dense thickets of *Acropora cervicornis* between 10 m and 25 m (Goreau and Goreau, 1973; Pang, 1973). Some of these thickets were destroyed, resulting in the deposition of coral rubble which buried other sessile invertebrates.

Received 26 August 1987; accepted 20 May 1988.

* Contribution No. 410 from the Australian Institute of Marine Science and No. 425 from the Discovery Bay Marine Laboratory, Jamaica.

Prior to Hurricane Allen, sponge populations on the fore-reef slope of Discovery Bay were large (Reiswig, 1973) and considered to be ecologically significant as they could filter a volume of water equivalent to the entire water column to a depth of 40 m each day (Reiswig, 1974). The only evidence of these populations in February 1986 was below 30 m depth where some of the extensive populations reported by Reiswig (1973) remained.

Reliable estimates of the growth rates of marine sponges generally are not available. Reiswig (1973), Dayton *et al.* (1974), and Wilkinson (1978) all attempted to determine growth rates by measuring sponges underwater, however their estimates were not particularly successful. More accurate estimates were obtained by Wilkinson and Vacelet (1979) who transplanted Mediterranean species onto plastic plaques for subsequent periodic measurement. These techniques, however, involved trauma to the specimens and were time consuming.

Sponge populations were surveyed on the north coast of Jamaica as part of a larger study (Wilkinson, 1987). The site chosen off the Discovery Bay Marine Laboratory was covered by a dense bed of *Acropora* rubble in excess of half a meter thick, which had accumulated during Hurricane Allen. This bed covered large areas with no evidence of the previous coral or sponge fauna. The site, however, did contain numerous small sponges and coral colonies growing on pieces of the rubble. This study reports the estimated growth rate of one sponge species from 20 m on the fore-reef slope off Discovery Bay. Four other species were collected, and speculative doubling rates are presented based on the rate estimated for the first species, *Pseudoceratina crassa*.

Materials and Methods

Specimens of five massive sponge species were collected in February 1986 from 20 m depth, approximately

1 km to the west of the Discovery Bay Marine Laboratory (see Goreau and Goreau, 1973, for site description). Care was taken to select only regular-shaped animals (presumably derived from a single larva) which were attached to rubble and without obvious signs of predation damage. The sponges were weighed after draining for approximately 20 seconds and the volume measured by displacement in water. Estimations of dry weight were made on 5 individuals of each species after drying for 36 h at 80°C.

The size-class structure of the *Pseudoceratina crassa* population was estimated using the MIX program of Macdonald and Pitcher (1979; Macdonald and Green, 1986). MIX is an interactive program used to fit distributions to grouped data by maximum likelihood estimation. The program has been used effectively in the analysis of fisheries size-frequency data where the groups represent successive year classes. For *P. crassa*, it was assumed that there were five size groupings representing the recruitment from five annual spawning events between Hurricane Allen and the date of collection. To test this assumption, all possible combinations of groups from two to ten were tried, but a significant fit was only obtained for five groups. The mean size of sponges in each size-class was determined from the significant fit obtained to the size-frequency data with the MIX program. These mean values for each size-class were analyzed using a least squares regression to provide an exponential growth model ($W_t = ae^{\alpha t}$) from which the relative growth rate α was estimated.

Growth rates for the other four sponge species could not be obtained by the same method due to the limited number of specimens. Growth rate approximations for these species were derived using the growth model from *P. crassa*. It was assumed that the average size at 50 days after spawning was the same for all species. Exponential growth curves were then derived using simultaneous equations starting with a wet weight at 50 days of 2.93 g (as for *P. crassa*) and the weight of the largest individuals at the date of collection. The age of these individuals was defined as the number of days between the first spawning after Hurricane Allen and the date of collection. Dates for spawning of these species were extracted from the few observations of mass release of sperm reported in the literature (Reiswig, 1983; Hoppe, 1988).

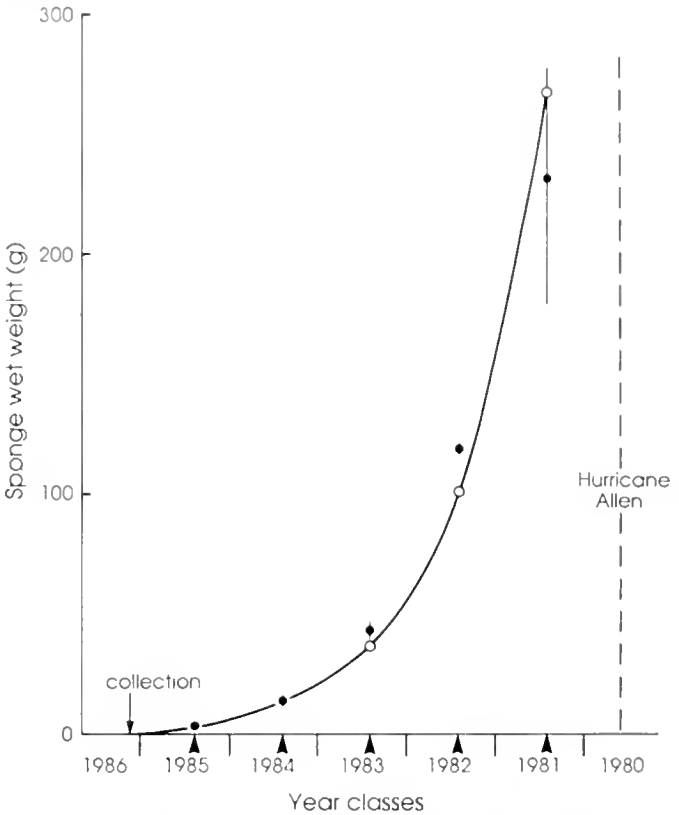

Figure 1. *Pseudoceratina crassa* growth curve prepared from MIX program analysis of sponge wet weights on the collection date in February 1986. The mean size for the five size-classes with standard errors are positioned at the suggested date of spawning (solid arrows) in May of each year. Hurricane Allen occurred on 6 August 1980. The exponential growth curve ($W_t = ae^{\alpha t}$, where $a = 2.567$, $\alpha = 0.00270$, and t = days since spawning) is represented by the curve drawn through the open circles, which are derived "mean sizes" for time year classes.

Results

The most prevalent sponge in this area, *Pseudoceratina crassa*, has an approximate doubling time of 8.5 months (257 days) with individuals after 5 years weighing, on average, 350 g wet weight (Fig. 1; Table I).

Growth rate estimates for the other four sponges suggest that the doubling times are between 7.6 and 10 months (232 and 304 days). These species were less abundant in the area surveyed, hence fewer samples were available for growth rate analysis. Confidence in these estimates is substantially lower than for *P. crassa*, especially for *Agelas dispar* (Table I).

The full data sets for the five species are listed in Figure 2 with the estimated mean size of each year-class. It was assumed that there were five spawning events after Hurricane Allen in August 1980, and that each spawning event contributed individuals to the population. In the case of *Ircinia felix*, the position is different in that there are possibly two annual sperm release events, one in October and another in February. Six year-classes are represented on Figure 2 assuming an October release, although it must be recognized that semi-annual classes could exist. The largest sponges are assumed to have arisen from larvae settling within two months of the hurricane, hence, the estimated growth rates are the most conservative. For the other species, there is a presumed

Table 1

Estimated growth rate parameters for sponge species at 20 m on the fore-reef slope of Discovery Bay, Jamaica

Sponge	Spawning date used	Abundance m^{-2}	No. collected	Doubling time days	Growth const. α	Growth const. a	Size g 5 years	Dry Wt. / Wet Wt.	Vol. / Wet Wt.
Pseudoceratina crassa	28 May	0.57	135	257	0.00270	2.567	354	0.175 ± .021	0.946 ± .023
Ircinia felix	14 February 1 October	0.12	54	235	0.00295	2.535	552	0.154 ± .032	n
Verongula ardis	14 March	0.05	39	232	0.00294	2.531	587	0.108 ± .023	0.927 ± .034
Smenospongia aurea	14 March	0.02	48	304	0.00228	2.621	168	0.155 ± .013	.930 ± .050
Agelas dispar	20 July	0.05	17	250	0.00277	2.557	404	0.150 ± .013	n

Spawning dates used in the exponential equations are from Reiswig (1983) and Hoppe (1988). Abundance reports incidence m^{-2} in 120 m^2 surveys reported in Wilkinson (1987). The doubling times and growth constants α and a are from the exponential equation $W_t = ae^{\alpha t}$ which was used to estimate size (wet weight) after 5 years. Dry weight to wet weight and volume to wet weight ratios plus standard deviations are included for comparison with other studies; n, no data available.

lag of 6.3 to 11.5 months between the date of the hurricane and the first spawning event.

Discussion

Hurricane Allen presented the opportunity to estimate the growth rates of some Caribbean reef sponges. These estimates, although approximate, represent rare examples of sponge growth rate statistics at the early stages of growth. A similar opportunity was used by Scoffin and Hendry (1984) to assess the effects of Hurricane Allen on the recruitment of sclerosponges to the Discovery Bay reef.

The estimated growth rates of the five species indicate doubling times in the range 232–304 days, *i.e.*, all increase by more than 100% per annum. These exceed the rates reported during studies of larger specimens of coral reef sponges (Reiswig, 1973; Wilkinson, 1978). These rates are only applicable to young sponges in the early exponential stage of growth, and cannot be extrapolated to larger sponges where proportional growth rates are considerably less (Reiswig, 1973). There is evidence in Figure 1 that the rate of growth of *Pseudoceratina crassa* is slowing down after four years with the fifth year-class sponges being 40 g (15%) smaller than sponges predicted from unrestricted exponential growth. A reduction in growth rates after the early, exponential phases of growth was observed by Reiswig (1973) for three large sponge species on the Discovery Bay reef.

These estimated growth rates are considered more useful than those recorded previously for coral reef sponges. The estimates are conservative as it is assumed that the larger sponges resulted from larvae settling out within the first year of Hurricane Allen. If the larger sponges resulted from later settlings, then more rapid growth rates would apply. The estimates were based on measurements of differences in biomass (both wet and dry weight measurements), whereas in previous studies growth rates were based on estimated changes in the size of large, irregular specimens underwater.

The assertion that these estimates may be more reliable depends on several assumptions:

(i) All sponges in the region surveyed were destroyed by the hurricane. The specimens collected originated from newly settled, individual larvae produced by undamaged populations from deeper water;
(ii) The individuals collected, particularly the large ones, originated from single larvae;
(iii) The sponge species examined produce recognizable size classes which can be related to annual or semi-annual spawning events;
(iv) The largest sponges resulted from larvae which settled out within the first year after Hurricane Allen.

With respect to assumption (i), destruction in the region surveyed in 1986 was extensive; no large corals (*e.g.*, *Montastrea annularis*) or sponges survived. The area is seaward of site B in Woodley *et al.* (1981) where there was extensive damage to gorgonian colonies. This site (similar in profile to E in Fig. 1 of Woodley *et al.*, 1981) was fully exposed to wave action because it slopes gently, thereby acting as the final repository for considerable amounts of *Acropora* rubble from shallower depths. Hence, it is unlikely that any sponge fragments survived in this habitat. All sponges appeared to be individuals that had settled on the rubble.

Of the five sponges present in sufficient numbers to warrant collection for this study, three form distinct,

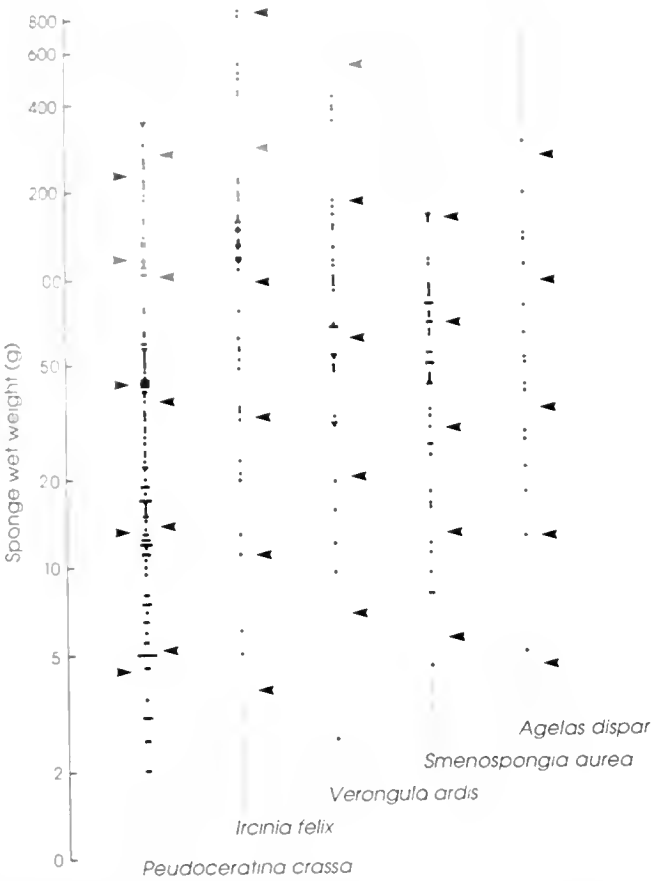

Figure 2. The data set of wet weights (natural logarithmic scale) of the five sponge species from 20 m depth on the Discovery Bay fore-reef. The arrows to the left of the *Pseudoceratina crassa* data set represent the sizes of the year-classes obtained from the MIX program, whereas the arrows to the right of each data set are the year-class sizes from exponential growth curves based on the curve derived from the *P. crassa* data.

massive shapes that vary little with size. *Smenospongia aurea*, *Verongula ardis*, and *Agelas dispar* all are erect, discrete sponges; the first two have a single osculum. It is assumed with confidence that the individual sponges of these three species grew from single larvae. This assumption is more difficult with the other two species. *Ircinia felix* forms irregular, hemispherical mounds which can fuse with adjacent specimens. *Pseudoceratina crassa* commences as a conical-shaped mound with a single oscule. These mounds divide as the sponge grows, eventually forming a series of similar-shaped mounds. Thus, in larger specimens it is difficult to differentiate between larger single sponges and smaller ones that have fused. In all of these sponges, however, it is unlikely that genetically compatible individuals have settled close enough to fuse when individual density is less than 1 m^{-2}. Therefore, the possibility that the larger specimens have formed from the fusion of smaller individuals is regarded as remote.

Knowledge on sponge age-classes [assumption (iii)] is lacking. Very little is known about sponge reproduction *in situ*, and even less is known of settlement from pelagic larvae. Most reports of periodicity in sponge breeding have come via divers' observations of mass releases of spermatozoa. In general, Caribbean sponges appear to have one or possibly two major spawning events *per annum* (Reiswig, 1983; Hoppe, 1988). For *P. crassa*, there is one report of several individuals spawning in May; another species of *Ircinia* produces mature sperm in September/October and again in February; other verongids like *S. aurea* and *V. ardis* spawn in February/March; and five of six reports for *Agelas* species report a single spawning event in July. From these meager observations, the only conclusion is that there is apparently only one and possibly two spawning events *per annum* for most Caribbean sponges.

After considering these assumptions and the associated constraints, these growth estimates can only be considered indications of the rates for these species until more accurate measures are obtained. If assumption (iv) is incorrect, then these rates underestimate *in situ* growth of these sponges. While the rates apply to only five species at one depth on the Discovery Bay fore-reef, they are indicative of three different Orders. These estimates exceed those reported previously for marine sponges. Reiswig (1973) reported that two species on the same reef had barely detectable growth rates, whereas another species, *Mycale laxissima*, had an annual growth rate of 60%. Wilkinson (1978) reported little or no growth for three species of Great Barrier Reef sponge, but *Neofibularia irata* had a mean growth rate of 33%. The doubling rates reported by Wilkinson and Vacelet (1979) varied from 19 weeks to 1 year, but these were for small Mediterranean sponges measured for the period of optimal growth.

The range of growth doubling times of 7.6 to 10 months at 20 m depth indicates that it will take a minimum of 4 to 6 more years for the sponge biomass to approach that reported to exist prior to the hurricane (Reiswig, 1973) or found on other Caribbean reefs at the same depth where individuals of all 5 species attain sizes in excess of 1 kg wet weight (Wilkinson, 1987). The species composition of the developing sponge population at Discovery Bay is considerably different to that studied by Reiswig (1973). In 1973, there were at least 100 sponge species on the fore-reef slope in front of Discovery Bay, whereas only 20 species were evident in an area of 120 m^2 in early 1986 (approximately half that found on other comparable Caribbean reefs; Wilkinson, 1987).

These apparently rapid rates of sponge growth indicate that there is an adequate supply of organic nutrient.

These species would rely almost entirely on the removal of organic matter from seawater for nutrition as none are phototrophic (Wilkinson, 1983). However, two of the species do have small populations of symbiotic cyanobacteria which may augment the amount of nutrient removed from the seawater through the translocation of fixed nutrient carbon (Wilkinson, 1979). These two sponges, *Ircinia felix* and *Verongula ardis*, showed the most rapid growth rates and it is possible that the increased growth over the other species may be attributable to supplemental nutrition from the symbionts.

Acknowledgments

This research was supported under the U. S./Australia Bilateral Agreement for Scientific and Technological Cooperation and by the Australian Institute of Marine Science. Special thanks are due to Dr. J. Woodley and staff at the Discovery Bay Marine Laboratory and to Madeleine Nowak. Dr. H. Reiswig provided valuable criticism of the manuscript.

Literature Cited

Dayton, P. K., G. A. Robilliard, and R. T. Paine. 1974. Biological accommodation in the benthic community at McMurdo Sound, Antarctica. *Ecol. Monogr.* **44:** 105–128.

Goreau, T. F., and N. I. Goreau. 1973. The ecology of Jamaican coral reefs. II. Geomorphology, zonation, and sedimentary phases. *Bull. Mar. Sci.* **23:** 399–464.

Hoppe, W. F. 1988. Reproductive patterns in three species of large coral reef sponges. *Coral Reefs* (in press).

Macdonald, P. D. M., and T. J. Pitcher. 1979. Age-groups from size-frequency data: a versatile and efficient method of analyzing distribution mixtures. *J. Fish. Res. Board Can.* **36:** 987–1001.

Macdonald, P. D. M., and P. E. J. Green. 1985. *User's Guide to Program MIX: an Interactive Program for Fitting Mixtures of Distributions.* Ichthus Data Systems, Ontario, Canada. 28 pp.

Pang, R. K. 1973. The ecology of some Jamaican excavating sponges. *Bull. Mar. Sci.* **23:** 227–243.

Reiswig, H. M. 1973. Population dynamics of three Jamaican Demospongiae. *Bull. Mar. Sci.* **23:** 191–226.

Reiswig, H. M. 1974. Water transport, respiration and energetics of three tropical marine sponges. *J. Exp. Mar. Biol. Ecol.* **14:** 231–249.

Reiswig, H. M. 1983. 1. Porifera. Pp. 1–21 in *Spermatogenesis and Sperm Function*, K. G. and R. G. Adiyodi, eds. John Wiley & Sons, New York.

Scoffin, T. P., and M. D. Hendry. 1984. Shallow-water sclerosponges on Jamaican reefs and a criterion for recognition of hurricane deposits. *Nature* **307:** 728–729.

Wilkinson, C. R. 1978. Microbial associations in sponges. I. Ecology, physiology and microbial populations of coral reef sponges. *Mar. Biol.* **49:** 161–167.

Wilkinson, C. R. 1979. Nutrient translocation from symbiotic cyanobacteria to coral reef sponges. Pp. 373–380 in *Biologie des Spongiaires*, C. Levi and N. Boury-Esnault, eds. Coll. Int. C.N.R.S., Paris, No. 291.

Wilkinson, C. R. 1983. Net primary productivity in coral reef sponges. *Science* **219:** 410–412.

Wilkinson, C. R. 1987. Interocean differences in size and nutrition of coral reef sponge populations. *Science* **236:** 1654–1657.

Wilkinson, C. R., and J. Vacelet. 1979. Transplantation of marine sponges to different conditions of light and current. *J. Exp. Mar. Biol. Ecol.* **37:** 91–104.

Woodley, J. D. 1980. Hurricane Allen destroys Jamaican coral reefs. *Nature* **287:** 387.

Woodley, J. D. *et al.* 1981. Hurricane Allen's impact on Jamaican coral reefs. *Science* **214:** 749–755.

CONTENTS

Volume 175 Number 2

THE BIOLOGICAL BULLETIN

OCTOBER, 1988

Published by the Marine Biological Laboratory

THE BIOLOGICAL BULLETIN

PUBLISHED BY
THE MARINE BIOLOGICAL LABORATORY

OCTOBER, 1988

Printed and Issued by
LANCASTER PRESS, Inc.
PRINCE & LEMON STS.
LANCASTER, PA

THE BIOLOGICAL BULLETIN

THE BIOLOGICAL BULLETIN is published six times a year by the Marine Biological Laboratory, MBL Street, Woods Hole, Massachusetts 02543.

Subscriptions and similar matter should be addressed to THE BIOLOGICAL BULLETIN, Marine Biological Laboratory, Woods Hole, Massachusetts. Single numbers, $20.00. Subscription per volume (three issues) $55.00 ($110.00 per year for six issues).

Communications relative to manuscripts should be sent to Dr. Charles B. Metz, Editor, or Pamela Chapp, Associate Editor, at the Marine Biological Laboratory, Woods Hole, Massachusetts 02543.

POSTMASTER: Send address changes to THE BIOLOGICAL BULLETIN, Marine Biological Laboratory, Woods Hole, MA 02543.

Second-class postage paid at Woods Hole, MA, and additional mailing offices.
ISSN 0006-3185

INSTRUCTIONS TO AUTHORS

The Biological Bulletin accepts outstanding original research reports of general interest to biologists throughout the world. Papers are usually of intermediate length (10–40 manuscript pages). Very short papers (less than 10 manuscript pages including tables, figures, and bibliography) will be published in a separate section entitled "Short Reports." A limited number of solicited review papers may be accepted after formal review. A paper will usually appear within four months after its acceptance.

The Editorial Board requests that manuscripts conform to the requirements set below; those manuscripts which do not conform will be returned to authors for correction before review.

1. ***Manuscripts.*** Manuscripts, including figures, should be submitted in triplicate. (Xerox copies of photographs are not acceptable for review purposes.) The original manuscript must be typed in double spacing (*including* figure legends, footnotes, bibliography, etc.) on one side of 16- or 20-lb. bond paper, 8½ by 11 inches. Manuscripts should be proofread carefully and errors corrected legibly in black ink. Pages should be numbered consecutively. Margins on all sides should be at least 1 inch (2.5 cm). Manuscripts should conform to the *Council of Biology Editors Style Manual*, 4th Edition (Council of Biology Editors, 1978) and to American spelling. Unusual abbreviations should be kept to a minimum and should be spelled out on first reference as well as defined in a footnote on the title page. Manuscripts should be divided into the following components: Title page, Abstract (of no more than 200 words), Introduction, Materials and Methods, Results, Discussion, Acknowledgments, Literature Cited, Tables, and Figure Legends. In addition, authors should supply a list of words and phrases under which the article should be indexed.

2. ***Figures.*** The dimensions of the printed page, 7 by 9 inches, should be kept in mind in preparing figures for publication. We recommend that figures be about 1½ times the linear dimensions of the final printing desired, and that the ratio of the largest to the smallest letter or number and of the thickest to the thinnest line not exceed 1:1.5. Explanatory matter generally should be included in legends, although axes should always be identified on the illustration itself. Figures should be prepared for reproduction as either line cuts or halftones. Figures to be reproduced as line cuts should be unmounted glossy photographic reproductions or drawn in black ink on white paper, good-quality tracing cloth or plastic, or blue-lined coordinate paper. Those to be reproduced as halftones should be mounted on board, with both designating numbers or letters and scale bars affixed directly to the figures. All figures should be numbered in consecutive order, with no distinction between text and plate figures. The author's name and an arrow indicating orientation should appear on the reverse side of all figures.

3. ***Tables, footnotes, figure legends, etc.*** Authors should follow the style in a recent issue of *The Biological Bulletin* in preparing table headings, figure legends, and the like. Because of the high cost of setting tabular material in type, authors are asked to limit such material as much as possible. Tables, with their headings and footnotes, should be typed on separate sheets, numbered with consecutive Roman numerals, and placed after the Literature Cited. Figure legends should contain enough information to make the figure intelligible separate from the text. Legends should be typed double spaced, with consecutive Arabic numbers, on a separate sheet at the end of the paper. Footnotes should be limited to authors' current addresses, acknowledgments or contribution numbers, and explanation of unusual abbreviations. All such footnotes should appear on the title page. Footnotes are not normally permitted in the body of the text.

4. ***A condensed title*** or running head of no more than 35 letters and spaces should appear at the top of the title page.

5. ***Literature cited.*** In the text, literature should be cited by the Harvard system, with papers by more than two authors cited as Jones *et al.*, 1980. Personal communications and material in preparation or in press should be cited in the text only, with author's initials and institutions, unless the material has been formally accepted and a volume number can be supplied. The list of references following the text should be headed LITERATURE CITED, and must be typed double spaced on separate pages, conforming in punctuation and arrangement to the style of recent issues of *The Biological Bulletin*. Citations should include complete titles and inclusive pagination. Journal abbreviations should normally follow those of the U. S. A.

Standards Institute (USASI), as adopted by BIOLOGICAL ABSTRACTS and CHEMICAL ABSTRACTS, with the minor differences set out below. The most generally useful list of biological journal titles is that published each year by BIOLOGICAL ABSTRACTS (BIOSIS List of Serials; the most recent issue). Foreign authors, and others who are accustomed to using THE WORLD LIST OF SCIENTIFIC PERIODICALS, may find a booklet published by the Biological Council of the U.K. (obtainable from the Institute of Biology, 41 Queen's Gate, London, S.W.7, England, U.K.) useful, since it sets out the WORLD LIST abbreviations for most biological journals with notes of the USASI abbreviations where these differ. CHEMICAL ABSTRACTS publishes quarterly supplements of additional abbreviations. The following points of reference style for THE BIOLOGICAL BULLETIN differ from USASI (or modified WORLD LIST) usage:

A. Journal abbreviations, and book titles, all underlined (for *italics*)

B. All components of abbreviations with initial capitals (not as European usage in WORLD LIST *e.g. J. Cell. Comp. Physiol.* NOT *J. cell. comp. Physiol.*)

C. *All* abbreviated components must be followed by a period, whole word components *must not* (*i.e. J. Cancer Res.*)

D. Space between all components (*e.g. J. Cell. Comp. Physiol.*, not *J.Cell.Comp.Physiol.*)

E. Unusual words in journal titles should be spelled out in full, rather than employing new abbreviations invented by the author. For example, use *Rit Vísindafjélags Islendinga* without abbreviation.

F. All single word journal titles in full (*e.g. Veliger, Ecology, Brain*).

G. The order of abbreviated components should be the same as the word order of the complete title (*i.e. Proc.* and *Trans.* placed where they appear, not transposed as in some BIOLOGICAL ABSTRACTS listings).

H. A few well-known international journals in their preferred forms rather than WORLD LIST or USASI usage (*e.g. Nature, Science, Evolution* NOT *Nature, Lond., Science, N.Y.: Evolution, Lancaster, Pa.*)

6. ***Reprints, charges.*** Authors will be charged the excess over $100 of the total of (a) $30 for each printed page beyond 15, (b) $30 for each table, (c) $15 for each formula more complex than a single line with simple subscripts or superscripts, and (d) $15 for each figure, with figures on a single plate all considered one figure and parts of a single figure on separate sheets considered separate figures. Reprints may be ordered at time of publication and normally will be delivered about two to three months after the issue date. Authors (or delegates for foreign authors) will receive page proofs of articles shortly before publication. They will be charged the current cost of printers' time for corrections to these (other than corrections of printers' or editors' errors).

Reference: *Biol. Bull.* **175:** 181–184. (October, 1988)

Morning Release of Larvae Controlled by the Light in an Intertidal Sponge, *Callyspongia ramosa*

SHIGETOYO AMANO

Cancer Research Institute, Kanazawa University, Kanazawa, Ishikawa 920, Japan

Abstract. The intertidal sponge *Callyspongia ramosa* releases larvae in the morning under natural light. The photic control of this morning release was studied under experimental light-dark (LD) cycles. Under LD 12:12h cycles (light period, from 6:00 to 18:00), release peaked about 6:00. But the release was not stimulated by the illumination in the morning because the sponge colonies released larvae even in the darkness. The experiments under various light regimes showed that the photic stimulus is not the onset of darkness but, unexpectedly, the onset of light the day before. In fact, *C. ramosa* colonies invariably released larvae about 24 hours after the onset of light under all illumination regimes tested. The tidal cycle and the daily cycle of the seawater temperature did not influence the time of release. Therefore, in nature, the dawning light most likely stimulates larval release on the next day. This photoadaptation in the larval release of *C. ramosa* suggests that the morning release is advantageous for their free-swimming larvae to seek out and settle on the suitable substratum in the intertidal region within their short dispersive period.

Introduction

Many sponges are phototrophic and some derive at least 50% of their energy requirements from large populations of photosynthetic symbionts, usually blue green algae (Wilkinson, 1983, 1987). Obviously these sponges must occupy a substratum of full sunlight. The free-swimming larvae of such species are probably capable of locating themselves on a habitat exposed to the sun in this dispersive period. On the other hand, the free-swimming larvae of the sponges adapted to the shady habitat must selectively settle themselves on a shaded substratum. The free-swimming larvae of many sponges respond to light (Warburton, 1966; Bergquist and Sinclair, 1968; Uriz, 1982a, b). However, it has not been shown experimentally that the larvae of phototrophic and non-phototrophic sponges show different patterns of behavior in habitat selection (Bergquist *et al.*, 1970; Fell, 1974).

Morning releases of larvae have been reported in several sponge species (Levi, 1951, 1956). *Halichondria panicea* (order Halichondrida) also releases larvae in the morning (Amano, 1986). It was shown that the stimulus for larval release in this sponge is the onset of darkness the evening prior to release, which occurs 15 hours later. In this report I show that *Callyspongia ramosa* (order Haploschlerida) releases larvae in the morning, but its stimulus for release is the onset of light the day before. This is quite different from *H. panicea*. The ecological significance of these photic controls of larval release and of the photoadaptations in the habitat selection of sponge larvae are discussed.

Materials and Methods

Callyspongia ramosa colonies were collected in June from rafts at the Breeding Center of Aomori Prefecture, in northern Japan, about three kilometers from the Asamushi Marine Biological Laboratory where all the experiments were performed. Sponge colonies were collected carefully to minimize damage. They were placed in water-tight containers under water, brought to the laboratory, and transferred into running seawater. Sponges were maintained in clean running seawater to ensure their health throughout the experiments.

In the early morning following collection, colonies releasing many larvae were selected. Larvae filled the mesohyle of such colonies. Usually colonies released larvae for more than ten days in the laboratory. The larvae released from a colony under experimental LD cycles were counted using the method described previously (Amano,

Received 23 May 1988; accepted 25 July 1988.

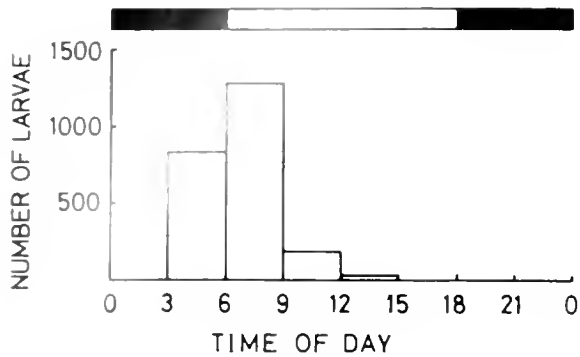

Figure 1. Typical larval release pattern of *Callyspongia ramosa* under LD 12:12h cycles (light period, from 6:00 to 18:00). The colony released largest number of larvae between 6:00 and 9:00, and the numbers decreased thereafter. The arithmetical mean of the release time (MRT) is 6:44. At the top, illumination schedule is shown: the blackened bar indicates the dark period and the white portion, the light period

1986). Briefly, the colony was fixed with a cotton thread in a photographic developing tank and supplied continuously with running seawater. Thus it could be illuminated or shielded from light at will without interrupting the seawater supply. The released larvae were washed with the outflow, caught by a piece of nylon mesh applied to a plastic vessel, and counted every three hours.

Results

Although the exact reproductive period of *C. ramosa* in nature is unknown, it released parenchymula larvae in June in the Asamushi Marine Biological Laboratory. The larvae ejected from a osculum swam just below the water surface. The dimensions of a typical larva were about 250 × 150 μm. The larvae were thickly covered with flagella except for a bare posterior pole, and the bare pole was encircled with a band of long flagella. They were dull yellow but contained reddish brown pigments in the posterior pole.

Under natural light, *C. ramosa* released larvae around dawn in the laboratory. This apparent diurnal periodicity was confirmed under artificial LD 12:12h cycles. Figure 1 shows a typical larval release of *C. ramosa* during a 24-hour-period under these conditions. Many larvae were released before 6:00, but most were released between 6:00 and 9:00; the numbers decreased gradually after 9:00. The mean release time (MRT) was arithmetically calculated with these data; the MRT of the larval release shown in Figure 1 is 6:44.

The results in Figure 1 suggest that the onset of light on that morning could not be a photic stimulus to the larval release because many larvae had been released before 6:00 while still dark. This suggestion is shown to be true in Figure 2. A sponge colony that had been under

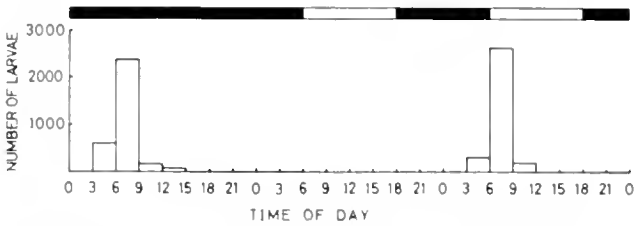

Figure 2. Inhibition of larval release brought about by continuous darkness on the day before. *Callyspongia ramosa* released larvae in the dark on the first day, but did not release on the second day despite illumination from 6:00 to 18:00. MRTs of the 1st and 3rd days are 7:14 and 7:26, respectively.

LD 12:12h cycles was kept in the dark on the first day. On the second and third days it was illuminated under LD 12:12h cycles again. On the first day, the colony released larvae in the dark as if it were still under a LD 12:12h cycle. It did not release on the second day, although it was illuminated from 6:00 to 18:00. This result was not brought about by the loss of release ability of the colony because it released larvae as usual on the third day. These results show that the time of release had been determined by the illumination on the day before. This conclusion is consistent with that of *Halichondria panicea* (Amano, 1986).

Figures 3 and 4 show the results of the experiments designed to determine which photic stimulus, the onset of light or the onset of dark on the day before, triggers larval release. In Figure 3, a colony was illuminated from 12:00 to 18:00; that is putting off of the onset of light by six hours. This putting off of the onset of light delayed the next day's larval release for about 4.5 hours. In Figure 4, a colony was illuminated from 6:00 to 12:00, that is advancing the onset of darkness by six hours. This advance, however, did not significantly advance the time of release on the next day. The delay of the larval release

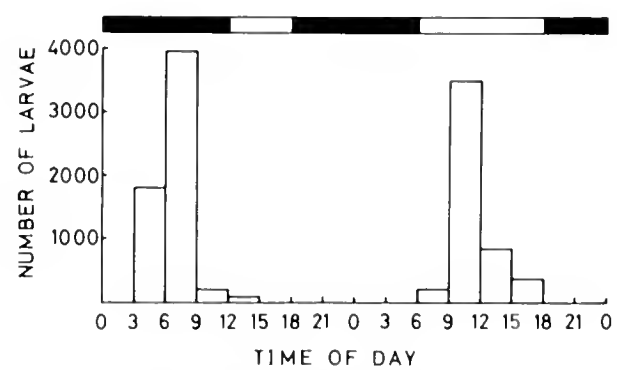

Figure 3. Delay of larval release brought about by six hours' putting off of the onset of light on the first day. The release on the second day was delayed for about 4.5 hours. MRTs of the 1st and 2nd days are 6:47 and 11:18, respectively.

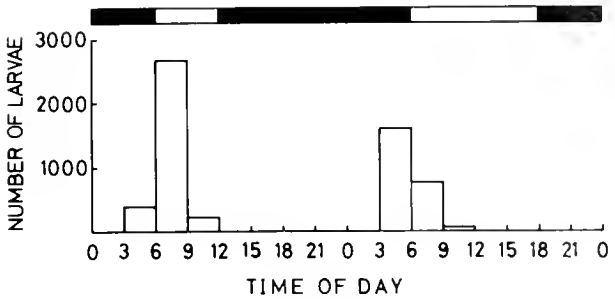

Figure 4. Although the onset of darkness was advanced for six hours, the colony released larvae about the same time on the second day as that under LD 12:12 h cycles. MRTs of the 1st and 2nd days are 7:26 and 5:32, respectively.

in Figure 3 was not a result of the shortening of light period because the colony in Figure 4 was also illuminated for six hours. Thus it is clear from these results that larval release was stimulated by the onset of light on the day before. This conclusion is distinctively different from that of *H. panicea* where the onset of darkness was the stimulus (Amano, 1986).

Results of Figure 5 confirm the above conclusion. If the onset of light is truely a stimulus, the time between photic stimulus and larval release must be about 24 hours because *C. ramosa* released larvae at about 6:00 under LD 12:12h cycles (light period, from 6:00 to 18:00). Instead, if the onset of dark were the stimulus, the duration should be about 12 hours. Preliminary experiments showed that a dark-adapted *C. ramosa* colony reacts to illumination for one hour. Figure 5 shows the result of one such experiment where a colony was illuminated from 17:00 to 18:00. Under these conditions it released larvae around 17:00 on the next day, that is, after about 24 hours.

Table I summarizes the results of the experiments presented in this paper and shows the temporal relationships

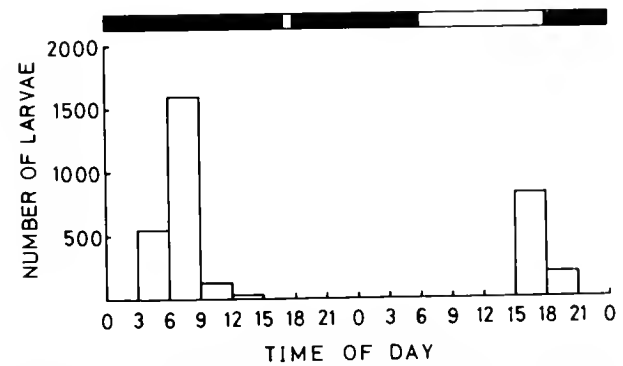

Figure 5. Larval release brought about by one-hour illumination. The colony released larvae about 24 hours after the illumination. MRTs of the 1st and 2nd days are 6:59 and 17:04, respectively.

Table I

Constant temporal relationship of larval release to onset of light on the day before under various illumination regimes in callyspongia ramosa

Hours from onset of light*	Hours from onset of dark*	Reference
24:44	12:44	Fig. 1
23:18	17:18	Fig. 3
23:32	17:32	Fig. 4
24:02	23:04	Fig. 5

* Duration between onset time of light or dark and arithmetical mean of release time.

between larval release and the two possible photic signals. Durations between the onset of light on the day before and larval release are constantly about 24 hours under all illumination regimes tested. On the other hand, the onset of dark has variable temporal relationships to larval release. Thus, at least under these experimental conditions, the larval release of *C. ramosa* is brought about by a photic stimulus, that is, the onset of light on the day before.

Discussion

Under natural illumination, *C. ramosa* releases larvae in the early morning with apparent diurnal periodicity. It is obvious from the results shown in this paper that the larval release is controlled by the light and does not depend on other possible environmental factors. Larval release is independent of the tidal cycle and the daily change of seawater temperature because it showed no temporal relationship to such factors during this study. Besides, it is not controlled by a circadian rhythm because a release peak occurred only once in the continuous darkness. It must be noted, however, that all of the results shown in this paper are based on laboratory experiments. I have yet to study larval release of a sponge in the field; it might be possible in a particular species only. The morning releases of larvae have been reported in several sponge species: *Halichondria panicea* (Amano, 1986), *Haliclona permolis* (Amano, unpub. data), *Oscarella lobularis*, *Hymeniacidon sanguinea*, and *Halisarca metschnikovi* (Levi, 1951, 1956). Thus the morning release of larvae is likely to be ubiquitous in viviparous sponges.

I have already shown that the onset of light on the day before is the photic stimulus to the larval release of *C. ramosa* (order Haploschlerida) (see Results). In fact, colonies of *C. ramosa* released larvae about 24 hours after the onset of light under all illumination regimes tested (Table I). In nature, the dawning light is probably a stimulus to the larval release of the next day. Therefore *C. ramosa* may release larvae a little earlier even on a dark, cloudy morning if the previous morning was clear. In

Halichondria panicea (order Halichondrida), however, the photic stimulus for its larval release is the onset of darkness on the previous day (Amano, 1986). Thus, the onset of light may be a photic stimulus in the order Haplosclerida and the onset of darkness may be a stimulus in the order Halichondrida, although more studies are required to verify this presumption.

Which receives the photic stimulus, a mother sponge or the larvae? The sponge has no ovary; larvae are enveloped by a layer of follicle cells and embedded in the mesohyle. The structure of the follicle and that of the mesohyle seem too simple to receive the photic stimulus and to perform complicated functions associated with larval release. It is more likely that the larvae receive the stimulus directly. Light can reach the larvae through the mesohyle because *C. ramosa* colonies are small and pale in color. When stimulated by the onset of light, mature larvae ready to be released may migrate toward an exhalant canal. Although almost nothing is known about their migration, the larvae must rupture the follicle and move toward an exhalant canal through the mesohyle (Brien and Meewis, 1938; Fell, 1969). *C. ramosa* larvae may require about twenty-four hours to reach the exhalant canal, that is to say, this is probably the lag time before release. To test this hypothesis, the migration of larvae within the mesohyle must be studied in detail during the twenty-four hours following the photic stimulation.

Although sessile animals of acquatic habitat belong to taxa which are very different phylogenetically, they may be grouped together ecologically as producers of dispersive propagules such as planktonic larvae (Sara, 1984). This has been an evolutionary trend, as dispersion and substrate occupation are obviously essential for the success of any sessile animal (Meadows and Campbell, 1972). In the sponge, all viviparous species produce free-swimming larvae as dispersive propagules. It is noteworthy that most intertidal sponges are viviparous and most oviparous sponges inhabit the deeper sea-floor (Reiswig, 1976; Watanabe, 1978; Simpson, 1980). Viviparity appears to be advantageous for the intertidal sponges to occupy a suitable substratum (Bergquist and Sinclair, 1968; Ayling, 1980). If they were oviparous, their eggs and developing embryos might be swept away from the intertidal region by strong currents and waves during a long embryonic period. Free-swimming larvae seem to be able to find and settle promptly on a suitable substratum within the dangerous intertidal region because they respond to light and gravity (Warburton, 1966; Bergquist *et al.*, 1970; Uriz, 1982a, b). The photic controls of larval release shown in this and in a previous paper (Amano, 1986) are probably two instances of the adaptation for efficient dispersion of the swimming larvae of these sessile sponges in the intertidal region.

Acknowledgments

Sincere thanks are expressed to Dr. Numakunai and other members of the Asamushi Marine Biological Laboratory for their hospitality and help during my stay. I am grateful to T. Mayama, S. Tamura, and M. Washio who collected the sponges.

Literature Cited

Amano, S. 1986. Larval release in response to a light signal by the intertidal sponge *Halichondria panicea*. *Biol. Bull.* **171:** 371–378.

Ayling, A. L. 1980. Patterns of sexuality, asexual reproduction and recruitment in some subtidal marine demospongiae. *Biol. Bull.* **158:** 271–282.

Bergquist, P. R., and M. E. Sinclair. 1968. The morphology and behaviour of larvae of some intertidal sponges. *N. Z. J. Mar. Freshwat. Res.* **2:** 426–437.

Bergquist, P. R., M. E. Sinclair, and J. J. Hogg. 1970. Adaptation to intertidal existance: reproductive cycles and larval behaviour in demospongiae. *Symp. Zool. Soc. Lond.* **25:** 247–271.

Brien, P., and H. Meewis. 1938. Contribution à l'étude de l'embryogénèse des Spongillidae. *Arch. Biol.* **49:** 177–250.

Fell, P. E. 1969. The involvement of nurse cells in oogenesis and embryonic development in the marine sponge, *Halichona ecbasis*. *J. Morphol.* **127:** 133–150.

Fell, P. E. 1974. Porifera. Pp. 51–132 in *Reproduction of Marine Invertebrates*, Vol. 1, A. C. Giese and J. S. Pearse, eds. Academic Press, NY.

Levi, C. 1951. L'oviparité chez les spongiaires. *C. R. Acad. Sci. Paris* **233:** 272–274.

Levi, C. 1956. Étude des *Halisarca* de Roscoff. Embryologie et systematique des démosponges. *Arch. Zool. Exp. Gen.* **93:** 1–181.

Meadows, P. S., and J. I. Campbell. 1972. Habitat selection by aequatic invertebrates. *Adv. Mar. Biol.* **10:** 271–382.

Reiswig, H. M. 1976. Natural gamete release and oviparity in Caribbean Demospongiae. Pp. 99–112 in *Aspects of Sponge Biology*, F. W. Harrison and R. R. Cowden, eds. Academic Press, NY.

Sara, M. 1984. Reproductive strategies in sessile macrofauna. *Boll. Zool.* **51:** 243–248.

Simpson, T. L. 1980. Reproductive processes in sponges: a critical evaluation of current data and views. *Int. J. Invertebr. Reprod.* **2:** 251–269.

Uriz, M. J. 1982a. Reproducción en *Hymeniacidon sanguinea* (Grant, 1826): biología de la larva y primeros estadios postlarvarios. *Inv. Pesq.* **46:** 29–39.

Uriz, M. J. 1982b. Morfología y comportamiento de la larva parenquímula de *Scopalina lophyropoda* Schmidt 1982 (*Demospongia, Halichondrida*) y formación del *rhagon*. *Inv. Pesq.* **46:** 313–322.

Warburton, F. E. 1966. The behaviour of sponge larvae. *Ecology* **47:** 672–674.

Watanabe, Y. 1978. The development of two species of *Tetilla* (demospongiae). *Nat. Sci. Rep. Ochanomizu Univ.* **29:** 71–106.

Wilkinson, C. R. 1983. Net primary productivity in coral reef sponges. *Science* **219:** 410–412.

Wilkinson, C. R. 1987. Interocean differences in size and nutrition of coral reef sponge populations. *Science* **236:** 1654–1657.

Reference: *Biol. Bull.* **175:** 185–192. (October, 1988)

Characterization of the Molt Stages in *Penaeus vannamei:* Setogenesis and Hemolymph Levels of Total Protein, Ecdysteroids, and Glucose

SIU-MING CHAN*, SUSAN M. RANKIN**, AND LARRY L. KEELEY

Laboratories for Invertebrate Neuroendocrine Research, Department of Entomology, Texas A&M University, Texas Agricultural Experimental Station, College Station, Texas 77843

Abstract. The molting cycle of *Penaeus vannamei* juveniles was characterized by distinct and predictable changes in the setae of pleopods. The molt pattern was diecdysic with a relatively short intermolt period (40%) and a long proecdysial period (>53%). The levels of both total protein and ecdysteroids increased in the hemolymph during proecdysis, whereas the level of hemolymph glucose was low at metecdysis and proecdysis and maximal during anecdysis. As revealed by SDS-PAGE, the relative concentrations of two polypeptides (32 kD; 175 kD) changed during the molting cycle.

Introduction

Molting in arthropods includes not only the act of ecdysis, but also new cuticle formation, apolysis, the immediate postecdysis, and tissue growth (Passano, 1960). This dynamic cycle has been divided into four phases in crustaceans: (1) metecdysis (stages A, B), the period immediately following ecdysis; (2) anecdysis (stage C), a period of tissue growth and accumulation of food reserves; (3) proecdysis (stage D), a period of active morphological and physiological changes in preparation of the next molt; and (4) ecdysis (stage E), the shedding of the old cuticle (Drach, 1939).

Several methods are used to determine the molt stages of crustaceans. These methods include histological examination of the integument, measurement of the size of the gastroliths or the regenerating pereiopods, and determination of setal development on the appendages. Determination of molt stages by the state of setogenesis on the appendages is rapid and inflicts little harm to the animals, even after repeated sampling. Setogenesis is used as a criterion to stage a number of decapods, including the natantians (Scheer, 1960; Kamiguchi, 1968), anomurans (Kurup, 1964), and macrurans (Aiken, 1973). Among the penaeids, criteria for assessing molt stages are described for *Penaeus duorarum* (Schafer, 1968), *Penaeus merguiensis* (Longmuir, 1983), *Penaeus esculentus* (Smith and Dall, 1985), *Penaeus stylirostris* (Huner and Colvin, 1979; Robertson *et al.*, 1987), and *Penaeus setiferus* (Robertson *et al.*, 1987).

Molting is stimulated in Crustacea by one or more of a group of closely related steroid hormones, the ecdysteroids (Skinner, 1985). Hemolymph ecdysteroids during the molting cycle have been measured in only a few decapods by use of radioimmunoassay (RIA) (Andrieux *et al.*, 1976; Chang *et al.*, 1976; McCarthy and Skinner, 1977; Keller and Schmid, 1979; Stevenson *et al.*, 1979; Chang and Bruce, 1980; Charmantier-Daures and De-Reggi, 1980; Hopkins, 1983; Jegla *et al.*, 1983; Soumoff and Skinner, 1983). No determinations are reported for penaeid shrimp. In most cases, hemolymph ecdysteroid titers increase rapidly during proecdysis; however, precise patterns are species-specific (*e.g.*, Stevenson, *et al.*, 1979; Chang and Bruce, 1980). Other hemolymph parameters, such as the levels of glucose (Telford, 1968) and protein (Dall, 1974) also undergo cyclic changes that correlate with the molt stage.

This paper describes the molting cycle of *Penaeus vannamei*, an economically important shrimp in the mariculture industry of the southern United States. We have characterized molt stages based on setogenesis of the

Received 10 March 1988; accepted 28 July 1988.

* Department of Wildlife and Fisheries Sciences, Texas A&M University.

** To whom correspondence should be addressed.

pleopods, determined hemolymph levels of protein, glucose, and ecdysteroids, and analyzed the hemolymph proteins by polyacrylamide gel electrophoresis (PAGE).

Materials and Methods

Animals

P. vannamei juveniles were purchased from Ocean Venture Inc. in Port Lavaca, Texas. They were held for two weeks in 250 gallon circular tanks for acclimation at 20–22°C and at a salinity of 28–30‰. Shrimp (11.5–13.0 cm total length) were maintained individually in plastic boxes (23 cm × 12.5 cm × 12 cm) and fed once daily with commercial maturation diet at a rate of 4% total body weight (Rangen Inc., Buhl, Idaho).

Setogenesis

To measure setogenesis, the distal third of the pleopod was excised, floated in saline on a microscope slide, and observed at 100× with a compound microscope. Photomicrographs were prepared from pleopods mounted in saline. Setal development was observed at 6-h intervals for 2 days after ecdysis and then twice daily until the next molt.

Hemolymph measurements

Forty μl of hemolymph were withdrawn through the arthropodial membrane of the fifth pereiopod using a chilled microsyringe. Hemolymph sampling was performed with minimal handling of animals and took <20 s. This brief period of handling precluded induction of an endocrine-dependent stress response that would influence the levels of hemolymph metabolites during the time of sampling. All sampling was performed 2–5 h after the onset of the photophase. Sampling of pleopods and of hemolymph at four-day intervals had no apparent effects on the animals. Results from both sexes were pooled since preliminary studies had indicated no sex-related differences in hemolymph metabolite levels.

Ecdysteroid titers were determined in the hemolymph by RIA. Ecdysone antiserum was a gift from Dr. W. E. Bollenbacher (University of North Carolina, Chapel Hill). 23,24 $^3H_2$(N) ecdysone (specific activity 58–60 Ci/m*M*) was purchased from New England Nuclear (Boston, MA); the ecdysone standard was purchased from Sigma Chemical Co. (St. Louis, MO). Ten μl of hemolymph were added to 150 μl methanol. After precipitation of protein for 15 minutes at 4°C, the sample was centrifuged for 5 minutes at 12,000 × *g*. The supernatant was collected and evaporated under nitrogen, and ecdysteroids were measured (Chang *et al.*, 1976).

Hemolymph total protein was measured using the Coomassie brilliant blue test (Bradford, 1976).

Hemolymph glucose was determined by the glucose oxidase procedure (Mark, 1959) using a commercial reagent kit (Sigma Chemical Co.).

Polyacrylamide gel electrophoresis (PAGE)

Hemolymph proteins were analyzed by slab gel electrophoresis (Laemmli, 1970). Native PAGE (6%), was performed with hemolymph mixed with a sample buffer (0.125 *M* Tris-HCl, pH 6.8) containing 0.01% bromphenol blue as the tracking dye. SDS-PAGE (10–15% linear gradient) was performed with hemolymph incubated in sample buffer containing 2% SDS and 1% 2-mercaptoethanol for 15 minutes in a boiling water bath. Electrophoresis was run at 50 V in the stacking gel and 100 V at the resolving phase. Gels were stained with Coomassie blue R for total protein or with dithiooxamide for copper (Whittaker, 1959).

Results

The molting cycle: setogenesis

Setae are external outgrowths from appendages such as uropods, pleopods, and antennule scales. In *P. vannamei*, the degree of setal development was not identical on different appendages and in different regions of the same appendage. For example, if pleopod setae were in stage D_0, most of the setae on the antennule scales were still in late anecdysis (C_3). Similarly, when the setae on the proximal portion of the pleopod entered proecdysis, the setae on the distal half of the pleopods were still at anecdysis. To standardize the criteria for determining molt stages, setogenesis was based on changes in the setae on the distal third of the pleopods.

Stage A (metecdysis). Stage A lasted about one day (Table I), and the newly molted animals were inactive and did not feed. The exoskeleton was soft, parchment-like, and uncalcified. The epidermis was transparent with little pigmentation. Setal lumens were filled with translucent fiber-like matrices (Fig. 1), and the epidermis near the setal base was less granular than that of later stages.

Stage B (metecdysis). The exoskeleton hardened, presumably due to deposition of calcium, and epidermal pigmentation increased. At this time, setal matrices appeared granular and began to retract from the setal lumens towards the bases of the setae. An internal cone (conical base) began to form in each seta during later Stage B.

Stage C (anecdysis). Calcification of the exoskeleton was completed. This stage occupied 10 to 15 days (35–40%) of the intermolt period (Table I). Animals were maximally active at this stage and resumed feeding. Most of the setal lumens were clear of setal matrix at this time.

Table I

Characteristics of the molting stages of juvenile Penaeus vannamei

Stage	Duration	Feeding/activity	Exoskeleton	Epidermis	Setal development
A	18–28 h (1–2%)	none/weak	soft	transparent	granular matrix fills lumen
B	23–40 h (3–4%)	none/restored	hardened	granular	granular matrix retracts; internal cone formation begins; setal organs become visible
C_1	1.5 days (5%)	restored/maximal	hard	granular	granular matrix retraction completed, internal cone formation completed
C_2	6–8 days (20%)	maximal/maximal	hard	granular	
C_3	4–7 days (15%)	maximal/maximal	hard	granules very dense	
D_0	3–6 days (15%)	decreasing/maximal	No new cuticle yet	retracts (apolysis)	
D_1	8–10 days (28%)	decreasing/maximal	New cuticle appears	invaginates	new setae begin to develop
D_2	2–3 days (6–7%)		Space forms between old and new cuticle	invaginates	new setae form barbules
D_3	1–2 days (3–4%)	no feeding, water is absorbed	old skeleton soft		old setal organs disappear, new setae fold
E	1–2 min	no feeding, body expands	old cuticle is shed		

Formation of internal cones was completed in the C_1 stage (Fig. 3). Setal organs, cylindrical structures that give rise to the setae (see Aiken, 1973), became clearly visible in the C_2 stage (Fig. 4). The C_3 stage differed from the C_2 stage (Fig. 4) in that during C_3 the setal bases were more dense and the setal organs more distinctive (Fig. 5), presumably due to mobilization of granules in the epidermis just before proecdysis.

Stage D (proecdysis). Proecdysis lasted 15 to 19 days and could be divided into stages D_0–D_3. Early proecdysis began with apolysis (Jenkin, 1966), the separation of the endocuticle from the epidermis. In *P. vannamei*, the process began first in the posterior region in the endopodites (Fig. 6) and was accompanied by the resorption and presumed decalcification of the exoskeleton. New cuticle was not present at the D_0 stage. As the epidermis retracted, it invaginated ($D_{1'}$) (Fig. 7) at the setal bases as new cuticle was deposited ($D_{1''}$). At the late $D_{1''}$ stage, the new epidermis continued to invaginate and new setae began to develop and protrude from the new cuticle (Fig. 8). At the D_2 stage (Fig. 9), new setae formed barbules and the setal spines extended into the base of the former seta. The epidermal retraction continued and resulted in large empty spaces between the old and new exoskeletons (D_3). Setal organs were no longer evident as discrete organs. Presumably as a result of muscular contraction, the new setae folded, and disrupted the regular pattern of setal arrangement (Fig. 10). Immediately before ecdysis, late proecdysis was characterized by absorption of water, expansion of the body, muscular contraction/relaxation, and breakage of the intercalary sclerites in the abdominal dip.

Stage E (ecdysis). As the animal shed the exuvium, the invaginated setae everted. Ecdysis lasted for less than 2 minutes (<1%). Early post-molt animals usually did not feed, although some newly molted animals consumed the old exuviae, possibly to recover calcium and other cuticular components.

The molting cycle: hemolymph ecdysteroids and metabolites

We measured levels of circulating ecdysteroids and metabolites during different stages of the molting cycle as determined by the criteria of setal formation and morphology described above.

Figure 11 shows the ecdysteroid levels in the hemolymph during each molt stage. Ecdysteroid titers were approximately 30 pg/μl during metecdysis (A and B). The titers dropped to a minimum of about 16 pg/μl at stage C_2, began to increase at C_3 and reached a maximum of approximately 200 pg/μl at $D_{1'}$. The increases in ecdysteroid titer correlated with the onset of proecdysis and the events related to new cuticle formation.

The pattern of hemolymph protein levels was similar to that of the ecdysteroids. Hemolymph protein levels were low during metecdysis (20 mg/ml) and anecdysis (C_1) and increased to a plateau (85–95 mg/ml) at the proecdysis (D_3) (Fig. 12).

The changes in levels of hemolymph glucose (Fig. 13) during the molting cycle did not resemble the S-pattern

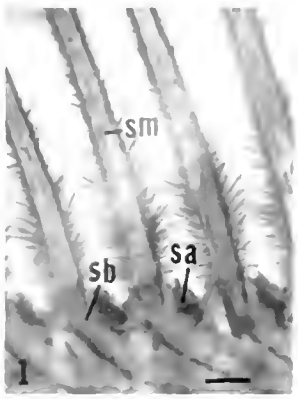

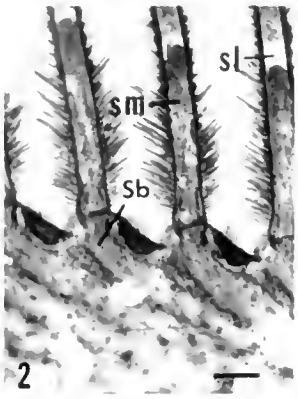

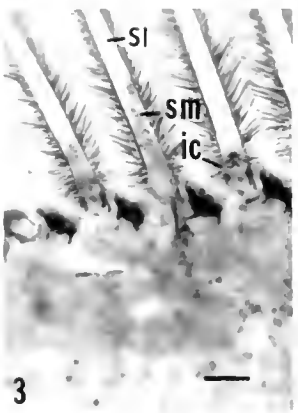

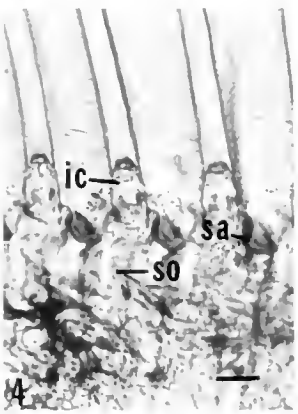

Figure 1. Early metecdysis, stage A. Most of the setal lumens are filled with setal matrix (sm). The bases of setae (sb) are agranular and setal articulations (sa) are opaque. (100 ×), scale bar = 45 μm.

Figure 2. Metecdysis, stage B. The setal matrix (sm) has begun to retract towards the base of the seta (sb), revealing the setal lumen (sl). (100 ×), scale bar = 45 μm.

Figure 3. Anecdysis, stage C_1. Retraction of setal matrix (sm) has neared completion and the setal lumens (sl) are almost empty. Formation of internal cones (ic) has been completed in most setae. (100 ×), scale bar = 45 μm.

Figure 4. Anecdysis, stage C_2. Setal organs (so), which give rise to the internal cones (ic), and setal articulations (sa) are evident. (100 ×), scale bar = 45 μm.

observed for the protein and ecdysteroid titers. The glucose levels were lowest immediately before and after the molt and increased significantly ($P < 0.05$; t-test) during anecdysis (C_3).

Thirteen proteins were detected in stained native gels; the dominant protein, #6, stained positively for copper with dithiooxamide (data not shown) and is therefore likely to be the respiratory protein, hemocyanin. No distinctive changes in proteins during the molting cycle were revealed by native gels. SDS-PAGE of hemolymph proteins of the molt cycle revealed more than 20 polypeptides (Fig. 14). No changes were observed in the major polypeptides; however, of the less abundant polypeptides, one small (32 kD) and one high molecular weight polypeptide (175 kD) changed in relative abundance during the molting cycle. The relative concentrations of these two polypeptides were low during late metecdysis (B) and anecdysis (C), and increased during proecdysis (D).

Discussion

The molting cycle in crustaceans is characterized by distinct morphological, physiological, and biochemical events. We have identified and characterized several of these parameters for the South American white shrimp, *P. vannamei*.

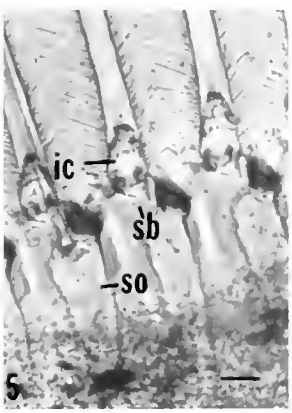

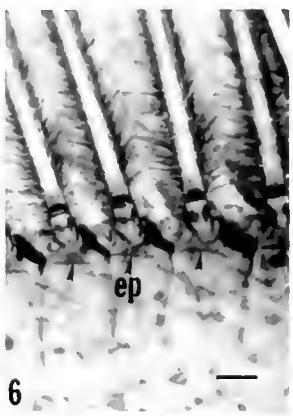

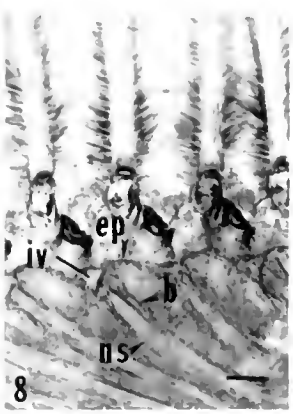

Figure 5. Anecdysis, stage C_3. Setal bases (sb) have become denser and setal organs (so) more distinct. Well-defined internal cones (ic) are evident. (100 ×), scale bar = 45 μm.

Figure 6. Proecdysis, stage D_0. Apolysis. The separation of the epidermis (ep) from the cuticle is evident. (100 ×), scale bar = 55 μm.

Figure 7. Proecdysis, stage D_1. Invagination (iv) of the epidermis (ep) has left a clear space between the old cuticle and the epidermis. The new setae (ns) and cuticle have begun to form. (100 ×), scale bar = 45 μm.

Figure 8. Proecdysis, stage D_2. The epidermis (ep) has continued to invaginate (iv); new barbules (b) have formed on some new setae (ns). (100 ×), scale bar = 45 μm.

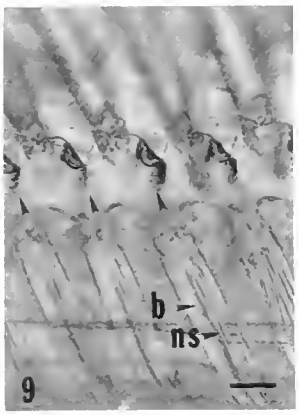

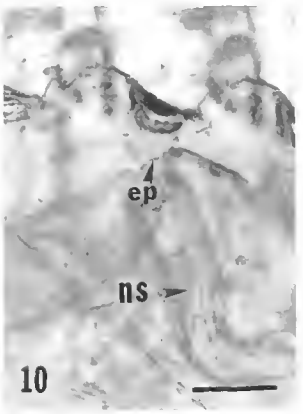

Figure 9. Proecdysis, stage D_2. New barbules (b) are present on all new setae (ns). (100×), scale bar = 30 μm.

Figure 10. Proecdysis, stage D_3. The pattern of new setae (ns) is interrupted by folds of the epidermis (ep). The animal is ready to molt in this stage. (120×) scale bar = 40 μm.

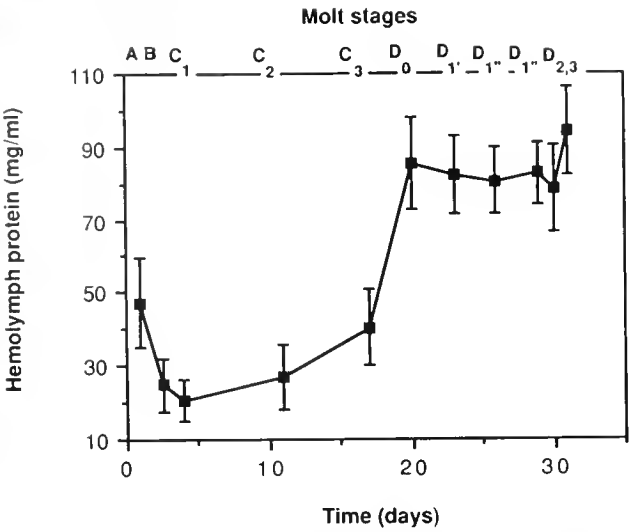

Figure 12. Total protein levels in the hemolymph of juvenile *P. vannamei* during the molting cycle. Values represent mean ± S.E.M. (n ≥ 12 for each point).

The crustacean molting cycle: setogenesis

Although setogenesis has been used as a criterion for molt staging for many years (see Drach, 1939), species variations in setal morphology and development result in differences among crustaceans in both staging criteria and in easily-defined subdivision of the molt stages. We have established criteria for the molt stages and substages in *P. vannamei*. These criteria include the discernment in the pleopods of the epidermis, setal lumens, internal cones, and setal organs (see Figs. 1–10). Similar criteria have been used to determine stages for the penaeidae shrimp *P. californiensis, P. stylirostris* (Huner and Colvin, 1979), *P. merguiensis* (Longmuir, 1983), *P. duorarum* (Schafer, 1968) and *P. esculentus* (Smith and Dall, 1985). Setogenesis in these shrimp species differs primarily in the degree of pigmentation in the appendages and in the duration of the molt stages. Furthermore, the complete retraction of the setal matrices was observed in other penaeids during anecdysis, whereas in some individuals of *P. vannamei* retention of setal matrices was observed. Deviations in setogenesis are even more pronounced in other decapods. For example, in the lobster *Panulirus marginatus*, internal cones are lacking; thus,

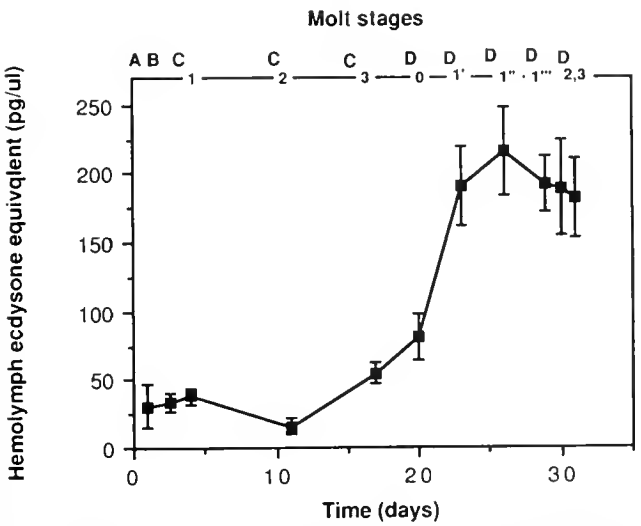

Figure 11. Ecdysteroid titers in the hemolymph of juvenile *P. vannamei* during the molting cycle. Each point represents the mean ± standard error of the mean (S.E.M.) (n ≥ 12 for each point).

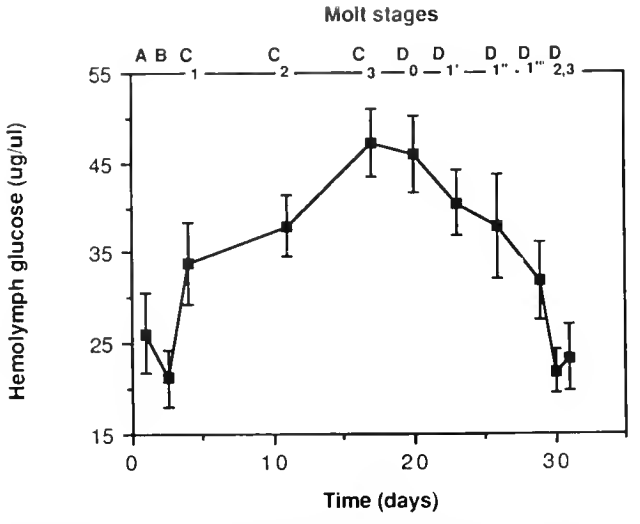

Figure 13. Total glucose levels in the hemolymph of juvenile *P. vannamei* during the molting cycle. Values represent mean ± S.E.M. (n ≥ 12 for each point).

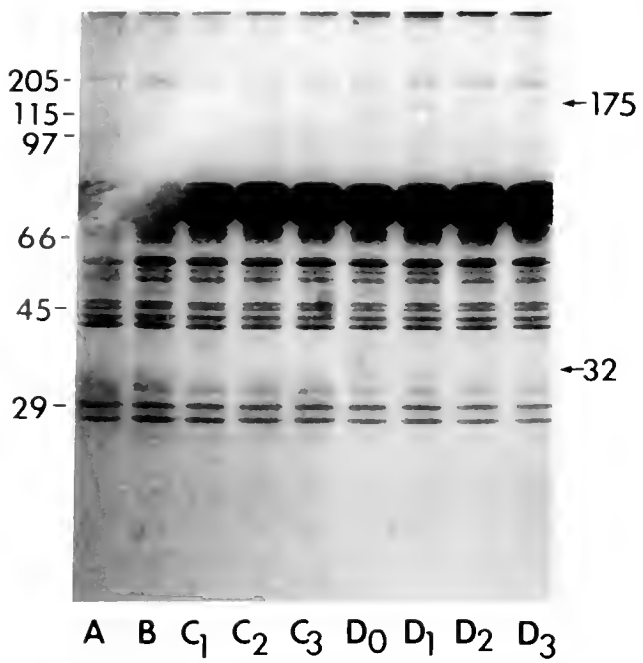

Figure 14. 10–15% linear gradient SDS-PAGE of hemolymph proteins from juvenile *P. vannamei* during the molting cycle. Values in the far left column indicate molecular weight determinations (kD). Arrows indicate polypeptides which increase in relative quantities as the molting cycle progresses. Letters (bottom) indicate the molt stage.

the distinction between stages B and C depends mainly on the thin and hollow appearance of the setal lumen in anecdysis (Lyle and MacDonald, 1983). These examples emphasize that molt staging must rely on a combination of setal characters. Furthermore, substaging varies according to the investigators. We found that the molting cycle in *P. vannamei* was readily divided into stages: A, B, C_{1-3}, and D_{0-3}. In the crayfish *Astacus leptodactylus*, the molting cycle was divided into A_{1-2}, B_{1-2}, C_{1-4}, and D_{0-4} (Van Herp and Bellon-Humbert, 1978). C_4 and D_4 stages were not described in *P. vannamei* because those putative stages were of extremely short duration.

Molt staging may be accomplished using setogenesis in a variety of appendages. These appendages include the pleopods, as demonstrated in *P. marginatus* (Lyle and MacDonald, 1983), *A. leptodactylus* (Van Herp and Bellon-Humbert, 1978) and *Orchestia cavimana* (Graf, 1972); the maxillae in *Chionoecetes opilio* (Moriyasu and Mallet, 1986); and the uropods in *Petrolisthes cinnectines* (Kurup, 1964), *P. stylirostris* (Huner and Colvin, 1979; Robertson *et al.*, 1987) and *P. setiferus* (Robertson *et al.*, 1987). We have used the pleopods for determination of molt stages in *P. vannamei* because removal of other appendages results in trauma or death, and because the relatively thin cuticle of the pleopods facilitates observations on setal development.

Two molting patterns have been defined for the crustacean molting cycle: (1) anecdysic that has a relatively long intermolt and (2) diecdysic that has a long premolt (Knowles and Carlisle, 1956). In general, crustaceans with an anecdysic molting cycle usually enter a terminal anecdysic (C_4) stage (Skinner, 1985). Whether the molting cycle of adult *P. vannamei* (which continue to molt throughout their life) is diecdysic or anaecdysic remains to be determined, but in juvenile *P. vannamei*, the premolt period occupied 50–55% of the molting cycle. Thus, the molting cycle of juvenile *P. vannamei* is diecdysic (Table 1). Our observations on durations of molt stages in juvenile *P. vannamei* are similar to those reported for juvenile *P. esculentus* (Smith and Dall, 1985); however, in juvenile *P. merguiensis* (Longmuir, 1983), juvenile *P. californiensis*, and juvenile *P. stylirostris* (Huner and Colvin, 1979) the D_0 stage is proportionally much longer.

The crustacean molting cycle: hemolymph ecdysteroids and metabolites

The titer of hemolymph glucose was low during stages A and B, rose gradually during stage C, reached a maximal concentration in early proecdysis (D_0, D_1), then declined in late proecdysis (Fig. 11). A similar situation was reported for *Carcinas maenas* (Spindler-Barth, 1976), although titers of circulating glucose in *C. maenas* were more than twice those reported here for *P. vannamei*. In contrast to this pattern, Telford (1968) demonstrated that hemolymph glucose titers increased shortly before ecdysis in three species of crabs. Maximal levels of glucose in *P. vannamei* during the intermolt probably resulted from an accumulation of food reserves during this period of active feeding. Likewise, the gradual decline in glucose titers during late proecdysis corresponded with reduced feeding. We believe that the glucose titers of *P. vannamei* correlate principally with the feeding pattern and do not reflect concurrent changes in metabolism. Since glucose levels were lowest just before and after ecdysis, it is unlikely that the glucose was essential for either chitin synthesis for the new cuticle or as a source of energy during molting. Gwinn and Stevenson (1973) have speculated that in *Orconectes limosus*, the major energy source is chitin because the chitin resorbed by the epidermis before molting provides sufficient material for both new chitin synthesis and energy for molting.

The use of the RIA to measure hemolymph ecdysteroid titers in decapods has been limited to only a few species, including the crayfish, *Orconectes sanborni* (Stevenson *et al.*, 1979) and *O. limosus* (Keller and Schmid, 1979; Jegla *et al.*, 1983), the lobster, *Homarus americanus* (Chang and Bruce, 1980), and the crabs *C. maenas* (Andrieux *et al.*, 1976), *Callinectes sapidus* (Soumoff and Skinner, 1983), *Gecarcinus lateralis* (McCarthy and

Skinner, 1977) *Uca pugilator* (Hopkins, 1983) *Pachygrapsus crassipes* (Chang *et al.*, 1976) and *P. maramoratus* (Charmantier-Daures and DeReggi, 1980). We have shown that in the shrimp, *P. vannamei*, ecdysteroid levels were low during metecdysis and anecdysis, began to rise at apolysis and reached a maximum during proecdysis (Fig. 11). Similar rapid increases in ecdysteroids occur in *C. sapidus* (Soumoff and Skinner, 1983), *O. limosus* (Keller and Schmid, 1979), *G. lateralis* (McCarthy and Skinner, 1977), and *P. crassipes* (Chang *et al.*, 1976). The increasing ecdysteroid titers at the end of anecdysis presumably initiated apolysis. The high ecdysteroid titer was maintained into late proecdysis (D_3) but had declined by early metecdysis (A). A similar decrease in ecdysteroid concentrations was reported for *C. sapidus* (Soumoff and Skinner, 1983), *Orchestia cavimana* (Graf and Delbecque, 1986) and *O. sanborni* (Stevenson *et al.*, 1979). The decrease in ecdysteroid concentrations may be in part the result of water uptake to achieve ecdysis. In all reported cases, however, the lowest ecdysteroid titer always occurs during anecdysis (stage C).

Identification of the specific ecdysteroids of *P. vannamei* remains to be determined. In *P. crassipes* (Chang *et al.*, 1976) and *Orconectes* sp. (Carlisle and Connick, 1973), both ecdysone and 20-hydroxyecdysone are found. Only 20-hydroxyecdysone is detected in *O. limosus* (Keller and Schmid, 1979), while both 20-hydroxyecdysone and Ponasterone A are found in *G. lateralis* (McCarthy and Skinner, 1977).

The increase in hemolymph ecdysteroids correlated with an increase in hemolymph protein content (*c.f.* Figs. 11, 12). A comparable pattern was reported for hemolymph protein in *Palaemon serratus* (Baldais *et al.*, 1984), *C. sapidus* (Soumoff and Skinner, 1983), and *O. sanborni* (Stevenson *et al.*, 1979). The increase in hemolymph protein concentration might result from increased protein synthesis (Gorell and Gilbert, 1971), reduced degradation of proteins and/or resorption of cuticular proteins (Travis, 1955).

Hemolymph proteins of several crustacean species have been separated and characterized by gel electrophoresis (Keer, 1969; Fielder *et al.*, 1971). The patterns vary for different species, but hemocyanin is the major protein detected in all cases and accounts for 80–95% of the total hemolymph protein. Since the major protein of juvenile *P. vannamei* stained positively for copper with dithiooximide (data not shown), and was similar in size (74–76 kD) to hemocyanin from *H. americanus* (Senkbell and Wriston, 1980) it is likely that it is hemocyanin. The rest of the proteins may consist of mostly free enzymes (Scheer, 1960). The increase in hemolymph protein observed in *P. vannamei* during the different molt stages (Fig. 12) likely resulted from a general increase in the quantities of the major proteins since no specific changes were observed in the major polypeptides on SDS-PAGE. However, two minor polypeptide subunits, one of low molecular weight (32 kD) and one of high molecular weight (175 kD), increased in relative abundance during proecdysis (Fig. 14). Although minor in quantities, these polypeptides could have important physiological functions, and play pivotal roles in the events of molting. The sources for any of these polypeptides are unknown.

In conclusion, the developmental stage of setae of the pleopods provides a rapid, accurate indication of the molt stage in juvenile *P. vannamei*. Because it is nonsacrificial, repeated measurements may be taken from the same animal to monitor the rate of development. In *P. vannamei*, setogenesis was used to define the molt stages and used, subsequently, to determine molt-related changes in the hemolymph concentrations of ecdysteroids, proteins, and glucose. It is now possible to use carefully staged animals when examining other physiological events such as reproduction.

Acknowledgments

This work was supported in part through institutional grant N A 85AA-D-SD128 to Texas A&M University by the National Oceanic and Atmospheric Administration's Sea Grant Program, Department of Commerce and by the Texas Advanced Technology Research Program. The research was conducted by the Texas Agricultural Experimental Station.

Literature Cited

Aiken, D. C. 1973. Proecdysis setal development and molt prediction in the American lobster (*Homarus americanus*). *J. Fish. Res. Board Can.* **30:** 1337–1344.

Andrieux, N., P. Porcheron, J. Berreur-Bonnenfant, and F. Dray. 1976. Determination du taux d'ecdysone au cours du cycle d'intermue chez le crabe *Carcinus maenas*: comparison entire individus sains et parasites par *Sacculina carcini*. *C. R. Acad. Sci. Paris* **283:** 1429–1432.

Baldais, L., P. Porcheron, J. Coimbra, and P. Cassier. 1984. Ecdysteroids in the shrimp *Palaemon serratus*: relations with molt cycle. *Gen. Comp. Endocrinol.* **55:** 437–443.

Bradford, M. M. 1976. A rapid and sensitive method for the quantitation of microgram quantities of protein utilizing the principle of protein-dye binding. *Anal. Biochem.* **72:** 248–254.

Carlisle, D. B., and R. O. Connick. 1973. Crustecdysone (20-hydroxyecdysone): site of storage in the crayfish *Orconectes propinquus*. *Can. J. Zool.* **51:** 417–420.

Chang, E. S. and M. J. Bruce. 1980. Ecdysteroid titers of juvenile lobsters following molt induction. *J. Exp. Zool.* **214:** 157–160.

Chang, E. S., B. A. Sage, and J. D. O'Connor. 1976. The qualitative and quantitative determination of ecdysone in tissue of the crab *Pachygrapsus crassipes*, following molt induction. *Gen. Comp. Endocrinol.* **30:** 21–33.

Charmantier-Daures, M., and M. DeReggi. 1980. Aspects préliminaries des variations hémolymphatiques du taux d'ecdystéroides chez *Pachygrapsus marmoratus* (Crustace, Decapode): Influence de la

régénération intensive et de l'ablation des organes Y. *Bull. Soc. Zool. Fr.* **105:** 81–86.

Dall, W., 1974. Indices of nutritional state in the western lobster, *Panulirus longipes* (Milne Edwards). I. Blood and tissue constituents and water content. *J. Exp. Mar. Biol. Ecol.* **16:** 167–180.

Drach, P., 1939. Mue et cycle d'intermue chez les crustacés décapodes. *Ann. Inst. Oceanogr. Paris N. S.* **19:** 103–391.

Fielder, D. R., K. R. Rao, and M. Fingerman, 1971. A female-limited lipoprotein and the diversity of hemocyanin components in the dimorphic variants of the fiddler crab, *Uca pugilator*, as revealed by disc electrophoresis. *Comp. Biochem. Physiol.* **39B:** 291–299.

Gorell, T. A., and L. I. Gilbert, 1971. Protein and RNA synthesis in the premolt crayfish *Orconectes virilis*. *Z. Vgl. Physiol.* **73:** 345–356.

Graf, F., 1972. Etude comparative de l'action de gus et le talitride eige *Orchestia* (Crustacés, Amphipodes). *C. R. Acad. Sci. Paris* **275:** 2045–2048.

Graf, F., and J. P. Delbecque, 1986. Ecdysteroid titer during the molt cycle of *Orchestia cavimana* (Crustacea, Amphipoda). *Gen. Comp. Endocrinol.* **61:** 22–32.

Gwinn, J. F., and J. R. Stevenson, 1973. Role of acetylglucosamine in chitin synthesis in crayfish. I. Correlation of ^{14}C-acetylglucosamine incorporation with stages of the molt cycle. *Comp. Biochem. Physiol.* **45B:** 769–776.

Hopkins, P. M., 1983. Patterns of serum ecdysteroids during induced and uninduced proecdysis in the fiddler crab, *Uca pugilator*. *Gen. Comp. Endocrinol.* **52:** 350–356.

Huner, J. V., and L. B. Colvin, 1979. Observations on the molt cycles of two species of juvenile shrimp, *Penaeus californiensis* and *Penaeus stylirostris* (Decapoda: Crustacea). *Proc. Natl. Shellfish. Assoc.* **69:** 77–84.

Jegla, T. C., C. Ruland, G. Kegel, and R. Keller, 1983. The role of the Y-organ and cephalic gland in ecdysteroid production and the control of molting in the crayfish, *Orconectes limosus*. *J. Comp. Physiol.* **152:** 91–95.

Jenkin, P. M., 1966. Apolysis in Arthopoda molting cycle. *Nature* **221:** 871.

Kamiguchi, Y., 1968. A new method for the determination of intermolt stage in the fresh water prawn *Palaemon paucidens*. *Zool. Mag.* **77:** 326–329.

Keller, R., and E. Schmid, 1979. *In vitro* secretion of ecdysteroids by Y-organ and lack of secretion by mandibular organs of crayfish following molt induction. *J. Comp. Physiol.* **130:** 347–353.

Keer, M. S., 1969. The hemolymph proteins of the blue crab *Callinectes sapidus* II. A lipoprotein serologically identical to oocyte lipovitellin. *Dev. Biol.* **20:** 1–17.

Knowles, F. G. W., and D. B. Carlisle, 1956. Endocrine control in the crustacea. *Biol. Rev.* **31:** 396–473.

Kurup, N. G., 1964. The intermolt cycle of an anomuran, *Petrolisthes cinctipes* Randall (Decapoda). *Biol. Bull.* **127:** 97–107.

Laemmli, U. K., 1970. Cleavage of structural proteins during the assembly of the head of bacteriophage T4. *Nature* **277:** 680–685.

Longmoir, E., 1983. Setal development, moult staging and ecdysis in the banana prawn *Penaeus merguiensis*. *Mar. Biol.* **77:** 183–190.

Lyle, W. G., and C. D. MacDonald, 1983. Molt stage determination in the Hawaiian spiny lobster *Panulirus marginatus*. *J. Crustacean Biol.* **3:** 208–216.

Mark, W., 1959. An improved glucose-oxidase method for determining blood C.S.F. and urine glucose level. *Clin. Chim. Acta* **4:** 395–402.

McCarthy, J. F., and D. M. Skinner, 1977. Proecdysial changes in serum ecdysone titer, gastrolith formation and limb regeneration following molt induction by limb autotomy and/or eyestalk removal in the land crab, *Gecarcinus lateralis*. *Gen. Comp. Endocrinol.* **33:** 278–292.

Moriyasu, M., and P. Mallet, 1986. Molt stages of the snow crab *Chionoecetes opilio* by observation of morphogenesis of setae on the maxilla. *J. Crustacean Biol.* **6:** 709–718.

Passano, L. M., 1960. Molting and its control. Pp. 473–536 in *The Physiology of Crustacea*, Vol. 1, T. H. Waterman, ed. Academic Press, New York.

Robertson, L., W. Bray, J. Leung-Trujillo, and A. L. Lawrence, 1987. Practical molt staging of *Penaeus setiferus* and *Penaeus stylirostris*. *J. World Aquaculture Soc.* **18:** 180–185.

Schafer, H. J., 1968. The determination of some stages of the molting cycle of *Penaeus duorarum*, by microscopic examination of the setae of the endopodites of pleopods. *U. S. Fish. Wildl. Serv. Fish. Bull.* **67:** 381–391.

Scheer, B. T., 1960. Aspects of the intermolt cycle in natantians. *Comp. Biochem. Physiol.* **1:** 3–18.

Senkbeil, E. G., and J. C. Wriston, 1980. Catabolism of hemocyanin in the American lobster, *Homarus americanus*. *Comp. Biochem. Physiol.* **69B:** 781–790.

Skinner, D. M., 1985. Molting and regeneration. Pp. 43–146 in *The Biology of Crustacea*, Vol. 9, D. E. Bliss and L. H. Mantel, eds. Academic Press, New York.

Smith, D. M., and W. Dall, 1985. Moult staging the tiger prawn *Penaeus esculentus*. Pp. 85–95 in *Second Australian National Prawn Seminar*, P. C. Rothlisberg, B. J. Hill, and D. J. Staple, eds. NPS2, Cleveland, Australia.

Soumoff, C., and D. M. Skinner, 1983. Ecdysteroid titers during the molt cycle of the blue crab resembles those of other crustaceans. *Biol. Bull.* **165:** 321–329.

Spindler-Barth, M., 1976. Changes in the chemical composition of the common shore crab, *Carcinus maenas*. *J. Comp. Physiol.* **105:** 197–205.

Stevenson, J. R., P. N. Armstrong, E. S. Chang, and J. D. O'Connor, 1979. Ecdysteroid titer during the molt cycle of crayfish *Orconectes sanborni*. *Gen. Comp. Endocrinol.* **39:** 20–25.

Telford, M., 1968. The identification of sugars in the blood of three species of Atlantic crabs. *Biol. Bull.* **135:** 674–584.

Travis, D. F., 1955. The molting cycle of the spiny lobster, *Panulirus argus* Latreille. IV. Post-ecdysial histological and histochemical changes in the hepatopancreas and integumental tissue. *Biol. Bull.* **113:** 451–479.

Van Herp, F., and C. Bellon-Humbert, 1978. Setal development and molt prediction in the larvae and adults of crayfish, *Astacus leptodactylus*. *Aquaculture* **14:** 289–301.

Whittaker, J. R., 1959. Localization of hemocyanin on starch gel electrophoretic pattern. *Nature* **184:** 194.

Reference: *Biol. Bull* **175**: 193–201. (October, 1988)

The Effect of Host Feeding on the Contribution of Endosymbiotic Algae to the Growth of Green Hydra

KENNETH W. DUNN*

Department of Ecology and Evolution, State University of New York, Stony Brook, New York 11794

Abstract. Previous work has shown that the advantage conferred by endosymbiotic algae on the growth of green hydra is most evident during periods of food shortage. This advantage disappears when hydra are amply fed. However, evidence is presented here which suggests that endosymbiotic algae are not sensitive to the nutritional needs of the host. In controlled feeding studies, green hydra produced more bud tissue than did aposymbionts at all feeding levels. *Per capita* algal contribution to host growth was independent of host feeding rate. Starvation had little effect on rates of algal photosynthesis. The algae of unfed hydra translocated a larger proportion of photosynthetically fixed ^{14}C to the host than did the algae in recently fed hydra. The differences in algal translocation were small, however, and unlikely to significantly affect hydra growth rates. Evidence is presented suggesting that the decrease in the rate of algal translocation in fed hydra may result from an increased algal demand for photosynthate to support the rapid algal growth that follows host feeding.

Introduction

Studies comparing the budding rates of green and aposymbiotic (algae-free) hydra show that possession of endosymbiotic algae increases the rate of hydra bud production. The advantage conferred by endosymbiotic algae was greatest when hydra received little food. There was no difference in budding rate between amply fed green and aposymbiotic hydra (Muscatine and Lenhoff, 1965a, 1965b, Stiven, 1965). A similar phenomenon occurs in the symbiosis between *Chlorella* and *Paramecium bursaria*. Endosymbiotic algae augment the ciliate's growth at low but not high concentrations of bacterial food (Karakashian, 1963). It is generally believed that the algae augment hydra growth by providing organic materials to the host (Muscatine and Lenhoff, 1965b, Smith *et al.*, 1969, Muscatine, 1971, Thorington and Margulis, 1981). The question then arises whether the endosymbiotic algae may increase the rate of photosynthate translocation during periods when the host is without food (Smith *et al.*, 1969, Mews, 1980).

Regulation of algal translocation according to host need suggests a high degree of coevolution between the symbionts. On the other hand, feeding the host stimulates algal growth (McAuley, 1981, 1982, 1985a, 1985b, 1986a, Bossert and Dunn, 1986, Dunn, 1987). If algae need much of their photosynthate to grow, they may necessarily translocate less carbon when growing rapidly (Pardy and White, 1977; Mews, 1980). Mews (1980) showed diminished translocation by the rapidly growing algae repopulating hydra that had been artificially depleted of algae. Thus the rate of algal carbon translocation may increase when the host is without food through a mechanism which involves no algal response to host need *per se*.

To determine if the contribution of algae to host growth is influenced by host nutritional state directly, rather than by algal growth rate, one would like to vary hydra food income while holding specific algal growth rate constant. It may be possible to accomplish this by studying hydra at "steady state" with their food incomes (Otto and Campbell, 1977, Gurkewitz *et al.*, 1980). Otto and Campbell (1977) showed that after ten days on a fixed feeding regime, hydra come to a "steady state" in which the specific growth rate of hydra cells is constant across feeding rates (see also Bosch and David, 1984). In the studies described here, bud production is measured in hydra at steady state with their feeding rates. Under

Received 12 February 1988; accepted 29 July 1988.

* Present address: Department of Pathology, College of Physicians and Surgeons, Columbia University, New York, New York 10032.

these conditions, the contribution of algae to host bud production was either independent of, or an increasing function of host feeding rate.

One might expect that starving hydra, because of their depressed growth rates, would receive more translocated carbon from their algae than do well fed hydra. Previous examinations of the distribution of photosynthetically fixed ^{14}C in green hydra have not supported this expectation. Similar percentages of fixed carbon were found to be translocated in hydra starved one and three days (Eisenstadt, 1971), and one and nine days (Mews, 1980). Although the percentage of fixed carbon translocated was unaffected by starvation, if algae increase their rate of photosynthesis during host starvation, the actual mass of carbon translocated may have varied with the rate of algal photosynthesis. This was not measured. In studies presented here, measurements of the percentage of photosynthetically fixed ^{14}C translocated from algae to host were taken alongside measurements of the rate of algal photosynthesis, measured with a polarographic oxygen electrode. Algal photosynthesis was unaffected by starvation. However, feeding induced small, brief declines in the percentage of ^{14}C translocated from algae to host to levels below the baseline characteristic of unfed hydra.

Thus: a. the contribution of algae to hydra growth, b. the rates of algal photosynthesis and, c. the percentages of fixed carbon translocated from algae to host, provide no evidence to support the idea that endosymbiotic algae respond according to host nutritional need.

Materials and Methods

Experimental organisms

The Carolina strain of *Hydra viridissima* was obtained from the Carolina Biological Supply Co. Aposymbiotic clones were derived from individuals whose algae were removed by the method of Pardy (1976).

Stock culture conditions

Hydra were maintained in M solution (Muscatine and Lenhoff, 1965a) minus Tris buffer at 17 degrees C under continuous illumination of 15 to 25 $\mu Em^{-2} s^{-1}$. Stocks were fed to repletion with freshly hatched *Artemia* nauplii every Monday, Wednesday and Friday for a period of several months before the start of any study. The culture dishes were rinsed 2 hours and 10 hours after feeding and were scrubbed once a week.

Maintenance of hydra on fixed feeding regimes

Experimental hydra were kept singly in 40 ml dishes. They were maintained on a fixed food income by pipetting a given number of freshly hatched *Artemia* nauplii directly onto the tentacles. Attached buds were not permitted to feed. Thus, bud production reflected parental investment only.

In the first study, 21 green hydra and 18 aposymbionts were fed between 1 and 5 nauplii apiece three times weekly. In the second, 23 green hydra and 20 aposymbionts were fed between 1 and 5 nauplii apiece six times weekly. In all cases the same feeding regime was enforced for ten days prior to the twenty-one day period of data collection. Ten days at a constant feeding rate has been found to be sufficient to equilibrate the size and budding rate of *Hydra attenuata* (Otto and Campbell, 1977). When experimental hydra refused to eat their alloted number of nauplii, subsequent meals were supplemented to compensate.

Measurements of hydra bud production

The number of detached buds was recorded daily for each hydra prior to feeding. On Monday, Wednesday, and Friday detached buds were removed, rinsed in distilled water, and lyophilized. Buds were later weighed individually on a Cahn G-2 microbalance.

Estimation of parental tissue

A positive relationship between parental size and feeding rate is characteristic of hydra at equilibrium with their feeding rates (Otto and Campbell, 1977, Gurkewitz *et al.*, 1980). To verify that this relationship existed in hydra whose bud production was to be measured, parental size had to be measured without harming the experimental hydra. Consequently, parental size was measured photographically. Hydra were photographed at the beginning, middle and end of each feeding experiment. Parental hydra volumes (exclusive of bud tissue) were computed from these photographs as previously described (Slobodkin and Dunn, 1983).

Calibration curves were constructed to convert photographic estimates of volume into masses. Budless adult hydra were each photographed twice, then lyophilized and weighed. Geometric mean regressions (Sokal and Rohlf, 1981) computed from these data explained 90% and 57% of the variation in the masses of green hydra and aposymbionts, respectively. These regressions were then used as calibration curves to estimate the mass of parental tissue of each experimental hydra from its photographic volume measurements.

Algal photosynthesis and translocation

To measure the effect of feeding on translocation of photosynthetically fixed carbon from algae to host, the

rates of photosynthesis and the distribution of photosynthetically fixed ^{14}C between algae and host were measured before and at various times after feeding.

Photosynthetic oxygen production was measured using a polarographic oxygen electrode chamber (volume = 6.4 ml) fitted with a YSI model 5331 oxygen probe (Dunn, 1986). Illumination from a Bausch and Lomb fluorescent lamp was passed through a Kodak 301A infrared cutoff filter to minimize heating of the incubation chamber. Photon flux at the experimental hydra was approximately 30 $\mu Em^{-2}\ s^{-1}$, an illumination level that caused no chamber heating. All incubations were done in 0.45 μ filtered M solution maintained at 17°C by circulating water from a constant temperature bath through the chamber water jacket.

For each experiment, 5 groups of 30 hydra each were assembled randomly from a pool of standard hydra (hydra with one fully formed bud) which had been unfed for 72 hours. One of these five groups was set aside for measurements on unfed hydra. The remaining 4 groups were fed and sequentially selected for measurement at the time points 12, 24, 36, and 48 hours after feeding. In one experiment hydra were fed one *Artemia* nauplius apiece and in a second, hydra were fed two nauplii apiece.

At each time point, hydra were placed in the respirometer, and all light was excluded from the chamber. Upon equilibration of the chamber temperature a constant rate of oxygen depletion was produced, reflecting respiration. Upon illumination a slower rate of oxygen depletion was immediately established and its slope, reflecting net photosynthesis (the combined rates of respiration and photosynthesis), was recorded for 15 minutes. At the end of this period, 50 μl of $Na_2{}^{14}CO_3$ (approximately 1 μCi per μl) was injected through a side port. Hydra were incubated in light in this solution for 45 minutes.

At the end of the incubation, the hydra were rinsed and then homogenized in a glass tissue homogenizer at 0°C. Algae were separated from host tissue by three rounds of centrifugation in M solution (at 600 *g*). Host and algal fractions were then frozen for later analyses. An average of 1.3% (±.15%, standard error) of the algae were found to be included in the host fraction.

At the end of each incubation, after hydra were removed from the chamber, the oxygen electrode was calibrated by means of measurements taken of air saturated distilled water at 17°C and of the deoxygenated solution after addition of a mixture of sodium dithionite and $CoCl_2$.

Additional ^{14}C partitioning data were collected in three more experiments in which hydra were otherwise treated as described above, but no respirometry data were collected. In one experiment, hydra were starved for 72 hours, then fed a single nauplius apiece. In a second experiment, hydra were starved for 72 hours, then fed *ad lib.* In the third experiment, hydra were starved for 120 hours, then fed *ad lib.*

Triplicate samples of both animal and algal fractions for each time point were prepared for liquid scintillation counting. 0.2 ml of 6 *N* acetic acid was added to 0.2 ml aliquots from each fraction. The mixture was then placed in a warm air stream and shaken intermittently over a period of 30 minutes to allow unfixed $^{14}CO_2$ to escape. A stable transparent mixture was obtained after addition of 10 ml of scintillation fluor (8 grams Omnifluor, 2 liters toluene, 1 liter Triton X-100) and 1.2 ml deionized water. Samples were counted with a Beckman LS-100C liquid scintillation counter. Counts per minute were corrected to disintegrations per minute by the external standards channel ratio method.

Of the radioactivity found in the host fraction, 84% was assumed to have been translocated from the algae, since the host fractions of three samples of green hydra incubated in darkness contained an average of 16% (±2%, standard error) of the radioactivity present in the host fraction of identically treated but illuminated green hydra. Likewise, a sample of aposymbionts incubated with radioactive sodium carbonate accumulated 16% of the radioactivity present in the host fraction of illuminated green hydra (after correcting for differences in protein content between the two).

Measurement of algal growth

Algal growth was estimated from four to eight hemacytometer counts of both the host and the algal fractions of a particular sample under 400× epifluorescence. To avoid bias, samples were analyzed without knowing their identity.

The data in Figure 7 on algal growth are also presented as part of another report (Dunn, 1987).

Protein determination

Triplicate protein determinations were made of both host and algal fractions by the method of Lowry *et al.* (1951) using bovine serum albumin as a standard. Sample absorption values were read at 750 nm to avoid interference from chlorophyll.

The difference between the protein content of hydra before and 12 hours after feeding (thus following regurgitation) was used as a measure of food intake for hydra fed *ad lib.* In the two experiments described above in which each hydra was fed one nauplius, the protein content of an individual *Artemia* nauplius was calculated according to this procedure to be 1.6 and 1.8 μg of protein

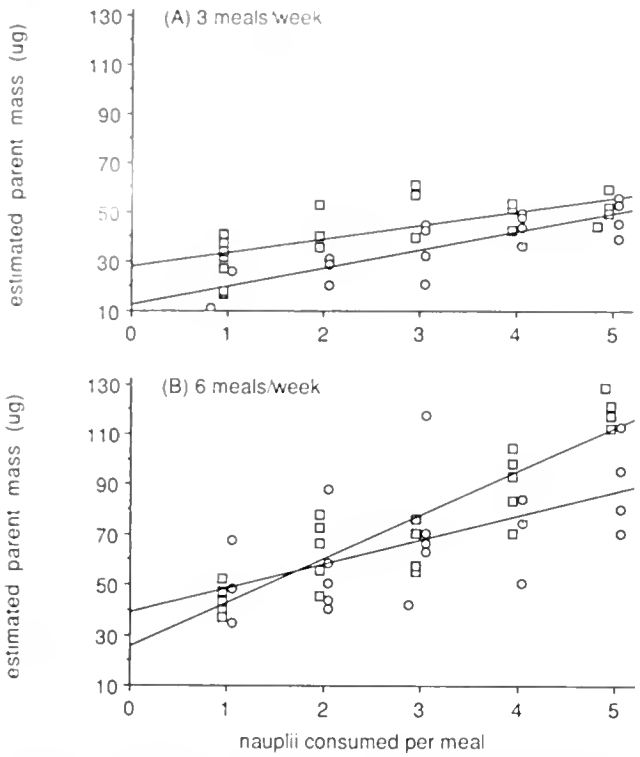

Figure 1. Estimated masses of green (□) and aposymbiotic (○) hydra at various steady state feeding rates for hydra fed three times weekly (A) and six times weekly (B). Masses were derived from photographic size estimates of parental tissue only (exclusive of bud tissue) by the method described in Slobodkin and Dunn (1983). Plotted values represent the means of determinations made at the beginning, middle, and end of the 21-day experiment. Least squares regressions (shown) yielded R^2 values of 0.51 and 0.82 for green hydra fed three times and six times weekly, respectively, and 0.69 and 0.33 for aposymbionts fed three times and six times weekly, respectively. In this and following figures, plotted values for green hydra and aposymbionts have been slightly offset horizontally for clarity.

per nauplius. These values agree well with a direct determination of 1.8 μg of protein per nauplius.

Results

The effect of feeding rate on hydra bud production

Parental body size of both green and aposymbiotic *Hydra viridissima* was an increasing function of steady state feeding rate (Fig. 1).

The experimental hydra produced more buds when provided with more food. For any food income, green hydra appeared to produce more buds than did aposymbiotic hydra (Fig. 2). (Because some of the cells of these meristic data have zero variance, the statistical significance of these regressions or the differences between them cannot be tested parametrically.) Bud size is likewise an increasing function of feeding rate for both forms of hydra (Fig. 3). The green hydra made larger buds than did the aposymbiont (ANCOVA, $P < .025$ in the low frequency feeding study, $P < .001$ in the high frequency feeding study).

To assess the contribution of algae to host growth, estimates of host tissue production were derived from measurements of the mass of buds produced. An average of 63% of the Carolina strain's protein was found in the host fraction when algae were removed by centrifugation. McAuley (1986b) showed that another 17% of hydra protein is lost by the host fraction to the algal fraction by this procedure. Accordingly, I assumed that 80% of the total protein produced by the Carolina strain is of host origin. Assuming that this protein ratio is proportional to the biomass ratio of host tissue to total hydra tissue, rough estimates of host tissue production can be made. Note that these estimates could be confounded by systematic variation in the biomass ratio with feeding rate (see Discussion).

When hydra were fed daily, the beneficial effect of algae on host tissue production was evident at all food lev-

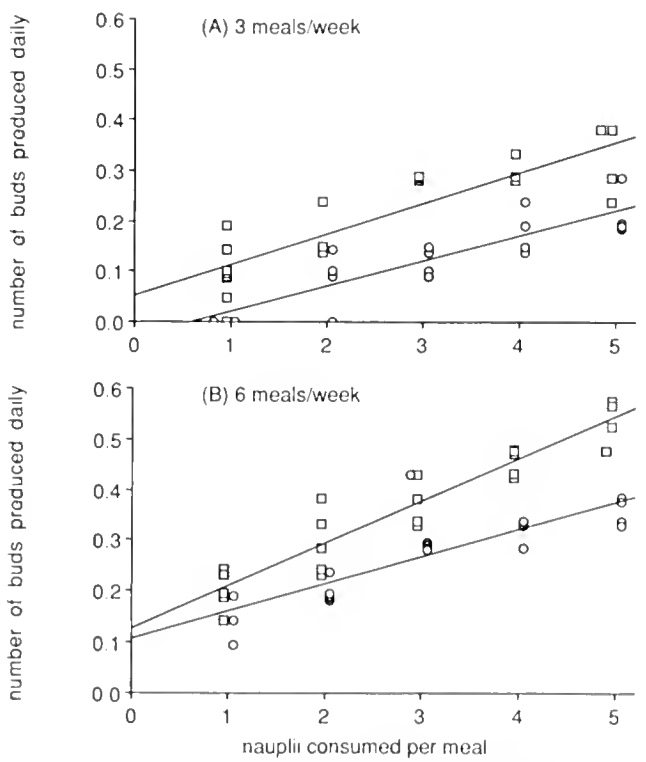

Figure 2. The numbers of buds produced by green (□) and aposymbiotic (○) hydra during 21 days at various steady state feeding levels for hydra fed three times (A) and six times weekly (B). Least squares regressions (shown) yielded R^2 values of 0.75 and 0.90 for green hydra fed three times and six times weekly, respectively, and 0.74 for aposymbionts fed three times or six times weekly, respectively.

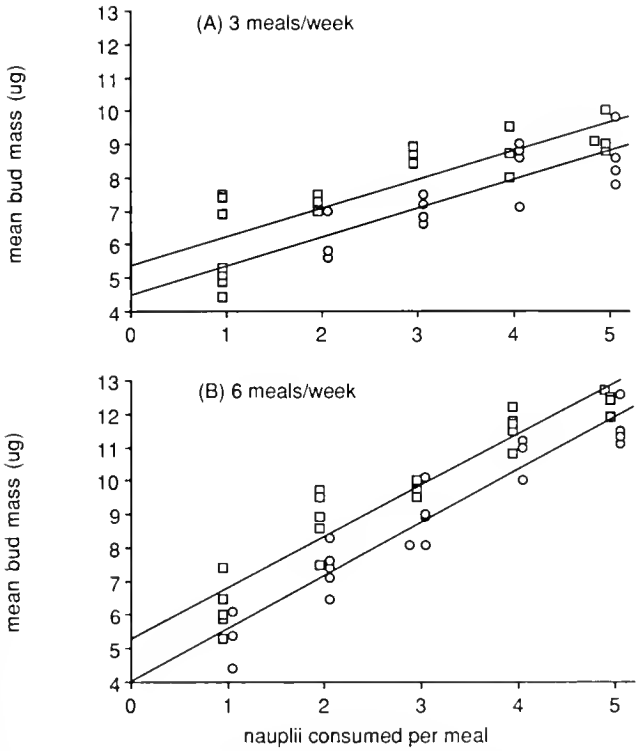

Figure 3. Mean masses of buds produced by green (□) and aposymbiotic (○) hydra during 21 days at various steady state feeding levels for hydra fed three times (A) and six times weekly (B). Least squares regressions (shown) yielded R^2 values of 0.70 and 0.90 for green hydra fed three times and six times weekly, respectively, and 0.65 and 0.91 for aposymbionts fed three times and six times weekly, respectively.

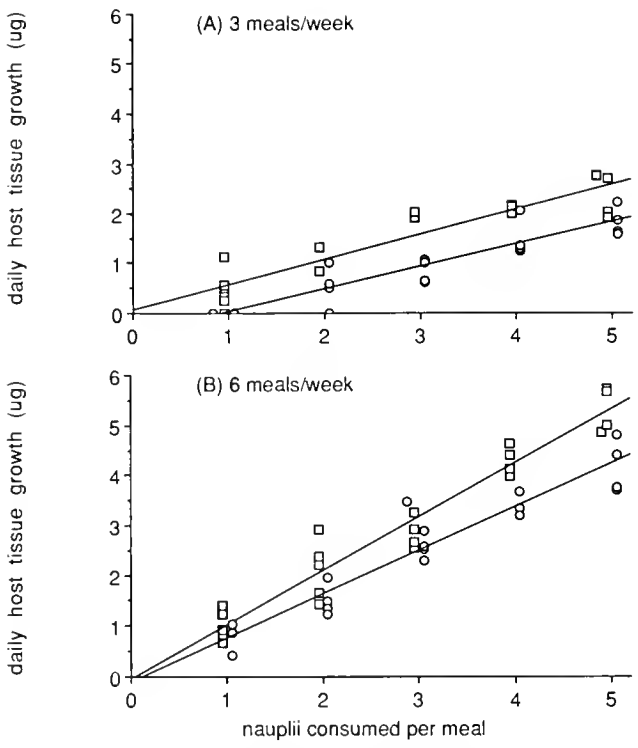

Figure 4. Estimated total amount of host tissue produced by green (□) and aposymbiotic (○) hydra during 21 days at various steady state feeding levels for hydra fed three times (A) and six times weekly (B). Least squares regressions (shown) yielded R^2 values of 0.85 and 0.94 for green hydra fed three times and six times weekly, respectively, and R^2 of 0.82 and 0.90 for aposymbionts fed three times and six times weekly, respectively.

els (Fig. 4b), and the benefit increased as food level increased (slopes differ significantly, $P < .05$, ANCOVA). For hydra fed every other day (Fig. 4a), green hydra produced more animal tissue than did aposymbionts ($P < .001$, ANCOVA), but the increment of difference was independent of food level (slopes do not differ significantly, $P > .25$, ANCOVA). There is no evidence at either feeding frequency that the contribution of algae to host tissue production increases as host food level decreases.

The effect of host feeding on algal photosynthesis

The rates of photosynthesis and of respiration were measured as a function of time after feeding for hydra consuming either one or two *Artemia* nauplii apiece. For each sample, the rate of gross photosynthesis was derived by subtracting the rate of oxygen depletion in the dark (due to respiration) from the rate of oxygen depletion in the light (due to the combination of respiration and photosynthesis). As shown in Figure 5, feeding appeared to have little effect on either the photosynthetic rates or the respiratory rates of starved hydra, at least at the level of resolution of twelve hours.

In all cases, hydra consumed oxygen, indicating that

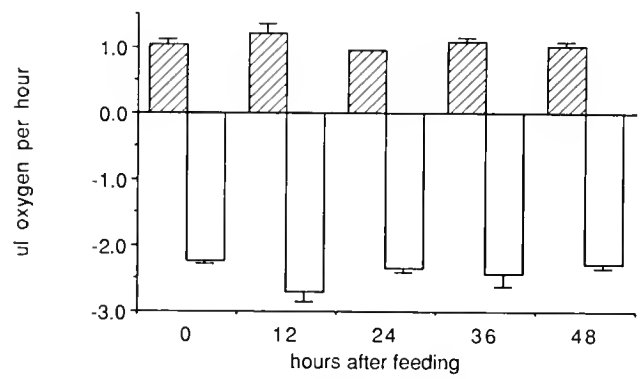

Figure 5. Gross photosynthetic oxygen production (hatched bars) and respiratory oxygen consumption (open bars) of samples of 30 hydra apiece at various times after feeding. Data shown are from two experiments. In one, hydra were fed a single *Artemia* nauplius apiece, in the other, hydra consumed an average of two nauplii apiece. Since no differences between the two feeding conditions were apparent, the data were pooled to yield the means and standard errors shown.

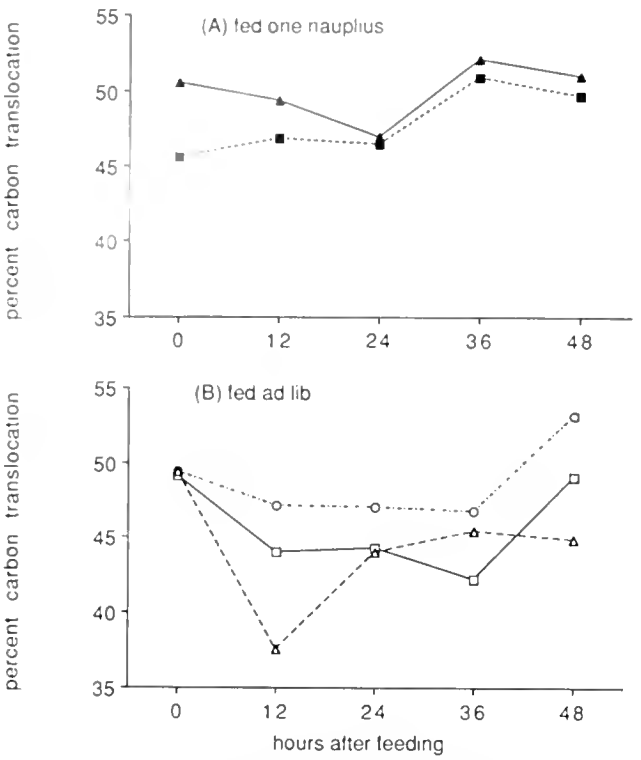

Figure 6. Percentage of photosynthetically fixed ^{14}C found in the host fraction of 30 hydra at various times after feeding. A. Each hydra fed one *Artemia* nauplius apiece. B. Hydra fed *ad lib*, each consuming two nauplii (○), or an average of three nauplii (△), or four nauplii (□). Hydra were starved for three days prior to experimental feeding in all cases except for the hydra which ate an average of three nauplii, which had been starved for five days.

30 $\mu Em^{-2} s^{-1}$ is below this association's light compensation point. Phipps and Pardy (1982) report a compensation point of 175 $\mu Em^{-2} s^{-1}$ for the Florida strain of *H. viridissima*.

The effect of feeding on photosynthate partitioning between host and algae

The percentage of fixed ^{14}C translocated from the algae to the host in a 45 minute incubation is plotted against time after feeding for five experiments (Figs. 6a, b). Initial values reflect translocation in hydra starved for three days (four experiments) or five days (one experiment).

The *ad lib* feeding experiments were characterized by a decline in the percentage of ^{14}C translocated during the interval from 12 to 36 hours following a meal (Fig. 6b). The mean percentage translocated during that interval varied inversely with both the average meal size of the hydra (Fig. 7a) and with the net algal growth rate during the interval (Fig. 7b). However, the mean percentage translocated was not related to the algal mitotic index (data not shown).

As in the studies of Eisenstadt (1971) and Mews (1980), extending the period of starvation beyond two days had little or no effect on translocation rates in hydra studied here; within 48 hours after feeding *ad lib*, translocation appears to stabilize near 50% (51.0 ± 2.1% at 48 hours, 48.7 ± 1.1% at 72 hours, and 49.4% at 120 hours, one sample).

Discussion

The effect of feeding rate on the contribution of endosymbionts to the growth of green hydra

Previous studies showed that the contribution of endosymbiotic algae to hydra budding increased at low food intakes. In the steady state feeding studies presented here, the difference in budding rate between green and aposymbiotic forms of the Carolina strain was either independent of, or an increasing function of, feeding rate. It may be that well-fed hydra enjoyed a greater benefit

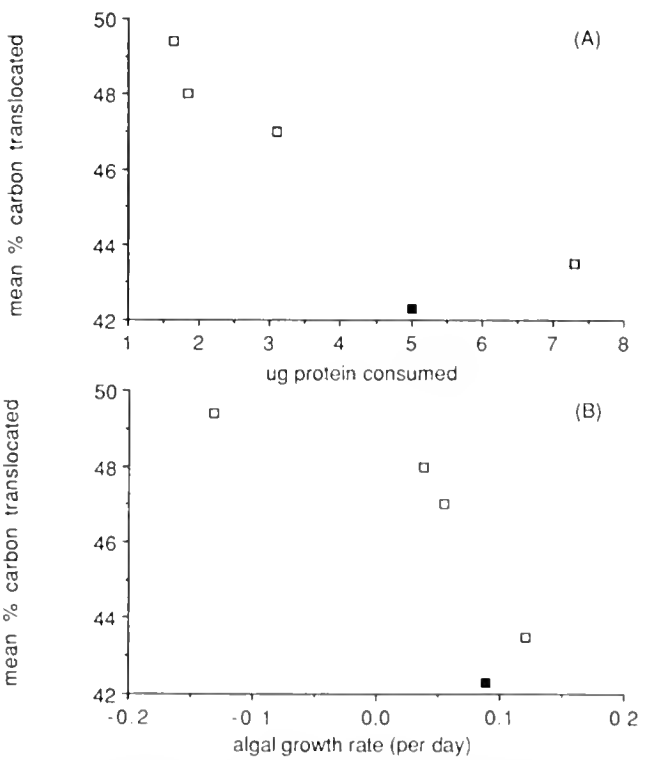

Figure 7. Mean percentage of photosynthetically fixed ^{14}C translocated to the host during the period from 12 to 36 hours after feeding as a function of the average amount of protein ingested by hydra in the immediately preceding meal (A), and as a function of the interval average algal growth rate (B). Hydra were starved for three days prior to experimental feeding in all cases except for one (■), in which hydra had been starved for five days.

from their algae by virtue of larger algal populations concommitant with their larger size.

Stiven (1965) found that the efficiency of bud production in green hydra (computed as calories of buds produced per calorie of *Artemia* nauplii consumed during a given interval of time, using the conversion coefficients given in Slobodkin, 1964) increased from 50% when fed daily to 61% when fed every other day. The beneficial effect of endosymbionts on the budding of the steady state hydra of the present study is likewise more obvious when feeding frequency is reduced from daily to semi-daily. However, it is less a consequence of an increase in the efficiency of green hydra than a consequence of the adverse effect of infrequent feeding on aposymbionts. Decreasing the feeding frequency from daily to semi-daily slightly increases the efficiency (calculated as above) of green hydra from 66% to 68% (not significant, $P > .75$, ANCOVA), but lowers aposymbiont budding efficiency from 43% to 35% (nearly significant, $.05 < P < .1$, ANCOVA).

For quantifying the beneficial effect of algae on the growth of hydra, the rate of host tissue production is an arguably better criterion than is the rate of bud production, which includes both host and algal components. However, the conclusion remains the same regardless of whether hydra growth is quantified in terms of number of buds, mass of buds, or mass of host tissue produced per day; the augmentation of hydra growth caused by algae is either independent of, or an increasing function of, hydra feeding rate.

However, it should be noted that an implicit assumption in the correction applied to convert the mass of buds produced into mass of host tissue produced is that the ratio of algal to host biomass is independent of hydra feeding rate. Large systematic variation in this ratio could seriously confound this correction. While no evidence exists that directly pertains to this, it is generally noted that starvation increases the ratio of algal to host biomass (Muscatine and Pool, 1979; Douglas and Smith; 1984, McAuley, 1985a; Muller-Parker and Pardy, 1987). If the same sort of variation occurs in steady state hydra such that the amount of algal tissue increases relative to host tissue at low feeding rates, it would only serve to accentuate the results already found, that is, the beneficial effect of algae increases with hydra feeding rate.

Many of the experimental hydra developed testes during the daily feeding experiments. This sexuality may have resulted from the constant feeding regime imposed on the hydra (Rutherford, *et al.*, 1983) since non-sexual animals were chosen for the experiment. Sexuality did not measurably affect asexual reproduction by these hydra. The proportion of the experimental interval in which hydra were observed to exhibit testes was not correlated to the efficiency of bud production of either form of *H. viridissima* (correlation coefficients were not significantly different from zero, $r^2 = .04$ for each form, arcsine-square-root transformed proportions).

The results suggest an increased contribution of endosymbionts to bud production seen at low host food levels (Muscatine and Lenhoff, 1965a, b; Stiven, 1965) may pertain only to hydra that are not at steady state with their feeding rates. The cell-specific growth rate of steady state hydra is independent of host feeding rate (Otto and Campbell, 1977), but the cell-specific growth rate of non-steady state hydra may vary with feeding rate. If this is true, it is possible that the beneficial effect of algae on host budding depends less on feeding rate *per se* than on the specific cellular growth rate of one or both symbionts.

The effect of host feeding on the rate of algal carbon translocation

The translocation data presented here qualititatively fit the model presented earlier in which algae translocate more carbon during periods of slow growth than during periods of rapid growth; the algae of unfed or poorly fed hydra translocated a larger proportion of their fixed carbon than algae in recently fed and well-fed hydra, respectively. The simplest interpretation of these data is that the algae in well-fed hydra retain more of their photosynthate to support their own rapid growth. Since the carbon fixation rates of endosymbionts are relatively constant regardless of host nutritional condition, slowly growing algae in poorly fed hydra may translocate more of their photosynthate.

Using ^{14}C as a tracer to estimate the rates of carbon translocation from algae to host incurs certain errors (see Mews, 1980; Muscatine *et al.*, 1984 for discussion). In particular, the specific activity of newly fixed carbon or of translocated carbon may both vary (*e.g.*, when hydra respiratory $^{12}CO_2$ production changes or if translocated carbon contains some variable fraction of previously fixed algal ^{12}C). Consequently, the amount of ^{14}C translocated may not be strictly proportional to the total amount of carbon translocated. Translocated carbon is quantified here as the percentage of fixed ^{14}C translocated from algae to host, a variable that is independent of variations in the specific activity of newly fixed carbon. Mews (1980) showed that the specific activity of translocated maltose varied with time of incubation as well as with intensity of illumination. These variables were carefully controlled in my studies, but comparisons of percent translocation rates in different incubations may still be compromised if the specific activity of translocated carbon varied despite these precautions. Muscatine *et al.* (1984) suggest that while the ^{14}C tracer technique may

be adequate for "short term relative comparisons," their "growth rate method" is to be preferred for estimation of absolute amounts of translocation integrated over protracted periods of time.

Considered quantitatively, the changes in percent translocation rates with host nutritional state were small. It seems unlikely that they explain the dramatic changes in the algal contribution to budding seen in the non-steady state feeding studies of Muscatine and Lenhoff (1965a, b) and Stiven (1965). During the 36 hour decline in percent translocation following feeding, the algae of hydra ingesting an average of four nauplii apiece translocated approximately 44% of their photosynthate, while those in hydra eating only one nauplius translocated approximately 49%. Assuming equivalent carbon fixation rates at these two feeding levels, this represents an 11% increase in the amount of photosynthate translocated. From Stiven's (1965) regressions, green hydra and aposymbionts produced buds at essentially the same rate when fed four nauplii a day. Green hydra receiving one nauplius a day produced buds 2.5 times as fast as did comparably fed aposymbionts. It seems unlikely that an 11% difference in carbon translocation could alone account for such a difference in host growth.

Muscatine and Lenhoff (1965b) found that populations of aposymbionts and green hydra grow identically when fed daily, but green hydra grow twice as fast as aposymbionts when fed every two days. We assume that hydra fed every other day receive translocated carbon as in the *ad lib* feeding experiments shown in Figure 6. Assuming that daily feeding maintains translocation rates at the levels observed from 12 to 24 hours after feeding, daily fed hydra receive only 5% less translocated carbon than hydra fed every 2 days. Again, it seems unlikely that a 5% difference in translocation rate could have such a dramatic effect on hydra growth rate.

Even considering possible differences in culture conditions between this and previous studies, these calculations suggest that the enhanced beneficial effect of algae on host budding (Muscatine and Lenhoff, 1965a, b; Stiven, 1965) at low feeding frequencies may depend on an algal factor other than carbon translocation. The importance of algal carbon translocation to the growth of regularly fed green hydra has been questioned by Mews and Smith (1982) and Muller-Parker and Pardy (1987). Mews and Smith (1982) found no relation between the rates of translocation and host budding in several artificial green hydra associations. In studies of an artificial association between aposymbiotic *H. viridissima* and algae isolated from symbiotic *Paramecium bursaria*, Muller-Parker and Pardy (1987) found that hydra raised at 30 $\mu Em^{-2} s^{-1}$ fixed almost four times as much carbon as those raised at 5 $\mu Em^{-2} s^{-1}$, but grew only 10% faster. They concluded that "the growth rates of fed hydra are regulated by factors other than light-dependent carbon fixation."

The light intensity in the studies reported here was below the association's compensation light intensity where photosynthetic oxygen production matches respiratory oxygen consumption. Therefore, hydra satisfied a certain fraction of their respiratory carbon requirement through feeding. If the experiments had been conducted at a higher illumination, algal photosynthesis and translocation may have satisfied the association's respiratory needs so that heterotrophy would not be required for maintenance. However, as discussed above, increased carbon translocation might not result in increased hydra growth.

The amount of algal disintegration in green hydra can be substantial and may increase when hydra are underfed (Dunn, 1987). Disintegration of algae may provide the host with a variety of nutrients, some of which may be more limiting to bud production than reduced carbon. Insofar as disintegrating algae are incapable of fixing carbon, this form of nutrient translocation will not be detectable in short-term radioactive carbon partitioning assays.

Acknowledgments

This research was supported by research grants from the National Science Foundation, the Mellon Foundation, and the Hudson River Foundation to L. B. Slobodkin and a grant from Sigma Xi to Kenneth Dunn. I am grateful to Leonard Muscatine for his encouragement and guidance during a nine-month stay in his laboratory at UCLA. I thank Heidi Chapnick, Jay Fader, and John LeGuyader for technical assistance. I also thank John McDonald for suggested improvements in the manuscript.

Literature Cited

Bosch, T. C. G., and C. N. David. 1984. Growth regulation in *Hydra*: relationship between epithelial cell cycle length and growth rate. *Dev. Biol.* **104**: 161–171.

Bosserl, P., and K. W. Dunn. 1986. Regulation of intracellular algae by various strains of the symbiote *Hydra viridissima*. *J. Cell Sci.* **85**: 187–196.

Douglas, A. E., and D. C. Smith. 1984. The green hydra symbiosis. VIII. Mechanisms in symbiont regulation. *Proc. R. Soc. Lond. B* **221**: 291–319.

Dunn, K. W. 1986. Adaptations to endosymbiosis in the green hydra, *Hydra viridissima*. Ph.D. dissertation, State University of New York, Stony Brook.

Dunn, K. W. 1987. Growth of endosymbiotic algae in the green hydra, *Hydra viridissima*. *J. Cell Sci.* **88**: 571–578.

Eisenstadt, E. 1971. Transfer of photosynthetic products from symbiotic algae to animal tissue in *Chlorohydra viridissima*. Pp. 202–

208 in *Experimental Coelenterate Biology*, H. M. Lenhoff, L. Muscatine and L. V. Davis, eds., University of Hawaii Press, Honolulu.

Gurkewitz, S., M. Chow, and R. Campbell. 1980. Hydra size and budding rate: influence of feeding. *Int. J. Invertebr. Reprod.* **2:** 199–201.

Karakashian, S. J. 1963. Growth of *Paramecium bursaria* as influenced by the presence of algal symbionts. *Physiol. Zool.* **36:** 52–67.

Lowry, O. H., N. J. Rosebrough, A. L. Farr, and R. J. Randall. 1951. Protein measurement with the Folin phenol reagent. *J. Biol. Chem.* **193:** 265–275.

McAuley, P. J. 1981. Control of cell division of the intracellular *Chlorella* symbionts in green hydra. *J. Cell Sci.* **47:** 197–206.

McAuley, P. J. 1982. Temporal relationships of host cell and algal mitosis in the green hydra symbiosis. *J. Cell Sci.* **58:** 423–431.

McAuley, P. J. 1985a. The cell cycle of symbiotic *Chlorella* I. The relationship between host feeding and algal cell growth and division. *J. Cell Sci.* **77:** 225–239.

McAuley, P. J. 1985b. The cell cycle of symbiotic *Chlorella* II. The effect of continuous darkness. *J. Cell Sci.* **77:** 241–253.

McAuley, P. J. 1986a. The cell cycle of symbiotic *Chlorella* III. Numbers of algae in green hydra digestive cells are regulated at digestive cell division. *J. Cell Sci.* **85:** 62–72.

McAuley, P. J. 1986b. Isolation of viable uncontaminated *Chlorella* from green hydra. *Limnol. Oceanogr.* **31**(1): 222–224.

Mews, L. K. 1980. The green hydra symbiosis. III. The biotrophic transport of carbohydrate from alga to animal. *Proc. R. Soc. Lond. B* **216:** 397–414.

Mews, L. K., and D. C. Smith. 1982. The green hydra symbiosis. VI. What is the role of maltose transfer from alga to animal? *Proc. R. Soc. Lond. B* **216:** 397–413.

Muller-Parker, G., and R. L. Pardy. 1987. Response of green hydra to feeding and starvation at four irradiances. *Biol. Bull.* **172:** 46–60.

Muscatine, L. 1971. Endosymbiosis of algae and coelenterates. Pp. 179–191 in *Experimental Coelenterate Biology*, H. Lenhoff, L. Muscatine and L. V. Davis, eds., Univ. of Hawaii Press, Honolulu.

Muscatine, L., P. G. Falkowski, J. W. Porter, and Z. Dubinsky. 1984. Fate of photosynthetic fixed carbon in light- and shade-adapted colonies of the symbiotic coral *Stylophora pistillata*. *Proc. R. Soc. Lond. B.* **222:** 181–202.

Muscatine, L., and H. M. Lenhoff. 1965a. Symbiosis of hydra and algae. I. Effects of some environmental cations on growth of symbiotic and aposymbiotic hydra. *Biol. Bull.* **128:** 415–424.

Muscatine, L., and H. M. Lenhoff. 1965b. Symbiosis of hydra and algae. II. Effects of limited food and starvation on growth of symbiotic and aposymbiotic hydra. *Biol. Bull.* **129:** 316–328.

Muscatine, L., and R. R. Pool. 1979. Regulation of numbers of intracellular algae. *Proc. R. Soc. Lond. B* **204:** 131–139.

Otto J. J., and R. D. Campbell. 1977. Tissue economics of hydra: regulation of cell cycle, animal size, and development by controlled feeding rates. *J. Cell Sci.* **28:** 117–132.

Pardy, R. L. 1976. The production of aposymbiotic hydra by the photodestruction of green hydra zoochlorellae. *Biol. Bull.* **151:** 225–235.

Pardy R. L., and B. N. White. 1977. Metabolic relationships between green hydra and its symbiotic algae. *Biol. Bull.* **153:** 228–236.

Phipps, D. W., Jr., and R. L. Pardy. 1982. Host enhancement of symbiont photosynthesis in the hydra algae symbiosis. *Biol. Bull.* **162:** 83–94.

Rutherford, C., D. Hessinger, and H. M. Lenhoff. 1983. Culturing sexually differentiated hydra. Pp. 71–78 in *Hydra Research Methods*, H. M. Lenhoff, ed., Plenum, New York.

Slobodkin, L. B. 1964. Experimental populations of Hydrida. *J. Anim. Ecol. Suppl.* **33:** 131–148.

Slobodkin, L. B., and K. W. Dunn. 1983. On the evolutionary constraint surface of hydra. *Biol. Bull.* **165:** 305–320.

Smith, D. C., L. Muscatine, and D. Lewis. 1969. Carbohydrate movement from autotrophs to heterotrophs in parasitic and mutualistic symbiosis. *Biol. Rev.* **44:** 17–90.

Sokal, R. R., and F. J. Rohlf. 1981. *Biometry, 2nd ed.* W. H. Freeman and Co., New York. 859 pp.

Stiven, A. 1965. The relationship between size, budding rate and growth efficiency in three species of hydra. *Res. Popul. Ecol.* **7:** 1–15.

Thorington, G., and L. Margulis. 1981. *Hydra viridis*: transfer of metabolites between hydra and symbiotic algae. *Biol. Bull.* **160:** 175–188.

Reference: *Biol. Bull.* 175: 202–211. (October, 1988)

Egg Capsule Catechol Oxidase from the Little Skate *Raja erinacea* Mitchill, 1825*

THOMAS J. KOOB[1] AND DAVID L. COX[1,2]

[1]*Mount Desert Island Biological Laboratory, Salsbury Cove, Maine and* [2]*Department of Biology, University of Oregon, Eugene, Oregon*

Abstract. A phenoloxidase was demonstrated in extracts of egg capsules tanning *in utero* and of nidamental glands from spawning little skate, *Raja erinacea*. The enzyme was identified as a catechol oxidase based on its ability to oxidize the *ortho*-diphenols pyrocatechol, 4-methylcatechol, 3,4-dihydroxyphenylalanine, 3-hydroxytyramine and *N*-acetyldopamine to their corresponding *ortho*-quinones and its relative inactivity against monophenols. 4-methylcatechol was oxidized at the greatest rate, while 3,4-dihydroxyphenylalanine, 3-hydroxytyramine and *N*-acetyldopamine were oxidized at slower rates. The nidamental gland enzyme was inhibited by cyanide, nitrogen, and diethyldithiocarbamate. Oxidase activity in crude extracts from nidamental glands was enhanced by addition of α-chymotrypsin, suggesting that the enzyme is produced in a latent form. Ammonium sulfate fractionation of nidamental gland and capsule extracts resulted in a fifteen-fold purification of the enzyme. This partially purified catechol oxidase from the nidamental gland exhibited optimal rates of oxidation at 0.5 *M* NaCl and pH 7.0. The enzyme, however, showed a wide tolerance for elevated salinity and alkaline pH. These observations indicate that the oxidase acts principally *in utero*, but may remain active in seawater following oviposition of the capsule. This enzyme plays a pivotal role during the formation of skate egg capsules by catalyzing the oxidation of capsular catechols to highly reactive quinones forming dark pigments which tan the capsular matrix.

Introduction

Oviparous elasmobranchs encapsulate eggs in curiously shaped, leathery capsules produced by specialized nidamental glands in the upper oviduct (for review of the structure and composition of these capsules see Hunt, 1985). These glands are highly developed during spawning and in some species are the predominant organs in the reproductive tract. The early structural studies of Perrevex (1884), Henneguy (1893), Borcea (1904, 1905), and Widakowich (1906) established that the nidamental glands of *Scyliorhinus canicula* and several other oviparous species have distinct glandular regions each with an extensive tubular system leading to lamellae at the lumenal surface. Typically, three regions were discriminated: an albumen-secreting zone, a mucous-secreting zone, and a shell-secreting zone. The tubules in the shell-secreting zone were bordered by epithelial cells which contained abundant cytoplasmic granules filled with the precursors of capsules. During capsule formation, these granules are secreted from the epithelial cell into the lumen where they coalesce and then are transported to the lamellae by ciliated tubule cells (Filhol and Garrault, 1938). Borcea (1905) and Widakowich (1906) showed how these lamellae mould the newly secreted capsular material and produce the layered organization of the capsular wall. This basic structure appears common to nidamental glands from both oviparous sharks and skates, having now been described in *Scyliorhinus canicula* (Perrevex, 1884; Henneguy, 1893; Borcea, 1904, 1905; Widakowich, 1906; Filhol and Garrault, 1938; Metten, 1939; Threadgold, 1957; Krishnan, 1959; Rusaouën, 1978), *Chiloscyllium griseum* (Nalini, 1940), *Raja batis*, and *Raja miraletus* (Filhol and Garrault, 1938). Although reduced in overall complexity and size, the nidamental glands of ovoviviparous and viviparous species also show similar tubular organization and lamellar systems (Borcea, 1905; Filhol and Garrault, 1938; Nalini, 1940; Prasad, 1945a, 1945b, 1948).

Rusaouën (1978) and Rusaouën *et al.* (1976) provided

Received 19 May 1987; accepted 28 July 1988.

* Portions of this work have appeared in abstract form; see Koob & Cox, 1984, 1985, and 1986a.

ultrastructural and histochemical evidence that six zones of secretory activity containing five types of secretory granules could be distinguished in the nidamental glands of *Scyliorhinus canicula*. Histochemical tests identified neutral and sulfated mucopolysaccharides, sulfated glycoproteins rich in tyrosine, a fibrillar collagenous protein, sulfhydryl groups, indole radicals, peroxidase, and phenoloxidase activities, each localized in granules of specific regions and cell types within the glands. In the shell secreting zone alone, Rusaouën (1978) found all of these components except the mucopolysaccharides. Her studies provide convincing evidence that the nidamental gland is an extremely complex organ which synthesizes a variety of secretory products and that capsule formation and composition are equally complex.

Formation of skate egg capsules begins in the nidamental gland with the secretion and assembly of capsular precursors. These materials are white when assembled but then gradually develop color with time *in utero*, eventually producing the deep greenish brown characteristic of skate capsules at oviposition. In *Raja erinacea*, the tanning of capsules *in utero* is coincident with the introduction of catechols into the capsular matrix (Koob and Cox, 1986b). An enzymic activity able to oxidize catechols to quinones has been demonstrated histochemically in tanning capsules and nidamental glands from several oviparous elasmobranchs. Brown (1955) reported that sections of newly formed *Raja* egg capsules turned brown upon incubation with tyrosine and that this reaction could be blocked by potassium cyanide. She believed that these results demonstrated a polyphenol oxidase which would oxidize the polyphenol present in the capsule to quinone which, in turn, would tan the capsule. A polyphenoloxidase was demonstrated histochemically in shell glands of *Scyliorhinus canicula* by incubating sections of fixed glands with catechol (Threadgold, 1957). Krishnan (1959) showed that both capsular material and sections of frozen glands from *Chiloscyllium griseum* oxidized catechol and that the capsule had chemical properties like other quinone tanned matrices. He suggested that capsule formation involved a form of quinone autotanning (*sensu* Smyth, 1954) catalyzed by a phenoloxidase. In *Scyliorhinus canicula* this enzyme is localized both to a narrow zone in the upper region of the nidamental gland and to a broad band in the caudal region (Rusaouën, 1978). Further information regarding the nature of this oxidase activity is lacking.

Therefore we set out to characterize the biochemical properties of the oxidase involved in forming egg capsules of the little skate, *Raja erinacea*. We were especially interested in defining the substrate specificity of the oxidative activity and in determining the sensitivity of this activity to inhibitors, salinity, pH, and urea to gain insight into the conditions within the tanning capsular matrix.

Materials and Methods

Selection of animals

Females of *Raja erinacea* were selected from otter trawl catches on the basis of ovarian size and color as viewed through the translucent ventral body wall. Bumpus (1898) showed that ripe females can be discriminated in this way. We found that females so selected will produce egg capsules during short term captivity (Koob *et al.*, 1986). Females landed with capsules *in utero* were also selected. Skates were maintained in 2400 l aquaria supplied with fresh circulating seawater and were fed Maine Gulf shrimp. Every twelve hours females were palpated for egg capsules in the uterus. Only females that produced eggs were used for collection of nidamental glands.

Egg capsule preparation

A female which had just completed secretion of egg capsules was sacrificed and the oviducts containing newly formed capsules were excised *in toto*. Later examination revealed that the egg capsules were fully formed but untanned at the anterior, more recently secreted end. The oviducts were ligated at the cervix and just cephalad to the nidamental gland to isolate the tanning capsule within the uterine portion of the oviduct. Ten ml of 1.0 *M* NaCl, 0.05 *M* NaH_2PO_4, pH 7.5 chilled to 4°C were introduced into each uterine lumen with a syringe *via* the cervical canal. After manipulating the buffer to thoroughly wash the uterine contents, it was collected through the opened upper oviduct. This uterine flush contained much particulate which was removed by centrifugation at 3,000 rpm and 4°C for 10 minutes. The capsules were then removed from the oviduct and placed into 60 ml of the same salt buffer at 4°C with occasional stirring for 15 minutes. This capsular wash was centrifuged as above to remove particulates. The attachment fibers from these capsules were then removed from the lateral seams and homogenized on ice in 30 ml of the 1.0 *M* NaCl buffer using a glass homogenizer. The homogenate was centrifuged at 37,000 × *g* for 15 minutes at 4°C. The supernatants from the uterine flush, capsular wash, and attachment fiber extract were assayed directly for oxidase activity.

A second, partially tanned capsule was removed from the uterus and extracted directly with 1.0 *M* NaCl, 0.05 *M* NaH_2PO_4, pH 7.0 by homogenization with a polytron (Brinkmann Instruments Inc., Westbury, New York). Following centrifugation at 37,000 × *g* and 4°C for 30

minutes, the extract was fractionated by differential ammonium sulfate precipitation as described below.

Nidamental gland preparation

Nidamental glands from spawning females were excised from the oviduct, minced over ice and disrupted with a glass homogenizer in 1.0 *M* NaCl, 0.05 *M* NaH_2PO_4, pH 7.0. The homogenate, which appeared gelatinous and slightly pink, was centrifuged at 37,000 × *g* and 4°C for thirty minutes. The pinkish supernatant was collected and analyzed directly for oxidase activity. This 1.0 *M* NaCl extract was subsequently fractionated by sequential precipitation at 5, 10, 20, 30, and 40% ammonium sulfate at neutral pH. Precipitates were collected by centrifugation at 4°C and 37,000 × *g* for thirty minutes, and redissolved in 1.0 *M* NaCl, 0.05 *M* NaH_2PO_4, pH 7.0. Not all the precipitate formed at low ammonium sulfate concentrations dissolved in the buffer, therefore it was necessary to clarify these solutions by centrifuging at 25,000 × *g* and 4°C for 15 minutes. Protein determinations were performed on diluted aliquots of the original extract and on the redissolved ammonium sulfate fractions (Lowry *et al.*, 1951).

Enzyme assay

Oxidase activity was measured in the various enzyme preparations by incubating diluted aliquots with 1 m*M* substrate in 0.5 *M* NaCl, 0.025 *M* NaH_2PO_4, pH 7.5 at ambient temperature and spectrophotometrically monitoring for increases in absorbance at product specific wavelengths. Substrates generally employed for oxidase assays were 3,4-dihydroxyphenylalanine (l-dopa) or 4-methylcatechol; other substrates tested were *p*-cresol, 3-hydroxytyramine, *N*-acetyldopamine and tyrosine (all obtained from Sigma Chemical Co., St. Louis, Missouri). Extinction coefficients for the substrates were from Waite (1976). For each assay the enzyme solution and diluent were mixed in 1 ml cuvettes. The reaction was initiated by adding substrate in a 0.01 *M* HCl stock solution and mixing. The change in absorbance at product specific wavelengths was recorded for periods up to 120 minutes. All assays were performed at room temperature in a reaction volume of 1 ml. The change in absorbance in the enzyme solutions was compared to that in control incubates which contained boiled enzyme, substrate, and buffer.

The kinetic parameters K_m and V_{max} were estimated by direct linear plots (Eisenthal and Cornish-Bowden, 1974) using only the initial, briefly linear reaction velocities from assays performed as described above. This limited the usable portion of such kinetic assays to about 30 seconds.

Inhibitors of other catechol oxidases were tested for effect on skate enzyme preparations. KCN or diethyldithiocarbamate was added to a final concentration of 50 μM and incubated 15 minutes at room temperature prior to the addition of 4-methylcatechol. In all other respects the assays were performed as above. Results from these assays were used to determine the type of inhibition observed and to estimate K_i, both by means of direct linear plots (Eisenthal and Cornish-Bowden, 1974). The effect of nitrogen on oxidase activity was estimated by extensive purging of reaction solutions prior to 4-methylcatechol addition and by assaying the reactions under nitrogen.

To examine the effects of salinity, pH, and urea on oxidase activity, the desired concentrations were effected by diluting the enzyme solution with concentrated stock buffers. NaCl concentration was varied from 0.25 *M* to 1.0 *M* in 0.05 *M* NaH_2PO_4, pH 7.0. pH was varied from 4.5 to 9.0 using three buffers: pH 4.5 to 6.0 in 0.05 *M* sodium acetate; pH 6.0 to 7.5 in 0.05 *M* sodium phosphate; and pH 7.5 to 9.0 in 0.05 *M* Tris. Urea concentrations were varied from 0 to 4.8 *M* in 0.05 *M* sodium phosphate, pH 7.0.

Gel electrophoresis

Discontinuous gel electrophoresis was performed by a modification of the method of Laemmli (1970) either with or without sodium dodecyl sulfate. Acrylamide and *N,N'*-methylene-bisacrylamide concentrations for the separating gel were 5% and 0.13% (w/v), respectively, those for the stacking gel were 3% and 0.08% (w/v). Electrode buffer was 0.025 *M* Tris, 0.192 *M* glycine, pH 8.3. To estimate protein molecular weights, gels and reservoir buffer included 0.1% SDS. Prior to such electrophoresis, samples and molecular weight standards (Pharmacia Inc., Piscataway, New Jersey) were heated for three minutes at 100°C in 2% SDS and 5% β-mercaptoethanol. Insoluble material was removed by centrifugation at 12,000 × *g* for three minutes. Electrophoresis was carried out at 15 mA per slab for 30 minutes after which current was doubled for three hours. During electrophoresis the apparatus was maintained at ambient seawater temperature (approximately 15°C). Proteins were visualized by fixing and staining gels overnight at ambient temperature in 0.5% (w/v) Coomassie brilliant blue G-250 dissolved in methanol:acetic acid:water (40:15:45, v/v), and were subsequently destained first in methanol:acetic acid:water (45:10:45, v/v) and then in 5% acetic acid. Catechol oxidase activity was localized by immersing unfixed native gels for one hour in a solution of 1 m*M* 4-methylcatechol, 0.5 *M* NaCl, 0.05 *M* NaH_2PO_4, pH 7.0.

Results

The uterine flush, capsular wash and attachment fiber extract catalyzed the conversion of 3,4-dihydroxyphe-

nylalanine to dopaquinone. The oxidase in the uterine flush oxidized 4-methylcatechol, l-dopa and *N*-acetyldopamine. All preparations showed an initial low rate of oxidation which eventually increased and became linear at the later time points. Boiling the extracts for one minute destroyed this activity indicating the enzymic nature of the oxidizing principle. These measurements showed that an oxidase was associated with tanning capsules *in utero*. Since this enzyme could be flushed from the uterine lumen without mechanical disruption of the capsular material, the enzyme obtained must have been on the capsule surface, on the surface of the uterine epithelium, or free in the uterine lumen.

Extracts of nidamental glands and tanning capsules from spawning females oxidized a variety of catechols (Fig. 1). Ammonium sulfate fractionation of 1.0 *M* NaCl extracts resulted in a significant enrichment in enzyme specific activity (Table I for data on shell gland extract). Catechol oxidase activity was found predominantly in precipitates formed at 5 and 10% $(NH_4)_2SO_4$. Most of the protein precipitated at higher concentrations. Based on specific activity, the enzyme was purified 15–20 fold with respect to the initial homogenate. Since both the 5% and 10% ammonium sulfate precipitates contained active catechol oxidase, they were combined for further characterization of the enzyme.

Discontinuous gel electrophoresis (Fig. 2) showed that ammonium sulfate fractionation produced a substantial purification of the shell gland catechol oxidase. The precipitate formed in 5% ammonium sulfate consisted mostly of material aggregated at the bottom of the sample well and several proteins having an apparent molecular weight around 63,000 daltons (Lane 2, Fig. 2). Material precipitated by 10% ammonium sulfate also contained aggregates in the sample well (Lane 3, Fig. 2), in addition to a predominant band with an estimated molecular weight of 85,000 daltons. Using 4-methylcatechol as substrate, catechol oxidase activity in this 10% ammonium sulfate fraction was localized not to the major protein, but in a slower migrating diffuse band between 440,000 and 230,000 daltons. This band was not visible when stained with Coomassie blue (Fig. 2). This indicated that the active enzyme preparation contains relatively little protein having catechol oxidase activity and that the predominant protein could be a contaminant or a reduced or inactive form of the enzyme. Most of the protein in the original extract precipitated at ammonium sulfate concentrations higher than 10%, appearing predominantly in the 20% fraction (Lane 4, Fig. 2). These data confirm the substantial purification of the enzyme by ammonium sulfate fractionation.

Partially purified oxidases in 1.0 *M* NaCl extracts of tanning capsules and nidamental glands were compared with respect to substrate specificities. The two enzymes

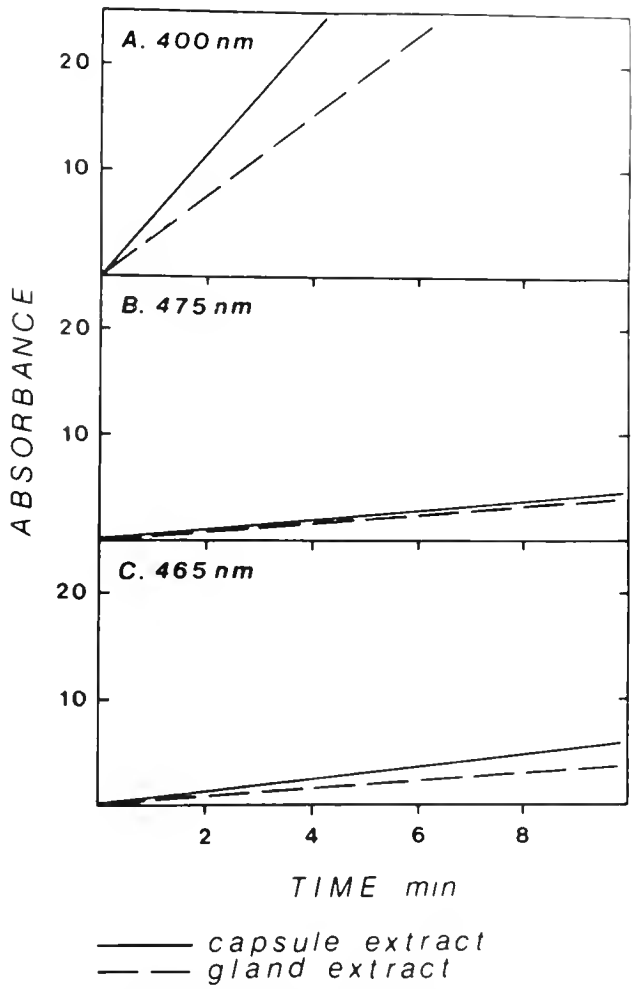

Figure 1. Oxidation of (A) 4-methylcatechol, (B) 3,4-dihydroxyphenylalanine, (C) 3-hydroxytyramine by partially purified extracts of tanning capsule and nidamental glands. Aliquots of redissolved 10% $(NH_4)_2SO_4$ precipitates of these extracts were incubated with 1 m*M* substrate in 0.5 *M* NaCl, 0.05 *M* NaH_2PO_4, pH 7.5 at ambient temperature. Absorbance was monitored at the indicated wavelengths. Values shown are means of triplicate analyses.

showed similar oxidative activities against 4-methylcatechol, 3-hydroxytyramine, and 3,4-dihydroxyphenylalanine (Fig. 1). Tyrosine was little affected by these enzymes.

The substrate specificity of the nidamental gland extract was examined in greater detail by determining its K_m and V_{max} for selected catecholic and phenolic compounds (Table II). Using the ratio V_{max}/K_m as an index of substrate preference (Segal, 1976), 4-methylcatechol was clearly the most favored substrate followed distantly by *N*-acetyldopamine and 3-hydroxytyramine. These data indicate that the nidamental gland enzyme has a strong preference for a methyl group substituted in *para* orientation to the first aromatic hydroxyl group. Chemical modification of the α-carbon by charged moieties

Table I

Catechol oxidase activity of ammonium sulfate fractions of the 1.0 M NaCl extract of Raja erinacea *shell glands*

Source	Oxidase activity (μM/min/ml)	Protein (mg/ml)	Specific activity (μM/min·mg)	Purification factor (Fold)
1.0 M NaCl extract	26.4 ± 0.8	12.5	2.1 ± 0.1	1
$(NH_4)_2SO_4$ fractions:				
5%	152.4 ± 7.2	3.8	39.7 ± 1.9	18.91
10%	160.4 ± 5.1	5.1	31.4 ± 0.2	14.95
20%	40.4 ± 1.2	19.0	2.1 ± 0.1	—
30%	trace	9.0	—	—
40%	—	5.5	—	—

such as the carboxyls or amines of dopa and 3-hydroxytyramine or even by the *N*-acetylethyl side chain of *N*-acetyldopamine markedly diminished the enzyme's catalytic efficiency. Monophenols such as *p*-cresol and tyrosine were little affected by the shell gland enzyme within the assay period.

Table III shows effects of inhibitors on the nidamental gland catechol oxidase. Like other phenoloxidases, the nidamental gland enzyme was inhibited by oxygen competitors such as cyanide and nitrogen. Diethyldithiocarbamate, a metal chelator especially effective against copper-containing enzymes, also inhibited the enzyme.

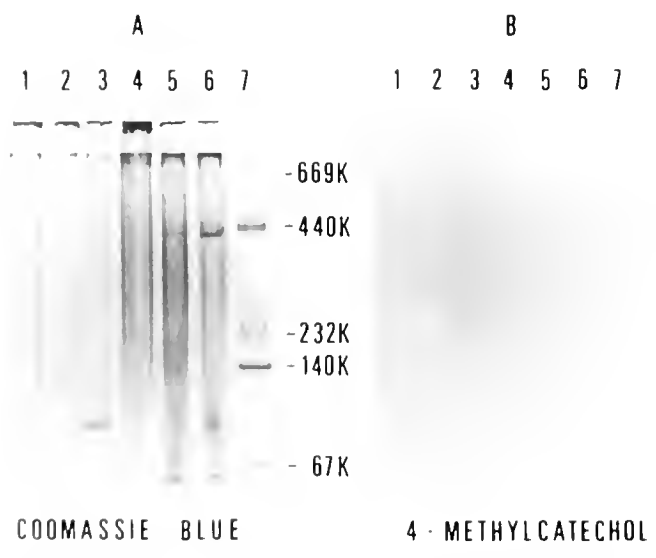

Figure 2. Polyacrylamide gel electrophoresis of ammonium sulfate fractions from nidamental gland extract. A: Coomassie blue R-250 stained SDS gel electrophoresis of mercaptoethanol reduced nidamental gland samples as follows: Lane (1) original extract; (2) 5% ammonium sulfate precipitate; (3) 10% ammonium sulfate precipitate; (4) 20% ammonium sulfate precipitate; (5) 30% ammonium sulfate precipitate; (6) 40% ammonium sulfate precipitate; and (7) molecular weight standards as indicated (from highest to lowest: thyroglobulin, ferritin, catalase, lactate dehydrogenase, and bovine serum albumin). B: 4-methylcatechol (1 m*M*) staining of a gel without detergent was carried out for 1 h at pH 7.5 and room temperature. Sample lane order is the same as for Coomassie blue stained gel.

Oxidase activity was sensitive to the pH of the reaction mixture (Fig. 3). Both partially purified extracts from nidamental gland and tanning capsules exhibited maximal oxidation rates at pH 7.0–7.5. Little oxidation occurred at or below pH 5.0. Enzyme in the capsule extract was also sensitive to alkaline pH, retaining only a small portion of its activity towards 4-methylcatechol and l-dopa at pH 8.0–8.5 (Fig. 3). The nidamental gland enzyme was apparently less sensitive to alkaline pH. Oxidation rates of 4-methylcatechol by the partially purified nidamental gland enzyme were substantially above the natural oxidation rate of this substrate (Fig. 3). Even at pH 9.0 the enzyme retained some of its activity. At alkaline pH these catechols rapidly oxidize, so measurement of enzymic activity at pH 8.0 to pH 9.5 is only an estimate. While it is clear that oxidase activity from both capsule and nidamental gland declines above pH 7.5, some oxidative activity is retained at the pH of seawater (8.0–8.5).

The concentration of sodium chloride in the catechol oxidase assay was varied from 0.25 *M* to 1.0 *M* in 0.05 *M* NaH_2PO_4, pH 7.0. Enzymatic activity at NaCl concentrations below 0.25 *M* could not be accurately measured because of the substantial increase in turbidity re-

Table II

Substrate preference of shell gland catechol oxidase from Raja erinacea

Substrate	K_m (m*M*)	V_{max}*	V_{max}/K_m
p-Cresol	0	0	0
L-Tyrosine	0	0	0
Pyrocatechol	3.1 ± .05	6.9 ± .24	2.2
4-Methylcatechol	1.1 ± .19	45.5 ± .46	41.4
L-Dopa	1.37 ± .07	3.1 ± .20	2.3
Dopamine	0.11 ± .01	0.7 ± .10	6.1
N-Acetyldopamine	0.60 ± .22	4.3 ± .48	7.2

* μmoles oxidized/min/mg protein.
n = 3.

Table III

Inhibitors of shell gland catechol oxidase. 4-methylcatechol was used as substrate in all assays

Inhibitor	Type	K_i (μM)
Cyanide	Noncompetitive	4.02 ± .03
Diethyldithiocarbamate	Noncompetitive	166 ± .04
N_2	Probably n.c.	not measured

n = 3.

sulting from protein precipitation. NaCl concentrations above 0.25 *M* had little effect on the rate of oxidation of 4-methylcatechol by the nidamental gland extract (Fig. 4). A slight increase in the oxidation rate was observed at 0.5 *M* and this was statistically different from the rate at 0.4 *M* and 1.0 *M*.

Urea inhibited catechol oxidase in the partially purified nidamental gland extract in a concentration-dependent manner (Fig. 5). At the lowest concentration examined, 0.15 *M*, a slight reduction in oxidase activity was detected. Fifty percent inhibition occurred at approximately 4.0 *M* urea. At the concentration of urea generally maintained in elasmobranch tissues the oxidation rate of 4-methylcatechol was reduced by about 10%.

Typically oxidation did not commence immediately upon addition of the substrate, but rather occurred only after a brief delay. The duration of this delay was reduced by incubating the extract with α-chymotrypsin prior to adding substrate to initiate the reaction (Fig. 6). When crude nidamental gland extracts were stored at 4°C for several hours, their oxidative activity increased. These results suggest that the enzyme is produced in a latent form and that some endogenous factor in the crude extract is able to activate the latent enzyme.

Discussion

These observations confirm the presence of a catechol oxidase in tanning capsules and mature nidamental glands of the little skate, *Raja erinacea*, and thus support previous reports that this type of enzyme might be involved in the formation of elasmobranch egg capsules. We biochemically identified this enzyme as a catechol oxidase on the basis of its ability to catalyze the conversion of *ortho*-diphenols to their corresponding quinones. The nidamental gland enzyme is markedly inhibited by both cyanide and nitrogen, as expected of any oxidase. The enzyme is also inhibited by diethyldithiocarbamate which suggests that like other phenoloxidases it may contain copper. The enzyme prefers catechols bearing a methyl side chain which lacks exposed charged groups. These substrate prejudices are similar to those reported for catechol oxidases from mussel byssus (Waite, 1985) and periostracum (Waite and Wilbur, 1976). While the native substrate for the catechol oxidase in the egg capsule has not been characterized, we have recently detected 3,4-dihydroxyphenylalanine in hydrolyzates of freshly oviposited capsules of *Raja erinacea* (Cox *et al.*, 1987). In addition, Hunt (1985) has reported identification of three catechols, including 3,4-dihydroxyphenylalanine, in hydrolyzates of egg capsules of *Scyliorhinus canicula*. It is uncertain whether these catechols are in-

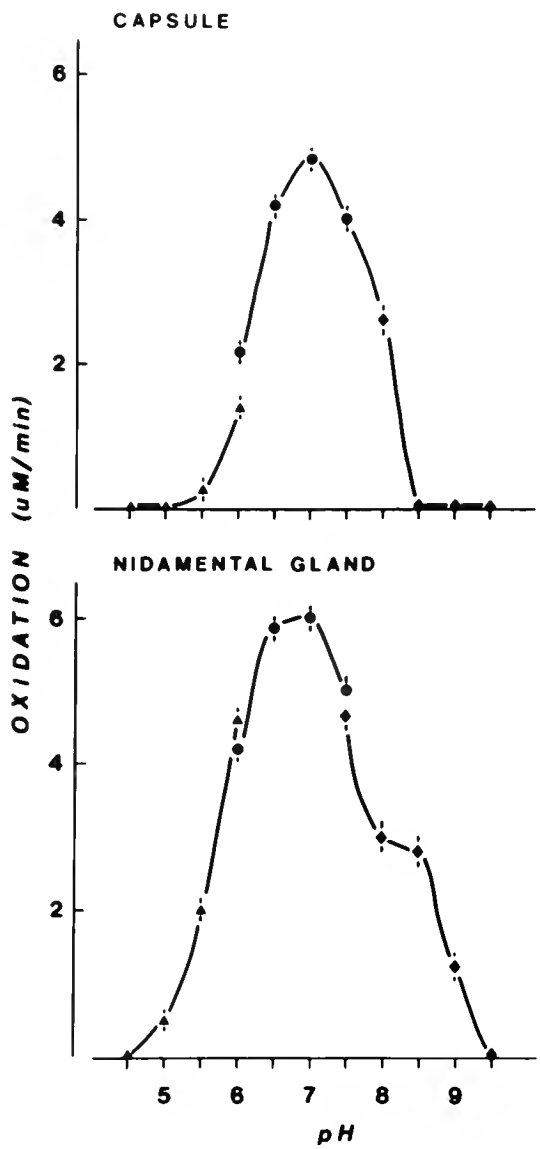

Figure 3. Effects of pH on oxidation rate of 4-methylcatechol by the capsule extract and nidamental gland extract. pH was varied from 5.0 to 8.5 using the three buffers: pH 4.5–6.0 in 0.05 *M* sodium acetate; pH 6–7.5 in 0.05 *M* sodium phosphate; pH 7.5–8.5 in 0.05 *M* Tris-HCl. Values shown are means of triplicate analyses of experimentals and boiled controls, and bars show the S.E.M.

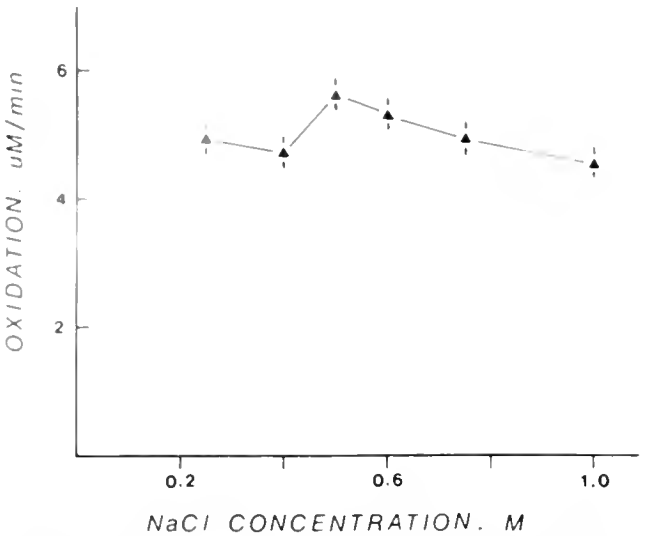

Figure 4. Effects of NaCl on the oxidation rate of 4-methylcatechol by the partially purified nidamental gland extract. NaCl was varied in 0.05 *M* NaH_2PO_4, pH 7.0. Values are means ± S.E.M. of triplicate analyses.

troduced as free amino acids or occur covalently bound to capsular proteins. Spectral analyses of intact capsular material suggested that the catechol in *Raja erinacea* capsules at oviposition is peptide bound (Koob, 1987). We have also shown that catechols are introduced into the capsular matrix following secretion and assembly of capsule precursors, while the formed capsules move into and reside in the uterine lumen. This accumulation of catechol is coincident with color development (Koob

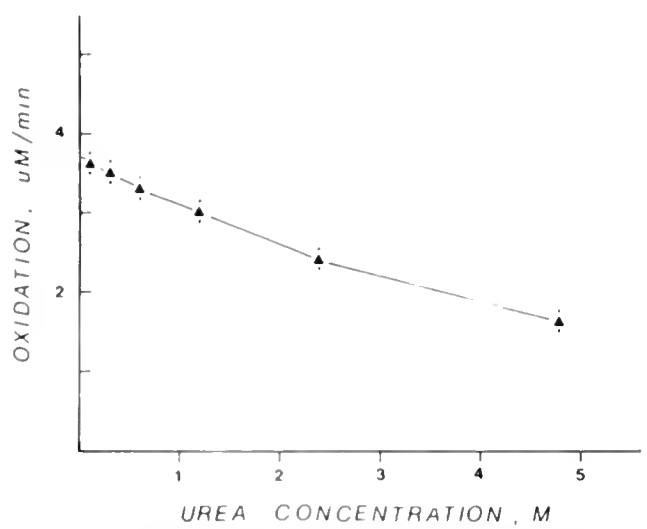

Figure 5. Effects of urea on the oxidation rate of 4-methylcatechol by the partially purified nidamental gland extract. Urea was varied in 0.5 *M* NaCl, 0.05 *M* NaH_2PO_4, pH 7.0. Values are means ± S.E.M. of triplicate analyses.

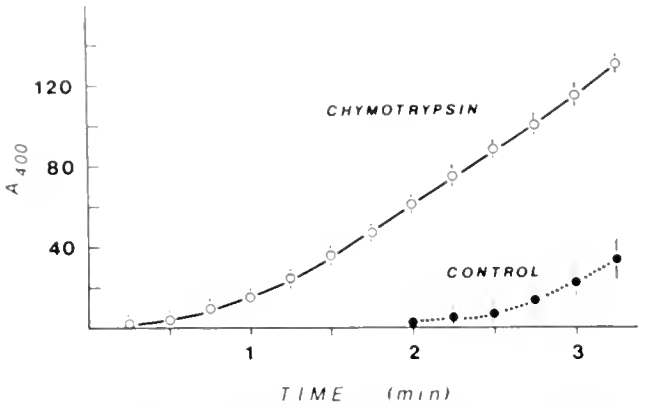

Figure 6. Initial rates of oxidation of 4-methylcatechol by extracts of nidamental glands with and without 40 μg of α-chymotrypsin. Aliquots of the 1.0 *M* NaCl extract were preincubated for 20 minutes at room temperature with 40 mg of α-chymotrypsin. Controls were incubated in parallel. Final assay conditions were 0.5 *M* NaCl, 0.05 *M* NaH_2PO_4, pH 7.5, and values presented are means ± S.E.M.

and Cox, 1986b). The presence of catechol oxidase in tanning capsules indicates that once catechols are introduced, they are susceptible to oxidation. These observations support Brown's (1955) original contention that this enzyme plays a pivotal role during the formation of skate egg capsules by catalyzing oxidation of catechols to highly reactive quinones forming dark pigments which tan the capsular matrix.

These experiments also establish the optimal conditions for assay of catechol oxidase from *Raja erinacea* nidamental glands. The partially purified enzyme exhibited maximal activity at 0.5 *M* NaCl and pH 7.0. Whether these conditions obtain in capsular material during tanning is not known, however, they closely resemble the osmolality and pH generally maintained in elasmobranch tissues. The sensitivity of the enzyme to urea is expected since renal and branchial enzymes from other elasmobranchs show identical inhibition by urea (Mályusz and Thiemann, 1976). We do not know whether urea is present in fluid bathing the tanning capsule or in the capsular material itself. The chemical conditions within the capsular matrix could be established during secretion of capsule precursors or alternatively could result from regulation of the intrauterine milieu.

The wide tolerance of nidamental gland catechol oxidase to alkaline pH and elevated salt concentrations provides evidence that the enzyme might remain active in seawater following oviposition of the capsule. Egg capsules of the little skate continue to tan during incubation by a process which may involve catechol oxidation (Koob, 1987). While it appears from the data presented here that catechol oxidase operates principally during capsular tanning *in utero*, it could also play a role in post-ovipositional tanning of the capsule.

One well characterized quinone tanning system that operates in seawater is the tanning of the attachment disc and byssus of *Mytilus edulis*. The byssal catechol oxidase displays optimum activity in salinity and pH near those of seawater (Waite, 1985). This enzyme's pH optimum (8.0) is slightly above that of the skate egg capsule enzyme, suggesting that the byssal enzyme may be more effective in seawater. Further study will be necessary to determine whether the egg capsule catechol oxidase in fact retains activity in seawater following oviposition. Such experiments will also furnish additional evidence regarding the role of this enzyme in the incubation-related tanning of the capsule.

The ability of α-chymotrypsin to shorten the delay in commencement of catechol oxidation by extracts of nidamental glands suggests that the egg capsule catechol oxidase is produced in a latent form which can be activated by proteolytic cleavage. Since this enzyme appears to auto-activate during storage as well as in the presence of substrate, these results also suggest that the gland produces a native activator. Whether the native activator resembles bovine α-chymotrypsin is not yet known. These observations are consistent with reports of latent phenoloxidases from both invertebrate and other vertebrate tanning systems.

For example, during sclerotization of the silkworm (*Bombyx mori*) cuticle, a latent phenoloxidase is activated by a serine protease (Dohke, 1973a, 1973b; Ashida and Dohke, 1980). A similar protease activates the prophenoloxidase of the arthropod immune response to invasive parasites (Ashida, 1971; Söderhäll, 1982; Ashida and Soderhall, 1984; Dularay and Lackie, 1985; Yoshida and Ashida, 1986; Saul and Sugumaran, 1987, 1988; for a review see Götz and Boman, 1985). In addition, *Mytilus edulis* produces a catechol oxidase that is latent towards catecholic substrates without prior activation by α-chymotrypsin (Waite, 1985). Among vertebrate tanning systems, the tyrosinase of amphibian skin is known to be produced in a latent form. Wittenberg and Triplett (1985a, b) have shown that detergents activate the latent tyrosinase from *Xenopus laevis*. This evidence is consistent with the preliminary data presented here. Together they implicate an activation process involving a zymogen of catechol oxidase during the formation of skate egg capsules.

Catechol oxidases have been detected in materials investing germ cells from many species and widely divergent taxa. Among fungi increases in phenoloxidase activity coincident with the development of fruiting-bodies have been noted for many species and have been investigated particularly in *Neurospora crassa* (Hirsch, 1954; Horowitz *et al.*, 1961), *Hypomyces solani* (Wilson, 1968), *Schizophyllum commune* (Phillips and Leonard, 1976, 1977; Leslie and Leonard, 1979), and *Agaricus bisporus* (Lindeberg, 1950; Turner, 1974; Rast *et al.*, 1981). Latent catechol oxidase has been identified as the predominant form of the enzyme in fruiting-bodies of *A. bisporus* (Yamaguchi *et al.*, 1970), though the mechanism of its activation has not been determined. The fruitbody phenoloxidase initiates melanization of propagule walls which is thought to confer protection from desiccation (reviewed by Sussman, 1968), lysis by other microorganisms (Potgieter and Alexander, 1966; Kuo and Alexander, 1967), and damage from ultraviolet light and other radiations (Sussman, 1968).

Seed coats of several wild legumes contain catechol oxidase. In *Pisum elatius*, for example, catechol oxidase activity in the seed coat rises sharply during the later developmental stages, especially during dehydration of the seed coat (Marbach and Mayer, 1975). The enzyme is believed to catalyze the generation of specific physicochemical properties important for dormancy and subsequent germination.

Catechol oxidases have also been detected in the eggshells and reproductive tracts of various invertebrates. Phenoloxidase activity has been histochemically demonstrated in both eggshells and vitellaria of many monogenetic and digenetic trematodes, and in certain cestodes (for a review see Clegg and Smyth, 1968; and Smyth and Halton, 1983). Recently, a dopa-rich eggshell precursor protein from the vitellaria of *Fasciola hepatica* has been purified and characterized (Waite and Rice-Ficht, 1987). Catechol oxidase activity has also been detected in the *Fasciola* vitellaria, and this enzyme has been partially purified (Cox and Waite, unpub. results). Like the elasmobranch egg capsule, the eggshells of many trematodes and cestodes appear to be stabilized by a form of sclerotization involving phenoloxidase catalyzed quinone tanning.

Egg cocoons of the leech *Erpobdella octoculata* undergo post-ovipositional hardening and darkening suggestive of some form of tanning. Knight and Hunt (1974) found the cocoons to be insoluble in the solutions used by Brown (1950a) with the exception of sodium hypochlorite. They also reported that the cocoons contain 3,4-dihydroxyphenylalanine and a catechol oxidase. Quinone tanning may occur in the egg cocoons of other annelids, but the evidence is as yet circumstantial (Brown, 1950b).

Among the Arthropoda, oothecae and left colleterial glands of the cockroaches *Blatta orientalis* (Pryor, 1940) and *Periplaneta americana* (Brunet, 1952) contain catechol oxidase which is believed to catalyze oxidation of 3,4-dihydroxybenzoic acid during the sclerotization of the ootheca. Likewise, eggshells of the house cricket, *Acheta domesticus*, reportedly contain a catechol oxidase (MacFarlane, 1960), while presence of the enzyme in shells of the mosquito, *Aedes aegypti*, has been in-

ferred (Walker and Menzer, 1969). Although several *o*- and *p*-diphenols have been extracted from eggshells and reproductive tracts of other insects, relatively little is known about the corresponding synthetic enzymes (for review of oothecal and eggshell proteins see Hinton, 1981).

To our knowledge, this is the first report of a catechol oxidase in egg capsules and oviduct of a vertebrate. The identification of catechol oxidase in egg capsules of *Raja erinacea* broadens the view that the products of this pathway possess particular properties adaptable to the needs of developing germ cells of fungi, plants, and animals.

Note added in proof

Inclusion of proteinase inhibitors (EDTA, benzamidine, N-ethylmaleimide and PMSF) during extraction of nidamental glands virtually eliminated catechol oxidase activity. The crude extract of one gland containing proteinase inhibitors contained less than 10% of the catechol oxidase activity found in the paired control gland extracted without proteinase inhibitors. These results support our suggestion that the egg capsule catechol oxidase is produced in a latent form requiring proteolytic activation.

Acknowledgments

These studies were supported in part by the Lucille P. Markey Charitable Trust and Mount Desert Island Biological Laboratory.

Literature Cited

Ashida, M. 1971. Purification and characterization of prephenoloxidase from hemolymph of the silkworm *Bombyx mori*. *Arch. Biochem. Biophys.* **144:** 749–762.

Ashida, M., and K. Dohke. 1980. Activation of prophenoloxidase by the activating enzyme of the silkworm *Bombyx mori*. *Insect Biochem.* **10:** 37–47.

Ashida, M., and K. Söderhäll. 1984. The prophenoloxidase activating system in crayfish. *Comp. Biochem. Physiol.* **77B:** 21–26.

Borcea, I. 1904. Sur la glande nidamentaire de l'oviducte des Élasmobranches. *C. R. Hebd. Seans. Acad. Sci.* **138:** 99–101.

Borcea, I. 1905. Recherches sur la système uro-genital des Élasmobranches. *Arch. Zool. Exp. Gen.* **4:** 199–484.

Brown, C. H. 1950a. A review of the methods available for the determination of the types of forces stabilizing structural proteins in animals. *Q. J. Microsc. Sci.* **91:** 331–339.

Brown, C. H. 1950b. Quinone tanning in the animal kingdom. *Nature* **165:** 275.

Brown, C. H. 1955. Egg capsule proteins of selachians and trout. *Q. J. Microsc. Sci.* **96:** 483–488.

Brunet, P. C. J. 1952. The formation of the ootheca by *Periplaneta americana*. II. The structure and function of the left colleterial gland. *Q. J. Microsc. Sci.* **93:** 47–69.

Bumpus, H. C. 1898. The breeding of animals at Woods Holl during the months of June, July and August. *Science* **8:** 850–858.

Clegg, J. A., and J. D. Smyth. 1968. Growth, development and culture methods: parasitic platyhelminths. Pp. 395–466 in *Chemical Zoology*, Vol. II, M. Florkin and B. T. Scheer, eds. Academic Press, New York and London.

Cox, D. L., R. P. Mecham, and T. J. Koob. 1987. Site-specific variation in amino acid composition of skate egg capsule (*Raja erinacea* Mitchell 1825). *J. Exp. Mar. Biol. Ecol.* **107:** 71–74.

Dohke, K. 1973a. Studies on prophenoloxidase-activating enzyme from cuticle of the silkworm *Bombyx mori*. I. Activation reaction by the enzyme. *Arch. Biochem. Biophys.* **157:** 203–209.

Dohke, K. 1973b. Studies on prophenoloxidase-activating enzyme from cuticle of the silkworm *Bombyx mori*. II. Purification and characterization of the enzyme. *Arch. Biochem. Biophys.* **157:** 210–221.

Dularay, B., and A. M. Lackie. 1985. Haemocytic encapsulation and the prophenoloxidase-activation pathway in the locust *Schistocerca gregaria* Forsk. *Insect Biochem.* **15:** 827–834.

Eisenthal, R., and A. Cornish-Bowden. 1974. The direct linear plot. A new graphical procedure for estimating enzyme kinetic parameters. *Biochem. J.* **139:** 715–720.

Filhol, J., and H. Garrault. 1938. La sécrétion de la prokératine et la formation de la capsule ovulaire chez les Sélaciens. *Arch. Anat. Microsc.* **34:** 105–145.

Götz, P. and H. G. Boman. 1985. Insect immunity. Pp. 453–485 in *Comprehensive Insect Physiology, Biochemistry and Pharmacology*, Vol. 3, G. A. Kerkut and L. E. Gilbert, eds. Pergamon Press, Oxford.

Henneguy, L. F. 1893. Sur la structure de la glande nidamentaire de l'oviducte des Sélaciens. *C. R. Soc. Philomatique* 8th ser., 5.

Hinton, H. E. 1981. *Biology of Insect Eggs*, Vol. 1. Pp. 201–210. Pergamon Press, Oxford.

Hirsch, H. M. 1954. Environmental factors influencing the differentiation of protoperithecia and their relation to tyrosinase and melanin formation in *Neurospora crassa*. *Physiologia Plantarum* **7:** 72–97.

Horowitz, N. H., M. Fling, H. L. Macleod, and Y. Watanabe. 1961. Structural and regulative genes controlling tyrosine synthesis in *Neurospora*. *Cold Spring Harbor Symp. Quant. Biol.* **26:** 233–238.

Hunt, S. 1985. The selachian egg case collagen. Pp. 409–434 in *Biology of Invertebrate and Lower Vertebrate Collagens*, A. Bairati and R. Garrone, eds. Plenum Press, New York and London.

Knight, D. P., and S. Hunt. 1974. Molecular and ultrastructural characterization of the egg capsule of the leech *Erpobdella octoculata* L. *Comp. Biochem. Physiol.* **47A:** 871–880.

Koob, T. J. 1987. Effects of oxidation and reduction on the spectral properties of the egg capsules of *Raja erinacea* Mitchill. *J. Exp. Mar. Biol. Ecol.* **113:** 155–166.

Koob, T. J., and D. L. Cox. 1984. Studies on skate (*Raja erinacea*) egg capsule formation. *Bull. Mt. Desert Is. Biol. Lab.* **24:** 78–80.

Koob, T. J., and D. L. Cox. 1985. Shell gland catechol oxidase from *Raja erinacea*. *Bull. Mt. Desert Is. Biol. Lab.* **25:** 132–134.

Koob, T. J., and D. L. Cox. 1986a. Effects of salinity, pH and urea on shell gland catechol oxidase of *Raja erinacea*. *Bull. Mt. Desert Is. Biol. Lab.* **26:** 113–116.

Koob, T. J., and D. L. Cox. 1986b. Studies on skate (*Raja erinacea*) egg capsule formation. II. Introduction of catechols occurs *in utero*. *Bull. Mt. Desert Is. Biol. Lab.* **26:** 109–112.

Koob, T. J., P. Tsang, and I. P. Callard. 1986. Plasma estradiol, testosterone, and progesterone levels during the ovulatory cycle of the skate (*Raja erinacea*). *Biol. Reprod.* **35:** 267–275.

Krishnan, G. 1959. Histochemical studies on the nature and formation of egg capsules of the shark *Chiloscyllium griseum*. *Biol. Bull.* **117:** 298–307.

Kuo, M.-J., and M. Alexander. 1967. Inhibition of the lysis of fungi by melanins. *J. Bacteriol.* **94:** 624–629.

Laemmli, U. K. 1970. Cleavage of structural proteins during the assembly of the head of bacteriophage T4. *Nature* **227:** 680–685.

Leslie, J. F., and T. J. Leonard. 1979. Monokaryotic fruiting in *Schizophyllum commune*: phenoloxidases. *Mycologia* **71:** 1082–1085.

Lindeberg, G. 1950. Phenol oxidases of the cultivated mushroom *Psalliota bispora f. albida*. *Nature* **166:** 739–741.

Lowry, O. H., N. J. Rosebrough, A. L. Farr, and R. J. Randall. 1951. Protein measurement with the Folin phenol reagent. *J. Biol. Chem.* **193:** 265–275.

Mályusz, M., and V. Thiemann. 1976. The effect of urea, thiourea and acetamide on the renal and branchial enzyme-pattern of the dogfish *Scyliorhinus canicula*. *Comp. Biochem. Physiol.* **54B:** 177–179.

Marbach, I., and A. M. Mayer. 1975. Changes in catechol oxidase and permeability to water in seed coats of *Pisum elatius* during seed development and maturation. *Plant Physiol.* **56:** 93–96.

McFarlane, J. E. 1960. Structure and function of the egg shell as related to water absorption by the eggs of *Acheta domesticus* (L.). *Can. J. Zool.* **38:** 231–241.

Metten, H. 1939. Studies on the reproduction of dogfish. *Phil. Trans. R. Soc. Lond.* **230B:** 217–238.

Nalini, K. P. 1940. Structure and function of the nidamental gland of *Chiloscyllium griseum*. *Proc. Indian Acad. Sci.* **12B:** 189–214.

Perrevex, E. 1884. Sur la formation de la coque des oeufs du *Scyllium canicula* et du *Scyllium catulus*. *C. R. Hebd. Seans. Acad. Sci.* **99:** 1080–1082.

Phillips, L. E., and T. J. Leonard. 1976. Extracellular and intracellular phenoloxidase activity during growth and development in *Schizophyllum*. *Mycologia* **68:** 268–276.

Phillips, L. E., and T. J. Leonard. 1977. On the oxidation of dihydroxyphenylalanine and benzidine in crude cell-free fungal extracts. *Mycologia* **69:** 413–416.

Potgieter, H. J., and M. Alexander. 1966. Susceptibility and resistance of several fungi to microbial lysis. *J. Bacteriol.* **91:** 1526–1532.

Prasad, R. R. 1945a. The structure, phylogenetic significance and function of the nidamental glands of some elasmobranchs of the Madras Coast. *Proc. Natl. Inst. Sci. India* **11:** 282–302.

Prasad, R. R. 1945b. Further observations on the structure and function of a few elasmobranchs of the Madras Coast. *Proc. Indian Acad. Sci.* **22B:** 368–373.

Prasad, R. R. 1948. Observations on the nidamental glands of *Hydrolagus colliei, Raja rhina* and *Platyrhinoids triseriatus*. *Copeia* **1948(1):** 54–57.

Pryor, M. G. M. 1940. On the hardening of the ootheca of *Blatta orientalis*. *Proc. R. Soc. Lond.* **128B:** 378–393.

Rast, D. M., H. Stüssi, H. Hegnauer, and L. E. Nyhlén. 1981. Melanins. Pp. 507–531 in *The Fungal Spore: Morphogenetic Controls*, G. Turian, and H. R. Hohl, eds. Academic Press, New York and London.

Rusaouën, M. 1978. Étude ultrastructurale des zones a sécrétions protéiques et glycoprotéiques de la glande nidamentaire de la rousette a maturité. *Arch. Anat. Microsc.* **67:** 107–119.

Rusaouën, M., J.-P. Pujol, J. Bocquet, A. Veillard, and J.-P. Borel. 1976. Evidence of collagen in the egg capsule of the dogfish, *Scyliorhinus canicula*. *Comp. Biochem. Physiol.* **53B:** 539–543.

Saul, S. J., and M. Sugumaran. 1987. Protease mediated prophenoloxidase activation in the hemolymph of the tobacco hornworm, *Manduca sexta*. *Arch. Insect Biochem. Physiol* **5:** 1–11.

Saul, S. J., and M. Sugumaran. 1988. Prophenoloxidase activation in the hemolymph of *Sarcophaga bullata* larvae. *Arch. Insect Biochem. Physiol.* **7:** 91–103.

Segal, I. H. 1976. *Biochemical Calculations. How to Solve Mathematical Problems in General Biochemistry*, 2nd ed. John Wiley & Sons, New York.

Smyth, J. D. 1954. A technique for the histochemical demonstration of polyphenoloxidase and its application to egg-shell formation in helminths and byssus formation in *Mytilus*. *Q. J. Microsc. Sci.* **95:** 139–152.

Smyth, J. D., and D. W. Halton. 1983. *The Physiology of Trematodes*, 2nd ed. Cambridge University Press, Cambridge.

Söderhäll, K. 1982. The prophenoloxidase activating system and melanization—a recognition mechanism of arthropods. A review. *Dev. Comp. Immunol.* **6:** 601–611.

Sussman, A. S. 1968. Longevity and survivability of fungi. Pp. 447–486 in *The Fungi. An Advanced Treatise. Vol. III. The Fungal Population*, G. C. Ainsworth, and A. S. Sussman, eds. Academic Press, New York and London.

Threadgold, L. T. 1957. A histochemical study of the shell gland of *Scyliorhinus caniculus*. *J. Histochem. Cytochem.* **5:** 159–166.

Turner, E. M. 1974. Phenoloxidase activity in relation to substrate and development stage in the mushroom, *Agaricus bisporus*. *Trans. Br. Mycol. Soc.* **63:** 541–547.

Waite, J. H. 1976. Calculating extinction coefficients for enzymatically produced *o*-quinones. *Anal. Biochem.* **75:** 211–218.

Waite, J. H. 1985. Catechol oxidase in the byssus of the common mussel, *Mytilus edulis* L. *J. Mar. Biol. Assoc. U. K.* **65:** 359–371.

Waite, J. H., and A. C. Rice-Ficht. 1987. Preselerotized eggshell protein from the liver fluke *Fasciola hepatica*. *Biochemistry* **26:** 7819–7825.

Waite, J. H., and K. M. Wilbur. 1976. Phenoloxidase in the periostracum of the marine bivalve *Modiolus demissus* Dillwyn. *J. Exp. Zool.* **195:** 359–367.

Walker, W. F., and R. E. Menzer. 1969. Chorionic melanization in the eggs of *Aedes aegypti*. *Ann. Entomol. Soc. Am.* **62:** 7–11.

Widakowich, V. 1906. Über Bau und Funktion des Nidamentalorgans von *Scyllium canicula*. *Z. Wiss. Zool.* **80:** 1–21.

Wilson, D. M. 1968. Physiology of sexual reproduction in *Hypomyces solani* f. sp. *cucurbitae*. V. Effect of tyrosinase. *Phytopathology* **58:** 1697–1699.

Wittenberg, C., and E. L. Triplett. 1985a. A detergent-activated tyrosinase from *Xenopus laevis*. I. Purification and partial characterization. *J. Biol. Chem.* **260:** 12,535–12,541.

Wittenberg, C., and E. L. Triplett. 1985b. A detergent-activated tyrosinase from *Xenopus laevis*. II. Detergent activation and binding. *J. Biol. Chem.* **260:** 12,542–12,546.

Yamaguchi, M., P. M. Hwang, and J. D. Campbell. 1970. Latent *o*-diphenol oxidase in mushrooms (*Agaricus bisporus*). *Can. J. Biochem.* **48:** 198–202.

Yoshida, H., and M. Ashida. 1986. Microbial activation of two serine enzymes and prophenoloxidase in the plasma fraction of hemolymph of the silkworm, *Bombyx mori*. *Insect Biochem.* **16:** 539–545.

Reference: *Biol. Bull.* 175: 212–217. (October, 1988)

Reciprocation, Reproductive Success, and Safeguards Against Cheating in a Hermaphroditic Polychaete Worm, *Ophryotrocha diadema* Åkesson, 1976

GABRIELLA SELLA

Department of Animal Biology, Via Accademia Albertina 17, University of Turin, 10123 Torino, Italy

Abstract. *Ophryotrocha diadema*, a simultaneous hermaphroditic polychaete worm, forms pairs in which both partners regularly alternate sex roles and trade eggs. Since *O. diadema* has a protandrous phase, safeguards against cheating by a non-reciprocating partner, either male or hermaphrodite, have evolved. Results of a mate choice experiment indicate that protandrous males are generally discarded as mates because they are unable to reciprocate with eggs. Reproductive success (measured by estimating the mean number of egg masses per individual per day) of hermaphrodites paired with males was significantly lower than the reproductive success of hermaphrodites paired with hermaphrodites. This indicates that *O. diadema* is able to time spawning activity according to the sexual condition of its partner. On the other hand, oogenesis and the production of multiple batches of mature oocytes is independent of the presence of a partner. Worms did not discard mates with substantially fewer eggs. The small size of clutches and the short interval between successive spawnings could be considered a form of egg parcelling, which would prevent exploitation of hermaphroditic individuals by partners unable to reciprocate.

Introduction

Ophryotrocha diadema Åkesson, 1976, is a small (4 mm long) simultaneous hermaphrodite which was discovered in 1976 by Reish and Åkesson among the fouling fauna in Los Angeles Harbor. Larvae are released from the egg case at a body length of 4 setigerous segments. Its sexual life begins with a protandrous phase, which lasts two to three weeks. The simultaneous hermaphroditic phase begins at the fourth week of life, at a body length of 14 setigers. Sperm are produced throughout life in the third and fourth setigers only, and eggs are produced from the fifth setiger onwards. Fecundity is age-dependent (Åkesson, 1976). In the first week of reproduction, cocoons contain 15–17 eggs. Maximum reproductive output (30–40 eggs/day) occurs four weeks after spawning begins and then slowly declines (Åkesson, 1982). Cocoons are released at intervals of about three days.

The main features of the mating system of *O. diadema* were described by Sella (1985) and can be summarized as follows:

(1) Pairs are formed preferentially between simultaneous hermaphrodites. Spawning synchronization is achieved by means of close mutual contact during a courtship lasting several hours.

(2) Partners repeatedly alternate sex roles with the same partner at intervals of about 30 hours. As one partner releases its eggs, the other fertilizes them. This alternate egg laying has been defined as egg trading by Fischer (1980) and Maynard Smith (1982, p. 160).

(3) Both partners care for the developing embryos.

This paper addresses the following question: does the mating system of *O. diadema* represent an evolutionarily stable strategy (ESS), *sensu* Maynard Smith (1982, p. 12) and Parker (1978), *i.e.*, a strategy such that, if all the members of a population adopt it, no mutant strategy is likely to invade it under the influence of natural selection? In the case of *O. diadema*, the mutant strategy would be reproducing only as a male. *O. diadema* eggs require greater nutritive resources than sperm (Sella, in prep.), so reproducing only as a female would probably be selected against.

Received 12 August 1987; accepted 12 July 1988.

A mating system involving reciprocity would not be stable if safeguards against non-reciprocating individuals had not evolved. Two partners have a common interest in reciprocating but there is a potential advantage in non-reciprocation. Since eggs require greater nutritive resources than sperm, a hermaphrodite could increase its fitness by fertilizing the eggs of other individuals on days when it has no mature eggs to give. For reciprocal spawning to be critical to reproductive success, there should be strong constraints on reproducing only as a male in both the protandrous and hermaphroditic phases. Therefore, reproductive success is expected to be significantly lower than average for those individuals that fail to reciprocate egg exchange. In *O. diadema* at each spawning, ovaries release all their mature eggs. Therefore, in order not to be a loser in egg trading, a hermaphrodite is expected to have evolved an ability to perceive how many eggs its partner has and, eventually, to discard a partner with substantially fewer eggs than it has.

To assess the evolutionary stability of the mating system of *O. diadema* I estimated the probability that subadults will succeed in mating with hermaphrodites, compared the reproductive success of a hermaphrodite mated to a male with that of a hermaphrodite paired to another hermaphrodite, and investigated whether worms can perceive egg loads of their partners and discard partners having fewer stored eggs.

Materials and Methods

Animals used in experiments were taken from laboratory populations originating from specimens of *O. diadema* collected in Los Angeles Harbor (Åkesson, 1976). Populations were reared according to the methods described by Åkesson (1976) and Sella (1985). They were placed in filtered sea water with a salinity of 34‰ at a constant temperature of 20°C and fed parboiled spinach.

A genetically determined yellow or white coloration of eggs permitted identification of the partners in a pair since both eggs and embryos are colored according to the mother's phenotype (Sella and Marzona, 1983). Therefore, color of eggs was used to infer which partner spawned eggs or fertilized them in a white and yellow worm pair. No difference in the mean number of eggs per cocoon was observed between yellow and white individuals (Åkesson, 1976; Sella, unpub.).

In all experiments, only virgin individuals of the same age were used, since both fecundity and fertility are age dependent in *O. diadema* (Åkesson, 1982). To obtain virgin individuals, individual males were reared in separate containers until they reached the length (14–15 setigers) at which oocyte production begins. Only when their first oocyte batch was mature, were they used in experiments. Therefore, the term "virgin worm" refers to a simultaneous hermaphrodite which is ready to spawn its first batch of eggs. Since body walls are transparent and ripe oocytes measure approximately 180 × 200 μm, oocyte growth (as well as embryo development) could be easily observed with a stereomicroscope at low magnification.

Although "reproductive success" generally is defined as the number of progeny that survive to reproduce, this number is often impossible to measure. When pairs are formed between two simultaneous hermaphrodites, approximately 95% of the eggs are fertilized and develop (Sella, in prep.). The mean number of eggs per cocoon per week has a standard error never greater than 1 (Åkesson, 1976). Therefore, if individuals of the same age are paired, reproductive success can be indirectly estimated by counting the cocoons released in a given time interval. The term "young male" refers to subadults 7–8 setigers long which have not yet reached the simultaneous hermaphroditic phase and release only sperm.

The following three experiments were conducted.

Mate selection

To study the intensity of sexual selection against males, 44 bowls each containing a yellow virgin hermaphrodite, a white virgin hermaphrodite, and a male six setigers long, were set up. Each hermaphrodite could choose to pair either with the male or with the other hermaphrodite. Animals were observed until a pair was formed in each bowl and courtship terminated with egg spawning by one of the two partners.

Reproductive success and failure to reciprocate

If reciprocal spawning is critical to mating success, reproductive success of a hermaphrodite mated to a young male is expected to be significantly lower than that of a simultaneous hermaphrodite paired with another simultaneous hermaphrodite. The reproductive success (number of cocoons spawned in 10 days) of a set of 72 pairs of yellow and white hermaphrodites was compared to a set of 72 pairs of young males and either yellow or white simultaneous hermaphrodites. In the latter situation, the simultaneous hermaphrodites can act only as females, since alternation of sex roles and reciprocation of fertilization is precluded. Each pair was kept in a separate container.

Ability to perceive partner's eggs load

There are two ovaries per setiger in *O. diadema*. Each ovary produces one or two mature oocytes at a time. Eggs are spawned only if a partner able to fertilize them is present. Isolated individuals accumulate ripe eggs in the coelomic cavity because they do not spawn. The experi-

Table I

Reproductive success (mean number of egg masses per individual) in 10-day interval (A) and mean interval between two successive spawnings (B) of simultaneous hermaphrodites paired with a simultaneous hermaphrodite or with a young male

	(A)		(B)	
Kind of pairs	N_A	$\bar{x}$ egg masses/ individual	N_B	$\bar{x}$ days between successive spawnings
♂ × ♂	144	2.1 ± 0.02	54	2.97 ± 0.20
♀ × ♂	72	1.8 ± 0.07	34	5.24 ± 0.26

(A) One-way ANOVA, $F_{1,142} = 7.58$; $0.005 < P < 0.01$

(B) One-way ANOVA, $F_{1,86} = 6.26$; $0.02 < P < 0.01$

N_A = number of sampled hermaphrodites; N_B = number of individuals from sample N_A which spawned twice during the experiment.

ment takes advantage of these characteristics to determine if an individual is able to perceive the number of eggs held by its partner and whether it can modulate its spawning behavior accordingly. Worms are expected to discard potential partners with fewer stored eggs.

Three equal groups of hermaphrodites with a different number of eggs in their coelomic cavity were allowed to choose their partner according to the number of mature eggs it had. The experiment lasted 124 hours. To obtain virgin individuals with different numbers of ripe oocytes, 3 groups of 100 virgin worms were isolated in separate containers for: (A) two weeks, (B) one week, and (C) one day, respectively, from the day the first ripe oocytes were visible through their body walls.

The experimental set up for matching individuals from groups A, B, and C was the following: in each of 50 Petri dishes filled with 30 ml of seawater, 6 individuals (2 from each group) were put together. A cellulose triacetate disc of the same size as the dish, printed with a millimeter grid, was placed beneath each dish to record the location of each pair upon its formation.

Results

Mate selection

Pairs between males and hermaphrodites formed in 14 bowls (32%) and pairs between hermaphrodites formed in 30 bowls (68%) out of 44. These values are significantly different than those expected (29.2 and 14.6) if mating choice had been random. (G test = 39.54; $P < 0.001$).

When hermaphrodites could choose between a male and another hermaphrodite, they preferred to mate with the hermaphrodite, *i.e.*, with a partner able to reciprocate eggs.

Reproductive success and failure to reciprocate

The mean number of egg masses each partner spawned in the set of simultaneous hermaphrodite pairs was significantly greater than the mean number each hermaphrodite spawned in the set of pairs between hermaphrodites and young males (Table I). Moreover, the mean number of days between successive spawnings of a simultaneous hermaphrodite mated to another hermaphrodite is significantly fewer than the mean interval between successive spawnings of an adult mated with young males (one-way ANOVA on data transformed in a $\sqrt{x + 0.5}$ scale) (Table I).

Therefore, the reproductive success of a simultaneous hermaphrodite is significantly influenced by the sexual phenotype (either male or hermaphrodite) of its partner. The number of spawned cocoons by a simultaneous hermaphrodite decreases when it cannot reciprocate because it has a young male as a partner.

Ability to perceive partner's egg load

Isolation treatment led to a significantly different number of ripe eggs accumulated in the coelomic cavity of worms from groups A, B, and C. (Table II). *A posteriori* comparisons among mean numbers of eggs (SS-STP test, Sokal and Rohlf, 1981, p. 245) from individuals which spawned eggs in groups A, B, and C are highly significant (Table II), thus indicating that egg accumulation in the coelomic cavity is significantly affected by the length of the isolation period.

The first pairs formed at the end of the first day after the beginning of the experiment and the first egg spawnings were observed during the second day.

Although the aim of this experiment was not to study reciprocation, it is worth observing that at the end of the experiment 67 of 110 pairs had reciprocated and that the

TABLE II

Mean number of eggs per cocoon laid by individuals isolated for 2 weeks (A), 1 week (B), and 1 day (C), after the first maturation of oocytes

	A	B	C
$\bar{x}$ ± S.E.	32.35 ± 1.51	24.46 ± 1.42	17.54 ± 1.03
N	60	53	46

One-way ANOVA, $F_{2,149} = 25.34$; $p < 0.001$

A posteriori comparisons among means, (SS-STP test):

comparisons	SS	
A *versus* B	1362.264	significant
B *versus* C	1227.5642	significant
C *versus* A	4986.718	significant
critical SS	591.43	

Table III

Frequency of pairs formed between individuals belonging to groups A, B, and C, in 6 days

Kinds of pairs	A × A	A × B	A × C	B × C	B × B	C × C	total
observed	9	33	33	30	3	2	110
expected	12.2	24.4	24.4	24.4	12.2	12.2	110

G-test, $G = 31.12$, $P < 0.01$

Numbers of individuals, out of 100, involved in pair formation either as males or as females from
group A = 84
group B = 69
group C = 67

Heterogeneity G-test, $G_2 = 9.3$, $P = 0.01$.

proportions of individuals acting only as fertilizers was not significantly different in all three groups (heterogeneity G test, $G_2 = 1.19$). Most fertilizers of pairs formed in the last two days of the experiment did not have the opportunity to reciprocate by spawning.

Expectations about pair formation were not fulfilled by the experimental data (Table III). Animals of group A, with the greatest number of oocytes, became involved in pair formation in a significantly greater number than animals of groups B and C, but they did not pair more frequently among themselves than with worms with a lower number of oocytes belonging to groups B and C. During the experiment no individual paired twice.

Pairing was not random. An excess of pairs were formed by individuals belonging to different groups and a deficiency of pairs were formed by individuals belonging to the same group compared with frequencies expected under the hypothesis of random mating.

Worms released all the eggs they currently had without parcelling them, irrespective of how many eggs their partners had, thus indicating that *O. diadema* does not select its mate by number of eggs.

Discussion

Simultaneous hermaphroditism with juvenile protandry would be an evolutionarily unstable reproductive strategy if males, competing for fertilization with hermaphrodites, had greater reproductive success than simultaneous hermaphrodites. This does not seem to happen in the mating system of *O. diadema* because there are strong constraints limiting reproductive success either as a non-reciprocating hermaphrodite or as a male. Hermaphrodites, which did not reciprocate because they mated with young males, laid fewer cocoons than reciprocating hermaphrodites. Males experience the following three selective constraints: (1) they are generally discarded as mates because they are unable to reciprocate; (2) if they are paired to a hermaphrodite, the number of egg masses laid by the hermaphrodite per day is less than the number of egg masses laid by a hermaphrodite paired with another hermaphrodite; and (3) they do not fertilize eggs as efficiently as hermaphrodites (Sella, in prep.). Therefore, one would expect a very brief protandrous phase, or for such a phase to be completely absent in the early part of the life cycle of *O. diadema*, because of the selective constraints against it. Indeed, the protandrous phase lasts about ¼ of the most fertile period of the life of *O. diadema*. Testes are comparable in size to ovaries, but, since they are present only in the third and fourth setigers throughout life, investment in testicular tissue may be much less. The return of this investment in juveniles is small, because they do not have many opportunities to pair, compared to the return of the same investment during the hermaphroditic phase, where opportunities to fertilize eggs are regularly offered to reciprocating individuals.

Despite the constraints on reproducing only as a male, 32% of young males engaged in mating competition with hermaphrodites succeeded in pairing with hermaphrodites. In another mate choice experiment described by Sella (1985), males succeeded in being the first to pair with hermaphrodites in three out of sixteen bowls. The difference between frequencies of males paired with hermaphrodites in both experiments is not statistically significant (heterogeneity G test, $G_1 = 1.04$). The only apparent competitive advantage that young males might have over hermaphrodites is their greater mobility, which could help them in searching for and courting a partner if population density were low. Ghiselin (1974, p. 194) advanced a similar hypothesis to explain the existence of small males associated with hermaphrodites in many animal groups; when adults have a mode of life in which motility is restricted, small males, able to capitalize on their motility, tend to evolve. Hermaphrodites of *O. diadema* and adults of other *Ophryotrocha* species have a restricted motility since they spend much of their time in egg brooding. Ghiselin (1974, p. 210), Gould (1977, p. 330), and Charnov (1982, p. 250) observed that

selective pressures favoring progenesis in males concomitantly increase as population density decreases. A hermaphrodite living in a low density population would incur some metabolic cost in searching for a better mate, and, at a certain stage of oogenesis, might be hormonally programmed to mate with the first available mate. In general, interstitial fauna are present at low densities (Svedmark, 1964). Unfortunately, nothing is known about the population structure of *O. diadema* in the field, apart from the original observation in Los Angeles Harbor that only 2 individuals of *O. diadema* were collected with more than 300 individuals of *O. labronica pacifica*. Since then, no additional specimens have been found in the same locality (D. Reish, pers. comm.).

It is difficult not to expect some form of egg parcelling in *O. diadema*, since it would prevent exploitation of hermaphroditic individuals by partners with no eggs. Although the excess of matings between individuals with a different number of oocytes observed in the third experiment merits further investigation, the results indicate that in *O. diadema* each partner releases all of its ripe eggs. The higher frequency of pairing by group A individuals may be explained by the greater number of accumulated eggs compressing coelomic walls and causing release of all the eggs. Results of the second experiment indicate that there is, at least, a sort of temporal parcelling of cocoon production: (1) time intervals between acts of egg laying by a worm are briefer if immediately reciprocated by an egg laying partner; (2) conversely, longer intervals between acts of egg-laying occur in matings with partners that do not lay eggs. The small size of the clutches and the short intervals between them can be considered a form of egg parcelling. It is interesting to observe that in other simultaneous hermaphroditic species of *Ophryotrocha* [*i.e.*, *O. hartmanni*, *O. maculata*, and *O. bacci* (Åkesson, 1973a, b)], egg masses contain only 20–40 eggs and in *O. gracilis* even fewer (Westheide, 1984). Intervals between successive spawnings in these species are not known. In contrast, in gonochoric and sequential hermaphroditic species of *Ophryotrocha*, egg masses contain a hundred eggs and are spawned only once every one or two weeks. Therefore, the previous doubt about the ability of *O. diadema* to parcel its clutches according to the reproductive behavior of its partner (Sella, 1985) needs to be corrected in light of these considerations.

In the simultaneous hermaphroditic coral reef fish *Hypoplectrus nigricans* a graded strategy of laying eggs in small batches, rather than all at once, has evolved to guard against cheating (Fischer, 1980). According to Maynard Smith (1982, p. 160), this form of egg parcelling can be regarded as a game of incomplete information, since each fish knows whether it has eggs to trade, but not if its partner has eggs. In *O. diadema*, sufficient information on the sexual condition of conspecifics (males, simultaneous hermaphrodites, or hermaphrodites temporarily out of eggs) could be obtained through pheromonal signals. In *Ophryotrocha puerilis*, the existence of sex attractants emanating from females has been observed repeatedly (Pfannenstiel, 1977, 1984; Marchionni and Rolando, 1981; Franke and Pfannenstiel, 1984; Grothe and Pfannenstiel, 1986; Berglund, in prep.). In the gonochoric species *O. robusta* and *O. labronica* (Rolando, 1984), as well as in *O. macrovifera* (Sella, unpub. obs.), pheromones have been hypothetized as the most likely explanation for sexual induction phenomena.

As both Axelrod and Hamilton (1981) and Maynard Smith (1982, p. 169) observed, an ability to discriminate between other members of the same species may extend the range of stable cooperation. This discrimination allows individuals to handle interactions with many other conspecifics in different ways. In *O. diadema*, the ability to recognize the sexual condition of the partner, and to time spawning activity accordingly, could both greatly reduce the risk of being cheated and enhance the evolutionary stability of the mating system.

Acknowledgments

This research has greatly benefited from critical comments by M. Ghiselin, B. Åkesson, W. D. Hamilton, from suggestions by an anonymous referee on an earlier paper (Sella, 1985), and by referees of the present paper. Financial support was supplied by the Italian Ministero della Pubblica Istruzione.

Literature Cited

Åkesson, B. 1973a. Morphology and life history of *Ophryotrocha maculata* sp. n. (Polychaeta, Dorvilleidae). *Zool. Scr.* **2**: 141–144.

Åkesson, B. 1973b. Reproduction and larval morphology of five *Ophryotrocha* species (Polychaeta, Dorvilleidae). *Zool. Scr.* **2**: 145–155.

Åkesson, B. 1976. Morphology and life cycle of *Ophryotrocha diadema*, a new polychaete species from California. *Ophelia* **15**: 23–35.

Åkesson, B. 1982. A life table study on three genetic strains of *Ophryotrocha diadema* (Polychaeta, Dorvilleidae). *Int. J. Invert. Reprod.* **5**: 59–69.

Axelrod, R., and W. D. Hamilton. 1981. The evolution of cooperation. *Science* **211**: 1390–1396.

Charnov, E. L. 1982. *The Theory of Sex Allocation*. *Monographs in Population Biology*, Vol. 18, Princeton University Press, Princeton, NJ. 355 pp.

Franke, H. D., and H. D. Pfannenstiel. 1984. Some aspects of endocrine control of Polychaete reproduction. *Fortsch. Zool.* **29**: 53–72.

Fischer, E. A. 1980. The relationship between mating system and simultaneous hermaphroditism in the coral reef fish *Hypoplectrus nigricans* (Serranidae). *Anim. Behav.* **28**: 620–633.

Ghiselin, M. T. 1974. *The Economy of Nature and the Evolution of Sex*. University of California, Berkeley, and Los Angeles. 343 pp.

Gould, S. J. 1977. *Ontogeny and Phylogeny.* Belknap Press of Harvard University Press, Cambridge, Massachusetts and London U.K. 501 pp.

Grothe, C. and H. D. Pfannenstiel. 1986. Cytophysiological study of neurosecretory and pheromonal influences on sexual development in *Ophryotrocha puerilis. Int. J. Invert. Reprod. Dev.* **10:** 227–239.

Marchionni, V. and A. Rolando. 1981. Sex reversal in *Ophryotrocha puerilis* induced by ethereal extracts of female phase individuals. *Boll. Zool.* **48:** 91–96.

Maynard Smith, J. 1982. *Evolution and the Theory of Games.* Cambridge University Press, U.K. 224 pp.

Parker, G. A. 1978. Selfish genes, evolutionary games, and the adaptiveness of behaviour. *Nature* **274:** 849–855.

Pfannenstiel, H. D. 1977. Experimental analysis of the "paarkultur-effect" in the protandric polychaete *Ophryotrocha puerilis* Clap. Mecz. *J. Exp. Mar. Biol. Ecol.* **28:** 31–40.

Pfannenstiel, H. D. 1984. Sex determination and intersexuality in polychaetes. *Fortschr. Zool.* **29:** 81–98.

Rolando, A. 1984. The sex induction hypothesis and reproductive behaviour in four gonochoristic species of the genus *Ophryotrocha* (Annelida, Polychaeta). *Monitore Zool. Ital. (N.S.)* **18:** 287–299.

Sella, G. 1985. Reciprocal egg trading and brood care in a hermaphroditic polychaete worm. *Anim. Behav.* **33:** 938–944.

Sella, G. and M. Marzona. 1983. Inheritance, maternal influence and biochemical analysis of an egg color polymorphism in *Ophryotrocha diadema. Experientia* **39:** 97–98.

Sokal, R. R. and F. J. Rholf. 1981. *Biometry*, second edition. W. H. Freeman and Co., San Francisco. 859 pp.

Svedmark, B. 1964. The interstitial fauna of marine sand. *Biol. Rev.* **39:** 1–42.

Westheide, W. 1984. The concept of reproduction in polychaetes with small body size: adaptation to interstitial environment. *Fortschr. Zool.* **29:** 265–287.

Reference: *Biol. Bull.* 175: 218–229. (October, 1988)

Geographically Widespread, Non-hybridizing, Sympatric Strains of the Hermaphroditic, Brooding Clam *Lasaea* in the Northeastern Pacific Ocean

DIARMAID Ó FOIGHIL* AND DOUGLAS J. EERNISSE**

Friday Harbor Laboratories, University of Washington, Friday Harbor, Washington 98250

Abstract. We have studied phenotypic variation in six enzymes of *Lasaea*, a taxonomically complex genus of small brooding clams, from nine northeastern Pacific sites. Each of the individuals examined produced one of five combinations of electromorph patterns. *Lasaea* phenotypes could be differentiated into two main types, one containing two and the other three phenotype combinations. Samples from each population contained from one to three phenotype combinations and there was no evidence for crossbreeding among phenotypes. These results are strongly at variance with random mating expectations and indicate that the phenotype combinations represent reproductively isolated strains. This is substantiated by a more detailed study of the McNeill Bay, British Columbia, population where both main strains coexist. Electrophoretic characterization of *Lasaea* from individual 100 cm^2 samples of barnacle cover revealed that strains are not spatially segregated. Progeny of (1) pair mating experiments, (2) brooding field individuals, and (3) specimens that reproduced in isolation, all perpetuated the maternal electromorphs. Data from previous studies of reproduction in northeastern Pacific *Lasaea* suggest that the formation of non-hybridizing strains has resulted either from the predominance of self-fertilization or as a result of pseudogamy combined with meiotic parthenogenesis. We currently favor the former hypothesis. The two main strains are largely conserved between geographically distant sites, despite the lack of a planktonic larval stage. Separation of the main strains in Victoria, British Columbia, populations on the basis of shell color phenotype is to some degree possible, but is often equivocal. Electrophoretic analysis (especially of reddish specimens) is necessary for their reliable identification.

Received 24 February 1988; accepted 29 July 1988.

* Present Address: Biology Department, University of Victoria, P. O. Box 1700, Victoria, British Columbia, Canada V8W 2Y2.

** Present Address: Museum of Zoology and Department of Biology, University of Michigan, Ann Arbor, Michigan 48109.

Introduction

Members of the taxonomically complex bivalve genus, *Lasaea*, are reproductively specialized, minute, intertidal, crevice dwellers (Keen, 1938; Oldfield, 1964; Glynn, 1965; Ponder, 1971) with a near-cosmopolitan distribution (Chavan, 1969). A prominent reproductive/developmental dichotomy exists within the genus. *Lasaea australis* (Lamarck, 1818) engages in random mating and broods its young to a straight-hinged, planktotrophic veliger stage of development (Ó Foighil, 1988). All congeners studied to date, release their young as crawl-away juveniles (Pelseneer, 1903; Oldfield, 1964; Glynn, 1965; Rosewater, 1975; Booth, 1979; Kay, 1979). There is as yet no evidence for cross-fertilization in *Lasaea* that have crawl-away juveniles (Crisp *et al.*, 1983; Ó Foighil, 1986a, Crisp and Standen, 1988), which together form a complex assembledge of nominal species and subspecies of unknown phylogenetic affinity.

Molluscan systematists have conventionally relied heavily on shell morphology to distinguish between species. There is great individual variation in *Lasaea* valves (Dall, 1899; Ponder, 1971; Roberts, 1984; Ó Foighil, 1986a), even among those collected from any particular site, and this poses a difficult taxonomic dilemma. Keen (1938) lists >40 species of *Lasaea*, distinguished from each other on the basis of slight differences in shell morphology and color. However, subsequent workers, have been unable to separate many of these nominal species

(Soot-Ryen, 1960; Barnard, 1964; Dell, 1964; Ponder, 1971; Haderlie and Abbott, 1980; Beauchamp, 1985). In the northeastern Pacific, Keen recognized two species, *L. subviridis* Dall, 1899 and *L. cistula* Keen, 1938. In a more recent worldwide review of *Lasaea*, Ponder (1971) concluded that most of the nominal species, including *L. subviridis* and *L. cistula*, are merely regional subspecies or ecotypes of the type species *L. rubra* (Montagu, 1803).

Population genetic studies of European *Lasaea* have revealed the existence of a variety of non-hybridizing, sympatric, genetic strains capable of reproducing in isolation (Crisp *et al.*, 1983, Crisp and Standen, 1988). These results have important implications for understanding morphological variation and systematic relationships within the genus. Crisp *et al.* (1983) concluded that the populations studied were composed of female, apomictic (*i.e.*, ameiotic) clones. However, Oldfield (1961) described European *Lasaea* as simultaneous hermaphrodites with minute sperm production, recently confirmed by McGrath and Ó Foighil (1986) and by D. J. Crisp and associates (pers. comm.). Crisp and Standen (1988) proposed that European *Lasaea* reproduce by a combination of pseudogamy and apomixis. As yet there is no available data on spawning and gamete interaction in European *Lasaea*. Thiriot-Quiévreux *et al.* (1988) found an unusually large chromosome complement ($100 \leq 2n \geq 120$) in Kerguelen *Lasaea* and proposed that this resulted from an apomictic mode of reproduction. However, re-examination of their histological material has revealed that Kerguelen *Lasaea* are simultaneous hermaphrodites with disproportionately tiny testicular *versus* ovarian tissue (Ó Foighil, unpub.). The presence of sperm in European and Kerguelen *Lasaea* leaves open the possibility of reproductive modes besides apomixis, including self-fertilization.

Considerable data are available on the reproduction of northeastern Pacific *Lasaea*. They brood their young to a crawl-away juvenile developmental stage (Keen, 1938; Glynn, 1965; Beauchamp, 1986; Ó Foighil, 1986b), are simultaneous hermaphrodites (Glynn, 1965; Ó Foighil, 1985a; Beauchamp, 1986), and can reproduce in isolation (Ó Foighil, 1986b, 1987). Isolated individuals simultaneously spawn sperm and eggs into the suprabranchial chamber, sperm attach to eggs by an acrosomal reaction, the male pronucleus is incorporated into the egg cytoplasm and the oocyte produces two polar bodies before first cleavage (Ó Foighil, 1987). A relatively tiny amount of testis is produced in the ovotestis, sperm occupy approximately 5% of gonadal volume, the rest being devoted to oogenesis (Ó Foighil, 1985a). This pattern of reduced sperm production is theoretically consistent with the hypothesis that self-fertilization is common (Heath, 1979; Fischer, 1981; Charlesworth and Charlesworth, 1981). Indeed, sperm production in the randomly mating *L. australis* is an order of magnitude greater (approximately 50% of gonadal volume) than in northeastern Pacific congeners (Ó Foighil, 1988). Several observations imply that cross-fertilization might be a relatively rare phenomenon in northeastern Pacific *Lasaea* populations. Sperm are present only in small numbers and have reduced motility (Ó Foighil, 1985a), and there is an apparent absence of specialized sperm transfer mechanisms typically found in cross-fertilizing brooding bivalves, such as spermatophores/spermatozeugmata (Coe, 1931; Ó Foighil, 1985b), dwarf/complemental males (Turner and Yakovlev, 1983; Ó Foighil, 1985c), and pseudocopulation (Townsley *et al.*, 1965).

In this study, we examined isozyme variation of four British Columbia (B. C.), Canada, and five California, U. S. A. populations of *Lasaea*. The F_1 progeny of adults from a B. C. site, either resulting from pairs or single individuals that reproduced when placed in isolation, or from broods collected from field individuals, were also characterized electrophoretically. We used isozyme data from adults and juveniles (1) to help identify the breeding system of *Lasaea* by comparing observed phenotype frequencies to random mating expectations and (2) to assess the systematic status of *Lasaea* populations using shell and protein phenotypes.

Materials and Methods

After collecting, adult nonbrooding animals were either analyzed electrophoretically within 2 days following storage in seawater tables or placed at −70°C until processed. Electrophoresis was performed at Friday Harbor Laboratories using 13% starch (Sigma hydrolyzed potato starch) gels, standard power supplies, and horizontal electrophoretic apparatus. Whole animals were individually homogenized with glass rods in an approximately equal volume of gel buffer and gels were run, not exceeding 200 volts, until the front had reached a preset "destiny" 80 mm from the origin. A single discontinuous Tris-citrate buffer system (electrode: 18.55 g boric acid/l and 2.4 g sodium hydroxide/l, pH 8.2; gel: 9.21 g tris/l and 1.05 g monohydrate citric acid/l, pH 8.7) was used for the following enzymes: esterase with α-naphtyl acetate substrate (EST; nonspecific), (leucine) aminopeptidase (LAP: E.C. 3.4.11.1), peptidase with glycyl-leucine substrate (PEP-GL), peptidase with leucyl-glycyl-glycine substrate (PEP-LGG), and peptidase with leucyl-valine and leucyl-tyrosine substrate (PEP-LVLT). In addition, phosphoglucomutase (PGM; E.C. 2.7.5.1) and glucose-phosphate isomerase (GPI; E.C. 5.3.1.9) were investigated using Crisp *et al.*'s (1983) discontinuous Tris-citrate buffer system. Most individuals showed no activity for PGM and the results for this enzyme are not presented. Enzyme staining assays for EST, LAP, and PGM

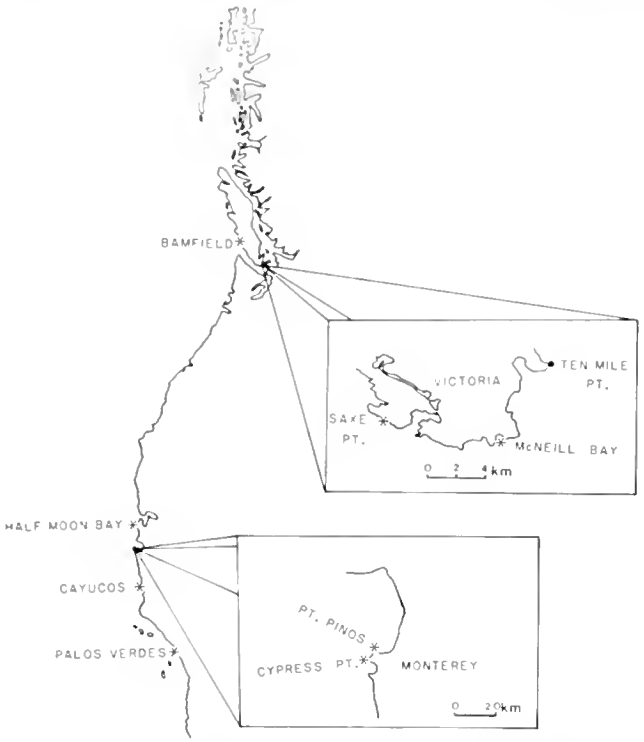

Figure 1. Sampling sites for northeastern Pacific *Lasaea* used in the electrophoretic study.

were as described by Ayala *et al.* (1972) and for GPI by Tracey *et al.* (1975). The PEP-GL, PEP-PP and PEP-LVLT staining assays consisted of 30 ml of a 2% agar solution (60°C) added to 20 mg of peptide substrate, 2000 units of peroxidase, 10 mg of O-Dianisidine, 5 mg of *Corotalus adamanteus* toxin, 0.5 ml of 0.1 *M* $MnCl_2$ and 20 ml of 0.1 *M* Na_2HPO_4 buffer.

At least one McNeill Bay individual of known protein phenotype was included per gel to provide a standard electromorph, and specimens from all nine populations were repeatedly run together on the same gels to verify electromorph scoring. The right valves of 73 McNeill Bay specimens were retained and analyzed for possible correlations of shell morphology and color to protein phenotype.

Subsequent to the initial electrophoretic survey of *Lasaea* from the nine study sites (Fig. 1), a more detailed investigation of the McNeill Bay population was performed. This involved electrophoretic characterization of the progeny of (1) pair mating experiments, (2) specimens that reproduced in isolation, (3) individuals that reproduced in the field. The degree of spatial overlap between strains in the McNeill Bay study site was also electrophoretically assessed.

In February 1987, non-brooding *Lasaea* adults were sampled from McNeill Bay and specimens were sorted according to shell color phenotype. Thirty pairs, each containing one white and one red shelled individual, were placed in separate culture vials containing 20 mls of 1 μm filtered seawater. *Lasaea* are positively thigmotactic (Morton, 1960) and each pair was positioned in close physical contact to ensure mutual attachment with byssal threads to facilitate potential cross-fertilization. The culture vials were maintained at 18°C and the clams were fed on cultured *Thalassiosira pseudonana* (strain 3H) and had salt water changes twice weekly. All individuals were checked weekly for brooding activity using a dissecting microscope (broods are visable through the translucent shells). Once a brooding individual was detected, the non-brooding partner was preserved at −70°C, as was the brooding parent when all the F_1 juveniles had been released from the brood chamber. The F_1 juveniles were cultured under the same conditions until September 1987, when parents, non-brooding partners, and the F_1 progenies of pairs containing adults of different enzyme phenotypes were electrophoretically analyzed. Originally, it was hoped to type the offspring (0.7–1.2 mm in valve lengths) using both LAP and PEP-GL enzyme assays, however, results were obtained only for the latter.

Ten red-shelled non-brooding adults collected from McNeill Bay in February 1987 were placed individually in culture vials and maintained in the laboratory, as previously described, until they released juveniles. In May 1987, 30 *Lasaea* adults brooding early embryos were selected from pooled McNeill Bay samples. They were also individually raised in laboratory conditions until juvenile release. Both sets of parents were then frozen at −70°C and electrophoretically characterized together with their offspring in September 1987 for the PEP-GL enzyme phenotypes.

Twenty five random 100 cm^2 samples of barnacle cover containing *Lasaea* were removed from the McNeill Bay site in October 1987 to investigate the degree of spatial overlap between strains. Samples were collected from the mid to high intertidal along an 80 m stretch of shore and were representative of the various crevice habitats available to *Lasaea* at the study site. All individuals in each sample were characterized for the PEP-GL phenotype after embryos had been dissected from brooding individuals.

Results

The electromorphs obtained from the survey of nine populations for EST, LAP, PEP-GL, and PEP-LGG are presented diagramatically in Figure 2. GPI was monomorphic in all individuals. PEP-LVLT phenotypes for each specimen were identical to the combined PEP-GL and PEP-LGG electromorphs for that individual and only one esterase presumed locus (EST) was consistently

Table I

Composite electromorph composition of the five Lasaea *strains observed in B.C. and California populations. Refer to Figure 2 for diagrammatic representation of electromorph patterns*

		Composite electromorph pattern			
	Strains	PEP-GL	PEP-LGG	LAP	EST
"A"	1	1	1	1	1
	2	2	1	2	1
	3	3	2	3	2
"B"	4	3	2	4	2
	5	3	3	4	2

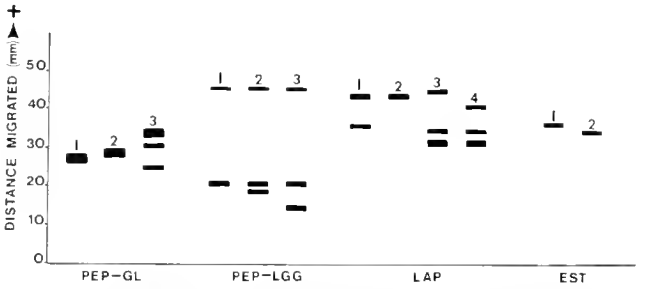

Figure 2. Diagrammatic representation of the total electromorph variation observed over four polymorphic gene-enzyme systems for northeastern Pacific *Lasaea*. Each electromorph pattern is individually numbered. For instance, the three PEP-GL protein phenotypes are labelled PEP-GL1, PEP-GL2, and PEP-GL3, respectively.

resolved in this study. Each *Lasaea* individual examined produced one of only five different composite electromorph patterns observed in this study (Table I). These patterns could be differentiated into two main sets ("A," "B") on the basis of similarity of the protein phenotypes. Patterns 1, 2 are of the "A" set and share identical PEP-LGG and EST phenotypes; "B" patterns 3, 4, 5 produce identical PEP-GL and EST phenotypes. Table II shows the distribution of the five composite electromorph patterns in the nine populations studied. The Bamfield, Pt. Pinos, and Palos Verdes samples were fixed for patterns 1, 4, and 2 respectively, while the remaining samples were polymorphic. The two main electromorph patterns ("A," "B") were respectively represented by patterns (1, 4) in both B. C. and California populations.

Genetic interpretation of these complex protein phenotypes is affected by the absence of expected heterozygous or homozygous phenotypes from polymorphic populations. For example, populations containing both "A" and "B" EST phenotypes (Table II) lacked obvious heterozygotes. Because all specimens had a single GPI band of identical mobility, we assume that all were homozygous at a single GPI coding locus. Genetic interpretation was more difficult for other, multiple-banded patterns and are thus provisional in nature. The three-banded PEP-GL 3 pattern (Fig. 2) probably does not represent a heterozygous phenotype for a dimer protein because the middle band is neither equidistant from, nor twice as prominent as, the two outlying bands (see Fig. 6). PEP-GL 1, 2 electromorphs share identical staining characteristics with the fastest of the three PEP-GL 3 bands and they may represent three alleles of a single locus (Fig. 2). The two slower PEP-GL 3 bands may represent a heterozygous monomer or two homozygous loci. PEP-LGG patterns 1, 2, and 3 all share an identical fast band which may represent a distinct locus (Fig. 2). It is unclear whether the slower PEP-LGG bands are products of one or more loci. Similarly, LAP 1 may represent a heterozygous monomer condition or else these individuals may be homozygous at two LAP loci (Fig. 2). The other LAP patterns 2, 3, and 4 do not appear to be consistent with a uniform heterozygous condition. Three potential loci may be represented by LAP 3 and 4; the three-banded patterns do not have the characteristics of a heterozygous dimer, the two slower bands are composed of a relatively weak faster band and a more pronounced slower one and probably do not represent a heterozygous monomer condition (Fig. 2).

None of the five composite electromorphs appeared to be the result of matings among electromorphs in any of the individuals characterized from the six populations that contained >1 strain. Assuming that these electromorph patterns have a similar genetic basis to that observed in other organisms, this is markedly at variance with random mating expectations. The observed and

Table II

Distribution of the five composite electromorph patterns (strains) in the nine Lasaea *populations studied. n = number of individuals analyzed per population*

		Frequency of *Lasaea* with each composite electromorph pattern per population				
		"A"		"B"		
Population	n	1	2	3	4	5
Bamfield	84	1.0	—	—	—	—
Saxe Point	78	0.15	—	0.71	0.14	—
McNeill Bay	140	0.29	—	0.63	0.08	—
Ten Mile Point	79	0.56	—	0.42	0.03	—
Half Moon Bay	19	—	—	—	0.63	0.37
Point Pinos	50	—	—	—	1.0	—
Cypress Point	25	—	—	—	0.64	0.36
Cayucos	54	0.04	—	—	0.72	0.24
Palos Verdes	14	—	1.0	—	—	—

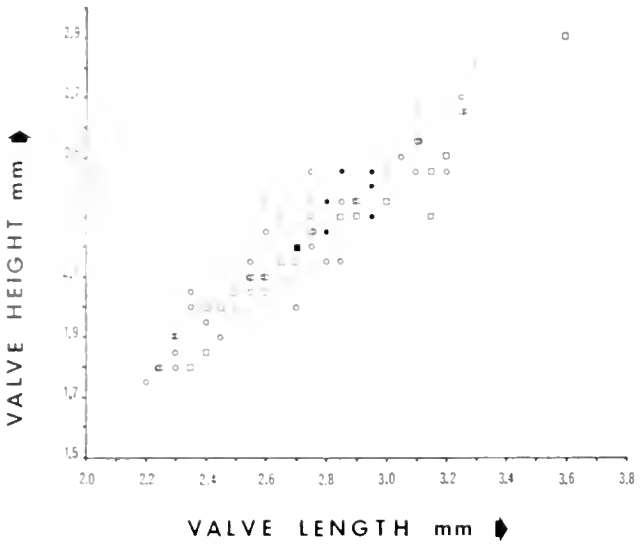

Figure 3. Plot of valve height against valve length for 73 McNeill Bay *Lasaea* characterized according to protein phenotype. Squares represent strain 1 animals (n = 27), solid squares are double scores, correlation coefficient (r) = 0.976. Circles represent strain 3 animals (n = 46), solid circles are double scores, r = 0.921 ($0.01 < P < 0.02$). When the large strain 1 individual (3.6 mm in length) is excluded, strain 1 r = 0.967 is not significantly different from 0.921 ($0.05 < P < 0.10$).

Hardy-Weinberg-Castle expected genotype frequencies for the EST locus of 140 McNeill Bay individuals characterized during the initial electrophoretic survey (Table II) are very different ($P < 0.001$). In addition, the apparent gametic disequilibrium between sympatric strains indicates that they are reproductively isolated.

The height and length of the right valves were positively correlated for 73 individuals from McNeill Bay, characterized according to protein phenotype and shell coloration. Although the height/length dimensions of strains 1, 3 overlap substantially (Fig. 3), their respective correlation coefficients (0.976 and 0.921) are significantly different ($0.01 < P < 0.02$) due to the presence of an unusually large (3.7 mm in length) strain 1 specimen. When this specimen is removed from the calculation, a correlation coefficient of 0.967 is obtained for strain 1, which is not significantly different from that of strain 3 ($0.05 < P < 0.10$). Individuals varied in shell coloration from totally white to totally red. Intermediate forms commonly occurred which were dorso-laterally red with white ventral patches. Some individuals appeared to have switched abruptly from forming a red shell to secreting a lighter zone of white growth. The height/length correlation coefficients do not differ significantly ($P > 0.50$) among white and predominantly red-shelled individuals (0.942 and 0.953 respectively) (Fig. 4). Anterio-dorsal shell margins varied considerably in shape within each strain and shell color group, *e.g.*, see specimens 2, 4, 5 and 31, 37, 38 (Fig. 5). There was no consistent difference in the maximum sizes attained by either protein phenotype or shell color groupings.

The relationship between shell color and protein phenotype was also investigated for *Lasaea* from Victoria's McNeill Bay population. Figures 5 and 6 show the right valves and the respective PEP-GL electromorphs for forty specimens (20 white; 20 predominantly red). The 20 white-shelled individuals, sorted before electrophoretic analysis, all exhibited the PEP-GL 3 electromorph. Four hundred and forty-one (441) adult specimens from McNeill Bay were typed for the PEP-GL 1 enzyme during the initial electrophoretic survey, and the subsequent investigation of spatial overlap between the two main strains. Of these, 272 and 169, respectively, expressed PEP-GL 3 and PEP-GL 1 phenotypes. If shell color is independent of PEP-GL protein phenotype, a ratio of 12.34 PEP-GL 3 to 7.66 PEP-GL 1 for the 20 white specimens in Figure 5 is expected (when analyzed by Chi square test: $P < 0.001$). The 19 predominantly red-shelled animals for whom electromorphs were obtained, contained both PEP-GL 1 (11 specimens) and PEP-GL 3 (8 specimens) patterns (expected ratios: 11.72 PEP-GL 3, 7.27 PEP-GL 1; Chi square test: $0.25 < P < 0.50$). Of these 19 predominently red animals, 11 were uniform in color and 8 had some white patches. Both of these two color subgroupings, however, were heterogenous in protein phenotype expression. Eight of the totally red specimens had the PEP-GL 1 pattern and four were type PEP-GL 3. Four of the eight mixed color individuals were PEP-GL 1 and the rest PEP-GL 3. Similar results were obtained when shell coloration and protein phenotypes of the Ten Mile Pt. population were investigated; white

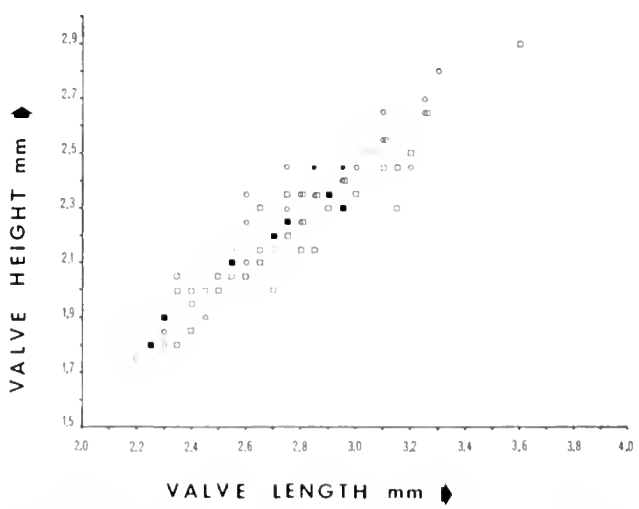

Figure 4. Plot of valve height against valve length for 73 McNeill Bay *Lasaea* characterized according to shell color. Squares represent predominently red individuals (n = 48), solid squares are double scores, correlation coefficient (r) = 0.953. Circles represent white shells (n = 25), solid circles are double scores, r = 0.942, ($P > 0.50$).

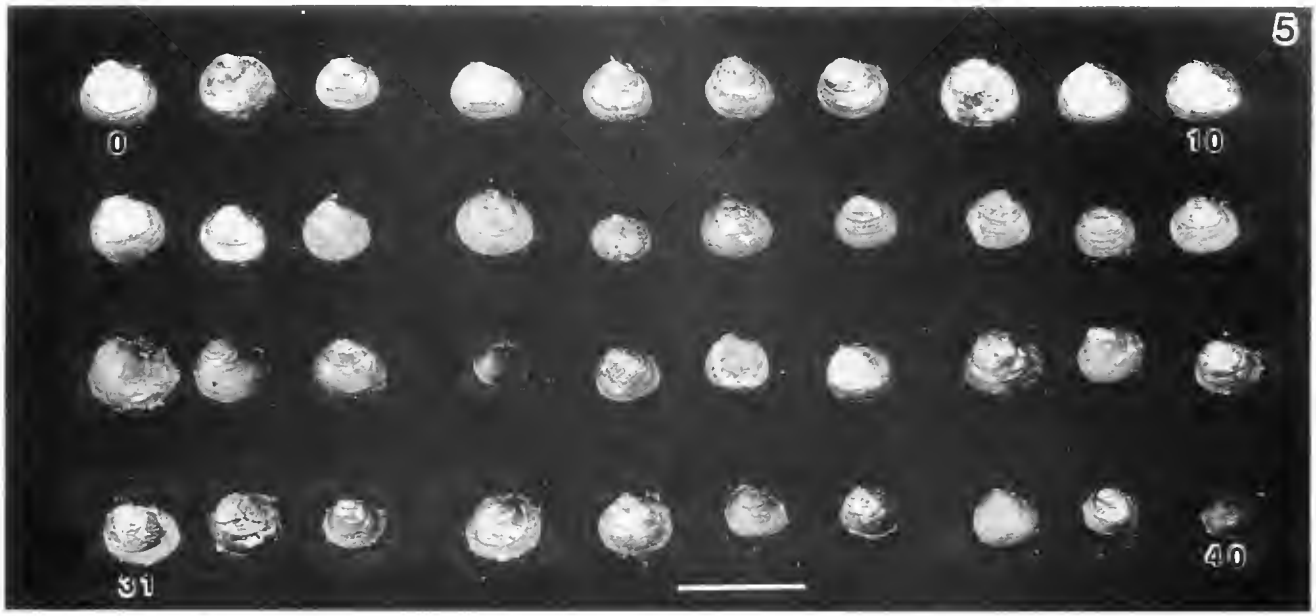

Figure 5. Right valves of 40 *Lasaea* individuals from McNeill Bay, Victoria. Specimens 1–20 (top two rows) have white shells and specimens 21–40 (bottom two rows) are predominantly or totally red. Scale = 5 mm.

individuals all expressed the PEP-GL 3 phenotype (15 specimens) and totally red or mixed color specimens produced either the PEP-GL 1 or PEP-GL 3 phenotypes (64 specimens).

No mortality of adult McNeill Bay *Lasaea* occurred during laboratory culture. Less than 5% of F_1 progeny died in culture, mainly as a result of premature release from the brood chamber before the development of valve opposition. Four of the 30 *Lasaea* pairs used in the pair mating experiments did not spawn while in the laboratory. One member of all remaining pairs released F_1 progeny, however, in eight of these pairs both adult specimens expressed the PEP-GL 3 electromorph. The remaining 18 pairs were composed of individuals exhibiting different PEP-GL phenotypes and in 17 of these cases the individual that initiated brooding expressed a PEP-GL 1 electromorph. When analyzed by Chi square test, this result is significantly different ($0.005 < P < 0.01$) from an expected ratio of 9 PEP-GL 1 to 9 PEP-GL 3, if precedence in the onset of brooding were independent of PEP-GL phenotype. Mean brood size was 17.8 ± 6.4 S.E. and a total of 330 F_1 progeny were typed for the PEP-GL enzyme. In all cases, the F_1 PEP-GL phenotypes were identical to those of the confirmed parents (brooding individuals) and did not reveal any evidence of cross-fertilization by the potential sperm donors (non-brooding partners) (see Fig. 7).

The 10 adult McNeill Bay *Lasaea* maintained in isolation during laboratory culture reproduced successfully. Eight and 2 individuals, respectively, expressed the PEP-GL 1 and PEP-GL 3 electromorphs. All 146 F_1 progeny (mean brood size of 14.6 ± 5.0 S.E.) perpetuated the parental PEP-GL phenotypes, including the 26 progeny of the 2 PEP-GL 3 parents. Assuming that the isolated PEP-GL 3 phenotype parents reproduced by self-fertilization, as previous cytological evidence would suggest (Ó Foighil, 1987), the result for the 26 F_1 progeny is significantly different from the 1:2:1 phenotype ratios expected if the PEP-GL 3 electromorph represented a heterozygous dimer protein, or if the 2 slow bands represented a heterozygous monomer protein (Chi square test, $P < 0.001$).

Eleven of the 30 brooding adults sampled in McNeill Bay in May 1987 expressed a PEP-GL 3 phenotype and the remainder exhibited the PEP-GL 1 electromorph. Altogether, 435 F_1 progeny (mean brood size = 14.5 ± 8.4 S.E.) were typed and all perpetuated the parental phenotypes, with a single exception. This exceptional individual occurred in a brood of 21 juveniles, 20 of which expressed the maternal PEP-GL 3 electromorph, the other produced the PEP-GL 1 phenotype. It is more likely that this individual resulted from inadvertent transfer between cultures, rather than from cross-fertilization between the strains, because it totally lacked the maternal phenotype for this brood.

Three hundred and one (301) individuals were characterized for the PEP-GL enzyme from the 25 samples of barnacle cover (100^2 cm^2) taken from McNeill Bay in October 1987. Both main *Lasaea* strains co-occurred in 18 of these samples (Figs. 8, 9) and there was no signifi-

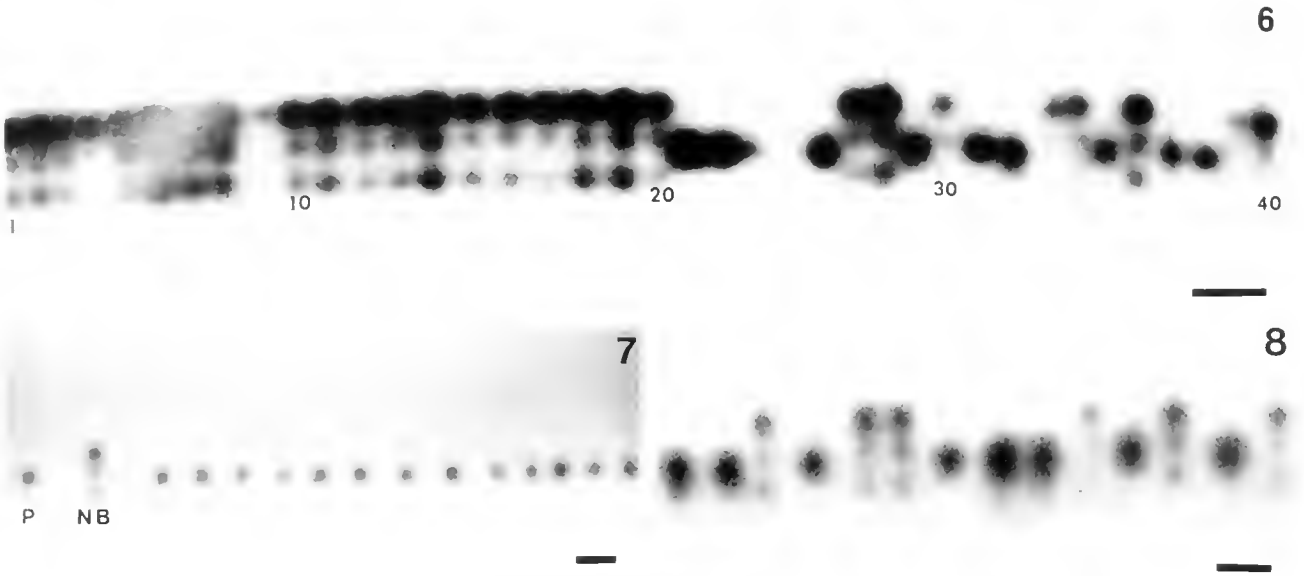

Figure 6. PEP-GI electromorphs of the same 40 *Lasaea* individuals in Figure 5. Specimens 1–20, 27, 28, 30, 33, 34, 36, 39, and 40 produced a PEP-GI 3 electromorph pattern. Individuals 21–23, 25, 26, 29, 31, 32, 35, 37, and 38 gave a PEP-GI 1 electromorph pattern. Specimen 24 gave no detectable result and specimen 25 was too faint to photograph well.

Figure 7. PEP-GI phenotypes of McNeill Bay *Lasaea* pair mating experiment showing parent (P), non-brooding partner (NB) and the 13 F1 progeny. Note that all offspring perpetuate the electromorph of the confirmed parent.

Figure 8. PEP-GI phenotypes of 14 McNeill Bay *Lasaea* recovered in a 100 cm^2 sample of barnacle cover. Both PEP-GI 1 (8) and PEP-GI 3 (6) phenotypes are expressed.

cant correlation between the distributions of the main strains ($r = 0.0399$, $P > 0.5$). It appears that the 2 main *Lasaea* strains are not segregated in McNeill Bay on this spatial scale and show a high degree of overlap.

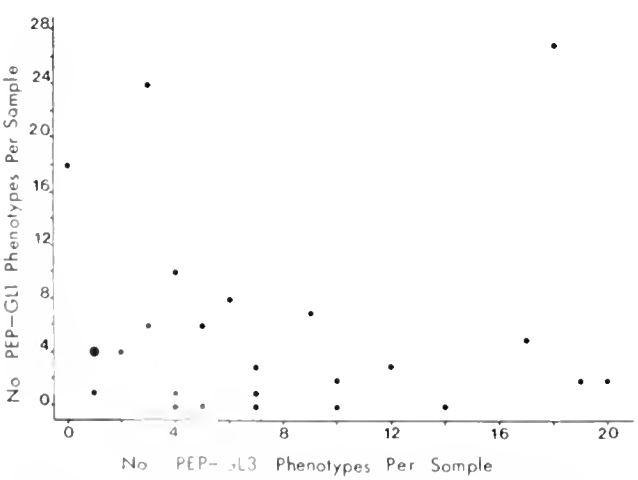

Figure 9. Relative numbers of PEP-GI 1 and PEP-GI 3 phenotypes in 25 100 cm^2 samples of barnacle cover from McNeill Bay, Victoria, B. C. Large circle = double score. Correlation coefficient (r) = 0.0399, $P > 0.5$.

Discussion

The absence of putative intermediate protein phenotypes and the consequent deviations from random mating expectations in spatially overlapping, sympatric field populations and in the progeny of pair mating experiments suggest that (1) several to many strains of *Lasaea* coexist and are widespread along the west coast of North America, and (2) if mating occurs between the various strains, it must be very rare. Population genetic structure of our study populations resemble those described by Crisp *et al.* (1983) and Crisp and Standen (1988) for European *Lasaea* but are markedly different from the randomly mating *L. australis* which has a planktotrophic larval development (Ó Foighil, 1988).

Formation of non-hybridizing, genetic strains can result from a number of reproductive modes, including apomixis, autosegregation, pseudogamy, and self-fertilization (Bell, 1982). Identifying the reproductive mode employed by *Lasaea* that lack dispersive larvae is proving to be problematical, due in part to the difficulty of identifying sperm in the ovotestis. In populations examined, a minute quantity of testis (averaging approximately 5% of gonadal volume) is produced in the posterio-ventral lobe of the ovotestis; the sperm heads vary

in shape and exhibit incomplete nuclear condensation (Pelseneer, 1903; Oldfield, 1961; Ó Foighil, 1985a, 1987; McGrath and Ó Foighil, 1986; Beauchamp, 1986). It is now apparent that both British and Kerguelen *Lasaea*, respectively, described by Crisp *et al.* (1983) and Thiriot-Quiévreux *et al.* (1988) as female, apomictic clones, are actually simultaneous hermaphrodites which appear identical to northeastern Pacific *Lasaea* in their gonadal and sperm morphologies (Oldfield, 1961; Ó Foighil, 1985a; McGrath and Ó Foighil, 1986; Ó Foighil, unpub.). Despite their unusual morphology, these sperm appear to be functionally mature and each is capable of swimming and undergoing an acrosomal reaction, binding to, and penetrating an egg (Ó Foighil, 1987).

Important data on post-spawning cytological events in isolated northeastern Pacific individuals are available (Ó Foighil, 1987), as reviewed in the introduction. These data, especially the evidence for production of two polar bodies before first cleavage, indicate that individuals from populations we studied reproduce not by apomixis but by automixis. Extrapolation to all northeastern Pacific strains assumes that results from these isolated individuals of unknown electrophoretic phenotype represent the norm. Additionally, since sperm were seen to penetrate eggs (Ó Foighil, 1987), these data suggest that the particular automitic mode must be either self-fertilization or meiotic parthenogenesis with some form of pseudogamy. In practice, self-fertilizing organisms and meiotic parthenogens are distinguished because the former produce both sperm and eggs, giving differentiation of gender at the gametic level (Bell, 1982).

Ideally, electrophoretic examination of the progeny of isolated heterozygous (Aa) adults could provide strong evidence for self-fertilization, or for some types of automictic parthenogenesis that have similar consequences to selfing (White, 1973; Suomalainen *et al.*, 1987), if the progeny do not deviate significantly from an expected 1AA:2Aa:1aa ratio. However, lack of segregation of the protein phenotypes in sampled populations makes positive identification of heterozygous loci difficult, because multiple bands on a gel that resemble typical heterozygous monomers or dimers could also be explained as the results of multiple loci. Similarly, if all progeny resemble their parent at a particular locus, as they did in our study and as reported by Crisp *et al.* (1983), this is not conclusive evidence for apomixis. Only a detailed study of male and female pronuclear interaction is likely to resolve the reproductive mode in these cases.

Crisp and Standen (1988) used a different buffer system from the one used by Crisp *et al.* (1983) and found non-segregating protein phenotypes they interpreted as suggestive evidence for fixed-heterozygosity at PGM and GPI loci of European *Lasaea* (*L. rubra*). They then concluded that *L. rubra* reproduces by a combination of pseudogamy and apomixis, citing Ó Foighil's (1987) description for sperm penetration in *L. subviridis* in support of this view. Although this remains a possibility, a number of important points need to be clarified before Crisp and Standen's (1988) interpretation can be accepted. Ó Foighil (1987) rejected apomixis in *L. subviridis*, not because of sperm penetration, but because the egg apparently undergoes a meiotic division before first cleavage, producing two polar bodies. It is quite possible that European *L. rubra* eggs are likewise meiotic. However, this remains to be established by observation of cytological events that occur before first cleavage. An alternate interpretation of the protein phenotype patterns observed by Crisp and Standen (1988) is that they represent multiple homozygous loci. C. Thiriot-Quiévreux (pers. comm.) found very high chromosome numbers in *L. rubra*, and these represent potential sources of such loci. Finally, pseudogamy is employed by all-female clones (Moore *et al.*, 1956; Kallman, 1962; Uzzell, 1964; Schultz, 1971, 1977; Kiester *et al.*, 1981; Stenseth *et al.*, 1985) or hermaphrodites (*e.g.*, the enchytraeid oligochaete *Lumricillus*, see Christensen and O'Connor, 1958; Christensen, 1980) that are sexual parasites of closely related cross-fertilizing species and are incapable of reproducing in isolation. *L. rubra* can reproduce in isolation to at least an F2 generation (Crisp *et al.*, 1983). The combination of pseudogamy with apomixis proposed by Crisp and Standen (1988) would indeed be noteworthy, if further substantiated, because we are presently unaware of any species where individuals are known to use their *own* sperm to initiate parthenogenic development.

Thiriot-Quiévreux *et al.* (1988) concluded that Kerguelen *Lasaea* were apomictic based on the absence of sperm and meiotic stages. It is now known that Kerguelen *Lasaea* are simultaneous hermaphrodites with greatly reduced sperm production (Ó Foighil, unpub.). Because of the relatively tiny testis, it is possible that sperm were overlooked by Thiriot-Quiévreux *et al.* (1988) in their chromosome preparations. We consider that a self-fertilizing mode of reproduction has yet to be ruled out for European and Kerguelen *Lasaea* populations. As is the case for northeastern Pacific congeners, a detailed cytological study is needed to firmly establish the reproductive mode of these populations.

Our present working hypothesis is that northeastern Pacific *Lasaea* reproduce by automixis, probably by self-fertilization. This interpretation is more parsimonious than that of pseudogamy combined with automictic parthenogenesis and, as discussed above, pseudogamy is only known to be employed by sexual parasites incapable of reproducing in isolation. If self-fertilization is in-

deed the predominate norm in northeastern Pacific *Lasaea* populations, heterozygous loci should be extremely rare within each strain, and each band in the complex multi-banded PEP-GL, PEP-LGG and LAP electromorph patterns recorded in this study should represent a separate homozygous locus. Each "B" strain typically yielded a greater number of protein phenotypes (*i.e.*, bands) than did each "A" strain in our study. One interesting possibility is that the strains differ in ploidy and perhaps one or more ploidy duplication events has been responsible, in part, for the reproductive isolation(s) of *Lasaea* strains (C. Moritz, pers. comm.). The only published work to date on *Lasaea* karyology is that of Thiriot-Quiévreux *et al.* (1988) who found a record (though variable) number of chromosomes for the class Bivalvia in Kerguelen *Lasaea* ($100 \leq 2n \leq 120$). A similarly high chromosome complement may be present in northeastern Pacific *Lasaea* (especially the "B" strains) and may represent a source of multiple homozygous loci.

Species that reproduce by self-fertilization still, in theory, retain the potential for cross-fertilization, and exclusively self-fertilizing populations [*e.g., Rivulus marmoratus* (Kallman and Harrington 1964; Vrijenhoek, 1985)] are thought to be extremely rare in nature (Bell, 1982). A mixed self- and cross-fertilizing mating pattern has the potential of creating a wide variety of new genotypes, as occasional outcrossing between inbred lineages will result in highly heterozygous progeny (Antonovics, 1968; Bucklin *et al.*, 1984). Cross-fertilizations in northeastern Pacific *Lasaea* populations might be exceptionally rare or absent, judging from the lack of intermediate protein phenotypes encountered in this study and the apparent absence of sperm transfer and sperm storage mechanisms that enable other suprabranchial brooding bivalves to cross-fertilize (Coe, 1931; Townsley *et al.*, 1965; Turner and Yakovlev, 1983; Ó Foighil, 1985b, c). Still, even rare cross-fertilization could provide an alternative mechanism, besides ploidy duplication, for the creation of new strains.

The majority of marine invertebrates including bivalves cross-fertilize, so it is interesting to consider how predominate self-fertilization might arise. Various genetic models of the evolution of self-fertilization predict that a history of inbreeding predisposes originally cross-fertilizing populations to the development of automixis (self-fertilization) by removing recessive deleterious alleles (Charlesworth and Charlesworth, 1981; Lande and Schemske, 1985; Uyenoyama, 1986). This forms the premise for Strathmann *et al.*'s (1984) hypothesis to account for the association of simultaneous hermaphroditism and brooding of young to a crawl-away juvenile stage in many marine invertebrate taxa. Strathmann *et al.* suggest that reduced dispersal promotes inbreeding which lowers heterozygosity, exposing deleterious homozygous combinations to selection and eventual elimination. Thus prolonged inbreeding dilutes the genetic penalty of inbreeding depression caused by self-fertilization. If a self-fertile individual happens to arise in an already inbred population, and it additionally produces relatively few sperm, it would then be at a reproductive advantage, because of the lowered cost of spermatogenesis and at a genetic advantage due to the reduced "cost of meiosis" (Williams, 1975; Maynard Smith, 1978; Bell, 1982). Indeed, the genetic advantage of a reduced "cost of meiosis" implies that once developed, the evolution of completely self-fertilizing lineages may be an irreversible step (Bull and Charnov, 1985). Strathmann *et al.* (1984) were concerned primarily with explaining hermaphroditism in groups that are normally gonochoric (*e.g.*, echinoderms, anemones, chitons, sipunculans, etc.), but they also point out that the basic model should apply to explaining exceptional self-fertilizers in hermaphroditic taxa that normally have effective blocks to self-fertilization (*e.g.*, tunicates, nudibranchs, certain bivalve taxa including *Lasaea*). The lack of a planktonic dispersive stage, simultaneous hermaphroditism, and apparent high level of self-fertilization of northeastern Pacific *Lasaea* are consistent with the proposal (Strathmann *et al.*, 1984; Eernisse, 1988) that having crawl-away offspring can lead to departure from cross-fertilization.

Cross-fertilizing marine invertebrate species that are typically sedentary as adults and lack a planktonic larval stage show significant interpopulational genetic divergence on a relatively small geographic scale (Berger, 1973, 1977; Snyder and Gooch, 1973; Campbell, 1978; Ward and Warwick, 1980; Bulnheim and Scholl, 1981; Burton, 1983; Janson and Ward, 1984; Palmer, 1984; Grant and Utter, 1988). Interpopulational genetic drift in these cases may originate from a founder effect (Holgate, 1966; Nei *et al.*, 1975) during an initial colonization, or a later genetic bottleneck event, that may be maintained and enhanced by infrequent genetic exchange with other populations over time. In contrast, our results for northeastern Pacific *Lasaea* show that some strains (1, 4) are present in geographically distant sites. A number of potential factors may have contributed to this, including alternative dispersal techniques such as byssus drifting (Lane *et al.*, 1985) and rafting (Highsmith, 1985) (short and long distances respectively), low rates of mutation, and a predominantly self-compatible reproductive mode. Self-fertilization is genetically conservative because new alleles formed by mutation are rapidly expressed in homozygous combinations and are thus directly exposed to selection (Bell, 1982). Newly formed populations will not experience a founder effect if the initial colonizers previously existed as reproductively isolated strains at the source site.

Taxonomic interpretations based on a small number

of loci can lead to a potentially serious bias (Nei, 1972). Even though we examined relatively few loci, it is clear that northeastern Pacific *Lasaea* populations are composed of a variety of reproductively isolated strains as Crisp *et al.* (1983) found for British populations. These strains are readily distinguishable by electrophoretic analysis.

Diagnostic separation of strains from Victoria, B. C. populations on the basis of shell phenotype appears unreliable, except for some apparent color differences between the strains. We can predict with a high degree of confidence that white-shelled *Lasaea* from Victoria will express particular protein electromorphs. However, specimens with the same protein phenotypes may also have mixed shell coloration (red/white) or totally red shells. Shell pigmentation is known to be light-induced in juvenile mussels (Trevelyan and Chang, 1987), and, in *Lasaea rubra hinemoa,* the extent of red coloration in the valves is thought to be related to the degree of exposure to sunlight (Ponder, 1971). This may also be the case for at least strain 3 of northeastern Pacific *Lasaea* because specimens recovered from deep crevices had the whitest shells. There may be a partial habitat difference between the two main strains in Victoria, with strain 3 occurring in both deep and shallow crevices and strain 1 found only in shallow crevices. Data from the laboratory pair mating experiments hint at physiological or spawning differences between the two main strains: 17 of the first individuals to spawn from the 18 heterogeneous pairs expressed a PEP-GL 1 phenotype.

Criteria used by Keen (1938) to separate two nominal *Lasaea* species in Californian populations are inadequate when applied to Victoria *Lasaea* of known protein phenotype. Keen (1938) distinguished *L. cistula* from *L. subviridis* by its smaller size, less oblique outline, darker color, higher umbones and by its more abrupt slope from the umbone to the anterior margin. However, Ponder (1971) and Beauchamp (1985) could not distinguish on morphological grounds two different forms of *Lasaea* in Californian populations. As in this present study, Ponder (1971) found Keen's (1938) distinguishing morphological characteristics to be highly variable among individual shells. For the present, it would appear that electrophoretic analysis is necessary for the reliable identification of northeastern Pacific *Lasaea* strains. Whether the two main strains detected in this study correspond to *L. subviridis* and/or *L. cistula* will require careful comparisons of any diagnostic morphological distinctions, should they be found, with existing type material for northeastern Pacific *Lasaea.*

There is as yet no evidence for cross-fertilization between the strains found in British (Crisp *et al.,* 1983) and northeastern Pacific *Lasaea* populations. Therefore the biological species concept (Mayr, 1957, 1963), which applies best to randomly mating organisms, would seem inappropriate for these populations. Ponder (1971) concluded that most nominal species of *Lasaea* are merely regional subspecies, or ecotypes of the type species *L. rubra.* Alternatively, one could conclude that every distinct electrophoretic strain is a distinct historical entity or, perhaps, species. Efforts to determine the level at which the category "species" best applies would best wait for reproductive investigations of other *Lasaea* populations and a better understanding of *Lasaea* historical relationships, which are undoubtedly complex among *Lasaea* that lack a dispersive larval stage (Ponder, 1971; Crisp *et al.,* 1983; Ó Foighil, 1986a; Thiriot-Quiévreux *et al.,* 1988). Resolution of these relationships will require a multidisciplinary approach applied to a variety of populations of this near-cosmopolitan genus.

Acknowledgments

Funding was provided by a University of Victoria graduate student fellowship and a Friday Harbor Laboratories post-doctorate fellowship to D. Ó Foighil; and NSF grant OCE-8415258 to R. R. Strathmann and D. J. Eernisse. We are indebted to D. J. Crisp for sending us an unpublished manuscript and to C. Thiriot-Quiévreux for letting us examine her histological material. A. R. Palmer, R. Grosberg, C. Moritz, F. Sly, R. R. Strathmann, and anonymous reviewers gave valuable comments on earlier drafts. We thank A. O. D. Willows, director of FHL, for the use of facilities.

Literature Cited

Antonovics, J. 1968. Evolution in closely adjacent plant populations. V. Evolution of self-fertility. *Heredity* **23:** 219–238.

Ayala, F. J., J. R. Powell, M. L. Tracey, C. A. Murao, and S. Perez-Salas. 1972. Enzyme variability in the *Drosophila willistoni* group. IV. Genic variation in natural populations of *Drosophila willistoni. Genetics* **70:** 113–139.

Barnard, K. H. 1964. Contributions to the knowledge of South African marine Mollusca. Pt. 5. Lamellibranchiata. *Ann. S. Afr. Mus.* **47:** 361–593.

Beauchamp, K. A. 1985. The reproductive ecology of a brooding, hermaphroditic clam, *Lasaea subviridis.* M. Sc. Thesis, University of California, Santa Cruz. 56 pp.

Beauchamp, K. A. 1986. Reproductive ecology of the brooding, hermaphroditic clam, *Lasaea subviridis. Mar. Biol.* **93:** 225–235.

Bell, G. 1982. *The Masterpiece of Nature.* Croom Helm, London. 635 pp.

Berger, E. M. 1973. Gene-enzyme variation in three sympatric species of *Littorina. Biol. Bull.* **145:** 83–90.

Berger, E. M. 1977. Gene-enzyme variation in three sympatric species of *Littorina.* II. The Roscoff population with a note on the origin of North American *L. littorea. Biol. Bull.* **153:** 255–264.

Booth, J. D. 1979. Common bivalve larvae from New Zealand: Leptonacea. *N. Z. J. Mar. Freshwater Res.* **13:** 241–254.

Bucklin, A., D. Hedgecock, and C. Hand. 1984. Genetic evidence of self-fertilization in the sea anemone *Epiactis prolifera. Mar. Biol.* **84:** 175–182.

Bull, J. J., and E. L. Charnov. 1985. On irreversible evolution. *Evolution* **39:** 1149–1155.

Bulnheim, H. P., and A. Scholl. 1981. Genetic variation between geographic populations of amphipods *Gammarus zaddachi* and *G. salinus*. *Mar. Biol.* **64:** 105–115.

Burton, R. S. 1983. Protein polymorphisms and genetic differentiation of marine invertebrate populations. *Mar. Biol. Lett.* **4:** 193–206.

Campbell, C. A. 1978. Genetic divergence between populations of *Ina [illegible]* (Gmelin). Pp. 157–170 in *Marine Organisms: Genetics, Ecology and Evolution*, B. Battagha and J. A. Beardmore, eds. Plenum Press, New York.

Charlesworth, D., and B. Charlesworth. 1981. Allocation of resources to male and female functions in hermaphrodites. *Biol. J. Linn. Soc.* **15:** 57–74.

Chavan, A. 1969. Leptonacea Gray 1847. Pp. 518–537 in *Treatise On Invertebrate Paleontology. Pt. N. Mollusca (2)*, R. C. Moore, ed. Geological Society of America and University of Kansas Press, Lawrence.

Christensen, B., and F. B. O'Connor. 1958. Pseudofertilization in the genus *Lumbricillus* (Enchytraeidae). *Nature* **181:** 1085–1086.

Christensen, B. 1980. Constant differential distribution of genetic variants in polyploid parthenogenetic forms of *Lumbricillus lineatus* (Enchytraeidae, Oligochaeta). *Hereditas* **92:** 193–198.

Coe, W. R. 1931. Spermatogenesis in the California oyster, *Ostrea lurida*. *Biol. Bull.* **61:** 309–315.

Crisp, D. J., A. Burlitt, K. Rodrigues, and M. D. Budd. 1983. *Lasaea rubra*: an apomictic bivalve. *Mar. Biol. Lett.* **4:** 127–136.

Crisp, D. J., and A. Standen. 1988. *Lasaea rubra* (Montagu) (Bivalvia: Erycinacea), an apomictic crevice-living bivalve with clones separated by tidal level preference. *J. Exp. Mar. Biol. Ecol.* **117:** 27–45.

Dall, W. H. 1899. Synopsis of the recent and tertiary Leptonacea of North America and the West Indies. *U. S. Natl. Mus. Proc.* **23:** 18–32.

Dell, R. K. 1964. Antartic and subantartic Mollusca: Amphineura, Scaphopoda and Bivalvia. *Discovery Rep.* **33:** 93–250.

Eernisse, D. J. 1988. Reproductive patterns in six species of *Lepidochitona* (Mollusca: Polyplacophora) from the Pacific coast of North America. *Biol. Bull.* **174:** 287–302.

Fischer, E. A. 1981. Sexual allocation in a simultaneously hermaphroditic coral reef fish. *Am. Nat.* **117:** 64–82.

Glynn, P. W. 1965. Community composition, structure, and interrelationships in the marine intertidal *Endocladia muricata–Balanus glandula* association in Monterey Bay, California. *Beaufortia* **148:** 1–198.

Grant, W. S., and F. M. Utter. 1988. Genetic heterogeneity on different geographic scales in *Nucella lamellosa* (Prosobranchia: Thaididae). *Malacologia* **28:** 275–287.

Haderlie, E. C., and D. P. Abbott. 1980. Bivalvia: the clams and their allies. Pp. 355–411 in *Intertidal Invertebrates of California*, R. H. Morris, D. P. Abbott and E. C. Haderlie, eds. Stanford University Press.

Heath, D. J. 1979. Brooding and the evolution of hermaphroditism. *J. Theor. Biol.* **81:** 151–155.

Highsmith, R. C. 1985. Floating and algal rafting as potential dispersal mechanisms in brooding invertebrates. *Mar. Ecol. Prog. Ser.* **25:** 169–179.

Holgate, P. 1966. A mathematical study of the founder principle of evolutionary genetics. *J. Appl. Probab.* **3:** 115–128.

Janson, K., and R. D. Ward. 1984. Microgeographic variation in allozyme and shell characters in *Littorina saxatilis* Olivi (Prosobranchia: Littorinidae). *Biol. J. Linn. Soc.* **22:** 289–307.

Kallman, K. D. 1962. Population genetics of the gynogenetic teleost *Mollienesia formosa* (Girard). *Evolution* **16:** 497–504.

Kallman, K. D., and R. W. Harrington. 1964. Evidence for the existence of homozygous clones in the self-fertilizing hermaphrodite teleost *Rivulus marmoratus* (Poey). *Biol. Bull.* **126:** 101–114.

Kay, E. A. 1979. *Hawaiian Marine Shells*. Bernice P. Bishop Museum Press, Honolulu. 620 pp.

Keen, A. M. 1938. New pelecypod species of the genera *Lasaea* and *Crassinella*. *Proc. Malacol. Soc. Lond.* **23:** 18–32.

Kiester, A. R., T. Nagylaki, and B. Shaffer. 1981. Population dynamics of species with gynogenetic sibling species. *Theor. Pop. Biol.* **19:** 358–369.

Lande, R., and D. W. Schemske. 1985. The evolution of self-fertilization and inbreeding depression in plants. I. Genetic models. *Evolution* **39:** 24–40.

Lane, D. J. W., A. R. Beaumont, and J. R. Hunter. 1985. Byssus drifting and the drifting threads of the young post-larval mussel *Mytilus edulis*. *Mar. Biol.* **84:** 301–308.

Maynard Smith, J. 1978. *The Evolution of Sex*. Cambridge University Press, Cambridge, U. K. 222 pp.

Mayr, E. 1957. Species concepts and definitions. Pp. 1–22 in *The Species Problem*, J. Huxley, A. C. Hardy and E. B. Ford, eds. Allen and Unwin Press, London.

Mayr, E. 1963. *Animal Species and Evolution*. Harvard University Press, Cambridge, Massachusetts.

McGrath, D., and D. Ó Foighil. 1986. Population dynamics and reproduction of hermaphroditic *Lasaea rubra* (Bivalvia: Galeommatacea). *Ophelia* **25:** 209–219.

Moore, B. P., G. E. Woodroffe, and A. R. Sanderson. 1956. Polymorphism and parthenogenesis in a ptinid beetle. *Nature* **177:** 847–848.

Morton, J. E. 1960. The responses and orientation of the bivalve *Lasaea rubra* (Montagu). *J. Mar. Biol. Assoc. U. K.* **39:** 5–26.

Nei, M. 1972. Genetic distance between populations. *Am. Nat.* **106:** 283–292.

Nei, M., T. Maruyama and R. Chakkaborty. 1975. The bottleneck effect and genetic variability in populations. *Evolution* **29:** 1–10.

Ó Foighil, D. 1985a. Fine structure of *Lasaea subviridis* and *Mysella tumida* sperm (Bivalvia: Galeommatacea). *Zoomorphology* **105:** 125–135.

Ó Foighil, D. 1985b. Sperm transfer and storage in the brooding bivalve *Mysella tumida*. *Biol. Bull.* **169:** 602–614.

Ó Foighil, D. 1985c. Form, function and origin of temporary dwarf males in *Pseudopythina rugifera* (Bivalvia: Galeommatacea). *Veliger* **27:** 72–80.

Ó Foighil, D. 1986a. Reproductive modes and their consequences in three galeommatacean clams: *Mysella tumida*, *Pseudopythina rugifera* and *Lasaea subviridis* (Mollusca: Bivalvia). Ph.D. Thesis, University of Victoria, 251 pp.

Ó Foighil, D. 1986b. Prodissoconch morphology is environmentally modified in the brooding bivalve *Lasaea subviridis*. *Mar. Biol.* **92:** 517–524.

Ó Foighil, D. 1987. Cytological evidence for self-fertilization in the brooding bivalve *Lasaea subviridis*. *Int. J. Invertebr. Reprod. Dev.* **12:** 83–90.

Ó Foighil, D. 1988. Random mating and planktotrophic larval development in the brooding hermaphroditic clam *Lasaea australis* (Lamarck, 1818). *Veliger* **31:** (in press).

Oldfield, E. 1961. The functional morphology of *Kellia suborbicularis* (Montagu), *Montacuta ferruginosa* (Montagu) and *M. substriata* (Montagu), (Mollusca, Lamellibranchiata). *Proc. Malacol. Soc. Lond.* **32:** 255–295.

Oldfield, E. 1964. The reproduction and development of some members of the Erycinidae and Montacutidae (Mollusca, Eulamellibranchiata). *Proc. Malac. Soc. Lond.* **36:** 79–120.

Palmer, A. R. 1984. Species cohesiveness and genetic control of shell color and form in *Thais emarginata* (Prosobranchia, Muricacea): preliminary results. *Malacologia* **25:** 477–491.

Pelseneer, P. 1903. Mollusques (amphineures, gastropodes et lamellibranches). in *Résultats du voyage du S. Y. Belgica.* Buschmann, Anvers.

Ponder, W. F. 1971. Some New Zealand and Subantartic bivalves of the Cyamiacea and Leptonacea with descriptions of new taxa. *Rec. Dom. Mus. Wellington* **7:** 119–141.

Roberts, D. 1984. A comparative study of *Lasaea australis, Vulsella spongarium, Pinna bicolor* and *Donacilla cuneata* (Mollusca: Bivalvia) from Princess Royal Harbor, Western Australia. *J. Moll. Stud.* **50:** 129–136.

Rosewater, J. 1975. An annotated list of the marine mollusks of Ascension Island, South Atlantic Ocean. *Smithson. Contrib. Zool.* **189:** 41 pp.

Schultz, R. J. 1971. Special adaptive problems associated with unisexual fishes. *Am. Zool.* **11:** 351–360.

Schultz, R. J. 1977. Evolution and ecology of unisexual fishes. Pp. 277–331 in M. K. Hecht, W. C. Steere and B. Wallace (eds.), *Evolutionary Biology.* Plenum Press, New York.

Snyder, T. P., and J. L. Gooch. 1973. Genetic differentiation in *Littorina saxatilis* (Gastropoda). *Mar. Biol.* **22:** 177–182.

Soot-Ryen, T. 1960. Pelecypods from Tristan da Cunha. *Res. Nor. Sci. Exped. Tristan da Cunha* **49:** 1–47.

Stenseth, N. C., L. R. Kirkendall, and N. Morgan. 1985. On the evolution of pseudogamy. *Evolution* **39:** 294–307.

Strathmann, R. R., M. F. Strathmann, and R. H. Empson. 1984. Does limited brood capacity link adult size, brooding and simultaneous hermaphroditism? A test with *Asterina phylactica*. *Am. Nat.* **123:** 796–818.

Suomalainen, E., A. Saura, and J. Lokki. 1987. *Cytology and Evolution of Parthenogenesis.* CRC Press, Boca Raton, Florida. 216 pp.

Townsley, P. M., R. A. Rickey, and P. C. Trussel. 1965. The laboratory rearing of the shipworm *Bankia setacea* (Tyron). *Proc. Natl. Shellfish. Assoc.* **56:** 49–52.

Thiriot-Quiévreux, C., J. Soyer, F. de Bovée and P. Albert. 1988. Unusual chromosome complement in the brooding bivalve *Lasaea*. *Lasaea consanguinea*. *Genetica* **76:** 143–151.

Tracey, M. L., K. Nelson, D. Hedgecock, R. A. Schleser and M. L. Pressick. 1975. Biochemical genetics of lobsters: genetic variation and the structure of the American lobster (*Homarus americanus*) populations. *J. Fish. Res. Board Canada.* **32:** 2091–2101.

Trevelyan, G. A. and E. S. Chang. 1987. Light-induced shell pigmentation in post-larval *Mytilus edulis* and its use as a biological tag. *Mar. Ecol. Prog. Ser.* **39:** 137–144.

Turner, R. D., and Y. M. Yakovlev. 1983. Dwarf males in the Teredinidae (Bivalvia; Pholadacea). *Science* **219:** 1077–1078.

Uyenoyama, M. K. 1986. Inbreeding and the cost of meiosis: the evolution of selfing in populations practicing biparental inbreeding. *Evolution* **40:** 388–404.

Uzzell, T. M. 1964. Relations of the diploid and triploid species of the *Ambystoma jeffersonium* complex (Amphibia, Caudata). *Copeia* **2:** 257–300.

Vrijenhoek, R. C. 1985. Homozygosity and interstrain variation in the self-fertilizing hermaphroditic fish, *Rivulus marmoratus*. *J. Hered.* **76:** 82–84.

Ward, R. D., and T. Warwick. 1980. Genetic differentiation in the molluscan species *Littorina rudis* and *Littorina arcana* (Prosobranchia: Littorinidae). *Biol. J. Linn. Soc.* **14:** 417–428.

White, M. J. D. 1973. *Animal Cytology and Evolution.* Cambridge University Press. 961 pp.

Williams, G. C. 1975. *Sex and Evolution.* Princeton University Press, Princeton, N. J. 255 pp.

Reference: *Biol. Bull.* 175: 230–239 (October, 1988)

Allelochemical Interactions Between Sponges and Corals

JAMES W. PORTER[1] AND NANCY M. TARGETT[2]

[1]*Zoology Department, University of Georgia, Athens, Georgia 30602, and* [2]*College of Marine Studies, University of Delaware, Lewes, Delaware 19958*

Abstract. The existence of chemical-biological interactions is routinely invoked to explain patterns of coexistence between neighboring organisms. This study characterizes the consequences of these interactions in interspecific space competition between the neighboring species *Plakortis halichondroides*, the liver sponge, and *Agaricia lamarcki*, the sheet coral. This sponge/coral association was studied *in situ* both at points of natural contact and following manipulations that artificially brought the sponge and coral together. *Plakortis* kills *Agaricia* upon direct contact and upon indirect contact (*i.e.*, waterborne metabolites only). *Plakortis* creates a dead zone of coral around its base as it overgrows the coral. The effect of either direct or indirect contact by *Plakortis* is to reduce: (1) the number of zooxanthellae in *Agaricia*, (2) the weight of chlorophyll *a* per unit area of the coral, and (3) the weight of tissue nitrogen per unit area of the coral.

The necrotic effect also evidences itself as changes in oxygen flux characteristics such as significant increases in the compensation point and the nocturnal respiration rate, and significant reductions in the maximum net and gross photosynthetic rates. As a consequence, the diel integrated production to respiration ratio falls below unity for *Agaricia* colonies in contact with *Plakortis;* this does not occur for coral without neighboring sponges.

Because direct contact between *Plakortis* and *Agaricia* is not necessary to effect stress in the coral, the presence of active chemical metabolites from *Plakortis* is suggested. Thus, mechanical abrasion is excluded as the sole mechanism of dominance by the sponge.

Introduction

Sessile and sedentary coral reef organisms frequently compete for space and food, adopting mechanisms to minimize fouling or overgrowth by epibionts and maximize their own space-capture abilities. Several biological mechanisms that mediate ecologically significant interactions among coral reef organisms have been described. For example, scleractinian corals effect extracoelenteric damage to neighbors via extended mesenterial filaments and long sweeper tentacles (Francis, 1973; Lang, 1973; Richardson *et al.*, 1979; Wellington, 1980; Sheppard, 1982). Likewise, hydrocorals and octocorals can move onto and spread across scleractinians, and thereby compete successfully for space with reef-building corals (Wahle, 1980; La Barre and Coll, 1982; Tursch and Tursch, 1982). Bryozoans employ sweeper appendages which are effective in competition and in prevention of fouling (Jackson, 1977). These structures are used in specific behaviors that involve the recognition of potential competitors and the direction of interference mechanisms against them.

Chemical defense mechanisms have also been suggested. These mechanisms have demonstrable effects on species distributions and individual survivorship in terrestrial plant communities (Fraenkel, 1969; Whittaker and Feeny, 1971; Rosenthal and Janzen, 1979; Meinwald, 1982; Targett and Isman, 1986), and have recently been reviewed in ecological contexts for marine communities (Barbier, 1981; Bak *et al.*, 1982; Fenical, 1982; Norris and Fenical, 1982; Palumbi and Jackson, 1982; Colwell, 1983; Faulkner and Ghiselin, 1983; Steinberg, 1984; Scheuer, 1985; Bakus *et al.*, 1986).

Unusual secondary metabolites have been isolated from numerous sessile solitary and colonial coral reef organisms (Tursch *et al.*, 1978; Cimino *et al.*, 1983; Sullivan *et al.*, 1983; Coval *et al.*, 1984; Bandurraga and Fenical, 1985; Kashman *et al.*, 1985; and Coll *et al.*, 1985). Animals that contain unusual secondary metabolites of-

Received 13 October, 1987, accepted 25 July 1988.

ten prove to be toxic in bioassay examinations (Bakus and Thun, 1979; Bakus, 1981; Coll *et al.*, 1982a, 1983; Targett *et al.*, 1983; Gerhart, 1984; McCaffrey and Endean, 1985; Thompson, 1985; Thompson *et al.*, 1985; LaBarre *et al.*, 1986a, b). In addition to their role in organism defense, secondary metabolites are also implicated in the maintenance living space (Jackson and Buss, 1975; Green, 1977; Jackson, 1977; Sheppard, 1979, 1982; Sammarco *et al.*, 1983).

Sponges are remarkable because they lack specialized organs and behaviors, and yet are successful in an environment where such adaptations are common. However, sponges do contain a variety of bioactive secondary metabolites. More than three dozen compounds with lethal or growth inhibitory properties are described from tropical sponges in reviews by Russell and Saunders (1967), Sigel *et al.* (1969), Martin and Padilla (1973), Baker and Murphy (1976), Hollenbeak *et al.* (1976), Faulkner (1977), Cimino (1977), Minale (1978), Kaul and Sinderman (1978), and Hashimoto (1979). These researchers characterize the compounds chemically and occasionally list effects on organisms of direct interest to man, but rarely include data on the ecological importance of the compound or demonstrate effects on other marine organisms likely to have frequent encounters with the species. Recent work continues to identify unusual secondary metabolites from sponges (*e.g.*, Fusetani *et al.*, 1981; Tachibana *et al.*, 1981; Carmely *et al.*, 1983; Cimino *et al.*, 1983; Gonzalez *et al.*, 1984; Nakatsu *et al.*, 1983, 1984; Manes *et al.*, 1985; Braekman *et al.*, 1985; Walker *et al.*, 1985; Nakamura *et al.*, 1986; Mayol *et al.*, 1986) and also identifies several ecological contexts in which the metabolites might function (Thompson *et al.*, 1982; Cimino *et al.*, 1982).

Sullivan *et al.* (1983) demonstrate that the burrowing sponge *Siphonodictyon* sp. secretes a guanidine-containing sesquiterpene, siphonodictidine, in its mucus. This compound kills adjacent coral tissue, thereby preventing the coral from overgrowing the sponge's oscular chimneys. The compound stimulates coral respiration and it has been speculated that increased respiration rate and decreased photosynthetic rate would probably result in death for the coral. However, Sullivan *et al.* (1983) point out that because so many factors can affect hard corals under aquarium conditions, one must be cautious in extrapolating to the long-term effects of siphonodictidine at subacute concentrations. Environmental information on the effects of these kinds of compounds *in situ* is needed.

In this paper, we characterize the consequences of chemical-biological interactions in interspecific space competition between the coral *Agaricia lamarcki* (Milne Edwards & Haime, 1848) and the sponge *Plakortis halichondroides* (Wilson, 1902). Interactions between *Plakortis* and *Agaricia* are common in St. Croix, U. S. Virgin Islands, and in Jamaica where *Plakortis* overgrows living coral, utilizing the newly dead coral skeletons as a primary point of attachment and growth (N. Targett, J. Neigel, J. Porter, unpub. data). Upon physical contact or proximity of less than five centimeters to the sponge, *Agaricia* bleaches and shows a marked necrosis in the region of contact (Fig. 1).

Figure 1. Natural associations of the sponge *Plakortis halichondroides* and the coral *Agaricia lamarcki* show a bleached area at the zone of contact. The necrotic area is evident in this photograph on the left side of the coral along the region adjacent to the sponge and above the 1.0 cm scale bar in the center. (Salt River Canyon, St. Croix, 25 m depth; photograph by R. S. Smith).

Using the *Plakortis/Agaricia* interaction as a basis for study, we: (1) describe the *in situ* effect of *Plakortis halicondroides* on *Agaricia lamarcki* both at points of natural contact and following manipulations that artificially bring together the sponge and coral, (2) quantify the *in situ* effects of direct sponge contact and indirect sponge contact (*i.e.*, exposure to whole sponge exudates only)

on photosynthetic and respiratory oxygen fluxes in the coral, and (3) suggest the long-term effects on tissue biomass, growth rate and survival of *Agaricia* colonies growing in association with *Plakortis* sponges.

Materials and Methods

Site description

This research was conducted utilizing the NOAA underwater habitat, Hydrolab, located at a depth of 17 m on the north coast of St. Croix, U. S. Virgin Islands. Experimental material and line transect data were collected from the east coral reef slope of the Salt River Canyon within the research area available from the habitat.

Field studies

Transects ten meters in length and two meters wide (for a total of 20 m^2 in each transect area) were layed parallel to depth contours at 20 and 30 m. The number of *Plakortis halichondroides* colonies within one meter of the line were counted. The number of times *P. halichondroides* grew within five centimeters of living tissue of *Agaricia lamarcki* was also noted. Additionally, a swimming census covering 1000 m^2 was conducted between the 20 and 30 m depth contours to record all species of scleractinian corals adjacent to *P. halichondroides* colonies.

Biomass determinations

Coral tissue was removed from the surface of the coral skeleton using a Water Pik (Johannes and Wiebe, 1970) with filtered seawater. The tissue slurry was homogenized for one minute in a blender and triplicate aliquots were removed for analysis of nitrogen content, zooxanthellae cell density, and chlorophyll *a* concentration. Standard protocols for sample preparation and analysis were used for fluorometric determination of chlorophyll *a* (Holm-Hansen *et al.*, 1965), hemocytometric counts of zooxanthellae (Muscatine *et al.*, 1984), and micro-Kjeldahl nitrogen digestions (Parsons *et al.*, 1984) as described for coral tissue analysis in Porter *et al.* (1984). Coral surface area was determined for *Agaricia lamarcki* using Marsh's (1970) aluminum foil overlay technique.

Oxygen flux determinations

Oxygen flux in three experimental chambers and ambient PAR light flux on a 4-π quantum sensor were recorded on a Datel magnetic tape data logger at four minute intervals during the 24-hour experimental incubations. Tapes from each experiment were read into a Tektronics 4054 microcomputer where consecutive readings were subtracted from one another. The result was then multiplied by the volume of water in the incubation chambers to give net rates of oxygen production or consumption. These oxygen flux values were normalized to biomass units of surface area, and mass of nitrogen and chlorophyll *a*.

Coral pieces were cut from larger colony rosettes and were used in physiological experiments after they had acclimated for 24 hours. Experimental corals were monitored prior to treatment as well as after treatment, and therefore each served as its own pre-treatment control.

Photosynthesis *versus* irradiance curves were constructed for each control or experimental condition by computing average fluxes over small intervals of irradiance (maximum interval 50 $\mu Em^{-2}\ s^{-1}$). These points were fitted to a hyperbolic tangent function (Jassby and Platt, 1976) which represented the best-fit for patterns of coral productivity (Porter, 1980; Chalker, 1980). The program derived from this function allowed accurate statistical determinations of (1) α the initial slope of the photosynthesis-irradiance curve, (2) I_c, the light compensation point, (3) I_k, the break point, where the P:I curve approached p max, (4) p_c net max and p_c gross max, the maximum net and gross coral head production, (5) r_c, coral nocturnal respiration rate, and (6) an integrated, diel P/R ratio. We have fully described the interpretive model for coral photosynthesis/respiration ratios elsewhere (Muscatine *et al.*, 1981; Muscatine *et al.*, 1984; Porter, 1985).

Experimental design

Eleven null hypotheses were formulated to investigate the consequences to *Agaricia lamarcki* of association with *Plakortis halichondroides*. These null hypotheses included information on biomass patterns (9–11), physiological rates (1–6), and carbon budget totals (7–8) for corals before and after contact with sponges (direct contact) or with sponge exudates (indirect contact). The following null hypotheses were advanced:

1. α Before = α After Exposure
2. I_k Before = I_k After Exposure
3. I_c Before = I_c After Exposure
4. p_c net max Before = p_c net max After
5. p_c gross max Before = p_c gross max After
6. r_c night Before = r_c night After
7. P/R Ratio Before = P/R Ratio After
8. P/R Ratio Exceeds 1.0 Before; Less Than 1.0 After
9. [Zooxanthellae] Before = [Zooxanthellae] After
10. [Pigment] Before = [Pigment] After
11. [Nitrogen] Before = [Nitrogen] After

The four experimental treatments listed below were designed to test these hypotheses, *i.e.*, they were designed to reject the contention that there were no significant

effects on coral biomass or oxygen flux patterns after contact with sponges. The *in situ* manipulations included:

1. Control, no contact or history of contact between *Plakortis halichondroides* and the examined *Agaricia lamarcki* colonies.
2. Indirect contact, *A. lamarcki* colonies in contact with seawater containing exudates from coarsely mashed *P. halichondroides*.
3. Direct contact, *A. lamarcki* colonies in physical contact with pieces of *P. halichondroides* cut from the reef and tied to the coral colonies for 24 hours prior to the oxygen flux measurements.
4. Direct contact, *A. lamarcki* colonies naturally occurring adjacent to uninjured *P. halichondroides* colonies on the reef.

Experimental condition (4) was of greatest ecological interest since, of the three experimental treatments, it most closely recorded conditions of natural contact on the reef.

Oxygen consumption by the electrodes (all experiments) and the injected sponge water (Experiment 2 only) were determined just prior to the experimental incubations. These chemical oxygen demands were added to oxygen fluxes inside the chambers to give the metabolic activity of the coral alone.

The injured and uninjured sponges used in the last two treatments (3 and 4, respectively) were removed from the coral's surface prior to oxygen flux measurements on the coral colony. Since sponge metabolic rates *per se* were not of direct interest in the experimental design, and since Reiswig (1971) has shown that small chambers are unsuitable for the determination of oxygen flux characteristics for sponges like *Plakortis* with high pumping rates, the metabolic activity of *Plakortis* was not determined.

As a control on the experimental method employed, the effects of contact with sponges such as *Agelas*, *Haliclona*, and *Verongula*, which did not cause bleaching and necrosis, were also monitored. Finally, to examine metabolites released from *P. halichondroides*, an *in situ* chemical sampling pump concentrated organic compounds from the water surrounding uninjured colonies of this species.

Results

Field studies

All coral species found in the transect area are overgrown and killed by *Plakortis halichondroides* (Table I). These fourteen species are from eight of the nine Caribbean coral families (the remaining family, the Acroporidae, was not found in this reef zone). The overgrown corals are more similar morphologically than taxonomically; they are all horizontally flattened, and as such, provide a level substratum on which *Plakortis* can grow. The only exception to this pattern is the finger coral, *Madracis mirabilis*, which is killed at the base of its branches in contact with the sponge.

Table I

Hermatypic scleractinian corals killed in situ *by* Plakortis halichondroides *(Wilson, 1902)*

I. Family Astrocoeniidae Koby, 1890
  1. *Stephanocoenia michelinii* Milne Edwards & Haime, 1848
II. Family Pocilloporidae Gray, 1842
  2. *Madracis decactis* (Lyman, 1859)
III. Family Agariciidae Gray, 1847
  3. *Agaricia agaricites* (Linnaeus, 1758)
  4. *Agaricia lamarcki* Milne Edwards & Haime, 1851
IV. Family Siderastreidae Vaughan & Wells, 1943
  5. *Siderastrea siderea* (Ellis & Solander, 1786)
V. Family Poritidae Gray, 1842
  6. *Porites astreoides* Lamarck, 1816
VI. Family Faviidae Gregory, 1900
  7. *Diploria labyrinthiformis* (Linnaeus, 1758)
  8. *Diploria strigosa* (Dana, 1846)
  9. *Colpophyllia natans* (Houttuyn, 1772)
  10. *Montastraea annularis* (Ellis & Solander, 1786)
  11. *Montastraea cavernosa* (Linnaeus, 1766)
VII. Family Meandrinidae Gray, 1847
  12. *Meandrina meandrites* (Linnaeus, 1758)
VIII. Family Mussidae Ortmann, 1890
  13. *Mycetophyllia lamarckiana* Milne Edwards & Haime, 1848–1849
  14. *Mycetophyllia ferox* Wells, 1973

Approximately one-third (34.0 ± 6.8%) of all *Plakortis* colonies occur on or directly adjacent to living coral (Table II). The remaining members of the population grow on stable substrata, many of which are recently dead coral plates. Almost half of the corals with sponges on or near them show signs of bleaching and necrosis (40.8 ± 3.4%, Table II), but all coral specimens show tissue death in the area directly underneath the sponge.

Biomass

Our results clearly demonstrate a marked effect on algal densities, algal pigment concentration, and coral tissue mass for all of the experimental conditions relative to the control condition (Table III). The number of zooxanthellae per unit area, and as a consequence, the chlorophyll *a* per unit area of coral, decreases by a factor of three after contact with injured sponges, uninjured sponges, and sponge water (Table III). The amount of chlorophyll *a* per algal cell does not follow a consistent pattern under the experimental treatments; only after exposure to sponge water does the mass of chlorophyll *a* per algal cell decline significantly (Table III).

Table II

Plakortis halichondroides [illegible] on density and interactions with scleractinian corals ($\bar{X} \pm$ one S.D., $n = 4$)

Station name	[illegible] number of sponge colonies per 20 m²	Total number of sponge colonies within 5 cm of coral	% of sponge population in contact with coral	Number of coral colonies within 5 cm of sponges	Number of coral colonies showing visible signs of stress	% of contacted corals showing signs of stress
20m Right	62	18	29	16	6	38
30m Left	39	13	33	13	5	38
30m Right	105	32	30	33	15	45
20m Left	90	40	44	36	15	42
	74 ± 29	26 ± 12	34.0 ± 6.9	24 ± 12	10 ± 5	40.8 ± 3.4

Nitrogen mass per unit area of coral tissue decreases by a factor of two (Table III). This effect cannot be explained solely by the loss of zooxanthellae since they constitute only 7% of the coral tissue biomass (Porter and Muscatine, in prep.). Coral tissue lysis also occurs (Fig. 2). The effect of these combined plant and animal tissue responses is to create a bleached zone, or necrotic halo, on the coral in the vicinity of the sponge that is visually obvious from a meter away (Fig. 1).

Oxygen flux

Contact with *Plakortis* effects both oxygen production and oxygen consumption (Fig. 3). Oxygen consumption more than doubles for corals in direct contact with injured or uninjured sponges, rising from approximately 6 to 12 $\mu gO_2 cm^{-2}\ h^{-1}$ (Table IV). Coral respiration rate stays the same during injection of sponge water in the short-term indirect contact experiments. However, the maximum net photosynthetic rate drops by almost half for both direct contact with injured or uninjured sponges and for indirect contact with sponge water. These lowered photosynthetic rates occur within eight minutes of injecting sponge water, suggesting that sponge metabolites rapidly diminish this coral species' photosynthetic capacity. Rising respiration rates and diminishing production rates tend to offset one another mathematically. And hence, only for indirect contact with sponge water, where production falls but respiration does not rise concomitantly, does the maximum gross production show a significant decline.

The compensation light intensity is significantly higher under all experimental treatments relative to the control (Fig. 3; Table IV). This demonstrates that more light is needed for corals near or adjacent to sponges to meet their basal metabolic demands through photosynthesis than for corals at a distance from sponges. Further, it suggests that coral production balances coral respiration later in the morning and stops earlier in the afternoon for corals near sponges (Fig. 3).

Given the lowered production rates and increased respiration rates observed under the experimental treatments, it is not surprising that coral P/R ratios are also substantially lower among corals in contact with sponges (Table IV). The overall effect is that while the integrated P/R ratio is always at or above unity in control corals, it is always below 1.0 in corals exposed to injured or uninjured sponges under field conditions (Table IV). P/R ratios below 1.0 are never found for this species in Jamaica,

Table III

Biomass variation ($\bar{X} \pm$ one S.D., $N = 3$) for colonies of the sheet-coral, Agaricia lamarcki *under different exposures to the liver sponge,* Plakortis halichondroides *(see Figs. 1 & 2)*

Characteristic	Units	Experimental treatment: No contact (Control)	Contact with sponge water	Contact with injured sponge	Contact with uninjured sponge
Zooxanthellae	10^6 cells cm^{-2}	1.04 ± 0.08	0.36 ± 0.08*	0.38 ± 0.06*	0.40 ± 0.14*
Pigments	pg Chl *a* cell^{-1}	10.02 ± 0.10	5.82 ± 0.93*	9.81 ± 4.05	10.57 ± 1.88
Pigments	μg Chl *a* cm^{-2}	10.39 ± 0.86	2.08 ± 0.13*	3.79 ± 1.61*	2.84 ± 1.00*
Nitrogen	mg TKN cm^{-2}	0.57 ± 0.06	0.25 ± 0.03*	0.25 ± 0.16	0.25 ± 0.10*

* Means significantly different from the Control ($P \leq 0.05$, ANOVA).

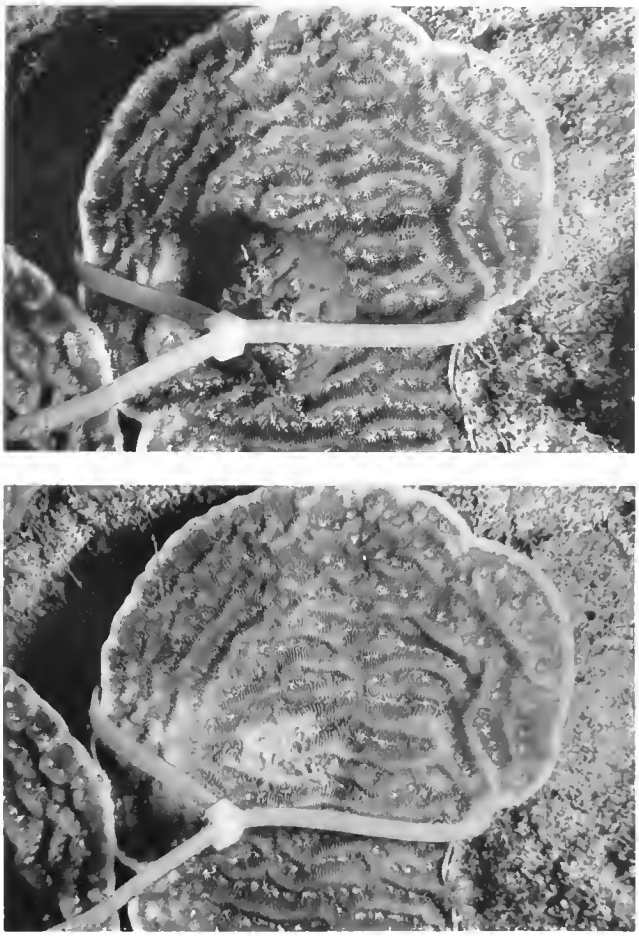

Figure 2. After two hours of experimentally induced contact between *Agaricia lamarcki* and *Plakortis halichondroides* (a, top), a bleached, necrotic area appears on the coral (b, bottom). (Salt River Canyon, St. Croix, 25 m depth; photograph by N. M. Targett).

even over greater depth ranges (Porter and Muscatine, in prep.), and therefore these values for coral colonies in contact with sponges are indicative of unsustainable carbon deficits.

In all cases, the differences observed between control and experimental coral oxygen flux patterns demonstrate significantly reduced photosynthetic capacity in coral colonies in contact with sponges or their metabolites. Therefore, the null hypotheses (no discernable effect) must be rejected for hypotheses (3) compensation point, (4) net production, (5) gross production, (6) nocturnal respiration rate, and (7) integrated P/R ratio under either field conditions or idealized "cloudless day" illumination. Hypothesis (8) P/R ratio > 1.0 is also falsified.

Other species of sponges (*Agelas conifera, Haliclona rubens,* and *Verongula* sp.) were also placed in contact with *Agaricia lamarcki.* They did not bleach the coral, thus indicating that mechanical irritation and pressure are not responsible for the effect observed with *P. halichondroides.*

Crude organic extracts were isolated from *Plakortis halichondroides* and coated onto synthetic cellulose pads, "tuffy sponges." When tied to living coral, these extract-soaked pads caused bleaching within 24 hours. Control pads (uncoated or coated with ether solvent only) produce no effect. While the exact nature of these organic compounds is still unknown, comparative thin layer chromatography of crude extracts from whole *P. halichondroides* and compounds isolated from waters surrounding uninjured *Plakortis* suggests that compounds in the surrounding water are the same as those produced naturally by the sponge.

Discussion

The sponge *Plakortis halichondroides* actively inhibits the metabolism and tissue survival of adjacent corals. Inhibition results from both direct and indirect contact (waterborne metabolites only) suggest that *Plakortis* uses allelochemicals as one means to secure and occupy space on the reef.

Plakortis halichondroides bleaches *Agaricia lamarcki* and causes marked tissue necrosis. The effects on coral biomass and coloration are sufficiently dramatic that it is possible to survey these interactions visually from some distance above the reef surface. The loss of zooxanthellae from corals following exposure to sponges or sponge exudates parallels the loss of symbiotic algae during other natural stresses such as abnormal temperatures, salinity fluctuations, or high rates of sedimentation (Porter, 1987).

These coral biomass reductions contribute to the profound effects that sponges have on coral oxygen metabolism. Parallelling the loss of zooxanthellae is a significant decline in primary production. Although the algae that remain appear to have normal concentrations of photosynthetic pigments, the few remaining zooxanthellae cannot compensate for the overall loss of algae. Further, despite the fact that there is significantly less coral tissue per unit area on corals adjacent to sponges than on corals without sponge contact, the respiration rate is still significantly higher. This respiratory increase suggests a stress or repair-metabolism response to the active sponge metabolites.

The overall effect on the P/R formula of decreasing the numerator and increasing the denominator is to lower the ratio below one for *Agaricia lamarcki.* These suboptimal values are not found in this photoautotrophic coral species. For example, even to depths of 50 m, *Agaricia* has an annual integrated P/R ratio of 1.13 (Porter and Muscatine, in prep.).

The ecological role of specific secondary metabolites

Table IV

Variation (x̄ ± 95% conf. limits, n = 6) in photosynthesis-light utilization characteristics for in situ *colonies of* Agaricia lamarcki *under different exposures to* Plakortis halichondroides *(see Fig. 3)*

Characteristic	Units	Experimental treatment			
		No contact (Control)	Contact with sponge water	Contact with injured sponge	Contact with uninjured sponge
α (cm^2)	μgO_2 cm^{-2} h^{-1} μE^{-1} m^2 s^{-1}	0.222 ± 0.046	0.140 ± 0.058	0.266 ± 0.141	0.303 ± 0.196
I_k (cm^2)	$\mu E m^{-2} s^{-1}$	137.82 ± 9.16	129.64 ± 27.93	109.40 ± 25.10	101.32 ± 36.12
I_c (cm^2)	$\mu E m^{-2} s^{-1}$	27.69 ± 1.70	60.54 ± 15.58*	76.90 ± 21.00*	85.84 ± 19.68*
P_c net max	μgO_2 cm^{-2} h^{-1}	24.88 ± 1.95	10.64 ± 2.22*	17.90 ± 4.19*	15.05 ± 7.12*
P_c gross max	μgO_2 cm^{-2} h^{-1}	30.66 ± 1.95	14.78 ± 2.22*	29.16 ± 4.19	30.98 ± 7.12
Average r_c night	μgO_2 cm^{-2} h^{-1}	5.77 ± 0.21	4.14 ± 0.29	11.26 ± 0.80*	15.93 ± 1.09*
P_c gross R_c 24 h	Ratio (field)	1.98 ± 0.51	1.37 ± 0.31	0.83 ± 0.34*	0.73 ± 0.23*

* Means significantly different from the Control ($P \leq 0.05$).

in marine organisms is known in only a few cases (Webb and Coll, 1983; Sullivan *et al.*, 1983; Morse and Morse, 1984; Targett *et al.*, 1986; Pawlik, 1986). In the boring sponge *Siphonodictyon*, mucus-borne metabolites kill corals (Sullivan *et al.*, 1983). Our study demonstrates that chemical-biological interactions are important in non-boring sponge species and in over-growth, not just anti-fouling, processes.

Several toxic exudates from soft corals appear to be responsible for causing localized mortality in hard corals, since extensive mortality of hard corals can occur even when direct contact is not established with the soft coral (Sammarco *et al.*, 1985). Coll *et al.* (1982b) isolated secondary metabolites from the water surrounding two species of octocorals that were identical to those isolated from the octocorals themselves. Flexibilide, dihydroflexibilide, sarcophine, and sarcophytoxide were isolated from crude extracts of *Simularia flexibilis* and *Sarcophyton crassocaula*, respectively, and from their surrounding water when sampled *in situ* (Coll *et al.*, 1982b). Flexibilide and sarcophytoxide cause death in scleractinian corals at concentrations > 10 ppm (Webb and Coll, 1983). These compounds are also structurally related to sinulariolide, a potent algal growth inhibitor (Tursch, 1976).

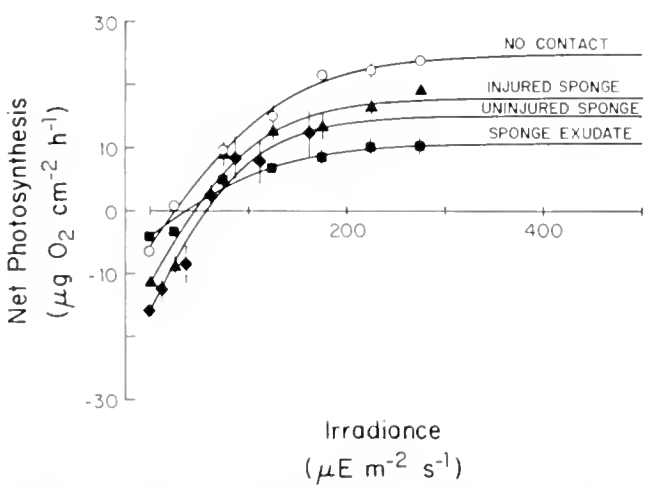

Figure 3. Net photosynthesis-irradiance curves are graphed for *Agaricia lamarcki* colonies (n = 3) from 20 m depth under different levels of contact with *Plakortis halichondroides*. The curves are fitted to a hyperbolic tangent function (see Table IV for the statistical comparisons between curves). Experimental Condition 1: control, no contact with *Plakortis* (open circles). Experimental Condition 2: indirect contact with water containing exudate from coarsely mashed *Plakortis* (solid squares). Experimental Condition 3: direct contact with injured *Plakortis* (solid triangles) (see Fig. 2). Experimental Condition 4: direct contact with uninjured *Plakortis* (solid diamonds) (see Fig. 1). Experimental Condition 4 most closely mimics conditions of natural contact on the reef.

The sponge *Plakortis halichondroides* contains numerous unusual secondary metabolites such as cyclic peroxides and aromatic lactones (Faulkner *et al.*, 1979; Stierle and Faulkner, 1980). It is possible that the cyclic peroxides cause the bleaching response described above and that the phenolic compounds contribute to tissue lysis. The closely related congener, *Plakortis zygompha*, contains (Z)-7-methyl-4-octen-3-one and several derivatives of 3-hydroxy-4-hydroxymethyl-4-pentenoic acid (Faulkner and Ravi, 1980). These may be involved in both the coral biomass changes and the oxygen flux modifications observed for the *Plakortis/Agaricia* association.

Between 30 and 40 percent of all *Plakortis* colonies on the reef are contiguous with scleractinian corals. Of these contacts, half show bleaching and necrosis on the coral tissue near the sponge; all show death of the coral tissue underneath the sponge. More importantly, based on the results of our *in situ* manipulations, the same effect is observable prior to the establishment of direct sponge-

coral contact. This implies that the sponge exudes waterborne metabolites which have a detrimental effect on coral respiration and photosynthesis. If even naturally low concentrations of these waterborne metabolites are effective at suppressing coral photosynthesis, then there is the distinct possibility that sponge exudates may influence ecosystem productivity in the deeper zones of the reef.

Plakortis kills and colonizes the dead skeletons of at least 14 scleractinian coral species. These species are distributed in all 8 Caribbean coral families located in the 20–30 m survey area. Our demonstration that toxins from *Plakortis* are so effective against corals, the otherwise most successful order of benthic invertebrates on the reef, suggests that further investigation of this interaction is warranted. Future research should focus on the mechanisms of action and chemical structure of the compounds that inhibit photosynthesis, stimulate respiration, and reduce coral colony biomass. The range of potency and the half-life of these allelochemicals once released into the water column is also of critical interest. Finally, information on the long-term survival of corals at varying distances from sponges, and the sources of mortality for *Plakortis* would be of great value to our understanding of the chemical ecology of this association. Allelochemistry gives *Plakortis* a measurable advantage in space competition with scleractinian corals, but is only one factor among many other biotic and abiotic factors which determine its population structure and dynamics.

Acknowledgments

We thank the Hydrolab staff for their support during Missions 84-10 and 85-4, and particularly thank aquanauts George Schmahl, Joe Schubauer, Paul Preston from 84-10, and Nick Vrolijk, Ray Jakubczak, and Robbie Smith from 85-4. We are also grateful to topside scientists Hany Salam (84-10 and 85-4) and Susan Sennett (85-4). Dr. Willard D. Hartman identified our *Plakortis* specimens. This work is supported by grants from the Hydrolab Program of NOAA and Office of Naval Research Grant Number N-000-14-84-K-0571.

Literature Cited

Bak, R. P. M., R. M. Termaat, and R. Dekker. 1982. The complexity of coral interactions: influence of time, location of interaction, and epifauna. *Mar. Biol.* **69:** 215–222.

Baker, J. T., and V. Murphy. 1976. *Compounds from Marine Organisms. Volume I* CRC Press, Cleveland. 226 pp.

Bakus, G. J. 1981. Chemical defence mechanisms and fish feeding behavior on the Great Barrier Reef, Australia. *Science* **211:** 497–499.

Bakus, G. J., N. M. Targett, and B. Schulte. 1986. Chemical ecology of marine organisms: an overview. *J. Chem. Ecol.* **12:** 951–987.

Bakus, G. J., and M. Thun. 1979. Bioassays on the toxicity of Caribbean sponges. *Collog. Internat. C. N. R. S.* **291:** 417–422.

Bandurraga, M. M., and W. Fenical. 1985. Isolation of the muricins: evidence of a chemical adaptation against fouling in the marine octocoral *Muricea fructicosa* (Gorgonacea). *Tetrahedron* **41:** 1057–1065.

Barbier, M. 1981. Marine chemical ecology: the roles of chemical communication and chemical pollution. Pp. 148–186 in *Marine Natural Products Chemical and Biological Perspectives Vol. IV*, P. J. Scheuer, ed. Academic Press, New York.

Braekman, J. C., D. Daloze, M. Kaisin, and B. Moussiaux. 1985. Ichthyotoxin sesterperenoids from New Guinean sponge *Carteriospongia foliasens. Tetrahedron* **41:** 4603–4614.

Carmely, S., Y. Loya, and Y. Kashman. 1983. Siphonellinol, a new triterpene from the marine sponge *Siphonochalina siphonella. Tetrahedron Lett.* **24:** 3673–3676.

Chalker, B. E. 1980. Modelling light saturation curves for photosynthesis: an exponential function. *J. Theoret. Biol.* **84:** 205–215.

Cimino, G. 1977. A survey of sesquiterpenoids from marine sponges. Pp. 61–86 in *Marine Natural Products Chemistry*, D. J. Faulkner and W. Fenical, eds. Plenum Press, New York.

Cimino, G., S. deRosa, S. deStefano, R. Self, and G. Sodano. 1983. The bromocompounds of the true sponge *Verongia aerophoba. Tetrahedron Lett.* **24:** 3029–3032.

Cimino, G., S. deRosa, S. deStefano, and G. Sodano. 1982. The chemical defense of four Mediterranean nudibranchs. *Comp. Biochem. Physiol.* **73B:** 471–474.

Coll, J. C., B. F. Bowden, D. M. Tapiolas, and W. C. Dunlap. 1982a. *In situ* isolation of allelochemicals released from soft corals (Coelenterata: Octocorallia): a totally submersible sampling apparatus. *J. Exp. Mar. Biol. Ecol.* **60:** 293–299.

Coll, J. C., B. F. Bowden, D. M. Tapiolas, R. H. Willis, P. Djura, M. Streamer, and L. Trott. 1985. Studies of Australian soft corals-XXXV: the terpenoid chemistry of soft corals and its implications. *Tetrahedron* **41:** 1085–1092.

Coll, J. C., S. LaBarre, P. W. Sammarco, W. T. Williams, and G. J. Bakus. 1982b. Chemical defenses in soft corals (Coelenterata: Octocorallia) of the Great Barrier Reef: a study of comparative toxicities. *Mar. Ecol. Progr. Ser.* **8:** 271–278.

Coll, J. C., D. M. Tapiolas, B. F. Bowden, L. Webb, and H. Marsh. 1983. Transformation of soft coral (Coelenterata: Octocorallia) terpenes by *Ovula ovum* (Mollusca: Prosobranchia). *Mar. Biol.* **74:** 35–40.

Colwell, R. R. 1983. Biotechnology in the marine sciences. *Science* **222:** 19–24.

Coval, S. J., P. J. Scheuer, G. K. Matsumoto, and J. Clardy. 1984. Two new xenicin diterpenoids from the octocoral *Anthelia edmondsoni. Tetrahedron* **40:** 3823–3828.

Faulkner, D. J. 1977. Interesting aspects of marine natural products chemistry. *Tetrahedron* **33:** 1421–1443.

Faulkner, D. J., R. W. Armstrong, P. Djura, M. D. Higgs, B. N. Ravi, D. B. Stierle, and S. J. Wratten. 1979. Some chemical constituents in Caribbean sponges. *Colloq. Internat. C. N. R. S.* **291:** 401–406.

Faulkner, D. J., and M. T. Ghiselin. 1983. Chemical defense and evolutionary ecology of dorid nudibranchs and some other opisthobranch gastropods. *Mar. Ecol. Progr. Ser.* **13:** 295–301.

Faulkner, D. J., and B. N. Ravi. 1980. Metabolites of the marine sponge *Plakortis zygompha. Tetrahedron Lett.* **21:** 23–26.

Fenical, W. 1982. Natural products chemistry in the marine environment. *Science* **215:** 923–928.

Fraenkel, G. 1969. Evolution of our thoughts on secondary plant substances. *Etomol. Exper. Appl.* **12:** 473–486.

Francis, L. 1973. Intraspecific aggression and its effect on the distribution of *Anthopleura elegantissima* and some related anemones. *Biol. Bull.* **144:** 73–92.

Fusetani, N., S. Matsunaga, and S. Konosu. 1981. Bioactive marine metabolites. II. Halistanol sulfate, an antimicrobial novel steroid sulfate from the marine sponge *Halichondria* cf. *moorei* Bergquist. *Tetrahedron Lett.* 22: [illegible] 1988.

Gerhart, D. J. 1984. Prostaglandin A_2: an agent of chemical defense in the Caribbean gorgonian *Plexaura homomalla*. *Mar. Ecol. Prog. Ser.* 19: 181–[illegible]

Gonzalez, V. [illegible] O. M. Estrada, J. D. Martin, V. S. Martin, C. Perez, and R. Perez. 1984. New antimicrobial diterpenes from the sponge *Spongia officinalis*. *Tetrahedron* 40: 4109–4113.

Green, G. 1977. Ecology of toxicity in marine sponges. *Mar. Biol.* 40: 207–215.

Hashimoto, Y. 1979. *Marine Toxins and Other Bioactive Marine Metabolites*. Japan Scientific Society Press, Tokyo. 369 pp.

Hollenbeak, K. H., F. J. Schmitz, and P. N. Kaul. 1976. Cardiotonic agents from marine sponges: isolation of histamine and N-methylated histamines. Pp. 282–287 in *Food and Drugs from the Sea, Proceedings 1974*. H. H. Webber and G. D. Ruggieri, eds. Marine Technology Society Press, Washington.

Holm-Hansen, O., C. J. Lorenzen, R. W. Holmes, and J. D. H. Strickland. 1965. Fluorometric determinations of chlorophyll. *J. Cons. Perm. Internat. Explor. Mer* 30: 3–15.

Jackson, J. B. C. 1977. Competition on marine hard substrata: the adaptive significance of solitary and colonial strategies. *Am. Nat.* 111: 743–767.

Jackson, J. B. C., and L. Buss. 1975. Allelopathy and spatial competition among coral reef invertebrates. *Proc. Natl. Acad. Sci. U.S.A.* 72: 5160–5163.

Jassby, A. D., and T. Platt. 1976. Mathematical formulation of the relationship between photosynthesis and light for phytoplankton. *Limnol. Oceanogr.* 21: 540–547.

Johannes, R. E., and W. J. Wiebe. 1970. Method for determination of coral tissue biomass and composition. *Limnol. Oceanogr.* 15: 822–824.

Kashman, Y., A. Groweiss, R. Lidor, D. Blasberger, and S. Carmely. 1985. Latrunculins: NMR study, two toxins and a synthetic approach. *Tetrahedron* 41: 1905–1914.

Kaul, P. N., and C. J. Sinderman, eds. 1978. *Drugs and Food from the Sea*. University of Oklahoma Press, Norman. 448 pp.

LaBarre, S. C., and J. C. Coll. 1982. Movement in soft corals: an interaction between *Nephthea brassica* (Coelenterata: Octocorallia) and *Acropora hyacinthus* (Coelenterata: Scleractinia). *Mar. Biol.* 72: 119–124.

LaBarre, S. C., J. C. Coll, and P. W. Sammarco. 1986a. Competitive strategies of soft corals (Coelenterata: Octocorallia): III. Spacing and aggressive interactions between alcyonaceans. *Mar. Ecol. Prog. Ser.* 28: 147–156.

LaBarre, S. C., J. C. Coll, and P. W. Sammarco. 1986b. Defensive strategies of soft corals (Coelenterata: Octocorallia) of the great Barrier reef. II. The relationship between toxicity and feeding deterrence. *Biol. Bull.* 171: 565–576.

Lang, J. C. 1973. Interspecific aggression by scleractinian corals. 2. Why the race is not only to the swift. *Bull. Mar. Sci.* 23: 260–279.

Manes, L. V., S. Naylor, P. Crews, and G. J. Bakus. 1985. Suvanine, a novel sesterterpene from an *Ircinia* marine sponge. *J. Org. Chem.* 50: 284–286.

Marsh, J. A. 1970. Primary productivity of reef-building calcareous red algae. *Ecology* 51: 255–263.

Martin, D. F., and G. M. Padilla. 1973. *Marine Pharmacognosy*. Academic Press, New York. 317 pp.

Mayol, L., V. Piccialli, and D. Sica. 1986. Metabolites from the marine sponge *Spongionella gra[illegible]*. *Tetrahedon* 42: 5369–5376.

McCaffrey, E. J., and R. Endean. 1985. Antimicrobial activity of tropical and subtropical sponges. *Mar. Biol.* 89: 1–8.

Meinwald, J. ed. 1982. The organic chemistry of animal defense mechanisms. *Tetrahedron* 38: 1855–1970.

Minale, L. 1978. Terpenoids from marine sponges. Pp. 175–240 in *Marine Natural Products. Chemical and Biological Perspectives, Vol. I*. P. J. Scheuer, ed. Academic Press, New York.

Morse, A. N. C., and D. E. Morse. 1984. Recruitment and morphosis of *Haliotis* larvae induced by molecules uniquely available at the surfaces of crustose red algae. *J. Exp. Mar. Biol. Ecol.* 75: 191–215.

Muscatine, L., P. W. Falkowski, J. W. Porter, and Z. Dubinsky. 1984. Fate of photosynthetically-fixed carbon in light- and shade-adapted colonies of the symbiotic coral, *Stylophora pistillata*. *Proc. R. Soc. Lond. B* 22: 181–202.

Muscatine, L., L. R. McCloskey, and R. E. Marian. 1981. Estimation the daily contribution of carbon zooxanthellae to coral animal respiration. *Limnol. Oceanogr.* 26: 601–611.

Nakamura, H., S. Deng, J. Kobayashi, Y. Ohizumi, and Y. Hirata. 1986. Dictyoceratin-A and -B, novel antimicrobial terpenoids from Okinawan marine sponge *Hippospongia* sp. *Tetrahedron* 42: 4197–4201.

Nakatsu, T., D. J. Faulkner, G. K. Matsumoto, and J. Clardy. 1984. Structure of the diterpene portion of a novel base from the sponge *Igelas mauritiana*. *Tetrahedron Lett.* 25: 935–9381.

Nakatsu, T., R. P. Walker, J. E. Thompson, and D. J. Faulkner. 1983. Biologically active sterol sulfates from the marine sponge *Toxadocia zumi*. *Experimentia* 39: 759–761.

Norris, J. N., and W. Fenical. 1982. Chemical defense in tropical marine algae. *Smithson. Contrib. Mar. Sci.* 12: 417–431.

Palumbi, S. R., and J. B. C. Jackson. 1982. Ecology of cryptic coral reef communities. II. Recovery from small disturbance events by encrusting bryozoa: the influence of "host" species and lesion size. *J. Exp. Mar. Biol. Ecol.* 64: 103–115.

Parsons, T. R., Y. Maita, and C. M. Lalli. 1984. *A Manual of Chemical and Biological Methods for Seawater Analysis*. Pergamon Press, Oxford. 173 pp.

Pawlik, J. R. 1986. Chemical induction of larval settlement and metamorphosis in the reef-building tube worm *Phragmatopoma californica* (Sabellariidae: Polychaeta). *Mar. Biol.* 91: 59–68.

Porter, J. W. 1980. Primary productivity in the sea: reef corals *in situ*. Pp. 403–410 in *Primary Productivity in the Sea*. P. G. Falkowski, ed. Plenum Press, New York.

Porter, J. W. 1985. The maritime weather of Jamaica: its effects on annual carbon budgets of the massive reef-building coral *Montastraea annularis*. *Proc. Fifth Internat. Coral Reef Congr., Tahiti* 6: 363–379.

Porter, J. W. 1987. Species profiles: life histories and environmental requirements of coastal fishes and invertebrates (South Florida). Reef-building corals. *U.S. Fish. Wildl. Serv. Biol. Rep.* 82: 1–23.

Porter, J. W., L. Muscatine, Z. Dubinsky, and P. G. Falkowski. 1984. Primary production and photoadaptation in light- and shade-adapted colonies of the symbiotic coral, *Stylophora pistillata*. *Proc. R. Soc. Lond. B* 216: 161–180.

Reiswig, H. M. 1971. *In situ* pumping activities of tropical Demospongia. *Mar. Biol.* 9: 38–50.

Richardson, C. A., P. Dustan, and J. C. Lang. 1979. Maintenance of living space by sweeper tentacles of *Montastrea cavernosa*, a Caribbean reef coral. *Mar. Biol.* 55: 181–186.

Rosenthal, G. A., and D. H. Janzen, eds. 1979. *Herbivores. Their Interactions with Secondary Plant Metabolites*. Academic Press, New York. 718 pp.

Russell, F. E., and P. R. Saunders, eds. 1967. *Animal Toxins*. Pergamon Press, New York. 428 pp.

Sammarco, P. W., J. C. Coll, and S. LaBarre. 1985. Competitive strategies of soft corals (Coelenterata: Octocorallia). II. Varible de-

fensive responses and susceptibility to scleractinian corals. *J. Exp. Mar. Biol. Ecol.* **91:** 199–216.

Sammarco, P. W., J. C. Coll, S. LaBarre, and B. Willis. 1983. Competitive strategies of soft corals (Coelenterata: Octocorallia): Allelopathic effects on selected scleractinian corals. *Coral Reefs* **1:** 173–178.

Scheuer, P. J., ed. 1985. The organic chemistry of marine products. *Tetrahedron* **41:** 979–1108.

Sheppard, C. R. C. 1979. Interspecific aggression between reef corals with reference to their distribution. *Mar. Ecol. Prog. Ser.* **1:** 237–247.

Sheppard, C. R. C. 1982. Coral populations on reef slopes and their major controls. *Mar. Ecol. Progr. Ser.* **7:** 83–115.

Sigel, M. M., L. L. Wellham, W. Lichter, L. E. Dudek, J. L. Gargus, and A. H. Lucas. 1969. Anticellular and antitumor activity of extracts from tropical marine invertebrates. Pp. 281–294 in *Food-Drugs from the Sea Proceedings, 1969*, H. W. Youngken, ed. Marine Technology Society Press, Washington.

Steinberg, P. D. 1984. Algal chemical defense against herbivores: allocation of phenolic compounds in the kelp *Alaria marginata*. *Science* **223:** 405–406.

Stierle, D. B., and D. J. Faulkner. 1980. Metabolites of three marine sponges of the genus *Plakortis*. *J. Org. Chem.* **45:** 3396–3401.

Sullivan, B., D. J. Faulkner, and L. Webb. 1983. Siphonodictidine, a metabolite of the borrowing sponge *Siphonodictyon* sp. that inhibits coral growth. *Science* **221:** 1175–1176.

Tachibana, K., P. J. Scheuer, Y. Tsukitani, H. Kikuchi, D. van Engen, J. Clardy, Y. Gopichand, and F. Schmitz. 1981. Okadaic acid, a cytotoxic polyether from two marine sponges of the genus *Halichondria*. *J. Am. Chem. Soc.* **103:** 2469–2471.

Targett, N. M., S. S. Bishop, O. J. McConnell, and J. A. Yoder. 1983. Antifouling agents against the benthic marine diatom *Navicula salinicola:* homarine from the gorgonians *Leptogorgia virgulata* and *L. setacea* and analogs. *J. Chem. Ecol.* **9:** 817–829.

Targett, N. M., and M. Isman, eds. 1986. Proceedings of the Second International Society of Chemical Ecology Meeting. *J. Chem. Ecol.* **12:** 949–1203.

Targett, N. M., T. Targett, N. Vrolijk, and J. Ogden. 1986. The effect of macrophyte secondary metabolites on feeding preferences of the herbivorous parrotfish *Sparisoma radians*. *Mar. Biol.* **92:** 141–148.

Thompson, J. E. 1985. Exudations of biologically-active metabolites in a sponge (*Aplysina fistularis*). I. Biological evidence. *Mar. Biol.* **88:** 23–26.

Thompson, J. E., R. P. Walker, D. J. Faulkner. 1985. Screening and bioassays for biologically active substances from forty marine sponge species from San Diego, Ca., U. S. A. *Mar. Biol.* **88:** 11–22.

Thompson, J. E., R. P. Walker, S. J. Wratten, and D. J. Faulkner. 1982. A chemical defense mechanism for the nudibranch *Cadlina luteomarginata*. *Tetrahedron* **38:** 1865–1873.

Tursch, B. 1976. Some recent developments in the chemistry of alcyonaceans. *Pure Appl. Chem.* **48:** 1–6.

Tursch, B., J. C. Braekman, D. Daloze, and M. Kaisin. 1978. Terpenoids from coelenterates. Pp. 247–296 in *Marine Natural Products. Chemical and Biological Perspectives Vol. II*, P. J. Scheuer, ed. Academic Press, New York.

Tursch, B., and A. Tursch. 1982. The soft coral community on a sheltered reef quadrat at Laing Island (Papua New Guinea). *Mar. Biol.* **68:** 321–332.

Wahle, C. E. 1980. Detection, pursuit and overgrowth of tropical gorgonians by milleporid hydrocorals: Perseus and Medusa revisited. *Science* **209:** 689–691.

Walker, R. P., J. E. Thompson, and D. J. Faulkner. 1985. Exudation of biologically active metabolites in a sponge *Aplysina fistularis*. II. Chemical evidence. *Mar. Biol.* **88:** 27–32.

Webb, L., and J. C. Coll. 1983. Effects of alcyonarian coral terpenes on scleractinian coral photosynthesis and respiration. *Toxicon Suppl.* **3:** 485–488.

Wellington, G. M. 1980. Reversal of digestive interactions between Pacific reef corals: mediation by sweeper tentacles. *Oecologia* **47:** 340–343.

Whittaker, R. H., and P. P. Feeny. 1971. Allelochemics: chemical interactions between species. *Science* **171:** 757–770.

Reference: *Biol. Bull.* 175: 240–245. (October, 1988)

A New Type of the Manifestation of Colony Specificity in the Compound Ascidian, *Botrylloides violaceus* Oka[1]

EUICHI HIROSE, YASUNORI SAITO, AND HIROSHI WATANABE

Shimoda Marine Research Center, University of Tsukuba, Shimoda 5-10-1, Shizuoka 415, Japan

Abstract. A new type of colony specificity (= allogeneic recognition) is shown for *Botrylloides violaceus*. All botryllid ascidians previously studied for colony specificity show allo-recognition reactions, manifested as fusion or nonfusion (rejection), both at the colonial margin (= growing edge) and at the cut surface. By contrast allorecognition in *Botrylloides violaceus* is absent at the cut surface, but present at the growing edge. Juxtaposition of cut surfaces resulted in fusion of the colonies regardless of origin, while juxtaposition of natural growing edges resulted in fusion or rejection, according to the genetic combination of colonies. Similar results occurred among the sibling colonies derived from the same mother colony, in which pairs tunic necrosis was observed in areas where the two colonies partially fused. These features of allogeneic rejection in *B. violaceus* were very similar to those of "nonfusion" in *Botrylloides simodensis*. In inter-specific combinations between *B. violaceus* and *B. simodensis*, a remarkable necrotic reaction was observed in the zone of contact when two colonies touched at their cut surfaces. When brought into contact at their growing edges, they resulted in "nonfusion" without a particular reaction.

Introduction

Colony specificity represented by allograft rejection has been demonstrated for many colonial forms of animals, from sponges to ascidians. Colony specificity in some compound ascidians is manifested by fusibility between colonies: two colonies either form a single mass (fusion) or do not fuse (rejection), when they come into contact. Some ascidian species do not show colony specificity, while others exhibit it (Koyama and Watanabe, 1982). In those that do, isogeneic colonies are always fusible at their natural growing edges, and allogeneic colonies are either fusible or not fusible.

Colony specificity in compound ascidians has been studied primarily in species of the family Botryllidae (botryllid ascidians). These species form sheet-like colonies in which zooids are buried in a gelatinous tunic. Zooids are arranged in rosettes or ladder-like systems with common cloacal apertures, and are connected to one another by a ramifying network of blood vessels which terminate in sausage-shaped *ampullae* at the periphery of the colony. All botryllid ascidians that have been studied so far exhibit colony specificity. In some of them, genetic control of their fusibility has been demonstrated (Oka and Watanabe, 1957, 1960, 1967; Sabbadin, 1962, 1982; Scofield *et al.*, 1982).

The morphology and cell biology of fusion and nonfusion (rejection) in botryllids have been studied in detail in four species: *Botryllus scalaris* (Saito and Watanabe, 1982), *B. primigenus* (Oka and Watanabe, 1967; Tanaka and Watanabe, 1973; Tanaka, 1973; Katow and Watanabe, 1980; Taneda and Watanabe, 1982), *B. schlosseri* (Milanesi *et al.*, 1978; Scofield and Nagashima, 1983), and *Botrylloides simodensis* (Mukai and Watanabe, 1974; Saito, 1976; *cf.* Saito *et al.*, 1981). The course of fusion is essentially the same in all these species. By contrast, the rejection reaction is initiated at distinctly different stages of fusion in different species. These facts imply that comparative studies of the processes of fusion and nonfusion in various species might be useful for analyzing the mechanism of allo-recognition, as well as for considerations of the evolution of colony specificity in botryllid ascidians. Here we have investigated the processes of fusion and nonfusion in the Japanese species *Botrylloides violaceus*, and found that this species shows

Received 7 January 1988; accepted 26 July 1988.

[1] Contribution number 484 from the Shimoda Marine Research Center.

Table I

Fusion experiments in Botrylloides violaceus *at the cut surface*

Combination	No. combination	Fusion	Nonfusion
Between colonies of the Shimoda population	112	112	0
Between colonies of the Asamushi population	27	27	0
Between the two populations	33	33	0

a new and instructive type of colony specificity previously undescribed for compound ascidians.

Materials and Methods

Colonies of *B. violaceus* were collected in the Shimoda Floating Aquarium (Shizuoka Prefecture) and in the vicinity of the Asamushi Marine Biological Station (Aomori Prefecture). The two collecting sites are about 1100 km apart in linear distance. *B. simodensis* colonies were also collected in the vicinity of the Shimoda Marine Research Center (Shizuoka Prefecture). To facilitate handling of the colonies, they were fixed on glass plates and reared in the culture boxes floated in the bay near the Shimoda Marine Research Center.

The fusibility of colonies was tested by fusion experiments. Procedures for fusion experiments were as follows: a piece was cut out of each of the two colonies between which fusibility was to be tested. The two similarly sized pieces (about 15 zooids) were placed in juxtaposition on a glass slide, and they were brought into contact with each other either at the cut surfaces or at the growing edges. The colonies on the glass slide were then kept in a moisture chamber for 30 minutes, so that the colonies might attach to the glass slides prior to their placement in running seawater. The experimental animals were observed under a binocular stereomicroscope each day. The paired colonies showed clear fusion or nonfusion reactions. Fusion here means the establishment of a common vascular system between the two colonies, and nonfusion the absence of it. In the latter case, several trials with the same combination of colonies were carried out to avoid the possibility of accidental failure of fusion.

Oozooids of *B. violaceus* were obtained from some colonies from the Shimoda Floating Aquarium population. In the fusion experiments of sibling colonies, a pair of oozooids derived from the same mother colony were placed on a glass slide so that they came into contact by their growing edges. Further experimental methods were the same as those just mentioned.

For histological studies, specimens in the process of fusion or nonfusion were fixed in a solution containing 2.5% glutaraldehyde and 0.45 *M* sucrose buffered with 0.1 *M* cacodylate at pH 7.4. The fixed specimens were then dehydrated through a butanol series, embedded in paraplast, sectioned at 5 μm and stained with Congo red, Delafield's hematoxylin, and eosin-orange G.

Results

Fusion experiments at the cut surface

When colonies of *Botrylloides violaceus* were apposed by their cut surfaces, we were surprised to note that all colonies fused (Table I). This was true both in intrapopulational and in interpopulational combinations. However, separation of such fused colonies between which the common vascular system had been established for a few days or more was occasionally observed. This suggests the presence of a kind of long term (or induced) allo-recognition. It should be noted, however, that in these experiments it was difficult to determine whether separation was caused by allo-recognition or by unsuitable conditions for long-term observation. By contrast, a rapid, necrotic xeno-graft rejection was observed between similarly juxtaposed pieces of *B. violaceus* and *B. simodensis* colonies. Blood cells from the blood vessels clustered in the tunic at the boundary between the colonies. The clusters of cells were observed as a clear *black line* along the boundary (Fig. 1). The area with the cell infiltration eventually degenerated and was apparently cleared from the area.

Fusion experiments at the growing edge

By contrast to the results with cut colonies, apposition of colonies by their naturally growing edges resulted either in fusion or nonfusion, depending on the particular combination of colonies employed. In the case of fusion,

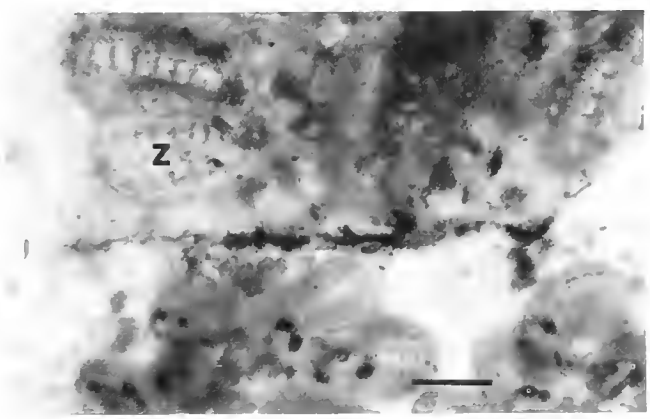

Figure 1. Xeno-rejection at the cut surface. Upper colony is *Botrylloides violaceus*, and lower colony is *B. simodensis*. Necrosis is observed along the boundary between the two colonies. z, zooid. Scale bar = 1 mm.

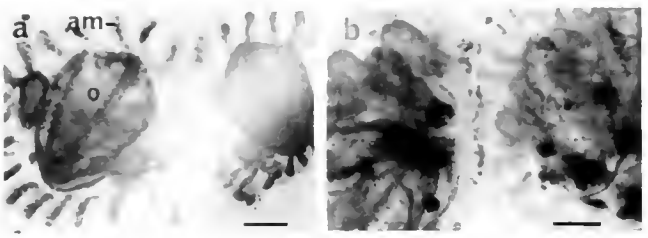

Figure 2. Fusion and nonfusion at the growing edge between sibling colonies of *Botrylloides violaceus*. a: Fusion, four days after settlement of the oozooids. Common vascular system has been established. b: Nonfusion, a week after settlement. am, ampullae; o, oozooid. Scale bars = 0.5 mm.

tip to side contacts occurred between ampullae of the two colonies, and then fusion took place at those sites to produce a common vascular system. In the case of nonfusion, ampullae of both colonies pushed against each other, but never penetrated the tunic of the facing colony. Although signs of rejection were not clearly visible in the contact area under the binocular stereomicroscope, the necrotic rejections were evident in subsequent histological sections of the rejection zone (below).

Similar experiments between sibling oozooids gave similar results (Fig. 2). Out of the 32 combinations studied, 14 resulted in fusion and 10 resulted in nonfusion. The results of the remaining eight combinations could not be assessed because of the degeneration or mechanical separation of the colonies.

All xenogeneic combinations between *B. violaceus* and *B. simodensis* resulted in nonfusion reactions similar to those in incompatible intraspecies pairs.

Histological observations

A frontal section of normal ampullae at the periphery of a colony is shown in Figure 3. The ampullae are buried in the tunic. Many blood cells are seen in the ampullar lumen, and are not usually seen in the tunic. Tunic (or "test") cells are dispersed throughout the tunic, and can be distinguished from blood cells by their morphology and staining characteristics. A cuticular layer is differentiated at the external surface of the tunic.

The histological features of fusion and nonfusion at the growing edge of *B. violaceus* were very similar to those of *B. simodensis* as reported by Saito (1976). In the case of fusion, the boundary between the two colonies disappeared and was filled with continuous test matrix containing normally distributed tunic cells (Fig. 4a–c). Fragments of cuticle were sometimes observed in the original boundary zone (Fig. 4b). In the case of nonfusion, the tunic layers sometimes fused, but only in small areas along the boundary. In the fused areas, tunic cells were considerably more abundant than usual (Fig. 4d). In addition, blood cells (particularly morula cells) infiltrated the tunic from the blood vessels in the contact areas (Fig. 4e). These cells were found clustered and disintegrated in the rejection zone. The disintegrated cells subsequently were released from the tunic in the form of massive aggregations (Fig. 4f).

Discussion

In *Botrylloides violaceus*, short term allo-recognition appears to be absent at the cut surface and present at the growing edge. This type of colony specificity has not been described previously. In compound ascidians previously studied, mechanisms of allo-recognition have been studied in *Didemnum moseleyi* (Mukai and Watanabe, 1974), *Perophora japonica* (Koyama and Watanabe,

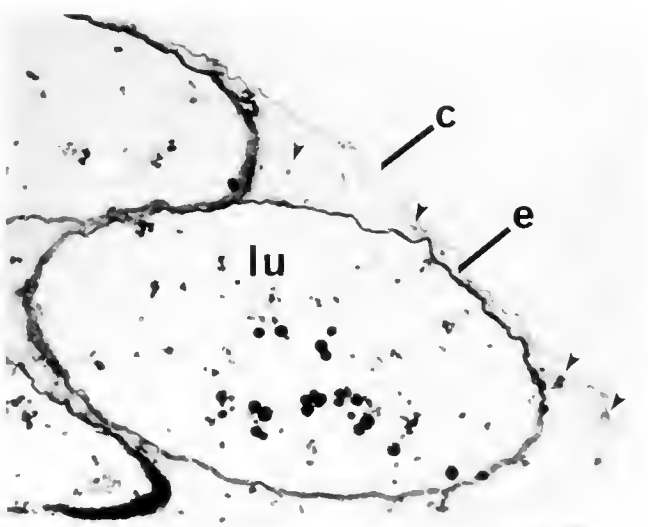

Figure 3. Frontal section through the periphery of a colony of *Botrylloides violaceus*. The substratum is to the bottom and the colony is growing to the right. Some of the tunic cells are pointed by arrow heads. c, cuticle; e, epithelium of ampulla; lu, lumen of ampulla with blood cells. Scale bar = 50 μm.

Figure 4. Histological aspects of fusion and nonfusion at the growing edge between sibling colonies of *Botrylloides violaceus*. a–c: Fusion. (a) Contact of colonies. Dissolution of cuticular layers occurs at the contact between colonies (arrow). (b) Fusion of colonies. Fragments of cuticle are still observed (arrow head). (c) Completely fused tunic. d–f: Nonfusion. (d) Partially fused tunic in which there are many tunic cells. (e) Blood cells infiltrate into the tunic and form a mass of cells (arrow heads). (f) The mass of destructed cells is removed to the outside of the tunic (arrow head). Scale bars = 50 μm.

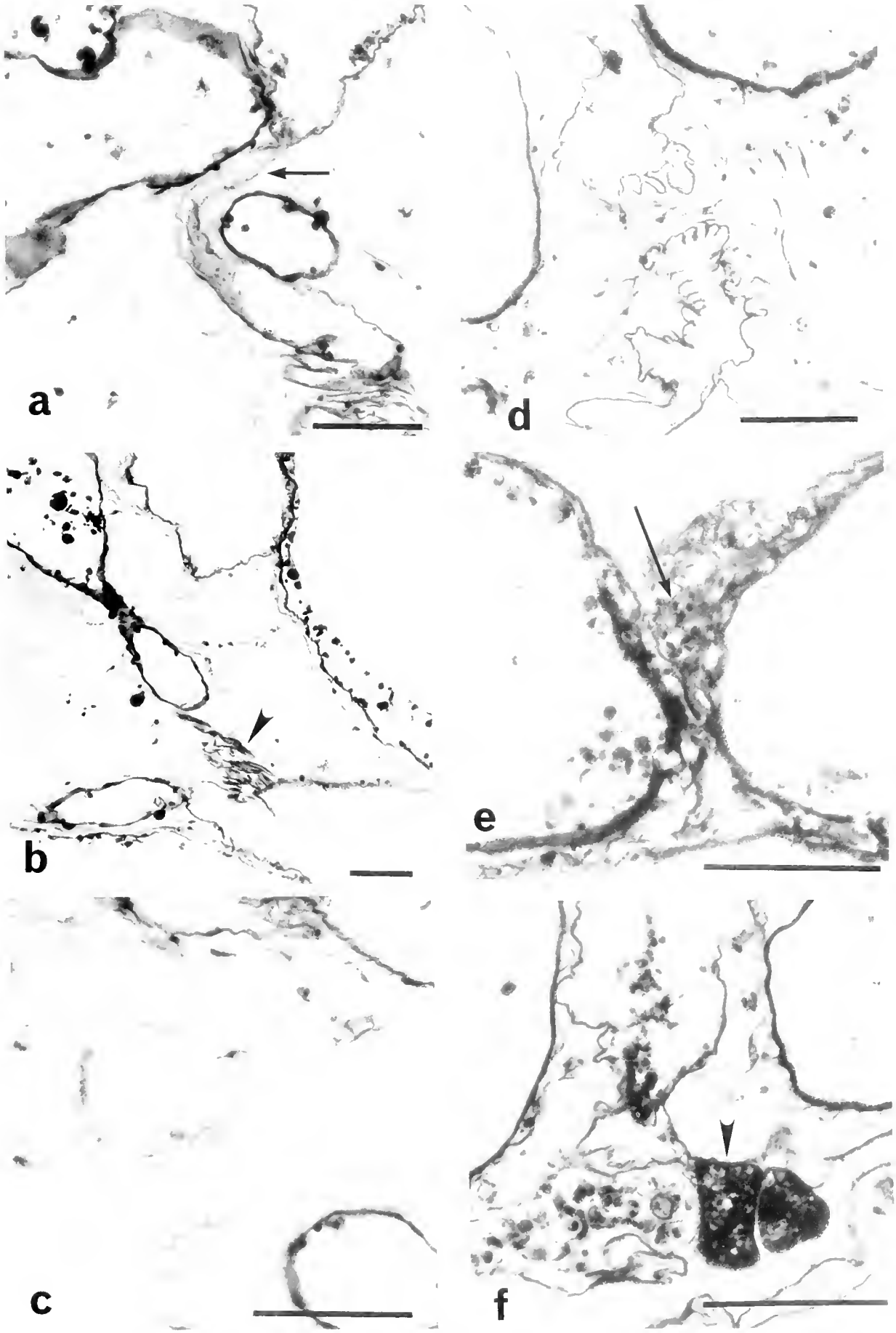
a
b
c
d
e
f

1981), *P. sagamiensis* (Kojima and Watanabe, 1982), *Symplegma reptans* (Mukai and Watanabe, 1974), *Botryllus scalaris* (Saito and Watanabe, 1982), *B. primigenus* (Oka and Watanabe, 1957), *B. schlosseri* (Bancroft, 1903; Sabadin, 1962; Scofield and Nagashima, 1983), and *Botrylloides simodensis* (Mukai and Watanabe, 1976). Although allo-recognition at the cut surface is uncertain in the two species of *Perophora* and *B. schlosseri*, all the other ascidians listed clearly have the capacity for allo-recognition, both at the cut surface and at the growing edge (reviewed by Watanabe and Taneda, 1982; Taneda *et al.*, 1985). On the other hand, in the species we and others found *lacking* colony specificity, *e.g.*, *Polycitor proliferus* (Oka and Usui, 1944; *cf.* Tokioka, 1953) and *Perophora multiclathrata* (Mukai and Watanabe, 1974; *cf.* Nishikawa, 1984), two colonies never fuse naturally at their growing edges, but invariably fuse at their cut surfaces, regardless of their origin. In *B. violaceus*, a colony invariably fuses with any other member of the same population or of another population at the cut surface. At the growing edge, however, colonies show fusion or nonfusion depending on the combination of colonies. From this we conclude that *B. violaceus* has a new type of colony specificity.

The nonfusion reaction observed at the growing edges of *B. violaceus* is similar to that of *B. simodensis*, which sometimes has been called "indifference." This term means nonfusion without particular reaction, such as the nonfusion of the ascidians lacking colony specificity, *e.g.*, *Perophora multiclathrata* (Mukai and Watanabe, 1974). In the nonfusion of both *B. simodensis* and *B. violaceus*, the necrotic reaction between two colonies is barely observable under a binocular stereomicroscope, but is clearly observed histologically. Consequently, the nonfusion of these species should be placed in a category other than indifference. We propose, therefore, to use the term "sub-cuticular rejection" to describe nonfusion reactions in these two species. In sub-cuticular rejection, the necrotic reaction with blood cell infiltration is limited to the tunic along the boundary between colonies, and never occurs in the ampullae and blood vessels.

In sub-cuticular rejection, allo-recognition appears to occur in the sub-cuticular region of the colonial margin because the reaction is limited to that area. In fact, *B. violaceus* may conduct allo-recognition *only* in the sub-cuticular region, since allo-recognition is absent at the cut surface in this species. The sub-cuticular region of tunic consists of tunicin fibers and tunic cells. Therefore, the tunic cells might play an important role for allo-recognition.

All botryllid ascidians studied with regard to colony specificity are capable of natural allo-recognition at the growing edge. The fusion reaction is essentially the same in all species studied, but the nonfusion reaction is initiated at different stages of the fusion process according to species (Table II). Taneda and his colleagues (1985) suggested that these differences depend upon the site in which allo-recognition initially occurs, and that the site has shifted to the surface of the colony during evolution. The nonfusion reaction initiated after ampullar fusion (in *B. scalaris*) seems to be a fundamental (or "primitive") type of allo-recognition in botryllids, and sub-cuticular rejection (in *B. violaceus* and *B. simodensis*) may be more advanced. Several species of botryllids, including *B. scalaris*, *B. primigenus*, *B. simodensis*, and *B. violaceus*, have also been studied in detail from the view point of life history (Saito and Watanabe, 1985), and their likely phylogenetic relationships have been outlined using rejection type as a reference point (Taneda *et al.*, 1985). From the presence of subcuticular rejection in this species, we deduce that *B. violaceus* may be an "advanced" species.

Table II

The stage at which the nonfusion reaction is initiated at the growing edge

Species	Stage	Reference
B. scalaris	ampullar fusion	Saito and Watanabe, 1982
B. primigenus	ampullar penetration	Taneda and Watanabe, 1982
B. simodensis	partial fusion of tunic	Saito, 1976
B. violaceus	partial fusion of tunic	

In *B. violaceus*, colony specificity is absent at the cut surface, although it is present at the growing edge. In this species, it is possible that the cells which have the capacity for allo-recognition distribute restrictedly in the sub-cuticular region. Therefore, in the case of cut surface contact, the cells having the capacity may not be exposed to allogeneic tissues, since the subcuticular region has been cut off. Then, the fusion would be allowed between allogeneic colonies. In the other botryllids, allo-recognition at the cut surface seems to occur mainly in blood vessels, but it can also occur between tunic cells (Tanaka and Watanabe, 1973; Tanaka, 1973). In *B. violaceus*, it appears that contact between allogeneic cells alone does not elicit rejection. In light of the phylogenetic position of this species, we suggest that the distribution of the allo-recognition site of botryllid ascidians has been extended from the blood cells to the sub-cuticular region, after which it has been lost except for the sub-cuticular region in *B. violaceus*.

In allogeneic fusion resulting from the contact of cut surfaces in *B. violaceus*, a natural separation of fused colonies was occasionally observed. This separation may be a manifestation of long term allo-recognition. If so, the separation may be comparable to that in *Botryllus scalaris* (Saito and Watanabe, 1982).

In xeno-grafts made at the cut surfaces between *B. vio-*

laceus and *B. simodensis*, necrosis occurred in both species. Thus, short term xeno-recognition is present between the two species.

A "single locus and multiple alleles model" has been proposed for the colony specificity of *B. primigenus* and *B. schlosseri*, (Oka and Watanabe, 1957, 1960, 1967; Sabbadin, 1962, 1982; Scofield *et al.*, 1982). According to this model, each colony has two alleles at one locus governing colony specificity, and colonies having at least one allele in common are fusible with one another. Mukai and Watanabe (1975) suggested that colony specificity in *B. simodensis* could also be explained by this model. The genetic system governing the colony specificity in *B. violaceus* is expected to be similar to this model, but further studies are required before reaching a definite conclusion.

Acknowledgments

We thank Professor H. Mukai for reading the manuscript and for providing critical comments. We also thank Mr. K. Anazawa for his assistance in performing fusion experiments, Dr. K. Numakunai of the Asamushi Marine Biological Station of Tohoku University and the members of the Shimoda Floating Aquarium for supplying *Botrylloides violaceus*, and the staff of the Shimoda Marine Research Center for their assistance throughout this experiment. This study was supported by Grant-in-Aid for General Scientific Research 61490004 to H. Watanabe from the Ministry of Education, Science and Culture of Japan.

Literature Cited

Bancroft, F. W. 1903. Variation and fusion of colonies in compound ascidians. *Proc. Calif. Acad. Sci.* **3**(Series 3): 137–186.

Katow, H., and H. Watanabe. 1980. Fine structure of fusion reaction in compound ascidian *Botryllus primigenus* Oka. *Dev. Biol.* **76:** 1–14.

Koyama, H., and H. Watanabe. 1981. Colony specificity in the colonial ascidian, *Perophora japonica*. *Annot. Zool. Jpn.* **54:** 30–41.

Koyama, H., and H. Watanabe. 1982. Colony specificity in the ascidian, *Perophora sagamiensis*. *Biol. Bull.* **162:** 171–181.

Milanesi, C., P. Burighel, G. Zaniolo, A. Sabbadin. 1978. The structure and the fate of the test cuticle during the fusion-nonfusion reaction in colonies of *Botryllus schlosseri* (Tunicata). *Boll. Zool.* **45:** 83–86.

Mukai, H., and H. Watanabe. 1974. On the occurrence of colony specificity in some compound ascidians. *Biol. Bull.* **147:** 411–421.

Mukai, H., and H. Watanabe. 1975. Fusibility of colonies in natural populations of the compound ascidian, *Botrylloides violaceus*. *Proc. Jpn. Acad.* **51:** 48–50.

Nishikawa, T. 1984. Ascidians from the Truck Islands, Ponape Island and Majuro Atoll (Tunicata, Ascidiacea). *Proc. Jpn. Soc. Syst. Zool.* **27:** 107–140.

Oka, H., and M. Usui. 1944. On the growth and propagation of the colonies in *Polycitor mutabilis* (*Ascidiae compositae*). *Sci. Rep. Tokyo Bunrika Daigaku* **7**(Series B): 23–53.

Oka, H., and H. Watanabe. 1957. Colony-specificity in compound ascidians as tested by fusion experiments (a preliminary report). *Proc. Jpn. Acad.* **33:** 657–659.

Oka, H., and H. Watanabe. 1960. Problems of colony-specificity in compound ascidians. *Bull. Mar. Biol. Stn. Asamushi* **10:** 153–155.

Oka, H., and H. Watanabe. 1967. Problems of colony specificity, with special reference to the fusibility of ascidians (in Japanese). *Kagaku (Tokyo)* **37:** 307–313.

Sabbadin, A. 1962. Le basi genetiche della capacitá di fusione fra colonie in *Botryllus schlosseri* (Ascidiacea). *Rend. Accad. Naz. Lincei* **32**(Ser. 8): 1031–1035.

Sabbadin, A. 1982. Formal genetics of ascidians. *Am. Zool.* **22:** 765–773.

Saito, Y. 1976. The mechanism of "self" and "not-self" recognition in the compound ascidian, *Botrylloides violaceus* Oka (in Japanese). Master's Thesis, Tokyo Kyoiku University.

Saito, Y., H. Mukai, and H. Watanabe. 1981. Studies on Japanese compound styelid ascidians. II. A new species of the genus *Botrylloides* and redescription of *B. violaceus*. *Publ. Seto Mar. Biol. Lab.* **26:** 357–368.

Saito, Y., and H. Watanabe. 1982. Colony specificity in the compound ascidian, *Botryllus scalaris*. *Proc. Jpn. Acad.* **58**(Ser. B): 105–108.

Saito, Y., and H. Watanabe. 1985. Studies on Japanese compound styelid ascidians. IV. Three new species of genus *Botrylloides* from the vicinity of Shimoda. *Publ. Seto. Mar. Biol. Lab.* **30:** 227–240.

Scofield, V. L., J. M. Schlumpberger, L. A. West, and I. L. Weissman. 1982. Protochordate allo-recognition is controlled by a MHC-like gene system. *Nature* **295:** 499–502.

Scofield, V. L., and L. S. Nagashima. 1983. Morphology and genetics of rejection reactions between oozooids from the tunicate *Botryllus schlosseri*. *Biol. Bull.* **165:** 733–744.

Tanaka, K., and H. Watanabe. 1973. Allogeneic inhibition in a compound ascidian, *Botryllus primigenus* Oka. I. Process and features of "nonfusion" reaction. *Cell. Immunol.* **7:** 410–426.

Tanaka, K. 1973. Allogeneic inhibition in a compound ascidian, *Botryllus primigenus* Oka. II. Cellular and humoral responses in "nonfusion" reaction. *Cell. Immunol.* **7:** 427–443.

Taneda, Y., and H. Watanabe. 1982. Studies on colony specificity in the compound ascidian, *Botryllus primigenus* Oka. I. Initiation of "nonfusion" reaction with special reference to blood cells infiltration. *Dev. Comp. Immunol.* **6:** 43–52.

Taneda, Y., Y. Saito, and H. Watanabe. 1985. Self or non-self discrimination in ascidians. *Zool. Sci.* **2:** 433–442.

Tokioka, T. 1953. *Ascidians of Sagami Bay*. Iwanami Shoten (Tokyo). 204–206.

Watanabe, H., and Y. Taneda. 1982. Self or non-self recognition in compound ascidians. *Am. Zool.* **22:** 775–782.

Reference: *Biol. Bull.* 175: 246–252. (October, 1988)

A New, Disjunct Species of Triclad Flatworm (Turbellaria: Tricladida) From a Spring in Southern New England

DOUGLAS G. SMITH

Museum of Zoology, University of Massachusetts, Amherst, Massachusetts 01003-0027 and Museum of Comparative Zoology, Harvard University, Cambridge, Massachusetts 02138

Abstract. An undescribed species of flatworm belonging to the genus *Polycelis* (family Planaridae) is reported from a spring in western Massachusetts. The new species represents the first recorded occurrence of *Polycelis* in eastern North America. The morphological uniqueness and geographical disjunction of the new species suggests that it has been isolated from congeneric forms for a considerable length of time. However, it is alternatively possible that the species' existence in western Massachusetts is the result of introduction from some as yet unknown "natural" range elsewhere. If in fact naturally occurring in New England, the new species could be a survivor of a pre-glacial fauna that survived glacial advances by living in groundwater habitats under the ice sheet.

Introduction

The freshwater flatworm genus *Polycelis*, as recently defined by Gourbault (1972) and Kenk (1973), is characterized by certain morphological features which vary little among described species. Within the genus, two subgenera are recognized (*Polycelis* and *Seidlia*), the basis of distinction being founded in the degree of musculature associated with the genital atrium (Kenk, 1953, 1973). Only a few species are presently assigned to *Seidlia*, in which the atrium is provided with an extensive and thick musculature. Apart from the differences in atrial musculature separating *Polycelis* (*sensu* stricto), without extensive atrial musculature, and *Seidlia*, the distinctions among the several known species in the genus are limited to differences in the shape and position of various components of the male reproductive system and, to a lesser extent, the presence or absence of muscular prostatic organs also known as adenodactyls.

The distribution of *Polycelis* covers a large portion of the Northern Hemisphere (Kenk, 1953; Ball, 1975). In North America, the known species are restricted to the western third of the continent. Kenk (1953) proposed that the North American distribution of *Polycelis* is a result of pre-glacial dispersal from Asia across the Bering Strait when a land bridge existed during periods of lower sea stands. According to Kenk (1953), subsequent glaciations have controlled or adjusted the distribution of certain species. Kenk's (1953) synthesis of *Polycelis* distribution has been adopted by Ball (1975).

Recent investigations of springs in western Massachusetts, in the northeastern United States, have revealed the existence of an undescribed species of *Polycelis*. The new species possesses, among other distinctive morphological features, a specialized gland situated near the reproductive structures, termed the ventral gland, which is unlike that of any other described species of *Polycelis* or any other known North American triclad species. This paper provides a description of the new species and attempts to explain the disjunct occurrence of the new species in New England.

Materials and Methods

The spring in which the new species was found is in Sunderland, Franklin County, Massachusetts and represents the type locality. The spring is the principal source of water for a state-owned fish hatchery. Specimens were collected on 25 August, 22 September, 30 October, 1987,

Received 26 February 1988; accepted 28 July 1988.

and 13 January, 1988. One hundred and fifty specimens were collected and examined. Of the series, 34 animals had fully formed reproductive organs.

Most specimens were killed in 2% nitric acid and fixed in FAA. A few specimens were maintained in laboratory conditions for behavioral observations. Twelve specimens were serially sectioned using conventional techniques and stained with Delafield's or Ehrlich's hematoxylin and eosin. Though most sections were of the sagittal plane, cross sections were prepared in two cases. An additional three specimens were dissected. The Holotype and the Paratypes (all slides) and a series of whole specimens have been deposited into the collections of the Museum of Comparative Zoology, Harvard University, Cambridge, Massachusetts. The remaining specimens and prepared slides have been deposited into the Museum of Zoology, University of Massachusetts, Amherst, Massachusetts.

Systematic Account and Results

Family Planariidae Stimpson, 1857

Genus *Polycelis* Ehrenberg, 1831

Polycelis remota, new species

Diagnosis

Polycelis remota is a medium sized species (maximum length, 17 mm) demonstrating characteristics representative of the genus, including the presence of an arc of eyespots following the anterior contour of the body of the animal, distinct cephalic auricles produced anterolaterally, testes situated ventrally, and pre-pharyngeal and paired oviducts uniting posteriorly of the penis bulb to form a common oviduct which descends to the genital atrium. Otherwise, it is distinct from all known species of *Polycelis* by the possession of a large, transverse muscular gland with a single exterior sucker-like organ situated always on the right ventral side of the animal, anterior and separate from the gonopore and its associated atrial cavities. The new species is further distinguished from all other known species of *Polycelis* by the peculiar seminal vesicle, by having a greatly elongated penis bulb, and by the position of the copulatory bursa which extends anterior of the posterior margin of the pharyngeal cavity.

Description

General characteristics of Holotype (living animal, 11.0 mm) (Fig. 1A, B). The anterior margin of the head forms a low inverted "V," and continues laterally with sub-triangular auricles. The neck region is posterior to auricles with slight constriction. The body widens posteriorly, reaching its greatest width in the region of pharynx. The posterior part of the animal tapers to a rounded point. Eyes are present and numerous, and extend across the margin of the head and along the lateral margins, exclusive of auricles, some distance posterior to auricles. The arc is interrupted at the midpoint of the anterior margin. The dorsal surface anterior to the pharyngeal region with the low median keel extending anteriorly to the apex of the anterior margin. The pharynx is single, medially placed, and occupies about one third of the length of the animal. The inner muscle layers of pharynx are composed of an outer, thin longitudinal layer and an inner, thick circular layer. Rhabdites are present along the margins of the animal. Both mouth and genital pores open ventrally on the midline. The color of the dorsal surface of animal, exclusive of the area of digestive caeca, is olive, and the digestive caeca are brown to yellowish-brown. The pharyngeal region is a lighter whitish-yellow. Ventrally, the animal is grayish-white, and the region of the atrium and gland is lighter. The pharynx is unpigmented.

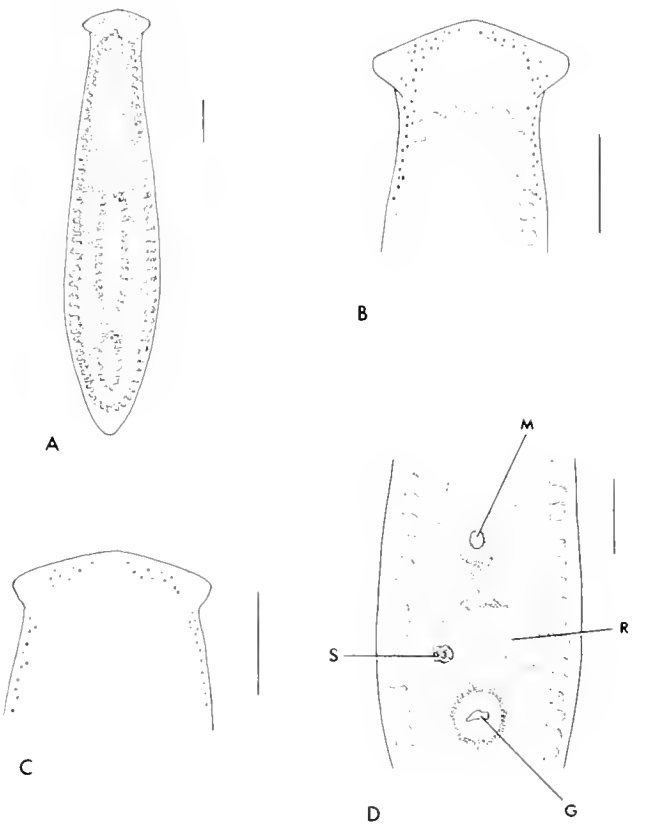

Figure 1. External characteristics of *Polycelis remota*: A, dorsal view of living animal; B, anterior end of living animal; C, anterior end of preserved animal; D, ventral view of posterior portion of preserved animal. Scale line equals 1 mm; G = gonopore, M = mouth pore, R = region of ventral gland, S = "sucker."

Anatomy of the Holotype (Figs. 1D, 2, 3a–d). In the

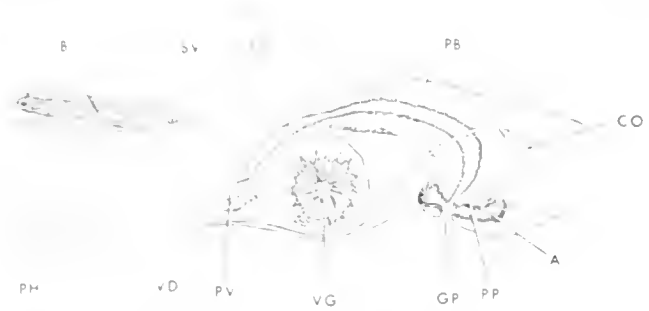

Figure 2. Sagittal view of posterior male and female reproductive structures of *Polycelis remota*, semi-diagrammatic: A = atrium, B = bursa, BD = bursa duct, CO = common oviduct, ED = ejaculatory duct, GP = gonopore, M = mouth pore, PB = penis bulb, PH = pharynx, PP = penis papilla, PV = papilla of vesicle, SV = seminal vesicle, VD = vas deferens (narrowed spermiductal vesicle), VG = ventral gland; stipple indicates presence of muscle tissue.

female reproductive system, the ovaries are situated ventrally and just posterior to first lateral digestive caecum and slightly to side of midline. Oviducts pass posteriorly and ventrally, medially to nerve cords, to a point just posterior of the ventral gland, under which they pass, and ascend on either side of the penis bulb. The right oviduct passes between the bursa duct and penis bulb. The two oviducts join posterior to the penis bulb to form a common oviduct which proceeds to female portion of the atrium. The copulatory bursa is a lobate, somewhat flattened sac placed dorsally and to right of the pharyngeal cavity. The bursa stalk or duct proceeds posteriorly from the bursa to the right of the penis bulb and joins the atrium ventrally along side the penis papilla. The histology of the bursa duct changes during its course. The duct wall is anteriorly similar to the bursa wall and contains a thick cellular lining composed of a tall, spacious, and densely staining columnar epithelium without a detectable muscle coat. The posterior portion of ventral gland is surrounded by a coat of connective tissue fibers; the inner epithelium is characterized by thin columnar cells which stain densely only at their bases.

The male reproductive system contains separate testes extending ventrally from between second and third digestive caeca posteriorly to near base of the pharynx. Up to eight testicular masses are evident at one time. The two vasa deferentia pass ventrally and posteriorly, and medially to the nerve cords near the distal third of the pharynx where the ducts enlarge to form spermiductal vesicles. The vesicles narrow somewhat and separately enter the seminal vesicle at approximately opposite lateral points on the vesicle. The seminal vesicle is large, oval, and situated immediately posterior to the pharyngeal cavity and has a spacious lumen. The vesicle wall is thinly lined with connective tissue, but a distinct muscle layer is not evident. The lumen is penetrated by lobes of villus-like tissue containing large, vacuolated cells presumed to be secretory. Ventrally, the lumen extends through a broad papilla into the ejaculatory duct, which is enclosed in a long and thickly muscularized penis bulb. The penis bulb extends posteriorly over the ventral gland and terminates in an expanded tip of a very short, conical, and unarmed penis papilla. The distal portion of the penial apparatus veers to the right, ending with the papilla facing and in close proximity to the opening of the bursa duct and near site of the gonopore. The genital atrium is narrow but cavernous; the region of the penis papilla has muscular walls. Glandular cells occupy deep pockets of the atrium to either side of penis papilla.

A structure, herein termed the ventral gland, occupies a position anterior of midpoint between the posterior pharyngeal cavity wall and the posterior tip of animal. The gland is large and crescent shaped; the apex of the crescent is pointed anteriorly. The structure is enclosed entirely by mesenchyme tissue. Its width equals about one half the body width of the animal. From left to right the gland is characterized by a thick muscle layer, at first opening dorsally, then closing to form a ring enclosing a nearly solid capsule. The muscle fibers are parallel to the long axis of the gland. The interior of the capsulated gland is comprised of bands of densely staining, apparent glandular cells arising in groups from the inner muscle margin and radiating inward, leaving a small, granule-filled lumen at the center. Invaginations are lined with large, cuboidal cells occasionally present on the inner muscle margin. Farther to the right of the animal, the dorsal musculature of gland capsule reopens, the ventral musculature splits, and the inner free portions of the ventral layer descend ventrally to form a secondary capsule communicating with the exterior. At the right extremity of gland, the secondary capsule, believed to represent a sucker-like organ, acquires an intrinsic thin musculature enclosing the sucker capsule and penetrating to basal papillae-like extensions that communicate with the exterior. Papillae-like extensions interrupt the epidermis and basement membrane of the body wall and contain, in addition to muscle fibers, intercellular spaces and elongated, apparent glandular cells.

Discussion

Variations

Lengths of animals collected ranged from 5 to 17 mm, however, only specimens 10 mm or greater in length had fully formed reproductive organs. The dorsal surface color, exclusive of the digestive caeca, varied from a very light olive in smaller specimens to brown in larger specimens. The area of the digestive caeca varied from reddish-brown to yellowish-brown, the color probably in-

fluenced by the contents of the caeca. Upon preservation, the anterior auricles become reduced and the eyes at the bases of the auricles become obscured (Fig. 1C). Within the female reproductive system, the ovaries are situated just slightly to the right or left of the midline. The size and the position of the copulatory bursa varies somewhat. The principal lobe is placed either to the left or right of the dorsal midline. The bursa duct passes either dorsally or laterally (right side) of the penis bulb. The male reproductive system of certain animals may have fewer testes, and lobes of the testes may occasionally extend dorsally. The posterior, enlarged vas deferens (spermiductal duct) sometimes continues a short distance posterior to the seminal vesicle before turning upward and anterior towards the point of union with the vesicle. Additional observations on cross sections of animals (Fig. 3e, f) confirm the position of the bursa duct on the right side of the penis bulb and the posterior orientation of the penis bulb and papilla. A single specimen contained two distinct penial complexes, neither functional, as the one embedded in the dorsal mesenchyme was connected to the single seminal vesicle whereas the one existing at the site of the gonopore originated blindly.

Ecology and habitat

The species was living in the spring and in the open stream and concrete lined raceways downstream from the spring for about 90 meters. Within this habitat the water temperature varied between 8.5° and 9.0°C on each collecting date. Specimens lived on the undersides of stones and cobbles and were more concentrated toward the spring itself. Farther downstream two other species of triclads were encountered. *Phagocata morgani morgani* (Stevens and Boring) was common in the 9.0° to 10.0°C zone and *Phagocata woodworthi* Hyman was found in the 10.0°C and higher zone. A certain amount of overlap was observed for all three species.

Living specimens moved by gliding over the substrate with their somewhat mobile auricles held slightly aloft. Copulation was not observed, however, unstalked cocoon-like structures were deposited by animals held in captivity. The capsules were bean shaped, translucent, and measured 0.3×0.7 mm.

Systematics and distribution

Little argument can be made to remove *P. remota* from *Polycelis* (*sensu* lato) as all the characters defining the genus are found without deviation in the described species. Similarities with other *Polycelis* species cease below the genus level, and *P. remota* can not be assigned to either of the recognized subgenera. Based on the morphological characters of *P. remota* assessed in this study, the species stands apart from all other described species of *Polycelis* to such an extent as to make phylogenetic hypotheses regarding its intergeneric relationships difficult.

Concerning the male reproductive system, the morphology of the seminal vesicle and its connection with the penis bulb is distinctive and cannot be easily derived from any known *Polycelis* species. Generally, in species of *Polycelis*, the seminal vesicle is enclosed in a definite muscle coat and empties directly into the ejaculatory duct without first passing through a papilla as found in *P. remota*. Probably the most problematic character in terms of evolutionary relationships is the ventral gland. The ventral gland may function as both a secretory gland and a holdfast that is employed during copulation; but this assumption remains to be proven as neither *in vivo* nor *in vitro* copulation has been observed. The gland can not be easily homologized with a true adenodactyl, as described by Kenk (1930) and Hyman (1951), because it is not associated with a cavity of any sort nor does it contain an apical, conical style or papilla typical of the solid adenodactyls found in other *Polycelis* species. Of the species of *Polycelis* in which typical adenodactyls are found, *P. felina* is the only one with adenodactyls situated away from the reproductive atrial cavity. However, in *P. felina*, these organs are posterior of the reproductive complex (Vandel, 1921; Dahm, 1958), whereas in *P. remota* the ventral gland is anterior.

Histologically and morphologically the ventral gland appears similar to the frontal musculo-glandular adhesive organs of dendrocoelid triclads as described by Hyman (1951). The morphology of the capsulated adhesive organ of *P. remota* somewhat resembles the anterior adhesive organ of *Procotyla fluviatilis* (Hyman, 1951; Fig. 21D). Ball (1974) argued that adhesive organs are derived features within the Tricladida. If this is true then there is little reason to dispute the derived nature of the ventral gland in *P. remota*. Thus, assuming that the ventral gland has evolved secondarily, the extreme length of the penis bulb and the displacement of the bursa to a more anterior position may have been merely a morphological adjustment to accomodate the ventral gland. Additionally, the size and complexity of the ventral gland represents more than a simple aberration or modification of some previously existing organ such as an adenodactyl or similar gland. It must be concluded that *P. remota*, though retaining the basic suite of *Polycelis* characters, has nonetheless undergone specialization during a long period of isolation.

Regarding the female reproductive system, the Palearctic species *P. nigra* and *P. tenuis* contain a bilobed bursa (Lender, 1936), which overlaps the pharyngeal

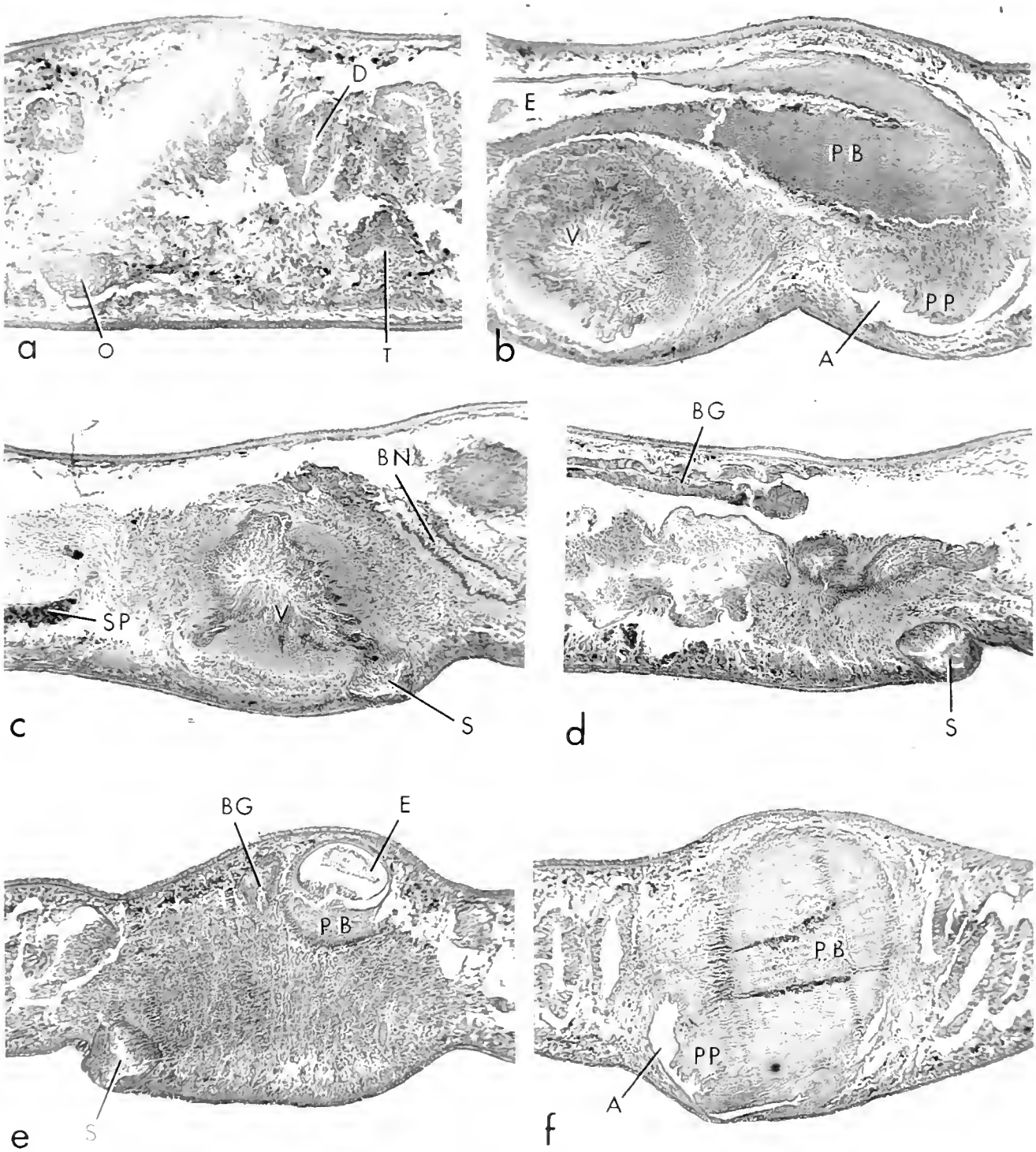

Figure 3. Reproductive anatomy of *Polycelis remota*. a–d, Holotype, sagittal view; a, anterior, left of midline; b, posterior, near midline; c, posterior, right of midline; d, posterior, right side; e–f, cross sections of specimen, posterior of pharynx, all figures ×95. A = atrium, BG = glandular portion of bursa duct, BN = nonglandular portion of bursa duct, D = digestive caecum, E = ejaculatory duct, O = ovary, PB = prostatic bulb, PP = penis papilla, S = "sucker," SP = spermiductal vesicle, T = testes, V = ventral gland.

cavity, an apparently unique feature in Planariidae besides *P. remota*. Whether the overlap of the pharyngeal cavity by the bursa in *P. remota* and the two Palearctic forms indicates a relationship among the three species is debatable. In *P. remota*, the overlap can be attributed to the position of the ventral gland which has displaced the seminal vesicle and the bursa farther anteriorly. In fact, the position and shape of each component of the entire posterior male and female secondary reproductive complex has been no doubt affected to some extent by the presence of the ventral gland.

Understanding the zoogeographical history of *P. remota* is complicated by not only unclear relationships within the genus, but by the fact that the species is thus far known from only the type locality. As discussed earlier, the species exists in a geographical area not previously known to be inhabited by *Polycelis*. Its presence in New England, an area presumably well sampled for most animal groups, can be explained by introduction from some presently unknown area or indicative of a natural but very restricted distribution. With respect to the possibility of introduction, artificial transfers of freshwater triclad flatworms are generally considered rare (Reynoldson, 1966) and have occurred for only a few wide ranging, ecologically generalistic species. Furthermore, species known to have resistant cocoons have not been found outside of their natural range (Ball and Fernando, 1969; Ball, 1974). Nonetheless, the terricolan triclad *Bipalium kewense* was first described from introduced material (Hyman, 1951) and its natural distribution was not understood for many years (Winsor, 1981).

The *P. remota* locality is the source of water for a fish hatchery that for many years has reared exotic species of trout (*Salmo trutta* and *S. gairdneri*). The former trout species was originally imported from Europe while the latter came from western North America, both regions known to have *Polycelis* species. The possibility of introduction with trout species declines as details of the distribution of *P. remota* within the spring are revealed. *P. remota* occurs only in the coldest section of the hatchery drainage, at or near the spring source, where the water temperature is well below regimes in which trout are maintained. The trout pens, farther downstream, have *P. m. morgani* and *P. woodworthi* populations, but rarely is *P. remota* found, and this species only occasionally occurs at the upstream most portion of the first pens in the system. Although introduction from some area containing as yet undiscovered populations of *P. remota* remains possible, the natural distribution theory has equally attractive arguments.

As previously discussed, the distinctive morphology of the reproductive system of *P. remota* suggests that the species has existed outside of the main body of the distribution of the genus for some time. Geographically, New England is situated far from regions where *Polycelis* spp. are found. Within North America, New England has been isolated hydrologically from other physiographic provinces for long periods of time by ancient boundary mountains of Paleozoic age. Species or species groups able to gain entry into provincial New England drainages during rare stream capture events could subsequently evolve independent of gene flow from contemporary forms elsewhere. In support of the prediction that the geographical and geological history of the New England province has favored the evolution of distinct forms is the presence of certain other freshwater invertebrate species apparently endemic to New England. The taxonomic and zoogeographic uniqueness of *P. remota* is characteristic of a group of relatively non-vagile endemic, plus a few non-endemic, invertbrates which have been hypothesized to have survived in the Pleistocene glaciers in subsurface environments (Holsinger, 1978, 1981; Smith, 1986) or periglacial refugia in southeastern New England (Smith, 1982, 1983). The species in this group that are geographically restricted to New England are likely relics of a preglacial fauna, possibly quite diverse, that was peculiar to the New England province. *Polycelis remota* is arguably a member of this group and survived the Pleistocene ice advances by existing in water laying near the surface or water continuously discharging from seepage environments beneath the glacial ice sheet.

Acknowledgments

I thank Roman Kenk for reading an early draft of the manuscript. I also thank the Massachusetts Division of Fish and Wildlife for allowing access to the Sunderland fish hatchery where the species was found.

Literature Cited

Ball, I. R. 1974. A contribution to the phylogeny and biogeography of the freshwater triclads (Platyhelminthes: Turbellaria). Pp. 339–401 in *Biology of the Turbellaria*, Nathan W. Riser and M. P. Morse, eds. McGraw-Hill Book Co., New York.

Ball, I. R. 1975. Nature and formulation of biogeographic hypotheses. *Syst. Zool.* **24:** 407–430.

Ball, I. R., and C. H. Fernando. 1969. Freshwater triclads (Platyhelminthes, Turbellaria) and continental drift. *Nature* **221:** 1143–1144.

Dahm, A. G. 1958. *Taxonomy and Ecology of Five Species Groups in the Family Planariidae.* Nya Litografen, Malmo. 241 pp.

Gourbault, N. 1972. Recherches sur les triclades paludicoles hypoges. *Mem. Mus. Nat. Hist. Nat. Ser. A Zool.* **73:** 1–249.

Holsinger, J. R. 1978. Systematics of the subterranean amphipod genus *Stygobromus* (Crangonyctidae), Part II: species of the eastern United States. *Smithson. Contrib. Zool.* **266:** 1–144.

Holsinger, J. R. 1981. *Stygobromus canadensis*, a troglobitic amphipod crustacean from Castleguard Cave, with remarks on the

concept of cave glacial refugia. *Proc. Int. Congr. Speleol.* **1**: 93–95.

Hyman, L. H. 1951. *The Invertebrates: Platyhelminthes and Rhynchocoela.* Vol. II. McGraw-Hill Book Co., New York. 550 pp.

Kenk, R. 1930. Beitrag zum system der Probursalter (Tricladida paludicola). *Z.* **89**: 145–162.

Kenk, R. 1953. The fresh-water triclads (Turbellaria) of Alaska. *Proc. U. S. N.* **103**: 163–186.

Kenk, R. 1973. Freshwater triclads (Turbellaria) of North America. V. the genus *Polycelis*. *Smithson. Contrib. Zool.* **135**: 1–15.

Lender, T. 1936. Sur *Polycelis nigra* (Ehrbg.) et *Polycelis tenuis* (Ijima) Turbellaries, Triclades. *Arch. Zool. Exp. Gen.* **78**: 49–56.

Reynoldson, T. B. 1966. The distribution and abundance of lake-dwelling triclads–towards a hypothesis. *Adv. Ecol. Res.* **3**: 1–71.

Smith, D. G. 1982. Distribution of the cambarid crayfish *Procambarus acutus acutus* (Girard) (Arthropoda: Decapoda) in New England. *Freshwater Biol.* **1**: 50–52.

Smith, D. G. 1983. A new species of fresh-water gammaroidean amphipod (Crangonyctidae) from southeastern New England. *Trans. Am. Microsc. Soc.* **102**: 355–365.

Smith, D. G. 1986. The occurrence of the troglobitic amphipod, *Stygobromus tenuis tenuis* (Smith) (Crangonyctidae) in the Taconic Mountains of southwestern Massachusetts (USA): a case for the existence of a subterranean refugium in a glaciated region. *Int. J. Speleol.* **14** (1984–1985): 31–37.

Vandel, A. 1921. Notes biologiques sur les Planaires des environs de Montpellier. *Bull. Biol. Fr. Belg.* **55**: 239–259.

Winsor, L. 1981. The taxonomy, zoogeography and biology of *Bipalium kewense* Moseley, 1878 (Tricladida, Terricola). *Hydrobiologia* **84**: 17.

Reference: *Biol. Bull.* **175:** 253–260. (October, 1988)

Temperature and Relative Humidity Effects on Aerial Exposure Tolerance in the Freshwater Bivalve *Corbicula fluminea*

ROGER A. BYRNE[1], ROBERT F. McMAHON[2], AND THOMAS H. DIETZ[1]

[1]*Department of Zoology and Physiology, Louisiana State University, Baton Rouge, Louisiana 70803, and* [2]*Section of Comparative Physiology, Department of Biology, Box 19498, The University of Texas at Arlington, Arlington, Texas 76019*

Abstract. The exposure tolerance, aerial respiratory behaviors, and the rates of water loss of the Asian freshwater clam, *Corbicula fluminea*, were assessed under three temperature conditions (15°, 25° and 35°C) and five relative humidity (RH) treatments (5%, 33%, 53%, 75% and 95%).

C. fluminea displayed low tolerance to aerial exposure (range of median tolerance times: 23.8–24.9 h at 35°C, 71.4–78.2 h at 25°C, and 248.5–341.6 at 15°C). Relative humidity had no effect on median tolerance time except at 15°C. Body size was reciprocally related to water loss rate at all temperatures, and on longevity at 25° and 35°C. Cumulative rates of water loss at 95% and 75% RH were lower than the other humidities at 15°C, but no differences were found at 25° or 35°C. Mantle edge exposure behavior was inhibited by low humidity and high temperature. Exposing mantle tissues did not increase rate of water loss except at humidities below which the behavior was very rare. The occurrence or extent of the behavior did not affect individual clam longevity. The results suggest that *C. fluminea* can detect rates of desiccation and make behavioral adjustments.

Introduction

The Asian clam, *Corbicula fluminea* (Müller) is a common inhabitant of freshwater habitats in the southern United States (McMahon, 1982, 1983a). Its migration to freshwater is relatively recent and evidence for its estuarine past exists in its higher blood osmolality and different ion ratios compared to other freshwater bivalves (Dietz, 1979). The adaptations displayed by *C. fluminea* for survival in freshwater must be recently evolved and may have arisen from estuarine/marine adaptations (Gainey, 1978). Furthermore, the adaptations of corbiculids are derived independently of those of another major freshwater bivalve family, the unionids.

Freshwater bivalve molluscs inhabiting shallow lentic or lotic habitats are subject to periodic emersion as water level drops. Typically, reduced water levels commonly occur during summer months when rainfall is lower and temperatures are higher. Emersion periods are not predictable in their duration or timing. As an adaptation to this stress, some freshwater bivalve species are capable of surviving up to a year out of water (Hiscock, 1953). McMahon (1979) showed that survivability of *C. fluminea* in air is affected by temperature and relative humidity. Associated with emersion are an array of behaviors which include gaping or mantle exposure. This appears to be associated with an aerial respiratory function (McMahon, 1979; McMahon and Williams, 1984). There is evidence that other freshwater bivalves can obtain oxygen directly across the valves (Collins, 1967; Dietz, 1974). Many intertidal marine bivalves maintain aerobic metabolism by continually gaping valves and allowing direct exchange of gasses with the atmosphere (Bayne *et al.*, 1976; Brinkhoff *et al.*, 1983; Shick *et al.*, 1986; for a review see McMahon, 1988). Exposure of large soft tissue surfaces to air should lead to water loss. Under prolonged aerial exposure conditions, *C. fluminea* must balance the advantages of maintaining an aerobic metabolic mode against the requirement to conserve water.

The aims of this study are to investigate the interrelationships of temperature and relative humidity on sur-

Received 20 February 1988; accepted 27 July 1988.

Abbreviations: RH: relative humidity, LSL: $\log_{10}$ shell length, ME: proportion of time spent with mantle exposed.

vivability of *C. fluminea* in air. We examined the effects of body size, and the occurrence and frequency of aerial respiratory behavior on water loss rates under these environmental conditions. We are particularly interested in the interplay between the requirement of preventing dehydration which necessitates valve closure and the metabolic advantages of maintaining contacts with the external environment.

Materials and Methods

Specimens of the Asian clam, *C. fluminea*, for all experiments were collected in June, 1985, from an outflow of Lake Benbrook, Tarrant County, Texas. Animals were maintained in filtered, aerated tapwater at laboratory temperatures (20°–23°C) for at least one week prior to use. A sample of 300 animals was used for the experiments, 20 per relative humidity/temperature combination. Each animal was identified by a lightly etched number on the left valve. The etchings removed the outer periostracal layer to reveal the light colored mineral underneath. It is unlikely that the etchings would have affected gas permeability. Specimens were blotted dry, weighed to the nearest 0.1 mg, and placed onto a desiccator plate in desiccators maintained at the appropriate relative humidity and temperature.

Five relative humidities were chosen, <5%, 33%, 53%, 75%, and >95%. These humidities were maintained in closed desiccators (plate diameter 190 mm) by using silica gel (<5%), supersaturated solutions of $MgCl_2 \cdot 6H_2O$ (33%), $Mg(NO_3)_2 \cdot 6H_2O$ (53%), NaCl (75%), and water (>95%). Salt solutions used to establish the various humidity values are from Wexler and Hasegawa (1954). Relative humidity was measured using a hygrometer (Airguide) and remained ±10% of the starting value during the experiments. Experiments were performed at 15°, 25°, and 35°C (±0.5°C), temperatures chosen to represent a range comparable with those experienced in the environment. Field observations show that individuals of this population when aerially exposed lie just beneath the surface of the sandy substratum, exposing little of the shell. Around 70–80% of the ventral aspect of the valve junction may be exposed. Under these conditions the effects of wind on evaporative loss are reduced and our design, which does not involve air movement, is appropriate.

Animals were reweighed at approximately 3, 6, or 12 hour intervals for 35°, 25°, and 15°C treatments, respectively. Prior to removing animals from the desiccators, the number of individuals exposing the mantle edge, a respiratory behavior, was noted, as were occasions when obvious quantities of fluid had been expelled. At death, the soft tissue was excised, dried to constant weight (>48 h, 90°C) and weighed. The shell was blotted dry and weighed. The experiment continued until all animals were dead.

The total available water [total weight at beginning of the experiment − (wet shell weight + dry tissue weight)], was calculated for each individual. Water loss was expressed as cumulative percent water lost (100 × weight lost since the start of the experiment/total available water). The points on the curves of the time course of cumulative water loss (Figs 1B, 2B, and 3B) represent values for a standard (grand mean sized) animal of 20.3 mm shell length. Values were derived by performing regression analyses of $\log_{10}$ shell length *versus* cumulative water loss at each sampling interval, and deriving an estimate for a 20.3 mm animal from the regression equation. The number of animals used for the regression analyses (the survivor number) ranged from 20 at the beginning to 3 near the end of the experiments. Of the approximately 150 separate regressions performed, 66% were significant ($P < 0.05$). A significant size relationship to cumulative water loss was more prevalent at 15°C and 25°C (85 and 93% of regressions performed, respectively) than at 35°C (33%). If no significant relationship was indicated ($P > 0.05$) then the mean water loss was utilized.

Hourly rates of water loss were calculated as the percent water lost/sampling interval duration and were categorized as to whether the animal was exposing mantle edge tissues, had closed valves, or had expelled fluid during the sampling interval. Analyses of variance using a repeated measures design on $\log_{10}$ transformed rates were performed, followed by Duncan's multiple range tests to determine differences between temperatures. Analyses of covariance were run with $\log_{10}$ shell length as the covariate and Duncan's multiple range tests were performed to detect relative humidity effects within each temperature. Student's *t*-tests were performed on paired comparisons of water loss rates when valves were closed, when exposing mantle tissues, and when fluid was expelled for each animal at each temperature/relative humidity combination. An index of individual clam behavior is the proportion of time a clam spends with mantle exposed (ME), exclusive of periods during which mantle fluid was expelled. A multiple regression relating clam longevity to relative humidity, $\log_{10}$ shell length, and ME was performed.

Median tolerance times (TLm or LT_{50}, the elapsed time to 50% mortality) were calculated from the mortality data using the SAS PROBIT procedure (SAS, Cary, NC). Probit analysis transforms the sigmoid time/mortality curve to a linear shape and, by means of linear regression, a mid-point or median value can be derived. Significant differences in median tolerance times were detected by non-overlap of 95% fiducial limits. Other statistical tests also utilized SAS procedures.

Results

There was a significant ($P < 0.05$) temperature effect on median tolerance time (TLm) (Table I) resulting in

Table I

Median tolerance times, time elapsed (hours) to 50% mortality as determined by probit analysis, for Corbicula fluminea *under various conditions of temperature and relative humidity*

	Median tolerance times (hours) relative humidity				
Temp.	<5%	33%	53%	75%	>95%
15°C	259.7 A	248.5 A	253.0 A	305.4 B	341.6 C
25°C	72.2 A	71.4 A	73.4 A	78.2 A	75.6 A
35°C	23.8 A	24.0 A	24.0 A	24.4 A	24.9 A

Different letters within a temperature treatment (rows) indicate non-overlap of 95% fiducial limits between those relative humidity treatments.

an approximately threefold increase in TLm with every 10°C decline in temperature. At 15°C, the TLm's at 75% and at 95% RH were significantly different ($P < 0.05$) from one another and both were higher than those at the other relative humidities. No such relationship of relative humidity to TLm was found at either of the other temperature treatments.

During emersion, *C. fluminea* displayed three categories of behavior. The first was simply the closed condition with valves tightly shut, displaying no tissue directly to the environment. The second behavior was that described by McMahon (1979) where the leading edge of the mantle tissue is protruded past slightly gaping valves so that moist tissue is exposed. This mantle edge exposure behavior has been linked to possible aerial oxygen uptake (McMahon and Williams, 1984). Under conditions of lower relative humidity the exposed tissues may appear dry, or a hardened mucus may form between the parted valves. Clams displaying these conditions also were scored as exposing mantle tissues. The third category of behavior was a complete or partial emptying of the mantle cavity water store. This was evidenced at higher humidities by a pool of fluid around the animal. At lower humidities the fluid may have dried, but evidence in the form of dried matter around the animal was an indication that fluid had been expelled.

Mantle edge exposure was influenced both by temperature and relative humidity (Figs 1A, 2A and 3A). High temperature (35°C) inhibited exposure (Fig. 3A), whereas at 25°C and 15°C mantle edge exposure was controlled primarily by relative humidity (Figs 2A and 1A). At 15°C (Fig. 1A) the behavior was observed at every relative humidity treatment. However, the incidence of mantle edge exposure was inhibited at humidities of 33% or lower. At 95% RH, approximately 40% of individuals were exposing tissue at any time. The initial incidence of mantle edge exposure behavior at 75% RH and 15°C was similar to that at 95% RH (Fig. 1A). At 53% RH mantle edge exposure behavior was reduced and occurred in two bouts, the first during the initial 100 hours of emersion and a second commenced after 200 hours. During these periods few (<20%) individuals were displaying the behavior. The incidence of the behavior was reduced even more at 33% and 5% RH.

At 25°C mantle edge exposure behavior, with one exception, was confined to relative humidities of 53% or greater (Fig. 2A). A distinct correlation existed between the frequency of mantle edge exposure behavior and relative humidity. Fifty to eighty percent of individuals at 95% RH were displaying the behavior between 24 and 54 hours of emersion. During the same period, individuals at 75% RH were exposing mantle 10–40% of the time, while 5–20% of those at 53% RH were exposing tissues.

At 35°C mantle edge exposure behavior was curtailed (Fig. 3A). The occurrences were limited to 53% RH and

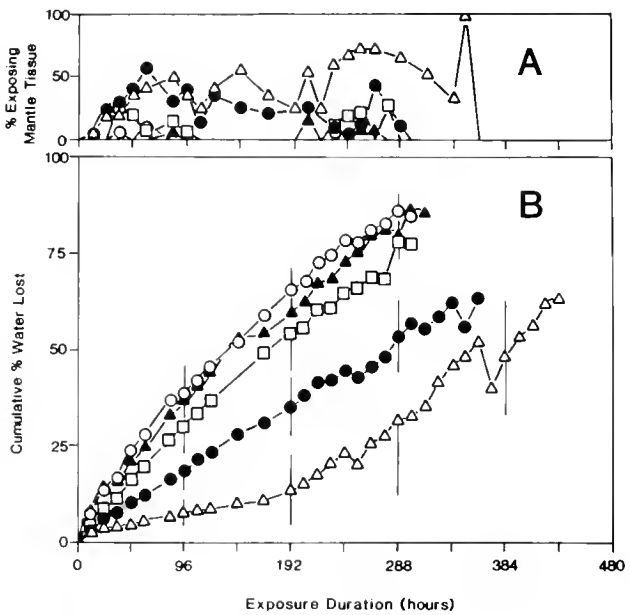

Figure 1. A. Time course of occurrence of mantle edge exposure behavior in *Corbicula fluminea* under five relative humidity treatments at 15°C. Mantle edge exposure behavior is quantified as the percent of individuals observed with mantle protruding at the close of a sampling interval. The abscissal scale is the same as for Figure 1B. Symbols represent △—>95% RH; ●—75% RH; □—53% RH; ○—33% RH; ▲—<5% RH.

B. Time course of cumulative percent body water lost for a standard sized (20.3 mm shell length) *Corbicula fluminea* under the same five relative humidity treatments at 15°C as in Figure 1A (symbols the same as Fig. 1A). The points represent estimations of the cumulative water lost for this standard sized animal based on linear regressions of $\log_{10}$ shell length on cumulative percent water lost where these regressions were significant ($P < 0.05$, 85% were significant). Where regressions proved not significant mean cumulative water loss is recorded. The number of animals ranged from 20 at the beginning of the experiment to 3 at the close. The vertical bars are standard errors of the estimate. For clarity, error bars were included at intervals. Declines in cumulative water lost were due to mortality.

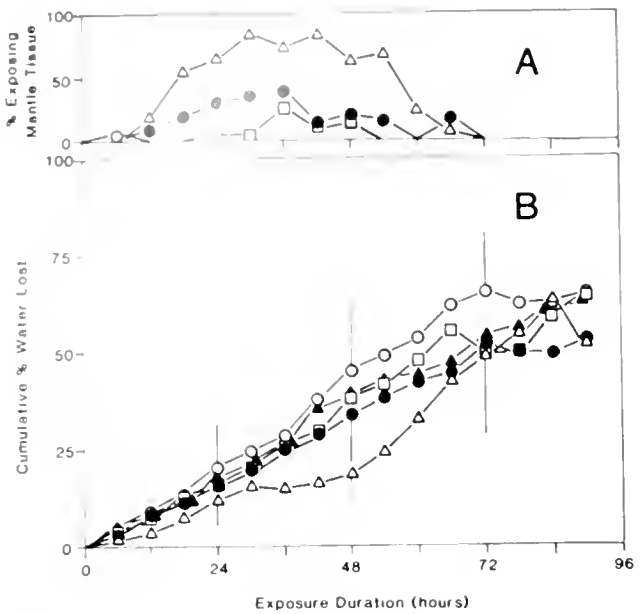

Figure 2. A. Time course of occurrence of mantle edge exposure behavior in *Corbicula fluminea* under five relative humidity treatments at 25°C. Mantle edge exposure behavior is quantified as in Figure 1A. The abscissal scale is the same as for Figure 2B. Symbols represent △—>95% RH; ●—75% RH; □—53% RH; ○—33% RH; ▲—<5% RH.

B. Time course of cumulative percent body water lost for a standard sized (20.3 mm shell length) *Corbicula fluminea* under the same five relative humidity treatments at 25°C as in Figure 2A (symbols the same as Figure 2A). Methods for calculating curves were the same as in Figure 1B. Approximately 93% of the size-water loss regressions were significant ($P < 0.05$). Declines in cumulative water lost were due to mortality.

above, with only single individuals recorded at 53%. The maximum occurrence was only 30% at 95% RH and less at the lower humidities. The incidences of the behavior were reduced during the period of accelerated water loss (see Fig. 3B), and ceased after 21 hours emersion.

At 15°C the pattern of cumulative water loss showed a distinct relative humidity effect (Fig. 1B). Cumulative water loss values for 5, 33, and 53% RH cluster together and display no differences at any interval. The curves for these treatments are approximately linear throughout the experiment. The curves for 75 and 95% RH are lower than the other relative humidity treatments. The 75% curve was linear whereas the 95% curve showed an initial slow increase followed by an acceleration to a higher loss rate later in the experiment.

At 25°C levels of water loss (Fig. 2B) were 2–6 times those at 15°C. Water loss levels for 5–75% RH were approximately linear and clustered together. At no time during the experiment was any significant difference ($P > 0.05$) found in water loss between the relative humidity treatments.

Cumulative water loss from clams at 35°C (Fig. 3B) was 2–3 times the 25°C values. Water loss was similar for all relative humidities and no significant differences ($P > 0.05$) were found between treatments. The curves of cumulative water loss were non-linear, showing an increase after 15–18 hours exposure, leveling off at 24 hours as mortality increased.

Overall hourly rates of water loss showed a threefold increase from 15°C to 25°C and a doubling from 25°C to 35°C (Fig. 4). The magnitude of these differences was reduced when rates of water loss during periods of valve closure were considered. When examining rates during both mantle exposure and fluid expulsion, in most cases temperature differences were more pronounced. There were significant differences ($P < 0.05$) between temperature treatments for all relative humidities and behavioral categories except for rates when fluid was expelled between 25° and 35°C at 33% and 53% RH.

No significant differences ($P > 0.05$) in overall rates of water loss existed between 5% and 53% RH treatments at 15°C (Fig. 4). The water loss rates at 75% and 95% RH were significantly less ($P < 0.05$) than the rates at the lower humidities. At 25°C and 35°C no differences in overall mean hourly water loss rates were found between the relative humidity treatments.

When rates of water loss after periods of valve closure

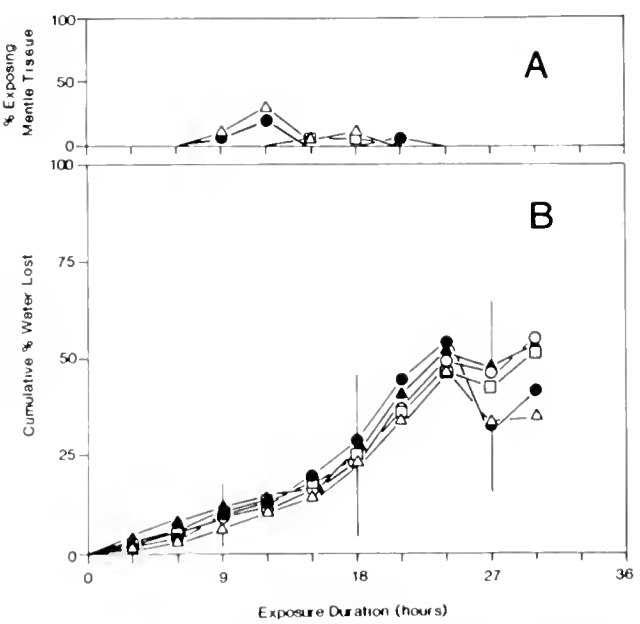

Figure 3. A. Time course of occurrence of mantle edge exposure behavior in *Corbicula fluminea* under five relative humidity treatments at 35°C. Mantle edge exposure behavior is quantified as in Figure 1A. The abscissal scale is the same as for Figure 3B. Symbols represent △—>95% RH; ●—75% RH; □—53% RH; ○—33% RH; ▲—<5% RH.

B. Time course of cumulative percent body water lost for a standard sized (20.3 mm shell length) *Corbicula fluminea* under the same five relative humidity treatments at 35°C as in Figure 3A (symbols the same as Fig. 3A). Methods for calculating curves were the same as in Figure 1B. Only 33% of size-water loss regressions were significant. Declines in cumulative water lost were due to mortality.

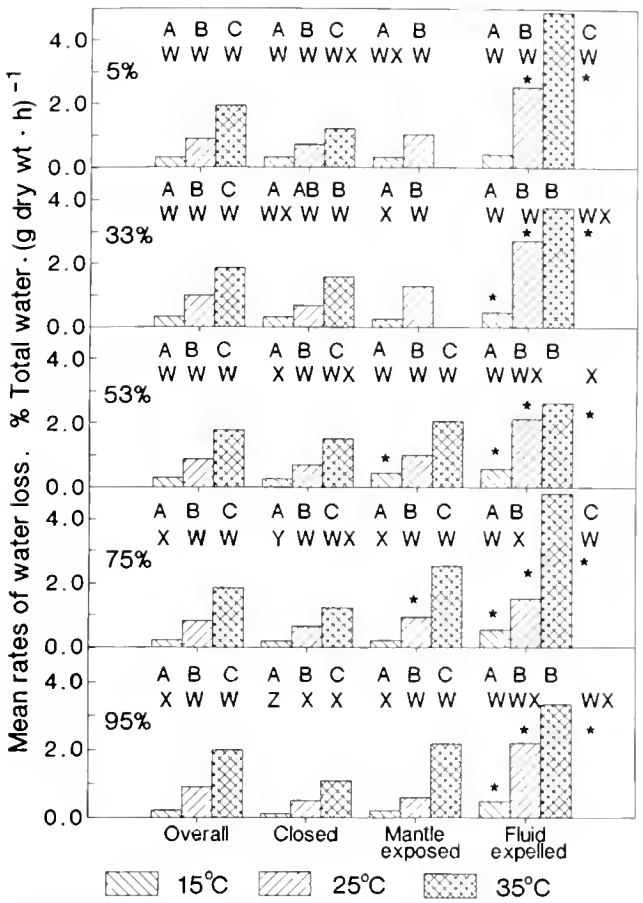

Figure 4. Mean rates of water loss for *Corbicula fluminea* at five relative humidity treatments (5%, 33%, 53%, 75%, and 95%) and three temperatures (15°C, 25°C, and 35°C). Rates of water loss are divided into four behavioral categories (overall average, with closed valves, with mantle exposed, and after fluid expulsion from the mantle cavity; see text). The letters A, B, and C refer to results of Duncan's multiple range tests comparing rates between temperatures, within a relative humidity and behavioral category. Categories marked with dissimilar letters denote significant differences ($P < 0.05$). The letters W, X, Y, and Z refer to results of Duncan's multiple range tests comparing rates between relative humidity treatments, within a temperature and behavioral category. Categories with dissimilar letters denote significant differences ($P < 0.05$). The asterisks denote significant differences ($P < 0.05$; paired 't' test) in mean rates between both the "mantle exposed" and "fluid expelled" behavioral categories and the "closed" category, within each temperature and relative humidity treatment.

(Fig. 4) were examined there were distinct relative humidity effects especially at 15°C. At this temperature the mean rate of water loss at 95% RH was only 40% of the 5% or 33% RH rate. These differences were less apparent at 25°C where the rate at 95% RH was significantly less than the other rates, but represented at most only a 30% reduction. At 35°C there was no consistent pattern of relative humidity effects on mean rates of water loss when valves were closed.

Rates of water loss after periods of mantle edge exposure (Fig. 4) showed no significant differences between relative humidity treatments at 25°C or 35°C, and no consistent relative humidity effect was found at 15°C. Similarly, rates when fluid was expelled showed no significant ($P > 0.05$) relative humidity effect at any temperature.

No significant differences were found between rates of water loss when valves were closed and rates when mantle edge tissue was exposed at 95% RH at any of the temperatures (Fig. 4). At 15°C when the mantle edge was exposed, the water loss rate was significantly higher than the rate at 53% RH when valves were closed, whereas at 25°C the loss rate when mantle was exposed was significantly higher at 75% RH. Rates of water loss when closed and when exposing mantle tissues were not significantly different at 35°C, at which temperature the behavior of exposing mantle tissues is non-existent at relative humidities below 53%, and is uncommon even at higher humidities. In most cases rates when fluid was expelled were significantly ($P < 0.05$) higher than when closed (Fig. 4). Only the rates at 15°C and 5% RH were not significantly different.

The multiple regression equation relating longevity to relative humidity, $\log_{10}$ shell length, and ME (mantle edge exposure behavior) is shown in Table IIA. Relative humidity had a significant ($P < 0.05$) effect on longevity at 15°C only, as would be expected from the median tolerance time statistics. Animal size had a significant negative effect at both 25°C and 35°C. No significant effect of

Table II

Multiple regression variable estimates relating Corbicula fluminea *aerial longevity (A) and mean water loss rate while closed (B), to relative humidity (RH), $\log_{10}$ shell length (LSL), and average proportion of time spent with mantle exposed (ME) (longevity only) at 15°, 25°, and 35°C*

	Intercept	RH	LSL	ME	R^2
		A. Longevity (hours)			
15°C	209.3*	0.897*	−2.6	21.7	0.22*
	(99.3)	(0.294)	(75.6)	(46.7)	
25°C	122.1*	0.069	−47.1*	−2.0	0.08
	(26.1)	(0.060)	(20.1)	(6.7)	
35°C	41.2*	0.006	−17.0*	1.5	0.12*
	(6.4)	(0.012)	(4.8)	(3.1)	
		B. Mean water loss rate (valves closed) (% body water · hour^{-1})			
15°C	0.959*	−0.0021*	−0.462*		0.52*
	(0.126)	(0.0003)	(0.097)		
25°C	3.40*	−0.0017*	−2.061*		0.36*
	(0.39)	(0.0007)	(0.304)		
35°C	4.18*	−0.0024	−2.077*		0.06
	(1.22)	(0.0023)	(0.927)		

Values in parentheses are standard errors of estimates. Asterisks indicate estimates significantly different from zero ($P < 0.05$).

mantle edge exposure behavior on clam longevity was noted at any of the temperatures.

Larger individuals lose water at a slower rate than smaller clams as there was a consistently significant ($P < 0.05$) negative effect of body size, as measured by the $\log_{10}$ of shell length, on mean water loss rate when valves were closed at all temperatures (Table IIB). There also was a significant effect of relative humidity at 15°C and 25°C, as would be expected from the results in Figure 4. Relative humidity had a significant effect on water loss after mantle edge exposure at 15°C and 25°C ($P < 0.05$).

Discussion

Temperature is the major factor affecting water loss rate, exposure tolerance, and mantle edge exposure behavior in *C. fluminea* under conditions of prolonged aerial exposure. The effects of relative humidity are less pervasive but significant. Whether water loss is determined as cumulative loss or mean hourly loss rates, relative humidity has little or no effect at 25 or 35°C. At 15°C a distinct mediating effect of higher relative humidities is detected. The major influence of relative humidity is on the incidence of mantle edge exposure behavior. Although temperature is dominant in determining the extent of this response, within a temperature treatment, increases in relative humidity increase the frequency of mantle edge exposure behavior. This indicates that specimens of *C. fluminea* can perceive desiccation and compensate behaviorally. This ability is further evidenced by examining rates of water loss in individuals with closed valves and after bouts of mantle edge exposure. Under conditions of high relative humidity there is no difference in rates of water loss within a temperature group. Significant increases in water loss rate occur only at relative humidities where mantle edge exposure behavior is transitional between being commonplace and being rare. Thus, under conditions where there are no adverse consequences of exposing tissues with regard to losing water, then the behavior is common. When water loss rates exceed rates when the animal has closed valves, then the behavior is inhibited.

The occurrence of a second period of mantle edge exposure behavior at the lower humidities suggests additional factors become important. When clams had lost 60–70% of body water, which corresponds to the total mantle cavity water store plus some hemolymph water (McMahon, 1983), a second bout of mantle edge exposure behavior is observed. In all cases this behavior is displayed in individuals close to death and might represent a loss of muscle tone associated with a weakened condition. Another possibility is that it represents a final gas exchange event prior to complete shutdown to conserve water.

Clams that expose tissues extensively do not survive longer than those that remain closed for extended periods. Furthermore, there is no relative humidity effect on median tolerance time at 25°C even though mantle edge exposure is significantly enhanced by higher relative humidity. Thus the adaptive significance to mantle edge exposure is obscure. McMahon and Williams (1984) showed a direct relationship between duration of mantle edge exposure behavior and aerial oxygen uptake. Other experiments (Byrne, unpub.) show that clams prevented from gaping their valves in air have a lower median tolerance time than those permitted to expose tissues (at 20°C and 95% RH the TLm is 154 hours when allowed to open valves, and is only 96 hours with valves prevented from opening, $P < 0.05$).

There are several adaptive explanations of mantle edge exposure behavior. First, it is possible that gas exchange necessary for the maintenance of aerobic metabolism may be accomplished with little exposure of tissues. The measurement of mantle edge exposure utilized here is essentially a "snapshot" of behavior. There is evidence (Byrne, unpub.) that clams, in addition to the more constant mantle edge exposure behavior also perform valve movements which ventilate the mantle cavity. Such behaviors are relatively short in duration and could be missed. Second, being out of water, there would be a buildup of metabolic waste products including dissolved CO_2 and concomitant acid-base problems as a result of reduction in gas exchange capability. Intermittent mantle edge exposure may aid gas exchange but may not significantly alter hemolymph solute concentrations, which might be the cause of the reduced survival time. Under aerial exposure conditions, blood osmolality increases threefold and calcium levels rise fourfold indicating mobilization of calcium carbonate from the shell (Byrne, unpub.). Third, the behavior may conserve energy stores. Even the most energy "efficient" anaerobic pathways are far less efficient than aerobic metabolism (Hochachka and Somero, 1984). Although the extent of the mantle edge exposure did not increase the survival time in air, the animal might have been conserving limited energy stores by maintaining aerobic metabolism. Whereas aerial survival would not be influenced by mantle edge exposure, subsequent abilities to resume aquatic existence would be enhanced in individuals that conserved substrates (McMahon, 1988).

The effect of body size on the ability to survive aerial exposure is two sided. There is a distinct reciprocal relationship between size and water loss rate. However, at 25 and 35°C there also is a negative relationship between individual clam longevity and size. The temperature effect is most severe at 35°C whereas size-dependent effects on water loss rates are significant at all temperatures. Thus, under short term conditions of aerial exposure, larger clams would have an adaptive advantage over smaller clams because of the larger clam's slower

rate of water loss. The effect of body size is not significant after periods of mantle edge exposure suggesting that evaporative water loss under these conditions is a simple function of the linear size of the exposed mantle, an almost two-dimensional surface, rather than being related to a surface area of the whole clam while valves are closed.

When compared to other freshwater bivalves, *C. fluminea* displays a low tolerance of aerial exposure. McMahon (1979) showed a somewhat longer aerial exposure tolerance for *C. fluminea* than reported here, but also found that relative humidity had an effect on median tolerance time at the lower temperature (20°C). Mantle edge exposure behavior was inhibited completely at the lower humidity (approximately 5% RH), but was common at the higher humidity (*ca.* 95% RH). The unionid *Ligumia subrostrata* could survive up to 40 days exposure under conditions of high relative humidity at temperatures of 22°–25°C (Dietz, 1974). An Australian unionid, *Hyridella australis,* apparently is capable of withstanding at least 60 days of exposure at room temperatures (Hiscock, 1953). *Sphaerium occidentale,* the fingernail clam, can survive aerial exposure for up to a month; the survival time is related to relative humidity (Collins, 1967). This species undergoes a period of aestivation during which the tolerance to aerial exposure is increased (McKee and Mackie, 1980). Non-aestivating *S. occidentale* has a median tolerance time at 20°C of 1–3 days, and aestivating clams 8–34 days, the range controlled by relative humidity. The record for exposure endurance is held by the African unionid, *Aspatharia petersi,* which has been reported to survive over a year out of water (Dance, 1958).

The lower tolerance of *C. fluminea* to exposure is similar to that of more marine/estuarine species. Median tolerance times for *Cerastroderma edule* at high relative humidity range from 129 h at 15°C to 9.5 h at 35°C (Boyden, 1972). These values are lower than those of *C. fluminea,* but represent an extended tolerance when compared to less-often exposed marine bivalves. *Cerastroderma glaucum,* found subtidally, has TLm's of 86.7, 42, and 9.7 h at 15, 25, and 35°C, respectively (Boyden, 1972). *Cerastroderma edule* gapes almost continuously when emersed and can survive 42.9% of tissue water loss, whereas *C. glaucum* remains closed on exposure and can withstand only 33% tissue water loss (Boyden, 1972). However, the high intertidal bivalve *Modiolus modiolus* air gapes while emersed and has a TLm of 9 days in air at 24.5°C (Lent, 1968). Survival time is associated with the volume of oxygen present in the atmosphere. Desiccation is an unavoidable side effect of an aerial respiratory adaptation (Lent, 1968).

Pulmonate snails represent a group of molluscs that have adapted to a range of habitats from completely terrestrial to obligate aquatic (McMahon, 1983b). Length of survival in air depends on the rate of water loss from the snail (Machin, 1975). Tolerance of a high loss of body water results in increased tolerance times. *Biomphalaria glabrata* can withstand 70% reduction in total body water and has a TLm of 64 days at 27°C at 96% RH (von Brand *et al.,* 1957). There are sharp distinctions of TLm between relative humidity treatments ranging down to 2.8 days at 15% RH (von Brand *et al.,* 1957). *Melampus bidentatus* can lose up to 78.5% of its body water (Price, 1980) and there is a major effect of body size in that larger snails can withstand in excess of 14 days exposure at 20°C and 97% RH whereas juvenile snails cannot survive 12 hours emersion without free water.

C. fluminea when aerially exposed under conditions of low humidity may form a hardened mucus between slightly parted valves. This is superficially similar to the epiphragm sometimes produced by estivating stylomatophoran snails which is thought to function in retarding evaporative water loss by reducing convective movement of air over moist tissues (Machin, 1975). The hardened mucus may perform a similar function in *C. fluminea* while also allowing a diffusive contact with the environment for gas exchange purposes.

It has been noted previously (McMahon, 1979, 1983a; McMahon and Williams, 1984) that *C. fluminea,* because of its relatively recent history in freshwater, displays physiological and behavioral adaptations that seem to be intermediate between those of more ancient freshwater forms such as the unionids and sphaeriids, and its estuarine and marine relatives. Its blood osmolality is higher, and the major hemolymph ions differ from those of unionids (Dietz, 1979). McMahon and Williams (1984) suggested that the respiratory adaptation to aerial exposure is intermediate between the continual gaping of some intertidal bivalves (*e.g., Cerastroderma edule*) and the closed valve response of unionids, or the transvalvular gas exchange capabilities of some sphaeriids. This intermediate nature also is evidenced in this study by the lower exposure tolerances found for this species when compared to most other freshwater bivalves, and the higher tolerance than that reported for most of estuarine/intertidal lamellibranchs.

There are two major problems facing a clam that has been exposed in air. First, there is the problem of maintaining metabolism and homeostasis without the normal modes of waste excretion, gas exchange, and ion regulation. Second, there is the loss of fluid either by passive surface evaporation or by active expulsion. Loss of nutritional opportunities frequently is regarded as not very significant owing to the overriding importance and immediacy of the other factors. However, in *C. fluminea,* carbohydrate stores are limited (Williams and McMahon, 1985) and prolonged emersion might cause severe carbohydrate depletion. Preserving water stores necessitates maintaining closed valves and preventing contact

with the external environment. Ameliorating internal conditions in the face of declining oxygen tensions, increasing carbon dioxide tensions, and increasing concentrations of metabolites requires some gas exchange with the environment and the consequent exposure of living tissues to a more or less arid atmosphere.

Corbicula fluminea possesses adaptations which enable it to survive periods of emersion longer than its estuarine relatives. Apparently *C. fluminea* can detect the loss of water and modify its gas exchange behavior accordingly. It can withstand a loss of up to 60% of its available water; however, it does not display the capabilities of some unionid species to withstand very long periods of aerial emersion. Unlike the marine and estuarine environments, freshwater animals may experience periods of emersion that are unpredictable either in timing or duration. Some unionid clams, with their long history in freshwater, appear to have evolved adaptations enabling them to withstand protracted exposure. *C. fluminea* in its own adaptations shows interesting modes of prolonging existence out of water. These adaptations, including the modification of the "gaping" behavior in response to temperature and relative humidity may be regarded as intermediate in nature between those of more ancient freshwater and estuarine forms, but might also be looked upon as novel adaptations to a new environment by a relatively recent invader.

Acknowledgments

We thank Edith Byrne, David Long, and Bruce Whitehead for assistance in data collection, Dr. Harold Silverman for critically reviewing the manuscript, and Vicki Lancaster for advice on statistics. This study forms part of a dissertation submitted by RAB to the Graduate School of Louisiana State University and A&M College in partial fulfillment of the Ph.D. degree. Supported by research grant from the University of Texas at Arlington to RFM and NSF grants DCB 83-03789 and DCB 87-01504 to THD.

Literature Cited

Bayne, B. L., C. J. Bayne, T. C. Carefoot, and R. J. Thompson. 1976. The physiological ecology of *Mytilus californianus* Conrad. 2. Adaptations to low oxygen tensions and air exposure. *Oecologia (Berl.)* 22: 211–228.

Boyden, C. R. 1971. Aerial respiration of the cockle *Cerastoderma edule* in relation to temperature. *Comp. Biochem. Physiol.* **43A:** 697–712.

von Brand, T., P. McMahon, and M. O. Nolan. 1957. Physiological observations on starvation and desiccation of the snail *Australorbis glabratus*. *Biol. Bull.* 113: 339.

Brinkhoff, N., K. Stockmann, and M. Grieshaber. 1983. Natural occurrence of anaerobiosis in mollusks from intertidal habitats. *Oecologia* 57: 151–155.

Collins, T. W. 1967. Oxygen-uptake, shell morphology and desiccation of the fingernail clam, *Sphaerium occidentale* Prime. Ph.D. Thesis. University of Minnesota. 166 pp. (*Diss. Abstr.* **28B:** 5238).

Dance, S. P. 1958. Drought resistance in an African freshwater bivalve. *J. Conchol.* **24:** 281–282.

Dietz, T. H. 1974. Body fluid composition and aerial oxygen consumption in the freshwater mussel, *Ligumia subrostrata* (Say): effects of dehydration and anoxic stress. *Biol. Bull.* **147:** 560–572.

Dietz, T. H. 1979. Uptake of sodium and chloride by freshwater mussels. *Can. J. Zool.* **57:** 156–160.

Gainey, L. F., Jr. 1978. The response of the Corbiculidae (Mollusca: Bivalvia) to osmotic stress: the cellular response. *Physiol. Zool.* **51:** 79–91.

Hiscock, I. D. 1953. Osmoregulation in Australian freshwater mussels (Lamellibranchiata). I. Water and chloride ion exchange in *Hyridella australis* (Lam.). *Aust. J. Mar. Freshwater Res.* **1:** 317–329.

Hochachka, P. W., and G. N. Somero. 1984. *Biochemical Adaptation.* Princeton University Press, Princeton, New Jersey. 537 pp.

Lent, C. M. 1968. Air-gaping by the ribbed mussel, *Modiolus demissus* (Dillwyn): effects and adaptive significance. *Biol. Bull.* **134:** 60–73.

Machin, J. 1975. Water relationships. In *Pulmonates* vol. 1. *Functional Anatomy and Physiology.* V. Fretter and J. Peake, eds. Academic Press, London.

McKee, P. M., and G. L. Mackie. 1980. Desiccation resistance in *Sphaerium occidentale* and *Musculium securis* (Bivalvia: Sphaeriidae) from a temporary pond. *Can. J. Zool.* **58:** 1693–1696.

McMahon, R. F. 1979. Tolerance of aerial exposure in the Asiatic freshwater clam, *Corbicula fluminea* (Müller). Pp. 227–241 in *Proceedings, First International Corbicula Symposium.* J. C. Britton, ed. Texas Christian University Research Foundation, Fort Worth.

McMahon, R. F. 1982. The occurrence and spread of the introduced Asiatic freshwater clam, *Corbicula fluminea* (Müller), in North America. *Nautilus* **96:** 134–141.

McMahon, R. F. 1983a. Ecology of an invasive pest bivalve, *Corbicula.* In *The Mollusca* vol. 6. *Ecology,* W. D. Russell-Hunter, ed. Academic Press, San Diego.

McMahon, R. F. 1983b. Physiological ecology of freshwater pulmonates. In *The Mollusca* vol. 6. *Ecology,* W. D. Russell-Hunter, ed. Academic Press, San Diego.

McMahon, R. F. 1988. Respiratory response to periodic emergence in intertidal molluscs. In *Physiological Compensation in Intertidal Animals Symposium.* R. Ellington and B. R. McMahon eds. *Am. Zool.* **28:** 97–114.

McMahon, R. F., and C. J. Williams. 1984. A unique respiratory adaptation to emersion in the introduced Asian freshwater clam *Corbicula fluminea* (Müller) (Lamellibranchia: Corbiculacea). *Physiol. Zool.* **57:** 274–279.

Price, C. H. 1980. Water relations and physiological ecology of the salt marsh snail, *Melampus bidentatus* Say. *J. Exp. Mar. Biol. Ecol.* **45:** 51–67.

Shick, J. M., E. Gnaiger, J. Widdows, B. L. Bayne, and A. de Zwaan. 1986. Activity and metabolism in the mussel *Mytilus edulis* L. during intertidal hypoxia and aerobic recovery. *Physiol. Zool.* **59:** 627–642.

Wexler, A., and S. Hasegawa. 1954. Relative humidity-temperature relationships of some saturated salt solutions in the temperature range 0 to 50°C. *J. Res. Nat. Bur. Stand.* **53:** 19–26.

Williams, C. J., and R. F. McMahon. 1985. Seasonal variation in oxygen consumption rates, nitrogen excretion rates and tissue organic carbon: nitrogen ratios in the introduced Asian freshwater bivalve, *Corbicula fluminea* (Muller) (Lamellibranchia: Corbiculacea). *Int. Malacol. Bull.* **3:** 267–268.

Reference: *Biol. Bull.* **175:** 261–273. (October, 1988)

Visual Spectral Sensitivities of Bioluminescent Deep-sea Crustaceans

TAMARA M. FRANK[1] AND JAMES F. CASE

Department of Biological Sciences and Marine Science Institute, University of California, Santa Barbara, California 93106

Abstract. The spectral sensitivities of eight species of deep-sea decapod shrimps (Family Oplophoridae) were determined from shipboard measurements of electroretinograms of dark-captured specimens. *Notostomus gibbosus* and *N. elegans* are maximally sensitive at 490 nm, and chromatic adaptation experiments indicate that a single visual pigment is present. Peak sensitivities of *Acanthephyra smithi* and *A. curtirostris* are at 510 nm, a longer wavelength than expected for such deep-sea dwellers. The four photophore-bearing species, *Systellaspis debilis, Janicella spinacauda, Oplophorus spinosus,* and *O. gracilirostris* have sensitivity maxima at 400 and 500 nm, and chromatic adaptation experiments indicate the presence of two visual pigments. This unusual short wavelength sensitivity may provide the basis for congener recognition based on the spectral bandwidth of luminescence.

Introduction

The light field in the deep-sea consists of essentially monochromatic light from two sources: (1) dim downwelling light with a chromatic spectrum centering on 475 nm (Jerlov, 1968; Dartnall, 1974; Cronin, 1986); and (2) bioluminescence, with spectra characteristically peaking at 460–490 nm (Herring, 1983; Widder *et al.*, 1983; Latz *et al.*, 1988). It has long been assumed that the visual systems of deep-sea organisms would also have monochromatic sensitivity, with visual pigment absorption maxima blue-shifted (as compared with shallow water species) for maximum sensitivity to the existing light regime (Bayliss *et al.*, 1936; Clarke, 1936; Goldsmith, 1972; Shaw and Stowe, 1982; Cronin, 1986). Almost all studies on deep-sea fish (Denton and Warren, 1957; Munz, 1957; Wald *et al.*, 1957; Denton and Shaw, 1963; Fernandez, 1978; Crescitelli *et al.*, 1985), cephalopods (Hara and Hara, 1979) and crustaceans (Fisher and Goldie, 1958, 1960; Denys and Brown, 1982) support this hypothesis, reporting single visual pigment systems with absorption maxima between 470 and 490 nm, in contrast with maxima of 490–550 for shallow water species (reviewed by Goldsmith, 1972; Lythgoe, 1972). However, these studies were performed on visual pigment extracts or *via* microspectrophotometry (MSP), which provide excellent information on the absorption characteristics of the visual pigments (see Menzel, 1979, for review of problems associated with extracts of invertebrate visual pigments), but may not necessarily reflect the physiological spectral sensitivity. For example, in the crayfish, *Procambarus*, the spectral sensitivity of the dark-adapted eye, measured electrophysiologically, peaks at about 570 nm (Wald, 1968), while the λ_{max} of the visual pigment is 530 nm; (Cummins and Goldsmith, 1981). Similar, though smaller, red shifts in spectral sensitivity are also found in the lobster, *Homarus*, (Wald and Hubbard, 1957; Wald, 1968) and the shrimp, *Palaemonetes*, (Fernandez, 1965; Wald and Seldin, 1968; Goldsmith and Fernandez, 1968). Goldsmith (1978) found that these shifts could be attributed to the filtering effects of red-leaky screening pigments. It is difficult, from pigment extract and MSP data, to accurately assess the degree of pre-retinal filtering and its effect on spectral sensitivity, but this must be taken into account before making any assessment of an organism's visual capacity.

Recording the electroretinogram, the mass response of a large number of photoreceptor cells to a flash of light, is a simple way to obtain physiologically relevant information about an organism's visual capabilities. For our

Received 24 December 1987; accepted 28 July 1988.

[1] Current Address: Department of Physiology, University of Connecticut Health Center, Farmington, CT 06032.

purposes, it is superior to intracellular recording methods because of the ease of working on a vibrating, unstable ship. Although data from this method cannot definitively establish whether one or several visual pigments are present, there is excellent evidence that ERG-determined peaks correspond to spectral cell types (Goldsmith and Fernandez, 1968; Stieve *et al.*, 1978; Laughlin *et al.*, 1980; Cummins and Goldsmith, 1981; Goldsmith, 1986) and this method is often the method of choice for comparative studies, particularly on previously untested organisms (Kobayashi and Ali, 1971; Iguchi *et al.*, 1982).

The first evidence for a short wavelength receptor in a deep-sea organism comes from Wald and Rayport's (1977) electrophysiological study of the alciopid worm *Vanadis*. Its dark-adapted spectral sensitivity curve exhibits a violet shoulder in addition to a blue-green peak, and response waveforms to 380 nm light are different from those to 480 nm light, arguing for the presence of two spectral classes of photoreceptor cells.

The fact that this is the only example of enhanced short wavelength sensitivity in deep-sea organisms may be because so few animals from this environment have been studied electrophysiologically. While both pigment extracts and MSP have proven successful in identifying dual red-shifted pigments in deep-sea fish (Denton *et al.*, 1970; O'Day and Fernandez, 1974; Partridge *et al.*, 1987), neither method has led to conclusive identification of the violet visual pigment (whose presence was verified with intracellular recordings) of some shallow water crustaceans (Goldsmith *et al.*, 1968; Goldsmith and Bruno, 1973; Cummins and Goldsmith, 1981; Martin and Mote, 1982; Cummins *et al.*, 1984). This may be due to the small quantity of pigment present, which would be swamped by the dominant pigment or its photoproducts during absorption measurements on extracts, or due to its location in small cells which may be inaccessible to, or overlooked by, MSP measurements.

Deep-sea crustaceans are useful subjects for exploratory electrophysiological studies of receptor systems of deep-sea animals, because they can be retrieved in good condition, and remain viable for many days under the proper maintenance conditions. Soft-bodied fish and invertebrates are generally dead upon retrieval or die within hours of capture. However, electrophysiological techniques have seldom been used with deep-sea crustaceans because they rarely survive transport to land-based labs in good condition. For this reason, we have developed a portable electrophysiological apparatus enabling shipboard measurements of spectral sensitivities of freshly caught specimens. Members of the family Oplophoridae were chosen for this study because (1) this family contains both photophore bearing and non-photophore bearing species, (2) their depth ranges are fairly well known, and (3) viable specimens could be obtained in sufficient numbers for a comprehensive study. An unexpected result of this work was the discovery of enhanced sensitivity to violet light in the four photophore bearing species examined. Preliminary reports have been presented in abstract form (Frank, 1986).

Materials and Methods

Specimen collection and maintenance

Specimens of the eight species of deep-sea shrimp used in this study (Table I) were collected during two cruises on the R.V. *New Horizon* off the southwest coast of Oahu, Hawaii, with an opening/closing 3.1 m Tucker Trawl, fitted with a thermally protected, light-tight collecting container (Childress *et al.*, 1977; Childress and Price, 1978). This container was closed at depth, ensuring recovery of healthy organisms whose eyes had not been irreparably damaged by surface light levels, a well known concern in working with deep-sea species (Loew, 1976; Nilsson and Lindstrom, 1983; Shelton *et al.*, 1985). The container was opened in a light tight room, and animals were sorted under dim red light. Experimental animals were maintained in chilled seawater (5°C) in light proof containers and studied within 24 hours of capture.

Dim red illumination was also used while setting up for experiments. Animals were mounted in a holder suspended in a 5°C seawater bath, allowing enough pleopod movement to maintain respiratory water currents across the gills. Temperature was maintained by pumping −1°C antifreeze from a Lauda cooler through cooling coils submerged in the seawater bath. The eyes were stabilized by gluing (Superglue) to small posts attached to the holding chamber on either side of the head.

Electrical recording

ERGs were recorded with 5 μm tip, glass insulated, metal microelectrodes (F. Haer & Co.), placed subcorneally with the aid of a dissecting microscope equipped with an infrared light source (Wratten Filter 89C) and an infrared image converter (FJW Industries). A reference electrode was placed in the other eye, and a silver-chloride electrode grounded the water bath. The electrodes were used with a Grass high impedance probe (Model HIP511, 10^7 *M* ohms impedance) to eliminate electrode polarization artifacts (Kugel, 1977). Signals were amplified with a Grass AC Pre-amplifier (Model HIP511J), with the low frequency filter set for minimal filtering (0.1–0.3 Hz) to minimize distortion due to AC-amplification.

Optical apparatus

Monochromatic test flashes were provided by an American ISA Monochromator (full width at half maximum intensity [FWHM] = 2 nm) with a tungsten - halogen light source powered by a Weston regulated power supply (Model 7521). Flash duration of 100 ms was controlled by a Uniblitz Shutter (Model 100-2) triggered by a Grass S44 Stimulator. Light intensity was controlled with a neutral density wedge and neutral density filters, and was calibrated at each wavelength with a UDT Optometer (United Detector Technology Model 61) and radiometric probe, with point calibrations referenced to NBS provided by UDT.

Test flashes were presented to the eye through one end of a branched quartz fiber optic light guide (Welch-Allen). The 2 mm output diameter of the light guide was large enough to illuminate the whole eye, and experiments showed that this light did not reach the reference eye.

The adapting light source for chromatic adaptation experiments was an incandescent light filtered by a 400 nm broadband filter (Melles Griot BG12, FWHM = 110) for violet adaptation, and a 520 nm broadband filter (M. G. VG6, FWHM = 90 nm) for green adaptation. The adapting light was delivered to the eye through one branch of the light guide, and test flashes were superimposed on this background light through the other branch. This ensured that both the adapting light and the stimulus light acted upon the same group of photoreceptor cells.

Experimental procedure

The eye was stimulated with 100 ms test flashes of monochromatic light adjusted for intensity until a defined criterion response was attained at each wavelength tested. The criterion was usually set 20 μV above baseline noise, ensuring that the intensity of the light flashes used was very near the threshold of sensitivity, so as not to light-adapt the eye. Signals were instantaneously analysed for peak to peak response height after digital conversion by an LSI/PDP 11 computer, and stored on magnetic tape (Lockheed Store 4 Recorder) for later waveform analysis. The order of the flashes was random, and the response to a standard flash of set wavelength and intensity was tested periodically throughout the experiment, to ensure the stability of the eye and to monitor the state of dark-adaptation. Spectral sensitivity measurements were started when the response to the standard flash was stable, for both dark-adapted and chromatically adapted eyes. Spectral sensitivity curves were generated as the reciprocal quanta needed to produce the criterion response at each wavelength. Absorptance spectra were constructed from Dartnall nomograms (Dartnall, 1953), using the analysis provided by Cornwall *et al.* (1984).

The inefficiency of the monochromator at shorter wavelengths limited the intensity of the adapting light that could be used. To ensure that a full spectral sensitivity curve could be measured, the intensity of the adapting light was adjusted so that a criterion response to 370 nm test flashes could still be elicited. Due to the varying sensitivity of some species to short wavelength light, the intensity of the adapting light necessarily varied between experiments.

Results

Notostomus gibbosus *and* N. elegans

The results for *N. gibbosus* and *N. elegans* were identical and will therefore be described together with no distinction made between species. The mean dark-adapted spectral sensitivity curve for *Notostomus* (Fig. 1A) shows that the sensitivity maximum occurred at about 490 nm. The absorptance spectrum for a 490 nm pigment with an optical density (O.D.) of .5 provides an excellent fit to the spectral sensitivity curve. Green chromatic adaptation uniformly depressed sensitivity across the spectrum (Fig. 1B), indicating that only one visual pigment is present in both species.

The dark-adapted response waveforms of the ERGs were identical at all wavelengths (Fig. 1C). Chromatic adaptation of the eyes with green light produced no discernible effects on the waveforms, supporting the conclusion that both species possess a single visual pigment.

Acanthephyra smithi *and* A. curtirostris

Although these two species have different depth distributions (Table I), their spectral sensitivities were identical, and will again be described with no distinction between species. Maximum sensitivity in the dark-adapted eye was at 510 nm (Fig. 2A). An absorptance spectrum, constructed based on the known absorption maximum (490 nm) and O.D. (.6) of *A. smithi* visual pigment (Hiller-Adams *et al.*, 1988), was offset from the spectral sensitivity curve by 20 nm.

Chromatic adaptation experiments indicate that only one visual pigment is present, as there were no selective effects of green and violet adaptation on the shape of the spectral sensitivity function; spectral sensitivity decreased uniformly across the spectrum (Fig. 2B, C).

The ERG response waveforms in dark-adapted eyes were identical at all wavelengths for individual specimens and adaptation with violet and green lights had no discernible effects on the shape of the response waveforms (Fig. 3). Lack of wavelength-specific effects of

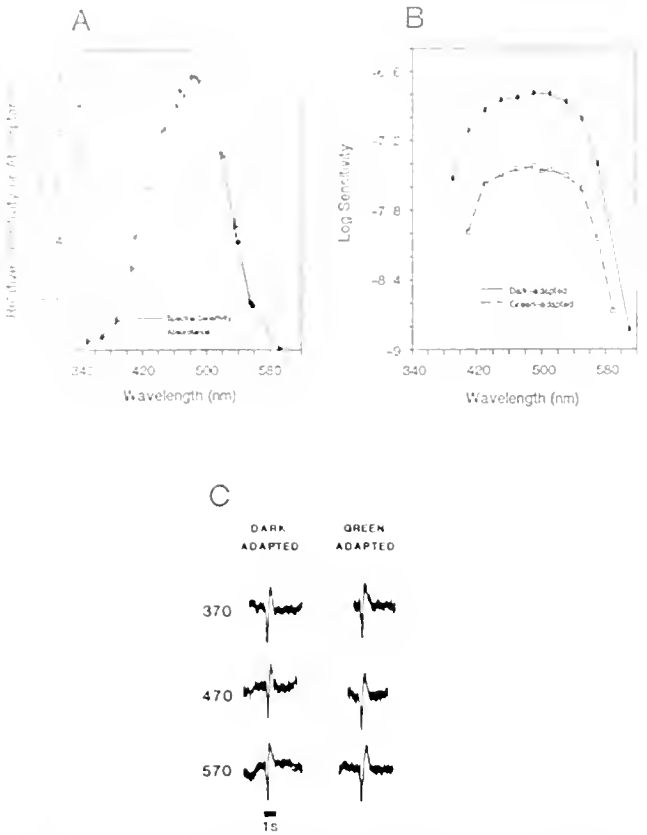

Figure 1. Spectral sensitivity of *Notostomus*. (A) Standardized mean spectral sensitivity curve (solid line) for *N. gibbosus* and *N. elegans* (n = 10). Criterion responses ranged from 20–50 μV. Standard errors are represented by vertical bars. Sensitivity is defined as the reciprocal of the quantum flux (photons/cm^2/s) required to elicit the criterion response at each wavelength. Maximum sensitivity centers on 490 nm. Dashed line represents the absorptance curve for a hypothetical rhodopsin with a λ_{max} of 490 nm, and an O.D. of .5. (B) Green chromatic adaptation had no effect on the spectral sensitivity of *Notostomus* (data from one specimen displayed). Results from four other specimens are the same. Sensitivity is displayed on a log scale so both curves could be displayed on the same axes. Intensity of adapting light was 1.1 × 10^{-6} μW/cm^2/s. (C) ERG response waveforms, matched for equal amplitude (50 μV), are identical at all wavelengths in the dark-adapted eye, and were not altered by green chromatic adaptation.

chromatic adaptation support the spectral sensitivity evidence that both species possess a single visual pigment.

Systellaspis debilis

Of fifteen *S. debilis* tested, 13 showed heightened sensitivity to violet light. Eight actually possessed two distinct peaks in the dark-adapted spectral sensitivity curves. The variation in the relative sizes of the two peaks (possibly due to variability in electrode location) and the absence of the heightened short wavelength sensitivity in two individuals (Fig. 4) made it inadvisable to combine all the dark-adapted data into one averaged curve. However, the location of the two sensitivity maxima at 400 and 500 nm, when present, was very consistent, as seen in the average curve for the eight specimens in which two maxima were present (Fig. 5A). Spectral sensitivity did

Table I

Depth distribution and bioluminescence mode

Species	Depth range (m)[1] Day	Night	Bioluminescence
Icanthephyra smithi	500–900	200–300	spew
Icanthephyra curtirostris	500–1200	500–1200	spew
Notostomus gibbosus	>900	>900[2]	spew
Notostomus elegans	>900	>900[2]	spew
Systellaspis debilis	620–900	100–300	spew photophores
Janicella spinacauda	500–600	30–250	spew photophores
Oplophorus spinosus	490–750	140–375	spew photophores
Oplophorus gracilirostris	490–650	60–750	spew photophores

[1] Zieman, 1975.
[2] J. Childress, pers. comm.

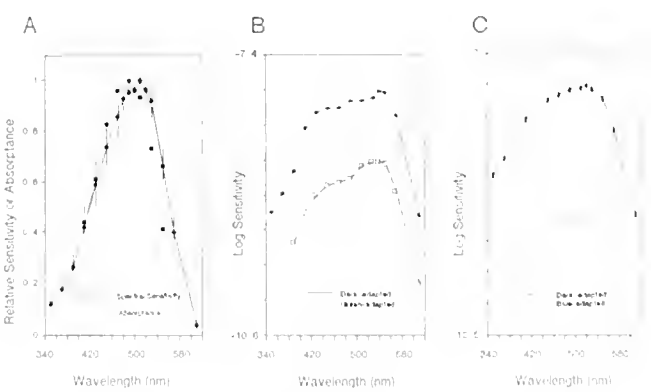

Figure 2. Spectral sensitivity of *Icanthephyra*. (A) Standardized mean spectral sensitivity curve for *I. curtirostris* and *I. smithi* (n = 14). Criterion responses ranged from 20–60 μV. Peak sensitivity centered on 510 nm. Absorptance spectrum (dashed line), was constructed based on the known absorption maximum (490 nm) and O.D. (.6) of *I. smithi* visual pigment (Hiller-Adams *et al.*, 1988). (B) Green chromatic adaptation did not diminish long wavelength sensitivity with respect to short wavelength sensitivity (data from one specimen). Results from three other specimens are the same. Intensity of adapting light was 3.2 × 10^{-5} μW/cm^2/s. (C) Similarly, violet chromatic adaptation did not enhance long wavelength sensitivity relative to short wavelength sensitivity (data from one specimen). Intensity of adapting light was 2.4 × 10^{-4} μW/cm^2/s.

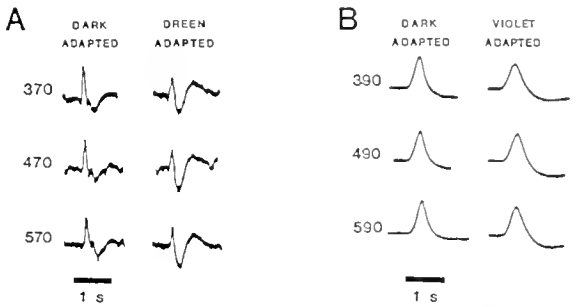

Figure 3. ERG response waveforms matched for equal amplitude (50 μV) in dark-adapted and chromatically adapted *Acanthephyra*. (A) Waveforms were identical across the spectrum in the dark-adapted eye. Upon green-adaptation, the responses were different from those in the dark-adapted eye, but were identical to each other. (B) Response waveforms from another dark-adapted specimen were also identical across the spectrum and adaptation with violet light did not affect their shape.

not appear to depend on the size of the criterion response for the range of criterion responses used (20–100 μV), as curves generated for an animal using two different criterion response levels were the same (Fig. 5B, C).

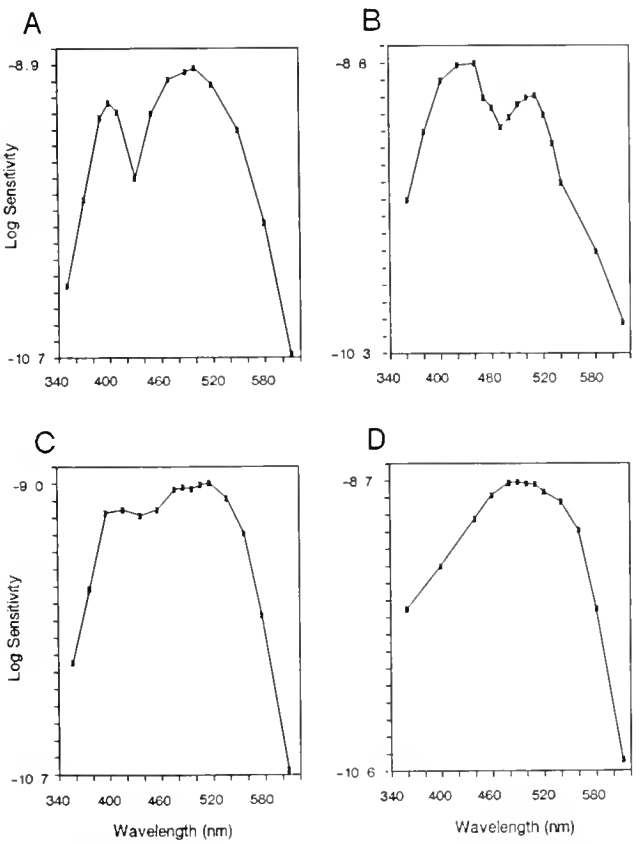

Figure 4. Dark-adapted spectral sensitivity curves from four specimens of *Systellaspis debilis*, demonstrating the variability in their spectral sensitivity. Criterion response = 50 μV.

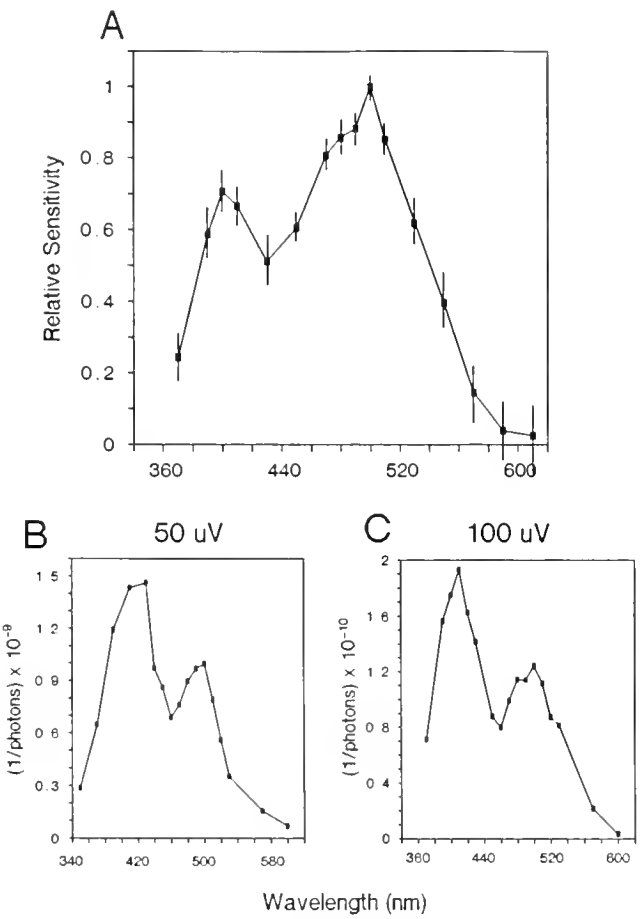

Figure 5. (A) Average standardized spectral sensitivity curve from only those dark-adapted *S. debilis* that possessed bimodal spectral sensitivity curves (n = 8). The two sensitivity maxima were consistently at 400 and 500 nm. (B, C) Dark-adapted spectral sensitivity curves for one preparation at two different criterion response levels were identical.

Results of chromatic adaptation experiments indicate that two visual pigments may be present. Under green adaptation, the spectral sensitivity curve was markedly depressed in the long wavelength part of the spectrum (Fig. 6A). Green adaptation also brought out the violet peaks in two specimens where there was no evidence of a short wavelength peak in the dark-adapted eye (Fig. 6B). The effect of violet adaptation was to depress the short wavelength peak with respect to the long wavelength peak, although the effects were not equally distinct in all experiments. The strongest effects were seen in those specimens that had large 400 nm peaks in the dark-adapted spectral sensitivity curves (Fig. 6C).

Differences in waveform responses to short *versus* long wavelength light suggest that the two putative pigments are in separate cells. Again, because of variability in electrode placement, the dark-adapted waveforms were not identical from animal to animal. In one specimen, the short wavelength response waveforms were distinctly

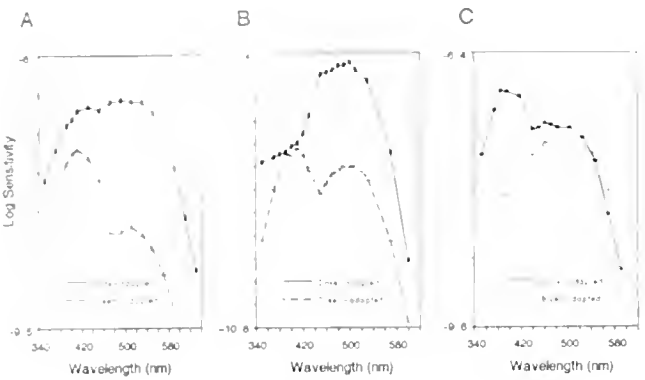

Figure 6. Effects of chromatic adaptation on the spectral sensitivity of *S. debilis*. (A) Green chromatic adaptation had a greater effect on the sensitivity of the blue-green receptors than the violet receptors, leading to a relative enhancement of the violet peak. (B) The dark-adapted spectral sensitivity curve for another preparation showed no distinct violet peak. Green adaptation depressed the sensitivity of the blue-green receptors, exposing the violet receptors and thereby producing a distinct violet peak in the spectral sensitivity function. (C) Blue adaptation had a greater effect on short wavelength sensitivity, depressing the sensitivity of the violet receptors to such an extent that only the blue-green peak is now visible. Results of four other green adaptation and four other blue adaptation experiments were consistent with the results shown. Intensities of adapting lights were (A) 1.2×10^{-4}, (B) 1.1×10^{-5}, and (C) 1.2×10^{-5} $\mu W/cm^2/s$.

different from the long wavelength responses in the dark-adapted eye (Fig. 7A). For another specimen, the waveforms were identical in the dark-adapted eye, but upon green chromatic adaptation, the short wavelength responses became markedly different from the long wavelength responses (Fig. 7B). Blue adaptation had either no effect when waveforms were identical in the dark-adapted eye, or actually diminished differences that were initially present in the dark adapted eye (Fig. 7C).

All of these results support the conclusion that *Systellaspis* possesses two spectral classes of receptor cells with different response characteristics: one with maximal blue-green sensitivity and the other maximally sensitive in the violet.

Janicella spinacauda

The dark-adapted spectral sensitivity curves of the four specimens tested displayed a consistent maximum at 500 nm in the blue-green, but the position of the short wavelength peak varied from 350 to 420 nm (Fig. 8A, B). No correlation could be found between these results and time of capture or time of experimentation.

The results of two chromatic adaptation experiments indicate that two visual pigments are present. The effect of green adaptation was to depress the blue-green peak with respect to the violet peak, as well as shift the short wavelength maximum from 350 to 410 nm (Fig. 8C). Violet adaptation selectively depressed the violet peak relative to the blue-green peak (Fig. 8D).

As in *Systellaspis*, the response waveforms were either distinctly different in the dark-adapted eye (Fig. 9A), or were identical in the dark-adapted state, and changed dramatically at the shorter wavelengths upon green adaptation (Fig. 9B). Conversely, violet chromatic adaptation had no selective effects on response waveforms that were identical in the dark-adapted eye (Fig. 9C).

These results indicate that *Janicella* also possesses two spectral classes of receptor cells.

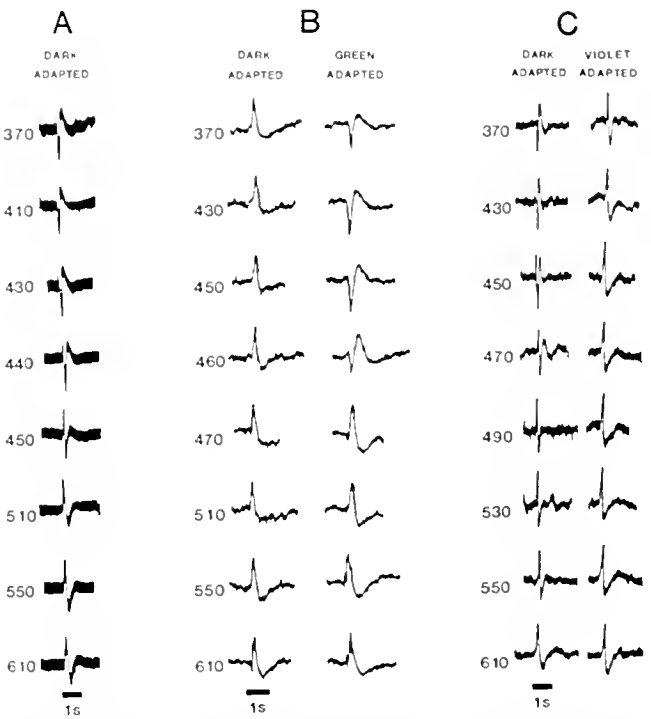

Figure 7. Effects of chromatic adaptation on the response waveforms matched for equal amplitudes in *S. debilis*. (A) Response waveforms of this specimen (criterion response = 40 μV) were distinctly different at different wavelengths. From 370 to 410 nm, the main component of the ERG was corneal positive (downward). Between 430 and 440 nm, a small corneal negative component preceded the larger positive portion. From 450 nm to 610 nm, the main component was corneal negative (upward). (B) Response waveforms (30 μV) in another preparation were identical at all wavelengths in the dark-adapted eye, with simple, monophasic, corneal negative waveforms. Green adaptation produced distinct wavelength specific effects. The waveforms from 350 to 450 nm were reversed in polarity, while the responses from 470 to 610 nm remained unchanged, with the transition occurring at 460 nm. (C) Dark-adapted response waveforms (50 μV) demonstrate the same differences as described in (A), with waveforms between 370 and 430 nm exhibiting one characteristic waveform, and responses between 470 and 610 nm exhibiting another. The transition from one type to the other occurred at 450 nm. Blue adaptation markedly altered the response waveforms between 370–450 nm; these waveforms became identical to the long wavelength responses, which were unaffected by blue adaptation.

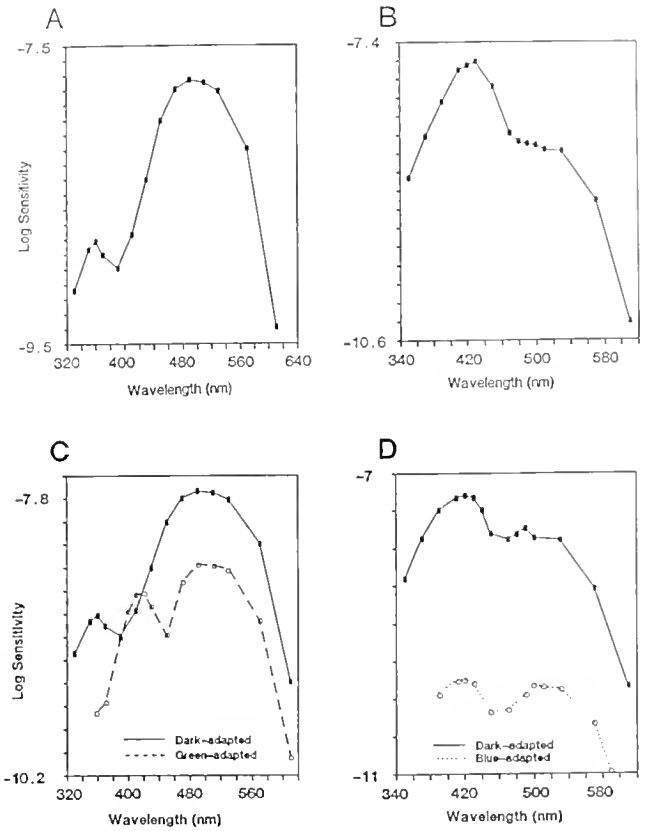

Figure 8. Dark-adapted spectral sensitivity curves for individual specimens of *Janicella spinacauda*. (A) The short wavelength sensitivity peaks at about 350 nm, while the long wavelength sensitivity peaks at 500 nm. (B) In another specimen, the short wavelength peak was at 420 nm, while the long wavelength sensitivity maximum was a shoulder rather than a distinct peak. (C) Green chromatic adaptation enhanced the relative size of the violet peak, as well as shifting the sensitivity maximum from 350 to 410 nm. Data from one specimen. Intensity of adapting light was 1.56×10^{-6} $\mu W/cm^2/s$. (D) Violet chromatic adaptation had a greater effect on short wavelength sensitivity, resulting in a relative enhancement of the blue-green peak. Data from one specimen. Intensity of adapting light was 1.2×10^{-3} $\mu W/cm^2/s$.

Oplophorus spinosus *and* O. gracilirostris

The results for *O. spinosus* and *O. gracilirostris* were the same, and will be discussed together with no distinction between species. Representative examples of dark-adapted spectral sensitivity curves for two specimens are shown in Figure 10 (A, B). The variability in these curves is similar to that seen in the previous two species.

Chromatic adaptation experiments again provide evidence that more than one visual pigment is present. Violet adaptation resulted in a small depression in the violet shoulder (Fig. 10C). The only specimen that had a distinct violet peak in its dark-adapted spectral sensitivity curve (see Fig. 10B) died during the chromatic adaptation experiment; therefore, the effects of violet adaptation are not as apparent as in *Systellaspis* or *Janicella*. The effects of green adaptation were much more dramatic. The sensitivity to long wavelength light was greatly diminished with respect to the short wavelength sensitivity, resulting in either two peaks, or, with more intense adaptation, a distinct peak at 400–410 nm, and a plateau centering at 500 nm (Fig. 10D).

The shapes of the response waveforms in dark-adapted and chromatically adapted eyes were the same as those described for *Systellaspis* and *Janicella* (Fig. 11C), again pointing to the presence of two spectral classes of receptor cells.

Oplophorus spinosus proved to be unusually robust, and in two instances we were able to record responses after the eye had recovered from chromatic adaptation. Green chromatic adaptation distinctly altered the shape of the spectral sensitivity curve as well as the response waveforms (Fig. 11A, C). Both the spectral sensitivity curve and the response waveforms, measured two hours after extinguishing the adapting light, were the same as those measured before chromatic adaptation (Fig. 11B, C). This indicates that waveform changes were due to the effects of the adapting light, and not to changes in electrode position or to degenerative changes in the eye during the course of an experiment.

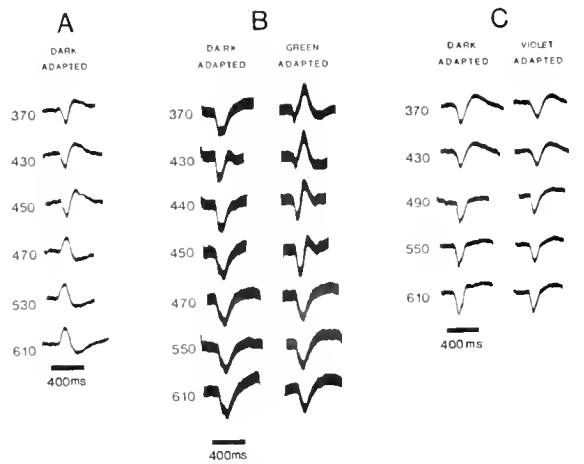

Figure 9. ERG response waveforms matched for equal amplitude in *J. spinacauda*. (A) The response waveforms (amplitude = 30 μV) in this dark-adapted preparation were markedly different between responses to short *versus* long wavelength light. The major component of the short wavelength responses (350–450 nm) was corneal positive (shown by the downward deflection), while the major component of the longer wavelength responses was negative. (B) In another preparation, the dark-adapted response waveforms (40 μV) were virtually identical, and were all corneal positive. Upon adaptation with green light, the waveforms between 370–450 nm were reversed in polarity, while the waveforms from 470–570 nm remained unchanged. (C) Dark-adapted waveforms in another preparation were virtually identical, and remain unchanged under a blue adapting light. Polarity differences in long wavelength response waveforms between different specimens are probably due to differences in the depth of the recording electrode (see Discussion).

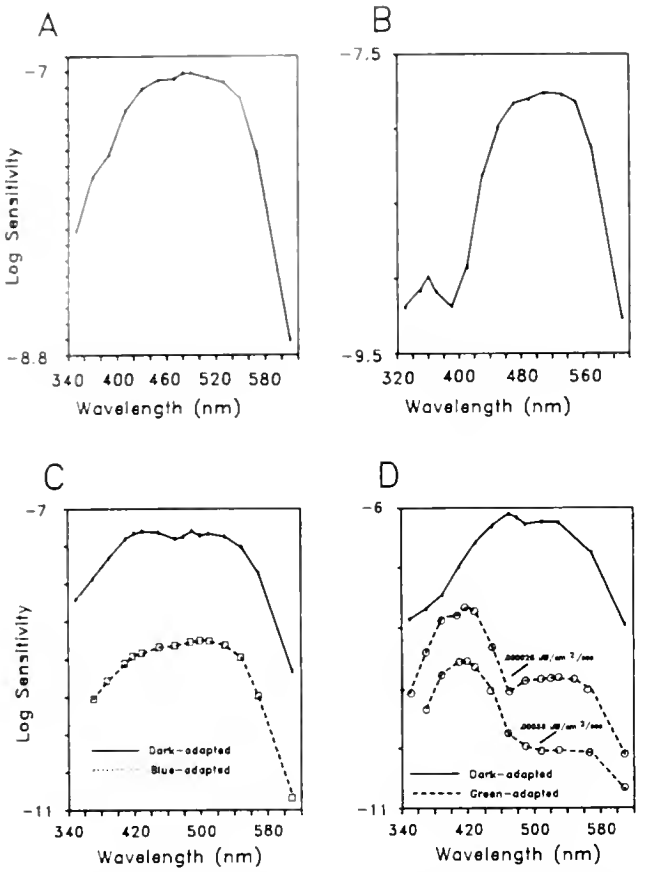

Figure 10. Dark-adapted spectral sensitivity curves for *Oplophorus*. (A) Six of the seven specimens tested possessed broad spectral sensitivity curves similar to the one shown, with small variations in sensitivity at the shorter wavelengths. (B) Only one distinctly bimodal spectral sensitivity curve was measured, with peaks at 350 and 500 nm. (C) Selective effects of violet adaptation are small but discernible; sensitivity was slightly more depressed at the shorter wavelengths, diminishing the small violet peak seen in the dark-adapted eye. Intensity of adapting light was 2.4×10^{-4} $\mu W/cm^2/s$. (D) Green adaptation selectively depressed sensitivity at the longer wavelengths, producing a much larger violet peak relative to the blue-green peak. Under a higher intensity adapting light, the blue-green peak was completely depressed in the same specimen. Results from four other specimens are compatible with those shown.

Discussion

In clear oceanic waters, the wavelength of maximum light transmittance is 510 nm in the surface layers, with the FWHM covering a spectral range from 440 to 600 nm. At 100 m depth, selective absorption and scattering have shifted the transmission maximum to 475 nm and narrowed the spectral distribution to a FWHM covering 440–500 nm (Jerlov, 1968; Dartnall, 1974; Jerlov, 1976; Cronin, 1986). The possibility that deep-sea organisms may have blue-shifted visual pigments as an adaptation for maximum sensitivity to this light regime (the Sensitivity Hypothesis) was first suggested by Clarke (1936) and Bayliss *et al.* (1936), and this idea of sensitivity peaks matching ambient light distribution has since been extended to other environments. Although Lythgoe (1968) has shown that the Sensitivity Hypothesis may not necessarily hold true for all shallow water species, which live in a very "complex" visual environment, it has been strongly supported by studies on organisms living in the

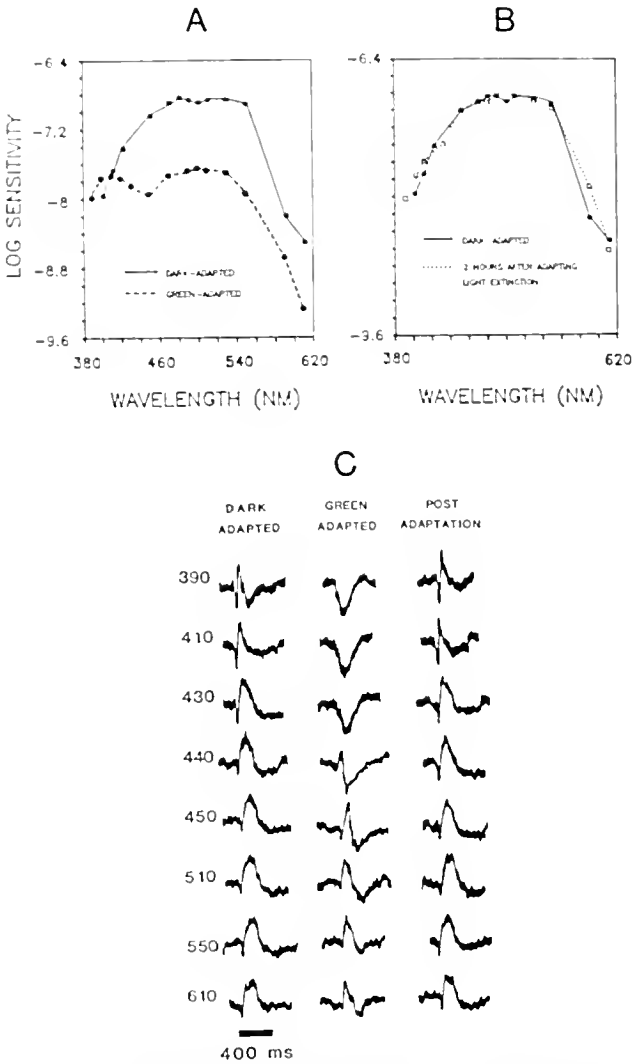

Figure 11. Effects of chromatic adaptation on spectral sensitivity and response waveforms in *Oplophorus*. (A) Green adaptation selectively depressed the long wavelength sensitivity, leading to a bimodal spectral sensitivity curve with maxima at 400 and 500 nm. (B) Two hours after the adapting light was turned off, the eye had recovered completely from the effects of the adapting light, and the spectral sensitivity function was identical to that of the dark-adapted eye. (C) Dark-adapted response waveforms for the same preparation shown above were slightly different at the shortest wavelengths. Green adaptation altered the response waveforms at the shorter wavelengths as previously described. Two hours after the adapting light was turned off, the response waveforms were again identical to those in the dark-adapted eye. Adapting light intensity $= 2.5 \times 10^{-4}$ $\mu W/cm^2/s$.; criterion response $= 40\ \mu V$.

"simpler" deep-sea visual environment. The visual pigments of most deep-sea species studied to date have peak absorption maxima clustered between 470 and 490 nm, which are about 10–20 nm shorter than those of their shallow water counterparts, thus supporting the Sensitivity Hypothesis (reviewed by Goldsmith, 1972; Cronin, 1986).

Single visual pigment systems

The results from two species in this study, *N. gibbosus* and *N. elegans*, support the Sensitivity Hypothesis. The maximum sensitivity of these species (490 nm) is at shorter wavelengths than those of shallow water crustaceans (510–550 nm), and fall into the same range as those of the deep-sea fish (Denton and Warren, 1957; Munz, 1957; Wald *et al.*, 1957; Denton and Shaw, 1963; Fernandez, 1978; Crescitelli *et al.*, 1985).

The spectral sensitivities of *A. curtirostris* and *A. smithi* peak at 510 nm, seemingly more appropriate for shallow water crustaceans than for species that maintain daytime depths of greater than 500 m. The absorptance spectrum matches the shape of the spectral sensitivity curve, but is offset by 20 nm. This suggests that these species may possess some type of non-moving distal pigment screen, as found in *A. purpurea* (Welsh and Chace, 1937), that would shift the sensitivity maximum away from the visual pigment absorption maximum. In crayfish and lobsters, this pigment screen is believed to be responsible for the 10–30 nm difference between the visual pigment absorption and the spectral sensitivity function (Goldsmith, 1978). Why such a screening pigment shield would be needed, particularly in *A. curtirostris*, which never migrates to shallower waters, remains obscure.

It is unlikely that self-screening by metarhodopsin contributed significantly to the long wavelength shift in spectral sensitivity. Although both species possess metarhodopsins with λ_{max} at shorter wavelengths (*A. curtirostris*—481 nm; *A. smithi*—483 nm; Hiller-Adams *et al.*, 1988) than those of their rhodopsins, so that self-screening by metarhodopsin would shift the spectral sensitivity to longer wavelengths, our experimental protocol ensured that the eye was fully dark-adapted before starting an experiment. According to Goldsmith (1978), self-screening by metarhodopsin should be negligible if: (1) the eye is dark-adapted, (2) near-threshold flashes are used to stimulate the eye (preventing isomerization of a sizable fraction of rhodopsin to metarhodopsin), and (3) the organism has other mechanisms than photo-regeneration for restoring a full titer of rhodopsin. The first two conditions were met by our experimental protocol, and while these two species have not been studied with respect to dark-regeneration, such a system was found in another oplophorid occupying the same depth range (Hiller-Adams *et al.*, 1988.) Additionally, specimens tested within three hours of capture demonstrated the same spectral sensitivity as those that were maintained in the dark for 24 hours before testing. Therefore, self-screening by metarhodopsin is not a reasonable explanation for the observed results.

The difference in the polarities of the representative response waveforms shown for *Notostomus* (Fig. 1) and *Acanthephyra* (Fig. 3) may be due to differences in the electrode depths from preparation to preparation. In both genera, preparations were found in which the response waveforms were of the opposite polarity to those shown in the figures, so these polarity differences are not species specific, but probably depend on the recording parameters. Konishi (1955), working with the lobster eye, showed that an electrode just beneath the corneal surface recorded a corneal negative response. With deeper insertion into the eye, the recorded response reversed in polarity to a corneal positive response. Since the depth of electrode penetration varied between preparations in our study, electrode position may explain the ERG polarity differences.

Dual visual pigment systems

The most interesting visual systems are found in the remaining four species, *S. debilis*, *J. spinacauda*, *O. spinosus*, and *O. gracilirostris*, which appear to possess a violet sensitive pigment in addition to one with maximal sensitivity in the blue-green. The variation in the shapes of the dark-adapted spectral sensitivity curves is much greater than in those of the single pigment species, and this may be due in part to the location of the electrode in the eye, particularly if different parts of the eye have different spectral sensitivities. Regional differences in spectral sensitivity have been found in the eyes of several species of insects (Walther, 1958; Ruck, 1965; Bennett and Ruck, 1970) and results of experiments on these insects are similar to ours. Goldsmith (1960) also reports that the relative contribution of the UV and green receptor systems to the ERG in the honeybee eye could be altered somewhat by moving the electrode to another part of the eye.

Due to our experimental protocol in testing the eye with a standard flash throughout the experiment, in addition to the fact that those crustaceans which had a distinct violet peak exhibited the same overall sensitivity as those which did not (see Fig. 4), we are confident that the differences in shapes of dark-adapted spectral sensitivity curves were not due to differences in the degree of dark-adaptation.

The conclusion that two visual pigments are present in these four species is strongly supported by the differential

effects of the different adapting lights on the shape of the spectral sensitivity curve. The selective effects of violet adaptation were generally not as great as those of green adaptation, and this can be attributed to the fact that all visual pigments possess a β-band that absorbs in the shorter wavelengths, meaning that violet adaptation would affect both receptor systems. However, the fact that violet adaptation had a stronger effect on the short wavelength system, so that differential effects in the shape of the spectral sensitivity functions could be seen, indicates that the violet peak is not due to the β-absorption band on the blue-green pigment as in the woodlouse *Porcellio* (Goldsmith and Fernandez, 1968). If this were the case, the sizes of the two peaks relative to each other would remain the same during all adaptation conditions.

Waveform differences between responses to short *versus* long wavelength light indicate that the two visual pigments are housed in different receptor cells. Single cells have never been shown to respond differentially to different wavelengths of light (Graham and Hartline, 1935; Naka and Rushton, 1966; Stark and Wasserman, 1974), and if several spectral mechanisms with different time courses contribute to the ERG, equal amplitude responses at all wavelengths can never be matched (Chapman and Lall, 1967). In several species of muscid flies, waveform differences between short and long wavelength responses were initially attributed to the presence of a red sensitive receptor in addition to short wavelength receptors (Autrum and Burkhardt, 1961; Burkhardt, 1962; Mazokhin-Porshnyakov, 1960). However, Goldsmith (1965) found that these differences were due to differences in the sizes of ganglionic on-off effects in the ERG, rather than the presence of several spectral classes of receptor cells. Crustacean ERGS do not exhibit these ganglionic on/off effects, since the ERG is a more purely retinal response (Naka and Kuwabara, 1956; Chapman and Lall, 1967; Goldsmith and Fernandez, 1968), and there is no experimental evidence for any contribution by the optic ganglion to the ERG (Ruck and Jahn, 1954; Konishi, 1955). Therefore, differences in waveform responses to short and long wavelength light in crustaceans, based on current knowledge, can only be attributed to two different populations of receptor cells with different membrane properties (Wald, 1968).

Further support for two spectral classes of receptor cells comes from the wavelength-specific effects of different adapting lights on response waveforms. These results can be explained by assuming that the visual pigments are housed in different receptor cells, and that the numeric distribution of the two receptor classes is not equal. This situation is found in crayfish and lobsters, where the long wavelength pigment occupies seven of the eight retinula cells present in each ommatidium, and the violet pigment occupies just one (Cummins and Goldsmith, 1981; Cummins *et al.*, 1984). A similar unequal distribution also appears to be present in our deep-sea species. The ERG responses in the dark-adapted eyes were generally characteristic of those attributed to the blue-green receptors. Upon green adaptation, the relative contribution of the violet receptors was enhanced, and distinct differences in response waveforms at the shorter wavelengths were observed. Conversely, violet adaptation had no affect on response waveforms, or diminished differences present at the shorter wavelengths in the dark-adapted eyes, as expected when the minor contribution of the violet receptors was further diminished.

The location of the violet receptor cells in an accessory eye would provide an explanation for the unusual "hyperpolarizing" responses seen to short wavelength light. All known microvillar photoreceptors, which are the type possessed by all crustaceans (Eakin, 1972), depolarize in response to light (reviewed by Jarvilehto, 1979), but an unusual orientation of the short wavelength receptors to the electrode could produce an apparently "hyperpolarizing" response. In the alciopid worm *Torrea*, which also has microvillar photoreceptors, responses from the main retina are depolarizing, while responses contributed by an accessory retina are hyperpolarizing, and this has been attributed to the reversed arrangement of the receptors of the accessory retina relative to the electrode position (Wald and Rayport, 1977).

Functions of two visual pigments in deep-sea organisms

Many other crustaceans, such as shallow water crabs (Wald, 1968; Hyatt, 1975; Martin and Mote, 1982), lobsters (Cummins *et al.*, 1984), estuarine shrimp (Wald and Seldin, 1968; Goldsmith and Fernandez, 1968), and crayfish (Goldsmith and Fernandez, 1968; Wald, 1968; Waterman and Fernandez, 1970; Cummins and Goldsmith, 1981) appear to possess a short wavelength visual pigment. The purpose of this pigment is not clear, although Hyatt (1975) feels that it may be a mechanism for hue discrimination in the fiddler crab. Even though the rationale for the pigment is not known, all of these species live in shallow or near-surface waters where UV light is abundant and may play some role in their visual environment. In insects, the presence of a UV peak has been closely correlated with some behavioral patterns. Behavioral studies on UV-sensitive pierid butterflies indicate that they visit violet and blue flowers more often than butterflies without the short wavelength sensitivity (Ilse, 1928; Eguchi *et al.*, 1982). Obara and Hidaka (1968) also report that male pierid butterflies approach females after identifying the UV patterns on their wings. However, the reason for a UV visual pigment among some nocturnal moths (Eguchi *et al.*, 1982; Mikkola,

1972) remains obscure, since UV light is absent in moonlight as well as in background galactic light at night (Munz and McFarland, 1973, 1977).

There is a similar absence of UV and near-UV light in the deep-sea. Although UV light may penetrate significantly in the surface layers (Jerlov, 1968; Dartnall, 1974; Jerlov, 1976), it is virtually absent by 500 meters—.09% of the 500 nm light present at the surface remains, while only .00007% of the 400 nm light is still present (Type 1 water, Table XXVI—Jerlov, 1976).

Bioluminescence, the other source of light in the deep-sea, is considered by some to be the major visual stimulus present in this environment (Beebe, 1935; Clarke and Hubbard, 1959; Jerlov, 1968). It is also the logical candidate to provide an explanation for the violet visual pigment, since the four species with the enhanced violet sensitivity possess photophores, while the four species without photophores are not violet sensitive. Examples of unusual visual systems correlated with bioluminescence are found in three species of malacosteid fish, which possess red-shifted visual pigments as an apparent adaptation for enhanced sensitivity to their own red bioluminescence (O'Day and Fernandez, 1974; Denton *et al.*, 1970; Bowmaker and Herring, unpub.). While the vast majority of bioluminescence emission maxima in the deep-sea, including those from the photophores of *S. debilis* and *O. spinosus*, are clustered around the same wavelengths as the downwelling illumination (460–490 nm), with no emission maxima below 430 nm (Herring, 1976; Herring, 1983; Widder *et al.*, 1983; Latz *et al.*, 1988), bioluminescence may still provide the explanation for the unusual violet pigment.

It has been suggested that the presence of two blue-green visual pigments in some species of deep-sea fish may serve as a system for discriminating between different bioluminescent organisms by using the spectral bandwidth as the basis for discrimination (Partridge *et al.*, 1988). The putative violet visual pigment may be serving the same purpose in these oplophorids. Spectra with broader spectral bandwidths would be more efficient in stimulating the violet-receptor, and in this manner could be distinguished from spectra with narrower bandwidths. The spectral emissions from most of the species with similar depth distributions as these oplophorids, including other crustaceans (except euphausiids), siphonophores, fish, and cephalopods, are remarkably similar, with the peaks lying between 465 and 485 nm, and FWHM covering 65–90 nm (Widder *et al.*, 1983; Herring, 1983; Latz *et al.*, 1988). However, the emissions from the photophores of *S. debilis* and *O. spinosus*, while peaking in the same range, have FWHMs of 48–58 nm (Herring, 1983; Latz *et al.*, 1988), and perhaps this difference in spectral bandwidth is enough to facilitate congener recognition. Additionally, the FWHM of their luminous secretion, which is thought to be used during escape responses, is between 65 and 75 nm, and could potentially be distinguished from the photophore emission to serve as warning signs to congeners.

Acknowledgments

We thank Dr. James Childress, his laboratory associates, and the captains and crews of the RV *New Horizon* for assistance with animal collection. We also thank Dr. Childress for generously providing shipboard laboratory space; Dr. Steve Bernstein for writing the digitizing program; and Mark Lowenstine, Robert Fletcher, and Joel Dal Pozzo for help in designing and building the portable ERG apparatus. Drs. Thomas Cronin, Edith Widder, and Michael Latz provided helpful comments and suggestions. This work was supported by a grant from the Office of Naval Research (N00014-84-K-0314) to J. F. Case, a National Science Foundation grant (OCE 85-000237) to J. J. Childress, and a UCSB patent fund grant and dissertation fellowship to T. M. Frank.

Literature Cited

Autrum, H., and D. Burkhardt. 1961. Spectral sensitivity of single visual cells. *Nature* **190:** 639.

Bayliss, L. E., R. J. Lythgoe, and K. Tansley. 1936. Some new forms of visual purple found in sea fishes, with a note on the visual cells of origin. *Proc. R. Soc. Lond. B* **816:** 95–113.

Beebe, W. 1935. *Half Mile Down* John Lane, London.

Bennett, R. R., and P. Ruck. 1970. Spectral sensitivities of dark- and light-adapted *Notonecta* compound eyes. *J. Insect Physiol.* **16:** 83–88.

Burkhardt, D. 1962. Spectral sensitivity and other response characteristics of single visual cells in the arthropod eye. *Symp. Soc. Exp. Biol.* **16:** 86–109.

Chapman, R. M., and A. B. Lall. 1967. Electroretinogram characteristics and the spectral mechanisms of the median ocellus and lateral eye in *Limulus polyphemus*. *J. Gen. Physiol.* **50:** 2267–2287.

Childress, J. J., A. T. Barnes, L. B. Quetin, and B. H. Robison. 1977. Thermally protecting cod ends for the recovery of living deep-sea animals. *Deep-Sea Res.* **25:** 419–422.

Childress, J. J., and M. H. Price. 1978. Growth rate of the bathypelagic crustacean *Gnathophausia ingens*. I. Dimensional growth and population structure. *Mar. Biol.* **50:** 47–62.

Clarke, G. L. 1936. On the depth at which fishes can see. *Ecology* **17:** 452–456.

Clarke, G. L., and C. J. Hubbard. 1959. Quantitative records of the luminescent flashing of oceanic animals at great depths. *Limnol. Oceanogr.* **4:** 163–180.

Cornwall, M. C., E. F. MacNichol, Jr., and A. Fein. 1984. Absorptance and spectral sensitivity measurements of rod photoreceptors of the tiger salamander, *Ambystoma tigrinum*. *Vision Res.* **24**(11): 1651–1659.

Crescitelli, F., M. McFall-Ngai, and J. Horowitz. 1985. The visual pigment sensitivity hypothesis: further evidence from fishes of varying habitats. *J. Comp. Physiol. A* **157:** 323–333.

Cronin, T. W. 1986. Photoreception in marine invertebrates. *Am. Zool.* **26:** 403–415.

Cummins, D. R., D-M. Chen, and T. H. Goldsmith. 1984. Spectral

sensitivity of the spiny lobster *Panulirus argus*. *Biol. Bull.* **166:** 269–276.

Cummins, D., and T. H. Goldsmith. 1981. Cellular identification of the violet receptor in the crayfish eye. *J. Comp. Physiol.* **142:** 199–202.

Dartnall, H. J. A. 1953. The interpretation of spectral sensitivity curves. *Br. Med. Bull.* **9:** 24–30.

Dartnall, H. J. A. 1974. Assessing the fitness of visual pigments for their receptor environments. Pp. 543–562 in *Vision in Fishes—New Approaches in Research*, M. Ali, ed. Plenum Press, New York.

Denton, E. J., J. B. Gilpin-Brown, and P. G. Wright. 1970. On the 'filters' in the photophores of mesopelagic fish and on a fish emitting red light and especially sensitive to red light. *J. Physiol. Lond.* **208:** 72–73.

Denton, E. J., and T. I. Shaw. 1963. The visual pigments of some deep-sea elasmobranchs. *J. Mar. Biol. Assoc. U. K.* **43:** 65–70.

Denton, E. J., and F. J. Warren. 1957. Photosensitive pigments in the retinae of deep-sea fish. *J. Mar. Biol. Assoc. UK* **36:** 651–662.

Denys, C. J., and P. K. Brown. 1982. Euphausiid visual pigments. *J. Gen. Physiol.* **80:** 451–471.

Eakin, R. M. 1972. Structure of invertebrate photoreceptors. Pp. 625–780 in *Handbook of Sensory Physiology, Vol. VII/1*, H. J. A. Dartnall, ed. Springer-Verlag, Berlin.

Eguchi, E., K. Watanabe, T. Hariyama, and K. Yamamoto. 1982. A comparison of electrophysiologically determined spectral responses in 35 species of Lepidoptera. *J. Insect Physiol.* **288:** 675–682.

Fernandez, H. R. 1965. A survey of the visual pigments of decapod crustaceans of S. Florida. *Ph. D. Thesis*, Univ. of Miami, Coral Gables, Florida.

Fernandez, H. R. C. 1978. Visual pigments of bioluminescent and nonbioluminescent deep-sea fishes. *Vision Res.* **19:** 589–592.

Fisher, L. R., and E. H. Goldie. 1958. The eye pigments of a euphausiid crustacean, *Meganyctiphanes norvegica* (M. Sars). *XV Intern. Cong. Zool. Lond. Proc.* 533–535.

Fisher, L. R., and E. H. Goldie. 1960. Pigments of compound eyes. *Prog. Photobiol. Proc. 3rd Int. Congr. Photobiol.* 153–154.

Frank, T. M. 1986. Visual spectral sensitivity of deep-sea decapod crustaceans. *Am. Zool.* **26A:** 35A.

Goldsmith, T. H. 1960. The nature of the retinal action potential, and the spectral sensitivities of ultraviolet and green receptor systems of the compound eye of the worker honeybee. *J. Gen. Physiol.* **43:** 775–799.

Goldsmith, T. H. 1965. Do flies have a red receptor? *J. Gen. Physiol.* **49:** 265–287.

Goldsmith, T. H. 1972. The natural history of invertebrate visual pigments. Pp. 727–742 in *Handbook of Sensory Physiology, Vol. VII/1*, H. J. A. Dartnall, ed. Springer-Verlag, New York.

Goldsmith, T. H. 1978. The effects of screening pigments on the spectral sensitivity of some crustacea with scotopic (superposition) eyes. *Vision Res.* **18:** 475–482.

Goldsmith, T. H. 1986. Interpreting trans-retinal recordings of spectral sensitivity. *J. Comp. Physiol. A* **159:** 481–487.

Goldsmith, T. H., and M. S. Bruno. 1973. Behavior of rhodopsin and metarhodopsin in isolated rhabdoms of crabs and lobsters. Pp. 147–153 in *Biochemistry and Physiology of Visual Pigments*, H. Langer, ed. Springer-Verlag, New York.

Goldsmith, T. H., A. F. Dizon, and H. R. Fernandez. 1968. MSP of photoreceptor organelles from the eyes of the prawn *Palaemonetes*. *Science* **161:** 468–470.

Goldsmith, T. H., and H. R. Fernandez. 1968. Comparative studies of crustacean spectral sensitivity. *Z. Vgl. Physiol.* **60:** 156–175.

Graham, C. H., and H. K. Hartline. 1935. The response of single visual sense cells to lights of different wavelengths. *J. Gen. Physiol.* **18:** 917–921.

Hara, T., and R. Hara. 1979. Retinochrome and rhodopsin in the extraocular photoreceptor of the squid, *Todares*. *J. Gen. Physiol.* **75:** 435–445.

Herring, P. J. 1976. Bioluminescence in decapod crustacea. *J. Mar. Biol. Assoc. U. K.* **56:** 1029–1047.

Herring, P. J. 1983. The spectral characteristics of luminous marine organisms. *Proc. R. Soc. Lond. B* **220:** 183–217.

Hiller-Adams, P., E. Widder, and J. F. Case. 1988. A microspectrophotometric study of visual pigments in deep-sea crustaceans. *J. Comp. Physiol. A* **163:** 63–72.

Hyatt, G. W. 1975. Physiological and behavioral evidence for color discrimination by fiddler crabs, Brachyura, Ocypodidae, genus *Uca*. Pp. 333–365 in *Physiological Ecology of Estuarine Organisms*, F. J. Vernberg, ed. University of S. Carolina Press, Columbia.

Ilse, D. 1928. Über den Farbensinn der Tagfalter. *Z. Vgl. Physiol.* **8:** 658–692.

Jarvilehto, M. 1979. Receptor potentials in invertebrate visual cells. Pp. 315–357 in *Handbook of Sensory Physiology, Vol. VII/6A*, H. Autrum, ed. Springer-Verlag, Berlin.

Jerlov, N. G. 1968. *Optical Oceanography*. Elsevier, Amsterdam. Pp. 114–131.

Jerlov, N. G. 1976. *Marine Optics*. Elsevier, Amsterdam. Pp. 134–135.

Kobayashi, H., and M. A. Ali. 1971. Electroretinographic determination of spectral sensitivity in albino and pigmented brook trout (*Salvelinus fontinalis*, Mitchill). *Can. J. Physiol. Pharmacol.* **49:** 1030–1037.

Konishi, J. 1955. Retinal and optic nerve response of the compound eye of spiny lobster, *Panulirus japonicus von Siebold*. *Rep. Fac. Fish. Univ. Mie* **2**(1): 138–144.

Kugel, M. 1977. The time course of the electroretinogram of compound eyes in insects and its dependence on special recording conditions. *J. Exp. Biol.* **71:** 1–6.

Latz, M. I., T. M. Frank, and J. F. Case. 1988. Spectral composition of bioluminescence of epipelagic organisms from the Sargasso Sea. *Mar. Biol.* **98:** 441–446.

Laughlin, S. B., A. D. Blest, and S. Stowe. 1980. The sensitivity of receptors in the posterior median eye of the nocturnal spider, *Dinopsis*. *J. Comp. Physiol.* **141:** 53–66.

Loew, E. R. 1976. Light, and photoreceptor degeneration in the Norway lobster, *Nephrops norvegicus*. *Proc. R. Soc. Lond. B* **193:** 31–44.

Lythgoe, J. N. 1968. Visual pigments and visual range underwater. *Vision Res.* **8:** 997–1011.

Lythgoe, J. N. 1972. The adaptation of visual pigments to the photic environment. Pp. 566–603 in *Handbook of Sensory Physiology, Vol. VII/1*, H. J. A. Dartnall, ed. Springer-Verlag, Berlin.

Martin, F. G., and M. I. Mote. 1982. Color receptors in marine crustaceans: a second spectral class of retinular cell in the compound eyes of *Callinectes* and *Carcinus*. *J. Comp. Physiol.* **145:** 549–554.

Mazokhin-Porshnyakov, G. A. 1960. System of colour vision of the fly, *Calliphora*. *Biophys.* **5:** 790–782.

Menzel, R. 1979. Spectral sensitivity and color vision in invertebrates. Pp. 503–580 in *Handbook of Sensory Physiology, Vol. VII/6A*, H. Autrum, ed. Springer-Verlag, Berlin.

Mikkola, K. 1972. Behavioral and electrophysiological responses of night-flying insects, especially Lepidoptera, to near UV and visible light. *Ann. Zool. Fennici* **9:** 225–254.

Munz, F. J. 1957. The photosensitive retinal pigments of marine and euryhaline teleost fishes. Ph. D. Thesis, Univ. of Cal., Los Angeles.

Munz, F. W., and W. N. MacFarland. 1973. The significance of spectral position in the rhodopsins of tropical marine fishes. *Vision Res.* **13:** 1829–1874.

Munz, F. W., and W. N. MacFarland. 1978. Evolutionary adapta-

tions of fishes to the photic environment. Pp. 193–274 in *Handbook of Sensory Physiology, Vol. VII/5*, F. Crescitelli, ed. Springer, Berlin.

Naka, K., and M. Kuwabara. 1956. The component analysis of the ERG from the compound eye of *Cambarus*. *Mem. Fac. Sci. Kyushu Univ., Series E* **22:** 75–86.

Naka, K. I., and W. A. H. Rushton. 1966. An attempt to analyze color reception by electrophysiology. *J. Physiol.* **185:** 556–586.

Nilsson, H. L., and M. Lindstrom. 1983. Retinal damage and sensitivity loss of a light-sensitive crustacean compound eye (*Cirolana borealis*): electron microscopy and electrophysiology. *J. Exp. Biol.* **107:** 277–292.

O'Day, W. T., and H. R. Fernandez. 1974. *Aristostomias scintillans* (Malacosteidae): a deep-sea fish with visual pigments apparently adapted to its own bioluminescence. *Vision Res.* **14:** 545–550.

Obara, Y., and T. Hidaka. 1968. Recognition of the female by the male, on the basis of UV reflection in the white cabbage butterfly, *Pieris rapae crucivora Boisduval*. *Proc. Jpn. Acad.* **44:** 829–832.

Partridge, J. C., S. N. Archer, and J. N. Lythgoe. 1987. Visual pigments in the individual rods of deep-sea fishes. *J. Comp. Physiol. A* **162:** 543–550 (1988).

Ruck, P. 1965. The components of the visual system of a dragonfly. *J. Gen. Physiol.* **49:** 289–307.

Ruck, P., and T. L. Jahn. 1954. Electrical studies on the compound eye of *Ligia occidentalis Dana* (Crustacea: Isopoda). *J. Gen. Physiol.* **37:** 825–849.

Scott, S., and M. I. Mote. 1973. Spectral sensitivity in some marine crustacea. *Vision Res.* **14:** 659–663.

Shaw, S. R., and S. Stowe. 1982. Photoreception. Pp. 291–358 in *The Biology of Crustacea, Vol. 3*, H. L. Atwood and D. C. Sandeman, eds. Academic Press, New York.

Shelton, P. M. J., E. Gaten, and C. J. Chapman. 1985. Light and retinal damage in *Nephrops norvegicus* (Crustacea). *Proc. R. Soc. Lond. B* **226:** 217–236.

Stark, W. S., and G. S. Wasserman. 1974. Wavelength-specific ERG characteristics of pigmented- and white-eyed strains of *Drosophila*. *J. Comp. Physiol.* **91:** 427–441.

Stieve, H., M. Bruns, and H. Gaube. 1978. Simultaneous recording by extra- and intracellular electrodes of light responses in the crayfish retina. *Vision Res.* **18:** 621–628.

Wald, G. 1967. Visual pigments in crayfish. *Nature* **215:** 1131–1133.

Wald, G. 1968. Single and multiple visual systems in arthropods. *J. Gen. Physiol.* **51**(2): 125–156.

Wald, G., P. K. Brown, and P. S. Brown. 1957. Visual pigments and depth of habitat of marine fishes. *Nature* **180:** 969–971.

Wald, G., and R. Hubbard. 1957. Visual pigment of a decapod crustacean: the lobster. *Nature* **180:** 278–280.

Wald, G., and S. Rayport. 1977. Vision in annelid worms. *Science* **196:** 1434–1439.

Wald, G., and E. B. Seldin. 1968. Spectral sensitivity of the common prawn, *Palaemonetes vulgaris*. *J. Gen. Physiol.* **51:** 694–700.

Walther, J. B. 1958. Changes induced in spectral sensitivity and form of retinal action potential of the cockroach eye by selective adaptation. *J. Insect Physiol.* **2:** 142–151.

Waterman, T. H. 1961. Light sensitivity and vision. Pp. 1–64 in *The Physiology of Crustacea, Vol. II, Sense Organs, Integration and Behavior*, T. H. Waterman, ed. Academic Press, New York.

Waterman, T. H., and H. R. Fernandez. 1970. E-vector and wavelength discrimination by retinular cells of the crayfish Procambarus. *Z. Vgl. Physiol.* **68:** 154–174.

Welsh, J. H., and F. A. Chace, Jr. 1937. Eyes of deep sea crustaceans. I. Acanthephyridae. *Biol. Bull.* **72:** 57–74.

Widder, E. A., M. I. Latz, and J. F. Case. 1983. Marine bioluminescence spectra measured with an optical multichannel detection system. *Biol. Bull.* **165:** 791–810.

Zieman, D. A. 1975. Patterns of vertical distribution, vertical migration, and reproduction in the Hawaiian mesopelagic shrimp of the family Oplophoridae. Ph. D. Thesis, University of Hawaii, Honolulu. Pp. 16–20.

Reference: *Biol. Bull.* 175: 274–283 (October, 1988)

Visual Spectral Sensitivity of the Bioluminescent Deep-sea Mysid, *Gnathophausia ingens*

TAMARA M. FRANK[1] AND JAMES F. CASE

Department of Biological Sciences and Marine Science Institute, University of California, Santa Barbara, California 93106

Abstract. The spectral sensitivity of the deep-sea mysid, *Gnathophausia ingens* (Family Lophogastridae), was measured by electroretinography on intact specimens. High sensitivity to orange light was found. This was an unexpected result for a species whose adult members are never found above 400 m. Results of chromatic adaptation and silent substitution experiments were not compatible with either a one pigment or dual pigment visual system, making this one of the more unusual visual systems ever described.

Introduction

In this, the second of two papers on the spectral sensitivities of deep-sea crustaceans, we report on the unusual visual system of the deep-sea mysid, *Gnathophausia ingens*, a species whose adult members are found below 400 m. This robust animal survives under laboratory conditions for over two years (Childress and Price, 1978), making it an ideal candidate for electrophysiological studies. Its visual system proved to be unlike any previously described crustacean visual system, including those of the deep-sea crustaceans described in our previous paper (Frank and Case, 1988). Prolonged laboratory maintenance was not responsible for the unusual results, since specimens tested three months after capture possessed identical threshold and spectral sensitivities to those tested within 24 hours of capture.

Materials and Methods

Animal collection and maintenance

Specimens of *Gnathophausia ingens* (Family Lophigastridae) were trawled from the deep basins near San Clemente and Santa Catalina Islands, using techniques described previously (Childress and Price, 1978; Frank and Case, 1988). The light-proof collecting vessel was opened in a light-tight room, and sorting was carried out under dim red light. Specimens were placed in light-proof containers for transport back to land, where they were maintained in a 4°C cold room. Earlier studies by Childress and Price (1978) demonstrated that these mysids could survive for over two years under the proper laboratory conditions, which included maintenance in regularly changed 4°C water and a weekly feeding of salmon and shrimp. Long-term observations of specimens kept in the dark with periodic exposures to white light indicated that, although they were healthy, serious damage to their eyes had occurred. Previously bright golden eyes turned white, and tail-flip responses to red light, present in freshly caught specimens, were no longer seen. Therefore, all specimens used in this study were protected from any exposure to white light. Animals were maintained in individual quart containers placed in a light tight box, and feeding and changing of maintenance water was carried out under infrared light with the aid of an infrared image converter (FJW Industries), or eventually, under dim red light once experiments confirmed very low sensitivity to light past 650 nm. Both sexes, ranging in size from 20 to 40 mm carapace length (instars 6 through 10—Childress and Price, 1983), were used for experiments.

Optical system and recording apparatus

Electroretinograms (ERGs) were recorded using the experimental set-up described in our previous study (Frank and Case, 1988). Chromatic adaptation experiments were conducted as previously described, with a 400 nm broadband filter (Melles Griot BG12, FWHM

Received 24 December 1987; accepted 28 July 1988.

[1] Current address: Department of Physiology, University of Connecticut Health Center, Farmington, CT 06032.

= 110 nm) for violet adaptation, a 520 nm broadband filter (M.G. VG6, FWHM = 90 nm) for green adaptation, and a 570 nm short wavelength cut-off filter (M.G. OG570) for orange adaptation.

Silent substitution experiments were conducted using a modification of the methods of Forbes *et al.* (1955) and Donner and Rushton (1959). The light output from two monochromators was controlled by two electromagnetic shutters (Uniblitz) connected in such a way that when one shutter opened, the other simultaneously closed. Light from the two monochromators was conducted to the eye through the two branches of a bifurcated light guide, ensuring that upon shifting illumination from one monochromator to the other, the same receptor field was illuminated. Thus, when the two light sources are matched for equal intensity and wavelength, switching from one monochromatic source to the other should produce no visual response: *i.e.*, the substitution should be "silent." Light intensity was controlled with glass neutral density filters and a neutral density wedge.

Experimental procedure

Test flashes of 100-ms duration were used, and were repeated at one minute intervals. The response to a standard flash of set wavelength and intensity was tested every five flashes to monitor the stability of the preparation. The reciprocal of the quantum flux ($\mu W/cm^2/s$) required to elicit a set criterion response (from 20 μV to 1 mV) at each wavelength, gave the spectral sensitivity function. Absorptance curves were constructed from Dartnall nomograms (1953), using methods described by Cornwall *et al.* (1984), by an iterative process to determine the best fit to the spectral sensitivity curve.

Excellent survivorship in the experimental chamber permitted three successive chromatic adaptation experiments on the same specimens. In these experiments, lasting up to 72 hours, spectral sensitivity curves from dark-adapted and chromatically adapted eyes were measured on the first day. After recovery in the dark for ten to twelve hours, another curve from the dark-adapted eye was measured. If this post-adaptation recovery curve was the same as the pre-adaptation curve (same threshold and spectral sensitivity), a second chromatic adaptation experiment (with a different color adapting light) was performed. Subsequent experiments were conducted as long as the recovery curve and the pre-adaptation curve were the same.

Silent substitution experiments were conducted by initially illuminating the eye with monochromatic light that produced a small response (50–100 μV). Light of such a low intensity was used to ensure that long term exposure would not completely photoadapt the visual pigment(s). To demonstrate that silent substitution was possible in this species with this apparatus, light of the same wavelength from another monochromator was substituted at various time intervals, and the intensity adjusted with a neutral density wedge until no response was seen. Subsequent silent substitutions were attempted with other wavelengths of light, using a neutral density wedge to make very small intensity adjustments.

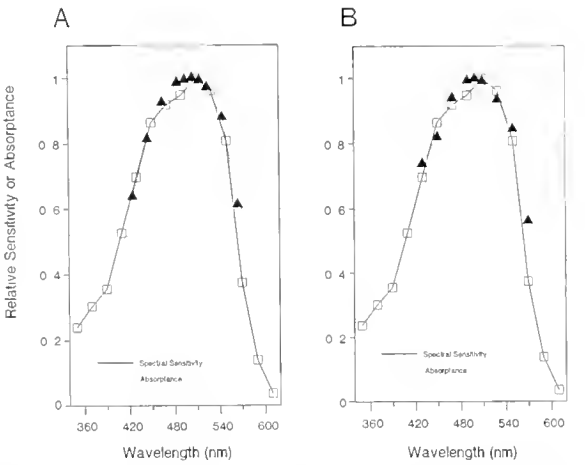

Figure 1. Solid line shows dark-adapted mean spectral sensitivity curve for *Gnathophausia ingens* (n = 25). Sensitivity is defined as the reciprocal of the relative number of quanta required to elicit a criterion response at each wavelength. Criterion responses were from 20 to 50 μV. Values from individual experiments were normalized before combining data. Standard errors are shown on the linear graph in Figure 3. The sensitivity maximum occurred around 510 nm. (A) Dotted line displays the absorptance spectrum for a hypothetical pigment with a λ_{max} of 505 nm and an O.D. of 1.2. The absorptance spectrum was calculated from the Dartnall nomogram, and plotted as the ratio of absorptance at selected wavelengths to that at 505 nm. (B) Dotted line shows the absorptance spectrum for two hypothetical pigments with λ_{max}s of 490 and 520 nm, and O.D.s of .5. Absorbance curves for the two pigments, obtained from Dartnall's template, were added together, and an absorptance curve was calculated from the result, normalized to the maximum value as above.

Regression analysis

The logarithmic spectral sensitivity values, measured at various wavelengths (every 10–20 nm from 350–610 nm) from chromatically adapted individuals, were subtracted from the values recorded from their dark-adapted eyes. The set of difference values from each animal was normalized, and the data from the same (adapting) color class were then averaged together. Linear regression lines were calculated for the mean values (Zar, 1974), and linear regression analyses were performed to determine whether the adapting lights had significant effects on the spectral sensitivities. The F-test was used to generate regressions that best fit the data. The T-test was used to determine whether the slopes of the regressions differed significantly from zero, which would indicate that the

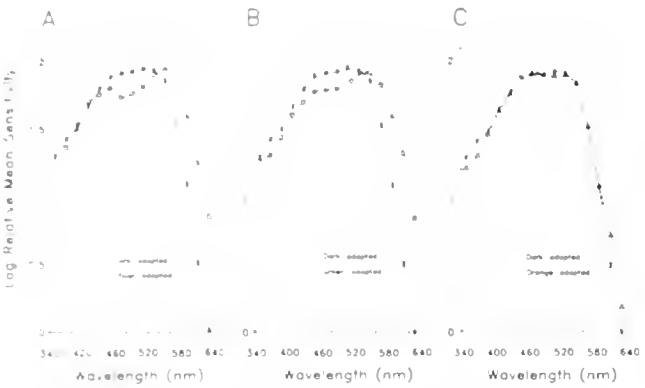

Figure 2. Effects of chromatic adaptation on the shape of the spectral sensitivity curve. Standard errors are shown in Figure 3. Values from individual experiments were normalized before combining data. (A) Average violet adapted curve (n = 11—dotted line) superimposed on the dark-adapted curve (solid line), displays two sensitivity maxima at 450 and 550 nm. (B) The effects of green adaptation (n = 7) were similar, but a short wavelength shoulder rather than a distinct peak was present. (C) Orange adaptation (n = 9) had no visible effect on the shape of the spectral sensitivity curve.

adapting light had a statistically significant effect on the shape of the spectral sensitivity curve.

Results

Spectral sensitivity

Spectral sensitivity curves were measured at criterion response amplitudes ranging from 20 μV to .5 mV. Because spectral sensitivity at all response levels was identical, only results obtained using the smallest criterion responses (from 20–80 μV) are presented, because more complete chromatically adapted curves were measured at these amplitudes.

Maximum sensitivity of dark-adapted eyes was at about 510 nm and the spectral sensitivity curve was much broader than those previously published for other crustaceans (see Fig. 2—data displayed on log scale for comparison with other published spectra). The shape of the curve is fairly well approximated by the absorptance spectrum of a single pigment present in a very high concentration (O.D. = 1.2—Fig. 1A) or by an absorptance spectrum arising from the presence of two pigments absorbing maximally at 490 and 520 nm (Fig. 1B).

Violet and green light adaptation altered the shape of the spectral sensitivity curve, but not in a manner consistent with a dual visual pigment system. Violet chromatic adaptation produced a bimodal curve with a small peak at 450 nm and a much larger 550 nm peak (Fig. 2A). Green adaptation affected the curve similarly, although the short wavelength sensitivity maximum was a shoulder rather than a peak (Fig. 2B). The effects of orange adaptation were very small (Fig. 2C); in individual animals, the curves measured under orange adaptation were identical to those measured in the dark-adapted eyes (see Fig. 5C). The chromatic adaptation results are presented on a log scale to be consistent with previously published spectral sensitivity curves on other crustaceans. However, when presented on a linear scale, the dramatic difference between the effectiveness of green and violet adaptation on altering the shape of the spectral sensitivity curve as compared with orange adaptation is much more visible (Fig. 3).

Regression analysis

Results of the linear regression analysis on the regression lines calculated for the mean difference values are shown in Figure 4. The fit to a single linear regression was poor for the data set obtained by subtracting values measured under violet adaptation from those measured in the dark-adapted eye, so these data were divided into two groups. The cut-off point for each group was chosen so that the regressions shown provided the best fit according to the F-test. The mean difference values for green adaptation were also best fit by two linear regressions, while a single regression provided the best fit to the mean difference data for orange adaptation. Both the long wavelength and short wavelength regression lines were significantly different from zero under violet adaptation ($P < .001$). Although the curve under green adaptation appears similar to that obtained under violet adaptation (Fig. 2A, B), only the long wavelength regression line (for points past 510 nm) was significantly different from zero. ($P < .001$). This indicates that green light did not have a statistically significant effect on spectral sensi-

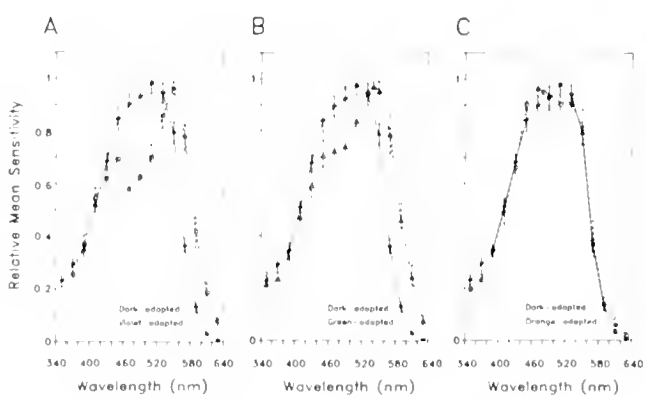

Figure 3. The effects of chromatic adaptation displayed on a linear scale, to accentuate the differences in the shapes of the chromatically adapted spectral sensitivity curves. Data are the same as those displayed in Figure 2. Bars indicate standard errors. The effects of violet and green adaptation were visibly greater and different from those of orange adaptation. A small shift in maximum sensitivity from 510 to 470 under orange adaptation is now visible.

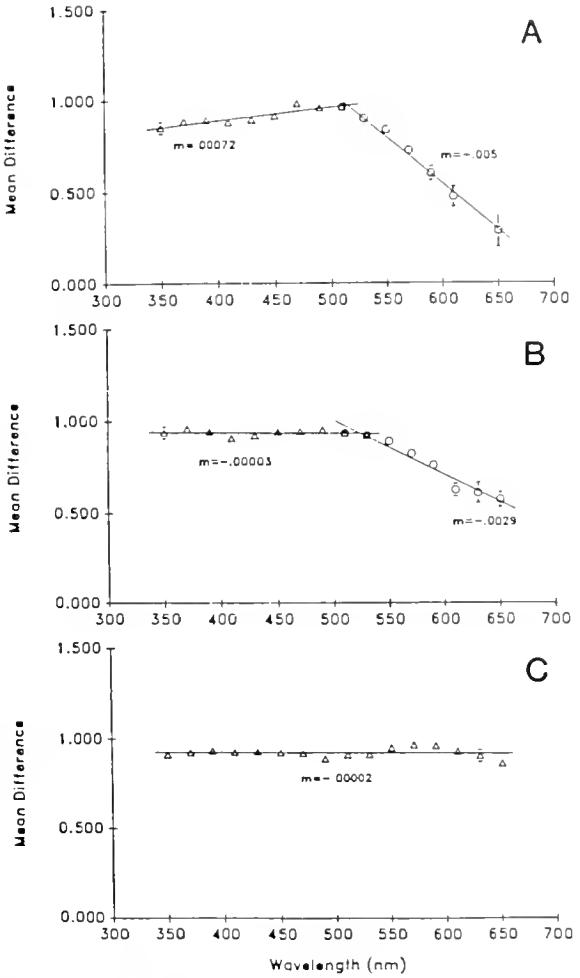

Figure 4. Statistical analysis of chromatic adaptation effects on spectral sensitivity. Each point is the mean of the difference values obtained by subtracting log light intensities required to elicit the criterion response during chromatic adaptation from those required in the dark-adapted eyes; difference values from individual animals were normalized before grouping into color classes. Standard errors are shown where they are larger than the point markers (.030). Slopes (m) of the regressions appear on each graph. (A) The mean difference values under violet chromatic adaptation (n = 11) were best fit by two regression lines. The regressions were generated using an iterative procedure in which data points were sequentially added or subtracted at 490, 510, 530, and 550 nm until the best fit was attained using the F-test. Both slopes are significantly different from zero (t = 5.89, d.f. = 7; t = 20, d.f. = 5; $P < 0.001$, both comparisons). (B) The mean difference data set for green adaptation was also best fit by two regressions. The slope of the regression from 350–530 nm is not significantly different from zero (t = .371, d.f. = 8); however, the slope of the line fitting data from 510–650 nm is (t = 11.2, d.f. = 6; $P < 0.001$). (C) The mean difference data for orange adaptation (n = 9) was best fit by one linear regression, the slope of which is not significantly different from zero (t = .110, d.f. = 14; $P \gg 0.10$).

tivity at the shorter wavelengths, but did significantly alter the shape of the spectral sensitivity curve at the longer wavelengths. The regression for the mean difference data under orange adaptation was not significantly different from zero, indicating that the shape of the spectral sensitivity curve under orange adaptation was the same as that of the dark-adapted eye.

The selective effects of the different colors were not due to intensity differences in the adapting lights. The effects were visible at the lowest intensities, and higher intensities only slightly enhanced these differences (Fig. 5). Selective effects were also not due to animal variability, as demonstrated by the results from three different chromatic adaptation experiments on one specimen (Fig. 6). This experiment also demonstrates that the results seen were not due to degenerative changes in the eye over time; complete recovery to the pre-adapted level after a sufficient dark interval can be seen (Figs. 6B, C).

Response waveforms

Analysis of the response waveforms indicates that a dual receptor system may be present, although again, the evidence is inconclusive. The ERGs were generally simple, monophasic, corneal-negative signals, characteristic of crustacean visual systems. Waveforms matched for equal amplitude in the dark-adapted eye were either similar (Fig. 7F), or, more commonly, were noticeably different only at the longest wavelengths (Fig. 7D). ERGS at the shorter wavelengths were simple in form, while at 550 to 570 nm, additional small waves appeared prior to the large wave. Occasional small positive shoulders preceding the larger negative waves were found at shorter wavelengths (Fig. 7A).

Violet, green, and orange adaptation had the same

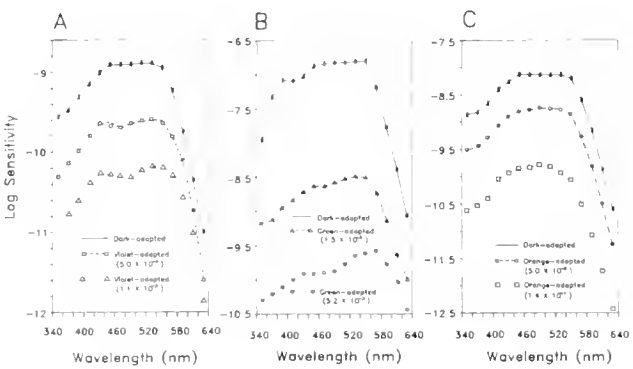

Figure 5. The effects of varying intensities of adapting lights on the spectral sensitivity function. Each graph represents data from one animal. The numbers below the plots indicate the quantum flux of the adapting light in $\mu W/cm^2/s$. (A) Violet adaptation at two different intensities produced essentially the same results. (B) The selective effects of green adaptation were more evident at the higher intensity, but were still visibly different from violet or orange adaptation at the lower intensity. (C) Selective effects of orange adaptation were not visible at either intensity, although the threshold was depressed by the same amount (1–2 log units) as under violet adaptation in A.

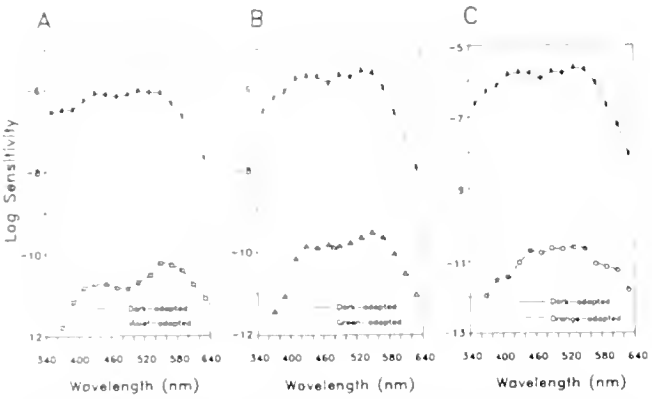

Figure 6. Selective effects of chromatic adaptation on the spectral sensitivity of one specimen. Each chromatically adapted curve is shown with the dark-adapted curve measured just prior to that chromatic adaptation experiment. The effect of the adapting light was to lower the sensitivity by approximately 4–5 log units in each experiment. The selective effects of the adapting lights are consistent with the results seen in the grouped data. (A) Blue adaptation produced two peaks at 450 and 550 nm. (B) Green adaptation similarly produced a relatively bimodal curve, with peak sensitivities at 430 and 550 nm. (C) Orange adaptation had no apparent effect on the shape of the spectral sensitivity function.

effects on the response waveforms. Under chromatic adaptation, all waveforms became biphasic, with a very small first wave (or cusp at the shortest wavelengths) followed by a second larger wave (Fig. 7B, E, G). The size of the first wave increased with increasing wavelength after 570 nm. Upon extinction of the adapting light, the response waveforms recovered to the pre-adapted state, indicating that the alteration in waveform was due to the adapting light (Fig. 7C).

Silent substitution

Substituting light from one monochromator to another did not produce a discernible dark period for *G. ingens*, since light of the same color could always be substituted without eliciting a response as long as the intensities were matched (Fig. 8A). When intensities were not properly matched, a distinct electrical signal was seen, the polarity of which depended on whether the substituting light was of a lower or a higher intensity. Silent substitution of 500 nm light for 400 nm light was always possible (Fig. 8B), indicating that the same receptor system was operating at these wavelengths. However, silent substitution was never possible between 500 and 600 nm (Fig. 8C), or 400 and 600 nm (Fig. 8D). An "on" response never completely disappeared before the "off" response became apparent. Increasing or decreasing the intensity only increased the size of the electrical signal. These results support the premise of two spectral classes of receptor cells, one dominating the responses in the blue-green, and the other operating primarily in the orange.

Discussion

Gnathophausia ingens is a deep-sea mysid whose depth distribution depends on its life history stage. The members of the size classes studied here (Instars 6–10) have a daytime depth range of 650–750 m (Childress and Price, 1978). They do not undergo a typical vertical migration, but instead disperse at night to depths between 400 and 900 m. This species possesses the typical crusta-

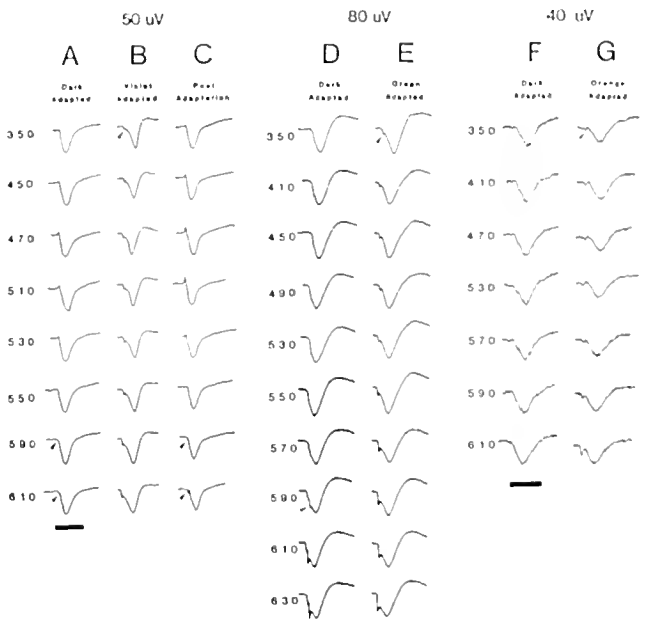

Figure 7. Response waveforms matched for equal intensity within one preparation. Data from three individuals are shown. The criterion response is shown at the top of each data set. Time bar designates 400 ms. (A) Dark-adapted waveforms were monophasic corneal-negative responses, indicated by the downward deflection, with a small corneal positive wave preceding the larger negative component at the shorter wavelengths, and a small corneal negative wave present at the longer wavelengths (arrows). (B) Violet adaptation changed all the response waveforms such that a small negative wave was present at all wavelengths (arrow), with the size of the wave increasing at the longer wavelengths. (C) Waveforms recorded two hours after extinction of the adapting light were identical to those in the dark-adapted eye. (D) The response waveforms recorded in the dark-adapted eye of another specimen were distinctly different at the longer wavelengths (arrow). The simple monophasic waveforms seen at the shorter wavelengths developed a small cusp by 590 nm, and two distinct waves were present at 610 and 630 nm. (E) The effects of a green adapting light were identical to those of the violet adapting light; the large corneal negative waves were preceded by a small corneal negative wave (arrow). The size of the small wave again increased with increasing wavelength. (F) The waveforms in this dark-adapted eye were virtually identical at all wavelengths. (G) Orange adaptation also produced the small corneal negative wave (arrow) at all wavelengths, and the small wave again increased in size at the longer wavelengths.

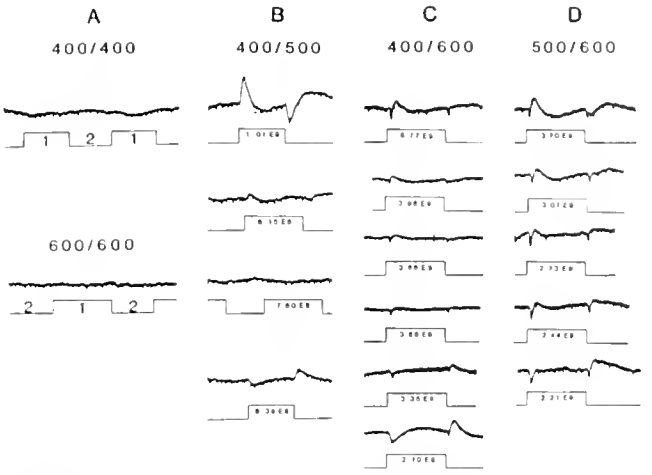

Figure 8. Results of silent substitution experiments for one specimen. The first number at the top of the graphs is the wavelength setting for Monochromator 1 (M1); the second number is for Monochromator 2 (M2). The square waves designate which monochromator was illuminating the eye for the responses seen. (A) Silent substitution was possible when M1 and M2 were set for the same wavelength, demonstrating that no discernible dark period was present during the substitution. The (1) under the square wave indicates that M1 was on at this time; when the square wave reverses polarity, light from M2 was substituted. (B) Silent substitution was also possible between 500 and 400 nm. The top figure shows the response when the intensity of the light from M1 was too high. There was a discernible "on" response at the start of the substitution, and an "off" response at the end. Responses were corneal positive in this specimen, as they were in several others, which can be attributed to the depth of the recording electrode (Konishi, 1955). The response was not a maintained "on" response for the duration of the stimulus due to the amplifier time constant. The intensity of the light from M1 is shown below the square wave pulse in photons/cm^2/s. With decreasing intensity of light, responses diminished until an intensity was reached at which no response was discernible (7.8×10^8 photons). For comparison, the last figure shows the off response when the intensity from M1 was too low and the on response upon substituting in light from M2. (C) Silent substitution was not possible between 400 and 600 nm light. Distinct on and off responses are visible in the first figure. With decreasing intensity, the on and off responses became smaller, but never disappeared. The smallest response was seen at 3.66×10^9 photons. Increasing the intensity increased the size of the on response, while decreasing the intensity produced a discernible off response. (D) Silent substitution was also not possible between 500 and 600 nm. The smallest response was at 2.73×10^9 photons, and increasing or decreasing the intensity from this value increased the size of the electrical signal.

cean spherical compound eye, but its visual physiology appears to be very unusual, and the results of this study are not entirely compatible with either a single or dual visual pigment system.

Spectral sensitivity

The absorptance curves in Figure 1 suggest two possible explanations for the unusually broad dark-adapted spectral sensitivity curve. A single pigment present in very high concentrations could give rise to such a broad spectral sensitivity curve, due to self-screening by rhodopsin. Such high concentrations of visual pigment have been found in several species of deep-sea fish (Denton and Warren, 1957) and crustaceans (Hiller-Adams *et al.*, 1988), and may increase sensitivity to light, a useful adaptation in the dimly lit deep-sea environment. However, two pigments with fairly close absorption maxima (490 and 520 nm) could also give rise to a broad spectral sensitivity curve, as demonstrated by the absorptance curve in Figure 1B.

The effects of chromatic adaptation do not support the single pigment/self-screening hypothesis. Only the response to orange adaptation is compatible with this hypothesis. The shift in maximal sensitivity is not significant, and the shape of the curve under orange adaptation is identical to the curve recorded from dark-adapted eyes in individual specimens. Under this hypothesis, the effects of green and violet adaptation should be the same as those of orange adaptation—decreasing sensitivity but not changing the position of peak sensitivity. However, violet and green light produced visible changes in the shape of the spectral sensitivity curve, and these changes were significant. Even when the adapting lights decreased the overall sensitivity by the same amount (see Fig. 6), the different colors had different effects on the spectral sensitivity. Therefore, a single visual pigment with a high optical density cannot alone explain the spectral sensitivity of *G. ingens*.

The spectral sensitivities of some shallow water lobsters, shrimp and crayfish are markedly shifted from the absorption maxima of their visual pigments (De Bruin *et al.*, 1957; Wald and Hubbard, 1957; Kennedy and Bruno, 1961; Goldsmith and Fernandez, 1968; Wald, 1968; Bruno *et al.*, 1977) and this has been attributed to selective filtering by screening pigments (Goldsmith, 1978; Cummins *et al.*, 1984). Although the eye of *Gnathophausia ingens* has not been investigated histologically, Elofsson and Hallberg (1977) and Hallberg (1977) have studied seven other species of deep-sea and shallow living mysids, and found several common characteristics. All possessed superposition eyes with a layer of red pigment cells around the proximal part of the rhabdom and below the basement membrane. In the deep-living species, the red pigment cells appeared to replace the darker retinular pigment found in other species.

Our gross histological examination of unfixed *G. ingens* eyes also revealed an abundance of red pigment cells. The eye also had a large eyeglow area, probably due to the presence of a tapetum or reflecting pigments. The eyeglow area did not change upon light adaptation, as it does in many insects and shallow living crustaceans with mobile proximal screening pigments (reviewed by Sta-

venga, 1979). This suggests that a dark proximal screening pigment is probably also absent in this species.

Due to the apparent lack of a proximal screening pigment in *Gnathophausia ingens*, the following discussion is based on the assumption that the red screening pigment is located around the proximal ends of the rhabdoms, as it is in the other deep-sea mysids lacking the proximal screening pigment (Elofsson and Hallberg, 1977; Hallberg, 1977). In this configuration, the red pigment would be in a position to filter light before it reached the visual pigment. MSP on a similar red pigment in the crab *Leptograpsus* showed that maximal absorbance was at 500 nm, with low absorbance in both the UV and red (Stowe, 1980); *i.e.*, UV and red light are not blocked by this pigment. Stowe has estimated that under strong light adaptation, when the pigment extends one third to one half way up the rhabdom, (as it does in the deep-sea mysid *Erythrops*—Hallberg, 1977), a "kink" would be seen in the spectral sensitivity curve at 380 nm. This is not the case in *G. ingens;* neither the dark-adapted or chromatically adapted eyes ever showed a violet sensitivity peak. Additionally, the long wavelength peak in *G. ingens* under violet and green adaptation always occurred between 530 and 550 nm. If a red-leaky screening pigment is responsible for the chromatically adapted spectral sensitivity (as it is in several species of muscid flies—Goldsmith, 1965), a red peak should be visible between 600 and 650 nm. Therefore, based on what is known about mysid screening pigments, the leaky screening pigment hypothesis also cannot provide an explanation for the spectral sensitivity of *G. ingens*.

In other species where there is good evidence for dual visual pigment mechanisms, the selective effects of chromatic adaptation are dramatic and undeniable under adapting lights that depressed sensitivity by 1–2 log units (Chapman and Lall, 1967; Goldsmith and Fernandez, 1968; Wald, 1968; Frank and Case, 1988). The effects of chromatic adaptation on *G. ingens* were not as distinct. Green and violet adaptation significantly changed the shape of the spectral sensitivity curve compared to orange adaptation (Fig. 4), but adapting lights that depressed sensitivity up to five log units never produced effects of the magnitude seen in other crustaceans. Additionally, we were never able to completely depress the short wavelength peak, which should be possible if a short wavelength pigment was present. Lall and Cronin (1987) describe a similar situation in the purple land crab (*Gecarcinus lateralis*). The spectral sensitivity of this species was much broader than the absorption maximum of a single visual pigment, but chromatic adaptation with different colors did not have pronounced selective effects. They suggest that this alone does not preclude the possibility of two receptor classes. Receptors containing visual pigments adjacent in the spectrum (such as blue *versus* green) would be difficult to isolate with ERGs, which are gross responses from the whole eye, and this problem would be compounded if one receptor class were numerically significantly inferior to the other class, as in the blue crab *Callinectes* (Martin and Mote, 1982).

Response waveforms

The shapes of the ERG response waveforms in the dark-adapted eye and under chromatic adaptation point towards the presence of a dual receptor mechanism, but there are inconsistencies. Under the dual receptor system hypothesis, at the shorter wavelengths, the 490 nm receptor cells would dominate the ERG. At longer wavelengths, the contribution of these shorter wavelength receptors would be diminished, and the contribution of the 520 nm receptors would become evident. The differences in response waveforms to long wavelength light (570–630 nm) and shorter wavelengths in the dark-adapted eye of *G. ingens* are consistent with this hypothesis (Fig. 7). Responses to shorter wavelengths were simple, monophasic corneal negative (downward) waveforms. At the longer wavelengths, the waveforms became more complex, with a very small negative wave preceding a much larger one. The fact that these small waves were only visible at the longest wavelengths in the dark-adapted eye, and that they became larger with increasing wavelength (Fig. 7A, D), supports the premise that they are due to the contribution of the long wavelength receptor system to the ERG.

The effects of green and violet chromatic adaptation on response waveforms are also compatible with this hypothesis. Green and violet adapting lights should and did selectively diminish the contribution of short wavelength receptors to the ERG, unmasking the contribution of the long wavelength receptors. Under these adapting lights, all waveforms were composed of a small wave preceding a larger wave, and the size of the small wave increased with increasing wavelength (Fig. 7B, E). Conversely, orange adaptation should diminish the contribution of the long wavelength receptors, and eliminate the small first waves that may have been present in the dark-adapted eye. However, this is not what occurred. The effects of orange adaptation were identical to those of violet and green adaptation; a small first wave was visible at all wavelengths and increased in size at longer wavelengths (Fig. 7G). This indicates that the small first waves are not produced by long wavelength receptor cells. These effects of orange adaptation are not consistent with the dual receptor system hypothesis, but there is currently no other physiological explanation for waveform differences in crustacean ERGs.

In insects, wavelength-specific waveform differences have been attributed to differences in the size of the gan-

glionic on/off effects in the ERG due to a leaky screening pigment. If a red leaky screening pigment is present, as in several species of muscid flies, then red stimulation would stimulate more receptors than expected, producing a larger on/off effect (Goldsmith, 1965). However, the ERG recorded in crustaceans is a more purely retinal response, with no evidence for any ganglionic component (Naka and Kawabara, 1956; Burkhardt, 1962; Chapman and Lall, 1967; Goldsmith and Fernandez, 1968). The small waves also occur only at the beginning of the response, indicating that they are not due to ganglionic contributions, since the "off" response is missing. Currently, the only explanation for waveform differences in dark-adapted crustacean eyes is that two different classes of receptor cells with different response characteristics are contributing to the ERG (Chapman and Lall, 1967; Fernandez and Goldsmith, 1968; Wald, 1968).

Silent substitution

The best evidence for a dual receptor mechanism in this species comes from the silent substitution experiments. The idea behind silent substitution (as described by Forbes *et al.*, 1955, and Donner and Rushton, 1959) is that if an eye is adapted to a steady monochromatic light, and this is replaced by a light of the same color from another source, a response will be seen if the intensity difference is within a detectable range for the eye. The substitution will only be silent when the eye can no longer detect an intensity difference, provided that the act of substitution does not produce a detectable dark period. If the lights are of different colors, the result will depend on the type of receptors contributing to the visual response. If only one type of receptor cell is present, then any two lights equally absorbed by the pigment can be silently substituted. Hence, in a single visual pigment system, an intensity can be found at each wavelength at which substitution will be silent. If more than one receptor type is contributing to the response, each with its own response characteristics, then in principle, substitution cannot be silent at all wavelengths. A response will be seen due to cessation of excitation of cells already responding, and the excitation of cells (with different membrane characteristics) previously not responding.

With our experimental design, we demonstrated that silent substitution was possible if monochromatic lights of the same colors were matched for equal intensities, indicating that an instrumental dark period was not discernible during the switch. Silent substitution was also possible between 400 and 500 nm, indicating that responses to these wavelengths are dominated by the same receptor cell class. However, 400 nm and 600 nm light could not be "silently" substituted at any intensity. Similarly, the substitution of 500 for 600 nm light always produced a discernible response. These results support the hypothesis that two receptor systems are present.

Autrum and Stumpf (1953) described the presence of a red receptor in *Musca*, basing their hypothesis partly on their heterochromatic flicker results that red light always elicited a response when substituted for blue or green light, while blue and green light intensities could be adjusted to achieve silent substitutions. However, this wavelength dependence was later attributed to stimulation of different numbers of ommatidia by red *versus* green light, due to the presence of a red leaky screening pigment (Goldsmith, 1965). Goldsmith found that it was possible to produce receptor components of equal size to green and red stimulation, but the on/off components, which are ganglionic in origin and depend on the number of receptors stimulated, could never be matched. This interpretation cannot explain our results, however, because we were working with a crustacean. As stated above, the ERG in crustaceans is a more purely retinal response, with no on/off component. Without the complicating on/off component, if a red-leaky accessory pigment was present, light intensities could be found at which weak stimulation of many receptors under red light would produce the same size response as stronger stimulation of fewer receptors under green light.

Unusual effects of adapting lights on portunid crabs (Wald, 1968; Leggett, 1979) have been attributed to the presence of a single visual pigment, whose absorption is modified by different colored filters abutting different rhabdoms upon light adaptation. Our results argue against this mechanism, as the difference in waveform responses and the inability to silently substitute between 400–500 nm *versus* 600 nm cannot be explained by a single photoreceptor class with colored filters.

We are confident that these remarkable results are not consequences of the experimental procedure. The identical apparatus was used to measure the spectral sensitivity of deep-sea oplophorids (Frank and Case, 1988) and provided clear evidence for either single or double visual pigment systems in those species, comparable to published results for shallow water crustaceans. The capture and maintenance of *Gnathophausia ingens* was identical to that of the oplophorids. The only difference is that some *G. ingens* specimens had been maintained in the laboratory for up to five months. However, both the spectral sensitivity and threshold sensitivity of specimens maintained for months in the laboratory were identical to those of specimens tested within twenty-four hours of capture, eliminating laboratory maintenance as an explanation for our unusual results.

The presence of a single highly concentrated visual pigment can be readily correlated with the deep-sea habitat of this organism, as mentioned above. However, the explanation for the long wavelength shift of peak sensi-

tivity to 510 nm, and therefore enhanced sensitivity to orange light, remains unknown. The life history of *Gnathophausia* provides no answer. The size classes used in this study are most often found above 400 m, and although smaller specimens are found at shallower depths, they are always deeper than 100 m, where the spectral distribution of light has already significantly narrowed towards the bluer wavelengths (Jerlov, 1968; Dartnall, 1974; Cronin, 1986).

The rational for the presence of two visual pigments, if they are indeed present, is even more difficult to conceive. Unexpected dual visual pigment systems have been found in several species of deep-sea fish (Denton *et al.*, 1970; O'Day and Fernandez, 1974; Bowmaker, Dartnall and Herring, unpub.; Partridge *et al.*, 1988), and may be present in some deep-sea crustaceans as well (Frank and Case, 1988). All these species possess photophores, and the cited authors have suggested that possession of dual visual pigments may play a role in congener recognition. However, *G. ingens* does not possess any photophores. It does emit a bioluminescent spew from the oral region with a peak spectral emission at 485 nm (Illig, 1905; Frank *et al.*, 1984). This is close to the peak sensitivity of one of its proposed visual pigments, but is also the same as most of the bioluminescence that has been measured from organisms obtained from these depths (Herring, 1976; Widder *et al.*, 1983), which would make congener recognition based on bioluminescence difficult.

In summary, various aspects of the visual physiology of *Gnathophausia ingens* support the premise of a dual receptor system, with maximum sensitivity at 490 nm and 520 nm. These are: (1) the unusually broad dark-adapted spectral sensitivity function; (2) the selective and statistically significant effects of violet and green adaptation on the shape of the spectral sensitivity curve; (3) wavelength specific differences in response waveforms in the dark-adapted eye; (4) effects of violet and green adaptation on the response waveforms; and (5) the inability to silently substitute between 400 and 600 nm light, and 500 and 600 nm light. However, other observations argue against this conclusion. These are: (1) the inability to significantly depress the 490 nm peak; (2) the insignificant effect of orange adaptation on the shape of the spectral sensitivity curve; and (3) the identical effects of violet, green, and orange adaptation on the shape of the response waveforms. We are left with the enigma of a deep-sea crustacean with unusually high sensitivity to orange light that cannot be explained by known combinations of visual and/or screening pigments.

Acknowledgments

We thank Dr. James Childress, his laboratory associates, and the captains and crews of the RVs *New Horizon* and *Velero IV* for assistance with animal collection. We thank Dr. Steven Bernstein, Mark Lowenstine, Robert Fletcher, and Joel Dal Pozzo for assistance with designing the experimental apparatus. Drs. Fred Crescitelli, Bruce Robison, and Edith Widder provided helpful comments and suggestions. This work was supported by a grant from the Office of Naval Research (N00014-84-K-0314) to J. F. Case, a National Science Foundation grant (OCE 85-000237) to J. J. Childress, and a UCSB research grant and dissertation fellowship to T. M. Frank.

Literature Cited

Autrum, H., and H. Stumpf, 1953. Elektrophysiologische Untersuchungen ueber das farbensehen von *Calliphora*. *Z. Vgl. Physiol.* **35:** 71–82.

Beebe, W. 1935. *Half Mile Down.* John Lane, London.

Bruno, M. S., S. N. Barnes, and T. H. Goldsmith. 1977. The visual pigment and visual cycle of the lobster, *Homarus*. *J. Comp. Physiol.* **120:** 123–142.

Burkhardt, D. 1962. Spectral sensitivity and other response characteristics of single visual cells in the arthropod eye. *Symp. Soc. Exp. Biol.* **16:** 86–109.

Chapman, R. M., and A. B. Lall. 1967. Electroretinogram characteristics and the spectral mechanisms of the median ocellus and lateral eye in *Limulus polyphemus*. *J. Gen. Physiol.* **50:** 2267–2287.

Childress, J. J., and M. H. Price. 1978. Growth rate of the bathypelagic crustacean *Gnathophausia ingens*. I. Dimensional growth and population structure. *Mar. Biol.* **50:** 47–62.

Cornwall, M. C., E. F. MacNichol Jr., and A. Fein. 1984. Absorptance and spectral sensitivity measurements of rod photoreceptors of the tiger salamander, *Ambystoma tigrinum*. *Vision Res.* **24**(11): 1651–1659.

Cronin, T. W. 1986. Photoreception in marine invertebrates. *Am. Zool.* **26:** 403–415.

Cummins, D. R., D-M. Chen, and T. H. Goldsmith. 1984. Spectral sensitivity of the spiny lobster, *Panulirus argus*. *Biol. Bull.* **166:** 269–276.

Dartnall, H. J. A. 1953. The interpretation of spectral sensitivity curves. *Br. Med. Bull.* **9:** 24–30.

De Bruin, G. H. P., and D. J. Crisp. 1957. The influence of pigment migration on vision of higher Crustacea. *J. Exp. Biol.* **34:** 447–463.

Denton, E. J., J. B. Gilpin-Brown, and P. G. Wright. 1970. On the "filters" in the photophores of mesopelagic fish and on a fish emitting red light and especially sensitive to red light. *J. Physiol.* **208:** 72–73.

Denton, E. J., and F. J. Warren. 1957. Photosensitive pigments in the retinae of deep-sea fish. *J. Mar. Biol. Assoc. U. K.* **36:** 651–662.

Donner, K. O., and W. A. H. Rushton. 1959. Retinal stimulation by light substitution. *J. Physiol.* **149:** 288–302.

Elofsson, R., and E. Hallberg. 1977. Compound eyes of some deep-sea and fiord mysid crustaceans. *Acta Zool. (Stockh.)* **58:** 169–177.

Forbes, A., S. Burleigh, M. Neyland. 1955. Electric responses to color shift in frog and turtle retina. *J. Neurophysiol.* **18:** 517–535.

Frank, T. M., E. A. Widder, M. I. Latz, and J. F. Case. 1984. Dietary maintenance of bioluminescence in a deep-sea mysid. *J. Exp. Biol.* **109:** 385–389.

Frank, T. M., and J. F. Case. 1988. Visual spectral sensitivities of bioluminescent deep-sea crustaceans. *Biol. Bull.* **175:** 255–267.

Goldsmith, T. H. 1965. Do flies have a red receptor? *J. Gen. Physiol.* **49:** 265–287.

Goldsmith, T. H. 1978. The effects of screening pigments on the spectral sensitivity of some crustacea with scotopic (superposition) eyes. *Vision Res* **18:** 475–482.

Goldsmith, T. H., and H. R. Fernandez. 1968. Comparative studies of crustacean spectral sensitivity. *Z. Vgl. Physiol* **60:** 156–175.

Hallberg, E. 1977. The fine structure of the compound eyes of mysids (Crustacea: Mysidacea). *Cell Tissue Res.* **184:** 45–65.

Herring, P. J. 1976. Bioluminescence in decapod crustacea. *J. Mar. Biol. Assoc. U.K.* **56:** 1029–1047.

Hiller-Adams, P., E. A. Widder, and J. F. Case. 1988. A microspectrophotometric study of visual pigments in deep-sea crustaceans. *J. Comp. Physiol.* **163:** 63–72.

Illig, G. 1905. Das leuchten der *Gnathophausen. Zool. Anz.* **28:** 662.

Jerlov, N. G. 1968. *Optical Oceanography.* Elsevier, Amsterdam.

Kennedy, D., and M. S. Bruno. 1961. The spectral sensitivity of crayfish and lobster vision. *J. Gen. Physiol.* **44:** 1089–1102.

Konishi, J. 1955. Retinal and optic nerve response of the compound eye of the spiny lobster, *Panulirus japonicus* von Siebold. *Rep. Fac. Fish. Univ. Mie* **2**(1): 138–144.

Lall, A. B., and T. W. Cronin. 1987. Spectral sensitivity of the compound eyes of the purple land crab *Gecarcinus lateralis. Biol. Bull.* **173:** 398–406.

Leggett, L. M. W. 1979. A retinal substrate for color discrimination in crabs. *J. Comp. Physiol.* **133:** 159–166.

Martin, F. G., and M. I. Mote. 1982. Color receptors in marine crustaceans: a second class of retinula cells in the compound eyes of *Callinectes* and *Carcinus. J. Comp. Physiol.* **145:** 549–554.

Naka, K., and M. Kuwabara. 1956. The component analysis of the ERG from the compound eye of *Cambarus. Mem. Fac. Sci. Kyushu Univ. Series E* **2**(2): 75–86.

O'Day, W. T., and H. R. Fernandez. 1974. *Aristostomias scintillans* (Malacosteidae): a deep-sea fish with visual pigments apparently adapted to its own bioluminescence. *Vision Res.* **14:** 545–550.

Partridge, J. C., S. N. Archer, and J. N. Lythgoe. 1988. Visual pigments in the individual rods of deep-sea fishes. *J. Comp. Physiol.* **162A:** 543–550.

Stavenga, D. G. 1979. Pseudopupils of compound eyes. Pp. 358–435 in *Handbook of Sensory Physiology, Vol. VII/6A.* Springer-Verlag, Berlin.

Stowe, S. 1980. Spectral sensitivity and retinal pigment movement in the crab, *Leptograpsus variegatus (Fabricius). J. Exp. Biol.* **87:** 73–98.

Wald, G. 1968. Single and multiple visual systems in arthropods. *J. Gen. Physiol.* **51**(2): 125–156.

Wald, G., and R. Hubbard. 1957. Visual pigment of a decapod crustacean: the lobster. *Nature* **180:** 278–280.

Widder, E. A., M. I. Latz, and J. F. Case. 1983. Marine bioluminescence spectra measured with an optical multichannel detection system. *Biol. Bull.* **165:** 791–810.

Zar, J. H. 1974. *Biostatistical Analysis.* W. D. McElroy and C. P. Swanson, eds. Prentice-Hall, Englewood Cliffs.

Reference: *Biol. Bull.* 175: 284–288 (October, 1988)

Fiber Types in the Limb Bender Muscle of a Crab (*Pachygrapsus crassipes*)

MICHAEL P. McDERMOTT AND PHILIP J. STEPHENS*

Villanova University, Department of Biology, Villanova, Pennsylvania 19085

Abstract. The bender muscle in the walking limb of the Pacific shore crab (*Pachygrapsus crassipes*) is composed of fibers with different structural (sarcomere length) and histochemical (NADH diaphorase and myofibrillar ATPase) properties. Slow fibers are located along the dorsal margin of the muscle and along the ventral margin in the distal portion of the muscle. The remaining bender muscle is composed of intermediate-type fibers, which can be differentiated into two groups based upon the pH sensitivity of the myofibrillar ATPase activity and the polysaccharide content of the fibers.

Introduction

Vertebrate motor neurons are considered to have a trophic influence on their target muscle fibers, since their physiological characteristics have a profound effect on the physiological properties and structural integrity of the muscle (Guth, 1968; Gutmann, 1976). Altering the firing activity or changing the motor supply can alter the contraction speed (Buller *et al.*, 1960; Buller and Lewis, 1965; Lomo *et al.*, 1974; Luff, 1975), calcium uptake (Sreter *et al.*, 1975), and energy metabolism (Buller *et al.*, 1969; Barany and Close, 1971; Pette, 1984) of the muscle fibers. Recently, work on invertebrates involving the fast excitor to the crayfish claw closer muscle has revealed that changing the firing patterns causes changes in the physiological (Lnenicka and Atwood, 1985; Pahapill *et al.*, 1986) and morphological (Lnenicka *et al.*, 1986) properties of the synapses (review: Atwood and Wojtowicz, 1986). As a prelude to a study of the effects of changing motor axon firing patterns on the properties of target muscle fibers, we have examined certain morphological and histochemical properties of the bender muscle in pristine walking limbs of the crab *Pachygrapsus crassipes*.

The skeletal muscles of crustaceans may be innervated by as few as three motor neurons (Wiersma and Ripley, 1952) and some evidence for trophic interactions between nerve and muscle comes from a close matching between motor neuron and muscle properties (Atwood, 1973). In the claw closer muscle, for example, there is a matching between muscle fiber type and the innervation patterns of the two excitatory motor neurons. In lobster, the innervation patterns of the two excitatory motor axons are matched with the oxidative capacity of the muscle fibers (Lang *et al.*, 1980). The oxidative capacity of fibers is low when innervated only by the fast axon, high when innervated only by the slow axon, and intermediate when innervated by both axons. In the crab closer muscle, a more detailed study has been performed on a small number of identifiable closer muscle fibers (Maier *et al.*, 1984). In this study the fast fibers in the crab closer muscle were divided into three sub-groups on the basis of the pH sensitivity of myofibrillar adenosine triphosphatase (ATPase) activity (Tse *et al.*, 1983). The slow and some fast (group II) closer muscle fibers are innervated by the fast and the slow excitatory axons, while the remaining fast muscle fibers are innervated by only the fast closer excitor.

In the present study we have examined certain structural and histochemical properties of fibers in the bender muscle in the walking limbs of the Pacific shore crab (*Pachygrapsus crassipes*). The limb bender muscle is innervated by two excitatory motor axons and by branches of the common inhibitor (Wiersma and Ripley, 1952). We show that the bender muscle is composed of slow and two types of intermediate fibers, and that these different types of fibers are regionally distributed within the bender muscle.

Materials and Methods

Crabs (*P. crassipes*) were obtained from the Pacific Biomarine Laboratories, Venice, California, and were

Received 13 October 1987; accepted 27 July 1988.

* To whom all correspondence should be sent

kept in the laboratory at 24°C. The animals were kept individually, and feeding (Purina rabbit chow) and subsequent seawater changes were performed every 2 to 3 days. Observations were made using autotomized, second and third walking limbs removed from crabs that had been acclimated to laboratory conditions for at least 4 weeks.

Certain histochemical properties were examined in frozen sections of the bender muscle. The cuticle of the carpus was reduced in thickness with a dental drill. The stretcher muscle was removed, and the bender muscle plus the remaining thin cuticle were mounted on a chuck in *Histo Prep* (Fisher Scientific) and immersed in liquid nitrogen; the tissue was allowed to equilibrate to −25°C in the cryostat. Sections (20 μm thick) were mounted on glass slides and air dried for 15 to 60 min.

Sections were stained for activity of the mitochondrial enzyme nicotinamide dehydrogenase (NADH) diaphorase using the method of Ogonowski and Lang (1979), and for calcium-activated myofibrillar adenosine triphosphatase (ATPase) activity with acidic or basic preincubation, using a modified procedure of Padykula and Herman (1955). Acidic preincubation was performed in a solution of 100 m*M* KCl and 100 m*M* Na-acetate at pH 5.0 for 10 min at room temperature. Preliminary experiments using pH 4.6 pre-incubation (Maier *et al.*, 1984) did not produce differentiation of muscle fibers in sections of the bender muscle. Alkaline preincubation was carried out in a solution of 18 m*M* $CaCl_2$ and 25 m*M* Na barbitol at pH 9.4 for 5 min, then transferred to the same solution containing 0.05% mercaptoethanol for 20 s. For both preincubation regimes, myofibrillar ATPase activity was determined as described by Maier *et al.* (1984). Sections were dehydrated in a graded series of ethanol, cleared in xylene, and mounted in Permount.

The polysaccharide content of bender muscle fibers was determined in unfixed, frozen sections using the method of Lillie and Fullman (1976); no counterstain was used.

Sarcomere length measurements were made from single bender muscle fibers fixed at resting length (O'Connor *et al.*, 1982). The cuticle over the stretcher muscle was removed. The underlying stretcher muscle, limb nerve, and connective tissue layer were carefully removed to expose the bender muscle. The preparation was bathed in a calcium-free, high magnesium crab saline for 1 h in an attempt to reduce muscle contraction during fixation. The carpus-propus joint was positioned so that the bender muscle was stretched and the preparation was immersed in Bouin's fixative for 36 h. The bender muscle was removed from the carpus and stored in 70% ethanol.

Sarcomere length measurements were made from single muscle fibers that had been teased into myofibrils in a drop of 70% alcohol on a glass slide. The myofibrils were examined under Nomarski optics and the length of five successive sarcomeres was measured using a calibrated ocular micrometer. Measurements were made from five different myofibrils and an average sarcomere length value was calculated for the muscle fiber. Measurements were made for 100 fibers removed from each bender muscle.

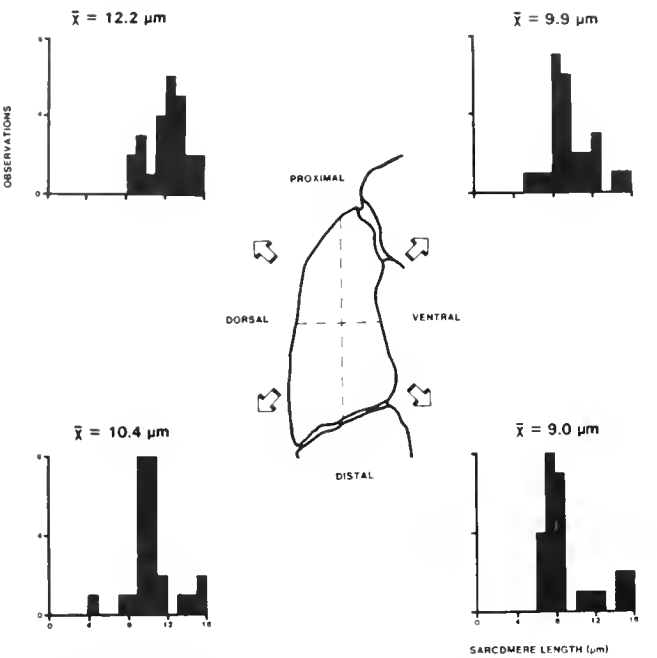

Figure 1. Sarcomere length measurements of 25 fibers removed from each quadrant of the bender muscle (inset diagram).

Results

The bender muscle is located in the carpopodite segment of the limb. In *P. crassipes*, the walking legs are compressed in the anterior-posterior direction, but the degree of compression of any one segment is not always constant. In the carpopodite, for example, the proximal region exhibits little compression and is essentially cylindrical (see Fig. 2). By contrast, the distal portion of the carpopodite is compressed to form flat anterior and posterior surfaces (see Figs. 3D and 4D). The inset of Figure 1 shows the orientation of the carpopodite. The limb is viewed from the anterior surface and is connected proximally to the meropodite and distally to the propodite. The other two surface are called dorsal and ventral.

Measurements made from 100 fibers removed from different areas in the bender muscle revealed an average sarcomere length of about 10.5 μm, with a range of 4 to 16 μm. In one preparation, the bender muscle was divided into four regions and measurements were made from each quadrant (Fig. 1—inset). The proximal-dorsal quadrant had fibers with the longest mean sarcomere

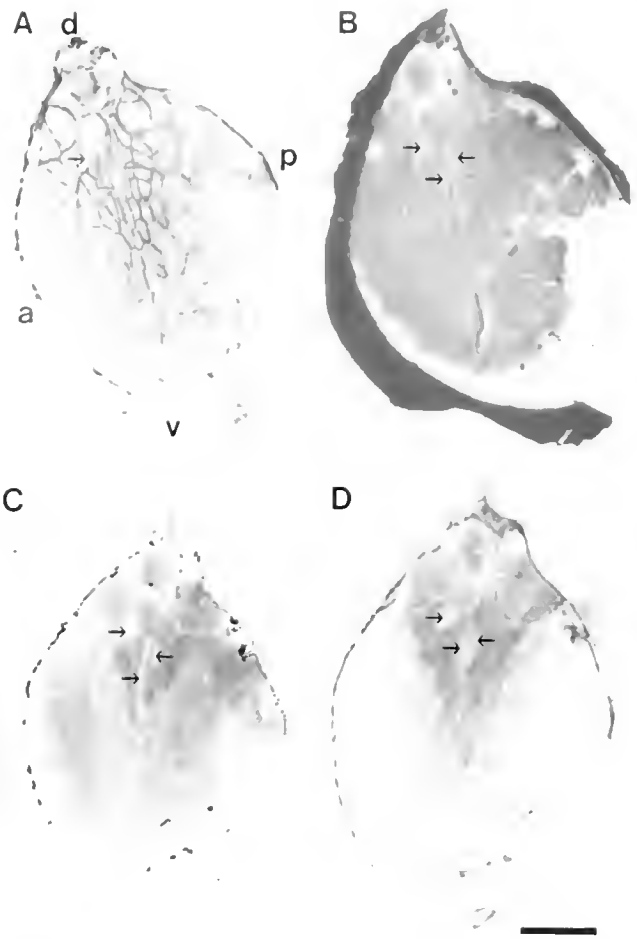

Figure 2. Histochemical properties of the bender muscle. Serial sections stained for NADH diaphorase activity (A), myofibrillar ATPase activity with alkaline (B) and acid (C) preincubation, and for polysaccharide content (D). a: anterior; d: dorsal; p: posterior; v: ventral. Calibration: 500 μm (A–C) and 415 μm (D).

length (12.2 μm; range 8 to 16 μm). The distal-dorsal quadrant contained a similar population of long-sarcomere fibers but also had some fibers with shorter (4 to 5 μm) sarcomeres. Fibers located on the ventral surface of the bender muscle had sarcomeres between 4 and 16 μm; the distal-ventral quadrant had a higher proportion of shorter-sarcomere (5 to 8 μm) fibers (Fig. 1).

Sections of the dissected carpopodite revealed that the bender muscle extends along the entire anterior surface and along some of the posterior surface of the segment (Fig. 2). The smaller stretcher muscle (which was removed prior to sectioning) is located along the posterior surface of the carpopodite and is confined to the ventral and central portion of the segment.

Bender muscle fibers can be differentiated by their contrasting histochemical properties. This can be seen in Figure 2, which shows four serial sections of the bender muscle taken at a level about one-third from the proximal end of the carpopodite. There is a population of muscle fibers that displays high NADH diaphorase activity, as seen by dark rings around the margin of individual fibers (Fig. 2A). In all preparations (n = 16), these types of fibers were located in the dorsal half of the muscle, on either side of the apodeme. With regard to myofibrillar ATPase activity, these same fibers stained poorly with alkaline preincubation (Fig. 2B) but well with acidic preincubation (Fig. 2C). Finally, these fibers had a high polysaccharide content (Fig. 2D).

Most of the other fibers in the bender muscle showed poor NADH diaphorase activity (Fig. 2A) and high alkaline myofibrillar ATPase activity (Fig. 2B). In all preparations (n = 16), staining for myofibrillar ATPase activity with acidic preincubation revealed that these fibers are not a homogeneous group. In Figure 2C there is one group of lighter staining fibers located towards the center of the muscle, and a second group of darker staining fibers around the peripheral margins of the muscle. A similar difference was also seen in sections stained for polysaccharide content (Fig. 2D). Fibers in the central portion of the muscle had a level of staining that was intermediate between fibers located more dorsally (dark staining) and fibers on the ventral margin of the muscle (light staining). Finally, in all preparations there were always some fibers that exhibited poor myofibrillar ATPase (at both pH levels) and NADH diaphorase activities (Fig. 2—arrows).

It is apparent that polysaccharide content may be correlated with the histochemical properties of most fibers in the bender muscle (Fig. 2). In all preparations (n = 16) fibers with high polysaccharide content (Fig. 2D) stained well for NADH diaphorase (Fig. 2A) and had high acid myofibrillar ATPase activity (Fig. 2C). Fibers with lower polysaccharide content (Fig. 2D) stained well for alkaline myofibrillar ATPase activity (Fig. 2B) and poorly for NADH diaphorase (Fig. 2A). We have used this correlation between fiber-type and polysaccharide content to differentiate fiber-types in the different regions of the bender muscle (Fig. 3); these observations were confirmed by examination of adjacent sections stained for NADH diaphorase activity (Fig. 4) and for myofibrillar ATPase activity with acid and alkaline pre-incubation (micrographs not shown).

Figures 3 and 4 each show four sections taken at different levels of the bender muscle; the inset numbers represent the level of the section of the carpopodite, with proximal as 0 and distal as 100. In the proximal portion of the muscle, fibers with high polysaccharide content and high NADH diaphorase activity form a "V-shaped wedge" around the apodeme in the dorsal portion of the muscle (Figs. 3A, B, and 4A, B). Intermediate staining fibers are located on either side of the "wedge," while poorly staining fibers are located mostly ventrally in the bender muscle (Fig. 3A, B).

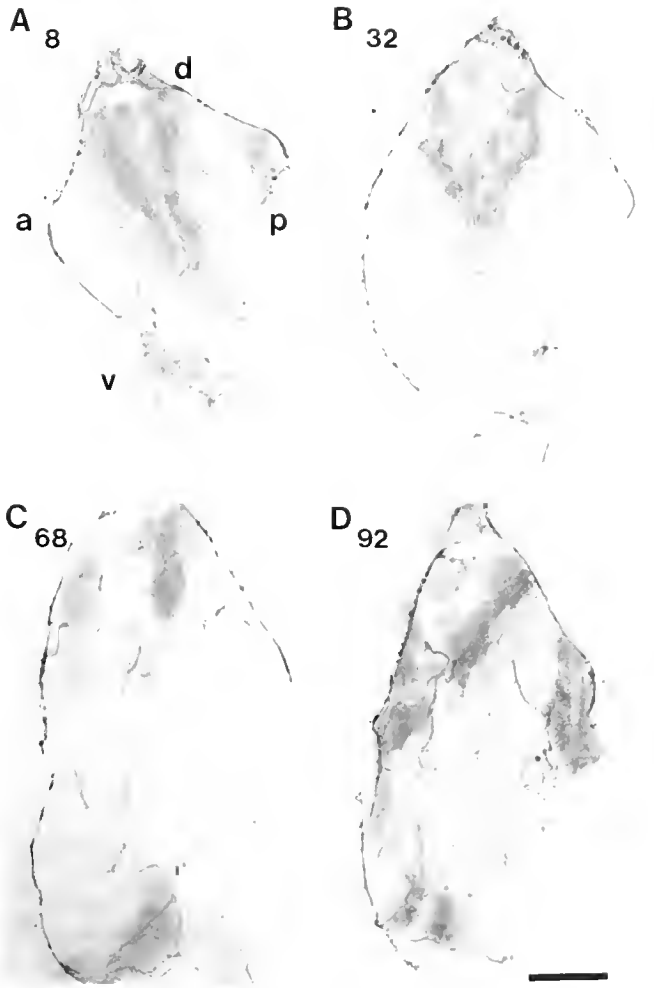

Figure 3. Polysaccharide content of bender muscle fibers. The inset numbers represent the level of sectioning in the muscle. 0 represents proximal, 100 represents distal. a: anterior; d: dorsal; p: posterior; v: ventral. Calibration: 500 μm.

In the distal half of the bender muscle, fibers with high polysaccharide content and high NADH diaphorase activity are located on the dorsal and ventral margins of the bender muscle (Figs. 3C, D, and 4C, D). Intermediate staining fibers are located mostly anteriorly, while poorly staining fibers are found mostly in the posterior-central portion of the bender muscle (Fig. 3C, D). The above staining profiles were consistent in all preparations (n = 16).

Discussion

The present study shows that the bender muscle in the walking limbs of *P. crassipes* is not composed of a uniform population of fibers. In other crustacean muscles a correlation has been found between fiber type, sarcomere length, NADH diaphorase activity and myofibrillar ATPase activity (Atwood, 1973; Ogonowski and Lang, 1979; Tse *et al.*, 1983; Maier *et al.*, 1984; Stephens *et al.*, 1985). Slow muscle fibers tend to have long sarcomeres (>10 μm), high NADH diaphorase activity, and high acid myofibrillar ATPase activity. In the proximal portion of the bender, fibers with long sarcomere lengths were found predominantly in the dorsal half of the muscle. The presumption that these fibers are slow is supported by the histochemical data, since there is a distinct population of muscle fibers with high NADH diaphorase activity and acid myofibrillar ATPase activity in this region (Fig. 2A, C). In the distal region of the muscle, however, presumptive slow fibers were concentrated in the dorsal, ventral and anterior portions of the muscle (Fig. 4C, D). It is interesting that NADH diaphorase activity in individual slow muscle fibers is confined to the peripheral margin (Figs. 2A and 4). A similar observation has been made in the tails of lobster (Ogonowski and Lang, 1979) and crab (Stephens *et al.*, 1985) and indicates that

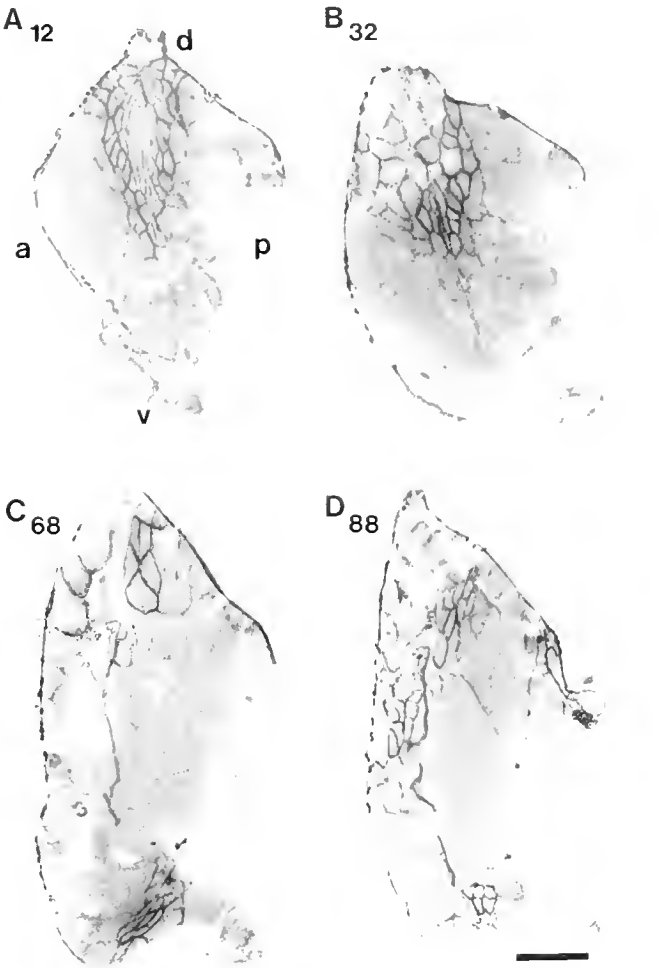

Figure 4. NADH diaphorase activity of bender muscle fibers. The inset numbers represent the level of sectioning in the muscle. 0 represents proximal, 100 represents distal. a: anterior; d: dorsal; p: posterior; v: ventral. Calibration: 500 μm.

the mitochondria containing this enzyme are concentrated in the peripheral margins of the slow fibers.

In many crustacean muscles, fast fibers have short sarcomeres (<4 μm), low NADH diaphorase activity and high alkaline myofibrillar ATPase activity. Our observations revealed no sarcomeres less than 4 μm in length (Fig. 1), indicating that the bender muscle contains no fast fibers. The remaining fibers in the bender muscle are therefore assumed to be intermediate-type fibers. The intermediate-type fibers appear to be concentrated ventrally in the proximal portion of the muscle (Fig. 2), and posteriorly in the distal portion of the muscle (Figs. 3 and 4).

In the present study we have found that the polysaccharide content is highest in slow fibers (Fig. 2). A similar correlation has been made between polysaccharide content and fiber-type in crab swimming muscles (Tse *et al.*, 1983). Furthermore, based on polysaccharide content there appear to be two types of intermediate fibers. Moreover, the distribution of the fibers with different polysaccharide content appears to be in line with those that exhibit contrasting acid ATPase activity (Figs. 2C, D). Fibers adjacent to the slow fibers have higher polysaccharide content and have a lighter staining profile for ATPase activity. Paradoxically, in some sections there were one or more fibers with intermediate polysaccharide content, and low NADH diaphorase and myofibrillar ATPase activities (Fig. 2—arrows). We have not been able to typify these fibers.

It may be argued that the polysaccharide content of the different fibers was influenced by the dissection procedure prior to freezing of the tissue. The dissection may have selectively stimulated one axon so that the innervated fibers could have been activated and thus could have decreased or depleted their polysaccharide stores. To examine this possibility, we froze several limbs immediately after autotomy. Although the presence of cuticle decreased the quality of the sections, no differences between the staining profiles of these sections and those from dissected preparations were observed (McDermott, unpub. observations). We conclude that the difference in the polysaccharide content of the various muscle fibers is not artifact.

Acknowledgments

This work was funded by a grant from the Research Corporation; the technical assistance of Ms. Louise diCola is gratefully acknowledged.

Literature Cited

Atwood, H. L., 1973. An attempt to account for the diversity of crustacean muscle. *Am. Zool.* **13:** 357–378.

Atwood, H. L., and J. M. Wojtowicz, 1986. Short-term and long-term plasticity and physiological differentiation of crustacean motor synapses. *Int. Rev. Neurobiol.* **28:** 275–361.

Barany, M., and R. I. Close, 1971. The transformation of myosin in cross-innervated rat muscles. *J. Physiol.* **213:** 455–474.

Buller, A. J., and D. M. Lewis, 1965. Further observations on mammalian cross-innervated skeletal muscle. *J. Physiol.* **178:** 343–358.

Buller, A. J., J. C. Eccles, and R. M. Eccles, 1960. Interaction between motor neurons and muscles in respect to the characteristic speed of their response. *J. Physiol.* **150:** 417–439.

Buller, A. J., W. F. H. M. Mommaerts, and K. Seraydarian, 1969. Enzymic properties of myosin in fast and slow twitch muscle of the cat following cross-reinnervation. *J. Physiol.* **205:** 581–597.

Guth, L., 1968. Trophic influences of nerve on muscle. *Physiol. Rev.* **48:** 645–687.

Gutmann, P. V., 1976. Neurotrophic relations. *Ann. Rev. Physiol.* **38:** 177–216.

Lang, F., M. M. Ogonowski, W. J. Costello, R. Hill, B. Roehrig, K. Kent, and J. J. Sellars, 1980. Neurotrophic influence on lobster skeletal muscle. *Science* **207:** 325–327.

Lnenicka, G. A., and H. L. Atwood, 1985. Age-dependent long-term adaptation of crayfish phasic motor axon synapses to altered activity. *J. Neurosci.* **5:** 459–467.

Lnenicka, G. A., H. L. Atwood, and L. Marin, 1986. Morphological transformation of synaptic terminals of a phasic motoneuron by long-term tonic stimulation. *J. Neurosci.* **6:** 2252–2258.

Lillie, R. D., and H. M. Fullman, 1976. *Histopathologic Technic and Practical Histochemistry* 4th Ed. McGraw-Hill, New York.

Lomo, T., R. H. Westgaard, and H. A. Dahl, 1974. Contractile properties of muscle: control by pattern of muscle activity in the rat. *Proc. R. Soc. Lond. (Biol.)* **187:** 99–103.

Luff, A. R., 1975. Dynamic properties of fast and slow skeletal muscles in the cat and rat following cross-innervation. *J. Physiol.* **248:** 83–96.

Maier, L., W. Rathmayer, and D. Pette, 1984. pH lability of myosin ATPase activity permits discrimination of different muscle fibre types in crustaceans. *Histochemistry* **81:** 75–77.

O'Connor, K., P. J. Stephens, and J. M. Leferovich, 1982. Regional distribution of muscle fiber types in the asymmetric claws of Californian snapping shrimp. *Biol. Bull.* **163:** 329–336.

Ogonowski, M. M., and F. Lang, 1979. Histochemical evidence for enzyme differences in crustacean fast and slow muscle. *J. Exp. Zool.* **207:** 143–151.

Padykula, H. A., and A. Herrmann, 1955. Factors affecting the activity of adenosine triphosphate and other phosphotases as measured by histochemical techniques. *J. Histochem. Cytochem.* **3:** 161–169.

Pahapill, P. A., G. A. Lnenicka, and H. L. Atwood, 1986. Neuronal experience modifies synaptic long-term facilitation. *Can. J. Physiol. Pharmacol.* **64:** 1052–1054.

Pette, D., 1984. Activity-induced fast to slow transitions in mammalian muscle. *Med. Sci. Sports. Exercise* **16:** 517–528.

Sreter, F. A., A. R. Luff, and J. Gergely, 1975. Effect of cross-reinnervation on physiological parameters and on properties of myosin and sarcoplasmic reticulum of fast and slow muscles of the rabbit. *J. Gen. Physiol.* **66:** 811–821.

Stephens, P. J., J. M. Leferovich, and P. Klainer, 1985. Neuromuscular relationships in the abdomen of the Californian shore crab *Pachygrapsus crassipes*. *J. Neurobiol.* **16:** 127–136.

Tse, F. W., C. K. Govind, and H. L. Atwood, 1983. Diverse fiber composition of swimming muscles in the blue crab, *Callinectes sapidus*. *J. Can. Zool.* **61:** 52–59.

Wiersma, C. A. G., and S. H. Ripley, 1952. Innervation patterns of crustacean limbs. *Comp. Oecol.* **2:** 391–405.

Reference: *Biol. Bull* 175: 289–300. (October, 1988)

A New Look at Insect Respiration[1]

KAREL SLÁMA

Insect Chemical Ecology Unit, UOCHB, Czechoslovak Academy of Sciences, 15800 Praha, Czechoslovakia

Abstract. A novel thermographic method has been used for simultaneously monitoring the passage of air through up to eight spiracles of endopterygote insects. Measurements on pupae of various lepidopteran species revealed active regulation of inspirations and expirations through one or two spiracles while the majority remained hermetically closed for prolonged periods. Because of subatmospheric hemocoelic pressure acting bellows-like on the large tracheae and air sacs, air is quickly sucked into the tracheal system whenever a spiracle opens. Large, mechanically produced positive peaks in hemocoelic pressure are associated with periodic outbursts of tracheal gases through specific spiracles. During the rhythmic pulsations in hemocoelic pressure, some spiracles open and close at different locations so that CO_2 is quickly ventilated. Spiracles on the same segment can function in synchrony with a spiracle on some other, even distant segment. In the period of subatmospheric hemocoelic pressure, the spiracles usually open in "twinkles" or flutters lasting only 50–300 ms. Some pupae, for example, diapausing *Manduca*, use only one "master spiracle" which opens for 200 ms about once a minute. Each opening is accompanied by a gulp of 500 nl of air sucked in by negative tracheal pressure. All other spiracles may be hermetically closed for 16 h or more.

It is concluded that insect respiration is controlled by a hitherto unknown, brain independent, neuromuscular mechanism (coelopulse) consisting of two main components: (a) a mechanism that integrates proprioceptive input to control the location and timing of the spiracular openings, and (b) a coordinated system of hemocoelic pressure control that regulates the force and direction of air flow through the spiracles. The results of this study question the general validity of the classical theory of insect respiration by simple gaseous diffusion.

Received 8 September 1987; accepted 26 July 1988.

[1] Dedicated to Prof. C. M. Williams of Harvard University on the occasion of his 70th birthday.

Introduction

Flying or running insects show regular pumping movements of the abdomen. These movements are associated with rhythmic changes of internal body (hemocoelic, intratracheal, or hemolymph) pressure which, acting on the walls of the tracheal sacs and tubes, produce bulk-flow of gases through the spiracles. This type of ventilation resembles ventilation of mammalian lungs by the respiratory muscles of the chest and diaphragm. The basic features of such convective tracheal ventilation have been reviewed by Babák (1912), Buck (1962), Mill (1974), Miller (1974, 1981), Kaars (1981) and Kestler (1985). The innervation and regulation of the spiracles has been described best by Miller (1981).

More complicated conditions have been encountered in immobile resting stages having very low respiratory exchange. It was believed until now that these stages—such as diapausing pupae—show no respiratory movements. Oxygen was expected to penetrate within the body by simple diffusion through the spiracles while CO_2 diffused in the opposite direction. Though this so called "diffusional theory of insect respiration" is generally associated with the late August Krogh, it was actually proposed over 150 years ago (see Wigglesworth, 1984). What Krogh accomplished was the measurement and mathematical calculations of diffusion rates of respiratory gases through the tracheal system. Subsequently, the general validity of Krogh's work has stood the test of time (see Buck, 1962, and Kestler, 1985).

In 1967 Schneiderman and his colleagues (Levy and Schneiderman, 1966; Brockway and Schneiderman, 1967) showed that discontinuous respiration was associated with specific changes in mechanical pressure within the tracheal system. Later Sláma (1976) observed that

certain immobile stages of insects exhibited rhythmic pulsations in hemocoelic pressure. Provansal *et al.* (1977) emphasized that these pulsations, which are currently known as the extracardiac pulsations, might be associated with regulation of water balance and tracheal ventilation. More recently I have used special isotonic strain-gauge transducers (Sláma, 1984a) and microrespirographs (Sláma, 1984b) to document that insects can actively and selectively control the bulk flow of gases through the spiracles. The homeostatic control of hemocoelic pressure on tracheal ventilation appeared to be effected by a novel, brain-independent, cholinergic circuitry with the centers located in thoracic ganglia of the ventral nerve cord (Sláma *et al.*, 1979; Sláma, 1986). Such an autonomic, parasympathetic-like nervous system has recently been found in various species and developmental stages of insects. It has been called the coelopulse system (Sláma, 1988b). Encouraged by these findings I have worked since 1979 on a method that could display the dynamics of respiration through the spiracles. This paper describes some initial results obtained with a microanemometric network that can monitor over prolonged periods the gas flow through one or more spiracles.

Material and Methods

The pupae of all the investigated species were obtained from our laboratory cultures. Larvae of *Actias selene* were fed fresh *Rhododendron sp.* leaves. Eggs were purchased from dealers, and the pupae were kept and measured at 25°C. *Sphinx ligustri* larvae were fed fresh leaves of *Ligustrum vulgare* outdoors in September. Diapausing pupae were stored at 5°C; measurements were made at room temperature (24–25°C). *Hyalophora cecropia* larvae were reared on willow (*Salix caprea*) and *Manduca sexta* larvae on an artificial diet at 25°C. Eggs of the latter two species were obtained courtesy of Prof. L. M. Riddiford and Dr. K. Hiruma of the University of Washington, Seattle. Diapausing pupae of these species were stored at 5°C; measurements were made at room temperature.

The spiracles to be measured were permanently equipped with male parts of small, plastic connectors manufactured from disposable tips of common automatic pipettes (Pipetman). Female parts of the conical fittings were fixed to 250 mm long anemometric tubings (teflon tubing 0.6 mm I.D.; 1.0 mm O.D.) leading to a multiple anemometric transducer (Fig. 1B). The fittings over the spiracles were smeared with silicone grease to insure a tight seal and easy installation or removal. Originally, the hemocoel of the pupae was connected by a steel needle with a special hydraulic transducer (Sláma, 1976), which could record simultaneously all respiration-dependent changes in hemocoelic pressure. It appeared, however, that the epidermal injury caused by penetration of the integument might cause long-lasting disturbances of respiratory functions, especially in diapausing pupae. After invention of a method for indirect recording of hemocoelic pressure from the body surface (Sláma, 1984a), the hydraulic transducers were usually replaced by noninvasive contact or isotonic transducers. In the present anemometric study I used the isotonic transducers in simple "pulling" version with the sensitive membrane attached to the tip of the abdomen. This served as an auxiliary detector for monitoring all relative changes in hemocoelic pressure, *e.g.*, inspirations, expirations, hermetical closure of all spiracles, or extracardiac pulsations in hemocoelic pressure.

The microanemometer setup for monitoring the passage of air through the spiracles consisted of four independent thermographic channels (4 resistant bridges). Each channel contained two matched thermographic elements (thermistors) connected in the neighboring branches of the Wheatstone's resistant bridge. The thermistors (type 10 NR 17A, Pramet Co., Šumperk, Czechoslovakia) were positioned within the transducer so that exactly half of their bodies protruded from the inside end of the anemometric tubing (O.D. of the selected thermistors was less than 300 μm, resistance from 280 to 480 Ohm) (see Fig. 1A). The movement of air in the tubing in either direction caused positive or negative temperature changes on slightly warmed body of the thermistor. This resulted in the respective + or − imbalance of the resistance bridge (bridge feeding 2 V AC of 5 kHz). After amplification and decoding of the signal, the recorder showed the respective + or − deviations from the midline. The two thermistors paired in one channel recorded the + and − changes with reversed polarity. When only one was connected to the spiracle while the other remained free as a control, the instrument selectively recorded inspirations and expirations in the opposite directions. This type of selective recording from up to four spiracles was predominantly used with developing pupae where inspirations alternated with frequent expirations (Figs. 1A, B).

The "nonselective" type of anemometric measurements involved situations when both thermistors of each pair terminated on the spiracles. In this case, each thermistor of the pair recorded movements of the same polarity (such as inspiration) in opposite directions from the midline. The responses were reversed with the reversed (expiratory) directions and, obviously, atypical or aberrant response occurred when both thermistors of a pair became activated at the same moment. In this way it was possible to record simultaneously from up to eight spiracles, provided that the polarity of responses was known (otherwise an inspiration in the + gate could be confused with

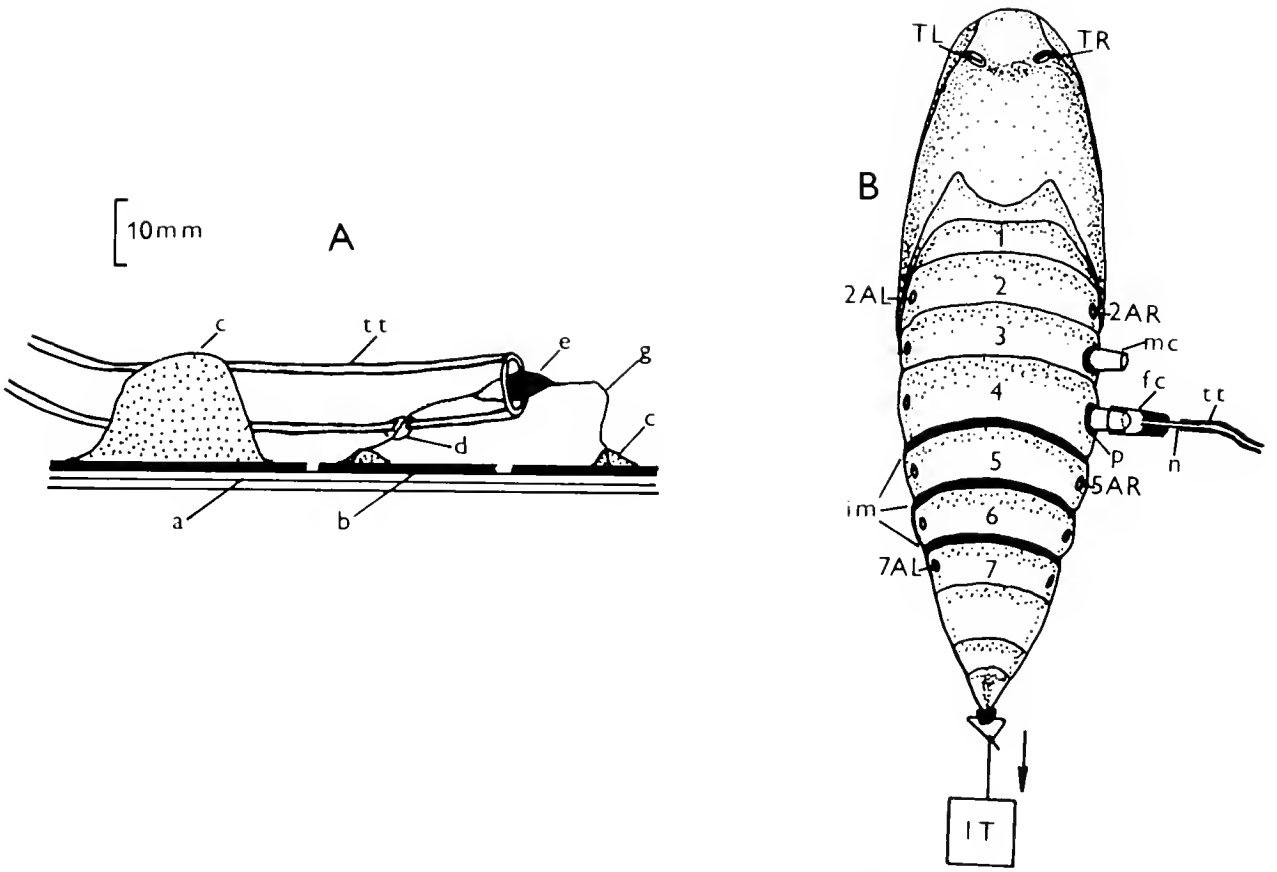

Figure 1. A—anemometric transducer formed by one thermistor (e) placed in the orifice of teflon tubing (tt) leading to the spiracle. B—a pupa with the system of spiracle identification, showing connectors of the anemometer tubings and the way of an isotonic transducer (IT) attachement. Legend: a—plastic plate of the printed circuits, b—etched circuitry, c—soldering, d—passage of thermistor wire through the wall of the tubing, e—thermistor, fc—female connector, g—silver wire of the thermistor used for positioning its body in the middle of the tubing section, im—intersegmental flexible membranes, mc—male connector permanently fixed around spiracles, n—stainless steel needle, p—paraffine wax seal, tt—teflon tubing.

an expiration in the − gate). Therefore, the anemometric measurements were always coupled with the direct or indirect transducers of hemocoelic pressure. This enabled clear distinction between the movement of air inside or outside of the body. A few examples of the combined anemo-tensiometric recording of the described type are shown in Figures 2 to 5.

The body of the anemometric transducer consisted of a printed circuit plate with the thermistors, resistors, and outlet cables, forming four complete thermographic units. It was maintained constantly within a thermostatted plastic box at 27°C ± 0.1°C. Details of manufacture, calibration, and performance of the instrument will be described in detail elsewhere (Sláma, 1988a). Measurements were made on a four-channel tensiometric unit M-1000 (Mikrotechna Co., Praha, Czechoslovakia) and a battery of linear recorders. Details of this electronic setup were described earlier (Sláma, 1984a, 1984b). The instrument was sensitive to a few nl of air movement; the frequency resolution was better than 4 Hz. The sample records shown in Figures 2 to 5 were selected from measurements on at least five pupae in each species.

Results

Respiration of developing adults of Actias selene

Pupae of the Chinese moon moth (*Actias selene*) develop without diapause. Preliminary recordings showed that they are breathing most of the time through the largest spiracles, located on the third abdominal segment. About midway in the pupal-adult transformation there are 30 to 40 min periods of relative ventilatory rest (at 25°C). The hemocoelic pressure shows slightly subatmospheric values (−300 to −500 Pa) and air is constantly

sucked in through one largely constricted spiracle (most commonly one of the thoracic or third abdominal). These resting periods regularly alternate with 15 to 20 min periods of intermittent pulsations in hemocoelic pressure. The pulsations are extracardiac. They are caused by contractions of the intersegmental abdominal muscles, the heart-beat operates independently on two different frequencies and causes 100-times smaller changes in hemocoelic pressure.

Figures 2A and B show ventilatory functions of three selected spiracles during the terminal part of one extracardiac pulsation. The lowest trace is an auxiliary record obtained from the isotonic transducer attached to the tip of the abdomen. This record shows the frequency of the extracardiac hemocoelic pulsation to vary from 26 to 18 strokes per min, and the amplitude of the associated abdominal movements from 5 to 15 μm. Another instructive feature of the record is the intervals when all spiracles are hermetically sealed (indicated by horizontal lines at the bottom of Fig. 2A and B). During this time, hemocoelic pressure decreases and the abdomen contracts with constant velocity of 84–90 μm · min^{-1}, which is proportional to the O_2 consumption rate. A further characteristic of the record is large inspirations of air (indicated by triangles). These are connected with a sudden increase of internal body volume, elevation of the subatmospheric hemocoelic pressure and, finally, with sudden elongation of the abdomen. This has been recorded by the transducer in Figures 2A and B.

The above relationships suggest that the record from the isotonic transducer can reveal many details related to the respiration dynamics of the investigated pupa. However, it does not show which of the spiracles was functioning. This information is partly provided by the anemometric records in Figures 2A and B. The spiracles on the third abdominal segment are most frequently used in this species. Each of the spiracles measured can function independently. Thus, the left thoracic spiracle (TL) was hermetically closed at the beginning of recording, it was slightly opened but held considerably constricted between the third and fifth min, and it opened after both 3A spiracles were tightly closed (Fig. 2B). This experiment does not determine how much the thoracic spiracular valves were opened during the maximum amplitude of the anemometric responses. It is also unknown whether some of the remaining intact spiracles would flutter at the same time. Nevertheless, the amplitudes showing the movement of up to ± 0.5 μl of air across the spiracular valve with every stroke of the intersegmental muscles (Figs. 2A, B) provide clear experimental evidence that hemocoelic pulsations may indeed cause a very efficient tracheal ventilation.

The comparison of anemometric records from the right and left 3A spiracles documents that each spiracle

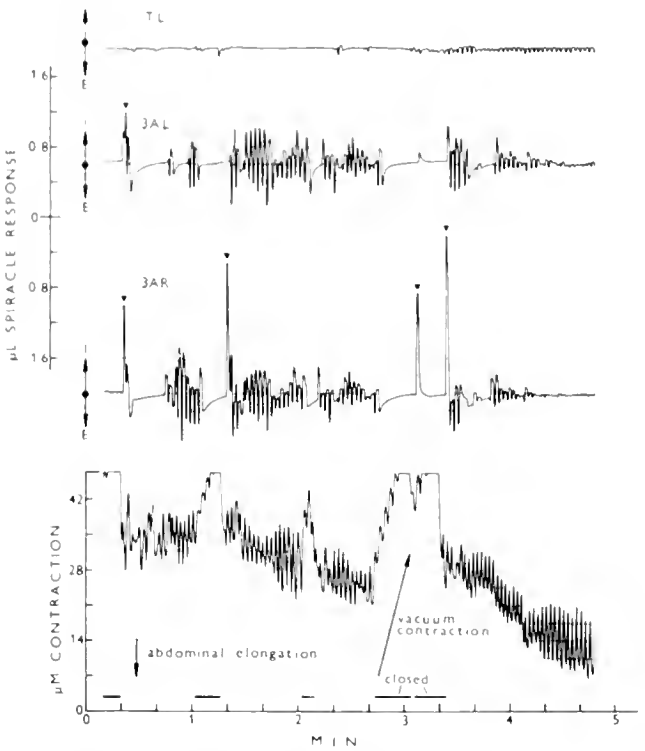

Figure 2A. *Actias selene*, midway during the pupal-adult transformation. Example of the selective recording of inspirations (I) and expirations (E) from three spiracles (TL-left prothoracic, 3 AL-left and 3 AR-right 3rd abdominal) during the second half-period of an extracardiac pulsation. Each of the three anemometric channels had one "active" thermistor connected with spiracle while the other was free. Lower trace shows relative changes of internal volume and hemocoelic pressure, recorded indirectly via an isotonic transducer attached to the tip of the abdomen. The heavy black lines on the bottom indicate periods when all spiracles are hermetically closed; triangles show larger inspirations of air.

can instantly open or close in full synchronization with individual strokes of the hemocoelic "hydraulic bellows." The frequency of 0.3 to 0.5 Hz (one stroke in 2–3 s) is sufficiently low to allow such synchronization. Although the 3AL and 3AR spiracles function in concert for some time, certain strokes are missing on one or another trace. Moreover, larger inspirations of 1.0 to 1.5 μl of air were realized selectively by a sudden 300 ms flutter of the 3AR valve, while the contralateral valve remained silent. These results show that functioning of the spiracular valves is controlled by a nervous system whose functions are precisely coordinated with nervous control of the extracardiac pulsations.

Respiration of diapausing cecropia pupae

Hyalophora cecropia invariably enters a prolonged pupal diapause which persists for at least 6 months at room

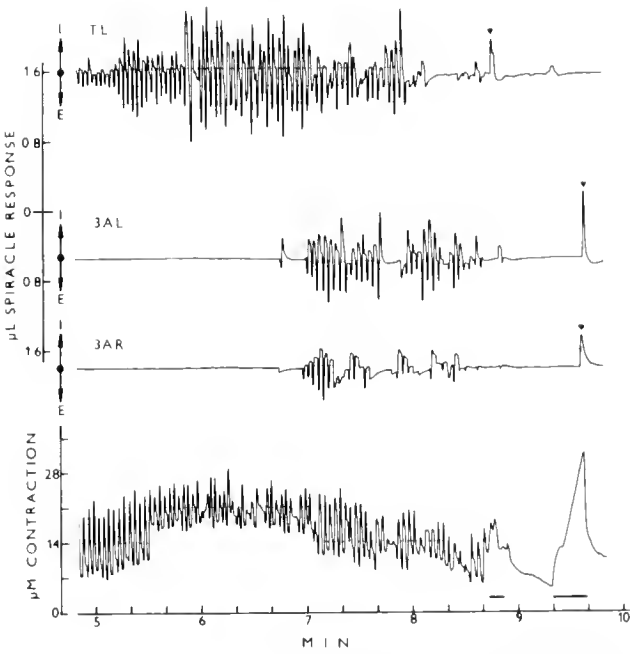

Figure 2B. Continuation of the recording from Figure 2A showing the terminal part of the extracardiac pulsation including ventilation of the left prothoracic spiracle.

temperature. In this case, anemometric recordings were preceded by one or more days of continuous monitoring of respiratory dynamics using the isotonic transducer alone (at 25°C). This was necessary to recognize possible abnormalities in respiratory functions resulting from the attachment of spiracles to anemometric tubing. The anemometric technique permits unrestrained movement of air across the spiracles. However, the records occasionally signaled suffocation or incomplete CO_2 ventilation after prolonged anemometric recordings. Usually this was recognized by supernumerary, out-of-schedule pulsations. In this case the connectors were dismantled for some time. In the majority of diapausing Cecropia pupae (15 specimens; some of them measured several times) there were regular bursts of CO_2 release at 5 to 7 h intervals. In addition, there were brief expiratory outbursts of intratracheal gases associated with abdominal rotation once per 12–16 h.

Figure 3 shows a typical sample of the combined tensio-anemometric recording during the interburst period. The lower trace from the isotonic transducer reveals relative changes of internal body volume. It shows that the spiracles were hermetically sealed most of the time (internal pressure was subatmospheric throughout). The closure is indicated by the periods when the abdomen retracts due to decreasing pressure with a constant speed of 3 µm per min. Volumetric calibration of this pupa under water revealed that 1 µm of abdominal contraction was equivalent to 240 nl of internal volume. Thus, isotonic transducer can be used as a rapid and simple detector of O_2 consumption rate. The constant rate of 3 $\mu m \cdot min^{-1}$ of abdominal retraction in Figure 3 corresponded to O_2 consumption of 720 $nl \cdot min^{-1}$ (43.2 $\mu l\ O_2 \cdot h^{-1}$).

The diapausing Cecropia pupae maintain subatmospheric hemocoelic pressure during the whole interburst period. Except for the CO_2 burst, they perform mechanical expiration only during a brief rotational response once per 12–16 h. In such prolonged inspirations, which is very common in all diapausing lepidopteran pupae, the anemometric network can be used for simultaneous recording from eight spiracles, as shown in Figure 3. In the upper part we find four anemometric traces corresponding to four pairs of eight reciprocal gates. Each trace is thus common to two spiracles whose inspirations are displayed in the opposite directions (see arrows in

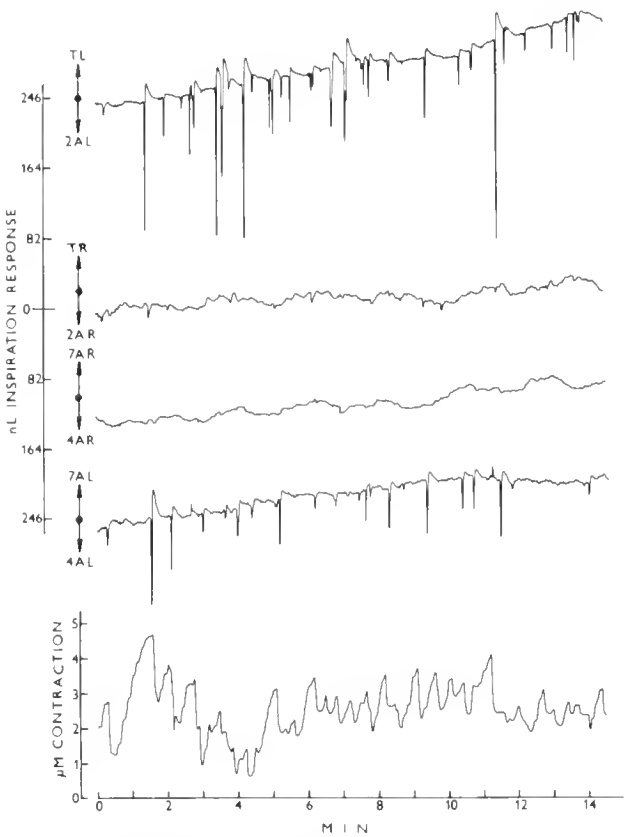

Figure 3. *Hyalophora cecropia*, diapausing male pupa during the interburst period (25°C). Recording of inspirations from eight spiracles (T-thoracic, AL-left, AR-right abdominal spiracles). Note that in contrast to single gate operation as shown in Figure 2, the two reciprocal gates of each channel record here inspirations in the opposite direction from the midline (see arrows). Lower trace from the isotonic transducer reveals intervals and magnitude of all inspirations, *i.e.*, sudden abdominal elongation. Hermetical closure of spiracles between inspirations is manifested by a steady upward movement of the pen driver (abdominal contraction due to decrease of hemocoelic pressure).

Fig. 3). The intervals and magnitudes of all inspirations in the body can be checked on lower trace from the isotonic transducer, as explained above. Accordingly, any sudden expiration of intratracheal gas, if present, should be recognized easily by instantaneous abdominal contraction, whereas passive inspirations are caused by abdominal elongation (for more details see Sláma, 1984a).

Figure 3 shows that the pupa used only two spiracles for periodic inspirations during the interburst period, *i.e.*, second and fourth left abdominal. Their function was coordinated with an accuracy of a few ms. With values of internal pressure ranging from −300 Pa to −2 kPa, the 2 AL spiracle showed larger inspirations up to 200 nl of air, while the 4 AL gave smaller and more variable responses of 20 to 50 nl at a time. This suggests that the aperture of each spiracle can be individually controlled. The general respiratory pattern of this pupa was that air was taken in discontinuously in sudden gulps lasting only 100–200 ms at more or less regular intervals of 3 to 4 per min. The intervals between inspirations could be prolonged by decreasing ambient temperature. For example, at 15°C the intervals were approximately twice as long as at 25°C. Near the CO_2 burst period, the passive respiratory movements often disappeared from the records though hemocoelic pressure remained slightly below barometric level. Gentle touching of the surface (causing small volumetric changes within the pupal body) always evoked an immediate anemometric response in one or both thoracic spiracles. This suggests that some spiracles can be maintained constricted, allowing a constant inflow of 720 nl·min^{-1} of air into the body.

Management of CO_2 by diapausing Cecropia pupae

Figure 4 shows the anemometric responses during the whole period of CO_2 burst in the same pupa used in Figure 3. The bottom trace from the isotonic transducer shows rather delicate extracardiac hemocoelic pulsation with an amplitude of only about 1 μm of abdominal movement and a frequency of 21–23 strokes per min. In principle, the movement of flexible abdominal segments acts bellows-like on the tracheae and produces the inflow or outflow of gas through any open spiracle. The amplitudes of the anemometric responses are directly proportional to the aperture of the spiracular valve. For example, a completely closed spiracle gives no response, a partly constricted one gives an intermediate response, and a fully opened spiracle should give the maximum response. In addition, amplitudes of the individual anemometric responses are weakened by an increasing number of spiracles that open simultaneously.

Some of the above outlined relationships are illustrated by the upper traces in Figure 4. The "nonselective" variant of the anemometric recording and slow chart speed do not show which of the two spiracle mates on each channel have actually responded. The arrangement of the pairs of spiracles shown in Figures 3 and 4 was made after the foregoing finding that the two spiracles of a pair did not function at the same time. Figure 4 shows that some spiracles, such as 7 AR and 4 AR remained closed throughout almost the entire period of the CO_2 burst. It also shows that the "master spiracles" from Figure 3 (2 AL and 4 AL) were probably functional during the initial half-period of the burst, whereas a larger thoracic spiracle (TR) opened at the end of the burst. Different amplitudes of the anemometric responses and permanent closure of some spiracles suggest that the spiracles cannot be maintained widely opened by high CO_2 concentration during the burst, as has been generally believed. In reality, some spiracles can be selectively ventilated at different sites and at determined periods of the CO_2 burst. The records of other burst periods in this and other pupae indicated that the pattern in Figure 4 is variable. This suggests that alteration of the spiracle opening sequence is under non-stereotyped physiological control.

Pupae of Cecropia and some other saturniids usually close all spiracles for 10 to 20 min after termination of a CO_2 burst, when internal pressure is close to atmospheric level. During this period, abdominal segments retract with the velocity of 5 to 12 μm·min^{-1} and hemocoelic pressure declines to −5 kPa or less. Such a large vacuum inside the body becomes sequentially reduced to the usual values by large inspirations of air, most frequently through thoracic or last abdominal plus thoracic spiracles. Sometimes more than 20 μl of air are taken in a single surge and sometimes more than 0.5 ml of air is taken in during one min. The process continues until hemocoelic pressure becomes adjusted to about −500 Pa. This is followed by the type of respiration as shown in Figure 3.

Respiration of diapausing Sphinx ligustri

Sphingid pupae typically show regular periods of inspirations that give the records of hemocoelic pressure a saw-tooth appearance. The records from isotonic transducers are mirror images of changes in hemocoelic pressure (see Sláma, 1984a), *i.e.*, the abdomen contracts slowly when hemocoelic pressure passively decreases. The bottom trace in Figure 5 shows the saw-tooth pattern in *Sphinx ligustri*. The teeth indicate intervals and size of the inspirations. A further peculiarity of sphingid pupae is the slowly expanding internal volume (visible as the slow decline tendency of the lower trace in Fig. 5). This is terminated once per several hours by a large expiration associated with abdominal rotation or, eventually, by a CO_2 burst. Useful information from this record are

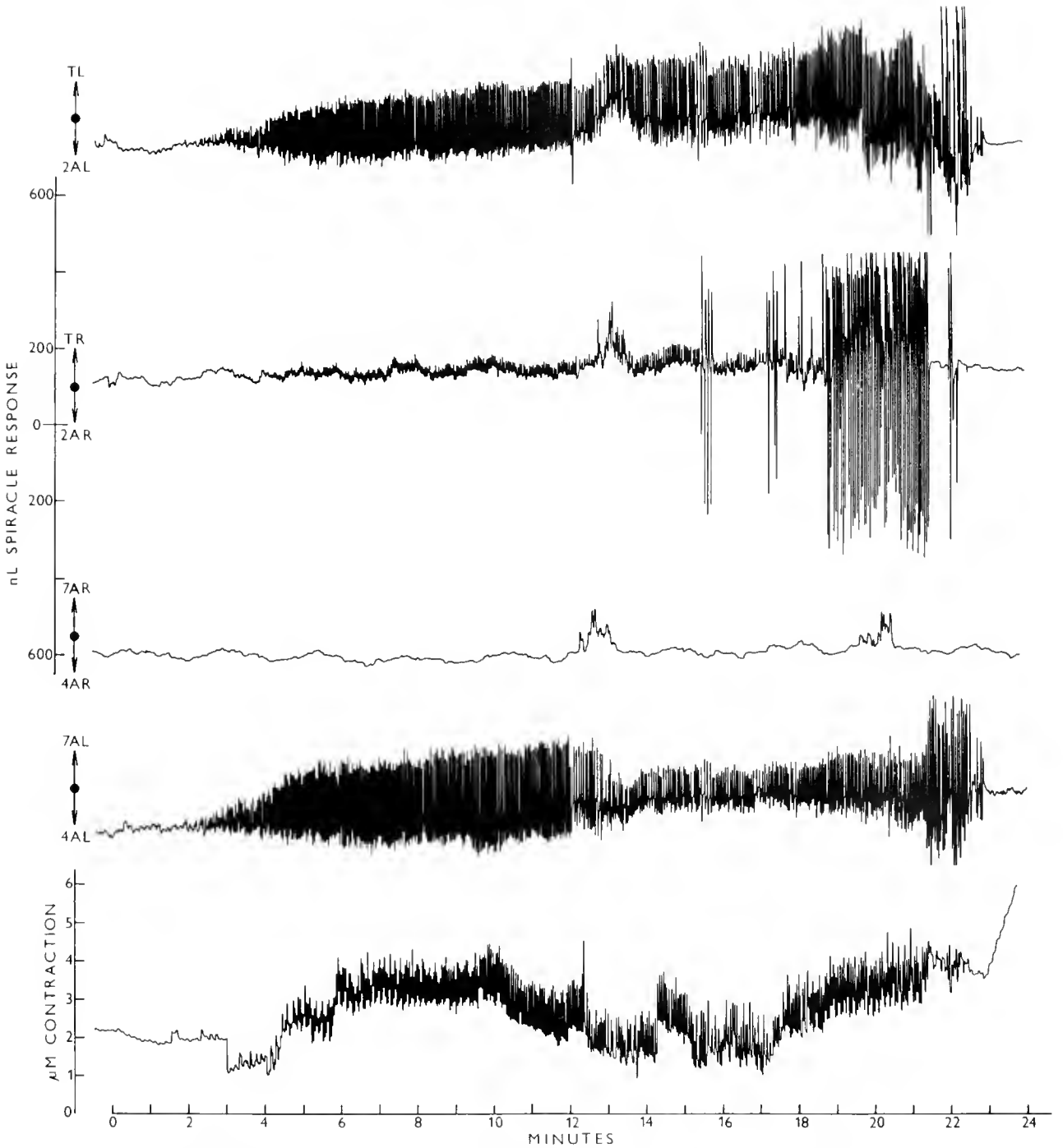

Figure 4. *Hyalophora cecropia*, the same preparation as in Figure 3, recording from eight spiracles during the 20-min period of CO_2 burst associated with an extracardiac pulsation (25°C). Each of the four anemometric traces gives unresolved responses from four pairs of spiracles (arrows indicate inspirations in the particular spiracles, but they may be expirations in the respective counterparts). The amplitudes of the anemometric responses are proportional to the degree of opening of the spiracular valves. Lower trace shows the bellows-like ventilatory movements of the distal abdominal segment.

more or less regular intervals of inspirations at 30 s, and the velocity of the constant abdominal contraction of 2.5 $\mu m \cdot min^{-1}$. Calibration of the pupa under water revealed that 1 μm of abdominal contraction was equivalent to 110 nl of air transported through the spiracle or 110 nl of O_2 consumed (O_2 consumption of 16.5 $\mu l \cdot h^{-1}$).

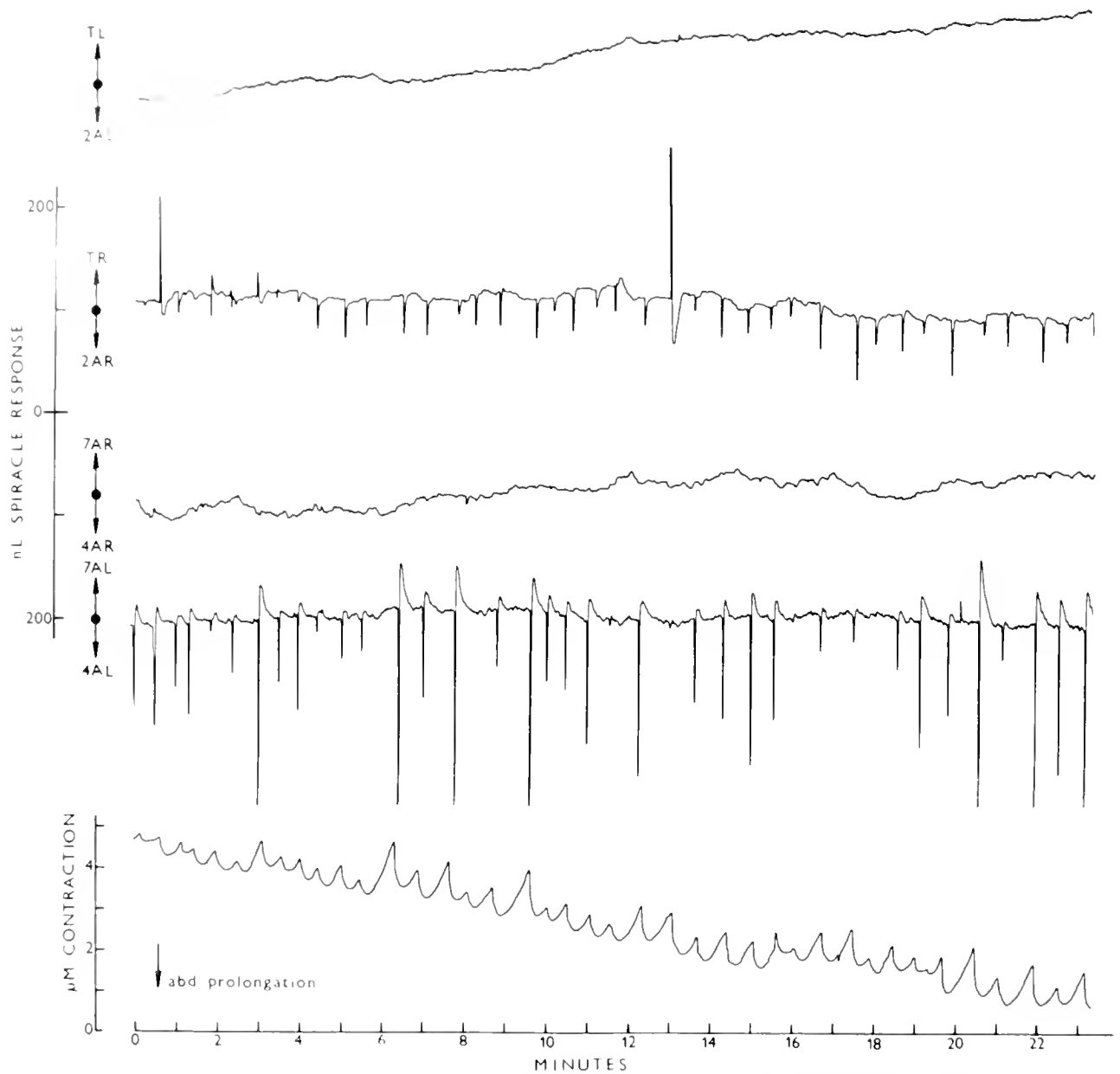

Figure 5. *Sphinx ligustri*, diapausing pupa. A sample from prolonged recordings between the CO_2 bursts during the period of discontinuous inspirations of air. Lower trace shows the characteristic "saw-tooth" pattern of hemocoelic pressure changes revealed indirectly by an isotonic transducer from the tip of the abdomen. Inspirations are indicated by sudden abdominal prolongation (sudden decrease of the internal vacuum). The anemometric traces show inspirations in eight spiracles indicated by the arrows. Note that only 4 AL and 2 AR spiracles were used for inspirations, the TR spiracle was used only twice, while the rest of spiracles were hermetically closed all time.

The anemometric traces (Fig. 5) document that this pupa also used inspirations through selected abdominal spiracles. Inspirations occurred only in 4 AL assisted by 2 AR. A sudden inspiration through the right thoracic spiracle occurred as the two abdominal spiracles go silent (around 13:00 min recording time). Such swift interplay between close or more distant spiracles is quite common. Direct evidence that it was not expiration through the paired 2 AR spiracle is provided by the tensiometric record below, which shows abdominal elongation due to volumetric increase, not contraction.

The pattern of inspirations in Figure 5 shows that the "master" and assisting spiracles taking part in discontinuous air intake are not only located on different body

segments, but can occur on contralateral sides. Moreover, the two functioning spiracles opened for a total of only 7 s of 22 min, while all other spiracles were hermetically closed. This pattern when all spiracles are closed while only two of them would flutter for no more than 0.53 per cent of time seems to be a common feature in diapausing pupae of Lepidoptera. It provides a serious argument against the belief that the pupa could breathe by simple diffusion of respiratory gases through spiracles. The situation in Fig. 5 cannot be taken as a stereotypic model for all pupae of a species. Other pupae of *S. ligustri* did not use 4 AL as the most active spiracle. Some used preferentially TR, 3 AL, or 7 AL.

The tobacco hornworm Manduca sexta

Large sphingid pupae (*Acherontia atropos, Herse convolvuli, Manduca sexta*) show very special respiratory scenarios during diapause. They maintain an internal vacuum and tend to use a single "master" spiracle for prolonged discontinuous inspirations, while all other spiracles are tightly closed. This often continues unaltered for periods of more than 15 h at room temperature or for several days at 5°C. Figure 6 shows a 24-min segment taken from an uninterrupted 48-h recording in diapausing *Manduca*. The bottom trace comes from the isotonic transducer. It shows regular inspirations at 1.5 to 2 min intervals. The inspirations have been associated with sudden increases of internal body volume which is manifested on the record by sudden elongations of the abdomen. After termination of the anemometric measurements, the hemocoel cavity of this pupa was connected with the hydraulic transducer for calibration of the system. The bottom trace in Figure 5 appeared as a mirror image of changes in hemocoelic pressure (for more details see Sláma, 1984a).

The records in Fig. 6 show that, of eight spiracles, the pupa inspired only through the left thoracic spiracle. All others were kept hermetically closed. Each inspiration lasted approximately 200 ms, the anemometer detected a rapid flow of 600 nl of air. Further measurements on this and other diapausing *Manduca* pupae revealed important biophysical data that can be summarized as follows: (a) the velocity of the steady abdominal contraction is 2 $\mu m \cdot min^{-1}$; (b) 1 μm of abdominal movement corresponds to 2.9 Pa change in hemocoelic pressure; (c) 1 μm of abdominal movement is equivalent to 150 nl of air inspired or O_2 consumed, and (d) the baseline hemocoelic pressure is 0.8 kPa under atmospheric level.

The above data reveal a hitherto unknown homeostatic mechanism. This mechanism regulates a constant body length within the limits of ± 5 μm (*i.e.*, 1/10000th of pupal length), maintains more or less constant body volume within the limits of ± 750 nl (*i.e.*, 1/13000th of body volume), or regulates hemocoelic pressure within the limits of ± 14.5 Pa (*i.e.*, 1.4 mm hydrostatic pressure). This illustrates remarkable accuracy in the underlying sensory and neurophysiological mechanisms.

Extensive anemometric studies with diapausing pupae of various lepidoptera consistently revealed subatmospheric hemocoelic pressures and predominantly closed tracheal systems. Air was mechanically sucked into the body whenever some spiracle opened while mechanical expiration was unusually rare. In certain cases, as in the pupa of *Manduca*, body volume remained constant for many hours in spite of a well-documented net inflow of air into the otherwise hermetically sealed pupal body. This effective nitrogen concentration within the closed pupal case has been studied intensively. Details will be described elsewhere.

Discussion

The mechanics of insect respiration and tracheal ventilation were studied some 80 years ago (for review see Babák, 1912). About 30 years ago, the discontinuous respiration of insects became a favorite subject of insect physiology (Punt, 1950; Schneiderman and Williams, 1955; Buck, 1962; Keister and Buck, 1964). Though it still is a favorite subject of more recent reviews (Miller, 1981; Kestler, 1985), few additional insights have been added since Schneiderman and his co-workers defined changes in intratracheal pressure, described the microcycles of suction respiration, and explained the basic mechanisms of spiracular functions (Levy and Schneiderman, 1966; Brockway and Schneiderman, 1967; Burkett and Schneiderman, 1966). The present study stems directly from these publications and confirms most, though not all, of the conclusions.

Information is available on neuromuscular control of spiracular functions and ventilatory movements (review by Miller, 1981). Anemometric techniques, combined with the direct or indirect detectors of hemocoelic pressure, now permit monitoring the actual passage of respiratory gases through individual spiracles. These techniques, in combination with very sensitive microrespirographic methods (see Sláma, 1984b), help to obtain simultaneous monitoring of the course of O_2 consumption, internal volume, and hemocoelic pressure changes and, most importantly, monitoring of the functioning spiracles (for more technical details see Sláma, 1984a, 1984b, 1988a).

August Krogh's pioneering work led to a theory of purely diffusive gas transfer within the tracheal system (Krogh, 1920). This model was subsequently corroborated by Weiss-Fogh (1964) who concluded that there were no reasons to assume mechanisms for insect respiration other than simple gaseous diffusion. The model

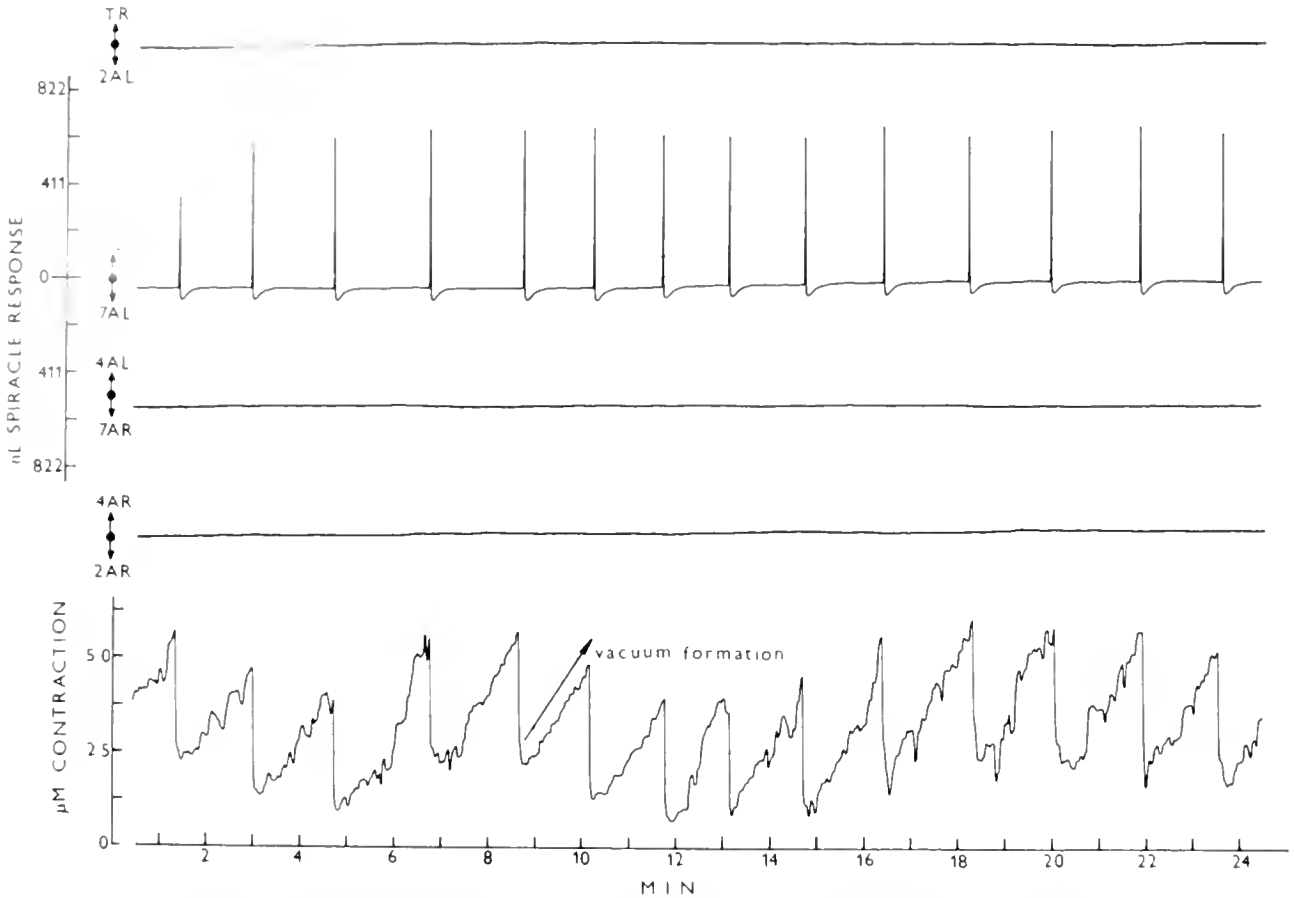

Figure 6. *Manduca sexta*, diapausing female pupa. Recording of regular inspirations from eight spiracles during the interburst period. Only left prothoracic spiracle was functional while all others were tightly sealed. The bottom trace from the isotonic transducer displays the associated pressoric or volumetric changes from movement of the tip of the abdomen.

was thoroughly analyzed by Buck (1962) and recently updated by Kestler (1985). The most important challenge to the diffusion theory has hitherto been the results of Hazelhoff. The latter's work is known mainly from the description of Prof. H. Jordan (see Jordan, 1927). Hazelhoff found that insect spiracles were completely closed most of the time—a finding that few have recognized but which is fully confirmed in the present study.

The diffusion theory of insect respiration was questioned in various review articles (Chauvin, 1949; Kuznetzoff, 1953; Buck, 1962; Miller, 1981; Kestler, 1985), but the critiques lacked experimental data. The original reasonings of Krogh (1920) supporting the purely diffusive made of insect respiration were based on the premise that immobile stages of insects did not show ventilatory movements. However, we see (Figs. 1A, B and 3) that immobile pupae do exhibit minute hemocoelic pulsations. These result in active tracheal ventilation. Buck (1962) postulated that a convective stream of intratracheal gas can be achieved by extremely small changes in internal pressure. Indeed, the changes in mechanical pressure associated with the described pulsations are so small (sometimes less than 5 Pa or less than 1 μm of integumental movement) that they can be visualized only via recently available electronic devices. This may explain why the existence of extracardiac pulsations in hemocoelic pressure remained unknown until 1976 (Sláma, 1976). Recent investigations show that the pulsations are present everywhere. They occur, for example, in immobile prepupae and in pupae of all major endopterygote groups, including Coleoptera, Lepidoptera, Hymenoptera, and Diptera (Sláma, 1984a). The widespread occurrence of these pulsations (ventilatory movements) in the immobile stages with low metabolic rates provides strong circumstantial evidence that simple diffusion principles are not satisfactory for the transport of gases through spiracles. However, the diffusion principles formulated by Krogh (1920) may find practical use for the internal transport of O_2 between tracheae and tissues. This view is consistent with the calculations of Buck

(1962), and of Kestler (1985), as well as with the recent views concerning respiratory functions of insect tracheoles (Wigglesworth, 1984).

To illustrate some arguments against the role of diffusion in the exchange of O_2, N_2, and CO_2 between the pupae and the environment, we may discuss again the case of *Manduca* in Figure 6. Here the unidirectional suction stream of air first passes through a narrow spiracular sieve into a cavity above the spiracular valve. The valve flutters only in the left thoracic spiracle for 100–200 ms about once per minute. Thus it opens only for approximately 0.5% of the time. During its opening, air is propelled inside vigorously by a 0.5 to 0.8 kPa pressure difference (according to preliminary calculations, the speed of the air stream is close to 20 $m \cdot s^{-1}$). All other spiracular valves are permanently and hermetically sealed for several hours, and at lower temperatures (5–10°C) they may be closed for several days. For obvious reasons, it is unrealistic to expect diffusion of the respiratory gases through just one spiracle that is sealed 99.5% of time and whenever it opens there is a fast stream of air.

The respiration pattern of *Manduca* is not restricted to the large-sized sphingid pupae. It is quite common among diapausing pupae in a number of lepidopteran families, including miniature pupae of Geometridae, where diffusion principles in respiration would be most likely. Reasons why lepidopteran pupae must live with closed spiracles, are still unknown. According to the literature (Buck, 1962; Kestler, 1985), the principal reason is water conservation.

The foregoing facts strongly argue that separate zones of the tracheal system can be ventilated by selective opening of the determined spiracles. Actual ventilation is brought about by genuine pulsations in hemocoelic pressure. These are generated in the majority of insect groups by contractions of the intersegmental muscles of the abdomen. Usually utilization of O_2, fixation of CO_2 in buffers, and hermetical closure of the spiracles, create subatmospheric pressures which are automatically conveyed to the gas-filled tracheae. An instantaneous inflow of fresh air occurs whenever a spiracle opens. This brief recapitulation of the observed respiratory relationships suggests that insects possess a neuromuscular mechanism for controlling inspirations and expirations through individual spiracles. The nervous system controlling opening or closing the spiracles has apparent motor outflow via a nerve system regulating the intersegmental muscles of the abdomen and, thereby, the hemocoelic pressure.

In *Tenebrio*, *Galleria*, and some other insects an autonomic (brain independent), parasympathetic-like nervous system regulating hemocoelic pressure has been described (Sláma *et al.*, 1979; Sláma, 1986). More recently, this mechanism has been termed the coelopulse system (from the Greek *koiloma* or Latin *coelom* for cavity and *pulsus* for beating or striking). It regulates certain homeostatic functions in reproducing adults of various insect groups (Sláma, 1988b). There is increasing evidence that insect respiration is regulated by the same coelopulse system that regulates hemocoelic pressure. The mechanism mutually determines the duration of the pressure pulsations, controls the level of the baseline hemocoelic pressure, and regulates the intervals of inspirations (see Sláma, 1984a). The present anemometric data show that it may also control the function of individual spiracles. Thus, the coelopulse mechanism of insect respiration is composed of two elements: (a) neuromuscular system regulating the opening or fluttering of spiracular valves (metameric system of unpaired central and transverse nerves innervating the spiracles, with the adjacent perisympathetic neurohaemal organs), and (b) what may be termed "hydraulic bellows" driven by the intersegmental muscles of the abdomen with nerve impulses coming from the thoracic ganglia (generating changes in hemocoel pressure that force the air in or out through the selected spiracle). These complex physiological functions can be compared to playing an accordion. There are two interconnected nerve functions: one is responsible for pulling the bellows and the other for pressing the right keys on the keyboard. We know the instrument but we must now learn to listen to the melody of different insects.

Acknowledgments

I am greatly indebted to Prof. C. M. Williams of Harvard University, Cambridge, Massachusetts, for valuable help in preparation of this manuscript; Prof. J. B. Buck of National Institutes of Health, Bethesda, Maryland, for helpful criticisms, and Dr. J. H. Willis of The University of Illinois, Urbana, Illinois, for suggesting the title.

Literature Cited

Babák, E. 1912. Die Mechanik und Innervation der Atmung. *Winterstein's Handb. Vergl. Physiol.* **I:** 265–640.

Brockway, A. F., and H. A. Schneiderman. 1967. Strain-gauge transducer studies on intratracheal pressure and pupal length during discontinuous respiration in diapausing silkworm pupae. *J. Insect Physiol.* **13:** 1413–1451.

Buck, J. 1962. Some physical aspects of insect respiration. *Annu. Rev Entomol* **7:** 27–56.

Burkett, B. N., and H. A. Schneiderman. 1974. Discontinuous respiration in insects at low temperatures: intratracheal pressure changes and spiracular valve behavior. *Biol. Bull.* **147:** 249–310.

Chauvin, R. 1949. *Physiologie de l'Insecte.* 2nd ed. Paris 1958.

Jordan, H. 1927. Die Regulierung der Atmung bei Insekten und Spinnen. *Z. Vegl. Physiol.* **5:** 179–190.

Kaars, C. 1981. Insects—spiracle control. Pp. 337–366 in *Locomo-*

tion and Energetics in Arthropods. C. Herreid and C. R. Fourtner, eds. Plenum, New York. [illegible]

Keister, M., and J. Buck, 1964. Respiration: some exogenous and endogenous effects [illegible] of respiration. Pp. 617–658 in *The Physiology of Insecta*, 3 [illegible] M. Rockstein, ed.

Kestler, P. 1985. [illegible] ation and respiratory water loss. Pp. 137–183 in *Environmental Physiology and Biochemistry of Insects*. K. H. Hoffmann [illegible] Springer, Berlin.

Krogh, A. 1920. Studien über Tracheenrespiration. II. Über Gasdiffusion in den Tracheen. *Pfluger's Arch. Gesamte Physiol. Menschen Tiere* **179**: 95–112.

Kuznetzoff, N. Y. 1953. *Osnovy fiziologii nasekomych* (Principles of Insect Physiology) Izd. Acad. Sci. Moscow, 402 pp. (In Russian.)

Levy, R. I., and H. A. Schneiderman, 1966. Discontinuous respiration in insects. IV. Changes in intratracheal pressure during the respiratory cycle of silkworm pupae. *J. Insect Physiol.* **12**: 465–492.

Mill, P. J. 1974. Respiration: aquatic insects. Pp. 403–467 in *The Physiology of Insecta*, 2nd ed., vol. 4, M. Rockstein, ed. Academic Press, New York, London.

Miller, P. L. 1974. Respiration—aerial gas transport. Pp. 345–402 in *The Physiology of Insecta*, 2nd ed., vol. 4, M. Rockstein, ed. Academic Press, New York, London.

Miller, P. L. 1981. Ventilation in active and inactive insects. Pp. 367–390 in *Locomotion and Energetics in Arthropods*, C. F. Herreid and C. R. Fourtner, eds. Plenum Press, New York, London.

Provansal, A., N. Baudry-Partiaoglou, and K. Sláma, 1977. Haemolymph pressure pulses in the metamorphosis of *Tenebrio molitor*. *Acta Entomol. Bohemoslov.* **74**: 362–374.

Punt, A. 1950. The respiration in insects. *Physiol. Comp.* **2**: 59–74.

Schneiderman, H. A., and C. M. Williams, 1955. An experimental analysis of the discontinuous respiration of the cecropia silkworm. *Biol. Bull.* **109**: 123–143.

Sláma, K. 1976. Insect haemolymph pressure and its determination. *Acta Entomol. Bohemoslov.* **73**: 65–75.

Sláma, K. 1984a. Recording of haemolymph pressure pulsations from the insect body surface. *J. Comp. Physiol. B* **154**: 635–643.

Sláma, K. 1984b. Microrespirometry in small tissues and organs. Pp. 101–129 in *Measurement of Ion Transport and Metabolic Rate in Insects*, I. J. Bradley and T. A. Miller, eds. Springer, New York, Berlin.

Sláma, K. 1986. Cholinergic control of extracardiac pulsations in insects. *Experientia* **42**: 54–56.

Sláma, K. 1988a. Microanemometric recording through the spiracles. *Acta Entomol. Bohemoslov.* (in press).

Sláma, K. 1988b. Role of the autonomic nervous system (coelopulse) in insect reproduction. *Proc. Int. Symp. Insect Reproduction*, Zinkovy 1987 (in press).

Sláma, K., N. Baudry-Partiaoglou, and A. Provansal-Baudez, 1979. Control of extracardiac haemolymph pressure pulses in *Tenebrio molitor* L. *J. Insect Physiol.* **25**: 825–831.

Weiss-Fogh, T. 1964. Diffusion in insect wing muscle, the most active tissue known. *J. Exp. Biol.* **41**: 229–256.

Wigglesworth, V. B. 1984. The physiology of insect tracheoles. *Adv. Insect Physiol.* **17**: 85–148.

Reference: *Biol. Bull.* **175:** 301–319. (October, 1988)

Abstracts of Papers Presented at the General Scientific Meetings of the Marine Biological Laboratory August 22–24, 1988

Abstracts are arranged alphabetically by first author within the following categories: cell biology, comparative and general physiology, developmental biology and fertilization, ecology, and neurobiology. Author and subject references will be found in the regular volume index in the December issue.

Cell Biology

The packing density of cytoskeletal polymers in axoplasm affects the resistance to polymer sliding. ANTHONY BROWN AND RAYMOND J. LASEK (Bio-architectonics Center, School of Medicine, Case Western Reserve University, Cleveland, OH 44106).

In the polymer sliding hypothesis of slow axonal transport, the rate of cytoskeletal polymer sliding is partly a function of the resistive drag that the polymers encounter as they slide past adjacent structures within the axon (Lasek 1986, *J Cell Sci.* [Suppl.] **5:** 161–179). A recent study of two side-by-side populations of axons that have different neurofilament transport rates has shown that the neurofilament density is higher in those axons with the slower rate (Price *et al.* 1988, *J Neurocytol.* **17:** 55–62). This suggests that an increase in polymer packing density may slow the rate of polymer sliding in axons. To test this, polymer sliding was mechanically induced *in vitro* by slowly stretching axoplasm extruded from squid giant axons (George and Lasek 1986, *Biol. Bull.* **171:** 469). The resistance to stretch was measured at various polymer packing densities. Cytoskeletal polymer density was increased by osmotically compressing axons with hypertonic sucrose solutions prior to extrusion of the axoplasm. With 1 *M* sucrose in seawater the mean axon volumes decreased by 63% (n = 9, minimum = 53%, maximum = 71%). Electron microscopy showed that the polymers were more densely packed. Axoplasm from these compressed axons showed a much greater resistance to polymer sliding. The mean modulus of elasticity, which is a measure of this resistance, was 13 dyn/min (minimum = 2 dyn/min, maximum = 30 dyn/min, n = 16) for untreated axoplasm and 60 dyn/min (minimum = 44 dyn/min, maximum = 77 dyn/min, n = 6) for axoplasm compressed with 1 *M* sucrose solutions. This indicates that compressing the axonal polymers more tightly together increases the resistive drag that they encounter during sliding. In this way, the external compressive forces on axons that pack axonal polymers *in situ* may increase the resistance to polymer sliding, thereby decreasing the rate of slow axonal transport.

Cell fusion and cell poration using a radiofrequency electric field. D. C. CHANG AND P. Q. GAO (Baylor College of Medicine).

Cell fusion and cell poration are important biological techniques that have a variety of applications in cell biology, molecular biology, and immunology. Recently we have developed a new method that induces cell fusion and cell poration using a pulsed radiofrequency (RF) electric field. This field is of high strength, typically 3–5 kV/cm. The pulse width is of the order of 100 microseconds, and the oscillating frequency varies from 50 kHz to 1 MHz. We have applied this new method to fuse and porate a number of cell types, including human red blood cells (RBC). Light microscopy using DIC optics and fluorescence microscopy were used to study the process of cell fusion induced by the RF field. Two types of fusion were observed in RBC. The first type is a membrane fusion in which the fusing cells retain their individual shapes, but a membrane-labelling dye can pass from one cell to another. The second type is a cytoplasmic fusion in which the fusing cells merge to become a single larger cell. The yield of cytoplasmic fusion is strongly dependent on the oscillating frequency of the applied RF field, with the highest yield at 100 kHz. Analysis by video microscopy of the fusion process shows that RBC first shrink in size following the RF pulses and then partially swell before fusion takes place. This observation suggests that the RF pulses may create large membrane pores which allow rapid exchange of intra- and extracellular substances. Using freeze-fracture electron microscopy, we have observed such pores. The pore size is large (up to 0.3 μm in diameter) so that large macromolecules such as coiled DNA can readily pass through the membrane of the porated cells. Our study suggests that the RF poration method will be highly useful for gene transfection or microinjection of biologically active substances (*e.g.*, antibodies or molecular markers).

Supported by the Advanced Research/Technology Program of Texas.

Ca^{2+}-dependent catecholamine modulation of sperm movement in Arbacia punctulata. LEONARD NELSON (Medical College of Ohio Toledo, OH 43699) AND LUCIO CARIELLO.

Sperm motility is a quantifiable phenomenon providing a readily accessible model for the analysis of complex regulatory mechanisms of cellular function. Bovine spermatozoa show saturable binding of radiolabeled norepinephrine with an affinity constant of about 0.5 n*M*. Coincubation of sperm cells with non-labeled compounds and blocking agents causes displacement of the bound isotope. Isoproterenol, dopamine, and epinephrine reduced the binding to a degree which suggested

that the challenging agents would effect the rate of sperm cell progression. Sea urchin sperm assay adapted to test the physiological responses revealed that *Urbacia* sperm [illegible]bited dose-, time-, and Ca^{2+}-dependent action. Norepinephri[illegible] proterenol, and dopamine increased the motile rate by 75 [illegible]at of the control sperm after 10 min of exposure, while epi[illegible] was without effect. Receptor blockers also induced increase[illegible]gressive movement. The α-adrenergic blocker phentolamine [illegible]nhanced isoproterenol's stimulation, while the β-blocker aten[illegible] stimulation was counteracted by the β-agonist norepinephrine. Propranolol, another β-blocker, moderately increased the motility while the mildly active α-adrenergic compound quinidine had no effect except when administered along with propranolol. Thus when β-adrenergic agonists occupy binding sites on the sperm cell surface, they prevent the stimulation due to agents which act as β-antagonists in neuromuscular systems. The α-blocker phentolamine, however, potentiates the action of the β-agonist isoproterenol.

The absence of Ca^{2+} or the presence of Ca^{2+}-channel blockers reduce the stimulatory effects of the catecholamines which appear to be involved in ion channel regulation. The catecholamines appear to interact with cell surface receptors that activate the adenylate cyclase/cyclic AMP second messenger system. Caffeine (an inhibitor of cAMP phosphodiesterase) and 8-Br-cyclic AMP reduce the stimulation caused by norepinephrine and atenolol. Epinephrine also depresses the stimulatory action of 8-Br-cyclic AMP.

Support by the Sage Foundation.

Initial studies of marine vertebrate lens cytoskeleton. NANCY RAFFERTY, KRIS LOWE, KEEN RAFFERTY, AND SEYMOUR ZIGMAN (University of Rochester Medical Center).

The anatomical nature of the lenses of marine vertebrates does not support a lens accommodative process that alters their shapes. Unlike the lenses of many terrestrial mammals, they are not elastic. However, accommodation is accomplished by translocation of the lens by retractor or protractor muscles in the eye. These lenses also resist swelling both in hypotonic media and when their Na/K ATPase is inhibited, which suggests cytoskeletal rigidity. Herein, we identify the cytoskeletal proteins in these lenses, and describe the structures of their cytoskeletons.

The lenses of teleosts and elasmobranchs were stained for actin using rhodamine phalloidin reagents. Morphological studies of the cytoskeleton were aided by electron microscopic examinations by using gold labelled antibodies. Lens extracts were examined by polyacrylamide gel electrophoresis (PAGE) with special attention to the cytoskeletal proteins, actin and vimentin. Immunoblotting was done with purified antibodies to actin and vimentin (Western blots).

Exposure of the lenses *in vitro* to near-UV radiation (365 ± 30 nm; .5 mW/cm^2) was used to study the induction of light-associated alterations of cytoskeletal elements.

Extracts of both dogfish and sea robin lenses were shown to contain both actin and vimentin by PAGE and immunoblotting. The antibodies against actin and vimentin were made in rabbits and mice, respectively; common antigenic determinants are thus present in the cytoskeletal elements of marine lenses.

Actin filaments were associated with the epithelial cell plasma membranes and in the perinuclear region. UV-exposure in dogfish appeared to cause depolymerization of the filaments. Immuno gold E.M. showed actin to be associated with the basal plasma membrane (in the dogfish). Teleost vimentin was found to be associated with the perinuclear network. PAGE plus immuno-b[illegible]otting resulted in bands proving that actin and vimentin were present in these lenses. Preliminary immunoblots suggest that some cytoskeletal elements may comigrate with the lens crystallins, especially in the cortex. The structure and chemistry of marine lens cytoskeletons appear to be similar to those of mammals. Thus, an altered cytoskeleton cannot explain the lack of swelling and accommodation in marine lenses.

Support: NIH and RPB, Inc.

Isolation of the dogfish erythrocyte marginal band using detergents. IVELISSE SANCHEZ AND WILLIAM D. COHEN (Hunter College, NY).

Isolation of the marginal band (MB) of microtubules from the erythrocytes of non-mammalian vertebrates is a useful approach to the molecular composition and the structural and mechanical properties of the nucleated erythrocyte cytoskeletal system. In our previous methods for MB isolation, proteases have been used to digest the cell surface-associated cytoskeletal network (SAC), containing actin and spectrin/fodrin-like proteins, that encloses the MB. In the present work, cytoskeletons were prepared from erythrocytes of the smooth dogfish (*Mustelus canis*) by lysis with Brij-58 in the presence of protease inhibitors, washed in microtubule stabilizing medium, and stored at −20°C in 50% (v/v) glycerol containing taxol to help stabilize the MB. This served as the standard starting material for testing potentially selective, non-proteolytic SAC solubilizing agents systematically. Various phosphates and reducing agents suggested by literature on the mammalian actin-spectrin network proved ineffective, as did numerous detergents used individually. However, MB release from cytoskeletons was obtained readily in Triton X-100 (0.1–0.4%) containing low concentrations of SDS (0.025–0.1%). Over 90% of the MBs can be liberated from cytoskeletons in 5–30 minutes, depending upon detergent concentrations. The MBs are sufficiently stable for isolation by centrifugation after sedimentation of nuclei. SAC dissolution and MB release are blocked by excess Triton and slowed by glycerol. Therefore, these reagents can be used to stop the release reaction during quantitative time-course studies. Added standard proteins are not proteolyzed during MB release, nor is release blocked by a protease inhibitor "cocktail," indicating that activation of endogenous proteases is not involved. As determined by SDS-PAGE, tubulin (four gel bands) is the dominant component of the isolated dogfish MB preparations. Results to date with amphibian and avian erythrocytes indicate that the method may be widely applicable to other species, and therefore useful for comparative studies.

Supported by MBRS-NIH S06RR08176-07 and NSF DCB8711810.

Assembly and changes in the fibrous substructure of the cleavage furrow in living cells. J. M. SANGER, J. S. DOMB, B. MITTAL, AND J. W. SANGER (University of Pennsylvania).

We have microinjected tracer amounts of fluorescently labeled myosin light chains, monomer actin, and phallotoxins into PtK_2 cells to observe the assembly of myosin and actin into the cleavage furrows of these cells. We selected large cells that often formed multipolar mitotic spindles and subsequently, multiple cleavage furrows that could be visualized with the fluorescent probes for myosin and actin. Mitotic cells that had been injected with fluorescent myosin light chains or fluorescent monomer actin had spindles whose fluorescence was brighter than that of the surrounding cytoplasm. The same was true of cells that had been injected with bovine serum albumin. In contrast, the fluorescence in spindles of cells that had been injected with F-actin probes, fluorescent phallotoxins, was approximately the same as in the cytoplasm adjacent to the spindle. We interpret this to mean that soluble proteins became concentrated in the mitotic spindle, whereas the actin that remains in the F-form during mitosis is present in the spindle at the same level as it is in the extra-spindle cytoplasm. In late anaphase, a band of

fluorescence was visible in the forming cleavage furrow of all cells that had been injected with one of the three probes for myosin and actin, but not in cells injected with bovine serum albumin. Fluorescent bands of actin and myosin formed not only between each group of separating chromosomes, but also midway between adjacent asters of multi-polar spindles. In one cell in which two mitotic spindles were oriented parallel to one another, four fluorescent bands formed: one between each of the two groups of separating chromosomes and one between each of the two pairs of adjacent asters. In a majority of exceptionally large cells, fibers were discernible in the cleavage furrows. In a few cases, the fibers appeared striated or beaded, in a manner similar to stress fibers in interphase cells. The fibers shortened and disassembled during cytokinesis and the fluorescently labeled proteins became localized on either side of the midbody and eventually were redistributed in the stress fibers of the daughter cells.

Cytoplasmic dynein is the motor for retrograde vesicle transport in squid axons. BRUCE J. SCHNAPP (Marine Biological Laboratory, Woods Hole, MA 02543).

Intracellular vesicles in axons move, without reversing, along uniformly oriented microtubules. A soluble fraction (S2) from extruded axoplasm was previously found to promote the bidirectional movement of plastic beads on purified microtubules *in vitro*. Two microtubule-based translocators were identified: an anterograde (+ end directed) motor, kinesin, and a retrograde motor whose purification and role in vesicle transport is described here. The retrograde motor in squid axoplasm is a microtubule-associated protein previously termed HMW1 (Vale *et al.* 1985, *Cell* **42**: 39–50). Like cytoplasmic dynein purified from bovine brain (Paschal *et al. J Cell Biol.* **105:** 1273–1282), HMW1 promotes microtubule sliding on glass, shows nucleotide-dependent binding to microtubules, is a 22s particle, and has a heavy chain of $M_r > 400{,}000$ that co-electrophoreses with axonemal dynein heavy chains. Like other dyneins, the heavy chain of HMW1 is specifically cleaved into two >200 kd fragments when irradiated with 254 nm light in the presence of 20 μM vanadate and 2 mM ATP, leading to inactivation of both motility and ATPase activity. UV-vanadate treatment of axoplasmic S2 completely blocks retrograde bead movement, indicating cytoplasmic dynein is the retrograde microtubule motor previously identified in this system.

Using KI-extracted vesicles whose movement is dependent on the addition of S2, vesicle movement was 63% retrograde when assayed on centrosome microtubules in control S2 (irradiated in the absence of vanadate) and 7% retrograde in the presence of S2 exposed to 20 μM vanadate during UV irradiation. In assays that quantified the absolute numbers of moving vesicles, the numbers of vesicles moving in the anterograde direction were unchanged by the UV-vanadate treatment. This indicates dynein operates specifically with a population of vesicles programmed to move toward the minus end of microtubules. Purified dynein, either alone or together with kinesin, did not promote vesicle movement, consistent with our previous finding (Schroer *et al.* 1988, *J. Cell Biol.*, in press) that soluble proteins, in addition to kinesin, are required for vesicle transport.

Comparative and General Physiology

The Limulus *amebocyte contains* α_2*-macroglobulin.* PETER B. ARMSTRONG (U. of California, Davis), JAMES P. QUIGLEY, AND FREDERICK R. RICKLES.

Alpha$_2$-macroglobulin, a protease-binding protein that is reactive with almost all endopeptidases, is present in high concentrations in the plasma of the horseshoe crab, *Limulus* (Quigley and Armstrong 1985, *J Biol. Chem.* **260:** 12715). Alpha-$_2$-macroglobulin was demonstrated by its ability to protect the active site of trypsin from inactivation by the macromolecular active site inhibitor, soybean trypsin inhibitor (Armstrong *et al.* 1985, *J. Exp. Zool.* **236:** 1), and by reaction with an antiserum prepared against purified *Limulus* α_2-macroglobulin. The blood cells also contain α_2-macroglobulin in a form that is released when washed cells are stimulated to undergo exocytosis by treatment with the ionophore, A23187. Alpha-$_2$-macroglobulin is detected in the materials released from the cells during degranulation both by activity in the soybean trypsin inhibitor-protection assay and by immunochemical staining of Western blots. The subunit molecular weight of the cell-associated α_2-macroglobulin, 185 kd, is identical to that of the plasma form. Although cells contain large quantities of the cytoplasmic marker enzyme (lactate dehydrogenase), none is released during ionophore-stimulated degranulation, indicating that cell lysis does not occur and is not responsible for the release of α_2-macroglobulin. The penultimate wash buffer lacks α_2-macroglobulin, demonstrating that the cells have been washed free of plasma proteins. We were unable to detect α_2-macroglobulin in Western blots of degranulated cells, indicating that most or all of the cell-associated α_2-macroglobulin is released during degranulation. The amount of α_2-macroglobulin contained within the cells of a given volume of blood is 2–5% of the quantity free in that volume of plasma. The distilled water lysates of N-ethylmaleimide-treated amebocytes used to detect endotoxin (*e.g., Limulus* amebocyte lysate or LAL) contain relatively large quantities of active α_2-macroglobulin. These preparations are essentially free of the principal plasma protein, hemocyanin, indicating that the cells have been well washed prior to lysis.

Supported by NIH Grant No. GM 35185.

Suppression of common mode signals within the electrosensory system of the little skate. DAVID BODZNICK (Wesleyan University) AND JOHN MONTGOMERY.

Elasmobranch fishes possess an acutely sensitive electrosensory system which can detect bioelectric fields produced by other animals. However, they produce bioelectric fields themselves (*e.g.*, during ventilation) which result in unwanted self-stimulation of the electroreceptors. Recordings from the brain show that central neurons are responsive to extrinsic fields, but manage to reduce the ventilatory modulation occurring in their afferent input. The likely basis of this suppression is that ventilatory stimulation is common mode to the receptors whereas extrinsic fields are differential (Montgomery 1984, *J. Comp. Physiol.* **155A:** 103–111; New and Bodznick 1987, *Neurosci. Abstr.* **13:** 399).

To test the hypothesis of common mode suppression, a stimulus was introduced via a gut electrode. The distribution of recorded electric fields, and recordings from primary afferents, show that this method provides a good common mode stimulus to all of the receptors (with the exception of the dorso-medial hyoid group which is above the water level in the tank). A 1 Hz sinusoid delivered through the gut electrode, was adjusted to give a 20 μV potential between the bath and a Ag/AgCl electrode placed in the interior of the body in the region of the electroreceptor clusters. This electrode also measures fluctuations in potential during normal ventilation which range from 0–60 μV. Defining the modulation produced by the gut electrode as noise, and the response to a 2 μV/cm uniform field as signal, the signal to noise ratio (S/N) in primary afferents ranged from 0.3 to 1.8 (mean 0.79, S.D. 0.32, n = 24). In the output neurons of the medullary nucleus the range of S/N was 0.7–65.8 (mean 4.8, S.D. 11.9, n = 29). The high values of S/N found in some central neurons is evidence that a common mode suppression mechanism functions to suppress CNS responses to ventilatory self stimulation.

Bacteriologic investigation of shell disease in the deep sea red crab, Geryon quinquedens. ROBERT BULLIS (Marine Biological Laboratory), LOUIS LEIBOVITZ, LARRY SWANSON, AND RANDY YOUNG.

We studied the [illegible] effects of pollution from sewage sludge dumping at site [illegible] cause of shell disease in crustaceans. Deep sea red crabs, *Geryon quinquedens*, chosen as a representative species, were collected from [illegible] continental shelf canyons which may have received dispersants from Dump site 106. Twenty crabs were examined representing populations that were close (Hudson canyon-8), intermediate (Block canyon-6), and relatively far (Atlantis canyon-6) from the dump site. All crabs examined exhibited darkly pigmented lesions of the exoskeleton which suggested crustacean shell disease. The lesions had a bimodal distribution pattern. A random unilateral hyperpigmentation was associated with apparent abrasions and scratches. A bilateral lesion symmetry was also observed. These bilateral lesions appeared to evolve as hyperpigmentation of the uniformly spaced microscopic sensory organelles located on the surface of the carapace. These pigmented areas became enlarged, confluent, and occasionally resulted in shell defects. Crabs with amputated appendages had lesions on the exposed proximal remaining articular surfaces. Cultures were taken from lesion and non-lesion areas on the crab on a variety of selective and non-selective media and incubated aerobically. Bacteria isolated presumptively included *Vibrio algmolyticus, Vibrio campbellii, Vibrio fluvialis, Flavobacter meningosepticum, Flavobacter breve,* and *Escherichia coli.* Several as yet unidentified fungi have been isolated. This study suggests that the shell disease lesions found in *Geryon* spp. are distinct from other previously described shell diseases, including "cigarette-burn disease."

This study is supported in part by a grant from the Division of Research Resources, National Institutes of Health (P40-RR1333-08).

Computer model of light-induced voltage response of the Hermissenda *type B photoreceptor based on seven light- and voltage-gated ionic conductances.* CHONG CHEN (Computation & Neural Systems, 216-76 Caltech, Pasadena, CA 91125), CHRISTOF KOCH, AND DANIEL L. ALKON.

Type B photoreceptors of a sea snail, *Hermissenda,* have been demonstrated as primary convergent neurons during associative conditioning. To understand its role in information processing and the underlying mechanism of ionic channel modulation, we implemented a mathematical model of the B-photoreceptor on a 3/160 SUN workstation. Hodgkin-Huxley-like equations are used to describe the kinetics of seven ionic conductances. The somata of the photoreceptor is approximated as a sphere of 30 μm in diameter. Three of the conductances are gated by light-induced chemical changes, $g_{Na}(L, V, t)$, $g_K(L, V, t)$, and a delayed $g_{DK}(L, V, t)$, where L is light, V is voltage, and t is time. The other four conductances are gated by voltage across the membrane, $g_{Ca}(V, t)$, $g_{Ca\text{-}K}(V, t)$, $g_A(V, t)$, and $g_K(V, t)$. A conductance (g) consists of activation (m), inactivation (h), and maximum conductance (g_{max}). Both m and h are described by first order differential equations of time, light, and voltage. By adopting experimental measurements of this and other preparations, the intracellular calcium that modulates some conductances is computed on the basis of the following processes: light-induced intracellular release, voltage-gated influx, diffusion, ion exchange, and intracellular buffering. The intracellular voltage clamp experiments performed with this model yield results comparable to laboratory recordings.

Isolation of a voltage-dependent calcium channel from the squid central nervous system. B. CHERKSEY, M. SUGIMORI, J.-W. LIN, AND R. LLINAS (NYU Medical Center, New York, NY 10016).

FTX, a low molecular weight factor purified from American funnel-web spiders, which specifically blocks the squid presynaptic calcium current (Sugimori *et al.* 1988, *Biol. Bull.* **175:** 302), was used to construct an affinity chromatography gel. Squid optic lobe homogenate was solubilized, reacted batchwise with the gel and the bound protein eluted, and reconstituted into lipid vesicles by sonication/dialysis. These vesicles were preloaded the with Quin-2. Addition of Ca^{++} to the external medium produced a rapid, sustained increase in the fluorescence not seen in control vesicles. Influx was blocked by 50 μM Cd^{++}. FTX blocked in a dose-dependent and competitive manner with external Ca^{++}. When a Nernst potential was established by valinomycin, the Ca^{++} influx into the vesicles was voltage dependent. Vesicles were also fused with lipid bilayers formed across the tip of a patch-clamp micropipette. Two types of channel-like activity were found. The first was characterized by voltage-dependent openings of 1–3 ms duration (mean). The opening probability, which was also voltage dependent, reached a maximum of 0.35 at a potential of 0 mV. The conductance was 15–20 pS in 80 mM Ba^{++} and 5–8 pS in 100 mM Ca^{++}. Comparison of the macroscopic currents obtained by summing multiple pulses reproduced closely the macroscopic Ica in squid terminal (Llinas *et al.* 1981, *Biophys. J.* **33:** 289). When the cytoplasmic face of the protein was exposed to high concentrations of Ba^{++}, extremely long mean open times (300 ms) were observed having a similar conductance. In symmetric Ba^{++} solutions, replacement of the cytoplasmic solution with Cs^{+} resulted in conversion of long openings to short openings. High internal calcium (100 mM) did not change the opening-time mode. We conclude that using an affinity gel based on FTX, it has been possible to isolate and partially purify a calcium channel with the properties expected for the presynaptic channel.

High ammonium background does not affect response function of narrowly tuned chemoreceptor cells. CARA M. COBURN, RAINER VOIGT, AND JELLE ATEMA (Boston University Marine Program, Marine Biological Laboratory).

We tested the effects of elevated ammonium (NH_4) background on the stimulus-response functions (S-R) of hydroxyproline- (Hyp), arginine- (Arg), and taurine-sensitive (Tau) cells of the lobster (*Homarus americanus*) medial antennule. NH_4 is a biologically relevant stimulus found in high levels in coastal waters.

Action potentials of single cells were recorded extracellularly using a suction electrode. Chemoreceptor cells were identified with a search stimulus (equimolar mixture of Hyp, Arg, and Tau; each at an applied peak concentration of $7 \times 10^{-5} M$) injected into a carrier flow of artificial seawater (ASW) which superfused the excised appendage. Individual responses to Hyp, Arg, and Tau ($7 \times 10^{-5} M$) were recorded to identify the best-stimulus. Then, S-R functions were determined for best-stimulus and NH_4 in ASW (7×10^{-9} to $7 \times 10^{-3} M$). After a 3-min adaptation to a $10^{-4} M$ NH_4 background, the S-R functions were redetermined. Finally, as a control for viability and NH_4 effects, S-R functions were repeated in ASW.

Ten Hyp cells were narrowly tuned (except one cell responded equally to Arg). Only one cell responded to high concentrations of NH_4 in ASW. None of the 10 cells tested altered S-R functions in the NH_4 background. Of two narrowly tuned Arg cells, one responded slightly to very high concentrations of NH_4 in ASW. Neither cell was affected by the NH_4 background. One of two narrowly tuned Tau cells was responsive to NH_4 in ASW. However, both cells showed a suppressed response in the NH_4 background.

We conclude that Hyp and Arg cells on the medial antennules are narrowly tuned and unaffected by even abnormally high NH_4 backgrounds. This characteristic makes them suitable for detection of chemical contrast. Similar effects have been described for chemoreceptor cells in other lobster chemoreceptor organs.

Supported by NSF (BNS-8512585) to JA.

Circulatory responses of bluefish to epinephrine, phentolamine, and atropine. STEPHEN H. FOX, CHRISTOPHER S. OGILVY, AND ARTHUR B. DUBOIS (John B. Pierce Foundation Laboratory, New Haven, CT 06519).

The cardiovascular responses to epinephrine, phentolamine, and atropine were studied in resting bluefish (*Pomatomus saltatrix*). Blood pressure and heart rate were monitored through a 1-mm tube placed in the ventral aorta. Change in mean blood pressure in mmHg in response to different doses of epinephrine chloride reached a maximum of 60 mmHg and had an ED50 of 5 μg/kg body weight. Following competitive blockade of the alpha adrenergic sympathetic system with phentolamine mesylate, 400 μg/kg intraarterially, the ED50 for epinephrine chloride increased to 15 μg/kg (n = 5). The phentolamine at this dose level dropped the resting blood pressure in fish lightly anesthetized with tricaine from a control of 83/54 to 64/45 ($P < 0.001$), and the heart rate remained unchanged (n = 9). But a dose of 200 μg/kg did not change the resting blood pressure or heart rate significantly (n = 4, $P = 0.2$). Atropine sulfate, 10 μg/kg, increased the heart rate from 48/min SE 4 to 87/min SE 12. Blood pressure increased from 98/61 to 112/81 (n = 5, $P < 0.02$). At 80 μg/kg, the heart rate increased from 42/min to 112/min and the blood pressure changed from 82/52, control, to 96/78. This tachycardia caused a significant increase in diastolic pressure (n = 5, $P < 0.01$). These results show that blood pressure and heart rate of bluefish are under tonic vagal and alpha adrenergic control, as in some other teleosts. This suggests the presence of well-developed parasympathetic and sympathetic regulation of the cardiovascular system in bluefish.

Calcium-dependent incorporation of serine into phosphatidylserine in the squid giant axon: physiological role in excitable membranes? P. G. HOLBROOK (Laboratory of Bioorganic Chemistry, National Institute of Diabetes, Digestive and Kidney Diseases, National Institutes of Health, Bethesda, Maryland 20892) AND R. M. GOULD.

Studies of the calcium-dependent, energy-independent incorporations of ^{14}C-labeled bases (choline, ethanolamine, and serine) into their respective phospholipids, phosphatidylcholine (PC), phosphatidylethanolamine (PE), and phosphatidylserine (PS) in subcellular fractions of whole rat brain demonstrated that these phospholipase-D type activities, known as the base-exchange enzymes, were enriched in both the microsomal and synaptosomal plasma membrane fractions and suggested that they might play a specific role in excitable membranes related to calcium-signaling (Holbrook and Wurtman 1988, *J. Neurochem.* **50:** 151–161). To obtain evidence that this type of activity is transported to nerve-endings, studies were initiated to establish whether serine-exchange activity was present in pure axoplasm extruded from the giant axon of the squid (*Loligo pealii*) (Holbrook and Gould 1986, *Biol. Bull.* **171:** 494). We report here that axoplasm incorporates ^3H-serine into PS at a rate which, when expressed on the basis of lipid phosphorous, is comparable to that observed in squid stellate ganglion and optic lobe. This incorporation meets accepted criteria for mediation via the base-exchange pathway: (1) it is stimulated by calcium and blocked by EGTA. (2) It has an alkaline pH optimum peaking at 8.6. The activity did not appear to saturate at the highest concentration of calcium tested (25 m*M*).

A bistable pigment system in Hermissenda *type A photoreceptors.* H.-P. HÖPP AND D. L. ALKON (Sect./Neural Systems, Lab. of Biophysics, NINCDS-NIH, Marine Biological Laboratory, Woods Hole, MA 02543).

On the basis of anatomy, electrophysiologic properties, and synaptic interaction, the five photoreceptors in each *Hermissenda* eye were previously distinguished (Alkon and Fuortes, 1972 *J. Gen. Physiol.* **60:** 631–649) as type A (2) and type B (3). White light elicits depolarizing generator potentials (with early transient and later sustained responses) from both types of cells. Following the offset of such light stimuli, however, type B cells show a long-lasting depolarization (LLD) while type A cells frequently exhibit long-lasting hyperpolarizations. In the present study, generator potentials of photoreceptors in isolated eyes, *i.e.*, with all synaptic interactions and impulse activity eliminated by axotomy, were exposed to a variety of light stimuli with different wavelength compositions.

After previous adaptation to white or orange light, both medial and lateral type A photoreceptors responded to blue light stimuli (blue edge filters, $\lambda_c = 530$ nm, 3.5×10^2 W/m^2) with a markedly reduced sustained depolarization. Additional stimulation resulted in a strong decrease or even complete disappearance of the early transient. The opposite effects, *i.e.*, increased sustained depolarization and reappearance or increase of the early transient, were elicited from blue adapted photoreceptors with white or orange light stimuli (orange edge filters, $\lambda_c = 540$ nm, 3.5×10^2 W/m^2). Typically, the offset of the blue light stimuli was followed by a prolonged depolarizing afterpotential (PDA) of up to 50 mV which could last for up to 3 hours and showed immediate restoration after exposure of the cell to white or orange light.

In contrast to these color-specific changes in light responses from type A cells, the responses of the three type B photoreceptors exhibited no comparable bistable changes over the wavelength range of 400 nm to 700 nm.

Using a double-pulse and a single-pulse paradigm, monochromatic light stimuli of equal duration and quantum flux (10 nm FWHM interference filters, $.9 \times 10^2$ W/m^2) were used to measure the spectral dependency of the decrease and increase in size of the early transient. The decrease was maximal at 470 nm while the increase was maximal at 570 nm. The existence of the two different wavelength maxima suggests two distinct visual pigment states with different absorption peaks.

Membrane conductance was reduced during the PDA evoked by blue light, suggesting the shutdown of an outward directed conductance as its underlying ionic mechanism. Furthermore, the strong increase in membrane conductance accompanying the early depolarizing transient was reduced and eventually eliminated as the early transient was reduced by the repetitive application of blue light. Conversely the same reduction in conductance reappeared as the early transient was restored with repetitive yellow light stimulation.

A thermostable rhodopsin-metarhodopsin conversion is thought to underly the color-specific regulation of the membrane potential and the conductances.

Supported by DFG Forschungsstipendium HO-989/1-1.

Organophosphorus acid (OPA) anhydrase from squid: a calcium-dependent P-F-splitting enzyme. FRANCIS C. G. HOSKIN, K. S. RAJAN, AND K. E. STEINMANN (Illinois Institute of Technology Center, Chicago, IL 60616).

The enzymes that hydrolyze the P-F bond of certain cholinesterase inhibitors (*e.g.*, diisopropylphosphorofluoridate, DFP; 1,2,2-trimethyl-

propyl methylphosphonofluoridate, Soman) are known as organophosphorus acid anhydrases (OPA anhydrase, formerly DFPase). They are categorized as "Mazur type" (cytosolic; Mn^{2+} stimulated; Soman/DFP hydrolysis ratios [illegible], mol. wt. 60–90,000) and "squid type" (limited to cephalopod hepatopancreas, and saliva; Mn^{2+} indifferent or slightly [illegible] Soman/DFP ≈ 0.25; mol. wt. 30,000; Hoskin *et al.* 1988 *Environ Appl Toxicol* **4**: S165–S172). We now find another property that distinguishes these two OPA anhydrases and may bear on the question of a physiological role for these unusual enzymes. The squid enzyme is non-competitively inhibited by EDTA (K_i ≈ 10^{-5} *M*). The inhibition is resolvable into fast and slow components ($t_{1/2}$ ≈ 1 h, reversible; $t_{1/2}$ ≈ 16 h, irreversible). The purified squid enzyme is inhibited 90%+ by EDTA, about 80% by EGTA, and not at all by the transition metal chelators 8-hydroxyquinoline-5-sulfonate and 1,10-phenanthroline, all at 10^{-4} *M*. EGTA followed by Ca^{2+} causes 80% recovery of activity, whereas EGTA and then Mg^{2+} causes 10% recovery. Identical results are obtained with freshly extruded axoplasm. In sharp contrast, Mazur type OPA anhydrase (various sources) is inhibited about 30% by all four chelators at 10^{-4} *M*, and is stimulated (many-fold) by Mn^{2+} and sometimes Mg^{2+} at 10^{-3} *M*. We conclude that squid type OPA anhydrase is a Ca^{2+} enzyme. We suggest that the Mazur type OPA anhydrases, while Mn^{2+} stimulated, are not divalent cation dependent. In view of a Ca^{2+} involvement in many cellular processes, these results imply a physiological role for squid type OPA anhydrase. The actual role, and the nature of the Ca^{2+} regulatory site, remain unknown.

Supported by a grant from Army Research Office.

A vibrating calcium-selective electrode for detecting extra-cellular calcium gradients. WIEL M. KÜHTREIBER, PHILIP C. WILLIAMS, AND LIONEL F. JAFFE (Marine Biological Laboratory, Woods Hole, MA 02543).

We have developed a vibrating, extracellular, calcium-selective microelectrode for measuring calcium gradients caused by localized calcium currents in or out of cells or tissues. The sensor is of the neutral carrier type and the electrode has a resistance of a few hundred Meg-Ohms. Gradients are measured by slowly vibrating the electrode and feeding its output into a phase-sensitive detector. In this way it is possible to measure calcium-fluxes smaller than 1 pmol/cm^2/s in a large background of other ions. Preliminary measurements with this new device on *Dictyostelium* and *Polysphondilium* show that these slime molds have large inward calcium currents ranging from about 1 to 3–30 pmol/cm^2/s at aggregation stages and at migrating slug stages, respectively. The influx just behind the front of the slug is two to three times the influx at more posterior locations. This area of reduced influx probably corresponds to the expected prestalk area of the slug. We have also detected calcium-fluxes in preliminary experiments on developing eggs of the fucoid seaweed *Pelvetia*, and in the growing pollentube of the tobacco plant. These feasibility studies show that the vibrating calcium-selective electrode produces biologically meaningful data. This device should provide a novel way to study the role of calcium fluxes in biological systems.

Supported by NIH-grants to LFJ

Hematopoietic chlamydiosis of the rock crab (Cancer irroratus) *and the jonah crab* (Cancer borealis). LOUIS LEIBOVITZ (Laboratory for Marine Animal Health, Marine Biological Laboratory).

The results of an approximate six-year study (1983–1988) of a previously unreported highly fatal transmissible disease of laboratory-maintained populations of rock and jonah crabs were reported. Hematopoietic tissues and circulating blood cells were primarily affected. The disease incidence was low in newly harvested wild crabs, which became infected rapidly when introduced into cannibalistic laboratory crab colonies. The percentage mortalities increased in direct proportion to the length of time crabs were maintained in the laboratory.

The disease was easily diagnosed by light microscopic examinations of fresh and fixed-stained blood smears and tissues demonstrating the pathognomonic, greatly swollen, immature and mature, infected circulating hemocytes. Such infected hemocytes were filled with fine basophilic *Chlamydia* that compressed and displaced the nuclei and cytoplasmic organelles of the host cells outwardly. As the disease continued, the crab's hematopoietic tissues were destroyed, and swollen cells frequently produced microscopic emboli and vascular occlusion. Infected cells frequently ruptured, releasing *Chlamydia* into the blood and tissue spaces.

Ultrastructural studies demonstrated oval or round developmental stages of *Chlamydia* sp. within infected host cells.

Reticulate stages ranged from a mean length of 560 nm and 475 nm in width; intermediate and condensing stages had a mean length of 422 nm and 354 nm in width; and elementary bodies had an approximate mean diameter of 214 nm.

This is the first report of a hematopoietic chlamydiosis, and chlamydiosis in crustacea. The specific features of the chlamydial agent, the importance of the disease, its epizootiology, and its comparative pathology were discussed.

This study is supported in part by a grant from the Division of Research Resources, National Institutes of Health (P40-RR1333-08).

The analysis of miniature synaptic potentials in the squid giant synapse. J.-W. LIN, M. SUGIMORI, AND R. LLINAS (Dept. of Physiology and Biophysics, NYU Medical Center, New York, NY 10016).

The miniature synaptic potentials recorded from the squid giant synapse have a near-symetrical waveform (Joyner *et al.* 1975, *Biophys J.* **15:** 37). Typically, it reaches peak amplitude in about 1 ms and decays in 5–6 ms. The time course can be approximated by a difference between two exponential functions, with a rising and a decay time constant, *i.e.*, $F(t) = a[e^{-t/td} - e^{-t/tr}]$. Synaptic noise simulated on the basis of this observation was then used to test the resolution of spectral analysis. Briefly, a fast Fourier transform was performed and a best fit of the spectra was located by searching through many time constant combinations. The results of the simulation show that the calculated time constants recreated the original miniature potential waveform satisfactorily as long as the standard deviation of the background noise was less than twice the miniature amplitude. Thus, only those experiments where a background noise level lower than 200 μV^2 were selected for spectral analysis, *i.e.*, with a standard deviation slightly larger than the minipotential amplitudes that has been estimated to be about 10 μV (Miledi 1967, *J. Physiol* **192:** 379; Augustine and Eckert 1984, *J. Physiol* **346:** 257). This procedure was applied to experimental data, where different levels of noise were evoked by presynaptic depolarizations, and the frequency characteristics of these spectra provided consistent time constants for each synapse. In one example, rise time constants of 0.2–0.3 ms and decay time constants of 1.5–1.6 ms were obtained from recordings where there was a 7-fold difference in transmitter release. Similar spectral consistency was obtained before and after FTX application, and provides an additional support for the presynaptic calcium conductance blockage role of this toxin (Sugimori *et al.* 1988, *Biol Bull* **175:** 302).

Effect of synapsin I and CAM kinase II on evoked and spontaneous transmitter release in the squid giant syn-

apse. R. LLINAS, M. SUGIMORI, J.-W. LIN, T. L. MCGUINNESS*, AND P. GREENGARD* (NYU Medical Center and *Rockefeller University).

Synapsin I, in its dephospho- and its phospho- form, and CAM kinase II were injected into the presynaptic terminal digits of the squid giant synapse. The location of these proteins was monitored with fluorescent microscopy. The effects of these injections on spontaneous transmitter release were studied using the technique described in an accompanying abstract (Lin *et al.* 1988, *Biol. Bull.* **175:** 300). The results indicated that dephosphosynapsin I reduced spontaneous and evoked quantal release in a manner which correlated temporally with its diffusion into the preterminal. Phosphosynapsin I showed no effect. By contrast, CAM kinase II did not modify spontaneous release if the presynaptic potential was negative to −70 mV. However, the low level of transmitter release produced by one second depolarizing pulses of the preterminal was increased by as much as 300% after the CAM kinase II injection. This indicated that a calcium entry, beyond that produced by the resting calcium conductance, is required for the injected CAM kinase II to increase transmitter release. The above results are consistent with the previous suggestion (Llinas *et al.* 1985, *PNAS* **82:** 3035) that these proteins control the availability of releasable vesicles by regulating the amount of vesicular caging by synapsin I whose binding to vesicles and to actin is phosphorylation-dependent (De Camilli and Greengard 1986, *Biochem. Pharmacol.* **35:** 4349).

Learning in the green crab. Electromyograms reveal that movement of the eye is not required for classical conditioning of the eye withdrawal reflex. RAFAEL H. LLINAS, RICHARD D. FEINMAN, ROBIN R. FORMAN, AND CHARLES I. ABRAMSON (SUNY Health Science Center at Brooklyn, Brooklyn, NY 11203).

The eye withdrawal reflex of the green crab, *Carcinus maenas,* can be conditioned according to a classical (Pavlovian) procedure by pairing a mild vibration to the carapace as a conditioned stimulus (CS) with an air puff to the eye as an unconditioned stimulus (US), (Abramson and Feinman 1988, *J. Neurosci.* **8:** 2908–2912). Eye retraction results from the activity of several muscles, the largest of which is the main abductor muscle, 19a. Stereotyped electrical activity in this muscle accompanies the eye retraction and can be recorded as electromyograms (EMG). The EMG record was used as an indicator of behavior to determine if the pattern of acquisition of conditioned responses was the same in an immobilized eye as in one that was freely moving. The results indicate that acquisition is the same in most cases and suggest that, as in many cases of classical conditioning, integration of the two sensory stimuli (CS and US) is sufficient for learning. Animals were assigned to either an experimental group with EMG leads implanted and the eye restrained, or to one of two control groups with freely moving eyes: either with EMG leads or unoperated. The pattern of acquisition for 5 of 8 experimental animals was the same as that for controls with moving eyes. Animals subjected to unpaired stimuli (fixed or moving eyes, with or without electrodes) showed few conditioned responses. After the acquisition trials, the eyes were freed, the wires were cut, and animals were returned to home tanks and later tested for behavioral responses in a sequence consisting of CS alone after 4 h and 24 h and a second period of paired training. Animals showed substantial retention and the second training period produced enhanced performance compared to training on the first day. The profile of behavior of all eight paired animals with fixed eyes was the same as that for animals with freely moving eyes. The unpaired animals that had been trained with eyes restrained were likewise indistinguishable from unpaired subjects with moving eyes.

This work was supported, in part, by funds from Margaret H. Morgan and from the Research Foundation of SUNY.

A histamine-gated anion channel suppresses lobster olfactory receptor cell activity. TIMOTHY S. MCCLINTOCK (The Whitney Laboratory).

Application of histamine to the soma of American lobster receptor cells suppressed both spontaneous and odor-evoked spiking as previously discovered in spiny lobster olfactory receptor cells (T. Bayer and B. W. Ache, unpub. data). In intracellular recordings, histamine caused an increase in conductance, a chloride-dependent change in membrane potential, and reductions in odor-evoked depolarizations. In isolated, voltage-clamped soma, pressure-applied histamine activated a largely chloride-dependent current. This current was not affected by external cobalt and cadmium (n = 2) or internal perfusion with 1 m*M* GTP-γ-S (n = 18) or GDP-β-S (n = 3). Applying histamine outside the patch pipette activated channels in outside-out patches but not in cell-attached patches (n = 19). Placing 1 mM GTP-γ-S in the pipette did not alter the activation of this channel in outside-out patches (n = 3). The mean slope conductance calculated from current-voltage relationships was 44 ± 6 pS. Extrapolated reversal potentials suggested that chloride was the major permeant ion present, but that some cation permeability also exists. In steady state concentrations of histamine, the probability of the channel being open began to rise rapidly between .1 μ*M* and 1 μ*M*, and appeared to saturate between 10 μ*M* and 100 μ*M* (n = 2). Channel opening evoked by 10 μ*M* histamine was blocked by 500 μ*M* cimetidine but not by 500 μ*M* pyrilamine. These results show that the modulatory action of histamine upon lobster olfactory receptor cells is mediated by a histamine-gated anion channel.

I thank the Grass Foundation and the NIMH for supporting this work, the members the 1988 Grass Fellow program, and B. W. Ache for advice.

Modification of the vestibulo-ocular reflex (VOR) after 6-OHDA induced catecholamine depletion in the CNS of goldfishes. JAMES G. MCELLIGOTT (Temple Univ. School of Medicine), MICHAEL WEISER, AND ROBERT BAKER.

The vestibulo-ocular reflex (VOR) helps to stabilize visual images on the retina during movements of the head. This compensatory reflex moves the eyes in a direction opposite to that of the head. Modification of the VOR provides an experimental paradigm for examining hypotheses about plasticity in the central nervous system (CNS). These experiments were designed to test the effects of depleting CNS catecholamines, especially norepinephrine (NE), on modifiability of the VOR in the goldfish. Past experimentation in various mammalian systems had shown that depletion of NE affects developmental plasticity in the visual system as well as VOR modifiability in cats. CNS catecholamines in the goldfish were depleted by small multiple injections of 6-OHDA into the brains of anesthetized goldfishes. Experimentation commenced two weeks after injection in order for CNS catecholamine depletion to occur. Eye movements were measured in chronically restrained alert animals. After initial measurements of the VOR gain (eye velocity/head velocity = 0.82), each fish underwent 4.5 hours of VOR gain modification. Gain was increased by presentation of visual stimuli in the presence of vestibular stimulation (⅛ Hz ± 20 degrees). Gain increased towards 2× and then towards 3× over a 4.5 hour period. In all cases, goldfishes (n = 4) produced robust VOR postmodification gain increases that averaged 2.6. When the brains of these animals were analyzed for catecholamine content by High Pressure Liquid Chromatography with Electrochemical Detection, there was a severe depletion

of brain NE to less than 4% for all brain regions measured as compared to controls. Thus, unlike other mammalian systems, 6-OHDA depletion of CNS NE in the goldfish does not noticeably influence VOR gain modifiability.

Physiologic mechanisms governing the cardiovascular compensation to gravity in bluefish. CHRISTOPHER S. OGILVY, STEPHEN H. FOX, AND ARTHUR B. DUBOIS (John B. Pierce Foundation Laboratory, New Haven, CT 06519).

Bluefish maintain ventral aortic blood pressure (BP) and develop a tachycardia during passive head-up tilting in air. This is true for unanesthetized or anesthetized fish despite a lower BP in anesthetized animals. Prior to tilting, we gave atropine sulfate (80 μg/kg) to block parasympathetic innervation to the heart, or phentolamine mesylate (400 μg/kg) to block alpha-adrenergic vasoconstriction. Or, we gave the neuromuscular junction blocking agent pancuronium bromide (100 μg/kg) to prevent body movements during tilting. In five fish, we transected the spinal cord 3 mm caudal to the obex before tilting. In others, the vagi were cut as well. After phentolamine, control BP was 73/47 mm Hg, and fell to 54/40.5 min into a 30° tilt, remaining low for the 30 min of tilting. Atropine increased the heart rate (HR) to 111 per min from a control of 42, and BP to 96/78 from a control of 82/52. HR remained unchanged during tilting, while BP decreased to 74/58 ($P < 0.05$) and remained low during the 30-min tilt. Flexion of the lower body musculature during tilting transiently increased the BP. Pancuronim prevented this and lowered BP during tilting. Cord transection without vagotomy lowered BP during the tilt despite an increase in HR. Cord section plus vagotomy produced a fall in BP and increase in HR. When these fish were tilted to 10° (2 min), 20° (2 min), or 30° (5 min), blood pressure fell precipitously and heart rate was unchanged. These results indicate that the cardiovascular reflex system in the bluefish is well developed and similar to that in land vertebrates. Upon tilting, there is inhibition of the vagus, with tachycardia, an apparent alpha adrenergic mediated vasoconstriction, and lower body muscular contractions. These aid venous return and maintain blood pressure to help perfuse the brain and other vital organs.

Further contributions to odor contrast detection in hermit crabs. LESLIE SAMMON, SOPHIL SANDERS, AND JELLE ATEMA (Boston University Marine Program, Marine Biological Lab, Woods Hole, MA 02543).

Hermit crabs (*Pagurus longicarpus*) are, in part, scavengers searching for food by smell in marsh environments with high organic backgrounds. We expect that the detection of chemical contrast is important for these animals. We tested their ability to locate upstream odor sources in the laboratory counting the fraction of individuals attracted through a slightly aversive dark corridor. We chose three odors that were highly attractive at different dilutions: shrimp juice (SJ) was most attractive (100% at 10^{-3} dilution) followed by fish juice (FJ; at 10^{-2}) and mussel juice (MJ, 100% at 10^{-1}). Response functions were essentially parallel: for all three odors 50% attraction occurred at 100× further dilution. Responses to control stimuli (seawater) averaged 25%.

In self-adapting backgrounds (10^{-4} dilution), all three response functions were suppressed (even below control values) for 10^{-5} and 10^{-4} stimulus dilutions, and reached 50% for 10^{-3} stimulus dilution. As expected, contrast detection is based here on intensity differences between stimulus and background.

In cross-adapting backgrounds, responses were expectedly unpredictable, since chemical contrast is now a function of both intensity and quality of stimulus and background. The weakest odor (MJ), when used as a background, suppressed responses to SJ more than responses to FJ. A background of the strongest odor (SJ) did not suppress responses to MJ, but did suppress responses to FJ, although FJ was a stronger stimulus than MJ. FJ backgrounds suppressed responses to SJ but not MJ, although SJ was a 100× stronger stimulus than MJ. In general, response functions for the weakest stimulus (MJ) were hardly suppressed by FJ or SJ, whereas response functions for the strongest stimulus (SJ) were strongly suppressed by FJ and MJ.

The results establish clearly that detection of chemical contrast between biologically relevant, complex odors is based on differences in both intensity and chemical composition of odors.

Supported by grants from NSF (BNS-8512585) to JA and Mt. Holyoke College to LS.

Blockage of calcium current by a factor from spider toxins. M. SUGIMORI, J.-W. LIN, B. CHERKSEY, AND R. LLINAS (Dept. Physiology and Biophysics, NYU Medical Center, New York, NY 10016).

A toxin fraction isolated from American funnel web spider venoms (FTX) blocks calcium currents in central neurons (Sugimori and Llinas 1987, *Neurosci. Abstr.*). This fraction has been recently shown to have a low molecular weight (200–300 dalton) (Cherksey *et al.* 1988, *Biol. Bull.* **175**: 298). When tested on transmission at the squid giant synapse, the toxin blocked synaptic transmission without affecting either sodium or potassium voltage-dependent conductances. The blockage occurred without affecting the pre- or post-fiber action potentials. Voltage-clamp experiments of the presynaptic terminal show that the inward calcium current is blocked at submicromolar concentrations by FTX within 5 to 10 minutes after direct application to the bath. The toxin was very slowly reversible, and its blockage was related in a competitive way to $[Ca^{2+}]$. Finally, pressure injection of glutamate in the area of the postsynaptic fiber demonstrated that FTX had no effect on the post synaptic potential generated, thereby indicating no effect of FTX on glutamate dependent post-synaptic channels.

Eye movement repertoire of the Cabazon sculpin, Scorpaenichthys marmoratus. MICHAEL WEISER, ANDREW BASS, JAMES G. MCELLIGOTT, AND ROBERT BAKER (NYU Medical Center, New York, New York).

Observation of eye movements in the Cabazon sculpin, a teleost, suggested goal-directed changes in gaze to attend small targets much like the oculomotor performance described for many foveated mammals. To test this hypothesis, spontaneous, optokinetic, and vestibular induced eye movements were quantitatively investigated employing the magnetic search coil technique. Saccades and fixation in the light were found in both the horizontal and vertical directions. Horizontal saccades occurred simultaneously in both eyes but often with disparate amplitude, direction, and velocity. Vertical saccades were independent of horizontal eye movements. Few spontaneous eye movements were observed in the dark. Visual following was elicited using either full field or subtended 5° targets delivered sinusoidally over a frequency range of 0.25 Hz to 1.0 Hz at 8–40°/s. Gain, measured as eye velocity/target velocity, was 0.6 and 0.4, respectively, throughout the frequency range. Smooth tracking was never elicited in the vertical direction. Vestibular evoked eye movements had a gain (eye velocity/head velocity) of 0.8 throughout the same frequency range. Combined visual and vestibular interaction produced eye movements at a gain of 1.0 from 0.063 Hz–2.0 Hz. Adaptive gain control of the vestibulo-ocular reflex towards a gain of 2.0 at 0.5 Hz (±10° amplitude) was examined after 3 h of training with a full field visual stimulus of 32°/s at a head velocity of 16°/s.

Vestibular evoked eye movements measured in the dark were increased from 0.8 to 1.8. We conclude that the oculomotor system of the Cabazon sculpin is remarkably robust, exhibiting more of the features described in foveated mammals than those reported in other teleosts as exemplified by the goldfish.

Stimulus/response coupling in sponge cell aggregation: differential effects of cocaine derivatives and non-steroidal antiinflammatory agents. GERALD WEISSMAN, REED BROZEN, GIULIA CELLI, AND PETER SANDS (Marine Biological Laboratory).

Dissociated marine sponge cells (*Microciona prolifera*) re-aggregate when protein kinase C and Ca fluxes elicit secretion of a species-specific aggregation factor. Aggregation is regulated by a guanine-nucleotide binding protein (G-protein) and is inhibited by pertussis toxin (Weissmann *et al.*, 1986 *PNAS* **83:** 2914–2918). Using quantitative aggregometry, we now show that agents which mimic binding of GTP to the G-protein (vanadate, >1 m*M*, fluoroaluminate, >5 m*M*) elicit aggregation of sponge cells exposed to sub-optimal amounts of Ca (5 m*M*) and ionomycin (1 μM). Arachidonic acid (20:4) had a similar effect. Cells treated with local anesthetics, *i.e.*, tetracaine (100 μM), dibucaine (150 μM), procaine (1 m*M*), or lidocaine (3.5 m*M*) failed to undergo normal aggregation in response to vanadate or arachidonate. Non-steroidal antiinflammatory drugs, *i.e.*, indomethacin (100 μM), piroxicam (100 μM), sodium salicylate (5 m*M*), or aspirin (5 m*M*) also inhibited aggregation. Neither class of drug inhibited aggregation induced by the direct activator of C-kinase, phorbol myristate acetate. The two groups of inhibitors differed in their mode of action with respect to the twin signals of protein kinase C and Ca movements (measured as ^{45}Ca efflux and appearance of ^{3}H-arachidonate in diacylglycerol on thin-layer chromatography in hexane:ether:acetic acid, 50:50:1). Whereas cocaine derivatives provoked enhanced ^{45}Ca fluxes from sponge cells exposed to Ca and ionomycin, aspirin-like drugs inhibited ^{45}Ca efflux. Moreover, whereas local anesthetics had no effect on diacylglycerol synthesis, aspirin-like drugs inhibited ^{3}H-arachidonate incorporation into diacylglycerol. The experiments not only suggest that cocaine derivatives exert their membrane effects at sites distal to C-kinase and that aspirin-like drugs work at the level of the G-protein, but that these primitive cells resemble human blood cells in their response to products of the coca plant or the willow.

Artificial diets of fish food are potentially useful for Hermissenda *mariculture.* EBENEZER YAMOAH, ALAN M. KUZIRIAN (Marine Biological Laboratory), DONNA MCPHIE, AND LOUIS MATZEL.

An advantage of using marine invertebrates as biomedical research models is their ability to be kept in laboratory culture. With the increasing dependence on closed-recirculating systems using natural or artificial seawater by non-coastal research laboratories, effective and efficient maintenance conditions are important.

The question of feeding density and growth rates for juveniles was addressed. Ten-day, post-metamorphic animals were kept in individual 5-ml flow-through test tubes in a 1-l container and fed 2–3 stalks of the coelenterate hydroid, *Tubularia* sp. (n = 10). Concurrently, animals were pooled in a 250-ml crystalizing dish with 10–12 hydroid stalks. All animals were kept in a 14°C incubator, their length measured, water changed, and food replenished every 3 days for 15 days. Instantaneous growth rates (K-values) for individually cultured and fed animals were compared with the multiple cultured animals. The data revealed no significant (Student *t*-test) differences between the two conditions (K-values: 13.4, 16.5, respectively).

Artificial fish food pellets were used by the Laboratory of Cellular and Molecular Neurobiology, NINCDS-NIH, Bethesda, MD, for maintenance of adult *Hermissenda*. Although artificial diets (microencapsulated food and amino acid suppliments) have been used for filter feeding larval and adult molluscs, this represented a unique opportunity to evaluate its use on a totally carnivorous species. Hard and soft fish food pellets, containing fish and shrimp meal, yeast, wheat-germ, seaweed meal, sucrose, vitamins, and trace elements were compared with a proven maintenance diet of crab viscera to test their ability to promote growth of healthy adult animals. Eight animals per feeding paradigm were fed either hard or soft fish pellets, or crab viscera. All animals were starved for five days, weighed, assigned to individual 50-ml flow-through test tubes, and fed (2 pellets/tube; viscera from 3 crabs split between 8 *Hermissenda*). Thereafter they were weighed, and fed every 3 days for 15 days. The following K-values based on weight gained (mg) were obtained: hard pellets, 2.18; soft pellets, 3.21; crab viscera, 4.30. Based on Student *t*-tests, the soft pellets were significantly better ($P < .05$) than hard, but not significantly less than the crab diet ($P > .1$). The hard pellets provided a significantly less effective diet than the crab ($P < .01$).

The results of the juvenile growth and culture conditions indicate that pooling of reasonable numbers of individuals and their food provides conditions which promote good growth. This is extremely important for ease of maintenance under mariculture conditions. The artificial diet study indicates that the soft fish food pellets provide adult growth rates comparable to that of crab viscera. They are somewhat better because the pellets foul the water much less than does crab viscera. The hard pellets which contain more crude protein (hard, 40%; soft, 35%) do not support comparably high growth rates. They probably are less palatable. This finding is important because it means there is a standard, extremely low maintenance diet potentially available that will provide consistant dietary conditions for *Hermissenda* mariculture.

E. Y. gratefully acknowledges the support provided by the American Society for Cell Biology, Minorities Student Program, and the Laboratory of Cellular and Molecular Neurobiology, NINCDS-NIH.

Some morphological and physiological properties of the sea robin Mauthner cell. STEVEN J. ZOTTOLI (Williams College), GRAEME W. DAVIS, AND SUSAN C. NORTHEN.

Comparative morphological studies of teleost fish have revealed differences in Mauthner cell (M-cell) size; somata can be categorized as either large or small. In addition, M-cells have not been found in certain fish. Most M-cell studies have been conducted on cyprinids which have M-cells in the large size class. We have analyzed the M-cell of the sea robin, *Prionotus carolinus*, to learn more about the properties of a cell in the small size category.

M-axons were identified as described previously (Zottoli and Agostini 1984, *Biol. Bull.* **167:** 535) using intracellular recordings with KCl electrodes in lightly anesthetized (0.007% MS-222) fish. M-axons could be activated by antidromic stimulation about halfway down the spinal cord but could not be activated further caudally. Morphological studies of the M-axons revealed a steady decrease in axonal size from the recording site in the medulla (40 μm) to halfway down the spinal cord (20 μm). Further caudally, it became increasingly difficult to distinguish the M-axons from other axons in the cord, suggesting that the M-axon does not extend the full length of the spinal cord.

Antidromic activation frequently resulted in a second component on the falling phase of the action potential. This later component may represent the spike generated at the initial segment which has traveled back passively to the axonal recording site. Double antidromic stimulation at 1/s resulted in blockage of the later component of the second

spike when the second stimulus was delivered approximately 10 ms or less after the first. The blocked component returned after increasing the frequency of stimulation. We speculate that this blockage is the result of a M-cell collateral inhibitory network similar to that described in the goldfish and that this network is common to M-cells independent of their size.

These results provide a first step in the analysis of a M-cell in the small size category and are a necessary prelude for comparative investigations of M-cell mediated behavior.

Supported by NINCDS Grant #NS 26032. Sue Northen was supported by the Ford-Mellon Research Scholar Program.

Developmental Biology and Fertilization

Protein phosphorylation during oocyte maturation in Spisula *and* Asterias. T. HANEJI AND S. S. KOIDE (The Population Council, New York, NY 10021).

Spisula oocytes were preincubated for 2 h with [^{32}P]phosphate at a concentration of 200 μCi/ml to radiolabel the adenosine triphosphate (ATP) pool. Maturation was induced with 5-hydroxytryptamine (5-HT) at a final concentration of 10 μM. After 10 and 30 min of treatment, oocytes were homogenized and the particulate fraction prepared. The phosphorylated proteins were separated by sodium dodecyl sulfate-polyacrylamide gel electrophoresis (SDS-PAGE) and the radiolabelled proteins analyzed by autoradiography. A marked increase in the radiolabelling of a protein with an estimated Mr of 30,000 occurred with the 5-HT-treated oocytes. A similar result was obtained with the particulate fraction of oocytes inseminated with sperm and incubated with [γ-^{32}P]ATP.

Maturation was induced in *Asterias* oocytes by treatment with 1-methyladenine for 10 and 30 min. Cytosol fraction was prepared and incubated with both [γ-^{32}P]ATP and [γ-^{32}P]GTP. The radiolabelled proteins were analyzed by SDS-PAGE and autoradiography. With [γ-^{32}P]ATP a marked increase in the incorporation of radioactivity occurred with proteins of estimated molecular weights of 70,000 and 62,000; whereas a marked increase in radiolabelling occurred with a protein of estimated Mr of 56,000 using [γ-^{32}P]GTP.

The present findings suggest that protein phosphorylation is an early biochemical event during the resumption of meiosis in *Spisula* and *Asterias* oocytes.

This study was supported by a grant No. Int 8211350 from NSF and GS PS 8712 from The Rockefeller Foundation.

Evidence for serotonin (5-HT$_{1A}$) receptor site on Spisula *oocyte*. A. L. KADAM, S. J. SEGAL, AND S. S. KOIDE (Population Council, New York).

Serotonin (5-hydroxytryptamine, 5-HT), a neurotransmitter, induces spawning when administered to *Spisula* and germinal vesicle breakdown (GVBD) of *Spisula* oocytes when added *in vitro* (Hirai *et al.*, 1988 *J. Exp. Zool.* **245:** 318). The present study was undertaken to determine the type of 5-HT receptor sites present on *Spisula* oocytes.

Oocyte maturation (GVBD) assay was performed by adding one drop containing about 2000 oocytes to 1.0 ml of artificial seawater (ASW) containing 5 μM concentration of test samples. After 30–40 min at ambient temperature, oocytes were scored for GVBD by light microscopy. Serotonin antagonist mianserin (5-HT$_1$), ketanserin (5-HT$_2$), metergoline (5-HT$_{1C}$) and its agonists 8-hydroxy-2-(di-n-propylamino)-tetralin (8-OH-DPAT) (5-HT$_{1A}$), RU-24969 (5-HT$_{1B}$), and 2-methylserotonin were used to determine the type of 5-HT receptor site on *Spisula* oocytes.

5-HT at a concentration of 5.0 μM induced GVBD in more than 90% of oocytes while 5-methoxytryptamine (5-MT) and 5-hydroxyindole acetic acid (5-HTAA) at the same dose did not induce GVBD. Mianserin, a 5-HT$_1$ antagonist, at 5.0 μM dose totally blocked 5-HT-induced GVBD. Ketanserin (5-HT$_2$) and metergoline (5-HT$_{1C}$) at the same dose failed to block 5-HT-induced GVBD. The 5-HT agonist, 8-OH-DPAT (5-HT$_{1A}$) induced GVBD in 80% of the oocytes; whereas RU-24969 (5-HT$_{1B}$) and 2-methyl-serotonin (5-HT$_3$) did not induce GVBD.

The present findings suggest that *Spisula* oocytes possess 5-HT$_{1A}$ receptor sites.

This study was supported by grant no. INT 82 11350 and NSF and GA PS 87123 from the Rockefeller Foundation. The 5-HT antagonists and agonists were obtained as gifts from Glaxo, Sandoz, Roussel UCLAF, and Farmitalia.

Stimulation of Spisula *sperm motility by serotonin (5-hydroxytryptamine).* A. L. KADAM, S. J. SEGAL, AND S. S. KOIDE (Population Council, New York).

Hirai *et al.* (*J. Exp. Zool.* **245:** 318, 1988) demonstrated that serotonin (5-HT) induces spawning when administered to male surf clam, *Spisula solidissima*. The present study was undertaken to determine the effect of 5-HT on *Spisula* sperm motility.

Spisula sperm were collected and diluted (1:500) with artificial seawater (ASW) and centrifuged at 300 $\times$ *g* for 5 min. The supernatant was recentrifuged at 1000 $\times$ *g* for 10 min at 4°C. The pellet of sperm was suspended in ASW to the original volume, refrigerated overnight, and used the next day for motility assay. Appropriate concentrations of test substances were added to 0.5 ml of sperm suspension. After 5 min of treatment, the percent motile sperm were estimated using the "cell soft" semen analyzer (Cryoresources). Motility was also determined using an axiovert microscope with video-enhancement (Zeiss). The oxygen consumption of treated and control sperm was measured by using the YSI oxygen meter (Clark type 02 electrode, Yellowstone Instrument Co.). Linear consumption of oxygen was recorded for 1 h. The fertilizing ability was assayed with washed *Spisula* oocytes and scored for germinal vesicle breakdown (GVBD) and embryo development by visual examination using an Axiovert microscope (Zeiss).

5-HT stimulated *Spisula* sperm motility. The effect was dose-dependent (1 μM = 45%; 2 μM = 77%; and 5 μM = 92%). 8-Hydroxy-2(di-n-propylamino)-tetralin, (8-OH-DPAT) (5-HT$_{1A}$ agonist), and 5-methoxytryptamine (5-MT) also stimulated sperm motility by 80% and 70%, respectively. RU-24969 (5-HT$_{1B}$) and 5-hydroxyindoleacetic acid (5-HIAA) had no effect on motility. Serotonin antagonists, mianserin (5-HT$_1$) and ketanserin (5-HT$_2$), at 5.0 μM concentration did not block 5-HT-induced sperm motility. 5-HT at 5.0 μM concentration did not stimulate sperm motility in sea urchin (*Arbacia*), parchment worm (*Chaetopterus*), and squid (*Loligo*). The oxygen consumption of 5-HT-stimulated *Spisula* sperm increased by 40% of the control value in 40 min. 5-HT-stimulated motile sperm retained their capacity to fertilize *Spisula* oocytes that developed normally.

In conclusion, 5-HT, 8-OH-DPAT, and 5-MT stimulate sperm motility in *Spisula*.

This study was supported by grant no. INT 82 11350 from NSF and GA PS 8712 from the Rockefeller Foundation. The 5-HT agonists and antagonists were gifts from Sandoz, Glaxo, Roussel, and Farmitalia.

The egg cortical endoplasmic reticulum. C. SARDET, M. TERASAKI, J. E. SPEKSNYDER, AND L. F. JAFFE (Station Zoologique, Villefranche-S-Mer, Laboratory of Neurobiology, NINCDS, NIH at Woods Hole, and Marine Biological Laboratory, Woods Hole).

Eggs of echinoderms, molluscs, amphibians, and mammals display numerous strands of endoplasmic reticulum (ER) immediately beneath the plasma membrane (Sardet 1984, *Dev. Biol.* **105:** 196; Charbonneau and Grey 1984, *Dev. Biol.* **102:** 90; Luttmer and Longo 1985, *Dev. Growth Differ.* **27:** 349; Speksnyder *et al.* 1986, *Progress in Developmental Biology*, part B, pp. 353–356). We have shown that this cortical ER can be retained in isolated cortices of sea urchin eggs as a honeycomb lattice encircling cortical granules (1). Using fluorescent dyes (Terasaki *et al.* 1986, *J. Cell Biol.* **103:** 1557), we have confirmed and extended these observations to several species of sea urchin eggs. A tubulovesicular network of rough ER adheres to the plasma membrane and is continuous with the cytoplasmic ER on which many organelles remain attached.

We have furthered our observations on cortical ER in eggs of the tunicate *Phallusia mammillata*, which do not have cortical granules. Cortices from these eggs are characterized by an extensive network of ER tubes and sheets, whose dynamics can be observed by fluorescence or DIC microscopy. Perfusion with hypotonic solution indicates that there are discrete anchorage points of the ER network to the plasma membrane. We could also localize microfilaments along the internal side of the plasma membrane using rhodamine-labeled phalloidin, and microtubules coursing along ER strands in the isolated cortex using immunofluorescence. The cortical ER network and microtubules were also observed by electron microscopy of replicas of fixed, rotary-shadowed whole mount preparations.

In view of the probable role of cortical ER in calcium regulation, its anchorage to the plasma membrane and its continuity throughout the cytoplasm, we must consider that the egg's ER may act as a scaffolding or framework able to control assembly-disassembly of associated cytoskeletal elements. These cytoskeletal elements as well as organelles may, in turn, move with respect to the ER.

A cell-free preparation of endoplasmic reticulum derived from eggs. M. Terasaki, C. Sardet*, and T. Reese (Laboratory of Neurobiology, NINCDS, NIH at Woods Hole, and *Station Zoologique, Villefranche-S-Mer).

The classic method for producing cell-free preparations of ER membranes is homogenization followed by differential centrifugation. This method has been useful, but (1) the continuity of the ER, which distinguishes it from other membranes, is not preserved, (2) other membranes may contaminate this fraction, and (3) compartmentation in the ER is difficult to study. A cell-free preparation of variably sized networks of tubular membranes was produced from sea urchin eggs (*Arbacia punctulata*) and tunicate eggs (*Phallusia mammillata*) by shearing attached eggs or by squashing eggs between two cover slips. The membranes which remain on the cover slip not associated with the cortices after washing were observed by fluorescent dye staining [DiOC6(3)], by video enhanced DIC, and by whole mount electron microscopy of glutaraldehyde-osmium-fixed and critical point dried samples. Ribosomes on many of the membranes were observed by EM and by staining with Hoechst dye 33258 at pH 2 (Hilwig and Gropp, *ECR* **91:** 457). Since some of the disadvantages of differential centrifugation can be avoided, this preparation makes possible new kinds of studies on activities of the ER, such as calcium regulation, protein or lipid synthesis, or protein filament binding and motility.

We used a different dye, DiIC16(3) (8 μg/ml for 1 min diluted just before use from 2.5 mg/ml ethanol stock), to examine the organization of the cortical ER in these cortices. This dye stains cortical ER but not cortical granules of sea urchin egg cortices. Comparison with phase contrast images shows that the ER often encircles cortical granules on the cortex, verifying the original observations of Sardet (1984, *DB* **105:** 196).

Diamino acids block plutei formation in developing Arbacia *mimicking other chemopreventive anticancer agents.* Walter Troll (NYU Medical Center, New York, NY) and Jessica A. Feinman.

Protease inhibitors and retinoids interfere with plutei development in *Arbacia punctulata* when added up to six hours after fertilization. The development of plutei is specifically modified without any effect on earlier differentiation. The protease inhibitor *e*-amino caproic acid (EAC) was effective at 0.1 *M* concentration while leupeptin, antipain, and α_1-antitrypsin, as well as retinoids, blocked plutei formation at m*M* concentrations. Similar concentrations of chemopreventive agents suppressed H-*ras* oncogene transformation of NIH 3T3 cells (Garte *et al.* 1987, *Cancer Res.* **47:** 3159–3162). We investigated lysine, the amino acid analog of EAC, and noted that it blocked plutei development at 1 m*M*, 100-fold lower concentration than the effective dose of EAC. The closely related amino acids hydroxylysine and ornithine also blocked plutei formation at m*M* concentrations. Other amino acids, including arginine, histidine, glutamic acid, and aspartic acid, were inactive. Thus, the diamino acids mimic the action of chemopreventive agents in blocking plutei development in *Arbacia*. It will be of interest to study these diamino acids further in their anticarcinogenic action in NIH 3T3 cells and in animal and carcinogenic model systems. They have the advantage that they are non-toxic and can be readily added to media or diets.

Supported by Center Grant ES-00260 from the National Institute of Environmental Sciences.

Ecology

Effect of tail regeneration on early fecundity in Capitella *sp. I and sp. II (Polychaeta).* Susan D. Hill (Michigan State University), Michael J. Ferkowicz, and Judith P. Grassle.

Capitella sp. I and sp. II are sibling species which co-occur in the vicinity of Woods Hole. Both species have comparatively large yolky eggs, and lecithotrophic larvae that colonize disturbed, organically rich habitats. Consequently, reduction in size of first brood or delay in first spawning may be significant in determining their rates of population increase in the field.

We investigated the effect of posterior segment amputation and subsequent regeneration on size of the first two broods and on time of emergence of the metatrochophore larvae. *Capitella* spp. I and II late juveniles and young females were paired according to size and stage of vitellogenesis. Animals in which oocytes were macroscopically undetectable were classified as juveniles; animals with visible oocytes were categorized by oocyte development. Tails were amputated at the 25th abdominal setiger from one of each pair. Each worm was mated with a male. Embryos in brood tubes produced by the first and second spawnings of each female were counted. Date of hatching of metatrochophores from the first brood tube was determined.

No significant difference was found in brood size in *Capitella* sp. I: regenerating worms produced as many eggs in their first and second broods as intact worms. *Capitella* sp. II worms that had their tails amputated as juveniles produced significantly fewer eggs in their first and second broods than did intact worms. *Capitella* sp. II females, in which oocytes were detectable at amputation, showed no reduction in either brood. It appears that, following amputation prior to vitellogenesis, *Capitella* sp. I produces its usual complement of eggs while *Capitella* sp. II reduces the number.

In both species, tail loss in [illegible] delays the production and hatching of the first brood of [illegible] phore larvae by several days, an important delay in species with short generation times.

Support for this research was provided by NSF OCE-8509169 (SDHH).

Marine policy implications related to the commercial value and scientific collecting of the whelk Busycon. HENRY M. KAPLAN, BARBARA C. BOYER, AND KRISTEN A. SANTOS (Union College).

This study examines socio-economic and ecological trends associated with fluctuations in the commercial value of the whelk *Busycon*, the basis of the New England conch fishery, and evaluates relevant marine policies. Interviews of fishermen, seafood buyers, and marine policy officials were conducted; information was also collected by setting our own conch traps for monitoring and research purposes. Results indicate a small but active conch industry in New England that has undergone significant price fluctuations and technological diversification. Specifically, within the last few years the price of conch has almost doubled and competition between conch pot fishermen and draggers now fishing for conch has increased. Depletion of foreign conch fisheries and overfishing of other domestic fishes have contributed to the increased activity in the New England conch industry. Ecological problems involving the possible depletion of the New England fishery and scientific collecting problems associated with scarcity and rising costs as well as changes and confusions regarding recent marine policies regulating the New England conch fishery are also examined.

The authors gratefully acknowledge the support of the Woods Hole Oceanographic Institution, the Marine Biological Laboratory, and Union College/Dana Fellowships.

Gray seal pups establish critical marine habitat in Nantucket Sound, U.S.A. DAVID PATON (Fayston, Vermont).

Halichoerus grypus birthings at Muskeget Island, Nantucket Sound, during the winter of 1987/1988 occurred during the last week of January. Surveys of the Nantucket and Martha's Vineyard Sounds, the Elisabeth Islands, and Nomans Island were begun in early November. Solitary males were seen at the North Shore of Muskeget in early December. Common seals arrived in numbers at this time and posted themselves at their usual hauling grounds. Aerial reconnaissance at elevations of 240 and 1000 meters were made with the Hasselblad 250 and 80 mm Zeiss lenses and Kodochrome ASA 64 film. The photographic transparencies were magnified and enhanced with digital techniques and flat plane microscopic objectives.

On 28 January, 10 males were grouped at the north shore of the south hook of the island upwind from 7 females and 2 white-coated pups. Sea birds flocked to the edge of the nursery grounds. Two males attended the shore near them. On 29 January, two placental remains showed at the middle of the bar. Two more white-coated pups were photographed. On the 30th the placentas had been removed except for red stains in the sand. During these three days, a small seal that had the pattern and shape of a molter was included in the nursery group. A high altitude reconnaissance was made of the area. No other white-pelt pups were detected. One week later eight swimming animals were seen near the island. Twenty-seven recent corpses were counted at the nursery; one of the five pups was reported dead by property owners. Molting pods chose Wasque Shoal and Muskeget Island north bar during April and May.

Andrews and Mott (1967) have established the continuous character of this species' use of these waters and shores. There is irrefutable evidence in these recent surveys that the life history of a pod of gray seals is begun here. The habitat includes pupping grounds, fishing, and molting haulouts (Boyd, 1961).

I wish to acknowledge Joe Costa, the Dickenson Trust, Ovide Fontier, the Holgate Family, and the VIPIRG Corporation for their support.

Preliminary report: composition of communities resident on Limulus *carapaces.* LINDA L. TURNER, CARRIE KAMMIRE, AND MARY ANNE SYDLIK (Eastern Michigan University).

Horseshoe crab (*Limulus polyphemus*) carapaces act as moving substrates for simple to complex assemblages of small marine organisms. Carapace communities are unique in two ways. First, maximum community age is constrained by horseshoe crab moult patterns. Second, horseshoe crabs spend most of the year buried offshore, then repeatedly move into subtidal eelgrass communities and harsher intertidal zones during the breeding season. These movements probably have a significant impact on carapace community composition and complexity.

Taxon frequency and diversity were determined by sampling 41 carapaces (intraocular distance range 21–41 cm) at Mashnee Dike, Cape Cod. Neither horseshoe crab size nor sex significantly influenced community structure. Barnacles (*Chthamalus* and *Balanus*) and slipper limpets (*Crepidula*) were the most common of the >10 faunal genera. More than 16 algal genera were present. Green blades, tubes, and branched filaments made up more than 50% of all algae. Brown and red filaments were intermediate and rare, respectively. *Punctaria* (brown blades) and *Chondrus* (red erect algae) were found only as germlings. Algal crusts (all orders) were relatively rare. The subtidal eelgrass community may have contributed up to eight faunal and twelve algal genera.

No significant changes in relative frequencies of algal orders were seen between 1–23 June 1988. There were shifts in the relative frequencies of algal morphologies over this period: blades and filaments alternately dominated, while *Chondrus*, *Codium*, and crusts exchanged subdominant positions.

The preliminary study suggests a possible optimum in taxon diversity. Eighty-three percent of samples bore between four and nine taxa per carapace (mean 6.3; range 1–13). Increases in taxa beyond five per carapace were due mainly to the addition of like organisms: two genera of barnacles instead of one; three species of branched filament rather than one.

Supported by NSF Grant BNS-8719325 to M.A. Sydlik.

Neurobiology

Effects of intracellular alien calcium chelators on transmitter release at the squid giant synapse. ELIZABETH M. ADLER (Univ. Toronto), STEVEN N. DUFFY, GEORGE J. AUGUSTINE, AND MILTON P. CHARLTON.

The molecular mechanisms underlying triggering of neurotransmitter release by calcium ions are poorly understood, in part because of a lack of information about the intracellular calcium transient that triggers release. As one approach to characterizing the calcium milieu of intracellular release sites, we injected a series of calcium chelators into the presynaptic terminal of the squid giant synapse. Transmitter release was assayed by measuring the postsynaptic electrical response elicited by action potentials in the presynaptic terminal.

As previously reported by Adams *et al.* (1985, *J. Physiol.* **369**: 145–159) injection of EGTA had little effect on neurotransmitter release.

We next examined BAPTA, which has an equilibrium affinity constant for calcium binding (K_D) similar to that of EGTA at physiological pH but binds calcium much more rapidly. BAPTA was highly effective in producing a rapid and reversible reduction in transmitter release. These changes in transmitter release were not caused by any changes in the presynaptic action potential. BAPTA derivatives with estimated intracellular K_Ds ranging from 1.8×10^{-7} *M* to 4.9×10^{-6} *M* were all highly effective at reducing transmitter release (*ca.* 80–90% reduction) at estimated presynaptic concentrations of several m*M*. At lower estimated concentrations (<1 m*M*), the order of buffer efficacy in blocking transmitter release was inversely proportional to K_D. A fourth derivative with an estimated intracellular K_D of 13 m*M* was less effective in reducing release (*ca.* 25% reduction in release at estimated presynaptic concentrations of 3 m*M*). We conclude that calcium binding rate is an important consideration when using calcium buffers to attenuate intracellular calcium transients.

Association of phospholipid metabolizing enzymes with axolemmal membranes (squid retinal fibers and garfish olfactory nerve) and axoplasmic vesicles from squid axoplasm. MARIO ALBERGHINA AND ROBERT M. GOULD (Institute for Basic Research in Developmental Disabilities, Staten Island, NY).

The neuronal perikarya is the acknowledged source of lipids and proteins used for the expansion and maintenance of the axonal membranes. However, the axon also contains lipid metabolizing enzymes. For example, we have shown that pure axoplasm from the giant axon of squid, *Loligo pealei*, will catalyze various reactions of phospholipid metabolism (Gould *et al.* 1983, *J. Neurochem.* **40**: 1300; Alberghina and Gould 1987, *Biol. Bull.* **173**: 439). To localize phospholipid metabolizing enzymes to axonal membranes, we measured their activities in fractions enriched in axolemmal membranes and axoplasmic vesicles. Axolemmal fractions from squid retinal fibers and garfish olfactory nerve were purified by published methods and characterized by marker enzyme content. Axoplasmic vesicles were separated from cytoskeletal proteins in extruded axoplasm by a potassium iodide treatment followed by sucrose density gradient centrifugation (Schroer *et al.* 1988, *J. Cell. Biol.*, submitted).

CDP-diacylglycerol: myo-inositol-3-phosphoryl-transferase (EC 2.7.8.11, PtdIns synthase), catalyzing the *de novo* synthesis of phosphatidylinositol, was enriched in the axolemmal fractions from both squid retinal fibers and garfish olfactory nerve. Purified axoplasmic vesicles had a high content of PtdIns synthase. AcylCoA:1-acyl-*sn*-glycero-3-phosphorylcholine acyltransferase (EC 2.3.1.23) was also present at high content in the axolemmal membrane-rich fractions of both squid retinal fibers and garfish olfactory nerve, and in axoplasmic vesicles from the squid giant axon.

Phospholipase A2 (EC 3.1.1.4), catalyzing the hydrolysis of the oleoyl group from exogenous phosphatidylcholine at neutral pH (7.4), was present in axolemmal fractions and in axoplasmic vesicles. Activities in all preparations were stimulated by added calcium (5 m*M*) and partially inhibited by EGTA (2 m*M*). Activities were not as enriched in axolemmal membranes and axoplasmic vesicle fractions as were the PtdIns synthase and acyltransferase activities. Our results indicate that membrane-associated (PtdIns synthase, acyltransferase and PLA2) and soluble (PLA2) enzymes of lipid metabolism are constituents of axonal processes.

Supported by grant NS 13980 from NINCDS (RMG).

Immunocytochemical characterization of the sonic motor nucleus of the toadfish, Opsanus tau. HARRIET BAKER (Cornell University), ANDREW BASS, AND ROBERT BAKER.

The sonic motor nucleus in toadfish is a midline nucleus that innervates a bilateral set of swimbladder "drumming" muscles. Intracellular recording from sonic motoneurons showed that the frequency of sonic motor discharge is determined by a rhythmic membrane hyperpolarization followed by a chemical and electrotonic depolarization. These observations imply inhibitory and excitatory "pacemaker" neurons. Intracellular injection of HRP and lesion experiments demonstrate that these neurons are localized both within and in the adjacent ventrolateral margin of the sonic motor nucleus. This study initiates the neurochemical characterization of the central components underlying sonic motor discharge. Using immunocytochemical techniques, GABA-, serotonin-, and catecholamine-containing elements were identified within and around the nucleus. Abundant GABA-like immunoreactivity was found in fibers and terminals throughout the nucleus. A few labeled perikarya, smaller in diameter than motoneurons, existed within the nucleus. Cells with processes directed into the nucleus were more numerous along the lateral margin. Surprisingly, serotonin-containing neurons, also of small diameter, were found within the nucleus characteristically at positions close to the midline or along the ventrolateral margin. The number of serotonin-containing fibers and terminals was small as compared to the extensive GABAergic termination. Catecholaminergic cells were dorsal and rostral to the nucleus and sent processes into the nucleus; however, terminals were even more sparse than observed for serotonin. These data suggest that GABA plays the important role in producing the inhibitory component of the sonic motor discharge. In contrast, given the sparsity of serotonin and catecholamine processes in the nucleus they are unlikely to represent the excitatory pacemaker neurons although they may play a modulatory role in determining the pattern of discharge.

Quinacrine blocks calcium currents in Paramecium. SUSAN R. BARRY (University of Michigan, Ann Arbor MI), JUAN BERNAL, AND BARBARA E. EHRLICH.

Paramecium calkinsi, a marine paramecium, contains voltage-sensitive calcium channels in the ciliary membrane. These channels are insensitive to the organic calcium channel blockers, D600, verapamil, and the dihydropyridine drugs. The only organic compounds that have been reported to block these channels are the calmodulin antagonist, W7, and its analogs. We report here that quinacrine hydrochloride may also block the voltage-sensitive calcium channel in paramecia.

A behavioral test was used initially to test the effects of quinacrine on calcium channels in paramecia. Paramecia were placed in a depolarizing solution containing 62.5 m*M* KCl, 62.5 m*M* NaCl, 1 m*M* $CaCl_2$, and 10 m*M* MOPS. When paramecia are depolarized in this solution, calcium channels in the ciliary membrane are transiently opened. Influx of calcium causes the cilia to reverse the direction of their stroke so that the paramecia swim backward for approximately seventy seconds. Quinacrine reduced the duration of backward swimming at a threshold concentration of approximately 1 μM. The duration of backward swimming was halved in 3 μM quinacrine while backward swimming was completely eliminated in 100 μM quinacrine. Quinacrine was three times more potent than W7 in inhibiting backward swimming. Since the duration of backward swimming has been correlated with calcium channel activity, quinacrine may reduce backward swimming by blocking calcium channels.

The effect of quinacrine on the calcium action potential in paramecia was also examined. The paramecia were impaled with single microelectrodes for stimulation and recording. Voltage-sensitive potassium channels were blocked by extracellular application of tetraethylammo-

nium chloride and intracellular application of cesium chloride. Thus, depolarization of the membrane produced an action potential whose magnitude and time course reflect the magnitude and time course of calcium influx. Addition of 50 or 100 μM quinacrine hydrochloride reduced both the amplitude and time course of the calcium action potential.

In conclusion, the calcium channels of paramecia are not blocked by the organic compounds that block metazoan calcium channels, but are blocked by quinacrine, a compound known to inhibit sodium channels in metazoan cells. These data show that quinacrine is an additional tool for the study of the voltage-sensitive calcium channel in paramecium.

This work was supported by NIH grant GM-39092 and NSF grant BNS 85-06778. BEE is a PEW Scholar in the Biomedical Sciences.

Neurophysiological correlates of sex differences in the sonic motor system of the midshipman, Porichthys notatus. ANDREW BASS (Cornell University) AND ROBERT BAKER.

In the sound-producing fish, *Porichthys notatus*, there are two classes of sexually mature males. A large size class (Type I) generates several types of "vocalizations" during the breeding season, unlike the smaller size class of males (Type II) and females which have not yet been found to be sonic. Previous studies have shown that the morphology of the central (sonic motor nucleus) and peripheral (swimbladder "drumming" muscles) components of the sonic motor system are similar in Type II males and females. In these studies all animals were acclimated to a temperature of 15°C. Surprisingly, sonic activity could be evoked in *all* classes of animals following midbrain stimulation and intracranial recording from exiting sonic motor nerves. A synchronous response was always evoked bilaterally in females and both classes of males. Intracellular recordings of synaptic and action potentials from every sonic motoneuron in Type II males and females, as in Type I males, exhibited a direct 1:1 correspondence with each evoked response. Temperature over a range of 6–24°C was then used as a physiological variable to further compare sex differences in functional organization. At the same temperature, the fundamental frequency in Type II males and females was similar but significantly lower than in Type I males. These data indicate that the sonic motor system of females and Type II males are qualitatively similar to that of Type I males, but there is a detectable difference in discharge frequency. We conclude that the central neuronal circuitry in Type II males and females can generate a rhythmic sonic output despite dramatic sex differences in the sizes of motoneurons, total muscle mass, and individual muscle diameter.

G-proteins modulate the calcium action potential in Paramecium calkinsi. JUAN BERNAL AND BARBARA EHRLICH (University of Connecticut, Farmington, CT).

Activation of voltage-dependent calcium channels initates backward swimming in *Paramecium*. The duration of backward swimming was modulated by G-proteins in the marine paramecium *Paramecium calkinsi* (McIlveen *et al.* 1987, *Biol. Bull.* 173: 445). With the aim to understand the mechanism of this modulation, we measured the effect of G-proteins on calcium action potentials in intact *Paramecium calkinsi*. First, we showed that this cell produces a calcium action potential under current clamp conditions. To isolate the calcium action potential, the paramecium was bathed in a sodium-free solution containing: (in mM) TEA-Cl, 125; KCl, 10; $CaCl_2$, 15; MOPS 10; pH 7.3. The electrodes were filled with CsCl (0.1 M or 2 M, pH 7.0). The amplitude of the calcium action potential increased when the extracellular calcium concentration was increased between 0.5 and 90 mM. In contrast, the calcium action potential in fresh water paramecia saturates at 1 mM calcium. The calcium action potential was blocked by W(12)Br (2 μM), a concentration which has been shown previously to block backward swimming and single calcium channel currents.

To test the hypothesis that G-proteins modulate the action potential, compounds of interest were injected into the cell. When GTPγS, a non-hydrolyzable analogue of GTP which activates G-proteins, was injected into the cell, the duration of calcium action potential was increased by 300%. This effect was maintained over 20 min. GDPβS, a non-hydrolyzable analogue of GTP which inhibits G-proteins, decreased the duration and amplitude of the calcium action potential. Five minutes after injection of GDPβS, the voltage response to a current pulse was reduced to the passive properties of the cell. These results suggest that G-proteins are involved in calcium action potential modulation. We are in the process of doing voltage clamp experiments to clarify the mechanism of the modulation of calcium action potential by G-proteins.

This work was supported by NIH grant GMS 39092. BEE is a PEW Scholar in the Biomedical Sciences.

A biologically motivated artificial neural network. DANIEL ALKON (Laboratory for Molecular and Cellular Neurobiology, NINCDS, NIH), KIM TIPLITZ BLACKWELL*, TOM P. VOGL*, VASSILIOS KOUNTOURIS*.

Most artificial neural networks utilize neuronal elements whose presynaptic strengths are modulated by the output, and are set by a number of different iterative, non-linear, or stochastic algorithms. The network described here, a dynamically stable associative learning (DYSTAL) network, is based on a biological neural network: the convergent visual and vestibular pathways which mediate associative learning of *Hermissenda crassicornis*. The response of these pathways to their preferred stimuli are of fixed synaptic strength. In addition, there are loci of convergence which are modified by repeated presentation of temporally related patterns.

By virtue of unique learning rules, the DYSTAL network displays a number of desireable features some of which may be found in other models but which have not previously been combined. The network is self-adapting and the strength (weight) associated with each synapse is adjusted by a rule that only requires information regarding the pre- and post-synaptic neurons involved. A consequence of self-adaptation is that the network can be scaled for the solution of large problems with only a linear increase in computation time, even on a serial machine. Finally, the network can associate different patterns which are presented sequentially.

The network was trained by presenting to the 3 by 3 input array either "T" or "E". The network was tested and was able to properly classify (distinguish) incomplete "T"s and "E"s. In addition, when presented with an ambiguous pattern (one which could be either a "T" or a "E") the network responds with the union of the patterns ("T") when trained to associate "T"s and "E"s, and with the intersection of the two ("I") when no association had been formed.

Clustering of presynaptic Ca channels at active zones of the squid giant synapse: EM analysis of active zone distribution in a fura-2 imaging specimen. JOANN BUCHANAN (Yale Univ. Medical School), GEORGE J. AUGUSTINE, MILTON P. CHARLTON, LUIS OSSES, AND STEPHEN J SMITH.

We have performed correlative light and electron microscopical studies of the distribution of active zones in the presynaptic terminal of the giant synapse. The goal of this study was to test the hypothesis that Ca channels are clustered at presynaptic active zones by comparing

* Environmental Research Institute of Michigan, Arlington, VA 22209.

the distribution of active zones to sites of Ca influx. This was accomplished by examining a squid giant synapse preparation which had been injected with the Ca indicator dye, fura-2, to study the pattern of Ca influx following presynaptic stimulation (see Smith *et al.* 1988, *Biol. Bull.* **175:** 311). Following physiological studies, the preparation was immersed in 2% glutaraldehyde in 0.1 *M* cacodylate buffer containing 0.8 *M* sucrose and further processed for electron microscopy. Thick sections (2 μm thickness) were cut through the 800 μm-long synapse, digitized, and reassembled with computer-aided reconstruction methods. At this level of resolution it was possible to visualize sites of synaptic contact along the synapse; the distribution of contacts was closely correlated with the longitudinal distribution of Ca influx sites detected with fura-2 in the living synapse. In addition, thin sections were collected at 50 μm intervals through the synapse and photographic montages were made to examine the distribution of active zones around the perimeter of the presynaptic terminal. It was found that the number of active zones in the region of the presynaptic terminal nearest the postsynaptic axon was 10-times greater than in the region away from the postsynaptic axon. This closely corresponds to the lateral gradients of Ca influx identified in the fura-2 measurements. These two findings demonstrate a close correlation between active zones and sites of Ca influx and therefore support the hypothesis that Ca channels are clustered at active zones.

Supported by Howard Hughes Medical Institute funds, NIH grant NS-21624, and MRC (Canada) funds.

Identification and characterization of peptidergic motoneurons in the buccal ganglia of Aplysia californica *using intracellular dye injections and immunocytochemistry.*

PAUL J. CHURCH AND MARK D. KIRK (Dept. of Biology, Boston University, Boston, MA 02215).

The Small Cardioactive Peptide *B* (SCP*B*) is present in buccal neurons of *Aplysia californica* and has physiological effects within the feeding system. Previous studies have localized SCP*B* to the identified neurons B1, B2, and B15, and shown its absence in B4/5 and B16. Immunocytochemical studies on juveniles have shown several small dorsal cells and three or four large ventral cells to contain SCP*B*, but the cells have yet to be characterized.

To determine the functional roles of SCP*B*ergic buccal neurons, we are identifying and physiologically characterizing the remaining buccal neurons with SCP*B*-like immunoreactivity. Ganglia from 115–600 gram animals were treated either as whole mounts or in 20 μm frozen sections. Cell identification was based on size, position, and physiology, combined with lucifer yellow injection.

SCP*B*-like immunoreactivity of the identified neurons B15, B1, and B2 was confirmed in adult animals. In addition, double label experiments show SCP*B*-like immunoreactivity in the motoneurons B6, B9, and B11, as well as a motoneuron with its soma located just medial to B6. An absence of staining has been demonstrated in B3, B7, B41, and B42. Consistant staining also appeared in several (approx. 25) small cells in the dorsal-rostral group as well as in at least one cell located peripherally at a branch point of the esophogeal nerve. Numerous processes in the neuropil, buccal nerves, and sheath above the commissural arch also show SCP*B*-like immunoreactivity. Staining was eliminated in preparations in which the primary antibody was preabsorbed to synthetic SCP*B*.

Supported by the Grass Foundation and NIH grant NS24662 to MDK.

Modulation of potassium channel inactivation in squid axons by ATP.

JOHN R. CLAY AND ETE Z. SZUTS (Marine Biological Laboratory, Woods Hole, MA).

We studied the effects of adenosine triphosphate (ATP) on the potassium ion current, I_K, in squid giant axons. Experiments were performed on internally perfused axons using a standard voltage-clamp technique. The internal perfusate contained 250 m*M* K glutamate, 25 m*M* K_2HPO_4, and 400 m*M* sucrose, to which 5 m*M* ATP (magnesium salt) was added. The pH of both the control and test solutions was adjusted to 7.2 with free glutamic acid. The external solution was filtered seawater to which 1 μ*M* tetrodotoxin was added to block the I_{Na} component. Temperature was maintained at 12 ± 0.1°C. The I_K component was elicited with 20 ms-duration depolarizing voltage-clamp steps to −40, −20, 0, 20, and 40 mV. The holding potential was either −90, −80, −70, −60, or −50 mV. We found no effect of ATP on I_K with holding potentials of −90 or −80 mV. However, ATP significantly reduced I_K from holding potentials of −60 or −50 mV without changing activation kinetics. The action of ATP could be described by a 10–15 mV shift of the inactivation parameter of the I_K channel along the voltage axis in the negative direction. Similar results were obtained with ATP-γ-S. ATP had no observable effect on I_{Na}. These results suggest that axoplasmic ATP regulates excitability of nerve axonal membrane. Specifically, loss of ATP results in a reduction of excitability. Our work is to be contrasted with the results of Bezanilla *et al.* (1986, PNAS **83:** 2743–2745), who report significant increases in I_K with ATP.

Octopine dehydrogenase activity in Loligo pealei: *an active cytoplasmic enzyme marker for subcellular studies.*

MICHAEL J. DOWDALL AND DAVID L. DOWNIE (Department of Zoology, University of Nottingham, U.K.).

Lactate dehydrogenase (LDH) is a classical cytoplasmic marker enzyme for subcellular fractionation. Synaptosomes from cephalopod optic lobe (Dowdall and Whittaker 1973, *J. Neurochem.* **20:** 921–935; Campbell and Dowdall 1976, *Exp. Brain Res.* **24:** 7) contain some 20% of the LDH in occluded form. However, since the activity of this enzyme in the optic lobe is only 5% of that found in mammalian brain, it is a relatively insensitive and inconvenient marker for quantitative studies with these tissues.

Octopine dehydrogenase (E.C. 1.5.1.11) (ODH) catalyses the reversible reductive condensation of L-arginine with pyruvic acid, using NADH as a co-factor, to form octopine. This enzyme has only been found in molluscan tissues and has been purified from the muscles of the scallop, *Pecten maximus* (van Thoai *et al.* 1969, *Biochim. Biophys. Acta* **191:** 46–57). Using essentially the same assay procedure of van Thaoi *et al* (1969) we have found considerable ODH activity in optic lobe and other tissues of *Loligo pealei*. The enzyme was readily extractable from squid tissues using 50 m*M* Tris buffer pH 7.4 containing 0.5% (w/v) Triton X-100 and in optic lobe ODH had Km's (m*M*) for pyruvate and L-arginine of 0.2 and 0.9, respectively. Optic lobe activity was 24.6 ± SD 3.5 μmol/min/g wet wt. (n = 4) at pH 6.6 and 25°C using 4 m*M* each of pyruvate and L-arginine, and 0.09 m*M* NADH. This was 15 times the LDH activity in this tissue using optimal assay conditions. Tentacle muscle and retinal fibers had comparable activities to optic lobe, whereas mantle muscle was approximately four times higher. Tissues with much lower activities included testes, sperm sacs, gill, hepatopancreas, giant axon, and fin nerve. In muscle, optic lobe, retinal fibers, testes, and gill, ODH activity was eight times or greater than that of LDH. This suggests that ODH rather than LDH plays a major role in energy metabolism in many tissues of *L. pealei*.

Subcellular fractionation of optic lobe showed ODH to have a classical cytoplasmic distribution with the synaptosomal fraction containing 20% of the activity in a 100% occluded form.

Supported by Travel Grants awarded to MJD from the Royal Society and the Wellcome Trust.

Protein synthesis in the giant axon and in nerve endings of the squid. ANTONIO GIUDITTA (Dept. General Physiology, University of Naples, Italy), ENRICO MUSCHIETTI, EMILIA CASTIGLI, AND BARRY B. KAPLAN.

Axons are generally believed to lack the system of protein synthesis. In accord with this view, the synthesis of axoplasmic protein by the isolated giant axon of the squid (Giuditta *et al.* 1968, *PNAS* **59**: 1284–1287) was attributed to the activity of periaxonal glial cells, from which newly made proteins are transferred to the axon (Lasek *et al.* 1977, *J. Cell Biol.* **74**: 501–523). However, our experiments demonstrate that polysomes carrying nascent peptide chains are present in squid axoplasm. Cleaned giant axons, still associated with intact giant axon systems, were incubated in Millipore-filtered seawater containing 100 μCi/ml ^{35}S-methionine (1 h at 20–22°C). Radioactive polysomes were purified from extruded axoplasm by sedimentation through a layer of 2 *M* sucrose and fractionated on 15–45% sucrose gradients. The radioactive polysomal profile was shifted to the top of the gradient by treatment of the resuspended pellet with RNase or EDTA. Cycloheximide (50 μg/ml) strongly inhibited the labelling of axoplasmic polysomes, while chloramphenicol (50 μg/ml) did not induce appreciable changes.

The occurrence of protein synthesis in a purified fraction of optic lobe synaptosomes (Hernandez *et al.* 1976, *Acta Cient. Venez.* **27**: 120–123) was confirmed by demonstrating ^{35}S-methionine incorporation into protein. The incorporation was linear for at least one hour, and dose-dependent in a limited protein concentration range. Cycloheximide was strongly inhibitory, while chloramphenicol induced only a limited degree of inhibition. Pretreatment of the synaptosomal fraction with RNase (10 μg/ml) did not affect incorporation, while hypo-osmotic shock completely abolished protein labelling. Strong inhibition was also induced by depolarizing conditions (100 m*M* KCl).

These data demonstrate that protein synthesis occurs in the giant axon axoplasm and that a similar process may be present in nerve endings.

Hemilabyrinthectomy and selective otolith lesion symptoms in the flatfish. WERNER GRAF AND ROBERT BAKER (Marine Biological Laboratory, Woods Hole, MA 02543).

During metamorphosis, flatfish tilt 90° to one side or the other to become bottom-adapted adult animals. In this position, the labyrinths are rotated 90° relative to their premetamorphic orientation in space. In this attitude the utriculus is least sensitive to small displacements, and therefore the other otoliths, in particular the sacculus, have been suggested to substitute for the alleged insensitivity of the utriculus. Nevertheless, the utricular nerve has the largest caliber by far of all labyrinthine nerve branches. In this context, we tested the relative contribution of the two labyrinths and single otolithic endorgans to maintain posture in the adult winter flounder, *Pseudopleuronectes americanus*. Hemilabyrinthectomy was either performed by central neurectomy of the labyrinthine nerve branches or by removal of the entire labyrinth via a lateral approach. Both methods yielded similar results. Lesions of the down-side labyrinth (n = 7) hardly resulted in any abnormal movement. In some cases, the animals spiralled towards the lesioned side as observed in upright fish. Extirpation of the up-side labyrinth, in contrast, produced dramatically different results (n = 14). The animals performed several full *pitch-down* rotations before settling on the tank floor. If "translated" into upright fish movement, this response could be described as a rotation about the dorso-ventral axis *away* from the lesioned side. Thus, two fundamental differences can be observed when comparing the hemilabyrinthectomy involving the up-side labyrinth in the adult flatfish to that of upright fish. First, a *change in direction* of the lesion symptoms from spiralling movements about the rostro-caudal axis to rotations about the dorso-ventral axis. Second, a *change of laterality* from body movements towards the lesioned side to rotations away from the lesion. Similar observations were made after hemilabyrinthectomy of the up-side labyrinth in two adult summer flounders, *Paralichthys dentatus*, a left-sided flatfish. Selective neurectomy of the utricular nerve produced identical body movements as those following hemilabyrinthectomy (up-side: n = 3; down-side: n = 1). Selective sacculus (up-side: n = 4) and lagena lesions (up-side: n = 2) produced movement patterns inconsistently or not at all. Thus, the utriculus retains its original functional role in respect to posture. In general, lesion symptoms were not pronounced but could be exacerbated by neurectomy of the optic nerves. We interpret the peculiar bilaterally asymmetric labyrinthine organization of the adult flatfish to be of fundamental importance for maintaining the flatfish as a flatfish.

Supported by NIH grant NS 20358.

Study of the resting conductance of the squid axon membrane. J. R. HUNT AND D. C. CHANG (Baylor College of Medicine).

Previous studies in this laboratory suggested that the resting conductance which determines the resting potential (V_{rest}) in the squid giant axon may be largely controlled by a pathway different than the delayed rectifier K channel. Because the resting conductance is very small, we developed a special voltage clamp procedure using extensive signal averaging to measure minute changes in conductance (g). This procedure consists of superimposing a 40 ms rectangular pulse with a series of small square pulses (±3 mV high, 1-ms wide). Thus, the slope conductance at a given potential can be determined directly from the current changes in response to the square pulses. Using this method, we measured the membrane conductance over a wide range of test potentials. The Na channel was blocked by externally applied tetrodotoxin. While conductance at depolarizing potentials was dominated by the delayed rectifier, at V more negative than the resting potential, we found a small component of K conductance (g_{K2}) which had V dependence deviated from the Hodgkin-Huxley equations describing the delayed rectifier. Our preliminary results of the ion selectivity measurements of g_{K2} show that the relative permeabilities of g_{K2} for K^+, Rb^+, NH_4^+, Na^+, Cs^+, and Li^+ ions are 1.0, 0.71, 0.14, 0.13, 0.10, and 0.09, respectively. We also determined the ion selectivity of the resting membrane by studying the effects of various ions on the V_{rest} of the axon. The ion selectivity of g_{K2} is qualitatively similar to that determined from V_{rest}. On the other hand, the ion selectivity of the resting membrane is known to be different than that of the delayed rectifier. For example, Cs^+ seems to be readily permeable to the resting membrane but is virtually impermeable to the delayed rectifier. This is not the case for g_{K2}. Hence, based on properties of both the V dependence and ion selectivity, it is reasonable to interpret that g_{K2} may be the major pathway for resting current.

Supported in part by NIH grant #NS25803-01.

Stereoscopy of high resolution video microscope images reconstructed from serial optical sections. SHINYA INOUÉ (Marine Biological Laboratory) AND TED INOUÉ.

We will demonstrate high-resolution stereoscopic video microscope images dynamically. The stereo-pair video pictures were obtained by reconstruction from through-focal, very thin optical sections (Inoué 1988, *Methods Cell Biol.* **30**: in press) stored on an optical memory disk recorder (OMDR). For images stored on the OMDR, and for intensity contours of microscope images, stereo pairs were reconstructed by shearing the image stack (Inoué and Inoué 1986, *Ann. NY Acad. Sci.* **483**: 392–404) with an Image-1/AT digital image processor (Universal Imaging Corp., Media, PA). The same processor compresses the left

and right images each to half height vertically but not horizontally, and places them in the top and bottom halves of the video field. A Stereographics processor re-expands and projects the left and right images alternately at 120 Hz as left and right circularly polarized images (Stereographics Corp., San Rafael, CA). Complementary filters worn by the observer provide striking, pseudocolor or monochrome, flickerless, dynamic stereoscopic images. Details of Golgi-stained neuronal processes and intensity contours of a human oral epithelial cell were projected at the meeting.

Supported by NIH grant GM 31617-07 and NSF grant DCB 8518672.

Contractility of the squid stellate ganglion. CLAUDIA M. NUÑO (Univ. Southern California), MARIA ELENA SANCHEZ, JOANN BUCHANAN, AND GEORGE J. AUGUSTINE.

Studies of synaptic transmission at the squid stellate ganglion sometimes are impeded by endogenous contractions of the ganglion. We characterized these contractions to identify experimental treatments that selectively eliminate movement without altering synaptic transmission. Contractions were detected in isolated stellate ganglia of *Loligo pealei* by using a fiber optic light collector and photodiode to measure changes in light transmission associated with movement. With such an arrangement rhythmic movements of the ganglion were readily detected. The amplitude, but not the frequency, of these signals depended upon the position of the fiber optic collector. Electron microscopy of the stellate ganglion identified two types of cells containing organized arrays of contractile filaments: smooth muscle cells of blood vessels and unidentified cells dispersed throughout the ganglion. Either of these cells could be involved in producing ganglion contractions.

Ion substitution and pharmacological experiments were used to examine the ionic basis of the ganglionic contractions. Removal of Na ions from the extracellular medium had effects that depended upon the nature of the substance used as a substitute for Na. Replacement of Na with Tris rapidly and reversibly abolished movements, while replacement with sucrose slowed contractions but did not entirely eliminate them. The Na channel blocker tetrodotoxin (1 μM) had no effect on contractions. In contrast, removal of Ca ions (with Mg as a substitute) completely eliminated contractions. Inorganic Ca channel blockers, such as Cd (2 mM) and Mn (12.5–25 mM), eliminated contractions, as did the dihydropyridine Ca channel blockers nitrendipine (10–20 μM) or nimodipine (20 μM). We conclude that Na ions play some role in generating movements, but are less important than Ca ions. Blockade of contractions by Tris is likely to be due to a secondary pharmacological action of this ion, rather than Na removal. Either Na or Ca could be involved in producing spontaneous electrical activity, while Ca might play some other role in excitation-contraction coupling. Of the several conditions that eliminate ganglion contractions, dihydropyridines are the only treatments which do not also affect synaptic transmission.

Supported by NIH grant NS-21624.

Multiple site optical recording from small ensembles of Aplysia californica *neurons in culture.* A. L. OBAID, T. D. PARSONS, AND B. M. SALZBERG (University of Pennsylvania School of Medicine).

Cell culture of 2-dimensional ensembles of identified invertebrate neurons permits one to construct truly simple "nervous systems" in a dish. We have consistently observed a wide variety of synaptic interactions in such preparations, using conventional electrophysiological techniques. These networks are uniquely amenable to study by means of multiple site optical recording of transmembrane voltage (MSORTV). We have used the potentiometric dye RH-155 and a 12×12 photodiode array to record changes in extrinsic absorption, at 700 ± 25 nm, from up to 9 neurons simultaneously. These optical signals provide a faithful representation of voltage changes at 124 loci during trials of 8-s duration. Rhythmic electrical activity is observed in many cells and connecting processes, in the absence of any electrical stimulation. This activity may be endogenous, or it may be light induced. In either case, computer averaging over spike occurrences in individual detector elements reveals complex correlations in the MSORTV records. These experiments suggest that multiple site optical recordings from small ensembles of interconnected neurons may help to unravel the intricate relationships that characterize even the simplest nervous systems.

We are grateful to Tom Capo and the Howard Hughes Medical Institute for providing us with juvenile *Aplysia*, to David Kleinfeld for introducing us to the *Aplysia* culture system, and to Larry Cohen and his co-workers for their generous provision of software for data acquisition and analysis. Supported by USPHS grants NS 16824 and HL 07499.

Electrical connections to cultured invertebrate neurons using multielectrode arrays. WADE REGEHR (Bell Labs, Murray Hill, NJ), YUAN LIU, MICHELLE MISCHKE, AND B. M. SALZBERG.

Recently it has become possible to culture a variety of invertebrate neurons from leech (*Hirudo medicinalis*), slug (*Aplysia californica*), and snail (*Helisoma trivolvis*). The ability to form small networks of synaptically connected identified neurons has facilitated the study of synaptogenesis and neuronal development. Using conventional electrophysiological techniques it is difficult to study more than 2 or 3 neurons for longer than several hours. For cultured neurons extracellular recording and stimulation is difficult, since the medium shunts the current flow to ground. Multielectrode arrays (Thomas 1972, *Exp. Cell Res.* **74**: 61–66; Pine 1980, *J. Neurosci. Methods* **2**: 19–31; Gross 1982, *J. Neurosci. Methods* **5**: 13–22) overcome these limitations. These planar arrays consist of 61 electrodes embedded in the bottom of a culture dish. Both the conductive leads and the insulation are transparent, making the dishes compatible with voltage-sensitive dyes and inverted microscopy. Large invertebrate neurons from *Aplysia*, leech, and *Helisoma*, grown on the array, form seals over dish electrodes. Action potentials have been recorded simultaneously from many neurons for up to two weeks, with signal-to-noise ratios as large as 500:1. The signals recorded from electrodes under cell bodies are essentially derivatives of the intracellular potential, while signals recorded from electrodes sealed under axon stumps are primarily due to active channels. Multielectrode arrays have also been used to stimulate neurons and to record the resulting action potential. While it is relatively easy to record action potentials, it is difficult to record post-synaptic potentials because of their small size and slow rate of rise. By improving the seal to tens of megohms it should be possible to record fast post-synaptic events.

We are grateful to Tom Capo and the HHMI for providing juvenile *Aplysia*. Supported by USPHS grant NS 16824 and Grass Foundation Fellowships to W.R. and Y.L.

Clustering of presynaptic Ca channels at active zones of the squid giant synapse: fura-2 movies of Ca influx. STEPHEN J. SMITH (Yale Univ. Medical School), GEORGE J. AUGUSTINE, JOANN BUCHANAN, MILTON P. CHARLTON, AND LUIS OSSES.

Recordings of fluorescence changes from intracellularly injected fura-2, a calcium indicator, were used to test the hypothesis that Ca channels at the giant synapse of *Loligo pealei* are localized at presynaptic active zones. A SIT video camera and an analog video disc recorder were used to record fluorescence images, which were subsequently ana-

lyzed using a digital video pr[illegible]. With excitation light of 380 nm wavelength, fluorescence de[illegible] the order of 25% were observed at the end of 0.5 s, 80 Hz ac[illegible]tial trains. With 350 nm excitation, fluorescence in[illegible]rved under the same conditions. These optical changes [illegible] effect complexation of fura-2 with Ca ions. At early times after pr[illegible]ptic stimulation, these indicator signals were localized to areas with high densities of active zones and synaptic contact, as determined in an accompanying light and electron microscopic histological study (see Buchanan *et al.* 1988, *Biol. Bull.* 175: 308). Later cytoplasmic Ca signals were more diffuse, probably reflecting diffusion of Ca ions away from Ca channels clustered at active zones. The patterns of early fluorescence change after action potential stimulation were consistent with the hypothesis that Ca channels cluster at active zones within the presynaptic membrane of this giant presynaptic terminal.

Supported by Howard Hughes Medical Institute funds, NIH grant NS-21624, and MRC (Canada) funds.

G-proteins in the squid Loligo pealeii: *characterization, quantitation, and examination of possible role in axonal transport.* STEVEN S. VOGEL (Columbia University), STEPHEN D. HESS, AND THOMAS S. REESE.

G-proteins have been implicated in mediating exocytosis. If they are involved in release of transmitter from synapses, we might expect them to be transported to, and enriched in, synaptic terminals. We used the giant axon and a synaptosome preparation from squid to examine this idea.

Using pertussis toxin (PTX) catalyzed [^{32}P]-ADP-ribosylation followed by SDS-PAGE, we find that optic lobe synaptosomes contain 28 pmoles ADP-ribose/mg protein in a M_r 40,000 protein. Synaptosomal labeling was enriched by a factor of 1.7 over optic lobe homogenate. Homogenates of giant axon had 0.68 ± 0.07 pmoles ADP-ribose/mg protein (n = 3) while extruded axoplasm had 0.32 ± 0.01 pmoles/mg (n = 3). It is now possible to calculate that 44% of the axonal G-protein is in axoplasm.

To determine whether G-proteins are transported to terminals, we cooled a 1 mm segment of axon to 4°C for 2 h while maintaining the rest at 16°C. Because transport is blocked at low temperatures, we expected a build-up of anterograde vesicles and a depletion of retrograde vesicles on the proximal side of the cold block (and the opposite on the distal side). Labeling in homogenates made from 5-mm segments just proximal to the block was consistently greater than in homogenates in comparable segments just distal to the block (6 of 7 experiments); without the cold block, labeling in both segments was the same. The build up of G-proteins on the proximal side was not correlated with any change in Coomassie staining including neurofilaments, actin, and tubulin. In one experiment, with three 2-mm segments on each side of the block, there was a build-up of G-protein on the proximal side, and a depletion on the distal side of the block.

Thus, squid nervous system contains PTX sensitive G-proteins that are concentrated in synaptosomes and transported to terminals by fast axonal transport.

S.S.V. received a 1988 Grass Fellowship.

Channels from smooth muscle sarcoplasmic reticulum are opened by inositol 1,4,5-trisphosphate and are inhibited by heparin. J. WAIRAS AND B. E. EHRLICH (University of Connecticut, Farmington, CT).

Inositol 1,4,5-trisphosphate (IP_3) has been implicated as the link between excitation and contraction in smooth muscle. However, the mechanism of the stimulation by IP_3 was unclear. We have found a novel channel in the sarcoplasmic reticulum (SR) of aortic smooth muscle that is opened by IP_3 and inhibited by heparin. This channel is quite different from the calcium release channel in SR from skeletal and cardiac muscle. Channel properties were determined by measuring calcium release from SR vesicles with the calcium indicator antipyrylazo III and by measuring calcium currents through single channels that had been incorporated into planar lipid bilayers. IP_3 activation of calcium release from aortic SR vesicles occurs at low concentrations of IP_3 ($K_{0.5}$ = 1 μM) and activation is specific. Several other inositol phosphates (inositol 1-phosphate, inositol 1,4-bisphosphate, inositol 1,3,4-trisphosphate, inositol 1,3,4,5-tetrakisphosphate; each at 20 μM) and caffeine (1–50 mM) did not initiate calcium release from these vesicles. Activation of the channels incorporated into bilayers were observed at 0.1 μM IP_3. In addition, IP_3 was only effective when added to one side of the bilayer showing that channels inserted preferentially in one orientation. These results contrast with those obtained with skeletal SR in which 1 mM caffeine induced calcium release and activated channels incorporated into planar bilayers. IP_3 (20 μM) activated neither calcium release nor channel activity in the bilayer with vesicles made from skeletal SR. Ruthenium red (1 μM) inhibited caffeine-induced calcium release from skeletal SR but 20 μM ruthenium red did not affect IP_3-induced calcium release from aortic SR. Similarly, only skeletal SR channel activity was inhibited by ruthenium red. Heparin (10 μg/ml) inhibited both calcium release and channel activity in aortic SR but concentrations 100 times larger were ineffective in skeletal SR assays. These results support the hypothesis that IP_3 is the trigger for contraction in smooth muscle.

This work was supported by NIH grant HL-33026 and GM-39092. BEE is a PEW Scholar in the Biomedical Sciences.

Voltage sensitive dye recording from the abdominal nerve cord of the American cockroach. JIAN-YOUNG WU, HANS-PETER HÖPP, CHUN XIAO, AND LARRY COHEN (Yale University School of Medicine).

Recently Yagodin, Pushkarev, and Slutsky reported that they were not able to measure voltage-sensitive dye signals from axons in insect nerve cord. We have tried to repeat this experiment using a microscope and 124 elements photodiode array to measure absorption signals from the abdominal chord of the American cockroach, *Periplaneta americana*. The cercal nerve was stimulated with a suction electrode and action potentials were also monitored by an extracellular electrode. In agreement with Yagodin *et al.*, when we used intact (non-desheathed) preparations, none of the 12 different dyes we tried penetrated the sheath and no signals were detected.

However, when the nerve cord was partially desheathed and then incubated in dye solution for 30 minutes, the axons appeared to be stained. Two oxonol dyes, RH479 and RH482, provided by Rina Hildesheim and Amiram Grinvald, gave absorption signals when the cercal nerve was stimulated. These signals could be detected in a single trial. We think these signals are real because if the stimulus intensity was reduced or the polarity reversed, the signal disappeared. The signal also disappeared if a wavelength which was not absorbed by the dye was used.

When we reduced the stimulus intensity so that there was only one all-or-none event on the electrical recording, we could not detect an optical signal. Thus the signal was not large enough to detect a single action potential from a single axon. With the stimulation paradigm and recording arrangement we used, only axons which receive excitatory synaptic connections from the cercal sensory fibers in the 6th abdominal ganglion, and ascend across the 5th abdominal ganglion would be detected. Furthermore, the stimulus was less than maximal. Thus we think that only a relatively small fraction of the axons in the cord generated the signals which we detected.

Supported by PHS grant NS08437.

Optical recording of membrane potential changes from single neurons with intracellular dyes. CHUN XIAO (Yale University) AND DEJAN ZECEVIC.

We investigated the absorption and fluorescence optical signals from individual neurons from the suboesophageal ganglion of *Helix aspersa* and the segmental ganglion of *Hirudo medicinalis* selectively stained by intracellular application of voltage sensitive dyes. We looked for optical signals that are large enough to allow the analyses of regional properties of neurons in the intact isolated ganglia.

The preparation was positioned on the microscope stage and its image was formed by 25×, 0.4 NA long working distance objective. In the plane of the magnified image we positioned the 12 × 12 array of photodiodes for multi-site recording of transmitted or fluorescence light intensity changes that correspond to changes in membrane potential.

In absorption measurements, negatively charged oxonol dye (JPW 1034) gave largest signals when applied from outside in both *Helix* and *Hirudo*. No signal occurred when dye was injected into the neurons. Photodynamic damage with this dye was relatively pronounced in leech neurons where it prevented extensive averaging. Fluorescence optical signals from intracellularly stained *Helix* neurons were obtained using positively charged styryl dyes RH461 and RH437. With RH437 we recorded absorption signals but the signal-to-noise ratio was not as good as in fluorescence. Improvement in dye structure, staining protocol, and measuring technology is needed to increase the resolution in order to record optically from dissociated neurons in culture and to record from individual cells in intact ganglia.

We are grateful to L. B. Cohen, B. Salzberg, and A. L. Obaid for valuable discussion. Supported by NIH grant NS-08437.

CONTENTS

Volume 175 Number 3

THE BIOLOGICAL BULLETIN

DECEMBER, 1988

Published by the Marine Biological Laboratory

THE BIOLOGICAL BULLETIN

PUBLISHED BY
THE MARINE BIOLOGICAL LABORATORY

DECEMBER, 1988

Printed and Issued by
LANCASTER PRESS, Inc.
PRINCE & LEMON STS.
LANCASTER, PA

THE BIOLOGICAL BULLETIN

THE BIOLOGICAL BULLETIN is published six times a year by the Marine Biological Laboratory, MBL Street, Woods Hole, Massachusetts 02543.

Subscriptions and similar matter should be addressed to THE BIOLOGICAL BULLETIN, Marine Biological Laboratory, Woods Hole, Massachusetts. Single numbers, $20.00. Subscription per volume (three issues), $50.00 ($10.00 per year for six issues).

Communications relative to manuscripts should be sent to Dr. Charles B. Metz, Editor, or Pamela Clapp, Associate Editor, at the Marine Biological Laboratory, Woods Hole, Massachusetts 02543.

POSTMASTER: Send address changes to THE BIOLOGICAL BULLETIN, Marine Biological Laboratory, Woods Hole, MA 02543.

Second-class postage paid at Woods Hole, MA, and additional mailing offices.
ISSN 0006-3185

INSTRUCTIONS TO AUTHORS

The Biological Bulletin accepts outstanding original research reports of general interest to biologists throughout the world. Papers are usually of intermediate length (10–40 manuscript pages). Very short papers (less than 10 manuscript pages including tables, figures, and bibliography) will be published in a separate section entitled "Short Reports." A limited number of solicited review papers may be accepted after formal review. A paper will usually appear within four months after its acceptance.

The Editorial Board requests that manuscripts conform to the requirements set below; those manuscripts which do not conform will be returned to authors for correction before review.

1. ***Manuscripts.*** Manuscripts, including figures, should be submitted in triplicate. (Xerox copies of photographs are not acceptable for review purposes.) The original manuscript must be typed in double spacing (*including* figure legends, footnotes, bibliography, etc.) on one side of 16- or 20-lb. bond paper, 8½ by 11 inches. Manuscripts should be proofread carefully and errors corrected legibly in black ink. Pages should be numbered consecutively. Margins on all sides should be at least 1 inch (2.5 cm). Manuscripts should conform to the *Council of Biology Editors Style Manual*, 4th Edition (Council of Biology Editors, 1978) and to American spelling. Unusual abbreviations should be kept to a minimum and should be spelled out on first reference as well as defined in a footnote on the title page. Manuscripts should be divided into the following components: Title page, Abstract (of no more than 200 words), Introduction, Materials and Methods, Results, Discussion, Acknowledgments, Literature Cited, Tables, and Figure Legends. In addition, authors should supply a list of words and phrases under which the article should be indexed.

2. ***Figures.*** The dimensions of the printed page, 7 by 9 inches, should be kept in mind in preparing figures for publication. We recommend that figures be about 1½ times the linear dimensions of the final publication desired, and that the ratio of the largest to the smallest letter or number and of the thickest to the thinnest line not exceed 1:5. Explanatory matter generally should be included in legends, although axes should always be identified on the illustration itself. Figures should be prepared for reproduction as either line cuts or halftones. Figures to be reproduced as line cuts should be unmounted glossy photographic reproductions or drawn in black ink on white paper, good-quality tracing cloth or plastic, or blue-lined coordinate paper. Those to be reproduced as halftones should be mounted on board, with both designating numbers or letters and scale bars affixed directly to the figures. All figures should be numbered in consecutive order, with no distinction between text and plate figures. The author's name and an arrow indicating orientation should appear on the reverse side of all figures.

3. ***Tables, footnotes, figure legends, etc.*** Authors should follow the style in a recent issue of *The Biological Bulletin* in preparing table headings, figure legends, and the like. Because of the high cost of setting tabular material in type, authors are asked to limit such material as much as possible. Tables, with their headings and footnotes, should be typed on separate sheets, numbered with consecutive Roman numerals, and placed after the Literature Cited. Figure legends should contain enough information to make the figure intelligible separate from the text. Legends should be typed double spaced, with consecutive Arabic numbers, on a separate sheet at the end of the paper. Footnotes should be limited to authors' current addresses, acknowledgments or contribution numbers, and explanation of unusual abbreviations. All such footnotes should appear on the title page. Footnotes are not normally permitted in the body of the text.

4. ***A condensed title*** or running head of no more than 35 letters and spaces should appear at the top of the title page.

5. ***Literature cited.*** In the text, literature should be cited by the Harvard system, with papers by more than two authors cited as Jones *et al.*, 1980. Personal communications and material in preparation or in press should be cited in the text only, with author's initials and institutions, unless the material has been formally accepted and a volume number can be supplied. The list of references following the text should be headed LITERATURE CITED, and must be typed double spaced on separate pages, conforming in punctuation and arrangement to the style of recent issues of *The Biological Bulletin*. Citations should include complete titles and inclusive pagination. Journal abbreviations should normally follow those of the U. S. A.

Standards Institute (USASI), as adopted by BIOLOGICAL ABSTRACTS and CHEMICAL ABSTRACTS, with the minor differences set out below. The most generally useful list of biological journal titles is that published each year by BIOLOGICAL ABSTRACTS (BIOSIS List of Serials; the most recent issue). Foreign authors, and others who are accustomed to using THE WORLD LIST OF SCIENTIFIC PERIODICALS, may find a booklet published by the Biological Council of the U.K. (obtainable from the Institute of Biology, 41 Queen's Gate, London, S.W.7, England, U.K.) useful, since it sets out the WORLD LIST abbreviations for most biological journals with notes of the USASI abbreviations where these differ. CHEMICAL ABSTRACTS publishes quarterly supplements of additional abbreviations. The following points of reference style for THE BIOLOGICAL BULLETIN differ from USASI (or modified WORLD LIST) usage:

A. Journal abbreviations, and book titles, all underlined (for *italics*)

B. All components of abbreviations with initial capitals (not as European usage in WORLD LIST *e.g. J. Cell Comp. Physiol.* NOT *J. cell. comp. Physiol.*)

C. *All* abbreviated components must be followed by a period, whole word components *must not* (*i.e. J. Cancer Res.*)

D. Space between all components (*e.g. J. Cell. Comp. Physiol.*, not *J.Cell.Comp.Physiol.*)

E. Unusual words in journal titles should be spelled out in full, rather than employing new abbreviations invented by the author. For example, use *Rit Vísindafjélags Islendinga* without abbreviation.

F. All single word journal titles in full (*e.g. Veliger, Ecology, Brain*).

G. The order of abbreviated components should be the same as the word order of the complete title (*i.e. Proc.* and *Trans.* placed where they appear, not transposed as in some BIOLOGICAL ABSTRACTS listings).

H. A few well-known international journals in their preferred forms rather than WORLD LIST or USASI usage (*e.g. Nature, Science, Evolution* NOT *Nature, Lond., Science, N.Y.; Evolution, Lancaster, Pa.*)

6. ***Reprints, charges.*** Authors will be charged the excess over $100 of the total of (a) $30 for each printed page beyond 15, (b) $30 for each table, (c) $15 for each formula more complex than a single line with simple subscripts or superscripts, and (d) $15 for each figure, with figures on a single plate all considered one figure and parts of a single figure on separate sheets considered separate figures. Reprints may be ordered at time of publication and normally will be delivered about two to three months after the issue date. Authors (or delegates for foreign authors) will receive page proofs of articles shortly before publication. They will be charged the current cost of printers' time for corrections to these (other than corrections of printers' or editors' errors).

CONTENTS

No. 1, August 1988

No. 2, October 1988

ECOLOGY AND EVOLUTION

GENERAL BIOLOGY

PHYSIOLOGY

ABSTRACTS

No. 3, December 1988

DEVELOPMENT AND REPRODUCTION

ECOLOGY AND EVOLUTION

PHYSIOLOGY

SHORT REPORTS

ABSTRACTS

Reference: *Biol. Bull.* **175**: 321–331. (December, 1988)

Regulation of Vitellogenesis in the Fiddler Crab, *Uca pugilator*

L. SCOTT QUACKENBUSH* AND L. L. KEELEY

Laboratories for Invertebrate Neuroendocrine Research, Department of Entomology, Texas A&M University, Texas Agricultural Experiment Station, College Station, Texas, 77843

Abstract. Protein synthesis was measured in ovary and hepatopancreas of intact and eyestalk-ablated fiddler crabs (*Uca pugilator*) *in vitro*. A crude extract of eyestalks from the shrimp *Penaeus setiferus* inhibited ovarian weight gain in eyestalk-ablated crabs. This crude eyestalk extract also inhibited *in vitro* protein synthesis in ovaries from intact and eyestalk-ablated crabs. A polyclonal antibody to crab vitellogenin was used to measure vitellogenin synthesis in ovaries, hepatopancreas, and hemolymph *in vitro*. Gonad-inhibiting hormone was partially purified from the crude eyestalk extract. The partially purified material inhibited vitellogenin synthesis in ovarian tissues *in vitro*.

Introduction

Panouse (1943) first observed accelerated gonadal growth in eyestalk-ablated shrimp, *Palaemon serratus*. Eyestalk ablation induces precocious gonadal development in almost all crustaceans (Charniaux-Cotton, 1985; Quackenbush, 1986; Fingerman, 1987). The endocrine nature of this response was confirmed by the implantation of sinus glands into eyestalk-ablated fiddler crabs (*Uca pugilator*). The implanted neurohemal organs suppressed gonadal development in eyestalk-ablated crabs (Brown and Jones, 1948). The rapid ovarian development that occurs after eyestalk ablation was attributed to the absence of a gonad-inhibiting hormone (GIH). The chemical characteristics of partially purified GIH resembles other peptide hormones produced in the eyestalk neurosecretory system (Charniaux-Cotton, 1985). GIH has not yet been fully characterized due in part to the difficulty in the bioassay of an inhibitory hormone (Channing *et al.*, 1985).

The ovaries and testes were accepted as the target tissues of GIH because they both develop rapidly after eyestalk ablation. Crude eyestalk extracts directly inhibit ovarian protein synthesis when tested *in vitro* (Gorell and Gilbert, 1971; Eastman-Reks and Fingerman, 1984). These reports confirmed that the eyestalk neuroendocrine system can directly suppress gonadal development in crustaceans. The primary product of ovarian protein synthesis is the egg yolk protein vitellin (Vn) (Eastman-Reks and Fingerman, 1984; Lui and O'Connor, 1976). However, it was generally accepted that the precursor to Vn, vitellogenin (Vg) was made in extra-ovarian tissues in crustaceans (Wallace *et al.*, 1967; Fielder *et al.*, 1971; Charniaux-Cotton, 1985). The demonstration that isolated ovaries synthesized Vg challenged the significance of extra-ovarian Vg synthesis (Lui and O'Connor, 1977). Both the hemocytes of the hemolymph and the hepatopancreas of crustaceans are capable of Vg synthesis and therefore also targets for GIH (Kerr, 1969; Souty and Picaud, 1984). The crustacean hepatopancreas synthesizes digestive enzymes and hemocyanin and may also produce Vg (Gibson and Barker, 1979; Senkbeil and Wriston, 1981; Paulus and Laufer, 1987; Tom *et al.*, 1987). An understanding of the relative contributions by the potential tissue sources of Vg is important to the development of a valid GIH bioassay.

This study was undertaken to determine if the hepatopancreas, hemolymph, and the ovaries of the fiddler crab (*Uca pugilator*) produced Vg. *In vitro* production of Vg was then used as a specific bioassay for the characterization and purification of GIH.

Received 17 November 1986; accepted 19 August 1988.

* Present Address: Department of Biological Sciences, Florida International University, Miami, Florida, 33199.

Abbreviations: ESE, eyestalk equivalents; GIH, gonad inhibiting hormone; HEPES, N-2-Hydroxyethylpiperazine-N-2-ethane sulfonic acid; IgG, immunoglobulin; mOS, milliosmoles; PBS, phosphate buffered saline; Rf, retention factor; Vg, vitellogenin; Vn, vitellin.

Materials and Methods

Animals

Fiddler crabs (*...ator*) were purchased monthly from Gulf Spe... (Panacea, Florida). Crabs were maintained in a recirculating seawater aquarium (25‰; 24°C) and fed daily with oatmeal. Crabs were eyestalk-ablated with fine scissors; the cut stumps were cauterized. To obtain ovaries with uniform oocyte diameters, the ovaries were dissected from crabs 8 days after eyestalk ablation. The average oocyte diameters from these animals were quite consistent (0.125 ± 0.001 mm; n = 60). The oocyte diameters of eggs just released and attached to pleopods of female crabs were 0.25 ± 0.01 mm (n = 90). Based on their size, the oocytes of crabs 8 days after eyestalk ablation were about halfway through secondary vitellogenesis. The ovaries from these ablated crabs were a characteristic deep purple color of vitellogenic fiddler crab eggs (Brown and Jones, 1948; Webb, 1977; Eastman-Reks and Fingerman, 1984). For all subsequent assays, ovaries were obtained from crabs 8 days after eyestalk ablation. Eyestalk-intact crabs provided ovarian tissues for controls, and the oocyte diameters from these animals were also recorded.

Eyestalk extract

Eyestalks from adult (>30 g) male and female *Penaeus setiferus* were obtained frozen from a commercial shrimp processor (Coastal Freezing, Port Aransas, Texas). One hundred eyestalks (22.25 g) were ground frozen in a mortar and pestle and extracted in distilled water. The extract was gently boiled for 5 min and then centrifuged at 10,000 × *g* for 30 min at 4°C. The supernatant (2 eyestalk equivalents/ml) was stored frozen at −4°C.

In vivo *GIH bioassay*

Crabs from the stock tank were eyestalk-ablated as described. One group (n = 10) had their ovaries removed and were weighed to the nearest 0.1 mg at the start of the experiment. Five other groups (all n = 10) were injected on alternate days for 15 days as described by Quackenbush and Herrnkind (1983). Four different doses of crude eyestalk ...tract and a saline control were tested for effects on ... weight gain after eyestalk ablation (Cooke *et al.*, 19...

In vivo *^{14}C leucine u... ...rom*

^{14}C leucine (270 μCi/m... ICN Radiochemicals, Irvine, California) was diluted ... old leucine (0.127 *M*) to achieve a final dose of leucin... 5 nmole/0.5 μCi/10 μl. Both intact and eyestalk-ablated crabs were injected with 10 μl of the stock ^{14}C leucine (5 nmole/0.5 μCi/10 μl) and held in dry containers after injection. Four hours or 24 hours after ^{14}C leucine injection a sample of hemolymph (50 μl) was removed from the crabs (n = 10; 2 replicates) and then added to small tubes containing 450 μl of extraction buffer (0.5 *M* NaCl; 0.5 *M* Tris; 5 mM EDTA; pH 7.0, Lui and O'Connor, 1976). The ovaries and the hepatopancreas from the crabs were then removed and separately homogenized in extraction buffer (n = 10; 2 replicates). Proteins from these extracts and the hemolymph samples were precipitated by the addition of three volumes of ice cold 100% $(NH_4)_2SO_4$, followed by centrifugation at 8000 × *g* for 5 min at 4°C. The resulting pellet of protein was resuspended and precipitated as described above twice more. The final pellets of protein were dissolved in phosphate-buffered saline (PBS, Quackenbush and Fingerman, 1985). Aliquots (100 μl) of the solubilized proteins were counted for ^{14}C leucine incorporation with a commercial scintillation fluor using liquid scintillation spectrometry. Counts per minute (CPM) were converted to disintegrations per minute (DPM) via an internally stored quench curve. Total protein of these samples was measured using the Bio-Rad Protein Reagent assay (Bio-Rad, Richmond, California) Bovine serum albumin (1 mg/ml) was used as a standard. Results from this assay are expressed as DPM/mg protein based on these determinations. Differences between treatment groups were tested using a standard *t*-test (Sokal and Rohlf, 1969).

In vitro *^{14}C leucine incorporation*

Tissues (ovary, hepatopancreas, or muscle) were removed from crabs by dissection under chilled saline. Tissue fragments (3–6 mm) were rinsed with saline and placed into a tissue culture media (n = 12; 2 replicates) (Reddy and Wyatt, 1967). The culture media consisted of amino acids, 0.066 *M* glucose, 0.033 *M* trehalose, 5 m*M* HEPES, and 0.001% ampicillin in crustacean saline (pH 8.2; 1100 mOS, Cooke *et al.*, 1977). Prior to use the media was filter sterilized (Nalgene, 20 μ filter). Eyestalk extracts (100 μl) or muscle extracts (100 μl) were added to the incubation media (2000 μl) that contained the crab tissue fragments. Finally, ^{14}C leucine (5 nmole/0.5 μCi/10 μl) was added to the incubation media. Beakers containing the media and tissue fragments were placed in a sealed chamber that was gassed with 95% O_2/5% CO_2 at 4 psi. During a 4-h incubation at 30°C, the beakers were gently agitated on an orbital shaker. At the termination of the incubation, tissues were removed from the media, rinsed with chilled saline, and then homogenized in ice cold extraction buffer. The tissue homogenates were centrifuged at 8000 × *g* for 15 min at 4°C. Proteins in the supernatant were precipitated by the addition of 3 vol-

umes of ice cold 100% $(NH_4)_2SO_4$ and then recentrifuged at 8000 × *g* for 15 minutes at 4°C. The pellet of protein was resuspended in extraction buffer, and the entire precipitation procedure was repeated twice more. The final pellet of protein was resuspended in PBS. Aliquots (100 μl) of the solubilized proteins were taken for the determination of both total protein and total ^{14}C leucine incorporation as described above. Differences between treatment groups were tested using a *t*-test (Sokal and Rohlf, 1969).

Time course of in vitro *^{14}C leucine incorporation*

Tissues were dissected (n = 12; 2 replicates) and incubated for 2, 4, 8, 16, or 22 hours as described above. At the termination of incubation, the tissues were rinsed with chilled crustacean saline, homogenized in 0.4 *N* perchloric acid and centrifuged at 2000 × *g* for 10 minutes at 22°C. The resulting pellet of protein was resuspended in 90% ethanol/1% sodium acetate and centrifuged as above. The resulting pellet of protein was retained and extracted in chloroform:methanol (2:1) and centrifuged as above. The final pellet of protein was air dried at 50°C and then dissolved in 1 *N* NaOH. Aliquots (100 μl) of the solubilized proteins were taken for total protein determination and total ^{14}C leucine incorporation as described above. Bovine serum albumin in 1 *N* NaOH served as the standard for the protein determinations. Differences between groups were tested with a *t*-test (Sokal and Rohlf, 1969).

Vn purification and antibody production

Uca pugilator vitellogenin was characterized as a large purple lipoprotein with two subunits of 100,600 and 125,000 daltons. This protein was about 90% of the total protein in crab ovaries (Eastman-Reks and Fingerman, 1984). We used a slight modification of the Eastman-Reks and Fingerman (1984) method to isolate vitellogenin from *Uca pugilator*. Ovaries from crabs (0.10 to 0.25 mm oocyte diameter) were pooled and homogenized in ice cold extraction buffer. Phenylmethonyl sulfonyl flouride (0.001%) was added to the extraction buffer just before use to inhibit general proteases. Ovarian proteins were extracted as above using 3 cycles of extraction buffer and ice cold 100% $(NH_4)_2SO_4$ precipitation. The final protein pellet was resuspended in PBS (2 mg/ml) and applied to a Sephadex G-200 column (2.5 cm × 20 cm; void volume = 18 ml with blue dextran). The protein extract retained the purple color characteristic of the crab ovaries and eggs. This characteristic color aided us in the purification procedure. The column was eluted with PBS (4 ml/h) at 4°C, 1-ml fractions were collected. Column fractions were monitored at 280 nm, and fractions with the characteristic purple color of crab ovaries were pooled and dried on a rotary evaporator (Speed-Vac, Savant Instruments, Hicksville, New York). Samples of this crude ovarian protein extract were characterized on 7% polyacrylamide gels. Sodium dodecyl sulfate was added to the protein sample and the polyacrylamide to dissassociate the large proteins into subunits (Hames and Rickwood, 1981). The crude extract was dominated by 2 bands of protein in the size range of vitellogenin characterized by Eastman-Reks and Fingerman, 1984. A preparative gel procedure was used to purify enough of the crude material from crab ovaries for rabbit immunization. Ovarian protein samples from the G-200 column were resuspended in a dissassociating buffer with sodium dodecyl sulfate. This was applied to a large preparative gel of 7% polyacrylamide (1.0 × 150 × 130 mm) in a single well which spanned the entire width of the gel (Hames and Rickwood, 1981, Laemmli, 1970). After the tracking dye eluted from the gel, a single vertical slice of the gel was removed and stained for proteins with 0.5% Coomassie Blue to determine mobilities of the proteins within the preparative gel. The remainder of the preparative gel was sliced horizontally (1-mm segments); the resulting gel segments were placed in an elution buffer of 0.05 m*M* ammonium acetate. Proteins were eluted from the gels into the buffer at 4°C for 24 hours. Proteins that eluted from the gels were freeze dried and stored at −4°C. Samples of the proteins eluted from the gel segments were characterized on another analytical 7% polyacrylamide gel with sodium dodecyl sulfate buffers. This procedure allowed us to obtain sufficient quantities of partially purified Vg for immunization procedures. The molecular weight of the Vg subunits were determined by comparison to standards simultaneously separated in analytical polyacrylamide gels of various percentages. Molecular weight standards were obtained from Bio Rad and used according to the instructions provided. Myosin (200,000), beta-galactosidase (116,250), phosphorylase-B (97,400), bovine serum albumin (66,200), and ovalbumin (42,699) were the protein standards used to calibrate the subunit molecular weight of ovarian proteins.

Serum was obtained from rabbits before immunization via ear vein puncture. Rabbits were immunized with 50 subepidermal injections (20 μl each) of complete adjuvant containing 40 μg egg yolk protein/ml as described previously (Quackenbush and Fingerman, 1985). Rabbits were bled each week via cardiac puncture. Whole blood was allowed to clot then centrifuged at 10,000 × *g* for 30 minutes at 4°C. The supernatant serum was stored at −72°C. Serum was screened against partially purified egg yolk proteins using Ouchterlony plates (Ouchterlony, 1949). Serum showing a precipitation line against partially purified egg yolk proteins was further purified. Positive serum was passed through a column of DEAE-Affi-Gel-Blue (Bio-Rad) to separate the IgG fraction

from other serum components. A column (14 ml bed volume) was prepared and used following methods described in Bio Rad Instruction 1062 (Bio Rad). Fractions containing IgG were pooled, aliquoted (0.5 mg/ml), and dried on a rotary evaporator. The antibody stocks were diluted with PBS containing 0.01% sodium azide for use in the assays.

Antibody characterization

Rabbits were immunized with either the high molecular weight Vg subunit (V_1) or the low molecular weight subunit (V_2). Since the hepatopancreas samples contained only V_2, only the antibodies against V_2 were characterized. Antibody characterization included Ouchterlony plates, immunoprecipitation, and western blotting. Extracts in PBS of gonad (100 μg/ml), hepatopancreas (110 μg/ml), and hemolymph (110 μg/ml) from both male and female crabs were tested against the antibody in Ouchterlony plates (1% agar in PBS). Extracts of gonad, hepatopancreas, and hemolymph (100 μg/300 μl) were incubated at 4°C for 18 hours with 10 μl of rabbit serum. The mixtures were then centrifuged at 8,000 × *g* at 4°C for 10 min and the resulting protein pellets washed with ice cold PBS 4 times. Pellets of immunoprecipitated protein were solubilized in electrophoresis buffer containing sodium dodecyl sulfate and separated on a 7% polyacrylamide gel. This assay should recover the proteins that the antibody recognizes and precipitated from the crude extracts containing several different proteins. Extracts of gonads and hepatopancreas from females in vitellogenesis were separated on a 7% polyacrylamide gel in sodium dodecyl sulfate. The gel was then electroblotted onto nitrocellulose paper (Towbin *et al.*, 1979; Douglas and King, 1984). The rabbit serum was incubated with the filter paper blots for 2 h in PBS. A goat anti-rabbit IgG antibody with peroxidase conjugated to the antibody was then incubated with the blots in PBS (Kirkegaard and Perry, Gaithersburg, Maryland). The blots were then stained with 4-chloro-1-napthol (Sigma Chemical Co, St. Louis, Missouri) and H_2O_2. This western blotting procedure was used to determine if the rabbit serum bound selectively to the V_2 proteins contained in these extracts, when it was challenged with all the different proteins in the crude extracts.

Immunoassay

The immunoassay consisted of a 4-h *in vitro* incubation as described above. Tissues were then homogenized in extraction buffer. Proteins were extracted with 3 cycles of extraction buffer and ice cold 100% $(NH_4)_2SO_4$. The final protein pellet was resuspended in 600 μl of PBS. Aliquots (100 μl) were taken from this solution for determination of total protein and ^{14}C leucine incorporation. Fifty μl of the rabbit serum (25 μg protein) was added to the remaining 400 μl of each tissue homogenate and the mixture was incubated at 4°C for 18 hours. After incubation, the tissue homogenates were centrifuged at 8000 × *g* at 4°C for 15 minutes. The supernatant was carefully removed, and 100 μl aliquots were taken for determination of total protein and ^{14}C leucine incorporation. The pellet of immunoprecipitated protein was washed four times with ice cold PBS. The final protein pellet was solubilized in 500 μl of 1 *N* NaOH, and aliquots of 100 μl were taken for determination of total protein and ^{14}C leucine incorporation. Differences between treatment groups were tested for significance with a *t*-test (Sokal and Rohlf, 1969).

GIH purification

Samples of crude *P. setiferus* eyestalks (3000 μl) were applied to a Sephadex G-25 column (2.5 cm × 20 cm; 43 ml void volume determined with blue dextran) and eluted in 0.05 m*M* ammonium acetate, pH 6.3 at 3.0 ml/h. Fractions (1 ml) were monitored at 280 nm, collected, and then bioassayed for their ability to effect Vg synthesis *in vitro*. The retention factor, Rf, was calculated based on the formula: column void volume/fraction elution volume. Standard peptides (1 mg/ml) were used to calibrate the column for size estimation. Standard peptides used were: aprotinin, 6500 daltons; insulin (beta subunit), 3496 daltons; and met-enkephalin, 537 daltons. The effect of crude eyestalk extract or partially purified GIH was quantified in all *in vitro* assays using the formula:

$$\% \text{ Inhibition} = \frac{\text{Control DPM/mg} - \text{Test DPM/mg}}{\text{Control DPM/mg}} \times 100$$

A unit of GIH activity was defined as that amount of protein that produced a 20% inhibition of ^{14}C leucine incorporation *in vitro*. Based on a *t*-test for percentages, a 20% inhibition was statistically significant at $P < 0.05$ (Sokal and Rohlf, 1969). Using these calculations, a single shrimp eyestalk had about 160 units of activity.

Results

In vivo *studies*

Crude extracts of *P. setiferus* eyestalks blocked the anticipated increase in ovarian weight gain of eyestalk ablated crabs (Fig. 1). This was attributed to the blockade of vitellogenesis. The shrimp eyestalk extract blocked vitellogenesis even though the remainder of the crab's endocrine system was intact. The extract was potent, only 0.0005 eyestalk equivalents was required to produce a

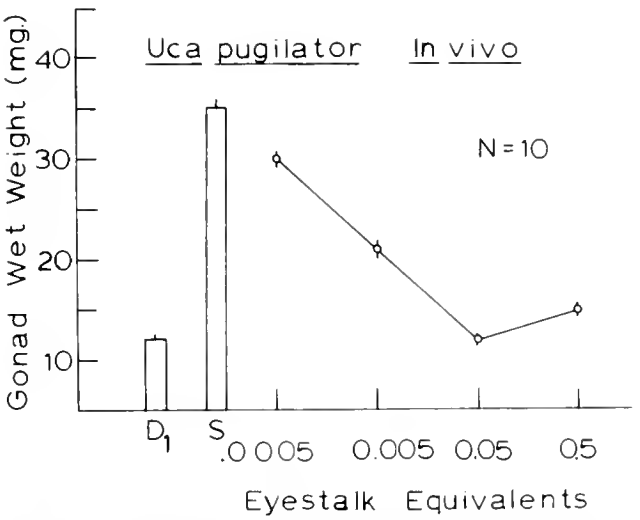

Figure 1. *In vivo* effects of crude shrimp eyestalk extract on ovarian growth of eyestalk ablated *Uca pugilator*. Extract dose was given in eyestalk equivalents, ovary wet weight was measured in milligrams. S = ovarian weight of crab injected with saline, D_1 = average ovarian wet weight for a group of crabs from which experimental crabs were selected at the start of the experiment. All values are the mean ± one standard error, n = 10, two replicates.

statistically significant inhibition of ovarian weight gain (*t*-test, $P < 0.05$).

The *in vivo* incorporation of ^{14}C leucine into proteins from the hepatopancreas, hemolymph, and ovaries was significantly higher in eyestalk-ablated crabs than intact crabs after 4 h (*t*-test, $P < 0.05$; Fig. 2). The average oocyte diameter of ovaries from eyestalk-ablated crabs (0.12 ± 0.01 mm) was twice the average oocyte diameter of ovaries in intact crabs (0.06 ± 0.01 mm). This may account for the significant differences in the incorporation of ^{14}C leucine, since the two groups of crabs had ovaries at different stages of vitellogenesis. Twenty-four hours after injection with ^{14}C leucine, incorporation of the labeled amino acid was about equal in the tissues from both intact and eyestalk-ablated crabs. Tissues from intact crabs had a significant increase in incorporation of labeled amino acid when incorporation time was increased from 4 to 24 hours (*t*-test, $P < 0.05$). The hepatopancreas and ovaries incorporated more labeled amino acid into proteins than the hemolymph in both groups of crabs.

In vitro *studies*

The time course of *in vitro* ^{14}C leucine incorporation was measured for muscle, hepatopancreas, and ovaries from intact and ablated crabs (Fig. 3). Incorporation of the labeled amino acid into muscle proteins was a control for non-specific binding of label and for the incorporation of label into proteins by a tissue that does not contain egg yolk proteins. There was a significant difference in the amount of label incorporated by ovary and hepatopancreas from intact crabs compared to these tissues from eyestalk-ablated crabs. The difference between the two groups was statistically significant at all measurements (*t*-test, $P < 0.01$–0.05). Initially, the ^{14}C leucine incorporation into proteins was about equal in the ovary and hepatopancreas from eyestalk ablated crabs. After 8 hours of incubation, the ovarian tissue continued to incorporate labeled amino acid into proteins; the hepatopancreas tissues did not increase their incorporation of labeled amino acid into proteins. The ovaries and hepatopancreas from intact crabs had about equal incorporation of labeled amino acid into proteins at 2 h and 8 h, though they had statistically different levels of incorporation of labeled amino acid into protein at 4 h (*t*-test, $P < 0.05$ at 4 h). After 8 h in the *in vitro* incubation, the tissues from the intact crabs followed the same pattern as the tissues from the eyestalk ablated crabs: the ovaries continued to incorporate label but the hepatopancreas did not increase incorporation of label. Variability in ^{14}C leucine incorporation into proteins increased with increased incubation times, as demonstrated by the increase in the standard deviations of these measurements (Fig. 3). This observation suggested that after 8 h of *in vitro* incubation the tissues were no longer uniformly active, and the assay would not produce an accurate pic-

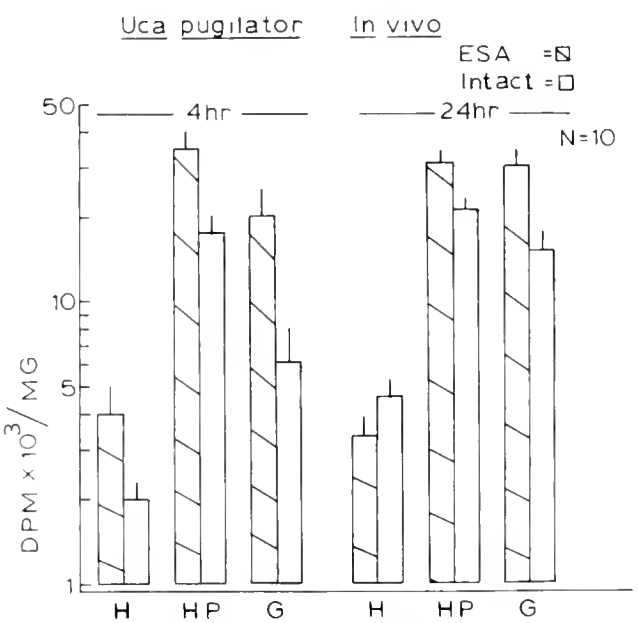

Figure 2. *In vivo* incorporation of ^{14}C leucine into proteins from the hemolymph (H), the hepatopancreas (HP), and ovary (G) of either intact (open bars) of eyestalk ablated (hatched bars) *Uca pugilator*. All values are the mean ± one standard error, n = 10 for each group, 2 replicates.

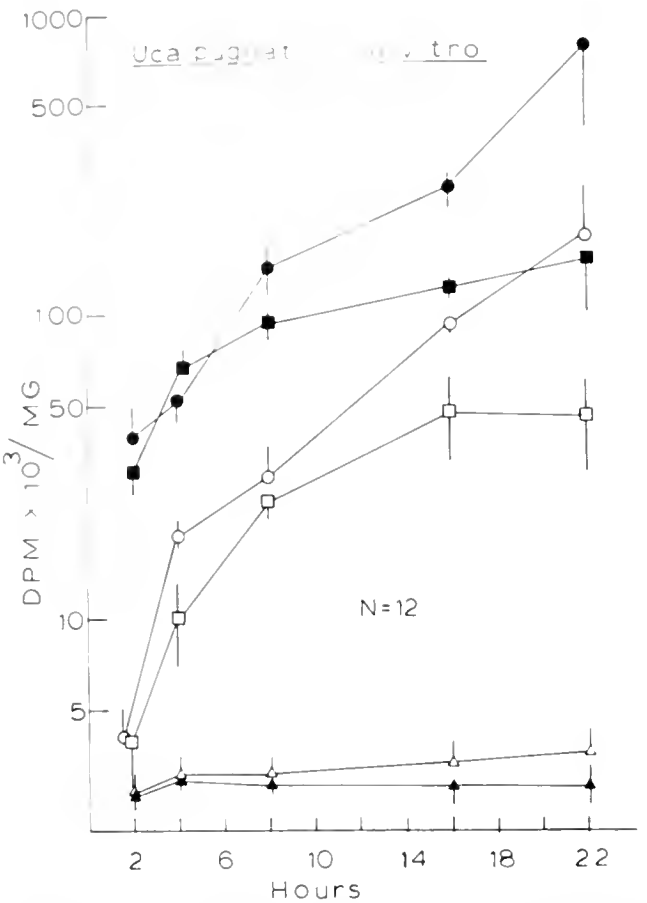

Figure 3. Time course of incorporation of ^{14}C leucine into proteins from muscle (triangles), ovaries (circles), and hepatopancreas (squares) from either intact crabs (open symbols) or eyestalk-ablated crabs (filled symbols) measured *in vitro*. All values are means ± one standard error, n = 12 for each group, 2 replicates.

ture of protein synthesis. A 4-h incubation time was used for all subsequent assays.

Crude shrimp eyestalk extracts were tested for their ability to affect *in vitro* protein synthesis in the ovaries from intact and eyestalk-ablated crabs (Fig. 4). The threshold for statistically significant inhibition of protein synthesis was the same regardless of the origin of the ovarian tissues (0.006 ESE, *t*-test for two percentages, $P < 0.05$). Maximum inhibition of the protein synthesis was produced by 0.05 ESE in ovaries from eyestalk ablated crabs. Protein synthesis in ovaries from intact crabs was maximally inhibited by 0.012 ESE. Ovaries from the intact crabs were more sensitive to the eyestalk extract than ovaries from ablated crabs. A dose of 0.012 ESE produced a significant greater inhibition in the ovaries from intact crabs than it did in the ovaries from eyestalk ablated crabs (*t*-test for two percentages, $P < 0.05$). The highest dose tested, 0.05 ESE, produced less, not more, inhibition of protein synthesis than a lower dose. This suggests that the crude extract probably contains many factors, perhaps even a factor that can increase protein synthesis *in vitro* (Charniaux-Cotton, 1985).

Vitellogenin purification and antibody characterization

The partially purified extract of ovaries from *Uca pugilator* was dominated by the two distinct bands of protein characteristic of the egg yolk proteins (Eastman-Reks and Fingerman, 1984; Fig. 5A, B). The molecular weights of the two groups of egg yolk proteins were 103,000 ± 1000 daltons, V_1, and 81,000 ± 1000 daltons, V_2 (n = 12 measurements, Fig. 5A, B). These bands of protein in the polyacrylamide gels clearly represent two classes of proteins, which each may contain several yet unresolved distinct polypeptides. The hepatopancreas extracts contained only the V_2 group of egg yolk proteins (n = 8; Fig. 5A, B). Both V_1 and V_2 are the dominant proteins of the egg yolk, they stain positive for both lipid and sugars, and they contain the purple pigment of the egg yolk. Thus, these proteins, V_1 and V_2 fulfill the criteria established for vitellogenin (Eastman-Reks and Fingerman, 1984; Wallace *et al.*, 1967).

The antiserum (#1790-12-4) to the V_2 protein group

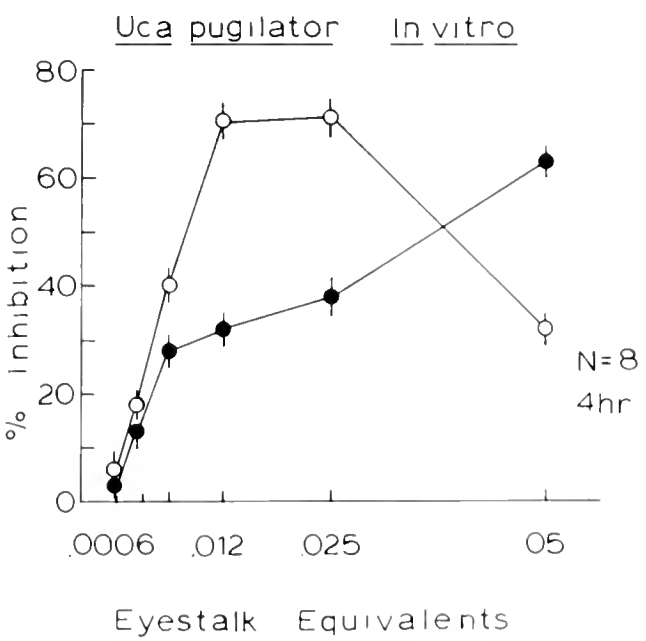

Figure 4. The *in vitro* inhibition of incorporation of ^{14}C leucine into ovarian proteins by crude shrimp eyestalk extract. Ovarian tissues from intact crabs (open circles) or eyestalk ablated crabs (filled circles) were tested. All values are means ± one standard error, n = 8 for each group, 2 replicates. An extract of shrimp tail muscle was used for a control for eyestalk extracts. Control injections were adjusted by dilution with crab saline to equal the total protein concentration of the injections of eyestalk extract. Percent inhibition was calculated as described in Materials and Methods.

reacted with crude extracts from female crab gonads, hepatopancreas, and hemolymph in Ouchterlony plates. The antiserum did not produce any reaction with similar extracts of tissue from male crabs. Therefore the antiserum was specific for female proteins (data not shown). The antiserum precipitated both V_1 and V_2 proteins from ovary extracts, but only V_2 proteins from hepatopancreas extracts (Fig. 5A). Thus when the antiserum was presented with crude tissue extracts containing many different proteins and some breakdown products of large proteins, the antiserum only precipitated the V_1 and V_2 proteins. The western blot of proteins from crude tissue extracts showed that the antiserum selectively bound to only the V_2 proteins in the hepatopancreas (Fig. 5C). The antiserum did bind to some low molecular weight proteins other than V_2 in the ovarian homogenate. The antiserum had low affinity for any of the other proteins known to be in these crude extracts (Fig. 5A–C). Thus this antiserum (#1790-12-4) was specific to female proteins, and relatively specific for V_1 and V_2 proteins from tissue extracts. The immunoprecipitation of both V_1 and V_2 from the ovarian tissue extracts suggests that these two proteins may be linked in the ovary.

The antibody was used to measure *in vitro* Vg synthesis in homogenates of ovaries, hepatopancreas and hemolymph (Table I). The ovary had more immunoprecipitatable protein than either the hepatopancreas or the hemolymph, consistent with the role of the ovary as a yolk storage site. However, the ^{14}C leucine content of the immunoprecipitated Vg was similar in both the ovary and hemolymph samples, suggesting that both ovary and hemolymph can produce new egg yolk proteins. Recovery of all the proteins and radioactive labeled amino acid was near 90% for these assays. Some label and protein was lost due to the procedures used. Though the amount of immunoprecipitated Vg was less in the hepatopancreas than the ovary, the Vg in the hepatopancreas had about three times the ^{14}C leucine incorporated into Vg than the ovary. This is consistent with the hepatopancreas as a site of Vg production but not Vg storage. Ovary, hepatopancreas, and hemolymph can incorporate ^{14}C leucine into new egg yolk proteins, the hepatopancreas incorporates much more than the other groups, whereas the ovary seems to retain more Vg than either the hepatopancreas and the hemolymph.

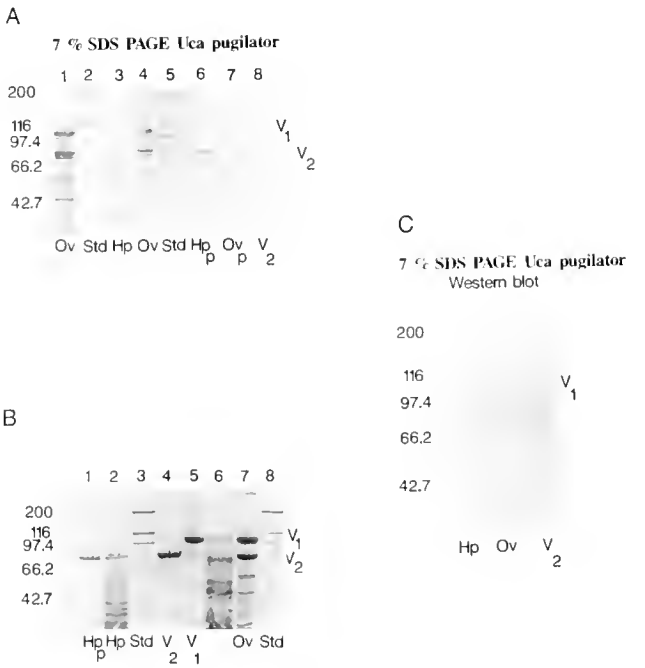

Figure 5. Isolation of egg yolk proteins from ovaries (Ov) and hepatopancreas (Hp) from the tissues of *Uca pugilator*. A. Proteins from crude extracts of ovary and hepatopancreas. Immunoprecipitates from these crude extracts of ovary (Ov_p) and hepatopancreas (Hp_p) are compared to the complete extracts and a sample of partially purified V_2 (V_2). In the sample of ovarian proteins the antibody precipitated both V_1 and V_2, but only V_2 was precipitated from the sample of hepatopancreas. The location of the molecular weight standards are labeled on the left side in daltons $\times 10^3$ B. Isolation of egg yolk proteins. Lane 7 contains a crude ovarian homogenate. Lane 6 contains the fraction with purple color from the G-200 column. Lanes 5 and 4 contain the proteins eluted from the preparative polyacrylamide gels, labeled V_1 and V_2 respectively. Lane 2 contains a crude extract of hepatopancreas, while lane 1 is the immunoprecipitated protein from this hepatopancreas homogenate. C. Western blot of a 7% polyacrylamide gel. Samples of crude ovarian and hepatopancreas extract were separated in a polyacrylamide gel, a sample of V_2 was run in the third lane. The polyclonal antibody to V_2 bound to a single band in the hepatopancreas sample, and to three bands in the ovarian sample. The antibody did not bind to V_1, though it was present in the ovarian sample.

Partial purification of GIH

Fractions from crude shrimp eyestalk extract were tested for their ability to inhibit *in vitro* ovarian protein synthesis. The values for immunoprecipitated Vg are given in Figure 6 and some values for non-specific inhibition are reported in Table II. Eighty-six percent of the inhibitory activity applied to the column was recovered in the 35 fractions that were tested (5 replicates). Three peaks of inhibitory activity were consistently resolved (fraction #29, Rf = 0.48; fraction #35, Rf = 0.41; and fraction 64, Rf = 0.23, 5 replicates). These fractions had 64% of all the inhibitory activity applied to the column. All three fractions had about the same specific activity (2200 ± 300 units/mg; 5 replicates), fraction 29 at Rf = 0.48 had the most protein (3 μg ± 0.7 μg; 5 replicates). The size of proteins eluting at fraction #29, Rf = 0.48 was estimated to be 3,300 ± 500 (5 replicates). This is a smaller size estimate for GIH that the GIH previously isolated from the lobster, *Panulirus argus*, (Quackenbush and Herrnkind, 1983). Based on the bioassay, the column chromatography produced a 37-fold purifica-

Table I

Immunoprecipitable [illegible] tissues of eyestalk ablated crabs [illegible]

	Proteins (mg)		
Sample	Ovary	Hepatopancreas	Hemolymph
Crude Extract	0.51 ± 0.09	0.55 ± 0.06	0.50 ± 0.01
Pellet	0.061 ± 0.04	0.045 ± 0.01	0.014 ± 0.01
Supernatant	0.421 ± 0.05	0.401 ± 0.02	0.390 ± 0.01
	DPM/MG/Hour		
Sample	Ovary	Hepatopancreas	Hemolymph
Crude Extract	5,611 ± 1,065	8,536 ± 1,425	1,448 ± 123
Pellet	865 ± 181	2,977 ± 755	792 ± 71
Supernatant	2,973 ± 1,208	3,803 ± 567	778 ± 79

All values are means ± one standard deviation, n = 12 for all cases, 2 replicates. Crude extract is the initial tissue homogenate. Pellet is the protein precipitated by the antibody to vitellogenin, Supernatant is the protein not precipitated by the antibody. Recovery of both label and protein was between 80–90% for these assays.

tion from the crude material (fraction #29, Rf = 0.48). Fraction #29 inhibited Vg ^{14}C leucine incorporation. It was specific to Vg proteins. Fraction #29 had no significant effect on ^{14}C leucine incorporation into proteins other than Vg, represented by the supernatant in the immunoassay (Table II). Both the crude starting material and material from the column void volume inhibited ^{14}C leucine incorporation into both Vg and non-Vg proteins, demonstrating non-specific protein synthesis inhibition (Table II, Fig. 6). Based on the size estimate for fraction #29 (3,300 ± 500 daltons) the material in this fraction was biologically active at 1.8×10^{-9} *M* protein.

Discussion

The primary source of crustacean egg yolk proteins was first suggested to be extra-ovarian (Wallace *et al.*, 1967). This hypothesis was consistent with the demonstrations of egg yolk protein synthesis in insects and vertebrates. However, evidence from histological studies of developing crustacean ovaries suggested that the ovaries were capable of producing proteins (Beams and Kessel, 1963; Ganion and Kessel, 1972; Wolin *et al.*, 1973; Schade and Schivers, 1980). Direct demonstration of protein synthesis by ovarian tissue supported the new view that the ovarian contribution to overall egg yolk protein synthesis was significant. The relatively slow rate of ovarian protein synthesis in isolated ovarian tissue supported the argument that extra-ovarian tissue also contributed to egg yolk protein synthesis (Lui and O'Connor, 1976, 1977; Eastman-Reks and Fingerman, 1985).

Ovarian egg yolk protein synthesis does not preclude extra-ovarian egg yolk protein synthesis. The unstated assumption in previous work was that egg yolk proteins in crustaceans were produced exclusively in a single tissue, as in insects and vertebrates. Insects produce vitellogenin exclusively in the fat body. A similar pattern was expected in arthropod relatives, the crustaceans. In the isopod, *Idotea bathica basteri*, and the amphipod, *Orchestia gammarella*, egg yolk proteins are produced in a subepidermal adipose tissue, the fat body (Blanchet-Tournier, 1982; Souty and Picaud, 1984). However, vitellogenin is also made in the ovaries of the crab *Pachygrapsus crassipes* (Lui and O'Connor, 1977) and in the hemocytes of the crab, *Callinectes sapidus* (Kerr, 1969). The subepidermal adipose tissues of a shrimp, *Parapenaeus longirostris*, and the hepatopancreas of the crabs, *Carcinus maenus* and *Libinia emarginata*, contain immunoreactive vitellin (Paulus and Laufer, 1987; Tom *et al.*, 1987). Together, these recent reports suggest several new sites for egg yolk protein synthesis.

In our study, immunoreactive Vg was found in the hemolymph, hepatopancreas, and ovaries of the crab, *Uca pugilator*. Each tissue was evaluated for its capacity to incorporate labeled amino acids into proteins and Vg

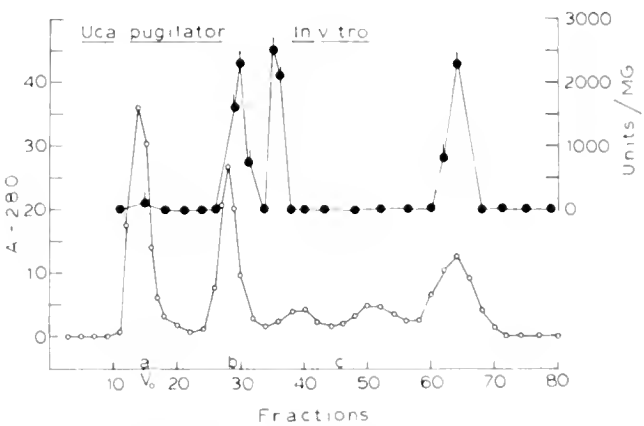

Figure 6. Immunoassay of the fractions of crude shrimp eyestalk extract after separation on G-25 Sephadex. Filled circles are the specific activity (Inhibition units/mg eyestalk extract protein) of the fractions for the inhibition of ^{14}C leucine incorporation into ovarian egg yolk proteins. Open circles are the absorbance (280 nm) of the fractions as they were eluted from the column. The column void volume is indicated by a V. The elution volumes of protein standards used to calibrate the G-25 Sephadex column are indicated by a = aprotinin, b = insulin beta chain, and c = met-enkephalin. The immunoassay values are means ± one standard error for n = 8 for each fraction, 4 replicates. Extracts of shrimp tail muscle were adjusted with crab saline to equal the protein concentrations of the various column fractions of shrimp eyestalk. These tail muscle extracts served as the controls in the *in vitro* assay. Percent inhibition of ^{14}C leucine incorporation into crab egg yolk proteins was calculated as described in Materials and Methods. Every other fraction was bioassayed, but some fractions (with no activity) were not plotted for clarity.

Table II

*Bioassay of shrimp (*Penaeus setiferus*) eyestalk extract on* in vitro *vitellogenin incorporation of labeled leucine in isolated ovarian fragments from the fiddler crab (*Uca pugilator*)*

	% Inhibition of protein incorporation of labeled leucine		
G-25 Fraction #	Pellet	Supernatant	
Crude material	64%*	22%*	
# 15 (void volume)	64%*	22%*	
# 22	6%	4%	
# 29	64%*	6%	Rf = 0.48
# 31	48%*	14%	
# 35	58%*	12%	
# 42	7%	10%	
# 52	5%	6%	
# 64	28%*	12%	
# 70	3%	5%	

All values are means, n = 8 for each fraction from 4 replicates. An * indicates a statistically significant difference between the fraction tested and a muscle extract control (t test for two percentages, $P < 0.05$). One unit of GIH activity produces a 20% inhibition of protein incorporation of labeled leucine, by definition. Crude material is the initial eyestalk extract; all test does were adjusted with saline to a protein concentration of 10 μg/ml. Fraction numbers in this table correspond with fraction numbers in Figure 6. Fractions were selected from a complete data set (35 fractions) as representative of the observations.

in vitro. Comparisons of protein synthesis in the tissues from *Uca pugilator* to other crustaceans is limited by the important variations in the reported methods, procedures, and other variables. Ovarian incorporation of labeled amino acids into egg yolk proteins from *Procambarus* sp. (477 DPM/mg/h) and *Pachygrapsus crassipes* (966 DPM/mg/h) were suggested to be too low to account for complete vitellogenesis (Lui and O'Connor, 1977). Incorporation of labeled amino acids into egg yolk proteins in the hepatopancreas of the fiddler crab (2927 DPM/mg/h) was more than three times the incorporation of labeled amino acids into egg yolk proteins in either the ovarian tissue or the hemolymph. This significant difference (*t*-test, $P < 0.05$) suggests that the hepatopancreas in the fiddler crab can contribute to overall egg yolk protein production.

The demonstrated role of the crustacean hepatopancreas is the synthesis and secretion of digestive enzymes (Gibson and Barker, 1979). This tissue is also a major site of lipid storage and carbohydrate metabolism (Chang and O'Connor, 1983; Sedlmeier, 1985). In the lobster, *Homarus americanus*, the hepatopancreas is the principal tissue source of hemocyanin synthesis (Senkbeil and Wriston, 1981). Eyestalk factors can affect lipid metabolism, protein synthesis, enzyme synthesis, and ribonucleic acid synthesis in the crustacean hepatopancreas (Fingerman *et al.*, 1967; O'Connor and Gilbert, 1968; Gorell and Gilbert, 1971; Bollenbacher *et al.*, 1972; Wormhoudt, 1974; Momin and Rangneker, 1975). In our study, eyestalk ablation significantly increased both *in vivo* and *in vitro* incorporation of labeled amino acids into proteins of the hepatopancreas. Crude extracts of eyestalks decreased protein synthesis in the hepatopancreas of the crayfish, *Orconectes virilis*, but increased ribonucleic acid synthesis in the hepatopancreas of the crayfish, *Procambarus clarkii* (Fingerman *et al.*, 1967; Gorell and Gilbert, 1971). Both protein synthesis and egg yolk protein synthesis in ovaries and hepatopancreas appear to be affected by the eyestalk endocrine system in crustaceans. The coordination of egg yolk protein synthesis in several tissues by the eyestalk endocrine system would be one mechanism to optimize the energy investment required for the production of many yolk-laden eggs.

Insects produce egg yolk proteins exclusively in the fat body (Downer and Laufer, 1983). Fiddler crabs can make egg yolk proteins in at least three sites: ovaries, hepatopancreas, and hemolymph. Other crustaceans appear to produce egg yolk proteins from several tissues as well (Blanchet-Tournier, 1982; Charniaux-Cotton, 1985; Fingerman, 1987). One hypothesis for these fundamental differences among the arthropods may be linked to the differences in life histories. Pterygote insects do not molt as adults, whereas most adult crustaceans continue to molt. Molting is a physiologically demanding process requiring extensive protein synthesis and lipid metabolism (Chang and O'Connor, 1983; Skinner, 1985). The repetitive egg yolk production of adult crustaceans which live for several years is an equally demanding physiological process. The mature ovary of a fiddler crab is 4–6% of the total body wet weight; the ovary contains about 30–40 mg of egg yolk proteins (Webb, 1977). During the reproductive period in the summer, a single female crab will produce two broods of several thousand eggs (Webb, 1977; Christy, 1978). The eyestalk endocrine system is capable of regulating both molting and ovarian development with inhibitory factors so that these two process do not occur simultaneously (Webb, 1977; Adiyodi, 1985). The established need for the synchronization of egg release or egg hatching to systematic environmental variation further constrains the production of mature oocytes (Hartnoll, 1969; Christy, 1982). Fiddler crabs precisely time the release of larvae to optimize their survival (Bergin, 1981; Christy, 1982). Both physiological and physical limitations may require that the massive egg yolk protein synthesis be completed quickly. Therefore, using several sites to synthesize egg yolk proteins may be one strategy to maximize both somatic growth and reproductive output within these constraints. The diversity of crustacean life histories and the habitats they exploit make this a testable hypothesis (Christy, 1982; Hartnoll, 1969).

The partially purified GIH inhibited egg yolk protein synthesis directly in the incubated ovaries. Use of antibody to Vg allows the specific measurement of egg yolk protein production. This Vg specific assay is a significant improvement over previous assays for GIH which were based on overall protein synthesis or simply ovarian wet weight changes (Bomirski *et al.*, 1981; Quackenbush and Herrnkind, 1983; Fastman-Reks and Fingerman, 1984; Charniaux-Cotton, 1985). The development of a bioassay for GIH or any inhibitory hormone requires adequate controls to detect the potential toxic effects of nonspecific agents that may be present in crude extracts (Channing *et al.*, 1985). Bomirski *et al.* (1981) found toxic fractions in their extraction of GIH from the crab, *Cancer magister*. The toxicity was attributed to the large amounts of protein they injected into their bioassay animals. They required a 0.5 ESE dose to produce a measurable response in the shrimp, *Crangon crangon*. The material we extracted from the shrimp eyestalks required only a 0.005 ESE dose *in vivo* and a 0.006 ESE dose *in vitro* to produce statistically significant inhibitory responses in *Uca pugilator*. The potency of the crude extract permitted much less total protein in our assays for GIH than previous assays required. This may have helped us avoid a non-specific protein-induced toxic effect of crude extracts. The partially purified GIH blocked incorporation of labeled amino acids into Vg, did not affect the incorporation of labeled amino acids into other proteins. Crude extract and a few fractions near the void volume of the column did have the ability to block labeled amino acid incorporation into both Vg and other proteins. This non-specific inhibition of incorporation of labeled amino acids serves as a control for non-specific effects in our *in vitro* assay system. Thus, with the *in vitro* assay procedure, we can measure specific inhibition of labeled amino acid incorporation into Vg, as well as the non-specific inhibition of incorporation of labeled amino acids into proteins that are not Vg. This *in vitro* procedure can now be used in the further characterization of eyestalk neurohormones.

Acknowledgments

This work was supported in part through an institutional grant NA-85AA-D-SD128 to Texas A & M University by the National Oceanic and Atmospheric Administration's Sea Grant Program, Department of Commerce, and by the Texas Advanced Technology Research Program. The research was conducted by the Texas Agricultural Experiment Station.

Literature Cited

Adiyodi, R. 1985. Reproduction and its control. Pp 147–217 in *The Biology of Crustacea*, volume 9, D. E. Bliss and L. H. Mantel, eds. Academic Press, New York.

Beams, H. W., and R. G. Kessel. 1963. Electron microscope studies on developing crayfish oocytes with special reference to the origin of yolk. *J. Cell Biol.* **18:** 621–649.

Bergin, M. 1981. Hatching rhythms in *Uca pugilator*. *Mar. Biol.* **63:** 151–158.

Blanchet-Tournier, M. F. 1982. Quelque aspects des interactions hormonales entre la mue et al vitellogenese chez le Crustacé Amphipode, *Orchestia gammarella*. *Reprod. Nutr. Dev.* **22:** 325–344.

Bollenbacher, W. E., S. M. Flechner, and J. D. O'Connor. 1972. Regulation of lipid synthesis during early premolt in decapod crustaceans. *Comp. Biochem. Physiol.* **42B:** 157–165.

Bomirski, A., M. Arendarczk, E. Kawainska, and L. H. Kleinholz. 1981. Partial characterization of crustacean gonad-inhibiting hormone. *Int. J. Invertebr. Reprod.* **3:** 213–219.

Brown, F. A. Jr., and G. M. Jones. 1948. Ovarian inhibition by a sinus gland principle in the fiddler crab. *Biol. Bull.* **96:** 228–232.

Chang, E. S., and J. D. O'Connor. 1983. Metabolism and transport of carbohydrates and lipids. Pp 263–287 in *The Biology of Crustacea*, volume 5, L. H. Mantel, ed. Academic Press, New York.

Channing, C. P., W. L. Gordon, W. K. Lui, and D. N. Ward. 1985. Physiology and biochemistry of ovarian inhibin. *Proc. Soc. Exp. Biol. Med.* **178:** 339–361.

Charniaux-Cotton, H. 1985. Vitellogenesis and its control in malacostracan crustacea. *Am. Zool.* **25:** 197–206.

Christy, J. H. 1982. Adaptive significance of semilunar cycles of larval release in fiddler crabs (Genus *Uca*): test of an hypothesis. *Biol. Bull.* **163:** 251–263.

Christy, J. H. 1978. Adaptive significance of reproductive cycles in the fiddler crab, *Uca pugilator*, a hypothesis. *Science* **199:** 453–455.

Cooke, I. M., B. Haylett, and T. Weatherby. 1977. Electrically elicited neurosecretory and electrical responses of the isolated crab sinus gland in normal and reduced calcium salines. *J. Exp. Biol.* **70:** 125–149.

Douglas, G. C., and B. F. King. 1984. A filter paper sandwich method using small volumes of reagents for the detection of antigens electrophoretically transferred onto nitrocellulose. *J. Immunol. Methods* **75:** 333–338.

Downer, R. G. H., and H. Laufer. 1983. *Endocrinology of Insects*. Alan Liss Inc., New York.

Fastman-Reks, S., and M. Fingerman. 1984. Effects of neuroendocrine tissue and cyclic AMP on ovarian growth *in vivo* and *in vitro* in the fiddler crab, *Uca pugilator*. *Comp. Biochem. Physiol.* **79A:** 679–684.

Fastman-Reks, S., and M. Fingerman. 1985. *In vitro* synthesis of vitellin by the ovary of the fiddler crab, *Uca pugilator*. *J. Exp. Zool.* **233:** 111–116.

Fielder, D. R., K. R. Rao, and M. Fingerman. 1971. A female-limited lipoprotein and the diversity of hemocyanin components in the dimorphic variants of the fiddler crab, *Uca pugilator*, as revealed by disc electrophoresis. *Comp. Biochem. Physiol.* **39B:** 291–297.

Fingerman, M. 1987. Endocrine mechanisms in crustaceans. *J. Crustacean Biol.* **7:** 1–24.

Fingerman, M., T. Dominiczak, M. Miyawaki, C. Oguro, and Y. Yamamoto. 1967. Neuroendocrine control of the hepatopancreas in the crayfish, *Procambarus clarkii*. *Physiol. Zool.* **40:** 23–30.

Ganion, L. R., and R. G. Kessel. 1972. Intracellular synthesis, transport and packaging of proteinaceous yolk in oocytes of *Oreonectes immunis*. *J. Cell Biol.* **52:** 420–437.

Gibson, R., and P. L. Barker. 1979. The decapod hepatopancreas. *Oceanog. Mar. Biol. Ann. Rev.* **17:** 285–316.

Gorell, T. A., and L. Gilbert. 1971. Protein and RNA synthesis in premolt crayfish, *Oreonectes virilis*. *Z. Vgl. Physiol.* **73:** 345–356.

Hames, B. D., and D. Rickwood. 1981. *Gel Electrophoresis of Proteins, a Practical Approach*. IRL Press, Washington, DC.

Hartnoll, R. G. 1969. Mating in the Brachyura. *Crustaceana* **16:** 161–181.

Kerr, M. S. 1969. The hemolymph proteins of the blue crab, *Callinectes sapidus*. II. A lipoprotein serologically identical to oocyte lipovitellin. *Dev. Biol.* **20:** 1–17.

Laemmli, U. K. 1970. Cleavage of structural proteins during assembly of the head of bacteriophage T4. *Nature* **227:** 680–685.

Lui, C. W., and J. D. O'Connor. 1976. Biosynthesis of lipovitellin by the crustacean ovary. II. Characterization of and *in vitro* incorporation of amino acids into purified subunits. *J. Exp. Zool.* **195:** 41–52.

Lui, C. W., and J. D. O'Connor. 1977. Biosynthesis of lipovitellin. III. The incorporation of labeled amino acids into purified lipovitellin of the crab, *Pachygrapsus crassipes*. *J. Exp. Zool.* **199:** 105–108.

Momin, M. A., and P. V. Rangneker. 1975. Histochemical localization of oxidative enzymes in the hepatopancreas of *Scylla serrata* (Forskal) (Brachyura:Decapoda). *J. Exp. Mar. Biol. Ecol.* **20:** 249–264.

O'Connor, J. D., and L. Gilbert. 1968. Aspects of lipid metabolism in crustaceans. *Am. Zool.* **8:** 529–539.

Ouchterlony, O. 1949. Antigen-antibody reactions in gels. II. Factors determining the site of the precipitate. *Ark. Kemi* **1:** 43–50.

Paulus, J. E., and H. Laufer. 1987. Vitellogenocytes in the hepatopancreas of *Carcinus maenus* and *Libinia emarginata*. *Int. J. Invert. Reprod. Dev.* **11:** 29–44.

Panouse, J. B. 1943. Influence d'ablation de pédoncle oculaire sur la croissance de l'ovaire chez la crevette, *Leander serratus*. *Comptes Rendu Acad. Sci. (Paris)* **217:** 553–555.

Quackenbush, L. S. 1986. Crustacean endocrinology: a review. *Can. J. Fish. Aqua. Sci.* **43:** 2271–2282.

Quackenbush, L. S., and M. Fingerman. 1985. Enzyme-linked immunosorbant assay of black pigment dispersing hormone from the fiddler crab, *Uca pugilator*. *Gen. Comp. Endocrinol.* **57:** 438–444.

Quackenbush, L. S., and W. F. Herrnkind. 1983. Partial characterization of eyestalk hormones controlling molt and gonadal development in the spiny lobster, *Panulirus argus*. *J. Crustacean Biol.* **3:** 34–44.

Reddy, S. R. R., and G. R. Wyatt. 1967. Incorporation of uridine and leucine *in vitro* by *Cercropia* silkmoth wing epidermis during diapause and development. *J. Insect Physiol.* **13:** 981–994.

Schade, M. L., and R. R. Shivers. 1980. Structural modulation of the surface and cytoplasm of oocytes during vitellogenesis in the lobster, *Homarus americanus*: an electron microscope protein tracer study. *J. Morphol.* **163:** 13–26.

Sedlmeier, D. 1985. Mode of action of the crustacean hyperglycemic hormone. *Am. Zool.* **25:** 223–232.

Senkbeil, E. G., and J. C. Wriston. 1981. Hemocyanin synthesis in the american lobster, *Homarus americanus*. *Comp. Biochem. Physiol.* **68B:** 163–171.

Skinner, D. M. 1985. Molting and regeneration. Pp 43–146 in *The Biology of Crustacea*, Vol. 9, D. E. Bliss and L. H. Mantel, eds. Academic Press, Orlando.

Sokal, R., and F. J. Rohlf. 1969. *Biometry*. Freeman Press, San Francisco.

Souty, C., and J-L. Picaud. 1984. Effet de l'injection d'une gonadotropin humaine sur la synthese et la libération de la vitellogénine par le tissu adipeaux du Crustacé Isopod marin, *Idotea bathica basteri* Audouin. *Gen. Comp. Endocrinol.* **54:** 418–421.

Tom, M., M. Goren, and M. Ovadia. 1987. Localization of the vitellin and its possible precursors in various organs of *Parapenaeus longirostris*. *Int. J. Invertebr. Reprod. Dev.* **12:** 1–12.

Towbin, H., T. Staehelin, and J. Gordon. 1979. Electrophoretic transfer of proteins from polyacrylamide gels to nitrocellulose sheets: procedure and some applications. *Proc. Natl. Acad. Sci.* **76:** 4350–4354.

Wallace, R. A., S. L. Walker, and P. V. Hauschka. 1967. Crustacean lipovitellin. Isolation and characterization of the major high density lipoprotein from eggs of decapoda. *Biochemistry* **6:** 1582–1590.

Webb, M. 1977. Eyestalk regulation of molt and vitellogenesis in *Uca pugilator*. *Biol. Bull.* **153:** 630–642.

Wolin, E. M., H. Laufer, and D. F. Albertini. 1973. Uptake of yolk protein, lipovitellin by developing crustacean oocytes. *Dev. Biol.* **35:** 160–170.

Wourmhoudt, A. 1974. Variations in the level of the digestive enzymes during the intermolt cycle of *Palaemon serratus*: influence of the season and effect of the eyestalk ablation. *Comp. Biochem. Physiol.* **49A:** 707–715.

Reference: *Biol. Bull.* 175: 332–342 (December, 1988)

Passive Suspension Feeding in a Sea Pen: Effects of Ambient Flow on Volume Flow Rate and Filtering Efficiency

BARBARA A. BEST[1]

Department of Zoology, Duke University, Durham, North Carolina 27706

Abstract. An integrative analysis of passive suspension feeding is developed and tested. It emphasizes the functional role of overall organism design in enhancing the hydromechanic conditions necessary for feeding. Feeding rate, defined as the total number of particles captured per time, is a function of the ambient flow speed which independently affects both the volume flow rate and the filtering efficiency. In the sea pen *Ptilosarcus gurneyi*, volume flow rate initially increases with increasing ambient flow speed, peaks, and then decreases as the animal deforms with the flow. Filtering efficiency, for a given filter geometry, decreases with increasing velocity. However, due to deformation of the filter with flow, higher filtering efficiencies are maintained as a result of the variable porosity filter. Feeding rate is strongly dependent on volume flow rates. The feeding rate initially increases with increasing ambient flow, but then peaks and decreases similar to the volume flow rate. Both volume flow rate and filtering efficiency depend upon the size of the organism and the relative position of the organism in the boundary layer.

Introduction

Aquatic suspension feeding organisms use an array of filtering elements to separate particles from the passing fluid medium. *Passive* suspension feeders rely solely on the relative movement of their filter and the particle-laden water for food capture. In many sessile and benthic organisms, the relative movement is generated by the ambient flow, leaving them highly dependent on the ambient flow for feeding. *Active* suspension feeders use cilia or muscles for pumping water past the filtering surface. This feeding may be augmented by the ambient velocity, which can be an order of magnitude greater than the self-generated currents (Merz, 1984; Okamura, 1984, 1987).

Recently a few studies have begun to examine and clarify particle capture mechanisms in biological systems. Particle size selection has been shown to depend on the diameter and spacing of the filtering elements, flow velocity past the elements, diameter of the particles, and surface chemistry of both particles and filtering elements (Rubenstein and Koehl, 1977; LaBarbera, 1978, 1984; Gerritsen and Porter, 1982). However, the most broad-scale aspects of filter feeding are still poorly understood, especially the functional role of overall organismal design in maintaining the organism's exposure to flow and in influencing the hydromechanical conditions which aid in particle capture. In some stony corals the branching pattern prevents the formation of stagnant zones within the colony. This assures adequate flow throughout (Chamberlain and Graus, 1975). In flexible organisms, their shape and exposure to flow depend on the flow velocity and the structure's response to drag forces imposed by the flow (Koehl, 1976; Patterson, 1984; Vogel, 1984), thereby changing the microenvironment around the filtering elements (Harvell and LaBarbera, 1985).

The present study emphasizes the effect of gross morphology on feeding performance in a particular suspension feeder to highlight the potential interactions between morphology and flow which may occur in a wide range of suspension feeders. The ecological consequence

Received 24 December 1987; accepted 16 September 1988.

[1] Present address: Orthopaedic Research Laboratory, Black Building 14-1412, Columbia University, 630 W. 168th St., New York, New York 10032.

of functional morphology is equated with "feeding rate" which is defined as the total number of particles caught per unit time. In this analysis, feeding rate is a function of three parameters: (1) the volume of water processed by the organism per unit time, (2) the proportion of particles removed per volume of water processed, (3) and the density of particles in the ambient water. The first two factors, the "accessibility" to flow and the "filtering efficiency" or proportion of particles retained, may both be influenced by the ambient velocity. For a benthic organism, several factors may affect the ambient velocity it experiences, including its own size and height above the substratum into the boundary layer (Nowell and Jumars, 1984).

This paper first describes an approach for examining the effect of structure-flow interactions on feeding. It then describes a series of field and laboratory studies of feeding rate in a passive suspension feeder which address these questions: (1) how does ambient flow speed independently affect volume flow rate and filtering efficiency, two components of feeding rate? (2) How are volume flow rates and filtering efficiency affected by organism size, as the organism grows and extends into a different ambient flow environment? (3) How does the structural response of the organism to ambient flow influence particle capture on the level of the filtering elements, or polyps?

Integrative analysis of suspension feeding

An approach useful for evaluating the effect of morphological features on the feeding rate of passive suspension feeders is presented. I first identify parameters (environmental and morphological) which may influence feeding and then define the relationships of these parameters. For example, an analysis of feeding mechanics encompasses several aspects of structural design which emphasize the interaction between animal structure and ambient flow:

(1) *Structural features related to maintaining filter surface area exposed to the flow.* Drag imposed by the flow will tend to deform flexible organisms. In organisms which require flow *through* the filter for feeding, it is the drag-induced pressure drop across the filter that drives the water through the filter; hence, the organism cannot "hide" from the flow and must have support structures to maintain the filter in the flow. In organisms which utilize flow over or around the filter, such as in gravitational deposition feeders, filter surface area or position in flow must be maintained.

(2) *Structural features which stabilize the filter in relation to changes in flow direction or amplitude.* For short-term fluctuations in current speed or direction, on the order of seconds to hours, the animal may stabilize the filter either by actively or passively re-orienting, and thus ensure proper exposure. For long-term fluctuation, from days to years, re-orientation and stabilization may occur via growth responses (*e.g.,* Wainwright and Dillon, 1969).

(3) *Flow-structure interactions related to particle capture.* Large scale features may pre-position particles before they contact the filter (Craig and Chance, 1981), or pre-condition the water and its flow characteristics, such as flow speed, through the filter (Harvell and LaBarbera, 1985).

The design aspects listed above all influence feeding. The first two aspects influence the volume of water processed by the organism and the last influences filtering efficiency. The total number of particles extracted per unit time is a function of the volume of water processed per unit time, the number of particles in the ambient water, and the proportion of particles removed per unit volume of water processed, and can be expressed as the equations given in Figure 1.

Structural and flow features can be identified which may affect either "accessibility" or "filtering efficiency" (refer to Fig. 1). For example, filtering efficiency depends on the flow pattern and particle paths around the filtering elements, and thus is a function of flow velocity around the elements; the size, spacing, orientation, and surface charge of elements; the diameter, density, motility, and surface charge of the particles; and possibly the frequency with which the elements are cleaned (Fuchs, 1964; Rubenstein and Koehl, 1977; Spielman, 1977; LaBarbera, 1978, 1984; Gudmundsson, 1981).

"Accessibility" can refer to the volume of water passing either through a filter or in close enough proximity that particle extraction is possible. In organisms where the flow is quasi-perpendicular to the filter, as in the sea pen *Ptilosarcus gurneyi,* access to flow is equated with volume flow rate. It is equal to the surface area of the filter exposed to the flow times the velocity of flow through that area (refer to Fig. 1). The surface area of the filter exposed to the flow is a function of the organism's vertical stance and orientation to the flow; the shape, size, and flexibility of the filter; the ambient velocity and the drag imposed by the flow; the position of the organism above the substratum and the presence of other organisms. The influence of most of these parameters on accessibility in the suspension feeding sea pen *Ptilosarcus gurneyi* is addressed in Best (1985, in prep.).

Having identified both flow characteristics and morphological features which may affect feeding rate, I examined the influence of flow velocity on both volume flow rate and filtering efficiency, with particular attention

Figure 1. Diagram of integrative method, showing relationships among parameters. See text for discussion.

to flow-structure interactions that change with ambient flow speed.

Materials and Methods

Experimental organism and morphology

The sea pen *Ptilosarcus gurneyi* (Cnidaria: Pennatulacea) was used in this study because it has a well-defined morphology which can be easily characterized on the basis of size and age (Birkeland, 1969, 1974). The upper portion of the organism, the rachis, contains the filtering elements—the polyps—which extend from the semi-circular horizontal plates termed "leaves" (Fig. 2). With an increase in ambient velocity, the flexible rachis bends downstream (Fig. 2). The polyps form a semi-cylindrical filter on the downstream side of the organism, extending the length of the rachis (Fig. 2). The height (vertical stance) of the rachis was the indicator of organism size. The rachis behaves as a single unit which orients to the flow (Best, 1985), ensuring water passage through the filter in the same direction—into the concave side of the semi-cylindrical filter. This sea pen feeds primarily on phytoplankton (Birkeland, 1969). Its bright orange color is the result of carotenoids incorporated from ingested dinoflagellates and can be passed on to the tissues of nudibranch predators (S. Kemp, pers. comm.).

Ptilosarcus gurneyi is a common inhabitant of soft-sediment environments in Puget Sound and the San Juan Archipelago, Washington. From an initial length of under 1 mm, *P. gurneyi* can grow to a total length of over 80 cm, extending over 40 cm above the benthic surface. Sea pens were hand collected from Lopez Sound by SCUBA diving and transported back to the Friday Harbor Laboratories of the University of Washington. Animals were maintained in running seawater.

Morphometrics

Photographs of organisms in the field were compared to photographs of fully expanded organisms in the laboratory. Since there were no differences detected in stance or body size between laboratory and field photographs, all morphometries were performed in the laboratory. With a Wild dissecting microscope, polyp sizes in small (3–10 cm rachis height) and large (20–30 cm rachis height) sea pens were measured. For each organism, polyp width, tentacle width and length, and pinnule length and spacing were measured to the nearest 0.01 mm. Polyps from the bottom, middle, and top of the rachis from each sea pen were examined.

Sea pens were placed in a large recirculating flow tank (working area of 32 by 34 cm; Vogel and LaBarbera, 1978), continuously supplied with fresh seawater. To examine spacing between polyps as a function of flow speed, close-up photographs of the sea pens were taken as they deformed under flow speeds up to 25 cm s^{-1}. From these photographs, the spacing between the leaves and the density of polyps were determined. Polyp density was calculated as the number of polyps cm^{-2} in the plane of the filter, approximating a plane perpendicular to the direction of flow.

Field velocities

Sea pens were studied within Lopez Sound where water depth averaged 10 m and the bottom consists of sandy-mud. To characterize the flow environment on the

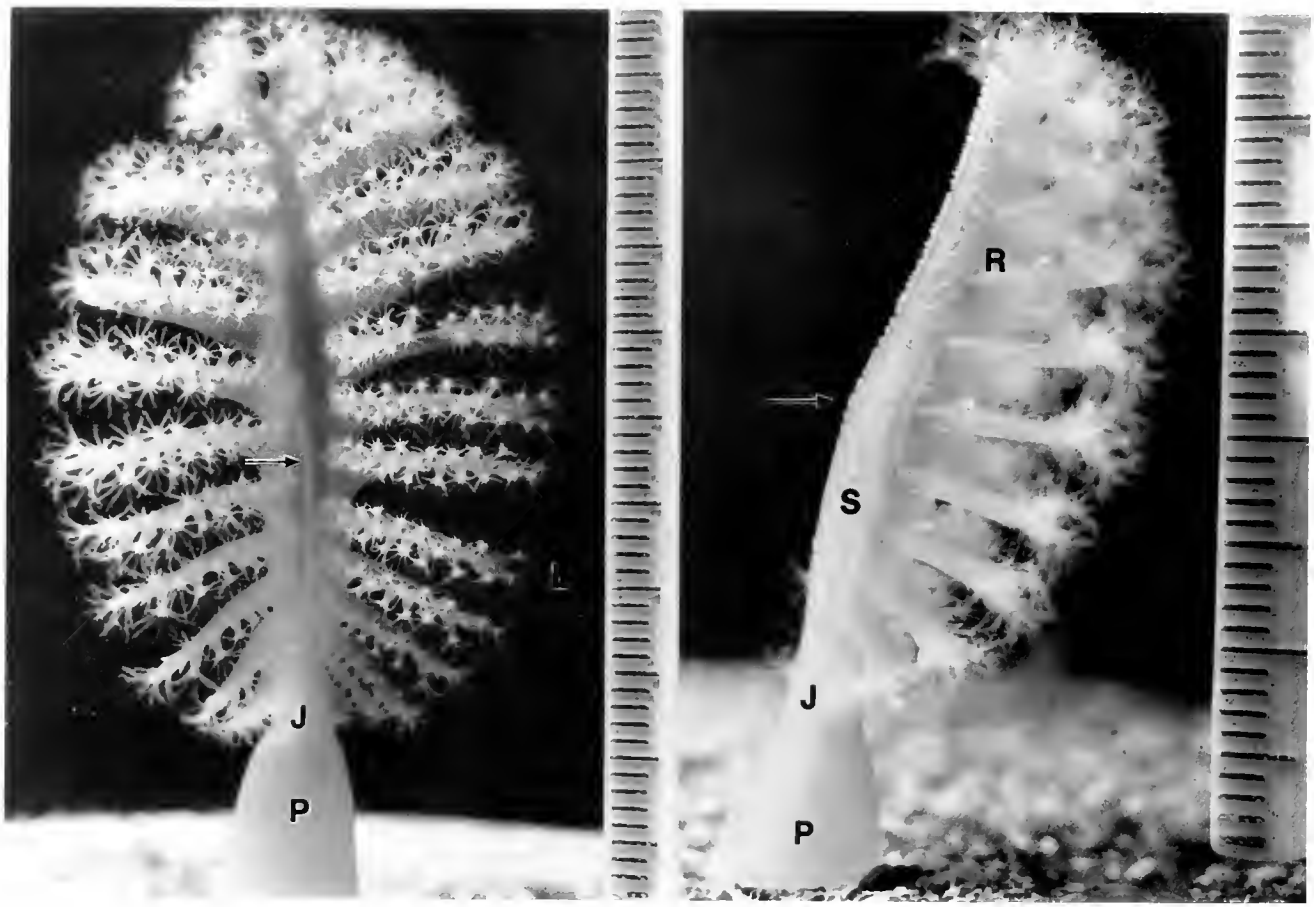

Figure 2. Photographs of small sea pens, *Ptilosarcus gurneyi*. Left. View of sea pen showing the array of polyps on the downstream side of the rachis (rachis height = 4.5 cm). "J" - Joint, "P" - Peduncle, "L" - Leaf. Arrow points to internal style visible through body wall. Note the parallel leaves "L" through which water would flow. Right. Side view of sea pen (rachis height = 3.0 cm). "P" - Peduncle, "J" - Joint, "S" - Siphonozooids, "R" - Rachis. Arrow points to the top rigid portion of the style. Flow is from left to right.

scale of the sea pens, a thermistor flow probe (LaBarbera and Vogel, 1976) was used to record local flow speeds at 18 cm above the substratum, the average height of the sea pens. Flow direction was also continuously monitored with a weather vane/potentiometer (Best, 1985). Velocity recordings were made over 6–8 hour periods, including one low and high tide, on three different days. To construct a velocity profile and determine the range of velocities experienced by small, medium, and large sea pens, velocity measurements were taken at different heights above the substratum.

Volume flow rates

There is a postural change in *Ptilosarcus gurneyi* with increasing flow speed. The area of the feeding filter oriented perpendicular to the current also changes with the flow speed. Therefore, it was necessary to measure directly the volume flow rate through the filter as a function of ambient flow speed.

Sea pens acclimated in the recirculating flow tank. An imaginary plane was established upstream of the organism and horizontal transects across this plane were made with a fluorescein dye injector. For each horizontal transect, it was noted for which points the dye, once released, subsequently passed through the filter of the downstream sea pen. Horizontal transects were spaced vertically every 1.0 cm for large and medium sea pens and 0.5 cm for small pens. From these transects an area on the imaginary plane was determined, representing the source of water actually passing through the filter. The volume flow rate was calculated by multiplying this area by the water flow speed through the plane (area $\times$ speed = volume time^{-1}). Flow speeds in the flow tank were measured with a thermistor flowmeter which had been calibrated with an electromagnetic water current meter

(Model 511, Marsh-McBirney Inc., with a precision ± 2%).

For each sea pen, flow rates were determined over a range of velocities, 1 to 25 cm s^{-1} for medium and large pens, 1 to 12 cm s^{-1} for small pens. Determinations of velocity-flow rates were repeated three times for a large and a small sea pen; replicated values were within 3% for the small sea pen and less than 6% for the large sea pen.

Velocity through rachis

A thermistor flow probe measured the flow speed between the leaves and through the mesh-work of polyps as sea pens were exposed to ambient speeds of 1 to 25 cm s^{-1} in the flow tank.

Filtering efficiency

In the field, water samples were collected upstream and downstream of sea pens from three size classes: a small sea pen with a rachis height of 7 cm, medium sea pen 15 cm high, and large sea pen 25 cm high. For each sea pen three concurrent upstream-downstream water samples were taken by SCUBA divers positioned on either side of the organism. Each diver held a transparent plastic tube, parallel to the current, either directly in front of the rachis or directly behind the rachis, at the same height. The tubes were held in place long enough to be flushed with seawater several times. Simultaneously, the ends of both tubes were sealed. Three sized tubes were used for the different sized sea pens, with 3 cm, 5 cm, and 7 cm diameters, respectively.

Upon leaving the water, the divers transferred the water samples into clean bottles, stored them on ice in the dark, and immediately took them to the laboratory for analysis.

In the laboratory each water sample was first filtered through a 163 μm Nitex filter. An Elzone 80XY particle counter (Particle Data, Inc.) was used to count the total number of particles in a 2 ml subsample, and to construct a size-frequency distribution of the particles into 128 particle size classes in the range 0–100 μm. Five subsamples were analyzed from each upstream and downstream field sample. The precision of counts from multiple subsamples is better than 5%.

To examine the effect of flow speed on particle retention, a laboratory experiment was conducted involving a medium-sized sea pen (rachis height = 12 cm). The sea pen was allowed to acclimate in the recirculating flow tank. A filtrate of natural particles—containing phytoplankton and particulates ranging from 1–80 μm in diameter—was added to the flow tank. A density between 3000–4000 particles ml^{-1} was maintained throughout the experiment. At each of three flow speeds, 1.5, 3.0, and 6.0 cm s^{-1}, water samples (40–70 ml) were collected concurrently with a suction device (5 mm diameter opening) immediately upstream and downstream of the rachis. Three sets of water samples were taken at each velocity.

In addition, experiments similar to the above were conducted with a medium sea pen feeding on one size range of particles, by adding only the chlorophycean phytoplankter *Dunaliella* (10 μm diameter) to the flow-tank. The water samples from the laboratory experiments were treated and analyzed for particle counts in the same manner as in the field experiment, but with 1 ml subsamples.

Filtering efficiency was calculated from the difference in particle counts from two samples, taken concurrently up- and downstream, and expressed as a percentage of the upstream count.

Results

Field velocities

Flows at the field site were relatively steady, hydraulically smooth and bidirectional, and changed orientation approximately 180° with the tides. The mean flow speed at 18 cm above the substratum ranged from 8 to 11 cm s^{-1}. The maximum speeds ranged from 13 to 17 cm s^{-1}. Over a 10 minute period, for a mean flow speed of 9.8 ± 0.42 cm s^{-1}, the turbulence intensity (standard deviation of the flow/mean flow speed) was 0.043. At 8 cm above the sediment—the approximate height of small sea pens—the mean flow speed ranged from 3 to 7 cm s^{-1} and the maximum speeds ranged from 8 to 10 cm s^{-1}. Velocity readings taken over a few minutes at 5, 10, 30, 50, and 100 cm above the substratum showed mean flow speeds of 6.5, 7.7, 8.7, 9.6, and 10.2 cm s^{-1}, respectively. Using the standard log layer equations for a geophysical boundary layer and the linear regression of the above means, the boundary shear velocity (u_*)—a measure of shear stress acting on the bed and a useful parameter of the flow field—was estimated to be 0.50 cm s^{-1}.

Morphometrics

Polyp width, the distance across the polyp between tentacle tips, is uniform throughout large sea pens and the middle and bottom regions of small sea pens (3.59 mm ± 0.157, n = 25). The very top 30–40 polyps on the small sea pens are slightly larger with a mean width of 3.88 mm ± 0.217 (Student's *t*-test, $t = 2.34$, $\alpha = 0.05$, n = 30). Tentacle length ranged from 1.4 to 1.9 mm, with a mean of 1.59 mm ± 0.13 (n = 30). The tentacle width was approximately 0.34 mm at its base and tapers to the

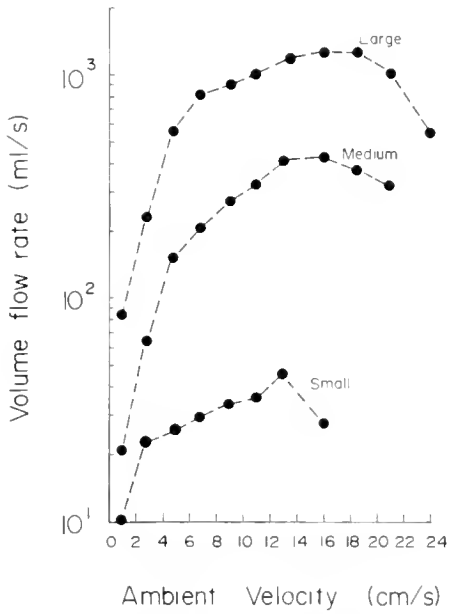

Figure 3. Volume flow rate as a function of ambient velocity. The volume of water passing through the rachis initially increases as velocity rises, then peaks and declines due to the postural change of a sea pen.

tip. Eleven to twelve pairs of pinnules project out along the length of the tentacle, increasing from a length of 0.07 mm at the tentacle base to 0.32 mm at the tentacle tip. These pinnules do not project laterally out from the tentacle, but are angled downstream. Pinnule width ranged from 0.03 to 0.05 mm. Spacing between pinnules ranged from 0.06 to 0.13 mm.

The spacing between the leaves, on the downstream side of the animal, was smaller in the small sea pens (3.8 mm mean spacing, 3.1–4.2 range, n = 6 organisms) than in the large sea pens (5.7 mm mean, 5.4–5.9 range, n = 7) in still water. With increasing flow speeds both small and large sea pens flex with the flow, resulting in a decreased spacing between leaves. At 13 cm s^{-1}, small sea pens had a mean spacing of 2.3 mm, range 2.6–2.8; large sea pens had a mean spacing of 3.9 mm, range 3.5–4.2. At 20 cm s^{-1}, large sea pens had a mean of 3.4 mm, range 3.2–3.6.

In still water polyp density, in the plane of the filter, is 30.2 ± 1.76 polyps cm^{-2} (n = 12) in large sea pens and 29.4 ± 2.35 polyps cm^{-2} (n = 12) in small sea pens. As ambient flow speed increases to 13 cm s^{-1}, polyp density does not change significantly in small sea pens. However, in large sea pens there is a significant increase in polyp density to 33.1 ± 0.13 polyps cm^{-2} (Student's *t*-test, $t = 3.58$, $\alpha = 0.05$, n = 24).

Volume flow rates

The volume of water flowing through the filter per unit time (volume flow rate) is dependent on both the ambient flow speed and the area of filter projected into the flow as determined by the posture of the organism (Best, 1985). As shown in Figure 3, the volume flow rate for a single organism increases with an increase in ambient flow until the organism becomes so bent back by the flow that more water tends to flow over rather than through the filter. The maximum volume flow rate, y (ml s^{-1}), attained for an organism is best fit by a linear function (stepwise multiple regression analysis) of its rachis height, χ (cm), where

$$y = -208.4 + 54.6\chi \quad (r = 0.93, n = 18).$$

The flow speeds at which these maximum volume flow rates occur are also related to the organism's size. For small sea pens, the maximum volume flow rates occur at flow speeds ranging between 6.5 and 8.5 cm s^{-1}, between 12 and 14 cm s^{-1} for medium sea pens, and between 14 and 18 cm s^{-1} for large sea pens.

Velocity through rachis and Reynolds number

Figure 4 shows the flow speed between the leaves and directly behind the polyps in relation to the ambient flow speed. As the ambient speed increases, the flow speed between the leaves and polyps also increases, but at a lower rate (slope of regression lines less than 1.0: for leaves, b = 0.55, $t_s = 8.58$, $t_{.05[6]} = 2.31$, $P < 0.05$; for polyps, b = 0.33, $t_s = 26.78$, $t_{.05[6]} = 2.31$, $P < 0.05$). At an ambient speed of 25 cm s^{-1}, the flow speed between the polyps is only 6–8 cm s^{-1}, and 11–13 cm s^{-1} between the leaves.

For an object moving relative to the ambient fluid, the relative importance of inertial and viscous forces acting on the object—and therefore the nature of flow around the object—is represented by the dimensionless parame-

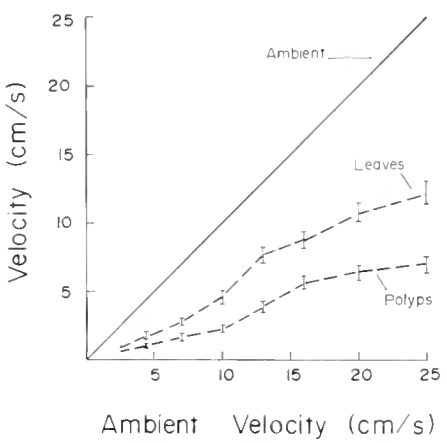

Figure 4. Flow velocities between leaves and behind the polyps as a function of ambient velocity. Note the much reduced flows occurring by the polyps.

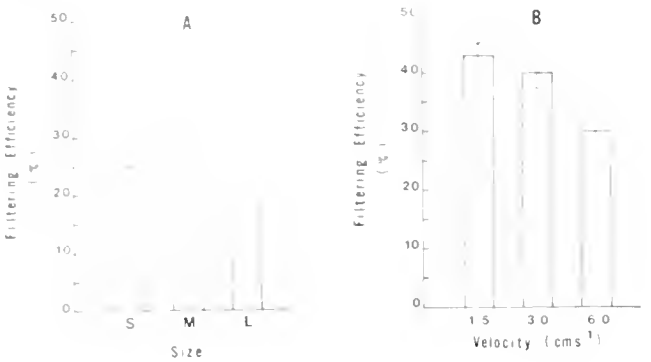

Figure 5. A. Filtering efficiency as a function of organism size. Filtering efficiency is calculated as the percentage difference in particle counts from upstream and downstream water samples taken in the field. Means ± SE are shown for 15 paired water samples (2 ml) analyzed for each small "S", medium "M", and large "L" sea pen. Field flow speeds for the small sea pen were approximately 5–6 cms $^{-1}$ and 8–9 cms $^{-1}$ for the medium and large sea pens. Particle retention in the small sea pen is significantly lower than the medium and large sea pens (2 × 2 G-test of independence, G = 56.6, α = 0.05) B. Filtering efficiency as a function of ambient flow speed. Filtering efficiency for a single sea pen feeding in the flow tank at three different speeds. Means ± SE are shown for 15 paired water samples (1 ml). Particle retention decreases with increasing velocity (ANOVA, $F_{2,44}$ = 75.52, $P \ll .001$, n = 45).

ter "Reynolds number" (Re). For medium and large sea pens, assuming the characteristic length to be the length of the rachis parallel to flow, the Reynolds number is around 8×10^2 to 1×10^4 for flows from 2 to 25 cm s^{-1}; for small sea pens the Reynolds number is around 2×10^2 to 3×10^3. However, due to the small size of the pinnules and tentacles (*i.e.*, small characteristic length) and the reduced flows over these structures, the nature of the flow is very different as reflected in the Reynolds number (Re: approximately 1–10 for tentacles, and 0.1–1.0 for the pinnules). Particle capture is occurring under low Reynolds number, viscous flow conditions.

Filtering efficiency

Figure 5A shows the filtering efficiencies—the percentage of particles present in the downstream water sample relative to the upstream sample—for the three different sized sea pens in the field. The small sea pen had the lowest retention of particles which was significantly different from the higher retentions of the medium and large sea pens (2 × 2 G-test of independence performed on raw particle counts, G = 56.6, α = 0.05). The relationship of filtering efficiency to ambient flow speed for one sea pen is shown in Figure 5B: the efficiency decreased from a mean of 42.8% ± 3.5% at a velocity of 1.5 cm s^{-1} to a mean of 29.9% ± 5.1% at a velocity of 6.0 cm s^{-1}. An ANOVA failed to show a significant difference in the number of particles in the upstream samples throughout the experiment ($F_{2,44}$ = 1.62, $P > 0.21$, n = 45), but did show a significant interaction between ambient flow speed and the number of particles in the downstream samples ($F_{2,44}$ = 75.52, $P \ll .001$, n = 45). Filtering efficiency decreases with increasing velocity.

The size-frequency distribution of particles in one set of upstream-downstream water samples taken in the field is shown in Figure 6; the difference between the area under these two curves represents the number of particles removed during one passage through the rachis. Every field feeding test failed to show a significant difference in the size-frequency distributions of the upstream-downstream water samples (G-test for goodness of fit), implying that no particle size selection was occurring. However, for the laboratory feeding experiments, there were significant differences (G-test for goodness of fit) in the size-frequency distributions of every upstream-downstream comparison (Table I). The mean particle size in the downstream sample was smaller than that for the upstream sample, implying that larger particles had a higher probability of being retained. The difference between the mean particle size of upstream-downstream samples increased as ambient flow speed increased (Table I), suggesting a greater selection for larger particles at higher ambient flow speeds.

Feeding performance

The total number of particles removed from the ambient water per unit time, the feeding rate, is equal to the product of volume flow rate and filtering efficiency. Feeding rates, calculated from these two independently measured parameters, of a large, medium, and small sea pen are shown in Figure 7, assuming an ambient particle concentration of 1000 particles ml^{-1} which is within the range of concentrations present in the field. Because filtering efficiencies were only measured for flow speeds up

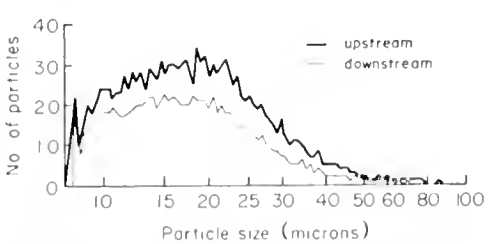

Figure 6. Size-frequency distribution of one set of upstream-downstream water samples from the field for a 15 cm sea pen in 6 cm s^{-1} flow. The total number of particles in 1 ml subsamples are shown. Note the similarity in curves; the size-frequency distributions are not significantly different (G-test for goodness of fit, G = 80.5, $\chi^2_{0.95[7]}$ = 93.9, $P > 0.1$).

Table I

Laboratory feeding experiments: differences in particle size distributions between paired upstream-downstream water samples

Ambient flow speed	Mean particle size (μm) Up	Down	G-test
1.0 cm s^{-1}	9.6	9.6	95.6*
	10.1	9.7	219.0*
	10.3	9.7	168.4*
	$\bar{x}$ = 10.0	9.7	
3.0 cm s^{-1}	10.1	9.6	195.6*
	10.3	9.6	231.2*
	10.3	9.9	377.8*
	$\bar{x}$ = 10.2	9.7	
6.0 cm s^{-1}	10.4	10.0	146.1*
	10.2	9.9	145.1*
	10.6	9.9	276.5*
	$\bar{x}$ = 10.5	9.9	

Means for each water sample are based on a count of 10,000 particles from natural filtrate. G-test for goodness of fit used to compare frequency distribution of 75 particle size classes (1–100 μm) of upstream and downstream water samples. G-test, $\chi^2_{.05[73]} = 93.9$, * significant at $\alpha = 0.05$.

around the polyps, coupled with polyp density, influence the size range of particles retained by the filter.

Size, flexibility, and volume flow rate

In many benthic communities, occupation of space above the substratum is at a premium (Jackson and Buss, 1975; Jackson, 1977; Sutherland and Karlson, 1977). Access to flow for these benthic organisms will depend on their protrusion above the substratum and the projected area of the filtering appendages relative to the flow direction. Volume flow rates are dependent on ambient flow speed and filter size, both of which increase as the organism grows. Volume flow rate refers to the volume of water which passes through the filter "boundary" of an organism per unit time.

For a sea pen, the volume flow rates initially increase with increasing flow speed, but then peak and decline due to deformation of the organism. The maximum volume flow rate and the ambient velocity at which it occurs are both dependent on organism size. As the animal bends in the flow, more water passes over it rather than

to 6 cm s^{-1} in the laboratory, filtering efficiency values for higher flow speeds were estimated to decrease to 20% in the absence of rachis deformation (closed circles). From the field experiments, efficiencies are known to remain around 30% (represented by open circles), probably due to a decrease in filter porosity as the rachis bends downstream. Feeding rate is largely determined by volume flow rate (compare Fig. 7 with Fig. 3); with increasing flow speed feeding initially increases, peaks, then decreases.

Discussion

Structure-flow interactions

Structure-flow interactions are important to suspension feeders which depend on relative movement of food particles past a filtering structure. (1) In flexible organisms, the drag forces on the organism will change the shape and vertical stance of the filter. These drag forces are dependent on the filter shape, size, orientation, and flexibility. The absolute (rachis height) and relative (degree of bending) vertical stance of the filter determine the volume of water flowing through the filter. (2) Flexibility regulates the speed and pattern of the flow past the filtering structures, and thus filtering efficiency. Efficiency depends on the packing array and density of polyps, which can change with ambient velocity. (3) Flow patterns

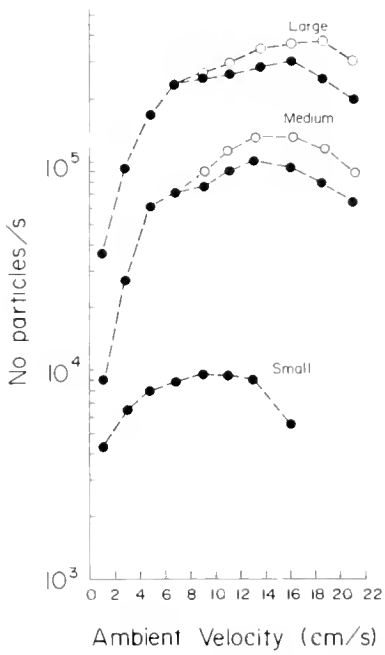

Figure 7. Feeding rate as a function of flow speed and rachis deformation. Using the determinations of volume flow rate and filtering efficiency, feeding rates of a large (rachis = 24 cm), medium (rachis = 15 cm), and small (rachis = 8 cm) sea pen are shown. Open circles represent feeding rates calculated using 30% efficiency at the higher flow speeds, as recorded in the field for medium and large sea pens; closed circles beneath the open circles represent feeding rates assuming that efficiency would continue to decrease to 20% at the higher flow speeds in the absence of rachis deformation.

through the rachis. Rachis flexibility prevents drag from rising exponentially (Best, in prep.), maintains lower velocities through the filter and past the polyps, and changes the porosity (polyp density) of the filter. Parameters influencing velocity advance—such as filter shape and size, drag, and structures resisting drag, are discussed in detail in Best (in prep.).

Ambient velocity, filter porosity, and filtering efficiency

Filtering efficiency, in engineering vernacular, is defined as the number of particles contacting a fiber relative to the number of particles which would have passed through the fiber area had the fiber not been there to divert streamlines (Fuchs, 1964; Spielman, 1977). Most biological filters are a composite of fibers of various dimensions and configurations that can change with organism growth and ambient flow. A more usable definition of efficiency for biological filters is the proportion of particles retained from a given volume of water within an organism's "access" to flow. For filters perpendicular to steady flows, access is the volume of water which passes through the filter's boundary. For filters perpendicular to oscillating flows or oriented parallel to flows, access is the volume of water passing sufficiently close to the filter from which particles *may* be extracted. Filtering efficiency depends on the position of fluid streamlines around the filtering elements and the particle paths around the filtering elements.

Rubenstein and Koehl (1977) were the first to compare filtering structures of aquatic organisms to manmade aerosol filters that have the potential of capturing particles by a number of non-sieving mechanisms (*e.g.*, Fuchs, 1964). Spielman (1977) extended the engineering analysis of particle capture by filters in aqueous media, leading to predictive models of the mechanisms, nature, and size of particles captured by these filters. The primary mechanism of particle capture for many biological filters appears to be by direct interception, aided possibly by electrostatic or London-van der Waals forces (for review see LaBarbera, 1984). This mechanism has been used to explain particle capture by brittle stars (LaBarbera, 1978), crinoids (Meyer, 1979), aquatic insects (Craig and Chance, 1981; Silvester, 1983), and cnidarians (Koehl, 1977; Patterson, 1984). As originally developed for *airborne* particles, capture by direct interception assumes that the center of a neutrally buoyant particle follows an undisturbed streamline around a filtering fiber; if the streamline and the center of the particle pass within one particle radius of a fiber, contact occurs and the particle is retained. As a *waterborne* particle approaches a fiber, it must deviate from the undisturbed streamline due to the slow drainage of fluid from the gap between the surfaces as the particle and fiber approach (Spielman, 1977). For contact to occur in aqueous media, the action of attractive forces (electrostatic or van der Waals forces) must be invoked to overcome the slow, viscous drainage. If the center of the particle passes within some critical distance, the attractive forces will be sufficient to insure contact with the fiber (Spielman, 1977). These models apply to single fibers and assume that all particles contacting the fiber remain caught.

In a test of Spielman's theories, LaBarbera (1984) found relatively good agreement between the predicted and actual size distribution of Sephadex beads (40–360 μm) caught by the brittle star *Ophiopholis aculeata*. Disagreements between observed and predicted distributions may be due to two factors. First, the model assumes a single filtering fiber, but brittle stars use an array of pinnules, resulting in flow interaction and changes in the direction of streamlines (Fuchs, 1964). Second, it is assumed that all particles contacting the fiber remain caught; this assumption has not been tested for a biological filter, especially when large active particles, such as zooplankton, are caught.

Direct interception is inversely dependent on flow velocity (Spielman, 1977). Contrary to the volume flow rate, filtering efficiency decreases with an increase in ambient flow speed, as shown in the laboratory experiment. In this laboratory experiment, I used a maximum flow speed of 6.0 cm s^{-1}. At speeds faster than this, the sea pen in the flow tank would begin to bend back significantly, increasing polyp density, and thus altering the geometry of the filter by compressing the polyps closer together. The laboratory experiment showed that, for a given porosity filter, a decrease in particle retention occurs with increasing ambient velocity.

The filtering network of *Ptilosarcus gurneyi* is not strictly two-dimensional. Water entering the rachis first passes between the leaves, and a velocity profile is established with the faster flow down the middle. On the downstream edge of the organism, the polyps extend between the leaves into the faster flow. The polyps, and their tentacles and pinnules, are oriented slightly downstream in such a way that they continually bisect the velocity distribution. In this way, the filtering elements are placed in the regions of "unfiltered" water, increasing the probability of particle contact.

In the field experiments, it was found that the medium and large sea pens had higher filtration efficiencies than the small sea pen, even though they were exposed to higher ambient flow speeds above the substratum. Under ambient flow, polyp density is higher in the larger sea pens, resulting in a lower "porosity" or spacing between the polyps. A lower filter porosity would increase the total filtering surface in a given volume, reduce the velocity

profile between neighboring filtering elements, and decrease the distance between particle streamlines and the element's surface. As ambient flow speed increased, sea pens are bent back by the flow, compressing the downstream array of polyps and decreasing porosity further. Structure-flow interactions therefore result in a "variable porosity filter" which can maintain a higher efficiency at higher ambient flow speeds.

Particle size selection

A review of Figure 6 reveals that, overall, the size distribution of particles retained follows closely the size distribution in ambient water. In fact, in the feeding experiments conducted in the field, there was no difference between upstream and downstream water samples in size distribution of particles. There was a difference detected in the laboratory experiments, perhaps because of the higher particle counts used to construct the distributions (10,000 particles in laboratory experiments *versus* 1500–3000 particles in field experiments). Although there was a preference towards the retention of larger particles in the laboratory experiments here and in LaBarbera's (1984) study with brittle stars, the distribution of particles retained still closely follows the availability of particles. There is no steep demarcation or stepped character in the distribution. Due to the mechanisms of particle capture operating in aqueous media, and the abundance of small particles in natural seawater (McCave, 1984), a high degree of selectivity for large particle sizes, to the exclusion of small particles, appears to be precluded. Whether or not an organism feeds on the small particles of detritus and phytoplankton in the sea, its filter will tend to collect these particles.

Feeding performance

Feeding performance is dependent on flow velocity in bryozoans (Okamura, 1984, 1985) and octocorals (Leversee, 1976; Patterson, 1984), and on swimming speed in juvenile fish (Friedland *et al.*, 1984). In the flexible bryozoans and octocorals studied, colony shape changed with ambient velocity; bryozoan branches collapsed inward and downstream (Okamura, 1984), while in octocorals individual polyps bent downstream (Patterson, 1984). These structural changes can influence feeding performance by altering both volume flow rate and filtering efficiency—two parameters influenced by ambient velocity and resulting structure-flow interactions. In this study I examined these two parameters independently. Feeding rate in the sea pen *Ptilosarcus gurneyi* is highly dependent on volume flow rate. Both feeding rate and volume flow rate initially increase sharply as flow speed increases, and then decrease as the upright posture decreases. Small sea pens have a lower feeding rate because of lower volume flow rates, due to smaller filters and lower ambient flow speeds near the substratum in the boundary layer. Filtering efficiency decreases with increasing flow speed, which may be compensated for by a change in filter porosity; polyps become more closely packed as flow speed increases.

Because feeding rate is dependent on a complex interplay of volume flow rates, filtering efficiencies, organism size and flexibility, and ambient velocity, competitive feeding interactions between organisms may be due not only to direct reduction of resource supplies, but may also be mediated by altering the ambient velocity. In the arborescent bryozoan *Bugula stolonifera*, Okamura (1984) found that feeding success in small colonies was reduced by both fast ambient flows and the presence of a large colony upstream. In the first case, fast ambient flows may have resulted in lower volume flow rates or reduced efficiencies. In the second case, the larger colony upstream may have depleted particles in the ambient water, or restricted the volume of water passing through the smaller colony.

Acknowledgments

I thank K. Loudon, S. Vogel, J. Voltzow, and S. Wainwright for their stimulating discussions and suggestions. The penultimate draft of the manuscript was improved by the helpful comments of two anonymous reviewers. This work was supported by a Cocos Foundation Training Grant in Morphology Grant and a Lerner-Gray Fund for Marine Research Grant.

Literature Cited

Best, B. A. 1985. An integrative analysis of passive suspension feeding: the sea pen *Ptilosarcus gurneyi* as a model organism. Ph.D. Dissertation, Duke University, Durham, NC.

Birkeland, C. 1969. Consequences of differing reproductive and feeding strategies for the dynamics of an association based on the single prey species, *Ptilosarcus gurneyi* (Gray). Ph.D. Dissertation, Univ. of Washington, Seattle, WA.

Birkeland, C. 1974. Interactions between a sea pen and seven of its predators. *Ecol. Monogr.* **44:** 211–232.

Chamberlain, J. A., and R. R. Graus. 1975. Water flow and hydromechanical adaptations of branched reef corals. *Bull. Mar. Sci.* **25(1):** 112–125.

Craig, D. A., and M. M. Chance. 1981. Filter feeding in larvae of Simuliidae (Diptera:Culicomorpha): aspects of functional morphology and hydrodynamics. *Can. J. Zool.* **60:** 712–724.

Friedland, K. D., L. W. Haas, and J. V. Merriner. 1984. Filtering rates of the juvenile menhaden *Brevoortia tyrannus* (Pisces:Clupeidae), with consideration of the effects of detritus and swimming speed. *Mar. Biol.* **84:** 109–117.

Fuchs, N. A. 1964. *Mechanics of Aerosols.* Pergamon, NY.

Gerritsen, J., and K. G. Porter. 1982. The role of surface chemistry in filter feeding by zooplankton. *Science* **216:** 1225–1227.

Gudmundsson, J. S. 1981 ...ate fouling. Pp. 357–387 in *Fouling of Heat Exchangers*, L. F. Somerscales and J. G. Knudsen, eds. Hemisphere.

Harvell, C. D., and N. ...arbera. 1985. Flexibility: a mechanism for control of ...es in hydroid colonies. *Biol. Bull.* **168**: 312–320.

Jackson, J. B. C. 1977. Habitat area, colonization, and development of epibenthic community structure. Pp. 349–358 in *Benthic Marine Organisms*, B. F. Keegan, P. O. Ceidigh, and P. J. Broaden, eds. Pergamon Press, Oxford.

Jackson, J. B. C., and L. W. Buss. 1975. Allelopathy and spatial competition among coral reef invertebrates. *Proc. Natl. Acad. Sci. U.S.A.* **72**: 5160–5163.

Koehl, M. A. R. 1976. Mechanical design in sea anemones. Pp. 23–31 in *Coelenterate Ecology and Behavior*, G. O. Mackie, ed. Plenum Press, NY.

Koehl, M. A. R. 1977. Effects of sea anemones on the flow forces they encounter. *J. Exp. Biol.* **69**: 87–105.

LaBarbera, M. 1978. Particle capture by a Pacific brittle star: experimental test of the aerosol suspension feeding model. *Science* **201**: 1147–1149.

LaBarbera, M. 1984. Feeding currents and particle capture mechanisms in suspension feeding animals. *Am. Zool.* **24**: 71–84.

LaBarbera, M., and S. Vogel. 1976. An inexpensive thermistor flowmeter for aquatic biology. *Limnol. Oceanogr.* **21**: 750–756.

Leversee, G. J. 1976. Flow and feeding in fan-shaped colonies of the gorgonian coral, *Leptogorgia*. *Biol. Bull.* **151**: 344–356.

McCave, I. N. 1984. Size spectra and aggregation of suspended particles in the deep ocean. *Deep-Sea Res.* **31(4A)**: 329–352.

Merz, R. A. 1984. Self-generated versus environmentally produced feeding currents: a comparison for the Sabellid polychaete *Eudistylia vancouveri*. *Biol. Bull.* **167**: 200–209.

Meyer, D. L. 1979. Length and spacing of the tube feet in crinoids (Echinodermata) and their role in suspension-feeding. *Mar. Biol.* **51**: 361–369.

Nowell, A. R. M., and P. A. Jumars. 1984. Flow environments of aquatic benthos. *Annu. Rev. Ecol. Syst.* **15**: 303–328.

Okamura, B. 1984. The effects of ambient flow velocity, colony size, and upstream colonies on the feeding success of bryozoa. I. *Bugula stolonifera* Ryland, an arborescent species. *J. Exp. Mar. Biol. Ecol.* **83**: 179–193.

Okamura, B. 1985. The effects of ambient flow velocity, colony size, and upstream colonies on the feeding success of bryozoa. II. *Conopeum reticulum* (Linnaeus), an encrusting species. *J. Exp. Mar. Biol. Ecol.* **89**: 69–80.

Okamura, B. 1987. Particle size and flow velocity induce an inferred switch in bryozoan suspension-feeding behavior. *Biol. Bull.* **173**: 222–229.

Patterson, M. R. 1984. Patterns of whole colony prey capture in the octocoral, *Heteroxenia fuscescens*. *Biol. Bull.* **167**: 613–629.

Rubenstein, D. I., and M. A. R. Koehl. 1977. The mechanisms of filter feeding: some theoretical considerations. *Am. Nat.* **111**: 981–994.

Silvester, N. R. 1983. Some hydrodynamic aspects of filter-feeding with rectangular-mesh nets. *J. Theor. Biol.* **103**: 265–286.

Sutherland, J. P., and R. H. Karlson. 1977. Development and stability of the fouling community at Beaufort, N. C. *Ecol. Monogr.* **47**: 425–446.

Spielman, L. A. 1977. Particle capture from low-speed laminar flows. *Annu. Rev. Fluid Mech.* **9**: 297–319.

Vogel, S. 1981. *Life in Moving Fluids: The Physical Biology of Flow*. Willard Grant Press, Boston. 357pp.

Vogel, S. 1984. Drag and flexibility in sessile organisms. *Am. Zool.* **24**: 37–44.

Vogel, S., and M. LaBarbera. 1978. Simple flow tanks for research and teaching. *Bioscience* **28**: 638–643.

Wainwright, S. A., and J. R. Dillon. 1969. On the orientation of sea fans. *Biol. Bull.* **136**: 130–139.

Reference: *Biol. Bull.* **175**: 343–348. (December, 1988)

Discocilia and Paddle Cilia in the Larvae of *Mulinia lateralis* and *Spisula solidissima* (Mollusca: Bivalvia)

BERNARDITA CAMPOS[1] AND ROGER MANN[2,*]

[1]*Institute of Oceanology, University of Valparaiso, P.O. Box 13-D, Vina del Mar, Chile, and* [2]*Virginia Institute of Marine Science, School of Marine Science, The College of William and Mary, Gloucester Point, Virginia 23062*

Abstract. The bivalve larval velum contains four bands of cilia: inner and outer preoral bands, an adoral band, and a postoral band. The preoral bands of compound cilia are generally considered to be used for both locomotion and food gathering. The adoral and postoral bands function in concert with the preoral bands in food gathering and transfer of food to the mouth. Cilia are usually described as cylindrical structures which taper to a blunt tip. Modified cilia with disc-shaped (discocilia) or paddle-shaped ends have been recorded in several invertebrate species. Here, for the first time, we demonstrate the presence of discocilia in the velum of *Mulinia lateralis* and paddle cilia in the velum of *Spisula solidissima*. Such cilia are restricted to the preoral bands and the central ciliary tuft. The presence of such cilia does not appear to increase the swimming velocity of these larvae in comparison to that of *Rangia cuneata* larvae of similar size. The possibility that these modified cilia have enhanced sensory capability remains to be tested.

Introduction

The larvae of bivalve molluscs are one of the major components of the meroplankton (Thorson, 1950). Most bivalve larvae develop from the fertilized egg to the veliger stage in twenty four hours or less. The veliger larva is characterized by a soft body enclosed by laterally compressed, semitransparent, paired valves and a protruding, oval, ciliated velum. The velum contains four bands of cilia: inner and outer preoral bands, an adoral band, and a postoral band (Elston, 1980; Waller, 1981). The preoral bands, consisting of compound cilia 20–80 μm long, are responsible for locomotion and food gathering. The adoral band, of shorter cilia approximately 8 μm long, transfer food particles to the mouth. The postoral band consists of complex cilia 15–20 μm in length. The efficiency of food concentration from the water depends on the harmonic beating of the preoral and postoral bands of cilia (Strathmann *et al.*, 1972; Strathmann and Leise, 1979).

Cilia are generally considered to be cylindrical structures with a constant diameter except for a tapering, blunt distal tip (Sleigh and Blake, 1977). Morphologically different cilia, discocilia, have been described for the polychaete *Lanice conchilega* (Pallas, 1776) by Heimler (1978). Tamarin *et al.* (1974) described cilia with "biconcave flattened discs or paddles," 1.33 μm in diameter in the ventral pedal groove of the juvenile mussel *Mytilus californianus* (Conrad, 1837) and ascribed to them a secretory function of adhesive material. Arnold and Williams-Arnold (1980) described discocilia in the embryo of the squid *Loligo pealei* (Lesueur, 1821); Matera and Davis (1982) observed paddle cilia in the rhinophore of the marine gastropod *Pleurobranchaea californica* (MacFarland, 1966); and ÓFoighil (1985) described papillae bearing cilia with bulbous tips of approximately 0.25 μm diameter in the mantle fold of temporary dwarf males of the bivalve *Pseudophythina rugifera* (Carpenter, 1864). In this report we describe, for the first time, the presence of modified cilia in the velum of larvae of two marine bivalves, the mactrids *Mulinia lateralis* (Say, 1882) and *Spisula solidissima* (Dillwyn, 1817).

Received 8 August 1988; accepted 29 September 1988.

* To whom correspondence should be sent.

Contribution number 1481 from the Virginia Institute of Marine Science, The College of William and Mary.

Materials and Methods

Mulinia lateralis adults were obtained from a cultured population at the Eastern Shore Laboratory of the Virginia Institute of Marine Science (VIMS), Wachapreague, VA. *Spisula solidissima* adults were obtained from a commercial fishing dock at Willis Wharf, VA. For comparison purposes a third mactrid, *Rangia cuneata* (Gray, 1831), was collected from the Rappahannock River, VA. All adult bivalves were maintained at the VIMS Wachapreague laboratory in water of appropriate salinity: 30 ppt for the marine stenohaline *S. solidissima*, 25 ppt for the euryhaline *M. lateralis*, and 10 ppt for the oligohaline *R. cuneata*. Adults were induced to spawn by thermal stimulation (24, 28, and 32°C for *S. solidissima*, *M. lateralis*, and *R. cuneata*, respectively). Larvae were cultured using the procedures of Culliney *et al.* (1975) and Chanley (1981) at the salinity of adult maintenance and temperatures of 23°C for *S. solidissima* and *M. lateralis*, and 25°C for *R. cuneata*. Water was changed every other day, at which time larvae were fed on mixtures of the phytoplankters *Pavlova* (*Monochrysis*) *lutheri* (Droop Green) (formerly *Monochrysis lutherii* Droop), *Isochrysis galbana* Parke, and *Isochrysis* aff. *galbana* (clone T-Iso). General procedures for phytoplankton culture followed the guidelines of Guillard (1983).

Preparation of larvae for scanning electron microscopy (SEM) followed the guidelines of Turner and Boyle (1975). Umbo stage larvae were siphoned from the culture container, retained on a 63 μm nylon mesh screen, thoroughly rinsed in 0.45 μm filtered water of the appropriate salinity, transferred to 10 ml of filtered seawater and relaxed by sequential additions of 1 ml of 8% (w/v) $MgCl_2$ in distilled water. Osmolarity of final relaxing solutions was not measured but relaxation was typically obtained following addition of 3–4 ml of $MgCl_2$ solution. Larvae were concentrated by centrifugation, and fixed for 2 hours with 2.5% chilled glutaraldehyde in distilled water buffered at pH 7.2 with 0.1 *M* sodium cacodylate. The fixative was subsequently pipetted off and the larvae subjected to three rinses, of 30 minutes each, of 3 ml of 0.1 *M* sodium cacodylate in 0.25 *M* NaCl. Larvae were post fixed for one hour in 5 ml of 1% OsO_4 in 0.19 *M* NaCl buffered at pH 7.2 with sodium cacodylate. Larvae were again rinsed, three times, in 0.1 *M* sodium cacodylate in 0.15 *M* NaCl, and stored overnight at 4°C. Dehydration was effected by 20-min exposures to a graded alcohol series (30, 50, 70, 90, 95, and 100%) followed by three changes in 100% acetone. Critical point drying was effected using a model 3000 Polaron dryer. Larvae were mounted on stubs using double sided adhesive tape, dessicated for a further 24 hours, coated with gold-palladium, and examined with an AMR model 1000 scanning electron microscope. Photographs were made with Polaroid 52 film.

Results

Figures 1 through 3 illustrate, with increasing magnification, the comparative morphology of the velum of the three species examined. In all species the postoral band consists of "typical" cylindrical cilia with distally tapering, blunted tips (Fig. 1A–C); however, the preoral bands exhibit species-specific differences. *Rangia cuneata* exhibit, again, "typical" cilia (Fig. 1C). The distal portions of the preoral cilia of *Spisula solidissima* and *Mulinia lateralis* terminate in biconcave paddles (Figs. 1A, 2A, 3A) or slightly inflated discs (discocilia, see Figs. 1B, 2B, 3B), respectively, the terminal structures measuring approximately 1–1.3 μm in diameter. A single preoral cilia in *M. lateralis* was observed with the disc 1–2 μm distal to the tip (Fig. 3B). The preoral cilia appear clustered and conform to the description of compound cilia as given by Waller (1981). The central ciliary tufts of the velum (Fig. 4) further exhibit species-specific cilia morphology; "typical" compound cilia in *R. cuneata* (Fig. 4B), cilia with terminal paddles in *S. solidissima*, and a mixture of cilia with terminal discs and discs 1–2 μm distal to the cilia tip in *M. lateralis* (Fig. 4A). In all three species the diameter of the ciliary shaft was between 0.2 and 0.4 μm.

Discussion

The comparatively rare occurrence of modified cilia in the animal kingdom prompts the question as to whether their presence is the result of artifacts during preparation for examination. Indeed, Ehlers and Ehlers (1978), examining flatworms, concluded that both paddle cilia and discocilia were absent in untreated tissue, but appeared only as artifacts after exposure to formaldehyde, sodium phosphate, and sodium cacodylate during preparation for SEM. Bergquist *et al.* (1977) contend that modified cilia observed in sponge larvae are real structures. Matera and Davis (1982), after a comprehensive study of *Pleurobranchaea californica* using light and transmission and scanning electron microscopy, rejected the conclusion of Ehlers and Ehlers (1978), noting that the paddle cilia can be seen with light microscopy in isosmotic seawater and made to straighten reversibly by exposure to hypertonic seawater. We also reject the conclusion of Ehlers and Ehlers (1978). In the present study discocilia or paddle cilia were a consistent characteristic of particular cilia bands within a species but not characteristic of the whole velum. Uniformity of cilia morphology throughout the velum, an observation consistent with the hypothesis of artifactural production during SEM preparation, was not

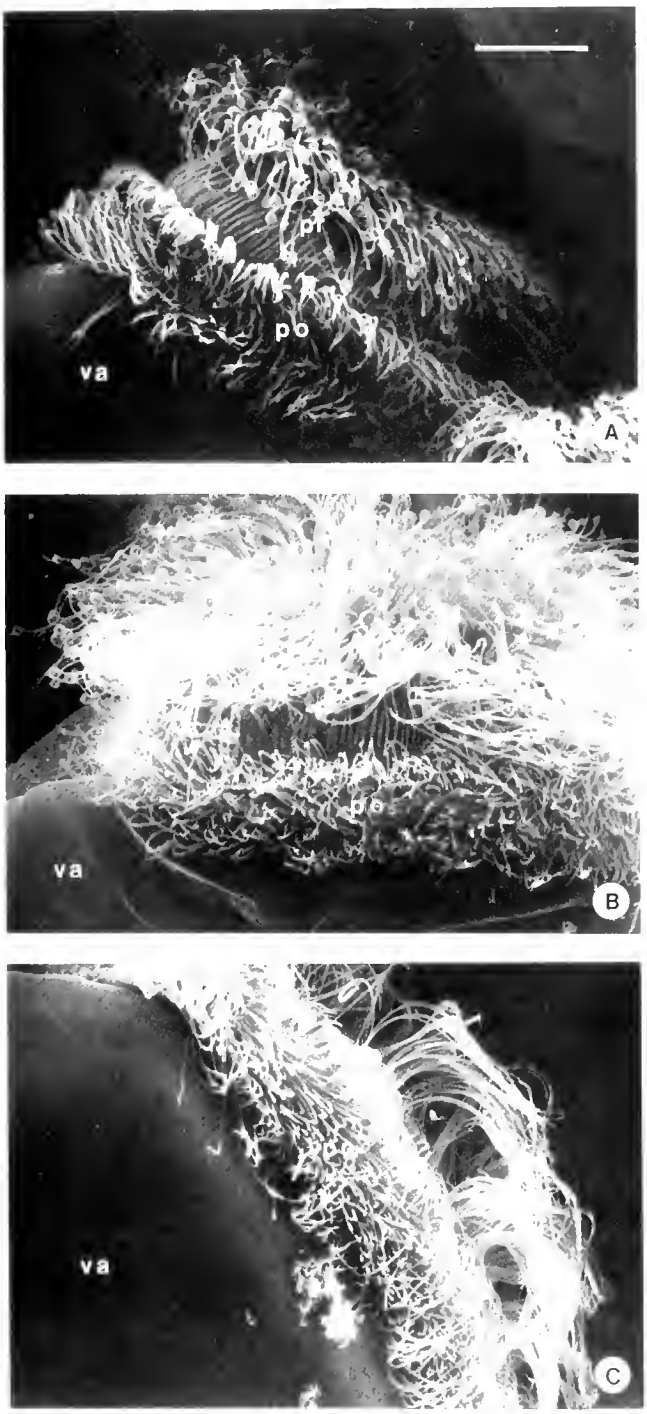

Figure 1. Scanning electron micrographs of the velum of (A) *Spisula solidissima*, (B) *Mulinia lateralis*, and (C) *Rangia cuneata* larvae. pr, preoral cilia; po, postoral cilia; va, valve. Scale bar = 20 μm

observed. The larvae used in this study were cultured at different salinities. The osmolarities of the final relaxing solutions were therefore different; however, larvae were fixed and subsequently processed identically and, in most instances, simultaneously. The question remains as to whether cilia morphology in these species will change with changing salinity; however, the ecological signifi-

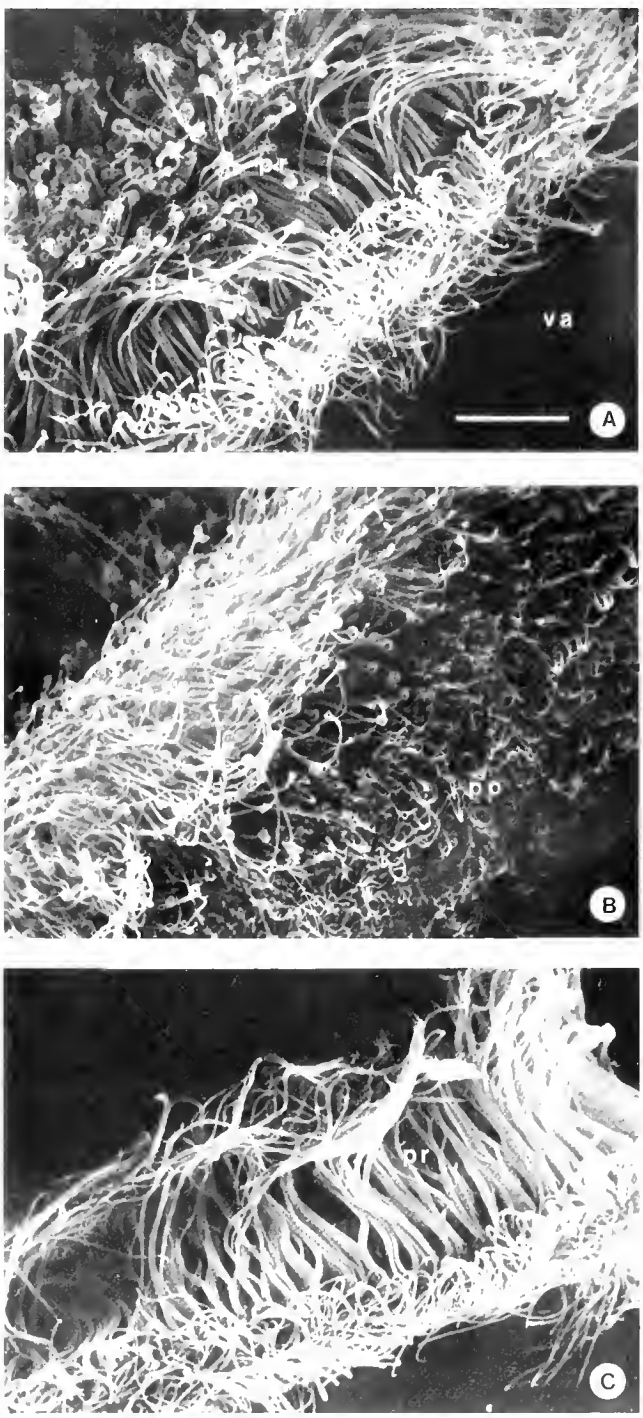

Figure 2. Scanning electron micrographs of the velum of (A) *Spisula solidissima*, (B) *Mulinia lateralis*, and (C) *Rangia cuneata* larvae. Details of the ciliary bands. pr, preoral cilia; po, postoral cilia; va, valve. Scale bar = 10 μm

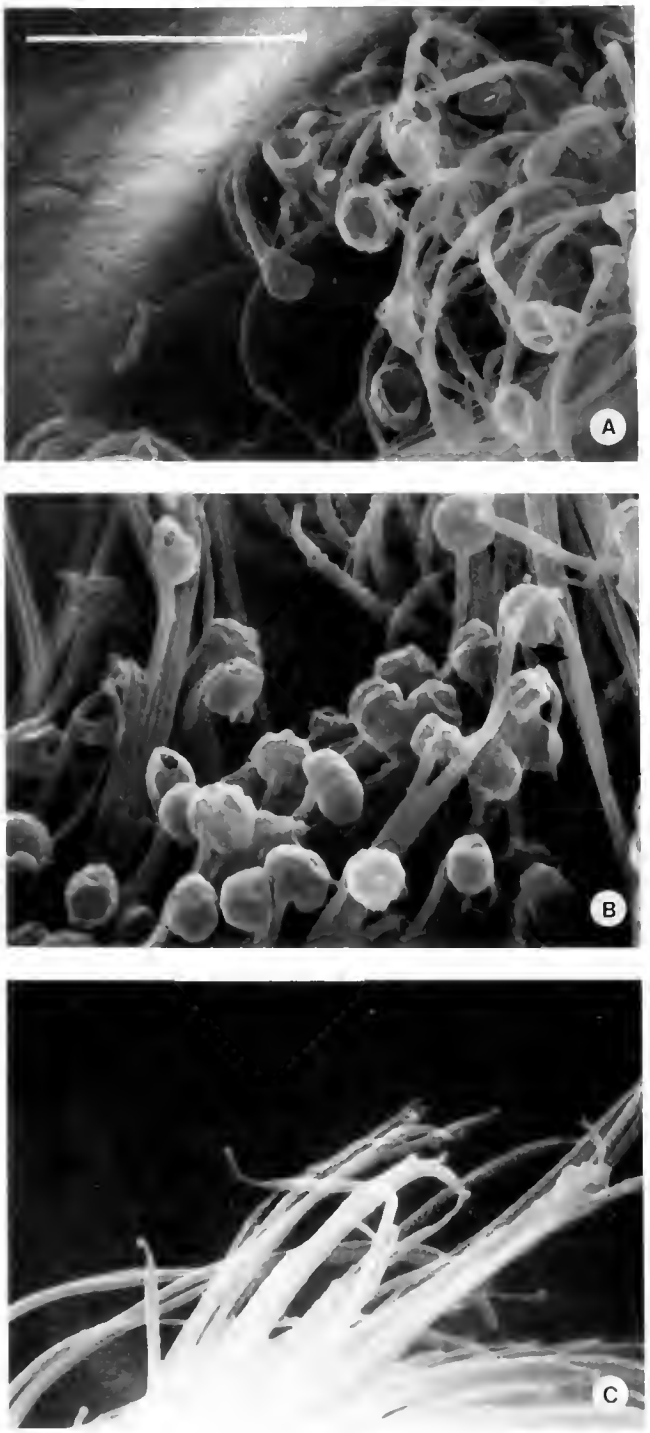

Figure 3. Scanning electron micrographs of the preoral velar cilia tips of (A) *Spisula solidissima*, (B) *Mulinia lateralis*, and (C) *Rangia cuneata* larvae. Note the biconcave paddles in *S. solidissima* and the terminal discs in *M. lateralis*. Arrow identifies a single disc distal to the cilia tip in *M. lateralis*. Scale bar = 10 μm.

cance of this question is probably minimal in that both the larvae and adults of these species exhibit distinctly different salinity optima (Campos, 1988) which are reflected in the culture conditions used here. In summary, we believe the paddle and discocilia described here to be genuine structures.

The function of the modified velar cilia is debatable. Matera and Davis (1982) concluded that previous literature "collectively indicate that dilations of ciliary membranes represent a common morphological specialization subserving chemosensation." The structures described by ÓFoighil (1985) are also appropriately located for sensory function. However, they are slightly smaller than previously described cilia modifications. Only the "secretory" cilia described by Tamarin *et al.* (1974) are thought to have a primary function that is other than sensory. As mentioned earlier, the primary function of the preoral bands in the bivalve larval velum is generally considered to be in locomotion and food gathering. The sensory function has received little attention; however, consideration of veliger swimming behavior, wherein larvae progress in a vertically oriented helix with the velum extended in the direction of motion (see Cragg and Gruffydd, 1975; Cragg, 1980; Mann and Wolf, 1983), suggests that such a function is reasonable. The ability to combine locomotion and chemosensation to direct oriented movement along a gradient of chemostimulant has yet to be demonstrated in bivalve larvae. Chemosensory responses associated with settlement and metamorphic inducers have been demonstrated in well-mixed laboratory containers (*e.g.*, Coon *et al.*, 1985), but responses to gradients *per se* remain untested. Despite the apparent lack of an organized nervous system in velar tissue Elston (1980) suggests that "a cell to cell transmission of impulses" would fulfill this sensory function.

The presence of paddle or discocilia do not appear to enhance rate of movement in the species examined here. In larger animals, paddle structures would generally be considered advantageous in overcoming drag and enhancing propulsion. Pelagic bivalve veliger larvae generally range in size from 75 to 400 μm maximum dimension and move at absolute velocities of less than 10 mm s^{-1}. At this size and velocity, Reynolds numbers are less than or approach 1, a region where viscous forces predominate in determining maximal velocity (see Vogel, 1981). In a complementary study (Campos, 1988) a comparison of rates of vertical displacement (time to ascend through a unit vertical distance while swimming in a helical pattern) was made for three size ranges of larvae for each of the species examined here at the temperature and salinity of culture. The "D" or straight hinge veliger larvae of *R. cuneata*, *M. lateralis*, and *S. solidissima* exhibited mean (n = 25) rates of 0.38, 0.25, and 0.26 mm s^{-1}, respectively. Comparable values for umbone larvae were 0.49, 0.49, and 0.40 mm s^{-1}, respectively. Mean values for pediveliger larvae of the three species were 0.45, 0.34, and 0.40 mm s^{-1}, respectively. Despite the

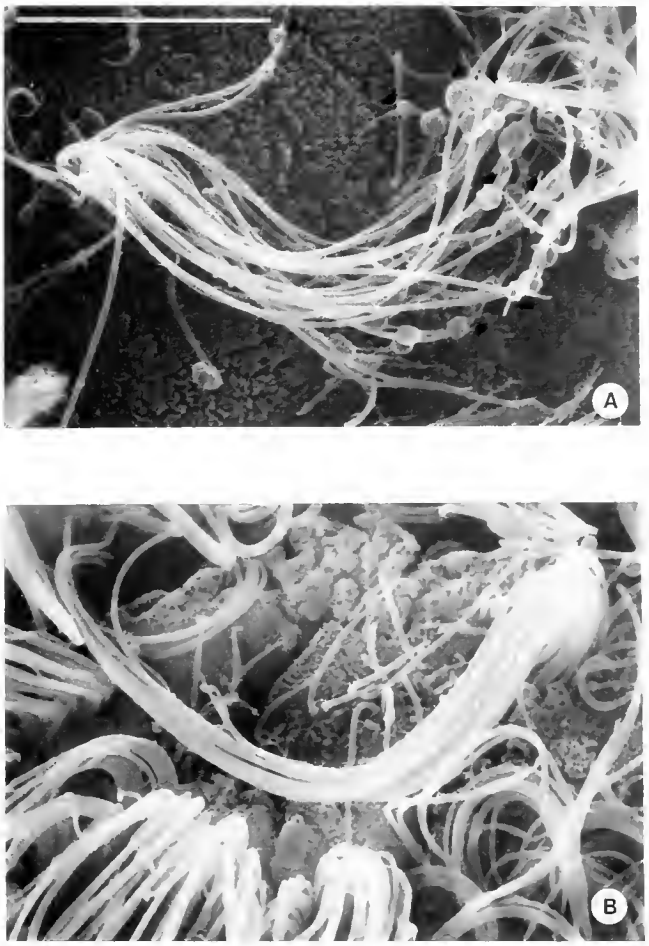

Figure 4. Scanning electron micrographs of the central ciliary tuft of (A) *Mulinia lateralis* and (B) *Rangia cuneata* larvae. Note the presence of both terminal discs and discs distal to the cilia tip (see arrows) in *M. lateralis*. Scale bar = 5 μm

fact that interspecific comparison is confounded by minor differences in morphometry, size, and, we suspect, specific gravity of larval stages, it is evident that the presence of discocilia and paddle cilia in *M. lateralis* and *S. solidissima*, respectively, does not apparently confer higher rates of vertical displacement when compared with *R. cuneata*. We did not compare absolute velocity (that which describes movement along the helical path rather than just vertical displacement) in the swimming study. Nonetheless, the ecologically meaningful value for vertical displacement (see discussion in Mann, 1986) suggests that the presence of modified cilia is not accompanied by greater ability to depth regulate in stratified water columns, an arguable advantage to any larvae encountering estuarine or shallow coastal environments.

Examination of previous descriptions of larvae or larval velar morphology for *Crassostrea virginica* Gmelin (Elston, 1980), *Ostrea edulis* Linne (Waller, 1981), and *Arctica islandica* Linne (Lutz *et al.*, 1982) have failed to demonstrate the presence of velar paddle cilia or discocilia—although in fairness only Waller (1981) provides micrographs of sufficient magnification and appropriate content for definitive statements. The taxonomic significance of these structures is also debatable. A significant component of bivalve taxonomy has historically focussed on adult shell characteristics and the present focus of larval taxonomy is on valve morphometry and hinge ultrastructure (see comments in Lutz *et al.*, 1982). Yet within one family, the Mactridae, we have examined three phylogenetically associated species and demonstrated the presence of three distinct cilia morphologies, each unique to one species. Clearly, determination of the frequency of occurrence, function, and taxonomic significance of these modified cilia in the bivalve larval velum awaits further investigation.

Acknowledgments

This work was supported in part by a Fulbright Fellowship to Bernardita Campos and funds provided by the Council on the Environment, Commonwealth of Virginia. We thank Prof. Ruth D. Turner for useful discussion on larval morphology, Mr. Michael Castagna for encouragement and use of facilities at the Wachapreague laboratory, Ms. Patrice Mason for assistance in electron microscopy, and an anonymous reviewer for constructive criticism of the manuscript.

Literature Cited

Arnold, J. M., and L. D. Williams-Arnold. 1980. Development of the ciliature pattern on the embryo of the squid *Loligo pealei*: a scanning electron microscope study. *Biol. Bull.* **159:** 102–116.

Bergquist, P. R., C. R. Green, M. E. Sinclair, and H. S. Roberts. 1977. The morphology of cilia in sponge larvae. *Tissue Cell* **9:** 179–184.

Campos, B. 1988. Swimming responses of larvae of three mactrid bivalves to different salinity gradients. M. A. thesis, College of William and Mary, Williamsburg, Virginia. 115 pp.

Chanley, M. H. 1981. Laboratory culture of marine bivalve molluscs. Pp. 233–249 in *Marine Invertebrates. Laboratory Animal Management*. National Academy Press, Washington, DC.

Coon, S. L., D. B. Bonar, and R. M. Weiner. 1985. Induction of settlement and metamorphosis of the Pacific oyster, *Crassostrea gigas* (Thunberg), by L-DOPA and catecholamines. *J. Exp. Mar. Biol. Ecol.* **94:** 211–221.

Cragg, S. M. 1980. Swimming behaviour of the larvae of *Pecten maximus* (L.) (Bivalvia). *J. Mar. Biol. Assoc. U. K.* **60:** 551–564.

Cragg, S. M., and Lld. Gruffydd. 1975. The swimming behaviour and pressure responses of the veliconcha larvae of *Ostrea edulis* L. Pp. 43–57 in *Proceedings 9th European Marine Biology Symposium*, H. Barnes, ed. Aberdeen University Press, Aberdeen, Scotland.

Culliney, J. L., P. J. Boyle, and R. D. Turner. 1975. New approaches and techniques for studying bivalve larvae. Pp. 257–271 in *Culture of Marine Invertebrate Animals*, W. Smith and M. Chanley, eds. Plenum Press, New York-London.

Ehlers, U., and B. Ehlers. 1978. Paddle cilia and discocilia—genuine structures? *Cell Tiss. Res.* **192:** 489–501.

Elston, R. 1980. Functional anatomy, histology and ultrastructure of

the soft tissues of the [illegible] ster *Crassostrea virginica* *Proc. Natl. Shellf. [illegible]* 93.

Guillard, R. R. 1983. [illegible] toplankton for feeding marine invertebrates. In *Nature of Marine Invertebrates*, C. J. Berg, ed. Hat[illegible] Publ. Co., Pennsylvania.

Heimler, W. 197[illegible] [illegible]nia—a new type of kinocilia in the larvae of *Pa[illegible]* (Polychaeta, Terebellomorpha). *Cell Tiss. Res.* **187**: 27[illegible]

Lutz, R. A., R. Mann, J. G. Goodsell, and M. Castagna. 1982. Larval and early post-larval development of the Ocean Quahog, *Arctica islandica*. *J. Mar. Biol. Assoc. U. K.* **62**: 745–769.

Mann, R. 1986. Sampling of bivalve larvae. Pp. 107–116 in North Pacific Workshop on stock assessment and management of invertebrates. *Can. Spec. Pub. Fish. Aquat. Sci.* **92**, G. S. Jamieson and N. Bourne, eds. Department of Fisheries and Oceans, Ottawa, Canada.

Mann, R., and C. C. Wolf. 1983. Swimming behaviour of larvae of the ocean quahog *Arctica islandica* in response to pressure and temperature. *Mar. Ecol. Prog. Ser.* **13**: 211–218.

Matera, E. M., and W. J. Davis. 1982. Paddle cilia (discocilia) in chemosensitive structures of the gastropod mollusk *Pleurobranchaea californica*. *Cell Tiss. Res.* **222**: 25–40.

ÓFoighil, D. 1985. Form, function, and origin of temporary dwarf males in *Pseudophyllina rugifera* (Carpenter, 1864) (Bivalvia: Galeommatacea). *The Veliger* **27**(3): 245–252.

Sleigh, M. A., and J. R. Blake. 1977. Methods of ciliary propulsion and their size limitations. Pp. 243–256 in *Scale Effects in Animal Locomotion*, T. C. Pedley, ed. Academic Press, New York.

Strathmann, R., and E. Leise. 1979. On feeding mechanisms and clearance rates of molluscan veligers. *Biol. Bull.* **157**: 524–535.

Strathmann, R., T. L. Jahn, and J. R. Fonseca. 1972. Suspension feeding by marine invertebrate larvae: clearance of particles by ciliated bands of a rotifer, pluteus and trochophore. *Biol. Bull.* **142**: 505–519.

Tamarin, A., P. Lewis, and J. Askey. 1974. Specialized cilia of the byssus attachment plaque forming region in *Mytilus californianus*. *J. Morphol.* **142**: 321–328.

Thorson, G. 1950. Reproductive and larval ecology of marine bottom invertebrates. *Biol. Rev.* **25**: 1–45.

Turner, R. D., and P. J. Boyle. 1975. Studies of bivalve larvae using the scanning electron microscope and critical point drying. *Bull. Am. Malac. Union* **1974**: 59–65.

Vogel, S. 1981. *Life in Moving Fluids*. Willard Grant Press, Boston. 352 pp.

Waller, T. R. 1981. Functional morphology and development of veliger larvae of the European oyster *Ostrea edulis* Linne. *Smithsonian Contr. Zool.* **328**: 1–70.

Reference: *Biol Bull* **175**: 349–354. (December, 1988)

Consequences of Supply-Side Ecology: Manipulating the Recruitment of Intertidal Barnacles Affects the Intensity of Predation Upon Them

PETER G. FAIRWEATHER*

Institute of Marine Ecology, University of Sydney, NSW 2006, Australia

Abstract. An experimental manipulation of barnacles successfully recruiting to two seashores tested the consequences of these variations to predation by whelks and the eventual population structure of the barnacles. Very young barnacle spat were removed from some areas with and without predatory whelks. The whelks moved away from areas without the juvenile barnacles, but stayed and ate barnacles present on the treatment with barnacle recruitment. Predation resulted in almost complete elimination of the cohort of barnacles. In contrast, barnacles survived and grew to reproductive sizes on areas initially without whelks but with recruits. Because of the movements of whelks and their predation on the barnacles, the final abundances of whelks and barnacles in each plot bore little relationship to their initial experimental treatments. Thus caution is needed in interpreting the causes of static patterns of abundance in the field, where the processes involved earlier are not definitely known. These results point to a need to incorporate variation in recruitment into models of biological interactions.

Introduction

An important development in marine ecology within the last five years has been the reappraisal of the incidence and implications of variation in larval settlement and recruitment (Lewin, 1986; Young, 1987; Underwood and Fairweather, 1988). Biological oceanographers and fisheries scientists (*e.g.*, Thorson, 1950; Coe, 1953; Ricker, 1954; Beverton and Holt, 1957; Loosanoff, 1966) have long focussed on the settlement from the water column of planktonic larvae of marine invertebrates and fishes, and their subsequent recruitment to adult populations (and hence to exploitable stocks). Field ecologists have recently turned their attention to the magnitudes of local variation in this recruitment (Victor, 1983; Caffey, 1985; Gaines and Roughgarden, 1985), and the consequences this has for diversity and abundance of marine species (Underwood and Denley, 1984; Connell, 1985; Peterson, 1986). This new emphasis has been termed "supply-side ecology" (Lewin, 1986). Specific theoretical models (Sale, 1982; Roughgarden, 1986; Menge and Sutherland, 1987) have been proposed incorporating such variation for the subsequent demography of these "open" populations and whether recruitment variation determines the size of populations. Variation in recruitment is considered an important alternative explanation for many ecological patterns (Underwood and Denley, 1984; Lewin, 1986). However, community ecologists have given less consideration to the consequences of this variation for biological interactions (such as predation or competition) among marine organisms (Underwood and Fairweather, 1988).

It has been shown experimentally that variation in the availability of different potential prey in a rocky intertidal area can greatly affect predation on them (Fairweather, 1985, 1987). One mechanism by which availability of prey might vary is via the settlement of their larvae and their recruitment as juveniles. In such circumstances, variation in the recruitment of particular prey species might also influence the outcome of predatory interactions and hence the structure of the community (Underwood and Fairweather, 1988). Although observations in other intertidal work suggest these effects (Fischer-Piette, 1935; Dayton, 1971; Menge, 1972; Morgan, 1972), no experiments involving manipulations of re-

Received 13 June 1988; accepted 19 August 1988.

* Present address: Centre for Environmental & Urban Studies, Macquarie University, NSW 2109, Australia.

cruitment have been [illegible]. Here I describe an experiment that simulates the failure of recruitment by an important member of a rocky intertidal community into areas with adult predators on two seashores in New South Wales, Australia. Species considered were the barnacle *Tesseropora rosea* (Krauss) and the muricid whelk *Morula marginalba* Blainville. *T. rosea* is the most abundant sessile animal at midtidal levels on shores exposed to wave action; *M. marginalba* is the most common predator in such areas (Denley and Underwood, 1979; Underwood, 1981a; Underwood *et al.*, 1983).

Materials and Methods

The experiment used simultaneous manipulations of recruitment and predation on small patches of rocky shore to test whether whelks are capable of responding to a simulation of an extreme case of recruitment variation. On some shores around Sydney, NSW, Australia (Underwood *et al.*, 1983), large areas of the midshore were devoid of nearly all animals that, prior to 1983, had supported dense populations of *Tesseropora* (from a settlement in 1978; Underwood and Denley, 1984) and their associated communities. The two seashores used were Green Point in Broken Bay (33°30′ S, 151°17′ E), and Maitland Bay (33°28′ S, 151°22′ E) on the open coast. I simulated the failure of barnacles to recruit by removing newly settled individuals surrounding selected pools on each shore. Two 400 m^2 sites at each of the two shores were chosen within which at least 24 slight depressions, pools, and small crevices could be found. All were separated by distances of at least 2 m. These crevices were suitable to shelter *Morula* (Moran, 1985), and a few animals had found refuge there. Around these pools were generally homogeneous bare areas of at least 1 m^2 with few prey (barnacles and gastropods) at a total density of only about 15 per m^2. In the first week of March, 1984, I noted a reasonably dense set of *Tesseropora* that had occurred about a week before at Maitland Bay (approximately 2000 per m^2) and Green Point (1100 per m^2). Spat at Green Point may have settled a week earlier than at Maitland Bay (pers. obs.).

At each site (two on each shore, consisting of 24 pools each), six pools were assigned to each of four treatments (see Fig. 1): a control with whelks and recruits present, a treatment with recruits removed but whelks present, a treatment with whelks absent, and a treatment with both whelks and recruits absent. Initially, the one- to two-week-old barnacles that comprised some 98% of the potential prey on all plots (although it is unusual for whelks to eat them so young; Fairweather, 1985). Barnacles were not seen being eaten by the whelks present at this time and probably very few were killed by predators during the first month (although mortality did occur). Barnacle

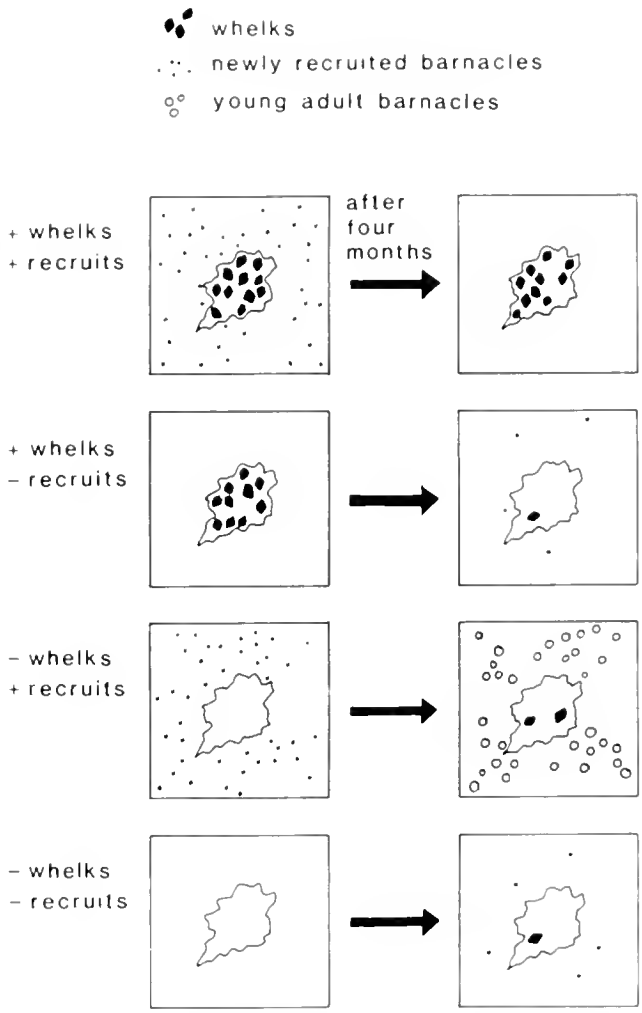

Figure 1. Pictorial representation of the initial and final configurations of the four treatments in the experiment. The whelks are shown hiding in the central crevice in each plot and the survival and growth of the barnacles is indicated by the number and sizes in each treatment (+ whelks/+ recruits are the control plots).

spat were removed from the appropriate plots by careful scraping with a knife on the 5th and 6th of March (so that <10% remained). The time taken to set this up, and to maintain and record these plots, prevented the use of more than one quadrat per treatment. Hence, each treatment pool was a replicate ($n = 6$, total sample size = 96). All whelks were removed from the study sites, and then fifty *Morula* (similar to the initial densities, see Fig. 2) were added to the 1-m^2 area surrounding each treatment pool with whelks.

The survivorship of recruits on a small (0.04 m^2), permanent quadrat within each plot was recorded at monthly intervals. The number of whelks staying in each plot was also recorded. The experiment ran for 18 weeks. The numbers of barnacles at each sampling time were analyzed using a four factor (Shores, Sites within Shores,

Table I

Examples of, a) analysis of variance of the numbers of Tesseropora *at the final date. n = 6. Sites is considered a random factor nested within Shores, other factors are considered fixed. NS = P > 0.05*

Source of variation	Degrees of freedom	Mean square	F-ratio	P	% of variation
Main Effects					
Shores, Sh	1	37	4	NS	0.8
Sites within Shores, Si(Sh)	2	10	1	NS	0.5
Predators, P	1	1204	143	<0.01	27.1
Recruits, R	1	771	1927	<0.001	17.3
Interaction					
Sh × P	1	88	11	NS	2.0
Sh × R	1	43	107	<0.01	1.0
Si(Sh) × P	2	8	1	NS	0.4
Si(Sh) × R	2	0	0	NS	0.0
P × R	1	1411	941	<0.001	31.7
Sh × P × R	1	81	54	<0.05	1.8
Si(Sh) × P × R	2	2	0	NS	0.1
Residual	80	10			17.4
Total	95				

b) Student-Newman-Keuls tests of mean numbers of barnacles surviving for the Sh × P × R interaction. "MB" = Maitland Bay, "GP" = Green Point, "+" = present, "−" = absent

Treatments								
Shore	MB	GP	GP	MB	GP	MB	GP	MB
Predators	−	−	+	+	−	−	+	+
Recruits	+	+	−	−	−	−	+	+
Means	18.5 >	12.3 >	2.8 =	2.5 =	2.1 =	2.0 =	1.3 =	0

Whelks, and Recruits), mixed model analysis of variance (after procedures in Underwood, 1981b) (see design in Table I). Differences among means were revealed by use of Student-Newman-Keuls tests on the means (Underwood, 1981b).

Results

Differences in the analyses among sites or shores are less relevant to the original hypothesis about recruitment, but may represent significant sources of variation in barnacle or whelk numbers. For example, in the final sample, Shores differed (see Tables I, II) in that there were more surviving barnacles in the plots from which whelks had been removed at Maitland Bay than at Green Point (as might be expected from the starting numbers *i.e.*, Fig. 2). Sites within each shore were not divergent (*i.e.*, despite different numbers of recruits initially, the two sites at each shore yielded a similar result). The treatment with recruits, but without whelks, had more barnacles than all other treatments, and this treatment at Maitland Bay had more than the corresponding treatment at Green Point (reflecting the initial numbers, see Table II, Fig. 2).

During the four-month experimental period, the number of whelks on plots declined rapidly where there were no recruits available as prey (Fig. 2a), while they did not move away from plots with juvenile barnacles. The whelks that disappeared were found in crevices outside the experimental plots and hence had not died. Thus, whelks responded readily and negatively to experimentally induced variation in recruitment of a major prey: the predators avoided the areas that simulated failures of recruitment.

Analyses of the number of barnacles present at the start of the experiment revealed significant differences between shores, and between plots where recruits were present and where they had been removed (see Tables I, II; Fig. 2b). In contrast, the final configuration of prey in plots was rather different from initial populations (Fig. 1). Numbers of recruits declined on all plots, but were annihilated by whelks (to local extinction at Maitland Bay and nearly so at Green Point; Fig. 2b). The rate of decline was greater at Maitland Bay. Some small recruitment (from the plankton) occurred subsequently on each shore, but at different times among the sites. After four months, there were again two statistically distinct groups of "barnacle" and "non-barnacle" plots, but densities of young *Tesseropora* in the controls had declined so much that these plots were indistinguishable from the "non-barnacle" group (Fig. 2b).

Discussion

The most direct test of whether variation in recruitment interacts with predation would include manipulation of the number of recruits to populations of prey and/or modifications of the timing of their arrival. Of course this would be difficult to do, especially regarding the timing of episodes of recruitment (because of uncertainty in the availability of larvae at any time). The plankton represents a "mystery stage" (Spight, 1975) in the life cycle of many marine organisms that is currently impossible to predict for these and other species (Underwood, 1979). The experiment used a somewhat less direct approach. By removing recruits as soon as they were observed, it was possible to create situations where a species had effectively "failed" to recruit, which could be compared to undisturbed areas with the "normal" number of recruits. This methodology is particularly applicable to sessile species such as barnacles, while it is difficult to increase the number of recruits to an area without great disturbance.

In this experiment, whelks left plots without recruits; *Morula* individuals migrated from unmanipulated areas without prey (Fairweather, 1988). These data suggest

Table II

Summary of analyses of variance [illegible] barnacles in the experiment

Date	Significant factors	Results
Mar. (initial)	Shores	MB > GP
	Recruits	+r > −r (= zero)
April	Shores	MB > GB
	Whelks × Recruits	−w/+r > +w/+r > +w/−r = −w/−r (= zero)
May	Sites	(undefined spatial variation)
	Whelks	+w > −w
	Recruits	+r > −r
June	Shores × Whelks	MB/−w > GP/−w > MB/+w > GP/+w
	Shores × Recruits	MB/+r > GP/+r > MB/−r > GP/−r
July (final)	Shores × Whelks × Recruits	MB/−w/+r > GP/−w/+r > other treatments

"w" = whelks, "r" = recruits, "+" = present, "−" = absent, "MB" = Maitland Bay, "GP" = Green Point. Results of Student-Newman-Keuls tests of differences among means are also given.

that persistent, dense aggregations of whelks require the natural equivalent of the treatment with recruitment and whelks initially. Where whelks remained, the barnacles suffered greater mortality than in areas without whelks. Thus the four different initial treatments changed into three sorts of communities (Fig. 1). Plots from which barnacles had been experimentally removed finished with no or few barnacles or whelks. Control plots finished with whelks but few or no barnacles, while plots which started with only barnacles remained that way (with some thinning). Very few whelks located these plots (Fig. 2a). Although this pattern could change if later migrations of whelks located plots with surviving barnacles, the results suggest that persistent and dense populations of barnacles require the natural equivalent of the treatment with recruitment in the absence of whelks. This situation does occur on the coast of New South Wales, but the locations of such patches vary through time (Fairweather, 1988).

The final abundances of predators and prey in the experimental communities, however, gave little indication of the interaction of predation with recruitment (see Fig. 1). Without direct knowledge of these processes during the previous four months, the pattern of these divergent plots could be mistakenly attributed to many combinations of the success or failure of recruitment, the intensity of predation, and other factors (such as physical disturbance) not considered here. It would be perilous to interpret any extant pattern of abundance of prey as being the result of present observable predatory interactions without experimental or historical evidence. Descriptive surveys of community structure cannot tell us much about the establishment or maintenance of these patterns (Wiens, 1981). Indeed, such observed interactions may constitute mere epiphenomena (Underwood *et al.*, 1983; Sutherland and Ortega, 1986; Weinberg *et al.*, 1986), in that any effects on demography and community relations of prey may be only transitory. The recent history of these processes acting on each site is important (Peterson and Black, 1988); to predict the abundance of either species in this experiment, the intensities of both processes involved must be known.

The consequences of this simulated recruitment failure go beyond direct effects on the demography of open populations (Roughgarden, 1986); variations in larval supply can set the scene for ecological interactions by determining the population sizes of the participants (Caffey, 1985). Most recent field studies concerning variation in the settlement, and subsequent recruitment, of planktonic larvae of benthic marine invertebrates have documented the magnitude of such variation (*e.g.*, Caffey, 1985; Connell, 1985; Gaines *et al.*, 1985; Peterson, 1986), or searched for its larger-scale oceanographic causes by looking at events in the plankton that influence the eventual numbers of recruits (*e.g.*, Gaines and Roughgarden, 1987; Peterman and Bradford, 1987; Shanks and Wright, 1987). More attention should be paid to the consequences of recruitment variation instead of only concentrating on the causes.

This third avenue of research is suggested by the results here (see also Underwood *et al.*, 1983; Sutherland and Ortega, 1986). We need to take variation in recruitment into account when considering possible outcomes of interactions like predation (Fairweather, 1985, 1987). There is a need for both theory and experiment incorporating variable recruitment in biological interactions as well as in demographic models, explicitly as a variable (Caffey, 1985; Underwood and Fairweather, 1988), not just characterized as consistently great or small (as in Roughgarden, 1986; Menge and Sutherland, 1987). In providing a variable input, recruitment has been shown here to influence the sorts of small scale interactions that organize intertidal assemblages.

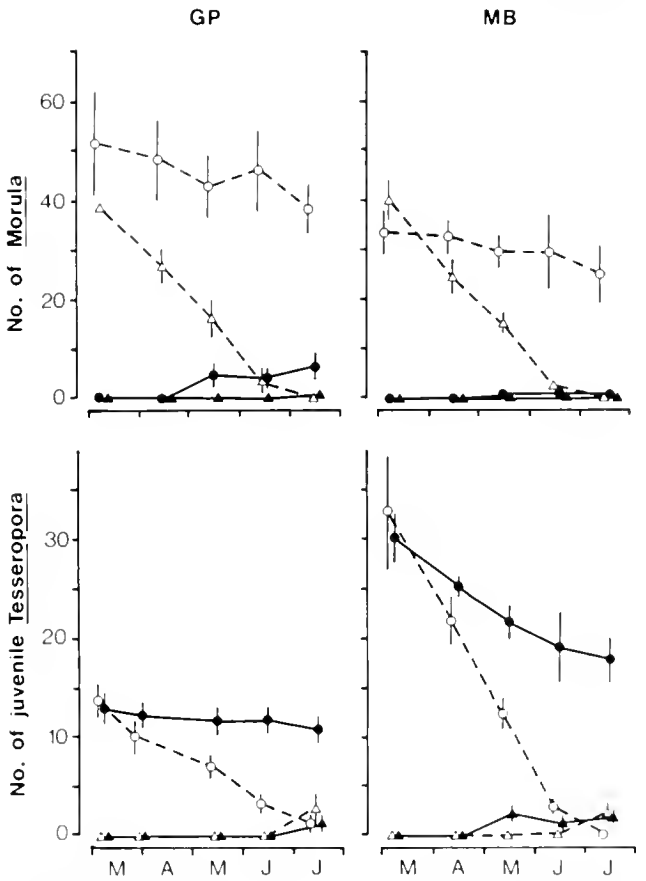

Figure 2. Densities of (a) whelks per m^2 and (b) barnacles per 0.04 m^2 during the experiment. GP denotes Green Point, MB = Maitland Bay, ○ = controls, ● = predators removed, △ = recruits removed, ▲ = predators and recruits removed. Means and their standard errors are shown as points and error bars, $n = 6$ replicate plots. Data for only one site are shown for each shore because the Sites factor was rarely significant in the analyses (see Table II).

Acknowledgments

Thanks to A. J. Underwood, P. D. Steinberg, G. P. Quinn, K. A. McGuinness, M. A. O'Donnell, and V. M. Nelson for advice on a draft, and to many others for discussions. Prof. J. Connell and an anonymous reviewer improved the clarity of the manuscript. L. Bragg drew the figures, and was supported by a Macquarie University Research Grant. This forms part of a Ph.D. thesis (University of Sydney) supported by a Commonwealth Postgraduate Research Award and a University of Sydney Research Grant.

Literature Cited

Beverton, R. J. H., and S. J. Holt. 1957. *On the Dynamics of Exploited Fish Populations.* HM Stationery Office, London.

Caffey, H. M. 1985. Spatial and temporal variation in the settlement and recruitment of intertidal barnacles. *Ecol. Monogr.* **55:** 313–335.

Coe, W. R. 1953. Resurgent populations of littoral marine invertebrates and their dependence on ocean currents and tidal currents. *Ecology* **34:** 225–229.

Connell, J. H. 1985. The consequences of variation in initial settlement vs. post-settlement mortality in rocky intertidal communities. *J. Exp. Mar. Biol. Ecol.* **93:** 11–45.

Dayton, P. K. 1971. Competition, disturbance and community organization: the provision and subsequent utilization of space in a rocky intertidal community. *Ecol. Monogr.* **41:** 351–389.

Denley, E. J., and A. J. Underwood. 1979. Experiments on factors influencing settlement, survival, and growth of two species of barnacles in New South Wales. *J. Exp. Mar. Biol. Ecol.* **36:** 269–293.

Fairweather, P. G. 1985. Differential predation on alternative prey, and the survival of rocky shore organisms in New South Wales. *J. Exp. Mar. Biol. Ecol.* **89:** 135–156.

Fairweather, P. G. 1987. Experiments on the interaction between predation and the availability of different prey on rocky seashores. *J. Exp. Mar. Biol. Ecol.* **114:** 261–273.

Fairweather, P. G. 1988. Correlations of predatory whelks with intertidal prey at several scales of time and space. *Mar. Ecol. Progr. Ser.* **45:** 237–243.

Fischer-Piette, E. 1935. Histoire d'une moulière: observations sur une phase desequilibre faunique. *Bull. Biol. Fr. Belg.* **69:** 152–177.

Gaines, S., and J. Roughgarden. 1985. Larval settlement rate: a leading determinant of structure in an ecological community of the marine intertidal zone. *Proc. Natl. Acad. Sci. USA* **82:** 3707–3711.

Gaines, S. D., and J. Roughgarden. 1987. Fish in offshore kelp forests affect recruitment to intertidal barnacle populations. *Science* **235:** 479–481.

Gaines, S., S. Brown, and J. Roughgarden. 1985. Spatial variation in larval concentrations as a cause of spatial variation in settlement for the barnacle, *Balanus glandula*. *Oecologia* **67:** 267–272.

Lewin, R. 1986. Supply-side ecology. *Science* **234:** 25–27.

Loosanoff, V. L. 1966. Time and intensity of setting of the oyster, *Crassostrea virginica*, in Long Island Sound. *Biol. Bull.* **130:** 211–227.

Menge, B. A. 1972. Foraging strategy of a starfish in relation to actual prey availability and environmental predictability. *Ecol. Monogr.* **42:** 25–50.

Menge, B. A., and J. P. Sutherland. 1987. Community regulation: variation in disturbance, competition, and predation in relation to environmental stress and recruitment. *Am. Nat.* **130:** 730–757.

Moran, M. J. 1985. The timing and significance of sheltering and foraging behaviour of the predatory intertidal gastropod *Morula marginalba* (Muricidae). *J. Exp. Mar. Biol. Ecol.* **93:** 103–114.

Morgan, P. R. 1972. The influence of prey availability on the distribution and predatory behaviour of *Nucella lapillus*. *J. Anim. Ecol.* **41:** 257–272.

Peterman, N. M., and M. J. Bradford. 1987. Wind speed and mortality rate of a marine fish, the northern anchovy (*Engraulis mordax*). *Science* **235:** 354–356.

Peterson, C. H. 1986. Enhancement of *Mercenaria mercenaria* densities in seagrass beds: is patterns fixed during settlement season or altered by subsequent differential survival? *Limnol. Oceanogr.* **31:** 200–205.

Peterson, C. H., and R. Black. 1988. Density-dependent mortality caused by physical stress interacting with biotic history. *Am. Nat.* **131:** 257–270.

Ricker, W. E. 1954. Stock and recruitment. *J. Fish. Res. Board Can.* **11:** 559–623.

Roughgarden, J. 1986. A comparison of food-limited and space-limited animal competition communities. Pp. 492–516 in *Community Ecology*, J. Diamond and T. J. Case, eds. Harper & Row, New York.

Sale, P. F. 1982. Stock-recruit relationships and regional coexistence

in a lotter[illegible]ation study. *Am. Nat.* **120**: 139–159.

Shanks, A. L., [illegible] 1987. Internal-wave-mediated shoa[illegible] megalopae, and gammarids and [illegible]es in the settling rate of intertidal barnacles. [illegible] **114**: 1–13.

Spight, T. M. 197[illegible] tors extending gastropod embryonic development and [illegible]e cost. *Oecologia* **21**: 1–16.

Sutherland, J. P., and S. Ortega. 1986. Competition conditional on recruitment and temporary escape from predators on a tropical rocky shore. *J. Exp. Mar. Biol. Ecol.* **95**: 155–166.

Thorson, G. 1950. Reproductive and larval ecology of marine bottom invertebrates. *Biol. Rev.* **25**: 1–45.

Underwood, A. J. 1979. The ecology of intertidal gastropods. *Adv. Mar. Biol.* **16**: 111–210.

Underwood, A. J. 1981a. Structure of a rocky intertidal community in New South Wales: patterns of vertical distribution and seasonal changes. *J. Exp. Mar. Biol. Ecol.* **51**: 57–85.

Underwood, A. J. 1981b. Techniques of analysis of variance in experimental marine biology and ecology. *Oceanogr. Mar. Biol. Ann. Rev.* **19**: 513–605.

Underwood, A. J., and E. J. Denley. 1984. Paradigms, explanations and generalizations in models for the structure of intertidal communities on rocky shores. Pp. 151–180 in *Ecological Communities: Conceptual Issues and the Evidence*, D. R. Strong *et al.*, eds. Princeton University Press, Princeton.

Underwood, A. J., E. J. Denley, and M. J. Moran. 1983. Experimental analyses of the structure and dynamics of mid-shore rocky intertidal communities in New South Wales. *Oecologia* **56**: 202–219.

Underwood, A. J., and P. G. Fairweather. 1988. Supply-side ecology and benthic marine assemblages. *Trends Ecol. Evol.* **3**: (in press).

Victor, B. C. 1983. Recruitment and population dynamics of a coral reef fish. *Science* **219**: 419–420.

Weinberg, J. R., H. Caswell, and J. B. Whitlach. 1986. Demographic importance of ecological interactions: how much do statistics tell us? *Mar. Biol.* **93**: 305–310.

Wiens, J. A. 1981. Single-sample surveys of communities: are the revealed patterns real? *Am. Nat.* **117**: 90–98.

Young, C. M. 1987. Novelty of "supply-side ecology." *Science* **235**: 415–416.

Reference: *Biol. Bull.* **175:** 355–360. (December, 1988)

Coordinated Interpersonal Timing of Down-Syndrome and Nondelayed Infants with Their Mothers: Evidence for a Buffered Mechanism of Social Interaction

MICHAEL JASNOW[1], CYNTHIA L. CROWN[2], STANLEY FELDSTEIN[2], LINDA TAYLOR[2], BEATRICE BEEBE[3], AND JOSEPH JAFFE[1]

[1]*Department of Psychiatry, Columbia University;* [2]*Department of Psychology, University of Maryland Baltimore County;* [3]*Ferkauf Graduate School of Psychology, Yeshiva University*

Abstract. A longitudinal study of four- and nine-month-old infants indicates that they coordinate the timing of their vocal behavior with that of their mothers and vice versa. Maternal interactions of Down-syndrome and nondelayed infants were analyzed and found not to differ with regard to such temporal coordination, indicating that it is independent of level of cognitive functioning. The capacity for coordinated timing is proposed as a mechanism for the facilitation of social interaction. Such coordination parallels temporal matching observed in a variety of species along the phylogenetic scale.

Introduction

Beginning at least with the work of the Gardeners (Gardner and Gardner, 1969; Gardner and Gardner, 1974), researchers have explored the extent to which animals can communicate as do human beings. Our research, on the other hand, has been concerned, in part, with the question of whether human social interaction is made possible, or facilitated by, capacities that are shared with other species and serve the same functions. We report here the results of a longitudinal study of the temporal structure of social communication between nondelayed and Down-syndrome infants in the first year of life and their mothers. The results suggest that coordinated interpersonal timing may serve as a mechanism for the facilitation of social interaction. We conclude that such timing shares features of functionally adaptive social predispositions present in other species.

Received 4 January 1988; accepted 27 September 1988.

Conversation is the primary mode of conspecific communication employed by homo-sapiens. Such exchange is an important mechanism serving the organization and maintenance of human society. In this respect, conversational exchange may be viewed as the functional analogue of the bird song and cricket chirp. While the information encoded in a chirp or a song sequence and a conversation may differ radically, the functional consequences of such a signal may be identical: facilitation of mating, bonding between infant and caretaker, guarding against predation, etc.. It is in this functional sense that we are considering a human vocal exchange as equivalent to vocal behaviors observed over a wide range of organisms. There is an extensive body of evidence (Feldstein and Welkowitz, 1987) showing that conversational exchange between adult speakers possesses a complex statistical temporal structure; a structure not entirely subsumed by the syntactic and semantic aspects of such an exchange. Of central interest to our investigation is coordinated interpersonal timing, which refers to an alteration in the temporal patterning of one speaker's behavior as a function of that of the other speaker.

Work with invertebrates, especially insects, and with simple vertebrate models, has begun to delineate a variety of genetic and neurologic factors that are responsible for the temporal organization of social behavior. Thus, for example, investigators (Zerhring *et al.*, 1984; Hamblen *et al.*, 1986) have isolated mutations mapped to a particular region of the X chromosome in *Drosophila*. Mutations on this locus increase, decrease, or destroy completely the temporal pattern of the male fly's mating song. A unique coding sequence that forms a portion of

this locus has recently been identified in several vertebrates (Schildberger, 1984). Groups of neurons that act as temporal filters have been identified in crickets (Schildberger, 1984). These filters are "tuned" to the temporal properties of the conspecific song. Temporal filters sensitive to biologically salient stimuli have also been identified in several species of toads (Rose and Capranica, 1984), the electric fish, *eigenmannia* (Partridge and Heiligenberg, 1981), and in rats (Rees and Moller, 1983).

The importance of a capacity for temporal attunement in terms of the organism's survival is not to be underestimated. Zelick (1986) emphasized the crucial ecological function served by the temporal patterning of vocalization in certain frogs and the electric organ discharge in the weakly electric fish. Both fish and frogs have adopted similar strategies of signal oscillator timing to avoid signal overlap and jamming between conspecifics. Lamprecht *et al.* (1985) detailed the utility of distance-call duets in bar-headed geese (*Anser indicus*).

In all of this work, the important variable is the temporal dimension of the signal. We emphasize that our investigation is concerned with precisely this dimension and not with the linguistic process. Obviously, language exhibits a range of phenomena that possess important temporal features. However, our analysis is not concerned with elucidating the temporal patterns of different linguistic processes such as phonemes, vowel recognition, or other more "molecular" linguistic features. Our method of analysis is neutral with respect to the content of the acoustic signal.

We wished to determine (a) whether human infants are attuned to the temporal properties of the vocal behavior of their adult partners in a dyadic exchange and (b) the extent to which adults interacting with an infant are similarly responsive to the temporal characteristics of the infant's vocal behavior. Finally, we examined the possibility of a relationship between the capacity for temporal attunement and cognitive development. Given that the capacity for coordinated timing appears to be expressed by organisms at various levels of the phylogenetic scale, we expected it to be independent of cognitive functioning. It was this conjecture that dictated our choice of infants with Down syndrome as one of our two groups of subjects (Gibson, 1978). We note that other investigators have utilized the impairment of cognitive functioning of persons with Down syndrome to disentangle the role played by cognitive functioning in a variety of human behaviors. Down syndrome offers a valuable window into the study of human development. The pattern of cognitive deficit associated with Down syndrome is fairly well understood, and a number of studies (Ciccheti and Serafica, 1981; Ciccheti and Sroufe, 1976; Serafica and Ciccheti, 1976; Spiker, 1983) of Down-syndrome infants and young children indicates that they show a pattern of delay rather than deficit in their social development. Workers such as Ciccheti and his colleagues (Ciccheti and Serafica, 1981; Ciccheti and Sroufe, 1976) have, in fact, used Down syndrome as a model for studying the interaction of social and cognitive development. Our choice of infants afflicted with the syndrome was motivated by the same rationale.

[1] Down syndrome refers to a genetically based condition that involves, among other problems, cognitive delay and/or retardation. The average Mental Development Index for the Down infant group was 64, which is inflated because no MDI < 50 could be calculated; the average for the nondelayed group was 110. Note that the name, Down's syndrome, has recently been changed to Down syndrome, making the use of Down or Down's equally acceptable.

Materials and Methods

Participants

The participants were two groups of caucasian mother-infant pairs. In one group of nine pairs, the infants were afflicted with Down syndrome (trisomy 21). Nine pairs of normal, nondelayed infants and their mothers comprised the other group. The infants with Down syndrome were recruited from community groups that provide services for such infants as well as from notices in the media. The nondelayed infants were recruited from notices placed in parent-child newsletters. All the mothers in the study were native speakers of English and were highschool graduates. At the initial session, each of the mothers was given a brief rating scale for depression (Radloff, 1977) and another for anxiety (Zuckerman and Lubin, 1965). None of the mothers used in the study were found to be clinically anxious and/or depressed. A medical history was obtained from each of the mothers concerning her own health, a history of the pregnancy, and her infant's health. To the best of our knowledge, none of the infants with Down syndrome used in this study presented any relevant health problems.

Procedure

The pairs were seen when the infants were within two weeks of being four months old, and within two weeks of being nine months old. On the second occasion, all the infants were given the Bayley Mental Development Scale (Bayley, 1969). Each of the mother-infant pairs engaged in a standard face-to-face play procedure for 12 minutes in the Interpersonal Communications Laboratory of the University of Maryland Baltimore County. At the four-month data point, the infant was seated in an infant seat directly across from its mother at an elevation

such that mother and infant could comfortably achieve eye-contact. At the nine-month point, the infant was seated in an infant chair again oriented in such a way as to make face-to-face interaction comfortable. Also at the nine-month point, the mothers were given a small hand puppet to use as a means of focusing the interaction. This procedure is a standard one and has been used in similar studies (Jasnow and Feldstein, 1986). Two-channel, 12-minute tape recordings were made of each mother-infant interaction. To minimize the spill of one person's voice into the microphone of the other person, contact microphones were used. If during the course of an interaction, the infant became fussy, the taping continued for 30 seconds. If at the end of the 30 seconds the baby was not reengaged, the taping was stopped until such time as the baby was able to continue.

Vocal analysis

The coding of the vocal behavior was accomplished via the direct input of two audio signals, representing the infant and adult, into a specialized computer system known as the Automated Vocal Transaction Analyzer (AVTA) (Jaffe and Feldstein, 1970). AVTA is a hardware and software system. The hardware component is an analogue-to-digital converter that "listens" to two channels of incoming audio signals to determine whether the signal in each channel is on or off. The audio signals represent the vocal behavior of the two partners. Both sequences of signals are sampled by the A-to-D converter every 250 milliseconds and are stored digitally in the computer in the form of one sequence of four numbers: one signal is on and the other is off, or vice versa; both are on; or both are off. The AVTA system transforms the decimal numbers into the set of dialogic vocal parameters defined below and summarizes them as frequencies, proportions, average durations, and standard deviations for a fixed time interval. The time sampling interval was five seconds because it is approximately equal to the mean plus one standard deviation of each parameter, with the exception of the turn. Inasmuch as the maternal average speaking turns were longer than five seconds, the same criterion yielded 30 seconds as the appropriate sampling unit for the adult turn.

The vocal parameters (Jaffe and Feldstein, 1970; Feldstein and Welkowitz, 1987) generated by the AVTA system are *speaking turns, vocalizations, pauses, switching pauses,* and *simultaneous speech.* Simultaneous speech had too low a rate of occurrence to be included in these analyses. A turn begins the instant a participant starts to vocalize alone and ends immediately prior to the instant that the other participant starts to vocalize alone. A vocalization is a segment of sound uninterrupted by any discernible silence. A pause is an interval of joint silence that is initiated and terminated by vocalizations of the same participant. A switching pause is a joint silence initiated by the participant who has the turn and terminated by a vocalization of the other participant (Fig. 1).

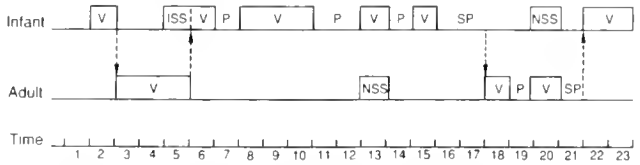

Figure 1. A diagramatic representation of a conversational sequence. The numbered line at the bottom represents time in 250-ms units. V stands for *vocalization,* P for *pause,* and SP for *switching pause* (the silence that occurs immediately prior to a change in the speaking *turn*). The arrows that point down denote the end of the infant's turns; the arrows that point up denote the end of the adult's turns. ISS and NSS stand for *interruptive* and *noninterruptive simultaneous speech,* respectively. (Adapted from Figure II-2 of Jaffe and Feldstein, 1970).

Statistical analyses

The dyadic time series was divided into five-second[2] segments, or time units, yielding 144 five-second units (over 12 min). A time-series regression (TSR) analysis (Ostrom, 1978) was computed for each parameter to assess the occurrence of coordinated interpersonal timing for each mother-infant pair. The TSR was accomplished by a three-step procedure. The series were first subjected to an ARIMA (SPSSX) modeling procedure for the purpose of "pre-whitening" the data. The ACF subprogram of SPSSX Trends was used to allow for visual and statistical checks to test which model parameters best fit to the data and met the assumptions made by the model. It was determined that the most useful parameter values were 2, 0, 0. Each series was prewhitened separately.

After the selection of the appropriate model, the TSR analyses were computed by the AREG subprogram of SPSSX Trends. It is the temporal coordination that occurs in the current 5- or 30-second sampling interval that was used in this report. In other words, we were concerned with the degree to which changes in one series are reflected by changes in the other series within the same time frame. This relationship is indexed by the standard-

[2] The five-second time unit was used for the TSR analyses of all the parameters but maternal speaking turns. Average values were computed for each parameter for every five seconds of interaction and for every 30 seconds in the case of maternal turns. Five seconds was chosen because it is approximately equal to the mean + 1 standard deviation for each parameter. Maternal speaking turns had a significantly greater mean value and thus 30 seconds was selected as a more appropriate time unit.

Table 1

Summary of Chi square analyses of the results of time-series regressions

Dyad type		T	P	SP	V
Four months					
	N	10	10	7	10
N: mother-infant	R	.52	.14	.07	.21
	χ^2	68.61	35.27	5.78*	126.47
	N	8	7	6	8
DS: mother-infant	R	.61	.15	.11	.21
	χ^2	100.85	28.53	17.48	64.63
Nine months					
	N	10	10	6	10
N: mother-infant	*R*	.63	.14	.14	.24
	χ^2	79.96	34.89	36.66	89.49
	N	10	9	5	9
DS: mother-infant	*R*	.89	.09	.07	.16
	χ^2	86.68	17.39	6.81*	30.33

* $P > .05$.

Note. *N* is the *df* for the Chi square. The *R* represents the average standardized partial regression coefficient. T stands for Turns, P for Pauses, SP for Switching Pauses, V for Vocalizations. The "N" stands for "Nondelayed," the "DS" stands for "Down's syndrome."

ized partial regression coefficient, which is used as a coefficient of coordinated timing.

We wanted two kinds of information. One was whether the group of dyads involving Down-syndrome infants and the group of dyads involving nondelayed infants each engaged in coordinated interpersonal timing. This information was provided by a meta-analytic approach in which standard normal deviate scores are obtained for the probability values associated with the regression coefficients. Each of these standard scores is squared to yield a Chi square with one degree of freedom. The Chi squares are then summed for each group of dyads to provide a Chi square test (with *df* equal to the number of Chi squares in the sum) of whether the regression coefficients in each group were significantly different from zero. Another was whether the two groups differed in terms of the extent with which they engaged in coordinated timing. Differences between the two groups of mother-infant pairs (nondelayed and delayed) and between the two age groups (four and nine months) were assessed by a split-plot analysis of variance.

Results

The Chi square analyses of the results indicate that mutual coordination occurred for all but one of the temporal parameters, at both 4 and 9 months, regardless of diagnosis (Table 1).

Given that the meta-analytic results demonstrate that temporal coordination occurred across all but one of the vocal behaviors, or parameters, the question is whether the two groups can be discriminated on the basis of their magnitudes of coordination. The analysis of variance of the pauses, switching pauses, and vocalizations yielded a significant main effect for diagnosis ($F[1, 17] = 4.34$, $P = .05$, $\epsilon = .40$), indicating that the dyads with the delayed infants seemed to engage in less coordination than their nondelayed counterparts. However, the occurrence of a significant interaction of diagnosis by age ($F[1, 17] = 4.34$, $P = .05$, $\epsilon = .40$) indicates that the apparent general difference between the two groups is primarily attributable to a significantly lower degree of coordination of the Down-syndrome dyads at four months of age. By the time the delayed infants reach nine months of age, their average degree of coordination with their mothers is similar to that of the nondelayed dyads (Fig. 2).

The results of the analysis of speaking turns (done separately because of the larger sampling interval) provide no evidence of a difference in degree of coordination between the dyads with the delayed infants and those with the nondelayed infants ($F[1, 17] = 0.00$, $P = .959$). Nor did the magnitude of coordination of either group of dyads change markedly with time ($F[1, 17] = 0.70$, $P = .415$).

Discussion

The results offer support for the hypothesis that infants and their mothers coordinate the temporal organization of their vocal behavior both when the infants are four

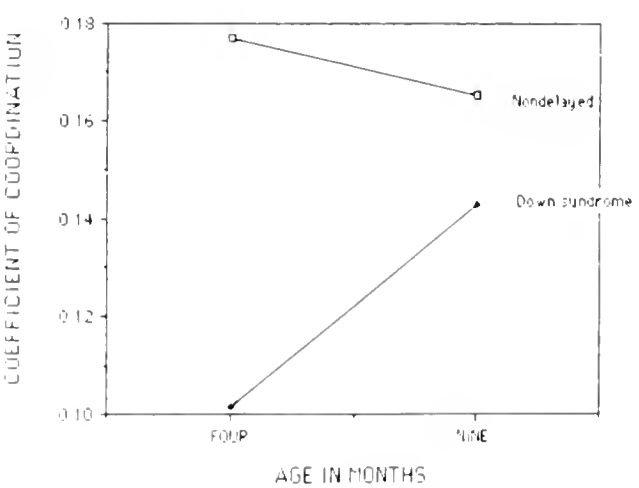

Figure 2. The interaction of the diagnosis by age, indicating that whereas the degree of coordinated interpersonal timing of the dyads with nondelayed infant is similar when the infants are four and nine months of age, that of the dyads with Down's syndrome infant increases significantly from four to nine months.

months and nine months old. They demonstrate that the temporal phenomenon found to characterize adult conversation (Partridge and Heiligenberg, 1981; Feldstein and Welkowitz, 1987) is present in adult-infant interactions from as early as four months of age and that the results are true not only for nondelayed infants, but also for infants afflicted with Down syndrome. Thus the study, having used a group about whose cognitive impairment there can be no doubt, represents a strong test of the proposition that coordinated interpersonal timing is independent of cognitive ability.

Note, however, that although coordination appears to be a general phenomenon detected in both groups at both ages, the two groups could be discriminated on the basis of the lower degree of coordination exhibited by the Down-syndrome infants and their mothers at four months of age. This finding of lower coordination at four months increasing, by nine months, to a level similar to that of the nondelayed dyads, is consistent with the findings from a wide array of studies about the social behavior of Down-syndrome infants. These studies (Cicchetti and Sroufe, 1976; Serafica and Cicchetti, 1976; Cicchetti and Serafica, 1981; Spiker, 1983) have shown that dysfunctional aspects of social behavior of Down-syndrome infants and young children are related to deviations in rate of development and not to deficits in development.

The capacity to process and respond to the temporal patterning of human vocalizations may enable the infant to select and "lock onto" a biologically important environmental stimulus. That this capacity is present in infants suffering from severe cognitive impairment suggests that it may be buffered against insults to the organism. In other words, it may be that the capacity functions to make social interaction possible. The underlying neuromechanisms responsible for such temporal sensitivity are not known. Workers such as Rose (1986) have observed that many different types of organisms employ the same set of neurons in the midbrain for processing certain varieties of temporal information. Rose speculated that similar mechanisms may be operative in human beings. Zelick (1986) pointed out that the behavior strategies adopted by certain frogs and the weakly electric fish to avoid signal jamming are quite similar, and suggested that common neuromechanisms may be responsible for the common behavioral strategy. Whether the mechanisms underlying the behaviors described in this report are similar to those that operate in nonhuman organisms remains open to investigation.

There is no doubt that the temporal patterning of social interaction is a fundamental aspect of behavior in any given ecological setting. Marler and Terrace (1984) noted that "The mechanisms that underlie imprinting and song learning cannot be understood without first acknowledging the pervasive role of unlearned, functionally adaptive predispositions to associate particular classes of stimuli" (p. 5). We conjecture that the responsivity to the temporal patterning of vocal behavior demonstrated by the findings presented here is an instance of such a functionally adaptive predisposition in human beings.

Acknowledgments

The study was supported by Research Grant No. 12-152 from the March of Dimes, by the Fund for Psychoanalytic Research, and, in part, by Research Grant No. R01-MH41675 from NIMH. The investigators are indebted to the Academic Computing Center of the University of Maryland Baltimore County for its generous contribution of computer time and services.

Literature Cited

Bayley, N. 1969. *Bayley Scales of Infant Development.* Psychological Corp.

Cicchetti, D., and F. Serafica. 1981. Interplay among behavioral systems: illustrations for the study of attachment, affiliation and wariness in young children with Down's syndrome. *Dev. Psychol.* **17:** 36–49.

Cicchetti, D., and A. Sroufe. 1976. The relationship between cognitive development in Down's syndrome infants. *Child Dev.* **47:** 920–929.

Feldstein, S., and J. Welkowitz. 1987. A chronography of conversation: in defense of an objective approach. Pp. 435–499 in *Nonverbal Behavior and Communication,* A. W. Siegman and S. Feldstein, eds. Erlbaum, Hillsdale, NJ.

Gardner, R. A., and B. T. Gardner. 1969. Teaching sign language to a chimpanzee. *Science* **165:** 664–672.

Gardner, B. T., and R. A. Gardner. 1974. Two-way communication with an infant chimpanzee. Pp. 171–184 in *Behavior of Nonhuman Primates,* Vol. 4, A. M. Schrier *et al.*, eds. Academic, New York.

Gibson, D. 1978. *Down's Syndrome: The Psychology of Mongolism.* Cambridge University Press, New York.

Hamblen, H., W. A. Zehring, C. P. Kyriacou, P. Reddy, Q. Yu, D. A. Wheeler, L. J. Zwiebel, R. J. Konopka, M. Rosbash, and J. C. Hall. 1986. Germ-line transformation involving DNA from the period locus in *Drosophila melangaster:* overlapping neural fragments that restore circadian and ultradian rhythmicity to per° and per⁻ mutants. *J. Neurogen.* **3:** 249–291.

Jaffe, J., and S. Feldstein. 1970. *Rhythms of Dialogue.* Academic, New York.

Jasnow, M. D., and S. Feldstein. 1986. Adult-like temporal characteristics of mother-infant vocal interactions. *Child Dev.* **57:** 754–761.

Lamprecht, J., A. Kaiser, A. Peters, and C. Kirchgessner. 1985. Distance call duets in bar-headed geese (*Anser indicus*): Cooperation through visual relief of the partner? *Z. Tierpsychol.* **70:** 211–218.

Marler, P., and H. Terrace, eds. 1984. *Dahlem Konferanzen* Springer-Verlag, Berlin.

Ostrom, C. W. 1978. *Time Series Analysis: Regression Techniques.* Sage, Beverly Hills, CA.

Partridge, B. L., and W. Heiligenberg. 1981. Pp. 309–319 in *Ad-*

vances in Psychobiol. M[illegible] J. P. Ewert *et al.* eds. Plenum, New York.

Radloff, L. 1977. [illegible] Scale: A self-report depression scale for research in [illegible] population. *Appl. Psychol. Measure.* **1:** 385–401.

Rees, A., and [illegible] Moller. 1983. Responses of neurons in the inferior coll[illegible] the rat to AM and FM tones. *Hear. Res.* **10:** 301–330.

Rose, G. 1986. A temporal processing mechanism for all species. *Brain Behav. Evol.* **28:** 134–144.

Rose, G., and R. Capranica. 1984. Accessing amplitude-modulated sounds by the auditory midbrain of two species of toads: matched temporal filters. *J. Comp. Physiol.* **154:** 211–219.

Schildberger, K. 1984. Temporal selectivity of auditory neurons in the cricket. *J. Comp. Physiol.* **155:** 171–185.

Serafica, F., and D. Cicchetti. 1976. Down's syndrome children in a strange situation: attachment and exploration behaviors. *Merrill-Palmer Q.* **22:** 137–150.

Shin, H. S., T. A. Bargiello, B. T. Clark, F. R. Jackson, and M. W. Young. 1985. An unusual coding sequence from a *Drosophila* clock gene is conserved in vertebrates (Letter). *Nature* **317:** 445.

Spiker, D. 1983. Early intervention for young children with Down's syndrome: new directions for enhancing parent child synchrony. In *Down's Syndrome: Advances in Biomedicine and the Behavioral Sciences.* S. Peuschel and J. Rynders, eds. The Ware Press, Cambridge, MA.

Zerhring, W. A., D. A. Wheeler, P. Reddy, R. J. Konopka, C. P. Kyriacou, M. Rosbash, and J. C. Hall. 1984. P-element transformation of period locus DNA restores rhythmicity to mutant, arhythmic *Drosophila melangaster*. *Cell* **39:** 369–376.

Zelick, R. 1986. Jamming avoidance in electric fish and frogs: strategies of signal oscillator timing. *Brain Behav. Evol.* **28:** 60–69.

Zuckerman, M., and B. Lubin. 1965. *Manual for the MACL.* Educational and Industrial Testing Service, San Diego, CA.

Reference: *Biol. Bull* **175**: 361–371. (December, 1988)

Intraspecific Variation in Growth and Reproduction in Latitudinally Differentiated Populations of the Giant Scallop *Placopecten magellanicus* (Gmelin)

B. A. MACDONALD AND R. J. THOMPSON

Marine Sciences Research Laboratory, Memorial University of Newfoundland, St. John's, Newfoundland A1C 5S7, Canada

Abstract. The giant scallop, *Placopecten magellanicus*, exhibits a discrete gametogenic cycle which varies between populations. In our study, spawning occurred later in scallops from New Jersey than in those from Newfoundland, but there is no latitudinal trend when data from the literature are considered. Reproduction is probably controlled by local environmental factors.

There was high intraspecific variation in shell and somatic growth rates, and in the production of somatic and germinal tissue. Reproductive output in particular showed great plasticity. Variation in these traits along a depth gradient on a micro-geographical scale was equal to or greater than variation on a latitudinal scale, although reproductive output in New Jersey scallops exceeded that of scallops from Newfoundland. Enhanced reproductive output was associated with reduced longevity.

Introduction

Many species of marine ectotherms are distributed over a wide latitudinal range and often display intraspecific variation in physiological characteristics and life-history strategies (Levinton, 1983). Such species are ideal candidates for determining which environmental factors, such as water temperature, that vary with latitude in a predictable manner may influence the growth and reproduction of individual animals. Causal relationships between water temperature and growth or reproductive output have proved difficult to establish unequivocally, owing to local variations in environmental conditions, such as food availability and temperature (Newell *et al.*, 1982; MacDonald and Thompson, 1985a). There is a need for studies in which intraspecific variation on a micro-geographic scale is examined for a number of characters and related to observations on latitudinally separated populations.

With some exceptions, the general consensus in the literature is that bivalve molluscs from low latitudes grow more rapidly at ambient temperature, attain a smaller maximum size, and have a shorter lifespan than do conspecifics from higher latitudes (Newell, 1964). This view is supported by studies on several species of bivalves, including *Siliqua patula* (Weymouth *et al.*, 1931) and *Mytilus edulis* (Seed, 1976), but clear latitudinal trends have not been observed in others, *e.g.*, *Mya arenaria* (Brousseau, 1979) and *Placopecten magellanicus* (Posgay, 1979). In *Macoma balthica* from North America, however, maximum size is greatest in populations from low latitudes, whereas in *M. balthica* from Europe growth is faster at intermediate latitudes (Gilbert, 1973; Bachelet, 1980; Beukema and Meehan, 1985).

There is an extensive literature on the gametogenic cycle and the timing of spawning in many bivalve species (Giese and Pearse, 1974; Sastry, 1979; Newell *et al.*, 1982). For several species in the northern hemisphere, spawning occurs at higher temperatures and later in the year in southern populations than in northern ones (Sastry, 1970, 1979; Seed, 1976; Barber and Blake, 1983), and is often more synchronized at higher latitudes (Ockelmann, 1958; Bricelj *et al.*, 1987). Unfortunately, there is very little information on intraspecific variation in reproductive output and reproductive effort in latitudinally separated populations (Bricelj *et al.*, 1987), yet these quantities are often more sensitive to environmental change than is shell growth, the most commonly measured variable (MacDonald and Thompson, 1985a, b).

Received 21 July 1988; accepted 20 September 1988.

The giant scallop *Placopecten magellanicus* is found only in the northwest Atlantic, between the Strait of Belle Isle, Newfoundland, and Cape Hatteras, North Carolina (Posgay, 1957; Porter, 1974). In previous papers, we have described how local variations in temperature and food supply can influence shell growth, somatic production, gametogenesis, and reproductive characteristics in populations from Newfoundland (MacDonald and Thompson, 1985a, b, 1986; MacDonald *et al.*, 1987). In this paper, we integrate this information with data from scallop populations in New Brunswick and New Jersey, to further our knowledge of intraspecific variation in *P. magellanicus*. The objectives are to establish whether growth and reproductive parameters show identifiable latitudinal trends, to determine which ones should be regarded as plastic or variable on a local scale, and to understand the possible adaptive value of the observed strategies.

Materials and Methods

Study sites and environmental data

Scallops were collected from Sunnyside (47°51′ N, 53°55′ W) in Trinity Bay, Newfoundland, by SCUBA divers, from St. Andrews (45°04′N, 67°04′W) in Passamaquoddy Bay, New Brunswick, and from a bed near Asbury Park (40°13′N, 73°47′W), New Jersey, (Fig. 1) using a modified Digby dredge. Collections were made approximately monthly between July 1982 and November 1983 at Sunnyside and New Jersey for determination of the gametogenic cycle. In 1983 a complete size range of scallops was obtained in the months immediately before and after spawning at Sunnyside (July/September), St. Andrews (July/November), and New Jersey (September/November), to measure the weight loss of the gonad on spawning. Samples were obtained from depths of 10 and 31 m in Sunnyside and St. Andrews but were only available from 31 m at the New Jersey site.

Seasonal water temperatures were recorded in Sunnyside using moored 180 d continuous recording thermographs (Ryan Instruments, Seattle, Washington) and in New Jersey by means of a maximum-minimum thermometer. Temperature cycles for St. Andrews were obtained from Forgeron (1959) and represent mean values for the 1957 and 1958 seasons combined. An approximation for water temperature at 10 m was calculated by averaging the temperature at the surface and the bottom (24 m).

Growth rates

Ages of individual scallops were estimated by interpreting external growth rings on the shell (Stevenson and Dickie, 1954) and growth increments on the calcareous portion of the ligament (Merrill *et al.*, 1966). Measurements of shell height [maximum distance between the dorsal (hinge) and ventral margin (Seed, 1980)] were recorded to the nearest 0.1 mm using vernier calipers. Mean shell heights for each age class were estimated using the von Bertalanffy equation:

$$H_t = H_\infty [1 - e^{-K(t - t_0)}]$$

where H_t = shell height at time t, H_∞ = mean asymptotic shell height, K = the Brody growth coefficient and t_0 = a parameter representing time when shell height equals zero. The von Bertalanffy functions were fitted by iteration, using the Marquardt algorithm available in the NLIN procedure of the Statistical Analysis System (SAS Institute Inc.).

Weights of the gonad and remaining (somatic) tissue were determined separately for individual scallops after drying at 90°C for 48 h. The mean somatic weight for

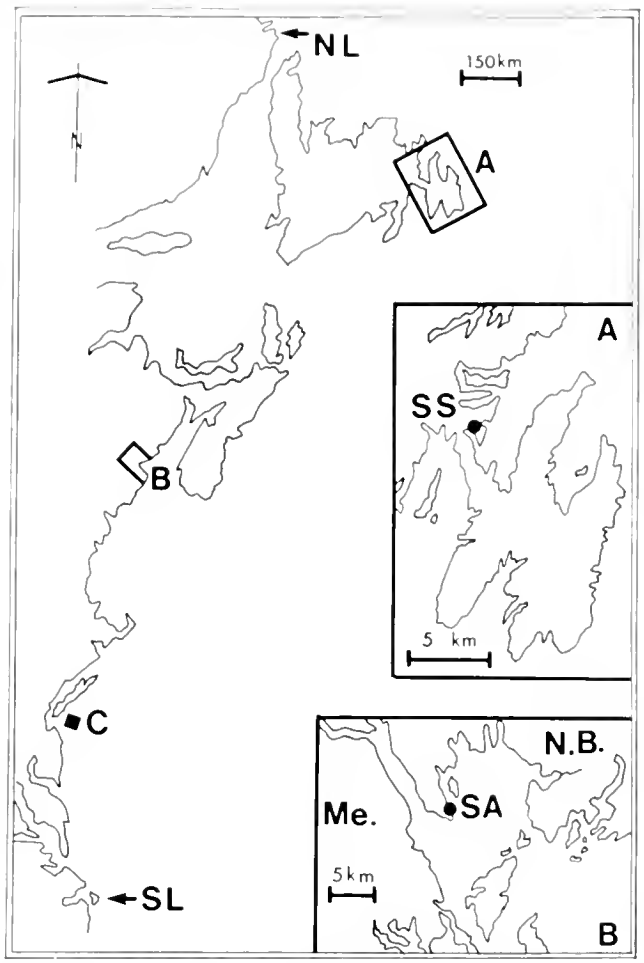

Figure 1. Sites from which scallops, *Placopecten magellanicus*, were collected. A—Avalon Peninsula, Newfoundland (SS = Sunnyside); B—Passamaquoddy Bay (SA = St. Andrews); C—New Jersey. NL—northern limit of distribution. SL—southern limit of distribution.

each age class was estimated using polynomial regression, which has some advantages over the von Bertalanffy function for describing somatic growth rates (MacDonald and Thompson, 1985a). Polynomial regression, which was computed by the General Linear Model (GLM) procedure of SAS, may be described by the following equation:

$$y = \beta_0 + \beta_1 x + \beta_2 x^2 + \beta_3 x^3 \cdots \beta_m x^m + \epsilon$$

where $\beta_0, \beta_1 \cdots \beta_m$ = population parameters, y = the predicted somatic weight for a given value of x (age) and ϵ = random error at observation x. Linear correlation between regressors (multicollinearity) was reduced by replacing values of x with $(x - \bar{x})$ (Neter *et al.*, 1983).

For predictive and comparative purposes, relationships between shell height and somatic or gonad weight were fitted by SAS (GLM procedure) to the allometric equation $y = ax^b$, where y is the predicted weight (g) at a given shell height x (mm), and a and b are fitted parameters. A linear form of this equation was obtained by transforming both variates to logarithms and fitting the data to a straight line by least squares regression. Owing to possible seasonal differences in shell and somatic growth rates, only those scallops collected from Sunnyside and New Jersey between July and December were used in comparisons with St. Andrews. Statistical comparisons between scallops from the three locations were only made on those individuals collected in 1983 ranging in age from two to eight years because these were the only age classes common to all three populations.

Gametogenic cycle and gamete volume fraction

To establish the gametogenic cycle, histological sections were prepared from the gonads of six male and six female scallops in each monthly sample from Sunnyside (10 m depth) and New Jersey. The proportions of the gonad occupied by developing gametes and mature gametes (the volume fractions) were estimated by a stereological procedure (Lowe *et al.*, 1982). The gamete volume fraction (GVF) was calculated as the sum of the values for developing and mature gametes (for details see MacDonald and Thompson, 1986).

Production

Somatic tissue production (Pg) was calculated from the increments in dry tissue weight between consecutive year classes, assuming that 1 g dry weight = 24.5 kJ (Thompson, 1977). Since *Placopecten magellanicus* has a discrete reproductive cycle and spawns only once a year, gamete production (Pr) was estimated from the weight loss of the gonad on spawning in scallops of given age (determined from the von Bertalanffy equation describing shell height as a function of age), and then converting to units of energy (1 g dry gametes = 26.0 kJ; MacDonald and Thompson, 1985b). Data from males and females were combined, because there were no consistent differences between the sexes in somatic or gonad growth curves (MacDonald and Thompson, 1985b).

Reproductive effort

Reproductive effort (RE), defined as the proportion of non-respired assimilation allocated to reproduction, was calculated for each age class:

$$RE = [Pr/(Pg + Pr)] \cdot 100$$

To compensate for differences in growth rate between populations, RE was also expressed as a function of somatic weight (MacDonald *et al.*, 1987). Furthermore, there were differences in longevity between populations (MacDonald and Thompson 1985a; this paper), so we also related RE to the proportion of the lifespan represented by any given age.

Results

Water temperature

Water temperatures were higher off New Jersey than at the more northerly sites, except in the summer, when the water at St. Andrews was warmer than elsewhere (Fig. 2). In New Jersey, the temperature reached 17°C in November, but never fell below 5°C during the winter, whereas at St. Andrews and particularly at Sunnyside, winter temperatures were much lower. The form of the temperature cycle was similar at St. Andrews and Sunnyside. Water temperatures in the shallower depths at these two locations generally exceeded those in deeper water, except during the winter (December–April), when the water columns were vertically mixed. Cumulative annual day degrees were estimated as 3180 for New Jersey, 2536 (10 m) and 2400 (31 m) for St. Andrews, and 1451 (10 m) and 957 (31 m) for Sunnyside.

Gametogenic cycle

Gametes observed in histological sections were divided into two categories: (1) developing gametes (DG), representing early stages, and (2) mature or ripe gametes (MG), (MacDonald and Thompson, 1986). Since the gametogenic cycles of Sunnyside scallops from 10 m and 31 m were similar (MacDonald and Thompson, 1986), only data from 10 m were used in comparisons with New Jersey scallops.

In both populations (Sunnyside and New Jersey), the seasonal cycles for GVF (TG; males and females combined) were very similar, although in both years Sunnyside scallops spawned two months earlier than those from New Jersey (Fig. 3). According to Dickie (1953)

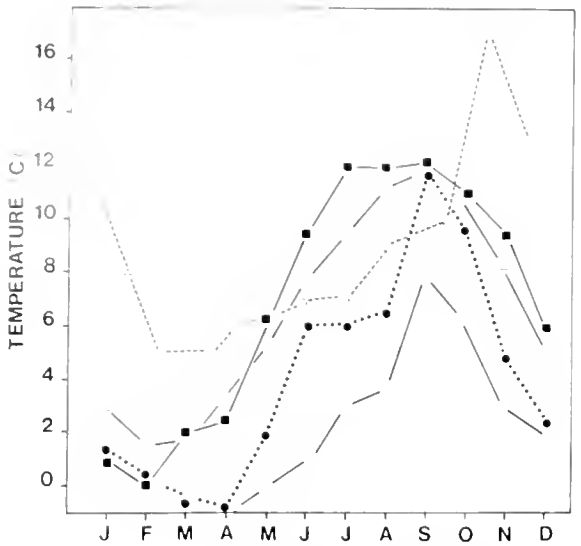

Figure 2. Water temperatures. ●---● Sunnyside (10 m); ○---○ Sunnyside (31 m); ■---■ St. Andrews (10 m); □---□ St. Andrews (31 m); △---△ New Jersey.

and Beninger (1987), spawning in *Placopecten magellanicus* from the St. Andrews area occurs at the same time as it does at Sunnyside, *i.e.*, late August to early September. Whereas gametogenesis began earlier in the year at Sunnyside than at New Jersey, mature (ripe) gametes did not appear in Sunnyside scallops until April, compared with January for New Jersey scallops in which mature gametes were present almost year-round. There was a small decrease in GVF (MG) during June and July in scallops from New Jersey, followed by an increase in August, which may suggest partial or dribble spawning (Newell *et al.*, 1982).

Shell growth

Von Bertalanffy equations were used to relate shell height to age for all age classes represented in each sample (Table I). There was a latitudinal gradient in longevity (Sunnyside > St. Andrews > New Jersey; see legend to Table I), although there was no clear trend for asymptotic height (H_∞). Shell height was greatest at Sunnyside (10 m) and least at New Jersey, with intermediate values in scallops from St. Andrews, but in deeper water (31 m) at Sunnyside H_∞ was relatively small. The Brody growth coefficient (K) was lower in the Sunnyside population (especially at 31 m) than in the others, indicating that scallops from Sunnyside reached asymptotic height relatively slowly compared with those from more southerly locations, but caution must be exercised in comparing growth coefficients when H_∞ values are different (see Discussion).

For a rigorous comparison of growth rates, polynomial regressions afford the advantage that they can be handled by linear models (MacDonald and Thompson, 1985a). Comparisons were made between scallops from 31 m at Sunnyside, St. Andrews, and New Jersey, and also between scallops from the shallowest depths from which they were obtained at each location, using data for individuals two to eight years old (Fig. 4, Table II). Scallops from 31 m at New Jersey and St. Andrews grew at similar rates but significantly faster than scallops from 31 m at Sunnyside. However, when scallops from the shallowest collection depths were compared, shell growth was similar at all three sites.

Somatic weight

Polynomial regressions of somatic weight against age were also compared (Fig. 5, Table II). For scallops from

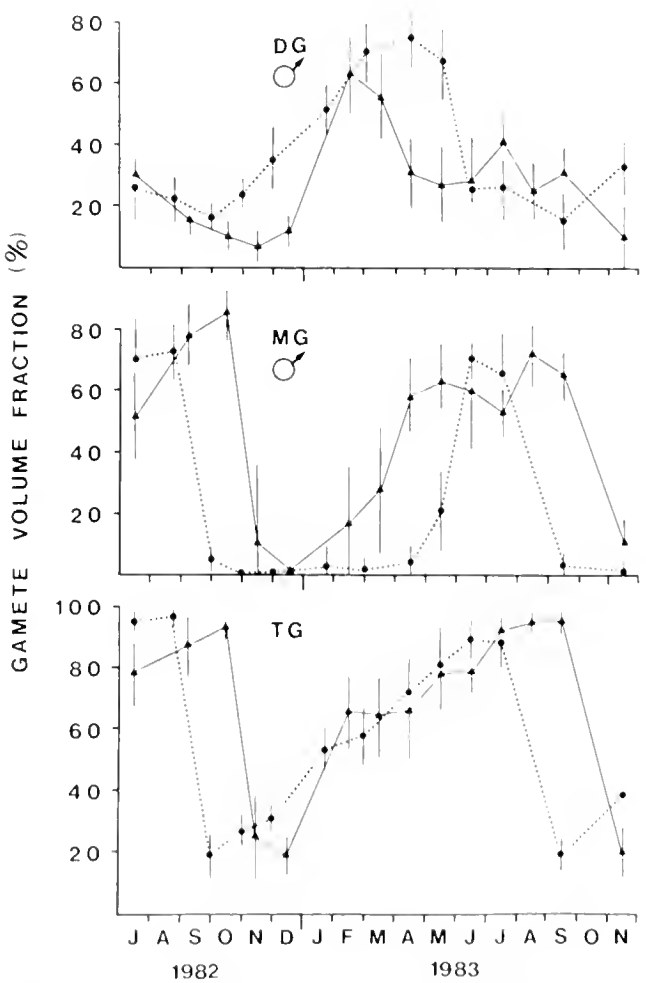

Figure 3. Gamete volume fraction for scallops, *Placopecten magellanicus*, from Sunnyside (10 m depth; ●---●) and New Jersey (▲---▲). Data for developing gametes (DG) and mature gametes (MG) are for males only, whereas data for total gametes (TG) are for males and females combined. Values are means ± 95% confidence limits.

Table I

Parameters (± 95% C.L.) of the von Bertalanffy equations describing shell height (H, mm) as a function of age (years) in Placopecten magellanicus *collected from depths of 10 m and 31 m in three locations*

	Sunnyside, Newfoundland		St. Andrews, New Brunswick		New Jersey	
	10 m	31 m	10 m	31 m	10 m	31 m
H_∞	176.5 ± 3.0	158.4 ± 3.3	166.9 ± 12.5	166.0 ± 8.1	—	155.9 ± 9.6
K	0.19 ± 0.013	0.16 ± 0.015	0.21 ± 0.033	0.21 ± 0.032	—	0.22 ± 0.04
t_0	0.55	0.10	0.51	0.53	—	0.32
r^2	0.97	0.97	0.96	0.98	—	0.95
n	272	243	83	73	—	145

The age classes found were 1–20 years at Sunnyside, 1–12 years at St. Andrews, and 1–10 years at New Jersey. r^2 = coefficient of determination, n = number of observations.

31 m, all regressions were significantly different, somatic weight being greatest at St. Andrews and least at Sunnyside. However, at the shallowest depths somatic weight was greater in scallops from St. Andrews and Sunnyside than in those from New Jersey. Significant differences were also observed between linear regressions of somatic weight against shell height (both variates transformed to logarithms), excepting the samples from the shallowest collections at Sunnyside and New Jersey (Tables II, III).

Production

There was a clear latitudinal trend in gamete production (Pr) by individual scallops from 31 m depth (New Jersey > St. Andrews > Sunnyside) which was also reflected in total production (Pg + Pr), but the greatest somatic production (Pg) was at St. Andrews and the least at Sunnyside (Fig. 6). Scallops from New Jersey also produced more gametes than those from shallow water (10 m) at the more northerly locations, and older individuals from New Jersey (>5 years) showed greater total production. For scallops from the shallowest depths at each site, Pg increased at higher latitudes (Sunnyside 10 m > St. Andrews > New Jersey), although the lowest values for Pg were observed in samples from 31 m at Sunnyside. All comparisons of gonad dry weight at any given shell height showed significant differences between populations, excepting that between Sunnyside (10 m) and New Jersey (Table II).

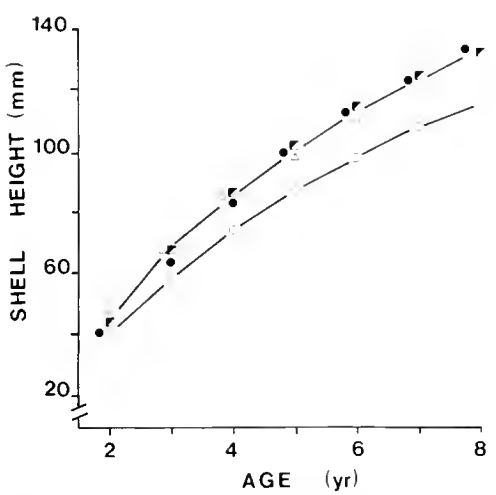

Figure 4. Shell growth in scallops, *Placopecten magellanicus*, from Sunnyside (● 10 m; ○ 31 m), St. Andrews (■ 10 m; □ 31 m) and New Jersey (△).

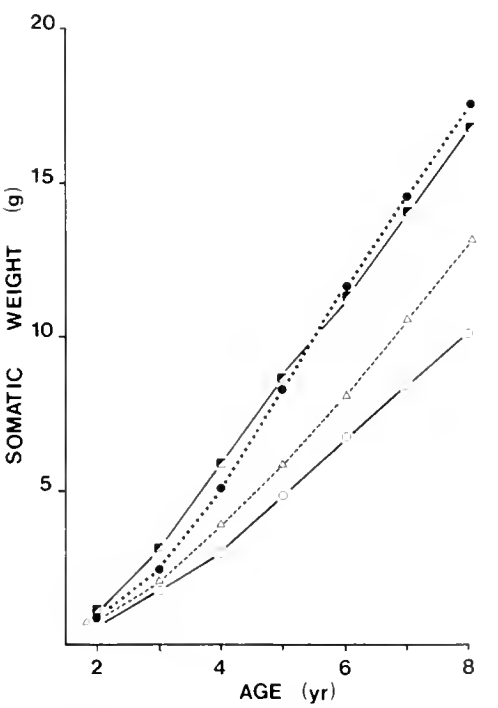

Figure 5. Somatic growth (dry tissue less gonad and shell) in *Placopecten magellanicus* from Sunnyside (●···● 10 m; ○---○ 31 m), St. Andrews (■---■ 10 m; □---□ 31 m), and New Jersey (△---△).

Table II

Summary of (a) t values for comparisons of polynomial regression equations (shell height and somatic weight against age) and (b) comparisons of allometric relationships between somatic weight, gonad weight, and shell height for populations of Placopecten magellanicus

		31 m vs 31 m vs 31 m			10 m vs 31 m+ vs 10 m		
		NF vs NJ	NJ vs NB	NF vs NB	NF vs NJ	NJ vs NB	NF vs NB
(a) Polynomial t values							
Shell Height vs. age	β_0	5.05***	0.69	4.11***	0.85	0.32	1.59
	β_1	4.37***	0.44	4.82***	1.41	0.58	1.12
	β_2	0.70	0.73	0.10	1.13	1.33	0.10
	β_3	1.84	1.29	0.88	0.87	1.31	0.39
Somatic Weight vs. age	β_0	3.58***	4.51***	7.71***	4.29***	7.06***	3.67***
	β_1	3.06**	1.22	5.47***	2.05	2.71**	0.73
	β_2	0.99	0.63	0.55	0.57	0.62	0.02
(b) Allometric regression t values							
Somatic Weight vs. Shell Height	log a	2.71**	11.10***	—	8.96***	10.12***	0.67
	b	0.59	1.54	2.48*	1.15	0.12	1.53
Gonad Weight vs. Shell Height	log a	—	8.00***	—	2.32	6.52***	—
	b	4.88***	0.45	5.64***	0.35	2.22	2.54*

Samples were collected from New Jersey (NJ; 31 m), St. Andrews, New Brunswick (NB; 10 and 31 m), and Sunnyside, Newfoundland (NF; 10 and 31 m). (*$P < 0.05$, **$P < 0.01$, ***$P < 0.001$, + indicates NJ sample).

The large reproductive output and low body weight of New Jersey scallops resulted in a higher turnover ratio [production: biomass ratio, (Pr & Pg)/B] than in individuals from the other populations (Fig. 7). At Sunnyside, production per unit weight was greater at 10 m than at 31 m, whereas at St. Andrews the turnover ratio for scallops less than 6 years old was independent of depth. With the exception of the New Jersey population, turnover ratio was a decreasing function of age.

Table III

Allometric relationships between tissue weight and shell height in Placopecten magellanicus *collected in 1983 from depths of 10 m and 31 m in three locations*

	Sunnyside, Newfoundland		St. Andrews, New Brunswick		New Jersey	
	10 m	31 m	10 m	31 m	10 m	31 m
Somatic						
log a	−4.67	−3.76	−4.77	−4.55	—	−4.94
b	2.77	2.28	2.83	2.72	—	2.86
r^2	0.97	0.83	0.99	0.99	—	0.93
n	93	97	83	75	—	48
Gonad						
log a	−6.29	−5.75	−9.96	−8.21	—	−7.89
b	3.29	2.87	5.05	4.16	—	4.18
r^2	0.83	0.60	0.92	0.93	—	0.95
n	41	48	43	41	—	24

Regressions are of the form $W = aH^b$, where W = dry weight (g) of the somatic tissue or of the gonad immediately before spawning, H = shell height (mm), a and b are fitted parameters.

Reproductive effort

There was considerable variation in RE between sites and between depths (Fig. 8). For all ages and sizes, RE at any given age or somatic weight was greatest in scallops from New Jersey, owing to higher Pr and lower Pg values than in individuals from the other populations. At Sunnyside, scallops from 10 m had a greater RE than those from 31 m. Reproductive effort was greater in young scallops (<5 years) from Sunnyside than in those from similar depths at St. Andrews, but lower in scallops older than 5 years. However, when expressed as a function of lifespan, RE was greatest in Sunnyside scallops and least in those from St. Andrews (Sunnyside 10 m > Sunnyside 31 m > New Jersey > St. Andrews 10 m > St. Andrews 31 m), *i.e.*, the maximum values observed for RE were in large, old individuals from the Newfoundland location.

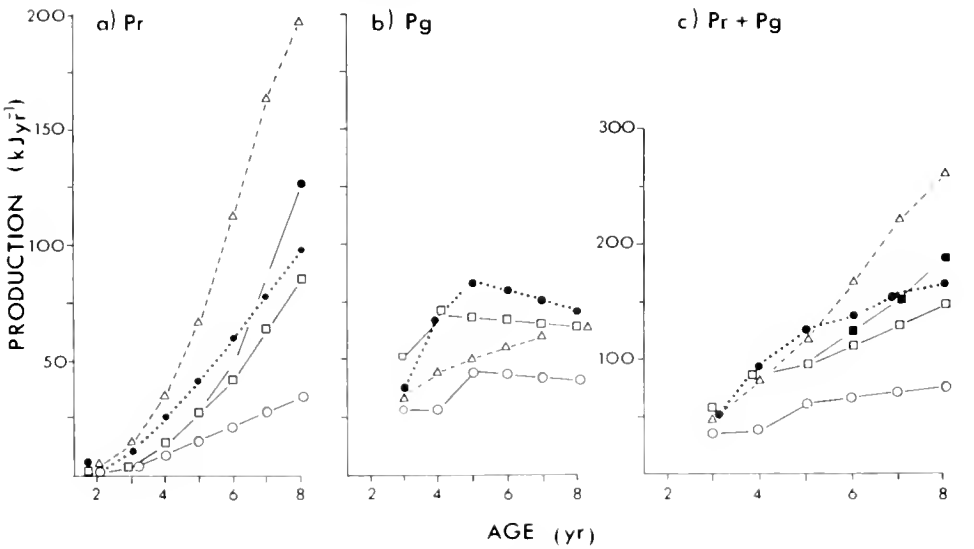

Figure 6. Gonad production (P_r), somatic production (P_g) and total production ($P_g + P_r$) by individual scallops, *Placopecten magellanicus*, from Sunnyside (●···● 10 m; ○---○ 31 m), St. Andrews (■---■ 10 m; □---□ 31 m), and New Jersey (△---△).

Discussion

In all the populations of *Placopecten magellanicus* examined here and in others described elsewhere (Thompson, 1977; Robinson *et al.*, 1981; Beninger, 1987) there is a discrete annual reproductive cycle with a well-synchronized spawning period. A slight decrease in GVF in New Jersey scallops during June and July may represent a minor spawning of the type described by Naidu (1970) for scallops from a bed in western Newfoundland, but we did not observe this phenomenon in Sunnyside scallops. In Newfoundland, scallops spawn in August–September (Naidu, 1970; this study). Beninger (1987) and Robinson *et al.* (1981) report a similar timing in *P. magellanicus* from the Bay of Fundy and from Maine, respectively. Our observation that the giant scallop spawns later in the year off the coast of New Jersey suggests that this species may be similar to the bay scallop *Argopecten irradians*, in which spawning occurs later in southern populations than in those further north (Sastry, 1970; Barber and Blake, 1983). Sastry (1970) attributed this latitudinal differentiation in the gametogenic cycle of *A. irradians* to differences in food supply, since the peak in phytoplankton availability occurs later at the southern location than the northern one. However, according to some reports, *P. magellanicus* spawns early (July) at the southern limit of its range (MacKenzie, 1979). On the north shore of the Gulf of St. Lawrence, which is close to the northern limit, spawning also takes place in July (Gaudet, pers. comm.). Thus, there are no clearly identifiable latitudinal trends in the timing of spawning, although the variation appears to be less than in some other bivalves, notably *Mytilus edulis*, in which the gametogenic cycle may be highly variable over a small geographic range (Lowe *et al.*, 1982; Newell *et al.*, 1982). Borrero (1987) found that the temporal variation across the intertidal zone in the reproductive cycle of the ribbed mussel *Geukensia demissa* may exceed that among latitudinally separated populations. As in other species, re-

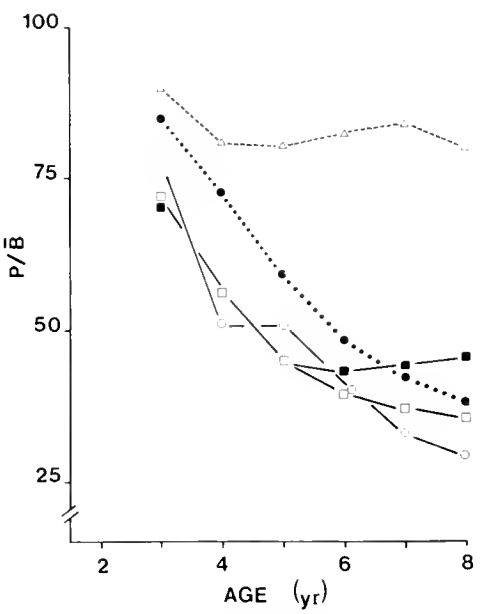

Figure 7. Turnover ratios (production: biomass P/B, where $P = P_g + P_r$) in scallops, *Placopecten magellanicus*, from Sunnyside (●···● 10 m; ○---○ 31 m), St. Andrews (■---■ 10 m; □---□ 31 m), and New Jersey (△---△).

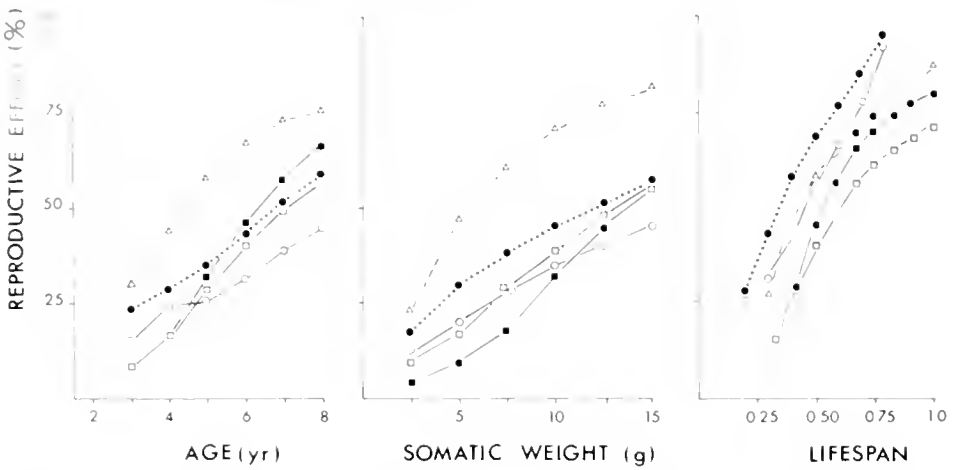

Figure 8. Reproductive effort, $100 \times P_r/(P_g + P_r)$, as a function of age, somatic weight and lifespan in the scallop *Placopecten magellanicus*. ●—● Sunnyside (10 m); ○---○ Sunnyside (31 m); ■---■ St. Andrews (10 m); □---□ St. Andrews (31 m); △---△ New Jersey.

production in *P. magellanicus* is probably controlled primarily by local environmental factors, especially food supply, which determines the nutrient reserve and hence the capability to initiate gamete development (Newell *et al.*, 1982).

Comparisons of shell growth rates from our own study and others show that differences in shell height at any given age in scallops from Newfoundland, New Brunswick, and Georges Bank are small (Fig. 9), and that there is as much variation between depths at several sites in eastern Newfoundland (MacDonald and Thompson, 1985a) as there is between populations at different latitudes. We have some evidence for an increase in asymptotic height in *Placopecten magellanicus* at higher latitudes, which is consistent with studies on some bivalve species, but not others (see Introduction). However, there is a clear differentiation in longevity, which is greater in northern than in southern populations.

Care must be taken when comparing shell growth rates from different populations, especially when the von Bertalanffy function is used. It is not appropriate to base comparisons on the parameter K when the asymptotic heights or lengths differ considerably between populations, because K is inversely related to H_∞ (Ralph and Maxwell, 1977; Haukioja and Hakala, 1979). Furthermore, K is a growth coefficient and should not be regarded as a growth rate *per se* (Ricker, 1975). Attempts to combine H_∞ and K into a single parameter have been made (Gallucci and Quinn, 1979; Appeldoorn, 1983), but this does not overcome the fundamental problem that the two are interdependent (Beukema and Meehan, 1985). Many of the literature values for von Bertalanffy parameters are of limited value for comparative purposes, since confidence limits are often not provided, but several statistical packages (including SAS) now include algorithms for handling nonlinear functions of the von Bertalanffy type and provide not only estimates of the parameters but also their variances. We circumvented the problems inherent in the von Bertalanffy function by also fitting polynomials to the shell growth data, which demonstrated that growth was slower at Sunnyside (especially at 31 m depth) than at more southerly

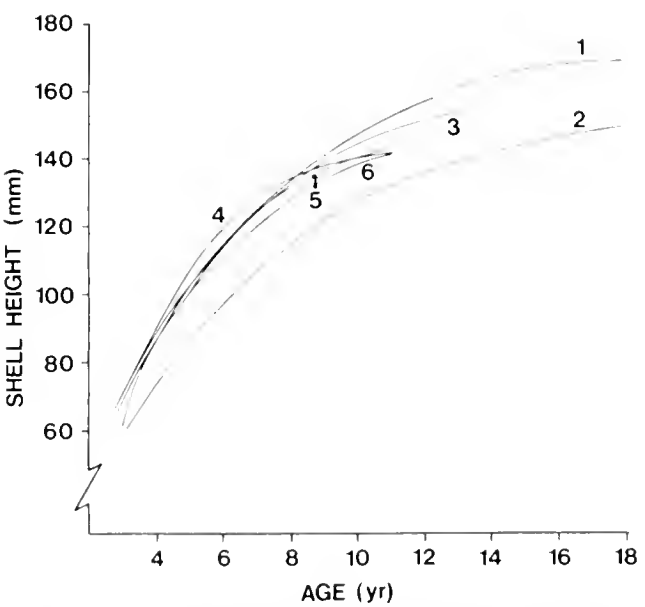

Figure 9. Shell growth curves for scallops, *Placopecten magellanicus*, from several locations. 1 = Sunnyside, Newfoundland, 10 m depth; 2 = Sunnyside, 31 m; 3 = St. Andrews, New Brunswick (all from MacDonald and Thompson, 1985a); 4 = Georges Bank (Brown *et al.*, 1972); 5 = Mid-Atlantic Bight (Serchuk *et al.*, 1982); 6 = New Jersey (this paper).

locations, but the problem with this approach is that the coefficients themselves have no biological significance.

There is considerable intraspecific variation in the somatic growth rate of *Placopecten magellanicus*, and in the production of somatic and germinal tissue, but only in reproductive output is there any evidence of latitudinal differentiation; scallops from New Jersey are more fecund than those from locations further north. For the most part, variation along a depth gradient on a microgeographic scale may be as great or greater than variation on a latitudinal scale (MacDonald and Thompson, 1985a, b; this study). Reproductive output in particular shows great plasticity, *viz.* the variation between years in shallow water at Sunnyside. Furthermore, MacDonald (1986) recorded greater shell growth rates, reproductive output, and somatic production in giant scallops maintained in suspended culture than in those growing on the bottom nearby.

These findings are consistent with observations on other bivalve species. In a comparison of several populations of *Argopecten irradians*, Bricelj *et al.* (1987) found the greatest differences in fecundity, timing of spawning, adductor muscle weight, and shell height to be between locations less than 2 km apart. In the weathervane scallop, *Patinopecten caurinus*, individuals from offshore beds show slower shell growth, a reduced asymptotic height and lower somatic and germinal production than is found in conspecifics from inshore areas, where food is more plentiful (MacDonald and Bourne, 1987). The growth of shell and somatic tissue is enhanced in the scallop *Chlamys islandica* by growing the animals in suspended culture (Wallace and Reinsnes, 1985). The mussel *Mytilus edulis* also exhibits considerable phenotypic variation in reproductive characteristics over a small geographic range (Bayne *et al.*, 1983). Similar observations have been made on fish (Kipling and Frost, 1969; Mann *et al.*, 1984).

According to Calow (1979), selection for enhanced reproductive output should result in a reduction in the lifespan, and there is a considerable body of evidence to support this position. Thus, in *Placopecten magellanicus*, the shift in emphasis from growth to reproduction occurs earlier in scallops from New Jersey than in those from more northerly locations, and total production is greater in the former than the latter, whereas longevity is reduced in these productive, fecund individuals from New Jersey. Further evidence comes from our observations on scallops from various depths at Sunnyside, Newfoundland. Since we were unable to resolve accurately growth lines for animals older than twenty years, these individuals were excluded from our analyses. However, we did record that a greater proportion (25%) of the total number of scallops (426) taken from 31 m depth fell into this category, compared with only 8.6% (n = 431) at 10 m. Thus on this extremely small geographic scale, longevity is reduced when food and temperature conditions are favorable and production (somatic and gonadal) by individual scallops is increased. Furthermore, MacDonald (1986) has demonstrated that asymptotic height decreases in *Placopecten magellanicus* grown in suspended culture, which is associated with greater production; and in a review of data from several species of limpets, Grahame and Branch (1985) describe a trend whereby longevity is a decreasing, non-linear function of reproductive output and of the growth coefficient K.

The importance of water temperature in determining geographic differentiation in growth rate and fecundity has been emphasized by Levinton (1983) and Lonsdale and Levinton (1985). The latitudinal variation in longevity which we have recorded in *Placopecten magellanicus* is certainly correlated with an observed temperature gradient, and at the Sunnyside site there is also an increase in longevity (associated with decreased production) in scallops from deeper, colder water.

There is little information on the degree to which intraspecific variation in growth and reproduction is environmentally induced or genetically determined. Levinton (1983) identified a genetic component to somatic growth differences among latitudinally separated sibling species in a genus of dorvilleid polychaete, and Lonsdale and Levinton (1986) described genetically based differentiation in both growth rate and fecundity along a latitudinal gradient in a harpacticoid copepod. Thompson and Newell (1985) recorded differentiation in the physiological response to high temperature in two latitudinally separated populations of the mussel *Mytilus edulis*, but were unable to determine whether this was genetic or a result of irreversible phenotypic adaptation. In a reciprocal transplant experiment, Widdows *et al.* (1984) found that most of the physiological variation between two populations of *M. edulis* was attributable to environmental rather than to genotypic factors, although acclimatization was not complete and a genetic component may therefore have been present. This is consistent with other observations on *M. edulis* demonstrating that most of the variation in tissue growth is accounted for by site rather than by stock (Mallet *et al.*, 1987). However, in another study in which reciprocal transplants were made between populations of *M. edulis*, Dickie *et al.* (1984) found a large environmental influence on growth combined with a significant genetic effect.

We have no information on genetic control of growth and reproduction in *Placopecten magellanicus*, but the considerable phenotypic plasticity in this species on a microgeographic scale suggests a strong environmental influence, especially since we have correlated changes in growth and reproduction with temperature and food conditions. This does not necessarily imply that local ge-

netic variability is of no importance, since genetic differentiation can still be significant when phenotypic variation in growth and reproductive traits is greater than the genetic component. The giant scallop exhibits a growth pattern described by Sebens (1987) as Type I indeterminate growth (plastic asymptotic growth), in which the size attained by an individual is largely governed by environmental conditions. Such phenotypic variability for a single species merits consideration in any analysis of the adaptive value of reproductive tactics, but has received little attention (Bayne *et al.*, 1983). In the same vein, Stearns (1976) has cautioned investigators against invoking evolutionary explanations to account for reproductive trends without first eliminating genetic and environmental factors, especially food. We conclude that growth and reproductive traits in *Placopecten magellanicus* are inter-related and highly variable on a temporal as well as a spatial scale, as they probably are in many other bivalve species; that local variability often exceeds variation along a latitudinal gradient; and that enhanced reproductive output is associated with reduced longevity.

Acknowledgments

We thank Dr. R. W. Elner, Dr. E. Gould, and Mr. R. Chandler for arranging scallop collections from St. Andrews and from New Jersey. Collections from Newfoundland were made by staff of the MSRL diving unit. Laboratory assistance was provided by Ms. J. Senciall. We thank Drs. B. L. Bayne, D. J. Innes, J. S. Levinton, and R. I. E. Newell for reviewing the manuscript. The work was supported by an NSERC operating grant to R.J.T. and by scholarships to B.A.M. from the Marine Sciences Research Laboratory and the Faculty of Graduate Studies, Memorial University of Newfoundland. This is Publ. No. D-32001-3-88 of the New Jersey Agricultural Experimental Station, supported by state funds. Marine Sciences Research Laboratory Contribution Number 731.

Literature Cited

Appeldoorn, R. S. 1983. Variation in the growth rate of *Mya arenaria* and its relationship to the environment as analyzed through principal components analysis and the ω parameter of the von Bertalanffy equation. *Fish. Bull.* **81:** 75–84.

Bachelet, G. 1980. Growth and recruitment of the tellinid bivalve *Macoma balthica* at the southern limit of its distribution, the Gironde Estuary (S.W. France). *Mar. Biol.* **59:** 105–117.

Barber, B. J., and N. J. Blake. 1983. Growth and reproduction of the bay scallop, *Argopecten irradians* (Lamarck) at its southern distributional limit. *J. Exp. Mar. Biol. Ecol.* **66:** 247–256.

Bayne, B. L., P. N. Salkeld, and C. M. Worrall. 1983. Reproductive effort and value in different populations of the marine mussel *Mytilus edulis* L. *Oecologia* **59:** 18–36.

Beninger, P. G. 1987. A qualitative and quantitative study of the reproductive cycle of the giant scallop, *Placopecten magellanicus*, in the Bay of Fundy (New Brunswick, Canada). *Can. J. Zool.* **65:** 495–498.

Beukema, J. J., and B. W. Meehan. 1985. Latitudinal variation in linear growth and other shell characteristics of *Macoma balthica*. *Mar. Biol.* **90:** 27–33.

Borrero, F. J. 1987. Tidal height and gametogenesis: reproductive variation among populations of *Geukensia demissa*. *Biol. Bull.* **173:** 160–168.

Bricelj, V. M., J. Epp, and R. E. Malouf. 1987. Intraspecific variation in reproductive and somatic growth cycles of bay scallops *Argopecten irradians*. *Mar. Ecol. Prog. Ser.* **36:** 123–137.

Brousseau, D. J. 1979. Analysis of growth rate in *Mya arenaria* using the von Bertalanffy equation. *Mar. Biol.* **51:** 221–227.

Brown, B. E., M. Parrack, and D. D. Flescher. 1972. Review of the current status of the scallop fishery in ICNAF division 5Z. ICNAF *Res. Doc.* 72/113, Serial No. 2829, 13 pp. (mimeo).

Calow, P. 1979. The cost of reproduction—a physiological approach. *Biol. Rev.* **54:** 23–40.

Dickie, L. M. 1953. Fluctuations in abundance of the giant scallop, *Placopecten magellanicus* (Gmelin), in the Digby area of the Bay of Fundy. *J. Fish. Res. Board Can. MS Rep. Biol. Sta.* No. **526.**

Dickie, L. M., P. R. Boudreau, and K. R. Freeman. 1984. Influences of stock and site on growth and mortality in the blue mussel (*Mytilus edulis*). *Can. J. Fish. Aquat. Sci.* **41:** 134–140.

Forgeron, F. D. 1959. Temperature and salinity in the Quoddy region. Pp. 1–23 in *Passamaquoddy Fisheries Investigations. Report to the International Joint Commission Ottawa and Washington.* Appendix 1: Oceanography.

Galluci, V. F., and T. J. Quinn. 1979. Reparameterizing, fitting and testing a simple growth model. *Trans. Am. Fish. Soc.* **108:** 14–25.

Giese, A. C., and J. S. Pearse. 1974. Introduction: general principles. Pp. 1–49 in *Reproduction of Marine Invertebrates*, Vol. 1, A. C. Giese and J. S. Pearse, eds. Academic Press, New York.

Gilbert, M. A. 1973. Growth rate, longevity and maximum size of *Macoma balthica* (L.). *Biol. Bull.* **145:** 119–126.

Grahame, J., and G. M. Branch. 1985. Reproductive patterns of marine invertebrates. *Oceanogr. Mar. Biol. Ann. Rev.* **23:** 373–398.

Haukioja, E., and T. Hakala. 1979. Asymptotic equations in growth studies—an analysis based on *Anodonta piscinalis* (Mollusca, Unionidae). *Ann. Zool. Fennici* **16:** 115–122.

Kipling, C., and W. E. Frost. 1969. Variations in the fecundity of pike *Esox lucius* L. in Windermere. *J. Fish. Biol.* **1:** 221–237.

Levinton, J. S. 1983. The latitudinal compensation hypothesis: growth data and a model of latitudinal growth differentiation based upon energy budgets. I. Interspecific comparison of *Ophryotrocha* (Polychaeta: Dorvilleidae). *Biol. Bull.* **165:** 686–698.

Lonsdale, D. J., and J. S. Levinton. 1985. Latitudinal differentiation in copepod growth: an adaptation to temperature. *Ecology* **66:** 1397–1407.

Lonsdale, D. J., and J. S. Levinton. 1986. Growth rate and reproductive differences in a widespread estuarine harpacticoid copepod (*Scottolana canadensis*). *Mar. Biol.* **91:** 231–237.

Lowe, D. M., M. N. Moore, and B. L. Bayne. 1982. Aspects of gametogenesis in the marine mussel, *Mytilus edulis* (L.). *J. Mar. Biol. Assoc. U. K.* **62:** 133–145.

MacDonald, B. A. 1986. Production and resource partitioning in the giant scallop *Placopecten magellanicus* grown on the bottom and in suspended culture. *Mar. Ecol. Prog. Ser.* **34:** 79–86.

MacDonald, B. A., and N. F. Bourne. 1987. Growth, reproductive output, and energy partitioning in weathervane scallops, *Patinopecten caurinus*, from British Columbia. *Can. J. Fish. Aquat. Sci.* **44:** 152–160.

MacDonald, B. A., and R. J. Thompson. 1985a. Influence of temperature and food availability on the ecological energetics of the giant

scallop *Placopecten magellanicus*. I. Growth rates of shell and somatic tissue. *Mar. Ecol. Prog. Ser.* **25:** 279–294.

MacDonald, B. A., and R. J. Thompson. 1985b. Influence of temperature and food availability on the ecological energetics of the giant scallop *Placopecten magellanicus*. II. Reproductive output and total production. *Mar. Ecol. Prog. Ser.* **25:** 295–303.

MacDonald, B. A., and R. J. Thompson. 1986. Influence of temperature and food availability on the ecological energetics of the giant scallop *Placopecten magellanicus*. III. Physiological ecology, the gametogenic cycle and scope for growth. *Mar. Biol.* **93:** 37–48.

MacDonald, B. A., R. J. Thompson, and B. L. Bayne. 1987. Influence of temperature and food availability on the ecological energetics of the giant scallop *Placopecten magellanicus*. IV. Reproductive effort, value and cost. *Oecologia* **72:** 550–556.

MacKenzie, C. L. 1979. Biological and fisheries data on sea scallop *Placopecten magellanicus* (Gmelin). U. S. Dept. of Commerce Tech. Rep. No. 19.

Mallet, A. L., C. E. A. Carver, S. S. Coffen, and K. R. Freeman. 1987. Winter growth of the blue mussel *Mytilus edulis* L.: importance of stock and site. *J. Exp. Mar. Biol. Ecol.* **108:** 217–228.

Mann, R. H. K., C. A. Mills, and D. T. Crisp. 1984. Geographical variation in the life-history tactics of some species of freshwater fish. Pp. 171–186 in *Fish Reproduction: Strategies and Tactics*, G. W. Potts and R. J. Wootton, eds. Academic Press, London.

Merrill, A. S., J. A. Posgay, and F. E. Nichy. 1966. Annual marks on shell and ligament of sea scallop *Placopecten magellanicus*. *Fish Bull.* **65:** 299–311.

Naidu, K. S. 1970. Reproduction and breeding cycle of the giant scallop *Placopecten magellanicus* (Gmelin) in Port au Port Bay, Newfoundland. *Can. J. Zool.* **48:** 1003–1012.

Neter, J., W. Wasserman, and M. H. Kutner. 1983. *Applied Linear Regression Models*. Irwin Publishers, Homeland, Illinois.

Newell, G. E. 1964. Physiological variation in intertidal molluscs. Pp. 59–87 in *Physiology of Molluscs*, Vol. 1, K. M. Wilbur and C. M. Yonge, eds. Academic Press, New York.

Newell, R. I. E., T. J. Hilbish, R. K. Koehn, and C. J. Newell. 1982. Temporal variation in the reproductive cycle of *Mytilus edulis* (L.) (Bivalvia: Mytilidae) from localities on the east coast of the United States. *Biol. Bull.* **162:** 299–310.

Ockelmann, K. W. 1958. The zoology of east Greenland. Marine Lamellibranchiata. *Medd. Gronl.* **122:** 1–256.

Porter, H. J. 1974. *The North Carolina Marine and Estuarine Mollusca—an Atlas of Occurrence*. University of North Carolina, Institute of Marine Sciences, Morehead City, North Carolina. 351 pp.

Posgay, J. A. 1957. The range of the sea scallop. *Nautilus* **71:** 55–57.

Posgay, J. A. 1979. Depth as a factor affecting the growth rate of the sea scallop. *Coun Meet. Int. Coun. Explor. Sea* C.M.-ICES/K:27.

Ralph, R., and J. G. H. Maxwell. 1977. Growth of two Antarctic lamellibranchs: *Adamussium colbecki* and *Laternula elliptica*. *Mar. Biol.* **42:** 171–175.

Ricker, W. E. 1975. Computation and interpretation of biological statistics of fish populations. *Bull. Fish. Res. Board Can.* **191:** 1–382.

Robinson, W. E., W. E. Wehling, M. P. Morse, and G. C. McLeod. 1981. Seasonal changes in soft-body component indices and energy reserves in the Atlantic deep-sea scallop, *Placopecten magellanicus*. *Fish. Bull.* **79:** 449–458.

Sastry, A. N. 1970. Reproductive physiological variation in latitudinally separated populations of the bay scallop, *Aequipecten irradians* Lamarck. *Biol. Bull.* **138:** 56–65.

Sastry, A. N. 1979. Pelecypoda (excluding Ostreidae). Pp. 113–292 in *Reproduction of Marine Invertebrates*, Vol. 5, A. G. Giese and J. S. Pearse, eds. Academic Press, New York.

Sebens, K. P. 1987. The ecology of indeterminate growth in animals. *Ann. Rev. Ecol. Syst.* **18:** 371–407.

Seed, R. 1976. Ecology. Pp. 13–65 in *Marine Mussels: Their Ecology and Physiology*, B. L. Bayne, ed. Cambridge University Press, Cambridge.

Seed, R. 1980. Shell growth and form in the Bivalvia. Pp. 23–68 in *Skeletal Growth of Aquatic Organisms*, D. C. Rhoads and R. A. Lutz, eds. Plenum Press, New York.

Serchuck, F. M., P. W. Wood, and R. S. Rak. 1982. Review and assessment of the Georges Bank, Mid-Atlantic and Gulf of Maine Atlantic sea scallop (*Placopecten magellanicus*) resources. NMFS/Woods Hole Ref. Doc. No. 82-06. 132 pp (mimeo).

Stearns, S. C. 1976. Life-history tactics: a review of the ideas. *Q. Rev. Biol.* **51:** 3–47.

Stevenson, J. A., and L. M. Dickie. 1954. Annual growth rings and rate of growth of the giant scallop, *Placopecten magellanicus* (Gmelin) in the Digby area of the Bay of Fundy. *J. Fish. Res. Board Can.* **11:** 660–671.

Thompson, R. J. 1977. Blood chemistry, biochemical composition and the annual reproductive cycle in the giant scallop, *Placopecten magellanicus*, from southeast Newfoundland. *J. Fish. Res. Board Can.* **34:** 2104–2116.

Thompson, R. J., and R. I. E. Newell. 1985. Physiological responses to temperature in two latitudinally separated populations of the mussel, *Mytilus edulis*. *Proc. 19th. Eur. Mar. Biol. Symp.*, pp. 481–495.

Wallace, J. C., and T. G. Reinsnes. 1985. The significance of various environmental parameters for growth of the Iceland scallop, *Chlamys islandica* (Pectinidae), in hanging culture. *Aquaculture* **44:** 229–242.

Weymouth, F., H. McMillan, and W. H. Rich. 1931. Latitude and relative growth of the razor clam *Siliqua patula* Dixon. *J. Exp. Biol.* **8:** 228–249.

Widdows, J., P. Donkin, P. N. Salkeld, J. J. Cleary, D. M. Lowe, S. V. Evans, and P. E. Thomson. 1984. Relative importance of environmental factors in determining physiological differences between two populations of mussels (*Mytilus edulis*). *Mar. Ecol. Prog. Ser.* **17:** 33–47.

Reference: *Biol. Bull.* 175: 372–377. (December, 1988)

Application of a Two-Dimensional Electrophoresis Method to the Systematic Study of Land Snails of Subgenus *Luchuphaedusa* from Southwestern Japan Islands

JUN-ICHI MIYAZAKI, REI UESHIMA, AND TAMIO HIRABAYASHI

Institute of Biological Sciences, The University of Tsukuba, Tsukuba-shi, Ibaraki 305, Japan

Abstract. A land snail, *Tyrannophaedusa (Luchuphaedusa) ophidoon* (family Clausiliidae), is classified into two types, large and small forms, according to shell size. Using a two-dimensional electrophoresis method, we compared the total protein components of the large form with seven members of *Luchuphaedusa* and three species of different subgenera of the same genus, and obtained the similarity ranging from 0.989 to 0.667. The similarity between the large form and *T. (Decolliphaedusa) bilabrata* was the lowest. Two species of the other subgenus, *Nesiophaedusa*, were very similar to the large form. The differences were very small between two specimens of the large form. The small form of *T. (L.) ophidoon* showed large differences from the large form. Thus, the relationship of the large and small forms is considered to be either closely related interspecific populations or distantly differentiated intraspecific populations, by comparing our result with available data obtained previously. Based on values of the similarity obtained, we discuss possible colonization patterns in *Luchuphaedusa*.

Introduction

Luchuphaedusa is a group of Japanese clausiliid snails originally described by Pilsbry (1901) as "section Luchuphaedusa." Kuroda (1963) placed this group in one of three subgenera in the genus *Tyrannophaedusa*. Based on Pilsbry's original description, this group has distinctive morphological characteristics in the shell aperture, the clausilium, and the plicae. In particular, the clausilium is very peculiar and unlike those of any closely related Clausiliid group.

Luchuphaedusa comprises eight species (two having one subspecies) and lives mainly on the Nansei Islands between the Pacific Ocean and the East China Sea (Kuroda, 1963). Only one species inhabits a small area of the Kyushu mainland; two species live on the western islands of Kyushu. Their distribution is distinctive and incompatible with biogeographical boundaries suggested by distributions of terrestrial vertebrates, avians, spiders, insects, and other land snails (Tokuda, 1978). Therefore, it is intriguing to investigate how these slow-moving animals have expanded their habitats, established their unique distribution, and speciated. There is no study so far concerning patterns of their expansion of distribution and speciation and the phylogenetic relationships of species belonging to this group.

T. (L.) ophidoon among *Luchuphaedusa* was originally described by Pilsbry (1905) as making up a distinctive "section Oophaedusa." This species has a peculiar shell shape which does not taper at the summit, while shells of other species are shaped like those of ordinary clausiliids. The species has been classified as the large or small form according to shell size (Pilsbry, 1905; Minato, 1985). Although Minato (1985) concluded that these two forms were conspecific, recent studies show that they are considerably different judging from some anatomical characters and allozyme variation (Ueshima, in prep.). Thus, these two forms are very ambiguous in their species identities. Therefore, it is intriguing to examine their characters from different viewpoints and to discuss the phylogenetic position of *T. (L.) ophidoon* in subgenus

Received 24 February 1988; accepted 18 August 1988.

Luchuphaedusa and taxonomic status of the two forms of this species relating to other species.

We have established a basis for elucidating the evolutionary process of *Luchuphaedusa* by analyzing protein constituents of whole bodies using two-dimensional electrophoresis. The method permits the simultaneous analysis of many characters (Aquadro and Avise, 1981; Miyazaki *et al.*, 1987) and avoids the need to consider intraspecific variation. This is in contrast to one-dimensional electrophoresis which analyzes variable proteins, *i.e.*, enzymes (Ayala *et al.*, 1974; Avise, 1975). We calculate the similarity among species based on two-dimensional electrophoretic patterns and discuss a radiation pattern and the relationships between these land snails.

Materials and Methods

Samples

Species used in this study are listed below. Three species belonging to two different subgenera of *Tyrannophaedusa*, including type species of respective subgenera, were also examined.

(i) *T. (L.) azumai azumai* and *T. (L.) ophidoon* (large and small forms) from Shimo Koshiki-jima Is.

(ii) *T. (L.) nesiothauma* and *T. (L.) oshimae* from Amami O-shima Is.

(iii) *T. (Nesiophaedusa) okinoerabuensis* from Okinoerabu-shima Is.

(iv) *T. (L.) callistochila*, *T. (L.) inclyta*, and *T. (N.) bernardi* from Okinawa Is.

(v) *T. (Decolliphaedusa) bilabrata* from Sho-o-cho, Okayama, Honshu.

The system of classification was according to Kuroda (1963), although some authors treat *Luchuphaedusa*, *Nesiophaedusa*, and *Decolliphaedusa* as full genera. *Nesiophaedusa*, consisting of two species, is endemic to Nansei Islands and is similar to *Luchuphaedusa* in general shell characteristics (Pilsbry, 1901). *Decolliphaedusa* is widely distributed in the southwestern area of Japan.

T. (L.) ophidoon is classified according to shell and anatomical characteristics into large and small forms. A recent study revealed that the large form was composed of two divergent populations inhabiting northern and southern parts of Shimo Koshiki-jima Island (Ueshima, in prep.). Thus, we used only the large form specimens from the southern part of the island to avoid confusion.

A distribution of members of *Luchuphaedusa* and *Nesiophaedusa* and localities where specimens were obtained are shown on the map in Figure 1.

Electrophoresis

Whole bodies of land snails, removed from their shells, were used for electrophoresis. One pair of specimens was used for each comparison.

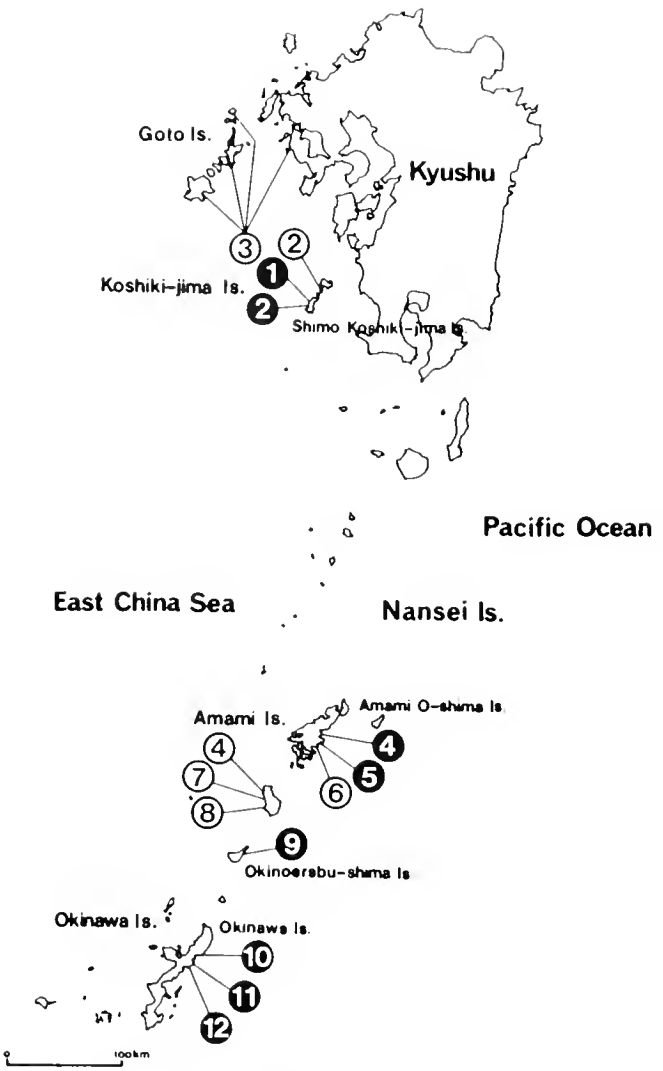

Figure 1. Map of southwestern Japan showing a distribution of members of *Luchuphaedusa* and *Nesiophaedusa* and localities of specimens used in this study. White numbers in closed circles represent islands where specimens for this study were obtained. Black numbers in open circles represent other areas in which members of *Luchuphaedusa* inhabit. 1, The large and small forms of *Tyrannophaedusa (Luchuphaedusa) ophidoon*; 2, *T. (L.) azumai azumai*; 3, *T. (L.) azumai uma*; 4, *T. (L.) nesiothauma*; 5, *T. (L.) oshimae*; 6, *T. (L.) mima mima*; 7, *T. (L.) mima tokunoshimana*; 8, *T. (L.) degenerata*; 9, *T. (Nesiophaedusa) okinoerabuensis*; 10, *T. (N.) bernardi*; 11, *T. (L.) callistochila*; 12, *T. (L.) inclyta*. *T. (Decolliphaedusa) bilabrata* is not included.

Sample solubilization and two-dimensional electrophoresis were carried out as described previously (Hirabayashi, 1981; Hirabayashi *et al.*, 1983; Oh-Ishi and Hirabayashi, 1988). In brief, the whole body was homogenized thoroughly in 20 volumes of an extraction medium containing 8 *M* guanidine HCl, which prevents protease activity completely. The homogenate was dialyzed against 5 *M* urea and 1 *M* thiourea and centrifuged

at 60,000 × *g* for 45 min. The supernatant (80 μl or 120 μl) was subjected to the first dimension isoelectric focusing with agarose gels for 12,500 V·h. The second dimension SDS-polyacrylamide gel electrophoresis was performed as described by Laemmli (1970), at 30 mA when the bromophenol tracking dye was in the stacking gel of 3% acrylamide and at 60 mA until the dye reached the lower end of the running gel of a concentration gradient of 12–20% acrylamide. After electrophoresis, proteins were stained by Coomassie brilliant blue as described by Stephano *et al.* (1986).

Analysis

A method for comparison between two specimens has been described (Miyazaki, 1987). For comparison of two-dimensional electrophoresis patterns, we used a triplet method in which two different samples to be compared (each 80 μl) and their mixture (60 + 60 μl) were focused and electrophoresed at the same time. One set composed of three patterns was examined on photographs. The overlapping of protein spots was confirmed on the mixture pattern after it was presumed from comparison between two individual patterns. A close examination of the mixture pattern is indispensable to identify subtle differences in positions of spots and to judge precisely the overlapping of spots, although only individual patterns were used for comparison by some authors (Ohnishi *et al.*, 1983a; Ohnishi *et al.*, 1983b; Williams, 1984).

In most cases we used the large form as a standard counterpart for comparison, because its taxonomic position relative to others is especially intriguing. About two to four hundred protein spots were examined on each electrophoretic pattern and the similarity was calculated as described by Aquadro and Avise (1981).

Results

Two typical sets for comparison between two-dimensional electrophoresis patterns are represented in Figure 2. Triplet patterns on the left are for investigating variation between different individuals of the large form of *Tyrannophaedusa (Luchuphaedusa) ophidoon* (Fig. 2a, b, c). Those on the right are for comparison between the large form of *T. (L.) ophidoon* and *T. (Nesiophaedusa) bernardi* (Fig. 2d, e, f). The pattern of *T. (N.) bernardi* (f in Fig. 2) is very different from that of the large form (d in Fig. 2). The patterns from different specimens of the large form from the same locality (a, c in Fig. 2) are very similar, showing almost no variation between individuals. Middle patterns (b, e in Fig. 2) of each set are derived from mixtures of two different samples.

The similarity was calculated according to the formula: $F = 2N_{xy}/(N_x + N_y)$, where F is the similarity between specimens x and y, N_{xy} is the number of spots shared by x and y, and N_x and N_y are the numbers of spots scored for x and y, respectively (Aquadro and Avise, 1981). The result of calculations is shown in Table 1. The similarity value between different specimens of the large form was very large (0.989), while the value between the large and small forms was smaller (0.913), suggesting that the large and small forms are definitely different populations. The result supports that *T. (Decolliphaedusa) bilabrata* is most divergent from *Luchuphaedusa*, because the similarity between *T. (D.) bilabrata* and the large form was the lowest (0.667) of all combinations examined. However, two species of other subgenus *Nesiophaedusa*, *T. (N.) okinoerabuensis* and *T. (N.) bernardi*, were more similar to the large form rather than some members of *Luchuphaedusa*, such as *T. (L.) inclyta*.

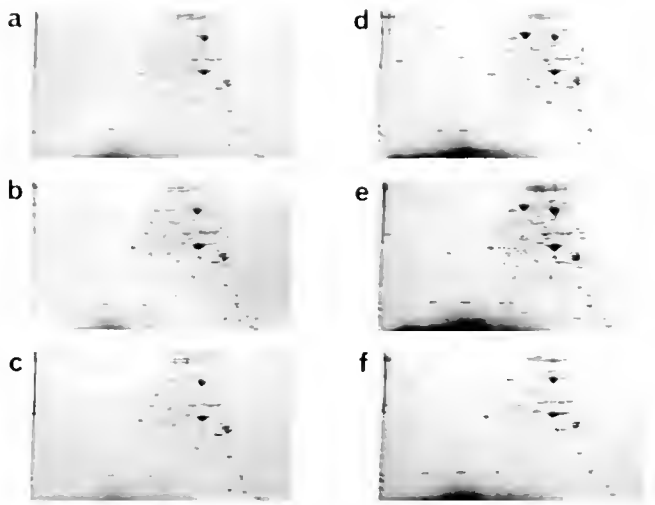

Figure 2. Two-dimensional electrophoresis patterns of whole bodies of land snails in genus *Tyrannophaedusa*. Electrophoresis was carried out as described previously (Hirabayashi, 1981; Oh-Ishi and Hirabayashi, 1988). Triplet patterns for investigating variation between different individuals of the large form of *T. (Luchuphaedusa) ophidoon* are represented on the left (a–c). Patterns from two different specimens of the same locality (a and c) and their mixture pattern (b) are shown. Triplet patterns for comparison between the large form of *T. (L.) ophidoon* and *T. (Nesiophaedusa) bernardi* are represented on the right (d–f), where d is the pattern of the large form, f is that of *T. (N.) bernardi*, e is that of their mixture.

Schematic drawing of a distribution of similarity values is shown in Figure 3. There were three large gaps of values; the first is between the large and small forms (0.076), the second between the small form and *T. (L.) azumai azumai* (0.067), and the third between *T. (L.) inclyta* and *T. (D.) bilabrata* (0.069). One may suppose that the large and small forms which live on Shimo Koshiki-jima Island (Fig. 1) are divergent from *T. (L.) azu-*

Table I

Similarity among land snails of Tyrannophaedusa

Combination		Similarity
	T. (L.) ophidoon (large form)	
a	vs. *T. (L.) ophidoon* (large form)	0.989
b	vs. *T. (L.) ophidoon* (small form)	0.913
c	vs. *T. (L.) azumai azumai*	0.846
d	vs. *T. (L.) nesiothauma*	0.834
e	vs. *T. (N.) okinoerabuensis*	0.824
f	vs. *T. (N.) bernardi*	0.795
g	vs. *T. (L.) callistochila*	0.768
h	vs. *T. (L.) oshimae*	0.766
i	vs. *T. (L.) inclyta*	0.736
j	vs. *T. (D.) bilabrata*	0.667
	T. (L.) callistochila	
k	vs. *T. (L.) oshimae*	0.878
l	vs. *T. (N.) okinoerabuensis*	0.833

Similarity is calculated according to Aquadro and Avise (1981). L., subgenus *Luchuphaedusa*, N., subgenus *Nesiophaedusa*; D., subgenus *Decolliphaedusa*.

mai azumai of this island, supporting a distinctive position of *T. (L.) ophidoon* as previously described by Pilsbry (1901). However, it should not be concluded unconditionally, because we do not compare directly the small form with *T. (L.) azumai azumai*. Similarly we cannot infer that *T. (L.) callistochila* and *T. (L.) oshimae* are very similar, simply because they were positioned so closely in Figure 3 (the upper line). Therefore, we made the direct comparison between *T. (L.) callistochila* and *T. (L.) oshimae* to learn whether they are closely similar or not. The result gave the largest similarity value (0.875) among values between different species (Table I), meaning that they are very similar as expected from their close positions in Figure 3 (the upper line). This situation is also supported by direct comparison between *T. (L.) callistochila* and *T. (N.)* okinoerabuensis, because they were positioned more distantly (Fig. 3, the upper line) and had a value of lower similarity (0.833) than *T. (L.) callistochila* and *T. (L.) oshimae*. The relationships of *oshimae* and *okinoerabuensis* to *callistochila* are also shown in Figure 3 (the lower line).

Discussion

Table I shows that the large form of *Tyrannophaedusa (Luchuphaedusa) ophidoon* is most similar to different specimens of the same form (similarity 0.989) and most different from species of another subgenus, *T. (Decolliphaedusa) bilabrata* (similarity 0.667). Therefore, relationships, which are considered to be most closely related or most differentiated, are demonstrated in the similarity values. This suggests that the two-dimensional electrophoresis method is suitable for systematic analysis and supports our previous conclusion that this method provides a valuable tool for systematics (Miyazaki *et al.*, 1987).

The method presents a debatable issue that species of the other subgenus, *Nesiophaedusa*, are more similar to the large form than some members of *Luchuphaedusa*. As reported by Pilsbry (1901), the general characters of shells are similar between *Nesiophaedusa* and *Luchuphaedusa*. We found no morphological differences except the clausilium. Therefore, *Luchuphaedusa* may be paraphyletic, since some members of *Luchuphaedusa* are less similar to the other member in this group than the members of the group *Nesiophaedusa*. From these considerations, we propose that *Nesiophaedusa* should be united with *Luchuphaedusa* as one subgenus. This is supported by our result that the similarity value of 0.833 is obtained between *T. (N.) okinoerabuensis* and *T. (L.) callistochila*, the type species of *Luchuphaedusa*. This value corresponds to those (0.824 and 0.795) among two species of *Nesiophaedusa* and the large form of *T. (L.) ophidoon* (Table I).

T. (L.) nesiothauma has a distinctive aperture by which it can be distinguished from other *Luchuphaedusa* species. But the result (Table I) shows that it is very similar to the large form of *T. (L.) ophidoon*. Therefore, it is necessary to examine how similar this species is to other members of *Luchuphaedusa* and to reconsider the taxonomic significance of its aperture difference.

Luchuphaedusa shows the peculiar distribution from Nansei Islands to a small area of the Kyushu mainland, which is not interrupted by biogeographical boundaries suggested by the data about other animals (Tokuda, 1978). Thus its radiation pattern is especially intriguing. Our result reveals a correlation between the similarity values and the arrangement of islands. Islands are located in the order of Amami O-shima Is., Okinoerabushima Is., and Okinawa Is. toward south from Shimo Koshiki-jima Is. (Fig. 1). The large form of *T. (L.) ophidoon* and two members which are most similar to that form inhabit Shimo Koshiki-jima Is. (Fig. 3, a, b, c). *T.*

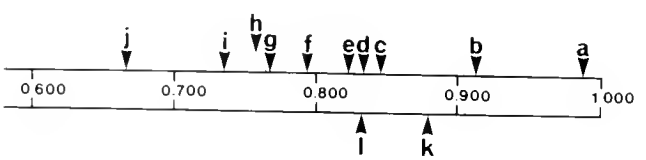

Figure 3. Schematic drawing of a distribution of similarity values among land snails. The similarity values to the large form of *Tyrannophaedusa (Luchuphaedusa) ophidoon*, which is a standard counterpart for comparison, are shown on the upper line, and those of *T. (L.) oshimae* and *T. (Nesiophaedusa) okinoerabuensis* to *T. (L.) callistochila* on the lower line. Letters correspond with those in Table I.

Table II

Distribution of the similarity values between intraspecific or interspecific populations

	Mouse		Fruit fly		Land snail	
Similarity	Intra	Inter	Intra	Inter	Intra	Inter
1.000–0.981			4		1	
0.980–0.961			1	2		
0.960–0.941	1		1	3		
0.940–0.921				6		
0.920–0.901	1			1	1*	
0.900–0.881			1	6		
0.880–0.861				5		1
0.860–0.841		1		6		1
0.840–0.821				8		3
0.820–0.801		1		2		

Figures represent the numbers of pairs which show the similarity within the range given in the left column. Intra and Inter indicate intraspecific and interspecific populations, respectively.

* Represents the position of the similarity between the large and small forms of *T. (L.) ophidoon*. The data on mice is from Aquadro and Avise (1981) and that on fruit flies (*Drosophila montium* species subgroup) is from Ohnishi *et al.* (1983b). Intraspecific populations were not found in ranges below 0.800.

(L.) nesiothauma, of which the similarity to the large form is higher next to the two above mentioned members, is an inhabitant of Amami O-shima Is. (Fig. 3, d). *T. (N.) okinoerabuensis* in Okinoerabu-shima Is. is less similar to the large form than *T. (L.) nesiothauma* (Fig. 3, e). *T. (L.) callistochila*, *T. (L.) inclyta*, and *T. (N.) bernardi*, which have the smaller similarity values to the large form, live on Okinawa Is. (Fig. 3, f, g, i). Therefore, the values show that the more remote the island is from Shimo Koshiki-jima Is., the lower similarity the species living on it has. This may be accounted for by sequential colonization of a single ancestor from either Shimo Koshiki-jima Is. or Okinawa Is., and by radiation within each island. *T. (L.) oshimae* is the only exception (Fig. 3, h) in this interpretation of radiation of these species. This species lives on Amami O-shima Is., but has significantly lower similarity than *T. (L.) nesiothauma*. After the main current of radiation was over, its ancestor may have come from some other island. The presumptive donor island is possibly Okinawa Is., because the species has the similarity value close to those of other members on this island. It is remarkably similar to *T. (L.) callistochila* in the protein constituent (Table I) and shell morphology.

The last problem concerns the taxonomic positions of the small and large forms of *T. (L.) ophidoon*. Their shell shapes are so peculiar that Pilsbry (1905) referred them to "section Oophaedusa" and included them as a single species. However, they are different to each other not only in shell size but also in anatomical and biochemical characteristics (Minato, 1985; Ueshima, in prep.). Our result also shows that they constitute considerably different populations, since there is a large gap (0.076) between the two forms (Fig. 3, the upper line). Therefore, it is questionable whether they should be included in the same species or not. When our result is compared with those reported by others using the two-dimensional electrophoresis method (Table II), the relationship between the large and small forms corresponds to that of closely related interspecific or distantly differentiated intraspecific populations. Data suggesting reproductive isolation between these two forms is under study of their allozyme variation (Ueshima, in prep.). Since available data from two-dimensional electrophoresis is insufficient, and since classification systems currently used are probably unique to different taxa, we can only assume taxonomic positions of organisms examined. Collection of data from other organisms by the two-dimensional electrophoresis method and investigation on other characteristics of the two forms are now being carried out to decide more precisely their taxonomic positions.

Acknowledgments

We express special thanks to Dr. Tetsuo Iwami (Tokyo Kasei Gakuin College) for his advice and encouragement throughout this work. We also thank Mr. Kunitsugu Kawabe and Dr. Sen Takenaka (The University of Tsukuba) for collecting specimens.

Literature Cited

Aquadro, C. F., and J. C. Avise. 1981. Genetic divergence between rodent species assessed by using two-dimensional electrophoresis. *Proc. Natl. Acad. Sci. USA* **78**: 3784–3788.

Avise, J. C. 1975. Systematic value of electrophoretic data. *Syst. Zool.* **23**: 465–481.

Ayala, F. J., M. L. Tracey, D. Hedgecock, and R. C. Richmond. 1974. Genetic differentiation during the speciation process in *Drosophila*. *Evolution* **28**: 576–592.

Hirabayashi, T. 1981. Two-dimensional gel electrophoresis of chicken skeletal muscle proteins with agarose gels in the first dimension. *Anal. Biochem.* **117**: 443–451.

Hirabayashi, T., R. Tamura, I. Mitsui, and Y. Watanabe. 1983. Investigation of actin in *Tetrahymena* cells. A comparison with skeletal muscle actin by a devised two-dimensional gel electrophoresis method. *J. Biochem.* **93**: 461–468.

Kuroda, T. 1963. [*Catalogue of the Non-marine Mollusks of Japan, Including the Okinawa and Ogasawara Islands*]. Mal. Soc. Jap. (In Japanese). 71 pp.

Laemmli, U. K. 1970. Cleavage of structural proteins during the assembly of the head of bacteriophage T4. *Nature* **227**: 680–685.

Minato, H. 1985. Two forms of *Euhuphaedusa ophidoon* (Pilsbry, 1905) from Shimokoshikijima Island, Kagoshima-ken (Pulmonata: Clausiliidae). *The Chiribotan* **16**: 79–82 (In Japanese).

Miyazaki, J.-I., K. Sekiguchi, and T. Hirabayashi. 1987. Application

of an improved method of two-dimensional electrophoresis to the systematic study of horseshoe crabs. *Biol. Bull.* **172:** 212–224.

Oh-Ishi, M., and T. Hirabayashi. 1988. Micro-two-dimensional gel electrophoresis with agarose gel in the first dimension. *Physio-chem. Biol.* **32:** 113–120.

Ohnishi, S., M. Kawanishi, and T. K. Watanabe. 1983a. Biochemical phylogenies of *Drosophila*: protein differences detected by two-dimensional electrophoresis. *Genetica* **61:** 55–63.

Ohnishi, S., K-W. Kim, and T. K. Watanabe. 1983b. Biochemical phylogeny of the *Drosophila montium* species subgroup. *Jpn. J. Genet.* **58:** 141–151.

Pilsbry, H. A. 1901. The land mollusks of the Loo Choo Islands: Clausiliidae. *Proc. Acad. Natl. Sci. Phila.* **53:** 409–424, Pls. 22–23.

Pilsbry, H. A. 1904 (1905). New Clausiliidae of the Japanese Empire-X. *Proc. Acad. Natl. Sci. Phila.* **56:** 809–838, Pls. 52–57.

Stephano, J. L., M. Gould, and L. Rojas-Galicia. 1986. Advantages of picrate fixation for staining polypeptides in polyacrylamide gels. *Anal. Biochem.* **152:** 308–313.

Tokuda, M. 1978. *Biogeography.* Tsukijishokan Inc., Tokyo. (In Japanese). 200 pp.

Williams, N. E. 1984. An apparent disjunction between the evolution of form and substance in the genus *Tetrahymena*. *Evolution* **38:** 25–33.

Reference: *Biol. Bull.* 175: 378–387. (December, 1988)

Sweeper Tentacles in a Gorgonian Octocoral: Morphological Modifications for Interference Competition

KENNETH P. SEBENS AND JULIA S. MILES

Northeastern University, Marine Science Center, Nahant, Massachusetts 01908

Abstract. Elongate tentacles serve an agonistic function in sea anemones and scleractinian corals. Although certain octocorals (soft corals: Octocorallia: Alcyonacea) produce and exude allelochemicals that damage neighboring scleractinian corals, no specialized structures used in agonistic behavior have previously been identified in this large cnidarian subclass. Here, we describe the first evidence of the occurrence and use of specialized agonistic structures, sweeper tentacles, in an octocoral. The encrusting gorgonian *Erythropodium caribaeorum* Pallas (Octocorallia: Gorgonacea) is abundant on shallow reefs in the Caribbean, and competes for space with numerous coral species, sea anemones, and other cnidarians. Zones of contact between this gorgonian and several coral species were observed and recent damage to the coral colonies was noted. Furthermore, the gorgonian develops fields of modified polyps along such borders. These polyps have elongate tentacles termed 'sweeper tentacles,' as in scleractinian corals. Such tentacles lack the side branches (pinnules) characteristic of octocorals in general, and bear a bulbous tip (acrosphere) densely packed with nematocysts. Transplant experiments showed damage to corals placed in contact with the gorgonian's sweeper tentacles and sweeper tentacles were induced when scleractinian corals contacted *Erythropodium* colony borders having exclusively normal tentacles. Thus, sweeper tentacles may contribute to the competitive success of this species in habitats where space is limiting and where there are a number of competing species, many with agonistic mechanisms of their own.

Introduction

Anthozoan coelenterates are important and abundant members of benthic marine communities from the arctic sublittoral to the extensive tropical coral reefs of the world. As sessile or sedentary animals with little or no ability to move, such species compete with each other and with members of other phyla for substratum on which to grow. Specialized structures and behaviors used in agonistic encounters were first identified in sea anemones from temperate rocky intertidal habitats. Species such as certain *Actinia* and *Anthopleura* (family Actiniidae) use inflated sacks protruding from below the tentacles, the acrorhagi, to damage neighboring individuals of the same or of other species (Abel, 1954; Bonnin, 1964; Francis, 1973; Williams, 1978; Sebens, 1984). This contact results in tissue necrosis where peels of ectoderm, filled with holotrichous nematocysts, adhere to the affected individual. Anemones forming clonal aggregations asexually show a specialization of function: edge individuals put more energy into producing and using acrorhagi than do center individuals, but forego sexual reproduction (Francis, 1976). There is typically a distinct size advantage when individuals compete in this manner, with the loser, usually the smaller individual, moving away from the region of encounter (Brace and Pavey, 1978; Brace, 1981; Ayre, 1982).

Scleractinian corals, including those species responsible for coral reef formation, compete for space either by direct overgrowth or by one of at least two specific agonistic mechanisms (reviewed by Lang, 1984; Lang and Chornesky, 1988). The first mechanism recognized was termed 'extra-coelenteric digestion' and is triggered when corals of two different species grow into contact (Lang, 1973). One of the species exudes mesenterial filaments, the coral's digestive organs, through the mouth or body wall and onto a neighbor's surface. Digestion of the neighbor's tissues takes place *in situ* resulting in a zone of naked coral skeleton that can then be overgrown. Coral species can be ranked in a clear dominance hierar-

Received 7 July 1988; accepted 28 September 1988.

chy (Lang, 1973) although a number of ecological factors also affect the outcome of competition by this method (Sheppard, 1979, 1982a, b, 1985; Wellington, 1980; Bak *et al.*, 1982; Logan, 1984, 1985).

A second mechanism of competition was identified for corals a few years later, the development of 'sweeper tentacles' (den Hartog, 1977; Richardson *et al.*, 1979; Wellington, 1980). Sweeper tentacles differentiate in response to several weeks of contact with corals of other species (Chornesky, 1983; Hidaka, 1985; Hidaka and Yamazoto, 1984; Hidaka and Miyazaki, 1984; Hidaka *et al.*, 1987) and can reach five to ten times the length of normal feeding tentacles, thus 'sweeping' an area adjacent to the coral border and causing tissue necrosis in neighboring polyps after contact. Elongate polyps on colonies of *Goniopora* (Sheppard, 1979, 1982b) may perform a similar function and are termed 'sweeper polyps.'

Anemone species in certain families (*e.g.*, Metridiidae) also use elongate tentacles for agonistic behavior. The 'catch tentacle' or 'fighting tentacle' is a longer and often thickened version of one of the feeding tentacles that can be induced to form by contact with genetically distinct conspecifics or with individuals of other species (Williams, 1975, 1980; Purcell, 1977; Watson and Mariscal, 1983; Fukui, 1986). The tip of this tentacle adheres to another individual contacted breaking off and causing tissue damage where it sticks. The agonistic function of these specialized tentacles is clear, resulting in clonal aggregations with spacing between neighboring clones, although habituation (Purcell and Kitting, 1982) and opposite sex tolerance (Kaplan, 1983) may allow for mingling of some clones.

Octocorals, another dominant group of benthic cnidarians, account for much of the biomass and species diversity on coral reefs as well as in steeply sloping deep sea habitats. Caribbean reefs support numerous species of gorgonians, most of which grow as upright branched colonies. Pacific reefs, on the other hand, lack abundant gorgonians but have numerous Alcyonacean octocorals, commonly termed soft-corals, filling similar roles. Octocorals show tissue rejection responses and cytotoxic effects, potential intraspecific competitive mechanisms, in transplant experiments (Theodor, 1970, 1976; Theodor and Senelar, 1975; Bigger and Runyan, 1979). Recent research has demonstrated that certain soft-corals also produce allelochemicals toxic to nearby scleractinian corals and to other soft-corals (Coll *et al.*, 1982; Sammarco *et al.*, 1983, 1985; LaBarre *et al.*, 1986). This competitive mechanism, as well as direct overgrowth, may account for the abundance of soft-corals in some shallow reef areas of the Pacific. However, soft-corals are susceptible to the agonistic mechanisms of scleractinian corals, and often show damage where such encounters occur (Sammarco *et al.*, 1985; LaBarre *et al.*, 1986). Octocorals were not previously known to develop specialized structures used in agonistic encounters. Elongate tentacles have been observed on several species of Gorgonacea and an Alcyonacea (several genera, Muzik, 1983, *T. reesii*, F. Bayer, pers. comm.), although potential agonistic use has not been tested.

Erythropodium caribaeorum Pallas, an encrusting gorgonian octocoral, is common on coral reefs throughout the Caribbean. It is the only gorgonian in this region that never produces upright processes but instead forms thin mat-like colonies overgrowing many other species which they contact. Large colonies are particularly abundant in surf-zone and shallow reef habitats (Karlson, 1980, 1983; Sebens, 1982) where the low colony profile may provide some protection from storm-induced damage. Observations of modified tentacles along edges of this species in contact with corals and other neighbors prompted our study of these structures and their function.

Materials and Methods

Surveys of sweeper tentacle occurrence were conducted in shallow back reef and fore reef habitats at Discovery Bay, Jamaica (March 1988), using snorkeling and SCUBA. Following a depth contour and proceeding in a predetermined direction, boundaries of all *Erythropodium* colonies encountered were examined for contact with other cnidarians. Linear measurements were made of each border where contact occurred. Both neighbors were examined for the presence of damaged areas and for specialized structures (sweeper tentacles, acrorhagi), although sweepers were frequently not visible in contracted colonies of *Erythropodium* and most coral species. Damaged areas were characterized by pallid tissue or denuded coral skeleton. If sweeper tentacles were noticed along a border with a non-cnidarian neighbor, that border was also measured and the condition of the neighbor noted.

Two series of transplant experiments were conducted over a 14 month period in the back-reef at Columbus Park, Discovery Bay, Jamaica (1–4 m depth). In each series, 16–18 large *Erythropodium* colonies were mapped and tagged. Branches or plates of the two corals most common in this habitat, *Madracis mirabilis* and *Agaricia agaricites*, were transplanted next to gorgonian colony edges; eight to ten corals were placed in zones without sweeper tentacles and the same number were placed into zones with obvious sweepers. Coral pieces were taken from large aggregations of branches or plates and were removed such that minimal living tissue areas were damaged. Transplants were positioned with tissues in close proximity but actual contact of the coral skeleton with the octocoral colony surface was minimized. Transplants were fixed in place using underwater epoxy (Pettit Co.), keeping the epoxy away from living surfaces of ei-

ther the transplant or *Erythropodium*. The side of each coral away from contact was the control for the transplant process. Nine colonies damaged during transplantation, possibly by inadvertent contact with epoxy, showed generalized necrosis over large areas of the colony in subsequent days to weeks and were omitted (<10 percent of transplants). Another 16 gorgonian colony edges without sweeper tentacles were designated as non-transplant controls for spontaneous sweeper tentacle formation by the gorgonian in regions without cnidarian neighbors.

The initial transplant experiments began in February 1987. A second set was initiated in February 1988. All transplants were examined over the first three days then at 5, 12, and 19 days for signs of new damage (white patches or peeling tissue) and for sweeper tentacle formation on either the corals or on the gorgonian. Night time observations were also made several times during the experiment. Damage was recorded as present or absent; in instances of sweeper tentacle induction, the number of modified polyps was recorded. In July 1987 and January 1988 the initial transplants were examined for evidence of overgrowth by either neighbor.

Results

In February 1986 we noticed extensive recent damage to coral colonies adjacent to *Erythropodium* in Discovery Bay, Jamaica (Fig. 1). Close-up photographs of these borders revealed polyps distinct from the normal polyps present on the rest of the *Erythropodium* colony. Normal polyps have eight tentacles of variable length, to approximately 2 cm, with numerous short side branches (pinnules) along their entire length. These tentacles are light to dark brown as a result of abundant symbiotic algae (zooxanthellae) in gastrodermal tissues. The modified tentacles, which we term 'sweeper tentacles' as in the scleractinian corals, were over three times as long as normal tentacles, lacked pinnules, were white to very light brown in color, and had a bulbous tip (acrosphere) (Fig. 2). All eight tentacles of modified polyps generally were of the 'sweeper' form although intermediate forms, where the proximal portion was pinnate and the distal was not, were also common. An extensive survey conducted in 1987 showed that most corals in contact with *Erythropodium* tentacles showed recent damage; almost all such damage was associated with the presence of sweeper tentacles (Table I).

Sweeper tentacles were observed in contact with a number of coral species, several sea anemone species, and a few other non-cnidarian organisms (Table I). Visible damage was observed only on the scleractinian corals which lack the ability to move away from the site of sweeper tentacle formation. Sea anemones are much more mobile and may be able to avoid damage either by movement or by postural changes. Either event can result in a gain of space for the gorgonian without extensive damage or death of the anemone. Sweeper tentacles appeared to be restricted to the edges near the zone of contact, although polyps one or more centimeters from the edge bore sweepers. Sweepers were never observed scattered over the colony far from the site of contact, as occurs in some scleractinians (Chornesky and Williams, 1983). One non-cnidarian group observed frequently in contact with *Erythropodium* borders bearing sweeper tentacles were crustose red algae (several undetermined species). At first we were skeptical that these algae were the only macroorganisms in contact along such borders. Small hydroids or other invertebrates could be present and hard to see, and might be the cause of the sweeper tentacle formation. However, subsequent detailed examination of several such borders and collected specimens observed in the laboratory convinced us that the algae were the only macroscopic occupants of such zones; yet they did not show obvious damage when adjacent to sweepers.

The series of transplant experiments replicated over two years (Table II, III) confirmed the agonistic function of this gorgonian's sweeper tentacles. Corals transplanted into contact with sweeper tentacles showed damage within a few days to a week. Corals transplanted into contact with *Erythropodium* borders with only normal tentacles showed few instances of damage until several weeks had passed. Furthermore, sweeper tentacles were observed in the latter transplant experiments after approximately three weeks of contact, demonstrating that contact with scleractinian corals can induce the formation of these modified structures in *Erythropodium*. Contingency table analyses of these experimental results are given in Tables II and III. Experiments begun in February 1987 were observed again in July 1987 and in January 1988. Although storms had dislodged many of the transplanted corals, of those that survived, all had been partially overgrown by *Erythropodium*. *Madracis mirabilis* developed sweeper tentacles along edges of contact with *Erythropodium* in three of the six surviving transplants, although damage to the *Erythropodium* was not obvious. We did not observe sweeper tentacle formation by *Agaricia* in the three week studies. The few colonies that survived five and eleven months were not examined at night when these tentacles are usually extended. Chornesky (1983) reports that *A. agaricites* did develop sweeper tentacles following prolonged contact with *Erythropodium*.

Sweeper tentacles differ structurally from normal tentacles in several ways (Fig. 3). First, pinnules are absent in sweeper tentacles, but can be seen in reduced form on nearby tentacles that appear intermediate between normal and sweeper tentacles, probably a transitional stage in their development. Several normal and sweeper tenta-

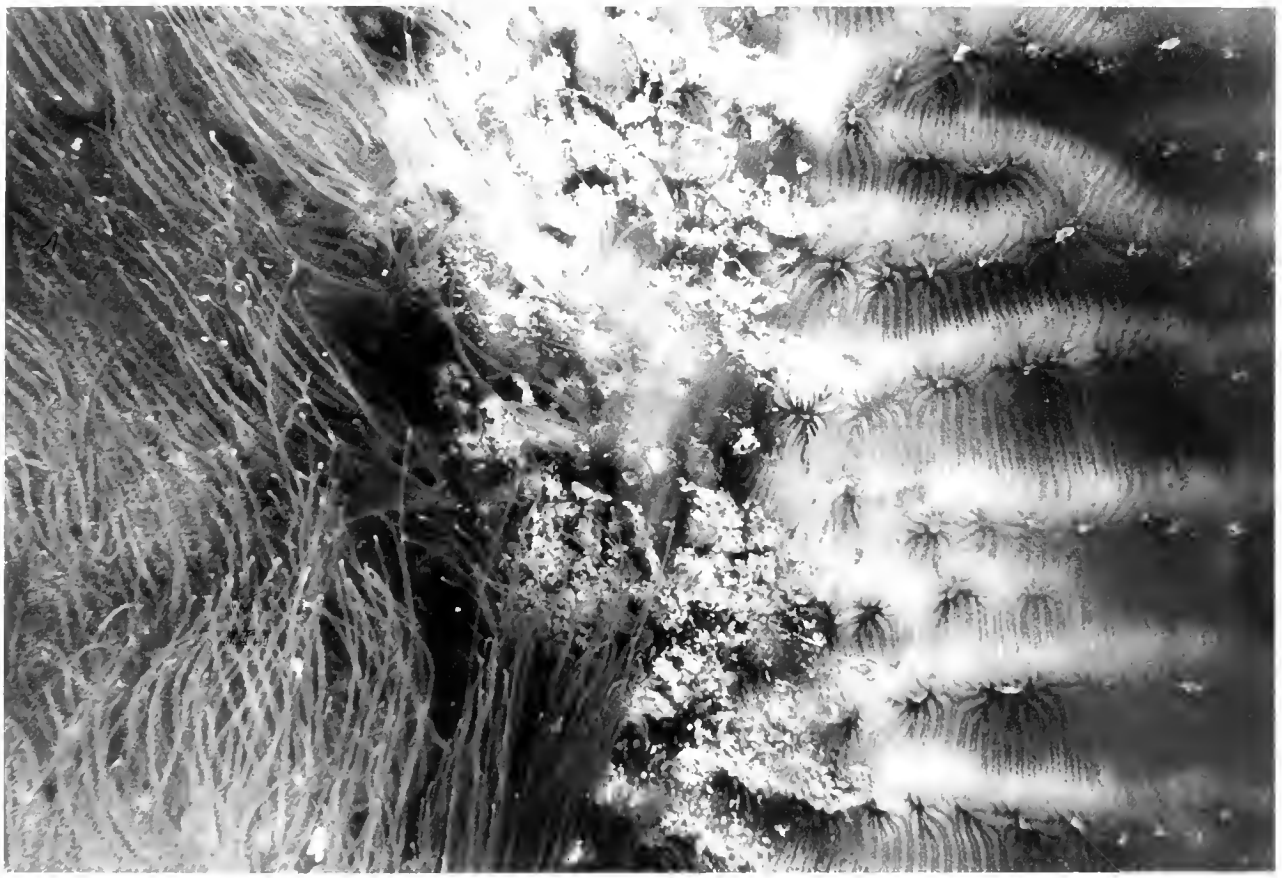

Figure 1. Damaged coral *Agaricia agaricites* adjacent to *Erythropodium* with sweeper tentacles at Discovery Bay, Jamaica, 4 m depth. Scale approximately 6 cm across photograph.

cles were examined at 400× using a compound microscope after relaxing them in 7.5% $MgCl_2$ mixed 50:50 with seawater at room temperature. The gastrodermal layer contained far fewer zooxanthellae in the sweeper tentacles, approximately 86–356 cells per mm relaxed tentacle length *versus* 520–896 cells per mm in normal tentacles (n = 3 each). The epidermal layer of the normal tentacles had few nematocysts, approximately 30–50 nematocysts over an entire tentacle surface (n = 3), whereas sweeper tentacles had a thickened epidermis composed primarily of nematocysts and enidoblasts (nematocyst forming cells). These were present by the hundreds and were too numerous to count in fresh preparations. The tip of a normal tentacle bears a small swelling, sometimes with a cluster of nematocysts, sometimes with very few. Sweeper tentacles form a bulbous tip (acrosphere) two to three times the diameter of the normal tentacle tip. The epidermal layer of the acrosphere is packed with nematocysts several layers deep. A fraction (<20%) of normal tentacles have an acrosphere as well; these may be intermediate forms developing into sweepers. It is likely that both the acrosphere and the epidermis along the entire sweeper tentacle length are involved in causing damage to neighboring cnidarians. All eight tentacles of each modified polyp become sweeper tentacles, and there appears to be some modification of the polyp itself as well, although it does not greatly elongate. Also, spicules of these polyps were clear compared to the deep red color of spicules in normal polyps.

Discussion

This study identified agonistic structures in the subclass Octocorallia, a modified polyp and tentacles that serve an agonistic function in competition for space with other anthozoan cnidarians and possibly with non-cnidarian space competitors as well. The sweeper tentacles of *Erythropodium* are much more numerous and extensive than sweeper tentacles we have observed on sclerartinian corals. Fields of sweeper tentacles (8 per polyp) on hundreds of polyps were common along edges in contact with both corals and anemones. These sweeper tentacles are able to kill tissue of adjacent scleractinians, potentially enabling *Erythropodium* to subsequently overgrow the denuded coral skeleton, an advance which may not have been possible while the coral edge was still alive. It

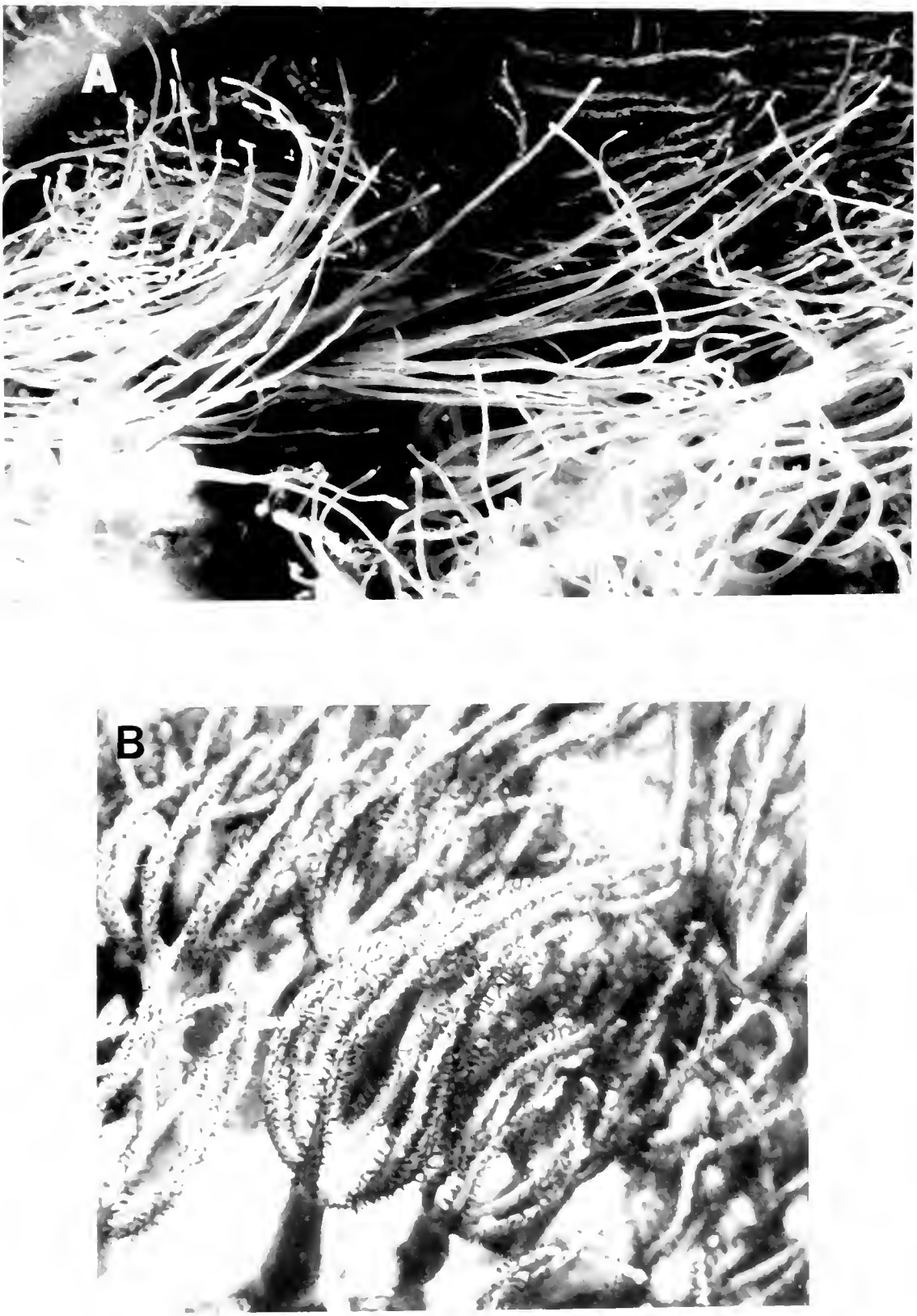

Figure 2. A. Sweeper tentacles of *Erythropodium* extended *in situ*. Scale approximately 2.2 cm across photograph. B. Normal pinnate tentacles, scale approximately 1.7 cm across photograph (Discovery Bay, Jamaica, 3 m depth).

Table I

Survey of interactions along Erythropodium *borders*

Species	Total	With sweepers			Without sweepers		
		N (S)	Dam	Length (cm, ±S.D.)	N	Dam	Length (cm ±S.D.)
Agaricia agaricites	37	28	26	5.6 ± 3.1	9	1	3.1 ± 2.9
Briareum asbestinum	14	0	0	—	14	0	2.5 ± 1.2
Condylactis gigantea	5	3	0	6.7 ± 2.9	2	0	16.0 ± 5.7
E. caribaeorum	7	7	0	4.4 ± 2.9	0	0	—
Heteractis lucida	35	28	0	11.2 ± 6.6	7	0	7.7 ± 2.2
Palythoa caribaeorum	6	0	0	—	6	0	4.2 ± 3.1
Porites astreoides	3	1	1	—	2	1	4.5 ± 0.7
Red crustose algae	52	52	0	2.9 ± 1.2	0	0	—

Surveys of *Erythropodium* borders (1987), noting the condition of neighboring cnidarian colonies or individuals (damaged or not), and the presence of sweeper tentacles on *Erythropodium*. Instances where sweeper tentacles were observed adjacent to non-cnidarian neighbors are also noted. Additional observations of sweeper tentacles and damage to adjacent colonies are given for other colonies examined, but which were not part of the systematic survey. Number of observations in parentheses. N = number of contacts, N (S) = number of contacts with sweeper tentacles on *Erythropodium*, Dam = number of cases where neighbor was damaged, length = mean length of border, S.D. = standard deviation.

Other borders with sweepers on *Erythropodium*: Corals: *A. agaricites* (5); *Diploria strigosa* (1); *Eusmilia fastigiata* (1); *Favia fragum* (1); *Madracis mirabilis* (2); *Meandrina meandrites* (2); *Montastrea annularis* (1); *M. cavernosa* (3); *Mycetophyllia* sp. (1); *P. astreoides* (6); *Porites furcata* (1); *Porites porites* (1); *Siderastrea siderea* (2); Anemones: *Aiptasia tagetes* (1); *Bartholomea annulata* (1); *H. lucida* (7); *Lebrunia danae* (1); *Telmatactis* sp. (2); Hydrozoa: *Millepora alcicornis* (3); *M. complanata* (4); unidentified hydroid (2); Sponges: *Chiona* sp. (1); *Iotrochota birotulata* (2); unid. green demosponge (1); Others: *didemnid* ascidian (1); *E. caribaeorum* (3); *P. caribaeorum*, zoanthid (5); *Paradiscosoma neglecta*, corallimorpharian (1); *Zoanthus solanderi*, zoanthid (1); algal mat (1).

Table II

Results of transplant experiments of corals into contact with Erythropodium *(1987 series)*

	Initial N	Week 1 (5 days)			Week 3 (19 days)		
		N	Dam	N (S)	N	Dam	N (S)
Erythropodium with *Madracis mirabilis*							
Edges with sweepers	10	8	6	—	6	6	—
opp. side controls	10	8	0	—	7	0	—
Edges without sweepers	10	8	2	0	7	2	2 (6, 5)
opp. side controls	10	8	0	—	6	0	—
Non-transplant controls	10	8	—	0	7	—	0
Erythropodium with *Agaricia agaricites*							
Edges with sweepers	8	8	5	—	8	8	—
opp. side controls	8	8	0	—	8	0	—
Edges without sweepers	8	8	3	0	8	7	4 (8, 3, 8, 10)
opp. side controls	8	8	0	—	8	0	—
Non-transplant controls	8	8	—	0	8	—	0

Results of 1987 transplant experiments at Columbus Park, Discovery Bay, Jamaica. Small plates or branches of the two most common coral species in this habitat, *Madracis mirabilis* and *Agaricia agaricites*, were transplanted into contact with *Erythropodium* edges initially with and without sweeper tentacles. N = number of surviving transplants, Dam = number with damage to corals in contact region, N (S) = number of edges with sweeper tentacles on *Erythropodium*. Numbers in parentheses are counts of polyps with newly developed sweeper tentacles along each edge where they developed during the experiment.

G-test for independence (with Yates' correction) show significantly greater occurrence of damage next to sweeper tentaeles than occurred on opposite sides of transplanted corals (opp. side controls, $G = 8.2$ ($P < 0.005$) at 5 days; $G = 11.9$, ($P < 0.005$) at 19 days for *M. mirabilis*. $G = 5.1$, ($P < 0.05$) at 5 days; $G = 14.7$, ($P < 0.005$) at 19 days for *A. agaricites*.) Damage next to edges without sweepers was not significant after 5 days for either species compared to opp. side controls, but was significant for *A. agaricites* after 19 days, $G = 11.2$, ($P < 0.005$). Damage frequency at edges with sweepers differed significantly from that at edges without sweepers for *M. mirabilis* only at 19 days, $G = 4.8$ ($P < 0.05$).

Table III

Results of transplant experiments of corals into contact with Erythropodium *(1988 series)*

	Initial N	Week 1 (4–5 days)			Week 3 (19 days)		
		N	Dam	N (S)	N	Dam	N (S)
Erythropodium with *Madracis mirabilis*							
Edges with sweepers	12	8	4	—	6	5	—
opp. side controls	12	8	0	—	6	0	—
Edges without sweepers	13	11	1	0	6	1	2 (2, 3)
opp. side controls	13	11	0	—	6	0	—
Non-transplant controls	13	13	—	0	13	—	0
Erythropodium with *Agaricia agaricites*							
Edges with sweepers	14	13	12	—	8	6	—
opp. side controls	14	13	0	—	8	0	—
Edges without sweepers	14	14	2	0	13	6	7 (10, 4, 3, 4, 5, >10, >10)
opp. side controls	14	14	0	—	13	0	—
Non-transplant controls	14	14	—	0	13	—	0

Results of 1988 transplant experiments of corals into contact with *Erythropodium*. Abbreviations same as Table I.

G-tests for independence (with Yates' correction) show significantly greater occurrence of damage next to sweeper tentacles than occurred on opposite sides of transplanted corals (opp. side controls; not sig. at 5 days, $G = 6.12$, ($P < 0.025$) at 19 days for *M. mirabilis*, $G = 22.4$, ($P < 0.005$) at 5 days, $G = 7.46$ ($P < 0.01$) at 19 days for *A. agaricites*). Damage next to edges without sweepers was not significant versus opposite side controls after 5 days for either species but was significant for *A. agaricites* after 19 days, $G = 6.16$, ($P < 0.025$). Damage frequency at edges with sweepers differed significantly from that at edges without sweepers for *A. agaricites* only at 5 days, $G = 14.94$ ($P < 0.005$) and not for *M. mirabilis* at either time.

is interesting that these structures were discovered in the only completely encrusting gorgonian species in the Caribbean; the encrusting habit brings the growing edges and tentacles into frequent contact with other competitors for primary space. The upright habit of other gorgonians allows them to avoid most such space competition on the primary substratum, although certain other upright cnidarian species, such as fire-corals (*Millepora* spp.), attack and take space from erect gorgonians then use the denuded gorgonian axis as substratum (Wahle, 1980).

Erythropodium is a common cnidarian on shallow Caribbean reefs, yet its ecology is poorly understood. It is avoided by most fish and invertebrate predators (Sebens, 1982) and contains potent toxins effective at least against vertebrate predators (Pawlik *et al.*, 1987). However, J. D. Witman (unpub. data) reports numerous observations of feeding on *Erythropodium* by the predatory gastropod *Cyphoma gibbosum* and Karlson (1983) notes predation by the sea urchin *Diadema antillarum* and by the fireworm *Hermodice carunculata*. In shallow habitats just behind the reef crest at Discovery Bay, Karlson (1980) observed *Erythropodium* overgrowing the zoanthids *Zoanthus solanderi* and *Palythoa caribaeorum* and the corals *Porites astreoides*, *P. porites*, *Agaricia agaricites*, *Siderastrea siderea*, and *Acropora palmata*, accounting for 73% of 37 mapped overgrowth interactions at his study site. *Erythropodium* also is an aggressive competitor for space in Lameshur Bay, St. John, U.S.V.I., where it overgrew four scleractinian species, two hydrocoral species, one zoanthid, an ahermatypic coral, and nine sponge species in quadrats monitored for two years (J. Witman, unpub. data, photographic monitoring of 32 0.25 m^2 quadrats at 6 m and 13 m depth, 1985–1987).

In our experiments, *Erythropodium* damaged and overgrew two coral species that are abundant on the same shallow reefs. Observations and surveys indicate that *Erythropodium* is a successful space competitor compared to most other coral species as well, based on incidence of damage and edge overlap. However, because of its non-rigid structure, it is difficult to tell whether any corals have damaged or taken space from *Erythropodium*. Certain edges in contact with corals and anemones were pale in color with widely spaced polyps, many of which remained retracted while all other polyps on the colony were fully expanded. It is possible that such zones represent areas where the colony has been injured and is retreating, resorbing tissue, and thus losing space to a superior competitor.

Sweeper tentacles of *Erythropodium* were observed frequently in contact with crustose red algae. All previous studies of cnidarian agonistic behaviors suggest that these behaviors are effective only against other cnidarians, except for studies in which algal growth was reduced in zones of contact with anthozoan tentacles (Bak and Borsboom, 1984; DeRuyter van Stevenink *et al.*, 1988). Reduced algal colonization also was noted in

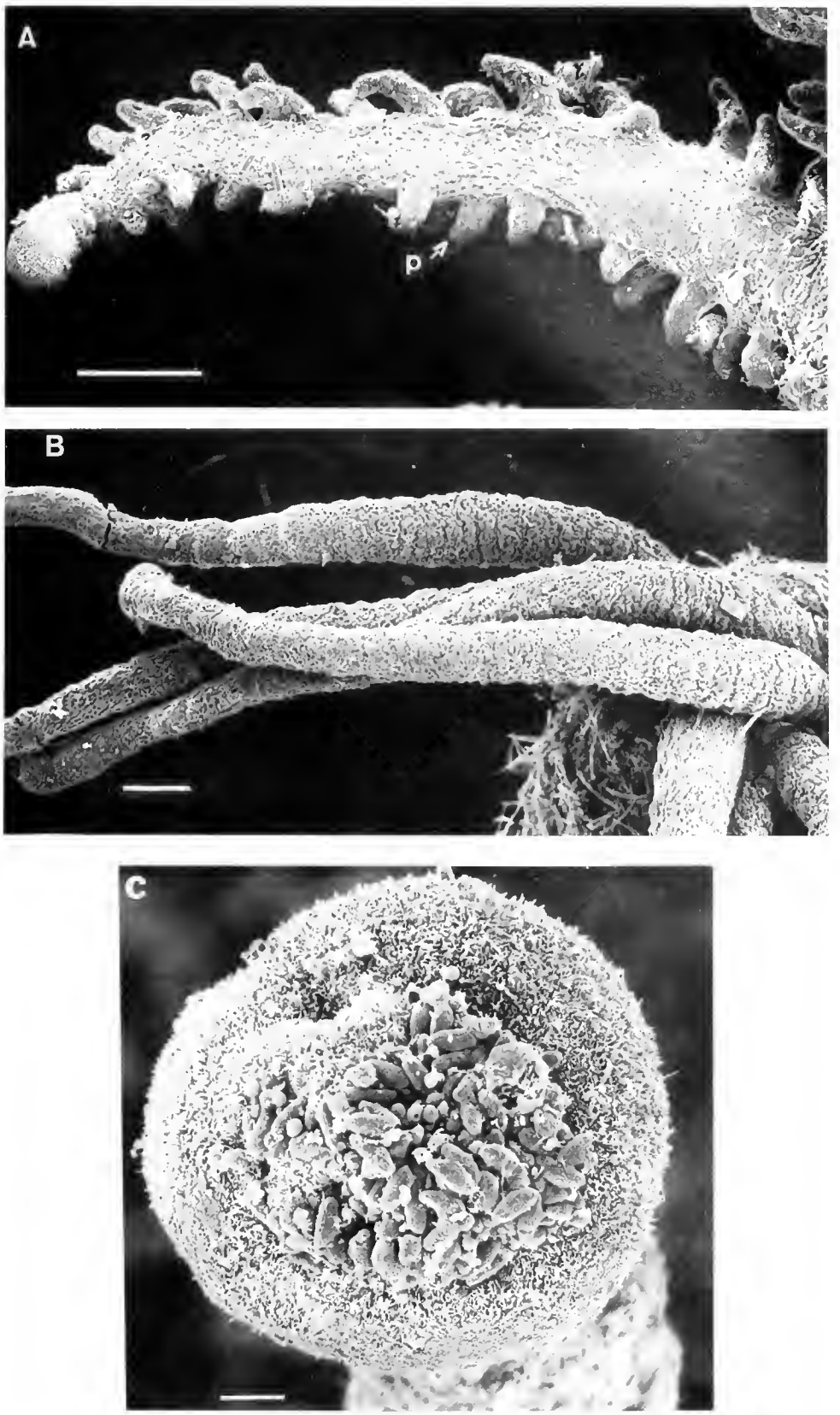

Figure 3. Scanning electron micrographs of normal (A) and sweeper (B) tentacles of *Erythropodium*. Note the absence of side branches (pinnules, P) on the sweeper tentacle and the knobbed tip (acrosphere) on both tentacles. Scale bars 100 μm in A, B. (C) Enlarged view of acrosphere from a sweeper tentacle with a central cluster of large nematocysts. Scale bar 10 μm.

scraped patches within a zoanthid bed (Sebens, 1982). Results such as these indicate that anthozoan mucus or nematocysts may have negative effects on adjacent algae and provide a possible explanation of why sweeper tentacles might form in response to crustose algae in this case. The need for such defense was illustrated by several observations of partial over growth by shelves of crustose algal thallus that had lifted off the substratum and had partially overgrown edges of corals and of several *Erythropodium* colonies in our study area.

Sweeper tentacles also were noted in several instances where two *Erythropodium* colonies contacted each other with no intervening substratum. Although the evidence is not experimental, it suggests that sweeper tentacles are used intraspecifically as well as interspecifically in this species. Corals also are able to recognize genetically different colonies or colony fragments, resulting in fusion or non-fusion at intraspecific colony borders (Hildeman *et al.*, 1979; reviewed by Lang and Chornesky, 1988). Intraspecific use of sweeper tentacles also has been observed (Sheppard, 1982; Hidaka and Yamazoto, 1984; Sebens, in Lang, 1984), and thus must involve colony genotypic recognition, as in the fusion process.

The development and use of sweeper tentacles is a newly recognized competitive mechanism in the subclass Octocorallia. Although 'sweeper tentacles' have been recorded in erect species including *Corallium* (Gorgonacea, Abel, 1970), *Bebryce, Cyclomuricea, Villogorgia,* and *Acalycigorgia* (Gorgonacea, Muzik, 1983, note photographs), and *Dendronephthya* (Alcyonacea, Muzik, 1983), each was described as a potential feeding structure and none have been demonstrated to have an agonistic function. Such tentacles are held well off the substratum, were not in potential contact with neighboring organisms, and were not devoid of pinnules. Alcyonacean octocorals in Australia produce allelochemicals that can damage adjacent anthozoans (Coll *et al.*, 1982; Sammarco *et al.*, 1983, 1985; LaBarre *et al.*, 1986). However, this competitive mechanism apparently does not rely on specialized structures. The delivery of nematocysts, and their toxins, to the surface of a competitor depends on structures that can span the distance between neighbors. Sweeper tentacles, several times as long as the feeding tentacles, are an obvious way to do this. Similarly, mesenterial filament extrusion by corals delivers both digestive enzymes and nematocysts to a neighbor's surface. Sea anemones with acrorhagi depend on inflation of acrorhagi and on extension and bending of the column to achieve this added reach.

The appearance of sweeper tentacles in relatively few families within three separate orders of the class Anthozoa (Actiniaria, Scleractinia, Gorgonacea) suggests that this competitive mechanism may have evolved independently several times. Tentacles are usually the first part of an anthozoan to contact a neighbor, and they already contain nematocysts used for feeding and for defense against predators. Therefore, feeding tentacles of edge polyps are a likely structure to develop a competitive or agonistic function. The feeding and defensive functions of tentacles can thus be considered pre-adaptations with regard to competition for space. Alternatively, they may represent a primitive character shared by all three orders but expressed in relatively few families, genera, and species. The discovery of sweeper tentacles in *Erythropodium* should stimulate examination of other gorgonian and alcyonacean species for the presence of similar structures. It may then be possible to determine whether this is a unique adaptation to local conditions in this species, or whether it is a more general phenomenon present in encrusting octocorals from other geographic regions or habitat types as well.

Acknowledgments

We thank R. Aronson and the East/West Program students for field assistance, and the Discovery Bay Marine Laboratory, University of the West Indies, for allowing use of facilities and boats. We also thank W. Fowle, M. P. Morse, and N. W. Riser for assistance with light and electron microscopy techniques, B. L. Thorne and J. Witman for improvements to the manuscript, and L. Chornesky and one other reviewer for many helpful suggestions. This is contribution No. 166 of Northeastern University's Marine Science Center and No. 460 of the Discovery Bay Marine Laboratory, Univ. of the West Indies.

Literature Cited

Abel, E. F. 1954. Ein Beitrag, zur Giftwirkung, Der Aktinien aund Funktion der Randsäckchen. *Zool. Anzeiger* **153:** 19–268.

Abel, E. F. 1970. Über den Tentakelapparat der Edelkoralle (*Corallium rubrum* L.) und seine Funktion beim Beutefangverhalten. *Oecologia* **4:** 133–142.

Ayre, D. J. 1982. Inter-genotype aggression in the solitary sea anemone *Actinia tenebrosa*. *Mar. Biol.* **68:** 199–205.

Bak, R. P. M., and J. L. A. Borsboom. 1984. Allelopathic interaction between a reef coelenterate and benthic algae. *Oecologia* **63:** 194–198.

Bak, R. P. M., R. M. Termaat, and R. Dekker. 1982. Complexity of coral interactions: influence of time, location of interaction and epifauna. *Mar. Biol.* **69:** 215–222.

Bigger, C. H., and R. Runyan. 1979. An *in situ* demonstration of self-recognition in gorgonians. *Dev. Comp. Immunol.* **3:** 391–597.

Bonnin, J. P. 1964. Recherches sur la "reaction d'aggression" et sur le fonctionnement des acrorrhages d'*Actinia equina* L. *Bull. Biol. France Belgium* **98:** 225–250.

Brace, R. C. 1981. Intraspecific aggression in the color morphs of the anemone *Phymactis clematis* from Chile. *Mar. Biol.* **64:** 85–93.

Brace, R. C., and J. Pavey. 1978. Size dependent dominance hierarchy in the anemone *Actinia equina*. *Nature* **273:** 752–753.

Chornesky, E. A. 1983. Induced development of sweeper tentacles on the reef coral *Agaricia agaricites*: a response to direct competition. *Biol. Bull.* **165:** 569–581.

Chornesky, E. A., and S. L. Williams. 1983. Distribution of sweeper

tentacles on *Montastrea cavernosa*. In *The Ecology of Deep and Shallow Reefs*, M. L. Reaka, ed. Symp. Ser. Undersea Res., N.O.A.A. Nat. Undersea Res. Prog. **1:** 61–67.

Coll, J. C., B. F. Bowden, D. M. Tapiolkas, and W. C. Dunlap. 1982. *In situ* isolation of allelochemicals released from soft corals (Coelenterate: Octocorallia): a totally submersible sampling apparatus. *J. Exp. Mar. Biol. Ecol.* **60:** 293–299.

Den Hartog, J. C. 1977. The marginal tentacles of *Rhodactis sanctithomae* (Corallimorpharia) and sweeper tentacles of *Montastrea cavernosa* (Scleractinia), their cnidom and possible function. Pp. 463–470 in *The Second Int. Coral Reef Symposium*, **1.** Univ. Miami Press, Miami, FL.

DeRuyter van Steveninck, E. D., L. L. Van Mulekon, and A. M. Breeman. 1988. Growth inhibition of *Lobophora variegata* (Lanoureux Womersley) by scleractinian corals. *J. Exp. Mar. Biol. Ecol.* **115:** 169–178.

Francis, L. 1976a. Social organization within clones of the sea anemone *Anthopleura elegantissima*. *Biol. Bull.* **150:** 361–376.

Francis, L. 1973b. Intraspecific aggression and its effects on the distribution of *Anthopleura elegantissima* and some related sea anemones. *Biol. Bull.* **144:** 73–92.

Fukui, Y. 1986. Catch tentacles in the sea anemone *Haliplanella luciae*: role as organs of social behavior. *Mar. Biol.* **91:** 245–251.

Hidaka, M. 1985. Nematocyst discharge, histoincompatibility, and the formation of sweeper tentacles in the coral *Galaxea fascicularis*. *Biol. Bull.* **168:** 350–358.

Hidaka, M., and K. Yamazato. 1984. Intraspecific interactions in a scleractinian coral, *Galaxea fascicularis*, induced formation of sweeper tentacles. *Coral Reefs* **3:** 77–85.

Hidaka, M., and I. Miyazaki. 1984. Nematocyst discharge and surface structure of the ordinary and sweeper tentacles of a scleractinian coral, *Galaxea fascicularis*. *Galaxea* **3:** 119–130.

Hidaka, M., I. Miyazaki, and K. Yamazoto. 1987. Nematocysts characteristic of the sweeper tentacles of the coral *Galaxea fascicularis* (Linnaeus) *Galaxea* **6:** 195–207.

Hildeman, W. C., C. H. Bigger, and I. S. Johnston. 1979. Histoincompatibility reactions and allogenic polymorphism among invertebrates. *Transplant Proc.* **11:** 1136–1141.

Kaplan, S. A. 1983. Intrasexual aggression in *Metridium senile*. *Biol. Bull.* **165:** 416–418.

Karlson, R. H. 1980. Alternative competitive strategies in a periodically disturbed habitat. *Bull. Mar. Sci.* **30:** 894–900.

Karlson, R. H. 1983. Disturbance and monopolization of a spatial resource by *Zoanthus sociatus* (Coelenterata: Anthozoa). *Bull. Mar. Sci.* **33:** 118–131.

LaBarre, S. C., J. C. Coll, and P. W. Sammarco. 1986. Competitive strategies of soft corals (Coelenterata: Octocorallia): III. Spacing and aggressive interactions between alcyonaceans. *Mar. Ecol. Prog. Ser.* **28:** 147–156.

Lang, J. C. 1973. Interspecific aggression by scleractinian reef corals. II. Why the race is not only to the swift. *Bull. Mar. Sci.* **23:** 260–279.

Lang, J. C., and E. A. Chornesky. 1988. Competition between scleractinian reef corals: a review of mechanisms and effects. In *Ecosystems of the World. Coral Reefs*, Z. Dubinsky, ed. Elsevier Press, Amsterdam.

Lang, J. C. 1984. Whatever works: the variable importance of skeletal and of non-skeletal characters in scleractinian taxonomy. *Paleontogr. Am.* **54:** 18–44.

Logan, A. 1984. Interspecific aggression in hermatypic corals from Bermuda. *Coral Reefs* **3:** 131–138.

Logan, A. 1985. Intraspecific immunological responses in five species of corals from Bermuda. In *Proc. Fifth Int. Coral Reef Congress*, Tahiti 1985, **6:** 63–68.

Muzik, K. 1983. Zoom and focus: octocorals. *Newton Graphic Sci. Mag.* (Japan) **3:** 30–35.

Pawlik, S. R., M. T. Burch, and W. Fenical. 1987. Patterns of chemical defense among Caribbean gorgonian corals: a preliminary survey. *J. Exp. Mar. Biol. Ecol.* **108:** 55–66.

Purcell, J. E. 1977. Aggressive function and induced development of catch tentacles in the sea anemone *Metridium senile* Coelenterata: Actiniaria. *Biol. Bull.* **153:** 355–368.

Purcell, J. E., and C. L. Kitting. 1982. Intraspecific aggression and population distributions of the sea anemone *Metridium senile*. *Biol. Bull.* **162:** 345–359.

Richardson, C. A., P. Dustan, and J. C. Lang. 1979. Maintenance of living space by sweeper tentacles of *Montastrea cavernosa*, a Caribbean reef coral. *Mar. Biol.* **55:** 181–186.

Sammarco, P. W., J. C. Coll, and S. LaBarre. 1985. Competitive strategies of soft corals (Coelenterata: Octocorallia). Coral Reefs **1:** 173–178.

Sammarco, P. W., J. C. Coll, and S. LaBarre, and B. Willis. 1983. Competitive strategies of soft corals (Coelenterata: Octocorallia): allelopathic effects on selected scleractinian corals. *J. Exp. Mar. Biol. Ecol.* **91:** 199–215.

Sebens, K. P. 1982. Intertidal distribution of zoanthids on the Caribbean coast of Panama: effects of predation and desiccation. *Bull. Mar. Sci.* **32:** 316–335.

Sebens, K. P. 1984. Agonistic behavior in the intertidal sea anemone *Anthopleura xanthogrammica*. *Biol. Bull.* **166:** 457–472.

Sheppard, C. R. C. 1979. Interspecific aggression between reef corals with reference to their distribution. *Mar. Ecol. Prog. Ser.* **1:** 237–247.

Sheppard, C. R. C. 1982a. Coral populations on reef slopes and their major controls. *Mar. Ecol. Prog. Ser.* **7:** 83–115.

Sheppard, C. R. C. 1982b. Reach of aggressively interacting corals, and relative importance of interactions at different depths. In *Proc. Fourth Int. Coral Reef Symp.*, Manila 1981, **2:** 363–368.

Sheppard, C. R. C. 1985. Unoccupied substrate in the Central Great Barrier Reef. *Mar. Ecol. Prog. Ser.* **25:** 259–268.

Theodor, J. L. 1970. Distinction between "self" and "not self" in lower invertebrates. *Nature* **227:** 690–692.

Theodor, J. L., and R. Senelar. 1975. Cytotoxic interactions between gorgonian explants: mode of action. *Cell. Immunol.* **19:** 194–200.

Theodor, J. L. 1976. Histo-incompatibility in a natural population of gorgonians. *Zool. J. Linn. Soc.* **58:** 173–176.

Wahle, C. M. 1980. Detection, pursuit, and overgrowth of tropical gorgonians by milleporid hydrocorals: Perseus and Medusa revisited. *Science* **209:** 689–691.

Watson, G. M., and R. N. Mariscal. 1983. The development of a sea anemone tentacle specialized for aggression: morphogenesis and regression of the catch tentacle of *Haliplanella luciae*. (Cnidaria, Anthozoa). *Biol. Bull.* **164:** 506–517.

Wellington, G. M. 1980. Reversal of digestive interactions between Pacific reef corals: mediation by sweeper tentacles. *Oecologia* **47:** 340–343.

Williams, R. B. 1980. A further note on catch-tentacles in sea anemones. *Trans. Norfolk Norwich Nat. Soc.* **25:** 84–86.

Williams, R. B. 1978. Some recent observations on the acrorhagi of sea anemones. *J. Mar. Biol. Assoc. U.K.* **58:** 787–788.

Williams, R. B. 1975. Catch tentacles in sea anemones: occurrence in *Haliplanella luciae* (Verrill) and a review of current knowledge. *J. Nat. Hist.* **9:** 241–248.

Reference: *Biol. Bull.* 175: 388–396 (December, 1988)

Gill Hemoglobin May Deliver Sulfide to Bacterial Symbionts of *Solemya velum* (Bivalvia, Mollusca)

JEANNETTE E. DOELLER[1], DAVID W. KRAUS[1], JAMES M. COLACINO[2], AND JONATHAN B. WITTENBERG[1]

[1]*Department of Physiology and Biophysics, Albert Einstein College of Medicine, Bronx, New York 10461 and* [2]*Department of Biological Sciences, Clemson University, Clemson, South Carolina 29634-1903*

Abstract. Two different hemoglobins occur in nearly equal concentrations in the gill of the bivalve mollusc, *Solemya velum* (total hemoglobin concentration is 200 μM/kg wet weight gill). A spectrophotometric study of intact gill filaments demonstrates that in the absence of sulfide, the gill hemoglobin may be oxygenated and deoxygenated, with part (5–20%) in the aquoferric form. In the presence of sulfide, about half of the gill hemoglobin is rapidly and reversibly converted to ferric hemoglobin, which then binds sulfide to form ferric hemoglobin sulfide (ferric hemoglobin with sulfide ligated to the heme iron in the distal ligand position); the balance continues to bind oxygen as oxyhemoglobin. *S. velum* inhabits reduced marine sediments where oxygen and hydrogen sulfide meet, and houses a dense population of intracellular chemoautotrophic sulfur-oxidizing symbiotic bacteria in its gill. We suggest that gill hemoglobins may mediate sulfide and oxygen delivery to the bacterial symbiont. Because sulfide is the dominant electron donor to fuel the *Solemya*/bacteria symbiosis, a cytoplasmic sulfide-binding protein that prevents the spontaneous reaction of sulfide with oxygen may be of utility in the nutrition of the animal.

Introduction

Intracellular chemoautotrophic bacteria, symbionts in the gills of certain molluscs, use the energy derived from the aerobic oxidation of sulfide (or other reductants) to fix carbon dioxide into organic compounds. Such bacterial symbionts form the primary base of the food chain of the dense populations of molluscs and giant tube worms at the deep sea hydrothermal vents (Cavanaugh *et al.*, 1981; Cavanaugh, 1985; Felbeck *et al.*, 1985). These symbiotic associations supply the majority of the carbon nutrition of the host (Cavanaugh, 1983; Felbeck, 1983; Dando *et al.*, 1985, 1986; Fisher and Childress, 1986; Anderson *et al.*, 1987; Southward, 1987).

Here we study the association between *Solemya velum*, an accessible small clam inhabiting the reduced sediment of eelgrass beds where oxygen and hydrogen sulfide meet, and chemoautotrophic bacteria housed in its gill (Cavanaugh, 1983). The gill obtains both sulfide and oxygen from the stream of seawater flowing through the mantle cavity, but the supply of sulfide and oxygen may be temporally separate as the animal moves within its burrow from the upper arms where oxygen predominates to the basal stem deeper in the sediment where sulfide predominates (Stanley, 1970; Jenner, 1977; Doeller, 1986). An intermittent supply suggests a need to store sulfide and oxygen in the gill. The diffusion path to the most remote bacterium housed in gill filament bacteriocytes is long (10–15 μm; Cavanaugh, 1983; Doeller, 1986), suggesting a need for facilitation of sulfide and oxygen diffusion to meet the demand by the symbionts.

Cytoplasmic hemoglobin is characteristic of the gills of most bivalves housing sulfur-oxidizing symbionts (Dando *et al.*, 1985; Wittenberg, 1985; *Lucinoma borealis* with symbionts may lack gill hemoglobin, Dando *et al.*, 1986; *Yoldia limatula* with few or no symbionts has gill hemoglobin at high concentration, Wittenberg, 1985; *Nucula proxima* with no symbionts has gill hemoglobin at low concentrations, Doeller, Kraus, and Smith, unpub. data). *S. velum* lacks a circulating hemoglobin (blood oxygen transport is assured by a circulating hemo-

Received 13 May 1988; accepted 18 August 1988.

cyanin, Mangum *et al.*, 1987), but has hemoglobin (200 μmol/kg wet weight gill) located in the bacteriocytes as well as other cells of the gill (Doeller, 1986). We have isolated two different cytoplasmic hemoglobins in roughly equal amounts from the gill. One reacts solely with oxygen and the other reacts with sulfide as well. In this paper we will show that about half of the hemoglobin in the living gill reacts with hydrogen sulfide, and argue that the sulfide-reactive hemoglobin serves to make sulfide available to the bacterial symbionts.

Materials and Methods

Animals

Solemya velum was collected from intertidal and subtidal sandy shoals near Morehead City, North Carolina, and from tidal mud flats near Woods Hole, Massachusetts. Average animal size was 1.7 cm long, with 0.04 g gill wet weight.

Isolation of Solemya *hemoglobins*

Gills were frozen in liquid nitrogen, pulverized, and extracted by a modification of the method of Schuder *et al.* (1979). The hemoglobin was fractionated with ammonium sulfate. Two different hemoglobin fractions were obtained by successive chromatography on Sephadex G100 and Sephadex DEAE A50 (Wittenberg and Wittenberg, 1981). The fraction emerging first from the DEAE column will be called Fraction I; that emerging second will be called Fraction II. Fraction I will be shown to react with sulfide.

Rates of oxygen dissociation

These were determined using a Gibson-Durrum stopped-flow spectrophotometer (Olson, 1981). The rate of oxygen dissociation from hemoglobin was determined by displacement of oxygen with carbon monoxide. A solution containing oxyhemoglobin (3 μ*M*) and oxygen (20 μ*M*) was mixed rapidly with a solution of carbon monoxide (1 m*M*) in the same buffer. Temperature was 20.0°C. The rate of the observed kinetic event was independent of carbon monoxide concentration (0.5–1 m*M*) and the rate of combination of carbon monoxide with deoxyhemoglobin is too fast to measure in our apparatus at these carbon monoxide concentrations.

Gas mixtures

Mixtures of oxygen, nitrogen, and carbon monoxide were prepared using a Tylan (Carson, CA) mass flow controller, humidified in a bubbler, and passed through the cuvette at a flow of 100 ml/min. Hydrogen sulfide and hydrogen cyanide were added to the humidified gas mixture from a gas-tight syringe (Hamilton) driven by a syringe pump.

Acquisition of optical spectra

In some experiments, optical spectra were acquired with a microspectrophotometer (Colacino and Kraus, 1984) and recorded from 440 to 400 nm at 2 nm intervals. Temperature was controlled at 20 ± 0.5°C. In subsequent experiments, optical spectra were acquired using a Cary model 14 recording spectrophotometer equipped with a Cary scattered transmission accessory and an Aviv digital data acquisition and analysis system (Lakewood, NJ). Optical spectra were recorded from 650 to 360 nm at 0.5 nm intervals. These experiments were performed near 24°C.

Optical spectra of purified hemoglobins

These were acquired using a thin-layer cell modified from Gill's (1981) design. Oxygenated and carbon monoxide hemoglobin were generated by exposing the hemoglobin to these gases. Deoxyhemoglobin was generated by exposing hemoglobin in a solution containing dithiothreitol to oxygen-free nitrogen. Dithiothreitol serves to reduce ferric hemoglobin to ferrous (deoxygenated) hemoglobin. Ferric hemoglobin sulfide was prepared from *Solemya* Hb I in two independent ways. In the first, ferric hemoglobin was exposed to hydrogen sulfide (0.4 torr) in nitrogen. In the second, oxyhemoglobin was exposed to a gas mixture containing oxygen (2 torr), hydrogen sulfide (0.4 torr), balance nitrogen.

Optical spectra of gill filaments

Freshly collected animals in seawater were cooled over ice. The gills were exposed after cutting the fused mantle tissue to open the valves. For experiments using the microspectrophotometer, 3–5 individual gill filaments (about 60–100 μm thick) were placed between two gas-permeable membranes (Teflon, 6 μm thick, Dilectrix Corp.) and held in a gas-tight cuvette (Colacino and Kraus, 1984). The ambient oxygen pressure or hydrogen sulfide pressure to achieve volume-average steady state half saturation of the total gill hemoglobin with oxygen or of about half the gill hemoglobin with hydrogen sulfide was calculated from absorbance changes at the wavelength pairs 415 and 430 nm, and 420 and 430 nm, respectively. The time to reach unchanging absorbance was less than 20 min. To obviate any complexities of dealing with oxygen and sulfide together during steady state measurements, the effect of sulfide on the gill hemoglobin was studied in gills held in nitrogen.

For experiments using the Cary spectrophotometer, approximately 30–50 individual gill filaments were cut

free from the central ligament of the gill and allowed to form a continuous layer of partially overlapping filaments (about 5–10 filaments or 100–200 μm thick) on the gas-permeable membrane window (MEM 213, 25 μm thick; General Electric Corp., Schenectady, NY) of the cuvette used in the Cary spectrophotometer. The sample was covered with a second membrane and the assembly was placed in a gas-tight cuvette. A single layer of parafilm was used to attenuate the Cary reference beam and to balance light scattering. The spectral contribution of hemoglobin in intact gill filaments is partially obscured by contributions from bacteria, mitochondria, other cell components, and by wavelength-dependent optical distortions. These unchanging contributions were cancelled by taking difference spectra constructed with computer assistance (Wittenberg and Wittenberg, 1986).

Results

Properties of the purified hemoglobins

Each component eluted from the Sephadex G100 column in a position near that expected for a monomeric hemoglobin of molecular weight about 17,000. The rate of oxygen dissociation, k′, for Hb I was 65 s^{-1}. This rate, although rapid, is characteristic of gill hemoglobins of many clams (Wittenberg, unpub.). The dissociation rate for Hb II was 35 s^{-1}. The combination rate constants have not yet been determined.

One of the purified hemoglobins, Hb I, when exposed to hydrogen sulfide (0.4 torr) at an oxygen pressure (2 torr) low enough to partially desaturate the hemoglobin, formed a spectral entity unequivocally identified as ferric hemoglobin sulfide; that is, ferric hemoglobin with sulfide ligated to the heme iron atom in the distal ligand position (Keilin, 1933). The product is identified by the following properties. The optical spectrum is identical to that of the product formed by reaction of ferric *Solemya* Hb I with hydrogen sulfide (see Fig. 2C, trace 2) and is closely similar to the spectrum reported by Keilin (1933) for ferric human hemoglobin sulfide. The spectrum is also nearly identical to those of ferric *Lucina pectinata* hemoglobin sulfide and ferric sperm whale myoglobin sulfide (Kraus and Wittenberg, in prep.). There was an insufficient quantity of isolated *Solemya* hemoglobin to allow chemical determination of the stoichiometry between sulfide and heme. Identity of ferric *Lucina pectinata* hemoglobin sulfide and ferric sperm whale myoglobin sulfide was established by demonstrating that one mole of sulfide was bound per mole heme (Kraus and Wittenberg, in prep.). The identity of ferric *Lucina* hemoglobin sulfide was confirmed by electron paramagnetic resonance (EPR) spectroscopy which gave the expected signature (Berzofsky *et al.*, 1971; Kraus and Wittenberg, in prep.).

In contrast to Hb I, *Solemya* Hb II remained in the oxygenated form when exposed to mixtures of hydrogen sulfide and oxygen. Neither purified hemoglobin formed the green compound, sulfhemoglobin, under the above conditions, although under these conditions, whale myoglobin was converted to sulfmyoglobin (Berzofsky *et al.*, 1971). In this report, the hemoglobin components will be called the sulfide-reactive and sulfide-unreactive hemoglobins.

Oxygen pressure to half saturate the gill hemoglobin in situ

The ambient oxygen pressure required to achieve volume-averaged half saturation of hemoglobin in respiring gill filaments was 6 ± 1 torr at 20°C (n = 26; Fig. 1A). This value reflects a balance between oxygen entry and oxygen utilization and will depend accordingly on the length of the diffusion path both external and internal to the tissue. It is not to be regarded as a fixed parameter of the reaction *per se*.

Hydrogen sulfide pressure to half saturate the gill hemoglobin in situ

The ambient hydrogen sulfide pressure required for half maximal spectral change in the Soret region of gill filaments exposed to hydrogen sulfide in nitrogen was 1.5 ± 0.5 torr at 20°C (n = 6; Fig. 1B). Not all of the gill hemoglobin reacts with sulfide, the balance remaining as deoxyhemoglobin; in these experiments, we did not determine the fraction reacting. The rate of sulfide consumption in the closely related clam *Solemya reidi* is large and of the same order as oxygen uptake (Anderson *et al.*, 1987). Accordingly, the value of 1.5 torr P_{H_2S} also depends on a balance between sulfide entry and utilization and on the diffusion path, and cannot be regarded as a fixed parameter of the reaction *per se*.

Identification of hemoglobin species formed in the gill

Oxyhemoglobin. We use difference spectra to examine the reaction of hemoglobin *in situ*. Figure 2A, trace 1, demonstrates that most of the gill hemoglobin reacted reversibly with oxygen. Carbon monoxide was used to convert the tissue hemoglobin to a common liganded form. Taking extinction coefficients determined for isolated *Solemya* hemoglobin, we estimate the amount of hemoglobin (hemoglobin concentration times pathlength for each preparation) in the tissue both from the direct spectrum of gill filaments exposed to carbon monoxide and from the difference spectrum: the spectrum of gill filaments in carbon monoxide minus the spectrum of the same array of gill filaments in air. This estimate agrees with an independent estimate from the difference

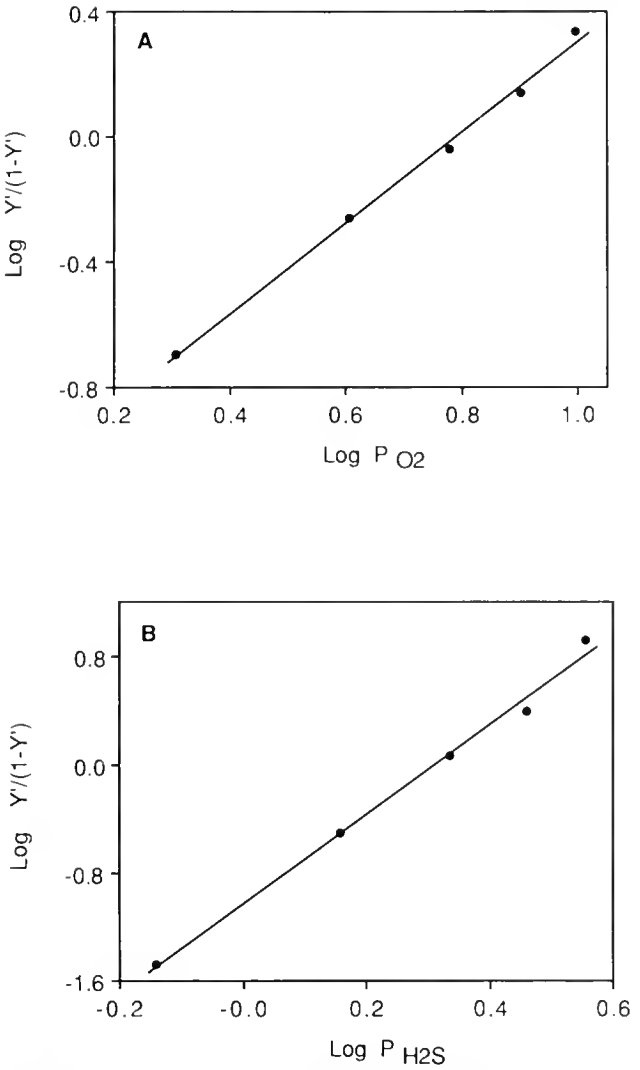

Figure 1. A. Hill plot showing the fractional saturation of the cytoplasmic hemoglobin in *Solemya* gill filaments as a function of external oxygen pressure. Data were acquired on the microspectrophotometer. Y' is defined as the fraction of the ligand-reactive hemoglobin undergoing reaction. The ambient oxygen pressure at half saturation is 6.1 torr in this representative experiment.

B. Hill plot showing the fractional ligation of sulfide to the cytoplasmic hemoglobin in *Solemya* gill filaments as a function of external hydrogen sulfide pressure. Data were acquired on the microspectrophotometer. Y' is defined as above. The ambient hydrogen sulfide pressure at half maximal spectral change is 1.8 torr in this representative experiment.

spectrum: gill filaments in air minus gill filaments in nitrogen.

Ferric hemoglobin sulfide—difference spectra. Hydrogen sulfide (0.7 torr) introduced into the flowing gas stream changed the optical spectrum of intact gill filaments either in the presence or absence of oxygen. The concentration of sulfide in water equilibrated with this gas mixture will be about 100 μM. It will be greater in buffered cytoplasm. The weak acid, H_2S, pK 7.0, decreased the pH of seawater equilibrated with this gas mixture by no more than 0.1 pH unit and is not expected to alter the pH of the strongly buffered cytoplasm appreciably.

The hydrogen sulfide-dependent reaction was followed at 435 nm, near the absorbance maximum of the difference spectrum between ferric hemoglobin sulfide and ferrous hemoglobin. Spectral change was most easily observed in gill filaments held at a gas phase oxygen pressure (about 60 torr) just low enough to bring about detectable deoxygenation of cytoplasmic hemoglobin in the thick preparation of filaments. Oxygen was removed from the gas stream after the spectral change was complete, simplifying analysis by removing the spectral contribution of oxyhemoglobin. A difference spectrum was constructed: the spectrum of gill filaments in hydrogen sulfide and nitrogen minus the spectrum of the same array of gill filaments previously exposed to nitrogen alone (Fig. 2B, trace 1). Spectral features near 422, 436, 566, and 582 nm are similar to features of the difference spectrum: purified ferric *Solemya* hemoglobin sulfide minus ferrous *Solemya* hemoglobin (Fig. 2A, trace 2). The amplitude of the difference spectrum of the gill (Fig. 2B, trace 1) corresponds to conversion of about half of the total hemoglobin in the gill to ferric hemoglobin sulfide.

Ferric hemoglobin. The feature near 405 nm in the difference spectrum (Fig. 2B, trace 1) varied in amplitude in experiments with different gills. We ascribe this feature to the removal of aquoferric hemoglobin (acid methemoglobin) initially present in the gill. This was estimated to vary from less than 5% to about 20% of the total ($n = 6$) and was estimated at approximately 10% in the particular gill figured (aquoferric hemoglobin will be converted to ferric hemoglobin sulfide). A difference spectrum: purified ferric *Solemya* hemoglobin sulfide minus the sum of the spectral contributions of ferrous *Solemya* hemoglobin (90%) and aquoferric *Solemya* hemoglobin (10%) (Fig. 2B, trace 2) is very similar to the difference spectrum of the gill (Fig. 2B, trace 1). The similarity of these two difference spectra (Fig. 2B1, 2B2) constitutes strong evidence that the form of hemoglobin generated by exposing gill filaments to sulfide is ferric hemoglobin sulfide and that a small amount of aquoferric hemoglobin is initially present in the gill.

Ferric hemoglobin sulfide—direct spectrum. The direct spectrum of the hemoglobin species generated by exposing gill filaments to hydrogen sulfide can be reconstructed by adding to the difference spectrum: gill filaments in hydrogen sulfide and nitrogen minus gill filaments in nitrogen (Fig. 2B, trace 1) the expected sum of the spectral contributions of ferrous *Solemya* hemoglobin (90%) and aquoferric *Solemya* hemoglobin (10%) estimated to be initially present in this particular gill (Fig.

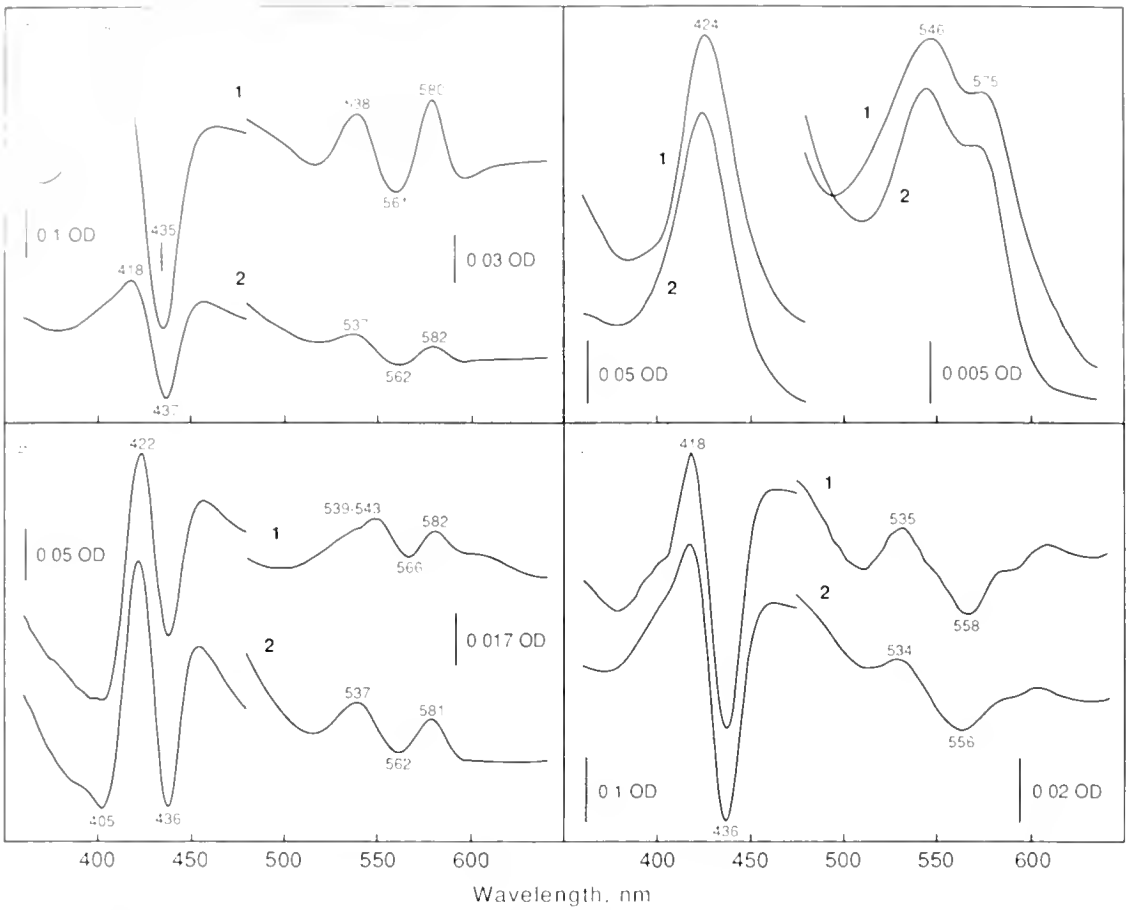

Figure 2. *Panel A Trace 1* Optical difference spectrum of intact gill filaments in oxygen (60 torr), balance nitrogen, minus a spectrum of the same specimen in nitrogen. *Trace 2* Optical difference spectrum of authentic ferric *Solemya* hemoglobin sulfide minus ferrous *Solemya* hemoglobin. The ordinate scale bars in all panels are those observed in the actual spectra of the gill filaments. The amplitude of the accompanying spectra of the purified components are adjusted to an equal amount of hemoglobin in the light path. Predictably, the spectra of oxyhemoglobin and ferric hemoglobin sulfide, both low spin ferric heme derivatives with similar ligands, have similar wavelength maxima (Perutz *et al.*, 1968). It is apparent that the molar extinction of the hemoglobin derivative in trace 2 is less than that in trace 1.

Panel B Trace 1 Optical difference spectrum of intact gill filaments allowed to react with hydrogen sulfide (0.7 torr) in the presence of oxygen, subsequently exposed to hydrogen sulfide in nitrogen, minus the spectrum of the same specimen previously exposed to nitrogen alone. The β-band includes a small contribution from a particle-bound (bacterial?) cytochrome *c*-like protein. This has the effect of shifting the apparent wavelength maximum toward longer wavelengths. This shift is reflected in the apparent wavelength maxima of Panel C, trace 1. *Trace 2* Optical difference spectrum of authentic ferric *Solemya* hemoglobin sulfide minus the sum of the spectral contributions of ferrous *Solemya* hemoglobin (90%) and aquoferric *Solemya* hemoglobin (10%).

Panel C Trace 1 Spectrum of the product formed when intact *Solemya* gill filaments are exposed to hydrogen sulfide, reconstructed by adding the computed spectrum of a mixture of ferrous *Solemya* hemoglobin (90%) and aquoferric *Solemya* hemoglobin (10%) to the difference spectrum of trace B1. *Trace 2* Optical spectrum of authentic ferric *Solemya* hemoglobin sulfide. Traces C1 and C2 are nearly indistinguishable.

Panel D Trace 1 Optical difference spectrum of intact *Solemya* gill filaments exposed first to a mixture containing hydrogen cyanide (0.2 torr) and oxygen (60 torr), balance nitrogen, and subsequently exposed to hydrogen cyanide (0.2 torr) in nitrogen, recorded after completion of the slow kinetic event (see text), minus the spectrum of the same specimen previously exposed to nitrogen alone. *Trace 2* Optical spectrum of authentic ferric *Solemya* hemoglobin cyanide minus ferrous *Solemya* hemoglobin. Traces D1 and D2 are sensibly the same.

Table I

Half-times of reactions of hemoglobin in gill filaments of Solemya velum

Ligand	$t_{1/2}$, addition		$t_{1/2}$, removal	
	H_2S absent	H_2S present	H_2S absent	
O_2	1.2 ± 0.2 (21)[a] 11 ± 5 (13)[b]	1.2 ± 0.2 (15)[a]	32 ± 9 (21)[a] 21 ± 12 (14)[b]	
	O_2 present	O_2 absent	O_2 present	O_2 absent
H_2S	62 ± 23 (6)[b]	163 ± 38 (3)[a]	178 ± 72 (4)[b] 196 ± 29 (9)[a]	340 (1)[b]
CN	50 ± 16 (4)[b]	830 (2)[b]	780 (1)[b]	—

Values are given as mean ± standard deviation. Bracketed values are number of determinations. The unit is seconds.

[a] Determined using the microspectrophotometer.

[b] Determined using the Cary model 14 spectrophotometer.

2C, trace 1). This reconstructed spectrum is nearly identical to the spectrum of ferric *Solemya* hemoglobin sulfide (Fig. 2C, trace 2) generated by exposing ferric *Solemya* hemoglobin to hydrogen sulfide (0.4 torr). This is strong additional evidence for the formation of ferric hemoglobin sulfide in the gill.

Kinetics of hemoglobin reactions in the gill

Oxygen. Oxygenation of previously anaerobic gills exposed to air proceeded with $t_{1/2} = 1.2$ s (a thin preparation examined in the microspectrophotometer) and 11 s (a thicker preparation examined in the Cary spectrophotometer; Table I). Deoxygenation proceeded with $t_{1/2} = 32$ s and 21 s (Table I) with the respective preparations. These rates are very slow compared to the rates of the reactions of isolated hemoglobin.

Hydrogen sulfide. Spectral change in gills exposed to hydrogen sulfide (0.5–3 torr) in nitrogen occurred with $t_{1/2} = 163$ s (these experiments were performed using the microspectrophotometer; Table I). When the gas stream was changed to air in this series of experiments, two distinct kinetic events were seen, with $t_{1/2} = 1.2$ s and $t_{1/2} = 196$ s, respectively (Table I). Absorption spectra at the end of the fast event indicated partial reoxygenation of the hemoglobin and those at the end of the slow event indicated fully oxygenated hemoglobin. We identify the rapid reaction as oxygenation of deoxyhemoglobin present in the tissue and identify the slow kinetic event as regeneration of oxyhemoglobin from ferric hemoglobin sulfide. We emphasize that each reaction corresponded to about half of the total hemoglobin in the gill.

In a separate series of experiments using the Cary spectrophotometer, hydrogen sulfide (0.7 torr) was introduced into the gas stream containing oxygen (60 torr), balance nitrogen. The hydrogen sulfide-dependent spectral change ($t_{1/2} = 62$ s; Table I) was more rapid than that observed in nitrogen. When hydrogen sulfide was removed from the oxygen-containing gas stream, oxyhemoglobin was regenerated in the gill with $t_{1/2} = 178$ s (Table I). We did not observe a fast kinetic event. We note that difference spectra showed that about half the hemoglobin was ferric hemoglobin sulfide and we assume that the balance remained oxygenated. As before, we interpret the kinetic event as regeneration of oxyhemoglobin from ferric hemoglobin sulfide.

The rate of reaction of oxyhemoglobin with hydrogen sulfide in the intact gill was much faster than the rate of reaction of purified oxy *Solemya* Hb I with hydrogen sulfide under equivalent conditions ($t_{1/2} \sim 400$–500 s; n = 2).

Cyanide. Cyanide binds very strongly to ferric hemoglobin and is useful for experiments with intact tissues because the undissociated acid diffuses rapidly into cells. Hydrogen cyanide introduced into the flowing gas stream was used to demonstrate ferric hemoglobin formation by trapping intracellular ferric hemoglobin as ferric hemoglobin cyanide. The reaction was followed at 420 nm, near the absorbance maximum of ferric hemoglobin cyanide. A relatively rapid kinetic event ($t_{1/2} = 50$ s; Table I) was observed in the presence of hydrogen cyanide (0.2 torr) and oxygen (60 torr), balance nitrogen. To identify the product and to simplify spectral analysis, oxygen was subsequently removed from the flowing gas stream and a difference spectrum was constructed: gill filaments in cyanide and nitrogen minus gill filaments previously exposed to nitrogen alone. This showed about half conversion of hemoglobin to ferric hemoglobin cyanide (n = 5). When gill filaments were exposed to hydrogen cyanide (0.2 torr) in nitrogen alone, only a slow kinetic event ($t_{1/2} \sim 830$ s; Table I) was seen, and a difference spectrum constructed at the end of this event indicated complete conversion of hemoglobin to ferric hemoglobin cyanide (n = 2). The differences in each case were nearly identical to the difference spectrum: authentic ferric *Solemya* hemoglobin cyanide minus ferrous *Solemya* hemoglobin (Fig. 1D, trace 2). We suggest that the fast kinetic event reflects conversion of the sulfide-reactive hemoglobin to ferric hemoglobin cyanide. The slow kinetic event includes the conversion of both hemoglobins to the same product.

Ferric hemoglobin cyanide formation was reversed and oxyhemoglobin was fully regenerated when cyanide was removed from the oxygen-containing gas stream.

Kinetics of ferric hemoglobin formation in the presence of hydrogen sulfide

The possibility arises that sulfide interacts nonenzymatically to accelerate the rate of formation of ferric he-

moglobin. To examine this possibility, gill filaments were exposed simultaneously to cyanide and oxygen in the gas stream and the rate of conversion of oxyhemoglobin to ferric hemoglobin cyanide was estimated. Hydrogen sulfide, subsequently introduced into the gas stream, did not accelerate ferric hemoglobin formation.

Discussion

The symbiotic association between the clam *Solemya velum* and the intracellular bacterial partner depends on both oxygen and hydrogen sulfide for its nutrition. Here we ask how the hemoglobin, so abundant in the bacteria-harboring gill, interacts with these two substrates. Hemoglobin in the respiring gill is half-saturated at an ambient oxygen pressure of about 6 torr. The oxygen pressure in the oxygenated upper arms of the *Solemya* burrow might be about 50–80 torr, as it is in the U-shaped burrows of other animals inhabiting reduced sediments (Mangum *et al.*, 1975; Mangum, 1976). This oxygen pressure is more than sufficient to provide extensive oxygenation of the gill hemoglobin. The reaction of gill hemoglobin with sulfide was studied in gills held in nitrogen. Half maximal spectral change occurred at a hydrogen sulfide pressure of 1.5 torr. The hydrogen sulfide concentration in the pore water of the sediments from which these animals were collected falls within the range of 30 μM to 3 mM (Fenchel and Reidl, 1970; Howarth and Teal, 1980) corresponding very approximately to a hydrogen sulfide pressure of 0.2 to 20 torr. This suggests that a substantial fraction of the gill hemoglobin would ligate hydrogen sulfide in the basal stem of the burrow.

In this study, we use difference spectroscopy to identify hemoglobin species present in the living gill. The majority of the hemoglobin in gill filaments exposed solely to air is oxygenated. On the other hand, we observed a mixture of about equal parts of oxyhemoglobin and of an additional species in gill filaments exposed to oxygen and hydrogen sulfide at relatively low partial pressures. We seek to identify this new species. For this purpose, we generated a difference spectrum between gill filaments containing this new species and the same gill filaments previously in nitrogen and show this difference to be identical to that formed between ferric *Solemya* hemoglobin sulfide and deoxyhemoglobin. Using the difference spectrum of gill filaments, we reconstructed the direct spectrum of the hemoglobin derivative formed in the presence of sulfide. This spectrum is indistinguishable from that of authentic ferric *Solemya* hemoglobin sulfide. The only other hemoglobin derivative likely to be formed under these conditions would be sulfhemoglobin. This latter species is green, with a characteristic and unmistakable spectrum (Berzofsky *et al.*, 1971) different from any seen here. We conclude that the hemoglobin species formed in the presence of hydrogen sulfide is ferric hemoglobin sulfide; that is, ferric hemoglobin with sulfide ligated to the heme iron atom in the distal ligand position (Keilin, 1933).

Only about half of the hemoglobin in intact gill filaments reacts to form ferric hemoglobin sulfide. The magnitude of the difference spectrum constructed at the end of the reaction with sulfide in the presence of oxygen corresponds to reaction of about half the hemoglobin in the gill. The rapid reoxygenation of deoxyhemoglobin in the gill at the end of the reaction with sulfide carried out in the absence of oxygen corresponds to the remaining half of the hemoglobin in the gill. These results suggest but do not prove that there are two differently reactive hemoglobin components in the gill. This suggestion is supported by experiments with cyanide. About half the hemoglobin reacts rapidly with cyanide in the presence of oxygen. The balance of hemoglobin, either in the presence or absence of oxygen, reacts ten times more slowly but under these forced conditions eventually is converted to ferric hemoglobin cyanide.

We suggest that the initial event in the formation of ferric hemoglobin sulfide is the conversion of ferrous to ferric hemoglobin. Difference spectroscopy of gill filaments demonstrates a standing crop of aquoferric hemoglobin, often about 10% of the total hemoglobin in the gill. When ligands for ferric hemoglobin, hydrogen sulfide or cyanide are added in the presence of oxygen, about half of the total hemoglobin is rapidly converted to the corresponding ligated ferric hemoglobin. The close similarity of the rates of reaction with the two very different ligands (Table I) suggests a common rate-limiting step which, we argue, is the formation of ferric hemoglobin. Subsequent ligation of hydrogen sulfide or cyanide will be rapid and independent of enzyme action.

The rate of formation of ferric hemoglobin sulfide ($t_{1/2}$ = 62 s) in the intact gill is much faster than the rate of the purely chemical event observed when purified Hb I is exposed to mixtures of oxygen and hydrogen sulfide ($t_{1/2} \approx$ 400–500 s), and is only 5 to 6-fold slower than the diffusion-limited ingress of oxygen in the same experimental series (Table I). Accordingly, we suggest that the conversion of ferrous to ferric hemoglobin is accelerated in the *Solemya* gill. The reverse reaction, reduction of ferric cytoplasmic hemoglobin, is known from studies of other tissues to require the action of enzyme systems (metmyoglobin or methemoglobin reductase).

Rapid conversion of ferrous to ferric cytoplasmic hemoglobin is unusual and is not encountered in tissues of any of the vertebrate and invertebrate species we have examined. In the presence of cyanide (1–10 mM, sufficient to inhibit most respiratory oxygen consumption), all hemoglobin in the tissue of the following species remained in the oxygenated form, with no detectable ferric

hemoglobin cyanide: the vertebrate tissues rat cardiac myocytes (Wittenberg and Wittenberg, 1986) and pigeon breast muscle (Wittenberg *et al.*, 1975); the molluses *Busycon canaliculatum* radular muscle, *Aplysia californica* buccal muscle, *Spisula solidissima* nerve, *Tellina alternata* nerve; the annelid *Arenicola cristata* body wall; the echiuran *Urechis caupo* body wall; and the insect *Gastrophilus intestinalis* tracheal cells (unpub. data).

Sulfide-binding components have been demonstrated in other invertebrates participating in sulfur-oxidizing symbioses. A component of the colorless blood plasma of the giant clam *Calyptogena magnifica* of the hydrothermal vents binds sulfide (Arp *et al.*, 1984). The blood hemoglobin of the giant tube worm *Riftia pachyptila* of the hydrothermal vents binds sulfide at a site believed to be remote form the heme (Arp *et al.*, 1987). Sulfide oxidation, presumptively to thiosulfate, has been noted in the animal tissues of *Solemya reidi* and the suggestion made that thiosulfate so formed is used by the symbionts (Powell and Somero, 1985, 1986).

We consider that the two hemoglobins found in the gill of *Solemya velum* may represent a division of labor in which the sulfide-reactive hemoglobin delivers sulfide and the sulfide-unreactive hemoglobin delivers oxygen to their respective consuming centers. We note the strong analogy with the nitrogen-fixing root nodules of legumes in which legume hemoglobin mediates oxygen delivery to the nitrogen-fixing bacterial symbionts (Appleby, 1984; Wittenberg, 1985). In the absence of sulfide, we envision a dynamic balance between ferric hemoglobin formation and removal in the gill, with about 5–20% of the total gill hemoglobin in the aquoferric form. In the presence of the natural substrate sulfide or the experimentally added cyanide, this balance is shifted and about half of the total hemoglobin (perhaps the sulfide-reactive component, Hb I) becomes trapped in the ligated form. Hemoglobins that ligate oxygen and sulfide, thereby preventing these molecules from interacting spontaneously, may be key features of the *Solemya*/bacteria symbiosis.

Acknowledgments

Some of the experiments reported here form part of the doctoral dissertation of J. E. Doeller (Clemson University, SC, 1986). This work was supported in part by Research Grant DMB 8703328 from the National Science Foundation (to JBW) and in part by Grant HL-19299 from the United States Public Health Service (to Dr. B. A. Wittenberg). J. B. Wittenberg is a Research Career Program Awardee 1-K6-733 of the United States Public Health Service, National Heart, Lung and Blood Institute. We thank Mr. John Valois and members of the Marine Resources Department, Marine Biological Laboratory, Woods Hole, MA, for supplying some of the animals used here. We thank Dr. E. E. Ruppert for bringing *S. velum* to our attention, Dr. J. Peisach for electron paramagnetic resonance spectroscopy, and Dr. B. A. Wittenberg for continuing discussions.

Literature Cited

Anderson, A. E., J. J. Childress, and J. A. Favuzzi. 1987. Net uptake of CO_2 driven by sulphide and thiosulfate oxidation in the bacterial symbiont-containing clam *Solemya reidi*. *J. Exp. Biol.* **133:** 1–31.

Appleby, C. A. 1984. Leghemoglobin and *Rhizobium* respiration. *Ann. Rev. Plant Physiol.* **35:** 443–478.

Arp, A. J., J. J. Childress, and C. R. Fisher, Jr. 1984. Metabolic and blood gas transport characteristics of the hydrothermal vent bivalve *Calyptogena magnifica*. *Physiol. Zool.* **57:** 648–662.

Arp, A. J., J. J. Childress, and R. D. Vetter. 1987. The sulphide-binding protein in the blood of the vestimentiferan tube-worm, *Riftia pachyptila*, is the extracellular haemoglobin. *J. Exp. Biol.* **128:** 139–158.

Berzofsky, J. A., J. Peisach, and W. E. Blumberg. 1971. Sulfheme proteins. I. Optical and magnetic properties of sulfmyoglobin and its derivatives. *J. Biol. Chem.* **246:** 3367–3377.

Cavanaugh, C. M. 1983. Symbiotic chemoautotrophic bacteria in marine invertebrates from sulfide-rich habitats. *Nature* **302:** 58–61.

Cavanaugh, C. M. 1985. Chemoautotrophic symbioses. In *The Hydrothermal Vents of the Eastern Pacific: An Overview*. M. L. Jones, ed. *Biol. Soc. Wash. Bull.* **6:** 373–388.

Cavanaugh, C. M., S. L. Gardiner, M. L. Jones, H. W. Jannasch, and J. B. Waterbury. 1981. Prokaryotic cells in the hydrothermal vent tube worm *Riftia pachyptila* Jones: possible chemoautotrophic symbionts. *Science* **213:** 340–342.

Colacino, J. M., and D. W. Kraus. 1984. Hemoglobin-containing cells of *Neodasys* (Gastrotricha, Chaetonotidae). II. Respiratory significance. *Comp. Biochem. Physiol.* **79A:** 363–369.

Dando, P. R., A. J. Southward, and E. C. Southward. 1986. Chemoautotrophic symbionts in the gills of the bivalve mollusc *Lucinoma borealis* and the sediment chemistry of its habitat. *Proc. R. Soc. Lond. B* **227:** 227–247.

Dando, P. R., A. J. Southward, E. C. Southward, N. B. Terwilliger, and R. C. Terwilliger. 1985. Sulphur-oxidiing bacteria and haemoglobin in gills of the bivalve mollusc *Myrtea spinifera*. *Mar. Ecol. Prog. Ser.* **23:** 85–98.

Doeller, J. E. 1986. A study of the gill hemoglobin in the nearly gutless bivalve *Solemya velum* Say (Protobranchia). Ph.D. Dissertation, Clemson University, South Carolina.

Felbeck, H. 1983. Sulfide oxidation and carbon fixation by the gutless clam *Solemya reidi*, an animal-bacterial symbiosis. *J. Comp. Physiol.* **152:** 3–11.

Felbeck, H., M. A. Powell, S. C. Hand, and G. N. Somero. 1985. Metabolic adaptations of hydrothermal vent animals. In *The Hydrothermal Vents of the Eastern Pacific: An Overview*. M. L. Jones, ed. *Biol. Soc. Wash. Bull.* **6:** 261–272.

Fenchel, T. M., and R. J. Reidl. 1970. The sulfide system: a new biotic community underneath the oxidized layer of marine sand bottoms. *Mar. Biol.* **7:** 255–268.

Fisher, C. R., and J. J. Childress. 1986. Translocation of fixed carbon from symbiotic bacteria to host tissues in the gutless bivalve *Solemya reidi*. *Mar. Biol.* **93:** 59–68.

Gill, S. J. 1981. Measurement of oxygen binding by means of a thin layer optical cell. *Methods Enzymol.* **76:** 427–438.

Howarth, R. W., and J. M. Teal. 1980. Energy flow in a salt march ecosystem: the role of reduced organic sulfur compounds. *Am. Nat.* **116:** 862–872.

Jenner, C. E. 1977. *Solemya* [illegible] a burrow-dwelling bivalve mollusc. *Assoc. Southeast* [illegible] *Bull.* **24:** 61a.

Keilin, D. 1933. On [illegible] combination of methaemoglobin with H_2S. *Proc. R. Soc. L.* [illegible] **113:** 393–404.

Mangum, C. P. [illegible] 6. Oxygenation of hemoglobin in lugworms. *Physiol. Z.* [illegible] **49:** 85–99.

Mangum, C. P., K. I. Miller, J. L. Scott, K. E. Van Holde, and M. P. Morse. 1987. Bivalve hemocyanin: structural, functional, and phylogenetic relationships. *Biol. Bull.* **173:** 205–221.

Mangum, C. P., B. R. Woodin, C. Bonaventura, B. Sullivan, and J. Bonaventura. 1975. The role of coelomic and vascular hemoglobin in the annelid family Terebellidae. *Comp. Biochem. Physiol.* **51A:** 281–294.

Olson, J. 1981. Stopped-flow, rapid mixing measurements of ligand binding to hemoglobin and red cells. *Methods Enzymol.* **76:** 631–651.

Peisach, J., W. E. Blumberg, B. A. Wittenberg, and J. B. Wittenberg. 1968. Electronic structure of protoheme proteins. III. Configuration of heme and its ligands. *J. Biol. Chem.* **243:** 1871–1880.

Powell, M. A., and G. N. Somero. 1985. Sulfide oxidation occurs in the animal tissue of the gutless clam, *Solemya reidi*. *Biol. Bull.* **169:** 164–181.

Powell, M. A., and G. N. Somero. 1986. Hydrogen sulfide oxidation is coupled to oxidative phosphorylation in mitochondria of *Solemya reidi*. *Science* **233:** 563–566.

Schuder, S., J. B. Wittenberg, B. Haseltine, and B. A. Wittenberg. 1979. Spectrophotometric determination of myoglobin in cardiac and skeletal muscle: separation from hemoglobin by subunit-exchange chromatography. *Anal. Biochem.* **92:** 473–481.

Southward, E. C. 1987. Contribution of symbiotic chemoautotrophs to the nutrition of benthic invertebrates. Pp. 83–118 in *Microbes in the Sea*, M. A. Sleigh, ed. Ellis Horwood Ltd., Chichester, England.

Stanley, S. M. 1970. *Relation of Shell Form to Life Habits of the Bivalvia (Mollusca)*. 296 pp. *The Geol. Soc. Am., Inc.* Colorado, Memoir **125.**

Wittenberg, J. B. 1985. Oxygen delivery to intracellular bacterial symbionts. In *The Hydrothermal Vents of the Eastern Pacific: An Overview*, M. L. Jones, ed. *Biol. Soc. Wash. Bull.* **6:** 301–310.

Wittenberg, J. B., and B. A. Wittenberg. 1981. Preparation of myoglobin. *Methods Enzymol.* **76:** 29–42.

Wittenberg, B. A., and J. B. Wittenberg. 1986. Oxygen pressure gradients in isolated cardiac myocytes. *J. Biol. Chem.* **260:** 6548–6554.

Wittenberg, B. A., J. B. Wittenberg, and P. R. B. Caldwell. 1975. Role of myoglobin in the oxygen supply to red skeletal muscle. *J. Biol. Chem.* **250:** 9038–9043.

Reference: *Biol. Bull.* **175**: 397–402. (December, 1988)

Biochemical Characteristics of the Pigmentation of Mesopelagic Fish Lenses

MARGARET MCFALL-NGAI[1,*], LIN DING[1], JAMES CHILDRESS[2], AND JOSEPH HORWITZ[1]

[1]*Jules Stein Eye Institute, University of California, Los Angeles, California 90024, and* [2]*Department of Biological Sciences, University of California, Santa Barbara, California 93106*

Abstract. We analyzed the biochemical, anatomical, and spectrophotometric characteristics of lens pigmentation in representatives of two mesopelagic fish families, the Opisthoproctidae and the Scopelarchidae. In small and large specimens of the opisthoproctid *Macropinna microstoma* and in the larval scopelarchid *Benthalbella infans*, the lens pigment was present in all layers of the lens as a freely diffusable chromophore. In contrast, the lenses in the adult specimens of the scopelarchid *Benthalbella dentata*, which have lenses averaging 6.7 mm in diameter, had a 2.4 mm-diameter pigmentless core. In this species, the chromophore was bound to one of the major structural proteins of the lens, gamma crystallin. Because the lens grows by the layering of new cells over older ones, such a pattern in *B. dentata* suggests that the lens pigment is not present in larvae of this species. The chromophores of all specimens were characterized by a single broad peak in the shorter-wavelength blue, near-UV portion of the spectrum.

Introduction

Pigmentation in the tissues of vertebrate and invertebrate visual systems is a common phenomenon, expressing itself most often in the cornea, lens, and retinal-associated cells (Muntz, 1972; Heinermann, 1984). In the lens, pigmentation occurs: (1) in many diurnally active animals (Walls and Judd, 1933; Cooper and Robson 1969a; Muntz, 1974), including both terrestrial and shallow water aquatic species; (2) as an age-related yellowing of the lens, which occurs in vertebrate species of long lifespan, independent of habitat (Cooper and Robson, 1969b; Zigman, 1971; Villermet and Weale, 1972); and (3) as a rare occurrence among animals in the mesopelagic zones of the ocean (from about 100–1000 m depth) (see for review, Heinermann, 1984).

The three types of lens pigmentation differ in their biochemical characteristics, their ontogenic pattern in the animal, and perhaps also in their function. In diurnally active animals, the lens pigment is present at all stages in the animal's life history as a soluble component of the lens cells; *i.e.*, it is freely diffusible through the numerous gap junctions between adjacent cells in the lens. Lenticular coloration in these species is thought to increase visual acuity by reducing chromatic aberration produced by the shorter wavelengths. In age-related pigmentation of the lens, while young lenses may be nearly colorless, yellowing intensifies with age. The older central portion of the lens is yellower than the younger, more peripheral lens layers (Mellerio, 1987). This age-associated yellowing of the lens probably results from accummulated, UV-induced modifications of the lens structural proteins, or crystallins, and may have no adaptive value (Zigman, 1971). The chromophores that occur in the lenses of diurnal animals and in the aging lens have simple spectra with absorbances in the short-wavelength blue and near-UV region of the spectrum. A recent study of the spectroscopy, ontogeny, and biochemistry of lens pigmentation in deep-sea hatchetfishes (Family Sternoptychidae) revealed a completely different pattern of pigmentation from those patterns reported for the more common types of lens pigmentation (McFall-Ngai *et al.*, 1986). Lens pigmentation in the deep-sea hatchetfish has an abrupt, age-dependent onset. It begins when the fish is about 38 mm SL (maximum SL about = 90 mm), and is restricted

Received 8 August 1988; accepted 26 September 1988.

* Address all correspondence to M. McFall-Ngai, Department of Biological Sciences, University of Southern California, Los Angeles, California 90089-0371.

Table I

Mesopelagic fish[illegible]ed in the present study

Family	Species	Capture site	n	SL range (mm)	Orbit diameters (mm)	Lens diameters (mm)
Opisthopr[illegible]tidae	*Macropinna microstoma*	SCB[1]	6	37–140	6.3–18.5	3.7–10.7
	Dolichopteryx sp.	SCB	1	70	ND[3]	~2
Scopelarchidae	*Benthalbella dentata*	SCB	2	202, 218	7.9, 8.1	6.6, 6.8
	B. infans	PRT[2]	2	39, 55	2.0, 2.8	1.4, 2.0
	Scopelarchus sp.	SCB	1	121	10.4	5.7

[1] San Clemente Basin.
[2] Puerto Rican Trench.
[3] Not determined.

to the peripheral cells of the lens that are laid down after the 38 mm stage. Further, the chromophore has a complex spectrum resembling that of carotenoid pigments and is associated specifically with alpha crystallin. Thus, it cannot diffuse between the cells. The biological significance of the pigment is unclear, although it certainly affects the optical function of the lens as a component of the visual system.

We analyzed the biochemical and spectrophotometric properties of the lens pigmentation in two other fish families, the Opisthoproctidae and the Scopelarchidae, that also occur in the mesopelagic zone. Our results indicate that representative species of two families have patterns of lens pigmentation unlike not only the type described in diurnally active animals and the age-related lens coloration, but also unlike those of the deep-sea hatchetfish. These differing patterns suggest that the lens pigmentation is a character that has arisen independently a number of times among the mesopelagic fishes.

Materials and Methods

Animals

Fishes were collected in the Eastern Pacific from the San Clemente Basin (Southern California) during cruises of the RV Velero IV in February and July 1984 and August 1985, and from the Caribbean Sea in the Puerto Rican Trench during a cruise of the RV Knorr in December 1985. The methods of capture and handling of the fishes were as previously described (McFall-Ngai *et al.*, 1986). The species analyzed in the present paper are: (1) Family Opisthoproctidae, *Macropinna microstoma* Chapman and *Dolichopteryx* sp.; (2) Family Scopelarchidae, *Benthalbella dentata* (Chapman), *B. infans* Zugmayer, and *Scopelarchus* sp. (Table I). All specimens were adults except those of *B. infans*, which were translucent larval fish. The lenses were removed through a superficial cut made around the edge of the cornea with a scalpel.

To compare the pigmentation patterns of these species with those of diurnally active animals and those with age-related lens pigmentation, we used lenses of *Spermophilus beecheyi*, the California ground squirrel, and normal human lenses, respectively. We obtained specimens of *S. beecheyi* from the laboratory of Dr. S. Fisher at the University of California, Santa Barbara; normal human lenses were from donors to the Jules Stein Eye Institute eye bank.

Spectral analyses of lenses and lens extracts

To determine the spectral characteristics of whole lenses, freshly dissected lenses were positioned in a quartz cuvette of 1-cm pathlength along the axis of the beam of a Shimadzu UV-160 spectrophotometer (for details, see McFall-Ngai *et al.*, 1986). Briefly, lenses were placed in holders that fit snuggly into the cuvette. The holders consisted of two pieces of black lucite with hemispherical depressions of various sizes to hold lenses of differing diameters. One-mm holes were drilled through the lucite at the center of the depressions to permit transmission of the beam. This configuration insured that the beam would go directly through the center of the lens. The lens was surrounded by fish ringer's solution to prevent optical aberrations. Spectral absorbances of a given whole lens were determined between 300 and 800 nm. The spectra of a given intact lens pair were then compared with extracts of the same lenses. One whole lens of each pair was homogenized and other lens was dissected into core and periphery, which were homogenized separately. Lens tissue was homogenized with a Wheaton tissue homogenizer in 50 m*M* sodium phosphate buffer (pH 7.4 at 20°C). The homogenate was spun at 4°C in 1.5 ml eppendorf tubes at 14,000 × *g* for 15 minutes in an Eppendorf 5414 tabletop centrifuge to pellet the insoluble material. The color of the pellet was noted and the spectrum of the supernatant fluid from each extract was determined between 300 and 800 nm. Lens extracts from

other specimens of the same species were frozen to determine the effect of freezing on the spectral characteristics.

During cruises in which a spectrophotometer was not available to measure whole lens spectra, lenses were removed from the eyes of specimens within one hour of trawl recovery, placed in vials with enough fish Ringers solution to cover them, and immediately frozen at −20°C. Within 1 to 2 weeks of collection, they were placed in a −80°C freezer until use. When analyzed, these lenses were thawed and extracted in the same manner as fresh lenses. The spectral absorbance of each supernatant fluid was determined from 300–800 nm using a Kontron Uvicon or a Shimadzu UV-160 spectrophotometer.

Biochemical analyses

Gel filtration of soluble extracts from frozen lens samples was performed at room temperature on a Pharmacia FPLC system with a Pharmacia HR-6 column in 20 m*M* Tris buffer with 0.1 *M* NaCl (pH 7.9 at 20°C) at a flow rate of 1 ml/min. The absorbance of each resulting fraction was determined between 300 and 800 nm on the Shimadzu UV-160. Samples in which the pigment occurred in the lowest molecular weight fraction resolved by the HR-6 column were subjected to further gel filtration on a Sephadex G-25 column (2.5 × 5 cm), at a flow rate of 1 ml/min with the same elution buffer as used on the FPLC HR-6 column. Fractions obtained by gel filtration were subjected to polyacrylamide gel electrophoresis in the presence of sodium dodecyl sulfate (SDS-PAGE) (Laemmli, 1970). Protein concentrations were determined spectrophotometrically using the difference in absorbance between 235 and 280 nm (Whittaker and Granum, 1980).

Results

General description of the visual system

All mesopelagic fish species analyzed in the present study have tubular, upwardly directed eyes. Such eyes, which are characteristic of certain families of fishes that occur in the lower portions of the mesopelagic zone (500–1000 m), are generally large relative to body size of the fish and have relatively large lenses, a much-reduced iris, and two photoreceptive areas—the ventral, main retina and the medial, accessory retina (Munk, 1966). Both visual and spectrophotometric analyses revealed yellow coloration in the lenses of *Macropinna microstoma*, *Benthalbella dentata*, and *B. infans*, but not in the lenses of *Dolichopteryx* sp. and *Scopelarchus* sp. Thus, not all tubular eyes have yellow lenses.

Table II

Peak wavelengths (λ_{max}) of the lens pigment of Macropinna microstoma *under different experimental conditions*

Specimen standard length (mm)	λ_{max} Intact lens	λ_{max} Lens total-soluble extract	λ_{max} Pigment-bearing gel filtration fraction
37	387	371	ND[1]
115	396	380	ND[1]
126	398	386	371

[1] Not determined.

Spectral characteristics of the lens pigments

Whole lenses. Macropinna microstoma was the only species with pigmented lenses that was obtained when a spectrophotometer was available for fresh whole lens spectral analyses. To determine whether the absorbance characteristics of the *M. microstoma* lens pigment changes during extraction, we compared the spectrum of an intact fresh lens to that of: (1) the total soluble lens extract and, (2) the partially purified pigment fraction of the total soluble extract, which had been obtained by gel filtration. Although the overall shapes of all of the spectra were the same, showing a single broad peak, this peak was shifted toward shorter wavelengths in the intact lenses of smaller specimens (Table II). In addition, the extracts and partially purified fractions of a given *M. microstoma* lens were also shifted several nanometers toward the shorter wavelengths relative to the intact lens spectrum of that same lens (Table II). Extracts and purified fractions that had been frozen had the same spectra as those that had not been frozen. Prolonged freezing did not affect pigment intensity or spectral quality.

Lens extracts

In the deep-sea fish and ground squirrel lenses, all the pigment was in the total soluble extract; the pellet of the insoluble lens material was white. However, in human lenses, because the pigment is associated with all proteins and these proteins gradually become insoluble with age, both pellet and supernatant fluid were a light yellow in older lenses.

The peak wavelengths of lens pigment absorbance, when corrected for scatter, were in the short-wavelength blue and long-wavelength ultraviolet portions of the spectrum in all fishes with yellow lenses (Fig. 1). The uncolored lenses of the opisthoproctid *Dolichopteryx* sp. and the scopelarchid *Scopelarchus* sp. showed no absorbance in these regions of the spectrum. In contrast to the complex, multipeaked spectrum of the hatchetfishes,

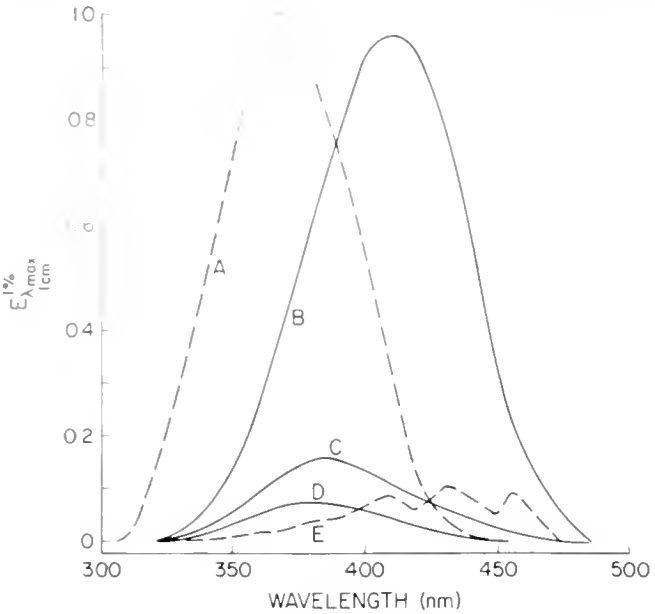

Figure 1. Comparison of the pigment intensity among the animals analyzed. A = *Spermophilus beecheyi*, B = *Benthalbella dentata*, C = *B. infans*, D = *Macropinna microstoma*, E = *Argyropelecus affinis*. Absorbances determined for a 1% solution of protein.

Argyropelecus ssp. (McFall-Ngai *et al.*, 1986), the absorbances of the lens pigments of *Benthalbella dentata*, *B. infans*, and, as mentioned above, *Macropinna microstoma* occur as single broad peaks, similar to that of the ground squirrel (Fig. 1). Although whole lenses of *Benthalbella* spp. were not available for spectral analysis, the whole lens extracts did not have a spectral peak markedly different from the purified fractions containing the chromophore. The age-related coloration of the human lens results in the elimination of wavelengths shorter than 350 nm. Because the scatter of the lens proteins themselves at this wavelength is so marked, no scatter-corrected pigment spectrum could be obtained for comparison.

Pigment distributions and intensities

The lenses of each species with yellow coloration were dissected to reveal pigment intensity in various layers of the lens. In the opisthoproctid, *Macropinna microstoma*, and the scopelarchid, *Benthalbella infans*, the pigment occurs in all layers of the lens. In contrast, in the scopelarchid, *B. dentata*, pigment is absent from portions of the lens core, or nucleus, measuring approximately 2.3–2.4 mm in diameter. In the 6.6 and 6.8 mm lenses of *B. dentata*, this unpigmented portion represents less than 5% of the total lens volume.

With the naked eye, *Benthalbella dentata* lens pigmentation appears more intense than that of either *B. infans* or *M. microstoma*. To quantify the intensity and compare it among the species with pigmented lenses, we determined the absorbance of the pigment at the peak wavelength for a 1% solution of the protein ($E^{1\%}_{\lambda max\ 1cm}$) (Table III). The intensity of the *B. dentata* lens pigment was similar to that of the ground squirrel, and was approximately 6–14 times stronger than that of the other mesopelagic fish lenses. The intensity differences can also be noted in the spectra (Fig. 1), when the spectra are normalized to protein concentration.

Biochemical analyses

The lenses of fishes are protein-rich tissues, about 50% of which is soluble protein with the remainder being mostly water (De Jong, 1981). Most of the soluble proteins are structural proteins called crystallins, which in fishes are of three primary types: alpha, beta, and gamma crystallins. In size exclusion chromatography (Fig. 2) of total soluble lens extracts, alpha crystallin, an 800 Kdal multimer, elutes first, followed by the beta crystallins, which are several oligomeric proteins ranging from approximately 50–150 Kdal. The gamma crystallins, monomers which average 20 Kdal, are the last proteins to elute. A non-protein, low molecular weight fraction appears last and includes absorbing materials around 1.5 Kdal, such as peptides and nucleic acids.

To determine whether the lens pigment is protein-associated in the opisthoproctid and scopelarchid species considered here, as in *Argyropelecus* spp. (McFall-Ngai *et al.*, 1986), we chromatographed the pigmented lenses, collected fractions, and measured the absorbances of the resultant fractions. Lenses of *Spermophilus beecheyi*, the pigment of which is known to be freely diffusable (*i.e.*, soluble but not associated with any protein species; Cooper and Robson, 1969a) were also chromatographed for comparison. The lens pigments of the opisthoproctid *Macropinna microstoma* and the scopelarchid *Benthalbella infans* eluted with the low molecular weight fraction in a similar manner to the lens pigment of *S. beecheyi*. Therefore, they were not protein associated in these fishes. In contrast, the lens pigment of *B. dentata* eluted with the gamma crystallin fraction (Fig. 2). SDS-PAGE of the pigment-containing fraction of *B. dentata* showed bands at an apparent molecular weight of approximately 20,000, characteristic of gamma crystallin, suggesting that the pigment is protein associated.

Discussion

The present study shows that the lens chromophores of the three species of mesopelagic fishes described herein differ in one or more of the following characteristics: (1) the appearance during ontogeny; (2) the biochemical as-

Table III

Spectral characteristics of three types of lens pigmentation

Class/type of lens pigmentation	Taxonomic affiliation	Species	λ_{max} of Chromophore	1% $E\lambda_{max}$ 1 cm
Deep-sea Teleosts	Order—Salmoniformes Family—Opisthoproctidae	*Macropinna microstoma* (70 mm SL)	377	.07
	Order—Aulopiformes Family—Scopelarchidae	*Benthalbella dentata* (202 mm SL)	412	.96
		Benthalbella infans (55 mm)	385	.16
	Order—Stomiiformes Family—Sternoptychidae	*Argyropelecus affinis*[1]	432	.10
Diurnal Species	Class—Mammalia Order—Rodentia	*Spermophilus beecheyi*	366	.99

[1] Strongest peak absorbance, McFall-Ngai *et al.* (1986).

sociation with a lens structural protein (crystallin); and, (3) the spectral quality.

The lens pigmentation pattern of one species, *Benthalbella dentata*, showed some similarities to the pattern previously described in the deep-sea hatchetfish, *Argyropelecus affinis* (McFall-Ngai *et al.*, 1986). Individuals of *A. affinis* smaller than 38 mm, with lenses ≤ 2.4 mm in diameter, had no lens pigment, while in those larger than 38 mm, newly synthesized, peripheral cells containing a chromophore bound to alpha crystallin surround the pigmentless core. Although small specimens of *B. dentata* were not available, the lenses of larger specimens also had a 2.4 mm core devoid of pigment. Furthermore, the pigment in the peripheral lens cells was bound to gamma crystallin, a molecule, like alpha crystallin, too large to traverse the cellular gap junctions. Thus, the characteristic distribution of lens pigment in *B. dentata* lenses suggests a similar ontogenic pattern to that of *A. affinis*. The presence of a colorless lens core and a chromophore bound to a crystallin are features of these two mesopelagic species not reported in any other pigmented eye lenses.

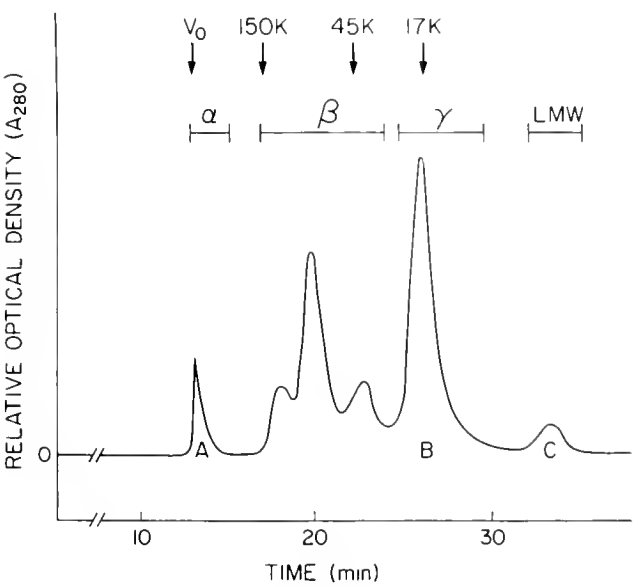

Figure 2. Typical gel filtration profile of fish lens crystallin proteins. The peak designated A, containing alpha crystallin, is the peak with which the chromophore of the *Argyropelecus affinis* lens elutes. The chromophore of *Benthalbella dentata* elutes with the gamma crystallins with the peak designated B. The chromophores of *B. infans* and *Macropinna microstoma* elute with the low molecular weight (LMW) fraction, designated C. The values across the top of the chromatogram [V_0 (void volume), 150K, 45K, and 17K] are molecular weight standards for the gel filtration column.

Our data suggest that the lens pigmentation of *B. infans*, for which only larval specimens were available, is ontogenetically and biochemically distinct from that described above for its congenor, *B. dentata*. In contrast with the unpigmented core of *B. dentata* lenses, the lenses of *B. infans* larvae, which were all 2.0 mm or less in diameter and destined to become the core of the adult lens, had an even distribution of pigment. These differences in lens pigmentation can only be reconciled within a single ontogenetic and biochemical pattern if, during the transition between larval and adult life, the pigment of *B. infans* is transported from the core to the periphery, and only there bound to gamma crystallin. In addition, the distinct spectra of the lens chromophores from these two species indicate either that the pigments are structurally distinct, or that the two species share a common pigment whose spectrum is altered in *B. dentata* by its association with the gamma crystallin.

Finally, the characteristics of lens coloration in the opistoproctid, *Macropinna microstoma*, were most like that of *Benthalbella infans*. In all specimens of *M. microstoma* the lens pigment was a freely diffusible molecular species that was evenly distributed throughout the lens. However, since no small specimens of the opistoproctid were available, we could not determine whether the pigment is produced continuously during lens growth (as appears to be the case for larval *B. infans*) or, alternatively, is synthesized late in lens development and diffuses into the previously unpigmented core regions. Regardless of the possible similarity of ontogenic appearance, the spectral characteristics of the lens chromophores of *M. microstoma* and *B. infans* suggest that the pigments are different.

The present study suggests that lens pigmentation has arisen a number of times in mesopelagic fishes. However, the biological function of such an adaptation remains unclear. Lens pigmentation does not correlate with the presence or absence of tubular eyes; *i.e.*, not all tubular eyes have yellow lenses (present study), while some yellow lenses occur in fishes with non-tubular eyes (Somiya, 1982). In addition, while the perception of intra- or interspecifically produced luminescence may be enhanced by the presence of yellow lenses in some species (Muntz, 1976), intraspecific communication as a function cannot be deduced from the occurrence of luminescence and lens pigmentation in the mesopelagic fishes studied thus far. For example, in *Benthalbella infans*, light organs are an adult character (Merrett *et al.*, 1973), but *B. dentata* and *Macropinna microstoma* have strong lens pigmentation and are not luminous. Furthermore, depending on the species, the lens may (Muntz, 1976) or may not (McFall-Ngai *et al.*, 1986) change the peak wavelength of visual pigment sensitivity. The only conclusion that can be made for all pigmented lenses of mesopelagic fishes is that the pigmented lens would filter out a portion of the downwelling light that impinges on the short-wavelength portion of the visual pigment curve. Thus, the function of the pigment may be similar to that suggested for the ground squirrel and other diurnal animals (Lythgoe, 1979)—to decrease chromatic aberration and increase acuity by the elimination of the higher energy wavelengths of the environment.

Acknowledgments

We thank E. G. Ruby for technical assistance during the cruises. We also thank R. Lavenberg of the Los Angeles County Museum of Natural History for identification of the fishes. We are grateful for discussions of the manuscript with E. G. Ruby and L. Holland. Special thanks are extended to the crews of the R/V Velero IV and the R/V Knorr for their assistance in collecting specimens. This work was supported by NIH grant EY 5905 to M. McFall-Ngai and NIH EY 3897 to J. Horwitz. The R/V Velero cruises were supported by NSF grants OCE 81 101 54 and OCE 85 002 37 to J. J. Childress, and the R/V Knorr cruise was supported by NSF grant OCE 84 162 06 to H. W. Jannasch of Woods Hole Oceanographic Institution.

Literature Cited

Cooper, G. F., and J. G. Robson. 1969a. The yellow colour of the lens of the grey squirrel. *J. Physiol.* **203:** 403–410.

Cooper, G. F., and J. G. Robson. 1969b. The yellow color of the lens of man and other primates. *J. Physiol.* **203:** 411–417.

De Jong, W. W. 1981. Evolution of lens and crystallins. Pp. 221–278 in *Molecular and Cellular Biology of the Eye Lens*, H. Bloemendal, ed. John Wiley and Sons, New York.

Heinermann, P. H. 1984. Yellow intraocular filters in fishes. *Exp. Biol.* **43:** 127–147.

Laemmli, U. K. 1970. Cleavage of structural proteins during the assembly of the head of bacterial phage T4. *Nature* **227:** 680–685.

Lythgoe, J. N. 1979. *The Ecology of Vision.* Clarendon Press, Oxford. xii + 244 pp.

McFall-Ngai, M., F. Crescitelli, J. Childress, and J. Horwitz. 1986. Patterns of pigmentation in the eye lens of the deep-sea hatchetfish, *Argyropelecus affinis* Garman. *J. Comp. Physiol. A.* **159:** 791–800.

Mellerio, J. 1987. Yellowing of the human lens: nuclear and cortical contributions. *Vis. Res.* **27:** 1581–1587.

Merrett, N. R., J. Badcock, and P. J. Herring. 1973. The status of *Benthalbella infans* (Pisces:Myctophoidei), its development bioluminescence, general biology and distribution in the eastern North Atlantic. *J. Zool. Lond.* **170:** 1–48.

Muntz, W. R. A. 1972. Inert absorbing and reflecting pigments. Pp. 529–565 in *Photochemistry of Vision. Handbook of Sensory Physiology, Vol. VII, 1*, H. J. A. Dartnell, ed. Springer, Berlin.

Muntz, W. R. A. 1974. The visual consequences of yellow filtering pigments in the eyes of fishes occupying different habitats. Pp. 271–287 in *Light as an Ecological Factor, Vol. II*, G. C. Evans, R. Bainbridge, and O. Rockham, eds. Blackwell Scientific, Oxford.

Muntz, W. R. A. 1976. On yellow lenses in mesopelagic animals. *J. Mar. Biol. Assoc. U. K.* **56:** 963–976.

Munk, O. 1966. Ocular anatomy of some deep-sea teleosts. *Dana Rep.* **70:** 1–62.

Somiya, H. 1982. 'Yellow lens' eyes of the stomiatoid deep-sea fish, *Malacosteus niger*. *Proc. R. Soc. Lond. B* **215:** 481–489.

Villermet, G. M., and R. A. Weale. 1972. Age, the crystallin lens of the rudd and visual pigments. *Nature* **238:** 345–346.

Walls, G. L., and H. D. Judd. 1933. The intra-ocular colour filters of vertebrates. *Brit. J. Ophthalmol.* **17:** 641–675.

Whittaker, J. R., and P. E. Granum. 1980. An absolute method for protein determination based on difference in absorbance at 235 and 280 nm. *Anal. Biochem.* **109:** 156–159.

Zigman, S. 1971. Eye lens color: formation and function. *Science* **171:** 807–809.

Reference: *Biol. Bull.* **175:** 403–409. (December, 1988)

Nitrogen Waste or Nitrogen Source? Urate Degradation in the Renal Sac of Molgulid Tunicates

MARY BETH SAFFO

Institute of Marine Sciences, University of California, Santa Cruz, CA 95064

Abstract. Two urate-producing ascidians, *Molgula manhattensis* and *M. occidentalis*, were tested for urate oxidase activity. Microradioassays were carried out on the wall and lumen fluid of the urate-containing, molgulid renal sac, on the renal sac endosymbiont *Nephromyces*, and on non-renal sac molgulid tissue. These assays indicate that urate is degraded enzymatically in the renal sac. However, this uricolytic activity is concentrated in *Nephromyces*, rather than in host renal sac tissue.

Thus, the urate "waste" of *Nephromyces*-infected *Molgula* is not stored permanently in the concretions in the renal sac lumen. Since molgulids are universally infected by *Nephromyces* in nature, renal sac function should be reassessed with attention to urate as a nitrogen source as well as a nitrogenous catabolite.

Introduction

The organs of many invertebrate animals have been named before their biological roles were well understood. This is especially true of invertebrate "renal" or "excretory" organs, whose names often reflect surmised, rather than demonstrated, functions (Barrington, 1979). Further, their convergent names mask the diversity of these structures among invertebrates, as well as the dissimilarities of these organs from vertebrate kidneys.

Several invertebrate organs have been assigned an excretory function largely because they contain nitrogenous catabolites which have been identified as excretory products in vertebrate kidneys. If such catabolites are present, need they be destined for excretion? Need they be "waste," whatever the structural, physiological, or ecological context of their production?

Tunicates (Urochordata) possess a number of so-called "renal" tissues (Berrill, 1950; Goodbody, 1974). The functions of these structures are not well understood, despite their functionally evocative names. Because a well-known nitrogenous catabolite, uric acid, has been found in the solid deposits ("concretions") of many of the renal tissues of ascidian tunicates (Azéma, 1928, 1937; Goodbody, 1965; Nolfi, 1970; Sabbadin and Tontodonati, 1967; Saffo, 1977), they often have been assumed to have an excretory function. But many of the features of these tissues seem at odds with such a function. The large renal sac of molgulid ascidians presents a particularly conspicuous puzzle.

First, as a major "excretory" product, uric acid is an unexpected nitrogenous catabolite for these low intertidal or subtidal animals, though evidence (Nolfi, 1970) for an exclusively purine origin for urate in the renal sac of *Molgula manhattensis* may diminish the energetic paradox posed by such a habit.

Second, the renal sac has no ducts or openings at any stage in its development (Saffo, 1978), leading earlier workers (Lacaze-Duthiers, 1874; Das, 1948) to the notion that the renal sac "excretes" urate waste by storing it rather than eliminating it.

Finally, a symbiotic fungus-like protist, *Nephromyces*, inhabits the renal sac lumen of all adult individuals of at least seven molgulid species (6 species of *Molgula*, 1 of *Bostrichobranchus:* Saffo, 1982, and unpub. data on *M. robusta*); earlier observations (Giard, 1888; Buchner, 1930, 1965) cite its presence as well in the renal sac of many other molgulid species. *Nephromyces* is usually present in large numbers in its hosts, especially in adults, with greatest densities typically in the immediate vicinity of the urate-containing, renal sac concretions.

Symbiotic (including parasitic) infection is unusual for excretory organs generally (Hochberg, 1982), and it remains undetected among "renal" tissues of non-molgulid ascidian families (Saffo, unpub. obs. on Ascidiidae and Corellidae).

Received 21 December 1987; accepted 18 August 1988.

Symbiotic infection is frequently associated with *extrarenal* urate deposits among invertebrates (Buchner, 1965). The guts of termites (Potrikus and Breznak, 1980, 1981; Breznak, 1982) and possibly anobiid beetles (Jurzitza, 1978) and the fat body of cockroaches (Mullins and Cochran, 1975a, b; Downer, 1982; Mullins, 1982); the parenchyma of the acoel flatworm *Convoluta* (Douglas, 1983); and the "concrement gland" of terrestrial prosobranch snails (Meyer 1925) all harbor endosymbionts in association with urate deposits. For each of these cases, it has been either suggested or shown that endosymbionts utilize the urate deposits of the host. Even without the involvement of symbionts, extrarenal urate might be neither permanently deposited nor excretory in function (Dresel and Moyle, 1950; Berridge, 1965; Duerr 1967, 1968; Gifford, 1968; Mullins and Cochran, 1975 a, b; Cochran, 1979; Buckner, 1982; Wolcott and Wolcott, 1984). Might *Nephromyces* also use the urate deposits of its host? Might urate be only a transient deposit in *Molgula*?

Goodbody (1965) searched for uricase activity in several ascidians. Using spectrophotometric assays, he found evidence for uricase in only a single ascidian, the styelid *Polycarpa obtecta*, despite examination of a number of ascidians, including *Molgula manhattensis*. However, Goodbody noted "the difficulties of proving a negative result," a problem underscored by the limited sensitivity of spectrophotometric methods for assay of uricase, and of the inclusiveness ("whole animals and portions of the tissues") of his samples.

Using more sensitive radioisotope methods and finer sample partitioning, I have re-investigated the possibility of urate degradation in *Molgula manhattensis* and *Molgula occidentalis*. I have assayed for urate oxidase activity in non-renal sac tissue of *Molgula*, and in both host (*Molgula*) and symbiont (*Nephromyces*) components of the renal sac wall and lumen.

Materials and Methods

Samples were assayed for urate oxidase (uricase; urate: oxygen oxidoreductase, E.C.1.7.3.3) activity with radioisotope methods modified from Friedman *et al.* (Friedman and Merril, 1973; Friedman and Johnson, 1977; Friedman *et al.*, 1985).

Assay method A provided preliminary estimates of uricolytic activity, (Table I) for later comparison with the definitive data (Table II) provided by method B. Method A was also used to compare the R_f values of degradation products of tissue samples with those of commercial urate oxidase. Individual tissue aliquots were incubated 20 to 40 minutes at room temperature (20–22°C) with 2-^{14}C-uric acid (Amersham, 50–51 mCi/mmole) dissolved in 0.03 *M* sodium borate buffer (pH 9.4; Truscoe, 1968). Reaction mixtures consisted of: 1 volume (3–10 μl) sample (buffer, enzyme, cell-free fluid or homogenized cell suspension); 1 volume 0.0010, 0.0012, or 0.0020 *M* ^{14}C-urate in pH 9.4 borate buffer; 2 volumes double-deionized water. Successive aliquots of the reaction mixture were spotted onto a cellulosic thinlayer chromatographic plate, which was developed for 90–120 minutes (to a distance of 14–17 cm) in 0.15 *M* NaCl: 95% ethanol (4:1) (Friedman and Merril, 1973). Each lane of the chromatogram was cut into 1 cm segments, which were assayed for the distribution of [^{14}C] with a liquid scintillation counter.

Assay method B was similar in general design to method A, except for modifications designed to minimize reagent and sample impurities, to maximize enzyme yield from tissue extracts, to standardize assay conditions, and to enable calculation of specific activities. ^{14}C-uric acid (Amersham; 51 mCi/mole) was purified chromatographically before assay to minimize the amount of ^{14}C-allantoin initially present in the urate reagent. Aliquots of the purified urate were resuspended in ultrapure (Milli-Q) water, titrated to pH 9.4 with NaOH, and kept at −70°C until use. Tissues were homogenized at 0°C in a pH 9.1 buffer containing 11.0 m*M* borate, 1.4 m*M* EDTA, and 0.18% Triton X-100 made up with Milli-Q water. To assess specific activity of urate oxidase, a small (2–10) μl aliquot of each tissue homogenate was analyzed for protein content using the method of Bradford (1976; Pierce Chemical Company). The major (15 μl) portion of tissue homogenate was added to 5.9×10^{-6} moles (10–18 μl) of purified ^{14}C-urate, and the resulting reaction mixture incubated at 26°C. Formation of ^{14}C-allantoin (or other reaction products) in these mixtures, and degradation of ^{14}C-urate, were followed for 20 to 40 minutes, using chromatographic methods described for method A.

Enzyme activity detected by method B was calculated from the greatest reaction rate (usually, but not always, the initial rate) observed during the first twenty minutes of incubation. Two measures of activity were calculated: μmoles reaction product/mg prot/min (specific activity) and μmoles reaction product/15 μl volume/min. Though specific activity was the preferred means of expressing activity, activity/volume/min was also included to better compare the significance of enzyme activity in two different sorts of samples: largely acellular fluid (centrifuged renal sac fluid) and tissue homogenates.

Two field-collected molgulid species were assayed for uricolytic activity: *Molgula occidentalis* from Alligator Harbor, on the Gulf Coast of Florida (Gulf Specimen Co., Panacea, Florida), and *Molgula manhattensis* from Woods Hole, MA; Stone Harbor, NJ; and San Francisco Bay, CA. As expected from earlier work (Saffo, 1982), all these field-grown *Molgula* individuals were infected with *Nephromyces*. Animals were maintained in running sea-

water or aerated aquaria and used in assays within a week after collection.

Parallel, laboratory-grown populations of *Nephromyces*-infected and *Nephromyces*-free *Molgula manhattensis* were also assayed to assess directly the impact of *Nephromyces* on urate metabolism in *Molgula*. These lab animals were raised in 0.5 μm-filtered seawater, using methods described previously (Saffo and Davis, 1982).

Several tissue types were analyzed. Each tissue was freshly dissected, or dissected and then frozen at −20°C for one hour and thawed at room temperature, just before use. Single tissue types from one to several (2–11 see Table II) animals were pooled for enzymatic assay. For each laboratory-raised animal, an aliquot of uncentrifuged renal sac fluid was examined by phase contrast microscopy at 400× to confirm the presence or absence of *Nephromyces* from *Nephromyces*-inoculated and uninoculated populations, respectively.

Renal sac samples were of four sorts: (1) fluid from the renal sac lumen, centrifuged 10 (method A) or 15 (method B) minutes at 1000 × *g* to remove suspended cells (which account for a substantial fraction of renal sac fluid volume in *Nephromyces*-infected *Molgula*), (2) *Nephromyces*, removed manually in *M. occidentalis* or collected as a pellet from centrifuged renal sac fluid in symbiont-infected *M. manhattensis*, (3) combined *Nephromyces*-fluid samples, using uncentrifuged renal sac fluid from infected *Molgula* (4) renal sac wall (host tissue: the layer of molgulid cells bounding the renal sac lumen, along with surrounding heart tissue) rinsed in sterile seawater or borate buffer to remove as much renal sac fluid and *Nephromyces* residue as possible and then homogenized in buffer.

Because of the minute volume of each sample, most samples could be assayed only once. Thus, each of the enzyme assays of a particular sort of tissue was carried out on material isolated from a different animal source.

Four other samples, serving as comparative controls, were spotted onto TLC plates and assayed for ^{14}C, with the first three followed over a time course similar to that of the tissue samples. (1) The neural gland complex and adjacent mantle tissue of *Molgula* provided molgulid, non-renal sac tissue. (2) A 6 mg/ml suspension of urate oxidase (Sigma Chemical Co., Type V, porcine liver: about 20 activity units/g protein) in borate buffer compared activity of purified urate oxidase with that of tissue samples. (3) ^{14}C-urate in borate buffer identified the extent of endogenous ^{14}C-allantoin impurity in the labeled uric acid substrate, as well as the rates of spontaneous, non-enzymatic degradation of ^{14}C-urate at alkaline pH (Friedman and Merril, 1973; Antia and Landymore, 1974). (4) Parallel TLC separations of unlabeled 0.01 *M* urate, 0.02 *M* allantoin, and 0.02 *M* urea, dissolved in borate buffer, assisted chromatographic localization of substrate and putative degradation products and provided non-isotopic controls for scintillation counting. Unlabeled uric acid was detected by absorption in ultraviolet light; unlabeled allantoin and urea were detected by the production of yellow color with Ehrlich reagent (4-Dimethylaminobenzaldehyde HCl; Sigma Chemical).

Results

Tables I and II provide clear evidence of enzyme-catalyzed uricolysis in *Nephromyces*-infected *Molgula occidentalis* and *Molgula manhattensis*. This activity is not distributed evenly throughout all molgulid tissues, or even throughout the entire renal sac. Rather, it is concentrated in *Nephromyces* cells.

Identity of uricolytic products

With an NaCl-95% ethanol solvent, the R_f of the peak of uricolytic product (Fig. 1) in the renal sac was quite similar to that of urate oxidase controls. Over two qualitative assays (Method A) and all time points (0, 3, 10, 20, 40 minutes), the urate oxidase-catalyzed reaction product (presumptive allantoin) showed a single [^{14}C] peak at R_f values of .82–.87. In 13 parallel assays, the [^{14}C] maximum of the *Nephromyces*-catalyzed reaction product peak showed an R_f value of 0.79–.87. R_f values for urate oxidase-catalyzed product in quantitative assays (Method B) ranged from .78–.81; those for *Nephromyces*-catalyzed product peak ranged from .75–.80.

In Method A, the R_f of ^{14}C-urate in borate buffer ranged from .43–.45. That of ^{14}C-urate incubated with tissue homogenates ranged from .40–.45. In Method B, the R_f of ^{14}C-urate in borate buffer was .41–.43. That of ^{14}C-urate incubated with tissue homogenates was .41–.44.

TLC separations of nonisotopic controls yielded R_f values of: 0.45–0.49 (urate), 0.80–.84 (allantoin), and 0.86–.90 (urea). TLC separations of unlabeled renal sac fluid yielded numerous UV-absorbent and UV-fluorescent compounds, of a wide range of R_f values. Though some of these compounds (those spanning R_f ranges of .75–.87) overlapped allantoin and urea in mobility, they did not react with Ehrlich's reagent.

Localization of uricolytic activity: assay method A (preliminary assays)

Results from method A were more variable than those from method B. Major complicating factors included variability in solubilization rates of the ^{14}C-urate substrate, and variability in effectiveness of physical methods for tissue homogenization from sample to sample. Nevertheless, enzymatic activity detected by these assays

Table I

Urate oxidase activity — Assay method A

Enzyme source	# Assays	Δ Product-cpm minute⁻¹sample⁻¹ (standard error)	% Individual assays showing uricolytic activity[a]
Controls			
Buffer	9	56 (±63)	0
Urate oxidase (porcine liver)	2	2,355 (±455)	100
Uninfected *Molgula manhattensis* (lab[c])			
Non renal sac	2	0	0
Renal sac wall	2	0	0
Renal sac fluid # 1	1	0	0
Renal sac fluid #2	1	156	—
Infected *Molgula manhattensis* (field[b] and lab[c])			
Non renal sac (field)	1	0	0
Non renal sac	5	0	0
Renal sac wall (field)	1	0.2	0
Renal sac wall	4	122 (±167)	50
Renal sac fluid (field)	1	34	0
Renal sac fluid #1	2	354 (±78)	100
Renal sac fluid #2	2	2,518 (±1036)	100
Nephromyces (field)	2	1,585 (±1648)	100
Nephromyces #1	2	576 (±517)	100
Nephromyces #2	2	25,894 (±7422)	100
Nephromyces (with fluid) (field)	4	989 (±540)	100
Nephromyces (with fluid)	2	2,110 (±1115)	100
Infected *Molgula occidentalis* (field)[b]			
Renal sac wall	1	0	0
Renal sac fluid	1	539	100
Nephromyces	1	772	100
Nephromyces (with fluid)	1	5,022	100

[a] % Individual assays with Δ product-cpm/min > parallel buffer control.

[b] Field-collected animals.

[c] Laboratory-raised animals.

indicated that urate oxidase activity was concentrated in *Nephromyces*.

Among samples from *Nephromyces*-infected *M. manhattensis* and *M. occidentalis*, all samples of *Nephromyces* cells showed high uricolytic activity. Uricolytic activity was also detected in five of six renal sac fluid samples, though activity per sample volume was always lower than that of parallel *Nephromyces* samples. Of host tissue, only two of six samples of renal sac wall, and no sample of nonrenal sac tissue, showed uricolytic activity.

In general, tissue samples from uninfected *M. manhattensis* showed no uricolytic activity. In the single possible exception to this pattern, one of the two uninfected renal sac fluid samples (renal sac fluid #2, Table I) assayed showed a rise in ^{14}C-product levels 1.2 times greater than that of the parallel buffer control, but only 0.75% and 7.7% that of parallel *Nephromyces* samples (*Nephromyces* #2) and of urate oxidase controls, respectively. Further, levels of ^{14}C-urate substrate fluctuated throughout incubation. Thus, the evidence for urate oxidase activity is ambiguous in this apparently aberrant assay.

Assay method B

Of seven samples of non-renal sac tissue, renal sac wall, and renal sac fluid assayed from uninfected *M. manhattensis* (see Table I), six showed no uricolytic activity. The seventh (one of two renal sac wall samples) showed miniscule urate oxidase activity: an increase in ^{14}C-product of only 60 dpm after 20 minutes' incubation, or about 10^{-3} the specific activity of commercially purified urate oxidase.

Even *Nephromyces*-infected *M. manhattensis* showed no consistent evidence for urate oxidase activity in host tissue. No urate oxidase activity at all was detected in non-renal sac tissues of infected *M. manhattensis*. Three samples of renal sac wall also showed no uricolytic activity, while one showed low activity (10^{-2} that of the urate oxidase control). Two samples of renal sac fluid showed no uricolytic activity, one showed low activity, and a fourth sample showed low uricolytic activity per sample volume, but high specific activity.

In contrast to the absent or spotty urate oxidase activity detected in *Molgula* tissue, all *Nephromyces* samples from *M. manhattensis* showed substantial urate oxidase activity, comparable to or even exceeding the specific activity of commercial urate oxidase.

Distribution patterns of urate oxidase activity in *Nephromyces*-infected *M. occidentalis* resembled those found in *Nephromyces*-infected *M. manhattensis*. Urate oxidase activity was absent in non-renal sac tissue and in one sample of renal sac wall. A second sample of renal sac wall, with small *Nephromyces* clumps adhering after rinsing, showed low urate oxidase activity, about a tenth that of commercial urate oxidase controls. Both samples of renal sac fluid showed relatively low urate oxidase activity per sample volume, but very high inferred or calculated specific activities. All *Nephromyces* samples showed very high specific activities for urate oxidase, either comparable to, or even far exceeding, those of the urate oxidase control.

Urate oxidase activity varied among *Nephromyces* samples from different sources of *Molgula*. The specific activities of urate oxidase measured from field-collected *M. manhattensis* (713–1567 μmoles/min/mg protein) were less than those from either laboratory-raised *M. manhattensis* (4800–6245 μmoles/min/mg) or *M. occidentalis* (4,103–23,696 μmoles/min/mg).

Table II

Urate oxidase activity: assay method B

Enzyme source	# Animals pooled per assay	# Assays (n)	Mean μmoles/min × 10^8 (standard error)	Specific activity: mean μmoles/mg prot/min × 10^5 (standard error)	% Assays with uricolytic activity[a]
Controls					
Buffer	—	3	0	0	0
Urate oxidase (porcine liver)					
0–2 mins	—	1	12,950	4,788	100
2–20 mins	—	1	1,310	490	100
Uninfected *Molgula manhattensis* (lab[c])					
Non renal sac	3–4	2	0 (0)	0 (0)	0
Renal sac fluid	5	2	1.35 (±1.35)	0.55 (±0.55)	0
Renal sac fluid	3–6	3	0 (0)	0 (0)	0
Infected *Molgula manhattensis* (field[b] and lab[c])					
Non renal sac (field and lab)	2–4	3	0 (0)	0 (0)	0
Renal sac wall					
field	2	2	0 (0)	0 (0)	0
lab	4	2	17 (±17)	15 (±15)	50
Renal sac fluid					
field	3	2	9 (±9)	18.5 (±18.5)	50
lab	4–11	2	76 (±76)	2,235 (±2235)	50
Nephromyces					
field	3	2	2,655 (±1761)	1,140 (±604)	100
lab	4–11	3	3,909 (±4256)	5,411 (±748)	100
Molgula occidentalis (field[b])					
Non renal sac	2	1	0	0	0
Renal sac wall[d]	1	2	115 (±115)	115 (±115)	50[d]
Renal sac fluid	1	2	511 (±485)	34,160[+e]	100
Nephromyces	1	3	7,518 (±3212)	14,116 (±9803)	100

[a] % of individual assays showing specific activity >0.
[b] Field-collected animals.
[c] Laboratory-raised animals.
[d] Clumps of *Nephromyces* adhering to wall in the sample showing uricolytic activity.
[e] Protein not detectable in one sample.

Discussion

The data presented in this report indicate that enzymatically catalyzed uricolysis takes place within the renal sac of *Molgula*. They further suggest that uricolytic activity is localized virtually exclusively within the renal sac symbiont, *Nephromyces*, rather than in host tissue. Indeed, the spotty presence of uricolytic activity in *Nephromyces*-infected molgulid tissue, coupled with the general absence of such activity in symbiont-free molgulid tissues, suggests that uricolytic activity detected in host tissue is not endogenous to *Molgula*, but rather arises largely or exclusively from *Nephromyces* contaminants.

Among symbiont-free molgulid tissue samples assayed by method B, no tissues except a single sample of renal sac wall showed any trace of urate oxidase activity. By comparison with urate oxidase controls, with *Nephromyces*, and with other organisms, the activity of even this sample is essentially zero: its value is smaller even than the urate oxidase activity detected in liver and kidney tissue of uricotelic animals (Saffo, 1989; in prep.; Scott *et al.*, 1969).

The low uricolytic activity detected in a small fraction of renal sac wall samples from infected *Molgula* seems best explained as the result of *Nephromyces* remnants occasionally remaining (in one case, visibly so) on the renal sac wall surface after rinsing.

By similar reasoning, uricolytic activity detected in several samples of renal sac fluid of infected animals must result, in some sense, from contamination by *Ne-*

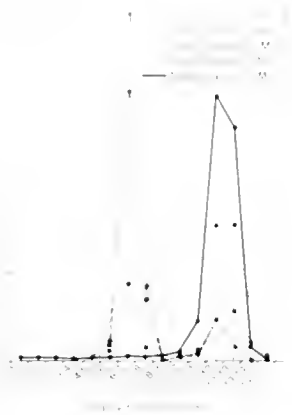

Figure 1. Incubation of ^{14}C urate with *Nephromyces*-renal sac fluid homogenate from field-collected *Molgula occidentalis*, compared with ^{14}C-urate incubated with commercial urate oxidase (assay method A). Distribution of radioactivity (measured as cpm) on thinlayer chromatogram after 0 and 20 minutes' incubation. Urate peak is 6–7 cm from origin; degradation product peak (allantoin) is 11–13 cm from origin.

phromyces. *Nephromyces* could give rise to uricolytic activity in the renal sac fluid in three possible ways. First, the symbiont might induce *Molgula* to produce uricolytic enzymes and to secrete them from the renal sac wall into the renal sac lumen. Since most renal sac wall samples lack detectable enzymatic uricolytic activity, this possibility seems unlikely. A second possibility is that the funguslike trophic stages of *Nephromyces* secrete degradative enzymes extracellularly, into the renal sac fluid, or that enzymatic contents of *Nephromyces* cells might be released naturally into the renal sac fluid as individual symbiont cells die. This possibility does not explain, however, the *absence* of urate oxidase activity from several samples of renal sac fluid drawn from infected *M. manhattensis*. Third, uricolysis in renal sac fluid could be an artifact of centrifugation: that is, the supernatant fluid could still contain intact cells of *Nephromyces* after centrifugation, or the *Nephromyces* cells could have lysed during centrifugation. The two nonuricolytic renal sac fluid samples from infected *M. manhattensis* would thus represent the only samples of renal sac fluid free of cells or cell contents. The discrepancy in these fluid samples, between uricolytic activity per volume (always low) and specific activity (much higher), is further suggestive of contamination of these samples with a small amount of protein.

The similarities between R_f values of urate degradation products resulting from catalysis by commercial urate oxidase and those catalyzed by *Nephromyces* are consistent with the notion that *Nephromyces* produces allantoin from urate—that is, that urate degradation in *Nephromyces* is catalyzed by urate oxidase. This need not mean that allantoin is the final product of urate degradation in *Nephromyces*. The apparent absence of allantoin from HPLC separations of renal sac fluid (Saffo, unpub.) underscores the possibility that allantoin may be only a transitional product of urate degradation in the renal sac.

The chromatographic data also leave open the possibility that additional compounds are produced from urate degradation. The NaCl-95% ethanol TLC solvent, used here because it yields widely different R_f values for urate and allantoin, does not separate allantoin distinctly from other, more polar compounds. For example, urea is only slightly more mobile than allantoin, yielding closely abutting allantoin and urea spots in TLC separations of allantoin-urea mixtures. Further, several compounds in the renal sac fluid overlap allantoin in mobility. Thus, the ^{14}C products of urate degradation seen in *Nephromyces* extracts might include urea or other compounds, in addition to allantoin.

Whatever may be the particular pathways of urate degradation in the renal sac, the general lesson remains clear. In *Nephromyces*-infected *Molgula*—that is, in *Molgula* in nature—urate is *not* a permanent deposit in the renal sac. Thus, uric acid cannot serve as a *permanent* repository for waste nitrogen in the renal sac. The role of urate production and of renal sac function in *Molgula* must be re-examined.

The high rates of uricolysis in *Nephromyces* and the symbiont's high densities in adult molgulids suggest that *Nephromyces* makes an important contribution to the function of the renal sac. Because of *Nephromyces'* widespread, probably universal, infection rate among adult *Molgula*, the metabolic activities of the symbiont and their specific effects on the physiology of *Molgula* merit careful scrutiny.

The present data suggest one aspect of *Nephromyces'* metabolism that is worth particular attention. For *Nephromyces*, renal sac urate is not nitrogen waste, but rather a potential *source* of carbon and nitrogen. Especially if the *Nephromyces*-molgulid symbiosis benefits the molgulid hosts (Saffo, 1984, 1986), could urate serve ultimately (albeit indirectly) as a nitrogen source for *Molgula*, as well as for *Nephromyces*? I am currently pursuing such views, tracing the fate of *Nephromyces* metabolites in and beyond the renal sac, determining whether carbon and nitrogen from urate degradation by *Nephromyces* is reincorporated by *Molgula*, and investigating the long-term consequences of *Nephromyces'* activities for the general biology of *Molgula*.

Acknowledgments

I thank Kristina Williams; Elizabeth Carter; D. Bradfute; D. Felix; J. Margolis; P. Sinnis; L. Stathoplos; and J. Whitbeck for experimental assistance; J. Wardrip and A. Whelan for graphics; and A. T. Newberry, W. B. Watt and an anonymous reviewer for editorial advice. Sup-

ported by grants from the Research Corporation; the American Philosophical Society; the Whitehall Foundation; and the National Science Foundation (PCM 84-10107 and DCB 85-40400), and by the Institute of Marine Sciences, UC Santa Cruz. Contribution No. 281 of the Tallahassee, Sopchoppy and Gulf Coast Marine Biological Association.

Literature Cited

Azéma, M. 1928. Quelques aspects de l'excrétion chez les Ascidies. *Bull. Assoc. Anat* **23:** 14–25.

Azéma, M. 1937. Le sang et l'excrétion chez les Ascidies. *Ann. Inst Ocean. Monaco* **17:** 1–150.

Barrington, E. J. W. 1979. *Invertebrate Structure and Function* Second Edition. John Wiley, New York. 765 pp.

Berridge, M. J. 1965. The physiology of excretion in the cotton stainer, *Dysdercus fasciatus* Signoret. *J. Exp. Biol.* **43:** 535–552.

Berrill, N. J. 1950. *The Tunicata* Ray Society, London. 354 pp.

Bradford, M. M. 1976. A rapid and sensitive method for the quantitation of microgram quantities of protein utilizing the principle of protein-dye binding. *Anal. Biochem* **72:** 248–254.

Breznak, J. A. 1982. Intestinal microbiota of termites and other xylophagous insects. *Annu. Rev. Microbiol.* **36:** 323–343.

Buchner, P. 1930. *Tier und Pflanze in Symbiose* Second Edition. Borntraeger, Berlin. Pp. 749–753.

Buchner, P. 1965. *Endosymbiosis of Animals with Plant Microorganisms.* Wiley-Interscience, New York. 909 pp.

Buckner, J. S. 1982. Hormonal control of uric acid storage in the fat body during last larval instar of *Manduca sexta. J. Insect Physiol* **28:** 987–994.

Cochran, D. G. 1979. Uric acid accumulation in young American cockroach nymphs. *Entomol. Exp. Appl* **25:** 153–157.

Das, S. M. 1948. The physiology of excretion in *Molgula* (Tunicata, Ascidiacea). *Biol. Bull* **95:** 307–319.

Douglas, A. E. 1983. Uric acid utilization in *Platymonas convolutae* and symbiotic *Convoluta roscoffensis. J. Mar. Biol. Assoc. (UK)* **63:** 435–447.

Downer, R. G. H. 1982. Fat body and metabolism. Pages 151–174 in *The American Cockroach,* W. J. Bell and K. G. Adiyodi, eds. Chapman and Hall, New York.

Dresel, E. I. B., and V. Moyle. 1950. Nitrogenous excretion of amphipods and isopods. *J. Exp. Biol* **27:** 210–225.

Duerr, F. 1967. The uric acid content of several species of prosobranch and pulmonate snails as related to nitrogen excretion. *Comp. Biochem. Physiol.* **22:** 333–340.

Duerr, F. 1968. Excretion of ammonia and urea in seven species of marine prosobranch snails. *Comp. Biochem. Physiol.* **26:** 1051–1059.

Friedman, T. B., and D. H. Johnson. 1977. Temporal control and urate oxidase activity in *Drosophila.* evidence of an autonomous timer in Malpighian tubules. *Science* **197:** 477–479.

Friedman, T. B., and C. R. Merril. 1973. A microradiochemical assay for urate oxidase. *Anal. Biochem* **55:** 292–296.

Friedman, T. B., G. E. Polanco, J. C. Appold, and J. E. Mayle. 1985. On the loss of uricolytic activity during primate evolution—I. Silencing of urate oxidase in a hominoid ancestor. *Comp Biochem. Physiol.* **81B:** 653–659.

Giard, A. 1888. Sur les *Nephromyces,* genre nouveau de champignons parasites du rein des Molgulidées. *C. R. Acad. Sci. (Paris)* **106:** 1180–1182.

Gifford, C. A. 1968. Accumulation of uric acid in the land crab, *Cardisoma guanhomi. Am. Zool.* **8:** 521–528.

Goodbody, I. 1965. Nitrogen excretion in Ascidiacea. II. Storage excretion and the uricolytic enzyme system. *J. Exp. Biol.* **42:** 299–305.

Goodbody, I. 1974. The physiology of ascidians. *Adv. Mar. Biol.* **12:** 1–149.

Hochberg, F. G. 1982. The "kidneys" of cephalopods: a unique habitat for parasites. *Malacologia* **23:** 121–134.

Jurzitza, G. 1979. The fungi symbiotic with anobiid beetles. Pp. 65–76 in *Insect-Fungus Symbiosis,* L. R. Batra, ed. Halsted/Wiley, New York.

Lacaze-Duthiers, H. 1874. Histoire des Ascides simples des Côtes de France. I. *Arch. Zool. Exp. Gén.* **3:** 304–313.

Meyer, K. F. 1925. The "bacterial symbiosis" in the concretion deposits of certain operculate land mollusks of the families Cyclostomatidae and Annulariidae. *J. Infect. Dis.* **36:** 1–107, plates 1–15.

Mullins, D. E. 1982. Osmoregulation and excretion. Pp. 117–149 in *The American Cockroach,* W. J. Bell and K. G. Adiyodi, eds. Chapman and Hall, New York.

Mullins, D. E., and D. G. Cochran. 1975a. Nitrogen metabolism in the American cockroach—I. An examination of positive nitrogen balance with respect to uric acid stores. *Comp. Biochem. Physiol* **50A:** 489–500.

Mullins, D. E., and D. G. Cochran. 1975b. Nitrogen metabolism in the American cockroach—II. An examination of negative nitrogen balance with respect to uric acid stores. *Comp. Biochem. Physiol.* **50A:** 501–510.

Nolfi, J. R. 1970. Biosynthesis of uric acid in the tunicate *Molgula manhattensis,* with a general scheme for the function of stored purines in animals. *Comp. Biochem. Physiol* **35:** 827–842.

Potrikus, C. J., and J. A. Breznak. 1980. Uric acid-degrading bacteria in guts of termites [*Reticulotermes flavipes* (Kollar)]. *Appl. Environ. Microbiol.* **40:** 117–124.

Potrikus, C. J., and J. A. Breznak. 1981. Gut bacteria recycle uric acid nitrogen in termites: a strategy for nutrient conservation. *Proc. Natl. Acad. Sci. (USA)* **78:** 4601–4605.

Sabbadin, A., and A. Tontodonati. 1967. Nitrogenous excretion in the compound ascidians *Botryllus schlossen* (Pallas) and *Botrylloides leachi* (Savigny). *Monitore Zool. Ital. (N.S.)* **1:** 185–190.

Saffo, M. B. 1977. Studies on the renal sac of *Molgula manhattensis* De Kay (Ascidiacea, Tunicata, phylum Chordata). Ph.D. thesis, Stanford University. Pp. 1–128.

Saffo, M. B. 1978. Studies on the renal sac of the ascidian *Molgula manhattensis.* I. Development of the renal sac. *J. Morphol* **155:** 287–310.

Saffo, M. B. 1982. Distribution of the endosymbiont *Nephromyces* Giard within the ascidian family Molgulidae. *Biol. Bull.* **162:** 95–104.

Saffo, M. B., and W. Davis. 1982. Modes of infection of the ascidian *Molgula manhattensis* by its endosymbiont *Nephromyces* Giard. *Biol Bull* **162:** 105–112.

Scott, P. J., L. P. Visentin, and J. M. Allen. 1969. The enzymatic characteristics of peroxisomes of amphibian and avian liver and kidney. *Ann. N.Y. Acad. Sci.* **168:** 244–264.

Truscoe, R. 1968. Effect of borate on urate oxidase activity. *Enzymologia* **34:** 325–343.

Wolcott, D. L., and T. G. Wolcott. 1984. Food quality and cannibalism in the red land crab, *Gecarcinus lateralis. Physiol. Zool* **57:** 318–324.

Reference: *Biol. Bull.* 175: 410–416 (December, 1988)

Evolutionary Temperature Adaptation of Agonist Binding to the A_1 Adenosine Receptor

JOSEPH F. SIEBENALLER[1] AND THOMAS F. MURRAY[2]

[1]*Department of Zoology and Physiology, Louisiana State University, Baton Rouge, Louisiana 70803, and* [2]*College of Pharmacy, Oregon State University, Corvallis, Oregon 97331*

Abstract. The effects of temperature on the binding of the agonist [^{3}H]cyclohexyladenosine to A_1 adenosine receptors were studied by equilibrium binding techniques in brain membranes from eight vertebrate species with average body temperatures from 1 to 40°C. K_d values for rat and chicken increased markedly as measurement temperature decreased. In contrast, the K_d values for six teleost species, including warm-adapted, cold-adapted, and deep-living species, were much less sensitive to temperature perturbation. At 5°C K_d values vary 30-fold among the species; however, at temperatures approximating the cell temperatures of the species there is only a four-fold range of values. Binding enthalpies varied in sign and magnitude among the species. Binding entropies were positive for all the species; values were largest for the warm-adapted species, and smallest for the deep-living fishes. B_{max} values were relatively insensitive to temperature changes. $MgCl_2$ significantly increased B_{max} values, and for two of three species, lowered K_d values. $MgCl_2$ did not alter the enthalpy changes. In equilibrium competition experiments at 5°C using brain membranes from the deep-living teleost *Antimora rostrata*, the adenosine analogs R-phenylisopropyladenosine, N-ethylcarboxamidoadenosine, and 2-chloroadenosine were approximately 23-fold more potent than S-phenylisopropyladenosine. Despite perturbation by low temperature of agonist binding to mammalian and avian A_1 adenosine receptors, agonist recognition and binding properties of the A_1 receptor have been retained in vertebrates adapted to different body temperatures. These adaptive trends mirror those noted in studies of soluble enzyme homologs and muscle actins from species adapted to different temperatures.

Received 7 July 1988; accepted 27 September 1988.

Introduction

Adenosine has been demonstrated to be a significant endogenous modulator in mammalian tissues, and influences numerous physiological processes including lipolysis, coronary vasodilation, platelet aggregation, and neuronal function in the central nervous system (Snyder, 1985; Stiles, 1986; Williams, 1987). Adenosine modulates cyclic adenosine monophosphate (cAMP[1]) accumulation by affecting adenylate cyclase activity through two distinct membrane-associated receptors. At A_1 receptors, adenosine inhibits adenylate cyclase activity. At A_2 receptors, adenosine stimulates cAMP production (Daly *et al.*, 1981). These receptors are distinguished on the basis of structure-activity profiles of adenosine agonist analogs. The rank order potency of adenosine analogs is R-phenylisopropyladenosine (R-PIA) ≥ 2-chloroadenosine (2-CADO) > N-ethylcarboxamidoadenosine (NECA) > S-phenylisopropyladenosine (S-PIA) at A_1 receptors and NECA > 2-CADO > R-PIA ≥ S-PIA at A_2 receptors (Daly, 1983 a,b; Stone, 1985; Williams, 1987).

A_1 adenosine receptors in central nervous tissue have a wide phylogenetic distribution among vertebrates (Siebenaller and Murray, 1986). Receptors were identified in brain membranes of eleven species representing six classes of vertebrates using the A_1-specific agonist [^{3}H]cyclohexyladenosine ([^{3}H]CHA) in assays at 22°C. Although all the vertebrates tested, including a number of cold-adapted marine fishes, displayed substantial amounts of specific [^{3}H]CHA binding, no specific bind-

[1] Abbreviations: 2-CADO, 2-chloroadenosine; cAMP, cyclic adenosine monophosphate; [^{3}H]CHA, [^{3}H]cyclohexyladenosine; EDTA, ethylenediaminetetraacetic acid; G protein, guanine nucleotide binding protein; NECA, N-ethylcarboxamidoadenosine; R-PIA, R-phenylisopropyladenosine; S-PIA, S-phenylisopropyladenosine; T_b, average body temperature.

ing could be detected in nervous tissue of molluscs or arthropods, the two invertebrate phyla tested (Siebenaller and Murray, 1986).

Ligand binding to the A_1 receptor is markedly sensitive to temperature perturbation (*e.g.*, Bruns *et al.*, 1980; Trost and Schwabe, 1981; Murphy and Snyder, 1982; Lohse *et al.*, 1984). In mammalian species, agonist binding is strongly perturbed by decreased temperatures (Murphy and Snyder, 1982); for example, optimal binding in rat adipocyte membranes is narrowly centered at 37°C (Trost and Schwabe, 1981). Agonist binding has a relatively large unfavorable enthalpy change and is strongly entropy-driven (Murphy and Snyder, 1982; Lohse *et al.*, 1984).

Because of the strong temperature dependence of agonist binding, and because ectothermic vertebrates have body temperatures spanning a broad range, a number of questions arise concerning A_1 adenosine receptors in ectotherms, particularly those living at cold temperatures. Do these receptors retain a high affinity for agonists at the average body temperature (T_b) of the species? Do A_1 receptors display the evolutionary conservation of ligand binding abilities documented for a variety of enzyme homologs in thermal adaptation? For example, in studies of homologs of M_4-lactate dehydrogenase from species with cell temperatures of −2 to 47°C, the K_m values of substrate and coenzyme are highly similar among species when measured at the T_b of the species, despite variation in K_m values with measurement temperature (Yancey and Somero, 1978; Graves and Somero, 1982; Hochachka and Somero, 1984; Yancey and Siebenaller, 1987). This selection for particular K_m values in evolutionary adaptation to temperature results in the preservation of the catalytic and regulatory functions of enzymes (Yancey and Somero, 1978; Graves and Somero, 1982; Hochachka and Somero, 1984; Siebenaller and Somero, 1988).

To elucidate the characteristics of A_1 adenosine receptors in evolutionary adaptation to temperature, a study was undertaken of the effects of temperature on binding of the A_1-specific agonist [^{3}H]CHA to brain membranes from species with body temperatures ranging from 1°C to 40°C, including a number of marine teleost fishes which differ in their depths of occurrence. [^{3}H]CHA was used as the ligand because of the problems associated with studying the binding of the endogenous agonist adenosine (Daly, 1983a).

Materials and Methods

Specimens

Demersal adult *Sebastolobus altivelis* and *S. alascanus* (Scorpaenidae) were taken by otter trawl at their typical depths of abundance off the coasts of Oregon and California. Demersal adult *Antimora rostrata* (Moridae), *Macrourus berglax* and *Coryphaenoides rupestris* (Macrouridae) were taken off the coast of Newfoundland, Canada. For comparisons these cold-adapted teleosts are grouped as shallow- or deep-living (Table I). Data on the depths of occurrence are from Wenner and Musick (1977), Sullivan and Somero (1980), Siebenaller *et al.* (1982), and Middleton and Musick (1986). Species which are common below approximately 600 m are considered deep-living. Brains were dissected and frozen in liquid nitrogen at sea and transported to the laboratory where they were stored at −80°C until used. Brains from *Epinephelus fulvus* (Serranidae) were provided by Dr. E. Pfeiler, University of Puerto Rico, Mayaguez, Puerto Rico, and shipped on dry ice. Frozen chicken (*Gallus domesticus*) and rat (*Rattus rattus*) brains were purchased from Pel-Freez Biologicals (Rogers, Arkansas). The T_b's of the species are given in Table I.

Chemicals

Radiolabeled [adenine-2,8-^{3}H]CHA (34.4 Ci/mmol) was purchased from DuPont NEN (Boston, Massachusetts). The R- and S-diastereomers of PIA and NECA were obtained from Research Biochemicals, Inc. (Wayland, Massachusetts). Adenosine deaminase (Sigma, Type VI), 2-CADO, and all other chemicals used were from Sigma Chemical Company (St. Louis, Missouri). Water was processed through a Milli-Q purification system (Millipore Corp., Bedford, Massachusetts).

Preparation of brain membranes

On the day of the experiment, frozen brain tissue was thawed and prepared in 50 m*M* Tris-HCl, pH 7.6 at 5°C, and 1 m*M* EDTA as described in Murray and Siebenaller (1987). Prior to the final resuspension of the tissue, the preparation was incubated with 2.5 IU/ml of adenosine deaminase at 20°C for 40 min. The final resuspension of the tissue was in 50 m*M* Tris-HCl, as indicated below.

Equilibrium binding assay for membrane bound A_1 adenosine receptors

The specific binding of the A_1-selective ligand [^{3}H]-CHA to brain membranes was determined using a rapid filtration assay described by Bruns *et al.* (1980) and Murray and Cheney (1982) with minor modifications. Assay conditions were chosen to be comparable to those used in a previous study of the two *Sebastolobus* species (Murray and Siebenaller, 1987).

Aliquots of brain membrane preparations (150–750 μg of protein) were incubated with [^{3}H]CHA and either buffer or competing compounds in a final volume of 1 ml. Samples were incubated in a circulating refrigerated

Table I

Thermodynamic [illegible] *and* B_{max} *values for [3H]CHA binding to A1 adenosine receptors in membranes from cold- and warm-adapted vertebrates with different body temperatures*

[illegible]	ΔG° (cal/mol)	ΔH° (cal/mol)	ΔS° (entropy units)	B_{max} (fmol/mg protein)
Warm-adapted				
Ra [illegible] (37°C)[a]	9,474 ± 68[b]	9,259 ± 1,644*[c,d]	63.3	420 ± 18.6[e]
Gallus gallus domesticus (40°C)	10,195 ± 223	6,731 ± 1,365*	60.8	216 ± 7.9
Hyperoplus lanceolatus (10 m; 24–25°C)	10,556 ± 74	3,190 ± 1,013*	49.4	288 ± 9.8
Cold-adapted shallow-living teleost fishes				
Sebastolobus alascanus (180–440 m; 4–7°C)	10,894 ± 6	1,219 ± 422*	34.8	179 ± 4.0
Macrourus berglax (400 m; 1–4°C)	11,075 ± 57	2,502 ± 845*	49.1	23 ± 0.9
Cold-adapted deep-living teleost fishes				
Sebastolobus altivelis (550–1200 m; 4–7°C)	10,762 ± 37	212 ± 526	39.4	211 ± 8.9
Coryphaenoides rupestris (1100–1700 m; 1–6°C)	10,634 ± 36	211 ± 809	39.0	71 ± 1.2
Antimora rostrata (1700 m; 1–4°C)	−10,405 ± 131	−3,773 ± 1,888	23.9	28 ± 2.9

[a] The range of body temperatures for the species, and for the marine fishes, the depth of occurrence are indicated.

[b] Mean of at least two determinations ± standard error.

[c] Calculated from the standard errors of the slopes of van't Hoff plots.

[d] * indicates ΔH° values not equal to zero ($P < 0.05$).

[e] Mean of determinations at all of temperatures ± standard error. The number of temperatures pooled for each species may be determined from Figure 1.

water bath (Model 2067, Forma Scientific, Marietta, Ohio) at the indicated temperatures for 2 h, since this time was found adequate in preliminary experiments for the binding reaction to achieve equilibrium at all temperatures. For each species except *Antimora rostrata*, experiments spanning the entire range of temperatures employed were performed in parallel to minimize variability in the treatment of the membrane preparations.

The binding reactions were terminated by filtration of the assay tube contents over No. 32 glass fiber filter strips (Schleicher and Schuell Inc., Keene, New Hampshire) using a cell harvester (model M-24R; Brandel Instruments, Gaithersburg, Maryland) under vacuum. Filters were then rinsed with four × 4-ml washes of ice-cold 50 m*M* Tris-HCl, pH 7.6 at 5°C, to remove unbound radioactivity. Filter disks were placed into counting vials to which was added 9 ml of Biocount (Research Products International Corp., Mount Prospect, Illinois). Filter-bound radioactivity was determined by liquid scintillation spectrometry (Beckman model LS8000) at an efficiency of 53% following overnight extraction at room temperature. The amount of radioligand bound was less than 10% of the total added in all experiments. Specific binding was defined as total binding minus binding occurring in the presence of 60 μ*M* R-PIA, and represented 95 to 85% of the total binding at the K_d values for [^{3}H]-CHA in all species.

Protein determination

Membrane protein content was assayed by the method of Lowry *et al.* (1951) following solubilization of the samples in 0.5 *M* NaOH. Bovine serum albumin (Sigma Chemical Company) was used as the standard.

Analysis

Each saturation binding isotherm of the agonist [^{3}H]-CHA to the A_1 receptor was analyzed using LUNDON-1 (Lundon Software, Inc., Cleveland, Ohio) iterative curve fitting routines (Lundeen and Gordon, 1985). The concentrations of [^{3}H]CHA used ranged from 0.08 n*M* to 24 n*M*.

Thermodynamic parameters were determined using the following equations:

$$K_a = 1/K_d$$

$$\Delta G^0 = -RT \ln K_a$$

$$\Delta G^0 = \Delta H^0 - T\Delta S^0$$

where K_a is the equilibrium association constant, K_d the

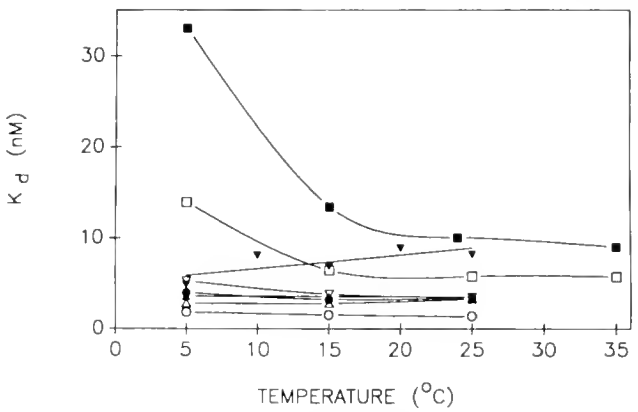

Figure 1. The effects of temperature on K_d of [^{3}H]CHA. Filled square: *Rattus rattus*, open square: *Gallus domesticus*, open inverse triangle: *Epinephelus fulvus*, open triangle: *Sebastolobus alascanus*, open circle: *Macrourus berglax*, filled triangle: *S. altivelis*, filled circle: *Coryphaenoides rupestris*; filled inverse triangle: *Antimora rostrata*. The standard error for each value is approximately 12% of the K_d. Each point represents at least two determinations.

apparent dissociation constant, ΔG^0 the standard free energy change, ΔH^0 the standard enthalpy change, ΔS^0 the standard entropy change, R the gas constant (1.987 cal mol^{-1} K^{-1}), and T the absolute temperature. Binding enthalpies were determined from van't Hoff plots of ln K_a *versus* the reciprocal absolute temperature using the integrated van't Hoff equation:

$$\ln K_a = -\Delta H^0/RT + \Delta S^0/R.$$

K_a values were calculated using the experimentally determined K_d at each temperature. The data were fit using a least squares linear regression.

For the [^{3}H]CHA competition experiments conducted at 5°C with *A. rostrata* brain membranes, IC_{50} values and slope factors were determined using the nonlinear least squares curve-fitting program LIGAND (Munson and Robard, 1980). Dissociation constants (K_i) were determined using the equation:

$$K_i = IC_{50}/[1 + ([L]/K_d)]$$

where [L] is the total [^{3}H]CHA concentration employed, K_d is the apparent dissociation constant of [^{3}H]CHA and IC_{50} is the concentration of inhibitor resulting in 50% inhibition of the specific binding (Cheng and Prusoff 1973).

Results

Effects of temperature on K_d and B_{max}

The effects of temperature at pH 7.6 on K_d of [^{3}H]-CHA values differed among the eight species studied (Fig. 1). Agonist binding in chicken and rat brain membranes was the most sensitive to temperature changes; K_d values increased 2- to 4-fold as temperature decreased from 35° to 5°C. In contrast, the K_d values for the six teleost fishes were much less sensitive to temperature; for five of these species, the K_d values changed less than 1.7 n*M* over the 20°C temperature range tested. The K_d values decreased with decreased measurement temperature for the preparations from *Antimora rostrata* and *Sebastolobus alascanus*. For *S. altivelis* and *Coryphaenoides rupestris* membranes, there were no changes in K_d over the temperature range 5–25°C. K_d values for *Epinephelus fulvus* and *Macrourus berglax* increased slightly with decreased temperature.

There is much less variation in K_d values at temperatures approximating the T_b's of the species (see Table I) than at an extreme measurement temperature such as 5°C. This is particularly apparent in comparing the K_d values of rat and chicken membranes at 35°C with the values for the cold-adapted fishes at 5°C (Fig. 1). There is a 30-fold range of values for all species at 5°C, and only a 4-fold range of K_d values at temperatures approximating the body temperatures of the species.

B_{max} values were relatively insensitive to temperature changes (*e.g.*, Fig. 3). The mean ± standard error of B_{max} values for all measurement temperatures pooled are presented in Table I.

Thermodynamic parameters

Binding enthalpies calculated from van't Hoff plots are given in Table I. A plot for representatives of the three groups of species is shown in Figure 2. The binding enthalpies differed among the species. The group of warm-adapted species, the rat, chicken, and *E. fulvus*, had the largest positive binding enthalpies. The two cold-adapted shallow-living fishes, *S. alascanus* and *M. berglax*, had

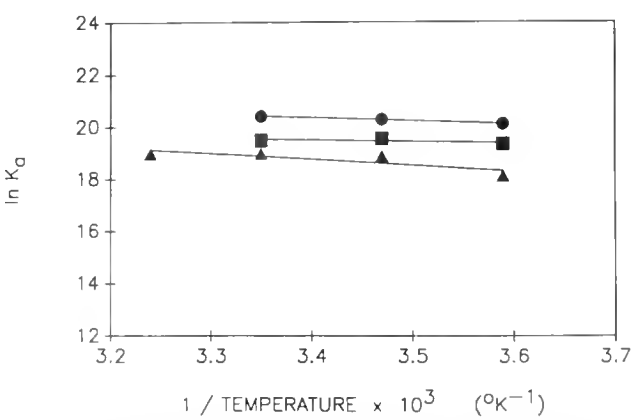

Figure 2. Van't Hoff plots for [^{3}H]CHA binding to brain membranes of *Coryphaenoides rupestris* (filled square); *Macrourus berglax* (filled circle); and *Gallus domesticus* (filled triangle).

Table II

Relative potencies of adenosine analogs as inhibitors of specific [^{3}H]CHA binding to Antimora rostrata brain membranes

Analog	K_i (n*M*)	Hill slope
R-PIA	4.5 ± 0.96	0.94 ± 0.16
S-PIA	115.9 ± 47.98	0.77 ± 0.24
NECA	4.6 ± 1.20	1.06 ± 0.23
2-CADO	4.3 ± 1.68	0.75 ± 0.17

Ten concentrations of each analog were incubated with 3.8 n*M* [^{3}H]CHA.

enthalpy changes of different signs. The cold-adapted deep-living species had enthalpies which were close to zero or negative; the 95% confidence limits for the negative enthalpy of *A. rostrata* overlap zero.

ΔG^0 values were calculated using the K_d values obtained at 5°C. ΔS^0 was determined from ΔH^0 and ΔG^0 (Table I). The ΔS^0 values for all species were positive. The warm-adapted species had the largest binding entropies (49 to 63 cal/mol deg). The shallow-living, cold-adapted macrourid *M. berglax* had a large entropy change, similar to that of the warm-adapted serranid *E. fulvus* (49 cal/mol deg). The species with negative or zero binding enthalpies had the smallest entropy changes (24–39 cal/mol deg).

The membrane preparations from *C. rupestris* were additionally assayed in 50 m*M* imidazole-HCl, pH 7.5 at 20°C, and the pH allowed to vary with assay temperature. The pK_a of imidazole changes −0.017 pH units/°C, in a manner similar to the change in blood pH with temperature (Yancey and Somero, 1978; White and Somero, 1982). The change in enthalpy obtained in this regime of varying pH was similar to that obtained at a constant pH using Tris-HCl buffer, and the data were pooled.

Agonist equilibrium competition profile at 5°C

The pharmacological profiles of [^{3}H]CHA binding sites in *S. alascanus* and *S. altivelis* brain membranes at 22°C have been shown to be those expected for A_1 adenosine receptors, based on the affinities, rank order potencies, and ability to discriminate between the R- and S-diastereomers of PIA (Siebenaller and Murray, 1986; Murray and Siebenaller, 1987). To determine whether the pharmacological profile is similar at cold temperature in a cold-adapted species with temperature-dependent binding characteristics different from warm-adapted species, equilibrium competition experiments were performed using *A. rostrata* brain membranes at 5°C (Table II). The potencies of R-PIA, NECA, and 2-CADO were similar. R-PIA was approximately 23-fold more potent than S-PIA. The nanomolar affinities and the discrimination between R- and S-PIA are consistent with an A_1 adenosine receptor.

Effects of $MgCl_2$

For *C. rupestris*, *M. berglax*, and *G. domesticus*, the effects of 5 m*M* $MgCl_2$ were tested. Divalent cations have been shown to influence binding to A_1 receptors in mammalian tissue (Goodman *et al.*, 1982; Ukena *et al.*, 1984), and teleost nervous tissue (Murray and Siebenaller, 1987). B_{max} values in the three species increased substantially in the presence of 5 m*M* $MgCl_2$ at all temperatures and this increase tended to be greater at higher temperatures (Fig. 3). Although binding affinities increased in the presence of $MgCl_2$ in the chicken and *C. rupestris* membranes, the binding enthalpies in the presence and absence of $MgCl_2$ do not differ for any of the three species (*t*-test for each species $P > 0.05$) (data not shown).

Discussion

The affinity for agonists of the mammalian A_1 adenosine receptor is markedly decreased at lowered temperatures (Bruns *et al.*, 1980; Murphy and Snyder, 1982; Lohse *et al.*, 1984). The A_1 adenosine receptor can exist in two affinity states for agonists (Lohse *et al.*, 1984; Ukena *et al.*, 1984). The decreased affinity at low temperature is characteristic of the high-affinity state of the A_1 receptor, which comprises 70 to 85% of the receptor population in rat brain at high temperatures (Lohse *et al.*, 1984). In contrast, agonist binding to the low affinity state was exothermic, and the proportion of the receptors

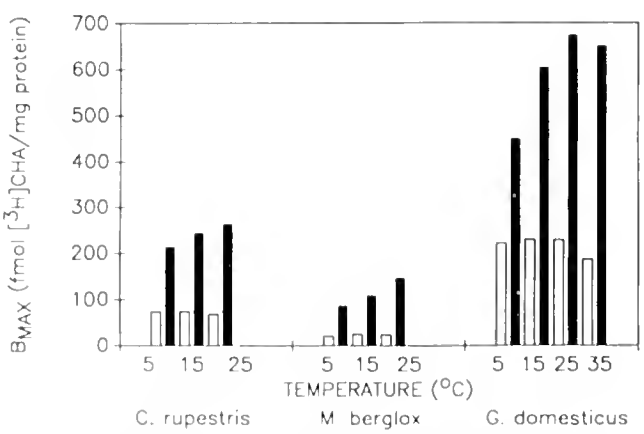

Figure 3. Effects of temperature and 5 m*M* $MgCl_2$ on B_{max} values of [^{3}H]CHA for *Coryphaenoides rupestris*, *Macrourus berglax*, and *Gallus domesticus* brain membranes. Open bars: no added $MgCl_2$; filled bars: 5 m*M* $MgCl_2$. Means of at least two experiments are shown; the standard error for each individual estimate of B_{max} is less than 9%; replicate estimates of B_{max} differ by less than 10%.

in the low affinity state increased at low temperatures (Lohse *et al.*, 1984).

The present study was undertaken to ascertain the pattern of temperature dependence of agonist binding to the A_1 receptor in vertebrates with different cell temperatures, particularly species with lowered body temperatures. With the protocol used, the data were consistently better fit by a one affinity state model (tested by a partial F-test, $P > 0.05$; see Hoyer *et al.*, 1984). Thus, this study cannot address potential temperature-dependent shifts among affinity states. Although the experimental protocol and incubation conditions of the present study differ in detail from that used in previous studies, the thermodynamic parameters obtained for rat (Table I) agree with those reported for mammalian nervous tissues by Murphy and Snyder (1982) (ΔH^0 13,200 cal/mol; ΔS^0 82 cal/mol deg at 25°C for CHA), and Lohse *et al.* (1984) for agonist binding to the high-affinity receptor subtype (ΔH^0 10,800 cal/mol; ΔS^0 76 cal/mol deg at 37°C for R-PIA binding).

Cold-adapted species retain high affinity binding at their T_b's, despite the strongly entropy-driven agonist binding displayed by such warm adapted species as the rat and chicken (Fig. 1; Table I). The affinity of agonist binding to the A_1 receptor in nervous tissue of cold-adapted ectotherms at their T_b's is comparable to that displayed by warm-adapted species at high temperatures. Although there is considerable variation in K_d values at different measurement temperatures, this variation is greatly reduced when comparisons are made at temperatures approximating the T_b's of the species. This contrast is most apparent when one compares the 30-fold range of values at 5°C to the 4-fold range of K_d values at temperatures approximating the cell temperatures of the species (Fig. 1; Table I).

$MgCl_2$ significantly increased B_{max} values (Fig. 3), and for the chicken and *C. rupestris* increased binding affinities. The binding enthalpies were not altered by $MgCl_2$; the Mg^{2+}-stimulated receptors have temperature-dependencies similar to the receptors treated with EDTA and incubated in the absence of $MgCl_2$.

The study at 5°C of *A. rostrata* (Table II) and previous studies of the *Sebastolobus* species (Siebenaller and Murray, 1986; Murray and Siebenaller, 1987) indicate that the pharmacological profile of A_1 receptors of deep-sea and cold-adapted fishes are comparable to those of mammals in terms of their affinities and in the discrimination of the R- and S-diastereomers of PIA, even when the receptors of a cold-adapted species are assayed at 5°C.

The A_1 receptors in vertebrates with widely different T_b's (1–40°C) have similar binding affinities for [^{3}H]-CHA at temperatures approximating the T_b's of the species. This is analogous to the evolutionary conservation of K_m values for enzyme homologs from species with different T_b's. At the T_b's of the species K_m values are highly similar, even though there is a strong temperature-dependence of substrate and coenzyme binding (Yancey and Somero, 1978; Graves and Somero, 1982; Hochachka and Somero, 1984; Yancey and Siebenaller, 1987). Conservation of K_m values, coupled with the similar *in vivo* substrate levels among species, results in the preservation of the regulatory and catalytic properties of the enzymes, and the sparing of cellular solvent capacity (*e.g.*, discussion in Hochachka and Somero, 1984).

The conservation of ligand recognition and binding affinity among receptors in species with different T_b's reflects the preservation during evolution of the interactions between agonist and receptor. Ligand binding to a receptor, such as the A_1 adenosine receptor which is coupled to adenylate cyclase, is but a single step in the function of the receptor—G protein—adenylate cyclase circuitry. Nonetheless, ligand recognition and binding are critical in the transmembrane signaling process.

The relative roles of enthalpy and entropy changes in establishing the net change in free energy vary systematically among species with different body temperatures (Table I) in a manner mirroring the adaptive changes in binding observed for actins from vertebrates with different body temperatures (Swezey and Somero, 1982). The differences among species in thermodynamic characteristics of agonist binding to the A_1 receptors may reflect a variety of factors which have yet to be evaluated. These factors may include differences (1) in the primary structure of the receptors, (2) in the carbohydrate moieties covalently bound to the receptor proteins, (3) in the lipid milieu of the membranes, and (4) in the interaction of the receptor with the inhibitory G protein (G_i), either in terms of the number and types of weak bonds involved in receptor protein-G_i binding, or in the relative quantities of G_i and A_1 receptor. It is likely that all of these may contribute to the adjustment of binding affinities with temperature, and indeed, in different evolutionary lineages, the relative importance of these mechanisms may differ.

Acknowledgments

This work was supported by NSF grants DCB-8416602 and DCB-8710155. Ship time on the R/V *Wecoma* cruises off the coast of Oregon were supported by these grants. Ship time on the R/V *Gyre* off the coast of Newfoundland was supported by NSF grant DMB-8502857 to Dr. A. F. Riggs. We thank Drs. A. Gibbs, E. Pfeiler, A. Riggs, and R. Noble for their help in obtaining specimens.

Literature Cited

Bruns, R. F., J. W. Daly, and S. H. Snyder. 1980. Adenosine receptors in brain membranes: Binding of N^6-cyclohexyl[^{3}H]adenosine

and 1,3-diethyl-8-[H]phenylxanthine. *Proc. Natl. Acad. Sci. USA* 77: 5547–5551.

Cheng, Y. C., and W. H. Prusoff. 1973. Relationship between the inhibition constant (K_i) and the concentration of inhibitor which causes 50% inhibition (I_{50}) of an enzymatic reaction. *Biochem. Pharmacol.* 22: 3099–3108.

Daly, J. W. 1983a. Adenosine receptors: characterization with radioactive ligands. Pp. 59–69 in *Physiology and Pharmacology of Adenosine Derivatives*, J. W. Daly, Y. Kuroda, J. W. Phillis, H. Shimizu, and M. Ui, eds. Raven, New York.

Daly, J. W. 1983b. Role of cAMP and adenosine receptors in physiological processes: Summary and prospectus. Pp. 275–290 in *Physiology and Pharmacology of Adenosine Derivatives*, J. W. Daly, Y. Kuroda, J. W. Phillis, H. Shimizu, and M. Ui, eds. Raven, New York.

Daly, J. W., R. F. Bruns, and S. H. Snyder. 1981. Adenosine receptors in the central nervous system: Relationship to the central action of methylxanthines. *Life Sci.* 28: 2083–2097.

Goodman, R. R., M. J. Cooper, M. Gavish, and S. H. Snyder. 1982. Guanine nucleotide and cation regulation of the binding of [^{3}H]cyclohexyladenosine and [^{3}H]diethylphenylxanthine to adenosine A_1 receptors in brain membranes. *Mol. Pharmacol.* 21: 329–335.

Graves, J. E., and G. N. Somero. 1982. Electrophoretic and functional enzyme evolution in four species of eastern Pacific barracudas from different thermal environments. *Evolution* 36: 97–106.

Hochachka, P. W., and G. N. Somero. 1984. *Biochemical Adaptation*. Princeton University Press, Princeton, New Jersey.

Hoyer, M. M., E. E. Reynolds, and P. B. Molinoff. 1984. Agonist-induced changes in the properties of *beta*-adrenergic receptors on intact S49 lymphoma cells. Time-dependent changes in the affinity of the receptor for agonists. *Mol. Pharmacol.* 25: 209–218.

Lohse, M. J., V. Lenschow, and U. Schwabe. 1984. Two affinity states of R_1 adenosine receptors in brain membranes. Analysis of guanine nucleotide and temperature effects on radioligand binding. *Mol. Pharmacol.* 26: 1–9.

Lundeen, J. E., and J. H. Gordon. 1985. Computer analysis of binding data. Pp. 31–49 in *Receptor Binding in Drug Research*, R. O'Brien, ed. Marcel Dekker, New York.

Middleton, R. W., and J. A. Musick. 1986. The abundance and distribution of the family Macrouridae (Pisces: Gadiformes) in the Norfolk Canyon area. *Fish. Bull.* 84: 35–62.

Munson, P. J., and D. Rodbard. 1980. LIGAND: a versatile computerized approach for characterization of ligand-binding systems. *Anal. Biochem.* 107: 220–239.

Murphy, K. M. M., and S. H. Snyder. 1982. Heterogeneity of adenosine A_1 receptor binding in tissue. *Mol. Pharmacol.* 22: 250–257.

Murray, J. F., and D. L. Cheney. 1982. Localization of N^6-cyclohexyl[^{3}H]adenosine binding sites in rat and guinea pig brain. *Neuropharmacology* 21: 575–580.

Murray, J. F., and J. F. Siebenaller. 1987. Comparison of the binding properties of A_1 adenosine receptors in brain membranes of two congeneric marine fishes living at different depths. *J. Comp. Physiol. B* 157: 267–277.

Siebenaller, J. F., and J. F. Murray. 1986. Phylogenetic distribution of [^{3}H]cyclohexyladenosine binding sites in nervous tissue. *Biochem. Biophys. Res. Commun.* 137: 182–189.

Siebenaller, J. F., and G. N. Somero. 1988. Biochemical adaptation to the deep sea. *Crit. Rev. Mar. Sci.* 1: in press.

Siebenaller, J. F., G. N. Somero, and R. L. Haedrich. 1982. Biochemical characteristics of macrourid fishes differing in their depths of distribution. *Biol. Bull.* 163: 240–249.

Snyder, S. H. 1985. Adenosine as a neuromodulator. *Ann. Rev. Neurosci.* 8: 103–124.

Stiles, G. L. 1986. Adenosine receptors: structure, function and regulation. *Trends Pharmacol. Sci.* 7: 486–490.

Stone, T. W. 1985. Summary of a symposium on purine receptor nomenclature. Pp. 1–5 in *Purines: Pharmacology and Physiological Roles*, T. W. Stone, ed. UCH Publishers, Deerfield Beach, Florida.

Sullivan, K. M., and G. N. Somero. 1980. Enzyme activities of fish skeletal muscle and brain as influenced by depth of occurrence and habits of feeding and locomotion. *Mar. Biol.* 60: 91–99.

Swezey, R. R., and G. N. Somero. 1982. Polymerization thermodynamics and structural stabilities of skeletal muscle actins from vertebrates adapted to different temperatures and pressures. *Biochemistry* 21: 4496–4503.

Trost, T., and U. Schwabe. 1981. Adenosine receptors in fat cells. Identification by (-)-N^6-[^{3}H]phenylisopropyladenosine binding. *Mol. Pharmacol.* 19: 228–235.

Ukena, D., E. Poeschla, and U. Schwabe. 1984. Guanine nucleotide and cation regulation of radioligand binding to R_1 adenosine receptors of rat fat cells. *Naunyn-Schmiedeberg's Arch. Pharmacol.* 326: 241–247.

Wenner, C. A., and J. A. Musick. 1977. Biology of the morid fish, *Antimora rostrata*, in the western North Atlantic. *J. Fish. Res. Board Can.* 34: 2362–2368.

White, F. N., and G. N. Somero. 1982. Acid-base regulation and phospholipid adaptations to temperature: time courses and physiological significance of modifying the milieu for protein function. *Physiol. Rev.* 62: 40–90.

Williams, M. 1987. Purine receptors in mammalian tissues: pharmacology and functional significance. *Ann. Rev. Pharmacol. Toxicol.* 27: 315–345.

Yancey, P. H., and J. F. Siebenaller. 1987. Coenzyme binding ability of homologs of M_4-lactate dehydrogenase in temperature adaptation. *Biochim. Biophys. Acta* 924: 483–491.

Yancey, P. H., and G. N. Somero. 1978. Temperature dependence of intracellular pH: its role in the conservation of pyruvate apparent K_m values of vertebrate lactate dehydrogenases. *J. Comp. Physiol.* 125: 129–134.

Reference: *Biol Bull* **175**: 417–429. (December, 1988)

The Fine Structure of the Amebocyte in the Blood of *Limulus polyphemus*. II. The Amebocyte Cytoskeleton: A Morphological Analysis of Native, Activated, and Endotoxin-Stimulated Amebocytes

FERN TABLIN[1] AND JACK LEVIN[2]

[1]*Department of Anatomy, School of Veterinary Medicine, University of California, Davis, California 95616, and* [2]*Departments of Laboratory Medicine and Medicine, University of California School of Medicine, San Francisco, California 94143 and the Veterans Administration Medical Center, San Francisco, California 94121*

Abstract. This study evaluates the structural organization of the cytoskeleton in native, activated, and endotoxin-activated amebocytes of the horseshoe crab, *Limulus polyphemus*. The discoid shape of native amebocytes appears to be maintained by a three-part arrangement consisting of a microtubule marginal band in a two-dimensional plane, an extensive actin-membrane array, and three-dimensional cortical actin array. This arrangement is disrupted during amebocyte activation in the absence of endotoxin, as the cortical actin array becomes diffuse and the cells form many pseudopodia. However, under these conditions the marginal band remains intact and continues to be located at the periphery of these cells. Amebocytes activated by bacterial endotoxin display a different cytoskeletal arrangement. After exposure to endotoxin, the cells displace their entire cortical actin array and marginal band to a more centralized location surrounding the nucleus.

Introduction

The amebocytes of the horseshoe crab, *Limulus polyphemus*, provide a useful model for the study of hemostasis and thrombosis. In *Limulus*, the amebocyte is the only type of circulating blood cell and is characterized by its large cytoplasmic granules, which contain the factors necessary for blood coagulation (Levin and Bang, 1964a, b, 1968; Murer *et al.*, 1975). Amebocytes are sensitive to the presence of bacterial endotoxins, which produce aggregation, activation, and degranulation (Bang, 1956, 1979; Levin and Bang, 1964a; Ornberg and Reese, 1981; Armstrong and Rickles, 1982). Amebocytes are also motile cells which can be observed in the abdominal spines (Bang, 1979) or isolated gill leaflets of young animals (Loeb, 1928; Armstrong, 1979). Studies of amebocytes treated with cytochalasin D have shown an inhibition of motility (Armstrong, 1979). This has led investigators to suggest that an actomyosin system is responsible for the generation of motile forces. Morphologic studies of activated amebocytes have demonstrated bundles of thin filaments within filopodia of motile cells (Armstrong, 1985). Studies of unactivated amebocytes have revealed a marginal band of microtubules (MB) present at the periphery of the cells (Dumont *et al.*, 1966; Nemhauser *et al.*, 1980). It has been suggested that the MB acts to stabilize the discoid shape of the amebocyte (Cohen and Nemhauser, 1985). In this report, we describe the cytoskeleton in native amebocytes and its subsequent rearrangement after activation and granule release in the absence or presence of bacterial endotoxin.

Received 6 May 1988; accepted 27 September 1988.

Materials and Methods

Horseshoe crabs (*Limulus polyphemus*) were obtained from the Department of Marine Resources, Marine Biological Laboratory, Woods Hole, Massachusetts.

Unactivated (native) amebocytes were obtained by

cardiac puncture with a sterile, endotoxin-free 18 gauge needle. Blood was allowed to drip directly into fixative or was aspirated briefly by a sterile, endotoxin-free syringe and concomitantly combined with fixative. Activated amebocytes were generated by taking hemolymph directly into a sterile, endotoxin-free syringe and allowing the cells to aggregate and adhere to the plastic surface. After activation was apparent, as demonstrated by visible aggregation of amebocytes, activated amebocytes were carefully discharged from the syringe directly into fixative. Endotoxin-activated cells were prepared by taking hemolymph directly into syringes containing endotoxin (*E. coli* B, 055:B5, Difco Laboratories, Detroit, Michigan, in 3% NaCl). The ratio of hemolymph to endotoxin-containing saline was 9:1; the final concentration of endotoxin was 1 μg/ml.

All cells were fixed with 2.5% glutaraldehyde and 0.5% tannic acid in 100 m*M* phosphate buffer, pH 7.0, at room temperature. Samples were washed in 100 m*M* phosphate buffer, and post-fixed in 2% osmium with 2% potassium ferrocyanide in 100 m*M* phosphate buffer. An additional population of native amebocytes also was fixed in 2% glutaraldehyde with 50 m*M* lysine (Boyles *et al.*, 1985) and stained with 1% osmium. All amebocytes were dehydrated and embedded in Epon 812. Thin sections were stained with saturated uranyl acetate (in 70% ethanol) and lead citrate and examined on a Hitachi 600 transmission electron microscope.

Nuclear profiles were measured by the use of concentric circle grids, and axial ratios (Q) were calculated according to the method of Elias and Hyde (1983). Axial ratios are defined as the quotient length/width. Determination of nuclear shape was made by the use of axial ratios, as described by Elias and Hyde (1983). These measurements were undertaken to allow us to evaluate whether cytoskeletal changes reflected direct cytoplasmic interactions or were secondary to an increase or decrease in the size of the nucleus, resulting in a subsequent displacement of any particular cytoplasmic structure.

Results

Native amebocytes

The native amebocyte is a discoid cell with a centrally located nucleus and prominent cytoplasmic granules (Fig. 1). The cytoskeleton can be divided into two major filamentous elements: thin (5–7 nm) filaments (presumably actin) and microtubules (25–28 nm).

Thin filaments were observed in several different arrays. There was a prominent cortical band of actin filaments, some of which were associated with the plasma membrane (Fig. 2A). A diffuse network of thin filaments also was located throughout the remainder of the cytoplasm. Polyribosomes were frequently found in association with these thin filaments. The actin array was best seen in cells that had been fixed in the presence of lysine, according to the method of Boyles *et al.* (1985). On rare occasions, wavy 10-nm filaments were seen in the cytoplasm. These filaments were often located near the cortical band of thin filaments, and may represent a minor population of intermediate filaments or aggregates of thin filaments (Fig. 2A).

Microtubules were present in the form of a marginal band, as has been observed by other investigators (Fawcett and Witebsky, 1964; Dumont *et al.*, 1966; Nemhauser *et al.*, 1980; Ornberg and Reese, 1981). The marginal band was located internally to the cortical actin array. Projections or "arms" were observed in association with microtubules in both longitudinal and cross-section. These projections often appeared to extend from one microtubule to another (Fig. 2B).

Native amebocytes contained a large population of granules that were randomly distributed in the cytoplasm, but which were always located internally to the marginal microtubule band and cortical actin array.

Activated amebocytes

Activated amebocytes, no longer discoid in shape, often developed multiple pseudopodia. Fine filopodia rarely were seen extending from the distal ends of pseudopodia.

The organization of actin in the activated amebocyte varied depending upon its location within the cell. The cortical actin filaments were diminished in number and no longer formed a distinct array. Small numbers of thin filaments (microfilaments) remained in association with the plasma membrane. Actin arrays, both within the body of the cell and within pseudopodia, were diffuse, with filaments forming a fine interconnecting meshwork (Fig. 3). This internal meshwork was similar to that observed in the cytoplasm of native amebocytes. Some areas contained microspikes, in which thin filaments formed discrete bundles, which often extended back into the body of the cell (Fig. 4). Fine filopodia were rarely observed; however, when present, they too contained bundles of microfilaments.

Microtubules were present as a marginal band (MB) within the body of the cells (Fig. 3). However, MB's also were observed within pseudopodia. This was detected primarily when a pseudopodium was extended within the same plane as the marginal band. (Data not shown.) Individual microtubules rarely were seen in pseudopodia.

Examinations of activated amebocytes revealed that many cells were undergoing exocytosis of granules. This

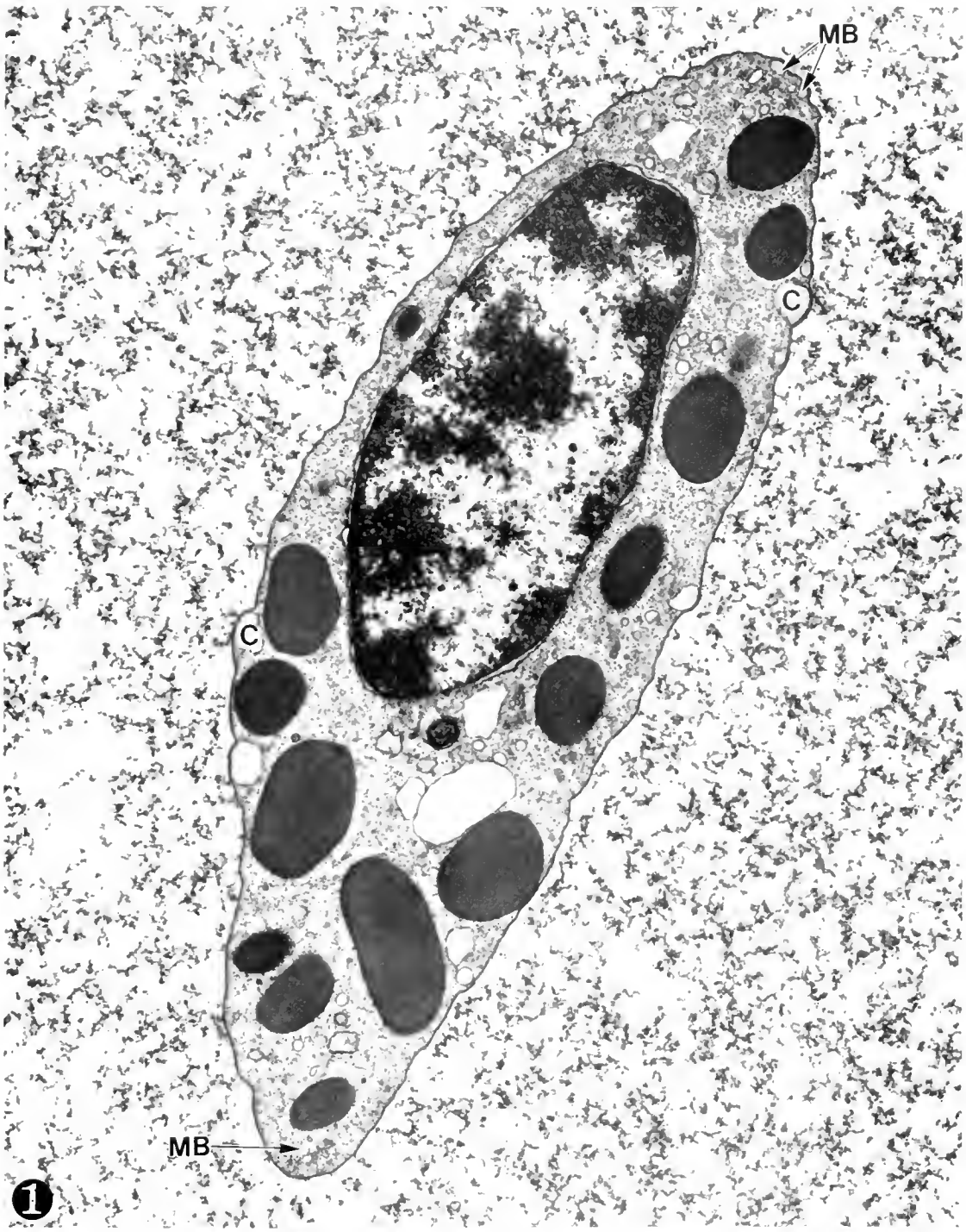

Figure 1. Native amebocytes are discoid in shape. The marginal band (MB) of microtubules is present in cross-section, at either end of the cell. Small cisternae (C) may represent intracellular calcium stores. Glutaraldehyde and tannic acid fixation (see Materials and Methods) was used for this and all subsequent studies, except for Figure 2A. × 21,000.

process appeared to be similar to that previously described by Ornberg and Reese (1981). Granules often were seen at the plasma membrane, and granule membrane-plasma membrane fusions also were observed. Asymmetric granules with narrow ends appeared to orient these ends toward the plasma membrane (Fig. 5).

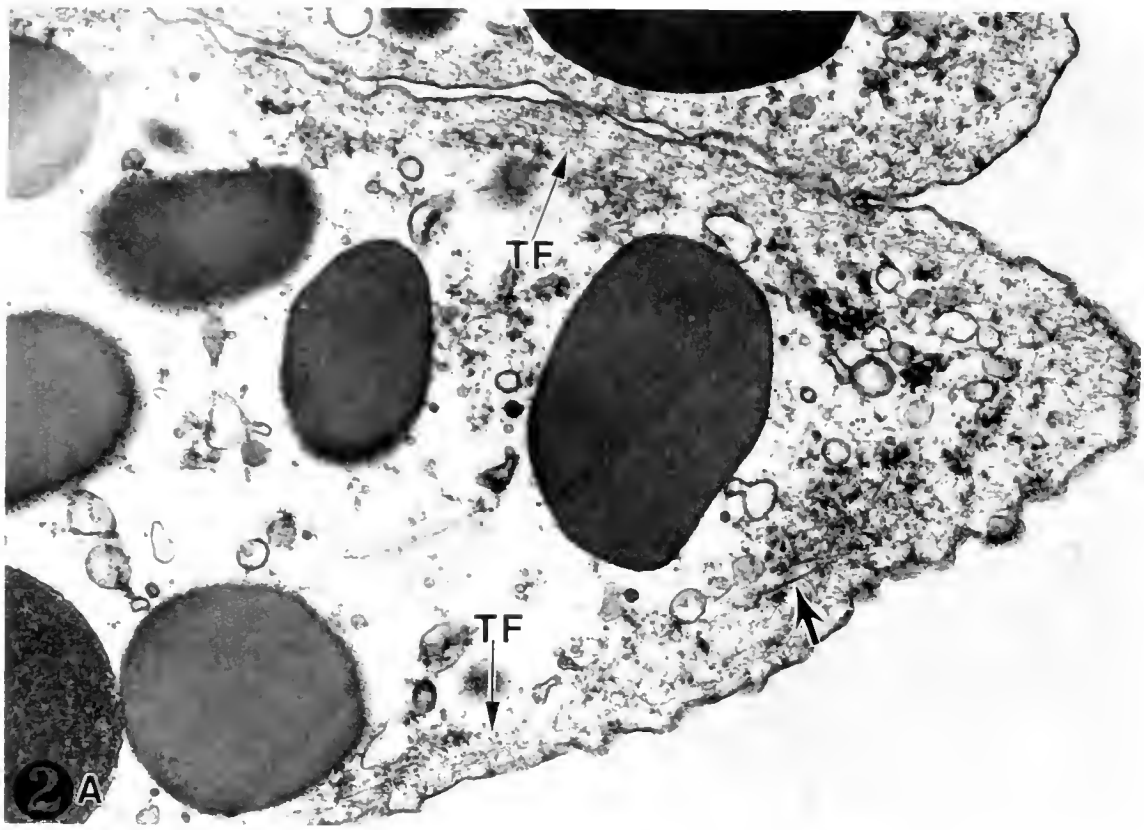

Figure 2A. Native amebocyte fixed by the method of Boyles *et al.* (1985) best reveals the cortical array of thin filaments (TF) which is present throughout the cell. In addition, short 10-nm filaments (▶) are seen among the cortical actin filaments. × 34,500. (Provided by Paula E. Stenberg, unpub. obs.)

This distinctive arrangement was observed in virtually all activated cells. Neither microtubules nor distinct arrays of thin filaments appeared to be associated with sites of exocytosis.

Endotoxin-activated amebocytes

Amebocytes exposed to bacterial endotoxin appeared to be rapidly activated and underwent extensive shape change and degranulation. Subsequently, most cells contained only a small residual population of granules which were located adjacent to the nucleus. In many cells, there was a coalescence of granules and granule membrane fusion was apparent. Unlike amebocytes activated by contact with an endotoxin-free surface (and in which exocytosis occurred following movement of granules to the plasma membrane [Fig. 5]), endotoxin-treated amebocytes appeared to secrete their granules from a more central location within the cell (Fig. 6).

Endotoxin-activated amebocytes were more spherical in shape, with numerous filopodia. Fine filopodia contained bundles of actin filaments, but the overall arrangement of thin filaments was vastly different from either native or surface-activated amebocytes (Fig. 6). Short pieces of thin filaments remained associated with the plasma membrane, and occasionally extended into the cytoplasm as isolated groups of two or three filaments, without apparent organization. A large area of cytoplasm between the plasma membrane and the now centrally located granules and nucleus contained sparse, randomly arranged thin filaments. At the outermost aspect of the centralized granules, there was a loosely organized bundle of actin filaments whose array was similar to the cortical actin seen in native cells (Fig. 6).

The MB surrounded the centralized granules and was located internally to the actin array. In cells that had undergone complete degranulation, the MB was now located adjacent to the nucleus (Fig. 7). The MB appeared to remain intact, and microtubules never were detected in other parts of the cells, under this experimental condition. MB's often were apparently twisted, with microtubules present in both longitudinal and tangential sections of the same cell. This distinct reorganization and central-

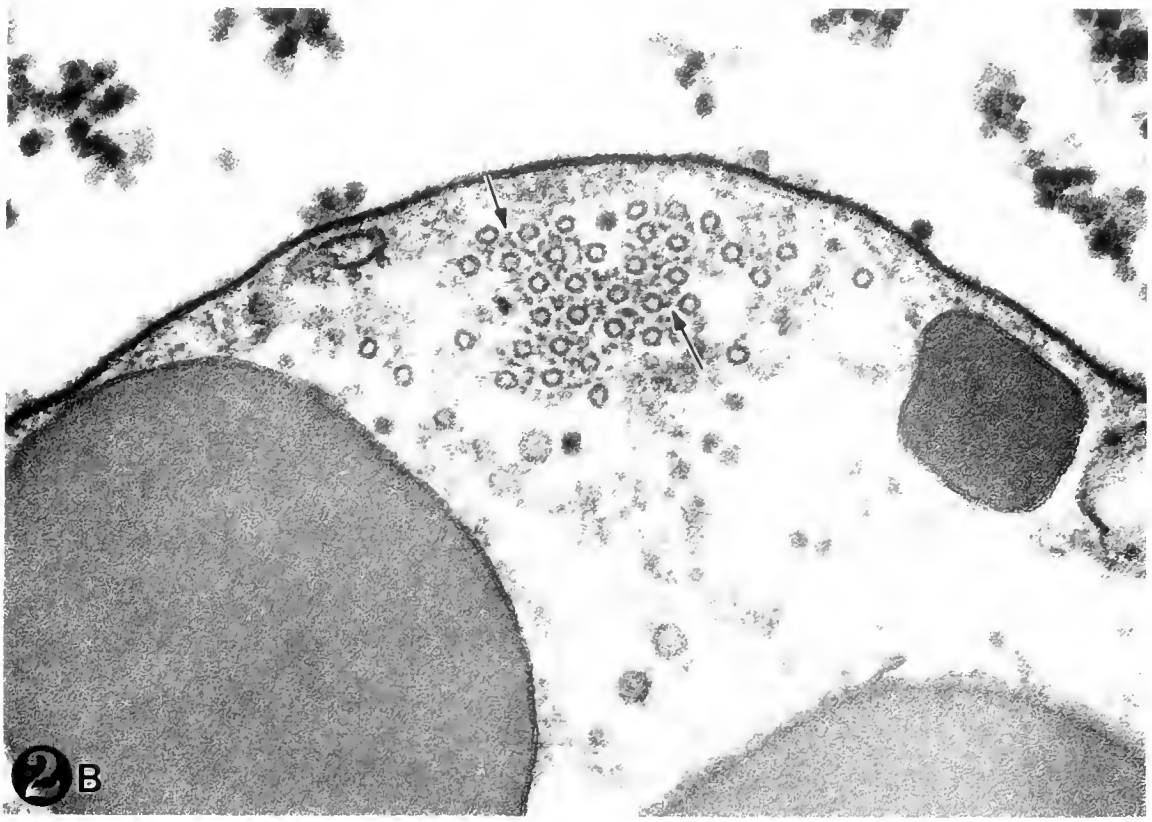

Figure 2B. A higher magnification of the marginal microtubule band (MB) in cross-section. Projections can be seen leading from one microtubule to another (▶). These projections may serve to stabilize the MB, and are likely related to microtubule-associated proteins present in other systems. × 104,000.

ization of the MB only occurred in endotoxin-activated cells.

Nuclear profiles

Amebocyte nuclei of cells studied under all three conditions (native, activated, and endotoxin-activated) had mean axial ratios of 1.67 (native, n = 30), 1.62 (activated, n = 29) and 1.50 (endotoxin-activated, n = 30). These values fit the axial ratios for an oblate ellipsoid, which is the most common nuclear shape of discoid cells (Elias and Hyde, 1983). The slightly smaller mean axial ratios of the nuclei in the endotoxin-activated cells may be due to the change in cell shape from discoid to a more spherical shape. These data were generated to determine if the nuclear profiles changed under the various conditions of the study, as we wished to know whether cytoskeletal changes were secondary to either an increase or decrease in nuclear size. Since nuclear axial ratios did not change appreciably under any of the experimental conditions, these data support our interpretation that the microtubule coil constricts around the nucleus in endotoxin-activated amebocytes.

Discussion

The discoid shape of native amebocytes has been observed with a variety of techniques, including high resolution differential interference contrast (DIC) microscopy (Armstrong, 1979) and electron microscopy (Copeland and Levin, 1985; Levin, 1985b). In this paper, we have presented data which suggest that the two major elements of the amebocyte cytoskeleton appear to act in tandem to maintain the discoid shape of the native amebocyte. The cortical actin array with its link to the plasma membrane, in association with the marginal microtubule band, appears to provide a tension arrangement similar to that proposed for nucleated erythrocytes by Cohen *et al.* (1982).

Following endotoxin-free activation of amebocytes, this arrangement becomes disrupted, and is accompanied by shape change. Shape change of endotoxin-free activated amebocytes is similar to that reported for surface-activated cells by Armstrong (1980). Under both conditions of endotoxin-free activation, cells extend pseudopodia and filopodia. It is interesting to note that while the actin array undergoes reorganization, the mar-

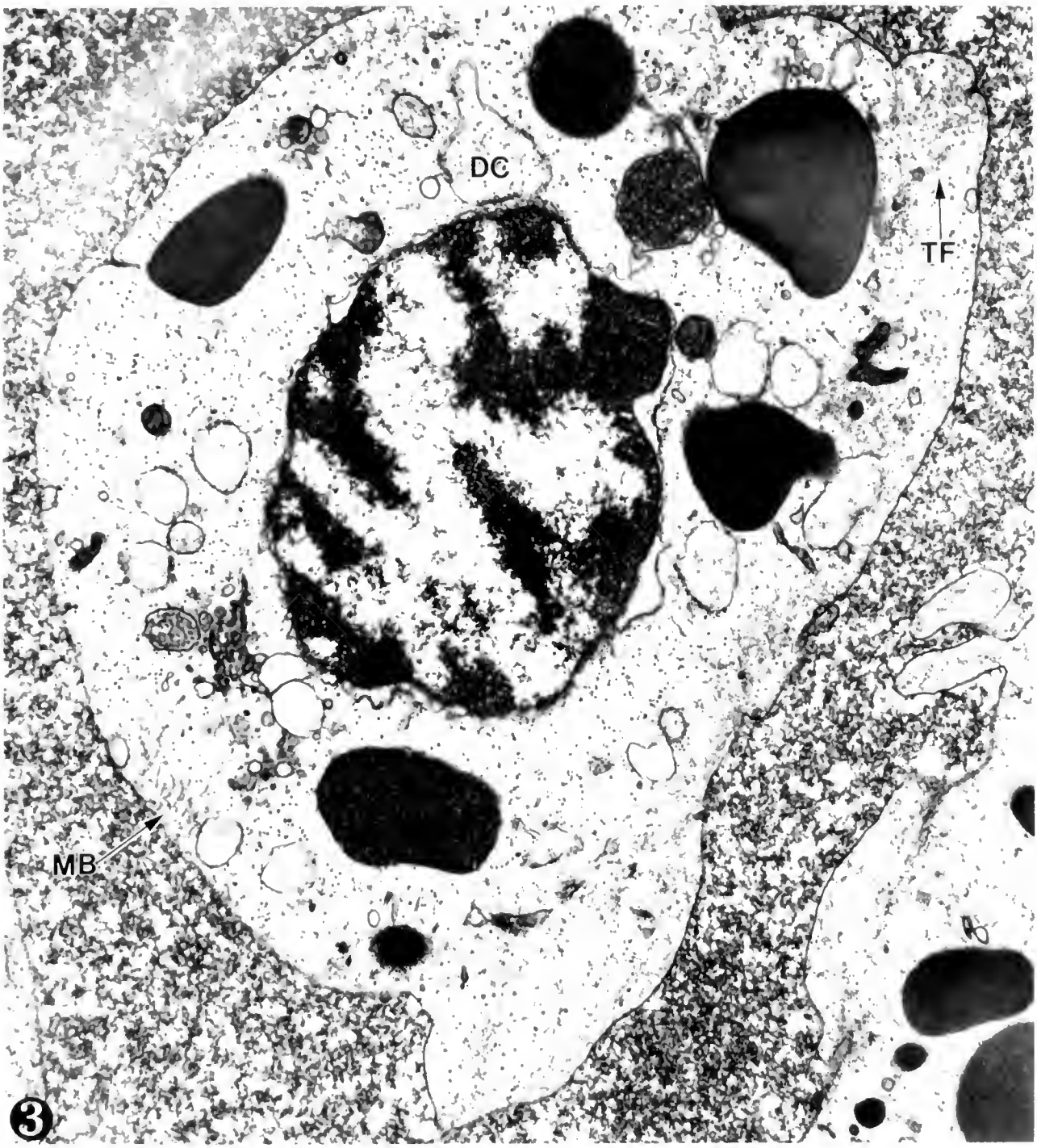

Figure 3. Following endotoxin-free aggregation, activated amebocytes are no longer discoid in shape, and many have secreted the contents of a variable number of their granules. Most cells have pseudopodia, which contain diffuse networks of thin filaments (TF). The MB, still intact, is only present in a tangential section. An area of plasma membrane invagination near a granule (upper left) indicates a likely site of exocytosis. Large irregular dilated cisternae (DC) may represent previous sites of exocytosis. ×21,000.

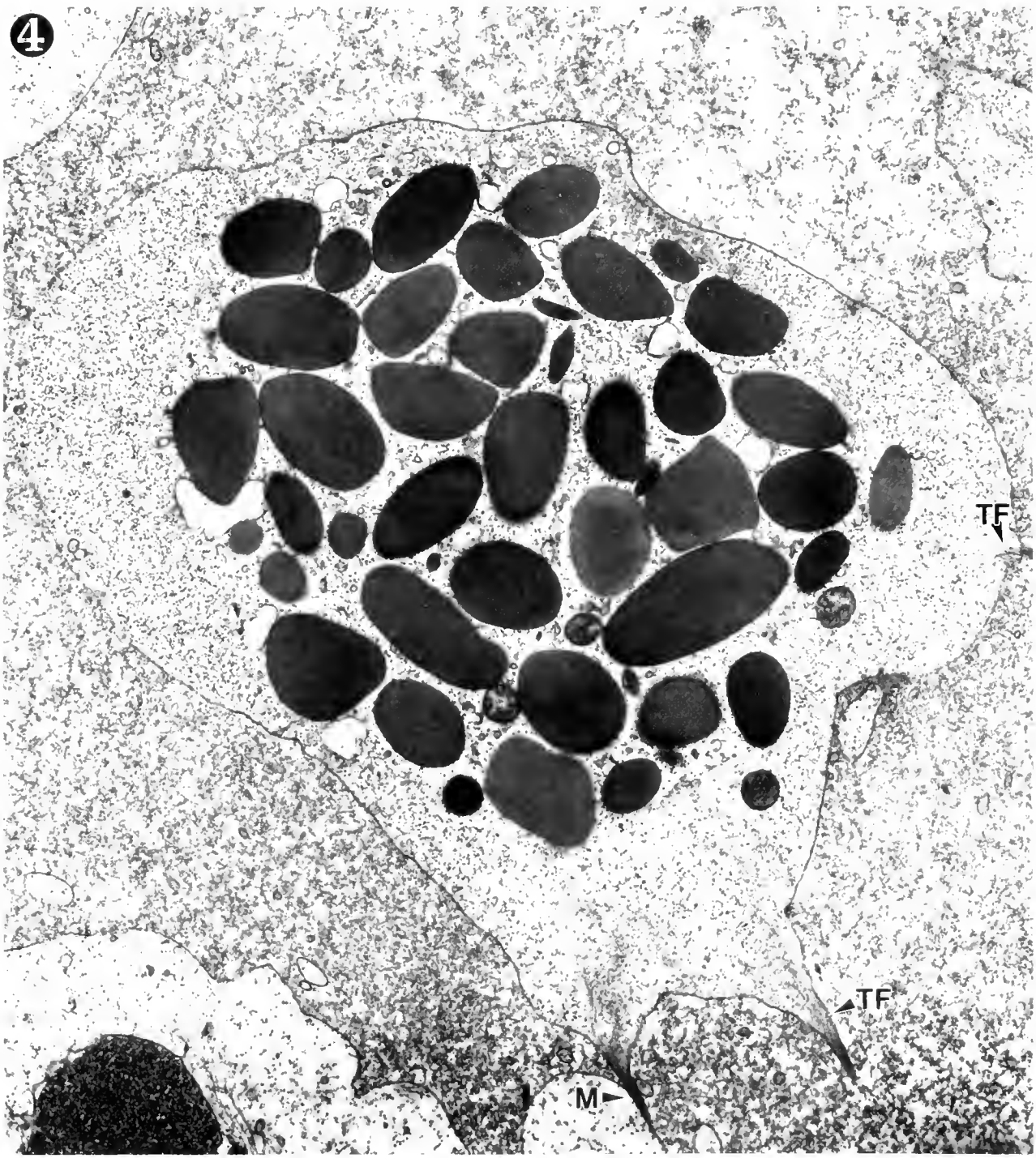

Figure 4. Activated amebocytes, in addition to developing pseudopodia, also produced microspikes (M), which contain fine bundles of thin filaments (TF), some of which remained bundled in the adjacent cytoplasm (▶). It is interesting to note that this cell, which has retained most of its granules, and the cell in Figure 3 were in the same group of surface-activated amebocytes, indicating that cells can undergo exocytosis at different rates. × 14,500.

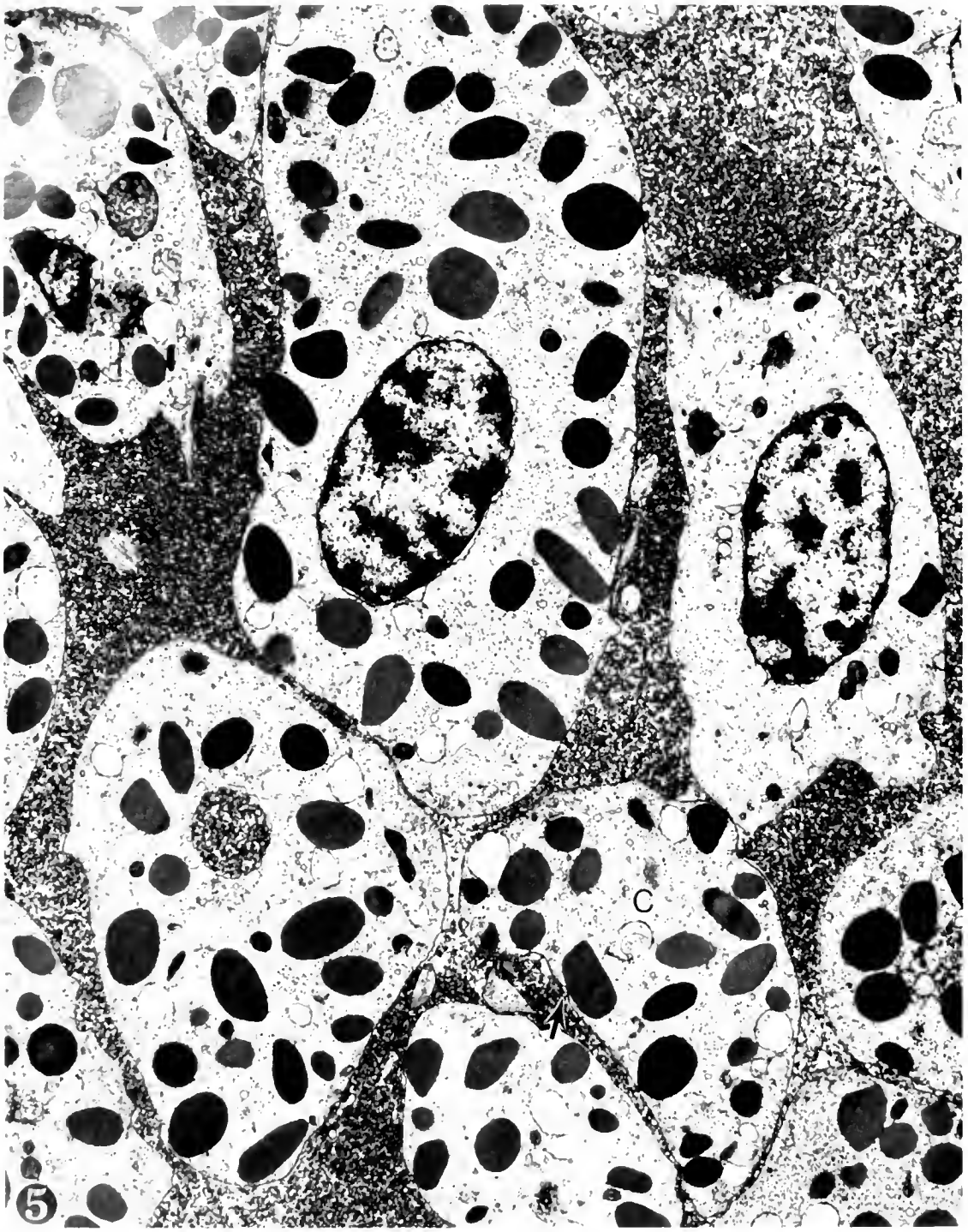

Figure 5. Surface-activated amebocytes demonstrate the distinctive orientation of granules towards the plasma membrane. Note that almost all of the granules are oriented with their "pointed" end toward the plasma membrane. One of the cells (C) (lower center) demonstrates the unusual observation of a granule which is oriented towards the plasma membrane along its broad side. However, an invagination of the plasma membrane appears to contact only one part of this granule (▶). A decrease in the density of cytoplasmic ground substance was apparent throughout the population of activated amebocytes. ×9600

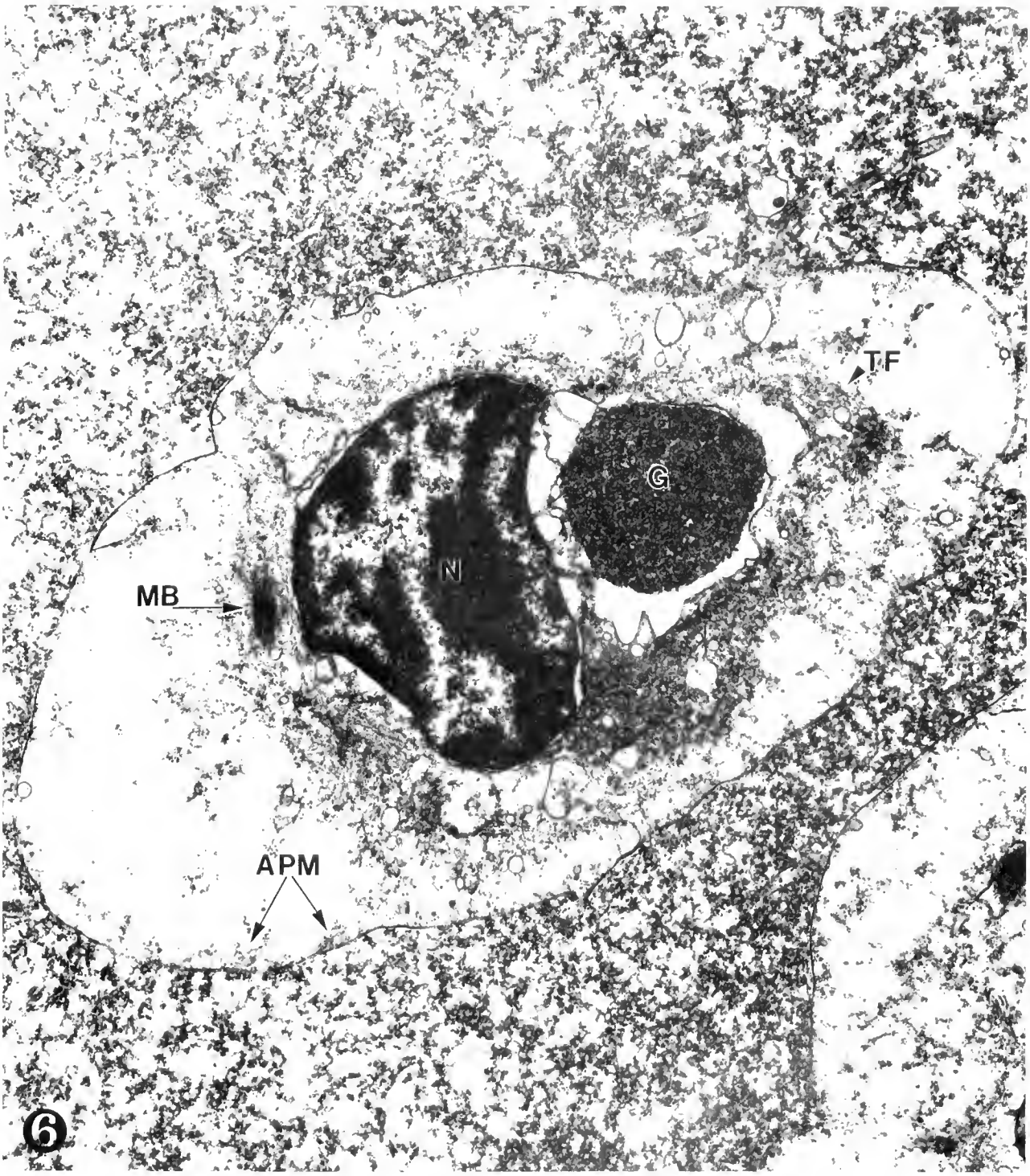

Figure 6. Endotoxin-activated cells usually contained fewer granules, and often were spherical in shape. A fine actin-plasma membrane (APM) network is still in place. However, the majority of the actin (TF), as well as the MB, is now located adjacent to the nucleus (N). A large granule (G) or fusion product of several granules can be seen next to the nucleus. Cytoplasmic ground substance appeared decreased, similar to that observed in surface-activated cells. × 17,200

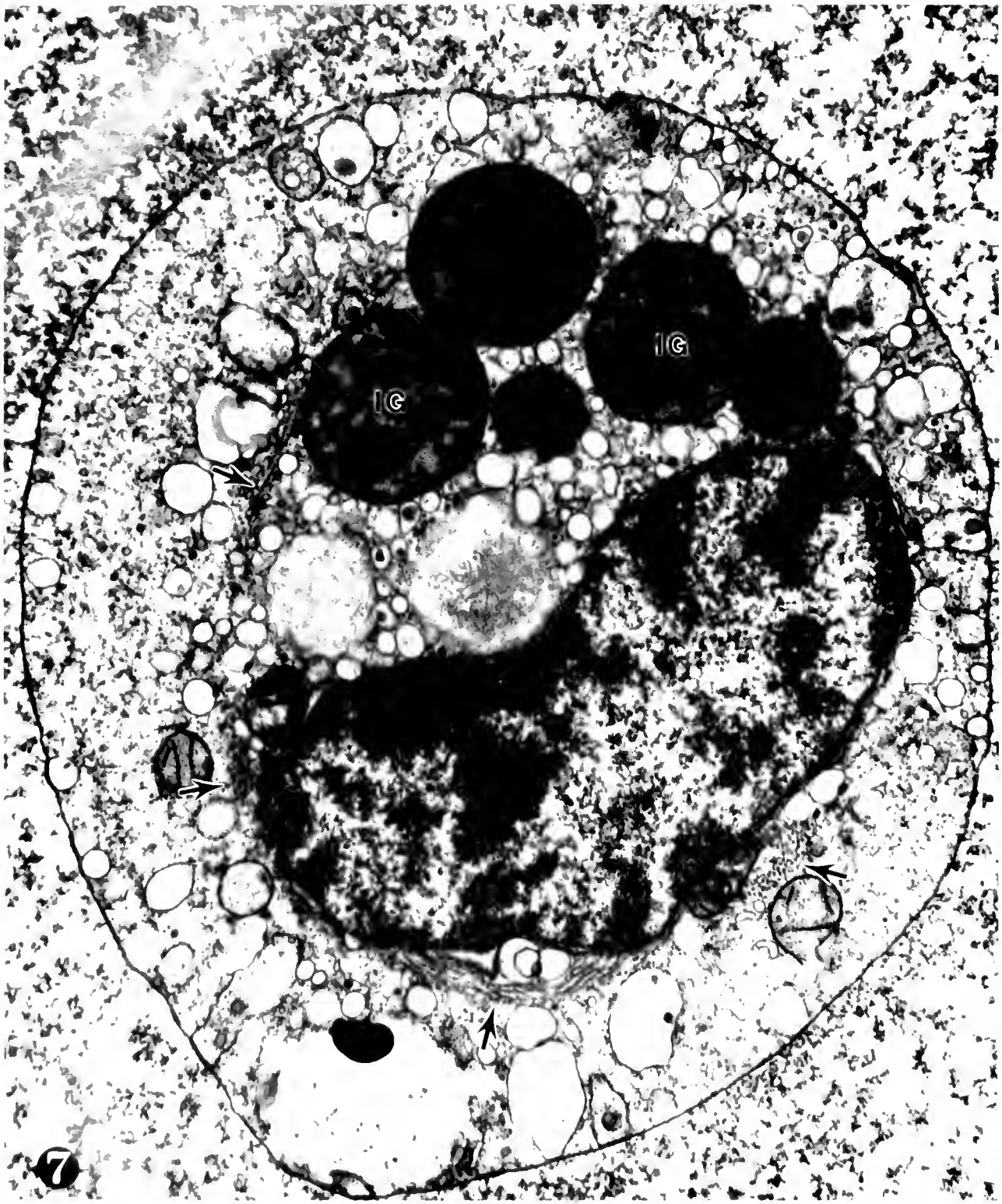

Figure 7. The rearrangement of the cortical actin network in endotoxin-activated cells may exert tension on the marginal band (▶), resulting in both constriction and twisting. This twist is illustrated by the various planes at which microtubules are present (MB). Several centralized immature granules (IG) are also present within the cytoplasm close to the nucleus. The apparent thickening of the granule membranes is likely due to the tangential nature of the section. × 24,800.

ginal band appears to remain quite stable. It may be held together by its projections which are most likely microtubule-associated proteins (Amos, 1977; Kim *et al.*, 1979). While a stable microtubule coil is often found in a variety of nucleated erythrocytes (cells which do not undergo exocytosis), it is not typical for cell systems in which the polarity of secretion is dependent upon a specific microtubule arrangement (Rindler *et al.*, 1987). In activated amebocytes, an entire marginal band may extend into a pseudopodium. We suspect that this is a tension related event in which the pseudopodium is extending within the same plane as the MB. In this case, the actin array reorganizes and extends into the pseudopodium, thus releasing the tension it may have previously exerted on the MB and allowing the MB to expand into the pseudopodium. Rare pieces of individual microtubules were observed within pseudopodia, likely due to a short unwinding of an end of the MB. However, we never observed the complete disassembly of the MB. Some types of invertebrate blood cells are extremely reactive to foreign surfaces (Belamarich, 1976). This is especially true of *Limulus* amebocytes (Armstrong, 1980) and also has been examined in lobster blood cells. However, in lobster blood cells, unlike *Limulus* amebocytes, the marginal microtubule band disassembles when the blood cells are activated by surface contact (Cohen, *et al.* 1983).

The changes detected in endotoxin-treated amebocytes were similar, in part, to the observations of Armstrong and Rickles (1982). They noted that amebocytes treated with endotoxin (1 μg/ml) developed a spherical appearance, a shape consistent with our observations. However, they believed that degranulation only occurred in a small percentage of cells. From our studies, it is apparent that after incubation with endotoxin, amebocytes undergo extensive degranulation as well as shape change. The development of a spherical shape was often accompanied by the presence of fine filopodia. We suggest that the spherical nature of the cells may be due to the vastly increased amount of plasma membrane now present as a result of granule membrane-plasma membrane fusion. This increase in plasma membrane could readily accommodate an increase in the overall volume of the cell, resulting in a large sphere in which thinning of the membrane-associated actin network has occurred. An alternative explanation for the change in plasma membrane-associated actin is that during activation, there is a lowering of the intracellular pH which could result in a net depolymerization of actin (Begg and Rebhun, 1979). This depolymerization in concert with a drop in intracellular pH might also be responsible for the apparent decrease in cytoplasmic ground substance seen in both activated states.

There is also displacement of the cortical actin array and MB to a more centralized location. The rearrangement of the MB to a more centralized location suggests constriction of the band, since it is no longer associated with the periphery of the cell, but now condensed around the nucleus. Furthermore, our determinations of mean caliper diameter, which indicated that the nuclear profiles did not change appreciably under any of our experimental conditions, confirmed that the MB had become constricted around the nucleus. Our observations of twisted marginal bands suggest that the movement of the cortical actin array to a perinuclear location likely exerts tension on the MB, resulting in constriction and twisting. However, not all condensed marginal bands were twisted after endotoxin-induced activation. We speculate that those MB that did twist may represent a less stiff population of microtubules. Marginal bands of dogfish thrombocytes also have been noted to constrict around the cell nucleus during activation and clotting (Shepro *et al.*, 1969).

The interactions between actin filaments and microtubules in normal or activated amebocytes are complex. This is suggested, in part, by their central redistribution and colocalization in the endotoxin-treated cells. If such an association was absent, one would predict that the actin arrays would remain associated with the plasma membrane actin. Actin and tubulin have been shown to colocalize in the fresh water ameba *Reticulomyxa* (Koonce and Schliwa, 1986), and some *in vitro* data suggest that microtubule-associated protein 2 can cross-link actin filaments and microtubules (Griffith and Pollard, 1982). However, there are no reported *in vivo* studies which document linkage either directly between actin and microtubules or via associated linking proteins. Therefore, the nature of the interaction between actin filaments and microtubules in *Limulus* amebocytes remains unknown.

Previous studies have compared *Limulus* amebocytes with anucleate mammalian platelets, with regard to their roles in hemostasis and thrombosis (Levin, 1985a). We also have noted some cytoskeletal similarities between the two cell types. Both amebocytes and human platelets (Fox *et al.*, 1984; Tuszynski *et al.*, 1985; Fox and Phillips, 1986) have an actin-membrane skeleton which appears to link the cytoskeleton with the plasma membrane. The extensive cortical actin array present in *Limulus* amebocytes has been detected in human (Fox and Phillips, 1983; Boyles *et al.*, 1985) and bovine (Tablin, pers. obs.) platelets.

A marginal band of microtubules is present in both cell types; but its properties and potential physiologic roles differ. In both amebocytes and platelets, the marginal microtubule band has been suggested to help maintain the discoid shape of the cells, in conjunction with

the actin filament-plasma membrane network (Nachmias, 1980; White *et al.*, 1984; Cohen and Nemhauser, 1985). However, the marginal microtubule band of amebocytes is an extremely stable structure which undergoes very little disruption under a range of stimuli. In contrast, the microtubule coil of both human and bovine platelets appears to be more responsive to physiological stimuli (Debus *et al.*, 1981; White, 1987). Although it appears that the *Limulus* amebocyte cytoskeleton does not play a role in exocytosis, there are suggestions that the human platelet microtubule coil may be important in the centralization of granules prior to secretion (Allen *et al.*, 1979; Stenberg *et al.*, 1984; White and Burris, 1984).

Further studies are needed to fully assess the amebocyte cytoskeleton and its related proteins, and to more completely compare amebocytes with mammalian platelets. We are currently biochemically characterizing amebocyte cytoskeletal components and their potential interactions.

Acknowledgments

We thank Marlene Castro and Susan Houghton for their excellent technical assistance. Extensive studies by Dr. Eugene Copeland at the Marine Biological Laboratory, Woods Hole, Massachusetts, established the basis for the techniques we used for the collection and fixation of *Limulus* amebocytes. This work was supported by a grant-in-aid from the American Heart Association (FT) and Research Grant HL 31035 from the National Heart, Lung, and Blood Institute, National Institutes of Health, Bethesda, MD. F.T. was the recipient of the Frederik B. Bang Fellowship from the Marine Biological Laboratory, during the performance of some of these studies.

Literature Cited

Allen, R. D., L. R. Zacharski, S. T. Widirstky, R. Rosenstein, L. M. Zaitlin, and D. R. Burgess. 1979. Transformation and motility of human platelets: details of the shape change and release reaction observed by optical and electron microscopy. *J. Cell Biol.* **83:** 126–142.

Amos, L. A. 1977. Arrangement of high molecular weight associated proteins on purified mammalian brain microtubules. *J. Cell Biol.* **72:** 642–654.

Armstrong, P. B. 1979. Motility of the *Limulus* blood cell. *J. Cell Sci.* **37:** 169–180.

Armstrong, P. B. 1980. Adhesion and spreading of *Limulus* blood cells on artificial surfaces. *J. Cell Sci.* **44:** 243–262.

Armstrong, P. B. 1985. Adhesion and motility of the blood cells of *Limulus*. Pp. 77–124 in *Blood Cells of Marine Invertebrates: Experimental Systems in Cell Biology and Comparative Physiology*, W. D. Cohen, ed. Alan R. Liss, New York.

Armstrong, P. B., and F. R. Rickles. 1982. Endotoxin-induced degranulation of the *Limulus* amebocyte. *Exp. Cell Res.* **140:** 15–24.

Bang, F. B. 1956. A bacterial disease of *Limulus polyphemus*. *Bull. Johns Hopkins Hosp.* **98:** 325–351.

Bang, F. B. 1979. Ontogeny and phylogeny of response to gram-negative endotoxins among the marine invertebrates. Pp. 109–123 in *Biomedical Applications of the Horseshoe Crab (Limulidae)*, E. Cohen *et al.*, eds. Alan R. Liss, New York.

Begg, D. A., and L. I. Rebhun. 1979. pH regulates the polymerization of actin in the sea urchin egg cortex. *J. Cell. Biol.* **83:** 241–248.

Belamarich, F. A. 1976. Hemostasis in animals other than mammals: the role of cells. Pp. 191–209 in *Progress in Hemostasis and Thrombosis*, Vol. 3, T. H. Spaet, ed. Grune and Stratton, New York.

Boyles, J., J. E. B. Fox, D. R. Phillips, and P. E. Stenberg. 1985. Organization of the cytoskeleton in resting discoid platelets: preservation of actin filaments by a modified fixation that prevents osmium damage. *J. Cell Biol.* **101:** 1463–1472.

Cohen, W. D., D. Bartelt, R. Jaeger, G. Langford, and I. Nemhauser. 1982. The cytoskeletal system of nucleated erythrocytes. I. Composition and function of major elements. *J. Cell Biol.* **93:** 828–838.

Cohen, W. D., I. Nemhauser, and M. Cohen. 1983. Marginal bands of lobster blood cells: disappearance associated with changes in cell morphology. *Biol. Bull.* **164:** 50–61.

Cohen, W. D., and I. Nemhauser. 1985. Marginal bands and the cytoskeleton in blood cells of marine invertebrates. Pp. 3–49 in *Blood Cells of Marine Invertebrates: Experimental Systems in Cell Biology and Comparative Physiology*, W. D. Cohen, ed. Alan R. Liss, New York.

Copeland, D. E., and J. Levin. 1985. The fine structure of the amebocyte in the blood of *Limulus polyphemus*. I. Morphology of the normal cell. *Biol. Bull.* **169:** 449–457.

Debus, E., K. Weber, and M. Osborn. 1981. The cytoskeleton of blood platelets viewed by immunofluorescence microscopy. *Eur. J. Cell Biol.* **24:** 45–52.

Dumont, J. N., E. Anderson, and G. Winner. 1966. Some cytologic characteristics of the hemocytes of *Limulus* during clotting. *J. Morphol.* **119:** 181–208.

Elias, H., and D. M. Hyde. 1983. *A Guide to Practical Stereology*. S. Karger, Basel, Switzerland. Pp. 45–82.

Fawcett, D. W., and F. Witebsky. 1964. Observations on the ultrastructure of nucleated erythrocytes and thrombocytes with particular reference to the structural basis of their discoidal shape. *Z. Zellforsch. Mikrosk. Anat.* **62:** 785–806.

Fox, J. E. B., and D. R. Phillips. 1983. Polymerization and organization of actin filaments within platelets. *Sem. Hematol.* **20:** 243–260.

Fox, J. E. B., J. K. Boyles, C. C. Reynolds, and D. R. Phillips. 1984. Actin filament content and organization in unstimulated platelets. *J. Cell Biol.* **98:** 1985–1991.

Fox, J. E. B., and D. R. Phillips. 1986. Actin-membrane interactions in platelets. Pp. 281–292 in *Membrane Skeletons and Cytoskeletal-Membrane Associations*, V. Bennett *et al.*, eds. Alan R. Liss, New York.

Griffith, L. M., and T. D. Pollard. 1982. The interaction of actin filaments with microtubules and microtubule-associated proteins. *J. Biol. Chem.* **257:** 9143–9151.

Kim, H., L. I. Binder, and J. L. Rosenbaum. 1979. The periodic association of MAP 2 with brain microtubules *in vitro*. *J. Cell Biol.* **80:** 266–276.

Koonce, M. P., and M. Schliwa. 1986. Reactivation of organelle movements along the cytoskeletal framework of a giant freshwater ameba. *J. Cell Biol.* **103:** 605–612.

Levin, J. 1985a. The role of amebocytes in the blood coagulation mechanism of the horseshoe crab *Limulus polyphemus*. Pp. 145–163 in *Blood Cells of Marine Invertebrates: Experimental Systems*

in Cell Biology and Comparative Physiology, W. D. Cohen, ed. Alan R. Liss, New York.

Levin, J. 1985b. The history of the development of the *Limulus* amebocyte lysate test. Pp. 3–28 in *Bacterial Endotoxins: Structure, Biomedical Significance and Detection with the Limulus Amebocyte Lysate Test*, J. W. ten Cate *et al.*, eds. Alan R. Liss, New York.

Levin, J., and F. B. Bang. 1964a. The role of endotoxin in the extracellular coagulation of *Limulus* blood. *Bull. Johns Hopkins Hosp.* **115:** 265–274.

Levin, J., and F. B. Bang. 1964b. A description of cellular coagulation in the *Limulus*. *Bull. Johns Hopkins Hosp.* **115:** 337–345.

Levin, J., and F. B. Bang. 1968. Clottable protein in *Limulus*: its localization and kinetics of its coagulation by endotoxin. *Thromb. Diath. Haemorrh.* **19:** 186–197.

Loeb, L. 1928. Amebocyte tissue and ameboid movement. *Protoplasma* **4:** 596–625.

Murer, E. H., J. Levin, and R. Holme. 1975. Isolation and studies of the granules of the amebocytes of *Limulus polyphemus*, the horseshoe crab. *J. Cell. Physiol.* **86:** 533–542.

Nachmias, V. T. 1980. Cytoskeleton of human platelets at rest and after spreading. *J. Cell Biol.* **86:** 795–802.

Nemhauser, I., R. Ornberg, and W. D. Cohen. 1980. Marginal bands in blood cells of invertebrates. *J. Ultrastruct. Res.* **70:** 308–317.

Ornberg, R. L., and T. S. Reese. 1981. Beginning of exocytosis captured by rapid-freezing of *Limulus* amebocytes. *J. Cell Biol.* **90:** 40–54.

Rindler, M. J., I. E. Ivanov, and D. D. Sabatini. 1987. Microtubule-acting drugs lead to the nonpolarized delivery of the influenza hemagglutinin to the cell surface of polarized Madin-Darby canine kidney cells. *J. Cell Biol.* **104:** 231–241.

Shepro, D., F. A. Belamarich, F. B. Merk, and F. C. Chao. 1969. Changes in thrombocyte ultrastructure during clot retraction. *J. Cell Sci.* **4:** 763–779.

Stenberg, P. E., M. A. Shuman, S. P. Levine, and D. F. Bainton. 1984. Redistribution of alpha granules and their contents in thrombin stimulated platelets. *J. Cell Biol.* **98:** 748–760.

Tuszynski, G. P., J. L. Daniel, and G. Stewart. 1985. Association of proteins with the platelet cytoskeleton. *Sem. Hematol.* **22:** 303–312.

White, J. G. 1987. The secretory pathway of bovine platelets. *Blood* **69:** 878–885.

White, J. G., and S. M. Burris. 1984. Morphometry of platelet internal contraction. *Am. J. Pathol.* **115:** 412–417.

White, J. G., S. M. Burris, D. Tukey, C. Smith, and C. C. Clawson. 1984. Micropipette aspiration of human platelets: Influence of microtubules and actin filaments on deformability. *Blood* **64:** 210–214

Reference: *Biol. Bull.* 175: 430–433. (December, 1988)

Independent Development of Bilaterally Homologous Closer Muscles in Lobster Claws

C. K. GOVIND AND JOANNE PEARCE

Life Sciences Division, Scarborough Campus, University of Toronto, 1265 Military Trail, Scarborough, Ontario, M1C 1A4, Canada

Abstract. The fiber composition of the closer muscle in the paired claws of the lobster *Homarus americanus* was determined in juvenile 8th and 9th stage animals following various experimental manipulations of the substrate and the claws in the early juvenile 4th and 5th stages. One of the paired muscles developed 90% fast fibers and 10% slow fibers, typical of a cutter claw. The other muscle varied in its fiber composition with fast fibers ranging from 10–90%. This range was categorized into three muscle types: a cutter with 70–90% fast fibers, a crusher with 10–30% fast, and an intermediate with 40–60% fast. The paired homologous claw closer muscles therefore develop such that one is preprogrammed as a cutter while the other is more plastic and develops along a gradient ranging from a cutter to a crusher.

Introduction

One of the puzzling aspects in the development of animals with bilateral symmetry is the appearance of asymmetry in homologous structures. An excellent example of such bilateral asymmetry is found in the enlarged chelipeds or claws of crustaceans such as male fiddler crabs, hermit crabs, snapping shrimps, and lobsters. In these, the paired claws consist of a major and a minor type. In the lobster, *Homarus americanus*, the asymmetry is expressed not only in the external morphology but in the fiber composition of the closer muscle as well (reviewed by Govind, 1984). Thus the major or crusher claw has a closer muscle comprised entirely of slow fibers; the minor or cutter muscle has predominantly fast fibers. Moreover, claw laterality is random (Herrick, 1911) and is determined during the juvenile 4th and 5th stages when the paired claws and closer muscles are still bilaterally symmetric (Emmel, 1908; Lang *et al.*, 1978). Once claw type is determined during the critical period, it is fixed for life (Emmel, 1908). The determination of claw type appears to initially involve the CNS and only later involves changes in the claw itself (Govind and Pearce, 1986). One of these changes is in the fiber composition of the closer muscle which may be bilaterally symmetric or asymmetric. By examining a large number of paired muscles in both configurations, we deduce that these bilaterally homologous muscles develop independently of each other. One of the paired muscles invariably develops as a cutter; the other muscle develops along a gradient ranging from a cutter to a crusher.

Received 1 June 1988; accepted 23 August 1988.

Materials and Methods

Larval lobsters (*Homarus americanus*) were obtained from the Massachusetts State Lobster Hatchery on Martha's Vineyard. They were reared at the Marine Biological Laboratory by procedures described previously (Lang, 1975) until the 8th or 9th stage, a period of three to four months from June to September. The molt history of each lobster and of its paired claws was recorded. Muscle fiber typing was performed histochemically by staining for myofibrillar ATPase activity via standard procedures (Ogonowski *et al.*, 1980). Cross-sections in the mid region of the claw, where the closer muscle had the largest area, were photographed and printed with a final enlargement of 100×. The percentage of fast and slow muscle fibers was calculated from these photographic prints by one of two methods, each of which yielded results varying by 2%. Thus the cross-sectional surface area occupied by each fiber type was calculated via (i.) a transparent acetate overlay marked in centimeter squares or (ii.) weighing "cut-outs" of the relevant areas.

The lobsters reported in this study came from a series of experiments in which the 4th and 5th stage were treated in various ways to control claw laterality. These treatments are classified under one of the following categories: (i.) no substrate in the 4th and 5th stages; (ii.) oyster chips provided at selected intervals during the 4th and 5th stages; (iii.) oyster chips provided in the 4th and 5th stages but with one of the claws immobilized by glueing it shut; or (iv.) oyster chips in the 4th and 5th stages but with one of the claws removed. All of these treatments, except the first, induced the development of paired asymmetric, cutter and crusher claws in the majority of lobsters (Govind and Kent, 1982). The first treatment suppressed the development of a crusher claw in a majority of lobsters, and instead produced lobsters with paired cutter claws. The present report quantitatively examines the fiber composition of the paired closer muscles from representative examples of lobsters reared under a variety of conditions. In this way the variability between bilaterally homologous muscles may be documented and developmental interactions between them noted.

Results and Discussion

The determination of claw type was usually made in the juvenile 8th or 9th stage on the basis of external morphology. At this stage the crusher appeared as a slightly stouter claw with a central molar-like tooth compared to the cutter which is a more slender claw and has a central incisor-like tooth (Herrick, 1911; Emmel, 1908). Occasionally, a claw appeared that was difficult to characterize as either a crusher or cutter since it had an external morphology intermediate to the two types. This unusual intermediate type as well as the usual cutter and crusher type claws were studied for the fiber composition of their closer muscles. However, in all cases the muscles were examined in bilaterally paired claws which included the asymmetric configuration of a cutter claw and either a crusher or an intermediate claw, and the symmetric configuration of paired cutter claws. Representative examples of the closer muscles from these three configurations of paired claws are shown in Figure 1. The percent composition of fast and slow fibers from the paired closer muscles of 35 animals is listed in Table I. The listing showed that one of the paired muscles was invariably a cutter type with a fairly constant composition of 90% fast and 10% slow fibers. The distribution of these fiber types was also constant; the fast muscle occupied most of the cross-sectional area while the slow muscle was restricted to a narrow ventral band (Fig. 1). The other claw of the homologous pair had a fast fiber composition ranging from 10 to 90%. In other words, the contralateral muscle was either another cutter muscle with 70–90% fast fibers, a crusher muscle with 10–30% fast, or an intermediate muscle with 50% fast.

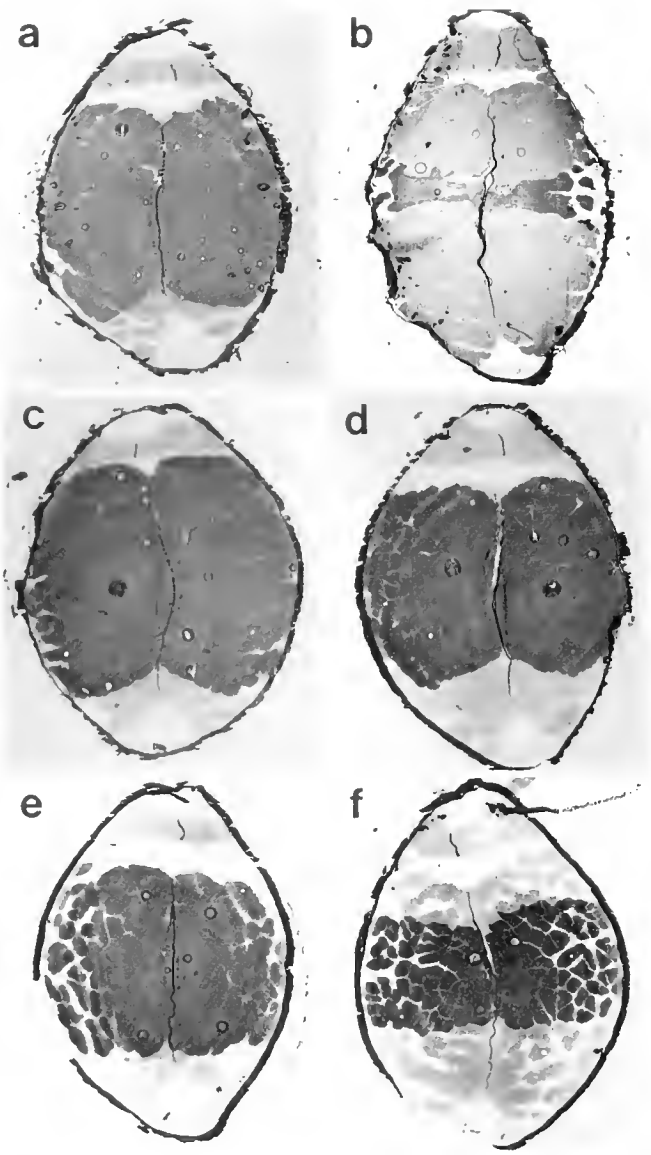

Figure 1. Representative cross-sections of bilaterally paired claws in juvenile 8th stage lobsters. In each section, the small, dorsally situated opener muscle stains lightly for myofibrillar ATPase activity, indicating slow fibers. The massive closer muscle has a mixture of light and dark staining indicating slow and fast fibers, respectively, which are classified into three types: a cutter type (a, c, d, e) with a majority of fast fibers, a crusher type (b) with a minority of fast fibers, and an intermediate type (f) with equivalent fast and slow fiber populations. The paired muscles therefore represent an asymmetric (a, b), symmetric (c, d), and intermediate (e, f) configuration in which one of the muscles is a cutter type (a, c, e) and the other is a crusher (b), another cutter (d), or an intermediate (f). Magnification = 25×.

The relationship between paired homologous muscles is better seen when the fiber composition of one muscle is plotted against that of its counterpart (Fig. 2); in this case the fast fiber composition was used. It became even more apparent that one of the paired muscles, either the

Table I

Muscle fiber composition in homologous claw closer muscles among juvenile 8th and 9th stage lobsters following various treatments in the 4th–5th stages

Treatment	Stage	Muscle 1		Muscle 2	
		% Fast	% Slow	% Fast	% Slow
No substrate in 4th, 5th	8	90	10	47	53
	8	90	10	85	15
	8	90	10	51	49
	8	90	10	30	70
	9	90	10	78	22
	9	93	7	50	50
	9	90	10	16	84
	9	90	10	72	28
	9	90	10	90	10
	9	90	10	26	74
	9	93	7	80	20
	9	90	10	90	10
Substrate					
in 4th	8	90	10	10	90
	8	90	10	50	50
	8	90	10	50	50
	8	85	15	48	52
in 5th	8	90	10	13	87
	8	90	10	90	10
	8	90	10	85	15
in early 5th	8	90	10	10	90
	8	93	7	15	85
	8	90	10	43	57
	8	83	17	83	17
in 4th, and 5th	9	90	10	90	10
	9	90	10	13	87
Substrate and one claw immobilized	8	91	9	48	52
	8	90	10	10	90
	8	90	10	50	50
	8	90	10	75	25
Substrate and one claw removed	8	90	10	45	55
	8	90	10	15	85
	8	90	10	40	60
	9	90	10	27	73
	9	90	10	56	64
	9	90	10	25	75

right or left one, was invariably of the cutter type with 90% fast fibers. The other muscle had a fast fiber population typical of a cutter, crusher, or intermediate type and therefore developed independently of its homologous counterpart.

How may such independent development of bilaterally homologous muscles occur? To formulate an hypothesis regarding this question, recognizing certain salient features about the development of paired homologous muscles is helpful. First, these lobsters did not develop paired crusher claws; nor has there been a single case of such a symmetrical configuration recorded in over 2000 laboratory-reared lobsters in the past 15 years in our facilities at the Marine Biological Laboratory. However, lobsters with paired crusher claws are occasionally found in the wild (Herrick, 1911) but even in these one of the paired closer muscles had approximately 40% fast fibers (Govind and Lang, 1979). Second, and as a corollary to the first point, is the fact that one of the paired claws invariably developed into a cutter. Third, not only did one claw become a cutter, but its closer muscle had almost a fixed fiber composition of 90% fast and 10% slow. In other words, the development of one of the paired muscles appeared to be a preprogrammed event. Fourth, the other (contralateral) muscle of a pair showed variability in its fiber composition. The variability was seen not only in that this second muscle became either a crusher, intermediate, or cutter type, but also in the fact that even as a cutter muscle its fast fiber composition ranged from 70–90% as compared to the almost fixed value of 90% for the preprogrammed cutter muscle. In this respect the second muscle of the homologous pair showed developmental plasticity. Thus, there appeared to be a divergence in the expression of phenotype between the paired homologous muscles in that while one muscle acquired its fiber composition according to a

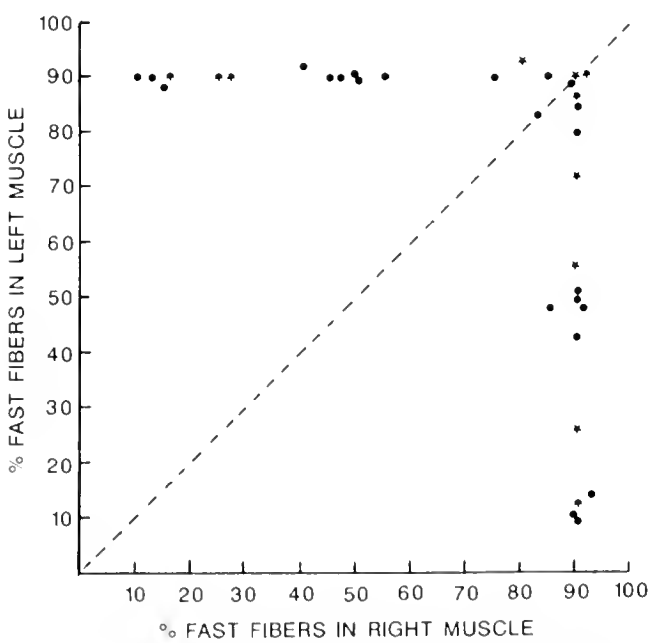

Figure 2. Relationship between the paired right and left closer muscles in terms of percent fast fibers in juvenile 8th (circles) and 9th (stars) stage lobsters. The broken line represents a line of symmetry where the paired muscles would be identical in fiber composition. The data points cluster about this line in the case of lobsters with paired cutter muscles but lie far from this line in the case of lobsters with paired cutter/crusher claws.

fixed program, its counterpart followed a more plastic route.

The initial decision for claw placement is made on the basis of differences in reflexive activity from the claws themselves (Govind and Pearce, 1986). Exercising one of the claws by making it reflexly grip an object causes that claw to develop into a crusher while the opposite claw becomes a cutter. However, when both claws were exercised neither became a crusher but both developed as cutters. These experiments suggest that neural input from the reflexively evoked claw activity impinging on the CNS, in this case the first thoracic ganglion, induces the side with the higher activity to become the crusher side while the opposite side becomes the cutter. When bilateral differences in neural input are minimal, the CNS fails to be lateralized and both sides develop into cutter types. Indeed, the cutter claw would represent a primitive type which would develop irrespective of any extrinsic influences such as reflexive claw activity. This would explain why when claw activity is minimized, such as when lobsters are reared without a substrate (Govind and Kent, 1982), both claws develop as cutters. For a crusher claw to develop, additional instructions must be superimposed onto the primitive cutter pattern—instructions which would promote the differentiation of slow fibers. These instructions would be restricted to one side as they arise because of bilateral differences. They would also have to be graded in nature to account for the fact that the second muscle may have a variable percentage of slow fibers.

Acknowledgments

We thank Dr. I. M. Campbell and C. Gee for critical comments, M. Syslow for generous supplies of larval lobsters, the Natural Sciences and Engineering Council, and the Muscular Dystrophy Association of Canada for financial support.

Literature Cited

Emmel, V. E. 1908. The experimental control of asymmetry at different stages in the development of the lobster. *J. Exp. Zool.* **5:** 471–484.

Govind, C. K. 1984. Development of asymmetry in the neuromuscular system of lobster claws. *Biol. Bull* **167:** 94–119.

Govind, C. K., and K. S. Kent. 1982. Transformation of fast fibres to slow prevented by lack of activity in developing lobster muscles. *Nature* **298:** 755–757.

Govind, C. K., and F. Lang. 1979. Physiological asymmetry in the bilateral crusher claws of a lobster. *J. Exp. Zool.* **207:** 27–32.

Govind, C. K., and J. Pearce. 1986. Differential reflex activity determines claw and closer muscle asymmetry in developing lobsters. *Science* **233:** 354–356.

Herrick, F. H. 1911. Natural history of the American lobster. *U. S. Bur. Fish.* **29:** 149–408.

Lang, F. 1975. A simple culture system for juvenile lobsters. *Aquaculture* **6:** 389–393.

Lang, F., C. K. Govind, and W. J. Costello. 1978. Experimental transformation of fiber properties in lobster muscle. *Science* **201:** 1037–1039.

Ogonowski, M. M., F. Lang, and C. K. Govind. 1980. Histochemistry of lobster claw closer muscles during development. *J. Exp. Zool.* **213:** 359–367.

Reference: *Biol. Bull.* 175: 434–438. (December, 1988)

A Comparative Study of Terrestrial Adaptations of the Gills in Three Mudskippers—*Periophthalmus chrysospilos, Boleophthalmus boddaerti,* and *Periophthalmodon schlosseri*

W. P. LOW, D. J. W. LANE, AND Y. K. IP

Department of Zoology, National University of Singapore, Kent Ridge, Singapore 0511

Abstract. The three mudskippers—*Periophthalmus chrysospilos, Boleophthalmus boddaerti,* and *Periophthalmodon schlosseri*—occupy the same macrohabitat in Singapore but have different behaviors. Correlations were made between differences in behavior and morphological adaptations of their gills to tolerate terrestrial exposure.

P. schlosseri has branched gill filaments, thick gill rods, and fused secondary lamellae which enable them to better adapt to a terrestrial than an aquatic environment. Of the three mudskippers, *P. chrysospilos* gills are the shortest. They are also bent and poorly developed for aquatic respiration. *B. boddaerti* gills consist of numerous long filaments and have the largest gill area of the three mudskippers. These features suggest that *B. boddaerti* gills function more efficiently as a respiratory organ in water than in air.

Gill surfaces of all three mudskippers are highly convoluted to increase surface area.

Introduction

The three mudskippers—*P. chrysospilos, B. boddaerti,* and *P. schlosseri*—were found at Pasir Ris, a small estuary at the east coast of Singapore. They differ markedly in size, microhabitat and behavior (Lee *et al.*, 1987; Siau and Ip, 1987). Maximum weights recorded in our laboratory for *P. schlosseri, B. boddaerti,* and *P. chrysospilos* were 110 g, 35 g, and 14 g, respectively. *B. boddaerti* and *P. schlosseri* inhabit mudflats which are periodically inundated by the tide. The former makes burrows on the lower region of the intertidal zone while the latter burrows on higher ground. At low tide, both are found on the mudflats. At high tide, *B. boddaerti* stays in its water-filled burrows and resurfaces only when the tide ebbs while *P. schlosseri* often swims with its snout and eyes above water along the water's edge. *P. chrysospilos* inhabits the littoral zone of the beach near the mudflats. At high and low tides, it rests on land next to water. Often, it clings to mangrove roots or tree trunks with only its tail fin dipped into water. When disturbed, both *P. schlosseri* and *P. chrysospilos* rapidly skim across the water surface in several bounds while *B. boddaerti* dives and remains submerged.

The feeding habits of the three mudskippers also differ (Khoo, 1966). *P. chrysospilos* tends to be carnivorous but takes some supplement of plant material. *P. schlosseri* is completely carnivorous. *B. boddaerti* is herbivorous. The latter mudskipper has a unique feeding behavior. On the surface of the mudflats, it makes rapid side-to-side movements of the head, skimming off a thin layer of mud and algae. Such feeding habit is followed by vibrating movements of the lips and operculae, during which the algae are presumably filtered (Khoo, 1966).

A problem that mudskippers face upon terrestrial exposure is the collapse of gills and the coalescence of their secondary lamellae, thus significantly reducing their functional respiratory area. Although the gill morphometry of *B. boddaerti* (Niva *et al.*, 1981; Hughes and Al-Kadhomiy, 1986), *B. chinensis,* and *P. cantonensis* (Tamura and Moriyama, 1976) have been studied, the structural adaptations of their gills to withstand terrestrial exposure has been mostly ignored. Thus, the present study was undertaken to examine the morphological ad-

Received 9 February 1987; accepted 6 September 1988.

aptations of the gills of *P. chrysospilos*, *B. boddaerti*, and *P. schlosseri* by scanning electron microscopy (SEM) with an attempt to correlate their unique gill structures to their different behaviors observed in their natural habitats.

Materials and Methods

Mudskippers ranging from young to fully grown adults (2–14 g for *P. chrysospilos*, 2–33 g for *B. boddaerti*, 3–110 g for *P. schlosseri*) were captured at Pasir Ris, Singapore, and maintained in the laboratory in 50% seawater (18‰ salinity). Fish were killed by pithing and the gills were dissected, washed with 0.85% sodium chloride solution, and immersed in 5% formalin made with 50% SW. After one day in the above mentioned solution, individual left arches were dehydrated through a graded ethanol series with a final change in acetone. The tissues were critical-point-dried with CO_2. Each arch was affixed onto a specimen stub with silver paint and then coated with a thin layer of gold using a JEOL Fine Coat JFC-1100 ion sputter. All specimens were viewed under a scanning electron microscope (JEOL JSM 35CF).

A specimen was chosen from each genera of captured mudskippers such that the three fishes were of similar weight to enable comparison of their gill parameters. Gill dimensions of all four left arches were measured following Hughes' (1984a) method. The filament length, secondary lamellar frequency, and area were calculated from measurements of every fifth filament in *P. chrysospilos* and *B. boddaerti*. Due to a substantial number of branched filaments, the filament length and the secondary lamellar frequency were obtained in *P. schlosseri* from measurements of every two filaments. The secondary lamellar area of this fish was determined from measurements of three filaments—one from the center (usually branched), and two from the mid-point between the center and the dorsal and ventral aspects of the arch. The filament number, filament length, and gill area from the left arches were doubled to account for the right arches.

Results

Preliminary observations of the mudskipper gills were performed immediately upon excision from the fish. These observations were then compared with the prepared samples for scanning electron microscopy (SEM) and it was ascertained that there was no macroscopic artifact caused by the preparation procedure.

P. chrysospilos has short and twisted filaments (Fig. 1). The secondary lamellae taper markedly towards the filament tip (Fig. 2). The gill rakers on all arches appear knob-like (Fig. 1). Branched gill filaments seldom occur. The filaments of *B. boddaerti* are arranged in a sheet-like fashion (Fig. 3). Unlike *P. chrysospilos*, the decrease in secondary lamellar size towards the filament tip is relatively gradual while the gill rakers are broad and leaf-like (Fig. 4). Like *P. chrysospilos*, branched gill filaments occur as exceptions. *P. schlosseri* is unique in having a substantial number of complexly branched filaments (Fig. 5), each with several filament tips. It also differs from the other two mudskippers in having conspicuously thick gill rods and extensive interlamellar fusions on the same filament (Fig. 6). Its gill rakers resemble those of *P. chrysospilos;* they too are knob-like (Fig. 5). The secondary lamellar surfaces of all three species are extensively folded (Fig. 7, 8, 9).

The measured total filament numbers, total filament lengths and total gill areas of the three mudskippers are presented in Table I.

Discussion

The secondary lamellar surface of all three mudskippers (Fig. 7, 8, 9) are highly folded. This greatly increases the gill surface area. Hence, the effective respiratory area of these mudskippers could be much larger than the apparent gill area reported. Being highly terrestrial, the gills of mudskippers constantly face the threat of desiccation. Thus, a primary concern would be to prevent desiccation of the respiratory surface. The raised ridges on gill epithelial cells suggest a mucus supporting function (Morgan and Tovell, 1973; Morris and Pickering, 1975). Such a mucus layer may act as an antidesiccant. It may also prevent frictional abrasion between the lamellae. A similar function has been proposed for the mucus layer on the surface microvilli of the rat mesothelium (Andrews and Porter, 1973).

There are several structural adaptations for physical support of the gills of *P. schlosseri* upon terrestrial exposure, one of which is its branched gill filaments (Fig. 5). As all of the *P. schlosseri* caught had branched gill filaments, it is improbable that these filaments had all undergone anomalous development or were subjected to physical damage as Hughes (1984b) suggested. If these same filaments were unbranched but retained their total length, they would be up to two and a half times longer than the average length of the rest of the filaments on the arch. A branched system accommodates a long filament length into shorter branches which can then derive maximal skeletal support from the gill rods. Furthermore, branched filaments naturally have more filament tips than unbranched ones. As secondary lamellae are added towards the tip of the gill filament, more tips would therefore increase the potential of generating a greater gill area.

Another adaptive feature of *P. schlosseri* gills is the extensive fusion of the secondary lamellae (Fig. 6). Fusion between secondary lamellae of adjacent filaments is not


1

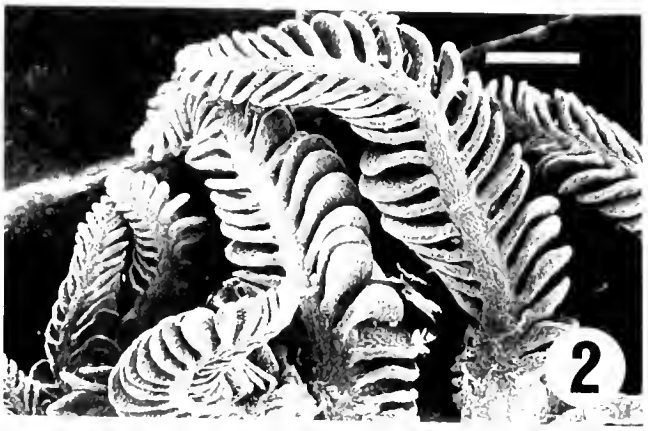
2

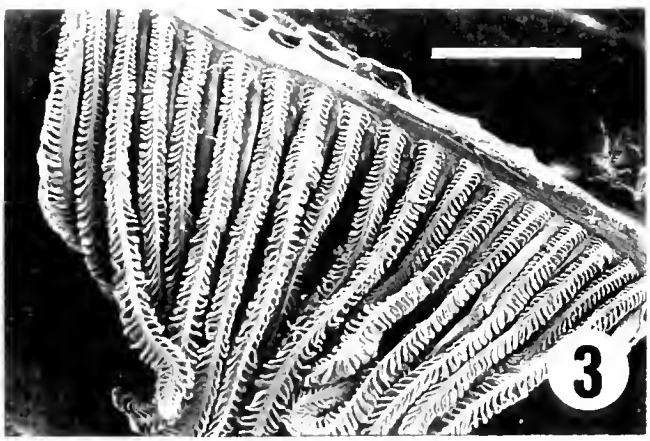
3

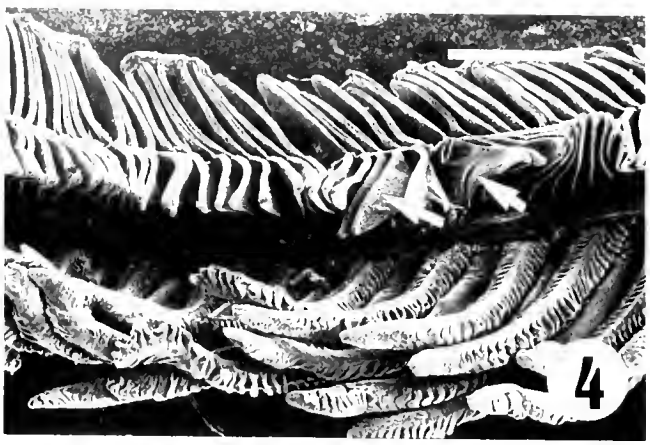
4

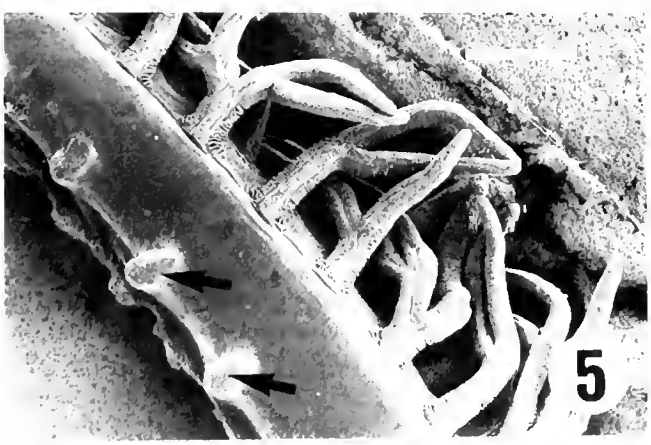
5


6


7

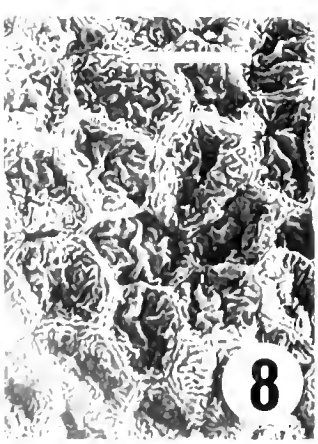
8


9

Table I

Comparison of various measured gill parameters of Periophthalmus chrysospilos, Boleophthalmus boddaerti *and* Periophthalmodon schlosseri

	P. chrysospilos	*B. boddaerti*	*P. schlosseri*
Body weight (g)	13.79	17.70	18.55
Total filament number	235	482	344
Total filament length (mm)	435.66	1295.7	521.6
Total gill area (mm^2)	1183.6	2631	1541

uncommon and in *Amia calva*, such consolidation prevents the secondary lamellae from coalescing upon air exposure (Daxboek *et al.*, 1981). The intrafilamentary secondary lamellar fusions in *P. schlosseri* also form a modified gill structure that imparts considerable support and prevents coalescence of the respiratory surfaces. Moreover, the spaces formed by such fusions may trap water within the fenestrae when the fish emerges from water. This trapped water may help reduce the danger of desiccation of the gills upon prolonged aerial exposure.

Although *P. schlosseri* gills may be capable of withstanding desiccation, they do not appear to be well adapted for aquatic respiration. First, they have fewer filaments, shorter filament length, and smaller gill area than the more aquatic *B. boddaerti*. Second, their intrafilamentary secondary lamellar fusions may prevent water from flowing between the lamellae, reducing the efficiency of the counter-current system of oxygen uptake from water. Finally, the presence of a mucus layer on the fused lamellae may further hinder aquatic gaseous exchange. Thus, all these factors may be partly responsible for the observed terrestrial behavior of *P. schlosseri*.

P. chrysospilos gills exhibit different features of terrestrial adaptation compared to *P. schlosseri*. Their secondary lamellae rapidly decrease in size towards the filament tip (Fig. 2). Therefore, even if the lamellae were to stick to each other upon terrestrial exposure, significant lamellar surface area will still be exposed for gaseous exchange. In contrast, their bent and twisted filaments (Fig. 1) result in their secondary lamellae not being oriented parallel to the respiratory water current, thus reducing the efficiency of the counter-current distribution mechanism. This problem is compounded by its relatively small filament number and short filament length (Table I). Moreover, it has the smallest gill area of the three mudskippers. All these indicate that its gills may play a relatively small role in respiration. Indeed, Tamura *et al.* (1976) showed that oxygen uptake by *P. cantonensis* gills in water was only 52% of the total amount of oxygen respired. As its gills are inefficient in aquatic respiration, it would then rather stay on land where its skin would be responsible for 76% of its oxygen uptake (Tamura *et al.*, 1976).

On the other hand, *B. boddaerti* gills appear better adapted for aquatic than aerial respiration. More of its secondary lamellae are aligned parallel to the respiratory water current (Fig. 3) than *P. chrysospilos;* thus *B. boddaerti* may be more efficient in utilizing the counter-current system for oxygen uptake. Moreover, it has the largest gill area (Table I) of the three mudskippers for gaseous exchange. However, it has the longest and greatest number of filaments; and the longer the filaments, the more likely they will collapse when removed from water. Furthermore, the secondary lamellae within the same filament show minimal tapering towards the filament tip compared to those of *P. chrysospilos*. Thus, when the lamellae coalesce, there will be a significant reduction in the respiratory area and this will limit the terrestrial affinity of *B. boddaerti*.

Figure 1. A gill arch from *Periophthalmus chrysospilos*. Note the bent and twisted filaments. The short and stumpy gill rakers are indicated by the arrows. Scale bar represents 500 μm.

Figure 2. Gill filaments of *P. chrysospilos*. The secondary lamellae decrease markedly in size towards the filament tip. Scale bar represents 200 μm.

Figure 3. The filaments on the gill arch of *Boleophthalmus boddaerti* are arranged in a sheet-like fashion. Scale bar represents 1000 μm.

Figure 4. The fourth gill arch of *B. boddaerti*. The leaf-like gill rakers are indicated by arrows. Scale bar represents 500 μm.

Figure 5. The gill filaments of *Periophthalmodon schlosseri* are complexly branched. The gill rods are conspicuously thickened compared to *P. chrysospilos* and *B. boddaerti*. The gill rakers are short and knob-like (arrows). Scale bar represents 1000 μm.

Figure 6. *P. schlosseri* is unique in having extensive interlamellar fusions on the filament. Scale bar represents 100 μm.

Figure 7. Higher magnification of the highly convoluted secondary lamellar surface in *P. chrysospilos*. Scale bar represents 10 μm.

Figure 8. The secondary lamellar surface is highly folded in *B. boddaerti*. Scale bar represents 10 μm.

Figure 9. The secondary lamellar surface of *P. schlosseri* bears conspicuous raised ridges which may indicate a mucus retaining function. The arrows indicate the interlamellar fusions. Scale bar represents 10 μm.

The behaviors of the mudskippers may also be related to the structure of the gill rakers. One possible function of the gill rakers is to minimize injury to the respiratory organs by straining large particles from the water current that enters the buccopharyngeal cavity away from the gills (Hughes and Morgan, 1973). However, the short and stumpy gill rakers of *P. schlosseri* (Fig. 5) and *P. chrysospilos* (Fig. 1) would be ineffective as a protective straining mechanism, hence, leading to their limited tendencies of submerging in silt-laden water. The gill rakers of *B. boddaerti* are broad and leaf-like (Fig. 4) and may act like a strainer when the mudskipper is in the water and when it feeds on the mudflat algae. Thus, it may be more adapted to entering water than *P. chrysospilos* and *P. schlosseri*. *B. boddaerti* from the Arabian Gulf has been studied by Hughes and Al-Kadhomiy (1986), but the behavior reported in their investigation is unlike the local species in that they were omnivorous and were found at the water's edge at high tide. Hence, it is very likely that the Arabian Gulf *B. boddaerti* is dissimilar to that in the present study.

Acknowledgment

This study was supported by grants RP 70/85 and RP 860337 from the National University of Singapore.

Literature Cited

Andrews, P. M., and K. R. Porter, 1973. The ultrastructural morphology and possible functional significance of mesothelial microvilli. *Anat. Rec.* **177**: 409–426.

Daxboeck, C., D. K. Barnard, and D. J. Randall, 1981. Functional morphology of the gills of the bowfin *Amia calva*, with special reference to their significance during air exposure. *Resp. Physiol.* **43**: 349–364.

Hughes, G. M. 1984a. Measurement of gill area in fishes: practices and problems. *J. Mar. Biol. Assoc. U. K.* **64**: 637–655.

Hughes, G. M. 1984b. General anatomy of the gills. Pp. 1–72 in *Fish Physiology*, Vol. X, W. S. Hoar, and D. J. Randall, eds. Academic Press, New York.

Hughes, G. M., and N. K. Al-Kadhomiy, 1986. Gill morphometry of the mudskipper *Boleophthalmus boddaerti*. *J. Mar. Biol. Assoc. U. K.* **66**: 671–682.

Hughes, G. M., and M. Morgan, 1973. The structure of fish gills in relation to their respiratory function. *Biol. Rev.* **48**: 419–475.

Khoo, K. G. 1966. Studies on the biology of Periophthalmidae fishes in Singapore. Honours thesis, National University of Singapore, Singapore.

Lee, C. G. L., W. P. Low, and Y. K. Ip, 1987. Na^+, K^+ and volume regulation in the mudskipper, *Periophthalmus chrysospilos*. *Comp. Biochem. Physiol.* **87A**(2): 439–448.

Morgan, M., and P. W. A. Tovell, 1973. The structure of the gill of the trout, *Salmo gairdneri* (Richardson). *Z. Zellforsch.* **142**: 147–162.

Morris, R., and A. D. Pickering, 1975. Ultrastructure of the presumed ion-transporting cells in the gills of ammocoete lampreys, *Lampetra fluviatilis* (L.) and *Lampetra planeri* (Bloch). *Cell Tiss. Res.* **163**: 327–341.

Niva, B., J. Ojha, and J. S. D. Munshi, 1981. Morphometries of the respiratory organs of an estuarine goby, *Boleophthalmus boddaerti*. *Jpn. J. Ichthyol.* **27**(4): 316–326.

Siau, H., and Y. K. Ip, 1987. Activities of enzymes associated with phosphoenolpyruvate metabolism in the mudskippers, *Boleophthalmus boddaerti* and *Periophthalmodon schlosseri*. *Comp. Biochem. Physiol.* **88B**(1): 119–125.

Tamura, S. O., H. Morii, and M. Yuzuriha, 1976. Respiration of the amphibious fishes *Periophthalmus cantonensis* and *Boleophthalmus chinensis* in water and on land. *J. Exp. Biol.* **65**: 97–107.

Tamura, O., and T. Moriyama, 1976. On the morphological feature of the gill of amphibious and air-breathing fishes. *Bull. Fac. Fish. Nagasaki Univ.* **41**: 1–8.

Reference: *Biol. Bull.* **175:** 439–445. (December, 1988)

Abstracts of Papers Presented at the MBL Centennial Symposium, "Ion Channels: Structure, Function, and Modulation"[1]

23–25 June 1988

Effects of external and internal Mg on the NMDA activated channel. P. ASCHER AND J. W. JOHNSON (Laboratoire de Neurobiologie, Ecole Normale Supérieure, 46, rue d'Ulm 75005, Paris, France).

It is now well established that the channels opened by N-methyl-D-aspartate (NMDA) in vertebrate central neurons are blocked by extracellular Mg in a voltage dependent way (4, 3). When single channel currents activated by NMDA are recorded in the presence of external Mg, the Mg block leads to characteristic bursts of openings (3, 2). The analysis of these bursts (1) has indicated that as a first approximation the block can be described as an open channel block in which the dissociation constant for Mg is:

$$K_{Mg} = 8.8 \exp(V/12.5)$$

where K_{Mg} is expressed in mM, and V is the membrane potential expressed in mV.

We have investigated the block of the NMDA activated channel by internal Mg. As first reported by Nowak *et al.* (4), this block was not accompanied by a flickering comparable to that observed for external Mg. The single channel current was decreased by internal Mg without any concomitant change of the mean open time. At Mg_i = 1 m*M* the block was only detectable at positive potentials. For Mg_i = 10 m*M* the single channel inward current was also substantially reduced at negative potentials. No voltage dependent block was observed when $(Ca)_i$ was increased to 1 m*M* in the absence of internal Mg. The single channel I–V relation in the presence of Mg_i = 1 m*M* was well described by assuming that the single channel current was reduced by a factor determined by the voltage dependent binding of Mg. The dissociation constant of Mg, K_{Mg}, was calculated as:

$$K_{Mg} = 12 \exp(-V/28)$$

where K_{Mg} is expressed in m*M*, and V in mV.

The block produced by internal Mg thus appears to involve a site that, when V = 0, has an affinity for Mg similar to that of the site involved in the block by external Mg. However, the fact that the block produced by internal Mg does not induce flickering of the single channel current suggests that both the on and off rates of Mg binding are faster in the case of the block by internal Mg.

The simplest interpretation of the voltage dependence of the external Mg block is that the binding site for external Mg is situated on the cytoplasmic side of the membrane (1). However, this interpretation is not compatible with the voltage dependence of the block by internal Mg.

In physiological conditions Mg is present on both sides of the membrane at m*M* concentrations and thus the NMDA channel will conduct current in a restricted voltage range centered near 0 mV. The block by external Mg appears to play an important physiological role, while the functional significance of the block by internal Mg remains to be established.

Literature Cited

(1) Ascher and Nowak 1988. *J. Physiol.* **399:** 247–266.
(2) Jahr and Stevens 1987. *Nature* **325:** 522–525.
(3) Mayer *et al.* 1984. *Nature* **309:** 261–263.
(4) Nowak *et al.* 1984. *Nature* **307:** 462–465.

Structure and regulation of the glycine receptor. H. BETZ, C.-M. BECKER, B. SCHMITT, G. GRENNINGLOH, A. RIENITZ, D. LANGOSCH, AND W. HOCH (ZMBH, Im Neuenheimer Feld 282, 6900 Heidelberg, FRG).

The postsynaptic glycine receptor complex of rat spinal cord is a ligand-gated chloride channel composed of polypeptides of Mr 48,000, 58,000, and 93,000. Molecular cloning data and crosslinking experiments indicate that it has a pentameric ion channel core structure assembled by Mr 48,000 and 58,000 polypeptides which are homologous to nicotinic acetylcholine and $GABA_A$ receptor subunits. The Mr 93,000 polypeptide is associated with cytoplasmic domains of the receptor and may serve as its anchor in the postsynaptic membrane.

During development of the rat spinal cord, the appearance of the adult postsynaptic glycine receptor complex is preceeded by the accumulation of a receptor species characterized by low antagonist affinity and altered immunogenicity. This "neonatal" form of the receptor is abundant in primary spinal cord cultures and may represent a functionally immature receptor species. Possible mechanisms generating glycine receptor heterogeneity during development were discussed.

[1] Abstracts are arranged alphabetically by first author. The generous support of the Monsanto Company is gratefully acknowledged.

Molecular properties of voltage-sensitive sodium and calcium channels. WILLIAM A. CATTERALL (Department of Pharmacology [illegible]-30, University of Washington, Seattle, WA 98[illegible]

The action [illegible] in most excitable cells results from an initial increase in Na [illegible] meability mediated by voltage-sensitive sodium channels fol[illegible]wed by a more prolonged increase in Ca permeability mediated by voltage-sensitive calcium channels. Sodium channels have five separate receptor sites for neurotoxins which have different effects on channel function. Na channels purified from rat brain using saxitoxin binding as an assay consist of three glycoprotein subunits [α(260 kDa), β1 (36 kDa), and β2 (33 kDa)] in 1:1:1 stoichiometry in a complex of 320 kDa. The β2 subunit is linked to α by disulfide bonds while β2 is noncovalently attached. The α subunit is a transmembrane glycoprotein which binds neurotoxins on its extracellular surface and can be phosphorylated by protein kinases on its intracellular surface. The β1 and β2 subunits are integral membrane glycoproteins. Incorporation of the purified Na channel into phospholipid vesicles of appropriate composition restores neurotoxin action at three receptor sites and selective ion flux. Fusion with planar bilayers and treatment with batrachotoxin results in single channels of 23 pS with the ion selectivity, toxin sensitivity, and voltage dependence of batrachotoxin-modified native Na channels. Selective removal of the β1, but not the β2, subunit from the purified complex causes loss of saxitoxin binding and ion conductance (1, 2).

cDNAs encoding the α subunit of the neuronal sodium channel have been identified, cloned, and sequenced (3, 4). They recognize mRNA of 9.0 kb in brain. This single mRNA, purified by hybrid selection or transcribed from cDNA, is sufficient to direct the synthesis of functional sodium channels in *Xenopus* oocytes, but the rate of inactivation is slow compared to native brain sodium channels or sodium channels synthesized from total brain mRNA. Co-expression of mRNAα and low molecular weight brain mRNA restores the rapid rate of sodium channel inactivation and enhances sodium channel expression suggesting that low molecular weight brain protein, possibly including β1 or β2 subunits, can modulate expression and function of the functionally autonomous α subunit. A model of sodium channel structure is developed in which the transmembrane pore is formed by the α subunit with the β1 and β2 subunits peripherally associated (1).

Voltage-sensitive calcium channels participate in the generation of action potentials in excitable cells and play a key role in regulating calcium influx into the cytoplasm. We have used high affinity binding of ^{3}H-labeled dihydropyridine calcium channel blockers to monitor purification of dihydropyridine-sensitive (L-type) calcium channels to homogeneity from skeletal muscle transverse tubules (5). Analysis by SDS-PAGE without reduction of disulfide bonds shows that the purified dihydropyridine-sensitive calcium channels contain polypeptide components of approximately 170 kDa, 54 kDa, and 30 kDa. Further analysis of the purified calcium channel by several specific labeling methods and SDS-PAGE after cleavage of disulfide bonds reveals two distinct high molecular mass polypeptides and an additional protein component of 27 kDa. α1, a 175 kDa subunit which is not N-glycosylated, contains the dihydropyridine binding site, cAMP-dependent protein kinase phosphorylation site(s) and substantial hydrophobic domain(s) labeled by a photoreactive hydrophobic probe. α2, a 143 kDa glycoprotein, has none of the properties characteristic of α1, but binds lectins and contains about 25% N-linked carbohydrate. α2 is a disulfide-linked to δ, a 24-27 kDa glycopeptide. α1 (175 kDa) and $\alpha 2\delta$ (170 kDa) migrate together when disulfide bonds are not reduced. β (54 kDa) contains a cAMP-dependent phosphorylation site, but is not N-glycosylated and does not have a hydrophobic domain. γ (30 kDa) has a carbohydrate content of about 30% and extensive hydrophobic domain(s). Precipitation with affinity-purified anti-α1 antibodies or α2-specific lentil lectin-agarose shows that $\alpha 1\alpha 2\beta\gamma\delta$ behaves as a complex (6). The purified calcium channel complex mediates ^{45}Ca influx after reconstitution into phospholipid vesicles (7). Calcium flux activity is increased by the dihydropyridine agonist Bay K 8644 and inhibited by PN200-110, verapamil, and D600 with apparent K_D values of 0.2, 1.5, and 1.0 μM. Calcium flux activity is increased eight-fold by phosphorylation of the α1 and β subunits with cAMP-dependent protein kinase. A model for subunit interaction and membrane insertion in which the α1 subunit is the central transmembrane component of an oligomeric calcium channel complex is proposed on the basis of these observations (6).

The complete primary structures of sodium channels from rat brain and calcium channels from skeletal muscle transverse tubules have been deduced from cDNA clones (8, 9). Each consists of four internally homologous domains with six proposed transmembrane segments, S1–S6. Mapping of functional sites on sodium channel α subunits with site-directed antibodies has revealed a cluster of 5 cAMP-dependent phosphorylation sites in the intracellular segment between domains I and II (10) and a site of covalent attachment of photoreactive scorpion toxin derivatives in the extracellular loop between transmembrane segments S5 and S6 of domain I (11). Antibodies to the intracellular segment between domains III and IV slow sodium channel inactivation in a voltage-dependent manner, suggesting a role for this region of the α subunit in channel inactivation (12). The highly conserved, α-helical S4 segments in each domain are postulated to transverse the membrane and form the voltage-sensing elements of the Na channel according to a Sliding Helix model of voltage-dependent gating (1). These results begin the development of a functional and topological map of the sodium channel α subunit and provide the basis for a similar analysis of the α1 subunit of the dihydropyridine-sensitive calcium channel. Such functional maps will help to define the molecular basis of electrical excitability.

Literature Cited

(1) Catterall 1986. *Ann. Rev. Biochem.* **55:** 953–985.
(2) Messner *et al.* 1986. *J. Biol. Chem.* **261:** 14882–14890.
(3) Goldin *et al.* 1986. *Proc. Natl. Acad. Sci. USA* **83:** 7503–7507.
(4) Auld *et al.* 1988. *Neuron* **1:** 449–461.
(5) Curtis and Catterall 1984. *Biochemistry* **23:** 2113–2118.
(6) Takahashi *et al.* 1987. *Proc. Natl. Acad. Sci. USA* **84:** 5478–5482.
(7) Curtis and Catterall 1986. *Biochemistry* **25:** 3077–3083.
(8) Noda *et al.* 1986. *Nature* **320:** 188–192.
(9) Tanabe *et al.* 1987. *Nature* **328:** 313–318.
(10) Rossie *et al.* 1987. *J. Biol. Chem.* **36:** 17530–17535.
(11) Tejedor and Catterall 1988. *Proc. Natl. Acad. Sci. USA* **85:** 8742–8746.
(12) Vassilev *et al.* 1988. *Science* **241:** 1658–1661.

Properties and regulation of chloride channels in salt-secreting epithelial cells. RAYMOND A. FRIZZELL (Department of Physiology and Biophysics, University of Alabama, Birmingham, AL 35294).

A Cl-selective apical membrane conductance appears to be the rate-determining step in NaCl secretion by a variety of epithelial tissues. This conductance is regulated by agonists which employ cyclic nucleotides and Ca as the intracellular mediators of their actions. Opening of anion-selective apical membrane channels permits Cl to diffuse down its electrochemical gradient from cell-to-lumen when regulatory pathways are activated. We have used a colonic tumor cell line (184) and human airway cell primary cultures to characterize some of the biophysical and regulatory properties of this channel. This agonist-activated channel is Cl-selective ($P_{Cl}/P_{Na} \sim 50$) and prefers halides in the order of decreasing ionic radius (I > Br > Cl > F). The channel shows

outward rectification, even with symmetrical salt concentrations bathing both sides of excised membranes and shows an open probability *versus* voltage relationship such that membrane depolarization induces an increase in channel open probability. The latter effect may help balance transapical Cl flow with alterations in the driving force for Cl exit at the apical membranes as Cl permeabilities change. This channel is inhibited by substituted disulfonic stilbenes in membrane vesicle, patch-clamp, and planar lipid bilayer preparations. The dinitryl stilbene analog, DNDS, is a reversible channel blocker, whereas the diisothiocynate derivative, DIDS, inhibits the channel irreversibly. These compounds should be useful in attempts to biochemically characterize this important conductance pathway. A defect in the activation of this channel contributes to the pathogenesis of cystic fibrosis (CF). Cell-attached recordings from human airway cells indicate that cAMP-dependent agonists activate Cl channels in normal, but not CF cells. In contrast, Ca-dependent channel activation pathways are intact. In excised membrane patches, the catalytic subunit of cAMP-dependent protein kinase activates Cl channels in membrane patches from normal, but not CF cells, suggesting that the CF defect lies in the apical membrane. Thus, the channel or an associated regulatory protein may not be an appropriate substrate for protein kinase A-mediated phosphorylation or, if phosphorylated, does not alter its conformation in a manner appropriate to permit Cl conduction.

Supported by NIH Grant DK38518 and by the Cystic Fibrosis Foundation.

Bacterial porins as models for voltage-gated channels. R. Michael Garavito (Department of Biochemistry and Molecular Biology, The University of Chicago, 920 East 58th Street, Chicago, IL 60637).

The structural motifs which make up membrane proteins are only now becoming known. With the elucidation of the structures of bacteriorhodopsin, at low resolution, and two bacterial photosynthetic reaction centers, the role of alpha helical secondary structure in creating polypeptide traverses across the lipid bilayer is now established. However there are classes of membrane proteins which apparently do not utilize alpha helices within the membrane. Several transmembrane channel-forming proteins from prokaryotic and eukaryotic systems contain almost no helical secondary structure but a substantial amount of beta sheet. How the beta strands are arranged within the transmembrane region is unclear.

Porins are transmembrane channel-forming proteins in the outer membrane of enterobacteria and are typified by their formation of nonspecific, water-filled pores. These pores allow the passive diffusion of small polar solutes across the lipid bilayer. Some porins also display voltage-induced channel closing (300 pS channel size). Most purified porins have a trimeric subunit structure (3×35–45 kDa) and display an appreciable amount of beta sheet as determined by circular dichroism, X-ray scattering, ATR-IR, and FTIR linear dichroism. The most recent work using FTIR (Nabedryk *et al* 1988, *Biophysical J* **53:** 671–676) suggests that while a significant number of beta strands are oriented perpendicular to the membrane plane, an equivalent number of strands are inclined quite far away from the membrane normal. The most plausible arrangement of the beta strands would be a sandwich-like packing of two near orthogonal sheets where one of the sheets would have its strands aligned along the membrane normal. Such supersecondary structures have often been seen in soluble proteins and are quite stable.

The molecular shape of the porin OmpF has now been elucidated at low resolution (15 Å) by a combination of neutron and X-ray diffraction and molecular replacement. The resulting maps clearly show the position of the three pores in the trimer and their passage through the membrane. The pores are independent and remain roughly 30 Å apart from each other as they pass through the protein. Their exit at the outer face of the protein is not clearly visible and may be the site of the channel gates. The exit of the pores on the periplasmic side of the protein is well defined and demonstrates that the pores remain physically independent. This pore topography is different from that proposed earlier by others using electron microscopic techniques and casts doubts on their interpretations. Tentative evidence also suggests that the pores are formed by the subunit interfaces of the trimer. Status of the current high resolution X-ray structural analysis was discussed.

Presynaptic facilitation, presynaptic inhibition, and the molecular logic of second messenger systems in Aplysia. Eric R. Kandel, David Sweatt, Andrea Volterra, Robert Hawkins, and Steven A. Siegelbaum (Center for Neurobiology and Behavior and Howard Hughes Medical Institute, Columbia University, College of Physicians and Surgeons, 722 West 168th Street, New York, NY 10032).

A striking feature of the organization of the brain is that some synaptic potentials are fast, lasting only milliseconds, whereas others are slow, lasting many seconds or even many minutes. One of the insights of the last several years is the realization that the two types of synaptic interactions involve different molecular mechanisms that serve different behavioral consequences, and are produced by proteins that derive from two distinct gene families.

In both types of synaptic actions, the receptor acted on by the transmitter has a double function: a recognition function at its receptor site as well as an effector function on ion channel activity. Thus, the receptor recognizes the transmitter and instructs the channel to open or close. In fast synaptic actions, like those involving the nicotinic ACh channels at the neuromuscular junction and the channels regulated in the central nervous system by glutamate, glycine, and GABA, the recognition function (receptor) and the effector function (channel) are carried out by different domains of a common multiple subunit protein. By contrast, slow synaptic actions involve separate proteins for recognition and effector functions: the proteins are often at some distance from one another. Remote receptors characterized to date typically consist of a single subunit with seven transmembrane spanning regions. They communicate with their channels via membrane transduction systems such as the GTP-binding proteins and diffusible internal second-messengers such as cAMP and the cAMP-dependent protein kinase.

Slow synaptic actions produced by remote receptors and second messengers have generated much interest because they fulfill quite different functions from the common fast synaptic actions. Whereas the fast synaptic actions produced by the directly acting receptors are utilized by the basic neural circuitry that *mediate behavior*, second messengers produce slow synaptic actions that tend to *modulate behavior* by altering the excitability of neurons and the strength of the synaptic connections of the basic neural circuitry. Specifically, modulatory synaptic pathways can serve as reinforcing stimuli in learning.

The finding that the receptor for the action of some transmitters modulates channel activity via an internal second messenger opens up the possibility for either synergistic or antagonistic interactions between different transmitters that target a common ion channel. For example, a small family of transmitters, each acting through its own independent remote receptors, may act synergistically to modulate the same channel via the same internal second messengers. Alternatively, the receptors could act on the channel antagonistically via different internal messengers.

We have found both of these situations in studies of the gill-withdrawal reflex of *Aplysia*. Here we have encountered an example in an

invertebrate of an observation well established in vertebrates, that stimuli that serve as reinforcers for learning can have two components: a prominent, facilitatory component, and a less obvious, inhibitory component. In vertebrates the facilitatory component is important for sensitization and classical conditioning of excitatory responses. The inhibitory component is important for inhibition and for conditioning of inhibitory responses. Both of these components are also evident in *Aplysia*. Strong stimuli to the tail serve as reinforcing stimuli for sensitization and classical conditioning of the reflex. These stimuli activate modulatory neurons that use the modulatory transmitters serotonin or the peptides SCP_A and SCP_B. The strong tail stimulus and the transmitter produce presynaptic facilitation at sensory-motor synapses by, in part, modulating a specific K^+ channel of the sensory neurons (the S channel) by a common second-messenger system: cyclic AMP (6). By contrast, weaker stimuli to the tail that produce inhibition of the reflex, activate modulatory neurons that use dopamine and the peptide FMRFamide. These weak stimuli and the inhibitory transmitter systems modulate the same S channel in the sensory neurons but now in the opposite way, to produce an inhibitory action on the sensory neuron that is mediated by the lipoxygenase metabolites of arachidonic acid. Dopamine, binding to a D_2-like receptor (19), and FMRFamide, have similar actions. We focus here on FMRFamide.

FMRFamide is of interest because it resembles the carboxy terminus of the met-enkephalin related peptide Tyr-Gly-Gly-*Phe-Met-Arg-Phe*. Moreover, Richard Scheller and his colleagues have studied the organization of the FMRFamide precursor polypeptide and have found important similarities with preproenkephalin, one of which is that multiple basic peptide units are interspersed with variable acidic spacers (7, 14). The FMRFamide gene in *Aplysia* encodes at least 19 individual FMRFamide sequences, a single FLRFamide sequence, and gives rise to multiple polyadenylated RNAs (16). Finally, this structural similarity between FMRFamide and the enkephalin peptides is preserved functionally. Just as enkephalins can produce presynaptic inhibition of nociceptive sensory neurons in vertebrates, FMRFamide produces presynaptic inhibition of sensory neurons in *Aplysia*.

Indeed, the action of FMRFamide and FMRFamidergic inhibitory interneurons is a mirror image of that of the facilitatory systems. As is the case for the facilitatory neurons, the inhibitory systems synapse onto the sensory neuron's cell body and presynaptic terminals. Moreover, we believe that the K^+ channels, modulated by serotonin and FMRFamide, exist not only in the cell body but also on the terminals, where their modulation plays a role in controlling synaptic strength (1). Thus, by investigating the logic whereby these two transmitters, acting through two different second messengers, interact within the cell to regulate channel function, these studies, in a larger sense, address how that interaction contributes to the up-and-down regulation of transmitter release. One final feature makes this interaction of further interest: the two actions are not symmetrical. While the modulatory effects of inhibition are more transient than those of facilitation, this transient inhibition can fully override the facilitation.

Thus, we have examined two questions: (1) how does each of the opposing modulatory systems produce their characteristic actions and (2) how does the inhibitory action override the facilitatory one when the two are presented together?

On the cellular level, the tail stimuli used for sensitization and classical conditioning activate a facilitatory system that contains both serotonergic and peptidergic neurons. The combined actions of these modulatory neurons increase the synaptic strength of the connection between the sensory neuron and the motor neuron by enhancing transmitter release from the terminals of the sensory neuron—a process we call presynaptic facilitation. Presynaptic facilitation involves protein phosphorylation through the cAMP-dependent protein kinase (5). Classical conditioning involves, in addition, a pairing specific, activity-dependent, enhancement of the presynaptic facilitation produced by sensitization.

Behavioral inhibition is reflected at the level of the sensory neuron by presynaptic inhibition of transmitter release, a mirror image process to presynaptic facilitation. This inhibition is induced by the peptide FMRFamide (11). Thus, we found that FMRFamide leads to a decrease in spontaneous transmitter release from the presynaptic terminal of the sensory neuron without affecting the size of the transmitter quanta, indicating that the sensitivity of receptors of the postsynaptic cell is not affected (8). In addition, the inhibition of synaptic transmission produced by FMRFamide is accompanied by a shortening of the duration of the action potential in the sensory neuron. This shortening is partly due to an increase in the sensory neuron of a specific K^+ current (the S current) (2, 3), and partly due to a depression of a specific Ca^{2+} current (4, 9). Finally, we have identified an interneuron, located within the left pleural ganglion, that shows FMRFamide immunoreactivity. This interneuron is activated by tail shock and simulates the presynaptic inhibitory action that tail shock produces (11).

What is the second messenger for this presynaptic inhibition? Whereas the facilitation is mediated through cyclic AMP-dependent protein phosphorylation, work carried out in collaboration with James Schwartz and his colleagues indicates that the inhibition is mediated through the lipoxygenase metabolites of arachidonic acid (15). Indeed, Mackey has now found that NDGA, which blocks the lipoxygenase pathway of arachidonic acid, also blocks the inhibitory consequence of tail stimuli (12).

Single channel recordings indicated that FMRFamide modulate the activity of the S-K^+ channel, one of the major targets of the facilitatory pathway. But whereas serotonin and cyclic AMP-dependent protein phosphorylation lead to closure of the S-K^+ channel, FMRFamide and lipoxygenase metabolites lead to an increase in probability that a channel is open. In addition, FMRFamide reverses the action of serotonin (or cAMP) by opening S-K^+ channels closed by serotonin or cAMP (2). Here, the results with FMRFamide parallel, on a single channel level, the ability of the inhibitory system to transiently override the behavioral facilitation. This override is also evident biochemically. Recent quantitative 2-D gel studies reveal that serotonin and cyclic AMP lead to an increase in the level of phosphorylation of 17 proteins in the sensory neurons. In the absence of serotonin, FMRFamide acts on 10 of these proteins and reduces their basal level of phosphorylation. But, in the presence of serotonin (or cAMP), FMRFamide will override the phosphorylation of all 17 proteins normally phosphorylated by serotonin (18). Thus, whereas serotonin and cyclic AMP work by activating a kinase (the cAMP-dependent protein kinase), FMRFamide acts in a novel way to either activate a phosphatase (perhaps an arachidonic acid specific-phosphatase) or to inhibit the cyclic AMP-dependent protein kinase. We are now performing biochemical experiments to distinguish between these two possibilities.

Presynaptic inhibition has two additional parallels to presynaptic facilitation. First, as is the case with presynaptic facilitation, presynaptic inhibition shows an activity-dependent enhancement (17). If the sensory neuron is active just before it is exposed to FMRFamide, the depression of transmitter release from the sensory neuron terminal is more powerful and more prolonged than if the sensory neuron is not active. This associative mechanism is characteristic of classical conditioning in the facilitating system, and suggests that the inhibitory component may have a comparable role in the associative inhibitory conditioning. Second, repeated presentation of FMRFamide produces a long-term depression of transmitter release, which persists over 24 hours. Unlike the short-term process, which does not require new protein synthesis, this long-term process resembles the long-term facilitation produced by serotonin in being selectively blocked by inhibitors of protein synthesis (13). We have recently identified specific patterns

of protein synthesis associated with long-term facilitation. It therefore also will be interesting to explore whether a complementary pattern of protein synthesis also accompanies the turning on of the long-term inhibitory pathway.

In a larger sense, these studies of behavioral sensitization and inhibition illustrate that environmental stimuli can act on single sensory neurons through two different modulatory systems, one facilitatory and one inhibitory. These modulatory systems use two different families of transmitters (including serotonin for facilitation and FMRFamide for inhibition), and engage two different second-messenger systems within the sensory neurons—the cAMP cascade for facilitation and the lipoxygenase pathway of arachidonic acid for inhibition. Therefore, our results suggest that these opposing behavioral events are represented within the nervous system by the activation of antagonistic modulatory systems and are rerepresented within single sensory neurons by the balance of actions of competing second-messenger systems. Thus, these results begin to reveal an unexpected richness at the cellular and molecular levels underlying the internal representation of external events.

Literature Cited

(1) Belardetti *et al.* 1986. *Proc. Natl. Acad. Sci. USA* **83:** 7094–7098.
(2) Belardetti *et al.* 1987. *Nature* **325:** 153–156.
(3) Brezina *et al.* 1987a. *J. Physiol.* **382:** 267–290.
(4) Brezina *et al.* 1987b. *J. Physiol.* **388:** 565–596.
(5) Castellucci *et al.* 1980. *Proc. Natl. Acad. Sci. USA* **77:** 7492–7496.
(6) Castellucci *et al.* 1986. Pp. 83–102 in *Coexistence of Neuronal Messengers: A New Principle in Chemical Transmission, Progress in Brain Research, Vol. 68*, T. Hokfelt, K. Fuxe and P. Pernow, eds. Elsevier, Amsterdam.
(7) Comb *et al.* 1982. *Nature* **295:** 663–666.
(8) Dale and Kandel 1988. *Soc. Neurosci. Abstr.* **14:** (in press).
(9) Edmonds *et al.* 1988. *Soc. Neurosci. Abstr.* **14:** (in press).
(10) Hille 1984. *Ionic Channels of Excitable Membranes*. Sinauer, Sunderland, MA.
(11) Mackey *et al.* 1987. *Proc. Natl. Acad. Sci. USA* **84:** 8730–8734.
(12) Mackey *et al.* 1988. *Soc. Neurosci. Abstr.* **14:** (in press).
(13) Montarolo *et al.* 1988. *Nature* **333:** 171–174.
(14) Noda *et al.* 1982. *Nature* **295:** 202–206.
(15) Piomelli *et al.* 1987. *Nature* **328:** 38–43.
(16) Scheller and Kirk 1987. *Trends Neurosci.* **10:** 46–52.
(17) Small *et al.* 1988. *Soc. Neurosci. Abstr.* **14:** (in press).
(18) Volterra *et al.* 1988. *Soc. Neurosci. Abstr.* **14:** (in press).
(19) Yaari 1988. *Soc. Neurosci. Abstr.* **14:** (in press).

Ion channels of Paramecium, *yeast, and* E. coli. C. KUNG (Laboratory of Molecular Biology and Department of Genetics, University of Wisconsin, Madison, WI).

We found gated ion channels in different microbes. Channels appear to have evolved early and exist in all cells.

At least seven types of channels are known to exist in *Paramecium*, a giant protozoan cell. Some mutations turn individual channel activity up; others turn them down or off. Mutants defective in the activities of their Ca^{++}-gated channels had single amino-acid substitutions in the third or fourth Ca^{++} binding pocket of their calmodulin.

The yeast plasma membrane was examined using the patch-clamp method, after removing the cell wall. Two types of channels have been discovered to date: (1) a depolarization-gated K^+-specific channel, 20 pS in conductance, blockable by Ba^{++} and quinidine; and (2) a mechanically gated poorly selective channel, 40 pS in conductance.

To study the ion channels of *E. coli*, we first grew the bacteria in cephalexin which blocks septation. We then converted the long filaments to large spheroplasts (3–10 μm diameter) with EGTA and lysozyme. Patch-clamp studies of these spheroplasts show that there are at least two types of voltage-gated channels. One of them is also gated by mechanical forces on the patch membrane. This channel has a very large conductance (800 pS) and almost no ion selectivity. Several pieces of evidence indicate that this channel exists in the outer membrane.

Ion channels in microbes are interesting in terms of their (1) physiological roles (osmoregulation, chemotaxis, energetics, sensory transductions?), (2) implications in terms of the evolution of senses, and (3) utility in expressing animal channel genes cloned into these microbes.

Supported by NIH GM22714, -36386, -37925, DK39121.

Regulation of neuronal ion channels and neuronal activity by protein phosphorylation. IRWIN B. LEVITAN, PETER H. REINHART, SUNG KWON CHUNG (Graduate Department of Biochemistry, Brandeis University, Waltham, MA 02254).

Work from a number of different laboratories over the last decade has provided convincing evidence that cyclic AMP-dependent protein phosphorylation can modulate ion channel properties, and that this form of channel regulation occurs in cells under physiological conditions. The active catalytic subunit of the cyclic AMP-dependent protein kinase is easily purified from mammalian heart or skeletal muscle. Because its active site has been very well conserved during evolution, this purified enzyme from mammalian sources can be used as a specific biochemical probe to examine regulation of ion channel properties in such diverse groups as mammals and molluscs.

We have examined the effects of the bovine heart catalytic subunit on calcium-dependent potassium channels from the nervous systems of snails and rats. Patch-clamp recordings from identified neurons in the garden snail *Helix* reveal the presence of a calcium-dependent potassium channel with a single channel conductance of about 75 pS. When patches containing these channels are detached from the cell, and the catalytic subunit of the cyclic AMP-dependent protein kinase together with ATP and magnesium is applied to what was formerly the cytoplasmic membrane surface, the activity of the channels increases dramatically. The results are consistent with the possibility that phosphorylation by the catalytic subunit increases the sensitivity of these calcium-dependent potassium channels to activation by calcium and/or voltage. Furthermore, these results indicate that the regulatable phosphorylation target is a membrane-associated protein which comes away with the membrane patch when it is pulled off the cell. These experiments have been extended by examining the activity of calcium-dependent potassium channels from snail neurons, reconstituted either in large planar bilayers or in smaller bilayers formed on the tips of patch electrodes. Under these conditions again the channel activity may be regulated by the addition of the catalytic subunit together with magnesium and ATP. These experiments allow the fundamental conclusion that the regulatable phosphorylation target is either the ion channel protein itself, or some regulatory element which is so intimately associated with the ion channel protein that it swims with it in the bilayer.

More recently we have extended these studies to plasma membrane fractions from rat brain. We have found at least three and probably more different calcium-dependent potassium channels from these partially purified plasma membrane preparations, which can be reconstituted in bilayers. These channels differ in their single channel conductances, in some kinetic properties, and in some aspects of their pharmacology, but they also share many features including calcium sensitivity and potassium selectivity. Furthermore several of these channels are subject to regulation by phosphorylation in the bilayer in the same way as the channel from *Helix* neurons. These studies raise the interesting

possibility that there exists in rat brain a *family* of calcium-dependent potassium channels, which may be closely related in some of their functional properties. Attempts are underway to purify and clone one or more of these calcium-dependent potassium channels, to determine the structural correlates of these functional similarities and distinctions.

Regulation of intracellular Ca^{2+} concentration in exocrine glands. A. MARTY, R. HORN[1], Y. P. TAN[2], AND J. ZIMMERBERG[3] (Laboratoire de Neurobiologie, Ecole Normale Superieure, 46 rue d'Ulm, 75005 Paris, France and [1]Roche Institute of Molecular Biology, Nutley, NJ 07110, [2]Physical Science Laboratory, N. I. H., Bethesda, MD 20892, and [3]Bogazici Universitesi, Bebek, Istanbul, Turkey).

Secreting cells of exocrine glands respond to muscarinic stimulation by releasing Ca^{2+} from internal stores. Several approaches were used to characterize the kinetics of this process. Experiments were performed at room temperature on cells from rat lacrimal glands which had been isolated using enzymatic treatment.

In one series of experiments, cells were loaded with the Ca^{2+} indicator fura2, and the internal Ca^{2+} concentration, Ca_i, was monitored following bath application of acetylcholine (ACh, 0.1–10 μM). Ca_i rose to an initial peak of 0.5 to 2 μM. This was followed either by a plateau corresponding to a somewhat lower Ca_i value or by a damped oscillation. Oscillations were mostly observed with ACh concentrations of 0.2–0.5 μM and had interpeak intervals of 7–15 s.

A second approach was to perform tight-seal whole cell recordings. Upon application of ACh, Ca^{2+}-dependent K^+ and Cl^- currents were activated. However this response was difficult to study quantitatively as it exhibited a pronounced rundown from one ACh application to the next. By varying the size of the recording pipette and that of the cell, evidence was gathered indicating that rundown was due to the loss of a water soluble substance (washout). Analyzing the time course of washout indicated that the washout molecule had a diffusion constant (and a molecular size) similar to glucose.

To obviate washout, we used a new method whereby the polyene antibiotic nystatin (50–100 μg/ml) was introduced into the recording pipette. The pipette-cell connection was then established by nystatin channels instead of using suction in the pipette. ACh-sensitive currents recorded with this method did not display washout. These currents rose abruptly after a marked delay (on the order of 1–5 s). The delay was a linear function of the inverse of the ACh concentration. The intercept of the line with the abscissa axis may reflect the dissociation constant of ACh for its receptor. The value was 0.25 μM.

Finally, short Ca^{2+} transients ("wavelets") were obtained in the conventional whole-cell recording mode by stimulating the cells with high Ca^{2+} or with inositoltrisphosphate in the pipette. These transients were attributed to Ca^{2+}-induced Ca^{2+} release in the endoplasmic reticulum. ACh-induced oscillations ("waves") may be due to the simultaneous recruitment of several wavelets. Feedback mechanisms likely to be involved in this coordination of Ca^{2+} transients are currently being investigated.

Feeling around inside a Ca^{2+}-activated K^+ channel in the dark. CHRISTOPHER MILLER, AND JACQUES NEYTON (Graduate Department of Biochemistry, Brandeis University, Waltham, MA).

Ion channels are unique among membrane transport proteins in that the very ion-transport function for which they are designed can be used to wheedle out clues about their molecular structures. For example, in the absence of direct structural information, we are nevertheless confident that these proteins are all built around a transmembrane pore structure through which ions diffuse passively. This fundamental structural motif of channels enables us to ask more refined questions about ion channel structure. The high-conductance Ca^{2+}-activated K^+ channel from rat skeletal muscle, reconstituted into planar phospholipid bilayer membranes, provides a good system to investigate the structure of the ion-diffusion pathway via a close examination of ion conduction, selectivity, and blocking of single channels. This highly K^+-selective channel accommodates several K^+ ions simultaneously in single-file within the narrow part of the pore. Barium blocks this channel by binding strongly in this narrow region of the pore, and we show here that discrete Ba^{2+} blocking can be used to gain a detailed picture of the pore. We use two types of experiments to attach questions of pore structure. First, we show that a Ba^{2+} ion inside the channel can be trapped by driving the channel into its "closed" conformation by hyperpolarizing or lowering Ca^{2+}. When closed, the channel does not permit the escape of Ba^{2+} to *either* side; this result implies that in the closed state, energy (or steric) barriers to ion movement are established on both sides of the conduction pathway. Second, we show that the rate of Ba^{2+} escape from the open pore is strongly affected by K^+ on the two sides of the membrane. A detailed examination of this phenomenon shows that the channel contains at least four K^+-binding sites, which are often occupied simultaneously. These sites are of inherently high affinity and selectivity for K^+, but the multiple occupancy leads to destabilization of the ions in the pore, and hence to the unusual combination of high conductance and extreme ionic selectivity shown by this channel.

Molecular studies of voltage-sensitive potassium channels. DIANE PAPAZIAN, THOMAS SCHWARZ, BRUCE TEMPEL, LESLIE TIMPE, YUH NUNG JAN, AND LILY JAN (Howard Hughes Medical Institute, University of California, San Francisco, CA 94143).

Voltage-sensitive potassium channels probably represent the most diverse group of ion channels found in most cell types studied in the animal and the plant kingdoms. Different combinations of potassium channels are found in different cells and are involved in a variety of cell functions. In the nervous system, they control excitability and modulate the strength of synaptic inputs; some of the potassium channels have been implicated in the processes of learning and memory. To better understand how these channels work and how the tremendous diversity of these channels is generated, one needs to study these channels biochemically. We have cloned the first such channel gene by taking advantage of *Drosophila* genetics (1) and found that alternative splicing at the *Shaker* locus provides one scheme for generating diversity (2, 3).

Although no potassium channels have been purified and characterized to the extent to allow for sequence comparison, identification of *Shaker* gene products as potassium channel proteins is possible by the following three criteria: (i) genetic and electrophysiological studies carried out previously by us, as well as other groups, showed that *Shaker* mutations affect a particular type of potassium channel (the A channel) that inactivates with a time constant of around 20 ms (4). (ii) Sequence comparison with the sodium channel gene and that of a dihydropyridine binding protein (likely part of a calcium channel) reveals a common motif: the so-called S4 sequence of around 20 amino acids, in which a basic residue (mostly arginine, and sometimes lysine) is present at every third position, alternating with two hydrophobic residues (5). This S4 sequence has been proposed to act as the voltage sensor of the channel. (iii) Functional expression of the potassium channel (A channel) in *Xenopus* oocytes has been demonstrated when mRNA tran-

scribed from a single species of *Shaker* cDNA is injected into the oocyte (3).

Different *Shaker* proteins arising from alternative splicing share a common core sequence containing multiple hydrophobic stretches that potentially can span the membrane, as well as a long stretch of hydrophilic sequence preceding the hydrophobic stretches (2); both are highly conserved in a homolog isolated from mouse brain cDNA libraries (6), suggesting that they are probably crucial for certain structural or functional aspects of this channel.

Literature Cited

(1) Papazian *et al.* 1987. *Science* **237**: 749–753.
(2) Schwarz *et al.* 1988. *Nature* **331**: 137–142.
(3) Timpe *et al.* 1988. *Nature* **331**: 143–145.
(4) Papazian *et al.* 1988. *Ann. Rev. Physiol* **50**: 379–394.
(5) Tempel *et al.* 1987. *Science* **237**: 770–775.
(6) Tempel *et al.* 1988. *Nature* **332**: 837–839.

The light-regulated, cyclic GMP-gated conductance in retinal rods and cones. K.-W. YAU (Howard Hughes Medical Institute and Department of Neuroscience, The Johns Hopkins University School of Medicine, Baltimore, MD 21205).

Retinal rods and cones respond to light with a membrane hyperpolarization, resulting from the decrease of an ionic conductance (the light-regulated conductance) in the outer segment. One proposed underlying mechanism is that light increases internal free Ca^{++} which then blocks the conductance; another is that light triggers the hydrolysis of cGMP, which supposedly keeps the conductance open in darkness.

We recently ruled out the Ca^{++} idea because: (1) intracellular Ca^{++} had little direct influence on the opening of the conductance in rods, and (2) Ca^{++} appeared to decrease rather than increase in the rod outer segment during illumination. The picture we derived is that in darkness there is a circulation of Ca^{++} at the outer segment, with a light-suppressible influx through the above conductance and an equal, light-insensitive efflux through a Na^{+}-Ca^{++} exchange carrier.

Using excised, inside-out membrane patches we found, as did Fesenko *et al.* (1985, *Nature* **313**: 310–313), that cGMP directly activates an ionic conductance in the rod outer segment membrane, with electrical properties similar to those of the light-sensitive conductance. The activation of the conductance by cGMP has a Hill coefficient as high as 3, indicating a minimum of three binding sites for cGMP per channel molecule. In the absence of divalent cations, cGMP-induced single-channel activity occurred in bursts of a few ms. This short burst duration suggests that cGMP is bound loosely to the channel, allowing the channel to track the internal cGMP concentration closely during phototransduction. In physiological conditions external divalent cations exert a flicker block on the channel, effectively converting it from a normal-size to a minute channel and consequently reducing the background open-channel noise in darkness. The blockage also underlies most of the characteristic outward rectification of the channel.

Using a truncated rod outer segment preparation we verified that the above cGMP-activated conductance can be suppressed by light, provided GTP is present. This requirement for GTP is consistent with the known involvement of a G-protein in the light-activated biochemical cascade leading to cGMP hydrolysis.

The Ca^{++} fluxes described above now appear to provide a negative feedback link between the conductance and the cGMP level, through an influence of Ca^{++} on cGMP metabolism. In darkness this feedback stabilizes the dark current; in the light this feedback underlies the phenomenon of light adaptation.

We also found a very similar phototransduction mechanism in cones. Interestingly, the cone conductance is a different molecular species in that it has slightly different electrical properties.

Three-dimensional structure of the acetylcholine receptor. N. UNWIN AND C. TOYOSHIMA (MRC Laboratory of Molecular Biology, Hills Road, Cambridge CB2 2QH, U. K.).

We study the structure of the acetylcholine receptor by electron image analysis of postsynaptic membranes from *Torpedo* electric organ crystallized in the form of long tubular vesicles. Earlier analyses revealed the pseudo-pentagonal configuration of the subunits around the central ion channel and identified the individual polypeptide chains. Recently we extended the resolution to about 18 A and examined the subunit configuration in the presence of the acetylcholine analogue, carbamylcholine. Desensitization, induced by the carbamylcholine, appears to be associated with a quaternary rearrangement involving predominantly the δ-subunit. Most recently, by helical reconstruction, we have observed the precise three-dimensional profile formed by the ion channel; it constricts sharply at the level of the phospholipid headgroups on either side of the bilayer.

INDEX

C

D

E

F

G

H

I

J

N

O

P

Q

R

S

T

U

V

W

X

Y

Z

CONTENTS